

# CHEM322 - Inorganic Chemistry

This text is disseminated via the Open Education Resource (OER) LibreTexts Project (<https://LibreTexts.org>) and like the hundreds of other texts available within this powerful platform, it is freely available for reading, printing and "consuming." Most, but not all, pages in the library have licenses that may allow individuals to make changes, save, and print this book. Carefully consult the applicable license(s) before pursuing such effects.

Instructors can adopt existing LibreTexts texts or Remix them to quickly build course-specific resources to meet the needs of their students. Unlike traditional textbooks, LibreTexts' web based origins allow powerful integration of advanced features and new technologies to support learning.



The LibreTexts mission is to unite students, faculty and scholars in a cooperative effort to develop an easy-to-use online platform for the construction, customization, and dissemination of OER content to reduce the burdens of unreasonable textbook costs to our students and society. The LibreTexts project is a multi-institutional collaborative venture to develop the next generation of open-access texts to improve postsecondary education at all levels of higher learning by developing an Open Access Resource environment. The project currently consists of 14 independently operating and interconnected libraries that are constantly being optimized by students, faculty, and outside experts to supplant conventional paper-based books. These free textbook alternatives are organized within a central environment that is both vertically (from advance to basic level) and horizontally (across different fields) integrated.

The LibreTexts libraries are Powered by [NICE CXOne](#) and are supported by the Department of Education Open Textbook Pilot Project, the UC Davis Office of the Provost, the UC Davis Library, the California State University Affordable Learning Solutions Program, and Merlot. This material is based upon work supported by the National Science Foundation under Grant No. 1246120, 1525057, and 1413739.

Any opinions, findings, and conclusions or recommendations expressed in this material are those of the author(s) and do not necessarily reflect the views of the National Science Foundation nor the US Department of Education.

Have questions or comments? For information about adoptions or adaptations contact [info@LibreTexts.org](mailto:info@LibreTexts.org). More information on our activities can be found via Facebook (<https://facebook.com/Libretexts>), Twitter (<https://twitter.com/libretexts>), or our blog (<http://Blog.Libretexts.org>).

This text was compiled on 01/18/2025



## TABLE OF CONTENTS

Licensing

What is Inorganic Chemistry?

Licensing

### Unit 1: Atomic Structure

- 1.1: Historical Development of Atomic Theory
  - 1.1.1: Early Experiments of Atomic Theory
  - 1.1.2: Discovery of Subatomic Particles
  - 1.1.3: Quantization of Energy and Bohr Model of the Atom
  - 1.1.4: Wave-Particle Duality
- 1.2: Electronic Structure of the Atom
  - 1.2.1: Wave Quantization and Particle in a Box
  - 1.2.2: The Schrodinger Equation
  - 1.2.3: Quantum Numbers and Atomic Wave Functions
- 1.3: Multi-Electron Atoms
  - 1.3.1: Orbital Energies
  - 1.3.2: Shielding
  - 1.3.3: Aufbau Principle
  - 1.3.4: Slater's Rules
- 1.4: Periodic Properties of the Elements
  - 1.4.1: Effective Nuclear Charge
  - 1.4.2: Ionization energy
  - 1.4.3: Electron Affinity
  - 1.4.4: Covalent and Ionic Radii
  - 1.4.5: Lanthanide Contraction
  - 1.4.6: The Uniqueness Principle
- 1.5: Unit 1 Practice Problems

### Unit 2: Molecular Structure

- 2.1: Chemical Bonding
  - 2.1.1: Types of Chemical Bonds
  - 2.1.2: Electronegativity and the Bonding Continuum
  - 2.1.3: Polarizability and Percent Ionic Character
- 2.2: Lewis Structures and Molecular Shape
  - 2.2.1: Lewis Electron-Dot Diagrams
  - 2.2.2: Formal Charge
  - 2.2.3: Resonance
  - 2.2.4: Expanded Octets
  - 2.2.5: Limitation of Lewis Theory
  - 2.2.6: Valence Shell Electron-Pair Repulsion
  - 2.2.7: Lone Pair Repulsion
  - 2.2.8: Multiple Bonds
  - 2.2.9: Electronegativity and Atomic Size Effects

- 2.2.10: Molecular Polarity

## Unit 3: Molecular Symmetry

- 3.1: Symmetry Elements and Operations LOs
  - 3.1.1: Definitions and Examples
- 3.2: Point Groups
  - 3.2.1: Molecular Point Groups
  - 3.2.2: Assigning Point Groups
  - 3.2.3: Chirality
- 3.3: Unit 3 Practice Problems

## Unit 4: Group Theory

- 4.1: Groups
  - 4.1.1: Properties of Groups
- 4.2: Representations and Character Tables
  - 4.2.1: Matrices
  - 4.2.2: Representations of Point Groups
  - 4.2.3: Character Tables
- 4.3: Application to Vibrational Spectroscopy
  - 4.3.1: Molecular Vibrations
- 4.4: Unit 4 Practice Problems

## Unit 5: Molecular Orbitals

- 5.1: Valence Bond Theory
  - 5.1.1: The Shapes of Molecules (VSEPR Theory) and Orbital Hybridization
- 5.2: Linear Combination of Atomic Orbitals
  - 5.2.1: Formation of Molecular Orbitals from Atomic Orbitals
  - 5.2.2: Molecular Orbitals from s Orbitals
  - 5.2.3: Molecular Orbitals from p Orbitals
  - 5.2.4: Molecular orbitals from d orbitals
  - 5.2.5: Nonbonding Orbitals and Other Factors
- 5.3: Diatomic MO Diagrams
  - 5.3.1: Homonuclear Diatomic Molecules
    - 5.3.1.1: Molecular Orbitals
    - 5.3.1.2: Orbital Mixing
    - 5.3.1.3: Diatomic Molecules of the First and Second Periods
    - 5.3.1.4: Photoelectron Spectroscopy
  - 5.3.2: Heteronuclear Diatomic Molecules
    - 5.3.2.1: Orbital ionization energies
    - 5.3.2.2: Polar bonds
    - 5.3.2.3: Ionic Compounds and Molecular Orbitals
- 5.4: Polyatomic MO Diagrams
  - 5.4.1: Ligand Group Orbitals and Generator Functions
  - 5.4.2: Polyatomic Molecules
    - 5.4.2.1: Bifluoride anion
    - 5.4.2.2: Carbon Dioxide
    - 5.4.2.3: H<sub>2</sub>O

- 5.4.2.4:  $\text{NH}_3$
- 5.4.3: Why is  $\text{BeH}_2$  Linear and  $\text{H}_2\text{O}$  Bent?
- 5.5: Pi Bonding and Hypervalency
  - 5.5.1:  $\text{BF}_3$
  - 5.5.2: Expanded Octets and Molecular Orbitals

## Unit 6: Solid State Chemistry

- 6.1: Solid State Structures
  - 6.1.1: Cubic Lattices and Close Packing
  - 6.1.2: Ionic Radii and Radius Ratios
- 6.2: Crystalline Solids
  - 6.2.1: Types of Crystalline Solids
  - 6.2.2: Alloys and Intermetallics
  - 6.2.3: The Imperfect Solid State
- 6.3: X-Ray Crystallography of Solids
  - 6.3.1: Miller Indices (hkl)
  - 6.3.2: X-rays and X-ray Diffraction
  - 6.3.3: Powder X-ray Diffraction
- 6.4: Energetics of Ionic Solids
  - 6.4.1: Lattice Enthalpies of Ionic Solids
  - 6.4.2: Born Haber Cycles
  - 6.4.3: Lattice Energies and Solubility
  - 6.4.4: Theoretical Lattice Energy Calculations
  - 6.4.5: Kapustinskii Equation
- 6.5: Band Theory and Conductivity
  - 6.5.1: Bonding in Metals and Semiconductors
  - 6.5.2: The Fermi Level
  - 6.5.3: Semiconductors- Band Gaps, Colors, Conductivity and Doping
  - 6.5.4: Periodic Trends- Metals, Semiconductors, and Insulators
  - 6.5.5: Semiconductor p-n Junctions
  - 6.5.6: Diodes, LEDs and Solar Cells
  - 6.5.7: Superconductors

## Unit 7: Acid-Base and Donor-Acceptor Chemistry

- 7.1: Acid Base Chemistry
  - 7.1.1: Arrhenius Model
  - 7.1.2: Brønsted-Lowry Model
  - 7.1.3: Metal Ions as Acids
  - 7.1.4: Autoionization and Solvent Leveling
  - 7.1.5: Lewis Model and Frontier Orbitals
- 7.2: Hard Soft Acid Base Theory
  - 7.2.1: Hard and Soft Acids and Bases
  - 7.2.2: Applications of Hard Soft Acid Base Theory
  - 7.2.3: Theoretical Interpretation of HSAB Theory
- 7.3: Unit 7 Practice Problems

## Unit 8: Electronic Structure of Coordination Complexes

- 8.1: Introduction to Coordination Complexes
  - 8.1.1: What are Coordination Complexes?
  - 8.1.2: History of Coordination Complexes
  - 8.1.3: Nomenclature and Ligands
  - 8.1.4: Coordination Numbers and Structures
  - 8.1.5: Isomerism
- 8.2: Crystal Field Theory
  - 8.2.1: Crystal Field Theory
  - 8.2.2: Crystal Field Stabilization Energy
  - 8.2.3: Non-octahedral Complexes
- 8.3: Crystal Field Theory and Magnetism
  - 8.3.1: Jahn-Teller Distortions
  - 8.3.2: Magnetism
  - 8.3.3: Magnetic Moments of Transition Metals
  - 8.3.4: Ferro-, Ferri- and Antiferromagnetism
- 8.4: Ligand Field Theory
  - 8.4.1: Ligand Field Theory
  - 8.4.2: The Spectrochemical Series
  - 8.4.3: Factors That Affect Ligand Field Splitting
  - 8.4.4: Octahedral vs. Tetrahedral Geometries
- 8.5: Absorption Spectroscopy of Coordination Complexes
  - 8.5.1: Absorption of Light
  - 8.5.2: Colors of Coordination Complexes
  - 8.5.3: Charge-Transfer Spectra
- 8.6: Tanabe Sugano Diagrams
  - 8.6.1: Tanabe-Sugano Diagrams
  - 8.6.2: Selection Rules
  - 8.6.3: Applications of Tanabe-Sugano Diagrams
  - 8.6.4: Tetrahedral Complexes

## Unit 9: Reactions of Coordination Complexes

- 9.1: Substitution Reactions
  - 9.1.1: Review of Reaction Thermodynamics and Kinetics
  - 9.1.2: Introduction to Substitution Reactions
  - 9.1.3: Ligand Substitution Mechanisms
  - 9.1.4: Some Reasons for Differing Mechanisms
    - 9.1.4.1: Dissociation
    - 9.1.4.2: Associative Mechanisms
  - 9.1.5: Thermodynamic Stability and Chelate Effect
  - 9.1.6: Kinetic Lability
  - 9.1.7: The Trans Effect
- 9.2: RedOx Reactions
  - 9.2.1: Redox Mechanisms
  - 9.2.2: Inner Sphere Electron Transfer
  - 9.2.3: Outer Sphere Electron Transfer
- 9.3: Unit 9 Practice Problems

## Unit 10: Organometallic Chemistry

- [10.1: Organometallic Complexes](#)
  - [10.1.1: Introduction to Organometallic Chemistry](#)
  - [10.1.2: Ligand Nomenclature and Classification](#)
  - [10.1.3: Survey of Common Organometallic Ligands](#)
  - [10.1.4: Electron Counting and the 18 Electron Rule](#)
- [10.2: Organometallic Reactions](#)
  - [10.2.1: Ligand Dissociation and Substitution](#)
  - [10.2.2: Oxidative Addition](#)
  - [10.2.3: Reductive Elimination](#)
  - [10.2.4: Migratory Insertion- 1,2-Insertions](#)
  - [10.2.5:  \$\beta\$ -Elimination Reactions](#)
  - [10.2.6: Organometallic Catalysts](#)

[Index](#)

[Glossary](#)

[Detailed Licensing](#)

[Detailed Licensing](#)

## Licensing

---

*A detailed breakdown of this resource's licensing can be found in [Back Matter/Detailed Licensing](#).*

## What is Inorganic Chemistry?

Where did the name "Inorganic Chemistry" come from? Well, the term "Organic Chemistry" literally means the *chemistry of life*. Organic chemistry is the study of carbon-based molecules because the first molecules that were isolated from living organisms contained carbon. On the other hand, minerals and other non-living things seemed to be made of other elements. For some time in our history, scientists believed that the chemical difference between living and non-living things was carbon. So, if "organic" molecules are the molecules of life, then is "inorganic chemistry" the "chemistry of death"? Almost? "Inorganic" chemistry historically meant the chemistry of "non-living" things; and these were non-carbon based molecules and ions.

The names "organic" and "inorganic" come from science history, and still today a generally-accepted definition of *Inorganic Chemistry is the study of non-carbon molecules, or all the elements on the periodic table except carbon* (Figure 1). But, this definition is not completely correct because the field of Inorganic Chemistry also includes organometallic compounds and the study of some carbon-based molecules that have properties that are familiar to metals (like conduction of electricity). This makes the field of inorganic chemistry very broad, and practically limitless. A great way to understand the breadth of the field is to take a look at the abstracts in the latest article of Inorganic Chemistry. Or, check out the 20 most-read articles from this past year using the links below.

**Inorganic**  
(not life)

**Life**

\* Lanthanide series

\*\* Actinide series

**Figure 1.** An illustration of the historic meaning of "organic" and "inorganic". The modern understanding of organic and inorganic chemistry is not consistent with these historical meanings.

### External links:

- The journal, Inorganic Chemistry: <https://pubs.acs.org/journal/inocaj>
- The latest issue of Inorganic chemistry: <https://pubs.acs.org/toc/inocaj/current>
- The most popular Inorganic Chemistry articles from the past month and the past year: <https://pubs.acs.org/action/showMostReadArticles?journalCode=inocaj>

### Practice

#### What are the Sub-Fields of Inorganic Chemistry?

To appreciate the breadth of Inorganic Chemistry, go to the most recent issue of Inorganic Chemistry and look at the titles and visual abstracts. Identify at least 4 sub-fields of Inorganic Chemistry.

**Answer**

There are a lot of correct answers here! The point here is that you notice that Inorganic Chemistry is a very broad field. It has something for almost everyone because many other fields overlap with Inorganic Chemistry. You might notice that some of the sub-fields you identified are also interdisciplinary fields between inorganic chemistry and another discipline. For a list of some of the subfields of Inorganic Chemistry, check this [Wikipedia article](#).



## Licensing

---

*A detailed breakdown of this resource's licensing can be found in [Back Matter/Detailed Licensing](#).*

## CHAPTER OVERVIEW

### Unit 1: Atomic Structure

- 1.1: Historical Development of Atomic Theory
  - 1.1.1: Early Experiments of Atomic Theory
  - 1.1.2: Discovery of Subatomic Particles
  - 1.1.3: Quantization of Energy and Bohr Model of the Atom
  - 1.1.4: Wave-Particle Duality
- 1.2: Electronic Structure of the Atom
  - 1.2.1: Wave Quantization and Particle in a Box
  - 1.2.2: The Schrodinger Equation
  - 1.2.3: Quantum Numbers and Atomic Wave Functions
- 1.3: Multi-Electron Atoms
  - 1.3.1: Orbital Energies
  - 1.3.2: Shielding
  - 1.3.3: Aufbau Principle
  - 1.3.4: Slater's Rules
- 1.4: Periodic Properties of the Elements
  - 1.4.1: Effective Nuclear Charge
  - 1.4.2: Ionization energy
  - 1.4.3: Electron Affinity
  - 1.4.4: Covalent and Ionic Radii
  - 1.4.5: Lanthanide Contraction
  - 1.4.6: The Uniqueness Principle
- 1.5: Unit 1 Practice Problems

---

Unit 1: Atomic Structure is shared under a [not declared](#) license and was authored, remixed, and/or curated by LibreTexts.

## 1.1: Historical Development of Atomic Theory

---

Learning objectives for this unit are to:

- Recall the key discoveries in atomic theory, including the quantization of light
  - Describe the relationship between electronic transitions in the atom and the absorption and emission of light energy and perform related calculations
  - Explain the concept of wave-particle duality
  - List the consequences of the Heisenberg Uncertainty Principle
- 

1.1: Historical Development of Atomic Theory is shared under a [CC BY-SA](#) license and was authored, remixed, and/or curated by LibreTexts.

## 1.1.1: Early Experiments of Atomic Theory

### Development of Atomic Theory

Since the ancient times, humans thought of explaining the material world in all of its complexity. The basic idea behind all element theories is that the matter that surrounds us is composed of more simple matter. This matter may be composed of even simpler matter. The most simple matter would be called an element.

The first element theories were one element theories: The greek philosopher Thales thought water was the only element, and everything was a form of water. Anaximenes thought air was the only element, and Heraclitus believed fire was the only element (Figure 1.1.1).



Figure 1.1.1 Thales (640-545 BC) (Attribution: Ernst Wallis et al [Public domain] [https://commons.wikimedia.org/wiki/File:Illustrerad\\_Verldshistoria\\_band\\_I\\_Ill\\_107.jpg](https://commons.wikimedia.org/wiki/File:Illustrerad_Verldshistoria_band_I_Ill_107.jpg)), Anaximenes (585-525 BC) (Attribution: [https://commons.wikimedia.org/wiki/File:Anaximenes\\_of\\_Miletus\\_Painting.jpg](https://commons.wikimedia.org/wiki/File:Anaximenes_of_Miletus_Painting.jpg)) and Heraclitus (544 – 483 BC) (Attribution: RoyFokker [CC BY-SA (<https://creativecommons.org/licenses/by-sa/4.0>)]]), respectively.

However, with only one element assumed it was difficult to explain the material world in all its complexity satisfactorily. This could be done more satisfactorily by a multi-element theory. The first philosopher who introduced a multi-element theory was Empedocles. He suggested a four-element theory with fire, air, water, and soil as the elements (Figure 1.1.2).



Figure 1.1.2 Empedocles (495 – 435 BC) (Attribution: Thomas Stanley, The history of philosophy, 1655 [Public domain] <https://commons.wikimedia.org/wiki/File:Philosophy.jpg>)

### First atomistic ideas



Figure 1.1.3 Democritus (460 – 370 BC) (Attribution: Strannik 92 [CC BY-SA (<https://creativecommons.org/licenses/by-sa/3.0/>)] <https://commons.wikimedia.org/wiki/File:Demokrit.jpg>)

The element theories of Thales, Anaximenes, Heraklitus, and Empedocles were all non-atomistic. This means that they did not include the idea that elements were made of small particles that were indivisible. The first greek philosophers that introduced atomistic element theory were Leukippes, and Democritus (Figure 1.1.3). They assumed that particles cannot be divided into smaller particles infinitely often. Ultimately, after many divisions, one would arrive at particles that could not be further divided, and these particles would be called atoms. Atomistic element theory allows for many different elements which helps to explain the complexity of the material world satisfactorily. However, Leukippes and Democritus did not know how many different elements there were, and how different atoms of different elements were actually distinguished. This question would not be answered until about 2000 years later.

## Modern Atomic Theories



Figure 1.1.4 Antoine Lavoisier, the father of modern chemistry, discovered the law of conservation of mass in 1774. (Attribution: Louis Jean Désiré Delaistre (1800–1871); drawing by Julien Léopold Boilly (1796–1874). [Public domain], [https://commons.wikimedia.org/wiki/File:Lavoisier\\_color.jpg](https://commons.wikimedia.org/wiki/File:Lavoisier_color.jpg))

Although the atomistic idea was already known in the antique, it became forgotten for a long time and was only reintroduced about 2000 years later with Dalton's atom hypothesis. What led to Dalton's atom hypothesis? The first discovery that was important to the development of modern atomic theory was the law of the conservation of mass by Antoine Lavoisier (Fig. 1.1.4). Historically, the conservation of mass and weight was kept obscure for millennia by the buoyant effect of the Earth's atmosphere on the weight of gases, an effect not understood until the vacuum pump first allowed the effective weighing of gases using scales. Until then, in many instances mass seemed to appear or disappear. For example, the mass of wood seems to disappear when it is burned. However, the mass of the wood actually does not disappear it is just converted into the mass of gases, mainly carbon dioxide. When scientists realized that mass never disappeared they could for the first time embark on quantitative studies of the transformations of substances. This in turn led to the idea of chemical elements, as well as the idea that all chemical processes and transformations are simple reactions between these elements. The **law of conservation of mass** states that the mass of a closed system of substances will remain constant, regardless of the processes acting inside the system. An equivalent statement is that matter cannot be created or destroyed, although it may change form. This implies that for any chemical process in a closed system, the mass of the reactants must equal the mass of the products.

## Law of Constant Composition

The discovery of the law of the conservation of mass led to the discovery of the law of the constant composition (also called law of definitive proportions) by Joseph Proust (Fig. 1.1.5). This law was the result of chemical analysis that determined the mass ratio of elements in pure substances. It was found that a pure substance always contains exactly the same proportion of elements by mass. For example the element analysis of pure substances containing the elements carbon and oxygen would be either 42.9% carbon and 57.1% oxygen or 27.3% carbon and 72.7% oxygen.



Figure 1.1.5 Joseph Proust (1754-1826) (Attribution: The original uploader was HappyApple at English Wikipedia. [Public domain] [https://commons.wikimedia.org/wiki/File:ust\\_joseph.jpg](https://commons.wikimedia.org/wiki/File:ust_joseph.jpg))

The law was questioned by Proust's fellow Frenchman Claude Louis Berthollet, who argued that the elements could combine in any proportion. The very existence of this debate was because at the time the distinction between pure chemical compounds and mixtures had not yet been fully developed. When two pure compounds of two different elements are mixed, then the mixture can have a continuous mass ratio between the two elements because compounds can be mixed at any ratio. So, for the example in the two compounds between carbon and oxygen, in mixtures of the two there could be carbon to oxygen ratios varying continuously between 27.7 % to 42.9% carbon, and 42.9% to 72.7% oxygen. It was an accomplishment of Proust that he was able to correctly distinguish between pure compounds and mixtures.

## The Law of Multiple Proportions



Figure 1.1.6 John Dalton 1766-1844 (Attribution: Charles Turner [Public domain] [https://commons.wikimedia.org/wiki/File:les\\_Turner.jpg](https://commons.wikimedia.org/wiki/File:les_Turner.jpg))

John Dalton (Fig. 1.1.6) discovered the law of multiple proportions by close analysis of Proust's law of constant composition. He noticed that if two elements form more than one compound between them, then the ratios of the masses of the second element which combines with a fixed mass of the first element will be the ratios of small whole numbers, also called integer numbers. Let us see what is the meaning of the law of the multiple proportions by an example:

### ✓ Example 1.1.1.1

The first compound contains 42.9% by mass carbon and 57.1% by mass oxygen.

The second compound contains 27.3% by mass carbon and 72.7% by mass oxygen.

Show that the data are consistent with the Law of Multiple Proportions!

#### Solution

In 100 g of the first compound (100 is chosen to make calculations easier) there are 57.1 g O and 42.9 g C.

The mass of O per gram C is:

$$57.1 \text{ g O} / 42.9 \text{ g C} = 1.33 \text{ g O per g C}$$

In 100 g of the second compound, there are 72.7 g O and 27.3 g C.

The mass of oxygen per gram of carbon is:

$$72.7 \text{ g O} / 27.3 \text{ g C} = 2.66 \text{ g O per g C}$$

Dividing the mass O per g C of the second (larger value) compound by the mass O per g C of the first compound gives:

$$2.66 : 1.33 = 2 : 1$$

2 and 1 are both integer numbers.

## Dalton's Atom Hypothesis

Dalton argued that atoms could explain the law of the multiple proportions. If one assumed that elements were made of the same type of indivisible particles, that are identical in mass and all properties then, because these particles can only come in integer numbers, different atoms can be combined to form compounds also only in integer numbers. Thus, in a pure compound atoms of unlike elements would be combined in small whole number ratios. Consequently a given compound always has the same relative number and types of atoms. Chemical reactions would involve reorganization of atoms, but the atoms would retain their identity. Atoms could be rearranged in a chemical reaction but not created or destroyed.

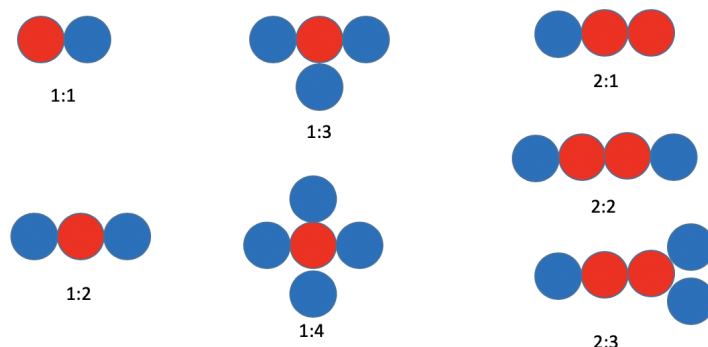


Figure 1.1.7 Illustration of the law of the multiple proportions for two generic, different atoms (red and blue balls).

Figure 1.1.7 is a simple illustration how atoms can explain the law of multiple proportions. The blue and red balls symbolize different atoms of different elements. It is possible to combine a red atom with one, two, three, or four blue atoms to make four different compounds. It is for example also possible to combine two red atoms with one, two or three blue atoms. In all of these compounds as well as in all other thinkable ones, the blue and red atoms can only be combined in integer numbers.

## Dalton's Atom Symbols

Dalton also thought of symbols for the atoms of the different elements. The symbols are different from the element symbols that are used today, but the concept is the same. You can see some of them in Figure 1.1.8. For example oxygen is represented by a white ball, while carbon is symbolized by a black ball. You can also see that Dalton already combined atom symbols of different elements to illustrate compounds. For example he combined one white ball with one black ball to indicate carbon monoxide, while he combined two white balls with one black ball to indicate carbon dioxide. In this case he correctly identified the ratios of atoms in the two compounds. However, you can see that this is not always the case. For example, he combined one hydrogen atom (white ball with a dot in the middle) with one oxygen atom to indicate the composition of water. However, as we know today, a water molecule has two hydrogen atoms and one oxygen atom. Why has he been right with the carbon-oxygen compounds, but wrong about the water? The answer is that at the time he could determine the atom ratios only from the law of the multiple proportions. At the time there was only one compound known that was made of hydrogen and oxygen, water, so he assumed the simplest atom ratio of 1:1. If he had known hydrogen peroxide, which has the composition  $\text{H}_2\text{O}_2$ , and thus half as much hydrogen per oxygen, he would have probably correctly assigned the correct hydrogen to oxygen ratio to water. In the case of the carbon oxides, he assigned the compositions correctly because both carbon monoxide and carbon dioxide were known at the time.

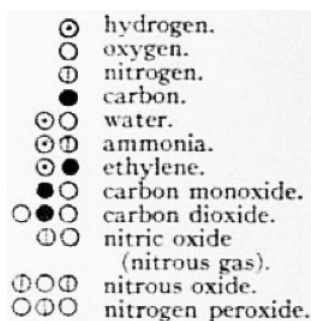


Figure 1.1.8 Dalton's atom symbols (Attribution: Encyclopædia Britannica, 1911 [Public domain]  
[https://commons.wikimedia.org/wiki/File:An\\_symbols.png](https://commons.wikimedia.org/wiki/File:An_symbols.png))

This page titled [1.1.1: Early Experiments of Atomic Theory](#) is shared under a [CC BY-SA 4.0](#) license and was authored, remixed, and/or curated by [Kai Landskron](#).

- [1.1: Historical Development of Atomic Theory](#) by [Kai Landskron](#) is licensed [CC BY 4.0](#).



## 1.1.2: Discovery of Subatomic Particles

### Subatomic Particles

Dalton's atomic theory stated that different elements were made of different atoms, but did not explain what made the atoms different. The answer is that atoms are composed of subatomic particles, protons, neutron, and electrons, and the number of the protons and electrons in an atom defines the element it represents. So after all, atoms are not so indivisible. However, an atom can still be seen as the smallest particle that represents the full properties of an element. If an atoms gets divided further into subatomic particles then these properties are being lost. To understand atoms further, we must therefore understand the subatomic particles they are made of. The first subatomic particle that was discovered was the electron. It was found through the investigation of so-called cathode rays which were a mysterious phenomenon at the time. Cathode rays occur when a high voltage of about 10-20 kV is applied to an evacuated tube (0.0001 mm Hg). You can see such a tube with a cathode ray going through in Figure 1.1.9. The big question was: What causes these rays?

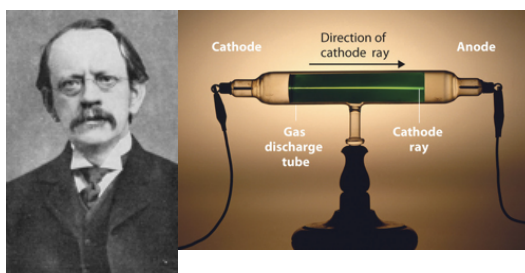


Figure 1.1.9 Joseph John Thomson (1856-1940) (Attribution: [https://commons.wikimedia.org/wiki/File:J\\_Thomson.jpg](https://commons.wikimedia.org/wiki/File:J_Thomson.jpg), PD-US-expired) and his experimental apparatus (Attribution: Chemlibetexts <https://chem.libretexts.org/@api/dek...338&height=228,creativecommons.org/licenses/by-nc-sa/3.0/us/>).

The answer was found by John Joseph Thomson. He applied electric and magnetic fields to these rays and found them deflected. When an electric field was applied the beam was deflected toward the positive pole. When an equally strong electric and magnetic field was applied, and the magnetic field was perpendicular to the electric field then these fields canceled out, and the rays were no longer deflected. Thomson concluded that these rays must consist of negatively charged particles emitted by the negatively charged electrode because they were attracted by the positive pole of the electric field: Electrons. Knowing the forces associated with the electrical and magnetic fields, he was able to calculate a mass to charge ratio of the electrons which is  $5.6857 \times 10^{-9} \text{ g/C}$ . After Thomson, Robert Millikan performed another experiment, the so-called oil drop experiment, that allowed to determine the charge and the mass of the electron. The charge of an electron is  $-1.6 \times 10^{-19} \text{ C}$ , and its mass is  $9.1 \times 10^{-28} \text{ g}$ .

### Thomson's plum pudding atomic model

The discovery of the electron led Thomson to the development of a first atomic model that would include a subatomic particle. It is named plum pudding model (Fig. 1.1.10). In the Thomson atom model electrons are embedded as little particles in a positively charged mass like raisins are embedded in a cake. This atom model is still far from the atom model that we accept today, but it represented an important step forward, because it introduced for the first time the idea that atoms are not indivisible, but contain subatomic particles.

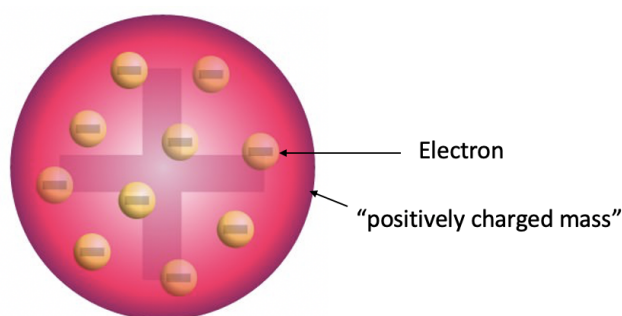


Figure 1.1.10 Thomson's plum pudding atomic model (Attribution: Fatfission (public domain) [https://commons.wikimedia.org/wiki/File:Plum\\_pudding\\_atom.svg](https://commons.wikimedia.org/wiki/File:Plum_pudding_atom.svg))

## Rutherford's Atom Model

Ernest Rutherford (Fig. 1.1.11) wanted to test Thomson's plum pudding atom model by experiment. To do so, he placed a photographic film around a gold foil (Figure 1.1.12). In the following he bombarded the gold foil with alpha radiation. Alpha radiation is a form of radioactivity and consists of helium nuclei, also called alpha-particles. It was known at this time the alpha-particles were positively charged and had a large mass compared to an electron. Rutherford's hypothesis was that if Thomson's atom model was true, then the alpha particles should all go straight through the gold foil like a bullet going through a plum pudding. Therefore, a blackening of the photographic film, which served as the alpha radiation detector, should only occur directly behind the gold film.

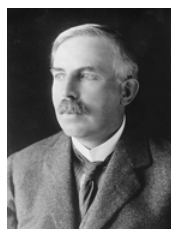


Figure 1.1.11 Sir Ernest Rutherford (1871-1931) who earned the Nobel prize for chemistry 1908. (Attribution: George Grantham Bain Collection (Library of Congress) [Public domain], commons.wikimedia.org/wiki/F...erford\_LOC.jpg)

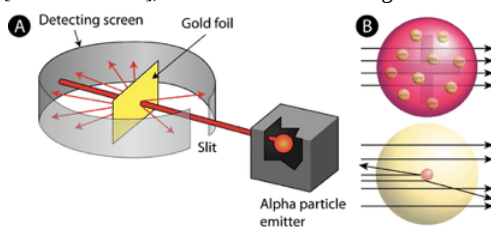


Figure 1.1.12 Rutherford's Gold Foil Experiment

However, what Rutherford observed was that while most of the alpha-particles went straight through the gold foil, some of them were deflected, and a few of them were even reflected. Rutherford concluded that Thomson's plum pudding model must be wrong. A bullet shot at a plum pudding would just never be reflected by the plum pudding and come back at you.

He suggested that the atom would be made of a positively charged nucleus where almost the entire mass of the atom would be concentrated. In the event of a collision between the alpha particle and that nucleus, the alpha particle would be reflected. In the event of an alpha particle passing by the nucleus close, the alpha particle would be deflected. In the event of an alpha particle passing the nucleus in larger distance, the alpha particle would pass the atom practically non-deflected. The observation that most of the alpha particles were not deflected led Rutherford to the conclusion that the overall atom must be much larger than the nucleus, in fact, the data allowed him to calculate that the radius of the atom would be about 10,000 times larger than the radius of the nucleus. This implies that the atoms would be mostly empty space. To explain the empty space, Rutherford assumed that the electrons would move in orbits around the nucleus like planets around the sun. This would be called the planetary model of the atom (Fig. 1.1.13).

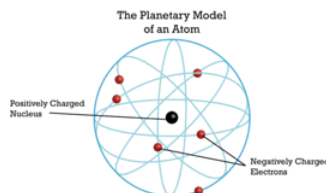


Figure 1.1.13 Rutherford's Atom Model

This page titled [1.1.2: Discovery of Subatomic Particles](#) is shared under a [CC BY-SA 4.0](#) license and was authored, remixed, and/or curated by [Kai Landskron](#).

- [1.1: Historical Development of Atomic Theory](#) by [Kai Landskron](#) is licensed [CC BY 4.0](#).

## 1.1.3: Quantization of Energy and Bohr Model of the Atom

### Bohr's Atom Model

Rutherford's atom model was another big step forward in the development of atomic theory, however there were inherent problems with it as it violated fundamental principles of physics. An electron in an orbit is a self-accelerating electrically charged particle, and according to the laws of physics such particles must emit electromagnetic radiation. However, under normal circumstances atoms do not emit electromagnetic radiation. Secondly, even if the electron emitted electromagnetic radiation, then this would mean that the electron would lose energy because electromagnetic radiation is a form of energy. However, an electron constantly losing energy would make it unstable in its orbit around the nucleus, and it should spiral downward closer to the nucleus until the atom was eventually collapsed. It is however, experimentally not observed that atoms collapse, they are quite stable species. These difficulties of the Rutherford atom model meant that it could not be the final answer to atomic structure. Niels Bohr (Fig. 1.1.14) was aware of the problems of the Rutherford model, and two new developments in physics, namely the concept of the quantization of energy and atomic spectra helped him to develop an improved atom model, known as Bohr model. To understand this model let us look first at the quantization of energy and atomic spectra.



Figure 1.1.14 Niels Bohr (1885 - 1962) (Attribution: Bain News Service, publisher Restored by: Bammesk [Public domain], commons.wikimedia.org/wiki/F...in\_-\_35303.jpg)

### Blackbody Radiation

The quantization of energy was discovered in the context of the physical phenomenon called “blackbody radiation”. Blackbody radiation is the electromagnetic radiation any object sends out due to its temperature (Fig. 1.1.15).



Figure 1.1.15 An example of blackbody radiation emitted by hot, volcanic lava. (Attribution: Hawaii Volcano Observatory (DAS) [Public domain], commons.wikimedia.org/wiki/F...hoehoe\_toe.jpg)

Its distribution of wavelengths follows curves that depend on the temperature and are shown in Figure 1.1.16. You can see that for each temperature the intensity first increases with increasing wavelength, then goes through a maximum, and finally decreases again. You can also see that the overall intensity of the blackbody radiation increases with temperature and that the maximum of the curve shifts to smaller wavelengths with increasing temperature. Objects at room temperature do not emit much blackbody radiation and the wavelengths are far longer than visible for the human eye. However, when an object is heated high enough, intensity increases and wavelength decreases, and the object starts to glow. For instance, lava (Figure 1.1.15) has a temperature high enough so that its blackbody radiation is visible for the human eye. With increasing temperature objects first glow red, then orange, then yellow, and eventually white. This is because red is the color associated with the largest wavelength, and as temperature increases other colors mix into red, until the object glows white. At extremely high temperatures the blackbody radiation also has a significant intensity in the UV region. Such temperatures occur in welding processes, for example, and for this reason welders need to wear glasses that block the UV radiation. The wavelength and intensity of blackbody radiation can be easily measured, but at the beginning of the 20th century there was no good explanation for its behavior. Classical theory predicted that intensity would continuously increase with decreasing wavelength at any temperature which was not in accordance with experimental observation.

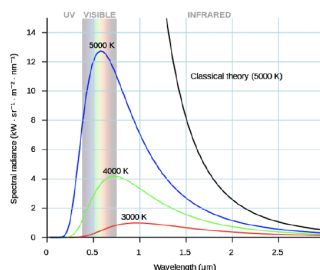


Figure 1.1.16 Experimentally measured intensity of blackbody radiation as a function of wavelength for 3000, 4000, and 5000 K vs. intensity predicted by classical theory (5000 K). (Attribution: Darrh Kule commons.wikimedia.org/wiki/File:Black\_body.svg)

To bring experiment and theory in accordance, Max Planck made the radical assumption that the energy associated with radiation of a given wavelength or a given frequency was quantized. It would be an integer multiple  $n$  of that frequency  $\nu$ , multiplied with proportionality constant  $h$ , known today as the Planck constant.

$$E = n h \nu$$

**Equation 1.1.1** The Planck-Einstein equation.

Using this assumption he was able to derive the Planck equation (Equation 1.1.2) which correctly describes the intensity and wavelength distribution of the blackbody radiation for any temperature. The correct description of blackbody radiation strongly supported Planck's assumption that energy was quantized, but it did not prove it or explain it. The proof and the explanation was found only later. Initially Planck assumed it merely to fit the data.

$$E(\lambda, T) = \frac{2hc^2}{\lambda^5} * \frac{1}{e^{\left(\frac{hc}{\lambda kT}\right)} - 1}$$

$h$  = Planck's constant =  $6.626 * 10^{-34} \text{ J} \cdot \text{s}$   
 $c$  = speed of light =  $2.997925 * 10^8 \text{ m / sec}$   
 $\lambda$  = wavelength (m)  
 $k$  = Boltzmann's constant =  $1.381 * 10^{-23} \text{ J/K}$   
 $T$  = temperature (K)

**Equation 1.1.2** Planck's equation

## Bohr's Atom Model

The second development that contributed to Bohr's atom model was the absorption and emission spectra of atoms. It was experimentally observed that under certain circumstances atoms would send out or absorb electromagnetic radiation of discrete wavelengths that were characteristic for an atom. For example, H atoms would absorb or emit at four discrete wavelengths in the visible region of the electromagnetic spectrum (Fig. 1.1.17).



Figure 1.1.17 The hydrogen emission spectrum in the visible region (Balmer series). (Attribution: Merikanto, Adrignola [CC0], commons.wikimedia.org/wiki/File:spectrum-H.svg)

This is known as the Balmer series named after its discoverer Johann Balmer. Friedrich Paschen and Chester Lyman later found that H also absorbs and emits at discrete wavelengths in the IR and UV region respectively. These wavelengths are known as the Paschen and Lyman series, respectively (Fig. 1.1.18).

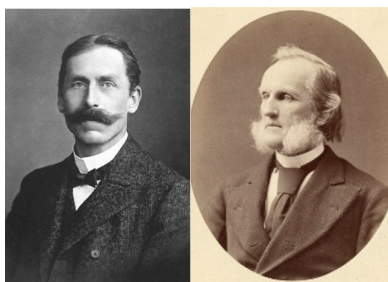


Figure 1.1.18 Friedrich Paschen (1865 – 1947) (Attribution: [www.maerkischeallgemeine.de](http://www.maerkischeallgemeine.de) [Public domain], [commons.wikimedia.org/wiki/File:F...n\\_Physiker.jpg](https://commons.wikimedia.org/wiki/File:F...n_Physiker.jpg)) and Chester Lyman (1814-1988) (Attribution: [commons.wikimedia.org/wiki/File:F...mith\\_Lyman.jpg](https://commons.wikimedia.org/wiki/File:F...mith_Lyman.jpg)), respectively.

For the absorption and emission spectra of H a simple mathematical relationship between the energies associated with the wavelengths can be found. The energy is proportional to a constant, today known as the Rydberg constant, times one over an integer number square minus one over another integer number square, whereby the second integer number would be larger than the first one (Eq. 1.1.3). The observation of integer numbers showed that also the energy and the wavelengths of the atomic absorption and emission spectra are quantized. The question was what the quantization of the absorption spectra meant for atomic structure.

$$\Delta E = R_H \left( \frac{1}{n_{low}^2} - \frac{1}{n_{high}^2} \right)$$

**Equation 1.1.3** Rydberg formula for the emission of light with particular energies.

Bohr answered the question the following way. He argued, that like in the Rutherford model the electrons would move in orbits around the nucleus. A balance of opposite centrifugal forces and Coulomb attractions would hold the electron stable in the orbit. However, because energy is quantized, also the angular momentum of the electron would be quantized, and thus, only discrete radii would be allowed. The most inner orbit would have the quantum number  $n=1$ , the next higher orbit the quantum number  $n=2$ , and so forth (Fig. 1.1.19).

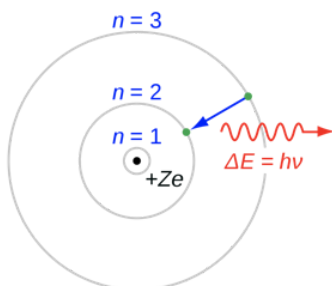


Figure 1.1.19 Bohr atom model (Attribution: JabberWok [CC BY-SA (<http://creativecommons.org/licenses/by-sa/3.0/>)], [commons.wikimedia.org/wiki/File:...atom\\_model.svg](https://commons.wikimedia.org/wiki/File:...atom_model.svg))

The quantization of the electron energies and the radii would be the explanation why electrons, despite self-accelerating, do not continuously emit electromagnetic radiation. Electromagnetic radiation is only emitted when an electron jumps from an outer orbit of higher energy to an inner orbit of lower energy. This radiation must have a discrete wavelength because the energy difference between two orbits is discrete. Vice versa, an atom can absorb electromagnetic radiation of specific wavelength and energy that is suitable to make the electron jump from an inner to an outer orbit. In sum, the quantization of the energy and the radii would explain the quantization of the absorption and emission spectra. The question is: Can the radii be calculated, and what are the associated energies of the electrons in the orbits?



#### Bohr's Postulates (1913)

1. An electron in an atom moves in a circular orbit about the nucleus under the influence of the Coulomb attraction between the electron and the nucleus, obeying the laws of classical mechanics.
2. Instead of the infinity of orbits which would be possible in classical mechanics, it is only possible for an electron to move in an orbit for which its orbital angular momentum  $L$  is an integral multiple of  $h/2\pi$ .

3. Despite the fact that it is constantly accelerating, an electron moving in such an allowed orbit does not radiate electromagnetic energy. Thus, its total energy  $E$  remains constant.
4. Electromagnetic radiation is emitted if an electron, initially moving in an orbit of total energy, discontinuously changes its motion so that it moves in an other orbit of total energy. The frequency of the emitted radiation is equal to the quantity divided by  $h$ .

To calculate the radii and energies of the electron in the H atom Bohr made two assumptions: Firstly, the centrifugal force associated with the electron moving in the orbit would be assumed equal to the Coulomb force between the electron and the proton so that the electron would be stable in the orbit. Secondly, the angular momentum of the electron would be quantized and an integer multiple of the Planck constant  $h$ . The factor  $2\pi$  is because  $E = h/2\pi \times$  angular frequency. The angular frequency (also called angular speed) is the angular displacement (in degree or rad) per time unit. Angular frequency is frequency  $\times 2\pi$ . We can rearrange this equation by solving it for  $v$  and then insert the equation into equation I giving the result as shown in Fig. 1.1.20.

I.

$$F_{cent} = F_{Coulomb}$$

$$\frac{mv^2}{r} = \frac{e^2}{4\pi\epsilon_0 r^2}$$

II.

$$2\pi r m v = n h$$

Solve for  $v$ :

$$v = \frac{n h}{2\pi r m}$$

↓ insert II. in I.

$$\frac{m n^2 h^2}{4\pi^2 r^3 m^2} = \frac{e^2}{4\pi\epsilon_0 r^2}$$

$v$  = velocity of the electron  
 $e$  = elementary charge =  $1.602176\ 53(14) \times 10^{-19}$  C  
 $\epsilon_0$  = dielectric constant of the vacuum  
 $m$  = mass of the electron

Figure 1.1.20 Derivation of the radii of the electron orbits (part 1).

We can then multiply this equation by  $4\pi\epsilon_0 r^2$ , divide by  $e^2$ , and multiply it by  $r$ . This gives us the term  $r = (n^2 h^2 \epsilon_0) / (\pi m e^2)$ . Analyzing the term shows us that  $r$  is only a function of the quantum number  $n$ , specifically the radius is proportional to  $n^2$  (Fig. 1.1.21). All other terms are constants, namely the Planck constant  $h$ , the dielectric constant of the vacuum,  $\pi$ , the mass of the electron, and the elementary charge. By inserting the quantum numbers into the equation we can calculate the actual values for the radii. For example, when we insert 1 for the quantum number  $n$ , we get the radius for the most inner orbit of the electron in the H atom. It is  $5.29 \times 10^{-11}$  m. If we inserted 2 for  $n$ , we would get the second radius, if we inserted 3, we would get the third radius and so on.

$$\frac{mn^2h^2}{4\pi^2r^3m^2} = \frac{e^2}{4\pi\epsilon_0r^2} \quad | \times 4\pi\epsilon_0r^2$$

$$\frac{n^2h^2\epsilon_0}{\pi m} = e^2 \quad | \div e^2 \quad | \times r$$

$$r = \frac{n^2h^2\epsilon_0}{\pi me^2}$$

$$\text{For the first radius (n=1): } r = \frac{1^2h^2\epsilon_0}{\pi me^2} = 5.29 \times 10^{-11} \text{ m}$$

Figure 1.1.21 Continuation of the derivation of the radii of the electron orbits.

Now let us calculate the energies of the electron on these radii. Generally, the overall energy of the electron is the sum of the kinetic and potential energies. The kinetic energy of a moving object is given by  $E_{\text{kin}} = \frac{1}{2}mv^2$ . We know that  $m$  must be the mass of the electron, but what is the velocity of the electron? We can derive it from equation I we previously used by solving it for  $v^2$  (Fig. 1.1.20). We can then insert the term for  $v^2$  into the equation  $E_{\text{kin}} = \frac{1}{2}mv^2$ , which gives  $E_{\text{kin}} = e^2/(8\pi\epsilon_0r)$ , Fig. 1.1.23.

Now let us consider the potential energy. The potential energy is the Coulomb energy between the proton and the electron in the H atom. The formula for the Coulomb energy of two particles having two opposite elementary charges is  $E_{\text{pot}} = -e^2/(4\pi\epsilon_0r)$ . Note that this energy has a negative algebraic sign because the forces between the proton and the electron are attractive (Fig. 1.1.23).

$$\begin{aligned} E &= E_{\text{kin}} + E_{\text{pot}} \\ E_{\text{kin}} &= \frac{1}{2}mv^2 & E_{\text{pot}} &= -\frac{e^2}{4\pi\epsilon_0r} \\ \text{Equation I: } \frac{mv^2}{r} &= \frac{e^2}{4\pi\epsilon_0r^2} \\ v^2 &= \frac{e^2}{4\pi\epsilon_0rm} \\ E_{\text{kin}} &= \frac{e^2}{8\pi\epsilon_0r} \end{aligned}$$

Figure 1.1.23 Derivation of kinetic, potential, and overall energies of the H electron (part 1).

We can now add up the kinetic and the potential energy to give the overall energy which is  $E = E_{\text{kin}} + E_{\text{pot}} = [e^2/(8\pi\epsilon_0r)] - [e^2/(4\pi\epsilon_0r)] = e^2/(\pi\epsilon_0r) (1/8 - 1/4) = -e^2/(8\pi\epsilon_0r)$ . We can then use the term we previously calculated for  $r$  (Fig. 1.1.21) and insert it into the term for the overall energy. As a result the overall energy becomes  $E = -(e^4m)/(8\epsilon_0^2n^2h^2)$ , Fig. 1.1.24. As we can see, the energies for the electrons in the different orbits are also only a function of the quantum number  $n$ , specifically, they are a function of  $1/n^2$ . Note also that the overall energy is negative. This is because the energy is a binding energy. Because of the negative algebraic sign, a higher quantum number  $n$  means a higher, because less negative energy. At very high quantum numbers  $n$  the value for  $E$  would approach zero, meaning that the binding energy for the electron would approach zero. The higher the orbit of the electron the more energy it has and the less strongly it is bound to the atom.

$$\begin{aligned} E &= E_{\text{kin}} + E_{\text{pot}} = \frac{e^2}{8\pi\epsilon_0r} - \frac{e^2}{4\pi\epsilon_0r} = \frac{e^2}{\pi\epsilon_0r} \left( \frac{1}{8} - \frac{1}{4} \right) = -\frac{e^2}{8\pi\epsilon_0r} \\ \text{B/c we had calculated before: } r &= \frac{n^2h^2\epsilon_0}{\pi me^2} \longrightarrow E = -\frac{e^4m}{8\epsilon_0^2n^2h^2} \end{aligned}$$

Figure 1.1.24 Continued derivation for the energies of the H electron.



Formula for energy of electron in a specific orbit:

$$E = -\frac{e^4 m}{8\epsilon_0^2 n^2 h^2}$$

Formula for energy difference between two orbits:

$$\Delta E = -\frac{e^4 m}{8\epsilon_0^2 n_{high}^2 h^2} - \left(-\frac{e^4 m}{8\epsilon_0^2 n_{low}^2 h^2}\right) = \frac{e^4 m}{8\epsilon_0^2 h^2} \left(\frac{1}{n_{low}^2} - \frac{1}{n_{high}^2}\right)$$

Empirically Rydberg found the H spectrum:

$$\Delta E = R_H \left(\frac{1}{n_{low}^2} - \frac{1}{n_{high}^2}\right)$$

Because  $\Delta E$  (theory) =  $\Delta E$  (empirical):

$$R_H = \frac{e^4 m}{8\epsilon_0^2 h^2}$$

Figure 1.1.25 Comparing derived energies of the H electron with those experimentally found in the H spectrum.

Finally let us calculate energy differences between electrons in different orbits. Subtraction of the terms for the energies of two electrons in two different orbits gives  $\Delta E = (e^4 m) / (8\epsilon_0^2 h^2) (1/n_{low}^2 - 1/n_{high}^2)$ , Fig. 1.1.25. The calculated and empirically found  $\Delta E$  match excellently, the empirically found Rydberg constant matches the theoretically derived constant  $(e^4 m) / (8\epsilon_0^2 h^2)$ . Thus experiment and theory are in accordance. Bohr's theory is able to explain the H spectra very well, and can predict both radii of electron orbits and energies. The Bohr model for the first time introduced the quantization of electron states in atoms, and in this regard it was a big step forward. However, there were still problems with Bohr's theory. It could only explain the H spectra well, but failed to explain the spectra of all other atoms. Secondly, Bohr's postulates seemed ad hoc and lacked an explanation. There was no good explanation why an electron in a quantized orbit would not emit electromagnetic radiation continuously. Thus, the Bohr model could still not be the final answer to atomic theory. In fact, it lacks to take an important property of the electron into account: The wave-particle dualism of the electron.

#### Problems with Bohr's Theory

1. It can explain only the H spectrum and fails to explain all the spectra of all other atoms.
2. Bohr's postulates are ad hoc. They lack an explanation.

Dr. Kai Landskron ([Lehigh University](#)). If you like this textbook, please consider to make a donation to support the author's research at Lehigh University: [Click Here to Donate](#).

This page titled [1.1.3: Quantization of Energy and Bohr Model of the Atom](#) is shared under a [CC BY-SA 4.0](#) license and was authored, remixed, and/or curated by [Kai Landskron](#).

- [1.1: Historical Development of Atomic Theory](#) by [Kai Landskron](#) is licensed [CC BY 4.0](#).



## 1.1.4: Wave-Particle Duality

### Wave Particle Dualism

The phenomenon of the wave-particle dualism was first discovered for electromagnetic radiation, and then extended to all other particles including the electron. It began with the investigation of the photoelectric effect by Albert Einstein (Fig. 1.2.1 and Fig. 1.2.2).

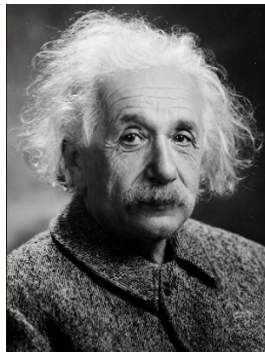


Figure 1.2.1 Albert Einstein, Nobel Prize 1921. (Attribution: Photograph by Orren Jack Turner, Princeton, N.J. Modified with Photoshop by PM\_Poon and later by Dantadd. [Public domain], commons.wikimedia.org/wiki/F...lanck\_1933.jpg)

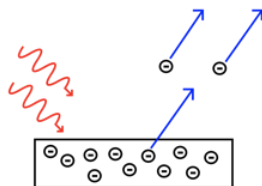


Figure 1.2.2 The photoelectric effect (Attribution: Wolfmankurd [CC BY-SA (<http://creativecommons.org/licenses/by-sa/3.0/>)]. commons.wikimedia.org/wiki/F...ric\_effect.svg)

The photoelectric effect occurs when a metal surface is irradiated by light. Above a certain frequency, or below a certain wavelength, light is able to eject electrons from the metal surface. The threshold frequency depends on the metal. Below the threshold frequency no electrons get ejected. Einstein investigated the maximum kinetic energy of the ejected electrons as a function of the frequency of the light. He found that there was a linear relationship. He analyzed the slope of this line and found that the slope was the Planck constant  $h$ . This would mean that electrons had an energy  $E = h\nu$  minus an energy  $E_B$  that would be needed to overcome the binding energy, also called the work function, of the electron in the metal (Figure 1.2.3, left).

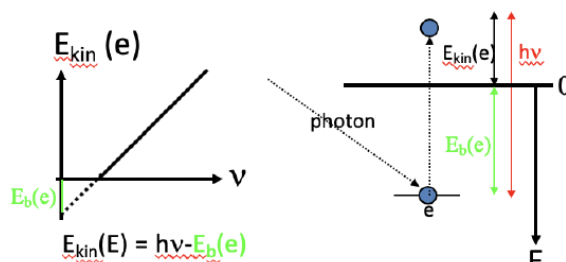


Figure 1.2.3 Maximum kinetic energy of the ejected electron as a function of the frequency of light (left), and mechanistic interpretation of the photoelectric effect (right).

The equation  $E = h\nu$  was previously derived by Planck (Fig. 1.2.4) based on the assumption that energy was quantized, and now Einstein had experimentally found it again in the quest to explain the photoelectric effect. This would mean that light was quantized. The quantization would be explained by the fact that light would not only have wave but also particle properties, and these particles would be called photons. Assuming photons the photoelectric effect could be easily explained (Figure 1.2.3, right). When light hits the metal surface the photon collides with the electron. Only when the photon had an energy larger than the work function of the metal, the electron would be ejected and would have a kinetic energy equal to the difference between the energy of the photon and the binding energy. The wave-particle dualism of light, and electromagnetic radiation in general can also be mathematically derived. Because mass can be converted into electromagnetic radiation according to the equation  $E = mc^2$ , and the

energy of electromagnetic radiation is  $E=h\nu$ ,  $mc^2=h\nu$ . We can solve the equation for  $\nu$ , and then it is  $\nu=mc^2/h$ . With  $\nu=c/\lambda$ , and solved for  $\lambda$ , the equation becomes  $\lambda=h/mc$ . This equation shows the wave particle-dualism of electromagnetic radiation because it relates a wavelength to a mass. In fact, the mass of the particle associated with electromagnetic radiation, the photon, is inverse proportional to the wavelength of the electromagnetic radiation. The discovery of the wave-particle dualism of electromagnetic radiation was a radically new concept that is difficult to grasp intellectually up to this date because the human mind tends to see waves and particles to be mutually exclusive. However, it is one of the most fundamental principles of nature. As we will see later, not only electromagnetic radiation shows the wave particle dualism, but all particles including electrons.

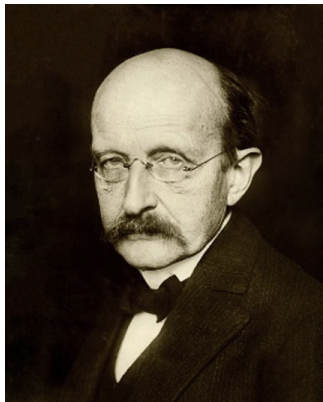


Figure 1.2.4 Max Planck, Nobel Prize 1918 (Attribution: commons.wikimedia.org/wiki/F...lanck\_1933.jpg)

### Wave Particle Dualism of Massive Particles

The wave-particle dualism was originally thought to be valid for the photon only. A young French physics PhD student, Louis De Broglie had the radical idea that not only the photon, but all particles would exhibit the wave particle dualism, including the electron. Einstein's formula  $\lambda = h/mc$  would just need to be slightly rearranged into  $\lambda = h/mv$ , whereby  $m$  would be the mass of the particle, and  $v$  would be the velocity of the particle. This idea was much disputed at the time, and Louis De Broglie's PhD thesis was almost not accepted. However, eventually the wave-particle dualism of the electron was proven by electron diffraction experiments, and Louis De Broglie was awarded the Nobel prize in 1929. Today, we believe that all particles show the wave-particle dualism, and no experiment up to this date indicates an exception.



Figure 1.2.5 Louis de Broglie 1892-1987, Nobel Prize 1929 (Attribution: Unknown commons.wikimedia.org/wiki/F...roglie\_Big.jpg, PD-US expired)

1.1.4: Wave-Particle Duality is shared under a CC BY-SA license and was authored, remixed, and/or curated by LibreTexts.

- 1.2: The quantum-mechanical model of the atom by Kai Landskron is licensed CC BY 4.0.

## 1.2: Electronic Structure of the Atom

---

Learning objectives for this unit are to:

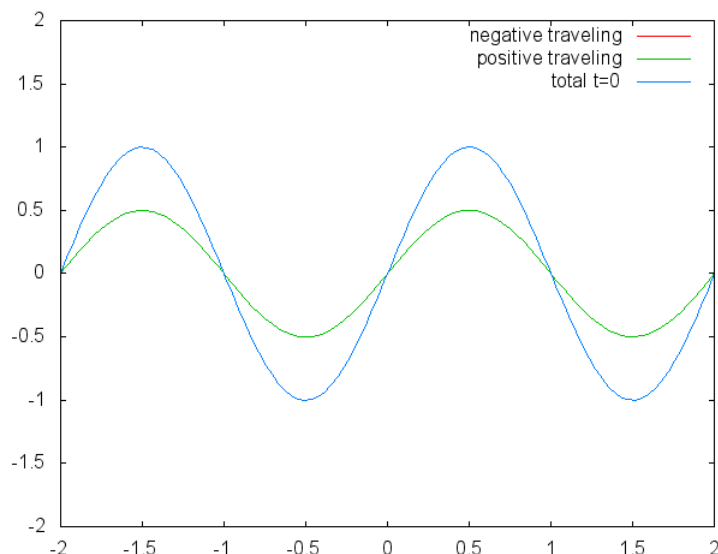
- Understand what information is contained in the Schrödinger equation
  - Qualitatively describe electrons in terms of the wavefunction,  $\psi(x)$ , including its angular and radial parts
  - Interpret radial wave function and radial probability graphs
  - Describe the location of an electron using quantum numbers
  - Predict the number of nodes from quantum numbers and sketch atomic orbital boundary surfaces
- 

1.2: Electronic Structure of the Atom is shared under a [CC BY-SA](#) license and was authored, remixed, and/or curated by LibreTexts.

## 1.2.1: Wave Quantization and Particle in a Box

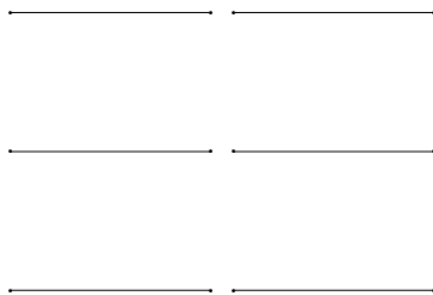
### Standing Waves

With the discovery of the wave-particle dualism of the electron, and the observation of the quantization of electronic states in atoms led physicists focus on a field in physics in which waves are quantized. The field of standing waves (Fig. 1.2.6).



**Figure 1.2.6** Two confined traveling waves (red and green) producing a standing wave (blue) due to their interference. (Attribution: Govindabalan [CC BY-SA (<https://creativecommons.org/licenses/by-sa/3.0>)], [commons.wikimedia.org/wiki/F...\\_animation.gif](https://commons.wikimedia.org/wiki/File:F..._animation.gif))

Standing waves are a quite common phenomenon. You can for example trigger a standing waves by plucking a guitar string. This causes the guitar string to vibrate in standing waves with discrete, quantized wavelengths. The vibration with the longest wavelength is the so-called ground vibration. Its wavelength is two times the length of the guitar string. In addition, so-called higher harmonics are possible. The first harmonic has a wavelength equal to the length of the guitar string, the second one, has a wavelength equal to two-thirds of the length of the string, the third one has a wavelength equal to half of the length of the string, the fourth one has a wavelength equal to one third of the length of the guitar string, and so fourth (Fig. 1.2.7).



**Figure 1.2.7** Standing waves (Attribution: Adjwilley [CC BY-SA (<https://creativecommons.org/licenses/by-sa/3.0>)], [commons.wikimedia.org/wiki/File:...n\\_a\\_string.gif](https://commons.wikimedia.org/wiki/File:...n_a_string.gif))

It can be easily seen that the possible wavelengths at which the string can vibrate follow the equation  $\lambda = 2L/n$ , whereby  $n$  is an integer, or a quantum number, and  $L$  is the length of the guitar string. Thus, we can say that the waves associated with the guitar string vibrations are quantized. Why are these waves called standing waves? This is because the positions of the crests and the troughs and the nodes do not move. They remain at the same position on the guitar string at any point in time. It should be said here

that the standing nature of the waves is actually an illusion. There are actually two waves traveling in opposite direction on the guitar string, and these waves interfere with each other so that a standing wave is produced (this is illustrated in Fig. 1.2.6). When the guitar string is plucked two waves are sent into opposite direction on the guitar string toward the two opposite ends on the guitar string. Once they have reached these ends they get reflected and sent into the opposite direction until they again reach the ends of the guitar string where they get reflected again. During this process, which happens over and over again, the two waves interfere and produce the standing wave. In sum, the fact that the wave is confined within the guitar string, leads to the quantized standing waves.

## Electron in a One-Dimensional Box

Let us now go from a vibrating guitar string to an electron in a one-dimensional box of length  $a$  having infinitely high walls. Inside the box the potential energy of the electron is zero, in the walls the potential energy is infinite (Figure 1.2.8).

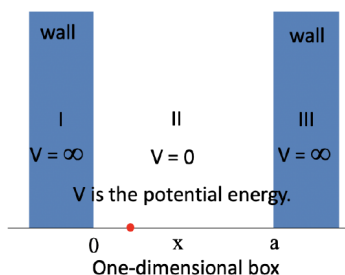


Figure 1.2.8 Electron (red dot) in a one-dimensional box with a potential energy  $V=0$  within the box and infinite potential energy within the walls (the walls may be thought infinitely high).

Due to its kinetic energy the electron can travel on a line within the box until it hits the wall (Fig. 1.2.9, A). At the wall it is getting reflected and forced to travel into the opposite direction until it again hits the wall where it reverses direction again, and so forth. Consider now that the electron does not only have particle, but also wave properties. Because of that also a wave travels along the line, gets reflected at the wall, travels into opposite direction, gets reflected again and so on. These waves can interfere with it other just like the waves traveling on the guitar string to produce a standing wave. Thus, the electron in the one-dimensional box should behave like a standing wave, and this wave should be quantized (Fig. 1.2.9, B-F).

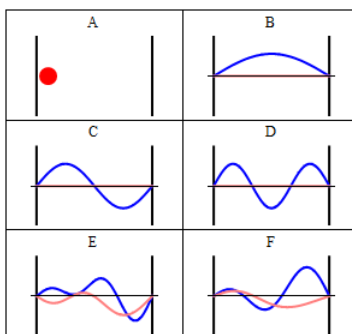


Figure 1.2.9 Electron traveling in a one-dimensional box acting as a standing wave (Attribution: Sbyrnes321 [CC0], commons.wikimedia.org/wiki/F...lAnimation.gif)

How can we mathematically describe the electron in the box as a standing wave? Generally, you can describe a standing wave by a wave function. A wave function tells the amplitude of the standing wave at a particular position in the one-dimensional box. How can we find the wave function? We can start out from a differential equation that is generally valid for standing waves (Eq. 1.2.1).

$$\frac{d^2\Psi(x)}{dx^2} = -\left(\frac{2\pi}{\lambda}\right)^2 \Psi(x)$$

**Equation 1.2.1** Standing wave differential equation.

It says that the second derivative of the amplitude of the wave function at the position  $x$  is equal to  $-(2\pi/\lambda)^2$  multiplied with the amplitude of the wave function at the position  $x$ . Let us now consider that the kinetic energy of the electron is  $E = 1/2mv^2$  and expand the equation by  $m$ .

$$\begin{aligned}
 E &= \frac{1}{2}mv^2 \\
 E &= (mv)^2/2m \rightarrow (mv)^2 = 2mE \rightarrow mv = [2mE]^{1/2} \longrightarrow \lambda = h/[2mE]^{1/2} \\
 \lambda &= h/mv \longrightarrow mv = h/\lambda
 \end{aligned}$$

**Equation 1.2.2** Solving for  $\lambda$  from kinetic energy equation and De Broglie equation.

Let us then solve the equation for  $(mv)$ . Now let us solve the De Broglie equation for  $mv$  and insert  $mv$  by  $h/\lambda$  in the previous equation. Finally, let us solve the equation by  $\lambda$  and we will get  $\lambda = h/[2mE]^{1/2}$ , Eq. 1.2.2. We can now substitute  $\lambda$  by  $h/[2mE]^{1/2}$  in the differential equation. Slightly rearranged this equation becomes the Schrödinger equation for the electron in the one-dimensional box (Equation 1.2.3).

$$\left[ \frac{d^2}{dx^2} \frac{-\hbar^2}{8\pi^2m} \right] \Psi(x) = E_{\text{kin}} \Psi(x)$$

**Equation 1.2.3** Schrödinger Equation for the electron in a 1-D box.

The Schrödinger equation is a differential equation. To get the wave function that describes the electron in the box we need to solve the differential equation. One possibility solve a differential equation is to guess its solution, and after that show that the solution is right. This is the approach we want to pursue here. A very general wave function is one that is a sum of a sinus term and a cosinus term of the coordinate  $x$  whereby we shall assume two general coefficients  $r$  and  $s$  in front of  $x$ , and two other general coefficients  $A$  and  $B$  in front of the sinus and the cosinus term, respectively.

$$\Psi = A \sin rx + B \cos sx$$

**Equation 1.2.4** Generic solution to the differential equation.

We can now think of so-called boundary conditions for the wave function which will make the wave function more specific. A boundary condition is a property the wave function must have to be a sensible solution to the differential equation. We can assume a first boundary condition which assumes that at the position  $x=0$  the amplitude of the wave function must be 0. This can be assumed because at these positions the "electron wave" gets reflected at the wall. That means that the wave function cannot have a cosinus term and thus  $B$  must be 0. If the wave function had a cosinus term it would not be 0 at  $x = 0$  because the cosinus of 0 is not 0.

$$B = 0 \quad \Psi = A \sin rx$$

**Equation 1.2.5** Boundary condition 1 for the wave function

The second boundary condition is that the amplitude of the wave function is zero at  $x = a$ . Again, this is because the electron hits the wall at  $x = a$  and reverses its direction. The sinus function is only zero at  $x = a$  when  $ra$  is an integer number  $n$  times  $\pi$ :  $ra=n\pi$ . This means that  $r$  must be  $n\pi/a$ .

$$ra = n\pi \quad \text{or} \quad r = n\pi/a$$

**Equation 1.2.6** Boundary condition 2 for the wave function

Thus, the wave function must be  $A=\sin(n\pi x/a)$ . We can see that the wave function that describes the electron as a standing wave in the one-dimensional box is quantized because the quantum number  $n$  appears.

$$\Psi = A \sin(n\pi x/a)$$

**Equation 1.2.7** The wave function considering boundary conditions 1 and 2.

Inserting the quantum numbers  $n$  into the wave functions produces all the standing waves the electron can adopt (Fig. 1.2.10). You can see that the number of nodes and the wavelengths of the waves depend on the quantum number  $n$ . For  $n = 0$  there is no node and the wavelength is twice the length of the box, for  $n = 2$  there is one node and the wavelength is equal to the length of the box, for  $n = 3$  there are three nodes and the wavelength of the wave is  $2/3$  of the lengths of the box and so forth. We can illustrate that the wave function describes the waves depicted in Figure 1.2.10 by an example. The amplitude for the wave for  $n=2$  is zero in the middle of the box where  $x = a/2$ . If we insert  $a/2$  into the equation for  $\Psi$  then  $\Psi = A \sin(n\pi 2a/a) = A \sin(n\pi) = 0$  because it is the property of a sinus function to be 0 at an integer number multiple of  $\pi$ . We could also insert other values for  $x$  and  $n$  into the wave function, and would get the expected amplitude. This shows that the wave function correctly represents the standing waves the electron can adopt.

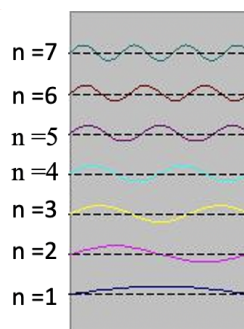


Figure 1.2.10 Standing waves corresponding to the wave function for different quantum numbers  $n$ .

We are still not quite finished with the wave function because we have not determined the parameter  $A$  in front of the sinus term. To obtain it we need to consider a third boundary condition (Eq. 1.2.8).

$$\int_0^a \Psi^2 dx = 1$$

#### Equation 1.2.8 Boundary condition 3.

It says that the integral of the square of the wave function over the length of the box must be equal to one. We can understand this boundary condition when we consider that the square of the wave function represents the probability to find the electron at a particular position in the box. The value the square of  $\Psi$  adopts at a position  $x$  within the box represents the probability to find the electron at this position when we consider the electron as a particle. This is called the Born interpretation of the wave function, named after the German physicist Max Born.

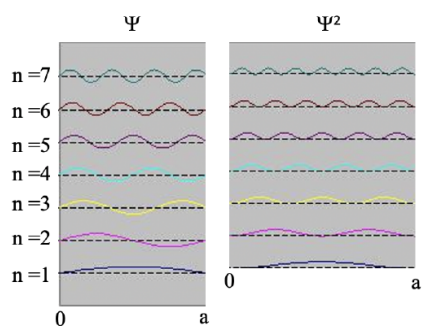


Figure 1.2.11 Standing waves corresponding to the wave function and its square.

Because the probability to find the electron anywhere in the box must be 100%, the integral of the square of the wave function over the entire box must be 100% or 1. One can show, and we omit the necessary mathematical steps for clarity here, that the boundary condition is only fulfilled when  $A$  is equal to the square root of  $2/a$ . The final wave function is then  $\psi$  is equal to  $\sqrt{2/a} \sin(n\pi x/a)$ . The factor square root of  $2/a$  is called the normalization constant of the wave function because it adjusts the amplitude of the wave function so that the probability to find the electron anywhere in the box is 100%.

Dr. Kai Landskron ([Lehigh University](#)). If you like this textbook, please consider to make a donation to support the author's research at Lehigh University: [Click Here to Donate](#).

This page titled [1.2.1: Wave Quantization and Particle in a Box](#) is shared under a [CC BY-SA 4.0](#) license and was authored, remixed, and/or curated by [Kai Landskron](#).

- [1.2: The quantum-mechanical model of the atom](#) by [Kai Landskron](#) is licensed [CC BY 4.0](#).



## 1.2.2: The Schrodinger Equation

### The Schrödinger Equation for the H Atom

Let us now go from an electron in a 1-dimensional box to the electron in the hydrogen atom. What is similar and what is different between these two cases. A similarity is that the electron is confined in an atom just like the electron is confined in the 1D box. Thus, like in the 1-dimensional box the electron should behave like a standing wave. While in the one-dimensional box there is only one coordinate to consider, there are three coordinates to consider for the electron in the atom. This is because an atom is spherical and thus three coordinates x, y, and z are necessary to describe a position within the atom. A second major difference is that the potential energy of the electron is zero at any position within the box, while it is not zero in the hydrogen atom. This is because in an atom there are attractive Coulomb forces between the nucleus and the electron. The further away the electron is from the nucleus the higher its potential energy. This is because it takes energy to pull the electron away from the nucleus.



Figure 1.2.12 Erwin Schrödinger (1887-1961), Nobel Prize 1933 (Attribution: Nobel foundation [Public domain] commons.wikimedia.org/wiki/F...ger\_(1933).jpg)

We therefore need to modify the Schrödinger equation that we used previously for the one-dimensional box the following way. Firstly, we need to expand the operator for the kinetic energy from one to three dimensions and introduce the coordinates y and z in addition to x. Secondly, we have to add an operator for the potential energy to the equation. The potential energy is the Coulomb energy between the proton and the electron. It is similar to the term we previously used for the calculation of the potential energy of the electron in the Bohr model. Instead of the radius r we use now the square root of the sum of the square of the three coordinates x, y, and z, to indicate the Coulomb energy of the electron at any position within the atom. Our wave function will now be a function of three coordinates x, y, and z. This means our wave function will now be three-dimensional and represent three-dimensional standing waves. Three-dimensional waves are harder to imagine compared to 1-dimensional ones, but have the same properties, which are that the position of the crests, troughs, and nodes does not move.

$$\left[ \left( \frac{d^2}{dx^2} + \frac{d^2}{dy^2} + \frac{d^2}{dz^2} \right) \frac{-\hbar^2}{8\pi^2m} + \frac{e^2}{4\pi\epsilon_0 \sqrt{x^2 + y^2 + z^2}} \right] \Psi(x,y,z) = E \Psi(x,y,z)$$

Operator for kinetic energy + Operator for potential energy  
(Coulomb energy)

**Equation 1.2.9** Schrödinger equation for the H atom.

In order to get the wave functions for the electron we need to solve the Schrödinger equation for the hydrogen atom. To do so, we need to think about the boundary conditions for the wave function. One condition is that the square of the wave function approaches zero when we go very far from the nucleus, and r, the distance from the nucleus approaches infinite. Secondly, like in the one-dimensional box, the integral over the square of the wave function must be one. This is because the probability to find the electron somewhere in the atom must be 100%. Thirdly, it would be sensible to assume that the wave function must be continuously differentiable and single valued (Fig. 1.2.13).

Boundary conditions for  $\Psi$ :

$$\Psi^2 = 0 \text{ for } r \rightarrow \infty$$

$$\int \Psi^2 dr = 1$$

-continuously differentiable and single valued

Figure 1.2.13 Boundary conditions for the wave function of the electron in the hydrogen atom.

## The Spherical Polar Coordinate System

The mathematical process to solve the Schrödinger equation is beyond the scope of this course and you are referred to Physical Chemistry classes and textbooks for the details. We shall only provide a brief outline of the process here. It is mathematically simpler to solve the Schrödinger equation in spherical polar coordinates instead of cartesian coordinates. Therefore, we obtain the solutions of the Schrödinger equation, the wavefunctions, in polar coordinates. The position of a point is specified by three numbers: the *radial distance* of that point from a fixed origin, its *polar angle* measured from a fixed zenith direction, and the *azimuthal angle* of its orthogonal projection on a reference plane that passes through the origin and is orthogonal to the zenith, measured from a fixed reference direction on that plane (Fig. 1.2.14).

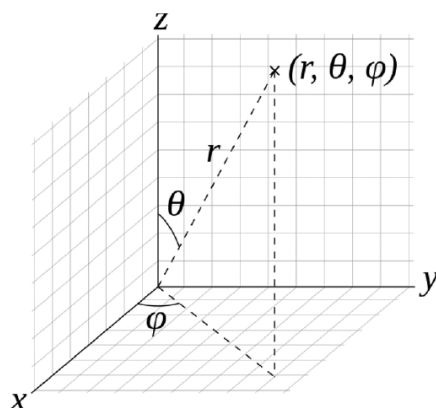


Figure 1.2.14 Illustration of the spherical polar coordinate system.

## Solutions of the Schrödinger Equation

The wavefunction is then a function of  $r$ ,  $\theta$  and  $\phi$ , in particular it is a product of a radial wave function which is function of  $r$ , a colatitude wave function, which is a function of  $\theta$ , and an azimuthal wave function which is a function of  $\phi$  (Eq. 1.2.10). You can see the explicit forms of the radial, colatitude, and azimuthal functions in Fig. 1.2.15.

$$\Psi(r, \theta, \phi) = R(r) \times \Theta(\theta) \times \Phi(\phi)$$

**Equation 1.2.10** The wave function for the electron in the H atom as a function of  $r$ ,  $\theta$  and  $\phi$

Radial wave function	→	$R_{n,l} = r^l L_{n,l} e^{-r/na_0}$
Colatitude wave function	→	$\Theta(\theta) = (-1)^m \sqrt{\frac{2l+1}{2\pi} \frac{(l-m)!}{(l+m)!}} P_l^m(\cos \theta).$
Azimuthal equation	→	$\Phi(\phi) = \frac{1}{\sqrt{2\pi}} e^{im\phi}.$

Figure 1.2.15 Explicit forms of the radial, colatitude and azimuthal functions

We do not need to understand all details here, but need to realize that these wavefunctions are functions of quantum numbers. In contrast to the electron in the one-dimensional box not only one, but three quantum numbers need to be considered. Beyond the quantum number  $n$ , which is called the principal quantum number, there is also a so-called orbital quantum number  $l$ , and a magnetic quantum number  $m$ . The quantum number  $n$  only occurs in the radial wave function, the quantum number  $l$  only occurs in the radial and colatitude function, and the quantum number  $m$  only occurs in the colatitude and the azimuthal part of the wave function. The values the orbital quantum number  $l$  can adopt depends on  $n$ , it can be between 0 and  $n-1$  for a given quantum number  $n$ . The magnetic quantum number  $m$  depends on the quantum number  $l$ , and can run from  $-l$  to  $+l$ . So, for example when  $n$  is equal to 2,  $l$  can vary between 0 and 1, and for  $l$  equal to 1,  $m$  can adopt any value between  $-1$  and  $+1$ , namely  $-1, 0, +1$ , and  $+2$  (Fig. 1.2.16).

Principal quantum number:  $n$   
 Orbital quantum number:  $l$  ( $l = 0, \dots, n-1$ )  
 Magnetic quantum number  $m$  ( $m = -l, \dots, +l$ )

Figure 1.2.16 The quantum numbers of the wave function of the H atom.

These wave functions have a particular name in chemistry. They are called orbitals. One can understand an orbital as the three-dimensional wave function that describes the electron in an atom as a standing wave. Thus, an orbital is a state the electron can adopt, and when we say that an electron is in a particular orbital we mean that the electron is in a particular state.

### The spin quantum number $s$

Within an orbital an electron can adopt two different spins described by the spin quantum number  $s$ . This quantum number is not a result of the Schrödinger equation, but was found experimentally. The spin quantum number  $s$  can adopt two values:  $+1/2$  and  $-1/2$ . We say an electron is spin up when  $s = +1/2$ , and spin down when  $s = -1/2$ .

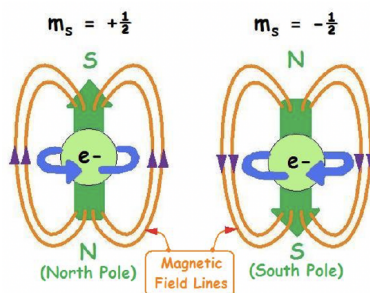


Figure 1.2.17 Electron spin (Attribution: Chemlibretexts.org  
 chem.libretexts.org/@api/dek...jpg?revision=1, CC BY-NC-SA 3.0)

The spin quantum number is understood most easily when you view the electron as a particle rotating around its own axis. A counter-clockwise rotation would be associated with  $s=+1/2$ , a clockwise rotation would be associated with  $s=-1/2$ . The rotation produces a magnetic field with the direction of the field lines depending on the direction of rotation.

Dr. Kai Landskron ([Lehigh University](#)). If you like this textbook, please consider to make a donation to support the author's research at Lehigh University: [Click Here to Donate](#).

This page titled [1.2.2: The Schrodinger Equation](#) is shared under a [CC BY-SA 4.0](#) license and was authored, remixed, and/or curated by [Kai Landskron](#).

- [1.2: The quantum-mechanical model of the atom](#) by Kai Landskron is licensed CC BY 4.0.

## 1.2.3: Quantum Numbers and Atomic Wave Functions

### 2.2.02: Quantum Numbers and Atomic Wave Functions

---

This page titled [1.2.3: Quantum Numbers and Atomic Wave Functions](#) is shared under a [CC BY-SA 4.0](#) license and was authored, remixed, and/or curated by [Kathryn Haas](#).

## 1.3: Multi-Electron Atoms

---

Learning objectives for this unit are to:

- Explain how and why  $Z$  affects the size and energy of atomic orbitals
  - Explain the meaning of effective nuclear charge ( $Z^*$ ) in terms of shielding
  - Rationalize electron configurations in terms of the Pauli Exclusion Principle, the Aufbau principle and Hund's rule (Pc and Pe)
  - Write electronic electron configurations for atoms, ions, and excited states
  - Use Slater's rules to calculate  $Z^*$
  - Understand how  $Z^*$  affects the relative energies of atomic orbitals
- 

1.3: Multi-Electron Atoms is shared under a [CC BY-SA](#) license and was authored, remixed, and/or curated by LibreTexts.

## 1.3.1: Orbital Energies

### Orbital Energies for the H Atom

The Schrödinger equation does not only allow to calculate the orbitals of the hydrogen atom, but also their energies. The energies of Bohr and Schrödinger model match:  $E = \text{constant}/n^2$ . This means that orbitals with the same quantum number  $n$  have the same energies. The energies are **not** a function of the quantum numbers  $l$  and  $m$ . The energies are negative because they are binding energies. In other words: Adding an electron to a proton is an exothermic process. The binding energy for the energy increases as the orbital energy decreases (Fig. 1.2.37).

shell	n	orbitals				
		s l = 0	p l = 1	d l = 2	f l = 3	
N	4	<div><div></div><div>4s</div></div>	<div><div><div></div><div></div><div></div></div><div>4p</div></div>	<div><div><div></div><div></div><div></div><div></div><div></div></div><div>4d</div></div>	<div><div><div></div><div></div><div></div><div></div><div></div><div></div></div><div>4f</div></div>	1/16 E <sub>1</sub>
M	3	<div><div></div><div>3s</div></div>	<div><div><div></div><div></div><div></div></div><div>3p</div></div>	<div><div><div></div><div></div><div></div><div></div><div></div></div><div>3d</div></div>	1/9 E <sub>1</sub>	
L	2	<div><div></div><div>2s</div></div>	<div><div><div></div><div></div><div></div></div><div>2p</div></div>	1/4 E <sub>1</sub> = -13.6 eV/4 = -3.4 eV		
K	1	<div><div></div><div>1s</div></div>	E <sub>1</sub> = -13.6 eV			

Figure 1.2.37 Orbital energies from the 1s orbital to 4f orbital. K, L, M, N indicate the shells associated with a quantum number  $n$ .

For the 1s orbital of H the energy is -13.6 eV, the energy of the 2s and the 2p orbitals are  $1/4$  of that, the energy of the 3s, 3p, and 3d orbitals are  $1/9$  of the energy of the 1s orbital and so forth. Note at  $1/4$  and  $1/9$ th of -13.6 eV is more than -13.6 eV due to the negative algebraic sign. The electron volt is a unit of energy. It is the amount of kinetic energy gained by a single unbound electron when it passes through an electrostatic potential difference of one volt, in vacuum.

$$1 \text{ eV} = 1.602176 \text{ } 53(14) \times 10^{-19} \text{ J.}$$

**Equation 1.2.23** The electron volt to joule unit conversion.

In other words, it is equal to one volt (1 volt = 1 joule per coulomb) times the charge of a single electron (in coulombs). It is a very small unit of energy which is practical for orbital energy calculations because the orbital energies are very small (Eq. 1.2.23).

### Multi-electron Atoms

Thus far we have only considered the orbitals for the hydrogen atom which contains only one electron. Can we also solve the Schrödinger equation for atoms that have more than one electron and get the exact energies of the orbitals? The answer is no, this mathematically not possible. The process is just already too complex even for only two electrons. The Schrödinger equation can only be solved for one electron systems. Therefore, the description of the atomic structure of all other atoms must work with approximations. Let us first consider the He atom. It has only one more electron than hydrogen. It is a useful approach to approximate multi-electron atoms as one-electron systems first, and then approximate the electron-electron interactions. Electron energies in an atom with more than one proton should follow the equation  $E_n = -Z^2 \times 13.6 \text{ eV}/n^2$ , whereby  $Z$  is the number of protons.

$$E_n = - \frac{Z^2 \text{ } 13.6 \text{ eV}}{n^2}$$

**Equation 1.2.24** The orbital energies for atoms with more than one proton

The binding energy of the electron increases proportionally to the square of the number of protons because the attractive Coulomb forces that act on the negatively charged electrons increases with the number of positively charged protons in the nucleus. One can experimentally measure the orbital energies via ionization energies. The energy required to remove an electron in a particular orbital from the atom is equal to the binding energy for the electron in that orbital. Therefore the ionization energy  $IE = -E_n$  ( $E_n =$

orbital energy). According to the Schrödinger model the orbital energy for a helium electron in a 1s orbital should be  $E_{1s} = -(2^2 \times 13.6 \text{ eV})/1^1 = -54.4 \text{ eV}$  (Eq. 1.2.25).

$$E_{1s} = -\frac{2^2 \times 13.6 \text{ eV}}{1^1} = -54.4 \text{ eV}$$

**Equation 1.2.25** Energy for a helium electron in a 1s orbital.

However, the experimentally measured ionization energy of the electron is +24.6 eV, which means that the real orbital energy is -24.6 eV, and not -54.4 eV. On the other hand, the ionization of a  $\text{He}^+$  ion is +54.4 eV which is exactly what we would expect. We can explain this phenomenon by the fact that the Schrödinger model works for a single electron only and must neglect electron interactions. In a  $\text{He}^+$  ion there is only one electron, therefore the Schrödinger model correctly predicts the energy of the electron. However, in a helium atom there are two electrons, and the Schrödinger model cannot account for the electron-electron interactions. Therefore, it does not give the correct energy for the electrons in a Helium atom. The electron-electron interactions can be viewed as shielding effects. This means that the first electron shields part of the nuclear charge from the second electron. Therefore, the second electron experiences a reduced Coulomb force from the nucleus. Because of the reduced Coulomb force, the binding energy is smaller. It is reduced from -54.4 eV to -24.6 eV. It should be pointed out that the two electrons in the 1s orbital of the He atom are indistinguishable, that means they both have the reduced binding energy. The binding energy only increases to -54.4 eV after one of the two electrons has been removed.

The net positive charge from the nucleus after accounting for shielding effects is called the effective nuclear charge. For the helium atom the effective nuclear charge is 1.34. We can calculate the effective nuclear charge from the experimentally measured first ionization energy. Solving the equation for  $Z_{\text{eff}}$  gives  $Z_{\text{eff}} = 1.34$  (Eq. 1.2.26).

$$E = -\frac{Z_{\text{eff}}^2}{n^2} \times 13.6 \text{ eV} = -24.6 \text{ eV} \quad \text{b/c } IE(\text{He}) = 24.6 \text{ eV}$$

$$Z_{\text{eff}} = \sqrt{n^2 \times \frac{24.6 \text{ eV}}{13.6 \text{ eV}}} = \sqrt{1^2 \times \frac{24.6 \text{ eV}}{13.6 \text{ eV}}} = 1.34$$

**Equation 1.2.26** Calculation of  $Z_{\text{eff}}$  in the Helium atom from first ionization energies.

---

Dr. Kai Landskron ([Lehigh University](#)). If you like this textbook, please consider to make a donation to support the author's research at Lehigh University: [Click Here to Donate](#).

---

This page titled [1.3.1: Orbital Energies](#) is shared under a [CC BY-SA 4.0](#) license and was authored, remixed, and/or curated by [Kai Landskron](#).

- [1.2: The quantum-mechanical model of the atom](#) by Kai Landskron is licensed [CC BY 4.0](#).

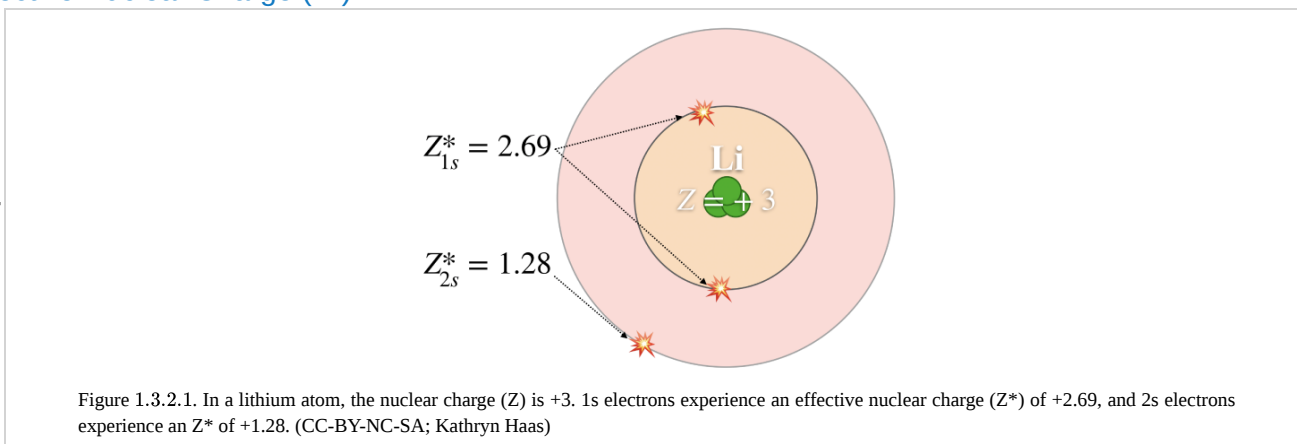
## 1.3.2: Shielding

### Introduction

Coulomb's Law is from classical physics; it tells us that particles with opposite electrostatic charge are attracted to each other, and the larger the charge on either particle or the closer the distance between them, the stronger the attraction. Coulomb's law explains why atomic size decreases as the charge on the nucleus increases, but it can't explain the nuances and variations in size as we go across the periodic table. Coulomb's Law also explains why electrons in different shells ( $n$ ), at different distances from the nucleus, have different energies. But on its own, Coulomb's law doesn't quite explain why electron subshells within a shell (like 2s vs. 2p) would have different energies. To explain these things, we need to consider how both electron **shielding** and **penetration** result in variations in effective nuclear charge ( $Z^*$ ) that depend on shell and subshell.

### Effective Nuclear Charge ( $Z^*$ )

Coulomb's law works well for predicting the



energy of an electron in a hydrogen atom (because H has only one electron). It also works for hydrogen-like atoms: any nucleus with exactly one electron (a  $\text{He}^+$  ion, for example, has one electron). However, Coulomb's law is insufficient for predicting the energies of electrons in multi-electron atoms and ions.

Electrons within a multi-electron atom interact with the nucleus and with all other electrons. Each electron in a multi-electron atom experiences both attraction to the nucleus and repulsion from interactions with other electrons. The presence of multiple electrons decreases the nuclear attraction to some extent. Each electron in a multi-electron atom experiences a different magnitude of (and attraction to) the nuclear charge depending on what specific shell and subshell the electron occupies. The amount of positive nuclear charge experienced by any individual electron is the **effective nuclear charge ( $Z^*$ )**.

For example, in lithium (Li), none of the three electrons "feel" the full +3 charge from the nucleus (see Figure 1.3.2.1). Rather, each electron "feels" a  $Z^*$  that is less than the actual  $Z$  and that depends on the electron's orbital. The actual nuclear charge in Li is  $Z = +3$ ; the 1s electrons experience a  $Z^* = +2.69$ , and the 2s electron experiences a  $Z^* = +1.28$ . In general, core electrons (or the electrons closest to the nucleus), "feel" a  $Z^*$  that is close to, but less than,  $Z$ . On the other hand, outer valence electrons experience a  $Z^*$  that is much less than  $Z$ .

In summary:

- Core electrons:  $Z^* \approx Z$
- Valence electrons:  $Z^* \ll Z$

### Shielding:

Shielding is the reduction of true nuclear charge ( $Z$ ) to the effective nuclear charge ( $Z^*$ ) by other electrons in a multi-electron atom or ion. Shielding occurs in all atoms and ions that have more than one electron. H is the only atom in which shielding does not occur.

**Explanation of shielding:** Electrons in a multi-electron atom interact with the nucleus and all other electrons in the atom. To describe shielding, we can use a simplified model of the atom: we will choose an electron-of-interest in a multi-electron atom and



treat all the "other" electrons as a group of spherically-distributed negative charge. Classical electrostatics allows us to treat spherical distribution of charge as a point of charge at the center of the distribution. Thus, we consider all the "other" electrons in our atom as a point of negative charge in the center of the atom. While the positive charge of the nucleus provides an attractive force toward our electron, the negative charge distribution at the center of the atom would provide a repulsive force. The attractive and repulsive forces would partially cancel each other; but since there are less "other" electrons than there are protons in our atom, the nuclear charge is never completely canceled. The "other" electrons partially block, or shield, part of the nuclear charge so that our electron-of-interest experiences a partially-reduced nuclear charge, the  $Z^*$ .

In reality, there is not a one-for-one "canceling" of the nuclear charge by each electron. Partly due to *penetration*, no single electron can completely shield a full unit of positive charge. Core electrons shield valence electrons, but valence electrons have little effect on the  $Z^*$  of core electrons. The ability to shield, and be shielded by, other electrons strongly depends on the electron orbital's average distance from the nucleus and its *penetration*; thus shielding depends on both shell ( $n$ ) and subshell ( $l$ ).

### Shielding depends on electron penetration

Coulomb's law shows us that distance of an electron from its nucleus is important in determining the electron's energy (its attraction to the nucleus). The shell number ( $n$ ) determines approximately how far an electron is from the nucleus *on average*. Thus, all orbitals in the same shell (s,p,d) have similar sizes and similar average distance of their electrons from the nucleus. But there is another distance-related factor that plays a critical role in determining orbital energy levels: *penetration*. **Penetration** describes the ability of an electron in a given subshell to penetrate into other shells and subshells to get close to the nucleus. Penetration is the **extent to which an electron can approach the nucleus**. Penetration depends on both the shell ( $n$ ) and subshell ( $l$ ).

The penetration of individual orbitals can be visualized using the radial probability functions. For example, Figure 1.3.2.2 below shows plots of the radial probability function of the 1s, 2s, and 2p orbitals. From these plots, we can see that the 1s orbital is able to approach the closest to the nucleus; thus it is the most penetrating. While the 2s and 2p have most of their probability at a farther distance from the nucleus (compared to 1s), the 2s orbital and the 2p orbital have different extents of penetration. Notice that the 2s orbital is able to penetrate the 1s orbital because of the central 2s lobe. The 2p orbital penetrates somewhat into the 1s, but it cannot approach the nucleus as closely as the 2s orbital can. While the 2s orbital penetrates more than 2p (the 2s orbital can approach closer to the nucleus), the 2p is slightly *closer on average* than 2s. The order of  $Z^*$  in 2s and 2p subshells depends on which factor (average distance or penetration) is more important. In the first two rows of the periodic table, penetration is the dominant factor that results in 2s having a lower energy than 2p (see Figure 1.3.2.4 for values).

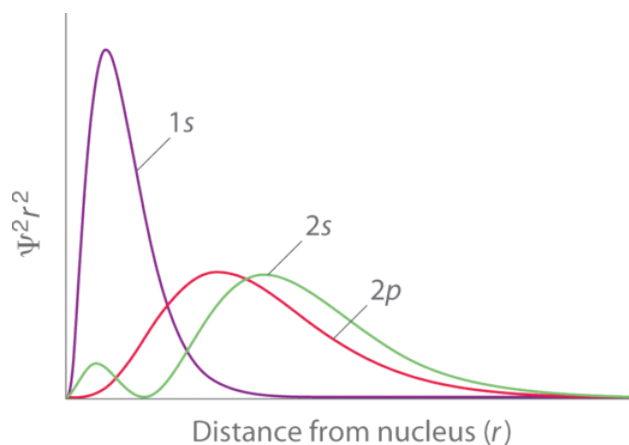


Figure 1.3.2.2. Orbital Penetration. A comparison of the radial probability distribution of the 2s and 2p orbitals for various states of the hydrogen atom shows that the 2s orbital penetrates inside the 1s orbital more than the 2p orbital does. Consequently, when an electron is in the small inner lobe of the 2s orbital, it experiences a relatively large value of  $Z^*$ , which causes the energy of the 2s orbital to be lower than the energy of the 2p orbital.

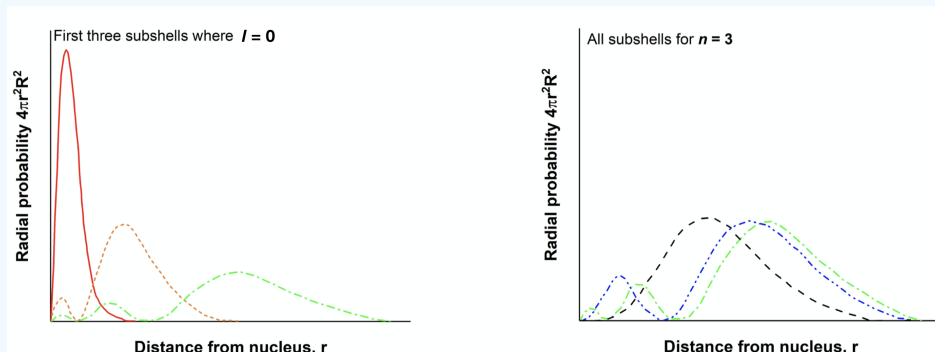
An electron orbital's penetration affects its ability to shield other electrons and affects the extent to which it is shielded by other electrons. In general, electron orbitals that have greater penetration experience stronger attraction to the nucleus and less shielding by other electrons; these electrons thus experience a larger  $Z^*$ . Electrons in orbitals that have greater penetration also shield other electrons to a greater extent.

Within the same shell value ( $n$ ), the penetrating power of an electron follows this trend in subshells ( $m_l$ ):

## Exercises

### ? Exercises

- Compare the 2s and 2p orbitals:
  - Which is closer to the nucleus on average?
  - Which is more penetrating?
  - Which orbital experiences a stronger  $Z^*$  and is thus lower in energy (consider your experience, but also inspect [Figures 1.1.2.3 and 1.1.2.4 from the previous page](#))? Please explain.
- Peruse the [Hyperphysics page \(click\)](#) that shows radial probability functions of several orbitals (click around on various orbitals). Compare the 2p and 3s orbitals:
  - Which is farther from the nucleus on average?
  - Which is more penetrating?
  - Which orbital is lower in energy?
- Which atom, Li, or N, has a stronger valence  $Z^*$ ? Explain why.
- Explain why 2s and 2p subshells are completely degenerate in a hydrogen atom.
- Which atom has a smaller radius: Be or F? Explain.
- Which electrons shield others more effectively: 3p or 3d?
- Use the clues given in the figures below to label the radial distribution functions shown.



- Examine the plots on the right in the previous question, above. Note that this is a plot showing the probability density for the 3s, 3p, and 3d subshells.
  - For which of these three functions is the highest probability density at the smallest  $r$  value (which is closest to the nucleus on average)? Is this the same subshell that penetrates most?
  - Use this example to describe how penetration and shielding result in a splitting of subshell energy level in multi-electron atoms.
- Explain why the ground state (most energetically favorable) electron configuration of Be is  $1s^2 2s^2$  rather than alternative configurations like  $1s^2 2s^1 2p^1$  or  $1s^2 2p^2$ .

#### Answer 1

- The 2s orbital is closer to the nucleus on average.
- The 2s orbital is more penetrating than 2p.
- You might "know" that the 2s orbital is lower in energy than 2p because 2s fills first. But a close inspection of [Figures 1.1.2.3 and 1.1.2.4 from the previous page](#) indicates that while the 2s and 2p elements are degenerate in Ne (element 10), for elements with atomic number 11 and greater 2p has a higher  $Z^*$  than 2s! This example illustrates that both average distance and penetration are factors in determining  $Z^*$ , and the factor that is more important may change as we increase in atomic number.

#### Answer 2

- The 3s orbital reaches farther away from the nucleus and is on average farther from the nucleus than 2p.

(b) The 3s orbital is more penetrating than 2p, even though 3s is farther on average!

(c) The 2p orbital is lower in energy than 3s; this is because 2p is still significantly closer to the nucleus on average and experiences a stronger  $Z^*$ . (Penetration is not the only consideration!)

### Answer 3

A nitrogen atom has a stronger effective nuclear charge ( $Z^*$ ) than lithium due to its greater number of protons; even though N also has more electrons that would shield the nuclear charge, each electron only partially shields each proton. This means that atoms with greater atomic number always have greater  $Z^*$  for any given electron.

### Answer 4

The hydrogen atom has only one electron; thus there is no shielding to consider. When there are not other electrons to shield the nucleus, penetration and shielding are irrelevant, and subshells within a shell are degenerate.

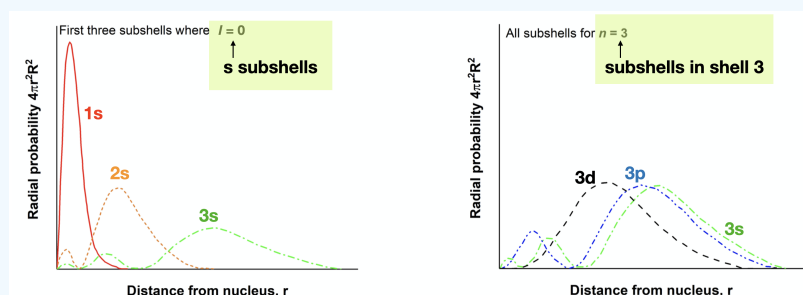
### Answer 5

Fluorine has a smaller radius than beryllium because F has a greater valence  $Z^*$  and therefore pulls the valence electrons closer to the nucleus and provides a smaller atomic radius.

### Answer 6

3p shields better than 3d because p orbitals penetrate more than d orbitals within the same shell.

### Answer 7



### Answer 8

3d is closest on average, but 3s penetrates most. The three subshells of  $n = 3$  differ in their average distance and in their ability to penetrate; these factors result in differences in the  $Z^*$  experienced by electrons in each orbital. We would expect 3s to be lowest in energy followed by 3p and then 3d.

### Answer 9

This question is asking why the 2s orbital fills in Be before 2p is occupied. This is a multi-electron atom, therefore core electrons shield the 2s and 2p orbitals to different extents. In Be we expect the 2s orbital to fill before 2p because 2s penetrates more and experiences a higher  $Z^*$ .

## References

1. Petrucci, Ralph H., William S. Harwood, F. Geoffrey Herring, and Jeffry D. Madura. General Chemistry: Principles and Modern Applications, Ninth Edition. Pearson Education Inc. Upper Saddle River, New Jersey: 2007.
2. Raymond Chang. Physical Chemistry for Biological Sciences. Sausalito, California: University Science Books, 2005
3. R. S. Mulliken, Electronic Structures of Molecules and Valence. II General Considerations, Physical Review, vol. 41, pp. 49-71 (1932)
4. Anastopoulos, Charis (2008). *Particle Or Wave: The Evolution of the Concept of Matter in Modern Physics*. Princeton University Press. pp. 236–237. ISBN 0691135126. <http://books.google.com/?id=rDEvQZhpltEC&pg=PA236>.

## Contributors and Attributions

- Sidra Ayub (UCD), Alan Chu (UCD)
- Emily V Eames (City College of San Francisco)

- Curated or created by [Kathryn Haas](#)

---

This page titled [1.3.2: Shielding](#) is shared under a [CC BY-SA 4.0](#) license and was authored, remixed, and/or curated by [Kathryn Haas](#).

- [2.2.4: Shielding](#) by [Kathryn Haas](#) is licensed [CC BY-NC-SA 4.0](#).

## 1.3.3: Aufbau Principle

[2.2.03: Aufbau Principle](#)

---

This page titled [1.3.3: Aufbau Principle](#) is shared under a [CC BY-SA 4.0](#) license and was authored, remixed, and/or curated by [Kathryn Haas](#).

### 1.3.4: Slater's Rules

#### Learning Objective

- To quantify the shielding effect experienced by atomic electrons.

We have previously described the concepts of electron shielding, orbital penetration and effective nuclear charge, but we did so in a qualitative manner. In this section, we explore one model for quantitatively estimating the impact of electron shielding, and then use that to calculate the effective nuclear charge experienced by an electron in an atom. The model we will use is known as Slater's Rules (J.C. Slater, *Phys Rev* **1930**, 36, 57).

#### Slater's Rules

The general principle behind Slater's Rule is that the actual charge felt by an electron is equal to what you'd expect the charge to be from a certain number of protons, but minus a certain amount of charge from other electrons. Slater's rules allow you to estimate the effective nuclear charge  $Z_{eff}$  from the real number of protons in the nucleus and the effective shielding of electrons in each orbital "shell" (e.g., to compare the effective nuclear charge and shielding 3d and 4s in transition metals). Slater's rules are fairly simple and produce fairly accurate predictions of things like the [electron configurations](#) and [ionization energies](#).

#### Slater's Rules

- Step 1:** Write the electron configuration of the atom in the following form:

(1s) (2s, 2p) (3s, 3p) (3d) (4s, 4p) (4d) (4f) (5s, 5p) . . .

- Step 2:** Identify the electron of interest, and ignore all electrons in higher groups (to the right in the list from Step 1). These do not shield electrons in lower groups
- Step 3:** Slater's Rules is now broken into two cases:
  - the shielding experienced by an s- or p- electron,
    - electrons within same group shield **0.35**, except the 1s which shield **0.30**
    - electrons within the n-1 group shield **0.85**
    - electrons within the n-2 or lower groups shield **1.00**
  - the shielding experienced by nd or nf valence electrons
    - electrons within same group shield **0.35**
    - electrons within the lower groups shield **1.00**

These rules are summarized in Figure 1.3.4.1 and Table 1.3.4.1.

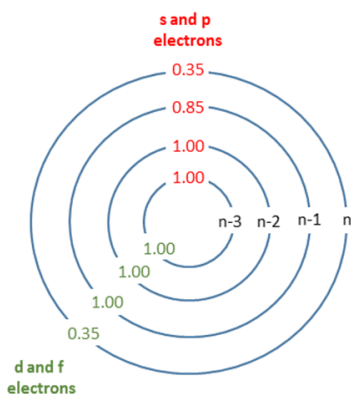


Figure 1.3.4.1: Graphical depiction of Slater's rules with shielding constants indicated.

Shielding happens when electrons in lower valence shells (or the same valence shell) provide a repulsive force to valence electrons, thereby "negating" some of the attractive force from the positive nucleus. Electrons really close to the atom (n-2 or lower) pretty much just look like protons, so they completely negate. As electrons get closer to the electron of interest, some more complex interactions happen that reduce this shielding.

Table 1.3.4.1: Slater's Rules for calculating shieldings

Group	Other electrons in the same group	Electrons in group(s) with principal quantum number $n$ and azimuthal quantum number $< l$	Electrons in group(s) with principal quantum number $n-1$	Electrons in all group(s) with principal quantum number $< n-1$
[1s]	0.30	-	-	-
[ns,np]	0.35	-	0.85	1
[nd] or [nf]	0.35	1	1	1

The shielding numbers in Table 1.3.4.1 were derived semi-empirically (i.e., derived from experiments) as opposed to theoretical calculations. This is because quantum mechanics makes calculating shielding effects quite difficult, which is outside the scope of this Module.

## Calculating $S$

Sum together the contributions as described in the appropriate rule above to obtain an estimate of the shielding constant,  $S$ , which is found by totaling the screening by **all electrons** except the one in question.

$$S = \sum n_i S_i \quad (1.3.4.1)$$

where

- $n_i$  is the number of electrons in a specific shell and subshell and
- $S_i$  is the shielding of the electrons subject to Slater's rules (Table 1.3.4.1)

### Example 1.3.4.1: The Shielding of 3p Electrons of Nitrogen Atoms

What is the shielding constant experienced by a 2p electron in the nitrogen atom?

**Given:** Nitrogen (N)

**Asked for:**  $S$ , the shielding constant, for a 2p electron (Equation 1.3.4.1)

**Strategy:**

- Determine the electron configuration of nitrogen, then write it in the appropriate form.
- Use the appropriate Slater Rule to calculate the shielding constant for the electron.

**Solution A** N:  $1s^2 2s^2 2p^3$

N:  $(1s^2)(2s^2, 2p^3)$

**Solution B**

$$S[2p] = \underbrace{0.85(2)}_{\text{the 1s electrons}} + \underbrace{0.35(4)}_{\text{the 2s and 2p electrons}} = 3.10$$

As Table 1.3.4.1 indicates,

- the 1s electrons shield the other 2p electron to 0.85 "charges".
- the 2s and 2p electrons shield the other 2p electron equally at 0.35 "charges".

### Exercise 1.3.4.1: The Shielding of valence $p$ Electrons of Bromine Atoms

What is the shielding constant experienced by a valence  $p$ -electron in the bromine atom?

**Answer**

$$S = 2 + 8 + 8 \times 0.85 + 10 + 4 \times 0.35 = 28.20$$

### Example 1.3.4.2: The Shielding of 3d Electrons of Bromine Atoms

What is the shielding constant experienced by a 3d electron in the bromine atom?

**Given:** Bromine (Br)

**Asked for:**  $S$ , the shielding constant, for a  $3d$  electron

**Strategy:**

- Determine the electron configuration of bromine, then write it in the appropriate form.
- Use the appropriate Slater Rule to calculate the shielding constant for the electron.

**Solution A** Br:  $1s^2 2s^2 2p^6 3s^2 3p^6 4s^2 3d^{10} 4p^5$

Br:  $(1s^2)(2s^2, 2p^6)(3s^2, 3p^6)(3d^{10})(4s^2, 4p^5)$

Ignore the group to the right of the  $3d$  electrons. These do not contribute to the shielding constant.

**Solution B**  $S[3d] = 1.00(18) + 0.35(9) = 21.15$

### Exercise 1.3.4.2: The Shielding of $3d$ Electrons of Copper Atoms

What is the shielding constant experienced by a valence  $d$ -electron in the copper atom?

**Answer**

$$S = 21.15$$

### Calculating $Z_{eff}$

One set of estimates for the effective nuclear charge ( $Z_{eff}$ ) was presented in Figure 2.5.1. Previously, we described  $Z_{eff}$  as being less than the actual nuclear charge ( $Z$ ) because of the repulsive interaction between core and valence electrons. We can quantitatively represent this difference between  $Z$  and  $Z_{eff}$  as follows:

$$S = Z - Z_{eff} \quad (1.3.4.2)$$

Rearranging this formula to solve for  $Z_{eff}$  we obtain:

$$Z_{eff} = Z - S \quad (1.3.4.3)$$

We can then substitute the shielding constant obtained using Equation 1.3.4.3 to calculate an estimate of  $Z_{eff}$  for the corresponding atomic electron.

### Example 1.3.4.3: The Effective Charge of $p$ Electrons of Boron Atoms

What is the effective nuclear charge experienced by a valence  $p$ - electron in boron?

**Given:** Boron (B)

**Asked for:**  $Z_{eff}$  for a valence  $p$ - electron

**Strategy:**

- Determine the electron configuration of boron and identify the electron of interest.
- Use the appropriate Slater Rule to calculate the shielding constant for the electron.
- Use the Periodic Table to determine the actual nuclear charge for boron.
- Determine the effective nuclear constant.

**Solution:**

**A** B:  $1s^2 2s^2 2p^1$ . The valence  $p$ - electron in boron resides in the  $2p$  subshell.

B:  $(1s^2)(2s^2, 2p^1)$

**B**  $S[2p] = 1.00(0) + 0.85(2) + 0.35(2) = 2.40$

**C**  $Z = 5$

**D** Using Equation 1.3.4.3  $Z_{eff} = 2.60$

### Exercise 1.3.4.3



What is the effective nuclear charge experienced by a valence d-electron in copper?

**Answer**

$$Z_{eff} = 7.85$$

## Summary

Slater's Rules can be used as a model of shielding. This permits us to quantify both the amount of shielding experienced by an electron and the resulting effective nuclear charge. Others performed better optimizations of  $Z_{eff}$  using variational [Hartree-Fock methods](#). For example, Clementi and Raimondi published "[Atomic Screening Constants from SCF Functions](#)." J Chem Phys (1963) 38, 2686–2689.

## References

- James L. Reed, "The Genius of Slater's Rules" , J. Chem. Educ., 1999, 76 (6), p 802
- David Tudela, "Slater's rules and electron configurations", J. Chem. Educ., 1993, 70 (11), p 956
- Kimberley A. Waldron, Erin M. Fehringer, Amy E. Streeb, Jennifer E. Trosky and Joshua J. Pearson, "Screening Percentages Based on Slater Effective Nuclear Charge as a Versatile Tool for Teaching Periodic Trends", J. Chem. Educ., 2001, 78 (5), p 635

## Contributors

- Brett McCollum ([Mount Royal University](#))

---

1.3.4: Slater's Rules is shared under a [CC BY-SA](#) license and was authored, remixed, and/or curated by LibreTexts.

## 1.4: Periodic Properties of the Elements

---

Learning objectives for this unit are to:

- Define the following atomic properties: ionization energy, electron affinity, electronegativity, atomic size
  - Recall the general trends in atomic properties
  - Rationalize or predict periodic trends in atomic radii, ionization energies, and electron affinities using the concepts of effective nuclear charge, electron shielding, electron penetration, and the lanthanide contraction.
  - Identify and utilize other periodic trends such as the “diagonal relationship” and the “uniqueness principle”
- 

1.4: Periodic Properties of the Elements is shared under a [CC BY-SA](#) license and was authored, remixed, and/or curated by LibreTexts.

## 1.4.1: Effective Nuclear Charge

### $Z^*$ modulates attraction

When valence electrons experience less nuclear charge than core electrons, different electrons experience different magnitudes of attraction to the nucleus. A modified form of Coulomb's Law is written below, where  $e$  is the charge of an electron,  $Z^*$  is the effective nuclear charge experienced by that electron, and  $r$  is the radius (distance of the electron from the nucleus).

$$F_{eff} = k \frac{Z^* e^2}{r^2}$$

This formula suggests that if we can estimate  $Z^*$ , then we can predict the attractive force experienced by, and the energy of, an electron in a multi-electron atom (ex. Li).

The attraction of the nucleus to valence electrons determines the atomic or ionic size, ionization energy, electron affinity, and electronegativity. The stronger the attraction, and the stronger  $Z^*$ , the closer the electrons are pulled toward the nucleus. This in turn results in a smaller size, higher ionization energy, higher electron affinity, and stronger electronegativity.

### General Periodic Trends in $Z^*$

Close inspection of Figure 1.4.1.3 and analysis of Slater's rules indicate that there are some predictable trends in  $Z^*$ . The data from Figure 1.4.1.3 is plotted below in Figure 1.4.1.4 to provide a visual aid to the discussion below.

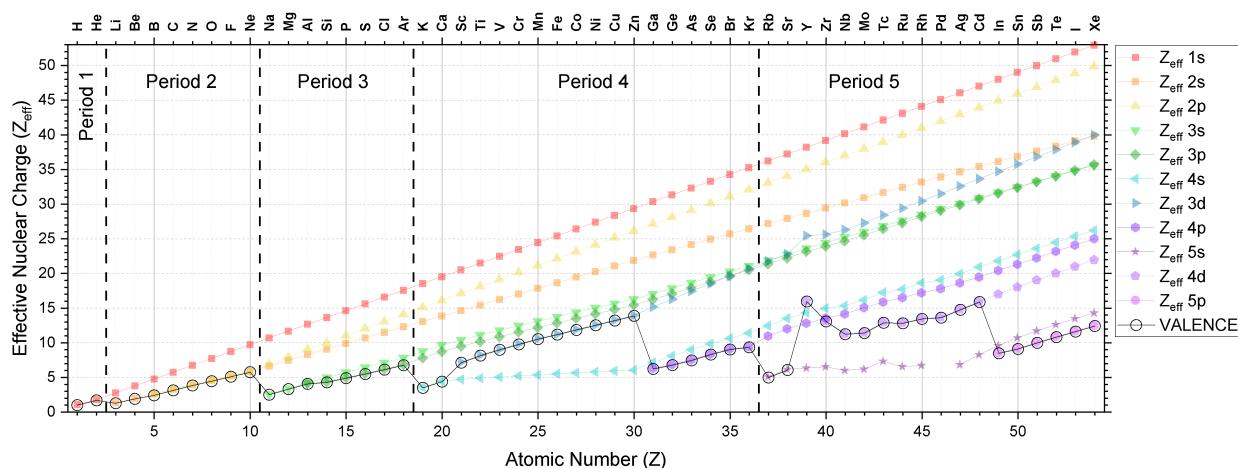


Figure 1.4.1.5: The  $Z^*$  values for electrons in each subshell of the first 54 elements (H to Xe). Each subshell is plotted as a different series (see legend) and the valence shell is highlighted by a solid black line with open circles. (Kathryn Haas; CC-NC-BY-SA)

### Trends in $Z^*$ for electrons in a specific shell and subshell

The  $Z^*$  for electrons in a given shell and subshell generally increases as atomic number increases; this trend holds true going across the periodic table and down the periodic table. Convince yourself that this is true for any subshell by examining Figure 1.4.1.4 (CC-BY-NC-SA; Kathryn Haas)

### Do you notice any exceptions to this general trend?

Inspection of Figure 1.4.1.4 should confirm for you that the  $Z^*$  increases as  $Z$  increases for electrons in any subshell (like the 1s subshell for example, which is plotted above as a red line with square points). You can see this trend as the positive slope in each series. There is one obvious exception in Period 5 in elements 39 (Y) to 41 (Nb); the  $Z^*$  of 4s actually decreases across these three elements as atomic number increases. There is also an exception between Y and Zr in the 3d subshell, and between Tc and Ru in the 5s subshell.

### For valence electrons:

It is useful to understand trends in valence  $Z^*$  because the valence  $Z^*$  determines atomic/ionic properties and chemical reactivity. The trends in the valence  $Z^*$  are not simple because as atomic number increases, the valence shell and/or subshell also changes. The valence  $Z^*$  is indicated in Figure 1.4.1.4 as a black line with open circles.

**Down the table:** As we go down a column of the periodic table, the valence  $Z^*$  increases. This is a simple trend because type of subshell is consistent and there is an increase only in shell and in atomic number,  $Z$ . This trend is best illustrated by inspection of Figure 1.4.1.3

**Across the table:** the trend depends on shell and subshell, but generally  $Z^*$  increases across a period.

**Periods 1-3 (s and p only):** As we go across the table in periods 1-3, the shell stays constant as  $Z$  increases and the subshell changes from s to p. In these periods, there is a gradual increase in valence  $Z^*$  as we move across any of the first three periods.

**Periods 4 and 5 (s, p, and d):** Now we have some more complex trends because valence subshell and shell are changing as we increase in atomic number. Notice that the valence  $Z^*$  generally increases going across a period as long as the subshell isn't changing; the exception is within the 4d subshell (elements 39-44 or Y-Ru). In general, going from an  $(n)s$  subshell to an  $(n-1)d$  subshell, there is a relatively large increase in valence  $Z^*$ . And in going from an  $(n-1)d$  subshell to an  $(n)p$  subshell, there is a relatively large decrease in  $Z^*$ .

**From one period to another:** From Figure 1.4.1.4 we can see that as we increase  $Z$  by one proton, going from one period to the next, there is a relatively large decrease in  $Z^*$  (from Ne to Na, for example). This is because as  $Z$  increases by a small interval, the shell number increases, and so the electrons in the valence shell are much farther from the nucleus and are more shielded by all the electrons in the lower shell numbers.

## Exercises

### ? Exercise 1.4.1.2

1. Compare trends in  $Z^*$  and atomic size. Explain how and why atomic size depends on  $Z^*$ .
2. Compare trends in  $Z^*$  and ionization energy. Explain how and why ionization energy depends on  $Z^*$ .

#### Answer

1. On the periodic table, atomic radius generally decreases across the periods (left to right) and increases down the groups. As atomic number increases across the periodic table, nuclear charge ( $Z$ ) increases and  $Z^*$  increases. In turn, the atomic radius decreases because the higher nuclear charge (and thus higher  $Z^*$ ) pulls electrons closer to the nucleus. Atomic radius increases down the periodic table because the shell number increases. Despite an increase in  $Z^*$  going down the periodic table, larger atomic radii result from electrons occupying higher shells.
2. Ionization energies (IE) are inversely related to atomic radius; IE increases across the periods and decreases down the groups. Since the nucleus holds valence electrons more strongly (due to higher  $Z^*$ ) across the periods, IE increases because valence electrons are harder to remove. Down the periodic table, larger atomic radii cause electrons in valence orbitals to be shielded by core electrons. Recall that shielding reduces the nuclear charge available to electrons in higher orbital levels, resulting in a lower  $Z^*$ . With more shielding and lower  $Z^*$ , the valence electrons are held less tightly by the nucleus such that ionization energy decreases (i.e., valence electrons are easier to remove).

## References

1. Petrucci, Ralph H., William S. Harwood, F. Geoffrey Herring, and Jeffry D. Madura. General Chemistry: Principles and Modern Applications, Ninth Edition. Pearson Education Inc. Upper Saddle River, New Jersey: 2007.
2. Raymond Chang. Physical Chemistry for Biological Sciences. Sausalito, California: University Science Books, 2005
3. R. S. Mulliken, Electronic Structures of Molecules and Valence. II General Considerations, Physical Review, vol. 41, pp. 49-71 (1932)
4. Anastopoulos, Charis (2008). *Particle Or Wave: The Evolution of the Concept of Matter in Modern Physics*. Princeton University Press. pp. 236–237. ISBN 0691135126. <http://books.google.com/?id=rDEvQZhpltEC&pg=PA236>.

## Contributors and Attributions

- Sidra Ayub (UCD), Alan Chu (UCD)
- [Emily V Eames](#) (City College of San Francisco)
- Curated or created by [Kathryn Haas](#)

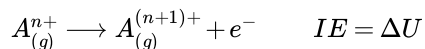
---

This page titled [1.4.1: Effective Nuclear Charge](#) is shared under a [CC BY-SA 4.0](#) license and was authored, remixed, and/or curated by [Kathryn Haas](#).

- [2.2.4: Shielding](#) by [Kathryn Haas](#) is licensed [CC BY-NC-SA 4.0](#).

## 1.4.2: Ionization energy

**Ionization energy** (IE) is the energy required to **remove an electron from a neutral atom or cation in its gaseous phase**. IE is also known as *ionization potential*.

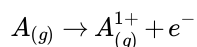


Conceptually, ionization energy is the affinity of an element for its outermost electron (an electron it already has in its valence shell).

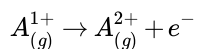
### 1<sup>st</sup>, 2<sup>nd</sup>, and 3<sup>rd</sup> Ionization Energies

The symbol  $I_1$  stands for the **first ionization energy** (energy required to take away an electron from a neutral atom, where  $n = 0$ ). The symbol  $I_2$  stands for the **second ionization energy** (energy required to take away an electron from an atom with a +1 charge,  $n = 2$ .)

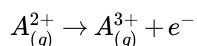
- **First Ionization Energy,  $I_1$**  (general element, A):



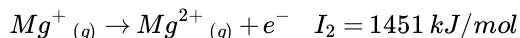
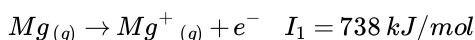
- **Second Ionization Energy,  $I_2$**  (general element, A):



- **Third Ionization Energy,  $I_3$**  (general element, A):



Each succeeding ionization energy is larger than the preceding energy. This means that  $I_1 < I_2 < I_3 < \dots < I_n$  will always be true. For example, ionization energy increases as succeeding electrons are taken away from Mg.



Ionization energy is correlated with the strength of attraction between the positively-charged nucleus and the negatively-charged valence electrons. The higher the ionization energy, the stronger the attractive force between nucleus and valence electrons, and the more energy is required to remove a valence electron. The lower the ionization energy, the weaker the attractive force between nucleus and valence electrons, and the less energy required to remove a valence electron.

### General periodic trends in electron affinity

In general, ionization energies increase from left to right and decrease down a group; however, there are variations in these trends that would be expected from the effects of penetration and shielding. The trends in **first ionization energy** are shown in Figure 1.4.2.1 and are summarized below.

- **Across a period:** As  $Z^*$  increases across a period, the ionization energy of the elements generally increases from left to right. However there are breaks or variation in the trends in the following cases:
  - IE is especially low when removal of an electron creates a newly empty p subshell (examples include  $I_1$  of B, Al, Sc)
  - IE energy is especially low where removal of an electron results in a half-filled p or d subshell (examples include  $I_1$  of O, S)
  - IE increases more gradually across the d- and f-subshells compared to s- and p- subshells. This is because d- and f- electrons are weakly penetrating and experience especially low  $Z^*$ .
- **From one period to the next:** There is an especially large decrease in IE with the start of every new period (from He to Li or from Ne to Na for example). This is consistent with the idea that IE is especially low when removal of an electron creates a newly empty s-subshell.
- **Noble gases:** The noble gases possess very high ionization energies. Note that helium has the highest ionization energy of all the elements.
- **Down a group:** Although  $Z^*$  increases going down a group, there is no reliable trend in IE going down any group; in some cases IE increases going down a group, while in other cases IE decreases going down a group.

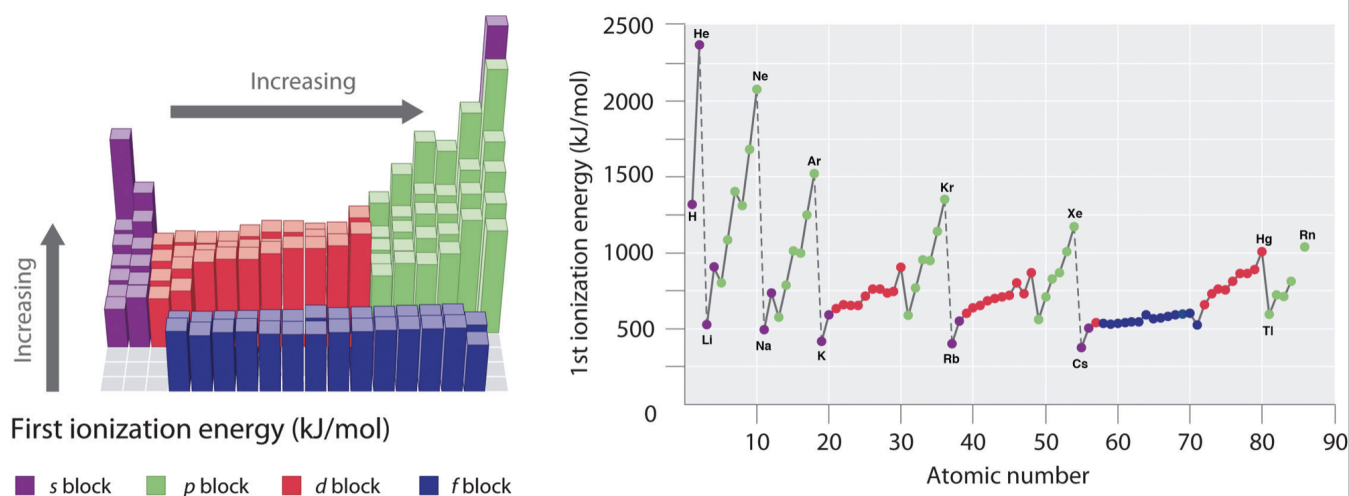


Figure 1.4.2.1: Graph showing the First Ionization Energy of the Elements. Left: ionization energies are mapped onto the periodic table, where the magnitude of ionization energy is depicted as a bar graph. Right: the first ionization energy is plotted against atomic number. In both panels the elements of the s-block are shown in purple, p-block are shown in green, d-block are shown in red, and f-block are shown in blue. (CC BY-NC-SA 3.0; anonymous)

Plots of the  $I_1$ ,  $I_2$ , and  $I_3$  of elements from hydrogen to krypton (first four periods) are shown in Figure 1.4.2.2. Notice that  $I_3 > I_2 > I_1$ . Also notice that trends mentioned above for  $I_1$  hold true for subsequent ionizations when electron configurations are considered!

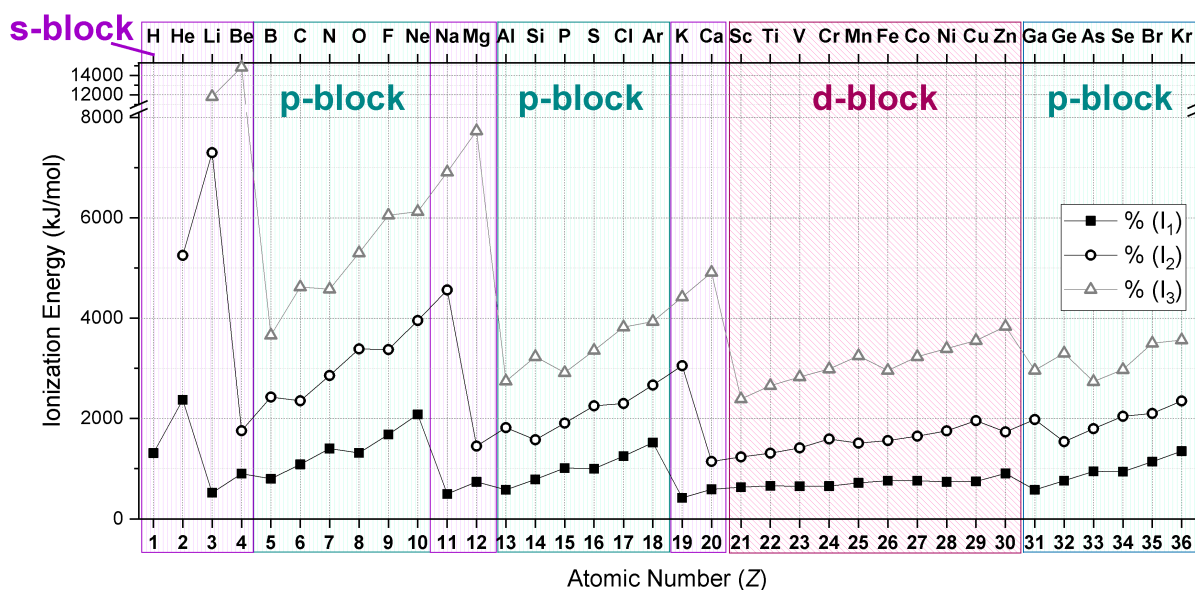


Figure 1.4.2.2. The first ( $I_1$ ), second ( $I_2$ ), and third ( $I_3$ ) ionization energies plotted for elements with  $Z = 1$  to 36 (H to Kr). The position of each element in its atomic form is indicated as s- p- or d-block. (CC-BY-NC-SA; Kathryn Haas)

This page titled [1.4.2: Ionization energy](#) is shared under a [CC BY-SA 3.0](#) license and was authored, remixed, and/or curated by [Kathryn Haas](#), [Swetha Ramireddy](#), [Bingyao Zheng](#), [Emily Nguyen](#), & [Emily Nguyen](#).

- [2.3.1: Ionization energy](#) by Bingyao Zheng, Emily Nguyen, Kathryn Haas, Swetha Ramireddy is licensed [CC BY-NC-SA 3.0](#).

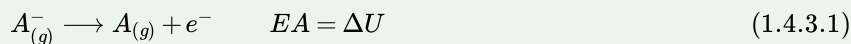
## 1.4.3: Electron Affinity

### Definitions of Electron Affinity

According to IUPAC, there are two different, but equivalent, definitions of **electron affinity (EA)**.<sup>1</sup>

#### Definition: Electron Affinity defined as removal of an electron

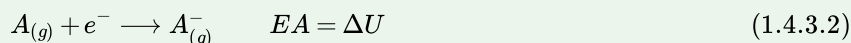
Electron affinity can be defined as the energy *required* when an electron is removed from a gaseous anion. The reaction as shown in equation 1.4.3.1 is *endothermic* (positive  $\Delta U$ ) for elements except noble gases and alkaline earth metals. Under this definition, the more positive the EA value, the higher an atom's affinity for electrons.



The reaction shown in Equation 1.4.3.1 is similar those that define **ionization energy**. For this reason, the EA is also described as the *zeroth ionization energy*.

#### Definition: Electron Affinity defined as addition of an electron

An alternate and more common definition is the microscopic reverse of Equation 1.4.3.1. This more common definition states that electron affinity is the energy *released* when an electron is added to a gaseous atom, as shown in Equation 1.4.3.2. The reaction as shown in equation 1.4.3.2 is *exothermic* (negative  $\Delta U$ ) for elements except noble gases and alkaline earth metals. The more negative this EA value, the higher an atom's affinity for electrons.



Conceptually, this second definition is quite similar to the concept of electronegativity; but unlike electronegativity, EA is a well-defined quantitative measurement.

### Trends in Electron Affinity

For this discussion, we will use the definition of EA that is consistent with it being a *zeroth ionization energy*: a more positive (larger) value means that the EA is higher (meaning stronger affinity toward an electron).

- **Across a period:** Similar to ionization energy, EA generally increases across a row of the periodic table; this observation is consistent with the increase in effective nuclear charge ( $Z^*$ ) from left to right across a period. However, there are variations across a period that are similar to variations in **ionization energy** and that can be explained by shielding, penetration, and electron configuration.
- **Down a group:** Like the case of **ionization energy** trends, EA does not consistently decrease going down a column of the periodic table despite the fact that  $Z^*$  increases down a group.

The trend in EA follows a zig-zag pattern similar to the one seen with ionization energies, except that it is displaced by one unit from the trend in  $I_1$ , two units from  $I_2$ , and so on. For example, EA peaks at F, while  $I_1$  peaks at Ne,  $I_2$  peaks at Na, and  $I_3$  peaks at Mg. A plot of EA for the first 13 elements is shown overlaid on plots of  $I_1$ ,  $I_2$  and  $I_3$  in Figure 1.4.3.1, where the shifts in the peaks and valleys within each zig-zag trend are indicated.



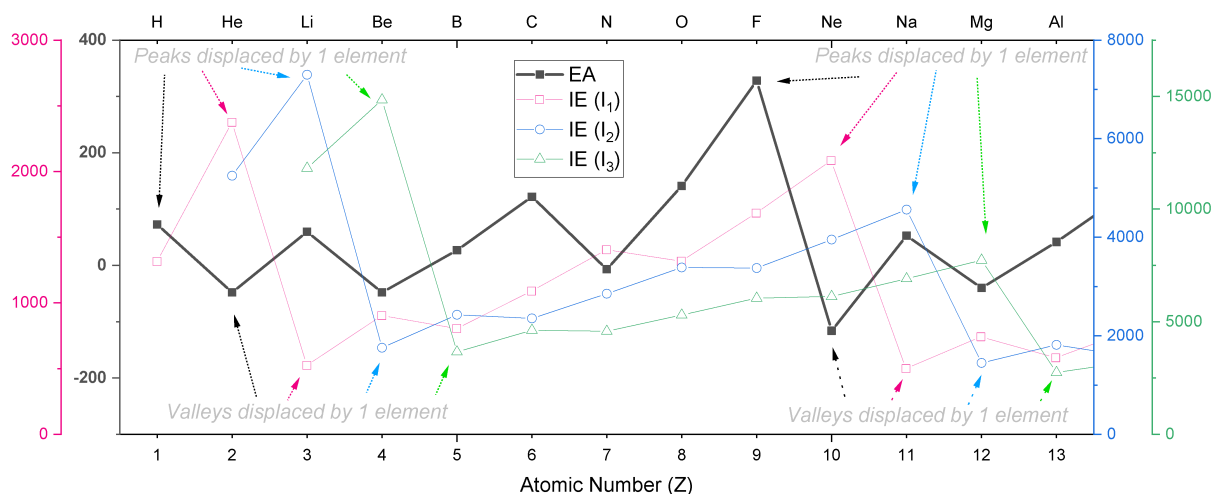


Figure 1.4.3.1. A plot of electron affinity (the zeroth ionization energy) is overlaid on plots of the first ( $I_1$ ), second ( $I_2$ ), and third ( $I_3$ ) ionization energies. Each plot is shown using separate y-axes. Trends in EA are similar to those in ionization energies, except that the peaks and valleys of the trends are shifted by one unit, as indicated. These plots are shown in units of kJ/mole. (CC-BY-NC-SA; Kathryn Haas)

## Sources

1. IUPAC. Compendium of Chemical Terminology, 2nd ed. (the "Gold Book"). Compiled by A. D. McNaught and A. Wilkinson. Blackwell Scientific Publications, Oxford (1997). Online version (2019-) created by S. J. Chalk. ISBN 0-9678550-9-8. doi.org/10.1351/goldbook.
2. Electron Affinity (data page), Wikipedia. en.Wikipedia.org/wiki/Electron\_affinity\_(data\_page) Accessed 12/3/19.

This page titled [1.4.3: Electron Affinity](#) is shared under a [CC BY-SA 4.0](#) license and was authored, remixed, and/or curated by [Kathryn Haas](#).

- [2.3.2: Electron Affinity](#) by Kathryn Haas is licensed [CC BY-NC 4.0](#).

## 1.4.4: Covalent and Ionic Radii

### Measurement of Radius

There are several methods that can be used to determine radii of atoms and ions:

- **Nonpolar atomic radii:** The radius of an atom is derived from the bond lengths within nonpolar molecules; one-half the distance between the nuclei of two atoms within a covalent bond.
- **van der Waals radius:** The radius of an atom is determined by collision with other atoms.
- **Crystal radii:** The atomic or ionic radius is determined using electron density maps from X-ray data.

The measurement of atomic or ionic size will depend on a number of factors, including the covalent character of bonding in any particular molecule, coordination number, physical state (liquid, solid, gas), the identity of nearby atoms/ions, variation in crystal structure, and distortions within regular crystal structures. You should keep in mind that the size of an atom or ion is a "fuzzy" measure, and the radius under a different set of conditions will probably change slightly.

Regardless, measured atomic and ionic radii reveal obvious trends across the periodic table and between atoms and ions. The relative atomic sizes shown in Figure 1.4.4.1 were derived from crystallographic data.<sup>1</sup>

### Trends in Atomic Radius

Atomic size generally decreases gradually from left to right across a period of elements. As nuclear charge ( $Z$ ) increases, we expect the effective nuclear charge ( $Z^*$ ) of the valence electrons to also increase. Increasing  $Z$  pulls electrons closer to the nucleus. However, with each additional unit of  $Z$ , there is also an additional electron. The change in size is a balance of a compression caused by increasing  $Z$  and an expansion in the number of electrons. As a result, the atomic radius decreases *gradually* across a period.

Atomic size generally increases going down a group. As valence electrons occupy higher level shells due to the increasing quantum number ( $n$ ), size increases despite the fact that  $Z$  and  $Z^*$  are increasing going down the group.

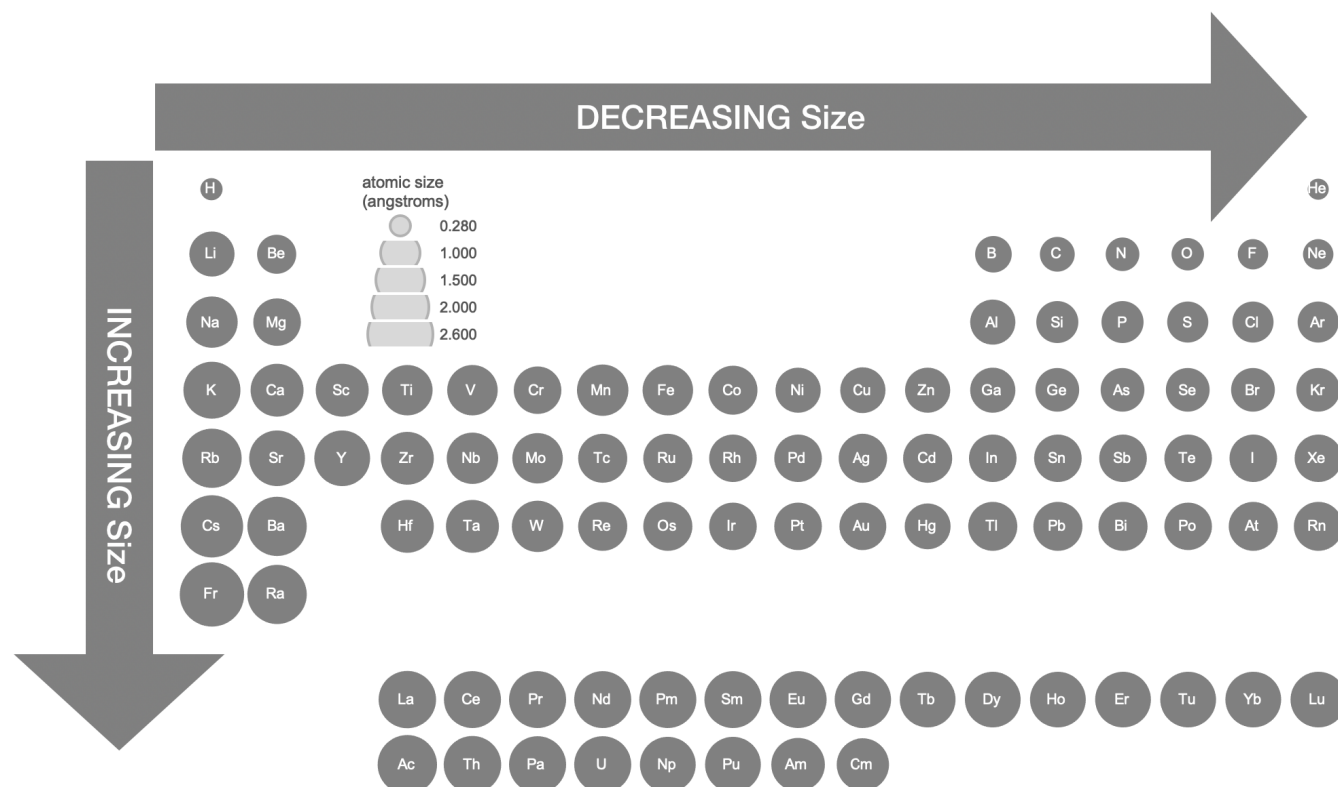


Figure 1.4.4.1. Atomic Radii Calculated from Crystallographic Data. Data from Cordero, Beatriz, Verónica Gomez, Ana E. Platero-Prats, Marc Reves, Jorge Echeverría, Eduard Cremades, Flavia Barragan, and Santiago Alvarez. "Covalent Radii Revisited." *Dalton Transactions*, no. 21 (2008): 2832–38. doi:10.1039/b801115j. (Kathryn Haas; CC-NC-BY-SA)



---

## References

1. Cordero, Beatriz, Veronica Gomez, Ana E. Platero-Prats, Marc Reves, Jorge Echeverria, Eduard Cremades, Flavia Barragan, and Santiago Alvarez. "Covalent Radii Revisited." *Dalton Transactions*, no. 21 (2008): 2832–38. doi:10.1039/b801115j.
2. R. D. Shannon (1976). "Revised effective ionic radii and systematic studies of interatomic distances in halides and chalcogenides". *Acta Crystallogr A*. **32** (5): 751–767. Bibcode:1976AcCrA..32..751S. doi:10.1107/S0567739476001551.
3. Wikipedia articles on [Atomic Radius](#) and [Ionic Radius](#).

---

This page titled [1.4.4: Covalent and Ionic Radii](#) is shared under a [CC BY-SA 4.0](#) license and was authored, remixed, and/or curated by [Kathryn Haas, Swetha Ramireddy, Bingyao Zheng, Emily Nguyen, & Emily Nguyen](#).

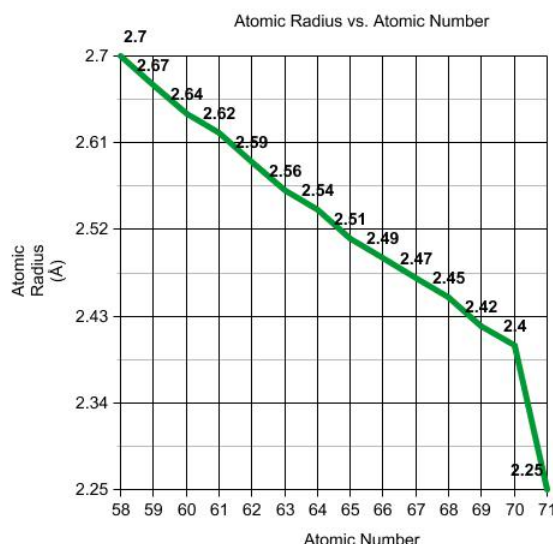
- [2.3.3: Covalent and Ionic Radii](#) by Bingyao Zheng, Emily Nguyen, Kathryn Haas, Swetha Ramireddy is licensed [CC BY-NC 4.0](#).

## 1.4.5: Lanthanide Contraction

The Lanthanide Contraction describes the atomic radius trend that the [Lanthanide](#) series exhibit. Another important feature of the The Lanthanide Contraction refers to the fact that the 5s and 5p orbitals penetrate the 4f sub-shell so the 4f orbital is not shielded from the increasing nuclear charge, which causes the atomic radius of the atom to decrease. This decrease in size continues throughout the series.

### Introduction

The Lanthanide Contraction applies to all 14 elements included in the [Lanthanide](#) series. This series includes Cerium(Ce), Praseodymium(Pr), Neodymium(Nd), Promethium(Pm), Samarium(Sm), Europium(Eu), Gadolinium(Gd), Terbium(Tb), Dysprosium(Dy), Holmium(Ho), Erbium(Er), Thulium(Tm), Ytterbium(Yb), and Lutetium(Lu). The atomic radius, as according to the Lanthanide Contraction, of these elements decreases as the atomic number increases. We can compare the elements Ce and Nd by looking at a [periodic table](#). Ce has an atomic number of 58 and Nd has an atomic number of 60. Which one will have a smaller atomic radius? Nd will because of its larger atomic number.

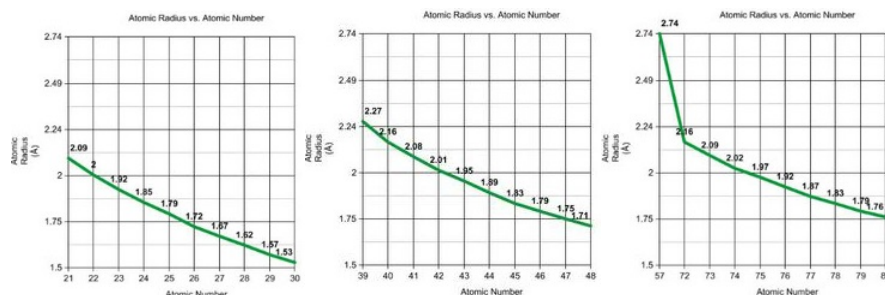


*The graph shows the atomic radius decreasing as the atomic number is increasing, Lanthanide Contraction.*

### Shielding and its Effects on Atomic Radius

The Lanthanide Contraction is the result of a poor shielding effect of the 4f electrons. The shielding effect is described as the phenomenon by which the inner-shell electrons shield the outer-shell electrons so they are not effected by nuclear charge. So when the shielding is not as good, this would mean that the positively charged nucleus has a greater attraction to the electrons, thus decreasing the atomic radius as the atomic number increases. The s orbital has the greatest shielding while f has the least and p and d in between the two with p being greater than d.

The Lanthanide Contraction can be seen by comparing the elements with f electrons and those without f electrons in the d block orbital. Pd and Pt are such elements. Pd has 4d electrons while Pt has 5d and 4f electrons. These 2 elements have roughly the same atomic radius. This is due to Lanthanide Contraction and shielding. While we would expect Pt to have a significantly larger radius because more electrons and protons are added, it does not because the 4f electrons are poor at shielding. When the shielding is not good there will be a greater nuclear charge, thus pulling the electrons in closer, resulting in a smaller than expected radius.



Row 1 of Periodic Table D block Row 2 Row 3

The graphs depict the atomic radii of the first three rows of transition metals. We can apply the same principle as applied with the elements Pd and Pt to whole rows and columns. As we can see by comparing Row 1 with Row 2, the atomic radii differ greatly between the elements, but if we compare Row 2 with Row 3, the atomic radii do not have much difference. Elements with atomic number 23 and 41 lie in the same column of the periodic table and have a significantly large difference in atomic radii (atomic radii increases from Row 1 to Row 2), but elements 41 and 73, also in the same column, only differ slightly. This is the cause of introducing 4f electrons in Row 3. In Row 3, we would expect the elements to carry on the same trend as was witnessed between Rows 1 and 2 (large increase in atomic radii) but we do not. This is because the 4f orbitals are not doing a great job of shielding.

## D Block Contraction (Scandide Contraction)

The d block contraction, also known as the Scandide Contraction, describes the atomic radius trend that the d block elements (Transition metals) experience. Normally the trend for atomic radius, moving across the periodic table is that the atomic radius decreases significantly. In the transition metals with D electrons as we move from left to right across the periodic table, the element's atomic radius only decreases slightly. This is because they have the same amount of s electrons, but are only differing in d electrons. These d electrons are in an inner shell (penultimate shell) and electrons are getting added to this shell, another shell is not created. The d electrons are not good at shielding the nuclear charge, so the atomic radius does not change much as electrons are added. Almost like disregarding the D electrons being added.

## Effects on Ionization Energy and Properties

As the proton number increases and the atomic radius decreases, the ionization energy increases. This is due to a more positively charged nucleus and a greater pull on the electrons by the nucleus. A greater pull is the result of an increased effective nuclear charge. Effective nuclear charge is caused by the nucleus having a more positive charge than the negative charge on the electron (net positive charge). The density, melting point, and hardness increase from left to right throughout the Lanthanide Series. The Lanthanide Contraction makes chemical separation of the Lanthanides easier. The Lanthanide Contraction, while making the chemical separation of Lanthanides easier, it makes the separation of elements following the series a bit more difficult.

## References

1. Petrucci, Harwood, Herring, and Madura. *General Chemistry Principles & Modern Applications*. 9th ed. Prentice Hall. Print.
2. Cotton, Simon. *Lanthanide and Actinide Chemistry*. Wiley. Print.

## Problems

1. What is the cause of Lanthanide Contraction?
2. Which element has a greater atomic radius Gd or Tb and why?
3. Which element has a smaller atomic radius Dy or Yb and why?
4. Why do elements in Rows 2 and 3 that are in the same column have similar atomic radii?
5. Place the following elements in order of increasing atomic radius: Eu, Ce, Pr, Ho.
6. Which one of the following has the lowest density: Tb, Pm, Er, Tm, Ce

Answers:

1. The Lanthanide Contraction is caused by a poor shielding effect of the 4f electrons.
2. Gd because as atomic number increases, the atomic radius decreases.
3. Yb because it has a larger atomic number.

4. Because the elements in Row 3 have 4f electrons. These electrons do not shield good, causing a greater nuclear charge. This greater nuclear charge has a greater pull on the electrons.
5. Ho, Eu, Pr, Ce
6. Ce

### Contributors and Attributions

- Amrit Paul Bains (UCD)

---

1.4.5: Lanthanide Contraction is shared under a [CC BY-SA 4.0](#) license and was authored, remixed, and/or curated by LibreTexts.

- [Lanthanide Contraction](#) is licensed [CC BY-NC-SA 4.0](#).

## 1.4.6: The Uniqueness Principle

The bonding characteristics of the elements do not vary gradually down the groups in the main group of the periodic table. Instead, there are significant discontinuities on moving between the first and second row elements and the second row elements and the rest of the periodic table. These differences are outlined below and depicted schematically in Figure 1.4.6.1.

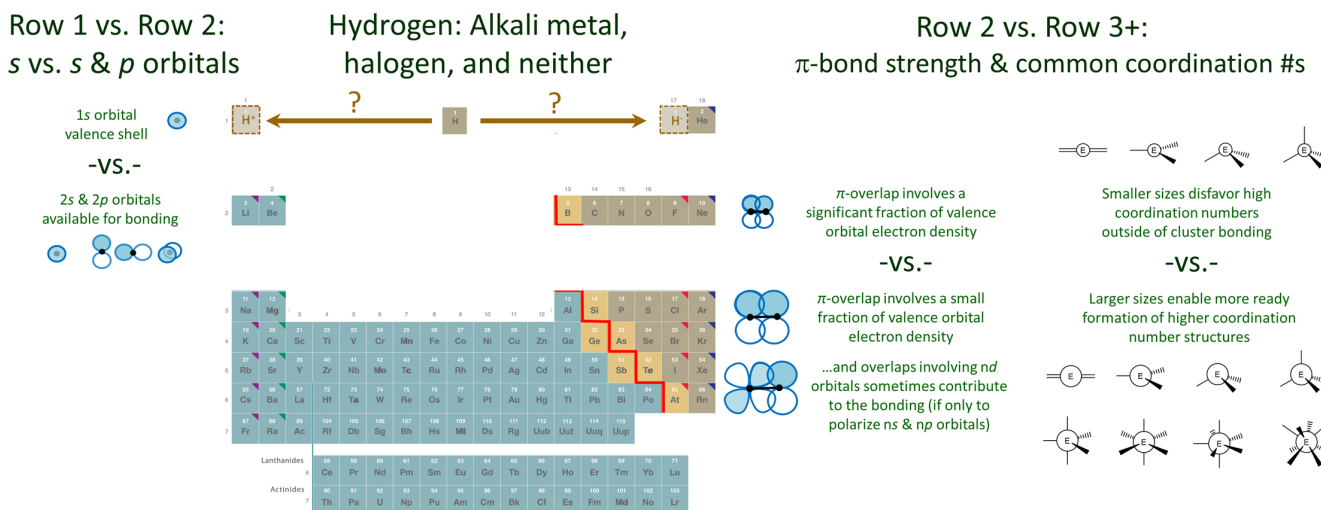


Figure 1.4.6.1. Factors that contribute to major differences in the chemical properties between the elements of the first two rows and between the row 2 elements and those in the rest of the periodic table. The image is adapted from [https://chem.libretexts.org/Bookshelves/General\\_Chemistry/Map%3A\\_Chemistry\\_-\\_The\\_Central\\_Science\\_\(Brown\\_et\\_al.\)/02\\_Atoms%2C\\_Molecules%2C\\_and\\_Ions/2.5%3A\\_The\\_Periodic\\_Table](https://chem.libretexts.org/Bookshelves/General_Chemistry/Map%3A_Chemistry_-_The_Central_Science_(Brown_et_al.)/02_Atoms%2C_Molecules%2C_and_Ions/2.5%3A_The_Periodic_Table). Otherwise this work by Stephen Contakes is licensed under a [Creative Commons Attribution 4.0 International License](#).

### The first row elements have a unique chemistry because their valence shell is only a 1s orbital.

In the case of He the 1s orbital is full, compact, and of low energy. Consequently He is extremely inert, to the point where no compounds of He are known.

Hydrogen's 1s orbital is comparatively higher in energy. As a result H is more reactive. It tends to lose or gain its single electron but can also contribute to multicenter bonding.

Because of its chemical versatility the location of H in the periodic table is ambiguous. Even though its electronegativity is much greater than that of lithium, it is usually placed at the head of the alkali metals. This placement is consistent with its possession of a single valence electron and the consequent readiness with which it loses an electron, particularly in aqueous media. However, hydrogen is also just short a single electron and so in other contexts it readily forms hydrides. Thus it might be placed at the head of the halogens. Although it is rare to place H above the halogens, in some tables H is placed above the table to emphasize this chemical versatility.

### According to the uniqueness principle the second row elements are unique in their ability to form strong multiple bonds and their resistance to serving as high coordination number centers.

There are three reasons why the second row elements differ significantly from their heavier congeners.

**1. Only the second row elements form strong  $\pi$ -bonds.** As depicted schematically in Figure 1.4.6.1, the second row elements are able to form strong  $\pi$  bonds since the fraction of electron density involved in the  $\pi$ -overlap is significant for the more compact orbitals and shorter bonds of the row 2 elements. In contrast, for row 3 and heavier elements, relatively little of the large and diffuse orbitals contributes to the overlap that stabilizes the  $\pi$ -bond. In consequence,  $\pi$ -bonds involving these elements are very weak and such bonds are *relatively* rare. This is because it is almost always more favorable for such elements to form multiple single bonds or engage in cluster bonding.

The tendency of Row 2 nonmetals to form strong  $\pi$  bonds in cases where their heavier congeners form extended structures is apparent from the common allotropes formed by the *p*-block nonmetals. As shown in Figure 1.4.6.2 Row 3+ elements have a greater tendency to form extended structures held together by single bonds than their Row 2 counterparts.



					18
					He(g)
13	14	15	16	17	
B <sub>∞</sub> (s)	C <sub>60</sub> (s) C <sub>∞</sub> (graphite) C <sub>∞</sub> (diamond)	N <sub>2</sub> (g)	O <sub>2</sub> (g)	F <sub>2</sub> (g)	Ne(g)
Al <sub>∞</sub> (s)	Si <sub>∞</sub> (s)	P <sub>4</sub> (s) P <sub>∞</sub> (s)	S <sub>8</sub> (s) S <sub>∞</sub> (s)	Cl <sub>2</sub> (g)	Ar(g)
Ga <sub>∞</sub> (s)	Ge <sub>∞</sub> (s)	As <sub>∞</sub> (s)	Se <sub>8</sub> (s) Se <sub>∞</sub> (s)	Br <sub>2</sub> (l)	Kr(g)
In <sub>∞</sub> (s)	Sn <sub>∞</sub> (s)	Sb <sub>∞</sub> (s)	Te <sub>∞</sub> (s)	I <sub>2</sub> (s)	Xe(g)

Red = contains multiple bonds      Green = cluster bonding  
 Blue = single bonds only              Orange = monatomic  
 Gray = clear metallic bonding

Figure 1.4.6.2. Characteristics of the common allotropes of selected *p* block elements. This work by Stephen Contakes is licensed under a [Creative Commons Attribution 4.0 International License](#).

As shown in Figure 1.4.6.3 the Row 2 element carbon forms sheetlike structures involving multiple bonding (graphite, fullerenes, nanotubes) as well as 3D networks held together by single bonds (the diamond structure), while its heavier congeners Si and Ge only form 3D networks. Similarly, nitrogen and oxygen form diatomic gases held together by multiple bonds, while their heavier congeners form clusters (P), layers (As, Sb), or chains (S, Se, Te) held together by single covalent bonds.

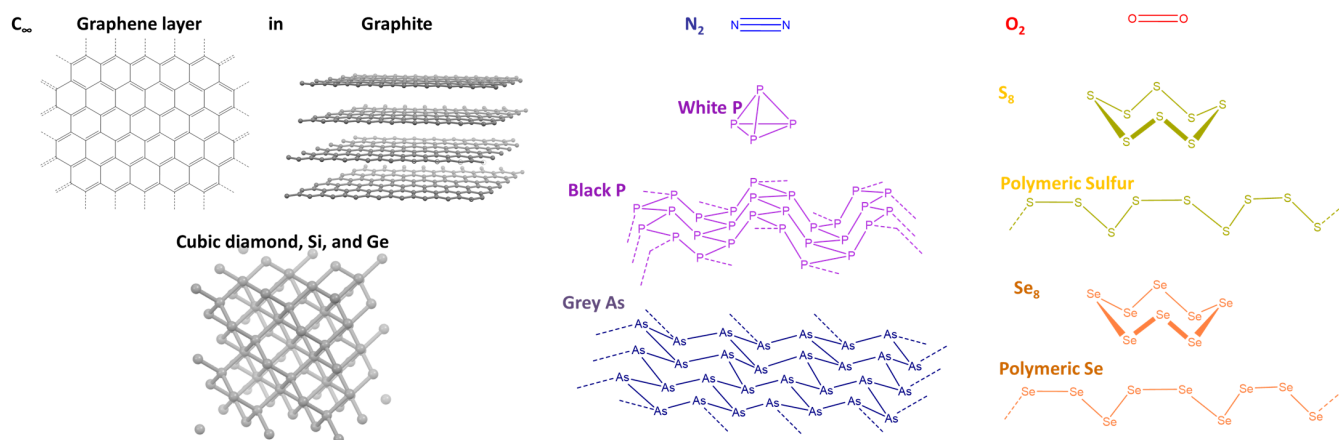


Figure 1.4.6.3. While row 2 elements like C, N, and O form structures held together by multiple bonds, their heavier congeners form singly bonded clusters, rings, chains, sheets, and networks. This work by Stephen Contakes is licensed under a [Creative Commons Attribution 4.0 International License](#).

2. **The valence shell of the second row elements lacks low-lying *nd* orbitals.** As a result, only the 2s and 2*p* type orbitals of second row elements significantly contribute to the bonding in their compounds. In contrast, the main group elements of row 3 and higher possess low lying unoccupied *nd* orbitals, which enable them to act as a  $\pi$  acid towards a ligand atom by forming  $d_{\pi} - p_{\pi}$  and  $d_{\pi} - d_{\pi}$  overlaps.

3. As depicted in Figure 1.4.6.1, **when second row elements serve as a central atom, they do not readily exhibit coordination numbers higher than four.** In contrast, the larger size of row 3 and heavier elements reduces the steric strain associated with the addition of multiple ligands about an element center. This makes it easier for these elements to form trigonal bipyramidal, octahedral, and other high coordination number structures.

## Contributors and Attributions

Stephen M. Contakes, Westmont College

1.4.6: The Uniqueness Principle is shared under a [CC BY-SA 4.0](#) license and was authored, remixed, and/or curated by LibreTexts.

- **8.1.1.2: There are qualitative differences between the chemistry of the elements in the first two rows and those in the rest of the periodic table** has no license indicated.

## 1.5: Unit 1 Practice Problems

### Unit 1A

#### Exercise 1

What is true about the Rutherford atom model?

- a. It explains why atoms do not send out electromagnetic radiation permanently
- b. It explains why alpha particles get scattered by atoms
- c. It explains the atomic spectrum of the hydrogen atom
- d. It explains the wave-particle dualism

**Answer**

- b) It explains why alpha particles get scattered by atoms

#### Exercise 2

The Bohr radius (the radius of the electron orbit for the H atom in its ground state) is  $5.29 \times 10^{-11}$  m. Calculate the radius of an electron in the third shell of the H atom according to the Bohr atom model.

**Answer**

$$r_3 = 3^2 \times 5.29 \times 10^{-11} \text{ m} = 47.61 \times 10^{-11} \text{ m}.$$

#### Exercise 3

The electron in an H atom undergoes an electronic transition from the 3<sup>rd</sup> to the 2<sup>nd</sup> shell. What frequency does the light that is emitted have? The energy of the electron in the first shell is  $-2.18 \times 10^{-18}$  J.

**Answer**

$$\text{Energy of electron in the 3}^{\text{rd}} \text{ shell: } E_3 = -2.18 \times 10^{-18} \text{ J} / 3^2 = -0.24 \times 10^{-18} \text{ J}$$

$$\text{Energy of electron in the 2}^{\text{nd}} \text{ shell: } E_2 = -2.18 \times 10^{-18} \text{ J} / 2^2 = -0.545 \times 10^{-18} \text{ J}$$

$$\text{Energy difference between the two electrons: } E_3 - E_2 = 0.305 \times 10^{-18} \text{ J}$$

$$\text{Frequency of emitted light: } \nu = (E_3 - E_2) / h = 0.305 \times 10^{-18} \text{ J} / 6.63 \times 10^{-34} \text{ Js} = 4.60 \times 10^{14} \text{ s}^{-1}$$

#### Exercise 4

What is the mass of a photon with a wavelength of 400 nm that travels through space?

**Answer**

$$\lambda = h/mc \rightarrow m = h/\lambda c = 6.63 \times 10^{-34} \text{ Js} / (400 \times 10^{-9} \text{ m} \times 3.00 \times 10^8 \text{ m/s}) = 5.525 \times 10^{-36} \text{ kg}.$$

#### Exercise 5

Two objects are moving at the same speed. Which (if any) of the following statements are true?

- a. The DeBroglie wavelength of the heavier object is longer than that of the lighter one.
- b. If one object has twice as much mass as the other, its wavelength is one-half of the other
- c. Doubling the speed of one of the objects will have the same effect on its wavelength as doubling its mass.

**Answer**

- a) If one object has twice as much mass as the other, its wavelength is one-half of the other

b) Doubling the speed of one of the objects will have the same effect on its wavelength as doubling its mass

#### Exercise 6

The power of a red laser with a wavelength of 630 nm) is 1.00 Watt (1.00 Js). How many photons per second does the laser emit?

**Answer**

$$v=c/\lambda = 3.00 \times 10^8 \text{ m/s} / 630 \times 10^{-9} \text{ m} = 4.76 \times 10^{14} \text{ s}^{-1}$$

$$E = h\nu = 6.63 \times 10^{-34} \text{ Js} \times 4.76 \times 10^{14} \text{ s}^{-1} = 3.157 \times 10^{-19} \text{ J}$$

$$\# \text{ photons} = 1 \text{ J} / 3.157 \times 10^{-19} \text{ J} = 3.2 \times 10^{18}$$

### Unit 1B

#### Exercise 7

Which of the following waves would you consider to be standing matter wave?

- a. The vibration of a drum.
- b. Sound traveling through open air.
- c. A tsunami.
- d. None of the above.

**Answer**

- a) The vibration of a drum.

#### Exercise 8

What are orbitals (more than one answer can be correct)?

- a. Wave functions that describe the electrons as three-dimensional standing matter waves in an atom.
- b. Spaces inside an atom in which the electron travels as a classical particle.
- c. Solutions of the Schrödinger equation for the hydrogen atom.

**Answer**

- a) Wave functions that describe the electrons as three-dimensional standing matter waves in an atom.
- c) Solutions of the Schrödinger equation for the hydrogen atom.

#### Exercise 9

Which quantum numbers  $l$  are allowed when the quantum number  $n$  is 4?

**Answer**

$l$  can be 3,2,1,0

#### Exercise 10

Which quantum numbers  $m$  are allowed when the quantum number  $l$  is 3?

**Answer**

-3,-2,-1,0,+1,+2,+3

### Exercise 11

What is true about the following wave function?

$$\Psi = \frac{1}{\sqrt{2\pi}} \frac{\sqrt{6}}{2} \cos \theta \frac{4}{81\sqrt{6}a_0^{3/2}} \left[ 6 - \frac{r}{a_0} \right] \frac{r}{a_0} e^{-r/3a_0}$$

- a. Its does not have angular nodes
- b. Its does not have spherical nodes
- c. Its amplitude is 0 at the nucleus
- d. The wave function represents an s orbital

**Answer**

- c) Its amplitude is 0 at the nucleus

### Exercise 12

The angular part of the wavefunction of an orbital has the following form:

$$\Theta\Phi(x, y, z) = \frac{1}{4} \sqrt{\frac{15}{\pi}} \frac{(x^2 - y^2)}{r^2}$$

Which planes are the planar nodes in this orbital?

**Answer**

The wavefunction is 0 for  $x=y$  and  $x=-y$ . So it is two planes that bisect the x and the y axis.

## Unit 1C

### Exercise 13

Order the following orbitals with respect to their penetration abilities:

4s, 4p, 4d, 4f

**Answer**

$4s > 4p > 4d > 4f$

### Exercise 14

What is the effective nuclear charge on an electron in an  $\text{He}^+$  ion?

**Answer**

$$\sigma = 0 \rightarrow Z_{\text{eff}} = Z = 2$$

### Exercise 15

Calculate the orbital energy of a 3p electron in a sulfur atom using the Slater rules.

**Answer**

$(1s^2) (2s^2 2p^6) (3s^2 3p^4)$

$$\sigma = 5 \times 0.35 + 8 \times 0.85 + 2 \times 1 = 10.55$$

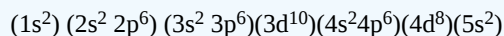
$$Z_{\text{eff}} = Z - \sigma = 16 - 10.55 = 5.45$$

$$E = -\frac{Z_{\text{eff}}^2 \times 13.6 \text{ eV}}{n^2} = -\frac{5.45^2 \times 13.6 \text{ eV}}{3^2} = -44.9 \text{ eV}$$

### Exercise 16

Calculate the orbital energy of a 3d electron in a palladium atom using the Slater rules.

**Answer**



$$\sigma = 9 \times 0.35 + 18 = 21.15$$

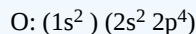
$$Z_{\text{eff}} = Z - \sigma = 46 - 21.15 = 24.85$$

$$E = -\frac{Z_{\text{eff}}^2 \times 13.6 \text{ eV}}{n^2} = -\frac{24.85^2 \times 13.6 \text{ eV}}{3^2} = -933 \text{ eV}$$

### Exercise 17

Calculate how much higher the first ionization energy of an oxygen atom is compared to a fluorine atom. Use the Slater rules to answer the question.

**Answer**



$$\sigma(2p_{\text{oxygen}}) = 5 \times 0.35 + 2 \times 0.85 = 3.45$$

$$Z_{\text{eff}}(2p_{\text{oxygen}}) = Z(2p_{\text{oxygen}}) - \sigma(2p_{\text{oxygen}}) = 8 - 3.45 = 4.55$$

$$E(2p_{\text{oxygen}}) = -\frac{Z_{\text{eff}}^2 \times 13.6 \text{ eV}}{n^2} = -\frac{4.55^2 \times 13.6 \text{ eV}}{2^2} = -70.4 \text{ eV}$$
  

$$\sigma(2p_{\text{fluorine}}) = 6 \times 0.35 + 2 \times 0.85 = 3.8$$

$$Z_{\text{eff}}(2p_{\text{fluorine}}) = Z(2p_{\text{fluorine}}) - \sigma(2p_{\text{fluorine}}) = 9 - 3.8 = 5.2$$

$$E(2p_{\text{fluorine}}) = -\frac{Z_{\text{eff}}^2 \times 13.6 \text{ eV}}{n^2} = -\frac{5.2^2 \times 13.6 \text{ eV}}{2^2} = -91.9 \text{ eV}$$
  

$$E(2p_{\text{fluorine}}) - E(2p_{\text{oxygen}}) = -91.9 \text{ eV} - (-70.4 \text{ eV}) = -21.5 \text{ eV}$$

$$\rightarrow \Delta IE = IE_{\text{fluorine}} - IE_{\text{oxygen}} = 21.5 \text{ eV}$$

Dr. Kai Landskron ([Lehigh University](#)). If you like this textbook, please consider to make a donation to support the author's research at Lehigh University: [Click Here to Donate](#).

This page titled [1.5: Unit 1 Practice Problems](#) is shared under a [CC BY-SA 4.0](#) license and was authored, remixed, and/or curated by [Kai Landskron](#).

- [Homework Problems Chapter 1](#) by [Kai Landskron](#) is licensed [CC BY 4.0](#).

## CHAPTER OVERVIEW

### Unit 2: Molecular Structure

#### 2.1: Chemical Bonding

##### 2.1.1: Types of Chemical Bonds

##### 2.1.2: Electronegativity and the Bonding Continuum

##### 2.1.3: Polarizability and Percent Ionic Character

#### 2.2: Lewis Structures and Molecular Shape

##### 2.2.1: Lewis Electron-Dot Diagrams

##### 2.2.2: Formal Charge

##### 2.2.3: Resonance

##### 2.2.4: Expanded Octets

##### 2.2.5: Limitation of Lewis Theory

##### 2.2.6: Valence Shell Electron-Pair Repulsion

##### 2.2.7: Lone Pair Repulsion

##### 2.2.8: Multiple Bonds

##### 2.2.9: Electronegativity and Atomic Size Effects

##### 2.2.10: Molecular Polarity

---

Unit 2: Molecular Structure is shared under a [not declared](#) license and was authored, remixed, and/or curated by LibreTexts.

## 2.1: Chemical Bonding

---

Learning objectives for this unit are to:

- Explain the thermodynamic driving force for the formation of chemical bonds
  - Compare and contrast ionic, covalent, and metallic bonds
  - Know that bonding is a continuum and explain or interpret information provided in a bonding triangle
  - Define electronegativity and identify regions of molecules with partial charge based on electronegativities
  - Define polarizability and relate polarizability to covalency
  - Define percent ionic character
- 

2.1: Chemical Bonding is shared under a [not declared](#) license and was authored, remixed, and/or curated by LibreTexts.



### 2.1.1: Types of Chemical Bonds

---

A **chemical bond** is the force that holds atoms together in a chemical compound. There are three idealized types of bonding. **Covalent bonding** is a type of chemical bonding in which electrons are shared between atoms in a molecule or polyatomic ion. **Ionic bonding** is a type of chemical bonding in which positively and negatively charged ions are held together by electrostatic forces. **Metallic bonding** is where all of the atoms in the metal share a few of their electrons which are free to circulate. One can relate the properties of materials to the type of bonding. Ionic compounds, for example, typically dissolve in water to form aqueous solutions that conduct electricity as the ions separate into solution. Solid ionic compounds do not conduct electricity or heat. In contrast, most covalent compounds that dissolve in water form solutions that do not conduct electricity because they go into the solvent as neutral molecules. The solids or liquids are not conductors. In metals, of course, the free electrons conduct electricity, and what is not obvious, also heat. Metals are good conductors of both. Further, in general, covalent compounds are volatile because the forces holding the neutral molecules together are relatively weak, whereas ionic compounds are not because the individual ions are strongly attracted to each other.

Despite the differences in the distribution of electrons between these idealized types of bonding, all models of chemical bonding have three features in common:

1. Atoms interact with one another to form aggregates such as molecules, compounds, and crystals because doing so lowers the total energy of the system; that is, the aggregates are more stable than the isolated atoms.
2. The type of bonding is determined by how the outermost electrons of an atom, the so called **valence** electrons of one atom interact with neighboring atoms. In ionic materials electrons are fully transferred. Covalent materials share electrons with neighboring atoms and metals share electrons over a wide region.
3. Energy is required to dissociate bonded atoms or ions into isolated atoms or ions. For ionic solids, in which the ions form a three-dimensional array called a *lattice*, this energy is called the lattice energy: the enthalpy change that occurs when a solid ionic compound (whose ions form a three-dimensional array called a lattice) is transformed into gaseous ions. For covalent compounds, this energy is called the bond energy: the enthalpy change that occurs when a given bond in a gaseous molecule is broken.
4. Each chemical bond is characterized by a particular optimal internuclear distance called the bond distance ( $r_0$ ), which is the lowest energy arrangement of the two atoms.

---

2.1.1: Types of Chemical Bonds is shared under a [not declared](#) license and was authored, remixed, and/or curated by LibreTexts.

## 2.1.2: Electronegativity and the Bonding Continuum

### Electronegativity

Electronegativity is the measure of the ability of an atom to attract electrons within a chemical bond. It is related to the electron affinity in the sense that both period properties measure the force by which an electron is attracted to a neutral atom. However, the electron affinity is associated with isolated atoms, that do not make bonds to neighbored atoms, while the electronegativity refers to atoms that are bonded to neighbored atoms. The importance of the electronegativity stems largely from its ability to predict and understand the nature of the bonding between atoms, in particular, covalent, ionic, and metallic bonding.

### Pauling Electronegativity Scale

Electronegativity was a concept first developed by Linus Pauling to describe the relative polarity of bonds and molecules. He argued that the electronegativity of an atom could be derived from bond energy differences between homoleptic and heteroleptic bonds (Eq. 1.3.1).

$$\chi(A)-\chi(B) = c [(E(A-B) - \{E(A-A) \cdot E(B-B)\}^{1/2}), \text{ eV}].$$

Here  $E(A-B)$ ,  $E(A-A)$  and  $E(B-B)$  are energies of A-B, A-A and B-B bonds respectively.  
c is a constant.

**Equation 1.3.1** Electronegativity according to Pauling, eV = electron volts.

For example, the energy required to break the bond in  $H_2$  is  $432 \text{ kJ mol}^{-1}$ , and for  $F_2$  it is  $159 \text{ kJ mol}^{-1}$ . However the energy required to break a bond in HF is  $565 \text{ kJ mol}^{-1}$ , which is much higher than expected just by averaging the energy of the two homonuclear bonds ( $296 \text{ kJ mol}^{-1}$ ). Pauling argued that the difference could be assigned to electrostatic attractions between the F and H “ends” of the molecule whereby the F end has more electron density and the H end has less electron density. The greater the difference between the average energy of the homoleptic bonds and the heteroleptic bonds, the greater the electronegativity difference between the atoms, and the greater the polarity of the heteroleptic bond.

First, Pauling used the arithmetic means of the heteroleptic bond energies, later he used the geometric means, because he found empirically that it worked better (Equation 1.3.1). The geometric mean of the homoleptic bond energies is the square root of the product of the homoleptic bond energies. This method only provided electronegativity differences. He therefore needed to define a reference atom with an arbitrarily defined electronegativity value, and then determine the electronegativity values of all other atoms relative to that value. He chose the most electronegative atom, the fluorine atom, as the standard and assigned a value of 4.0. The values of all other atoms vary between 0.7 (Fr) and 3.44 (O), and are shown in the periodic table on the below (Fig. 1.3.6).

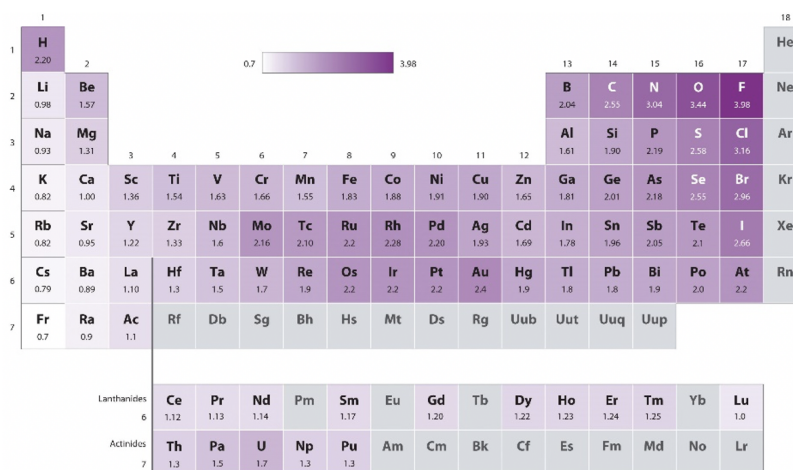


Figure 1.3.6 Periodic trends of electronegativity (Attribution: Chemlibretexts <https://chem.libretexts.org/@api/dek...jpg?revision=1> <http://creativecommons.org/licenses/by-nc-sa/3.0/us/>)

What are the periodic trends? One can see that within a period the electronegativity values of the main group elements strictly increase with the group number. Note though that the noble gases do not have a Pauling electronegativity because, with few exceptions, noble gases do not make compounds and thus no bond energies are available for them. We can also see that for main group elements the electronegativity strictly decreases down a group. This makes the fluorine the most electronegative atom, and

the cesium the least electronegative atom. Cesium has an electronegativity value of 0.7. We ignore the radioactive francium here. For the d-block, the trends are less strict, but there is a tendency of electronegativity increase from group 3 to group 11. All group 12 elements have smaller electronegativities compared to their neighbored group 11 elements. What about trends within a group? In group 3 to group 5 there is a small decrease in electronegativity down a group. For group 6 and 9, the period 5 elements have higher values than their neighbored elements in period 4 and 6. For group 10 to 12 the electronegativity increases down a group. The d-block element with the highest electronegativity is the gold, it has a value of 2.4. Note that this is similar to the electronegativity of non-metals such as I, S, and P. For these reasons, sometimes gold can behave like a non-metal in compounds with very low electronegativity. For example, there is the compound cesium auride (CsAu) which is a transparent, ionic crystalline compound due to the high electronegativity difference between cesium and gold. The f-block elements generally have low electronegativity.

### Allred-Rochow Electronegativity Scale

The Pauling electronegativity scale is derived from empirical data on bond energies. It works very well in practice and it is up to date the most used electronegativity scale. However, it does not relate electronegativity to other periodic properties, and the quantum-mechanical model of the atoms. One electronegativity scale that addresses this short-coming the Allred-Rochow scale. It relates the electronegativity to the Coulomb force that acts on an electron on the surface of an atom. The Coulomb force is proportional to the effective nuclear charge  $Z^*$  and inverse proportional to the atomic radius square.  $Z^*/r^2$  is multiplied with a factor of 3590 and a value of 0.744 is added to this term. These numbers are empirically chosen so that the values of the Allred-Rochow scale become comparable to the Pauling scale.

$$\text{Allred-Rochow: } \chi = [0.744 + 3590 \cdot Z^*/r^2]$$

Here  $Z^*$  is effective nuclear charge and  $r$  is atomic radius.

#### Equation 1.3.2 Allred-Rochow definition of electronegativity

### Mulliken Electronegativity Scale

Another frequently used scale is the Mulliken electronegativity scale. The Mulliken scale relates the electronegativity to the sum of the first ionization energy IE and the first electron affinity EA. We would intuitively agree that the ability of an atom to attract electrons within a chemical bond is the higher, the harder it is to remove an electron from an isolated atom, and the easier it is to add an electron to an isolated atom. The numbers 0.118 and -0.207 are empirically chosen to make comparisons to the Pauling scale possible. The Mulliken scale is related to the Allred-Rochow scale in the sense that you can explain ionization energies and electron affinities of atoms with the concept of the effective nuclear charge.

$$\text{Mulliken: } \chi = [0.118 \cdot (IE + EA) - 0.207]$$

Here IE is ionization energy and EA is electron affinity of an atom

#### Equation 1.3.3 Mulliken definition of electronegativity

### Allen Electronegativity Scale

Another electronegativity scale has been developed by Leland C. Allen. It designed for main group elements in particular. It argues that the electronegativity is proportional to the average energy of the s and p valence electrons in the atom. This electronegativity concept also has a relationship to that of Allred-Rochow, because orbital energies can be calculated from the effective nuclear charge.

$$\text{Allen: } \chi = [(m e_p + n e_s) / (m + n)]$$

Here  $e_p$  is the energy of p-electrons and  $e_s$  is the energy of s-electrons;  $m$  and  $n$  are populations of p- and s-orbitals respectively.

#### Equation 1.3.4 Leland C. Allen definition of electronegativity

Overall, you can see that the electronegativity scales are inter-related, they say essentially the same, but present electronegativity from a somewhat different perspective.

### Electronegativity of the Elements and Chemical Bonding

One of the most powerful attributes of electronegativity is that it can predict what type of chemical bond is to expect in elements and compounds. Let us first look at the bonding between elements.

1

2

3

4

5

6

7

8

9

10

11

12

13

14

15

16

17

18

19

20

21

22

23

24

25

26

27

28

29

30

31

32

33

34

35

36

37

38

39

40

41

42

43

44

45

46

47

48

49

50

51

52

53

54

55

56

57

58

59

60

61

62

63

64

65

66

67

68

69

70

71

72

73

74

75

76

77

78

79

80

81

82

83

84

85

86

87

88

89

90

91

92

93

94

95

96

97

98

99

100

101

102

103

104

105

106

107

108

109

110

111

112

113

114

115

116

117

118

119

120

121

122

123

124

125

126

127

128

129

130

131

132

133

134

135

136

137

138

139

140

141

142

143

144

145

146

147

148

149

150

151

152

153

154

155

156

157

158

159

160

161

162

163

164

165

166

167

168

169

170

171

172

173

174

175

176

177

178

179

180

181

182

183

184

185

186

187

188

189

190

191

192

193

194

195

196

197

198

199

200

201

202

203

204

205

206

207

208

209

210

211

212

213

214

215

216

217

218

219

220

221

222

223

224

225

226

227

228

229

230

231

232

233

234

235

236

237

238

239

240

241

242

243

244

245

246

247

248

249

250

251

252

253

254

255

256

257

258

259

260

261

262

263

264

265

266

267

268

269

270

271

272

273

274

275

276

277

278

279

280

281

282

283

284

285

286

287

288

289

290

291

292

293

294

295

296

297

298

299

300

301

302

303

304

305

306

307

308

309

310

311

312

313

314

315

316

317

318

319

320

321

322

323

324

325

326

327

328

329

330

331

332

333

334

335

336

337

338

339

340

341

342

343

344

345

346

347

348

349

350

351

352

353

354

355

356

357

358

359

360

361

362

363

364

365

366

367

368

369

370

371

372

373

374

375

376

377

378

379

380

381

382

383

384

385

386

387

388

389

390

391

392

393

394

395

396

397

398

399

400

401

402

403

404

405

406

407

408

409

410

411

412

413

414

415

416

417

418

419

420

421

422

423

424

425

426

427

428

429

430

431

432

433

434

435

436

437

438

439

440

441

442

443

444

445

446

447

448

449

450

451

452

453

454

455

456

457

458

459

460

461

462

463

464

465

466

467

468

469

470

471

472

473

474

475

476

477

478

479

480

481

482

483

484

485

486

487

488

489

490

491

492

493

494

495

496

497

498

499

500

501

502

503

504

505

506

507

508

509

510

511

512

513

514

515

516

517

518

519

520

521

522

523

524

525

526

527

528

529

530

531

532

533

534

535

536

537

538

539

540

541

542

543

544

545

546

547

548

549

550

551

552

553

554

555

556

557

558

559

560

561

562

563

564

565

566

567

568

569

570

571

572

573

574

575

576

577

578

579

580

581

582

583

584

585

586

587

588

589

590

591

592

593

594

595

596

597

598

599

600

601

602

603

604

605

606

607

608

609

610

611

612

613

614

615

616

617

618

619

620

621

622

623

624

625

626

627

628

629

630

631

632

633

634

635

636

637

638

639

640

641

642

643

644

645

646

647

648

649

650

651

652

653

654

655

656

657

658

659

660

661

662

663

664

665

666

667

668

669

670

671

672

673

674

675

676

677

678

679

680

681

682

683

684

685

686

687

688

689

690

691

692

693

694

695

696

697

698

699

700

701

702

703

704

705

706

707

708

709

710

711

712

713

714

715

716

717

718

719

720

721

722

723

724

725

726

727

728

729

730

731

732

733

734

735

736

737

738

739

740

741

742

743

744

745

746

747

748

749

750

751

752

753

754

755

756

757

758

759

760

761

762

763

764

765

766

767

768

769

770

771

772

773

774

775

776

777

778

779

780

781

782

783

784

785

786

787

788

789

790

791

792

793

794

795

796

797

798

799

800

801

802

803

804

805

806

807

808

809

810

811

812

813

814

815

816

817

818

819

820

821

822

823

824

825

826

827

828

829

830

831

832

833

834

835

836

837

838

839

840

841

842

843

844

845

846

847

848

849

850

851

852

853

854

855

856

857

858

859

860

861

862

863

864

865

866

867

868

869

870

871

872

873

874

875

876

877

878

879

880

881

882

883

884

885

886

887

888

889

890

891

892

893

894

895

896

897

898

899

900

901

902

903

904

905

906

907

908

909

910

911

912

913

914

915

916

917

918

919

920

921

922

923

924

925

926

927

928

929

930

931

932

933

934

935

936

937

938

939

940

941

942

943

944

945

946

947

948

949

950

951

952

953

954

955

956

957

958

959

960

961

962

963

964

965

966

967

968

969

970

971

972

973

974

975

976

977

978

979

980

981

982

983

984

985

986

987

988

989

990

991

992

993

994

995

996

997

998

999

1000

Figure 1.3.7 Pauling electronegativity values for the elements (Attribution: Ck12.org [https://www.ck12.org/flx/show/default/image/user%3Ack12editor/201411241416847232690011\\_ab8840393ea93a2a7c9fc01e395da3b2-201411241416847569430107.png](https://www.ck12.org/flx/show/default/image/user%3Ack12editor/201411241416847232690011_ab8840393ea93a2a7c9fc01e395da3b2-201411241416847569430107.png) <https://creativecommons.org/licenses/by-nc/3.0/legalcode>)

In the depicted periodic table (Figure 1.3.7) you can see the type of chemical bonding between atoms indicated by different colors. There is metallic bonding in metals, indicated by the color blue. In metallic bonds the electrons are shared between atoms but are delocalized over many atoms in the metal. The green color indicates covalent bonding seen in non-metals. In covalent bonding the electrons are shared, but localized in between typically two atoms. Metalloids have chemical bonding with a mix of covalent and metallic character shown in orange. There is electron-sharing with a moderate degree of delocalization. The Pauling electronegativity values of the elements are written underneath the element symbols.

Can we relate the electronegativity values to the chemical bonding in the elements? We can clearly see that elements with high electronegativity values significantly above 2.0, the non-metals, tend to make covalent bonds in between them. All metalloids with a hybrid covalent-metallic character, have intermediate electronegativity around 2.0. Most metals have low electronegativity values below 2.0 except noble metals like Pt and Au. Overall, we can say that there is a clear relationship between the bonding type in an element and its electronegativity. Now let us see if electronegativity can also predict chemical bonding in compounds.

### Ketelaar's Triangle

The ability of electronegativity to predict the bonding type in compounds can be understood by Ketelaar's triangle, named after J.A.A. Ketelaar.

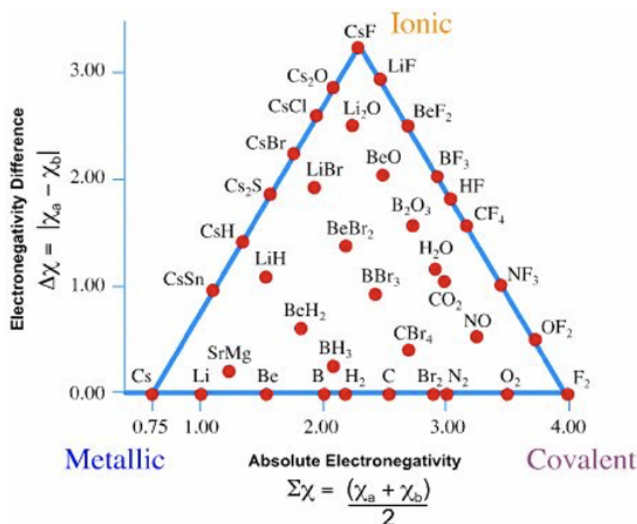


Figure 1.3.8 Ketelaar's Triangle (Attribution: Chemlibretexts <https://chem.libretexts.org/@api/dek...jpg?revision=2> <http://creativecommons.org/licenses/by-nc-sa/3.0/us/>)

You can see that Ketelaar's triangle has three corners (Figure 1.3.8). Two of the corners are occupied by the elements F and Cs, and the third corner is occupied by CsF. All elements are located on the horizontal edge of the triangle, and there many compound indicated by dots either on the two other edges or within the triangle. There are no compounds or elements outside of the triangle. How can we understand this triangle and what does it say about the relationship between bonding character and electronegativity? To understand this, look at the two axes. The horizontal x-axis represents the average electronegativity of the atoms in an element

or a compound. The vertical y-axis represents the electronegativity difference between the atoms in the elements or the compound. For elements the electronegativity difference between the atoms is zero, because in an element all atoms are of the same type. Therefore, all the elements lie on the horizontally oriented edge of the triangle. Because Cs is the element with the lowest electronegativity, it lies furthest to the left on this edge. Fluorine is the element with the highest electronegativity, and thus lies the furthest on the right side. The other elements are located in between the cesium and the fluorine on the edge. The higher the electronegativity of the elements, the further right their position on this edge of the triangle.

For compounds, the electronegativity difference between atoms is never exactly zero, therefore all compounds are located above the horizontal edge of the triangle. The compound with the highest electronegativity difference is the CsF. Its average electronegativity is the sum of the electronegativity of Cs and F divided by 2. Therefore, CsF defines the third corner of the triangle. All other compounds must lie on the edges or within the triangle. All cesium compounds are located on the edge between the Cs and CsF, and all the fluorine compounds are located on the edge between CsF and F<sub>2</sub>. The compounds of all other elements are inside the triangle. The position of the compound on or in the triangle defines its bonding character. The closer the position of the compound toward the Cs corner, the more metallic, the closer the position is to the F<sub>2</sub> corner, the more covalent, and the closer it is to the CsF corner, the more ionic. For example Li<sub>2</sub>O is located close to CsF, and the bonding would be predominantly ionic, although there is also a small degree of covalent and metallic bonding. In contrast to that, SrMg has mostly metallic bonding, a little bit of covalent bonding, and even less ionic bonding. The bonding situation in LiH is in between metallic and ionic, with a little bit of covalent bonding character mixed in. Note that a 100% ionic bond is not possible because the electronegativity difference is finite, and thus there must always be a certain degree of electron sharing. In contrast to that, a 100% covalent bond is possible because electrons can be equally shared between two atoms when the electronegativity difference is zero.

The take home message is that in compounds and elements there is usually a mix of bonding types, and not a single bonding type, even though one bonding type may strongly dominate. The concept of electronegativity, and Ketelaar's triangle in particular, is extremely helpful to predict to which degree the three bonding types are present in a substance.

---

Dr. Kai Landskron ([Lehigh University](#)). If you like this textbook, please consider to make a donation to support the author's research at Lehigh University: [Click Here to Donate](#).

---

This page titled [2.1.2: Electronegativity and the Bonding Continuum](#) is shared under a [CC BY 4.0](#) license and was authored, remixed, and/or curated by [Kai Landskron](#).

- [1.3: Periodic Properties of Atoms](#) by Kai Landskron is licensed [CC BY 4.0](#).

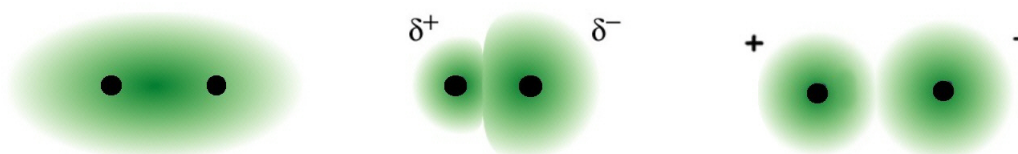
## 2.1.3: Polarizability and Percent Ionic Character

Having now revised the basics of trends across and down the Periodic Table, we can use the concepts of Effective Nuclear Charge and Electronegativity to discuss the factors that contribute to the types of bonds formed between elements.

### Fajans' Rules

Rules formulated by Kazimierz Fajans in 1923, can be used to predict whether a chemical bond is expected to be predominantly ionic or covalent, and depend on the relative charges and sizes of the cation and anion. *If two oppositely charged ions are brought together, the nature of the bond between them depends upon the effect of one ion on the other.*

non-polar covalent polar covalent ionic



Fajan's rules for predicting whether a bond is predominantly Covalent or Ionic

Covalent	Ionic
Small cation ( $< \sim 100$ pm)	Large cation ( $> \sim 100$ pm)
Large anion	Small anion
High charges	Low charges

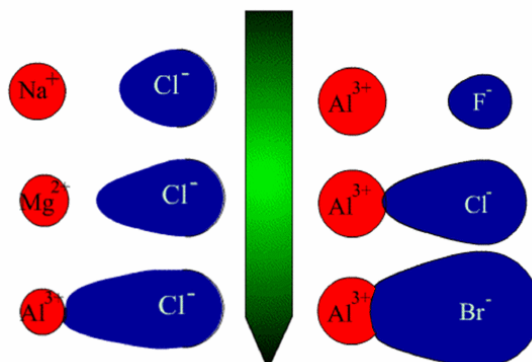
Although the bond in a compound like  $X^+Y^-$  may be considered to be 100% ionic, it will always have some degree of covalent character. When two oppositely charged ions ( $X^+$  and  $Y^-$ ) approach each other, the cation attracts electrons in the outermost shell of the anion but repels the positively charged nucleus. This results in a distortion, deformation or polarization of the anion. If the degree of polarization is quite small, an ionic bond is formed, while if the degree of polarization is large, a covalent bond results.

The ability of a cation to distort an anion is known as its polarization power and the tendency of the anion to become polarized by the cation is known as its polarizability. The polarizing power and polarizability that enhances the formation of covalent bonds is favoured by the following factors:

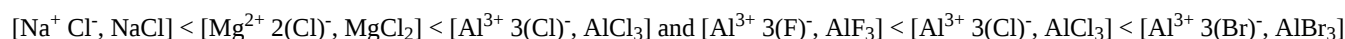
- Small cation: the high polarizing power stems from the greater concentration of positive charge on a small area. This explains why LiBr is more covalent than KBr ( $\text{Li}^+$  90 pm cf.  $\text{K}^+$  152 pm).
- Large anion: the high polarizability stems from the larger size where the outer electrons are more loosely held and can be more easily distorted by the cation. This explains why for the common halides, iodides, are the most covalent in nature ( $\text{I}^-$  206 pm).
- Large charges: as the charge on an ion increases, the electrostatic attractions of the cation for the outer electrons of the anion increases, resulting in the degree of covalent bond formation increasing.

Reminder. Large cations are to be found on the bottom left of the periodic table and small anions on the top right. The greater the positive charge, the smaller the cation becomes and the *ionic potential* is a measure of the charge to radius ratio.





The cation charge increases (size decreases) and on the right, the anion size increases, both variations leading to an increase in the covalency. Thus covalency increases in the order:



Electronic configuration of the cation: for two cations of the same size and charge, the one with a pseudo noble-gas configuration (with 18 electrons in the outer-most shell) will be more polarizing than that with a noble gas configuration (with 8 electrons in the outermost shell). Thus zinc (II) chloride (  $\text{Zn(II)} 1s^2 2s^2 2p^6 3s^2 3p^6 3d^{10}$  and  $\text{Cl}^- 1s^2 2s^2 2p^6 3s^2 3p^6$  ) is more covalent than magnesium chloride (  $\text{Mg(II)} 1s^2 2s^2 2p^6$  ) despite the  $\text{Zn}^{2+}$  ion (74 pm) and  $\text{Mg}^{2+}$  ion (72 pm) having similar sizes and charges.

From an MO perspective, the orbital overlap disperses the charge on each ion and so weakens the electrovalent forces throughout the solid, this can be used to explain the trend seen for the melting points of lithium halides.

$\text{LiF} = 870^\circ\text{C}$ ,  $\text{LiCl} = 613^\circ\text{C}$ ,  $\text{LiBr} = 547^\circ\text{C}$ ,  $\text{LiI} = 446^\circ\text{C}$

*It is found that the greater the possibility of polarization, the lower is the melting point and heat of sublimation and the greater is the solubility in non-polar solvents.*

#### ✓ Example 2.1.3.1:

The melting point of KCl is higher than that of AgCl though the crystal radii of  $\text{Ag}^+$  and  $\text{K}^+$  ions are almost the same.

Solution:

When the melting points of two compounds are compared, the one having the lower melting point is assumed to have the smaller degree of ionic character. In this case, both are chlorides, so the anion remains the same. The deciding factor must be the cation. (If the anions were different, then the answer could be affected by the variation of the anion.) Here the significant difference between the cations is in their electronic configurations.  $\text{K}^+ = [\text{Ar}]$  and  $\text{Ag}^+ = [\text{Kr}] 4d^{10}$ . This means a comparison needs to be made between a noble gas core and pseudo noble gas core, which as noted above holds that the pseudo noble gas would be the more polarizing.

#### Percentage of ionic character and charge distribution

Based on Fajan's rules, it is expected that every ionic compound will have at least some amount of covalent character. The percentage of ionic character in a compound can be estimated from dipole moments. The bond dipole moment uses the idea of electric dipole moment to measure the polarity of a chemical bond within a molecule. It occurs whenever there is a separation of positive and negative charges. The bond dipole  $\mu$  is given by:

$$\mu = \delta d$$

A bond dipole is modeled as  $+\delta - \delta^-$  with a distance  $d$  between the partial charges. It is a vector, parallel to the bond axis and by convention points from minus to plus (note that many texts appear to ignore the convention and point from plus to minus). The SI unit for an electric dipole moment is the coulomb-meter, (C m). This is thought to produce values too large to be practical on the molecular scale so bond dipole moments are commonly measured in Debye, represented by the symbol, D.

Historically the Debye was defined in terms of the dipole moment resulting from two equal charges of opposite sign and separated by 1 Ångstrom ( $10^{-10} \text{ m}$ ) as 4.801 D. This value arises from  $(1.602 \times 10^{-19} \times 1 \times 10^{-10}) / 3.336 \times 10^{-30}$  where  $D = 3.336 \times 10^{-30} \text{ C m}$

(or  $1 \text{ C m} = 2.9979 \times 10^{29} \text{ D}$ ).

Typical dipole moments for simple diatomic molecules are in the range of 0 to 11 D (see Table below).

The % ionic character =  $\mu_{\text{observed}} / \mu_{\text{calculated}}$  (assuming 100% ionic bond) \* 100 %

#### ✓ Example 2.1.3.12:

From the Table below the observed dipole moment of KBr is given as 10.41 D, ( $3.473 \times 10^{-29}$  coulomb metre), which being close to the upper level of 11 indicates that it is a highly polar molecule. The interatomic distance between  $\text{K}^+$  and  $\text{Br}^-$  is 282 pm. From this it is possible to calculate a theoretical dipole moment for the KBr molecule, assuming opposite charges of one fundamental unit located at each nucleus, and hence the percentage ionic character of KBr.

Solution

dipole moment  $\mu = q * e * d$  coulomb metre

$q = 1$  for complete separation of unit charge

$e = 1.602 \times 10^{-19} \text{ C}$

$d = 2.82 \times 10^{-10} \text{ m}$  for KBr (282 pm)

Hence calculated  $\mu_{\text{KBr}} = 1 * 1.602 \times 10^{-19} * 2.82 \times 10^{-10} = 4.518 \times 10^{-29} \text{ Cm}$  (13.54 D)

The observed  $\mu_{\text{KBr}} = 3.473 \times 10^{-29} \text{ Cm}$  (10.41 D)

the % ionic character of KBr =  $3.473 \times 10^{-29} / 4.518 \times 10^{-29}$  or  $10.41 / 13.54 = 76.87\%$  and the % covalent character is therefore about 23% (100 - 77).

Given the observed dipole moment is 10.41 D ( $3.473 \times 10^{-29}$ ) it is possible to estimate the charge distribution from the same equation by now solving for  $q$ :

Dipole moment  $\mu = q * e * d$  Coulomb meters, but since  $q$  is no longer 1 we can substitute in values for  $\mu$  and  $d$  to obtain an estimate for it.

$q = \mu / (e * d) = 3.473 \times 10^{-29} / (1.602 \times 10^{-19} * 2.82 \times 10^{-10})$

thus  $q = 3.473 \times 10^{-29} / (4.518 \times 10^{-29}) = 0.77$  and the  $\delta^-$  and  $\delta^+$  are -0.8 and +0.8 respectively.

#### ✓ Example 2.1.3.3:

For HI, calculate the % of ionic character given a bond length = 161 pm and an observed dipole moment 0.44 D.

Solution

To calculate  $\mu$  considering it as a 100% ionic bond

$\mu = 1 * 1.602 \times 10^{-19} * 1.61 \times 10^{-10} / (3.336 \times 10^{-30}) = 7.73 \text{ D}$

the % ionic character =  $0.44 / 7.73 * 100 = 5.7\%$

The calculated % ionic character is only 5.7% and the % covalent character is (100 - 5.7) = 94.3%. The ionic character arises from the polarizability and polarizing effects of H and I. Similarly, knowing the bond length and observed dipole moment of HCl, the % ionic character can be found to be 18%. Thus it can be seen that while HI is essentially covalent, HCl has significant ionic character.

Note that by this simplistic definition, to achieve 100 % covalent character a compound must have an observed dipole moment of zero. Whilst not strictly true for heteronuclear molecules it does provide a simple qualitative method for predicting the bond character.

## Contributors and Attributions

- [Template:Lancashire](#)



This page titled [2.1.3: Polarizability and Percent Ionic Character](#) is shared under a [CC BY-NC-SA 4.0](#) license and was authored, remixed, and/or curated by [Robert J. Lancashire](#).

- [Polarizability](#) by [Robert J. Lancashire](#) is licensed [CC BY-NC-SA 4.0](#).

## 2.2: Lewis Structures and Molecular Shape

---

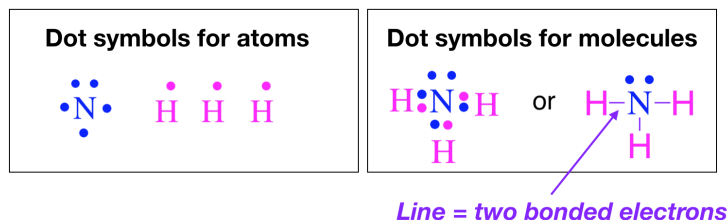
Learning objectives for this unit are to:

- Use Lewis structures in conjunction with formal charge and VSEPR to predict and draw 3-dimensional representations of molecules
  - Predict distortions from ideal geometry based on electronegativity and atom size
  - Draw reasonable equivalent and inequivalent resonance structures of molecules
  - Predict or explain experimental bond lengths and bond angles based on Lewis structures and resonance
- 

2.2: Lewis Structures and Molecular Shape is shared under a [not declared](#) license and was authored, remixed, and/or curated by LibreTexts.

## 2.2.1: Lewis Electron-Dot Diagrams

In 1916, Gilbert Lewis Newton introduced a simple way to show the bonding between atoms in a molecule through Lewis electron dot diagrams. Creating Lewis diagrams is rather simple and requires only a few steps and some accounting of the valence electrons on each atom. Valence electrons are represented as dots. When two electrons are paired (lone pairs), they are represented by two adjacent dots located on an atom, and when two paired electrons are shared between atoms (bonds), they are shown as lines. For example, below are the electron dot structures of atoms and the Lewis electron dot structures of the molecules. These diagrams are helpful because they allow us to show how atoms are connected, and when coupled with [Valence Shell Electron Repulsion Theory \(VSEPR\)](#), we can use Lewis structures to predict the shape of the molecule.



The drawing of Lewis electron-dot structures is guided largely by the **octet rule**: that atoms form bonds to achieve eight electrons in their valence shell. For many elements, a full valence shell has an electron configuration of  $s^2p^6$ , or eight electrons. A common exception to this rule is the first row elements, H and He. These two elements have  $n = 1$  as their valence shell, and so they have only two electrons in a full valence shell ( $1s^2$  electron configuration). Although H and He are exceptions to the "octet rule", they still form bonds to achieve a full valence shell. It may be better to think of this as the "full valence" rule of bonding. We will see many more violations to the "octet" rule as we progress through this course. In the case of metals and metalloids, breaking of the rules is particularly common. (CC-BY-NC-SA; Kathryn Haas)

### Common Violations of the Octet Rule

- **Less than eight electrons (hypovalency):** H and He are examples of elements that cannot have more than two electrons in their full valence shell. Additionally, there are cases where a valid Lewis structure contains atoms with **hypovalency**: *partially-filled valence shells*. This is common in atoms with few valence electrons, such as beryllium and boron
- **More than eight electrons (hypervalency):** This is a case where an element has more than eight electrons in its valence shell. It is common for larger atoms ( $n \geq 3$ ), and it is discussed further in [Section 3.3.3](#).

There are different rules for counting electrons depending on the purpose of the counting. These are the rules for counting for "octets". The rules for calculation of an atom's formal charge are **different** and are described in [Section 3.3.1](#). When an atom is part of a molecule, all electrons that are associated with the atom are counted as contributing to the atom's valence. This includes electrons that are lone pairs on the atoms, and *all* electrons that are shared in bonds. If four electrons are shared between two atoms, it is a double bond. If six electrons are shared between atoms, it is a triple bond.

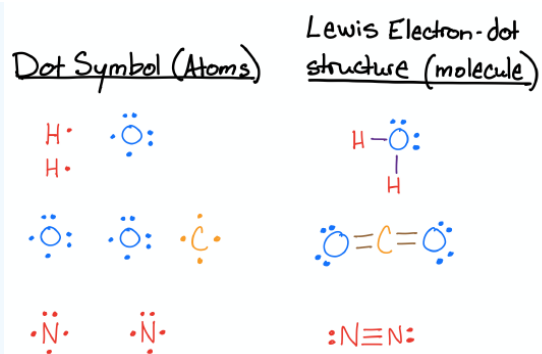
Electrons in valence (octet) = total unbonded electrons on the atom + total bonded electrons (2 electrons per bond)

Even if you're an old pro at drawing Lewis structures, it's a good idea to polish up. Please complete the practice exercises below. You should get out an actual piece of paper (I know...just do it. It's good for you.) and a writing tool and try to complete each problem before checking the answer.

### Exercise 2.2.1.1

Draw the Lewis structures for  $\text{H}_2\text{O}$ ,  $\text{CO}_2$ , and  $\text{N}_2$ .

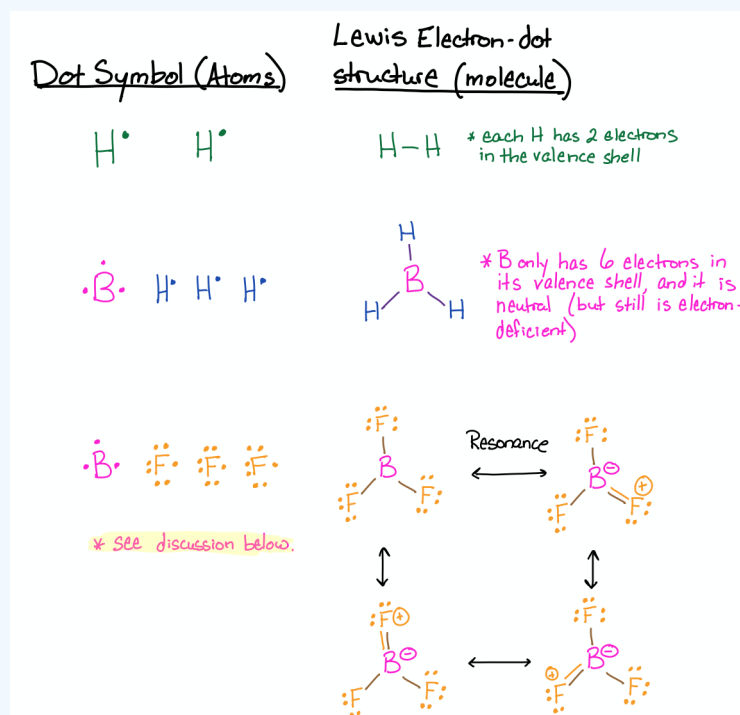
**Answer**



### Exercise 2.2.1.2

Draw the Lewis structures for  $\text{H}_2$ ,  $\text{BH}_3$  and  $\text{BF}_3$ .

Answer



These three examples include atoms that have less than eight electrons in their valence shell. In the case of H, it is satisfied with only two electrons in its valence, as was discussed earlier in this section. The case of  $\text{BH}_3$  was also discussed above. In the Lewis structure of  $\text{BH}_3$ , the boron can only have six electrons in its octet and it is neutral in charge. The boron is electron deficient even though it has neutral charge.

The case of  $\text{BF}_3$  deserves a discussion: If you are unfamiliar with resonance and formal charge, see Sections 3.3.1 (Formal Charge) and 3.3.2 (Resonance) first and come back to this afterward. You might have drawn the  $\text{BF}_3$  structure similar to the one that is drawn for  $\text{BH}_3$ , where boron has three bonds and only six electrons in its valence shell. If you did that, then you are correct; but if you only gave this structure, then your answer is not complete. There are three other correct ways to draw structure. Since F has lone pairs of electrons, other valid Lewis structures would each have a double bond to one of the fluorines (three total). All of these structures are called resonance structures, and based on the four of them, we could predict that  $\text{BF}_3$  would have B-F bonds that have some double-bond character. In fact, this is the case for  $\text{BF}_3$ ; it has bond lengths that are shorter than single bonds, but longer than double bonds. Read more about it on its [Wikipedia page here \(click\)](https://en.wikipedia.org/wiki/Boron_trifluoride).

## Outside Resources

- [en.Wikipedia.org/wiki/Lewis\\_structures](https://en.wikipedia.org/wiki/Lewis_structures)

## Contributors and Attributions

- Modified from [Lewis Structures](#) by Andrew Iskandar, University of California, Davis
- Curated or created by [Kathryn Haas](#)

---

This page titled [2.2.1: Lewis Electron-Dot Diagrams](#) is shared under a [CC BY-NC-SA 4.0](#) license and was authored, remixed, and/or curated by [Kathryn Haas](#).

- [3.1: Lewis Electron-Dot Diagrams](#) by [Kathryn Haas](#) is licensed [CC BY-NC 4.0](#).
- [3.3: Lewis Electron-Dot Diagrams](#) by [Kathryn Haas](#) is licensed [CC BY-NC-SA 4.0](#).

## 2.2.2: Formal Charge

The formal charge of an atom in a molecule is the *hypothetical* charge the atom would have if we could redistribute the electrons in the bonds evenly between the atoms. Another way of saying this is that formal charge results when we take the number of valence electrons of a neutral atom, subtract the nonbonding electrons, and then subtract the number of bonds connected to that atom in the Lewis structure.

### Calculating Formal Charges

We calculate the formal charge of an atom in a molecule or polyatomic ions as follows:

$$\text{Formal Charge} = (\text{valence electrons of the "free" element}) - (\text{unshared electrons}) - (\text{bonds}).$$

We can double-check formal charge calculations by determining the sum of the formal charges for the whole structure. The sum of the formal charges of all atoms in a molecule must be zero; the sum of the formal charges in an ion should equal the charge of the ion.

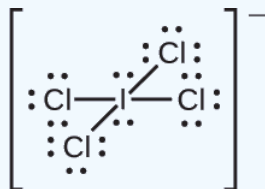
We must remember that the formal charge calculated for an atom is not the *actual* charge of the atom in the molecule. Formal charge is only a useful bookkeeping procedure; it does not indicate the presence of actual charges.

#### ✓ Calculating Formal Charge from Lewis Structures

Assign formal charges to each atom in the [interhalogen ion](#)  $\text{ICl}_4^-$ .

##### Solution

We divide the bonding electron pairs equally for all I–Cl bonds:



We assign lone pairs of electrons to their atoms. Each Cl atom now has seven electrons assigned to it, and the I atom has eight.

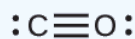
Subtract this number from the number of valence electrons for the neutral atom:

- I:  $7 - 8 = -1$
- Cl:  $7 - 7 = 0$

The sum of the formal charges of all the atoms equals  $-1$ , which is identical to the charge of the ion ( $-1$ ).

#### ? Exercise 2.2.2.1

Calculate the formal charge for each atom in the carbon monoxide molecule:



##### Answer

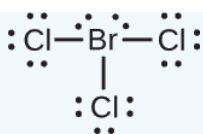
C  $-1$ , O  $+1$

#### ✓ Example: Calculating Formal Charge from Lewis Structures

Assign formal charges to each atom in the interhalogen molecule  $\text{BrCl}_3$ .

##### Solution

Assign one of the electrons in each Br–Cl bond to the Br atom and one to the Cl atom in that bond:



Assign the lone pairs to their atom. Now each Cl atom has seven electrons and the Br atom has seven electrons.

Subtract this number from the number of valence electrons for the neutral atom. This gives the formal charge:

- Br:  $7 - 7 = 0$
- Cl:  $7 - 7 = 0$

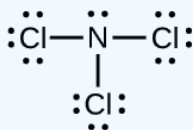
All atoms in  $\text{BrCl}_3$  have a formal charge of zero, and the sum of the formal charges totals zero, as it must in a neutral molecule.

### ? Exercise 2.2.2.2

Determine the formal charge for each atom in  $\text{NCl}_3$ .

**Answer**

N: 0; all three Cl atoms: 0



2.2.2: Formal Charge is shared under a [CC BY-NC-SA 4.0](https://creativecommons.org/licenses/by-nc-sa/4.0/) license and was authored, remixed, and/or curated by LibreTexts.

- 7.5: Formal Charges and Resonance by OpenStax is licensed [CC BY 4.0](https://creativecommons.org/licenses/by/4.0/). Original source: <https://openstax.org/details/books/chemistry-2e>.

## 2.2.3: Resonance

Resonance structures are a set of two or more Lewis Structures that collectively describe the electronic bonding a single polyatomic species including fractional bonds and fractional charges. Resonance structures are capable of describing delocalized electrons that cannot be expressed by a single Lewis formula with an integer number of covalent bonds.

### Sometimes One Lewis Structure Is Not Enough

Sometimes, even when **formal charges** are considered, the bonding in some molecules or ions cannot be described by a single Lewis structure. Resonance is a way of describing delocalized electrons within certain molecules or polyatomic ions where the bonding cannot be expressed by a single Lewis formula. A molecule or ion with such delocalized electrons is represented by several contributing structures (also called resonance structures or canonical forms). Such is the case for **ozone** ( $O_3$ ), an allotrope of oxygen with a V-shaped structure and an O–O–O angle of  $117.5^\circ$ .

#### Ozone ( $O_3$ )

1. We know that ozone has a V-shaped structure, so one O atom is central:



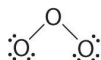
2. Each O atom has 6 valence electrons, for a total of 18 valence electrons.

3. Assigning one bonding pair of electrons to each oxygen–oxygen bond gives



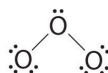
with 14 electrons left over.

4. If we place three lone pairs of electrons on each terminal oxygen, we obtain

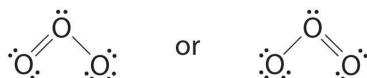


and have 2 electrons left over.

5. At this point, both terminal oxygen atoms have octets of electrons. We therefore place the last 2 electrons on the central atom:



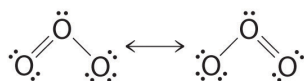
6. The central oxygen has only 6 electrons. We must convert one lone pair on a terminal oxygen atom to a bonding pair of electrons—but which one? Depending on which one we choose, we obtain either



Which is correct? In fact, neither is correct. Both predict one O–O single bond and one O=O double bond. As you will learn, if the bonds were of different types (one single and one double, for example), they would have different lengths. It turns out, however, that both O–O bond distances are identical, 127.2 pm, which is shorter than a typical O–O single bond (148 pm) and longer than the O=O double bond in  $O_2$  (120.7 pm).

Equivalent Lewis dot structures, such as those of ozone, are called **resonance structures**. The position of the *atoms* is the same in the various resonance structures of a compound, but the position of the *electrons* is different. Double-headed arrows link the different resonance structures of a compound:





The double-headed arrow indicates that the actual electronic structure is an *average* of those shown, not that the molecule oscillates between the two structures.

*When it is possible to write more than one equivalent resonance structure for a molecule or ion, the actual structure is the average of the resonance structures.*

### The Carbonate ( $\text{CO}_3^{2-}$ ) Ion

Like ozone, the electronic structure of the carbonate ion cannot be described by a single Lewis electron structure. Unlike  $\text{O}_3$ , though, the actual structure of  $\text{CO}_3^{2-}$  is an average of *three* resonance structures.

1. Because carbon is the least electronegative element, we place it in the central position:

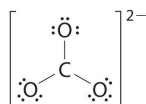


2. Carbon has 4 valence electrons, each oxygen has 6 valence electrons, and there are 2 more for the  $-2$  charge. This gives  $4 + (3 \times 6) + 2 = 24$  valence electrons.

3. Six electrons are used to form three bonding pairs between the oxygen atoms and the carbon:

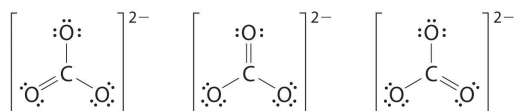


4. We divide the remaining 18 electrons equally among the three oxygen atoms by placing three lone pairs on each and indicating the  $-2$  charge:

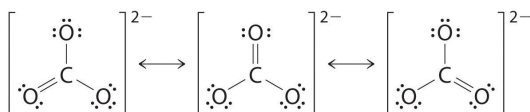


5. No electrons are left for the central atom.

6. At this point, the carbon atom has only 6 valence electrons, so we must take one lone pair from an oxygen and use it to form a carbon–oxygen double bond. In this case, however, there are *three* possible choices:



As with ozone, none of these structures describes the bonding exactly. Each predicts one carbon–oxygen double bond and two carbon–oxygen single bonds, but experimentally all C–O bond lengths are identical. We can write resonance structures (in this case, three of them) for the carbonate ion:

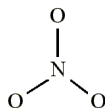


The actual structure is an average of these three resonance structures.

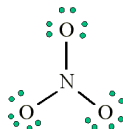
### The Nitrate ( $\text{NO}_3^-$ ) ion

1. Count up the valence electrons:  $(1 \times 5) + (3 \times 6) + 1(\text{ion}) = 24$  electrons

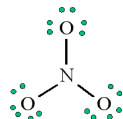
2. Draw the bond connectivities:



3. Add octet electrons to the atoms bonded to the center atom:

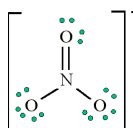


4. Place any leftover electrons (24-24 = 0) on the center atom:



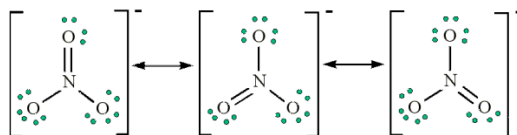
5. Does the central atom have an octet?

- **NO**, it has 6 electrons
- Add a multiple bond (first try a double bond) to see if the central atom can achieve an octet:



6. Does the central atom have an octet?

- YES
- Are there possible resonance structures? YES



Note: We would expect that the bond lengths in the  $\text{NO}_3^-$  ion to be somewhat shorter than a single bond.

### Warning

For second period elements you cannot exceed the octet, even if additional double or triple bonds would reduce the formal charges in the structure.

### Example 2.2.3.1: Benzene

Benzene is a common organic solvent that was previously used in gasoline; it is no longer used for this purpose, however, because it is now known to be a carcinogen. The benzene molecule ( $\text{C}_6\text{H}_6$ ) consists of a regular hexagon of carbon atoms, each of which is also bonded to a hydrogen atom. Use resonance structures to describe the bonding in benzene.

**Given:** molecular formula and molecular geometry

**Asked for:** resonance structures

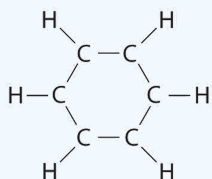
**Strategy:**

- Draw a structure for benzene illustrating the bonded atoms. Then calculate the number of valence electrons used in this drawing.

- B. Subtract this number from the total number of valence electrons in benzene and then locate the remaining electrons such that each atom in the structure reaches an octet.
- C. Draw the resonance structures for benzene.

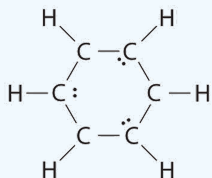
**Solution:**

A Each hydrogen atom contributes 1 valence electron, and each carbon atom contributes 4 valence electrons, for a total of  $(6 \times 1) + (6 \times 4) = 30$  valence electrons. If we place a single bonding electron pair between each pair of carbon atoms and between each carbon and a hydrogen atom, we obtain the following:



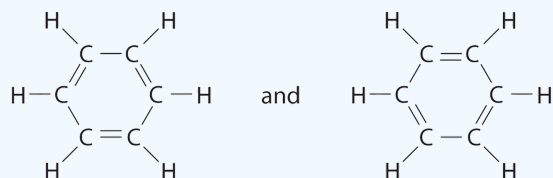
Each carbon atom in this structure has only 6 electrons and has a formal charge of +1, but we have used only 24 of the 30 valence electrons.

B If the 6 remaining electrons are uniformly distributed pairwise on alternate carbon atoms, we obtain the following:

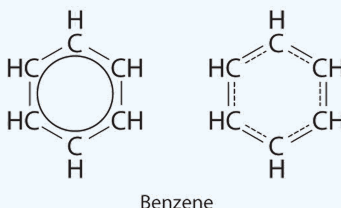


Three carbon atoms now have an octet configuration and a formal charge of -1, while three carbon atoms have only 6 electrons and a formal charge of +1. We can convert each lone pair to a bonding electron pair, which gives each atom an octet of electrons and a formal charge of 0, by making three C=C double bonds.

C There are, however, two ways to do this:



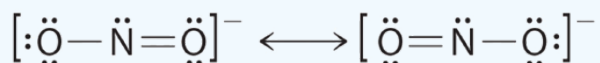
Each structure has alternating double and single bonds, but experimentation shows that each carbon-carbon bond in benzene is identical, with bond lengths (139.9 pm) intermediate between those typically found for a C-C single bond (154 pm) and a C=C double bond (134 pm). We can describe the bonding in benzene using the two resonance structures, but the actual electronic structure is an average of the two. The existence of multiple resonance structures for aromatic hydrocarbons like benzene is often indicated by drawing either a circle or dashed lines inside the hexagon:



**Exercise 2.2.3.1: Nitrate Ion**

The sodium salt of nitrite is used to relieve muscle spasms. Draw two resonance structures for the nitrite ion ( $\text{NO}_2^-$ ).

**Answer**



Resonance structures are particularly common in oxoanions of the *p*-block elements, such as sulfate and phosphate, and in aromatic hydrocarbons, such as benzene and naphthalene.

#### How do resonance structures represent the true structure?

If several reasonable resonance forms for a molecule exists, the "actual electronic structure" of the molecule will probably be intermediate between all the forms that you can draw. The classic example is benzene in Example 2.2.3.1. One would expect the double bonds to be shorter than the single bonds, but if one overlays the two structures, you see that one structure has a single bond where the other structure has a double bond. The best measurements that we can make of benzene do not show two bond lengths - instead, they show that the bond length is intermediate between the two resonance structures.

Resonance structures is a mechanism that allows us to use all of the possible resonance structures to try to predict what the actual form of the molecule would be. Single bonds, double bonds, triple bonds, +1 charges, -1 charges, these are our limitations in explaining the structures, and the true forms can be in between - a carbon-carbon bond could be mostly single bond with a little bit of double bond character and a partial negative charge, for example.

### Summary

Some molecules have two or more chemically equivalent Lewis electron structures, called resonance structures. Resonance is a mental exercise and method within the [Valence Bond Theory](#) of bonding that describes the delocalization of electrons within molecules. These structures are written with a **double-headed arrow** between them, indicating that none of the Lewis structures accurately describes the bonding but that the actual structure is an average of the individual resonance structures. Resonance structures are used when one Lewis structure for a single molecule cannot fully describe the bonding that takes place between neighboring atoms relative to the empirical data for the actual bond lengths between those atoms. The net sum of valid resonance structures is defined as a resonance hybrid, which represents the overall delocalization of electrons within the molecule. A molecule that has several resonance structures is more stable than one with fewer. Some resonance structures are more favorable than others.

2.2.3: Resonance is shared under a [CC BY-NC-SA 4.0](#) license and was authored, remixed, and/or curated by LibreTexts.

- [3.3B: Resonance](#) is licensed [CC BY-NC-SA 4.0](#).
- [8.6: Resonance Structures](#) is licensed [CC BY-NC-SA 3.0](#).

## 2.2.4: Expanded Octets

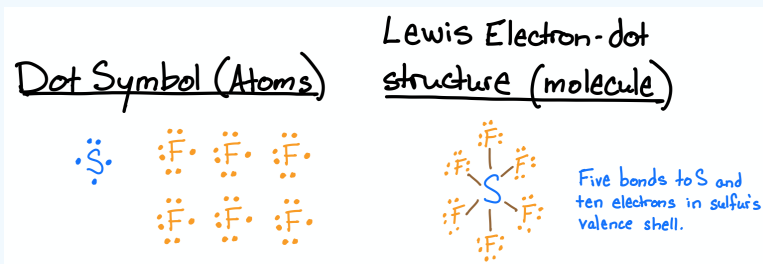
### Hypervalency

The octet rule applies well to atoms in the second row of the periodic table, where a full valence shell includes eight electrons with an electron configuration of  $s^2p^6$ . Even elements in the third and fourth row are known to follow this rule *sometimes*, but not always. In larger atoms, where  $n \geq 3$  the valence shell contains additional subshells: the  $d$ ,  $f$ ,  $g$ ... subshells. Therefore, atoms with  $n \geq 3$  can have higher valence shell counts by "expanding" into these additional subshells. When atoms contain more than eight electrons in their valence shell, they are said to be **hypervalent**. Hypervalency allows atoms with  $n \geq 3$  to break the octet rule by having more than eight electrons. This also means they can have five or more bonds; something that is nearly unheard of for atoms with  $n \leq 2$ . Complete the exercises below to see examples of molecules containing hypervalent atoms.

#### Exercise 2.2.4.1

Draw the Lewis structures for  $\text{SF}_6$ .

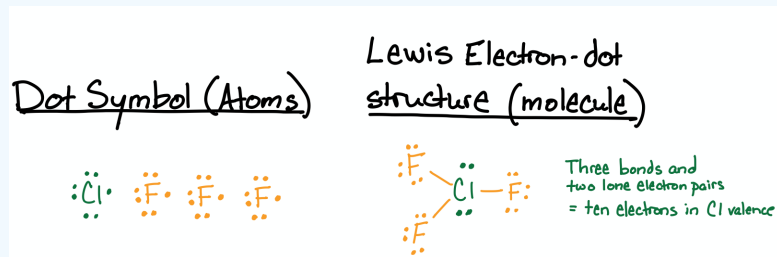
Answer



#### Exercise 2.2.4.2

Draw the Lewis structure for  $\text{ClF}_3$ .

Answer



Is hypervalency real? Not exactly. Hypervalency is a concept associated with hybrid orbital theory and Lewis theory. It's useful for some simple things, like predicting how atoms are connected and predicting molecular shape. But the idea that the  $d$ -orbitals are involved in bonding isn't accurate according to wave mechanics.

For main group molecules, chemists (like Pauling) thought a long time ago that hypervalence is due to expanded  $s^2p^6$  octets. The consensus is now clear that  $d$  orbitals are **NOT** involved in bonding in molecules like  $\text{SF}_6$  any more than they are in  $\text{SF}_4$  and  $\text{SF}_2$ . In all three cases, there is a small and roughly identical participation of  $d$ -orbitals in the wavefunctions. This has been established in both MO and VB theory. However using hybrid orbitals with  $d$ -orbital contributions equips us with a language which can pragmatically describe the geometries of highly coordinated substances.

While hybrid orbitals are a powerful tool to describe the geometries and shape of molecules and metal complexes. However, in "real" molecules, their significance may be debated. Often with a more realistically molecular orbitals approach is needed. However, from an epistemologically simple point of view, bonding theories can only be judged by their predictions. To the extent that hybridization can explain the shapes of  $\text{PF}_5$  and  $\text{SF}_6$ , valence bond theory is a perfectly good theory. To the extent that if you

write out the valence bond wavefunction using hybridized orbitals and calculate energies and other properties à la Pauling (i.e., ionization energy and electron affinities) and find them to be off from experimental results (by tens of kcal/mol), then valence bond theory is not accurate.

*Bonding theories can only be judged by their predictions.*

### An Alternate View of Expanded Octets

Another way to represent main group compounds with more than four bonds is to include ionic bonding character. This allows for compounds with more than 4 bonds to the central atom to not exceed their octets. For example, the Lewis structure of SF<sub>6</sub> can be redrawn with two ionic S-F bonds and four covalent S-F bonds as shown in Figure 2.2.4.1. In this picture the central S atom has six F atoms coordinated, but only shares four bonding pairs of electrons and has a complete (non-expanded) octet. Considering all the possible resonance structures for SF<sub>6</sub>, each S-F bond is  $\frac{2}{3}$  covalent and  $\frac{1}{3}$  ionic.

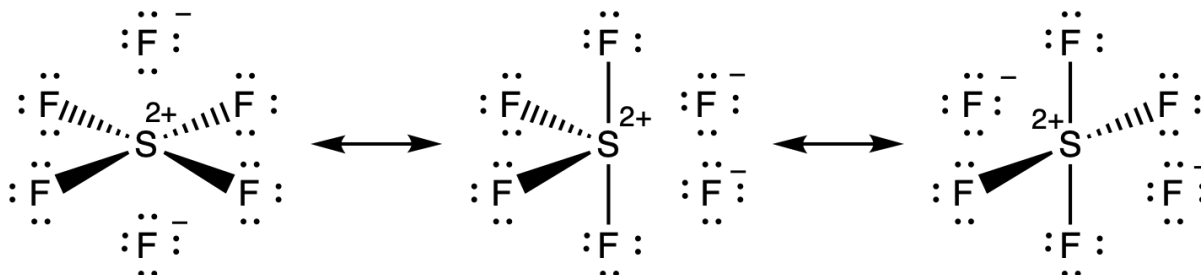


Figure 2.2.4.1: Three of the 15 possible resonance structures for sulfur hexafluorophosphate with four covalent and two ionic S-F bonds. (CC BY-NC-SA; Catherine McCusker)

### Additional Resources

- Gillespie, R. The Octet Rule and Hypervalence: Two Misunderstood Concepts. *Coord. Chem. Rev.* **2002**, 233–234, 53–62. [https://doi.org/10.1016/S0010-8545\(02\)00102-9](https://doi.org/10.1016/S0010-8545(02)00102-9).

### Contributors and Attributions

- Modified by Catherine McCusker, ETSU

This page titled 2.2.4: Expanded Octets is shared under a CC BY-NC-SA 4.0 license and was authored, remixed, and/or curated by Kathryn Haas.

- 3.3C: Expanded Octets by Kathryn Haas is licensed CC BY-NC-SA 4.0.
- 3.1.2: Breaking the octet rule with higher electron counts (hypervalent atoms) by Kathryn Haas is licensed CC BY-NC 4.0.

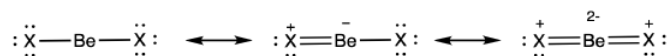
## 2.2.5: Limitation of Lewis Theory

Two notable cases where Lewis theory fails to predict structure is in the cases of beryllium (Be) and boron (B). These two atoms are in period 2 ( $n = 2$ ) of the periodic table and their atoms have the valence electron configurations of  $2s^2$  and  $2s^2 2p^1$ , respectively.

### Beryllium

#### Prediction based on Lewis structure:

The Lewis electron dot structures are shown below for  $\text{BeX}_2$ , where X is one of the halogens, F or Cl.



Each of the structures above would predict a linear geometry for the  $\text{BeX}_2$  molecule. Together the three resonance structures suggest partial double-bond character in the Be-X bond, which results in an intermediate bond length between a single and double bond.

There are issues with each of these resonance structures. The structure on the left would predict only four electrons around Be; thus, the atom does not fulfill the octet rule. The structure on the right suggests multiple bonds for the halogen (X) and high separation of charge with formal charge on each atom. The structure in the middle is a mix of these problems. None of these situations is ideal according to Lewis theory. Further, experimental data is not consistent with any of these structures or their resonance hybrid (except in the case of  $\text{BeCl}_2$  at very high temperatures).

It turns out that the monomer of  $\text{BeX}_2$  (shown above) does exist, but only at very high temperatures and low pressures. Even under extreme conditions, the monomer is not particularly stable due to the electron deficiency around Be.

### $\text{BeF}_2$

At ambient temperature and pressure,  $\text{BeF}_2$  is a solid that looks similar to quartz (Figure 2.2.5.1). The Be is four-coordinate with tetrahedral geometry; each F is two-coordinate and the Be-F bond length is 1.54 Å. This structure is possible due to an extended 3-dimensional network in the solid where adjacent  $\text{BeF}_2$  units are bonded to one another, as shown in Figure 2.2.5.1.

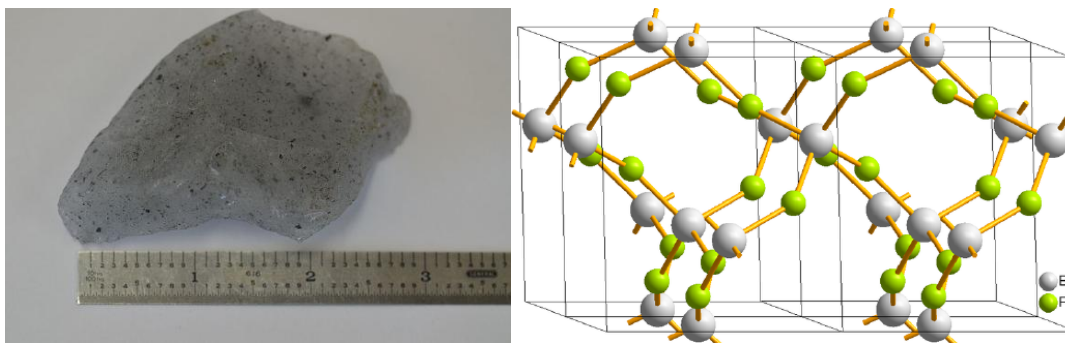


Figure 2.2.5.1: (left) A nugget of beryllium fluoride obtained from Materion. Black spots are carbon (CC BY-SA 3.0; Bckelleher via Wikipedia). (right)  $\text{BeF}_2$  structure (CC BY-SA 3.0 Unported; MaterialsScientist via Wikipedia)

In the liquid phase,  $\text{BeF}_2$  has a fluctuating tetrahedral structure where Be and F ions exchange. The vapor phase is reached at temperatures higher than 1000 °C (at ~ 1 atm). In the vapor phase,  $\text{BeF}_2$  exists as a monomer with linear geometry and a bond length of 1.43 Å, consistent with a double bond between Be and F.

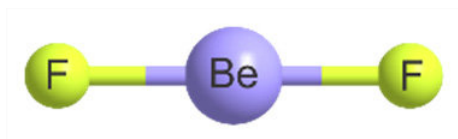


Figure 2.2.5.2: Geometries of  $\text{BeF}_2$ . (CC BY; Ibon Alkorta and Anthony C. Legoe via Inorganics)

## BeCl<sub>2</sub>

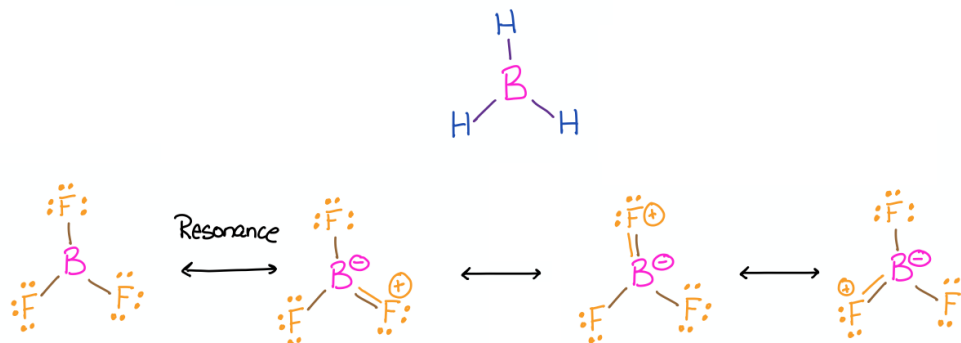
At ambient temperature and pressure, BeCl<sub>2</sub> is a solid. As in BeF<sub>2</sub> described above, BeCl<sub>2</sub> has four-coordinate, tetrahedral Be and two-coordinate F. In contrast to BeF<sub>2</sub>, solid BeCl<sub>2</sub> is a 1-dimensional polymer consisting of edge-shared tetrahedral.

In the gas phase, BeCl<sub>2</sub> exists as a dimer with two chlorine atoms bridging two Be atoms. In the dimer, the Be atoms are 3-coordinate. Bridging Cl atoms are two-coordinate, while terminal Cl atoms are one-coordinate. At higher temperatures in the vapor phase, the linear monomer also exists.

## Boron (2s<sup>2</sup>2p<sup>1</sup>)

Prediction based on Lewis structures:

Lewis structures of BH<sub>3</sub> and BF<sub>3</sub> were described in [Exercise 3.1.2](#), and are drawn again below for convenience.



**Figure 2.2.5.3:**  
Lewis structures of  $\text{BH}_3$  and  $\text{BF}_3$

## Boron trihalides (ex. BF<sub>3</sub>)

Boron trihalides, like BF<sub>3</sub>, have properties that are largely predicted by Lewis structures and VSEPR theory. The Lewis structure for BF<sub>3</sub> includes several resonance structures. The structure with only single bonds is the most common representation for this molecule because the charge separation shown in the other structures is considered to be unfavorable. The highly polarized B-F bond has a dipole moment that lies opposite of the indicated formal charges shown in the resonance structures with double bonds between boron and fluorine.

The resonance hybrid of BF<sub>3</sub> predicts partial double bond character between boron and fluorine, thus a bond length shorter than a single bond. Using the Lewis structures and VSEPR theory, we would predict a trigonal planar geometry around boron. In fact, the actual structure of BF<sub>3</sub> is a monomer with trigonal planar geometry and with bond length that is shorter than a single bond. The case is similar to structures of other boron trihalides as well.

Boron trihalides are electron deficient at the boron center and react readily with Lewis bases. In other words they are strong Lewis acids (electrophiles).

## Boron trihydride (BH<sub>3</sub> is really B<sub>2</sub>H<sub>6</sub>)

The properties of boron trihydride (BH<sub>3</sub>) are not predicted by the simple predictions made through Lewis structures and VSEPR. The monomer, BH<sub>3</sub>, is not stable, but when dissolved in the presence of a Lewis base, BH<sub>3</sub> can form a stable acid-base adduct. In its pure form, the compound actually exists as a dimeric gas with a molecular unit of B<sub>2</sub>H<sub>6</sub> (try drawing a valid Lewis structure for that!). Its unexpected structure includes two H's that bridge the two boron atoms in 3-center-2-electron bonds. You can read more about B<sub>2</sub>H<sub>6</sub> on the Wikipedia page for Diborane.

This page titled [2.2.5: Limitation of Lewis Theory](#) is shared under a [CC BY-NC-SA 4.0](#) license and was authored, remixed, and/or curated by [Kathryn Haas](#).

- [3.1.4: Lewis Fails to Predict Unusual Cases - Boron and Beryllium](#) by [Kathryn Haas](#) is licensed [CC BY-NC 4.0](#).



- [3.3D: Limitation of Lewis Theory](#) by [Kathryn Haas](#) is licensed [CC BY-NC-SA 4.0](#).

## 2.2.6: Valence Shell Electron-Pair Repulsion

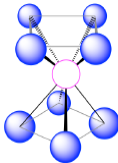
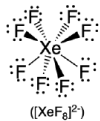
### Introduction to VSEPR

The **Valence Shell Electron Repulsion (VSEPR)** model can predict the structure of most molecules and polyatomic ions in which the central atom is a nonmetal; it also works for some structures in which the central atom is a metal. VSEPR builds on Lewis electron dot structures (discussed in [Section 3.1](#)); Lewis structures alone predict only connectivity while the Lewis structure and VSEPR together can predict the geometry of each atom in a molecule. The main idea of VSEPR theory is that pairs of electrons (in bonds and in lone pairs) repel each other. The pairs of electrons (in bonds and in lone pairs) are called "groups". Because electrons repel each other electrostatically, the most stable arrangement of electron groups (i.e., the one with the lowest energy) is the one that minimizes repulsion. Groups are positioned around the central atom in a way that produces the molecular structure with the lowest energy. In other words, the repulsion between groups around an atom favors a geometry in which the groups are as far apart from each other as possible. Although VSEPR is simplistic because it does not account for the subtleties of orbital interactions that influence molecular shapes, it accurately predicts the three-dimensional structures of a large number of compounds.

We can use the VSEPR model to predict the geometry around the atoms in a polyatomic molecule or ion by focusing on the number of electron pairs (groups) around a *central atom* of interest. Groups include bonded and unbonded electrons; a single bond, a double bond, a triple bond, a lone pair of electrons, or even a single unpaired electron each count as one group. The molecule or polyatomic ion is given an  $AX_mE_n$  designation, where **A** is the central atom, **X** is a bonded atom, **E** is a nonbonding valence electron group (usually a lone pair of electrons), and  $m$  and  $n$  are integers. The number of groups is equal to the sum of  $m$  and  $n$ . Using this information, we can describe the molecular geometry around a central atom, that is, the arrangement of the *bonded atoms* in a molecule or polyatomic ion. The geometries that are predicted from VSEPR when a central atom has only bonded groups ( $n = 0$ ) are listed below in Table 2.2.6.1. The cases where lone pairs contribute to the total groups ( $n \geq 1$ ) are discussed in the [next section about lone pair repulsion](#).

Table 2.2.6.1. Geometries predicted using VSEPR theory (bonded groups only).

Groups around central atom ( $m + n$ )	Geometry Name	Geometry Sketch	Predicted bond Angle	Example
2	linear		180°	$\text{:O=C=O:}$ (CO <sub>2</sub> )
3	trigonal plane		120°	$\begin{array}{c} \text{:Cl:} \\   \\ \text{:Cl-B-Cl:} \\   \\ \text{:Cl:} \end{array}$ (BCl <sub>3</sub> )
4	tetrahedron		109.5°	$\begin{array}{c} \text{H} \\   \\ \text{H-C-H} \\   \\ \text{H} \end{array}$ (CH <sub>4</sub> )
5	trigonal bipyramid		90° and 120°	$\begin{array}{c} \text{:F:} \\   \\ \text{:F-P-F:} \\   \\ \text{:F:} \end{array}$ (PF <sub>5</sub> )
6	octahedron		90°	$\begin{array}{c} \text{:F:} \\   \\ \text{:F-S-F:} \\   \\ \text{:F:} \end{array}$ (SF <sub>6</sub> )
7	pentagonal bipyramid		90° and 72°	$\begin{array}{c} \text{:F:} \\   \\ \text{:F-Zr-F:} \\   \\ \text{:F:} \end{array}$ ([ZrF <sub>7</sub> ] <sup>3-</sup> )

Groups around central atom ( $m + n$ )	Geometry Name	Geometry Sketch	Predicted bond Angle	Example
8	square antiprism		70.5°, 99.6° and 109.5°	 (XeF <sub>8</sub> ) <sup>2-</sup>

## Practice

### 📌 VSEPR to predict Molecular Geometry

You can follow these four steps to predict the geometry around an atom using VSEPR:

1. Draw the Lewis electron structure of the molecule or polyatomic ion.
2. For the central atom of interest, assign the AX<sub>m</sub>E<sub>n</sub> designation and the total number of groups ( $m+n$ ).
3. Determine the electron group arrangement around the central atom that minimizes repulsions.
4. Describe the molecular geometry.

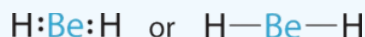
Use the procedure above to complete the exercises below

### ? Exercise 2.2.6.1

Predict the geometry around the central atom in BeH<sub>2</sub> and CO<sub>2</sub>.

#### Answer BeH<sub>2</sub>

1. The central atom, beryllium, contributes two valence electrons, and each hydrogen atom contributes one. The Lewis electron structure is

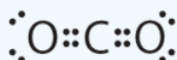


#### Lewis structure

2. There are two groups around the central atom, and both groups are single bonds. Thus BeH<sub>2</sub> is designated as AX<sub>2</sub>.
3. We see from Table 2.2.6.1 that the arrangement that minimizes repulsions places the groups 180° apart.
4. From Table 2.2.6.1 we see that with two bonding pairs, the molecular geometry that minimizes repulsions in BeH<sub>2</sub> is *linear*.

#### Answer CO<sub>2</sub>

1. The central atom, carbon, contributes four valence electrons, and each oxygen atom contributes six. The Lewis electron structure is



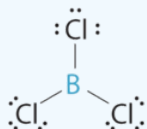
2. The carbon atom forms two double bonds. Each double bond is counted as one group, so there are two groups around the central atom. Once again, both groups around the central atom are bonds, so CO<sub>2</sub> is designated as AX<sub>2</sub>.
3. Like BeH<sub>2</sub>, the arrangement that minimizes repulsions places the groups 180° apart.
4. VSEPR only recognizes groups around the *central* atom (the carbon). Thus the lone pairs on the oxygen atoms do not influence the molecular geometry. With two bonded groups on the central atom and no lone pairs, the molecular geometry of CO<sub>2</sub> is linear (Table 2.2.6.1). The structure of CO<sub>2</sub> is shown in Table 2.2.6.1

### ? Exercise 2.2.6.2

Predict the geometry around the central atom in  $\text{BCl}_3$  and  $\text{CO}_3^{2-}$ .

Answer  $\text{BCl}_3$

1. The central atom, boron, contributes three valence electrons, and each chlorine atom contributes seven valence electrons. The Lewis electron structure is

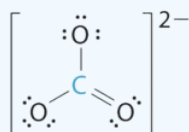


Lewis structure

2. There are three groups around the central atom and all are single bonds. The structure is designated as  $\text{AX}_3$ .
3. To minimize repulsions, the groups are placed  $120^\circ$  apart (Table 2.2.6.1).
4. From Table 2.2.6.1 we see that with three bonding pairs around the central atom, the molecular geometry of  $\text{BCl}_3$  is trigonal planar.

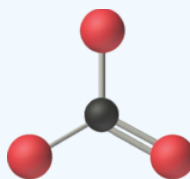
Answer  $\text{CO}_3^{2-}$

1. The central atom, carbon, has four valence electrons, and each oxygen atom has six valence electrons. The Lewis electron structure of one of three resonance forms is represented as



Lewis structure

2. The structure of  $\text{CO}_3^{2-}$  is a resonance hybrid. It has three identical bonds, each with a bond order of  $1\frac{1}{3}$ . All electron groups are bonds. With three bonding groups around the central atom, the structure is designated as  $\text{AX}_3$ .
3. We minimize repulsions by placing the three groups  $120^\circ$  apart (Table 2.2.6.1).
4. We see from Table 2.2.6.1 that the molecular geometry of  $\text{CO}_3^{2-}$  is trigonal planar with bond angles of  $120^\circ$ .



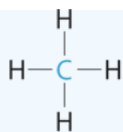
Molecular geometry  
(trigonal planar)

### ? Exercise 2.2.6.3

Predict the geometry around the central atom in  $\text{CH}_4$ ,  $\text{PCl}_5$  and  $\text{SF}_6$ .

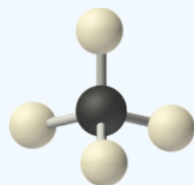
Answer  $\text{CH}_4$

1. The central atom, carbon, contributes four valence electrons, and each hydrogen atom has one valence electron, so the full Lewis electron structure is



#### Lewis structure

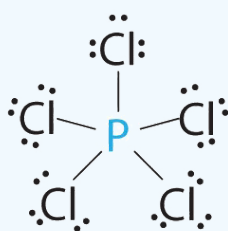
2. There are four electron groups around the central atom. All electron groups are bonding pairs, so the structure is designated as  $\text{AX}_4$ .
3. As shown in Table 2.2.6.1 repulsions are minimized by placing the groups in the corners of a tetrahedron with bond angles of  $109.5^\circ$ .
4. With four bonding pairs, the molecular geometry of methane is *tetrahedral* (Table 2.2.6.1).



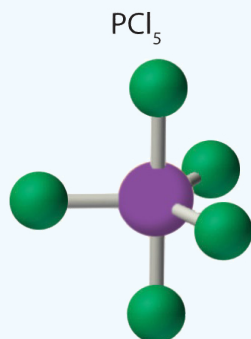
Molecular geometry  
(tetrahedral)

#### Answer $\text{PCl}_5$

1. Phosphorus has five valence electrons and each chlorine has seven valence electrons, so the Lewis electron structure of  $\text{PCl}_5$  is

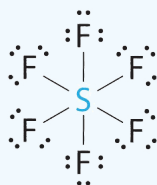


2. There are five bonding groups around phosphorus, the central atom. All electron groups are bonds, so the structure is designated as  $\text{AX}_5$ .
3. The structure that minimizes repulsions is a *trigonal bipyramid*, which consists of two trigonal pyramids that share a base (Table 2.2.6.1).
4. The molecular geometry of  $\text{PCl}_5$  is *trigonal bipyramidal*, as shown below. The molecule has three atoms in a plane in *equatorial* positions and two atoms above and below the plane in *axial* positions. The three equatorial positions are separated by  $120^\circ$  from one another, and the two axial positions are at  $90^\circ$  to the equatorial plane. The axial and equatorial positions are not chemically equivalent.



#### Answer $\text{SF}_6$

1. The central atom, sulfur, contributes six valence electrons, and each fluorine atom has seven valence electrons, so the Lewis electron structure is



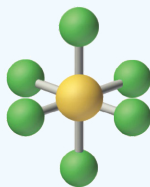
### Lewis structure

With an expanded valence, this species is an exception to the octet rule.

2. There are six electron groups around the central atom, each a bonding pair. We see from Figure 2.2.6.2 that the geometry that minimizes repulsions is *octahedral*.

3. With only bonding pairs,  $\text{SF}_6$  is designated as  $\text{AX}_6$ . All positions are chemically equivalent, so all electronic interactions are equivalent.

4. There are six nuclei, so the molecular geometry of  $\text{SF}_6$  is octahedral.



Molecular geometry  
(octahedral)

This page titled [2.2.6: Valence Shell Electron-Pair Repulsion](#) is shared under a [CC BY-NC-SA 4.0](#) license and was authored, remixed, and/or curated by [Kathryn Haas](#).

- [3.2: Valence Shell Electron-Pair Repulsion](#) by [Kathryn Haas](#) is licensed [CC BY-NC-SA 4.0](#).

## 2.2.7: Lone Pair Repulsion

In the [previous section](#), we saw how to use VSEPR to predict the geometry around a central atom based on the number of groups attached to a central atom. However, our previous discussion was limited to the simple cases where all of the groups were bonded groups (i.e., in the designation  $AX_mE_n$ ,  $n=0$ ). When all of the groups are bonds, the geometries can be predicted using information in [Table 3.2.1 in the previous section](#). Now we will consider cases where one or more of these groups are lone pairs.

### Lone pairs have stronger repulsive forces than bonded groups.

When one or more of the groups is a lone pair of electrons (non-bonded electrons), the experimentally-observed geometry around an atom is slightly different than in the case where all groups are bonds. The actual bond angles are similar, but not exactly the same, as those predicted based on the *total number of groups* (the "parent" geometry). When there is a mixture of group types (**lone pairs (E)** and **bonded groups (X)**) there are three different types of angles to consider: bond angles between two bonded atoms (**X-X** angles), angles between a bonded atom and a lone pair (**X-E** angles), and angles between two lone pairs (**E-E** angles). Empirical evidence shows the following trend in the degree of bond angles around atoms with a mixture of group types:

*Trend in bond angles:*



Using empirical evidence as a guide, we can predict that lone pairs repel other electron groups more strongly than bonded pairs. The molecular geometry of molecules with lone pairs of electrons is better predicted when we consider that electronic repulsion created by lone pairs is stronger than the repulsion from bonded groups. It is difficult to predict the exact bond angle based on this principle, but we can predict approximate angles, as described and summarized below in Table 2.2.7.1.

Table 2.2.7.1: Predictions of molecular geometry and bond angles around atoms with a mixture of bonded (X) and unbonded (E) electron groups.

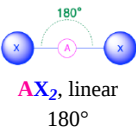
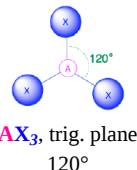
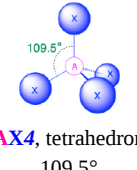
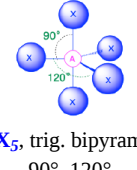
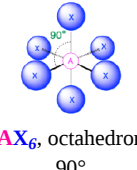
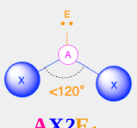
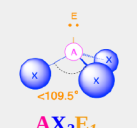
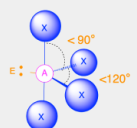
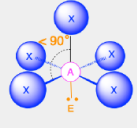
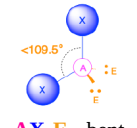
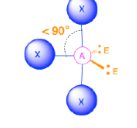
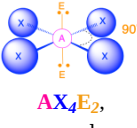
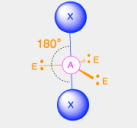
Electron Groups ( $m + n$ )					
	2 (steric number = 2)	3 (steric number = 3)	4 (steric number = 4)	5 (steric number = 5)	6 (steric number = 6)
... Parent Geometry (0 lone pairs) $AX_m$	 $AX_2$ , linear 180°	 $AX_3$ , trig. plane 120°	 $AX_4$ , tetrahedron 109.5°	 $AX_5$ , trig. bipyramid 90°, 120°	 $AX_6$ , octahedron 90°
... 1 lone pair $AX_mE_1$		 $AX_2E_1$ , bent <120°	 $AX_3E_1$ , trig. pyramid <109.5°	 $AX_4E_1$ , see-saw <90°, <120°	 $AX_5E_1$ , square pyramid 90°, <90°
... 2 lone pairs $AX_mE_2$			 $AX_2E_2$ , bent <109.5°	 $AX_3E_2$ , T-shape <90°	 $AX_4E_2$ , square plane 90°
... 3 lone pairs $AX_mE_3$				 $AX_2E_3$ , linear 180°	

Table 2.2.7.1 summarizes the geometries and bond angles predicted for nearest-neighbor bonded groups on central atoms with a mixture of lone pairs and bonded groups. The table does not cover all possible situations; it only includes cases where there are two bonded groups in which an X-X angle is measurable between nearest-neighbors. A more detailed description of some selected cases is given below.

### Two Electron Groups ( $m + n = 2$ )

(Steric number = 2) In the case that there are only two electron groups around a central atom, those groups will lie  $180^\circ$  from one another. This results in a linear molecular geometry with  $180^\circ$  bond angles.

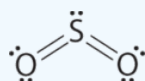
### Three Electron Groups ( $m + n = 3$ )

(Steric number = 3) In the case that there are three electron groups around a central atom, those groups will lie approximately  $120^\circ$  from one another in space. This results in an electronic geometry that is approximately **trigonal planar**. There are two different molecular geometries that are possible in this category:

- When all of the electron groups are bonds ( $m = 3$  or  $AX_3$ ), the molecular geometry is a **trigonal plane** with  **$120^\circ$**  bond angles.
- When there is one lone pair ( $m=2, n=1$  or  $AX_2E_1$ ), the molecular geometry is **bent** with a bond angle that is slightly **less than  $120^\circ$** .

#### ✓ $AX_2E$ Molecules: Example $SO_2$

1. The central atom, sulfur, has 6 valence electrons, as does each oxygen atom. With 18 valence electrons, the Lewis electron structure is shown below.



2. There are three electron groups around the central atom: two double bonds and one lone pair. We initially place the groups in a trigonal planar arrangement to minimize repulsions (Table 2.2.7.1).

3. With two bonding pairs and one lone pair, the structure is designated as  $AX_2E$ . This designation has a total of three electron pairs, two X and one E. The lone pair occupies more space around the central atom than a bonding pair (even double bonds!). Bonding pairs and lone pairs repel each other electrostatically in the order  $BP-BP < LP-BP < LP-LP$ . In  $SO_2$ , we have one  $BP-BP$  interaction and two  $LP-BP$  interactions.

4. The molecular geometry is described only by the positions of the nuclei, *not* by the positions of the lone pairs. Thus, with two nuclei and one lone pair the shape is **bent**, or *V shaped*, which can be viewed as a trigonal planar arrangement with a missing vertex. The O-S-O bond angle is expected to be less than  $120^\circ$  because of the extra space taken up by the lone pair.

### Four Electron Groups ( $m + n = 4$ )

(Steric number = 4) In the case that there are four electron groups around a central atom, those groups will lie approximately  $109.5^\circ$  from one another in space. This results in an electronic geometry that is approximately **tetrahedral**. There are three different molecular geometries that are possible in this category:

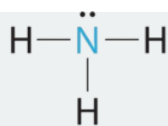
- When all electron groups are bonds ( $m=4$  or  $AX_4$ ), the molecular geometry is a **tetrahedron** with bond angles of  **$109.5^\circ$** .
- When there is one lone pair ( $m=3, n=1$  or  $AX_3E_1$ ), the molecular geometry is a **trigonal pyramid** with bond angles of **slightly less than  $109.5^\circ$** .
- When there are two lone pairs ( $m=2, n=2$  or  $AX_2E_2$ ), the molecular geometry is **bent** with bond angles of **slightly less than  $109.5^\circ$** .

#### ✚ $AX_3E$ Molecules: Example $NH_3$

One of the limitations of Lewis structures is that they depict molecules and ions in only two dimensions. With four electron groups, we must learn to show molecules and ions in three dimensions.

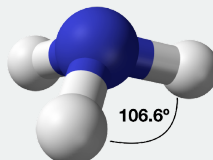
1. In ammonia, the central atom, nitrogen, has five valence electrons and each hydrogen donates one valence electron, producing the Lewis electron structure





### Lewis structure

2. There are four electron groups around nitrogen, three bonding pairs and one lone pair. Repulsions are minimized by directing each hydrogen atom and the lone pair to the corners of a tetrahedron.
3. With three bonding pairs and one lone pair, the structure is designated as  $\text{AX}_3\text{E}$ . This designation has a total of four electron pairs, three X and one E. We expect the LP–BP interactions to cause the bonding pair angles to deviate significantly from the angles of a perfect tetrahedron.



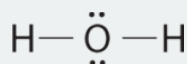
#### *The Difference in the Space Occupied by a Lone Pair of Electrons and by a Bonding Pair*

As with  $\text{SO}_2$ , this composite model of electron distribution and negative electrostatic potential in ammonia shows that a lone pair of electrons occupies a larger region of space around the nitrogen atom than does a bonding pair of electrons that is shared with a hydrogen atom.

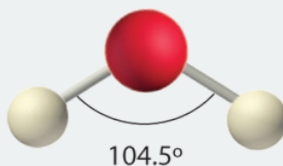
4. There are three nuclei and one lone pair, so the molecular geometry is *trigonal pyramidal*. In essence, this is a tetrahedron with a vertex missing. However, the H–N–H bond angles are less than the ideal angle of  $109.5^\circ$  because of LP–BP repulsion. The bond angles in ammonia are  $106.6^\circ$ .

### $\text{AX}_2\text{E}_2$ Molecules: Example $\text{H}_2\text{O}$

1. Oxygen has six valence electrons and each hydrogen has one valence electron, producing the Lewis electron structure



2. There are four groups around the central oxygen atom, two bonding pairs and two lone pairs. Repulsions are minimized by directing the bonding pairs and the lone pairs to the corners of a tetrahedron.
3. With two bonding pairs and two lone pairs, the structure is designated as  $\text{AX}_2\text{E}_2$  with a total of four electron pairs. Due to LP–LP, LP–BP, and BP–BP interactions, we expect a significant deviation from idealized tetrahedral angles.
4. With two hydrogen atoms and two lone pairs of electrons, the structure has significant lone pair interactions. There are two nuclei about the central atom, so the molecular shape is *bent*, or *V shaped*, with an H–O–H angle that is even less than the H–N–H angles in  $\text{NH}_3$ , as we would expect because of the presence of two lone pairs of electrons on the central atom rather than one. This molecular shape is essentially a tetrahedron with two missing vertices.



### Five Electron Groups ( $m + n = 5$ )

(Ste  
ric  
nu  
mb  
er =

5)  
In  
the  
cas  
e  
tha  
t  
ther  
e  
are  
five  
elec  
tron  
gro  
ups  
aro  
und

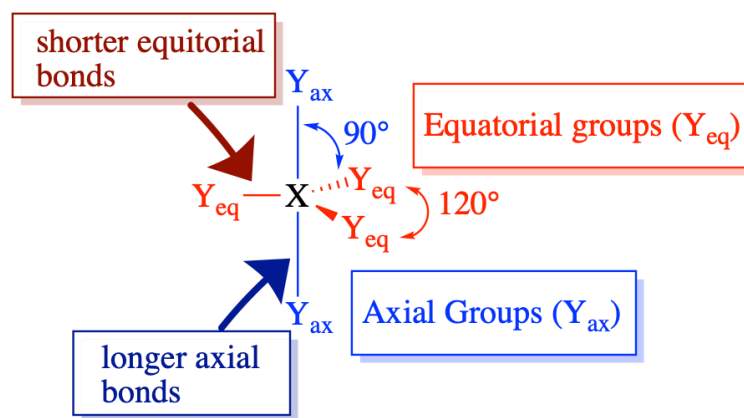


Figure: Trigonal pyramidal molecules (steric number 5) possess different bond angles and lengths for axial (ax) and equatorial (eq) pendant atoms. (CC-BY-NC-SA; Kathryn Haas).

a central atom, there are two different types of positions around the central atom: equatorial positions and axial positions. The three equatorial ligands are 120° from one another and are 90° from each of the two axial ligands. The axial positions have three adjacent groups oriented 90° away in space. Axial groups are thus more crowded than the equatorial positions with only two adjacent groups at 90°. The crowding of axial positions results in slight differences in bond distances; crowded axial groups have longer bonds than the less crowded equatorial groups. Lone pairs of electrons generally prefer to occupy equatorial positions rather than axial positions. The justification for this preference, according to VSEPR theory, is that the lone electron pairs are more repulsive than bonding electron pairs, and thus the lone pairs prefer the less crowded equatorial positions.

The arrangement of five groups around a central atom results in a **trigonal bipyramidal** electronic geometry. There are four different molecular geometries that are possible in this category, depending upon the number of bonded groups and lone pairs of electrons:

- When all electron groups are bonds ( $m=5$  or  $AX_5$ ), the molecular geometry is a **trigonal bipyramid** with bond angles of **120°** and **90°** between adjacent ligands.
- When there is one lone pair ( $m=4$ ,  $n=1$  or  $AX_4E_1$ ), the lone pair occupies one of the equatorial positions. The molecular geometry is called a **see saw** with bond angles of **slightly less than 120°** and **slightly less than 90°**.
- When there are two lone pairs ( $m=3$ ,  $n=2$  or  $AX_3E_2$ ), each lone pair occupies one of the three equatorial positions. The molecular geometry is **T-shaped** with bond angles of **slightly less than 120°** and **slightly less than 90°**.
- When there are three lone pairs ( $m=1$ ,  $n=3$  or  $AX_1E_3$ ), the lone pairs occupy the three equatorial positions. The molecular geometry is **linear** with bond angles of **180°**.

#### AX<sub>4</sub>E Molecules: SF<sub>4</sub>

1. The sulfur atom has six valence electrons and each fluorine has seven valence electrons, so the Lewis electron structure is



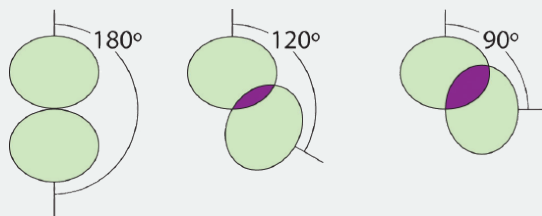
#### Lewis structure

With an expanded valence, this species is an exception to the octet rule.

2. There are five groups around sulfur, four bonding pairs and one lone pair. With five electron groups, the lowest energy arrangement is a trigonal bipyramid.

3. We designate SF<sub>4</sub> as AX<sub>4</sub>E; it has a total of five electron pairs. However, because the axial and equatorial positions are not chemically equivalent, where do we place the lone pair? If we place the lone pair in the axial position, we have three LP–BP repulsions at 90°. If we place it in the equatorial position, we have two 90° LP–BP repulsions at 90°. With fewer 90° LP–BP repulsions, we can predict that the structure with the lone pair of electrons in the *equatorial position* is *more stable than the one*

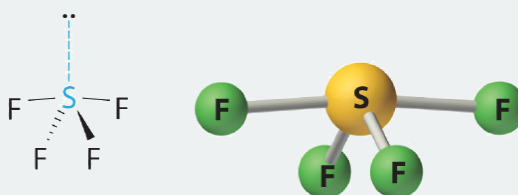
with the lone pair in the axial position. We also expect a deviation from ideal geometry because a lone pair of electrons occupies more space than a bonding pair.



*Illustration of the Area Shared by Two Electron Pairs versus the Angle between Them*

At  $90^\circ$ , the two electron pairs share a relatively large region of space, which leads to strong repulsive electron–electron interactions.

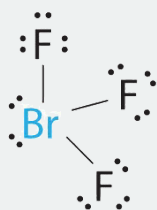
4. With four nuclei and one lone pair of electrons, the molecular structure is based on a trigonal bipyramid with a missing equatorial vertex; it is described as a *seesaw*. The  $F_{\text{axial}}\text{--S--}F_{\text{axial}}$  angle is  $173^\circ$  rather than  $180^\circ$  because of the lone pair of electrons in the equatorial plane.



**Molecular geometry (seesaw)**

### $AX_3E_2$ Molecules: $\text{BrF}_3$

1. The bromine atom has seven valence electrons, and each fluorine has seven valence electrons, so the Lewis electron structure is

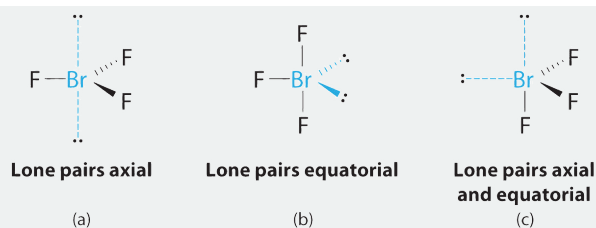


### **Lewis structure**

Once again, we have a compound that is an exception to the octet rule.

2. There are five groups around the central atom, three bonding pairs and two lone pairs. We again direct the groups toward the vertices of a trigonal bipyramid.

3. With three bonding pairs and two lone pairs, the structural designation is  $AX_3E_2$  with a total of five electron pairs. Because the axial and equatorial positions are not equivalent, we must decide how to arrange the groups to minimize repulsions. If we place both lone pairs in the axial positions, we have six LP–BP repulsions at  $90^\circ$ . If both are in the equatorial positions, we have four LP–BP repulsions at  $90^\circ$ . If one lone pair is axial and the other equatorial, we have one LP–LP repulsion at  $90^\circ$  and three LP–BP repulsions at  $90^\circ$ :



#### Interactions

90° LP-LP	0	0	1
90° LP-BP	6	4	3

Structure (c) can be eliminated because it has a LP-LP interaction at 90°. Structure (b), with fewer LP-BP repulsions at 90° than (a), is lower in energy. However, we predict a deviation in bond angles because of the presence of the two lone pairs of electrons.

4. The three nuclei in  $\text{BrF}_3$  determine its molecular structure, which is described as *T shaped*. This is essentially a trigonal bipyramid that is missing two equatorial vertices. The  $\text{F}_{\text{axial}}\text{-Br-F}_{\text{axial}}$  angle is  $172^\circ$ , less than  $180^\circ$  because of LP-BP repulsions.

*Because lone pairs occupy more space around the central atom than bonding pairs, electrostatic repulsions are more important for lone pairs than for bonding pairs.*

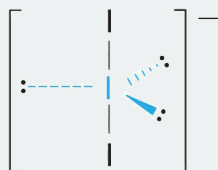
#### $\text{AX}_2\text{E}_3$ Molecules: $\text{I}_3^-$

1. Each iodine atom contributes seven electrons and the negative charge one, so the Lewis electron structure is



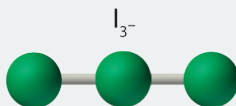
2. There are five electron groups about the central atom in  $\text{I}_3^-$ , two bonding pairs and three lone pairs. To minimize repulsions, the groups are directed to the corners of a trigonal bipyramid.

3. With two bonding pairs and three lone pairs,  $\text{I}_3^-$  has a total of five electron pairs and is designated as  $\text{AX}_2\text{E}_3$ . We must now decide how to arrange the lone pairs of electrons in a trigonal bipyramid in a way that minimizes repulsions. Placing them in the equatorial positions eliminates  $90^\circ$  LP-LP repulsions and minimizes the number of  $90^\circ$  LP-BP repulsions.



The three lone pairs of electrons have equivalent interactions with the three iodine atoms, so we do not expect any deviations in bonding angles.

4. With three nuclei and three lone pairs of electrons, the molecular geometry of  $\text{I}_3^-$  is linear. This can be described as a trigonal bipyramid with three equatorial vertices missing. The ion has an I-I-I angle of  $180^\circ$ , as expected.



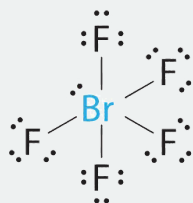
#### Six Electron Groups ( $m + n = 6$ )

(Steric number = 6) In the case that there are six electron groups around a central atom, the nearest groups will lie approximately  $90^\circ$  from one another in space. This results in an electronic geometry that is approximately **octahedral**. There are three relevant molecular geometries in this category:

- When all electron groups are bonds ( $m=6$  or  $AX_6$ ), the molecular geometry is an **octahedron** with bond angles of  **$90^\circ$**  between adjacent bonds.
- When there is one lone pair ( $m=5$ ,  $n=1$  or  $AX_5E_1$ ) we now distinguish between the axial and equatorial positions; the lone pair is considered to be in one of the axial positions, while the bond directly opposite of the lone pair is the axial bond. The molecular geometry is a **square pyramid** with bond angles of  **$90^\circ$**  between adjacent equatorial bonds and **slightly less than  $90^\circ$**  between the axial bond and equatorial groups.
- When there are two lone pairs ( $m=4$ ,  $n=2$  or  $AX_4E_2$ ), the lone pairs are opposite of one another and each occupy an axial position. The molecular geometry is **square planar** with bond angles of  **$90^\circ$** .

#### AX<sub>5</sub>E Molecules: BrF<sub>5</sub>

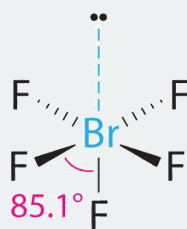
1. The central atom, bromine, has seven valence electrons, as does each fluorine, so the Lewis electron structure is



#### Lewis structure

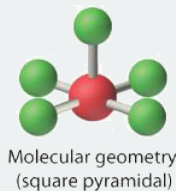
With its expanded valence, this species is an exception to the octet rule.

2. There are six electron groups around the Br, five bonding pairs and one lone pair. Placing five F atoms around Br while minimizing BP–BP and LP–BP repulsions gives the following structure:



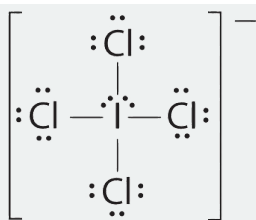
3. With five bonding pairs and one lone pair, BrF<sub>5</sub> is designated as AX<sub>5</sub>E; it has a total of six electron pairs. The BrF<sub>5</sub> structure has four fluorine atoms in a plane in an equatorial position and one fluorine atom and the lone pair of electrons in the axial positions. We expect all  $F_{\text{axial}}\text{--Br--}F_{\text{equatorial}}$  angles to be less than  $90^\circ$  because of the lone pair of electrons, which occupies more space than the bonding electron pairs.

4. With five nuclei surrounding the central atom, the molecular structure is based on an octahedron with a vertex missing. This molecular structure is **square pyramidal**. The  $F_{\text{axial}}\text{--Br--}F_{\text{equatorial}}$  angles are  $85.1^\circ$ , less than  $90^\circ$  because of LP–BP repulsions.

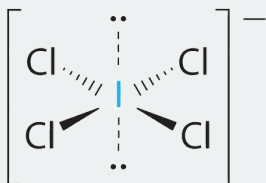


#### AX<sub>4</sub>E<sub>2</sub> Molecules: ICl<sub>4</sub><sup>–</sup>

1. The central atom, iodine, contributes seven electrons. Each chlorine contributes seven, and there is a single negative charge. The Lewis electron structure is

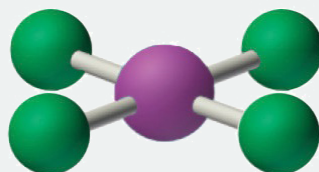


2. There are six electron groups around the central atom, four bonding pairs and two lone pairs. The structure that minimizes LP–LP, LP–BP, and BP–BP repulsions is



3.  $\text{ICl}_4^-$  is designated as  $\text{AX}_4\text{E}_2$  and has a total of six electron pairs. Although there are lone pairs of electrons, with four bonding electron pairs in the equatorial plane and the lone pairs of electrons in the axial positions, all LP–BP repulsions are the same. Therefore, we do not expect any deviation in the Cl–I–Cl bond angles.

4. With five nuclei, the  $\text{ICl}_4^-$  ion forms a molecular structure that is *square planar*, an octahedron with two opposite vertices missing.



## Summary

The arrangement of bonded atoms in a molecule or polyatomic ion is crucial to understanding the chemistry of a molecule, but Lewis electron structures give no information about **molecular geometry**. The **valence-shell electron-pair repulsion (VSEPR) model** allows us to predict which of the possible structures is actually observed in most cases. VSEPR is based on the assumption that pairs of electrons occupy space, and the lowest-energy structure is the one that minimizes repulsions between electron pairs. In the VSEPR model, the molecule or polyatomic ion is given an  $\text{AX}_m\text{E}_n$  designation, where A is the central atom, X is a bonded atom, E is a nonbonding valence electron group (usually a lone pair of electrons), and  $m$  and  $n$  are integers. Each group around the central atom is designated as a bonding pair (BP) or lone (nonbonding) pair (LP). From the BP and LP interactions we can predict both the relative positions of the atoms and the angles between the bonds, called the **bond angles**. From this we can describe the **molecular geometry**. The VSEPR model can be used to predict the shapes of many molecules and polyatomic ions, but it gives no information about bond lengths and the presence of multiple bonds. A combination of VSEPR and a bonding model, such as Lewis electron structures, is necessary to understand the presence of multiple bonds.

The relationship between the number of electron groups around a central atom, the number of lone pairs of electrons, and the molecular geometry is summarized in Table 2.2.7.1.

## Example Exercises

### ✓ Example 2.2.7.1

Using the VSEPR model, predict the molecular geometry of each molecule or ion.

1.  $\text{PF}_5$  (phosphorus pentafluoride, a catalyst used in certain organic reactions)
2.  $\text{H}_3\text{O}^+$  (hydronium ion)

**Given:** two chemical species

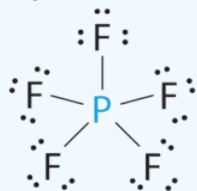
**Asked for:** molecular geometry

**Strategy:**

- Draw the Lewis electron structure of the molecule or polyatomic ion.
- Determine the electron group arrangement around the central atom that minimizes repulsions.
- Assign an  $AX_mE_n$  designation; then identify the LP–LP, LP–BP, or BP–BP interactions and predict deviations in bond angles.
- Describe the molecular geometry.

**Solution:**

- A** The central atom, P, has five valence electrons and each fluorine has seven valence electrons, so the Lewis structure of  $PF_5$  is



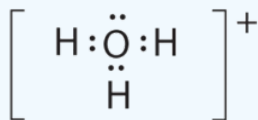
**B** There are five bonding groups about phosphorus. The structure that minimizes repulsions is a trigonal bipyramid.

**C** All electron groups are bonding pairs, so  $PF_5$  is designated as  $AX_5$ . Notice that this gives a total of five electron pairs. With no lone pair repulsions, we do not expect any bond angles to deviate from the ideal.

**D** The  $PF_5$  molecule has five nuclei and no lone pairs of electrons, so its molecular geometry is trigonal bipyramidal.



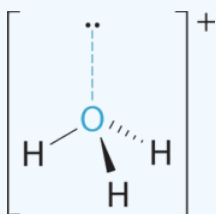
- A** The central atom, O, has six valence electrons, and each H atom contributes one valence electron. Subtracting one electron for the positive charge gives a total of eight valence electrons, so the Lewis electron structure is



**B** There are four electron groups around oxygen, three bonding pairs and one lone pair. Like  $NH_3$ , repulsions are minimized by directing each hydrogen atom and the lone pair to the corners of a tetrahedron.

**C** With three bonding pairs and one lone pair, the structure is designated as  $AX_3E$  and has a total of four electron pairs (three X and one E). We expect the LP–BP interactions to cause the bonding pair angles to deviate significantly from the angles of a perfect tetrahedron.

**D** There are three nuclei and one lone pair, so the molecular geometry is *trigonal pyramidal*, in essence a tetrahedron missing a vertex. However, the H–O–H bond angles are less than the ideal angle of  $109.5^\circ$  because of LP–BP repulsions:



### ? Exercise 2.2.7.2

Using the VSEPR model, predict the molecular geometry of each molecule or ion.

- $\text{XeO}_3$
- $\text{PF}_6^-$
- $\text{NO}_2^+$

#### Answer a

trigonal pyramidal

#### Answer b

octahedral

#### Answer c

linear

### ✓ Example 2.2.7.3

Predict the molecular geometry of each molecule.

- $\text{XeF}_2$
- $\text{SnCl}_2$

**Given:** two chemical compounds

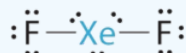
**Asked for:** molecular geometry

**Strategy:**

Use the strategy given in Example 2.2.7.1

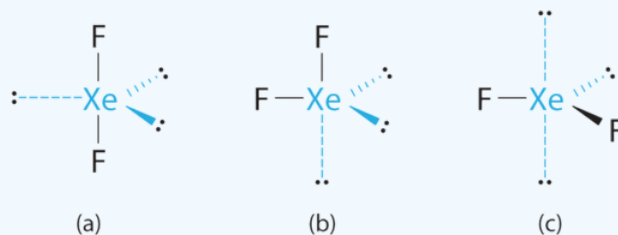
**Solution:**

- A** Xenon contributes eight electrons and each fluorine seven valence electrons, so the Lewis electron structure is



**B** There are five electron groups around the central atom, two bonding pairs and three lone pairs. Repulsions are minimized by placing the groups in the corners of a trigonal bipyramid.

**C** From B,  $\text{XeF}_2$  is designated as  $\text{AX}_2\text{E}_3$  and has a total of five electron pairs (two X and three E). With three lone pairs about the central atom, we can arrange the two F atoms in three possible ways: both F atoms can be axial, one can be axial and one equatorial, or both can be equatorial:



#### Interactions

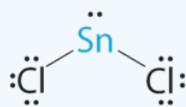
90 LP-LP	0	2	2
----------	---	---	---

The structure with the lowest energy is the one that minimizes LP-LP repulsions. Both (b) and (c) have two  $90^\circ$  LP-LP interactions, whereas structure (a) has none. Thus both F atoms are in the axial positions, like the two iodine atoms around the central iodine in  $\text{I}_3^-$ . All LP-BP interactions are equivalent, so we do not expect a deviation from an ideal  $180^\circ$  in the F-Xe-F bond angle.



**D** With two nuclei about the central atom, the molecular geometry of  $\text{XeF}_2$  is linear. It is a trigonal bipyramid with three missing equatorial vertices.

2. **A** The tin atom donates 4 valence electrons and each chlorine atom donates 7 valence electrons. With 18 valence electrons, the Lewis electron structure is



**B** There are three electron groups around the central atom, two bonding groups and one lone pair of electrons. To minimize repulsions the three groups are initially placed at  $120^\circ$  angles from each other.

**C** From B we designate  $\text{SnCl}_2$  as  $\text{AX}_2\text{E}$ . It has a total of three electron pairs, two X and one E. Because the lone pair of electrons occupies more space than the bonding pairs, we expect a decrease in the  $\text{Cl-Sn-Cl}$  bond angle due to increased LP-BP repulsions.

**D** With two nuclei around the central atom and one lone pair of electrons, the molecular geometry of  $\text{SnCl}_2$  is bent, like  $\text{SO}_2$ , but with a  $\text{Cl-Sn-Cl}$  bond angle of  $95^\circ$ . The molecular geometry can be described as a trigonal planar arrangement with one vertex missing.

### ? Exercise 2.2.7.4

Predict the molecular geometry of each molecule.

- $\text{SO}_3$
- $\text{XeF}_4$

**Answer a**

trigonal planar

**Answer b**

square planar

This page titled [2.2.7: Lone Pair Repulsion](#) is shared under a [not declared](#) license and was authored, remixed, and/or curated by [Kathryn Haas](#).

- [3.2.1: Lone Pair Repulsion](#) by [Kathryn Haas](#) has no license indicated.
- [3.2.2: Multiple Bonds](#) by [Kathryn Haas](#) has no license indicated.

## 2.2.8: Multiple Bonds

In the previous sections, we saw how to predict the approximate geometry around an atom using VSEPR theory, and we learned that lone pairs of electrons slightly distort bond angles from the "parent" geometry. This page discusses the effect of multiple (double and triple) bonds between bonded atoms.

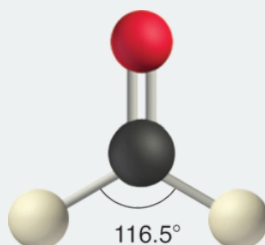
### Double and triple bonds are more repulsive than single bonds

VSEPR theory predicts that double and triple bonds have stronger repulsive forces than single bonds. Like lone pairs of electrons, multiple bonds occupy more space around the central atom than a single bond. The result is that bond angles are slightly distorted compared to the parent geometry. Since a multiple bond has a higher electron density than a single bond, its electrons occupy more space than those of a single bond. Double and triple bonds distort bond angles in a way similar to what lone pairs do. Due to the stronger repulsion, double and triple bonds occupy positions similar to those of lone pairs in groups with 5 and 6 electron groups.

#### Examples 2.2.8.1

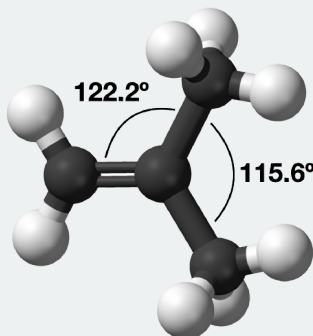
##### CH<sub>2</sub>O

In a molecule such as CH<sub>2</sub>O (AX<sub>3</sub>), whose structure is shown below, the double bond repels the single bonds more strongly than the single bonds repel each other. This causes a deviation from ideal geometry (an H–C–H bond angle of 116.5° rather than 120°).



##### 2-methylbutene

In the molecule, CH<sub>2</sub>C(CH<sub>3</sub>)<sub>2</sub>, the methyl–C–methyl bond angle is 115.6°, which is less than the 120° bond angle that would be expected of the parent geometry. On the other hand, the acetyl–C–methyl bond angle is greater than 120°, with an actual bond angle of 122.2°.



### Atoms with both lone pairs and multiple bonds

In general, we expect that a lone pair has slightly greater repulsive force than a multiple bond, and that a multiple bond has slightly greater repulsive force than a single bond. The **order of expected repulsive force** is:

lone pair > double or triple bond > single bond

## Examples 2.2.8.1

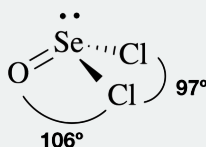
### $\text{IO}_2\text{F}_2^-$

With five electron groups, the  $\text{IO}_2\text{F}_2$  molecule has an approximately trigonal bipyramidal electronic (parent) geometry. The central iodine atom has a single bond to each of the fluorine atoms, a double bond to each oxygen, and a lone pair. The lone pair and the double bonds will occupy more space around iodine than each of the single bonds. Thus, we expect the lone pair and double bonds to occupy equatorial positions around the iodine. The  $\text{O}=\text{I}=\text{O}$  bond angle is  $102^\circ$  (*much* smaller than the  $120^\circ$  angle expected from the parent geometry). This dramatically smaller angle is a result of the increased repulsion between the lone pair and the double bond.



### $\text{SeOCl}_2$

With four electron groups, the  $\text{SeOCl}_2$  molecule has four electron groups and approximately tetrahedral electronic (parent) geometry. It has both a lone pair and a double bond on the central selenium atom. The two chlorine atoms are singly bonded to selenium, while the oxygen is double bonded. The lone pair is most repulsive, followed by the double bonded oxygen, and then the chlorine bonds. This gives a  $\text{Cl}-\text{Se}-\text{Cl}$  bond angle of  $97^\circ$  and a  $\text{Cl}-\text{Se}-\text{O}$  bond angle of  $106^\circ$ ; both angles are less than the  $109.5^\circ$  angles expected for the ideal tetrahedral geometry.



## Practice

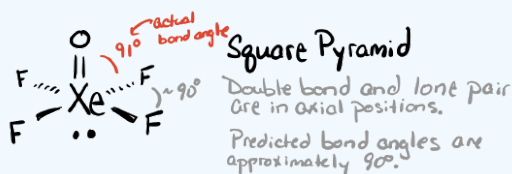
### ? Exercise 2.2.8.1

Use VSEPR theory to predict the geometries and draw the structures of the following.

- $\text{XeOF}_4$
- $\text{NO}_2^-$
- $\text{SOCl}_2$
- $\text{IOF}_3^-$

#### Answer a

This molecule has six electron groups around the central Xe atom (steric number 6), and thus has an approximately octahedral electronic (parent) geometry. There is a double bond to O and a lone pair, both of which are more strongly repulsive than the single bonds to F. The double bond and lone pair will be directly opposite to each other, designated as axial positions. The result is a square pyramidal molecular geometry. VSEPR theory predicts  $\text{F}-\text{Xe}-\text{F}$  bond angles of  $90^\circ$ . As a general rule, lone pairs are slightly more repulsive than multiple bonds, and so we might expect the  $\text{O}-\text{Xe}-\text{F}$  bond angles to be  $<90^\circ$ ; *however in this case the actual  $\text{O}-\text{Xe}-\text{F}$  bond angle is observed to be  $91^\circ$  (you could not have predicted the latter).*



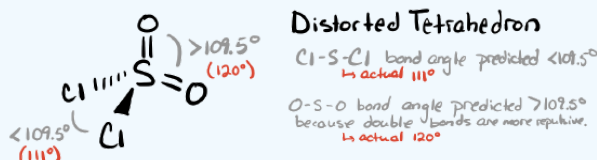
### Answer b

This molecule has three electron groups around the central atom: one lone pair and two double bonds to oxygen atoms. This results in an approximately trigonal planar electronic (parent geometry). We expect the lone pair to be slightly more repulsive than double bonds, and so we expect the O—N—O bond angle to be slightly less than  $120^\circ$ . *The actual O—N—O angle is  $115^\circ$ .*



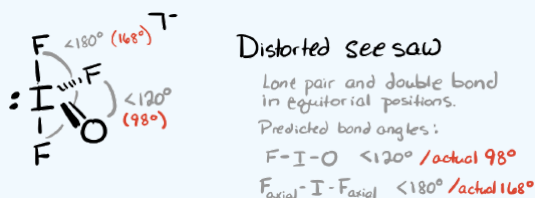
### Answer c

This molecule has four electron groups (steric number 4) with an approximately tetrahedral electronic (parent) geometry. Each double bonded oxygen will take up more space around the central S than the single bonded Cl atoms. We should expect the double bonds to repel each other more strongly than they repel each single bond, with the least repulsive interaction being between the two single bonds. The bond angle for Cl—S—Cl is expected to be  $<109.5^\circ$  according to VSEPR theory (however, it is actually  $111^\circ$ ). We would expect the bond angle for O—S—O to be larger than the angle for Cl—S—Cl and for Cl—S—O. The O—S—O bond angle is predicted to be  $>109.5^\circ$  (and the actual bond angle is  $120^\circ$ ). The molecular geometry is a distorted tetrahedron.



### Answer d

This molecule has five electron groups (steric number 5) with an approximately trigonal bipyramidal electronic (parent) geometry. There is one lone pair, a double bond to O, and three single bonds to F atoms around the central I atom. The lone pair and double bond are most repulsive, and should occupy the less crowded equatorial positions rather than the more crowded axial positions. This results in a seesaw molecular geometry. With the more repulsive lone pair and the strongest equatorial repulsive force being between the double bond and lone pair, we should expect the  $F_{\text{equatorial}}\text{—I—O}$  bond angle to be less than the  $120^\circ$  angle expected for the parent geometry (*it is actually much less, at  $98^\circ$* ). Due to repulsion between the axial F atoms and both the lone pair and double bond, we should expect the F—S—F bond angles to be compressed. The  $F_{\text{axial}}\text{—I—F}_{\text{axial}}$  is actually  $168^\circ$ .



## References

- Miessler, G.; Fischer, P.J.; Tarr, D. (2014). Inorganic Chemistry. New Jersey: Prentice-Hall. pp. 55

This page titled 2.2.8: Multiple Bonds is shared under a [not declared](#) license and was authored, remixed, and/or curated by Kathryn Haas.

- 3.2.2: Multiple Bonds by Kathryn Haas has no license indicated.

## 2.2.9: Electronegativity and Atomic Size Effects

### Introduction

We saw in previous sections how **lone pairs of electrons** and **multiple bonds** distort bond angles between non-central atoms (ligands) around a central atom. This section describes how ligand **electronegativity and size also influence bond angles and molecular geometry**. Electronegativity is generally correlated with atomic size going down any group of the periodic table. There are some cases where bond angles can be predicted by these correlations. However, size and electronegativity can also work as competing factors in determining bond angles.

### Electronegativity and Size Influence Bond Angles

Let's begin by examining the bond angles of several trigonal pyramidal molecules. The molecules shown in Figure 2.2.9.2 each have three identical "pendant groups" on the central atom (Figure 2.2.9.2). *Pendant atoms or pendant groups* are the atoms, or groups of atoms, that are bonded directly to the central atom. The molecules shown here are arranged according to the size of the central and pendant atoms. Central atoms increase in size going down this figure, and pendant atoms increase in size going across from left to right. The bond angles and bond lengths are labeled in each case.

What trends can you identify?

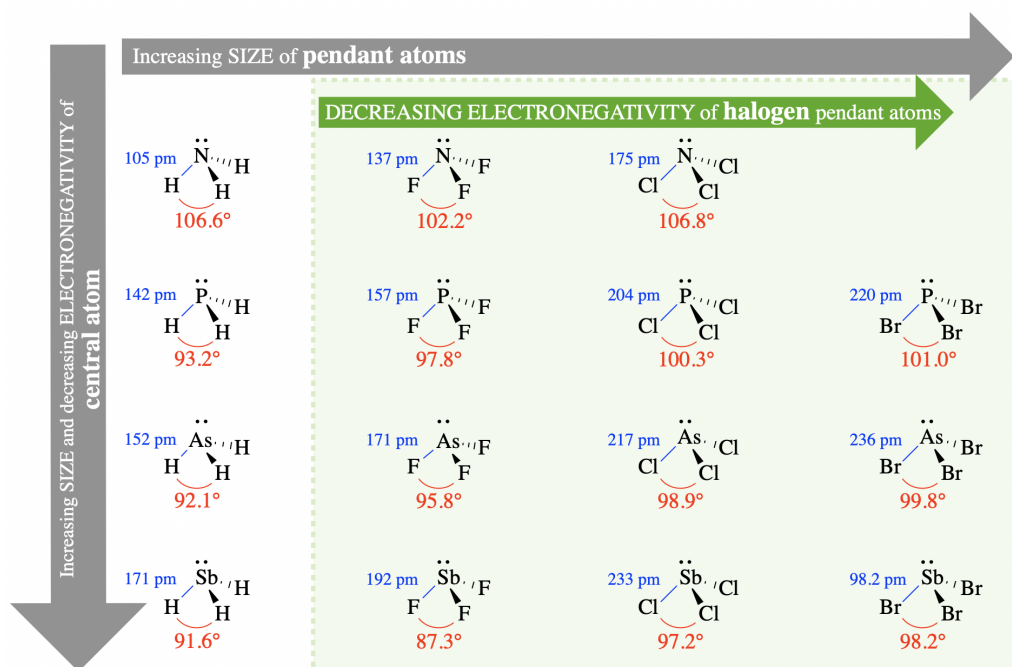


Figure 2.2.9.2: Several molecules with trigonal pyramidal electronic geometry are shown arranged according to size of the central atom (increasing size of central atom from top to bottom) and pendant atom (increasing size of pendant atoms from left to right). Bond angles and bond lengths are indicated. (Kathryn Haas; CC-NC-BY-SA)

### Trends in Size

First, let's examine how the size of the central and pendant groups might influence bond angle. In VSEPR theory, **the size of atoms (or groups of atoms) will affect bond angles due to changes in steric interactions between pendant groups**.

#### Size of the central atom

Examine the relationship between the size of the central atom and the bond angles in Figure 2.2.9.2 (go down any column in the figure). For example, compare  $\text{NH}_3$ ,  $\text{PH}_3$ ,  $\text{AsH}_3$ , and  $\text{SbH}_3$ , with bond angles 106.6°, 93.2°, 92.1°, and 91.6°, respectively. In this series, the size of the central atom increases from N to Sb while the size of the pendant atom (hydrogen) remains constant. As the size of the central atom increases, the bond angles decrease; thus, we observe a negative relationship between size of the central atom and the bond angle in these molecules. This relationship is explained by sterics. As the central atom increases in size, the bond lengths also increase and the pendant atoms are farther from each other in space. In VSEPR theory, this will reduce steric

interactions between the pendant groups. Since the lone pair on these molecules is more repulsive than bonded groups, the decrease in steric interactions between bonded groups results in a decrease in bond angles.

### Size of the pendant atoms (or groups)

Examine the relationships between size of the halogen pendant atoms and bond angle in Figure 2.2.9.2 (go across any row within the shaded region). For example, compare  $\text{PF}_3$ ,  $\text{PCl}_3$ , and  $\text{PBr}_3$ , with bond angles  $97.8^\circ$ ,  $100.3^\circ$ , and  $101.0^\circ$ , respectively. In this series, the size of the pendant atom increases from F to Br while the central atom remains constant (phosphorous). *As the size of pendant atoms increases, the bond angle increases; thus, we observe a direct relationship between size of the pendant group and the bond angle in these molecules.* Again, we can explain this using sterics. As the size of the pendant atoms increases, sterics between the pendant groups will increase (despite small changes in bond length). Increased steric interactions between pendant groups will prefer larger bond angles between the groups.

This trend fails, however, if we consider the molecules with hydrogen as the pendant atoms. Notice, for example, that H is the smallest pendant atom. If we consider the trend described above, we should assume that  $\text{XH}_3$  (where X is a variable atom) would have the smallest bond angle in the series of  $\text{XH}_3$ ,  $\text{XF}_3$ ,  $\text{XCl}_3$ , and  $\text{XBr}_3$ . However this is not the case of  $\text{NH}_3$ ,  $\text{NF}_3$ , and  $\text{NCl}_3$ , with bond angles  $106.6^\circ$ ,  $102.2^\circ$ , and  $106.8^\circ$ , respectively. To explain the variation in these bond angles, we need to consider electronegativity.

### Trends in Electronegativity

Now let's examine how electronegativity influences bond angles around a central atom. In VSEPR theory, **electronegativity of atoms/groups will affect bond angles due to changes in the distribution of electron pairs around the central atom (and thus changes in the severity of electron pair repulsion)**. This really comes down to bond polarity caused by the difference in electronegativity between the central atom and pendant groups (bond polarity in the context of valence bond theory). In a polar bond, the more electronegative atom will pull electron density towards itself. When a pendant atom is more electronegative, it will pull the bonded electron pair towards itself and away from the central atom; this will reduce the electron pair repulsion between bonded electron pairs on the central atom. A decrease in electron pair repulsion on the central atom should decrease bond angles between the groups (Figure 2.2.9.3).

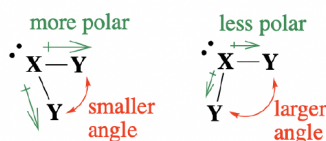


Figure 2.2.9.3. When electron pairs are distributed away from the central atom, repulsions are decreased, allowing smaller bond angles. (Kathryn Haas; CC-NC-BY-SA)

Electronegativity is an alternative explanation to the trends we already examined above in Figure 2.2.9.2. For example, when we compare the halogen pendant atoms (shaded region in Figure 2.2.9.2), the electronegativity of pendant groups decreases, bond polarity of the bonds decreases, and bond angles increase going from left to right and from F to Br. As more electron density remains on the central atom, electron repulsion between the bonded pairs increases and bond angles increase.

The electronegativity argument can also be used to explain the fact that  $\text{NH}_3$  ( $106.6^\circ$ ) has a larger bond angle than  $\text{NF}_3$  ( $102.2^\circ$ ). This particular case illustrates how electronegativity and size can be competing factors. While electronegativity differences seem to dominate in the case of  $\text{NH}_3$  ( $106.6^\circ$ ) compared to  $\text{NF}_3$  ( $102.2^\circ$ ), size differences still dominate in the cases of other  $\text{XH}_3$  and  $\text{XF}_3$  examples in Figure 2.2.9.2.

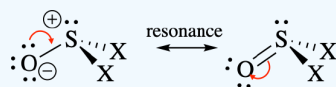
#### ? Exercise 2.2.9.1

Predict the geometry and approximate bond angles. Then put the molecules in each series in order of smallest to largest bond angle. Defend your answer.

- The X-S-X bond angle in  $\text{OSF}_2$ ,  $\text{OSCl}_2$ ,  $\text{OSBr}_2$
- $\text{H}_2\text{O}$ ,  $\text{H}_2\text{S}$ ,  $\text{H}_2\text{Se}$ ,  $\text{H}_2\text{Te}$
- $\text{H}_2\text{O}$ ,  $\text{OF}_2$ ,  $\text{OCl}_2$

**Answer (a)**

**Geometry and predicted bond angles:** These are molecules with steric number 4. They can be written as two different resonance structures, and the resonance hybrid would have double bond character between S and O.



We would expect a trigonal pyramidal geometry with all bond angles  $<109.5^\circ$  because the lone pair is more repulsive than bonds. Because the double bond is more repulsive than single bonds, we should also expect the O-S-X bond angles to be greater than the X-S-X bond angles.

**Trend:** This is a series of molecules that varies in the identity of the pendant atoms; the variation is within the halogens. The size of the halogens increases, and the electronegativity decreases in the order F, Cl, Br. Both size and electronegativity would lead us to conclude that the X-S-X bond angles would increase in the order  $\text{OSF}_2 < \text{OSCl}_2 < \text{OSBr}_2$

Explanation: (1) Increasing electronegativity of the pendant atom ( $\text{F} > \text{Cl} > \text{Br}$ ) increases the polarity of the bond and reduces the electron density of the bonded pair on the central atom. This reduces the e-e repulsions of adjacent bonded electron pairs on S, allowing the halogens to become closer. The more electronegative pendant atoms can have smaller bond angles. (2) Increasing size of pendant atoms ( $\text{F} < \text{Cl} < \text{Br}$ ) increases steric repulsions and increases bond angle. Both explanations lead to the same predicted trend.

The actual measured X-S-X bond angles are  $\text{OSF}_2$  ( $92.3^\circ$ ) /  $\text{OSCl}_2$  ( $96.2^\circ$ ) /  $\text{OSBr}_2$  ( $98.2^\circ$ ). The trend in these bond angles is consistent with the prediction.

#### Answer (b)

**Geometry and predicted bond angles:** These are molecules with steric number 4, bent molecular geometry, with predicted bond angles  $<109.5^\circ$  because the two lone pairs are each more repulsive than the bonds. There are two lone pairs and two single bonds to H around each central atom.

**Trend:** This is a series of molecules that varies in the identity of the central atom. The central atom increases in the order  $\text{O} < \text{S} < \text{Se} < \text{Te}$ , where Te is the largest element and O is the smallest. Arguments based on size would lead us to predict that the pendant groups of  $\text{H}_2\text{Te}$  would be less sterically crowded and thus have a smaller bond angle than the pendant groups of  $\text{H}_2\text{O}$ . The electronegativity decreases in the order  $\text{O} > \text{S} > \text{Se} > \text{Te}$ , where O is the most electronegative element and Te is the least. Thus, we expect the bonding electron pairs to be closer to the central atom on O than they would be on Te; we should expect  $\text{H}_2\text{Te}$  to have the least electron pair repulsions and thus smallest bond angle in this series, while  $\text{H}_2\text{O}$  would have the strongest electron pair repulsions and largest bond angles.

Both arguments lead to the same conclusion, that the order of increasing bond angle is  $\text{H}_2\text{Te} < \text{H}_2\text{Se} < \text{H}_2\text{S} < \text{H}_2\text{O}$ .

The actual measured bond angles are  $\text{H}_2\text{Te}$  ( $90.2^\circ$ ) /  $\text{H}_2\text{Se}$  ( $90.6^\circ$ ) /  $\text{H}_2\text{S}$  ( $92.1^\circ$ ) /  $\text{H}_2\text{O}$  ( $104.5^\circ$ ). The trend in these bond angles is consistent with prediction.

#### Answer (c)

**Geometry and predicted bond angles:** These are molecules with steric number 4, bent molecular geometry, with predicted bond angles  $<109.5^\circ$  because the two lone pairs are each more repulsive than the bonds. There are two lone pairs and two single bonds to H around each central atom. (This is similar to the case in (b)).

**Trend:** This is a series of molecules that varies in the identity of the pendant atoms; two of the molecules have halogens, and the other has hydrogen pendant atoms. This is a case where size and electronegativity will be conflicting factors because trends in electronegativity do not mirror the trend in size.

- **Size:** The size of pendant atoms increases in the order  $\text{H} < \text{F} < \text{Cl}$  where H is smallest and Cl is largest. Prediction of bond angles based on size alone would lead to the predicted order of increasing bond angle  $\text{H}_2\text{O} < \text{OF}_2 < \text{OCl}_2$ .
- **Electronegativity:** The electronegativity decreases in the order  $\text{F} > \text{Cl} > \text{H}$  where F has the greatest electronegativity and H has the least. Since we expect the most electronegative pendant atoms to have the smallest bond angles, prediction based on electronegativity alone would lead to the predicted order of increasing bond angle  $\text{OF}_2 < \text{OCl}_2 < \text{H}_2\text{O}$ .

The points above illustrate how the two different arguments would lead to different predictions about the trend in bond angle. This makes it difficult to predict the actual order of increasing bond angle. However, we saw above in the example of  $\text{NH}_3$  vs  $\text{NF}_3$  that electronegativity is more important than size; yet in the case of  $\text{NH}_3$  vs  $\text{NCl}_3$ , the much larger size of the



pendant atom is more important. If we apply this lesson to the current problem, we might predict the order  $\text{OF}_2 < \text{H}_2\text{O} < \text{OCl}_2$ , and in fact this more nuanced prediction, based on a similar case, matches the actual order for measured bond angles:  $\text{OF}_2$  ( $103.3^\circ$ )  $< \text{H}_2\text{O}$  ( $104.5^\circ$ )  $< \text{OCl}_2$  ( $110.9^\circ$ ).

## Group Electronegativities

You probably heard the terms "electron donating group" and "electron withdrawing group" from your coursework in Organic Chemistry. For example, the acid trifluoroacetic acid (TFA) is more acidic than acetic acid due to the electron withdrawing effects of the  $\text{CF}_3$  group compared to  $\text{CH}_3$ .  $\text{CF}_3$  is an electron withdrawing group, while  $\text{CH}_3$  is an electron donating group. In other words,  $\text{CF}_3$  is more electronegative than  $\text{CH}_3$ .

The electron withdrawing ability (electronegativity) of groups can be estimated and compared, just as they are with atoms. Although there is no one scale that is used for group electronegativities, and published values even for the same groups vary widely, there are reliable trends within similar groups. The same size and electronegativity factors discussed above that affect bond angles for *pendant atoms*, also can be used to rationalize distorted bond angles for *pendant groups* around a central atom.

### ? Exercise 2.2.9.2

Consider the relative electronegativities and sizes of the pendant atoms/groups in the following examples. Is the trend in bond angles what you would expect from the relative group electronegativities and relative sizes? What, if any, is the more dominant factor in determining the trend?

- $\text{N}(\text{CH}_3)_3$  has an C-N-C bond angle of  $110.9^\circ$ , while  $\text{N}(\text{CF}_3)_3$  has a bond angle of  $117.9^\circ$ .
- The X-S-X bond angles in molecules of the form  $\text{SO}_2(\text{X})_2$  are:  $\text{SO}_2(\text{OH})_2$   $101.3^\circ$ ;  $\text{SO}_2(\text{CF}_3)_2$   $102.0^\circ$ ;  $\text{SO}_2(\text{CH}_3)_2$   $102.6^\circ$ .

#### Answer (a)

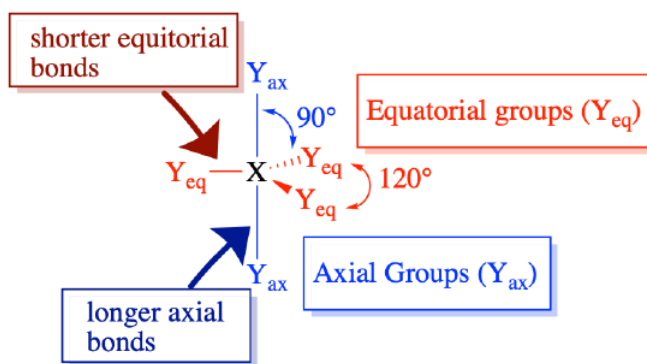
Add texts here. Do not delete this text first.

#### Answer (b)

Add texts here. Do not delete this text first.

## Special case of electronegativity and size in steric number 5 (trigonal bipyramid)

Molecules with steric number 5 are interesting because they possess two different types of positions (equatorial and axial). These positions have unique bond angles and bond lengths. Pendant atoms/groups have different preferences for the axial and equatorial positions that depend somewhat on their electronegativity.



Molecules with steric number 5 possess different bond angles and lengths for axial (ax) and equatorial (eq) pendant atoms. (CC-BY-NC-SA; Kathryn Haas)

In a previous section, we discussed the preference of **lone pairs** and **multiple bonds** for the equatorial positions in trigonal bipyramidal molecules. VSEPR theory rationalizes this by assuming that lone pairs and multiple bonds are more repulsive than the electron pairs in single bonds. Equatorial positions are less crowded (with only two closest neighbors at  $90^\circ$ , and two farther neighbors at  $120^\circ$ ) compared to axial positions (with three closest neighbors at  $90^\circ$ ), thus the more repulsive groups prefer the less crowded equatorial positions.



Pendant groups that are more electronegative result in weaker electron pair repulsion around the central atom, while groups that are less electronegative result in stronger electron-pair repulsion around the central atom (as described above). The result for steric number 5: **bonding pairs to less electronegative elements are more repulsive, and generally prefer equatorial positions**. Still, lone pairs and multiple bonds are more repulsive than single bonds and would show a stronger preference for equatorial positions.

## Examples and Nuances

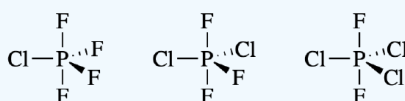
### ? Exercise 2.2.9.3

Some examples of molecule that demonstrate the equatorial preference of less electronegative groups are below. Predict (draw) their structures.

- $\text{PF}_4\text{Cl}$ ,  $\text{PF}_3\text{Cl}_2$ , and  $\text{PF}_2\text{Cl}_3$
- $\text{PF}_4(\text{CH}_3)$ ,  $\text{PF}_3(\text{CH}_3)_2$ , and  $\text{PF}_2(\text{CH}_3)_3$

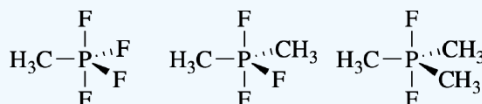
#### Answer (a)

Cl is less electronegative than F; thus we expect Cl to have stronger preference for the equatorial positions.

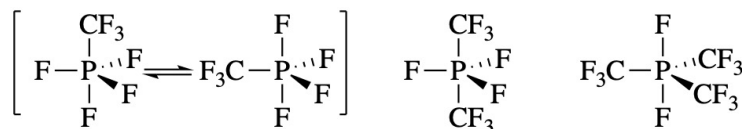


#### Answer (b)

$\text{CH}_3$ , an electron donating group, is less electronegative than F. We expect  $\text{CH}_3$  to have a stronger preference for the equatorial positions.



In the exercise above, the structures can be explained by the electronegativity of the pendant groups; less electronegative groups prefer the equatorial positions. There are other similar molecules for which explanations (or predictions) are difficult. For example, the series of molecules below seems to have completely random placement of F and  $\text{CF}_3$  groups. **These structures could not be predicted based on VSEPR theory**. It seems that in this case, the more symmetrical arrangements of pendant groups is preferred.



## References and resources

- Pauling, L. (1932). "The Nature of the Chemical Bond. IV. The Energy of Single Bonds and the Relative Electronegativity of Atoms". *J. Am. Chem. Soc.* **54**(9): 3570–3582. doi:[10.1021/ja01348a011](https://doi.org/10.1021/ja01348a011).
- Housecroft, Catherine E. et. al. "Inorganic Chemistry" 3rd Edition. Pearson Education Limited 2008. Chapter 2.5 "Electronegativity Values" pgs. 42-44
- International Union of Pure and Applied Chemistry. "Electronegativity". [goldbook.iupac.org/E01990.html](http://goldbook.iupac.org/E01990.html).

## Acknowledgment

- Matthew Salem (UC Davis) ([Pauling Electronegativity](#))
- Introduction to Inorganic Chemistry Wikibook ([https://chem.libretexts.org/Bookshel...\\_Bond\\_Strength](https://chem.libretexts.org/Bookshel..._Bond_Strength))
- Curated or created by [Kathryn Haas](#)

This page titled [2.2.9: Electronegativity and Atomic Size Effects](#) is shared under a [not declared](#) license and was authored, remixed, and/or curated by [Kathryn Haas](#).

- [3.2.3: Electronegativity and Atomic Size Effects](#) by [Kathryn Haas](#) has no license indicated.

## 2.2.10: Molecular Polarity

Dipole moments occur when there is a separation of charge. They can occur between two ions in an ionic bond or between atoms in a covalent bond; dipole moments arise from differences in electronegativity. The larger the difference in electronegativity, the larger the dipole moment. The distance between the charge separation is also a deciding factor in the size of the dipole moment. The dipole moment is a measure of the polarity of the molecule.

### Introduction

When atoms in a molecule share electrons unequally, they create what is called a dipole moment. This occurs when one atom is more electronegative than another, resulting in that atom pulling more tightly on the shared pair of electrons, or when one atom has a lone pair of electrons and the difference of electronegativity vector points in the same way. One of the most common examples is the water molecule, made up of one oxygen atom and two hydrogen atoms. The differences in electronegativity and lone electrons give oxygen a partial negative charge and each hydrogen a partial positive charge.

### Dipole Moment

When two electrical charges, of opposite sign and equal magnitude, are separated by a distance, an electric dipole is established. The size of a dipole is measured by its dipole moment ( $\mu$ ). Dipole moment is measured in Debye units, which is equal to the distance between the charges multiplied by the charge (1 Debye equals  $3.34 \times 10^{-30} \text{ C m}$ ). The dipole moment of a molecule can be calculated by Equation 2.2.10.1:

$$\vec{\mu} = \sum_i q_i \vec{r}_i \quad (2.2.10.1)$$

where

- $\vec{\mu}$  is the dipole moment vector
- $q_i$  is the magnitude of the  $i^{\text{th}}$  charge, and
- $\vec{r}_i$  is the vector representing the position of  $i^{\text{th}}$  charge.

The dipole moment acts in the direction of the vector quantity. An example of a polar molecule is  $\text{H}_2\text{O}$ . Because of the lone pair on oxygen, the structure of  $\text{H}_2\text{O}$  is bent (via VSEPR theory), which means that the vectors representing the dipole moment of each bond do not cancel each other out. Hence, water is polar.

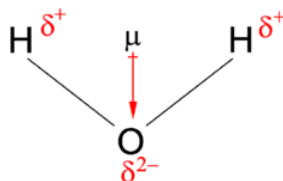


Figure 2.2.10.1: Dipole moment of water. The convention in chemistry is that the arrow representing the dipole moment goes from positive to negative. Physicist tend to use the opposite orientation.

The vector points from positive to negative, on both the molecular (net) dipole moment and the individual bond dipoles. Table A2 shows the electronegativity of some of the common elements. The larger the difference in electronegativity between the two atoms, the more electronegative that bond is. To be considered a polar bond, the difference in electronegativity must be large. The dipole moment points in the direction of the vector quantity of each of the bond electronegativities added together.

It is relatively easy to measure dipole moments: just place a substance between charged plates (Figure 2.2.10.2); polar molecules increase the charge stored on the plates, and the dipole moment can be obtained (i.e., via the capacitance of the system). Nonpolar  $\text{CCl}_4$  is not deflected; moderately polar acetone deflects slightly; highly polar water deflects strongly. In general, polar molecules will align themselves: (1) in an electric field, (2) with respect to one another, or (3) with respect to ions (Figure 2.2.10.2).

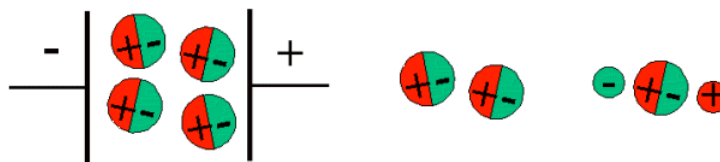


Figure 2.2.10.2: Polar molecules align themselves in an electric field (left), with respect to one another (middle), and with respect to ions (right)

Equation 2.2.10.1 can be simplified for a simple separated two-charge system like diatomic molecules or when considering a bond dipole within a molecule

$$\mu_{\text{diatomic}} = Q \times r \quad (2.2.10.2)$$

This bond dipole is interpreted as the dipole from a charge separation over a distance  $r$  between the partial charges  $Q^+$  and  $Q^-$  (or the more commonly used terms  $\delta^+$  -  $\delta^-$ ); the orientation of the dipole is along the axis of the bond. Consider a simple system of a single electron and proton separated by a fixed distance. When the proton and electron are close together, the dipole moment (degree of polarity) decreases. However, as the proton and electron get farther apart, the dipole moment increases. In this case, the dipole moment is calculated as (via Equation 2.2.10.2):

$$\begin{aligned} \mu &= Qr \\ &= (1.60 \times 10^{-19} \text{ C})(1.00 \times 10^{-10} \text{ m}) \\ &= 1.60 \times 10^{-29} \text{ C} \cdot \text{m} \end{aligned}$$

The Debye characterizes the size of the dipole moment. When a proton and electron are 100 pm apart, the dipole moment is 4.80  $D$ :

$$\begin{aligned} \mu &= (1.60 \times 10^{-29} \text{ C} \cdot \text{m}) \left( \frac{1 \text{ D}}{3.336 \times 10^{-30} \text{ C} \cdot \text{m}} \right) \\ &= 4.80 \text{ D} \end{aligned}$$

4.80  $D$  is a key reference value and represents a pure charge of +1 and -1 separated by 100 pm. If the charge separation is increased then the dipole moment increases (linearly):

- If the proton and electron are separated by 120 pm:

$$\mu = \frac{120}{100}(4.80 \text{ D}) = 5.76 \text{ D} \quad (2.2.10.3)$$

- If the proton and electron are separated by 150 pm:

$$\mu = \frac{150}{100}(4.80 \text{ D}) = 7.20 \text{ D} \quad (2.2.10.4)$$

- If the proton and electron are separated by 200 pm:

$$\mu = \frac{200}{100}(4.80 \text{ D}) = 9.60 \text{ D} \quad (2.2.10.5)$$

#### ✓ Example 2.2.10.1: Water

The water molecule in Figure 2.2.10.1 can be used to determine the direction and magnitude of the dipole moment. From the electronegativities of oxygen and hydrogen, the difference in electronegativity is 1.2e for each of the hydrogen-oxygen bonds. Next, because the oxygen is the more electronegative atom, it exerts a greater pull on the shared electrons; it also has two lone pairs of electrons. From this, it can be concluded that the dipole moment points from between the two hydrogen atoms toward the oxygen atom. Using the equation above, the dipole moment is calculated to be 1.85  $D$  by multiplying the distance between the oxygen and hydrogen atoms by the charge difference between them and then finding the components of each that point in the direction of the net dipole moment (the angle of the molecule is 104.5°).

The bond moment of the O-H bond = 1.5  $D$ , so the net dipole moment is

$$\mu = 2(1.5) \cos\left(\frac{104.5^\circ}{2}\right) = 1.84 \text{ D}$$

## Polarity and Structure of Molecules

The shape of a molecule and the polarity of its bonds determine the OVERALL POLARITY of that molecule. A molecule that contains polar bonds might not have any overall polarity, depending upon its shape. The simple definition of whether a complex molecule is polar or not depends upon whether its overall centers of positive and negative charges overlap. If these centers lie at the same point in space, then the molecule has no overall polarity (and is non polar). If a molecule is completely symmetric, then the dipole moment vectors on each molecule will cancel each other out, making the molecule nonpolar. A molecule can only be polar if the structure of that molecule is not symmetric.

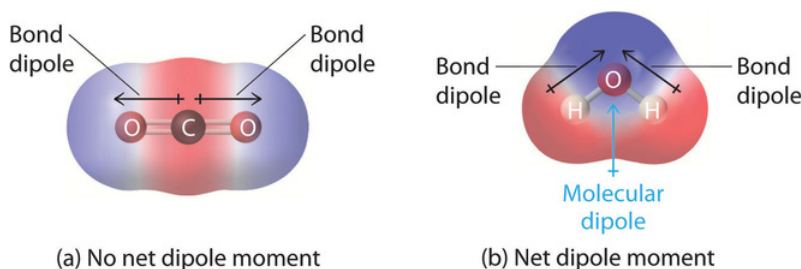


Figure 2.2.10.3: Charge distributions of  $\text{CO}_2$  and  $\text{H}_2\text{O}$ . Blue and red colored regions are negatively and positively signed regions, respectively. (CC BY-SA-NC 3.0; anonymous)

A good example of a nonpolar molecule that contains polar bonds is carbon dioxide (Figure 2.2.10.3a). This is a linear molecule and each  $\text{C}=\text{O}$  bond is, in fact, polar. The central carbon will have a net positive charge, and the two outer oxygen atoms a net negative charge. However, since the molecule is linear, these two bond dipoles cancel each other out (i.e. the vector addition of the dipoles equals zero) and the overall molecule has a zero dipole moment ( $\mu = 0$ ).

*Although a polar bond is a prerequisite for a molecule to have a dipole, not all molecules with polar bonds exhibit dipoles*

For  $\text{AB}_n$  molecules, where  $A$  is the central atom and  $B$  are all the same types of atoms, there are certain molecular geometries which are symmetric. Therefore, they will have no dipole even if the bonds are polar. These geometries include linear, trigonal planar, tetrahedral, octahedral and trigonal bipyramidal.

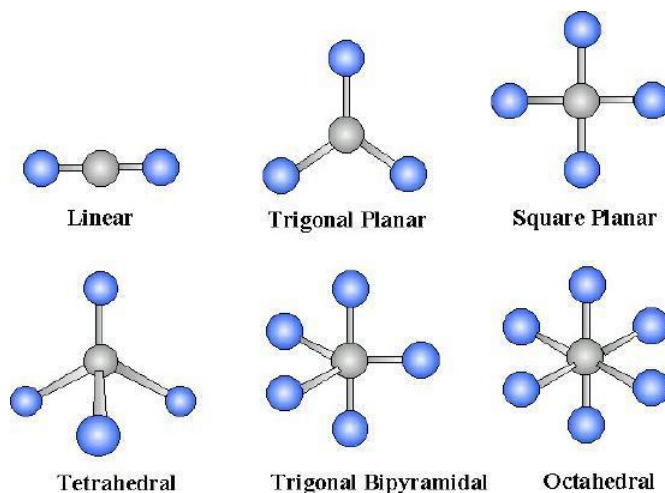
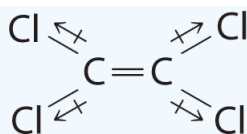


Figure 2.2.10.4: Molecular geometries with exact cancellation of polar bonding to generate a non-polar molecule ( $\mu = 0$ )

### ✓ Example 2.2.10.3: $\text{C}_2\text{Cl}_4$

Although the  $\text{C}-\text{Cl}$  bonds are rather polar, the individual bond dipoles cancel one another in this symmetrical structure, and  $\text{Cl}_2\text{C}=\text{CCl}_2$  does not have a net dipole moment.

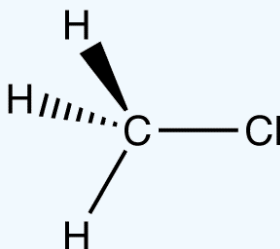


### ✓ Example 2.2.10.3: CH<sub>3</sub>Cl

C-Cl, the key polar bond, is 178 pm. Measurement reveals 1.87 D. From this data, % ionic character can be computed. If this bond were 100% ionic (based on proton & electron),

$$\mu = \frac{178}{100}(4.80 \text{ D})$$

$$= 8.54 \text{ D}$$



Although the bond length is **increasing**, the dipole is **decreasing** as you move down the halogen group. The electronegativity decreases as we move down the group. Thus, the greater influence is the electronegativity of the two atoms (which influences the **charge** at the ends of the dipole).

Table 2.2.10.1: Relationship between Bond length, Electronegativity and Dipole moments in simple Diatomics

Compound	Bond Length (Å)	Electronegativity Difference	Dipole Moment (D)
HF	0.92	1.9	1.82
HCl	1.27	0.9	1.08
HBr	1.41	0.7	0.82
HI	1.61	0.4	0.44

## References

1. Housecroft, Catherine E. and Alan G. Sharpe. *Inorganic Chemistry*. 3rd ed. Harlow: Pearson Education, 2008. Print. (Pages 44-46)
2. Tro, Nivaldo J. *Chemistry: A Molecular Approach*. Upper Saddle River: Pearson Education, 2008. Print. (Pages 379-386)

This page titled [2.2.10: Molecular Polarity](#) is shared under a [not declared](#) license and was authored, remixed, and/or curated by [Kathryn Haas](#).

- [Dipole Moments](#) by Delmar Larsen, Mike Blaber is licensed [CC BY 4.0](#).

## CHAPTER OVERVIEW

### Unit 3: Molecular Symmetry

3.1: Symmetry Elements and Operations LOs

3.1.1: Definitions and Examples

3.2: Point Groups

3.2.1: Molecular Point Groups

3.2.2: Assigning Point Groups

3.2.3: Chirality

3.3: Unit 3 Practice Problems

---

Dr. Kai Landskron ([Lehigh University](#)). If you like this textbook, please consider to make a donation to support the author's research at Lehigh University: [Click Here to Donate](#).

---

Unit 3: Molecular Symmetry is shared under a [CC BY 4.0](#) license and was authored, remixed, and/or curated by LibreTexts.

## 3.1: Symmetry Elements and Operations LOs

---

Learning objectives for this unit are to:

- Define and identify the basic symmetry elements and operations: E (identity),  $\sigma$  (mirror plane and reflection),  $C_n$  (rotational axis),  $S_n$  (improper rotational axis), and i (inversion)
  - Apply symmetry elements and operations to molecular structures.
- 

3.1: Symmetry Elements and Operations LOs is shared under a [not declared](#) license and was authored, remixed, and/or curated by LibreTexts.


### 3.1.1: Definitions and Examples

#### Symmetry in Chemistry

Symmetry is actually a concept of mathematics and not of chemistry. However, symmetry, and the underlying mathematical theory for symmetry, group theory, are of tremendous importance in chemistry because they can be applied to many chemistry problems. For example it helps us to classify the structures of molecules and crystals, understand chemical bonding, predict vibrational spectra, and determine the optical activity of compounds. We will therefore first discuss the general foundations of symmetry and group theory, and then apply them to chemical problems, in particular chemical bonding.

Let us first find a definition for symmetry. Symmetry is very familiar to us as we associate symmetry with beauty, but very familiar things are not necessarily easy to define scientifically. One common definition is that symmetry is the self-similarity of an object. The more similar parts it has the more symmetric it appears. For example, we would argue that the two wings of the butterfly depicted look similar. If the left wing was very different from the right wing the butterfly would look less symmetric.



Figure 2.1.1 Symmetry depicted through an image of a butterfly (Attribution: Chemlibretexts   
<https://chem.libretexts.org/@api/dek...jpg?revision=2> <http://creativecommons.org/licenses/by-nc-sa/3.0/us/>)

How can we measure the self-similarity, or symmetry of an object quantitatively? We can do this using the concept of the symmetry operation. It is defined as a movement of an object into an equivalent indistinguishable orientation. The number and kind of symmetry operations that can be carried out defines the symmetry of the object.

#### Definition: Symmetry Operation

Movement of an object into an equivalent indistinguishable orientation

Symmetry operations are carried out around so-called symmetry elements. A symmetry element is a point, line, or plane about which a symmetry operation is carried out. Let us understand now what symmetry elements and operations exist.

#### Definition: Symmetry Element

A point, line or plane about which a symmetry operation is carried out

#### The Identity Operation ( $E$ )

The most simple operation is the identity operation. It can be denoted by the Schoenflies symbol  $E$ . Schoenflies symbols are the most common symbols to denote a symmetry operation. The identity operation says that each object is self-similar to itself when you do not move it in any way. This is a trivial statement, but as we will see later, the identity operation is necessary to make the mathematical framework of symmetry, group theory, complete. The identity operation is present in any object. In the example of the depicted snail shell it is the only operation (Fig. 2.1.2).





Figure 2.1.2 Snail shell (Attribution: Petr Kratochvil <http://res.publicdomainfiles.com/pdf...8045418010.jpg>)

## The Proper Rotation Operation

The proper rotation operation is a counter-clockwise rotation about a proper rotational axis by an angle of  $360^\circ$  over an integer number  $n$ . After that rotation the object must be indistinguishable from its original form. That means that the object after the rotation must superimpose the original object before the rotation. For example, when  $n=4$ , then we rotate around  $90^\circ$ , and after that the object must superimpose its original form. The proper rotational axis is the symmetry element associated with the proper rotation operation. It's Schoenflies symbol is  $C_n$ , whereby  $n$  is called the order of the rotational axis. A proper rotational operation has the symbol  $C_n^m$ , whereby  $m$  counts the number of times the operation is carried out. Overall we rotate by an angle of  $360^\circ \times m/n$  when we carry out an operation  $C_n^m$ . This means that when  $m=n$ , then we have rotated around  $360^\circ$  (Fig. 2.1.3). Then all points in the object are at their original position. It is as though we had done nothing with the object. We can also say we have reached the identity  $E$ . In mathematical form we can say that  $C_n^n = E$ . If we rotated one more time,  $C_n^{(n+1)}$ , then this would be equal to rotating only one time, and thus  $C_n^{(n+1)} = C_n^1$ . For example if  $n=4$ , then rotating four times around  $90^\circ$  will produce the identity. We have rotated around  $4 \times 90^\circ = 360^\circ$  which is the same as though we had not rotated at all, because all points in the object are in their original position after a  $360^\circ$  rotation. If we rotated 5 times around  $90^\circ$ , it would be the same as rotating only one time.

$$\begin{aligned} C_n^m &= 360^\circ \times \frac{m}{n} \\ C_n^n &= E \\ C_n^{n+1} &= C_n^1 \end{aligned}$$

Figure 2.1.3 Properties of the proper rotation operation

If an object has several axes with different order  $n$ , then the one with the highest order is called the *principal axis*. If there is more than one axis of the same order, then they get distinguished by primes if they are not conjugate. We will learn about the exact definition of conjugation somewhat later, we can however often see by inspection if two axes are conjugate. This is usually the case when they pass through the object in an equivalent way, and rotate the object in an equivalent way. Axes that pass through less many bonds, get less many primes. This is just a convention, but you have to follow it. An additional rule is that an axis which is in the same position as the principal axis gets the least number of primes. For example, a square planar molecule such as  $\text{PtCl}_4^{2-}$  has a  $C_4$  principal axis standing perpendicular to the square plane of the molecule. There is an additional  $C_2$  axis where the  $C_4$  axis runs. It is present because one can also rotate around  $180^\circ$ , and not only around  $90^\circ$ . This  $C_2$  axis does not get any prime. You can see that there are four additional  $C_2$  axes, two of them are denoted  $C_2'$ , and two others are denoted  $C_2''$ . You can see that the two axes which only have one prime pass through two Pt-Cl bonds, while the ones that have two primes, do not pass through any bonds. The two  $C_2'$  axes are conjugate, meaning that they transform the object in an equivalent way. The two  $C_2''$  axes are also conjugate.

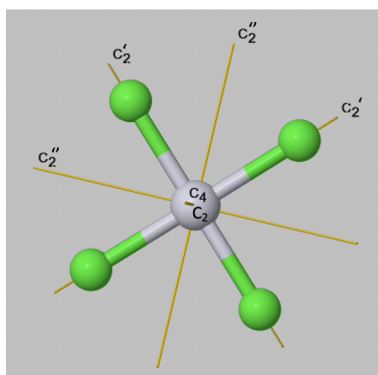


Figure 2.1.4 Proper rotational axes in the  $\text{PtCl}_4^{2-}$  molecular anion. (Attribution: symotter.org/gallery)

We can now think about how we can write out the axes and their associated proper rotational operations in a systematic way. Let us first look at the symmetry elements, the proper axes: We conventionally write the principal axis first, and then all other axes from their highest to their lowest order. When there are axes of the same order, those with the least number of primes get denoted first, and those with the highest number of primes last. If there are conjugate axes then their number is placed in front of their Schoenflies symbol. For the proper axes of the  $\text{PtCl}_4^{2-}$  the notation would therefore be:  $C_4, C_2, 2C_2', 2C_2''$ . Now let us see how to denote the rotation operations that are associated with these symmetry elements. The notation follows the same rules as for the symmetry elements. In addition, we have to consider that we must not count identical operations twice, we also do not denote the operations that are the same as the identity. For the  $C_4$  axis there are four operations until we reach the identity.  $C_4^1, C_4^2, C_4^3$ , and  $C_4^4$ . For each of the  $C_2, C_2'$ , and  $C_2''$  elements there are two operations until the identity is reached.  $C_2^1, C_2^2, C_2'^1, C_2'^2, C_2''^1, C_2''^2$ . The  $C_4^4$ , the  $C_2^2$ , the  $C_2'^2$ , and the  $C_2''^2$  are the same as the identity and therefore we do not consider them. In addition we can see that the  $C_4^2$  is the same as the  $C_2^1$ . This is because the  $C_4$  and the  $C_2$  axes are in the same location, and rotating two times around  $90^\circ$  is the same as rotating one time around  $180^\circ$ . By convention we eliminate the operation associated with the higher order, thus the  $C_4^2$ . The overall notation would then be:  $C_4^1, C_4^3, C_2^1, 2C_2'^1, 2C_2''^1$  (Fig. 2.1.5).

Rotation symmetry operations are:  $C_4^1, C_4^3, C_2^1, 2C_2'^1, 2C_2''^1$   
 $(C_4^4 = E, C_4^2 = C_2^1, C_2^2 = E, C_2'^2 = E, C_2''^2 = E)$

Figure 2.1.5 Proper rotation operations in  $\text{PtCl}_4^{2-}$

## The Reflection Operations ( $\sigma$ )

Let us look at reflection operations which are carried out around reflection planes, or mirror planes. Mirror planes have the Schoenflies symbol  $\sigma$ . When we carry out a reflection operation, then we move any point of the object to the other side of the mirror plane. There are two types of mirror planes, so-called horizontal mirror planes and vertical mirror planes. A horizontal mirror plane always stands perpendicular to the principal axis. For example in the depicted  $\text{BH}_3$  molecule there is a horizontal mirror plane that stands perpendicular to a  $C_3$  principal axis (Fig. 2.1.6). A horizontal mirror plane has the Schoenflies symbol  $\sigma_h$ .

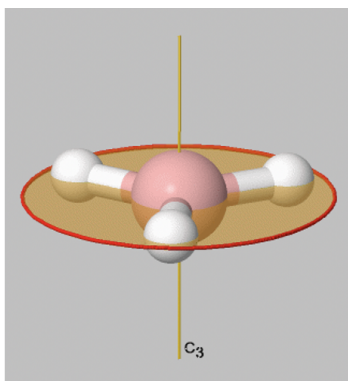


Figure 2.1.6 Visual depiction of the horizontal mirror plane of  $\text{BH}_3$ ,  $\sigma_h$  (Attribution: symotter.org/gallery)

A vertical mirror plane has the property that it contains the principal axis, this means that it is part of the principal axis. It is denoted  $\sigma_v$ . The  $\text{BH}_3$  molecule has three vertical axes that pass through the three B-H bonds. You can see that each of them contain

the principal  $C_3$  axis (Fig. 2.1.7). The three vertical mirror planes are conjugate, and therefore they are not distinguished by primes. We can write a coefficient 3 in front of the symbol  $\sigma_v$  to indicate that there are three conjugate vertical mirror planes.

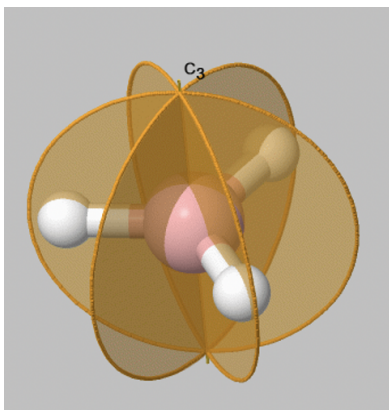


Figure 2.1.7 Visual depiction of the vertical mirror planes of  $BH_3$ , 3  $\sigma_v$  (Attribution: symotter.org/gallery)

Now let us look at how many symmetry operations are associated with a particular mirror plane. Fortunately, things are simple here: There is only one reflection operation associated with one mirror plane. This because reflecting two times at a mirror plane produces the identity  $E$ :  $\sigma_v^2 = E$ . More generally, when we reflect  $n$  times, and  $n$  is an even number then this is the same as the identity or,  $\sigma_v^n = E$  ( $n$  is even). When  $n$  is odd the reflecting  $n$  times is the same as reflecting only one time or,  $\sigma_v^n = \sigma_v^{-1}$  ( $n$ =odd).

The horizontal mirror plane of the  $BH_3$  molecule deserves an additional comment. Carrying out the horizontal reflection does not change the position of any atom. It is important to understand why the operation does exist despite the fact it does not change the position of any atom. The criterion is not whether the position of an atom is changed, but whether the position of the points in the object changes. In the case of the  $BH_3$  molecule the part of the molecule that is located above the mirror plane will be located below the mirror plane after the reflection operation has been carried out. Vice versa any part of the molecule that was formerly below the mirror plane will be located above the mirror plane after the reflection operation has been carried out. For example the lower half of the B atom will be above the mirror plane, and the half above the plane will be below the plane after the execution of the reflection operation.

Like non-conjugate proper rotations are distinguished by primes, also non-conjugate vertical mirror planes must be distinguished by primes. The smaller the number of bonds the vertical mirror plane contains, the larger the number of primes.

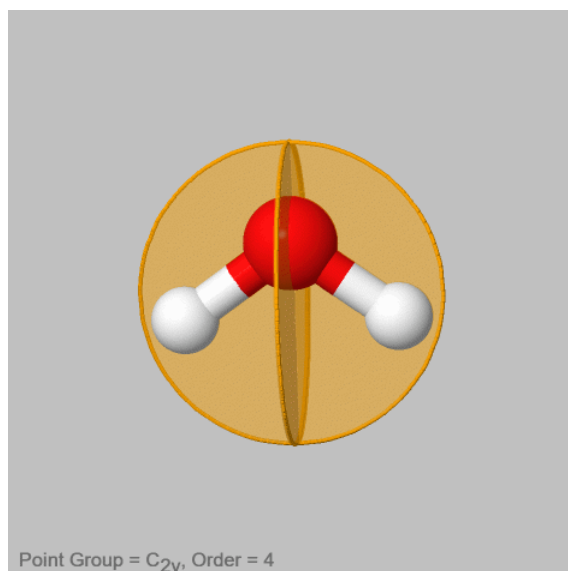


Figure 2.1.8 Non-conjugate vertical mirror planes of  $H_2O$  (Attribution: symotter.org/gallery)

For example in the water molecule (Fig. 2.1.8) there are two non-conjugate vertical mirror planes. One contains the two O-H bonds, the other stands perpendicular to the first mirror plane. It is easy to see that these two mirror planes will not move the points in the atom in an equivalent way, and therefore they are not conjugate. The first mirror plane does not change the position of any

atom, while the second one swaps the positions of the two hydrogen atoms. Therefore, the second mirror plane not containing any O-H bonds gets one prime the one that contains the O-H bonds do not get a prime.

### Dihedral Reflection Planes ( $\sigma_d$ )

A special case of a vertical mirror plane is a dihedral mirror plane, denoted  $\sigma_d$ . A dihedral mirror plane bisects the angle between two conjugate  $C_2$  axes.

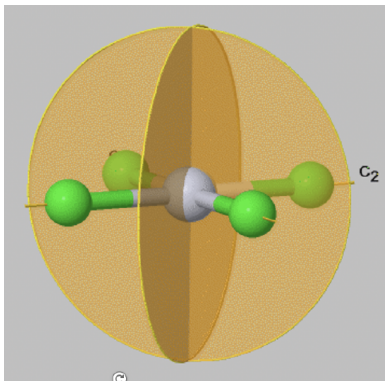


Figure 2.1.9 Dihedral mirror planes of  $\text{PtCl}_4^{2-}$  (Attribution: symotter.org/gallery)

For example, in the  $\text{PtCl}_4^{2-}$  anion (Fig. 2.1.9) there are two vertical mirror planes that bisect the angle between the two conjugate  $C_2$  axes that pass through the Pt-Cl bonds. Therefore, these mirror planes are vertical mirror planes  $\sigma_d$ .

### The Inversion Operation ( $i$ )

Let us look next at the inversion operation which is symbolized by a Schoenflies symbol  $i$ . The symmetry element associated with an inversion, is the inversion center, also called center of symmetry. It is a single point. When an inversion operation is performed, then each point of the object is moved through the inversion center to the other side. Each coordinate in the object ( $x,y,z$ ) is inverted into the coordinates ( $-x,-y,-z$ ).

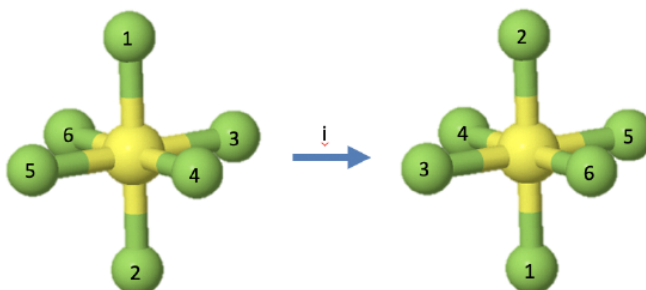


Figure 2.1.10 The inversion operation for  $\text{SF}_6$  (Attribution: symotter.org/gallery)

For example, the octahedral molecule  $\text{SF}_6$  has an inversion center in the center of the molecule (Fig. 2.1.10). When the inversion operation is carried out, then each fluorine atom is moved through the inversion center to the other side. This means that the fluorine atoms 1 and 2 swap up their positions, the fluorine atoms 3 and 5 swap up their positions, and so do the fluorine atoms 4 and 6. The sulfur atom does not change its position. There is only one inversion operation associated with each inversion center. Inverting two times, or more generally, an integer number of two times produces the identity. Inverting an odd number of times is the same as inverting one time.

### The Rotation-Reflection Operation ( $S_n$ )

The rotation-reflection operation  $S_n$  is the most complex symmetry operation. It is carried out in two steps. First, a rotation around an improper axis is carried out. The angle is determined by the order  $n$  of the improper axis, and is  $360^\circ/n$ . This axis is called improper, because the object does not need to superimpose the original object after the rotation. Achieving superposition requires the second step which is the reflection at a mirror plane that stands perpendicular to the improper axis. Only after the second step the operation is complete. The presence of the rotation-reflection does not require a proper rotational axis or a regular mirror plane  $\sigma$  to exist, however it also do not preclude their existence.

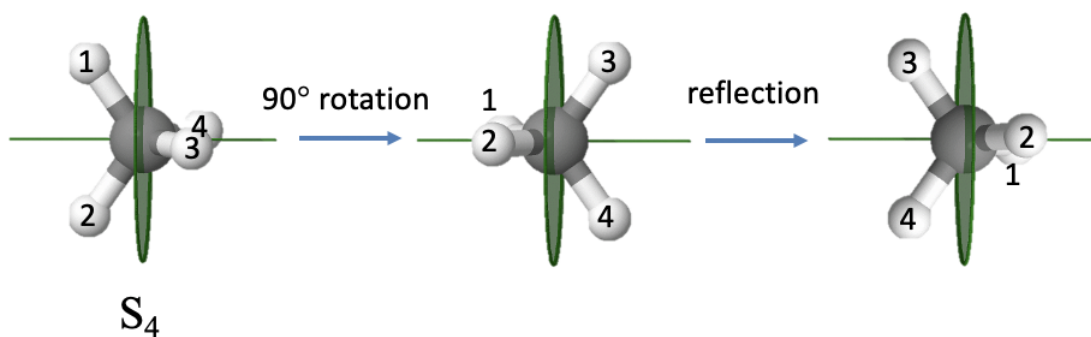


Figure 2.1.11 The improper  $S_4$  rotation for  $\text{CH}_4$  (Attribution: symotter.org/gallery)

An example of a molecule with an improper axis is the methane molecule (Fig. 2.1.11). It has an  $S_4$  improper axis. The axis bisects the H-C-H tetrahedral bond angle. The order of the axis is four which requires that we rotate by  $90^\circ$  around this axis. You can see that after we carry out the rotation, the molecule does not superimpose the original molecule. Only after we reflect the rotated molecule at a mirror plane standing perpendicular to the improper axis the molecule superimposes the original molecule.

### Properties of the Rotation-Reflection Operation ( $S_n$ )

The rotation-reflection has a number of interesting properties. One of the them is that an  $S_1$  operation is the same as a reflection. This is because the order 1 implies a rotation around  $360^\circ$  which produces the identity, and all points within the object are in their original position. This is the same as though we had not rotated at all. This means actually we only did the second step, the reflection, and therefore the  $S_1$  is identical to a “regular” reflection. The second property is that an  $S_2$  operation is the same as an inversion. When you rotate around  $180^\circ$  and then reflect perpendicular to the improper axis of rotation, the positions of the points in the object change exactly the same way as they do when you invert through an inversion center.

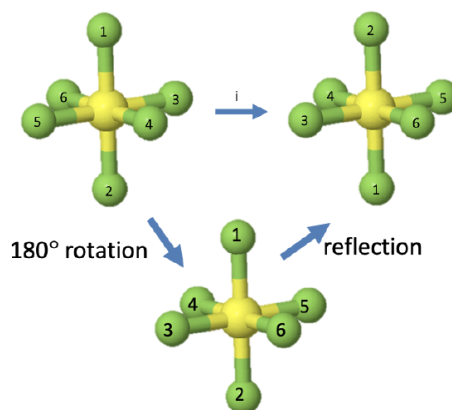


Figure 2.1.12 Rotation-Reflection operations for  $\text{SF}_6$  (Attribution: symotter.org/gallery)

Look for example at the  $\text{SF}_6$  molecule again (Fig. 2.1.12) which has an inversion center in the center of the atom. We previously saw that when we carry out the inversion, the atoms 1 and 2 swap their position, and so do the atoms 3 and 5, as well as the atoms 4 and 6. Let us carry out the rotation-reflection, and see if the atoms change the same way. Firstly we rotate  $180^\circ$  around an axis that goes through the atoms 1 and 2. This leaves the positions of the atoms 1 and 2 unchanged, but swaps up the positions of the atoms 3 and 5, as well as the atoms 4 and 6. Next we must do a reflection at a plane that stands perpendicular to the improper axis. It is the plane defined by the atoms 3, 4, 5, and 6. Reflection at this plane does not change the positions of the atoms 3, 4, 5, and 6, but it swaps up the positions of the atoms 1 and 2, which lie above and below the plane, respectively. We can see that the positions of the atoms are the same as after the inversion.

The fact that we can express a reflection by an  $S_1$  rotation-reflection, and an inversion by a  $S_2$  rotation-reflection means that the reflection and the inversion are not independent symmetry operations, and we would not need them. The symmetry of an object could be fully described by the identity, proper rotations, and rotation-reflections. However, by convention, we use reflections and inversions instead of  $S_1$  and  $S_2$ , simply because it is easier for the human mind to perform 1-step operations, rather than 2-step operations.

Improper rotations have different properties depending on whether the order of the axis is even or odd. For even orders, the presence of an  $S_n$  improper rotational axis implies that there must also be a proper rotational axis with an order  $n/2$ . For improper

axes of even orders  $n$  the identity is produced after  $n$  rotation-reflections (Fig. 2.1.13).

$S_n$  with  $n$  even  $\rightarrow$  molecule contains  $C_{n/2}$

$$S_n^n = E$$

Figure 2.1.13 Properties of improper rotations with even order  $n$

For improper axes of odd order  $n$ , carrying out the rotation-reflection  $n$  times is the same as carrying out a reflection at a horizontal mirror plane. We need to do the rotation-reflection  $2n$  times to reach the identity (Fig. 2.1.14).

$S_n$  with  $n$  odd  $\rightarrow$  molecule contains  $C_n$  and  $\sigma_h$

$$S_n^n = \sigma_h$$

$$S_n^{2n} = E$$

Figure 2.1.14 Properties of improper axes of odd order  $n$

### Rotation-Reflections of $PF_5$ (an example with odd order)

Let us show these properties using two examples. Let us first look at an example with an improper rotation of odd order. The  $PF_5$  molecule has trigonal bipyramidal shape with three F atoms in the equatorial plane, and two additional F atoms above and below the plane. The F atoms have been numbered from 1 to 5 as indicated by the subscripts that follow the element symbol (Fig. 2.1.15). The  $PF_5$  has an improper rotational axis  $S_3$  that stands perpendicular to the equatorial plane going through the P-F<sub>1</sub> and P-F<sub>2</sub> bonds. Let us carry out the  $S_3$  symmetry operations step by step and see how the atoms move.

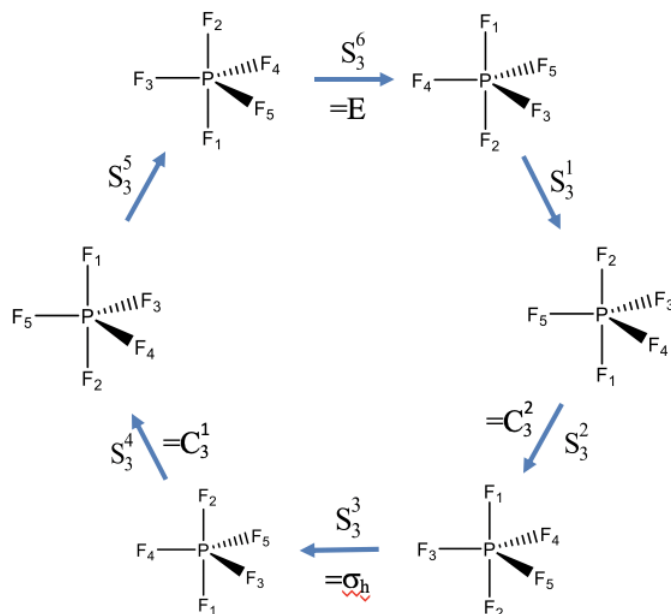


Figure 2.1.15  $S_3$  symmetry operations for  $PF_5$

We would expect that after we carry out the operation six times the identity will be produced. After three rotation-reflections we would expect that the object has been moved the same way a horizontal mirror plane would do. After the first rotation-reflection the atoms F<sub>1</sub> and F<sub>2</sub> have swapped their positions, and the three F atoms in the equatorial plane have been rotated by 120 degrees counter-clockwise. The F<sub>5</sub> atom now occupies the position of the F<sub>4</sub>, the F<sub>4</sub> has been rotated into the position of the F<sub>3</sub>, and the F<sub>3</sub> has been moved into the position of the F<sub>5</sub>. The second  $S_3$  operation again swaps up the F<sub>2</sub> and F<sub>1</sub> atoms, and rotates the remaining F atoms by 120°. Now the F<sub>5</sub> atoms points toward us, the F<sub>4</sub> atom points away from us, and the F<sub>3</sub> atoms is in the paper plane. Carrying out the operation a third time again swaps the F<sub>1</sub> and F<sub>2</sub> and rotates F<sub>3</sub>, F<sub>4</sub>, and F<sub>5</sub> counter-clockwise by 120°. Now let us compare the position of the atoms with the atom positions of the molecule we started with. We see that the position of the equatorial F atoms are same as in the beginning, but the position of the axial F<sub>1</sub> and F<sub>2</sub> atoms have been swapped up. This is equivalent to a reflection at a horizontal mirror plane located within the equatorial plane. This horizontal mirror plane would only swap up the axial F atoms, but would not move the equatorial ones. The  $S_3^4$  operation again swaps up the position of the F<sub>1</sub> and the F<sub>2</sub> atoms, and rotates the equatorial F atoms by 120° counter-clockwise. Now, F<sub>4</sub> points toward us, F<sub>3</sub> points away, and F<sub>5</sub> is in the paper plane. After the fifth rotation-reflection F<sub>1</sub> and F<sub>2</sub> are again swapped so that F<sub>1</sub> is below and F<sub>2</sub> is above the equatorial plane.



The atoms  $F_3$ ,  $F_4$  and  $F_5$  are rotated so that  $F_3$  is in the paper plane,  $F_5$  points toward us, and  $F_4$  points away from us. The sixth rotation-reflection again swaps up  $F_1$  and  $F_2$ , and rotates the other F atoms around  $120^\circ$  counter-clockwise. We can now see that the produced molecule is the same as the one we started with, and the identity has been produced.

It is also noteworthy that the  $S_3^2$  and the  $S_3^4$  operation can be expressed by simpler operations, namely  $C_3^2$  and  $C_3^1$  proper rotation operations. We can understand this considering that an  $S_3^2$  operation requires that we reflect two times, and reflecting two times is just like not reflecting at all. So effectively, we only have two rotations around  $120^\circ$  which is equivalent to  $C_3^2$ . Similarly, the  $S_3^4$  operation requires to reflect four times, which is the same as not reflecting at all. Thus, effectively, we only rotate four times around  $120^\circ$ . This is the same as rotating only one time around this angle, which is equivalent to a  $C_3^1$  operation.

Using similar considerations, we can also understand why the  $S_3^3$  operation is equivalent to a  $\sigma_h$ . In this case, we rotate  $3 \times 120^\circ = 360^\circ$ , and rotating around  $360^\circ$  is the same as not rotating at all. In addition, we carry out a reflection three times. Reflecting an odd number of times is the same as reflecting only one time. Thus overall, we effectively carry out a single reflection only.

Overall, only the  $S_3^1$  and the  $S_3^5$  operations are unique, all others can be expressed by other, simpler operations.

### Rotation-Reflections of $CH_4$ (an example with even order)

Let us illustrate the properties of an improper rotational axis with even order using the example methane (Fig. 2.1.16).

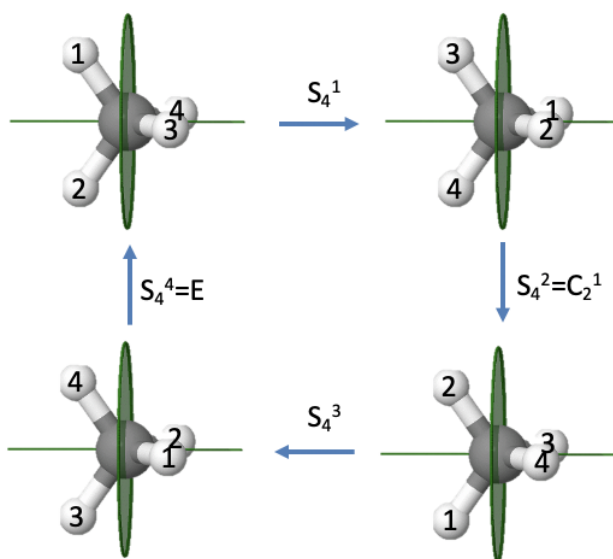


Figure 2.1.16  $S_4$  symmetry operations for  $CH_4$  (Attribution: symotter.org/gallery)

We previously saw that the methane molecule has an  $S_4$  improper axis. Executing the symmetry operation once moves the H atoms 1 and 2 to the right, whereby atom 1 points to the back and atom 2 points to the front. After the second rotation-reflection the atoms 1 and 2 are reflected back to the left side, but because we have rotated two times by  $90^\circ$  atom 2 points up, and atom 1 points down. Similarly, atoms 3 and 4 are reflected back to the right side, but atom four points toward us and atom 3 points to the back. After three rotation-reflections, the atoms 1 and 2 are again on the right side with atom 2 pointing to the back and atom 1 pointing to the front. Atoms 3 and 4 are on the left with atom 4 pointing up, and atom 3 pointing downward. After the operation is carried out four times, all atoms are back in their original position, meaning the identity has been produced. This is what we expected for an improper rotation of even order. We can see in addition that the  $S_4^2$  operation is the same as an  $C_2$  operation. Rotating two times about  $90^\circ$  is the same as rotating about  $180^\circ$ . Reflecting two times is the same as not reflecting at all. Therefore, effectively, we only rotated by  $180^\circ$  which is the same as what a  $C_2^1$  operation does. Because an  $S_4^2$  can be expressed by a  $C_2^1$ , and an  $S_4^4$  is the same as the identity, only the  $S_4^1$  and the  $S_4^3$  are unique symmetry operations.

### The Symmetry of a Molecule

We have now discussed all types of symmetry elements and operations that can exist in an object. Next, let us think about how we can define the overall symmetry of an object. The **overall symmetry** of an object is defined as the sum of all the symmetry operations for this object. If two objects have exactly the same symmetry elements and operations then their symmetry is the same. Using the mathematical language of group theory, the mathematical theory for symmetry, we can say they belong to the same point group. The name point group comes from the fact, that it has at least one invariant point. The number of symmetry operations

belonging to a point group is called the order of the point group. Let us see next what different point groups we know and how we can systematically classify them.

---

Dr. Kai Landskron ([Lehigh University](#)). If you like this textbook, please consider to make a donation to support the author's research at Lehigh University: [Click Here to Donate](#).

---

This page titled [3.1.1: Definitions and Examples](#) is shared under a [CC BY 4.0](#) license and was authored, remixed, and/or curated by [Kai Landskron](#).

- [2.1: Symmetry Elements and Operations](#) by Kai Landskron is licensed [CC BY 4.0](#).



## 3.2: Point Groups

---

Learning objectives for this unit are to:

- Identify which symmetry elements are possessed by a molecule or other object and use this information to assign the molecule or object to a point group
  - Use point groups to determine polarity and chirality of molecules
- 

3.2: Point Groups is shared under a [not declared](#) license and was authored, remixed, and/or curated by LibreTexts.

## 3.2.1: Molecular Point Groups

### Introduction

In group theory, molecules or other objects can be organized into point groups based on the type and number of symmetry operations they possess. Every molecule in a point group will have all of the same symmetry operations as any other molecule in that same point group. The most common, and chemically relevant point groups are described below.

### The Low Symmetry Point Groups

#### $C_1$ Point Group

Overall, we divide point groups into three major categories: High symmetry point groups, low symmetry point groups, dihedral point groups, and rotational point groups. Let us begin with the low symmetry point groups. As the name says, these point groups only have few symmetry elements and operations. The point group  $C_1$  is the point group with the lowest symmetry. Molecules that belong to this point group only have the identity as symmetry element.

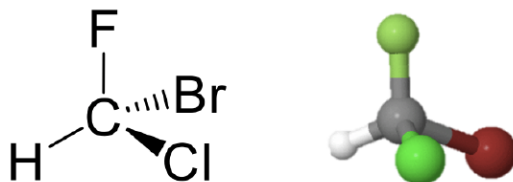


Figure 3.2.1.1  $C_1$  point group of bromochlorofluoromethane (Attribution: symotter.org/gallery)

An example is the bromochlorofluoromethane molecule (Figure 3.2.1.1). It has no symmetry element except the identity ( $E$ ). The name  $C_1$  comes from the symmetry element  $C_1$ . A  $C_1$  operation is the same as the identity.

#### $C_s$ Point Group

The point group  $C_s$  has a mirror plane in a addition to the identity. An example is the 1,2-bromochloroethene molecule (Figure 3.2.1.2).

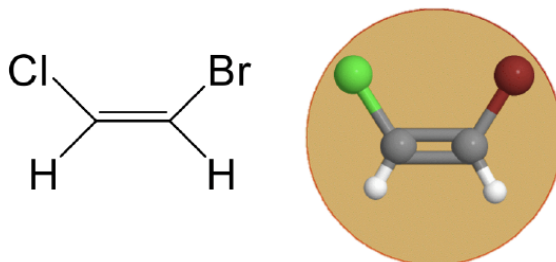


Figure  
3.2.1.2  
 $C_s$   
point group of 1,  
2-bromochloroethene  
(Attribution:  
symotter.org/gallery  
)

This is a planar molecule and the mirror plane is within the plane of the molecule. This mirror plane does not move any atoms when the reflection operation is carried out, nonetheless it exists because any point of the molecule above the mirror plane will be found below the mirror plane after the execution of the operation. Vice versa, any point below the mirror plane will be above the mirror plane. This mirror plane does not have a vertical or horizontal mirror plane designation because no proper rotational axes exist.

### $C_i$ Point Group

The point group  $C_i$  has the inversion as the only symmetry element besides the identity. The point group  $C_i$  is sometimes also called  $S_2$  because an  $S_2$  improper rotation-reflection is the same as an inversion. An example is the 1,2-dibromo 1,2-dichloro ethane (Figure 3.2.1.3).

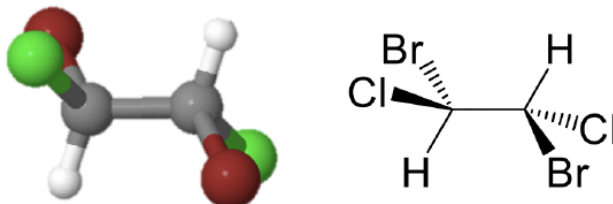


Figure 3.2.1.3 The  $C_i$  point group: 1,2-dibromo-1,2-dichloroethane (Attribution: symotter.org/gallery)

This molecule looks quite symmetric, but it has inversion center in the middle of the carbon-carbon bond as the only symmetry element. Upon execution of the inversion operation, the two carbons swap up their positions, and so do the two bromine, the two chlorine, and the two hydrogen atoms.

### The High Symmetry Point Groups

The symmetry elements of the high symmetry point groups can be more easily understood when the properties of platonic solids are understood first. Platonic solids are polyhedra made of regular polygons. In a platonic solid all faces, edges, and vertices (corners) are symmetry-equivalent. We will see that this is a property that can be used to understand the symmetry elements in high symmetry point groups. There are only five possibilities to make platonic solids from regular polygons (Figure 3.2.1.4).


 File:Platonic Solids Transparent.svg

Figure 3.2.1.4 The platonic solids (Attribution: Drummyfish [CC0] [https://commons.wikimedia.org/wiki/File:Platonic\\_Solids\\_Transparent.svg](https://commons.wikimedia.org/wiki/File:Platonic_Solids_Transparent.svg))

The first possibility is to construct a tetrahedron from four regular triangles. The second platonic solid is the octahedron made of eight regular triangles. The third possibility is the icosahedron made of twenty triangles. In addition, six squares can be connected to form a cube, and twelve pentagons can be connected to form a dodecahedron. There are no possibilities to connect other regular polygons like hexagons to make a platonic solid.

### The $T_d$ Point Group

The tetrahedron, as well as tetrahedral molecules and anions such as  $CH_4$  and  $BF_4^-$  belong to the high symmetry point group  $T_d$  (Note that only tetrahedral molecules where all four outer atoms/groups are the same will be in the  $T_d$  point group). Let us find the symmetry elements and symmetry operations that belong to the point group  $T_d$ . First, we should not forget the identity operation,  $E$ . Next, it is useful to look for the principal axes.

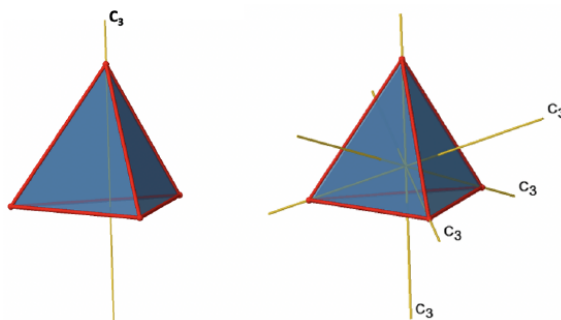


Figure 3.2.1.5 The  $C_3$  axes in a tetrahedron (Attribution: symotter.org/gallery)

The tetrahedron has four principal  $C_3$  axes (Figure 3.2.1.5). It is a property of the high-symmetry point groups that they have more than one principal axis. The  $C_3$  axes go through the vertices of the tetrahedron. Because each  $C_3$  axis goes through one vertex, there are four vertices, and we know that in a platonic solid all vertices are symmetry-equivalent, we can understand that there are four  $C_3$  axes. How many unique  $C_3$  operations are associated with these axes? After three rotations around  $120^\circ$  we reach the identity. Therefore  $C_3^3=E$ , and we only need to consider the  $C_3^1$  and the  $C_3^2$  rotation about  $120$  and  $240^\circ$  respectively. Because there are four  $C_3$  axes, there are four  $C_3^1$  and four  $C_3^2$  operations and eight  $C_3$  operations overall. In addition to the  $C_3$  axes there are  $C_2$  axes (Figure 3.2.1.6).

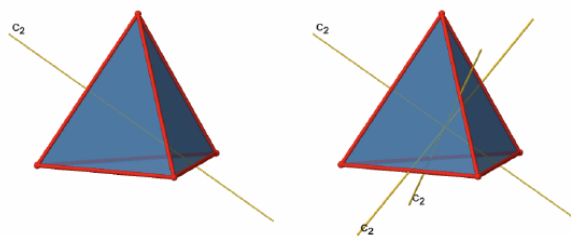


Figure 3.2.1.6 The  $C_2$  axes in a tetrahedron belonging to the point group  $T_d$  (Attribution: symmotter.org/gallery)

You can see that a  $C_2$  axis goes through two opposite edges in the tetrahedron. Because a tetrahedron has six edges, and each  $C_2$  axis go through two edges there are  $6/2=3$   $C_2$  axes. There is only one  $C_2$  symmetry operation per  $C_2$  axis because we produce the identity already after two rotations. Therefore there are three  $C_2^1$  operations overall.

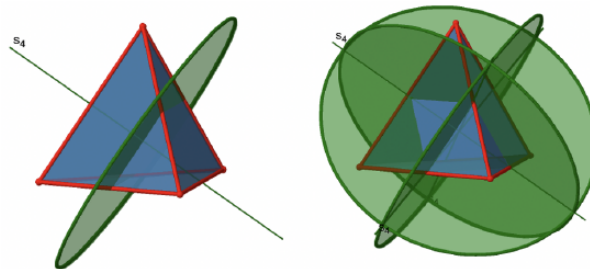


Figure 3.2.1.7 The  $S_4$  axes in a tetrahedron (Attribution: symmotter.org/gallery)

In addition, the  $T_d$  point group has  $S_4$  improper rotation reflections. Like the  $C_2$  axes, they pass through the middle of two opposite edges. This also means that they are superimposing the  $C_2$  axes. Because there are six edges, and two  $S_4$  axes per edge there are  $6/2=3$   $S_4$  axes (Figure 3.2.1.7). How many operations are associated with these  $S_4$  axes? The order of the axes are even, and therefore we need four  $S_4$  operations to produce the identity. The  $S_4^2$  operation is the same as a  $C_2^1$  operation because reflecting two times is equivalent to not reflecting at all, and rotating two times by  $90^\circ$  is the same as rotating about  $180^\circ$ . Therefore overall, only  $S_4^1$  and  $S_4^3$  operations are unique operations.  $S_4^2$  and  $S_4^4$  can be expressed by the simpler operations  $C_2^1$  and  $E$  respectively. Because there are 3  $S_4$  axes, there are three  $S_4^1$  and three  $S_4^3$  operations. Overall there are six  $S_4$  operations.

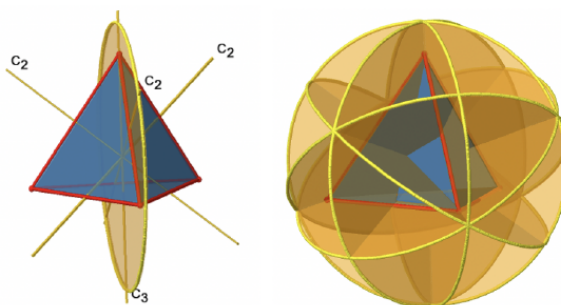


Figure 3.2.1.8 The mirror planes and  $C_2$  axes in a tetrahedron belonging to the point group  $T_d$  (Attribution: symmotter.org/gallery)

There are also mirror planes (Figure 3.2.1.8). The planes contain a single edge of the tetrahedron, thereby bisecting the tetrahedron. There are six edges in a tetrahedron, and therefore there are  $6/1=6$  mirror planes. These planes are dihedral planes because each plane contains a  $C_3$  principal axis and bisects the angle between two  $C_2$  axes. Overall, there are three  $C_2$  axes and three  $C_2$  operations. There is one reflection operation per mirror plane because reflecting two times produces the identity. Therefore, there are six  $\sigma_d$  reflection operations.

#### 📌 Symmetry Operations in the $T_d$ Point Group

Every molecule or object in the  $T_d$  point group has the following symmetry operations:

- $E$ , 8  $C_3$ , 3  $C_2$ , 6  $S_4$ , and 6  $\sigma_d$

### The Octahedral Point Group $O_h$

Another high symmetry point group is the point group  $O_h$ . Both the octahedron as well as the cube belong to this point group despite their very different shape Figure 3.2.1.9 Because they belong to the same point group they must have the same symmetry elements and operations. There are many octahedrally shaped molecules, such as the  $SF_6$ .

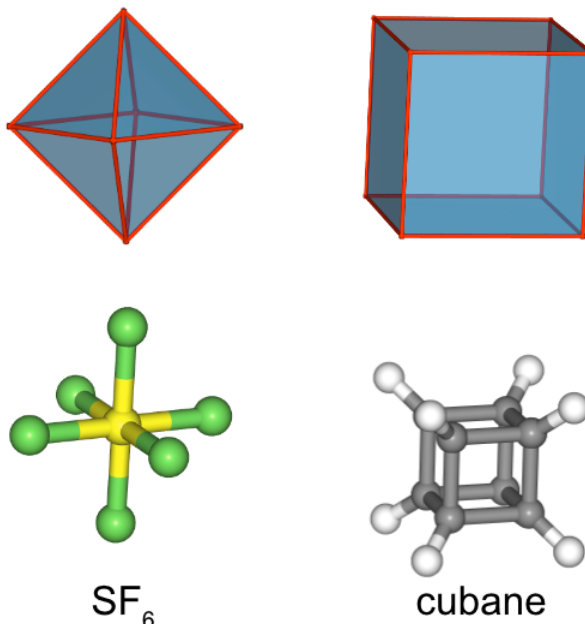


Figure 3.2.1.9:  $SF_6$  and cubane with cubic and octahedral shape, respectively, belong to the point group  $O_h$  (Attribution: symmotter.org/gallery)

Molecules with cubic shapes are far less common, because a cubic shape often leads to significant strain in the molecule. An example is cubane  $C_8H_8$ . Let us determine the symmetry elements and operations for the point group  $O_h$  using the example of the octahedron. If we used the cube, we would get exactly the same results.

There are three  $C_4$  principal axes in the octahedron. They go through two opposite vertices of the octahedron (Figure 3.2.1.10). There are three  $C_4$  axes because an octahedron has six vertices which are all symmetry-equivalent because the octahedron is a platonic solid.

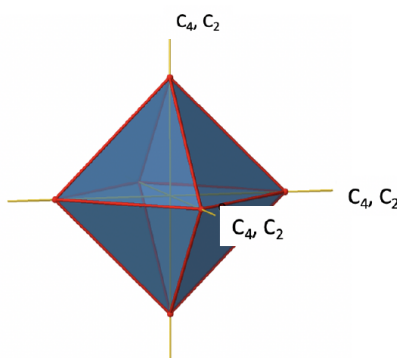


Figure 3.2.1.10: The  $C_4$  and  $C_2$  axes in the octahedral point group  $O_h$  (Attribution: symmotter.org/gallery)

We can see that there are also  $C_2$  axes where the  $C_4$  axes run. This is because rotating two times around  $90^\circ$  is the same as rotating around  $180^\circ$ . What are the symmetry operations associated with these symmetry elements? Rotating four times around  $90^\circ$  using the  $C_4$  axes produces the identity. So we have to consider the operations  $C_4^1$ ,  $C_4^2$ ,  $C_4^3$  and  $C_4^4$ . How many of these are unique?  $C_4^4$  is the same as the identity, so it is not unique. In addition a  $C_4^2$  is identical to a  $C_2^1$ , and thus  $C_4^2$  is also not unique, and can be expressed by the simpler operation  $C_2^1$ . That leaves the  $C_4^1$  and the  $C_4^3$  as the only unique symmetry operations. Because we have

three  $C_4$  axes, there are  $2 \times 3 = 6$   $C_4$  operations, in detail there are  $3C_4^1$  and three  $C_4^3$  operations. In addition, there are the three  $C_2^1$  operations belonging to the three  $C_2$  axes.

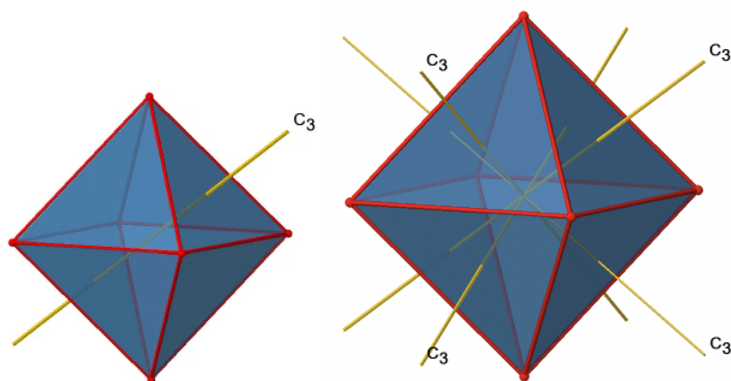


Figure 3.2.1.11: The  $C_3$  axes in the octahedral point group  $O_h$  (Attribution: symmotter.org/gallery)

In addition, there are four  $C_3$  axes (Figure 3.2.1.11). They are going through the center of two opposite triangular faces of the octahedron. You see above a single  $C_3$  axis, and on the right hand side all four of these axes. How can we understand that there are four axes? An octahedron has overall eight triangular faces, and each  $C_3$  axis goes through two opposite faces, so there are  $8/2 = 4$   $C_3$  axes. Each  $C_3$  axis has the  $C_3^1$  and the  $C_3^2$  as unique symmetry operations. The  $C_3^3$  is the same as the identity. So overall we have  $4 \times 2 = 8$  operations, four of them are  $C_3^1$ , and four of them are  $C_3^2$ .

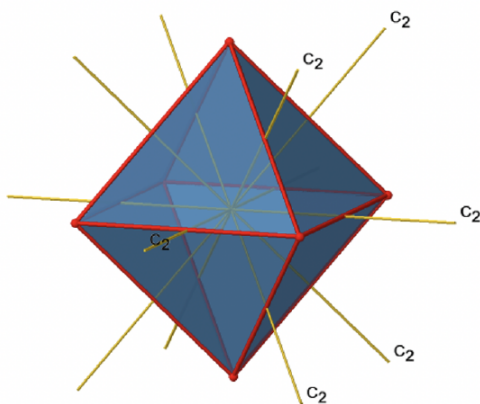


Figure 3.2.1.12: The  $C_2'$  axes in the octahedral point group  $O_h$  (Attribution: symmotter.org/gallery)

In addition to the  $C_2$  axes that superimpose the  $C_4$  axes, there are  $C_2'$  axes which go through two opposite edges of the octahedron (Figure 3.2.1.12). How many of them are there? An octahedron has twelve edges, and because each  $C_2'$  passes through two edges, there must be  $12/2 = 6$   $C_2'$  axes. These axes have primes because they are not conjugate to the  $C_2$  axes that superimpose the  $C_4$  axes. For each  $C_2'$  axis there is only the  $C_2'^1$  as the unique symmetry operation, and therefore there are overall 6  $C_2'^1$  symmetry operations.

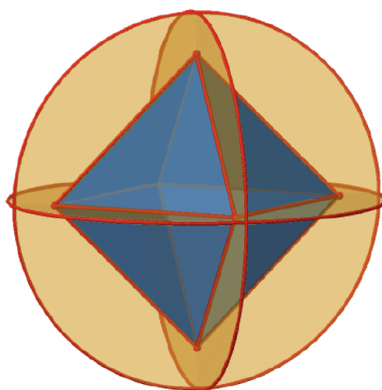


Figure 3.2.1.13: The horizontal mirror planes in the octahedral point group  $O_h$  (Attribution: symotter.org/gallery)

Let us look at the horizontal mirror planes next (Figure 3.2.1.13). There are horizontal mirror planes that stand perpendicular to the  $C_4$  principal axes. Note that this mirror plane also contains two axes, in addition to the one to which it stands perpendicular. Because it contains two principal  $C_4$  axes, it has also properties of a vertical mirror plane. Nonetheless, we call it a horizontal mirror plane because it stands perpendicular to the third  $C_4$ . The horizontal properties trump the vertical ones, so to say. You can see that a single mirror plane contains four edges of the octahedron. Because there are twelve edges, there are  $12/4=3$  horizontal mirror planes. There is one mirror plane per principal  $C_4$  axis. There are three horizontal reflection operations because there is always only one reflection operation per mirror plane

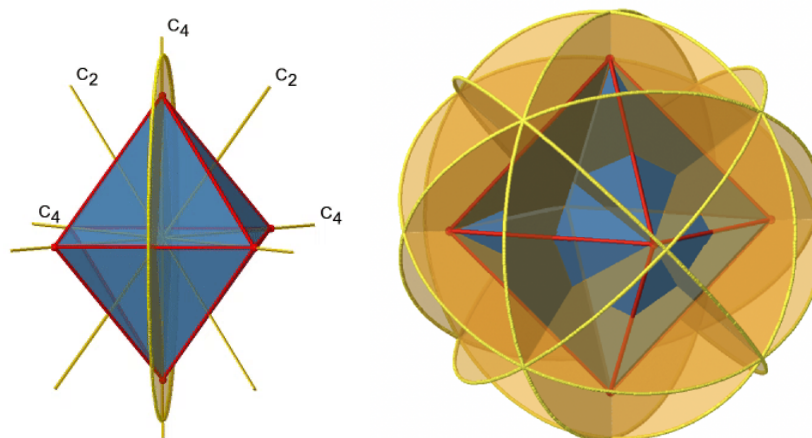


Figure 3.2.1.14: The vertical mirror planes in the octahedral point group  $O_h$  (Attribution: symotter.org/gallery)

Next let us look for vertical mirror planes (Figure 3.2.1.14). You can see that - contrast to the horizontal mirror planes - it does not contain any edges. Rather, it cuts through two opposite edges. You can see that this plane contains a  $C_4$  axis, but it does not stand perpendicular to the other two  $C_4$  axes. Therefore it has only the properties of a vertical mirror plane. You can see however, that the mirror plane bisects the angle between two  $C_2'$  axes which also depicted. This makes the vertical mirror planes dihedral mirror planes,  $\sigma_d$ . How many of them do we have? As previously mentioned, each mirror plane cuts through two opposite edges. There are twelve edges in an octahedron, and thus there are  $12/2=6$  dihedral mirror planes. You can see all of them on the right side of Figure 3.2.1.14 Each mirror plane is associated with one reflection operation, therefore there are six dihedral reflection operations.

Next we can ask if the point group  $O_h$  has an inversion center? Yes, there is one in the center of the octahedron (Figure 3.2.1.15)!



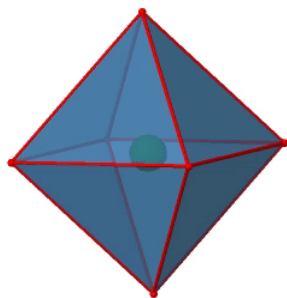


Figure 3.2.1.15: The inversion center of the octahedral point group  $O_h$  (Attribution: symotter.org/gallery)

Each point in the octahedron can be moved through the inversion center to the other side, and the produced octahedron will superimpose the original one. There is always one inversion operation associated with an inversion center.

Next, let us look for improper rotations. You can see an  $S_6$  improper rotation operation below (Figure 3.2.1.16 left).

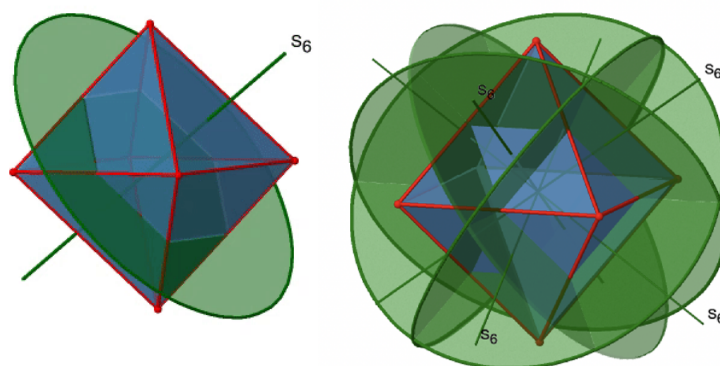


Figure 3.2.1.16: The  $S_6$  improper rotation element of the octahedral point group  $O_h$  (Attribution: symotter.org/gallery)

The improper  $S_6$  axis passes through the centers of two opposite triangular faces. One can see that rotation about  $60^\circ$  alone does not make the octahedron superimpose. The reflection at a plane perpendicular to the improper axis is required to achieve superposition. Overall, the rotation-reflection swaps up the position of the two opposite triangular faces. How many  $S_6$  improper axes are there? Since each  $S_6$  passes through two faces, and an octahedron has 8 faces there must be  $8/2=4$   $S_6$  axes. You can see all of them above (Fig. 2.2.31, right). Note that they are in the same position as the  $4C_3$  axes we previously discussed. How many unique operations are associated with them? For an  $S_6$  axis we need to consider operations from  $S_6^1$  to  $S_6^6$ .  $S_6^6$  is the same as the identity so it is not unique. The  $S_6^2$  is the same as a  $C_3^1$  because rotating two times round  $60^\circ$  is the same as rotating around  $120^\circ$ , and reflecting twice is the same as not reflecting at all. Similarly, an  $S_6^4$  is the same as a  $C_3^2$ . Rotating four times by  $60^\circ$  is the same as rotating two times by  $120^\circ$  and reflecting four times is the same as not reflecting at all. Further, an  $S_6^3$  is the same as an inversion. After three  $60^\circ$  rotations we have rotated by  $180^\circ$ . If we reflect after that, then this is the same as an  $S_2^1$  operation which is the same as an inversion. Therefore, only the  $S_6^1$  and the  $S_6^5$  operations are unique, all other operations can be expressed by simpler operations.



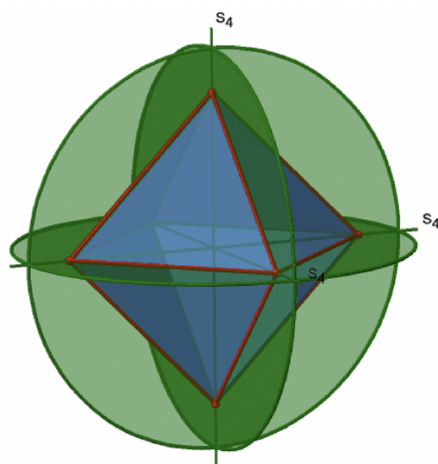


Figure 3.2.1.17: The  $S_4$  improper axis of the octahedral point group  $O_h$  (Attribution: symotter.org/gallery)

The octahedron also has  $S_4$  improper axes, and you can see one of them in Figure 3.2.1.17, right). It goes through two opposite corners of the octahedron. The  $S_4$  improper axis seemingly does the same as the  $C_4$  axis that goes through the same two opposite vertices, but actually does not. While rotating around  $90^\circ$  already makes the octahedron superimpose with its original form, executing the reflection operation after the rotation swaps up the position of the two vertices, and generally all points of the octahedron above and below the plane, respectively. Overall the  $S_4$  moves the points within the object differently compared to the  $C_4$  which makes it an additional, unique symmetry element. There are overall three  $S_4$  improper axes because the octahedron has six vertices and one  $S_4$  passes through two vertices.

#### Symmetry Operations in the $O_h$ Point Group

Every molecule or object in the  $O_h$  point group has the following 48 symmetry operations:

- E, 8  $C_3$ , 6  $C_2$ , 6  $C_4$ , 3  $C_2$  ( $C_4^2$ ), i, 6  $S_4$ , 8  $S_6$ , 3  $\sigma_h$ , and 6  $\sigma_d$

#### The $I_h$ Point Group

The two remaining platonic solids, the icosahedron and the dodecahedron, belong both to the icosahedral point group  $I_h$ . This is despite they are made of different polygons. Because they belong to the same point group, they have exactly the same symmetry operations. An example for a molecule with icosahedral shape is the molecular anion  $B_{12}H_{12}^{2-}$ . Examples of molecules with dodecahedral shape include dodecahedrane ( $C_{20}H_{20}$ ) and buckminsterfullerene ( $C_{60}$ ). Let us determine the symmetry elements and symmetry operations for the example of the icosahedron. We could also use the dodecahedron, and the results would be the same. The principal axes of the icosahedron are the  $C_5$  axes. You can see one of them, going through the center of the pentagon comprised of five triangular faces below (Figure 3.2.1.18).

Figure 3.2.1.18: One of the  $C_5$  axes of the icosahedron stands perpendicular to the paper plane going through the center of a pentagon of the icosahedron (Attribution: symotter.org/gallery)

You can understand that there is a  $C_5$  when considering that there are five triangular faces making a pentagon. The  $C_5$  axis sits in the center of the pentagon. We can see that when we rotate around this  $C_5$  axis, then the produced icosahedron superimposes the original one. The  $C_5$  axis goes through two opposite vertices of the icosahedron. Because an icosahedron has 12 vertices, there must be six  $C_5$  axes overall. You can see all of them below (Figure 3.2.1.19). There are four unique symmetry operations associated with a single  $C_5$  axis, namely the  $C_5^1$ , the  $C_5^2$ , the  $C_5^3$ , and the  $C_5^4$ . The  $C_5^5$  is the same as the identity. Because there are six  $C_5$  axes, there are overall  $6 \times 4 = 24$   $C_5$  symmetry operations.

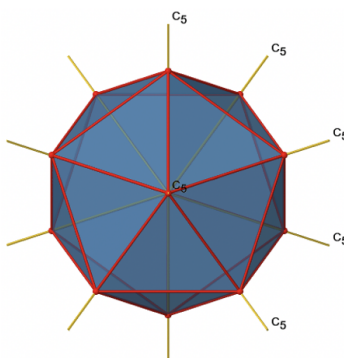


Figure 3.2.1.19: The  $C_5$  axes of the icosahedron (Attribution: symotter.org/gallery)

Figure 3.2.1.20: One of the  $C_3$  axes of the icosahedral point group (Attribution: symotter.org/gallery)

In addition, there are  $C_3$  axes. One of them is shown below, and you can see that it passes through the centers of two opposite triangular faces (Figure 3.2.1.20). As one rotates by  $120^\circ$  the atoms on the triangular faces change their position, and the resulting icosahedron superimposes the original one. As the name icosahedron says, there are twenty faces overall.

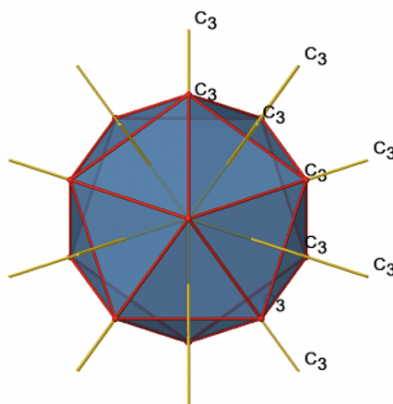


Figure 3.2.1.21: The  $C_3$  axes of the icosahedral point group (Attribution: symotter.org/gallery)

Because one  $C_3$  passes through two opposite axes, there are  $20/2=10$   $C_3$  axes overall (Figure 3.2.1.21). Each  $C_3$  axis is associated with two symmetry operations, namely  $C_3^1$ , and  $C_3^2$ . Thus, there are overall  $10 \times 2 = 20$   $C_3$  symmetry operations.

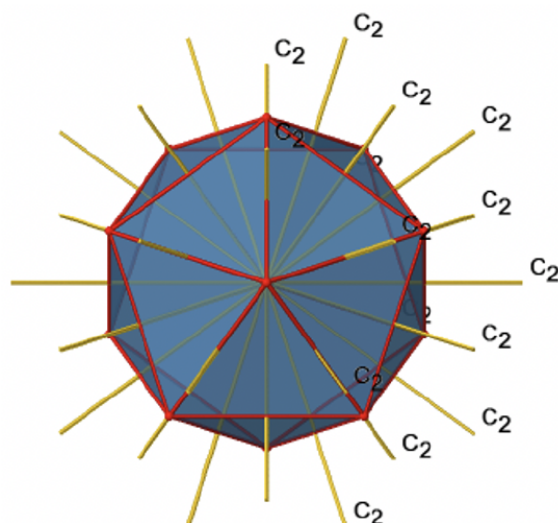


Figure 3.2.1.22: The  $C_2$  axes of the icosahedral point group (Attribution: symotter.org/gallery)

There are also  $C_2$  axes (Figure 3.2.1.21). They pass through the centers of two opposite edges of the icosahedron. Rotating around the  $C_2$  axis shown makes the icosahedron superimpose. An icosahedron has overall 30 edges. Because one  $C_2$  axis passes through the centers of two opposite edges, we can understand that there are  $30/2=15$   $C_2$  axes. There is one unique  $C_2$  operation per axis, and therefore there are 15  $C_2$  operations.

We have now found all proper rotations. Let us look for mirror planes, next. You can see a mirror plane below (Figure 3.2.1.22).

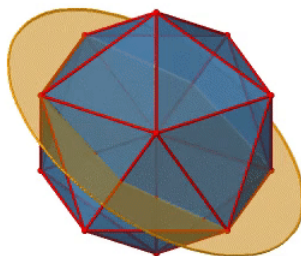


Figure 3.2.1.22: A mirror plane in the icosahedral point group (Attribution: symotter.org/gallery)

It contains two opposite edges. It also bisects two other edges. An icosahedron has overall 30 edges, therefore there are  $30/2=15$  mirror planes. You can see all of them below (Figure 3.2.1.23).

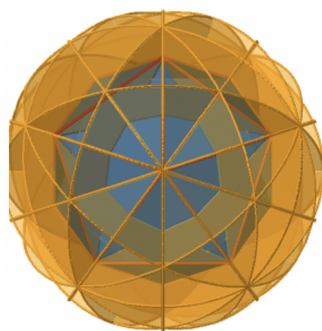


Figure 3.2.1.23: All the mirror planes in the icosahedral point group (Attribution: symotter.org/gallery)

The icosahedron also has an inversion center in the center of the icosahedron (Figure 3.2.1.24). As we carry out the associated symmetry operation, all points in the icosahedron move through the inversion center to the other side.

Figure 3.2.1.24: The inversion center in the icosahedron (Attribution: symotter.org/gallery)

Let us now look for improper rotations. The improper rotational axes with the highest order are  $S_{10}$  axes. They are located in the same position as the  $C_5$  axes, and go through two opposite corners (Figure 3.2.1.25).

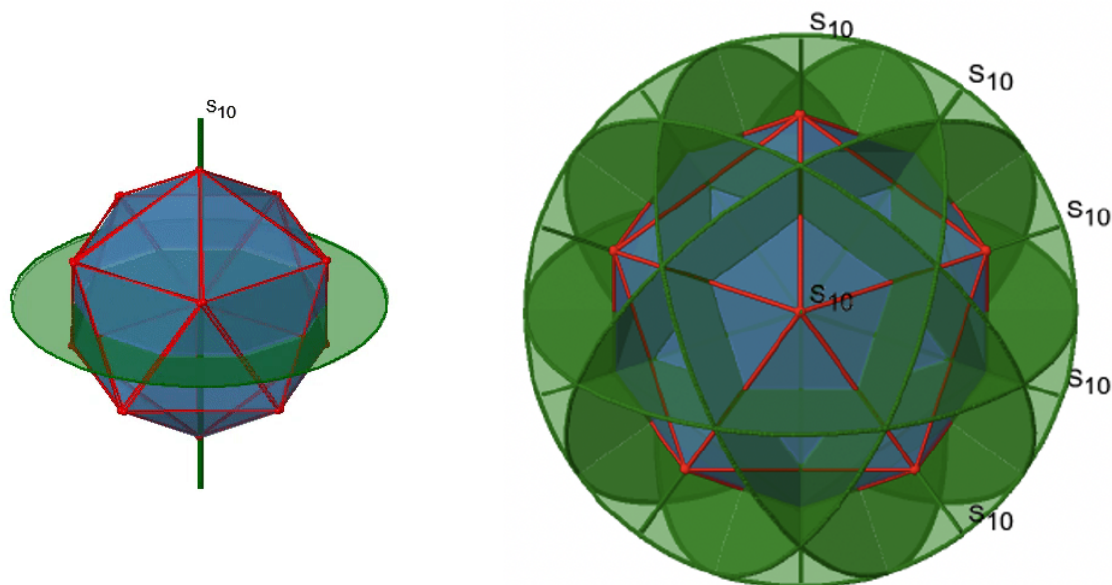


Figure 3.2.1.25: The  $S_{10}$  improper rotational axes in the icosahedral point group (Attribution: symotter.org/gallery)

The  $S_{10}$  exists because in an icosahedron there are pairs of co-planar pentagons that are oriented staggered relative to each other. The rotation around  $36^\circ$  brings one pentagon in eclipsed position relative to the other, but superposition is only achieved after the reflection at the mirror plane perpendicular to the rotational axis. Because one  $S_{10}$  passes through two opposite vertices, and there are 12 vertices there are 6  $S_{10}$  improper axes. For each axis there are four unique symmetry operations, the  $S_{10}^1$ , the  $S_{10}^3$ , the  $S_{10}^7$ , and the  $S_{10}^9$ . Therefore, there are overall  $4 \times 6 = 24$  operations possible.

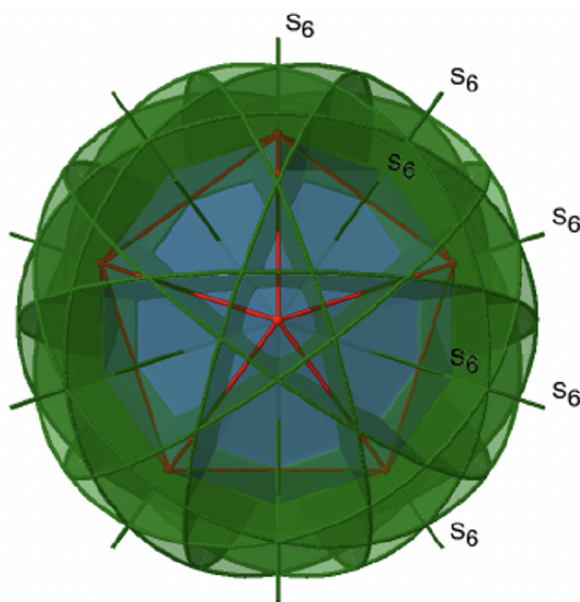


Figure 3.2.1.26: The  $S_6$  rotation-reflections in the icosahedral point group (Attribution: symotter.org/gallery)

Are the lower order improper rotational axes? Yes, there are  $S_6$  axes that pass through the centers of two opposite triangular faces (Figure 3.2.1.26). This symmetry element exists because the two triangular faces are in staggered orientation to each other. Rotation alone brings one face in eclipsed orientation relative to the other, but reflection at a mirror plane perpendicular to the axis is required to achieve superposition. The  $S_6$  axes are in the same location as the  $C_3$  axes. There are 10  $S_6$  axes because there are twenty faces and one axis passes through two opposite faces. Only the  $S_6^1$  and the  $S_6^5$  operations are unique  $S_6$  operations, all others can be expressed by simpler operations. Therefore there are overall  $10 S_6^1 + 10 S_6^5 = 20 S_6$  operations.

We have now found all symmetry operations for the  $I_h$  symmetry. There are overall 120 operations making the point group  $I_h$  the point group with the highest symmetry.

#### 📌 Symmetry Operations in the $I_h$ Point Group

Every molecule or object in the  $I_h$  point group has the following 120 symmetry operations:

- E, 24  $C_5$ , 20  $C_3$ , 15  $C_2$ , i, 24  $S_{10}$ , 20  $S_6$ , and 15  $\sigma$

### Rotational Point Groups

After having discussed high and low symmetry point groups, let us next look at rotational point groups. Unlike the high symmetry point groups, these only have a single proper rotational axis. The presence or absence of reflection planes further defines this class of point groups

#### $C_n$ Point Groups

In the most simple case the point groups do not have any additional symmetry element such as mirror planes or improper rotations. These point groups are called pure rotation groups and denoted  $C_n$  whereby n is the order of the proper rotation axis. An example is the hydrogen peroxide molecule  $H_2O_2$  (Figure 3.2.1.27). It has a so-called roof-structure due to its non-planarity. One hydrogen atom points toward us, and the other points away from us. This structure is due to the two electron-lone pairs at each  $sp^3$ -hybridized oxygen atom. These electron-lone pairs consume somewhat more space than the H atoms, and there is electrostatic repulsion between the electron lone pairs. Therefore, the electron lone pairs at the different oxygen atoms try to achieve the greatest distance from each other. This forces the H-atoms out of the plane, leading to the roof-structure of the hydrogen peroxide. Because the  $H_2O_2$  molecule is not planar, it only has a single  $C_2$  axis, but no other symmetry element besides the identity. The  $C_2$  axis passes through the center of the O-O bond. Execution of the  $C_2$  operation swaps up both the O and the H atoms.

Figure 3.2.1.27: The  $C_2$  rotational axis of hydrogen peroxide (Attribution: symotter.org/gallery)

### $C_{nv}$ Point Groups

Another class of groups are the pyramidal groups, denoted  $C_{nv}$ . They have  $n$  vertical mirror planes containing the principal axis  $C_n$  in addition to the principal axis  $C_n$ . Generally molecules belonging to pyramidal groups are derived from an  $n$ -gonal pyramid. An  $n$ -gonal pyramid has an  $n$ -gonal polygon as the basis which is capped. For example a trigonal pyramid has a triangular basis which is capped, a tetragonal pyramid has a square which is capped, and so on. The proper axis associated with a specific pyramid has the order  $n$  and goes through the tip of the pyramid and the center of the polygon. An example of a molecule with a trigonal pyramidal shape is the  $\text{NH}_3$  (Figure 3.2.1.28).

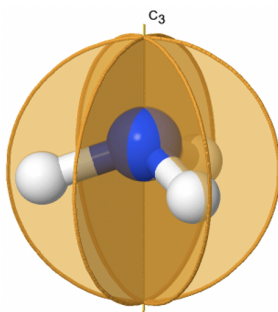


Figure 3.2.1.28:  $C_3$  axis and vertical mirror planes in  $\text{NH}_3$  (Attribution: symotter.org/gallery)

The three H atoms form the triangular basis of the pyramid, which is capped by the N atom. The  $\text{NH}_3$  molecule belongs to the point group  $C_{3v}$ . The  $C_3$  axis goes through the N atom which is the tip of the pyramid, and the center of the triangle defined by the H atoms. There are three vertical mirror planes that contain the  $C_3$  axis. Each of them goes through an N-H bond.

### $C_{nh}$ Point Groups

If we add a horizontal mirror plane instead of  $n$  vertical mirror planes to a proper rotational axis  $C_n$  we arrive at the point group type  $C_{nh}$ . The presence of the horizontal mirror planes also generates an improper axis of the order  $n$ . This is because when one can rotate and reflect perpendicular to the rotational axes independently, then it must also be possible to do it in combination. An example of a molecule belong to a  $C_{nh}$  group is the trans-difluorodiazene  $\text{N}_2\text{F}_2$  (Figure 3.2.1.29). It is a planar molecule with a  $C_2$  axis going through the middle of the N-N double bond, and standing perpendicular to the plane of the molecule. The horizontal mirror plane stands perpendicular to the  $C_2$  axis, and is within the plane of the molecule. There is an additional inversion center because an  $S_2$  must exist which is the same as an inversion center. The inversion center is in the middle of the N-N bonds. Overall, the molecule has the symmetry  $C_{2h}$ .

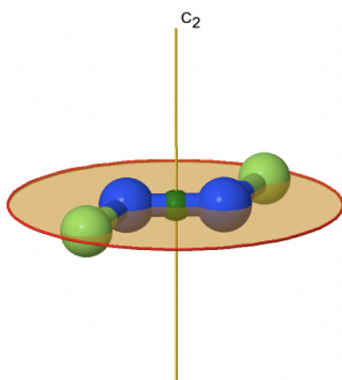


Figure 3.2.1.29:  $C_2$  axis and horizontal mirror plane in trans- $\text{N}_2\text{F}_2$  (Attribution: symotter.org/gallery)

### $S_{2n}$ Point Groups

The category of rotational point groups to be discussed are the improper rotation point groups. They only have one proper rotational axis, and an improper rotational axis that has twice the order of the proper rotational axis (Figure 3.2.1.30). There may be an inversion center present depending on the order of the proper and improper axes. Molecules that fall into these point groups are rare. An example the tetramethylcycloocta-tetraene molecule (Figure 3.2.1.30).

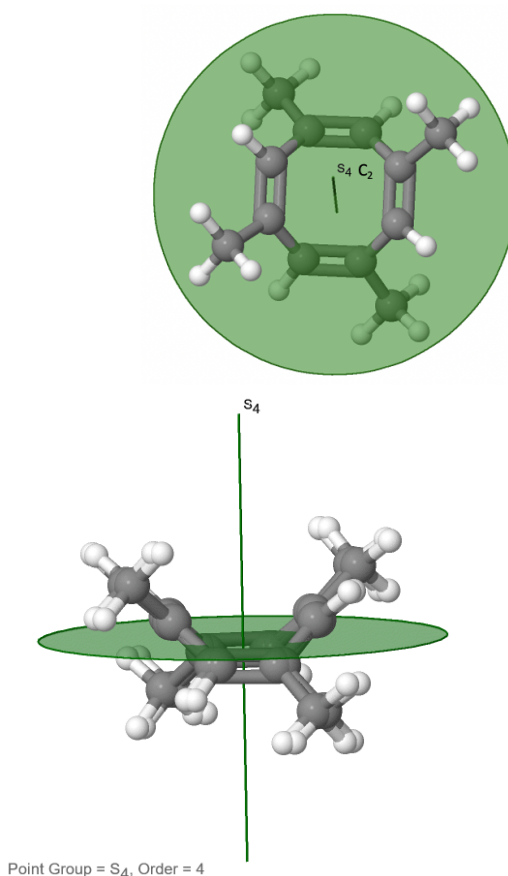


Figure 3.2.1.30: The  $S_4$  and an  $C_2$  axes of tetramethyl cycloocta-tetraene

It has an  $S_4$  and an  $C_2$  axis as the only symmetry elements besides the identity. Rotating by  $90^\circ$  alone does not superimpose the molecule because two C-C double bonds lie above the plane and two below the plane. In addition, two opposite methyl groups lie above and below the plane respectively. Therefore it needs the additional reflection to achieve superposition. There is also a  $C_2$  axis which is in the same locations as the  $S_4$  axis.

## Dihedral Groups

### $D_n$ Point Groups

Dihedral groups are point groups that have  $n$  additional  $C_2$  axes that stand perpendicular to the principal axis of the order  $n$ . If there are no other symmetry elements, then the point group is of the type  $D_n$ . For example in the point group  $D_3$  there is a  $C_3$  principal axis, and three additional  $C_2$  axes, but no other symmetry element (Fig. 2.2.75). The tris-oxalatoferrate(III) ion belongs to this point group (Figure 3.2.1.31). You can see that the  $C_3$  axis stands perpendicular to the paper plane, and there are three  $C_2$  axes in the paper plane.

Figure 3.2.1.31: The tris-oxalatoferrate(III) ion and its symmetry elements. (Attribution: symotter.org/gallery)

### $D_{nh}$ Point Groups

If a horizontal mirror plane is added to the  $C_n$  axis and the  $n$   $C_2$  axes we arrive at the  $D_{nh}$  point groups. The addition of the horizontal mirror plane generates further symmetry elements namely an  $S_n$  and  $n$  vertical mirror planes. An example for a molecule belonging to this class of point group is  $PF_5$  (Figure 3.2.1.32). It has a trigonal bipyramidal shape. The  $C_3$  axis goes through the axial F atoms of the molecule, and the three  $C_2$  axes go through the three equatorial F atom. The horizontal mirror plane stands



perpendicular to the principal  $C_3$  axis and is located within the equatorial plane of the molecule. In addition, there are the vertical mirror planes that contain the  $C_3$  axis, and go through the three equatorial P-F bonds. There is also an  $S_3$  axis which superimposes the  $C_3$  axis.

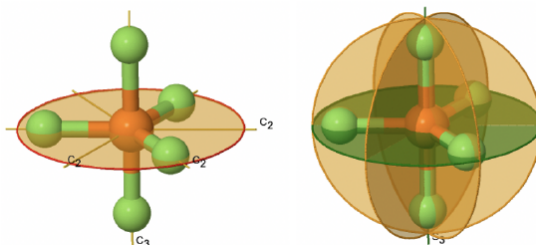


Figure 3.2.1.32: The  $PF_5$  molecule belonging to the point group  $D_{3h}$  and its symmetry elements. (Attribution: symotter.org/gallery)

### $D_{nd}$ Point Groups

If we add  $n$  vertical mirror planes to the principal axis and the  $n$   $C_2$  axes, we arrive at the point group  $D_{nd}$ . The vertical mirror planes are dihedral mirror planes because they bisect the angle between the  $C_2$  axes. An example is the ethane molecule in staggered conformation which has the symmetry  $D_{3d}$  (Figure 3.2.1.33). The  $C_3$  axis goes along the C-C bond, and the  $3C_2$  axes pass through the middle of the carbon-carbon bond, and bisect the angle between two hydrogens and one carbon atom. The three dihedral mirror planes pass through the C-H bonds. In addition, the ethane molecule has an  $S_6$  axis, and an inversion center.



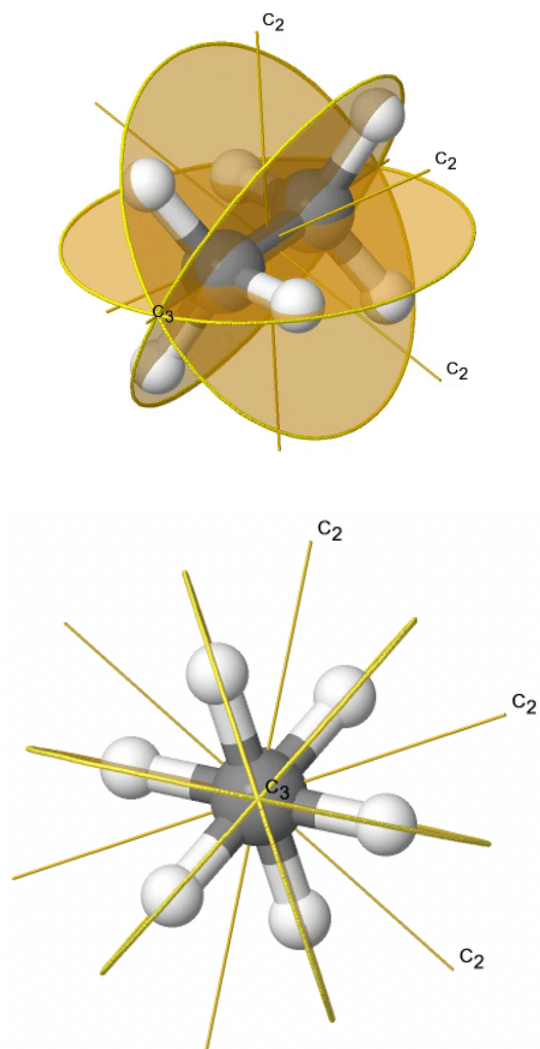


Figure 3.2.1.33: The ethane molecule in the staggered conformation belongs to the point group type  $D_{nd}$  (Attribution: symotter.org/gallery)

## Linear Point Groups

The principal rotation axis in a linear molecule is a  $C_\infty$  axis, meaning the molecule can be rotated along its bond axis an infinitely small amount and remain unchanged. Linear molecules can be subdivided based on the presence or absence of a horizontal reflection plane and inversion center.

### $C_{\infty v}$ point groups

A special  $n$ -gonal polygon is the cone. A cone can be conceived as an  $n$ -gonal pyramid with an infinite number  $n$  of corners at the base (Figure 3.2.1.34).

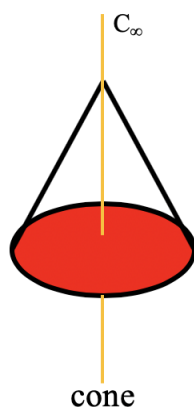


Figure 3.2.1.34: Cone having a proper rotational axis with infinite order.

In this case the order of the rotational axis that passes through the tip of the cone and the center of the circular basis is infinite. This also means that there is an infinite number of vertical mirror planes that contain the  $C_\infty$  axis. The point group describing the symmetry of a cone is called the linear point group  $C_{\infty v}$ . Polar, linear molecules such as CO, HF,  $N_2O$ , and HCN belong to this point group. You can see the HCN molecule with its  $C_\infty$  axis and its infinite number of vertical mirror planes below (Figure 3.2.1.35). The infinite number of mirror planes, shown in blue are forming a cylinder that surround the molecule.

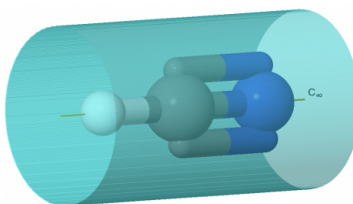


Figure 3.2.1.35:  $C_\infty$  axis of the HCN molecule.

### $D_{\infty h}$ point groups

A special case of a  $D_{nh}$  group is the linear group  $D_{\infty h}$ . An object that has this symmetry is a cylinder. A cylinder can be conceived as a prism with an infinite number of vertices. Thus, the principal axis that passes through a cylinder has infinite order. Because of the infinite order of the principal axis, there is an infinite number of  $C_2$  axes that stand perpendicular to the principal axis. You can see one such  $C_2$  going through the cylinder (Figure 3.2.1.36).

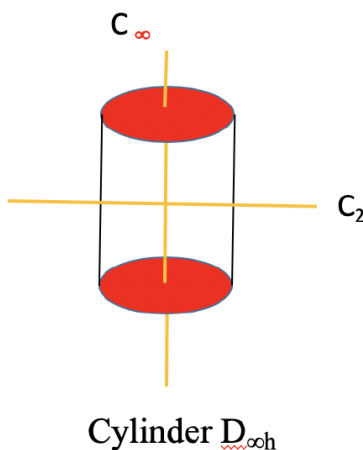


Figure 3.2.1.36: Cylinder as an example of linear group  $D_{\infty h}$ .

There is now also an improper axis of infinite order, as well as an infinite number of vertical mirror planes. Non-polar linear molecules like  $H_2$ ,  $CO_2$ , and acetylene  $C_2H_2$  belong to the point group  $D_{\infty h}$ . You can see the  $C_\infty$  axis passing through a  $CO_2$  molecule below (Figure 3.2.1.37). You can see the infinite number of vertical mirror planes as a blue cylinder. The infinite number of  $C_2$  axes is shown a yellow lines going around the molecule.

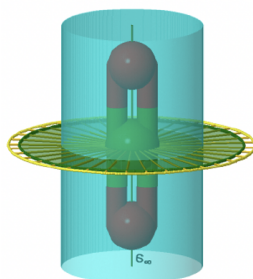


Figure 3.2.1.37: C<sub>∞</sub> in a CO<sub>2</sub> molecule.

Dr. Kai Landskron ([Lehigh University](#)). If you like this textbook, please consider to make a donation to support the author's research at Lehigh University: [Click Here to Donate](#).

This page titled [3.2.1: Molecular Point Groups](#) is shared under a [CC BY-NC-SA 4.0](#) license and was authored, remixed, and/or curated by [Kai Landskron](#).

- [2.2: Point Groups](#) by Kai Landskron is licensed [CC BY 4.0](#).
- [4.2: Point Groups](#) by Kai Landskron is licensed [CC BY-NC-SA 4.0](#).

## 3.2.2: Assigning Point Groups

[Click here](#) to see a lecture on this topic.

### Introduction

A **Point Group** describes all the symmetry operations that can be performed on a molecule that result in a conformation indistinguishable from the original. Point groups are used in Group Theory, the mathematical analysis of groups, to determine properties such as a molecule's molecular orbitals.

### Assigning Point Groups

While a point group contains all of the symmetry operations that can be performed on a given molecule, it is not necessary to identify all of these operations to determine the molecule's overall point group. Instead, a molecule's point group can be determined by following a set of steps which analyze the presence (or absence) of particular symmetry elements.

#### Steps for assigning a molecule's point group:

1. Determine if the molecule is of high or low symmetry.
2. If not, find the highest order rotation axis,  $C_n$ .
3. Determine whether the molecule has any  $C_2$  axes perpendicular to the principal  $C_n$  axis. If so, then there are  $n$  such  $C_2$  axes, and the molecule is in the  $D$  set of point groups. If not, it is in either the  $C$  or  $S$  set of point groups.
4. Determine whether the molecule has a horizontal mirror plane ( $\sigma_h$ ) perpendicular to the principal  $C_n$  axis. If so, the molecule is either in the  $C_{nh}$  or  $D_{nh}$  set of point groups.
5. Determine whether the molecule has a vertical mirror plane ( $\sigma_v$ ) containing the principal  $C_n$  axis. If so, the molecule is either in the  $C_{nv}$  or  $D_{nd}$  set of point groups. If not, and if the molecule has  $n$  perpendicular  $C_2$  axes, then it is part of the  $D_n$  set of point groups.
6. Determine whether there is an improper rotation axis,  $S_{2n}$ , collinear with the principal  $C_n$  axis. If so, the molecule is in the  $S_{2n}$  point group. If not, the molecule is in the  $C_n$  point group.

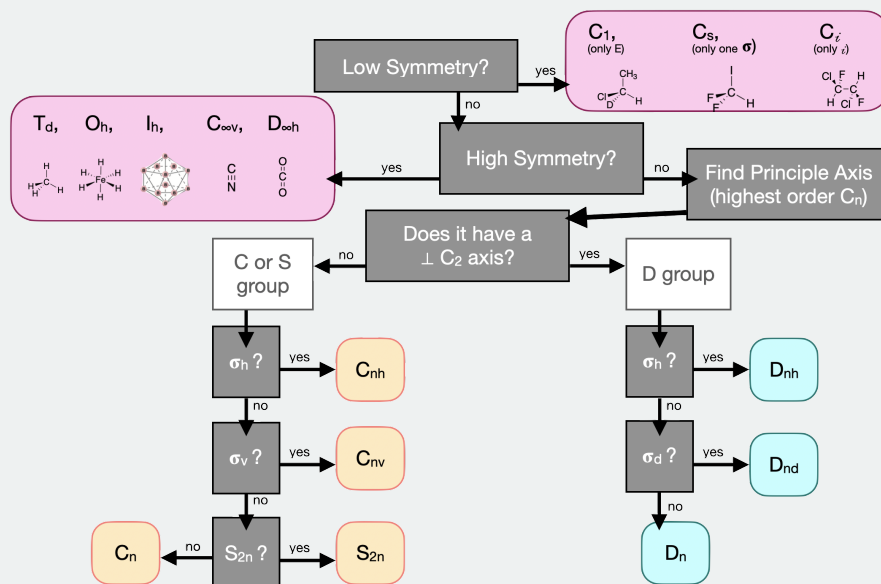


Figure 3.2.2.1: Decision tree for determining a molecule's point group (CC-BY-NC-SA; Kathryn Haas)

#### ✓ Example 3.2.2.1

Find the point group of benzene ( $C_6H_6$ ).

**Answer**

**Solution**

1. Benzene is neither high nor low symmetry
2. Highest order rotation axis:  $C_6$
3. There are 6  $C_2$  axes perpendicular to the principal axis
4. There is a horizontal mirror plane ( $\sigma_h$ )

Benzene is in the  $D_{6h}$  point group.

## See Also

[Symmetry Gallery](#)

This page titled [3.2.2: Assigning Point Groups](#) is shared under a [not declared](#) license and was authored, remixed, and/or curated by [Kathryn Haas](#).

- [4.2: Point Groups](#) by [Kathryn Haas](#) has no license indicated.

### 3.2.3: Chirality

#### Introduction

Around the year 1847, the French scientist Louis Pasteur provided an explanation for the optical activity of tartaric acid salts. When he carried out a particular reaction, Pasteur observed that two types of crystals precipitated. Patiently and carefully using tweezers, Pasteur was able to separate the two types of crystals. Pasteur noticed that the types rotated plane-polarized light by the same amount but in different directions. These two compounds are called enantiomers.

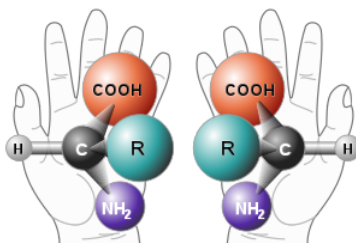


Figure 3.2.3.1: Two enantiomers of an amino acid (with side chain R).

#### What is chirality?

A molecule is **chiral** (or **dissymmetric**) if it is non-superimposable on its mirror image. The two mirror images of a chiral molecule are called enantiomers. Enantiomers have the same physical properties (e.g., melting point, etc.). They differ in their ability to rotate plane polarized light and in their reactivity with other chiral molecules. Due to their ability to rotate plane polarized light, they are referred to as being *optically active*.

#### Using Symmetry to Determine Chirality

There are some general rules of thumb that help determine whether a molecule is chiral or achiral. The point group of the molecule, and the symmetry operations within that point group, can give clues as to whether the molecule is chiral.

##### Symmetry operations of chiral molecules

A chiral molecule cannot possess a plane of symmetry ( $\sigma$ ), a center of inversion ( $i$ ), or an improper rotation ( $S_n$ ). Due to the fact that all groups that lack both  $\sigma$  and  $i$  also lack  $S_n$ , **a molecule that belongs to any group that lacks  $S_n$  is chiral.**

An example of an inorganic coordination complex is tris(ethylenediamine)cobalt(III) (Figure 3.2.3.1). Figure 3.2.3.1 shows the two enantiomers of tris(ethylenediamine)cobalt(III): the  $\Delta$  and  $\Lambda$  isomers.

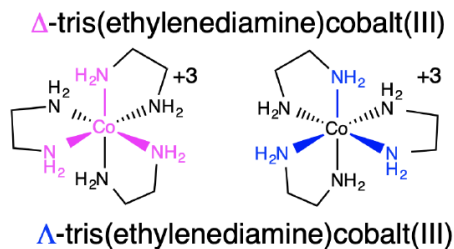


Figure 3.2.3.2: Two chiral enantiomers of tris(ethylenediamine)cobalt(III).

You can visualize the  $\Lambda$  and  $\Delta$  isomers by imagining that the ligands around the metal centers are blades of a fan. To push the air toward you, you would need to rotate the  $\Delta$  isomer clockwise, and the  $\Lambda$  isomer counter-clockwise.

##### Exercise 3.2.3.1

Which point groups are possible for chiral molecules?

**Answer**

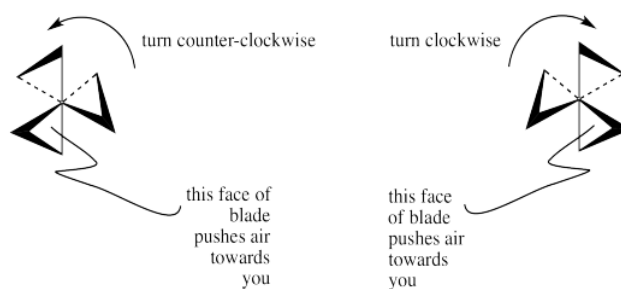


Figure 3.2.3.3: Another way of thinking about the chirality of the two chiral enantiomers of tris(ethylenediamine)cobalt(III) shown in Figure 3.2.3.2. This figure was taken from [Structure and Reactivity in Organic, Biological, and Inorganic Chemistry](#).

As a result of the previous discussion, there are a few classes of point groups that lack an improper axis. Those classes are  $C_1$ ,  $C_n$ , and  $D_n$ .

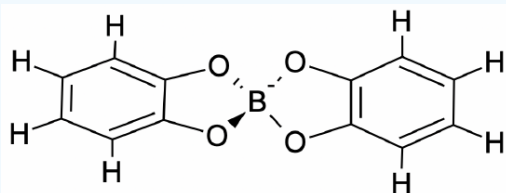
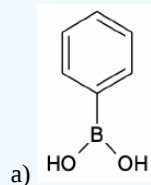
This page titled [3.2.3: Chirality](#) is shared under a [CC BY-NC 4.0](#) license and was authored, remixed, and/or curated by [Kathryn Haas](#).

- [4.4.1: Chirality](#) by [Kathryn Haas](#) is licensed [CC BY-NC 4.0](#).

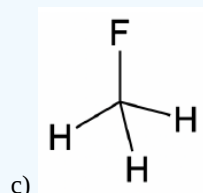
### 3.3: Unit 3 Practice Problems

#### Exercise 1

Determine all symmetry elements and all unique symmetry operations of the following molecules:

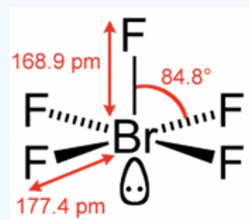


Note: The boron is tetrahedrally coordinated by O.

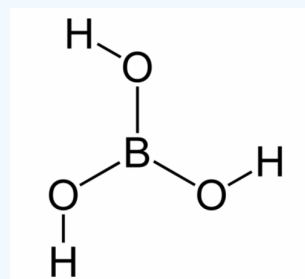


d) ethane (staggered conformation)

e) bromine tetrafluoride

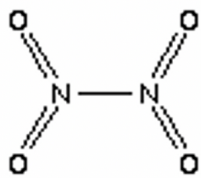


f) Boric acid



g) Dinitrogen tetroxide





h)  $\text{PtCl}_4^{2-}$  (square planar)

i) bromobenzene

j)  $\text{SF}_4$

k)  $\text{ClF}_3$

l)  $\text{CO}_2$

m) benzene

### Answer

Elements:  $E, C_2, \sigma_v, \sigma_v'$

a) Operations:  $E, C_2, \sigma_v, \sigma_v'$

Elements:  $E, S_4, C_2, 2\sigma_v$

b) Operations:  $E, S_4^1, S_4^3, C_2, 2\sigma_v$

Elements:  $E, C_3, 3\sigma_v$

c) Operations:  $E, C_3^1, C_3^2, 3\sigma_v$

Elements:  $E, C_3, 3 C_2, i, S_3, 3\sigma_d$

d) Operations:  $E, C_3^1, C_3^2, i, 3 C_2^1, S_6^1, S_6^5, 3\sigma_d$

Elements:  $E, C_4, C_2, 2 \sigma_v, 2 \sigma_v'$

e) Operations:  $E, C_4^1, C_4^3, C_2^1, 2\sigma_v, 2 \sigma_v'$

Elements:  $E, C_3, \sigma_h, S_3$

f) Operations:  $E, C_3^1, C_3^2, \sigma_h, S_3^1, S_3^5$

Elements:  $E, C_2, C_2', C_2'', i, \sigma_h, 2\sigma_v$

g) Operations:  $E, C_2^1, C_2'^1, C_2''^1, i, \sigma_h, 2\sigma_v$

Elements:  $E, C_4, C_2, 2C_2', 2C_2'', i, S_4, \sigma_h, 2\sigma_v, 2\sigma_d$

h) Operations:  $E, C_4^1, C_4^3, C_2^1, 2C_2'^1, 2 C_2''^1, i, S_4^1, S_4^3, \sigma_h, 2\sigma_v, 2\sigma_d$

Elements:  $E, C_2, \sigma_v, \sigma_v'$

i) Operations:  $E, C_2^1, \sigma_v, \sigma_v'$

Elements:  $E, C_2, \sigma_v, \sigma_v'$

j) Operations:  $E, C_2^1, \sigma_v, \sigma_v'$

Elements:  $E, C_2, \sigma_v, \sigma_v'$

k) Operations:  $E, C_2^1, \sigma_v, \sigma_v'$

Elements:  $E, C_\infty, \infty C_2, \infty \sigma_v, \sigma_h, S_\infty, i$

l) Operations:  $E, \infty C_\infty, \infty C_{2\perp}, \infty \sigma_v, \sigma_h, \infty S_\infty, i$

Elements:  $E, C_6, C_3, C_2, 6C_2', \sigma_h, 6\sigma_v, i, S_6, S_3$

m) Operations:  $E, C_6^1, C_6^5, C_3^1, C_3^2, C_2^1, 6C_2'^1, \sigma_h, 6\sigma_v, i, S_6^1, S_6^5, S_3^1, S_3^5$

## Exercise 2

When is a molecule chiral?

- a) It has no mirror planes
- b) It has no inversion center
- c) It has no principal axis
- d) It has no rotation reflections (improper rotations)

**Answer**

- d) It has no rotation reflections (improper rotations)

## Exercise 3

If a molecule has a principal axis  $C_n$ , and  $n$  additional  $C_2$  axes standing perpendicular to  $C_n$  then it belongs to

- a) A dihedral point group
- b) A rotational point group
- c) A low symmetry point group
- d) A high symmetry point group

**Answer**

- a) A dihedral point group

## Exercise 4

Which of the following molecules are chiral:

- a)  $CH_4$
- b)  $CHCl_3$

- c) HCFCIBr
- d) HOF
- e) BHFCI

**Answer**

- c) HCFCIBr

### Exercise 5

Determine the point groups of the molecules at [symmetry.otterbein.edu/challenge/index.html](http://symmetry.otterbein.edu/challenge/index.html) until you feel that you can determine point groups effortlessly

---

Dr. Kai Landskron ([Lehigh University](#)). If you like this textbook, please consider to make a donation to support the author's research at Lehigh University: [Click Here to Donate](#).

---

This page titled [3.3: Unit 3 Practice Problems](#) is shared under a [CC BY 4.0](#) license and was authored, remixed, and/or curated by [Kai Landskron](#).

- [Homework Problems Chapter 2](#) by [Kai Landskron](#) is licensed [CC BY 4.0](#).

## CHAPTER OVERVIEW

### Unit 4: Group Theory

#### 4.1: Groups

##### 4.1.1: Properties of Groups

#### 4.2: Representations and Character Tables

##### 4.2.1: Matrices

##### 4.2.2: Representations of Point Groups

##### 4.2.3: Character Tables

#### 4.3: Application to Vibrational Spectroscopy

##### 4.3.1: Molecular Vibrations

#### 4.4: Unit 4 Practice Problems

---

Unit 4: Group Theory is shared under a [not declared](#) license and was authored, remixed, and/or curated by LibreTexts.

## 4.1: Groups

---

Learning objectives for this unit are to:

- Know the four requirements of mathematical groups
  - Multiply symmetry operations and construct group multiplication tables
  - Determine the inverse of any operation in a group
  - Prove that operations in a group are associative
  - Determine the order of a group
  - Determine if a group is abelian or non-abelian
- 

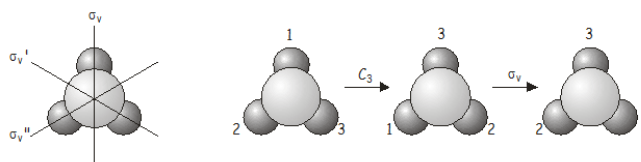
4.1: Groups is shared under a [not declared](#) license and was authored, remixed, and/or curated by LibreTexts.

## 4.1.1: Properties of Groups

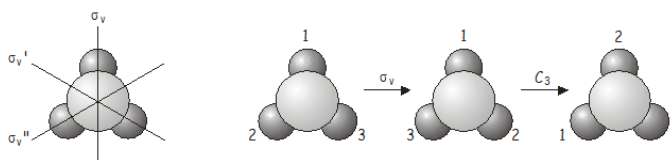
[Click here](#) to see a lecture on this topic.

### Group Multiplication

Now we will investigate what happens when we apply two symmetry operations in sequence. As an example, consider the  $NH_3$  molecule, which belongs to the  $C_{3v}$  point group. Consider what happens if we apply a  $C_3$  rotation ( $120^\circ$  counter-clockwise) followed by a  $\sigma_v$  reflection (reflection over the  $\sigma_v$  axis). We write this combined operation  $\sigma_v C_3$  (when written, symmetry operations operate on the thing directly to their right, just as operators do in quantum mechanics – we therefore have to work backwards from right to left from the notation to get the correct order in which the operators are applied). As we shall soon see, the order in which the operations are applied is important.



The combined operation  $\sigma_v C_3$  is equivalent to  $\sigma_v''$  (note the double prime on  $\sigma_v''$ !), which is also a symmetry operation of the  $C_{3v}$  point group. Now let's see what happens if we apply the operators in the reverse order, i.e.,  $C_3 \sigma_v$  ( $\sigma_v$  followed by  $C_3$ ).



Again, the combined operation  $C_3 \sigma_v$  is equivalent to another operation of the point group, this time  $\sigma_v'$  (note the single prime on  $\sigma_v'$ !).

There are two important points that are illustrated by this example:

1. The order in which two operations are applied is important. For two symmetry operations  $A$  and  $B$ ,  $AB$  is not necessarily the same as  $BA$ , i.e. symmetry operations do not in general **commute**. In some groups the symmetry elements do commute; such groups are said to be **Abelian**.
2. If two operations from the same point group are applied in sequence, the result will be equivalent to another operation from the point group. Symmetry operations that are related to each other by other symmetry operations of the group are said to belong to the same **class**. In  $NH_3$ , the three mirror planes  $\sigma_v$ ,  $\sigma_v'$  and  $\sigma_v''$  belong to the same class (related to each other through a  $C_3$  rotation), as do the rotations  $C_3^+$  and  $C_3^-$  (anticlockwise and clockwise rotations about the principal axis, related to each other by a vertical mirror plane).

### Four Properties of Mathematical Groups

Now that we have explored some of the properties of symmetry operations and elements and their behavior within point groups, we are ready to introduce the formal mathematical definition of a group. The definitions below will be put into the context of *molecular symmetry*.

A mathematical group is defined as a set of elements ( $A_1, A_2, A_3 \dots$ ) together with a rule for forming combinations  $A_i A_j \dots$ . For our purposes,  $A_1, A_2, A_3$ , etc. are symmetry elements and  $A_i, A_j$ , etc. are symmetry operations described in a [previous section](#). The elements of the group and the rule for combining them must satisfy the following four criteria.

1. The group must include the **identity**  $E$ , which commutes with other members of the group. In other terms,  $E A_i = A_i$  for all the elements of the group. Application of the identity operation before or after another operation,  $A_i$ , results in the same outcome as  $A_i$  alone.
2. The elements must satisfy the group property that the combination of any pair of elements is also an element of the group. For example, in the  $C_{3v}$  point group, a  $C_3$  rotation followed by a  $\sigma_v$  gives another operation that is already part of the

group: a  $\sigma_v$  ”.

3. Each symmetry operation  $A_i$  must have an inverse  $A_i^{-1}$ , which is also an element of the group, such that

$$A_i A_i^{-1} = A_i^{-1} A_i = E$$

The inverse  $g_i^{-1}$  effectively 'undoes' the effect of the symmetry operation  $g_i$ . For example, in the  $C_{3v}$  point group, the inverse of  $C_3^+$  is  $C_3^-$ .

4. The rule of combination must be associative

$$(A_i A_j)(A_k) = A_i(A_j A_k)$$

Or  $A(BC) = (AB)C$ . In other words, the order of operations should not matter.

Group theory is an important area in mathematics, and luckily for chemists the mathematicians have already done most of the work for us. Along with the formal definition of a group comes a comprehensive mathematical framework that allows us to carry out a rigorous treatment of symmetry in molecular systems and learn about its consequences.

Many problems involving operators or operations (such as those found in quantum mechanics or group theory) may be reformulated in terms of matrices. Any of you who have come across transformation matrices before will know that symmetry operations such as rotations and reflections may be represented by matrices. It turns out that the set of matrices representing the symmetry operations in a group obey all the conditions laid out above in the mathematical definition of a group, and using matrix representations of symmetry operations simplifies carrying out calculations in group theory. Before we learn how to use matrices in group theory, it will probably be helpful to review some basic definitions and properties of matrices.

\*This page was adapted from [here \(click\)](#).

### Contributors and Attributions

- [Claire Vallance](#) (University of Oxford)
- Curated or created by [Kathryn Haas](#)

---

This page titled [4.1.1: Properties of Groups](#) is shared under a [not declared](#) license and was authored, remixed, and/or curated by [Kathryn Haas](#).

- [4.3: Properties and Representations of Groups](#) by [Kathryn Haas](#) has no license indicated.

## 4.2: Representations and Character Tables

---

Learning objectives for this unit are to:

- Perform matrix multiplication
  - Recognize square, diagonal, and identity matrices
  - Construct transformation matrices for symmetry operations
  - Understand and extract information from character tables, including the order of the group, the number of classes of symmetry operations, and the meaning of the characters
  - Explain the difference between reducible and irreducible representations
  - Generate representations using a variety of basis sets, including xyz coordinate vectors, rotational vectors, and atomic orbitals
  - Perform calculations to demonstrate that two irreducible representations are orthogonal
  - Know the information indicated by the Mulliken symbols and be able to assign Mulliken symbols to irreducible representations
- 

4.2: Representations and Character Tables is shared under a [not declared](#) license and was authored, remixed, and/or curated by LibreTexts.



## 4.2.1: Matrices

The symmetry of molecules is essential for understanding the structures and properties of organic and inorganic compounds. The properties of chemical compounds are often easily explained by consideration of symmetry. For example, the symmetry of a molecule determines whether the molecule has a permanent dipole moment or not. The theories that describe optical activity, infrared and ultraviolet spectroscopy, and crystal structure involve the application of symmetry considerations. Matrix algebra is the most important mathematical tool in the description of symmetry.

The properties of symmetry groups are organized in character tables (discussed later in this chapter). Character tables are constructed based on matrices. This page is a brief description of matrices and matrix multiplication.

### What is a matrix?

An  $m \times n$  matrix **A** is a rectangular array of numbers with  $m$  rows and  $n$  columns. The numbers  $m$  and  $n$  are the dimensions of **A**. The numbers in the matrix are called its entries. The entry in row  $i$  and column  $j$  is called  $a_{ij}$ .

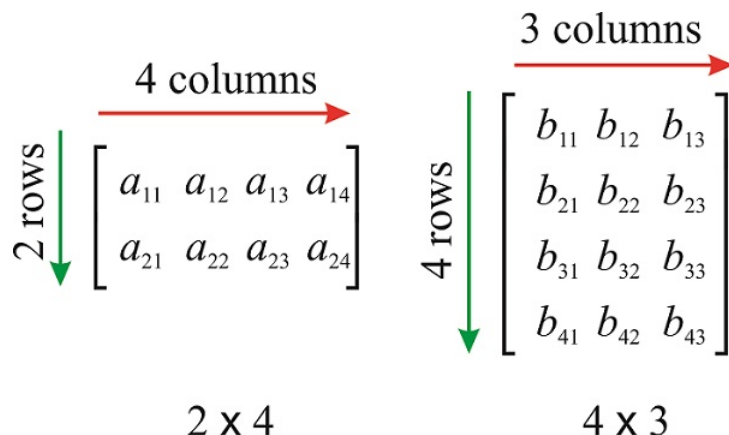


Figure 4.2.1.1: Matrices of different dimensions

Some types of matrices have special names:

- A square matrix:

$$\begin{pmatrix} 3 & -2 & 4 \\ 5 & 3i & 3 \\ -i & 1/2 & 9 \end{pmatrix}$$

with  $m = n$

- A rectangular matrix:

$$\begin{pmatrix} 3 & -2 & 4 \\ 5 & 3i & 3 \end{pmatrix}$$

with  $m \neq n$

- A column vector:

$$\begin{pmatrix} 3 \\ 5 \\ -i \end{pmatrix}$$

with  $n = 1$

- A row vector:

$$(3 \quad -2 \quad 4)$$

with  $m = 1$

- The identity matrix:

$$\begin{pmatrix} 1 & 0 & 0 \\ 0 & 1 & 0 \\ 0 & 0 & 1 \end{pmatrix}$$

with  $a_{ij} = \delta_{i,j}$ , where  $\delta_{i,j}$  is a function defined as  $\delta_{i,j} = 1$  if  $i = j$  and  $\delta_{i,j} = 0$  if  $i \neq j$ .

- A diagonal matrix:

$$\begin{pmatrix} a & 0 & 0 \\ 0 & b & 0 \\ 0 & 0 & c \end{pmatrix}$$

with  $a_{ij} = c_i \delta_{i,j}$ .

- An upper triangular matrix:

$$\begin{pmatrix} a & b & c \\ 0 & d & e \\ 0 & 0 & f \end{pmatrix}$$

All the entries below the main diagonal are zero.

- A lower triangular matrix:

$$\begin{pmatrix} a & 0 & 0 \\ b & c & 0 \\ d & e & f \end{pmatrix}$$

All the entries above the main diagonal are zero.

- A triangular matrix is one that is either lower triangular or upper triangular.

### The Trace of a Matrix

The trace of an  $n \times n$  square matrix  $\mathbf{A}$  is the sum of the diagonal elements, and formally defined as  $Tr(\mathbf{A}) = \sum_{i=1}^n a_{ii}$ .

For example,

$$\mathbf{A} = \begin{pmatrix} 3 & -2 & 4 \\ 5 & 3i & 3 \\ -i & 1/2 & 9 \end{pmatrix}; Tr(\mathbf{A}) = 12 + 3i$$

### Singular and Nonsingular Matrices

A square matrix with nonzero [determinant](#) is called *nonsingular*. A matrix whose determinant is zero is called *singular*. (Note that you cannot calculate the determinant of a non-square matrix).

For a 2x2 matrix,

$$\mathbf{B} = \begin{pmatrix} a & b \\ c & d \end{pmatrix}; det(\mathbf{B}) = ad - cb$$

For a 3x3 matrix,

$$\mathbf{C} = \begin{pmatrix} a & b & c \\ d & e & f \\ g & h & i \end{pmatrix}$$

$$det(\mathbf{C}) = a \begin{vmatrix} e & f \\ h & i \end{vmatrix} - b \begin{vmatrix} d & f \\ g & i \end{vmatrix} + c \begin{vmatrix} d & e \\ g & h \end{vmatrix}$$

$$det(\mathbf{C}) = aei - ahf - bdi + bgf + cdh - cge$$

### The Matrix Transpose

The matrix transpose, most commonly written  $\mathbf{A}^T$ , is the matrix obtained by exchanging  $\mathbf{A}$ 's rows and columns. It is obtained by replacing all elements  $a_{ij}$  with  $a_{ji}$ . For example:

$$\mathbf{A} = \begin{pmatrix} 3 & -2 & 4 \\ 5 & 3i & 3 \end{pmatrix} \rightarrow \mathbf{A}^T = \begin{pmatrix} 3 & 5 \\ -2 & 3i \\ 4 & 3 \end{pmatrix}$$

## Matrix Multiplication

To multiply two matrices, the number of vertical columns in the first matrix must be the same as the number of rows in the second matrix. If  $\mathbf{A}$  has dimensions  $m \times n$  and  $\mathbf{B}$  has dimensions  $n \times p$ , then the product  $\mathbf{AB}$  is defined, and has dimensions  $m \times p$ .

$$c_{ij} = \sum a_{ij} \times b_{ij}$$

The entry  $a_{ij} \times b_{ij}$  is obtained by multiplying row  $i$  of  $\mathbf{A}$  by column  $j$  of  $\mathbf{B}$ , which is done by multiplying corresponding entries together and then adding the results:

$$c_{11} = a_{11}b_{11} + a_{12}b_{21} + a_{13}b_{31} + a_{14}b_{41}$$

$$\begin{bmatrix} a_{11} & a_{12} & a_{13} & a_{14} \\ a_{21} & a_{22} & a_{23} & a_{24} \end{bmatrix} \begin{bmatrix} b_{11} & b_{12} & b_{13} \\ b_{21} & b_{22} & b_{23} \\ b_{31} & b_{32} & b_{33} \\ b_{41} & b_{42} & b_{43} \end{bmatrix} = \begin{bmatrix} c_{11} & c_{12} & c_{13} \\ c_{21} & c_{22} & c_{23} \end{bmatrix}$$

$2 \times 4 \qquad 4 \times 3 \qquad 2 \times 3$

$$c_{22} = a_{21}b_{12} + a_{22}b_{22} + a_{23}b_{32} + a_{24}b_{42}$$

$$\begin{bmatrix} a_{11} & a_{12} & a_{13} & a_{14} \\ a_{21} & a_{22} & a_{23} & a_{24} \end{bmatrix} \begin{bmatrix} b_{11} & b_{12} & b_{13} \\ b_{21} & b_{22} & b_{23} \\ b_{31} & b_{32} & b_{33} \\ b_{41} & b_{42} & b_{43} \end{bmatrix} = \begin{bmatrix} c_{11} & c_{12} & c_{13} \\ c_{21} & c_{22} & c_{23} \end{bmatrix}$$

Figure 4.2.1.1: Matrix multiplication

### ✓ Example 4.2.1.1

Calculate the product

$$\begin{pmatrix} 1 & -2 & 4 \\ 5 & 0 & 3 \\ 0 & 1/2 & 9 \end{pmatrix} \begin{pmatrix} 1 & 0 \\ 5 & 3 \\ -1 & 0 \end{pmatrix}$$

#### Solution

We need to multiply a  $3 \times 3$  matrix by a  $3 \times 2$  matrix, so we expect a  $3 \times 2$  matrix as a result.

$$\begin{pmatrix} 1 & -2 & 4 \\ 5 & 0 & 3 \\ 0 & 1/2 & 9 \end{pmatrix} \begin{pmatrix} 1 & 0 \\ 5 & 3 \\ -1 & 0 \end{pmatrix} = \begin{pmatrix} a & b \\ c & d \\ e & f \end{pmatrix}$$

To calculate  $a$ , which is entry (1,1), we use row 1 of the matrix on the left and column 1 of the matrix on the right:

$$\begin{pmatrix} 1 & -2 & 4 \\ 5 & 0 & 3 \\ 0 & 1/2 & 9 \end{pmatrix} \begin{pmatrix} 1 & 0 \\ 5 & 3 \\ -1 & 0 \end{pmatrix} = \begin{pmatrix} a & b \\ c & d \\ e & f \end{pmatrix} \rightarrow a = 1 \times 1 + (-2) \times 5 + 4 \times (-1) = -13$$

To calculate  $b$ , which is entry (1,2), we use row 1 of the matrix on the left and column 2 of the matrix on the right:

$$\begin{pmatrix} 1 & -2 & 4 \\ 5 & 0 & 3 \\ 0 & 1/2 & 9 \end{pmatrix} \begin{pmatrix} 1 & 0 \\ 5 & 3 \\ -1 & 0 \end{pmatrix} = \begin{pmatrix} a & b \\ c & d \\ e & f \end{pmatrix} \rightarrow b = 1 \times 0 + (-2) \times 3 + 4 \times 0 = -6$$

To calculate  $c$ , which is entry (2,1), we use row 2 of the matrix on the left and column 1 of the matrix on the right:

$$\begin{pmatrix} 1 & -2 & 4 \\ 5 & 0 & 3 \\ 0 & 1/2 & 9 \end{pmatrix} \begin{pmatrix} 1 & 0 \\ 5 & 3 \\ -1 & 0 \end{pmatrix} = \begin{pmatrix} a & b \\ c & d \\ e & f \end{pmatrix} \rightarrow c = 5 \times 1 + 0 \times 5 + 3 \times (-1) = 2$$

To calculate  $d$ , which is entry (2,2), we use row 2 of the matrix on the left and column 2 of the matrix on the right:

$$\begin{pmatrix} 1 & -2 & 4 \\ 5 & 0 & 3 \\ 0 & 1/2 & 9 \end{pmatrix} \begin{pmatrix} 1 & 0 \\ 5 & 3 \\ -1 & 0 \end{pmatrix} = \begin{pmatrix} a & b \\ c & d \\ e & f \end{pmatrix} \rightarrow d = 5 \times 0 + 0 \times 3 + 3 \times 0 = 0$$

To calculate  $e$ , which is entry (3,1), we use row 3 of the matrix on the left and column 1 of the matrix on the right:

$$\begin{pmatrix} 1 & -2 & 4 \\ 5 & 0 & 3 \\ 0 & 1/2 & 9 \end{pmatrix} \begin{pmatrix} 1 & 0 \\ 5 & 3 \\ -1 & 0 \end{pmatrix} = \begin{pmatrix} a & b \\ c & d \\ e & f \end{pmatrix} \rightarrow e = 0 \times 1 + 1/2 \times 5 + 9 \times (-1) = -13/2$$

To calculate  $f$ , which is entry (3,2), we use row 3 of the matrix on the left and column 2 of the matrix on the right:

$$\begin{pmatrix} 1 & -2 & 4 \\ 5 & 0 & 3 \\ 0 & 1/2 & 9 \end{pmatrix} \begin{pmatrix} 1 & 0 \\ 5 & 3 \\ -1 & 0 \end{pmatrix} = \begin{pmatrix} a & b \\ c & d \\ e & f \end{pmatrix} \rightarrow f = 0 \times 0 + 1/2 \times 3 + 9 \times 0 = 3/2$$

The result is:

$$\begin{pmatrix} 1 & -2 & 4 \\ 5 & 0 & 3 \\ 0 & 1/2 & 9 \end{pmatrix} \begin{pmatrix} 1 & 0 \\ 5 & 3 \\ -1 & 0 \end{pmatrix} = \begin{pmatrix} -13 & -6 \\ 2 & 0 \\ -13/2 & 3/2 \end{pmatrix}$$

#### ✓ Example 4.2.1.2

Calculate

$$\begin{pmatrix} 1 & -2 & 4 \\ 5 & 0 & 3 \end{pmatrix} \begin{pmatrix} 1 \\ 5 \\ -1 \end{pmatrix}$$

#### Solution

We are asked to multiply a  $2 \times 3$  matrix by a  $3 \times 1$  matrix (a column vector). The result will be a  $2 \times 1$  matrix (a vector).

$$\begin{pmatrix} 1 & -2 & 4 \\ 5 & 0 & 3 \end{pmatrix} \begin{pmatrix} 1 \\ 5 \\ -1 \end{pmatrix} = \begin{pmatrix} a \\ b \end{pmatrix}$$

$$a = 1 \times 1 + (-2) \times 5 + 4 \times (-1) = -13$$

$$b = 5 \times 1 + 0 \times 5 + 3 \times (-1) = 2$$

The solution is:

$$\begin{pmatrix} 1 & -2 & 4 \\ 5 & 0 & 3 \end{pmatrix} \begin{pmatrix} 1 \\ 5 \\ -1 \end{pmatrix} = \begin{pmatrix} -13 \\ 2 \end{pmatrix}$$

Need help? The link below contains solved examples: Multiplying matrices of different shapes (three examples): <http://tinyurl.com/kn8ysqq>

External links:

- Multiplying matrices, example 1: <http://patrickjmt.com/matrices-multiplying-a-matrix-by-another-matrix/>
- Multiplying matrices, example 2: <http://patrickjmt.com/multiplying-matrices-example-2/>
- Multiplying matrices, example 3: <http://patrickjmt.com/multiplying-matrices-example-3/>

## The Commutator

Matrix multiplication is not, in general, commutative. For example, we can perform

$$\begin{pmatrix} 1 & -2 & 4 \\ 5 & 0 & 3 \end{pmatrix} \begin{pmatrix} 1 \\ 5 \\ -1 \end{pmatrix} = \begin{pmatrix} -13 \\ 2 \end{pmatrix}$$

but cannot perform

$$\begin{pmatrix} 1 \\ 5 \\ -1 \end{pmatrix} \begin{pmatrix} 1 & -2 & 4 \\ 5 & 0 & 3 \end{pmatrix}$$

Even with square matrices, that can be multiplied both ways, multiplication is not commutative. In this case, it is useful to define the **commutator**, defined as:

$$[\mathbf{A}, \mathbf{B}] = \mathbf{AB} - \mathbf{BA}$$

### ✓ Example 4.2.1.3

Given  $\mathbf{A} = \begin{pmatrix} 3 & 1 \\ 2 & 0 \end{pmatrix}$  and  $\mathbf{B} = \begin{pmatrix} 1 & 0 \\ -1 & 2 \end{pmatrix}$

Calculate the commutator  $[\mathbf{A}, \mathbf{B}]$

**Solution**

$$[\mathbf{A}, \mathbf{B}] = \mathbf{AB} - \mathbf{BA}$$

$$\mathbf{AB} = \begin{pmatrix} 3 & 1 \\ 2 & 0 \end{pmatrix} \begin{pmatrix} 1 & 0 \\ -1 & 2 \end{pmatrix} = \begin{pmatrix} 3 \times 1 + 1 \times (-1) & 3 \times 0 + 1 \times 2 \\ 2 \times 1 + 0 \times (-1) & 2 \times 0 + 0 \times 2 \end{pmatrix} = \begin{pmatrix} 2 & 2 \\ 2 & 0 \end{pmatrix}$$

$$\mathbf{BA} = \begin{pmatrix} 1 & 0 \\ -1 & 2 \end{pmatrix} \begin{pmatrix} 3 & 1 \\ 2 & 0 \end{pmatrix} = \begin{pmatrix} 1 \times 3 + 0 \times 2 & 1 \times 1 + 0 \times 0 \\ -1 \times 3 + 2 \times 2 & -1 \times 1 + 2 \times 0 \end{pmatrix} = \begin{pmatrix} 3 & 1 \\ 1 & -1 \end{pmatrix}$$

$$[\mathbf{A}, \mathbf{B}] = \mathbf{AB} - \mathbf{BA} = \begin{pmatrix} 2 & 2 \\ 2 & 0 \end{pmatrix} - \begin{pmatrix} 3 & 1 \\ 1 & -1 \end{pmatrix} = \begin{pmatrix} -1 & 1 \\ 1 & 1 \end{pmatrix}$$

$$[\mathbf{A}, \mathbf{B}] = \begin{pmatrix} -1 & 1 \\ 1 & 1 \end{pmatrix}$$

## Multiplication of a vector by a scalar

The multiplication of a vector  $\vec{v}_1$  by a scalar  $n$  produces another vector of the same dimensions that lies in the same direction as  $\vec{v}_1$ ;

$$n \begin{pmatrix} x \\ y \end{pmatrix} = \begin{pmatrix} nx \\ ny \end{pmatrix}$$

The scalar can stretch or compress the length of the vector, but cannot rotate it (figure [\[fig:vector\\_by\\_scalar\]](#)).

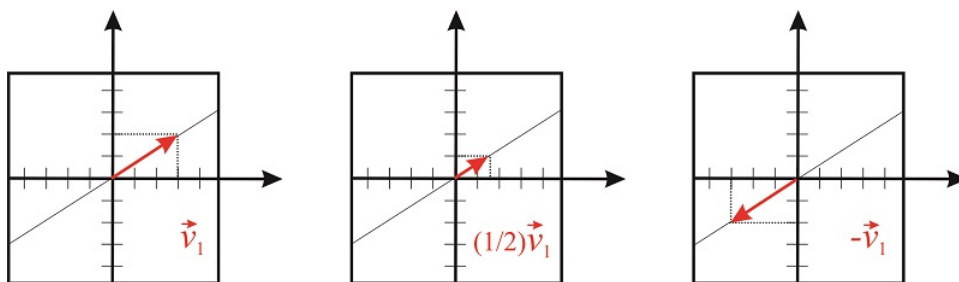


Figure 4.2.1.2: Multiplication of a vector by a scalar

### Multiplication of a square matrix by a vector

The multiplication of a vector  $\vec{v}_1$  by a square matrix produces another vector of the same dimensions of  $\vec{v}_1$ . For example, we can multiply a  $2 \times 2$  matrix and a 2-dimensional vector:

$$\begin{pmatrix} a & b \\ c & d \end{pmatrix} \begin{pmatrix} x \\ y \end{pmatrix} = \begin{pmatrix} ax + by \\ cx + dy \end{pmatrix}$$

For example, consider the matrix

$$\mathbf{A} = \begin{pmatrix} -2 & 0 \\ 0 & 1 \end{pmatrix}$$

The product

$$\begin{pmatrix} -2 & 0 \\ 0 & 1 \end{pmatrix} \begin{pmatrix} x \\ y \end{pmatrix}$$

is

$$\begin{pmatrix} -2x \\ y \end{pmatrix}$$

We see that  $2 \times 2$  matrices act as operators that transform one 2-dimensional vector into another 2-dimensional vector. This particular matrix keeps the value of  $y$  constant and multiplies the value of  $x$  by  $-2$  (Figure 4.2.1.3).

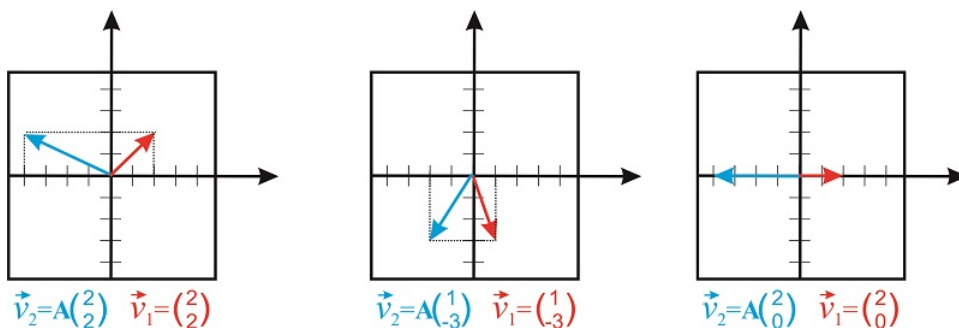


Figure 4.2.1.3: Multiplication of a vector by a square matrix

Notice that matrices are useful ways of representing operators that change the orientation and size of a vector. An important class of operators that are of particular interest to chemists are the so-called symmetry operators.

### Attribution

This page was adapted from [Matrices \(click here\)](#), contributed by Marcia Levitus, Associate Professor (Biodesign Institute) at Arizona State University.

Curated or created by [Kathryn Haas](#)

This page titled [4.2.1: Matrices](#) is shared under a [not declared](#) license and was authored, remixed, and/or curated by [Kathryn Haas](#).

- [4.3.1: Matrices](#) by [Kathryn Haas](#) has no license indicated.

## 4.2.2: Representations of Point Groups

### Symmetry Operations: Matrix Representations

A **symmetry operation**, such as a rotation around a symmetry axis or a reflection through a plane, is an operation that, when performed on an object, results in a new orientation of the object that is indistinguishable from the original. For example, if we rotate a square in the plane by  $\pi/2$  or  $\pi$ , the new orientation of the square is superimposable on the original one (Figure 4.2.2.1).

If rotation by an angle  $\theta$  of a molecule (or object) about some axis results in an orientation of the molecule (or object) that is superimposable on the original, the axis is called a rotation axis. The molecule (or object) is said to have an  $n$ -fold rotational axis, where  $n$  is  $2\pi/\theta$ . The axis is denoted as  $C_n$ . The square of Figure 4.2.2.1 has a  $C_4$  axis perpendicular to the plane because a  $90^\circ$  rotation leaves the figure indistinguishable from the initial orientation. This axis is also a  $C_2$  axis because a  $180^\circ$  degree rotation leaves the square indistinguishable from the original square. In addition, the figure has several other  $C_2$  axis that lie on the same plane as the square:

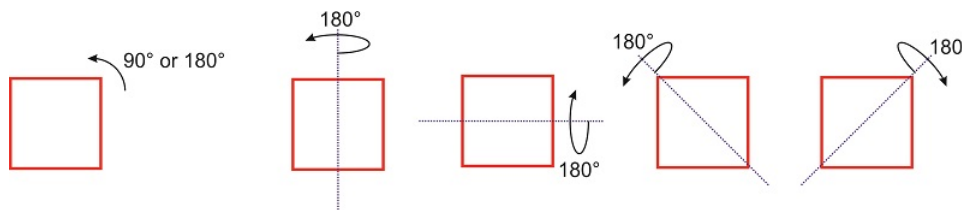


Figure 4.2.2.1: Symmetry operations performed on a square

A symmetry operation moves all the points of the object from one initial position to a final position, and that means that symmetry operators are  $3 \times 3$  square matrices (or  $2 \times 2$  in two dimensions). Each symmetry operation can be expressed as a **transformation matrix** where the vector  $(x', y', z')$  represents the new coordinates of the point  $(x, y, z)$  after the symmetry operation.

$$[\text{New Coordinates}(x', y', z')] = [\text{Transformation Matrix}] \times [\text{Old Coordinates}(x, y, z)]$$

We will use the example of water, which is in the  $C_{2v}$  point group, to illustrate how transformation matrices can be used to represent the symmetry of a group.

Figure 4.2.2.2 shows the three symmetry elements of the molecule of water ( $\text{H}_2\text{O}$ ). This molecule has only one rotation axis, which is 2-fold, and therefore we call it a “ $C_2$  axis.” It also has two mirror planes, one that contains the two hydrogen atoms ( $\sigma_{yz}$ ), and another one perpendicular to it ( $\sigma_{xz}$ ). Both planes contain the  $C_2$  axis.

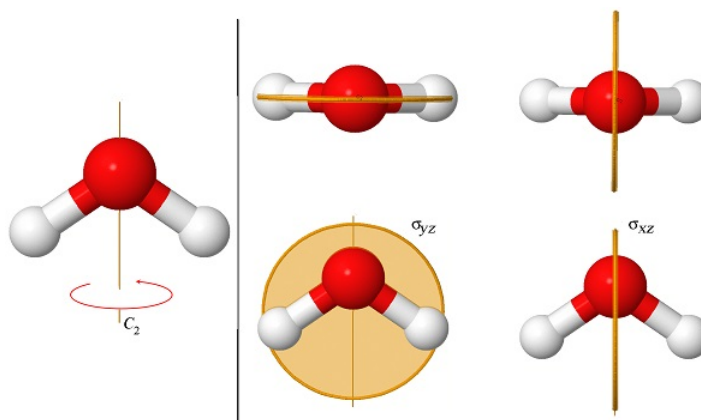


Figure 4.2.2.2: The symmetry elements of the molecule of water

#### Transformation Matrix of $C_2$ rotation

A 2-fold rotation around the  $z$ -axis changes the location of a point  $(x, y, z)$  to  $(-x, -y, z)$  (see Figure 4.2.2.3). By convention, rotations are always taken in the counterclockwise direction.

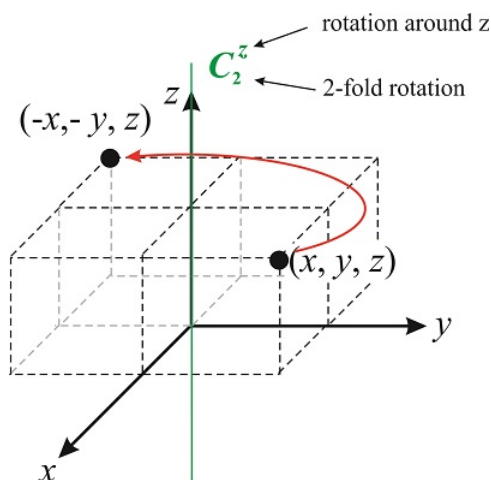


Figure 4.2.2.3: A 2-fold rotation around the z-axis

What is the matrix that represents the  $C_2$  rotation? The matrix transforms the vector  $(x, y, z)$  into  $(-x, -y, z)$ , so

$$C_2(x, y, z) = (-x, -y, z)$$

$$\begin{pmatrix} a_{11} & a_{12} & a_{13} \\ a_{21} & a_{22} & a_{23} \\ a_{31} & a_{32} & a_{33} \end{pmatrix} \begin{pmatrix} x \\ y \\ z \end{pmatrix} = \begin{pmatrix} -x \\ -y \\ z \end{pmatrix}$$

We know the matrix is a  $3 \times 3$  square matrix because it needs to multiply a 3-dimensional vector. In addition, we write the vector as a vertical column to satisfy the requirements of matrix multiplication.

$$\begin{pmatrix} a_{11} & a_{12} & a_{13} \\ a_{21} & a_{22} & a_{23} \\ a_{31} & a_{32} & a_{33} \end{pmatrix} \begin{pmatrix} x \\ y \\ z \end{pmatrix}$$

$$a_{11}x + a_{12}y + a_{13}z = -x$$

$$a_{21}x + a_{22}y + a_{23}z = -y$$

$$a_{31}x + a_{32}y + a_{33}z = z$$

and we conclude that  $a_{11} = -1$ ,  $a_{12} = a_{13} = 0$ ,  $a_{22} = -1$ ,  $a_{21} = a_{23} = 0$  and  $a_{33} = 1$ ,  $a_{31} = a_{32} = 0$ . The transformation matrix of the  $C_2$  operation of the  $C_{2v}$  point group is:

$$C_2 = \begin{pmatrix} -1 & 0 & 0 \\ 0 & -1 & 0 \\ 0 & 0 & 1 \end{pmatrix} \quad (4.2.2.1)$$

### Transformation Matrix of $\sigma_{xz}$ reflection

Rotations are not the only symmetry operations we can perform on a molecule. Figure 4.2.2.4 illustrates the reflection of a point through the  $xz$  plane. This operation transforms the vector  $(x, y, z)$  into the vector  $(x, -y, z)$ . Symmetry operators involving reflections through a plane are usually denoted with the letter  $\sigma$ , so the operator that reflects a point through the  $xz$  plane is  $\hat{\sigma}_{xz}$ :

$$\sigma_{xz}(x, y, z) = (x, -y, z)$$



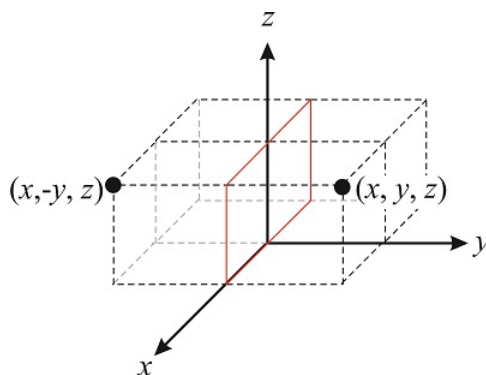


Figure 4.2.2.3: A reflection through the  $xz$  plane

Following the same logic we used for the rotation matrix, we can write the  $\sigma_{xz}$  transformation matrix as:

$$\sigma_{x,z} = \begin{pmatrix} 1 & 0 & 0 \\ 0 & -1 & 0 \\ 0 & 0 & 1 \end{pmatrix} \quad (4.2.2.2)$$

This is true because

$$\begin{pmatrix} 1 & 0 & 0 \\ 0 & -1 & 0 \\ 0 & 0 & 1 \end{pmatrix} \begin{pmatrix} x \\ y \\ z \end{pmatrix} = \begin{pmatrix} x \\ -y \\ z \end{pmatrix}$$

#### ? Exercise 4.2.2.1

Find the transformation matrix of the identity ( $E$ ) and the  $\sigma_{y,z}$  operations under the  $C_{2v}$  point group.

**Answer**

The transformation matrix for  $E$  is  $\begin{pmatrix} 1 & 0 & 0 \\ 0 & 1 & 0 \\ 0 & 0 & 1 \end{pmatrix}$ .

The transformation matrix for  $\sigma_{v(yz)}$  is  $\begin{pmatrix} -1 & 0 & 0 \\ 0 & 1 & 0 \\ 0 & 0 & 1 \end{pmatrix}$ .

### Characters

For a square matrix, the **character** is the trace of the matrix. For the  $C_2$  operation, with the transformation matrix

$$\begin{pmatrix} -1 & 0 & 0 \\ 0 & -1 & 0 \\ 0 & 0 & 1 \end{pmatrix},$$

the trace is  $(-1) + (-1) + 1 = -1$ .

The set of characters for a point group is called a **reducible representation ( $\Gamma$ )**. The reducible representation for the  $C_{2v}$  point group is:

$C_{2v}$	$E$	$C_2$	$\sigma_v$	$\sigma'_v$
$\Gamma$	3	-1	1	1

### ? Exercise 4.2.2.1

Prove that the characters in the reducible representation for  $C_{2v}$  are correct:

$C_{2v}$	$E$	$C_2$	$\sigma_v$	$\sigma'_v$
$\Gamma$	3	-1	1	1

**Answer**

For the  $E$  operation, with the transformation matrix  $\begin{pmatrix} 1 & 0 & 0 \\ 0 & 1 & 0 \\ 0 & 0 & 1 \end{pmatrix}$ , the trace is  $1 + 1 + 1 = 3$ .

For the  $C_2^z$  operation, with the transformation matrix  $\begin{pmatrix} -1 & 0 & 0 \\ 0 & -1 & 0 \\ 0 & 0 & 1 \end{pmatrix}$ , the trace is  $(-1) + (-1) + 1 = -1$ .

For the  $\sigma_{v(xz)'}^z$  operation, with the transformation matrix  $\begin{pmatrix} 1 & 0 & 0 \\ 0 & -1 & 0 \\ 0 & 0 & 1 \end{pmatrix}$ , the trace is  $1 + (-1) + 1 = 1$ .

For the  $\sigma_{v(yz)''}$  operation, with the transformation matrix  $\begin{pmatrix} -1 & 0 & 0 \\ 0 & 1 & 0 \\ 0 & 0 & 1 \end{pmatrix}$ , the trace is  $-1 + 1 + 1 = 1$ .

This gives the reducible representation

$C_{2v}$	$E$	$C_2$	$\sigma_v$	$\sigma'_v$
$\Gamma$	3	-1	1	1

## Reducible and Irreducible Representations

Let us now go back and look in more detail at the transformation matrices of the  $C_{2v}$  point group that we derived above. If we look at the matrices carefully we see that they all take the same block diagonal form (a square matrix is said to be **block diagonal** if all the elements are zero except for a set of submatrices lying along the diagonal).

$$E = \begin{pmatrix} [1] & 0 & 0 \\ 0 & [1] & 0 \\ 0 & 0 & [1] \end{pmatrix}, C_2 = \begin{pmatrix} [-1] & 0 & 0 \\ 0 & [-1] & 0 \\ 0 & 0 & [1] \end{pmatrix}, \sigma'_{v(xz)} = \begin{pmatrix} [1] & 0 & 0 \\ 0 & [-1] & 0 \\ 0 & 0 & [1] \end{pmatrix}, \sigma_{v(yz)''} = \begin{pmatrix} [-1] & 0 & 0 \\ 0 & [1] & 0 \\ 0 & 0 & [1] \end{pmatrix}$$

All the non-zero elements become 1x1 matrices that each represent individual  $x, y, z$  coordinates. In other words, the element  $a_{11}$  represents  $x$ ,  $a_{22}$  represents  $y$ , and  $a_{33}$  represents  $z$ . The matrix elements for  $x$  from each transformation matrix combine to form an irreducible representation of the  $C_{2v}$  point group. Likewise, the matrix elements for  $y$  combine to form a second irreducible representation, and the same is true for  $z$  elements. These irreducible representations are shown below:

$C_{2v}$	$E$	$C_2$	$\sigma_v$	$\sigma'_v$	Coordinate Used
	1	-1	1	-1	$x$
	1	-1	-1	1	$y$
	1	1	1	1	$z$
$\Gamma$	3	-1	1	1	

The irreducible representations add to form the reducible representation,  $\Gamma$ . This  $\Gamma$ , which is the set of 3x3 matrices, can be reduced to the set of 1x1 matrices of the irreducible representations. The irreducible representations cannot be reduced further, hence their name.

## Sources & Attribution

- Parts of this page was adapted from [Matrices \(click here\)](#) (Symmetry Operators), contributed by Marcia Levitus, Associate Professor (Biodesign Institute) at Arizona State University.
- Parts of this page were adapted from [Reductions of Representations](#), contributed by

[Claire Vallance](#) (University of Oxford)

- Curated or created by [Kathryn Haas](#)

---

This page titled [4.2.2: Representations of Point Groups](#) is shared under a [not declared](#) license and was authored, remixed, and/or curated by [Kathryn Haas](#).

- [4.3.2: Representations of Point Groups](#) by [Kathryn Haas](#) has no license indicated.

## 4.2.3: Character Tables

### Introduction to Character Tables, using $C_{2v}$ as example

A character table is the complete set of irreducible representations of a symmetry group. In the [previous section](#), we derived three of the four irreducible representations for the  $C_{2v}$  point group. These three irreducible representations are labeled  $A_1$ ,  $B_1$ , and  $B_2$ . The fourth irreducible representation,  $A_2$ , can be derived using the properties (or "rules") for irreducible representations listed below.

#### Properties of Characters of Irreducible Representations in Point Groups

1. There is always a totally symmetric representation in which all the characters are 1.  
*e.g. In  $C_{2v}$ ,  $A_1$  is totally symmetric.*
2. The order of the group ( $h$ ) is the total number of symmetry operations in the group.  
*e.g. In  $C_{2v}$ ,  $h = 4$*
3. Similar operations are listed as classes (R) and appear as columns in the table.  
*e.g. In  $C_{2v}$ , there are four classes of operations,  $E$ ,  $C_2$ ,  $\sigma_{v(xz)}$ , and  $\sigma'_{v(yz)}$*
4. The number of irreducible representations (rows) must equal the number of classes (columns). This results in all character tables being square.  
*e.g. In  $C_{2v}$ , there are four classes and four irreducible representations.*
5. The sum of squares of all characters under  $E$  is equal to the order of the group:  $h = \sum [\chi_i]^2$   
*e.g. In  $C_{2v}$ ,  $h = 1^2 + 1^2 + 1^2 + 1^2 = 4$*
6. For any irreducible representation ( $i$ ), the sum of squares of its characters multiplied by the number of operations in the class is the order of the group:  $h = \sum [\chi_i(R)]^2$   
*e.g. For  $A_2$  in  $C_{2v}$ ,  $h = (1 \times 1)^2 + (1 \times 1)^2 + (-1 \times 1)^2 + (-1 \times 1)^2 = 4$*
7. Irreducible representations are orthogonal. For any two representations ( $i$  and  $j$ ):  $\sum [\chi_i * (R) \chi_j(R)] = 0$   
*e.g. For  $B_1$  and  $B_2$  of  $C_{2v}$ ,  $[1 \times 1] + [-1 \times -1] + [1 \times -1] + [-1 \times 1] = 0$*

The complete character table for  $C_{2v}$  is given below.

$C_{2v}$	$E$	$C_2$	$\sigma_v$	$\sigma'_v$	$h = 4$	
$A_1$	1	1	1	1	$z$	$x^2, y^2, z^2$
$A_2$	1	1	-1	-1	$R_z$	$xy$
$B_1$	1	-1	1	-1	$x, R_y$	$xz$
$B_2$	1	-1	-1	1	$y, R_x$	$yz$

The various sections of the table are as follows:

- i. The first element in the table gives the name of the point group, usually in Schoenflies ( $C_{2v}$ ) notation.
- ii. Along the first row are the symmetry operations of the group,  $E$ ,  $C_2$ ,  $\sigma_v$  and  $\sigma'_v$ , followed by the order of the group,  $h$ .
- iii. In the first column are the irreducible representations of the group, represented by Mulliken Labels. In  $C_{2v}$  the irreducible representations are  $A_1$ ,  $A_2$ ,  $B_1$  and  $B_2$ . The Mulliken labels indicate the symmetry of each representation (explained further below).
- iv. The characters ( $\chi$ ) of the irreducible representations under each symmetry operation are given in the bulk of the table.
- v. The final column(s) of the table lists a number of functions that transform as the various irreducible representations of the group. These are the Cartesian axes ( $x, y, z$ ), the Cartesian products ( $z^2, x^2 + y^2, xy, xz, yz$ ), and the rotations ( $R_x, R_y, R_z$ ) (explained further below).

### Another example: $C_{3v}$

The  $C_{3v}$  point group has three classes of operations:  $E$ ,  $C_3$ , and  $\sigma_{v(xz)}$ . The derivation of transformation matrices for  $E$  and  $\sigma_{v(xz)}$  is similar to the case for  $C_{2v}$ . However, the  $C_3$  operation does not give simple 1 or -1 characters. If we carry out a rotation about  $z$  by an angle  $\theta$ , our  $x$  and  $y$  axes are transformed onto new axes  $x'$  and  $y'$ . The new axes can each be written as a linear combination of our original  $x$  and  $y$  axes. The derivation of the rotation matrices will not be covered in this text, but is described [elsewhere](#):

$$\begin{aligned}x' &= x \cos \theta + y \sin \theta \\y' &= -x \sin \theta + y \cos \theta\end{aligned}$$

For a  $C_3$  rotation counterclockwise through  $120^\circ$  (or  $\frac{2\pi}{3}$ ):

$$\begin{aligned}x' &= x \cos(2\pi/3) + y \sin(2\pi/3) = -\frac{1}{2}x - \frac{\sqrt{3}}{2}y \\y' &= -x \sin(2\pi/3) + y \cos(2\pi/3) = \frac{\sqrt{3}}{2}x - \frac{1}{2}y\end{aligned}$$

The transformation matrices for symmetry operations of  $C_{3v}$  are as follows:

$$E = \begin{pmatrix} 1 & 0 & 0 \\ 0 & 1 & 0 \\ 0 & 0 & 1 \end{pmatrix} \quad C_3 = \begin{pmatrix} [-\frac{1}{2} & -\frac{\sqrt{3}}{2}] & 0 \\ [\frac{\sqrt{3}}{2} & -\frac{1}{2}] & 0 \\ 0 & 0 & 1 \end{pmatrix} \quad \sigma'_{v(xz)} = \begin{pmatrix} 1 & 0 & 0 \\ 0 & -1 & 0 \\ 0 & 0 & 1 \end{pmatrix}$$

The  $C_3$  transformation matrix contains off-diagonal entries, and therefore it cannot be block diagonalized as 1x1 matrices. However, the first two lines can be diagonalized as a 2x2 and the last line as a 1x1 matrix (Figure 4.2.3.1):

**2x2 matrices**

$$E = \begin{pmatrix} 1 & 0 & 0 \\ 0 & 1 & 0 \\ 0 & 0 & 1 \end{pmatrix} \quad C_3 = \begin{pmatrix} [-\frac{1}{2} & -\frac{\sqrt{3}}{2}] & 0 \\ [\frac{\sqrt{3}}{2} & -\frac{1}{2}] & 0 \\ 0 & 0 & 1 \end{pmatrix} \quad \sigma'_{v(xz)} = \begin{pmatrix} 1 & 0 & 0 \\ 0 & -1 & 0 \\ 0 & 0 & 1 \end{pmatrix}$$

Figure 4.2.3.1: The  $C_3$  transformation matrix contains off-diagonal entries, and therefore it cannot be block diagonalized as 1x1 matrices. However, the first two lines can be diagonalized as a 2x2 and the last line as a 1x1 matrix. (CC-BY-NC-SA; Kathryn Haas)

The character from a 2x2 matrix is the sum of the trace of that matrix. So, for the  $C_3$  operation, the 2x2 matrix gives the character -1 (from  $-\frac{1}{2} + -\frac{1}{2}$ ).

The character table for  $C_{3v}$  is shown below.

$C_{3v}$	$E$	$2C_3$	$3\sigma_v$	$h = 6$
$A_1$	1	1	1	$z, z^2, x^2 + y^2$
$A_2$	1	1	-1	$R_z$
$E$	2	-1	0	$(x, y), (xy, x^2 + y^2), (xz, yz), (R_x, R_y)$

## Additional features of character tables

### Additional Features of Character Tables

- Symmetry operations of the same class are grouped into the same column (class) in the character table and not listed separately.  
e.g. In the  $C_{3v}$  point group, there are four operations:  $E$ ,  $C_3$ ,  $C_3^2$ , and  $\sigma_v$ . The  $C_3$  and  $C_3^2$  operations are listed together in the character table as  $2C_3$ .
- If there are multiple  $C_2$  axes (in a  $D$  group), the  $C_2$  axes that are perpendicular to the principle axis are labeled with primes (e.g.  $C_2'$  and  $C_2''$ ); when there are multiple types of perpendicular  $C_2$  axes, one prime ( $C_2'$ ) means that it passes through more atoms, while a double prime ( $C_2''$ ) means it goes between atoms.
- Mirror planes that are perpendicular to the principle axis are "horizontal" mirror planes and are designated with an  $h$  subscript ( $\sigma_h$ ). Mirror planes that are in-plane with the principle axis are "vertical" mirror planes,  $\sigma_v$ . When there are two types of vertical mirror planes, those that run through more atoms are  $\sigma_v$  while those that run between atoms are "dihedral",  $\sigma_d$ .
- Matching the symmetry operations listed in the character table to the symmetry operations of a molecule can confirm its point group.

5. Irreducible representations are each assigned a Mulliken label, listed in the left-hand column, that indicates the symmetry of that representation as follows:

Mulliken Labels	meaning
<i>A</i>	singly degenerate (1x1), symmetric to principle axis
<i>B</i>	singly degenerate (1x1), antisymmetric to principle axis
<i>E</i>	doubly degenerate (2x2)
<i>T</i>	triply degenerate (3x3)
Subscripts and superscripts	meaning
1	symmetric to $\sigma_v$ or perpendicular to $C_2$
2	anti-symmetric to $\sigma_v$ or perpendicular to $C_2$
<i>g</i>	symmetric to inversion center
<i>u</i>	anti-symmetric to inversion center
'	symmetric to $\sigma_h$
''	anti-symmetric to $\sigma_h$

6. The right-hand columns of the character table list a number of functions that transform as the various irreducible representations of the group. These are the Cartesian axes ( $x, y, z$ ), the Cartesian products ( $z^2, x^2 + y^2, xy, xz, yz$ ), and the rotations ( $R_x, R_y, R_z$ ). These expressions indicate the properties of orbitals within the symmetry group. The *s*-orbital, which is totally symmetric, corresponds to the irreducible representation that possesses symmetry of  $x^2, y^2$  and  $z^2$  combined. The *p*-orbitals each possess the symmetry of the corresponding axis (e.g.  $p_x$  corresponds to the  $x$  axis). Each of the *d*-orbitals possess the symmetry of the corresponding binary product (e.g.  $d_{xy}$  corresponds to the binary product,  $xy$ , in the character table).

The functions listed in the final column of the table are important in many chemical applications of group theory, particularly in spectroscopy. For example, by looking at the transformation properties of  $x, y$  and  $z$  (sometimes given in character tables as  $T_x, T_y, T_z$ ) we can discover the symmetry of translations along the  $x, y$ , and  $z$  axes. Similarly,  $R_x, R_y$  and  $R_z$  represent rotations about the three Cartesian axes. The transformation properties of  $x, y$ , and  $z$  can be used to determine whether or not a molecule is IR-active or whether or not it can absorb a photon of  $x$ -,  $y$ -, or  $z$ -polarized light and undergo a spectroscopic transition. The Cartesian products play a similar role in determining selection rules for Raman transitions, which involve two photons.

A visual summary of the sections and their significance is given in Figure 4.2.3.2 Character tables for common point groups are given in the [References section of LibreTexts Bookshelves](#).

Point Group (Shoenflies notation)  $C_{2v}$

Symmetry operations (R) organized into **classes**

Order of the group  $h = 4$

	E	$C_2$	$\sigma_v(xz)$	$\sigma_v'(yz)$		
<b>A<sub>1</sub></b>	1	1	1	1	<b>z</b>	$x^2, y^2, z^2$
<b>A<sub>2</sub></b>	1	1	-1	-1	<b>R<sub>z</sub></b>	<b>xy</b>
<b>B<sub>1</sub></b>	1	-1	1	-1	<b>x, R<sub>y</sub></b>	<b>zx</b>
<b>B<sub>2</sub></b>	1	-1	-1	1	<b>y, R<sub>x</sub></b>	<b>yz</b>

**Characters ( $\chi$ )**

**Mulliken labels ( $i,j,..$ )** ..tell us "at a glance" about the symmetry of a representation

**Labels**  
 A = 1x1, symmetric to principle axis  
 B = 1x1, anti-symmetric to principle axis  
 E = 2x2  
 T = 3x3

**Subscripts and superscripts**  
 1 = symmetric to  $\sigma_v$  or  $\perp C_2$   
 2 = anti-symmetric to  $\sigma_v$  or  $\perp C_2$   
 g = symmetric to inversion center  
 u = anti-symmetric to inversion center  
 ' = symmetric to  $\sigma_h$   
 " = anti-symmetric to  $\sigma_h$

**Quadratic functions (translations):**  
 Symmetry of d-orbitals.  
 Raman active modes.

**Linear functions (transformations):**  
 x, y, z axes and rotations around axes ( $R_x, R_y, R_z$ ).  
 Symmetry of the p-orbitals.  
 IR active modes.

Figure 4.2.3.2: Visual summary of the sections of a character table and their meaning. (CC-BY-NC-SA; Kathryn Haas)

### Contributors and Attributions

- Curated or created by [Kathryn Haas](#)
  - [Claire Vallance](#) (University of Oxford)
- adapted from [Character Tables \(click here\)](#)

This page titled [4.2.3: Character Tables](#) is shared under a [not declared](#) license and was authored, remixed, and/or curated by [Kathryn Haas](#).

- [4.3.3: Character Tables](#) by [Kathryn Haas](#) has no license indicated.

## 4.3: Application to Vibrational Spectroscopy

---

Learning objectives for this unit are to:

- Know the number of expected vibrational modes in a molecule containing "N" atoms
  - Generate reducible representations using a degrees of freedom basis set or a simple bond stretching basis set
  - Decompose reducible representations within a point group into their irreducible components using the great orthogonality theorem
  - Assign the irreducible representations to translations, rotations and vibrations
  - Determine which vibrational modes are IR active and Raman active
  - Use Mulliken symbols to predict the molecular deformations that correspond to a particular vibrational mode
  - Apply the selection rules for IR and Raman active modes to experimental scenarios
- 

4.3: Application to Vibrational Spectroscopy is shared under a [not declared](#) license and was authored, remixed, and/or curated by LibreTexts.



### 4.3.1: Molecular Vibrations

Symmetry and group theory can be applied to understand molecular vibrations. This is particularly useful in the context of predicting the number of peaks expected in the infrared (IR) and Raman spectra of a given compound.

We will use water as a case study to illustrate how group theory is used to predict the number of peaks in IR and Raman spectra.

#### How many IR and Raman peaks would we expect for $H_2O$ ?

To answer this question with group theory, a pre-requisite is that you **assign the molecule's point group and assign an axis system** to the entire molecule. By convention, the  $z$  axis is collinear with the principle axis, the  $x$  axis is in-plane with the molecule or the most number of atoms. It is a good idea to stick with this convention (see Figure 4.3.1.1).

**What is the point group for  $H_2O$ ? (click to see answer)**

$H_2O$  has the following operations:  $E$ ,  $C_2$ ,  $\sigma_v$ ,  $\sigma'_v$ . The point group is  $C_{2v}$ .

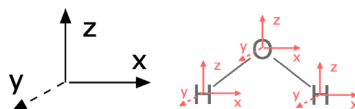


Figure 4.3.1.1: The first step to finding normal modes is to assign a consistent axis system to the entire molecule and to each atom. (CC-BY-SA; Kathryn Haas)

Now that we know the molecule's point group, we can use group theory to determine the symmetry of all motions in the molecule, or the symmetry of each of its degrees of freedom. Then we will subtract rotational and translational degrees of freedom to find the vibrational degrees of freedom. The number of degrees of freedom depends on the number of atoms ( $N$ ) in a molecule. Each atom in the molecule can move in three dimensions ( $x, y, z$ ), and so the number of degrees of freedom is three dimensions times  $N$  number of atoms, or  $3N$ . The total degrees of freedom include a number of vibrations, three translations (in  $x, y$ , and  $z$ ), and either two or three rotations. Linear molecules have two rotational degrees of freedom, while non-linear molecules have three. The vibrational modes are represented by the following expressions:

$$\begin{aligned}\text{Linear Molecule Degrees of Freedom} &= 3N - 5 \\ \text{Non-Linear Molecule Degrees of Freedom} &= 3N - 6\end{aligned}$$

**Our goal is to find the symmetry of all degrees of freedom, and then determine which are vibrations that are IR- and Raman-active.**

#### STEP 1: Find the reducible representation for all normal modes $\Gamma_{modes}$ .

The first major step is to **find a reducible representation ( $\Gamma$ )** for the movement of all atoms in the molecule (including rotational, translational, and vibrational degrees of freedom). We'll refer to this as  $\Gamma_{modes}$ . To find normal modes using group theory, **assign an axis system** to each individual atom to represent the three dimensions in which each atom can move. Each axis on each atom should be consistent with the conventional axis system you previously assigned to the entire molecule (see Figure 4.3.1.1).

$\Gamma_{modes}$  is the sum of the **characters (trace) of the transformation matrix** for the entire molecule (in the case of water, there are 9 degrees of freedom and this is now a 9x9 matrix). Let's walk through this step-by-step. The transformation matrix of  $E$  and  $C_2$  are shown below:

$$E = \begin{pmatrix} 1 & 0 & 0 & 0 & 0 & 0 & 0 & 0 & 0 \\ 0 & 1 & 0 & 0 & 0 & 0 & 0 & 0 & 0 \\ 0 & 0 & 1 & 0 & 0 & 0 & 0 & 0 & 0 \\ 0 & 0 & 0 & 1 & 0 & 0 & 0 & 0 & 0 \\ 0 & 0 & 0 & 0 & 1 & 0 & 0 & 0 & 0 \\ 0 & 0 & 0 & 0 & 0 & 1 & 0 & 0 & 0 \\ 0 & 0 & 0 & 0 & 0 & 0 & 1 & 0 & 0 \\ 0 & 0 & 0 & 0 & 0 & 0 & 0 & 1 & 0 \\ 0 & 0 & 0 & 0 & 0 & 0 & 0 & 0 & 1 \end{pmatrix} \begin{pmatrix} x_{oxygen} \\ y_{oxygen} \\ z_{oxygen} \\ x_{hydrogen-a} \\ y_{hydrogen-a} \\ z_{hydrogen-a} \\ x_{hydrogen-b} \\ y_{hydrogen-b} \\ z_{hydrogen-b} \end{pmatrix} = \begin{pmatrix} x'_{oxygen} \\ y'_{oxygen} \\ z'_{oxygen} \\ x'_{hydrogen-a} \\ y'_{hydrogen-a} \\ z'_{hydrogen-a} \\ x'_{hydrogen-b} \\ y'_{hydrogen-b} \\ z'_{hydrogen-b} \end{pmatrix}, \chi = 9$$

$$C_2 = \begin{pmatrix} -1 & 0 & 0 & 0 & 0 & 0 & 0 & 0 & 0 \\ 0 & -1 & 0 & 0 & 0 & 0 & 0 & 0 & 0 \\ 0 & 0 & 1 & 0 & 0 & 0 & 0 & 0 & 0 \\ 0 & 0 & 0 & 0 & 0 & 0 & -1 & 0 & 0 \\ 0 & 0 & 0 & 0 & 0 & 0 & 0 & -1 & 0 \\ 0 & 0 & 0 & 0 & 0 & 0 & 0 & 0 & 1 \\ 0 & 0 & 0 & -1 & 0 & 0 & 0 & 0 & 0 \\ 0 & 0 & 0 & 0 & -1 & 0 & 0 & 0 & 0 \\ 0 & 0 & 0 & 0 & 0 & 1 & 0 & 0 & 0 \end{pmatrix} \begin{pmatrix} x_{oxygen} \\ y_{oxygen} \\ z_{oxygen} \\ x_{hydrogen-a} \\ y_{hydrogen-a} \\ z_{hydrogen-a} \\ x_{hydrogen-b} \\ y_{hydrogen-b} \\ z_{hydrogen-b} \end{pmatrix} = \begin{pmatrix} x'_{oxygen} \\ y'_{oxygen} \\ z'_{oxygen} \\ x'_{hydrogen-a} \\ y'_{hydrogen-a} \\ z'_{hydrogen-a} \\ x'_{hydrogen-b} \\ y'_{hydrogen-b} \\ z'_{hydrogen-b} \end{pmatrix}, \chi = 1$$

It is unnecessary to find the transformation matrix for each operation since it is only the TRACE that gives us the character, and any off-diagonal entries do not contribute to  $\Gamma_{modes}$ . The values that contribute to the trace can be found simply by performing each operation in the point group and assigning a value to each individual atom to represent how it is changed by that operation. If the atom moves away from itself, that atom gets a character of zero (this is because any non-zero characters of the transformation matrix are off of the diagonal). If the atom remains in place, each of its three dimensions is assigned a value of  $\cos\theta$ . For the example of  $H_2O$  under the  $C_{2v}$  point group, the axes that remain unchanged ( $\theta = 0^\circ$ ) are assigned a value of  $\cos(0^\circ) = 1$ , while those that are moved into the negative of themselves (rotated or reflected to  $\theta = 180^\circ$ ) are assigned  $\cos(180^\circ) = -1$ . The character for  $\Gamma$  is the sum of the values for each transformation.

**Let's walk through the steps to assign characters of  $\Gamma_{modes}$  for  $H_2O$  to illustrate how this works:**

For the operation  $E$ , performed on  $H_2O$ , all three atoms remain in place. The three axes  $x, y, z$  on each atom remain unchanged. Thus, each of the three axes on each of three atom (nine axes) is assigned the value  $\cos(0^\circ) = 1$ , resulting in a sum of  $\chi = 9$  for the  $\Gamma_{modes}$ .

For the operation  $C_2$ , the two hydrogen atoms are moved away from their original position, and so the hydrogens are assigned a value of zero. The oxygen remains in place; the  $z$ -axis on oxygen is unchanged ( $\cos(0^\circ) = 1$ ), while the  $x$  and  $y$  axes are inverted ( $\cos(180^\circ)$ ). The sum of these characters gives  $\chi = -1$  in the  $\Gamma_{modes}$ .

Now you try! Find the characters of  $\sigma_{v(xz)}$  and  $\sigma_{v(yz)}$  under the  $C_{2v}$  point group. Compare what you find to the  $\Gamma_{modes}$  for all normal modes given below.

$C_{2v}$	$E$	$C_2$	$\sigma_v$	$\sigma'_v$
$\Gamma_{modes}$	9	-1	3	1

(4.3.1.1)

**STEP 2: Break  $\Gamma_{modes}$  into its component irreducible representations.**

Now that we've found the  $\Gamma_{modes}$  (4.3.1.1), we need to break it down into the individual irreducible representations ( $i, j, k, \dots$ ) for the point group. We can do this systematically using the following formula:

$$\# \text{ of } i = \frac{1}{h} \sum (\# \text{ of operations in class}) \times (\chi_i) \times (\chi_i) \quad (4.3.1.2)$$

In other words, the number of irreducible representations of type  $i$  is equal to the sum of the number of operations in the class  $\times$  the character of the  $\Gamma_{modes} \times$  the character of  $i$ , and that sum is divided by the order of the group ( $h$ ).

Using equation 4.3.1.2 we find that for all normal modes of  $H_2O$ :

$$\Gamma_{modes} = 3A_1 + 1A_2 + 3B_1 + 2B_2 \quad (4.3.1.3)$$

Notice there are 9 irreducible representations in Equation 4.3.1.3. These irreducible representations represent the symmetries of all 9 motions of the molecule: vibrations, rotations, and translations.

### ? Exercise 4.3.1.1: Derive the irreducible representation in equation 4.3.1.3.

Derive the nine irreducible representations of  $\Gamma_{modes}$  for  $H_2O$ , expression 4.3.1.3

#### Hint

To find the number of each kind of irreducible representation that combine to form the  $\Gamma_{modes}$ , we need the characters of  $\Gamma_{modes}$  that we found above (4.3.1.), the  $C_{2v}$  character table (below), and equation 4.3.1.2

$C_{2v}$	$1E$	$1C_2$	$1\sigma_v$	$1\sigma'_v$	$h = 4$	
$A_1$	1	1	1	1	$z$	$x^2, y^2, z^2$
$A_2$	1	1	-1	-1	$R_z$	$xy$
$B_1$	1	-1	1	-1	$x, R_y$	$xz$
$B_2$	1	-1	-1	1	$y, R_x$	$yz$

In the  $C_{2v}$  point group, each class has only one operation, so the number of operations in each class (from equation 4.3.1.2) is **1** for each class. This has been explicitly added to the character table above for emphasis.

#### Answer

The number of  $A_1 = \frac{1}{4}[(1 \times 9 \times 1) + (1 \times (-1) \times 1) + (1 \times 3 \times 1) + (1 \times 1 \times 1)] = 3A_1$

The number of  $A_2 = \frac{1}{4}[(1 \times 9 \times 1) + (1 \times (-1) \times 1) + ((-1) \times 3 \times 1) + ((-1) \times 1 \times 1)] = 1A_2$

The number of  $B_1 = \frac{1}{4}[(1 \times 9 \times 1) + ((-1) \times (-1) \times 1) + (1 \times 3 \times 1) + ((-1) \times 1 \times 1)] = 3B_1$

The number of  $B_2 = \frac{1}{4}[(1 \times 9 \times 1) + ((-1) \times (-1) \times 1) + ((-1) \times 3 \times 1) + (1 \times 1 \times 1)] = 2B_2$

### STEP 3: Subtract rotations and translations to find vibrational modes.

Because we are interested in molecular vibrations, we need to subtract the rotations and translations from the total degrees of freedom.

$$\text{Vibrations} = \Gamma_{modes} - \text{Rotations} - \text{Translations}$$

In the example of  $H_2O$ , the total degrees of freedom are given above in equation 4.3.1.3 and therefore the vibrational degrees of freedom can be found by:

$$H_2O \text{ vibrations} = (3A_1 + 1A_2 + 3B_1 + 2B_2) - \text{Rotations} - \text{Translations} \quad (4.3.1.4)$$

But which of the irreducible representations are ones that represent rotations and translations? The symmetry of rotational and translational degree modes can be found by inspecting the right-hand columns of any character table. Rotational modes correspond to irreducible representations that include  $R_x$ ,  $R_y$ , and  $R_z$  in the table, while each of the three translational modes has the same symmetry as the  $x$ ,  $y$  and  $z$  axes. For a non-linear molecule, subtract three rotational irreducible representations and three translational irreducible representations from the total  $\Gamma_{modes}$ .

In the specific case of water, we refer to the  $C_{2v}$  character table:

$C_{2v}$	$E$	$C_2$	$\sigma_v$	$\sigma'_v$	$h = 4$	
$A_1$	1	1	1	1	$z$	$x^2, y^2, z^2$
$A_2$	1	1	-1	-1	$R_z$	$xy$
$B_1$	1	-1	1	-1	$x, R_y$	$xz$
$B_2$	1	-1	-1	1	$y, R_x$	$yz$

In  $C_{2v}$ , translations correspond to  $B_1$ ,  $B_2$ , and  $A_1$  (respectively for  $x, y, z$ ), and rotations correspond to  $B_2$ ,  $B_1$ , and  $A_1$  (respectively for  $R_x, R_y, R_z$ ). Subtracting these six irreducible representations from  $\Gamma_{modes}$  will leave us with the irreducible representations for vibrations.

$$\begin{aligned}
 H_2O \text{ vibrations} &= \Gamma_{modes} - \text{Rotations} - \text{Translations} \\
 &= (3A_1 + 1A_2 + 3B_1 + 2B_2) - (A_1 + B_1 + B_2) - (A_2 + B_1 + B_2) \\
 &= 2A_1 + 1B_1
 \end{aligned}$$

**The three vibrational modes for  $H_2O$  are  $2A_1 + 1B_1$ .** Note that we have the correct number of vibrational modes based on the expectation of  $3N - 6$  vibrations for a non-linear molecule.

#### STEP 4: Determine which of the vibrational modes are IR-active and Raman-active.

The next step is to determine which of the vibrational modes is IR-active and Raman-active. To do this, we apply the IR and Raman Selection Rules below:

##### IR and Raman Selection Rules

###### Infrared selection rules:

If a vibration results in the change in the molecular dipole moment, it is IR-active. In the character table, we can recognize the vibrational modes that are IR-active by those with symmetry of the  $x, y$ , and  $z$  axes.

In  $C_{2v}$ , any vibrations with  $A_1$ ,  $B_1$  or  $B_2$  symmetry would be IR-active.

###### Raman selection rules:

If a vibration results in a change in the molecular polarizability, it will be Raman-active. In the character table, we can recognize the vibrational modes that are Raman-active by those with symmetry of any of the binary products ( $xy, xz, yz, x^2, y^2$ , and  $z^2$ ) or a linear combination of binary products (e.g.  $x^2 - y^2$ ).

In  $C_{2v}$ , any vibrations with  $A_1$ ,  $A_2$ ,  $B_1$  or  $B_2$  symmetry would be Raman-active.

In our  $H_2O$  example, we found that of the three vibrational modes, two have  $A_1$  and one has  $B_1$  symmetry. Both  $A_1$  and  $B_1$  are IR-active, and both are also Raman-active. **There are two possible IR peaks and three possible Raman peaks expected for water.\***

\*It is important to note that this prediction tells only what is possible, but not what we might actually see in the IR and Raman spectra. For example, if the two IR peaks overlap, we might actually notice only one peak in the spectrum. Or, if one or more peaks is off-scale, we wouldn't see it in actual data. Group theory tells us what is *possible and allows us to make predictions or interpretations of spectra*.

#### Summary of Analysis for Water

Each molecular motion for water, or any molecule, can be assigned a symmetry under the molecule's point group. For water, we found that there are a total of 9 molecular motions;  $3A_1 + A_2 + 3B_1 + 2B_2$ . Six of these motions are not the translations and rotations. The remaining motions are vibrations; two with  $A_1$  symmetry and one with  $B_1$  symmetry.

We can tell what these vibrations would look like based on their symmetries. The two  $A_1$  vibrations must be completely symmetric, while the  $B_1$  vibration is antisymmetric with respect to the principal  $C_2$  axis.

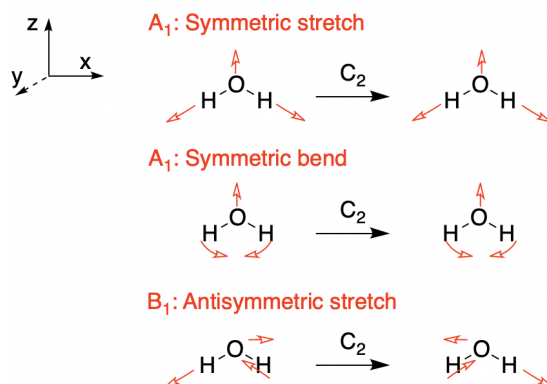


Figure 4.3.1.2: Illustration of the vibrational motions of water. The antisymmetric stretch has  $B_1$  symmetry, while the symmetric stretch and symmetric bend both have  $A_1$  symmetry. ([Click here to see animation](#)) (CC-BY-NC-SA; Kathryn Haas)

Table 4.3.1.1: Summary of the Symmetry of Molecular Motions for Water

All Motions (step 2 above)	Translations (x,y,z)	Rotations ( $R_x, R_y, R_z$ )	Remaining Vibrations	Description of Vibration
$3A_1$	$1A_1$		$2A_1$	One is a symmetric stretch. The other is a symmetric bend. Both are <i>IR-active</i> and <i>Raman-active</i>
$A_2$		$1A_2$		
$3B_1$	$1B_1$	$1B_1$	$1B_1$	Antisymmetric stretch that is <i>IR-active</i> and <i>Raman-active</i> .
$2B_2$	$1B_2$	$1B_2$		

### ? Exercise 4.3.1.2

Find the symmetries of all motions of the square planar complex, tetrachloroplatinate (II). Determine which are rotations, translations, and vibrations. Determine which vibrations are IR and Raman active.

#### Answer

The point group of  $[\text{PtCl}_4]^{2-}$  is  $D_{4h}$  ([refer to its character table](#)). There are five atoms and 15 vectors ( $x, y, z$  for each atom  $\times$  5 atoms).

**STEP 1:** The first major step is to **find a reducible representation ( $\Gamma$ )** for the movement of all atoms in the molecule.

$$\begin{array}{c|cccccccccccc}
 C_{2v} & E & 2C_4 & C_2 & 2C'_2 & 2C''_2 & i & 2S_4 & \sigma_h & 2\sigma_v & 2\sigma_d \\
 \hline
 \Gamma_{\text{modes}} & 15 & 1 & -1 & -3 & -1 & -3 & -1 & 5 & 3 & 1
 \end{array} \quad (4.3.1.5)$$

**STEP 2:** Break  $\Gamma_{\text{modes}}$  into its component irreducible representations.

Following the process described earlier, we come to  $A_{1g} + A_{2g} + B_{1g} + B_{2g} + E_g + 2A_{2u} + B_{2u} + 3E_u$ . This accounts for all modes of movement, including rotations and translations.

**STEP 3:** Subtract rotations and translations to find vibrational modes.

The translations are  $A_{2u} + E_u$  and the rotations are  $A_{2g} + E_g$ .

The remaining normal modes are:  $A_{1g} + B_{1g} + B_{2g} + A_{2u} + B_{2u} + 2E_u$

**STEP 4:** Determine which of the vibrational modes are IR-active and Raman-active:

$A_{2u} + E_u$  are IR-active. Since  $A_{2u}$  is singly degenerate and  $E_u$  is doubly degenerate, we expect three possible IR bands.

$A_{1g} + B_{1g} + B_{2g}$  are Raman-Active. Each of these is singly degenerate, so we expect three possible Raman bands.

## Selected Vibrational Modes

The interpretation of CO stretching vibrations in an IR spectrum is particularly useful. Symmetry and group theory can be applied to predict the number of CO stretching bands that appear in a vibrational spectrum for a given metal coordination complex. A classic example of this application is in distinguishing isomers of metal-carbonyl complexes. For example, the *cis*- and *trans*- isomers of square planar metal dicarbonyl complexes ( $\text{ML}_2(\text{CO})_2$ ) have a different number of IR stretches that can be predicted and interpreted using symmetry and group theory. Another example is the case of *mer*- and *fac*- isomers of octahedral metal tricarbonyl complexes ( $\text{ML}_3(\text{CO})_3$ ). Structures of the two types of metal carbonyl configurations and their isomers are shown in Figure 4.3.1.1. The isomers in each case can be distinguished using vibrational spectroscopy.

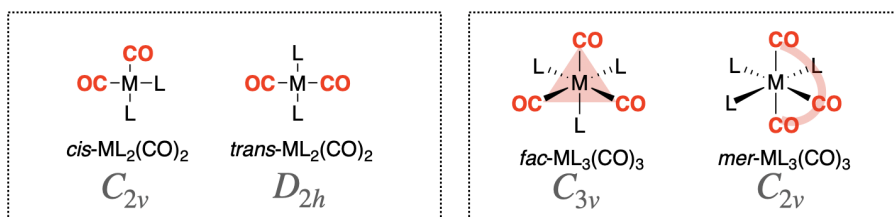


Figure 4.3.1.3: *Cis*- and *trans*- isomers of square planar metal dicarbonyl complexes ( $\text{ML}_2(\text{CO})_2$ ) are shown in the left box. *Mer*- and *fac*- isomers of octahedral metal tricarbonyl complexes ( $\text{ML}_3(\text{CO})_3$ ) are shown in the right box. The point group for each of the general structures is also shown. (CC-BY-NC-SA; Kathryn Haas)

### EXAMPLE 1: Distinguishing *cis*- and *trans*- isomers of square planar metal dicarbonyl complexes

General structures of the *cis*- and *trans*- isomers of square planar metal dicarbonyl complexes ( $\text{ML}_2(\text{CO})_2$ ) are shown in the left box in Figure 4.3.1.1. We can use symmetry and group theory to predict how many carbonyl stretches we should expect for each isomer following the steps below.

#### Step 1: Assign the point group and Cartesian coordinates for each isomer.

The *cis*-isomer has  $C_{2v}$  symmetry and the *trans*-isomer has  $D_{2h}$  symmetry. We assign the Cartesian coordinates so that  $z$  is colinear with the principle axis in each case. For the  $D_{2h}$  isomer, there are several orientations of the  $z$  axis possible. The axes shown in Figure 4.3.1.2 will be used here.

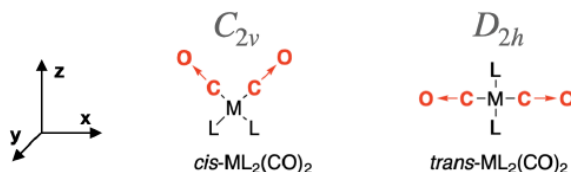


Figure 4.3.1.4: *Cis*- and *trans*- isomers of square planar metal dicarbonyl complexes ( $\text{ML}_2(\text{CO})_2$ ) are shown and oriented with respect to the Cartesian coordinates shown at the left so that the highest-order rotation axis is colinear with  $z$  and the molecule is co-planar with the  $xz$  plane. The vector along each C—O bond is shown using a red arrow ( $\rightarrow$ ). These vectors represent the direction of C—O stretching motions. (CC-BY-NC-SA; Kathryn Haas)

#### Step 2: Produce a reducible representation ( $\Gamma$ ) for CO stretches in each isomer

First, assign a vector along each C—O bond in the molecule to represent the direction of C—O stretching motions, as shown in Figure 4.3.1.2 (red arrows  $\rightarrow$ ). These vectors are used to produce a reducible representation ( $\Gamma$ ) for the C—O stretching motions in each molecule. Using the symmetry operations under the appropriate character table, assign a value of 1 to each vector that remains in place during the operation, and a value of 0 if the vector moves out of place. There will be no occasion where a vector remains in place but is inverted, so a value of -1 will not occur.

##### *cis*- $\text{ML}_2(\text{CO})_2$ :

For *cis*-  $\text{ML}_2(\text{CO})_2$ , the point group is  $C_{2v}$  and so we use the operations under the  $C_{2v}$  character table to create the  $\Gamma_{\text{cis-CO}}$ .

$C_{2v}$	$E$	$C_2$	$\sigma_v(xz)$	$\sigma'_v(yz)$
$\Gamma_{\text{cis-CO}}$	2	0	2	0

### trans- ML<sub>2</sub>(CO)<sub>2</sub>:

For trans- ML<sub>2</sub>(CO)<sub>2</sub>, the point group is  $D_{2h}$  and so we use the operations under the  $D_{2h}$  character table to create the  $\Gamma_{trans-CO}$ .

$D_{2h}$	$E$	$C_2(z)$	$C_2(y)$	$C_2(x)$	$i$	$\sigma(xy)$	$\sigma(xz)$	$\sigma(yz)$
$\Gamma_{trans-CO}$	2	0	0	2	0	2	2	0

### Step 3: Break each $\Gamma$ into its component irreducible representations

Each  $\Gamma$  can be reduced using inspection or by the systematic method [described previously](#).

In the case of the *cis*- ML<sub>2</sub>(CO)<sub>2</sub>, the CO stretching vibrations are represented by  $A_1$  and  $B_1$  irreducible representations:

$C_{2v}$	$E$	$C_2$	$\sigma_v(xz)$	$\sigma'_v(yz)$	
$\Gamma_{cis-CO}$	2	0	2	0	
$A_1$	1	1	1	1	$z, x^2, y^2, z^2$
$B_1$	1	-1	1	-1	$x, R_y, xz$

(4.3.1.6)

In the case of *trans*- ML<sub>2</sub>(CO)<sub>2</sub>, the CO stretching vibrations are represented by  $A_g$  and  $B_{3u}$  irreducible representations:

$D_{2h}$	$E$	$C_2(z)$	$C_2(y)$	$C_2(x)$	$i$	$\sigma(xy)$	$\sigma(xz)$	$\sigma(yz)$	
$\Gamma_{trans-CO}$	2	0	0	2	0	2	2	0	
$A_g$	1	1	1	1	1	1	1	1	$x^2, y^2, z^2$
$B_{3u}$	1	-1	-1	1	-1	1	1	-1	$x$

These irreducible representations correspond to the symmetries of only the selected C—O vibrations. Since these motions are isolated to the C—O group, they do not include any rotations or translations of the entire molecule, and so we do not need to find and subtract rotationals or translations (unlike the previous cases where all motions were considered).

### Step 4: Determine which vibrational modes are IR-active and/or Raman-active

Apply the infrared selection rules [described previously](#) to determine which of the CO vibrational motions are IR-active and Raman-active. The two isomers of ML<sub>2</sub>(CO)<sub>2</sub> are described below.

In the case of the *cis*- ML<sub>2</sub>(CO)<sub>2</sub>, the CO stretching vibrations are represented by  $A_1$  and  $B_1$  irreducible representations. The characters of both representations and their functions are shown above, in [4.3.1.6](#) (and can be found in the  $C_{2v}$  character table). Under  $C_{2v}$ , both the  $A_1$  and  $B_1$  CO vibrational modes are IR-active and Raman-active. Therefore, two bands in the IR spectrum and two bands in the Raman spectrum are possible.

In the case of the *trans*- ML<sub>2</sub>(CO)<sub>2</sub>, the CO stretching vibrations are represented by  $A_g$  and  $B_{3u}$  irreducible representations. The characters of both representations and their functions are shown above, in [4.3.1.6](#) (and can be found in the  $D_{2h}$  character table). Under  $D_{2h}$ , the  $A_g$  vibrational mode is Raman-active only, while the  $B_{3u}$  vibrational mode is IR-active only. Therefore, only one IR band and one Raman band are possible for this isomer.

## Summary

It is possible to distinguish between the two isomers of square planar ML<sub>2</sub>(CO)<sub>2</sub> using either IR or Raman vibrational spectroscopy. The *cis*- ML<sub>2</sub>(CO)<sub>2</sub> can produce two CO stretches in an IR or Raman spectrum, while the *trans*- ML<sub>2</sub>(CO)<sub>2</sub> isomer can produce only one band in either type of vibrational spectrum. If a sample of ML<sub>2</sub>(CO)<sub>2</sub> produced two CO stretching bands, we could rule out the possibility of a pure sample of *trans*-ML<sub>2</sub>(CO)<sub>2</sub>.

### ? Exercise 4.3.1.3

Repeat the steps outlined above to determine how many CO vibrations are possible for *mer*-ML<sub>3</sub>(CO)<sub>3</sub> and *fac*-ML<sub>3</sub>(CO)<sub>3</sub> isomers (see Figure 4.3.1.1) in both IR and Raman spectra. Could either of these vibrational spectroscopies be used to distinguish the two isomers?

**Answer**

Step 1: Assign the point group and Cartesian coordinates for each isomer.

The *fac*-isomer is  $C_{3v}$ . The *mer*-isomer is  $C_{2v}$ .

Step 2: Produce a reducible representation for CO stretches in each isomer.

Step 3: Break each into its component irreducible representations.

Step 4: Determine which vibrational modes are IR-active and/or Raman-active.

**For *fac*- $\text{ML}_3(\text{CO})_3$** , the point group is  $C_{3v}$  and so we use the operations under the  $C_{3v}$  character table to create the  $\Gamma_{\text{fac-CO}}$ . Then break it into its irreducible representations and determine which are IR and Raman active:

$C_{3v}$	$E$	$2C_2$	$3\sigma_v$
$\Gamma_{\text{fac-CO}}$	3	0	1

This reduces to  $A_1 + E$ . Both of these are IR active, and since one is singly degenerate while the other is doubly degenerate, we expect three possible IR bands from this isomer. Both vibrational modes are also Raman active, and again we would expect three possible bands in the Raman spectrum.

**For *mer*- $\text{ML}_3(\text{CO})_3$** , the point group is  $C_{2v}$  and so we use the operations under the  $C_{2v}$  character table to create the  $\Gamma_{\text{mer-CO}}$ . Then break it into its irreducible representations and determine which are IR and Raman active:

$C_{2v}$	$E$	$C_2$	$\sigma_v(xz)$	$\sigma'_v(yz)$
$\Gamma_{\text{mer-CO}}$	3	1	3	1

This reduces to  $2A_1 + B_1$ ; both  $A_1$  and  $B_1$  are IR and Raman active. So this isomer would have three possible IR bands and three possible Raman Bands.

These two isomers have the same number of possible bands in both IR and Raman spectroscopy. It would not be straightforward to distinguish them from each other based on the number of possible bands in the vibrational spectrum.

This page titled [4.3.1: Molecular Vibrations](#) is shared under a [CC BY-NC 4.0](#) license and was authored, remixed, and/or curated by [Kathryn Haas](#).

- [4.4.2: Molecular Vibrations](#) by Kathryn Haas is licensed [CC BY-NC 4.0](#).



## 4.4: Unit 4 Practice Problems

### Exercise 1

Can the following matrices be multiplied and if so what is the product matrix?

a) 
$$\begin{bmatrix} 2 & 1 & 0 \\ 5 & 9 & 1 \\ 2 & 2 & 3 \end{bmatrix} \begin{bmatrix} 0 & 3 & 1 \\ 4 & 1 & 2 \\ -1 & -1 & 3 \end{bmatrix}$$

b) 
$$\begin{bmatrix} 3 & 1 & 0 \end{bmatrix} \begin{bmatrix} 4 \\ 2 \\ 1 \end{bmatrix}$$

c) 
$$\begin{bmatrix} 1 & 2 & 3 & 4 \\ 4 & 3 & 2 & 1 \end{bmatrix} \begin{bmatrix} 1 & 4 \\ 2 & 3 \\ 3 & 2 \\ 4 & 1 \end{bmatrix}$$

d) 
$$\begin{bmatrix} 2 & -1 \\ 1 & 1 \end{bmatrix} \begin{bmatrix} 1 & 5 & 8 \\ 2 & 2 & 4 \\ 1 & 8 & 1 \end{bmatrix}$$

**Answer**

a) 
$$\begin{bmatrix} 2 & 1 & 0 \\ 5 & 9 & 1 \\ 2 & 2 & 3 \end{bmatrix} \begin{bmatrix} 0 & 3 & 1 \\ 4 & 1 & 2 \\ -1 & -1 & 3 \end{bmatrix} = \begin{bmatrix} 2 \times 0 + 1 \times 4 + 0 \times (-1) & 2 \times 3 + 1 \times 1 + 0 \times (-1) & 2 \times 1 + 1 \times 2 + 0 \times 3 \\ 5 \times 0 + 9 \times 4 + 1 \times (-1) & 5 \times 3 + 9 \times 1 + 1 \times (-1) & 5 \times 1 + 9 \times 2 + 1 \times 3 \\ 2 \times 0 + 2 \times 4 + 3 \times (-1) & 2 \times 3 + 2 \times 1 + 3 \times (-1) & 2 \times 1 + 2 \times 2 + 3 \times 3 \end{bmatrix} = \begin{bmatrix} 4 & 7 & 4 \\ 35 & 23 & 26 \\ 5 & 5 & 15 \end{bmatrix}$$

b) 
$$\begin{bmatrix} 3 & 1 & 0 \end{bmatrix} \begin{bmatrix} 4 \\ 2 \\ 1 \end{bmatrix} = \begin{bmatrix} 3 \times 4 + 1 \times 2 + 0 \times 1 \end{bmatrix} = \begin{bmatrix} 14 \end{bmatrix}$$

c) 
$$\begin{bmatrix} 1 & 2 & 3 & 4 \\ 4 & 3 & 2 & 1 \end{bmatrix} \begin{bmatrix} 1 & 4 \\ 2 & 3 \\ 3 & 2 \\ 4 & 1 \end{bmatrix} = \begin{bmatrix} 1 \times 1 + 2 \times 2 + 3 \times 3 + 4 \times 4 & 1 \times 4 + 2 \times 3 + 3 \times 2 + 4 \times 1 \\ 4 \times 1 + 3 \times 2 + 2 \times 3 + 1 \times 4 & 4 \times 4 + 3 \times 3 + 2 \times 2 + 1 \times 1 \end{bmatrix} = \begin{bmatrix} 30 & 20 \\ 20 & 30 \end{bmatrix}$$

d) 
$$\begin{bmatrix} 2 & -1 \\ 1 & 1 \end{bmatrix} \begin{bmatrix} 1 & 5 & 8 \\ 2 & 2 & 4 \\ 1 & 8 & 1 \end{bmatrix}$$

These two matrices cannot be multiplied.

## Exercise 2

Determine the irreducible representations for the following orbitals in the point group  $D_{2h}$ .

The z axis is defined as the axis of the principal  $C_2$  axis.  $C_2'$  is defined as the axis rotating around y.  $\sigma_v$  is defined as the xz plane.

	E	$C_2$	$C_2'$	$C_2''$	i	$\sigma_h$	$\sigma_v$	$\sigma_v'$
a) 2s								
b) $2p_x$								
c) $2p_y$								
d) $2p_z$								
e) $3d_{z^2}$								
f) $3d_{x^2-y^2}$								
g) $3d_{xy}$								
h) $3d_{yz}$								
i) $3d_{xz}$								

### Answer

	E	$C_2$	$C_2'$	$C_2''$	i	$\sigma_h$	$\sigma_v$	$\sigma_v'$
a) 2s	1	1	1	1	1	1	1	1
b) $2p_x$	1	-1	-1	1	-1	1	1	-1
c) $2p_y$	1	-1	1	-1	-1	1	-1	1
d) $2p_z$	1	1	-1	-1	-1	-1	1	1
e) $3d_{z^2}$	1	1	1	1	1	1	1	1
f) $3d_{x^2-y^2}$	1	1	1	1	1	1	1	1
g) $3d_{xy}$	1	1	-1	-1	1	1	-1	-1
h) $3d_{yz}$	1	-1	-1	1	1	-1	-1	1
i) $3d_{xz}$	1	-1	1	-1	1	-1	1	-1

## Exercise 3

Determine the matrix representations of the symmetry elements of the following point groups:

a)  $D_2$

Define principal  $C_2$  axis as the axis running along z.  $C_2'$  runs along x.

b)  $C_3$

If we define the principal  $C_3$  axis running along the z axis:

### Answer

$$\begin{array}{ccc}
 \begin{matrix} 1 & 0 & 0 \\ 0 & 1 & 0 \\ 0 & 0 & 1 \end{matrix} & \begin{matrix} -1 & 0 & 0 \\ C_2: 0 & -1 & 0 \\ 0 & 0 & 1 \end{matrix} & C_2': \begin{bmatrix} 1 & 0 & 0 \\ 0 & -1 & 0 \\ 0 & 0 & -1 \end{bmatrix} \\
 \\ 
 \begin{matrix} -1 & 0 & 0 \\ C_2'': 0 & 1 & 0 \\ 0 & 0 & -1 \end{matrix} & & \\
 \text{a)} & & 
 \end{array}$$

$$\begin{array}{ccc}
 \begin{matrix} 1 & 0 & 0 \\ E: 0 & 1 & 0 \\ 0 & 0 & 1 \end{matrix} & \begin{matrix} -\frac{1}{2} & -\frac{\sqrt{3}}{2} & 0 \\ C_3^1: \frac{\sqrt{3}}{2} & -\frac{1}{2} & 0 \\ 0 & 0 & 1 \end{matrix} & \begin{matrix} -\frac{1}{2} & \frac{\sqrt{3}}{2} & 0 \\ C_3^2: -\frac{\sqrt{3}}{2} & -\frac{1}{2} & 0 \\ 0 & 0 & 1 \end{matrix} \\
 \text{b)} & & 
 \end{array}$$

Dr. Kai Landskron ([Lehigh University](#)). If you like this textbook, please consider to make a donation to support the author's research at Lehigh University: [Click Here to Donate](#).

This page titled [4.4: Unit 4 Practice Problems](#) is shared under a [CC BY 4.0](#) license and was authored, remixed, and/or curated by [Kai Landskron](#).

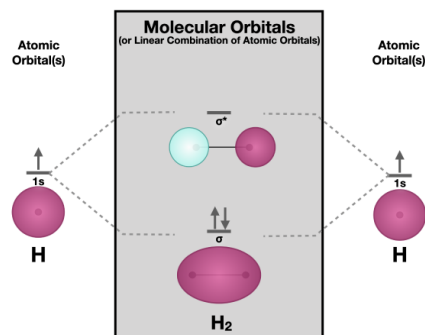
- [Homework Problems Chapter 2](#) by [Kai Landskron](#) is licensed [CC BY 4.0](#).

## CHAPTER OVERVIEW

### Unit 5: Molecular Orbitals

#### Molecular Orbital Theory

*Molecular Orbital (MO) Theory* is a sophisticated bonding model. It is generally considered to be more powerful than *Lewis* and *Valence Bond Theories* for predicting molecular properties; however, this power comes at the price of complexity. In its full development, MO Theory requires complex mathematics, though the ideas behind it are simple. Atomic orbitals (AOs) that are localized on individual atoms combine to make molecular orbitals (MOs) that are distributed over the molecule. The simplest example is the molecule dihydrogen ( $H_2$ ), in which two independent hydrogen 1s orbitals combine to form the  $\sigma$  bonding MO and the  $\sigma^*$  antibonding MO of the dihydrogen molecule (see figure). The MO's are also called Linear Combinations of Atomic Orbitals (LCAO).



#### 5.1: Valence Bond Theory

##### 5.1.1: The Shapes of Molecules (VSEPR Theory) and Orbital Hybridization

#### 5.2: Linear Combination of Atomic Orbitals

##### 5.2.1: Formation of Molecular Orbitals from Atomic Orbitals

##### 5.2.2: Molecular Orbitals from s Orbitals

##### 5.2.3: Molecular Orbitals from p Orbitals

##### 5.2.4: Molecular orbitals from d orbitals

##### 5.2.5: Nonbonding Orbitals and Other Factors

#### 5.3: Diatomic MO Diagrams

##### 5.3.1: Homonuclear Diatomic Molecules

##### 5.3.1.1: Molecular Orbitals

##### 5.3.1.2: Orbital Mixing

##### 5.3.1.3: Diatomic Molecules of the First and Second Periods

##### 5.3.1.4: Photoelectron Spectroscopy

##### 5.3.2: Heteronuclear Diatomic Molecules

##### 5.3.2.1: Orbital ionization energies

##### 5.3.2.2: Polar bonds

##### 5.3.2.3: Ionic Compounds and Molecular Orbitals

#### 5.4: Polyatomic MO Diagrams

##### 5.4.1: Ligand Group Orbitals and Generator Functions

##### 5.4.2: Polyatomic Molecules

##### 5.4.2.1: Bifluoride anion

##### 5.4.2.2: Carbon Dioxide

##### 5.4.2.3: $H_2O$

##### 5.4.2.4: $NH_3$

##### 5.4.3: Why is $BeH_2$ Linear and $H_2O$ Bent?

#### 5.5: Pi Bonding and Hypervalency

##### 5.5.1: $BF_3$

##### 5.5.2: Expanded Octets and Molecular Orbitals

This page titled [Unit 5: Molecular Orbitals](#) is shared under a [CC BY-SA 4.0](#) license and was authored, remixed, and/or curated by [Kathryn Haas](#).

## 5.1: Valence Bond Theory

---

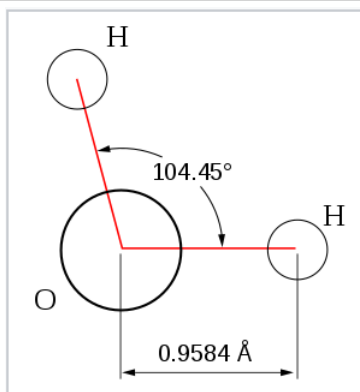
Learning objectives for this unit are to:

- Construct simple diagrams to explain the hybridization of atomic orbitals
  - Identify the hybrid orbitals used to describe the bonding in covalent compounds based on the VSEPR molecular geometry
  - Use words and pictures to develop valence bond descriptions of the bonding in covalent compounds
  - Calculate the percent s-character in a hybrid orbital based on the bond angle
  - Predict or explain experimental bond angles in molecules based on the percent s-character in hybrid orbitals and Bent's rules
- 

5.1: Valence Bond Theory is shared under a [not declared](#) license and was authored, remixed, and/or curated by LibreTexts.

### 5.1.1: The Shapes of Molecules (VSEPR Theory) and Orbital Hybridization

The Valence Shell Electron Pair Repulsion (VSEPR) theory is a simple and useful way to predict and rationalize the shapes of molecules. The theory is based on the idea of minimizing the electrostatic repulsion between electron pairs, as first proposed by Sidgwick and Powell in 1940,<sup>[9]</sup> then generalized by Gillespie and Nyholm in 1957,<sup>[10]</sup> and then broadly applied over the intervening 50+ years.<sup>[11]</sup>



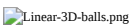





Geometry of the water molecule





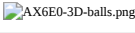
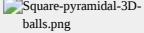
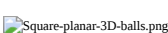
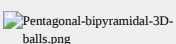
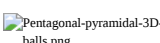

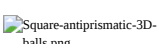
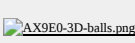
To use the VSEPR model, one begins with the Lewis dot picture to determine the number of lone pairs and bonding domains around a central atom. Because VSEPR considers all bonding domains equally (i.e., a single bond, a double bond, and a half bond all count as one electron domain), one can use either an octet or hypervalent structure, provided that the number of lone pairs (which should be the same in both) is calculated correctly. For example, in either the hypervalent or octet structure of the  $\text{I}_3^-$  ion above, there are three lone pairs on the central I atom and two bonding domains. We then follow these steps to obtain the **electronic geometry**:

- Determine the number of lone pairs on the central atom in the molecule, and add the number of bonded atoms (a.k.a. bonding domains)
- This number (the *steric number*) defines the electronic shape of the molecule by minimizing repulsion. For example a steric number of three gives a trigonal planar electronic shape.
- The angles between electron domains are determined primarily by the electronic geometry (e.g.,  $109.5^\circ$  for a steric number of 4, which implies that the electronic shape is a tetrahedron)
- These angles are adjusted by the hierarchy of repulsions: (lone pair - lone pair) > (lone pair - bond) > (bond - bond)

The **molecular geometry** is deduced from the electronic geometry by considering the lone pairs to be present but invisible. The most commonly used methods to determine molecular structure - X-ray diffraction, neutron diffraction, and electron diffraction - have a hard time seeing lone pairs, but they can accurately determine the lengths of bonds between atoms and the bond angles.

The table below gives examples of electronic and molecular shapes for steric numbers between 2 and 9. We are most often concerned with molecules that have steric numbers between 2 and 6.

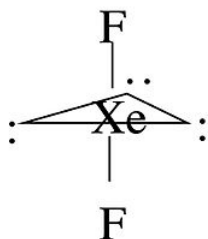
Bonding electron pairs	Lone pairs	Electron domains (Steric #)	Shape	Ideal bond angle (example's bond angle)	Example	Image
2	0	2	linear	$180^\circ$	$\text{CO}_2$	
3	0	3	trigonal planar	$120^\circ$	$\text{BF}_3$	
2	1	3	bent	$120^\circ$ ( $119^\circ$ )	$\text{SO}_2$	
4	0	4	tetrahedral	$109.5^\circ$	$\text{CH}_4$	
3	1	4	trigonal pyramidal	$109.5^\circ$ ( $107^\circ$ )	$\text{NH}_3$	
2	2	4	bent	$109.5^\circ$ ( $104.5^\circ$ )	$\text{H}_2\text{O}$	

Bonding electron pairs	Lone pairs	Electron domains (Steric #)	Shape	Ideal bond angle (example's bond angle)	Example	Image
5	0	5	trigonal bipyramidal	90°, 120°, 180°	PCl <sub>5</sub>	
4	1	5	seesaw	180°, 120°, 90° (173.1°, 101.6°)	SF <sub>4</sub>	
3	2	5	T-shaped	90°, 180° (87.5°, < 180°)	ClF <sub>3</sub>	
2	3	5	linear	180°	XeF <sub>2</sub>	
6	0	6	octahedral	90°, 180°	SF <sub>6</sub>	
5	1	6	square pyramidal	90° (84.8°), 180°	BrF <sub>5</sub>	
4	2	6	square planar	90°, 180°	XeF <sub>4</sub>	
7	0	7	pentagonal bipyramidal	90°, 72°, 180°	IF <sub>7</sub>	
6	1	7	pentagonal pyramidal	72°, 90°, 144°	XeOF <sub>5</sub> <sup>-</sup>	
5	2	7	planar pentagonal	72°, 144°	XeF <sub>5</sub> <sup>-</sup>	
8	0	8	square antiprismatic		XeF <sub>8</sub> <sup>2-</sup>	
9	0	9	tricapped trigonal prismatic		ReH <sub>9</sub> <sup>2-</sup>	

From the Table, we see that some of the molecules shown as examples have bond angles that depart from the ideal electronic geometry. For example, the H-N-H bond angle in ammonia is 107°, and the H-O-H angle in water is 104.5°. We can rationalize this in terms of the last rule above. The lone pair in ammonia repels the electrons in the N-H bonds more than they repel each other. This lone pair repulsion exerts even more steric influence in the case of water, where there are two lone pairs. Similarly, the axial F-S-F angle in the "seesaw" molecule SF<sub>4</sub> is a few degrees less than 180° because of repulsion by the lone pair in the molecule.

### Geometrical isomers

For some molecules in the Table, we note that there is more than one possible shape that would satisfy the VSEPR rules. For example, the XeF<sub>2</sub> molecule has a steric number of five and a trigonal bipyramidal geometry. There are three possible stereoisomers: one in which the F atoms occupy axial sites, resulting in linear molecule, one in which the F atoms occupy one equatorial and one axial site (resulting in a 90° bond angle), and one in which the F atoms are both on equatorial sites, with a F-Xe-F bond angle of 120°.



The observed geometry of XeF<sub>2</sub> is linear, which can be rationalized by considering the orbitals that are used to make bonds (or lone pairs) in the axial and equatorial positions. There are four available orbitals, s, p<sub>x</sub>, p<sub>y</sub>, and p<sub>z</sub>. If we choose the z-axis as the axial direction, we can see that the p<sub>x</sub> and p<sub>y</sub> orbitals lie in the equatorial plane. We assume that the spherical s orbital is shared equally by the five electron domains in the molecule, the two axial bonds share the p<sub>z</sub> orbital, and the three equatorial bonds share the p<sub>x</sub> and p<sub>y</sub> orbitals. We can then calculate the bond orders to axial and equatorial F atoms as follows:

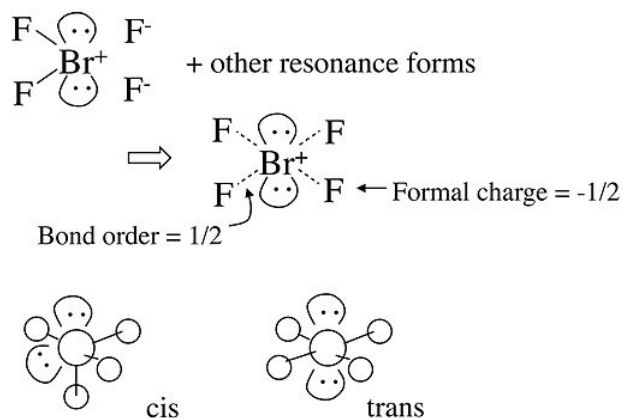


*axial*:  $\frac{1}{5} + \frac{1}{2}p_z = 0.7$  bond (formal charge = -0.3)

*equatorial*:  $\frac{1}{5}s + \frac{1}{3}p_x + \frac{1}{3}p_y = 0.867$  bond (formal charge = -0.122)

Because fluorine is more electronegative than a lone pair, it prefers the axial site where it will have more negative formal charge. In general, by this reasoning, lone pairs and electropositive ligands such as  $\text{CH}_3$  will always prefer the equatorial sites in the trigonal bipyramidal geometry. Electronegative ligands such as F will always go to the axial sites.

In the case of the  $\text{BrF}_4^-$  anion, which is isoelectronic with  $\text{XeF}_4$  in the Table, the electronic geometry is octahedral and there are two possible isomers in which the two lone pairs are *cis* or *trans* to each other. In this case, lone pair - lone pair repulsion dominates and we obtain the *trans* arrangement of lone pairs, giving a square planar molecular geometry.



## Orbital hybridization

The observation of molecules in the various electronic shapes shown above is, at first blush, in conflict with our picture of atomic orbitals. For an atom such as oxygen, we know that the 2s orbital is spherical, and that the 2p<sub>x</sub>, 2p<sub>y</sub>, and 2p<sub>z</sub> orbitals are dumbbell-shaped and point along the Cartesian axes. The water molecule contains two hydrogen atoms bound to oxygen not at a 90° angle, but at an angle of 104.5°. Given the relative orientations of the atomic orbitals, how do we arrive at angles between electron domains of 104.5°, 120°, and so on? To understand this we will need to learn a little bit about the quantum mechanics of electrons in atoms and molecules.

The atomic orbitals  $\psi$  represent solutions to the **Schrödinger wave equation**,

$$E\psi = \hat{H}\psi \quad (5.1.1.1)$$

Here E is the energy of an electron in the orbital, and  $\hat{H}$  is the Hamiltonian operator.

By analogy with classical mechanics, the Hamiltonian is commonly expressed as the sum of operators corresponding to the kinetic and potential energies of a system in the form

$$\hat{H} = \hat{T} + \hat{V} \quad (5.1.1.2)$$

where  $\hat{V} = V(\mathbf{r}, t)$  is the potential energy, and

$$\hat{T} = \frac{\hat{\mathbf{p}} \cdot \hat{\mathbf{p}}}{2m} = \frac{\hat{p}^2}{2m} = -\frac{\hbar^2}{2m} \nabla^2, \quad (5.1.1.3)$$

is the kinetic energy operator in which  $m$  is the mass of the particle and the momentum operator is:

$$\hat{p} = -i\hbar\nabla, \text{ where } \nabla = \frac{\delta}{\delta x} + \frac{\delta}{\delta y} + \frac{\delta}{\delta z} \quad (5.1.1.4)$$

Here  $\hbar$  is  $h/2\pi$ , where  $h$  is Planck's constant, and the Laplacian operator  $\nabla^2$  is:

$$\nabla^2 = \frac{\delta^2}{\delta x^2} + \frac{\delta^2}{\delta y^2} + \frac{\delta^2}{\delta z^2} \quad (5.1.1.5)$$

Although this is not the technical definition of the Hamiltonian in classical mechanics, it is the form it most commonly takes in quantum mechanics. Combining these together yields the familiar form used in the Schrödinger equation:

$$\hat{H} = \hat{T} + \hat{V} = \frac{\hat{\mathbf{p}} \cdot \hat{\mathbf{p}}}{2m} + V(\mathbf{r}, t) = -\frac{\hbar^2}{2m} \nabla^2 + V(\mathbf{r}, t) \quad (5.1.1.6)$$

For hydrogen-like (one-electron) atoms, the Schrödinger equation can be written as:

$$E\psi = -\frac{\hbar^2}{2\mu} \nabla^2 \psi - \frac{Ze^2}{4\pi\epsilon_0 r} \psi \quad (5.1.1.7)$$

where  $Z$  is the nuclear charge,  $e$  is the electron charge, and  $\mathbf{r}$  is the position of the electron. The radial potential term on the right side of the equation is due to the Coulomb interaction, i.e., the electrostatic attraction between the nucleus and the electron, in which  $\epsilon_0$  is the dielectric constant (permittivity of free space) and

$$\mu = \frac{m_e m_n}{m_e + m_n} \quad (5.1.1.8)$$

is the 2-body reduced mass of the nucleus of mass  $m_n$  and the electron of mass  $m_e$ . To a good approximation,  $\mu \approx m_e$ .



Erwin Schrödinger as a young scientist

This is the equation that Erwin Schrödinger famously derived in 1926 to solve for the energies and shapes of the s, p, d, and f atomic orbitals in hydrogen-like atoms. It was a huge conceptual leap for both physics and chemistry because it not only explained the quantized energy levels of the hydrogen atom, but also provided the theoretical basis for the octet rule and the arrangement of elements in the periodic table.

The Schrödinger equation can be used to describe chemical systems that are more complicated than the hydrogen atom (e.g., multi-electron atoms, molecules, infinite crystals, and the dynamics of those systems) if we substitute the appropriate potential energy function  $V(\mathbf{r}, t)$  into the Hamiltonian. The math becomes more complicated and the equation must be solved numerically in those cases, so for our purposes we will stick with the simplest case of time-invariant, one-electron, hydrogen-like atoms.

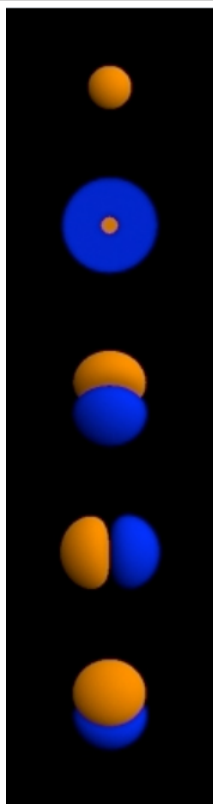
Without going into too much detail about the Schrödinger equation, we can point out some of its most important properties:

$$E\psi = -\frac{\hbar^2}{2\mu} \nabla^2 \psi - \frac{Ze^2}{4\pi\epsilon_0 r} \psi \quad (5.1.1.9)$$

- The equation derives from the fact that the total energy ( $E$ ) is the sum of the kinetic energy (KE) and the potential energy (PE). These three quantities are represented mathematically as **operators** in the equation.
- On the left side of the equation, the total energy operator ( $E$ ) is a scalar that is multiplied by the wavefunction  $\psi$ .  $\psi$  is a function of the spatial coordinates ( $x, y, z$ ) and is related to the probability that the electron is at that point in space.
- The first term on the right side of the equation represents the kinetic energy (KE). The kinetic energy operator is proportional to  $\nabla^2$  (the Laplacian operator) which takes the second derivative (with respect to three spatial coordinates) of  $\psi$ . Thus, the Schrödinger equation is a **differential equation**.
- The second term on the right side of the equation represents the Coulomb potential (PE), i.e. the attractive energy between the positively charged nucleus and the negatively charged electron.
- The solutions to the Schrödinger equation are a set of **energies**  $E$  (which are scalar quantities) and **wavefunctions** (a.k.a. **atomic orbitals**)  $\psi$ , which are functions of the spatial coordinates. You will sometimes see the energies referred to as

*eigenvalues* and the orbitals as *eigenfunctions*, because mathematically the Schrödinger equation is an eigenfunction-eigenvalue equation. Although  $\psi$  is a function of the coordinates,  $E$  is not. So an electron in a  $2p_z$  orbital has the same total energy  $E$  ( $= PE + KE$ ) no matter where it is in space.

- These  $E$  values and their associated wavefunctions  $\psi$  are catalogued according to their **quantum numbers**  $n$ ,  $l$ , and  $m_l$ . That is, there are many solutions to the differential equation, and each solution ( $\psi(x,y,z)$  and  $E$ ) has a unique set of quantum numbers. Some sets of orbitals are **degenerate**, meaning that they have the same energy (e.g.,  $2p_x$ ,  $2p_y$ , and  $2p_z$ ).
- The solutions  $\psi(x,y,z)$  to the Schrödinger equation (e.g., the  $1s$ ,  $2s$ ,  $2p_x$ ,  $2p_y$ , and  $2p_z$  orbitals) represent **probability amplitudes** for finding the electron at a particular point  $(x,y,z)$  in space. A probability amplitude can have either **+** or **- sign**. We typically represent the different signs by shading or by  $+$  and  $-$  signs on the two lobes of a  $2p$  orbital.
- The square of the probability amplitude,  $\psi^2$ , is always a positive number and represents the **probability** of finding the electron at a point  $x,y,z$  in space. Because the total probability of finding the electron somewhere is 1, the wavefunction must be **normalized** so that the integral of  $\psi^2$  over the spatial coordinates (from  $-\infty$  to  $+\infty$ ) is 1.
- The solutions to the Schrödinger equation are **orthogonal**, meaning that the product of any two (integrated over all space) is zero. For example the product of the  $2s$  and  $2p_x$  orbitals, integrated over the spatial coordinates from  $-\infty$  to  $+\infty$ , is zero.



The shapes of the first five atomic orbitals:  $1s$ ,  $2s$ ,  $2p_x$ ,  $2p_y$ , and  $2p_z$ . The colors denote the sign of the wave function.

Orbital hybridization involves making *linear combinations* of the atomic orbitals that are solutions to the Schrödinger equation. Mathematically, this is justified by recognizing that the Schrödinger equation is a *linear* differential equation. As such, any sum of solutions to the Schrödinger equation is also a valid solution. However, we still impose the constraint that our hybrid orbitals must be **orthogonal** and **normalized**.

#### Rules for orbital hybridization:

- Add and subtract atomic orbitals to get hybrid orbitals.
- We get the same number of orbitals out as we put in.
- The energy of a hybrid orbital is the weighted average of the atomic orbitals that make it up.
- The coefficients are determined by the constraints that the hybrid orbitals must be orthogonal and normalized.

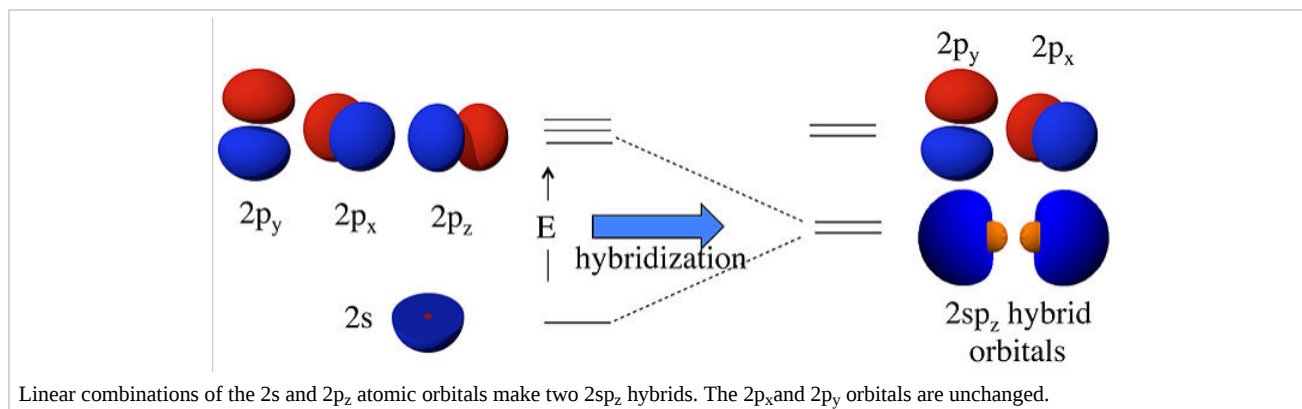
For **sp hybridization**, as in the  $\text{BeF}_2$  or  $\text{CO}_2$  molecule, we make two linear combinations of the  $2s$  and  $2p_z$  orbitals (assigning  $z$  as the axis of the Be-F bond):

$$\psi_1 = \frac{1}{\sqrt{2}}(2s) + \frac{1}{\sqrt{2}}(2p_z) \quad (5.1.1.10)$$

$$\psi_2 = \frac{1}{\sqrt{2}}(2s) - \frac{1}{\sqrt{2}}(2p_z) \quad (5.1.1.11)$$

Here we have simply added and subtracted the 2s and 2p<sub>z</sub> orbitals; we leave it as an exercise for the interested student to show that both orbitals are normalized (i.e.,  $\int \psi_1^2 d\tau = \int \psi_2^2 d\tau = 1$ ) and orthogonal (i.e.,  $\int \psi_1 \psi_2 d\tau = 0$ ).

What this means physically is explained in the figure below. By combining the 2s and 2p<sub>z</sub> orbitals we have created two new orbitals with large lobes (high electron probability) pointing along the z-axis. These two orbitals are degenerate and have an energy that is halfway between the energy of the 2s and 2p<sub>z</sub> orbitals.



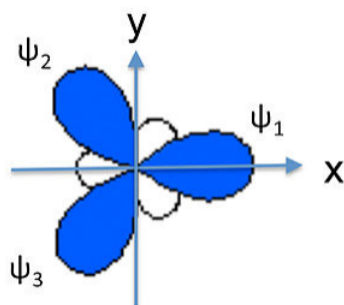
For an isolated Be atom, which has two valence electrons, the lowest energy state would have two electrons spin-paired in the 2s orbital. However, these electrons would not be available for bonding. By **promoting** these electrons to the degenerate 2sp<sub>z</sub> hybrid orbitals, they become unpaired and are prepared for bonding to the F atoms in BeF<sub>2</sub>. This will occur if the **bonding energy** (in the promoted state) exceeds the promotion energy. The **overall bonding energy**, i.e., the energy released by combining a Be atom in its ground state with two F atoms, is the difference between the bonding and promotion energies.

We can similarly construct **sp<sup>2</sup> hybrids** (e.g., for the BF<sub>3</sub> molecule or the NO<sub>3</sub><sup>-</sup> anion) from one 2s and two 2p atomic orbitals. Taking the plane of the molecule as the xy plane, we obtain three hybrid orbitals at 120° to each other. The three hybrids are:

$$\psi_1 = \frac{1}{\sqrt{3}}(2s) + \frac{\sqrt{2}}{\sqrt{3}}(2p_x) \quad (5.1.1.12)$$

$$\psi_2 = \frac{1}{\sqrt{3}}(2s) - \frac{1}{\sqrt{6}}(2p_x) + \frac{1}{\sqrt{2}}(2p_y) \quad (5.1.1.13)$$

$$\psi_3 = \frac{1}{\sqrt{3}}(2s) - \frac{1}{\sqrt{6}}(2p_x) - \frac{1}{\sqrt{2}}(2p_y) \quad (5.1.1.14)$$



These orbitals are again degenerate and their energy is the weighted average of the energies of the 2s, 2p<sub>x</sub>, and 2p<sub>y</sub> atomic orbitals.

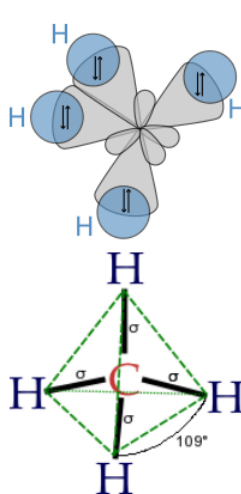
Finally, to make a sp<sup>3</sup> hybrid, as in CH<sub>4</sub>, H<sub>2</sub>O, etc., we combine all four atomic orbitals to make four degenerate hybrids:

$$\psi_1 = \frac{1}{2}(2s + 2p_x + 2p_y + 2p_z) \quad (5.1.1.15)$$

$$\psi_2 = \frac{1}{2}(2s - 2p_x - 2p_y + 2p_z) \quad (5.1.1.16)$$

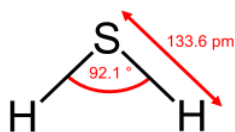
$$\psi_3 = \frac{1}{2}(2s + 2p_x - 2p_y - 2p_z) \quad (5.1.1.17)$$

$$\psi_4 = \frac{1}{2}(2s - 2p_x + 2p_y - 2p_z) \quad (5.1.1.18)$$



The lobes of the **sp<sup>3</sup> hybrid** orbitals point towards the vertices of a tetrahedron (or alternate corners of a cube), consistent with the tetrahedral bond angle in CH<sub>4</sub> and the nearly tetrahedral angles in NH<sub>3</sub> and H<sub>2</sub>O. Similarly, we can show that we can construct the trigonal bipyramidal electronic shape by making sp and sp<sup>2</sup> hybrids, and the octahedral geometry from three sets of sp hybrids. The picture that emerges from this is that the atomic orbitals can hybridize as required by the shape that best minimizes electron pair repulsions.

Interestingly however, the bond angles in PH<sub>3</sub>, H<sub>2</sub>S and H<sub>2</sub>Se are close to 90°, suggesting that P, S, and Se primarily use their p-orbitals in bonding to H in these molecules. This is consistent with the fact that the energy difference between s and p orbitals stays roughly constant going down the periodic table, but the bond energy *decreases* as the valence electrons get farther away from the nucleus. In compounds of elements in the 3rd, 4th, and 5th rows of the periodic table, there thus is a *decreasing tendency to use s-p orbital hybrids in bonding*. For these heavier elements, the bonding energy is not enough to offset the energy needed to promote the s electrons to s-p hybrid orbitals.



This page titled [5.1.1: The Shapes of Molecules \(VSEPR Theory\) and Orbital Hybridization](#) is shared under a [CC BY-SA 4.0](#) license and was authored, remixed, and/or curated by [Chemistry 310 \(Wikibook\)](#) via [source content](#) that was edited to the style and standards of the LibreTexts platform.

- **1.3: The Shapes of Molecules (VSEPR Theory) and Orbital Hybridization** by [Chemistry 310](#) is licensed [CC BY-SA 4.0](#). Original source: [https://en.wikibooks.org/wiki/Introduction\\_to\\_Inorganic\\_Chemistry](https://en.wikibooks.org/wiki/Introduction_to_Inorganic_Chemistry).

## 5.2: Linear Combination of Atomic Orbitals

---

Learning objectives for this unit are to:

- Compare and contrast valence bond theory and molecular orbital theory
  - Classify MOs according to the type of atomic orbital interaction (s, p, d, and nb)
  - Predict the strength of different MOs (s, p, and d) based on orbital overlap
  - Sketch MOs that form from combinations of particular atomic orbital interactions
  - Explain the stabilization of bonding molecular orbitals and destabilization of antibonding molecular orbitals relative to the component atomic orbitals.
- 

5.2: Linear Combination of Atomic Orbitals is shared under a [not declared](#) license and was authored, remixed, and/or curated by LibreTexts.

### 5.2.1: Formation of Molecular Orbitals from Atomic Orbitals

---

Molecular orbital theory extends from quantum theory and the atomic orbital wavefunctions ( $\psi$ ) described by the Schrödinger equation. While the Schrödinger equation defines a  $\Psi$  for electrons in individual atoms, we can approximate the molecular wavefunction (what  $\Psi$  would look like if we combined the  $\psi$  of individual atoms). The addition or subtraction of wavefunctions is termed **linear combination of atomic orbitals** (LCAO). Molecular orbital theory is applied to LCAO to describe bonding.

The LCAO for the wavefunction of two atoms ( $\psi_a$  and  $\psi_b$ ) is represented by the general expression below. The coefficients  $c_a$  and  $c_b$  quantify the contribution of each atomic  $\psi$  to the molecular  $\Psi$ .

$$\Psi = c_a\psi_a + c_b\psi_b$$

For two atomic  $\psi$ s to form a bond, three conditions must be satisfied:

- First, the **distance between the atoms** must be small enough to provide good overlap. This is because the two orbitals must be able to overlap using regions of  $\psi^2$  where the probability of finding electrons is significant. If atoms are not close enough,  $\psi_a$  and  $\psi_b$  cannot interact productively. At the same time, the atoms must be far enough apart that their nuclei do not repel each other.
- The **symmetry of the orbitals** must be compatible such that regions of  $\psi_a$  and  $\psi_b$  with the same sign constructively interfere more than regions with opposite sign destructively interfere. In other words, for a productive interaction, there must be a relatively high probability of finding an electron between the two nuclei, and this depends on the symmetry (and sign of the  $\psi$ ) of the atomic orbitals.
- Third, the **energies of the atomic orbitals** must be similar. Orbitals with similar energy combine to make the most stable bonding molecular orbitals. Atomic orbitals with very different energies form less stable bonding interactions, and the larger the difference in the atomic orbitals, the weaker the bonding interaction will be.

Atomic orbitals combine to form molecular orbitals when these three conditions are met. The result is a set of bonding molecular orbitals that are lower in energy than the original atomic orbital energies.

---

This page titled [5.2.1: Formation of Molecular Orbitals from Atomic Orbitals](#) is shared under a [CC BY-SA 4.0](#) license and was authored, remixed, and/or curated by [Kathryn Haas](#).

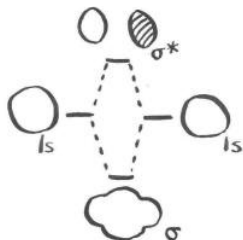
- [5.1: Formation of Molecular Orbitals from Atomic Orbitals](#) by [Kathryn Haas](#) is licensed [CC BY-SA 4.0](#).

## 5.2.2: Molecular Orbitals from s Orbitals

In the case of the hydrogen molecule, we took two atomic orbitals and combined them to form two molecular orbitals. These new molecular orbitals had different wavelengths than the two atomic orbitals: one had a longer wavelength and was a little lower in energy, while the other had a shorter wavelength and was a little higher in energy. If we take into account the energy of the two original atomic wavefunctions, and compare them to the total energy of the two new molecular wavefunctions, there is no change overall.

We started with two atomic orbitals, and by combining them we produced two molecular orbitals. Both of these ideas are useful in considering the formation of more complex molecules from individual atoms.

- The average energy of the orbitals has remained almost constant.
  - Also, the number of wavefunctions has remained constant.



Of course, from the point of view of the two real electrons, some remarkable changes have occurred. Both of these electrons have adopted a longer wavelength and a lower energy and that has made all the difference. There is an occupied molecular orbital and an unoccupied molecular orbital; only the occupied orbital makes a real energetic contribution to the overall stability of the molecule. The unoccupied orbital is completely imaginary.

A bonding picture of  $\text{He}_2$  would look exactly the same, because it would also involve the overlap of 1s electrons on one atom with 1s electrons on the other atom. There would be a different electronic energy, however. That difference would affect the prospects of helium-helium bond formation.

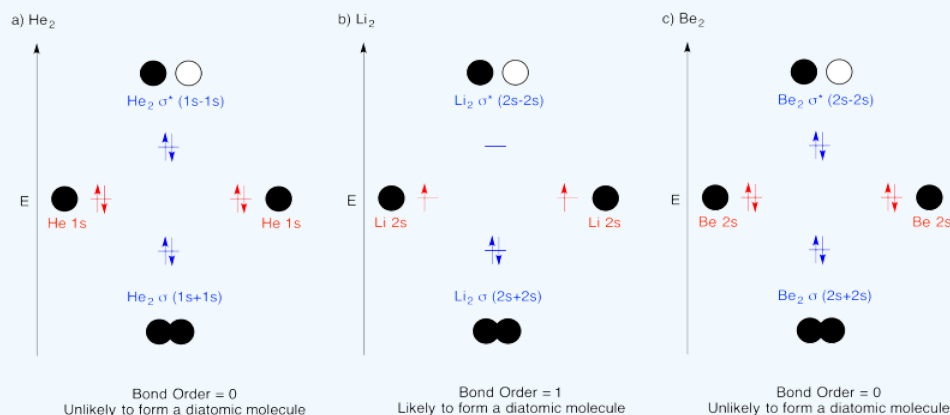
- The electrons have lower kinetic energy in the bond than they had before bonding.
- Electronic energy has decreased. A stable bond has formed.

### ? Exercise 5.2.2.1

Construct molecular orbital diagrams for the following diatomic species and discuss the likelihood of bond formation in each case.

- $\text{He}_2$ .
- $\text{Li}_2$ .
- $\text{Be}_2$ .

#### Answer





---

This page titled [5.2.2: Molecular Orbitals from s Orbitals](#) is shared under a [CC BY-NC 3.0](#) license and was authored, remixed, and/or curated by [Chris Schaller & Kathryn Haas](#).

## 5.2.3: Molecular Orbitals from p Orbitals

### Bonding with P-orbitals

#### Sigma bonding with p-orbitals

Other diatomic molecules in the upper right corner of the periodic table can be constructed in a similar way. Look at dinitrogen,  $N_2$ . We can think about how dinitrogen would form if two nitrogen atoms were placed close enough together to share electrons. Nitrogen has more electrons than hydrogen, so this interaction is more complicated.

In our qualitative examination of bonding in main group diatomics, we will take the approach used in Lewis structures and just look at the valence electrons. A quantitative molecular orbital calculation with a computer would not take this shortcut, but would include all of the electrons in the atoms that are bonding together.

Nitrogen has five valence electrons, and these electrons are found in the 2s and 2p levels. There are three possible atomic orbitals in the 2p level where some of these electrons could be found:  $p_x$ ,  $p_y$  and  $p_z$ . We need to look at the interaction between the s and  $p_x$ ,  $p_y$  and  $p_z$  orbitals on one nitrogen atom with the s and  $p_x$ ,  $p_y$  and  $p_z$  orbitals on the other nitrogen. That process could be extremely complicated, but:

- Orbital interactions are governed by symmetry.

Orbitals interact most easily with other orbitals that have the same element of symmetry. For now, we can simplify and say that orbitals on one atom only interact with the same type of orbitals on the other atom.

- s orbitals interact with s orbitals. We can already see how that will work out in dinitrogen, because that is what happened in dihydrogen.
- $p_x$  orbitals interact with  $p_x$  orbitals.
- $p_y$  orbitals interact with  $p_y$  orbitals.
- $p_z$  orbitals interact with  $p_z$  orbitals.

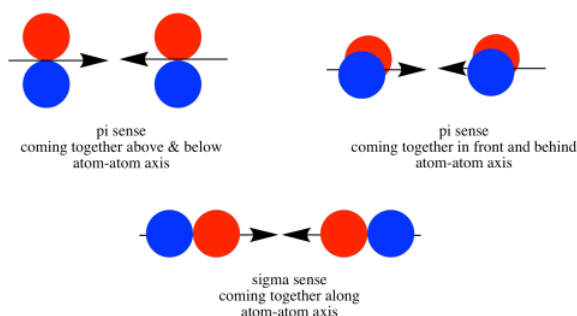
Another complication here is that the s and p orbitals do not start out at the same energy level. When the orbitals mix, one combination goes up in energy and one goes down. Does the s antibonding combination go higher in energy than the combinations from p orbitals? Do the p bonding combinations go lower in energy than the combinations from s orbitals? We will **simplify** and **assume** that the s and p levels remain completely separate from each other. This is not always true, but the situation varies depending on what atoms we are dealing with.

- The combination of one s orbital with another is just like in hydrogen. Two original orbitals will combine and rearrange to produce two new orbitals.
- There is a bonding combination in which the orbitals are in phase. The new orbital produced has a longer wavelength than the original orbital. It is lower in energy.
- There is an antibonding combination in which the orbitals are out of phase. The new orbital produced has a shorter wavelength than the original orbital. It is higher in energy.

In considering the interaction of two p orbitals, we have to keep in mind that p orbitals are directional. A p orbital lies along a particular axis: x, y or z. The three p orbitals on nitrogen are all mutually perpendicular (or orthogonal) to each other. That situation is in contrast to s orbitals, which are spherical and thus look the same from any direction.

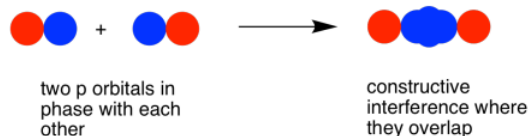


We first need to define one axis as lying along the N-N bond. It does not really matter which one. We arbitrarily say the N-N bond lies along the z axis. The  $p_z$  orbitals have a different spatial relationship to each other compared to the  $p_y$  and  $p_x$ . The  $p_z$  orbitals lie along the bond axis, whereas the  $p_y$  and  $p_x$  are orthogonal to it.

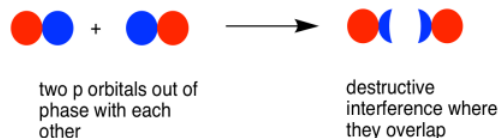


As the nitrogen atoms are brought together, one lobe on one  $p_z$  orbital overlaps strongly with one lobe on the other  $p_z$  orbital. The other lobes point away from each other and do not interact in any obvious way.

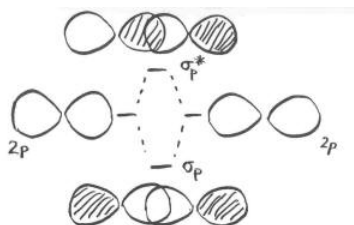
As with the s orbital, the  $p_z$  orbitals can be in-phase or out-of-phase. The in-phase combination results in constructive interference. (Here, "in-phase" means the lobes that overlap are in-phase; for that to happen the two p orbitals are actually completely out-of-phase with each other mathematically, so that one orbital is the mirror image of the other.) This combination is at a longer wavelength than the original orbital. It is a lower energy combination.



The out-of-phase combination (meaning in this case that the overlapping lobes are out-of-phase) results in destructive interference. This combination is at shorter wavelength than the original orbital. It is a higher energy combination.



As a result, we have two different combinations stemming from two different p orbitals coming together in two different ways. We get a low-energy, in-phase, bonding combination and a high-energy, out-of-phase, antibonding combination.

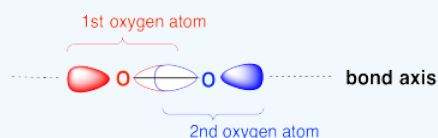


What about those other p orbitals, the ones that do not lie along the bond axis? We'll take a look at that problem on the next page.

### ? Exercise 5.2.3.2

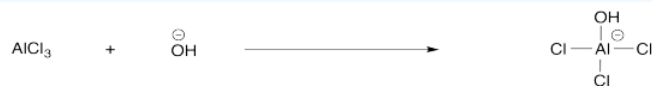
Draw an MO cartoon of a sigma bonding orbital formed by the overlap of two p orbitals between two oxygen atoms. Label the positions of the oxygen nuclei with the symbol "O". Label the O-O bond axis.

**Answer**



### ? Exercise 5.2.3.3

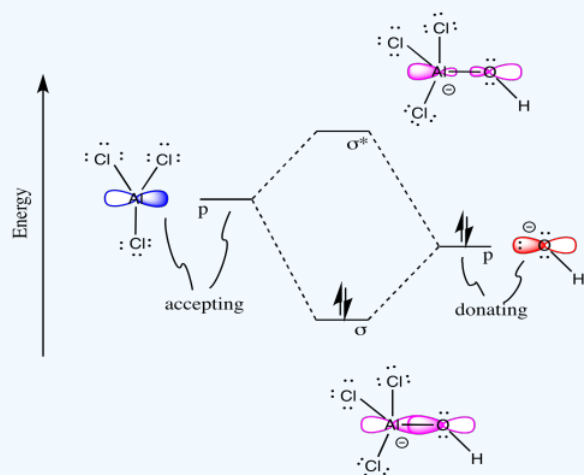
Chemical reactions can be described by MO diagrams too! Consider the following reaction in which a new sigma bond is formed.



Draw an MO diagram for the reaction above. In other words, start from the one frontier MO on each reactant to build the MO's of the new sigma bond in the product.

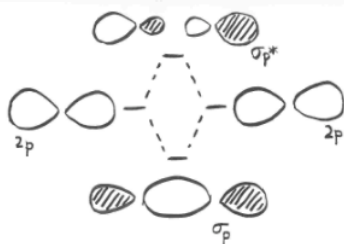
- o Draw the orbital from the base (hydroxide) that is likely to donate its electrons.
- o Draw the orbital from the acid (aluminum chloride) that is likely to accept electrons.
- o Complete the MO mixing diagram of these two orbitals:
  - Label the electron donating orbital
  - Label the electron accepting orbital
  - Populate the MO mixing diagram with electrons
- o Draw a cartoon showing each reactant and product MO that contributes to the bonding interaction.

**Answer**

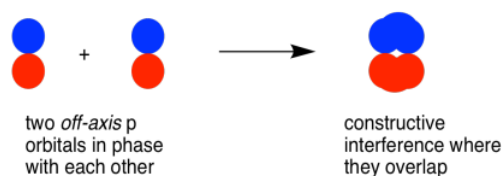


### Pi-bonding with p-orbitals

Earlier, we saw that p orbitals that lie along the same axis can interact to form bonds.



Parallel, but not collinear, p orbitals can also interact with each other. They would approach each other side by side, above and below the bond axis between the two atoms. They can be close enough to each other to overlap, although they do not overlap as strongly as orbitals lying along the bond axis. They can make an in-phase combination, as shown below.

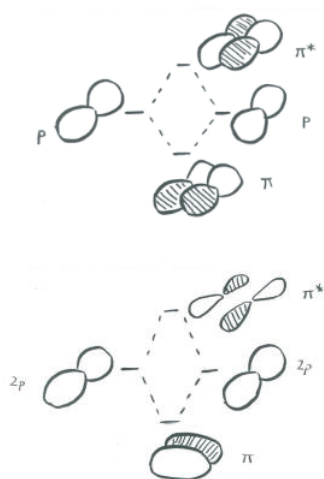


They could also make an out-of-phase combination, as shown below.



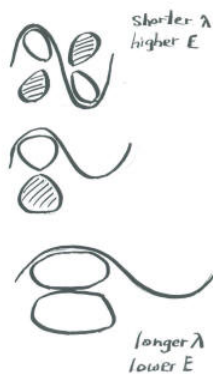
- parallel p orbitals can overlap to produce bonding and antibonding combinations.
- the resulting orbitals contain nodes along the bond axis.
- the electron density is found above and below the bond axis.
- this is called a p ( $\pi$ ) bond.

The illustration above is for one set of p orbitals that are orthogonal to the bond axis. The second picture shows the result of the constructive (or destructive) interference. A similar picture could be shown for the other set of p orbitals.

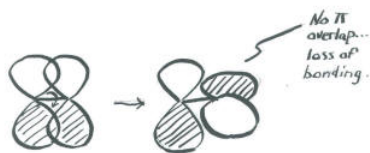


In a main group diatomic species like dinitrogen, one p orbital lying along the bond axis can engage in  $\sigma$  bonding. The two p orbitals orthogonal to the bond axis can engage in p bonding. There will be both bonding and antibonding combinations.

Just as the sigma-bonding orbitals display progressively shorter wavelengths along the bonding axis as they go to higher energy, so do the pi bonding orbitals. In other words, there are more nodes in the higher-energy orbitals than in the lower-energy ones.



An important consequence of the spatial distribution or "shape" of a p orbital is that it is not symmetric with respect to the bond axis. An s orbital is not affected when the atom at one end of the bond is rotated with respect to the other. A p orbital is affected by such a rotation. If one atom turns with respect to the other, the p orbital would have to stretch to maintain the connection. The orbitals would not be able to overlap, so the connection between the atoms would be lost.



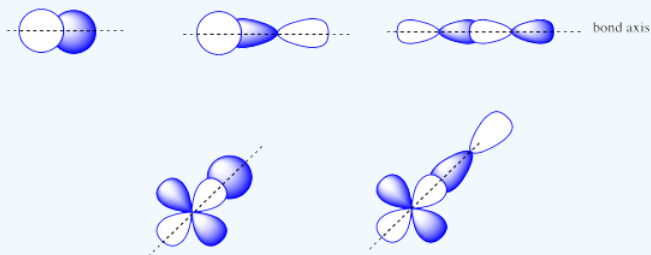
#### ? Exercise 5.2.3.4

The combinations of \_\_\_\_\_ atomic orbitals leads to  $\sigma$  orbitals.

Draw pictures.

**Answer**

The combinations of  $s + s$  OR  $s + p$  OR  $p + p$  OR  $s + d$  OR  $p + d$  atomic orbitals can lead to  $\sigma$  orbitals.



#### ? Exercise 5.2.3.5

The combinations of \_\_\_\_\_ atomic orbitals leads to  $\pi$  orbitals.

Draw pictures.

**Answer**

The combinations of side by side  $p + p$  or  $p + d$  atomic orbitals leads to  $\pi$  orbitals.



### ? Exercise 5.2.3.6

Which molecular orbital is typically the highest in energy?

- a. p
- b.  $\sigma$
- c.  $\pi^*$
- d.  $\pi$
- e.  $\sigma^*$

**Answer**

e)  $\sigma^*$

### ? Exercise 5.2.3.7

Why would a *core* 1s orbital not interact with a *valence* 2s orbital?

Hint: Why is a  $\text{Li}_2\text{O}$  bond stronger than a  $\text{K}_2\text{O}$  bond?

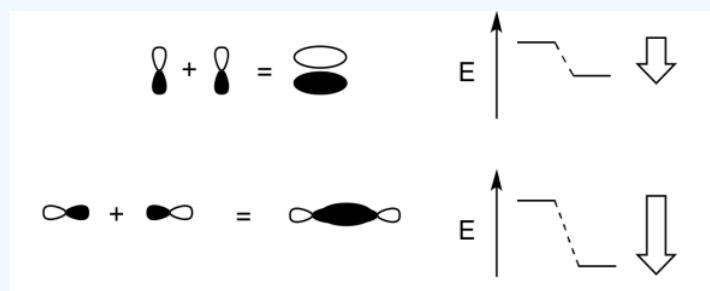
**Answer**

$\text{Li}^+$  and  $\text{O}^{2-}$  are more similar in size than  $\text{K}^+$  and  $\text{O}^{2-}$ , so the bond between  $\text{Li}^+$  and  $\text{O}^{2-}$  is stronger.

The energy difference between any core orbitals and valence orbitals is too large, so they cannot interact. In order for orbitals to interact, the orbitals need to have the same symmetry, be in the same plane, and be similar in energy.

### ? Exercise 5.2.3.8

Add a few words to explain the ideas conveyed in these drawings.



**Answer**

When two parallel p orbitals combine out-of-phase, destructive interference occurs.

There is a node between the atoms.

The energy of the electrons increases.

When two parallel p orbitals combine in-phase, constructive interference occurs.

There is no node between the atoms; the electrons are found above and below the axis connecting the atoms.

The energy of the electrons decreases.

### Attribution

Chris P Schaller, Ph.D., (College of Saint Benedict / Saint John's University)

Curated or created by Kathryn Haas

This page titled [5.2.3: Molecular Orbitals from p Orbitals](#) is shared under a [CC BY-NC 3.0](#) license and was authored, remixed, and/or curated by [Chris Schaller](#).

- [5.1.2: Molecular Orbitals from p Orbitals](#) by [Chris Schaller](#) is licensed [CC BY-NC 3.0](#).



## 5.2.4: Molecular orbitals from d orbitals

In transition metals and other heavier elements, the  $d$  orbitals may combine with other orbitals of compatible symmetry (and energy) to form molecular orbitals. Generally, there are three types of bonding and antibonding interactions that may occur with  $d$  orbitals: sigma ( $\sigma$ ), pi ( $\pi$ ), and delta ( $\delta$ ) bonds.

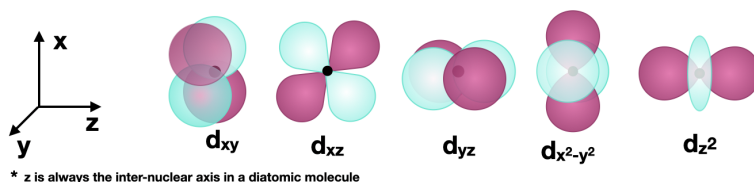


Figure 5.2.4.1: The five  $3d$  orbitals are shown. The orientation of the axes is consistent and the  $z$  axis is horizontal for convenience in drawing bonding along the  $z$  axis (see examples below). (CC-BY-SA; Kathryn Haas)

### Sigma ( $\sigma$ ) bonding with $d$ orbitals

$\sigma$  bonds are symmetric with respect to the inter-nuclear axis (in a diatomic molecule, this is the  $z$  axis). An example of a  $\sigma$  bond formed by  $d$  orbitals is that of two  $d_{z^2}$  orbitals (see Figure 5.2.4.2). If a bonded atom is in a position other than on the  $z$  axis (in an octahedral geometry, for example),  $\sigma$  bonds can also form. For example, two  $d_{x^2-y^2}$  orbitals on atoms bonded along the  $x$  or  $y$  axes could also form a  $\sigma$  bond.

$d$  orbitals can also form  $\sigma$  bonds with other types of orbitals with the appropriate symmetry. Examples of orbitals with appropriate symmetry are the  $s$  orbital and certain  $p$  orbitals on another atom, as shown below in Figure 5.2.4.2

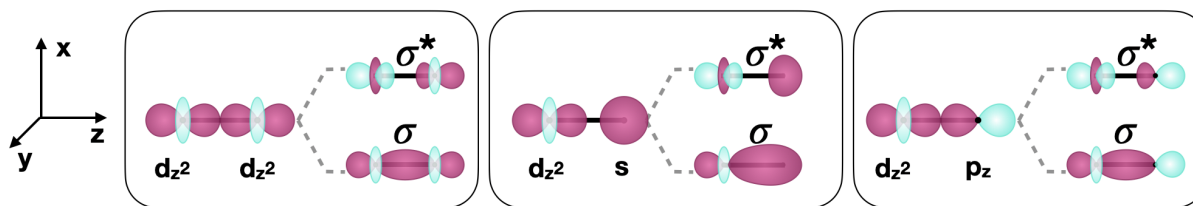


Figure 5.2.4.2: Selected examples of  $\sigma$  bonds involving  $d$  orbitals along the  $z$  internuclear axis (shown as a bold horizontal line) between two atoms. (CC-BY-SA; Kathryn Haas)

### Pi ( $\pi$ ) bonding with $d$ orbitals

$\pi$  bonds are those with one node that is in-plane with the internuclear axis. A  $\pi$  bond can form between two  $d$  orbitals or between  $d$  orbitals and other types of orbitals with comparable symmetry. An example of a  $\pi$  bond between two  $d$  orbitals is that formed by two  $d_{xz}$  orbitals along the  $z$  axis (shown in Figure 5.2.4.3).  $d$  orbitals can also form  $\pi$  bonds using  $p$  orbitals with compatible symmetry, as shown in Figure 5.2.4.3

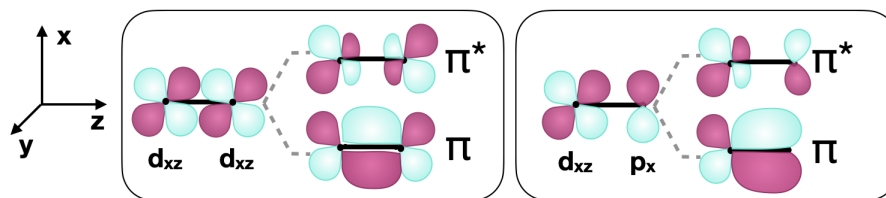


Figure 5.2.4.3: Selected examples of  $\pi$  bonds involving  $d$  orbitals along the  $z$  internuclear axis (shown as a bold horizontal line) between two atoms. (CC-BY-SA; Kathryn Haas)

### Delta ( $\delta$ ) bonding with $d$ orbitals

$\delta$  bonds are those with two nodes that are in-plane with the internuclear axis.  $\delta$  bonds can form between two  $d$  orbitals with appropriate symmetry. For example, when two atoms bond along the  $z$  axis, the  $d_{xy}$  orbitals and the two  $d_{x^2-y^2}$  orbitals can form  $\delta$  bonds (Figure 5.2.4.4).

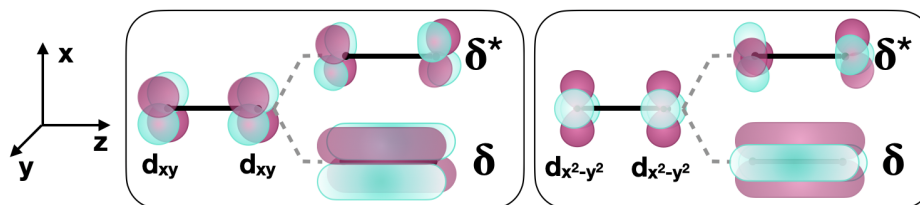


Figure 5.2.4.4: Selected examples of  $\delta$  bonds involving  $d$  orbitals along the  $z$  internuclear axis (shown in bold horizontal line) between two atoms. (CC-BY-SA; Kathryn Haas)

### Incompatible orbitals

In the descriptions above, we focused on how bonds (and antibonds) can be formed with  $d$  orbitals. All bonding and non-bonding interactions require that orbitals have compatible symmetry to form productive interactions. It is worth mentioning that orbitals with symmetry that is incompatible with the  $d$  orbitals will not have bonding or antibonding interactions with  $d$  orbitals. The figure below shows several sets of orbitals that are incompatible for bonding.

Curated or created by [Kathryn Haas](#)

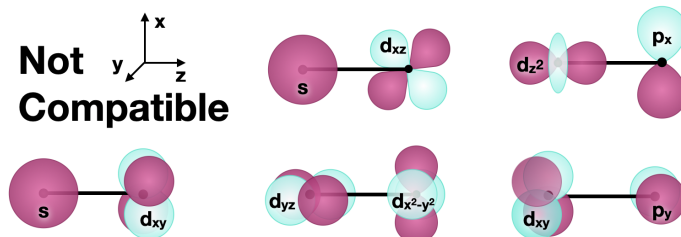


Figure 5.2.4.5: Several incompatible pairs of orbitals. (CC-BY-SA; Kathryn Haas)

This page titled [5.2.4: Molecular orbitals from d orbitals](#) is shared under a [CC BY-SA 4.0](#) license and was authored, remixed, and/or curated by [Kathryn Haas](#).

- [5.1.3: Molecular orbitals from d orbitals](#) by [Kathryn Haas](#) is licensed [CC BY-SA 4.0](#).

## 5.2.5: Nonbonding Orbitals and Other Factors

The simplest case is when there is an even number of atomic orbitals that all combine to form strong bonding and antibonding orbitals. But what if there is an uneven number of atomic orbitals? Or what if there are some orbitals that don't meet the criteria for bonding? Or what if the bonding interactions are weak? In these cases, there will be molecular orbitals on the molecule that have non-bonding character.

It is important to note that the bonding, non-bonding, and antibonding nature of orbitals exist on a spectrum. Some bonding and anti-bonding orbitals may have some non-bonding character depending on where their energies lie with respect to the original atomic orbital energies. When molecular orbitals have energies similar to their original atomic orbitals, they will have some non-bonding character. The closer the energies of atomic and molecular orbitals, the more non-bonding the molecular orbitals.

### Two major factors to consider

**Uneven number of atomic orbitals:** In the case that there is an uneven number of atomic orbitals with compatible symmetry, orbitals with non-bonding character will form. For example, in the case where three atomic orbitals combine, the most common result is formation of a low-energy bonding orbital, a high energy antibonding orbital, and a non-bonding orbital of intermediate energy (Figure 5.2.5.1).

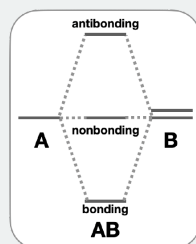


Figure 5.2.5.1. This figure illustrates the most common case for three atomic orbitals that combine to form three molecular orbitals; formation of one low-energy bonding, one high-energy antibonding, and one intermediate energy non-bonding molecular orbital. (CC-BY-NC-SA, Kathryn Haas)

**Differences in energy:** Combination of orbitals with different energies may lead to orbitals with non-bonding character. Atomic orbitals that have similar energies will have the strongest interactions, and result in bonding molecular orbitals with much lower energies than the component atomic orbitals. On the other hand, atomic orbitals with very unequal energies have a weaker interaction because the molecular orbitals are closer in energy to the atomic orbital energies, thus there is less energy benefit to putting electrons in the bonding molecular orbitals (Figure 5.2.5.2). When bonding or antibonding orbitals are close to the energies of the contributing atomic orbitals, those molecular orbitals may have some non-bonding character.

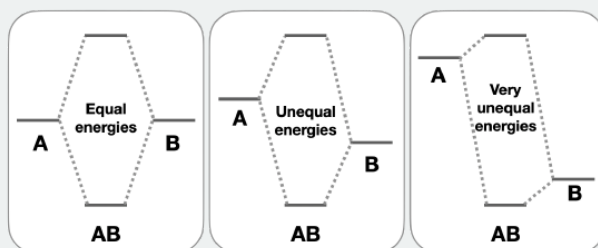


Figure 5.2.5.2. This figure illustrates how relative energies of atomic orbitals result in molecular orbitals that are more or less favorable. The greater the energy difference between atomic orbitals and the bonding molecular orbital, the more energetically favorable it is for bonding to occur. (CC-BY-NC-SA, Kathryn Haas)

This page titled [5.2.5: Nonbonding Orbitals and Other Factors](#) is shared under a [CC BY-SA 4.0](#) license and was authored, remixed, and/or curated by [Kathryn Haas](#).

- [5.1.4: Nonbonding Orbitals and Other Factors](#) by [Kathryn Haas](#) is licensed [CC BY-SA 4.0](#).

## 5.3: Diatomic MO Diagrams

---

Learning objectives for this unit are to:

- Derive molecular orbital energy diagrams for homonuclear and heteronuclear diatomic molecules, taking into account atomic orbital overlap and mixing of molecular orbitals
  - Predict the bond orders for homonuclear and heteronuclear diatomic molecules and ions, and correlate bond lengths, strengths, and stabilities of molecules with bond order
  - Predict the magnetic properties of molecules (diamagnetic/paramagnetic) based on the MO diagram
  - Identify the HOMO and LUMO on an MO diagram
  - Explain the origin and consequences of sp mixing
- 

5.3: Diatomic MO Diagrams is shared under a [not declared](#) license and was authored, remixed, and/or curated by LibreTexts.

## SECTION OVERVIEW

### 5.3.1: Homonuclear Diatomic Molecules

In this section you will be introduced to the molecular orbital diagrams of several homonuclear diatomic molecules. Homonuclear diatomic molecules are molecules made of exactly two identical atoms, and they are relatively simple.

#### 5.3.1.1: Molecular Orbitals

#### 5.3.1.2: Orbital Mixing

#### 5.3.1.3: Diatomic Molecules of the First and Second Periods

#### 5.3.1.4: Photoelectron Spectroscopy

---

This page titled [5.3.1: Homonuclear Diatomic Molecules](#) is shared under a [CC BY-SA 4.0](#) license and was authored, remixed, and/or curated by [Kathryn Haas](#).

### 5.3.1.1: Molecular Orbitals

There are several cases where our more elementary models of bonding (like Lewis Theory and Valence Bond Theory) fail to predict the actual molecular properties and reactivity. A classic example is the case of  $O_2$  and its magnetic properties. At very cold temperatures,  $O_2$  is attracted to a magnetic field, and thus it must be paramagnetic (unpaired electrons give rise to magnetism). Watch the [video below](#)!



The magnetic properties of  $O_2$  are easily rationalized by its **molecular orbital diagram**. A molecular orbital diagram is a diagram that shows the relative energies and identities of each molecular orbital in a molecule. Figure 5.3.1.1 shows a simplified and generic molecular orbital diagram for a second-row homonuclear diatomic molecule. The diagram is simplified in that it assumes that interactions are limited to degenerate orbitals from two atoms ([see next section](#)).

There are some things you should note as you inspect Figure 5.3.1.1 (and keep these in mind as you draw your own diagrams!). First, notice that there are the **same number of molecular orbitals as there are atomic orbitals**. Second, notice that **each orbital in the diagram is rigorously labeled** using labels ( $\sigma$  and  $\pi$ ) that include the subscripts  $u$  and  $g$ . These labels and subscripts indicate the symmetry of the orbitals. The  $\sigma$  symbol indicates that the orbital is symmetric with respect to the internuclear axis, while the  $\pi$  label indicates that there is one node along that axis. The  $g$  and  $u$  stand for *gerade* and *ungerade*, the German words for *even* and *uneven*, respectively. The subscript  $g$  is given to orbitals that are *even*, or *symmetric*, with respect to an inversion center. The subscript  $u$  is given to orbitals that are *uneven*, or *antisymmetric*, with respect to an inversion center. The pictures of calculated molecular orbitals are shown in Figure 5.3.1.1 to illustrate the symmetry of each orbital.

Another important thing to notice is that the diagram in Figure 5.3.1.1 lacks electrons (because it is generic for any second-row diatomic molecule). If this were a *complete* molecular orbital diagram it would **include the electrons for each atom and for the molecule**. Electrons in molecular orbitals are filled in the same way an atomic orbital diagram would be filled, where electrons occupy lower energy orbitals before higher energy orbitals, and electrons occupy empty degenerate orbitals before pairing. A complete molecular orbital diagram would show whether the molecule is diamagnetic or paramagnetic. It can also be used to calculate the bond order of the molecule (the number of bonds between atoms) using the formula below:

$$\text{Bond order} = \frac{1}{2} \left[ \left( \begin{array}{c} \text{number of electrons} \\ \text{in bonding orbitals} \end{array} \right) - \left( \begin{array}{c} \text{number of electrons} \\ \text{in antibonding orbitals} \end{array} \right) \right]$$

In general, non-valence (core) electrons can be ignored because they contribute nothing to the bond order. In fact, many molecular orbital diagrams will ignore the core orbitals, as they are insignificant for bonding interactions and reactivity.

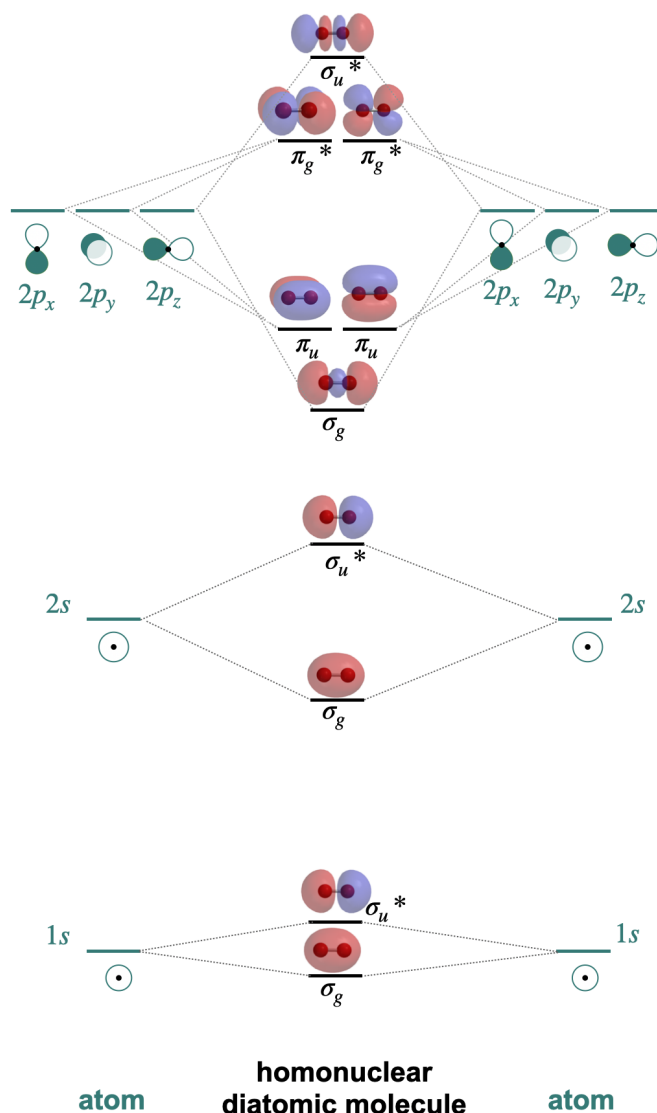


Figure 5.3.1.1.1: A generic molecular orbital diagram for a homonuclear diatomic molecule of second-row elements assuming no orbital mixing (interactions are formed by orbitals of the same energy from each atom). (CC-BY-NC-SA, Kathryn Haas)

Now, to see how this molecular orbital diagram can explain the magnetic behaviour of  $O_2$ , complete the example below.

#### ✓ Example 5.3.1.1.1

Let's change Figure 5.3.1.1.1 to make it specific for  $O_2$ . Re-draw the MO diagram (no need to draw the shapes of orbitals). Fill in the correct number of electrons for each oxygen atom on either side of the diagram. Then, fill in the total molecular electrons in the center. Calculate the bond order and determine whether it is diamagnetic or paramagnetic.

#### Solution

The diagram in Figure 5.3.1.1.1 includes core orbitals (the 1s) and valence electrons (2s, 2p). Therefore, we will consider all the electrons in an oxygen atom and a dioxygen molecule. An oxygen atom has eight total electrons. So we fill eight electrons into the atomic orbitals for the oxygen atom on the right, and eight electrons into the atomic orbitals for oxygen on the left. The total number of electrons for the molecule is sixteen, so fill in 16 electrons into the molecular orbitals, being sure to apply Hund's rule and the Aufbau principle. The result is a diagram that looks like the one drawn below in Figure 5.3.1.1.2

The bond order is calculated using the molecular orbitals (we can ignore atomic orbitals). There are 10 electrons in binding orbitals and 6 electrons in antibonding orbitals. This gives a bond order of  $\frac{1}{2}(10 - 6) = 2$ . This bond order is consistent with valence bond theory!

This diagram indicates that dioxygen is paramagnetic; it has two unpaired electrons in the  $\pi^*$  orbitals. This paramagnetic electron configuration explains why dioxygen is attracted to magnetic fields!

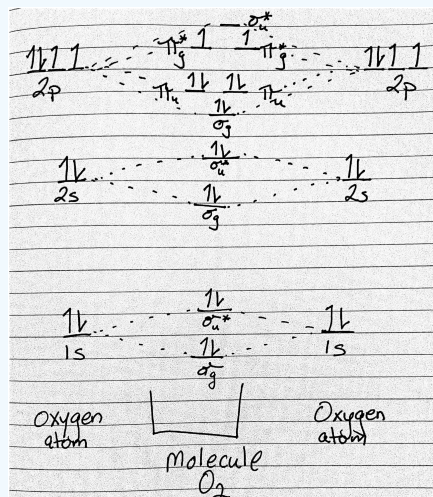


Figure 5.3.1.1.2: Hand-drawn molecular orbital diagram for dioxygen. (CC-BY-SA; Kathryn Haas)

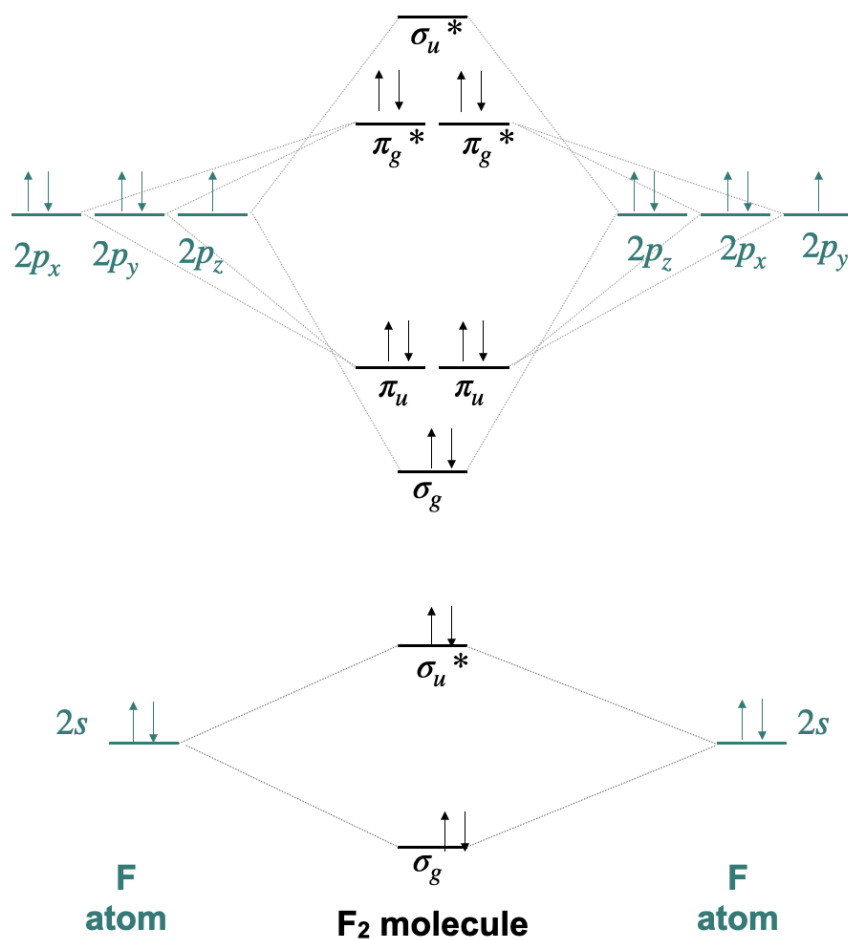
### ? Exercise 5.3.1.1.1

Draw the molecular orbital diagram for  $F_2$ ; be sure to label your orbitals with the appropriate symmetry and count your orbitals to make sure that the total number of atomic orbitals and molecular orbitals is the same. As a shortcut, include only the valence orbitals and electrons. What is the bond order? Is the molecule diamagnetic or paramagnetic?

#### Answer

The valence orbitals on an F atom are 2s and 2p. And, there are seven valence electrons in F. This gives fourteen total valence electrons. The MO diagram of the valence molecular orbitals can be constructed by combining the valence 2s and valence 2p orbitals from each F atom. The bond order is 1 and the molecule is diamagnetic.





This page titled 5.3.1.1: Molecular Orbitals is shared under a CC BY-SA 4.0 license and was authored, remixed, and/or curated by Kathryn Haas.

- 5.2.1: Molecular Orbitals by Kathryn Haas is licensed CC BY-SA 4.0.

### 5.3.1.2: Orbital Mixing

In the [previous section](#), we introduced a simplified molecular orbital (MO) diagram, assuming that interactions were limited to degenerate orbitals of compatible symmetry. A version of that *simplified* diagram for second-row homonuclear diatomics is shown on the left side of Figure 5.3.1.2.1 (only valence orbitals shown).

In reality, orbitals of compatible symmetry can combine, or mix, even when they have different energies. When sets of orbitals mix, it has the effect of decreasing the energy of the lower-energy set and increasing the energy of the higher-energy set. There are two ways to explain mixing, described in the points below. The diagram on the right of side of Figure 5.3.1.2.1 shows how energy levels are affected by orbital mixing.

- Starting from the simplified MO diagram and mixing molecular orbitals of like symmetry:** If we start with the "no mixing" simplified diagram shown on the left, we can pick out the orbitals with like symmetry and consider what will happen if these molecular orbitals mix. For example, starting from the MO diagram on the left side of Figure 5.3.1.2.1 we see that there are two  $\sigma_g$  orbitals that have identical symmetry (hence they have identical symmetry labels). Upon mixing, the lower-energy  $\sigma_g(2s)$  will decrease in energy while the higher-energy  $\sigma_g(2p)$  will increase in energy. Likewise, there are two  $\sigma_u^*$  orbitals that will mix, decreasing the energy of  $\sigma_u^*(2s)$  while increasing the energy of  $\sigma_u^*(2p)$ .
- Starting from and mixing atomic orbitals of compatible symmetry:** Starting from the atomic orbitals, we can select the orbitals that have compatible symmetry to make productive interactions, and combine them as a set to make molecular orbitals. From the two sets of atomic orbitals on the right panel in Figure 5.3.1.2.1, there are two sets of four orbitals with compatible symmetry; one is the set of two  $2s$  and two  $2p_z$  orbitals. These four orbitals can combine to form molecular orbitals with  $\sigma$  symmetry. They combine to form one lowest-energy bonding  $\sigma_g$ , a highest-energy  $\sigma_u^*$ , and two orbitals with intermediate energy ( $\sigma_g$ , and  $\sigma_u^*$ ). This treatment can be expressed as the linear combination of four atomic orbitals:

$$\Psi = c_1\psi(2s_a) \pm c_2\psi(2s_b) \pm c_3\psi(2p_a) \pm c_4\psi(2p_b)$$

where the coefficients  $c_1 = c_2$  and  $c_3 = c_4$  for homonuclear diatomic molecules.

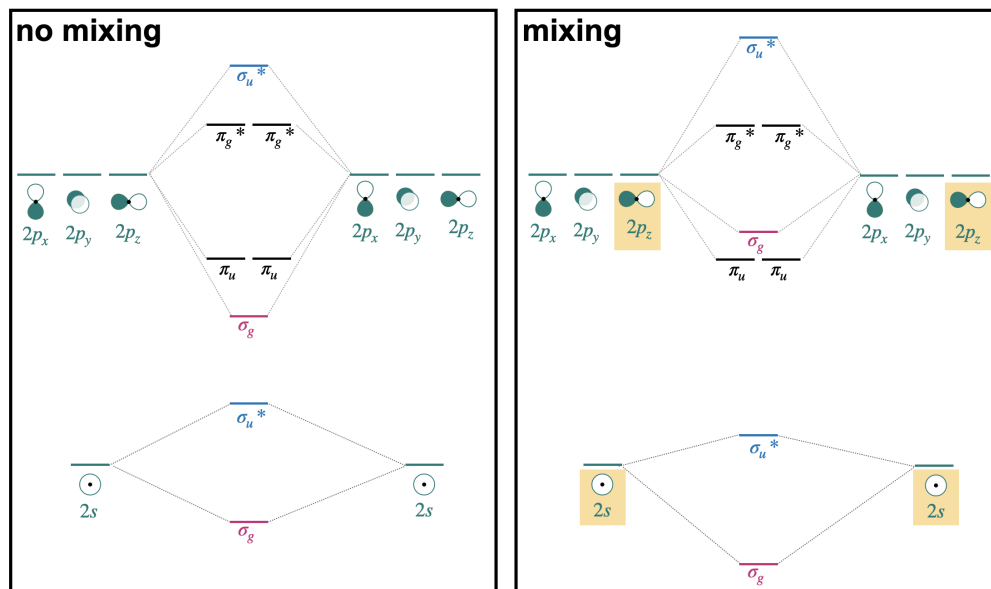


Figure 5.3.1.2.1: Mixing of orbitals with like symmetry affects the energies of molecular orbitals. The simplified case where no mixing occurs is shown on the left. The effects of mixing are shown on the right. The  $\sigma_g$  orbitals of like symmetry are highlighted in fuchsia and the  $\sigma_u^*$  orbitals of like symmetry are highlighted in blue. A group of atomic orbitals of similar symmetry are highlighted in yellow boxes; these atomic orbitals combine to give all  $\sigma$  molecular orbitals. (CC-BY-SA, Kathryn Haas)

In the case of homonuclear diatomic molecules of the second row, orbital mixing has important consequences for the energetic order of the  $\sigma_g(2p)$  and  $\pi_u(2p)$  orbitals. This will be discussed in the next section.

This page titled [5.3.1.2: Orbital Mixing](#) is shared under a [CC BY-SA 4.0](#) license and was authored, remixed, and/or curated by [Kathryn Haas](#).

- 5.2.2: Orbital Mixing** by [Kathryn Haas](#) is licensed [CC BY-SA 4.0](#).

### 5.3.1.3: Diatomic Molecules of the First and Second Periods

#### First Period Homonuclear Diatomic Molecules

In the first row of the periodic table, the valence atomic orbitals are  $1s$ . There are two possible homonuclear diatomic molecules of the first period:

**Dihydrogen,  $H_2$  [ $\sigma_g^2(1s)$ ]:** This is the simplest diatomic molecule. It has only two molecular orbitals ( $\sigma_g$  and  $\sigma_u^*$ ), two electrons, a bond order of 1, and is diamagnetic. Its bond length is 74 pm. MO theory would lead us to expect bond order to decrease and bond length to increase if we either add or subtract one electron. The calculated bond length for the  $H_2^+$  ion is approximately 105 pm.<sup>1</sup>

**Dihelium,  $He_2$  [ $\sigma_g^2\sigma_u^{*2}(1s)$ ]:** This molecule has a bond order of zero due to equal number of electrons in bonding and antibonding orbitals. Like other noble gases, He exists in the atomic form and does not form bonds at ordinary temperatures and pressures.

#### ? Exercise 5.3.1.3.1

Draw the complete molecular orbital diagrams for  $H_2$  and for  $He_2$ . Include sketches of the atomic and molecular orbitals.

Answer

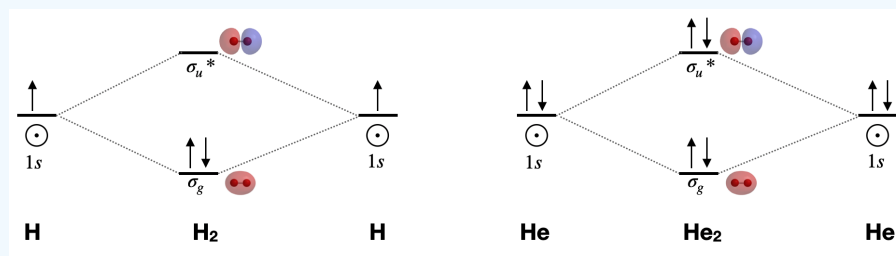


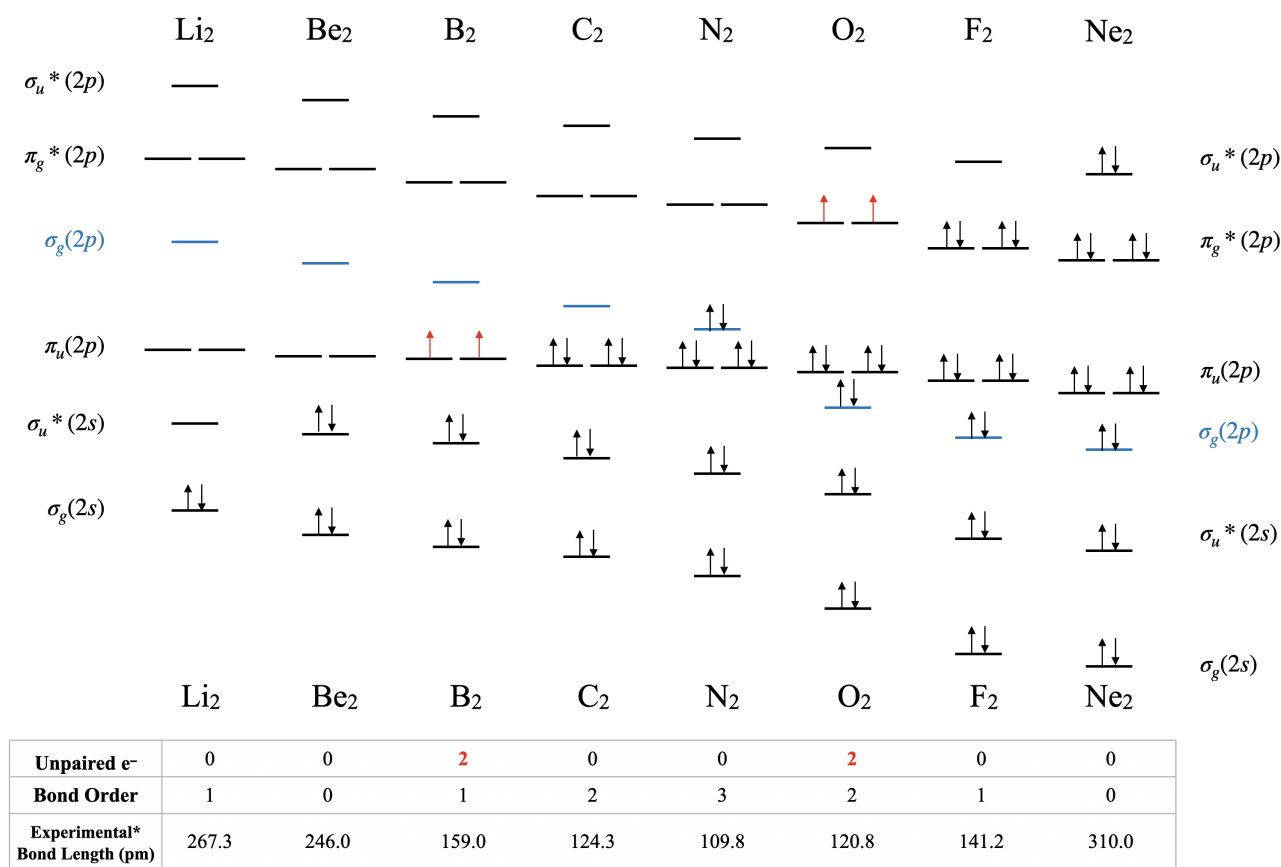
Figure for Exercise 5.3.1.3.1: Molecular orbital diagrams for dihydrogen and dihelium. Molecular orbital surfaces calculated using Spartan software. (CC-BY-NC-SA; Kathryn Haas)

A complete molecular orbital diagram includes all atomic orbitals and molecular orbitals, their symmetry labels, and electron filling.

#### Second Period Homonuclear Diatomic Molecules

The second period elements span from Li to Ne. The valence orbitals are  $2s$  and  $2p$ . In their molecular orbital diagrams, non-valence orbitals ( $1s$  in this case) are often disregarded in molecular orbital diagrams.

Orbital mixing has significant consequences for the magnetic and spectroscopic properties of second period homonuclear diatomic molecules because it affects the order of filling of the  $\sigma_g(2p)$  and  $\pi_u(2p)$  orbitals. Early in period 2 (up to and including nitrogen), the  $\pi_u(2p)$  orbitals are lower in energy than the  $\sigma_g(2p)$  (see Figure 5.3.1.3.1). However, later in period 2, the  $\sigma_g(2p)$  orbitals are pulled to a lower energy. This lowering in energy of  $\sigma_g(2p)$  is not unique; all of the  $\sigma$  orbitals in the molecule are pulled to lower energy due to the increasing positive charge of the nucleus. The  $\pi$  orbitals in the molecule are also affected, but to a much lesser extent than  $\sigma$  orbitals. The reason has to do with the high penetration of  $s$  atomic orbitals compared to  $p$  atomic orbitals (recall our previous discussion on [penetration and shielding](#), and its effect on [periodic trends](#)). The  $\sigma$  molecular orbitals have more  $s$  character and thus their energy is more influenced by increasing nuclear charge. As nuclear charge increases, the energy of the  $\sigma_g(2p)$  orbital is lowered significantly more than the energy of the  $\pi_u(2p)$  orbitals (Figure 5.3.1.3.1).



\*Experimental bond lengths from “List of Experimental Diatomic Bond Lengths”, NIST, <https://cccbdb.nist.gov/diatomicepibondx.asp>

Figure 5.3.1.3.1: Molecular orbital energy-level diagrams for the diatomic molecules of the period 2 elements. Unlike earlier diagrams, only the valence molecular orbital energy levels for the **molecules** are shown here (atomic orbitals not shown for simplicity). For Li<sub>2</sub> through N<sub>2</sub>, the  $\sigma_g(2p)$  orbital is higher in energy than the  $\pi_u(2p)$  orbitals. In contrast, from O<sub>2</sub> onward, the  $\sigma_g(2p)$  orbital is lower in energy than the  $\pi_u(2p)$  orbitals because the nuclear charge increases across the row. The experimental bond lengths correlate with the calculated bond order. (CC-BY-NC-SA, Kathryn Haas)

**Lithium, Li<sub>2</sub> [ $\sigma_g^2(2s)$ ]:** This molecule has a bond order of one and is observed experimentally in the gas phase to have one Li-Li bond.

**Diberyllium, Be<sub>2</sub> [ $\sigma_g^2\sigma_u^{*2}(2s)$ ]:** This molecule has a bond order of zero due to the equal number of electrons in bonding and antibonding orbitals. Although Be<sub>2</sub> does not exist under ordinary conditions, it can be produced in a laboratory and its bond length measured (Figure 5.3.1.3.2). Although the bond is very weak, its bond length is surprisingly ordinary for a covalent bond of the second period elements.<sup>2</sup>

**Diboron, B<sub>2</sub> [ $\sigma_g^2\sigma_u^{*2}(2s)\pi_u^1\pi_u^1(2p)$ ]:** The case of diboron is one that is much better described by molecular orbital theory than by Lewis structures or valence bond theory. This molecule has a bond order of one. The molecular orbital description of diboron also predicts, accurately, that diboron is paramagnetic. The paramagnetism is a consequence of orbital mixing, resulting in the  $\sigma_g$  orbital's being at a higher energy than the two degenerate  $\pi_u^*$  orbitals.

**Dicarbon, C<sub>2</sub> [ $\sigma_g^2\sigma_u^{*2}(2s)\pi_u^2\pi_u^2(2p)$ ]:** This molecule has a bond order of two. Molecular orbital theory predicts two bonds with  $\pi$  symmetry, and no  $\sigma$  bonding. C<sub>2</sub> is rare in nature because its allotrope, diamond, is much more stable.

**Dinitrogen, N<sub>2</sub> [ $\sigma_g^2\sigma_u^{*2}(2s)\pi_u^2\pi_u^2\sigma_g^2(2p)$ ]:** This molecule is predicted to have a triple bond. This prediction is consistent with its short bond length and bond dissociation energy. The energies of the  $\sigma_g(2p)$  and  $\pi_u(2p)$  orbitals are very close, and their relative energy levels have been a subject of some debate (see next section for discussion).

**Dioxygen,  $O_2$**  [ $\sigma_g^2 \sigma_u^{*2} (2s) \sigma_g^2 \pi_u^2 \pi_g^{*1} \pi_g^{*1} (2p)$ ]: This is another case where valence bond theory fails to predict actual properties. Molecular orbital theory correctly predicts that dioxygen is paramagnetic, with a bond order of two. Here, the molecular orbital diagram returns to its "normal" order of orbitals where orbital mixing could be somewhat ignored, and where  $\sigma_g(2p)$  is lower in energy than  $\pi_u(2p)$ .

**Difluorine,  $F_2$**  [ $\sigma_g^2 \sigma_u^{*2} (2s) \sigma_g^2 \pi_u^2 \pi_g^{*2} \pi_g^{*2} (2p)$ ]: This molecule has a bond order of one and like oxygen, the  $\sigma_g(2p)$  is lower in energy than  $\pi_u(2p)$ .

**Dineon,  $Ne_2$**  [ $\sigma_g^2 \sigma_u^{*2} (2s) \sigma_g^2 \pi_u^2 \pi_g^{*2} \pi_g^{*2} \sigma_u^{*2} (2p)$ ]: Like other noble gases, Ne exists in the atomic form and does not form bonds at ordinary temperatures and pressures. Like  $Be_2$ ,  $Ne_2$  is an unstable species that has been created in extreme laboratory conditions and its bond length has been measured (Figure 5.3.1.3.2)

### ? Exercise 5.3.1.3.2

Draw the complete molecular orbital diagram for  $O_2$ . Show calculation of its bond order and tell whether it is diamagnetic or paramagnetic.

#### Answer

$O_2$  is paramagnetic with a bond order of 2. Its  $\sigma_g(2p)$  molecular orbital is lower in energy than the set of  $\pi_u(2p)$  orbitals.

$$\text{Bond order} = \frac{1}{2} \left[ \left( \begin{array}{c} 8 \text{ electrons in} \\ \text{valence bonding orbitals} \end{array} \right) - \left( \begin{array}{c} 4 \text{ electrons in} \\ \text{valence antibonding orbitals} \end{array} \right) \right]$$

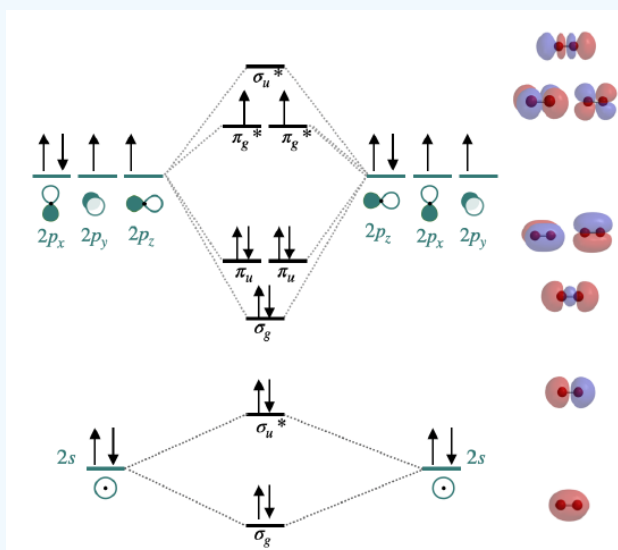


Figure for Exercise 5.3.1.3.2. Molecular orbital diagram of  $O_2$ . (CC-BY-NC-SA, Kathryn Haas)

### ? Exercise 5.3.1.3.3: The Peroxide Ion

Use a qualitative molecular orbital energy-level diagram to predict the electron configuration, the bond order, and the number of unpaired electrons in the peroxide ion ( $O_2^{2-}$ ).

#### Answer

This diagram looks similar to that of  $O_2$ , except that there are two additional electrons.

$(\sigma_g(2s))^2 (\sigma_u^*(2s))^2 (\sigma_g(2p))^2 (\pi_u(2p))^4 (\pi_g(2p))^4$ ; bond order of 1; no unpaired electrons.

## Bond Lengths in Homonuclear Diatomic Molecules

The trends in experimental bond lengths are predicted by molecular orbital theory, specifically by the calculated bond order. The values of bond order and experimental bond lengths for the second period diatomic molecules are given in Figure 5.3.1.3.1, and shown in graphical format on the plot in Figure 5.3.1.3.2. From the plot, we can see that bond length correlates well with bond

order, with a minimum bond length occurring where the bond order is greatest ( $N_2$ ). The shortest bond distance is at  $N_2$  due to its high bond order of 3. From  $N_2$  to  $F_2$  the bond distance increases despite the fact that atomic radius decreases.

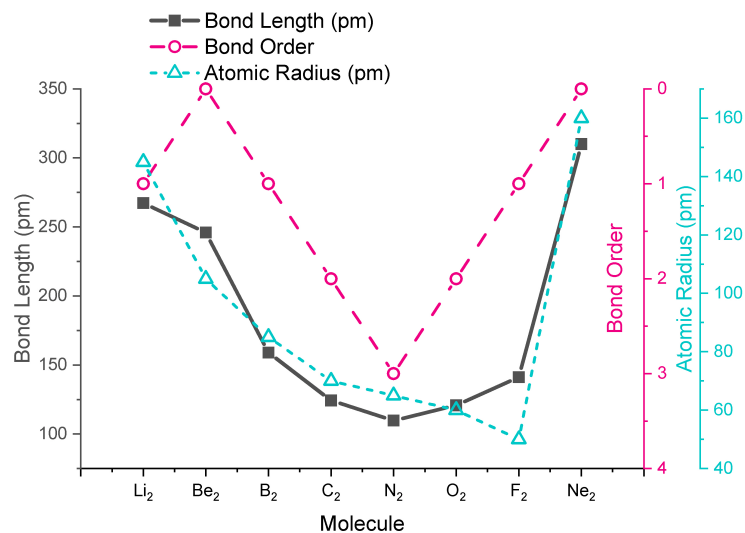


Figure 5.3.1.3.2: Overlaid plots of bond length (black squares), bond order (pink circles), and atomic radius (teal triangles) versus atomic number for second period homonuclear diatomic molecules. (CC-BY-NC-SA; Kathryn Haas)

## References

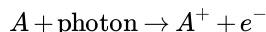
1. NIST, Calculated Geometries available for  $H_2^+$  (Hydrogen cation)  $2\Sigma_g^+$   $D_{\infty h}$ , available at <https://cccbdb.nist.gov/diatomiceqbondx.asp>
2. Merritt, J. M.; Bondybey, V. E.; Heaven, M. C., Beryllium Dimer-Caught in the Act of Bonding. *Science* **2009**, 324 (5934), 1548-1551.

This page titled 5.3.1.3: Diatomic Molecules of the First and Second Periods is shared under a CC BY-SA 4.0 license and was authored, remixed, and/or curated by Kathryn Haas.

- 5.2.3: Diatomic Molecules of the First and Second Periods by Kathryn Haas is licensed CC BY-SA 4.0.
- 5.P: Problems is licensed CC BY-SA 4.0.

### 5.3.1.4: Photoelectron Spectroscopy

A photoelectron spectrum can show the relative energies of occupied molecular orbitals by ionization. The *ionization energy* is a direct measure of the energy required to just remove the electron concerned from its initial level to the vacuum level (free electron). Photoelectron spectroscopy measures the relative energies of the ground and excited positive ion states that are obtained by removal of single electrons from the neutral molecule.



The information obtained from photoelectron spectroscopy is typically discussed in terms of the electronic structure and bonding in the ground states of neutral molecules, with ionization of electrons occurring from bonding molecular orbitals, lone pairs, antibonding molecular orbitals, or atomic cores. These descriptions reflect the relationship of ionization energies to the molecular orbital model of electronic structure.

Ionization energies are directly related to the energies of molecular orbitals (by [Koopmans' theorem](#)).

#### Example: Photoelectron spectrum of dihydrogen

The molecular orbital description of dihydrogen involves two  $1s$  atomic orbitals generating two molecular orbitals: a bonding  $\sigma_g$  and an antibonding  $\sigma_u^*$ . The two electrons occupy the  $\sigma_g$  bonding orbital, leaving the molecule with a bond order of one (Figure 5.3.1.4.1). The PES spectrum of dihydrogen (Figure 5.3.1.4.1) has a single band that corresponds to the ionization of one electron from the  $\sigma_g$ . The multiple peaks are due to electrons ejecting from a range of stimulated vibrational energy levels. When extensive vibrational structure is resolved in a PES molecular orbital, then the removal of an electron from that molecular orbital induces a significant change in the bonding (in this case an increase in the bond length due to decrease in bond order).

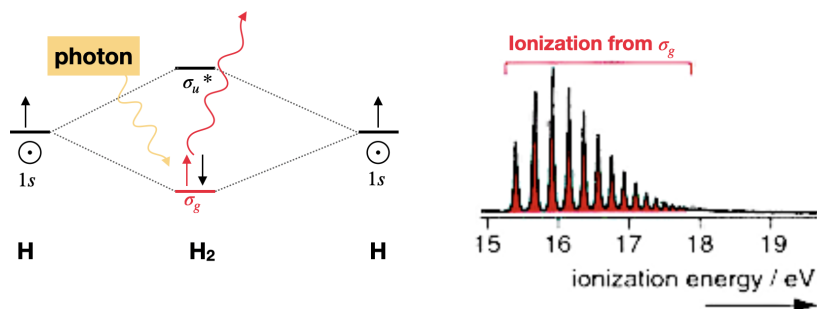


Figure 5.3.1.4.1: The molecular orbital diagram and photoelectron spectrum of dihydrogen. (CC-BY-NC-SA; Libretexts)

#### Example: Photoelectron spectrum of dinitrogen

Diatomic nitrogen is more complex than hydrogen since multiple molecular orbitals are occupied. Five molecular orbitals are occupied; two of them are degenerate. Three bands in the photoelectron spectrum correspond to ionization of an electron in  $\sigma_g(2p)$ ,  $\pi_u(2p)$  and  $\sigma_u^*(2s)$  molecular orbitals. Ionization of the fourth type of orbital,  $\sigma_g(2s)$ , does not appear in Figure 5.3.1.4.2 because it is either off scale or because the incident light  $h\nu$  used did not have sufficient energy to ionize electrons in that deeply stabilized molecular orbital. Note that extensive vibrational structure for the  $\pi_u(2p)$  band indicates that the removal of an electron from this molecular orbital causes a significant change in the bonding.

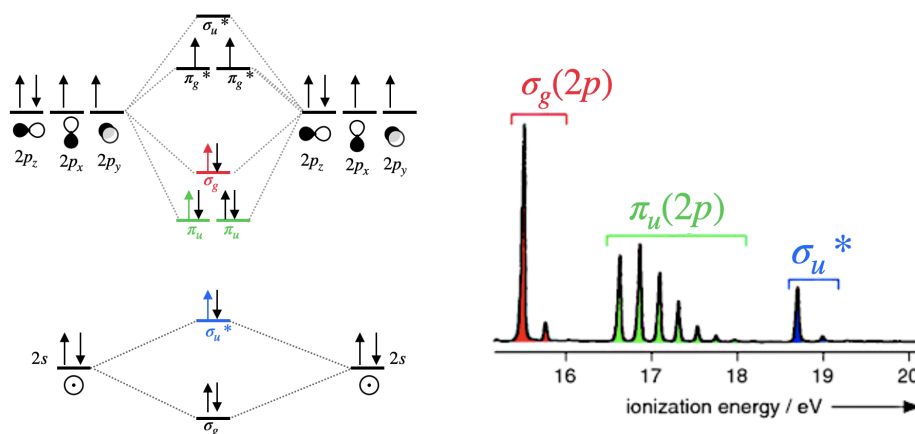


Figure 5.3.1.4.2: The molecular orbital diagram and photoelectron spectrum of dinitrogen. (CC-BY-NC-SA; Libretexts)

From the photoelectron spectrum of dinitrogen, we can see that the electrons in the  $\sigma_g(2p)$  orbital can be ionized using less energy than required to ionize electrons in the  $\pi_u(2p)$  orbital. This is evidence for  $\sigma_g(2p)$  existing at a higher energy than the  $\pi_u(2p)$  orbitals.

This page titled [5.3.1.4: Photoelectron Spectroscopy](#) is shared under a [CC BY-SA 4.0](#) license and was authored, remixed, and/or curated by [Kathryn Haas](#).

- [10.4: Photoelectron Spectroscopy](#) by Roger Nix is licensed [CC BY 4.0](#).



## SECTION OVERVIEW

### 5.3.2: Heteronuclear Diatomic Molecules

Diatomic molecules with two non-identical atoms are called **heteronuclear** diatomic molecules. When atoms are not identical, the molecule forms by combining atomic orbitals of unequal energies. *The result is a polar bond in which atomic orbitals contribute unevenly to each molecular orbital.*

The application of molecular orbital theory to heteronuclear diatomic molecules is similar to the case of homonuclear diatomics, except that the atomic orbitals from each atom have different energies and contribute unequally to molecular orbitals. Recall that atomic orbitals must have compatible symmetry and similar energy to combine into molecular orbitals. In the case where atomic orbitals of like symmetry have different energies, they combine less favorably than orbitals that are closer to one another in energy. As a general rule, orbitals that have energy differences of greater than 10-14 eV do not combine favorably. In the molecular orbital diagram, the closer a molecular orbital is to an atomic orbital, the more that atomic orbital contributes to the molecular orbital. This last point is helpful for back-of-the napkin estimations of what the molecular orbitals "look" like.

In this section, you should learn how to generate molecular orbital diagrams of heteronuclear diatomic molecules. To approach such a problem, we must start with a knowledge of the relative energies of electrons in different atomic orbitals. In other words, we need knowledge of the orbital potential energies (or orbital ionization energies).

#### 5.3.2.1: Orbital ionization energies

#### 5.3.2.2: Polar bonds

#### 5.3.2.3: Ionic Compounds and Molecular Orbitals

---

#### Sources:

- Gray, Harry. *Electrons and Chemical Bonding*, Benjamin, 1964.
- Miessler, Gary L, and Donald A. Tarr. *Inorganic Chemistry*. Upper Saddle River, N.J: Pearson Education, 2014. Print.

---

This page titled [5.3.2: Heteronuclear Diatomic Molecules](#) is shared under a [CC BY-SA 4.0](#) license and was authored, remixed, and/or curated by [Kathryn Haas](#).

### 5.3.2.1: Orbital ionization energies

To generate molecular orbital diagrams of heteronuclear diatomic molecules, we must start with a knowledge of the relative energies of electrons in different atomic orbitals. In other words, we need knowledge of the orbital potential energies (or orbital ionization energies).

#### Orbital Ionization Energies

There are two approaches you can use to "know" or estimate the atomic orbital energy levels.

1. Use a table of atomic orbital ionization energies, like those found in Table 5.3.2.1.1
2. When you do not have access to a table of values like the one below, use periodic trends in electronegativity and/or ionization energies as your guide to approximate relative values for different atoms.

Table 5.3.2.1.1: These are one-electron ionization energies of the valence orbitals calculated by average energies of both the ground-state and ionized-state configurations. (From Harry Gray, "Electrons and Chemical Bonding," Benjamin, 1964, Appendix) Values are expressed in eV.

Atom	1s	2s	2p	3s	3p	4s	4p	Atom	3d	4s	4p
H	-13.64							Sc	-4.71	-5.70	-3.22
He	-24.55							Ti	-5.58	-6.08	-3.35
Li		-5.46						V	-6.32	-6.32	-3.47
Be		-9.30						Cr	-7.19	-6.57	-3.47
B		-14.01	-8.31					Mn	-7.93	-6.82	-3.60
C		-19.47	-10.66					Fe	-8.68	-7.07	-3.72
N		-25.54	-13.14					Ni	-10.04	-7.56	-3.84
O		-32.36	-15.87					Cu	-10.66	-7.69	-3.97
F		-46.37	-18.72								
Ne		-48.48	-21.57								
Na				-5.21							
Mg				-7.69							
Al				-11.28	-5.95						
Si				-15.00	-7.81						
P				-18.72	-10.17						
S				-20.71	-11.65						
Cl				-25.29	-13.76						
Ar				-29.26	-15.87						
K						-4.34					
Ca						-6.08					
Zn						-9.42					
Ga						-12.65	-5.95				
Ge						-15.62	-7.56				
As						-17.61	-9.05				
Se						-20.83	-10.79				
Br						-24.05	-12.52				
Kr						-27.52	-14.26				

This page titled 5.3.2.1: Orbital ionization energies is shared under a CC BY-SA license and was authored, remixed, and/or curated by Kathryn Haas.

- 5.3: Heteronuclear Diatomic Molecules by Kathryn Haas is licensed CC BY-SA 4.0.

### 5.3.2.2: Polar bonds

#### Molecular orbital diagrams for heteronuclear diatomic molecules

The molecular orbital diagram of a heteronuclear diatomic molecule is approached in a way similar to that of a homonuclear diatomic molecule. The orbital diagrams may also look similar. A major difference is that the more electronegative atom will have orbitals at a lower energy level. Two examples of heteronuclear diatomic molecules will be explored below as illustrative examples.

##### Carbon monoxide MO diagram

Carbon monoxide is an example of a heteronuclear diatomic molecule where both atoms are second-row elements. The valence molecular orbitals in both atoms are the  $2s$  and  $2p$  orbitals. The molecular orbital diagram for carbon monoxide (Figure 5.3.2.2.1) is constructed in a way similar to how you would construct dicarbon or dioxygen, except that the oxygen orbitals have a lower potential energy than analogous carbon orbitals. The labeling of molecular orbitals in this diagram follows a convention by which orbitals are given serial labels according to type of orbital ( $\sigma$ ,  $\pi$ , etc.). The lowest energy orbitals of any type are assigned a value of 1 and higher energy orbitals of the same type are assigned by increasing intervals (..2, 3, 4...). The orbital labeling system described previously is inappropriate for heteronuclear diatomic molecules that cannot be assigned  $g$  and  $u$  subscripts.

A consequence of unequal atomic orbital energy levels is that orbital mixing is significant. Notice the order of the molecular orbitals labeled  $1\pi$  and  $3\sigma$  in Figure 5.3.2.2.1. This is a similar order of  $\pi$  and  $\sigma$  orbitals to the one we saw in the case of the  $\sigma_g$  and  $\pi_u$  orbitals of  $N_2$  and lighter diatomics of the second period. Because the oxygen  $2p_z$  orbital is close in energy to both the carbon  $2p_z$  and carbon  $2s$ , these three orbitals will have significant interaction (mixing). The result is an increase in the energy of the  $3\sigma$  orbital and a decrease in energy of the  $2\sigma^*$  orbital, resulting in the diagram shown in Figure 5.3.2.2.1.

In the case of carbon monoxide (Figure 5.3.2.2.1), atomic orbitals contribute unequally to each molecular orbital. For example, because the  $2s$  orbital of oxygen is very close in energy to the  $2\sigma$  molecular orbital, it contributes to that molecular orbital more than the  $2s$  orbital from carbon. Notice the shape of this  $2\sigma$  orbital and how it is unevenly distributed over the two atoms; it is more heavily distributed on the oxygen because it is most like the oxygen  $2s$ . This is in line with the assumption that electron density is distributed more on oxygen because it is more electronegative than carbon. Likewise, the  $1\pi$  orbitals are unevenly distributed, with more distribution close to the oxygen.

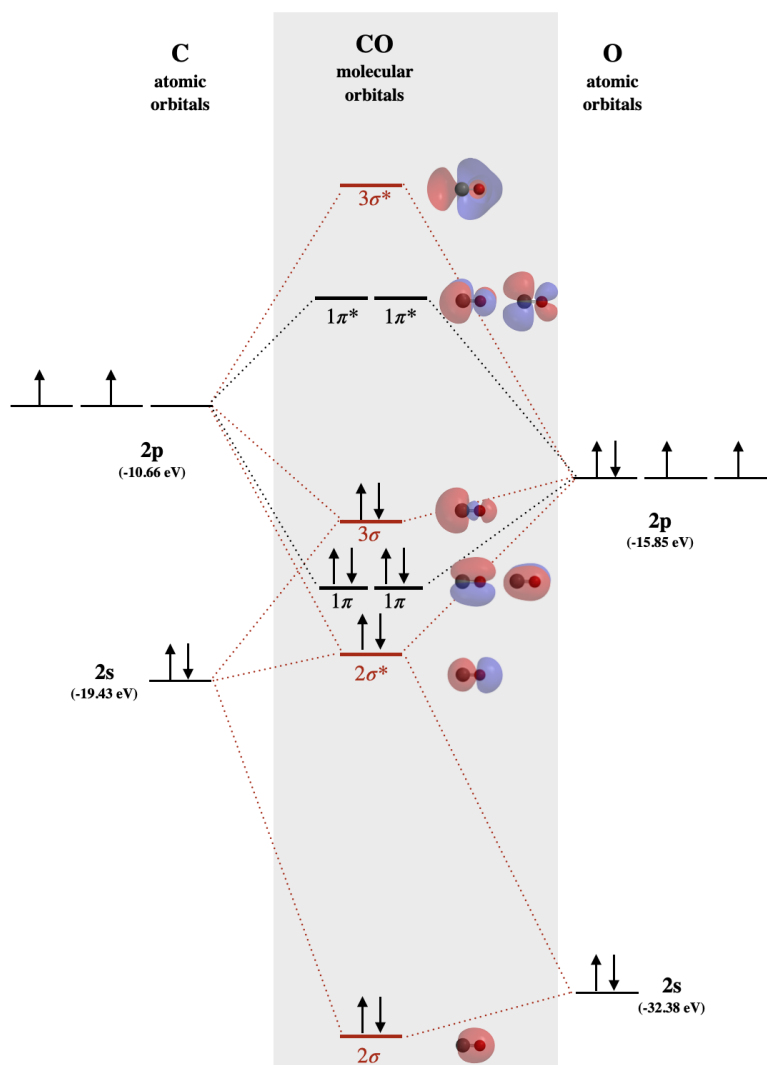


Figure 5.3.2.2.1: Molecular orbital diagram of carbon monoxide. The labeling of molecular orbitals in this diagram follows a convention by which orbitals are given serial names according to the type of orbital ( $\sigma$ ,  $\pi$ , etc.). The lowest energy orbitals of any type are assigned a value of 1 and higher energy orbitals of the same type are assigned by increasing intervals (...2, 3, 4...). The orbital labeling system described previously is inappropriate for heteronuclear diatomic molecules that cannot be assigned  $g$  and  $u$  subscripts. Molecular orbital surfaces were calculated using Spartan software. (Kathryn Haas, CC-BY-NC-SA)

### ? Exercise 5.3.2.2.1

Examine the shape of the  $3\sigma$  orbital of carbon monoxide in Figure 5.3.2.2.1. Describe what ways this shape is different from the shape of the  $\sigma_g$  orbitals from second period homonuclear diatomic molecules (see Fig. 5.2.1.1). Rationalize these differences. Both orbitals are re-created below for convenience.



### Answer

The  $3\sigma$  orbital is like the  $\sigma_g$  in that it has three lobes and two nodes distributed along the internuclear bond. They are different in their distribution. The two external lobes of  $\sigma_g$  are evenly distributed because they are an equal combination of

two  $p_z$  orbitals (one from each atom). The  $3\sigma$  orbital is more heavily distributed toward the carbon atom, the less electronegative atom, than toward the oxygen. The unequal distribution of  $3\sigma$  is apparent in the unequal sizes of its exterior lobes and the uneven shape of the interior lobe. The heavier distribution within the exterior lobe on carbon is caused by the mixing of the carbon  $2s$  orbital with carbon and oxygen  $2p_z$  orbitals. The uneven shape of the interior lobe, where it leans toward oxygen, is best explained by the fact that the  $3\sigma$  orbital is closer in energy to the oxygen  $2p_z$  than the carbon  $2p_z$ .

### Hydrogen fluoride MO diagram

Hydrogen fluoride is an example of a heteronuclear diatomic molecule in which the two atoms are from different periods. In this case, the valence orbital of H is  $1s$  while those of F are  $2s$  and  $2p$ . The molecular orbital diagram for HF is shown in Figure 5.3.2.2.2

Three of these orbitals have compatible symmetry for mixing; these are the hydrogen  $1s$ , fluorine  $2s$ , and fluorine  $2p$ . However, the extent to which they will interact depends on their relative energies. Fluorine is more electronegative than H, and the fluorine atom has a higher first ionization energy than does hydrogen. From these trends, we can expect that the fluorine valence orbitals are lower in energy than that of hydrogen. From Table 5.3.1, we find that the  $1s$  orbital of H ( $-13.6$  eV) is higher in energy than both fluorine orbitals ( $-18.7$  and  $-40.2$  eV, respectively for  $2p$  and  $2s$ ). The energies of hydrogen  $1s$  and fluorine  $2p$  are a good match for combination; however, the fluorine  $2s$  orbital is much too different to create a productive interaction. Therefore, we expect that the fluorine  $2s$  will create a non-bonding molecular orbital, while the  $1s$  and  $2p_z$  orbitals combine to make  $\sigma$  bonding and  $\sigma^*$  antibonding molecular orbitals. The remaining  $2p_x$  and  $2p_y$  orbitals do not have compatible symmetry for bonding with hydrogen, and they will form non-bonding  $\pi$  molecular orbitals. The non-bonding orbitals will have similar energy and character as their component atomic orbitals.

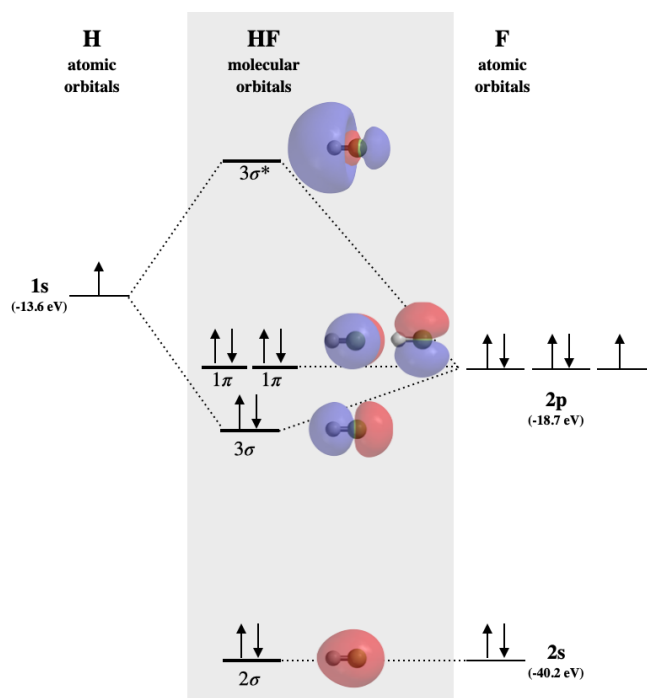


Figure 5.3.2.2.2: Molecular Orbital diagram of hydrogen fluoride. Molecular orbitals calculated using Spartan software. (Kathryn Haas, CC-BY-NC-SA)

### Chemical reactions take place at the HOMO and LUMO orbitals

Knowledge of molecular orbital diagrams, and the shapes of molecular orbitals, can be used to accurately explain and predict chemical reactivity. Chemical reactions take place using the highest occupied molecular orbitals (HOMO) of a nucleophile or Lewis base, and the lowest unoccupied molecular orbital (LUMO) of an electrophile or Lewis acid.

*Lewis bases react using electrons in the HOMO, while Lewis acids react using the empty LUMO.*

### Example: Reactivity of CO with metal ions

CO is an excellent ligand for many metal ions. In fact, the strong affinity between CO and the heme iron (Fe) ions in hemoglobin can explain the mechanism of carbon monoxide poisoning. When CO binds in place of  $O_2$  to hemoglobin, that hemoglobin can no longer carry  $O_2$  to tissue cells. CO binding to hemoglobin is strong and practically irreversible. When CO binds to metal ions, it does so through the carbon atom. This is contrary to expectations based on the Lewis structure and the known bond polarity, where electron density is polarized toward oxygen. The distribution of the electron density of the HOMO of CO can explain this observation!

#### ? Exercise 5.3.2.2.2

Refer to the MO diagram for CO. Identify the HOMO and explain why CO bonds to metal ions through the carbon atom rather than through the oxygen atom.

#### Answer

In the interaction between CO and a metal ion, CO would act as a Lewis base; thus it will react using electrons in its HOMO. The MO diagram for CO is shown in Figure 5.3.2.1 the HOMO is the  $3\sigma$  orbital (also discussed in ? Exercise 5.3.2.2.1). The electron density of that MO is centered around the carbon atom, thus the carbon atom will be a better Lewis base than the O atom.

This page titled [5.3.2.2: Polar bonds](#) is shared under a [CC BY-SA 4.0](#) license and was authored, remixed, and/or curated by [Kathryn Haas](#).

- [5.3.2: Polar bonds](#) by [Kathryn Haas](#) is licensed [CC BY-SA 4.0](#).

### 5.3.2.3: Ionic Compounds and Molecular Orbitals

Ionic interactions lie at one extreme on a spectrum of bonding. On the opposite end of the spectrum are the non-polar covalent bonds (e.g., homonuclear diatomics). In these molecules, molecular orbitals are formed by equal-energy atomic orbitals, resulting in electron density evenly distributed over the molecule. In the middle of the spectrum are the cases of polar covalent bonds (e.g., heteronuclear diatomics), in which atomic orbitals of unequal energies contribute unequally to molecular orbitals, resulting in uneven distribution of electron density across the molecule. In the case of polar bonds, the electron density is shifted toward the more electronegative atom since that atom contributes more to the lowest energy bonding molecular orbitals. Molecular orbital diagrams can be drawn for ionic compounds as if they are extremely polar bonds in which electrons are not only shifted toward, but are transferred completely to the more electronegative atom.

#### Example: NaCl

In NaCl, the sodium  $3s$  orbital ( $-5.2$  eV) is significantly higher in energy than the chlorine valence orbitals. The chlorine  $3s$  and  $3p_z$  orbitals have compatible symmetry, yet only the  $3p_z$  orbital ( $-13.8$  eV) is close enough in energy to interact with the Na  $3s$ ; still, the energy difference is large enough to make bonding weak. The Na  $3s$  orbital combines with Cl  $3p_z$  to form the molecular orbitals labeled  $4\sigma$  and  $4\sigma^*$  in Figure 5.3.2.3.1. The  $4\sigma$  orbital is weakly bonding, but is very close in energy to the Cl  $3p_z$  orbital, and is mostly Cl-like in character. Notice that all  $\sigma$  orbitals look very much like either  $s$  or  $p$  orbitals centered on the Cl atom, while the  $4\sigma^*$  orbital is centered almost entirely on Na. The lack of molecular orbitals that are distributed over both atoms at once is consistent with a lack of significant covalent bond character in NaCl. The bonding here is characterized by transfer of one electron from Na to Cl and is almost entirely electrostatic. Bonding that is mostly electrostatic in character is non-directional, unlike true covalent bonding.

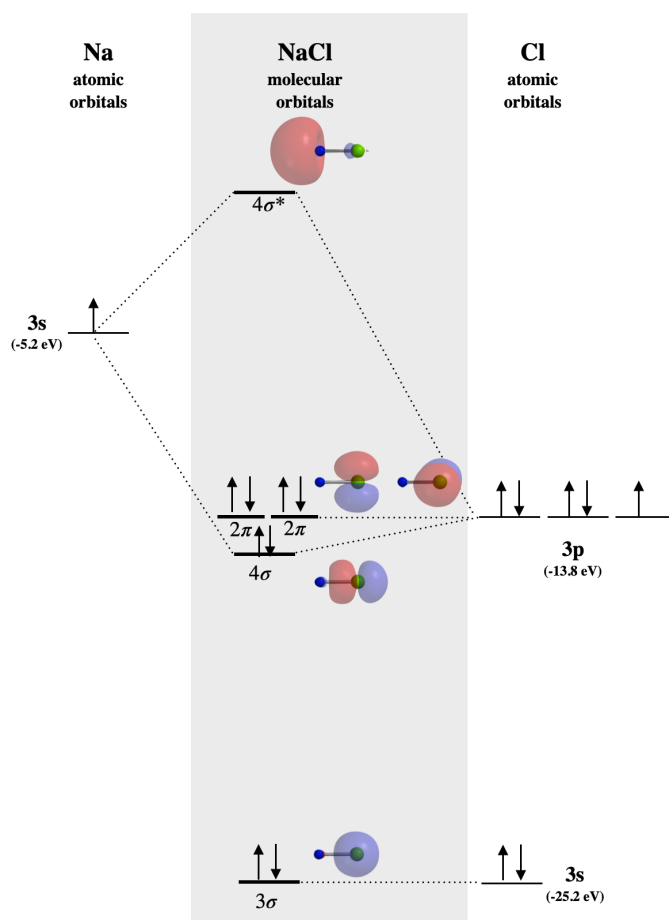


Figure 5.3.2.3.1: The molecular orbital diagram for sodium chloride. Molecular orbital surfaces calculated using Spartan software indicate almost no covalent nature of bonding. (CC-BY-NC-SA, Kathryn Haas)

### ? Exercise 5.3.2.3.1

Draw the molecular orbital diagram for LiF. Make sure to label all molecular orbitals appropriately, and specify whether they are mostly bonding, non-bonding, or antibonding. Identify the HOMO and LUMO. Sketch the approximate shapes of all orbitals.

#### Answer

We expect LiF to be an ionic compound because the energy difference in valence orbitals is at least 10-14 eV. (See Table 5.3.1) There are a variety of ways used to label molecular orbitals. In the figure below, we are using the convention of labeling each type of orbital with numbers starting from the lowest-energy orbitals. The  $1\sigma$  orbital would be mostly F  $1s$  in character and is not shown. The  $2\sigma$  orbital is mostly non-bonding in nature, although it has a very small contribution from  $2s$  of Li due to compatible symmetry. The  $3\sigma$  orbital is slightly bonding but it is mostly F  $2p$  in character. The two  $1\pi$  orbitals are completely non-bonding. The  $3\sigma^*$  orbital is antibonding.

- HOMO is  $1\pi$
- LUMO is  $3\sigma^*$

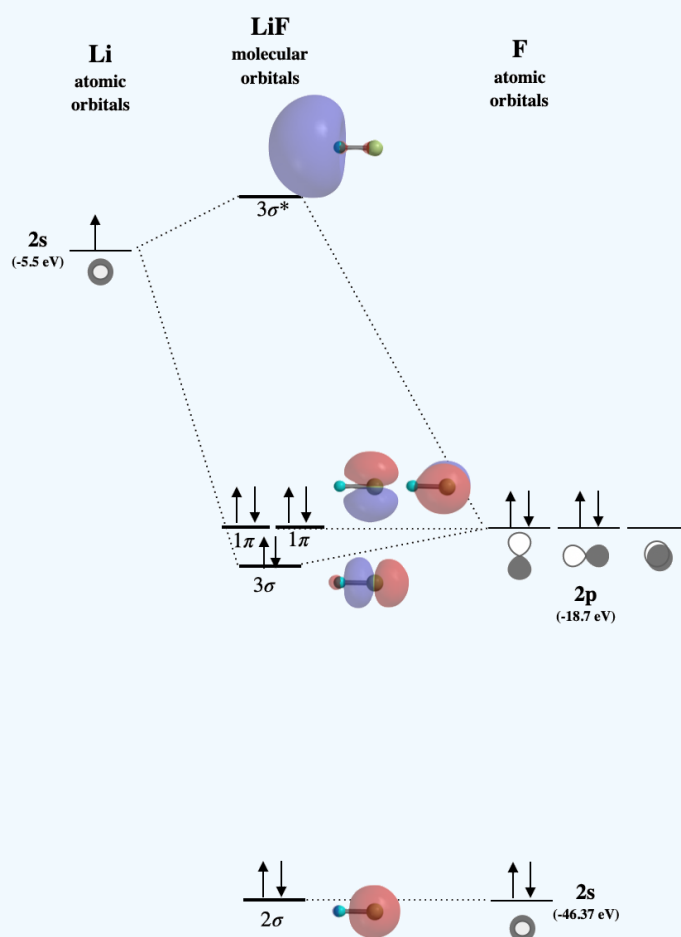


Figure for Exercise 5.3.2.3.1: Molecular orbital diagram for the ionic compound, LiF. (CC-BY-NC-SA, Kathryn Haas)

This page titled [5.3.2.3: Ionic Compounds and Molecular Orbitals](#) is shared under a [CC BY-SA 4.0](#) license and was authored, remixed, and/or curated by [Kathryn Haas](#).

- [5.3.3: Ionic Compounds and Molecular Orbitals](#) by Kathryn Haas is licensed [CC BY-SA 4.0](#).



## 5.4: Polyatomic MO Diagrams

---

Learning objectives for this unit are to:

- Use group theory and the central atom generator function method to determine the symmetries of and draw pictures of ligand group orbitals (LGOs)
  - Derive molecular orbital energy diagrams for polyatomic molecules based on the interactions between the central atom AOs and the LGOs
  - Use MO diagrams to determine or rationalize bond order (bond length/strength), magnetism, and reactivity of molecules
  - Generate and interpret Walsh correlation diagrams for two different geometric arrangements of atoms
- 

5.4: Polyatomic MO Diagrams is shared under a [not declared](#) license and was authored, remixed, and/or curated by LibreTexts.

### 5.4.1: Ligand Group Orbitals and Generator Functions

So far we have examined the Molecular Orbital (MO) diagrams for diatomic molecules. These molecules can be classified in two different groups, those that contain hydrogen (and thus only have the hydrogen 1s orbital available to make MOs) and those that do not. For the second group, the general diagram developed in previous sections containing  $\sigma$ - and  $\pi$ -bonding and antibonding MOs will generally apply, although there can be subtle differences for heteronuclear diatomics that contain atoms with vastly different electronegativity values. The number of diatomic molecules is incredibly small compared to the number of molecules containing three or more atoms. It would be impractical to create and refer to general MO diagrams for all of the different possible combinations, so developing a method to quickly develop MO diagrams for these larger molecules is highly desirable. The method described will use group theory to do just that. For our purposes, we are only going to consider molecules that have a central atom surrounded by either hydrogen or a halide (which can be treated like hydrogen but with three lone pair). In other words, there will be no  $\pi$ -bonding in these molecules. While this again is a relatively small subset of all known molecules, it will provide a basis for the development and understanding of MO diagrams. As this course is not entirely dedicated to MO diagrams, it makes sense to take this limited approach. Larger molecules with  $\pi$ -bonding (and in some cases  $\delta$ -bonding) requires advanced computational methods to develop MO diagrams.

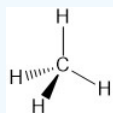
The starting point to this approach is drawing a proper three-dimensional structure of the molecule of interest. From there, the point group of the molecule must be determined. Once the symmetry of the molecule is known, the symmetry of the central atom's atomic orbitals (AOs) can be described using the appropriate symmetry labels. These are found in what is known as a character table and will be called the generator functions. The ligand group orbitals (LGOs) are then derived using a graphical approach. Combination of the generator functions and LGOs in an appropriate way gives the desired MO diagram. Using this technique, you should be able to quickly (albeit crudely) derive an MO diagram to help understand the symmetry and relative energy of the frontier orbitals, often the highest occupied molecular orbital (HOMO) and the lowest unoccupied molecular orbital (LUMO), the orbitals most responsible for chemical reactivity and spectroscopy. At this point, this approach likely seems somewhat vague at best. Rather than continue in a long narrative of the process, it is likely more effective to work through an example. This example will work through several steps that will be summarized at the end.

#### Step 1 - Drawing the structure and determining the hybridization of the central atom

##### Exercise 5.4.1.1

Using VSEPR, draw the three-dimensional structure of methane ( $\text{CH}_4$ ).

**Answer**



##### Exercise 5.4.1.2

What orbitals need to be used for hybridization of the central carbon atom?

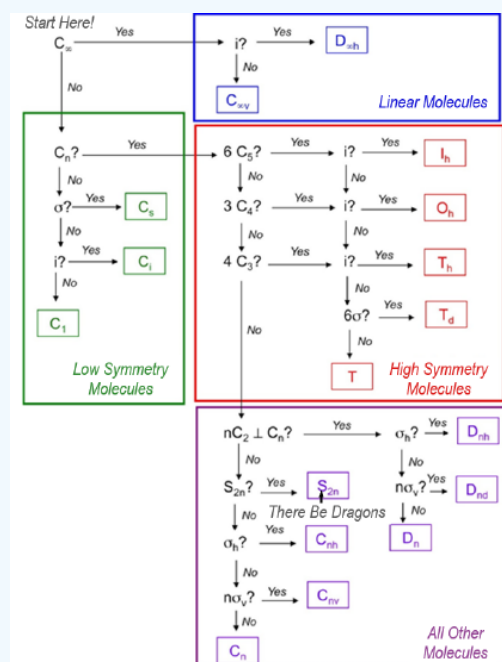
**Answer**

The carbon would be classified as  $\text{AX}_4\text{E}_0$  since it is bonded to the four hydrogen atoms and has no lone pair. Based on this the carbon would have to be  $\text{sp}^3$  hybridized, which means you will need to account for the s- and all three p-orbitals on the carbon atom.

#### Step 2 - Determine the point group of the molecule and assign the generator functions

### Exercise 5.4.1.3

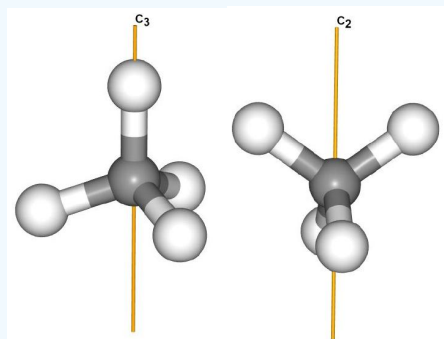
What is the point group of methane?



### Answer

Methane does not have an infinite rotation axis.

There is at least one rotation axis (in fact several). The highest order rotation axis is  $C_3$ , which can be thought of as any C-H bond. While not important for this application, there are also several  $C_2$  axes that pass between two C-H bonds.



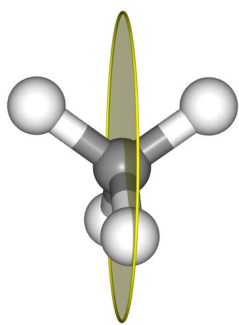
There are not 6  $C_5$  axes.

There are not 3  $C_4$  axes.

There are 4  $C_3$  axes as each of the C-H bonds is a  $C_3$  axis.

There is not an inversion center (it would have to be the unique carbon atom, and none of the hydrogen atoms have another hydrogen atoms directly across from it).

There are 6  $\sigma$ .



The point group of methane is  $T_d$ .

At this point we need to turn to the [character table](#) for the point group of methane. Character tables have many uses, most of which are not applicable to this course. As such, character tables have a lot of information that will not find necessary. Shown below are two different representations for the character table for the  $T_d$  point group. The first is the full character table while the second is an abbreviated character table that will be more useful for our purposes.

$T_d$	E	8 $C_3$	3 $C_2$	6 $S_4$	6 $\sigma_d$	Linear Functions	Quadratic Functions
$A_1$	+1	+1	+1	+1	+1		$x^2 + y^2 + z^2$
$A_2$	+1	+1	+1	-1	-1		
E	+2	-1	+2	0	0		$(2z^2 - x^2 - y^2, x^2 - y^2)$
$T_1$	+3	0	-1	+1	-1	$(R_x, R_y, R_z)$	
$T_2$	+3	0	-1	-1	+1	$(x, y, z)$	$(xy, xz, yz)$

Table 5.4.1.1: Full character table for the  $T_d$  point group.

You may notice that this point group has an improper rotation (even though we did not find it when assigning the point group) and that the mirror planes are designated as  $\sigma_d$ . While significant and useful, there is much more information here than we need. The abbreviated character table will give us all of the information that is necessary. The table has been contracted to include on the symmetry labels (beneath  $T_d$ ) and the corresponding orbitals that go with those labels. Note that some of the labels do not correspond to orbitals. The Orbitals column in the abbreviated character table corresponds to the Linear Functions column above. The  $(x, y, z)$  translates to the  $(p_x, p_y, p_z)$ . The s orbital is always assigned to the row that only contains values of +1 beneath the symmetry operations. That is not significant for our purposes, but worth mentioning.

$T_d$	Orbitals
$A_1$	s
$A_2$	
E	
$T_1$	
$T_2$	$(p_x, p_y, p_z)$

Table 5.4.1.2 Abbreviated character table for the  $T_d$  point group.

#### Exercise 5.4.1.4

What are the symmetry labels for the orbitals on carbon used to make methane.

**Answer**

$s - a_1$

$p_x - t_2$

$p_y - t_2$

$p_z - t_2$

These are now our generator functions for making the LGOs. Note that the convention is a switch to lower case when assigning symmetry to orbitals.

### Step 3 - Making the LGOs

Now that we have the generator functions, we can make the LGOs. This is done pictorially essentially asking the questions "What would the hydrogen 1s orbitals have to look like in order to interact in a constructive way with the carbon orbital in question?" To do this, it is very important to define the axes of your molecule before you start considering potential interactions. Due to the high symmetry of the molecule we will slightly break from convention in order to maximize orbital interactions. In group theory, the principle axis is always assigned as the z-axis, but in this case, we will assign the axes to the  $C_2$  axes in the molecule. To begin with, let's consider the s-orbital of carbon which is labeled  $a_1$ . The s-orbital is a sphere with the same sign for the wave function in all directions (Fig. 5.4.1.1).

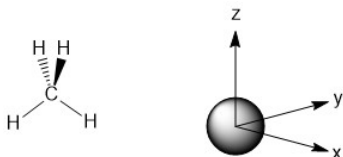


Figure 5.4.1.1: The  $a_1$  orbital for the carbon atom in methane.

Once the axes and the orbital on carbon are drawn we want to consider what the signs for the wave functions on each hydrogen atom would have to be in order to have constructive overlap. In this case, the symmetric  $a_1$  orbital of carbon will be able to interact with all of the hydrogen atoms in a constructive manner if they have the same sign for their wave functions (Fig. 5.4.1.2). This generates a LGO for the hydrogen atoms that has  $a_1$  symmetry. Although it is comprised of AOs from four hydrogen atoms, we now treat this as a single orbital for all of the hydrogen atoms hence the LGO designation.

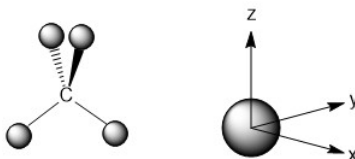


Figure 5.4.1.2 The LGO for the hydrogen atoms that has  $a_1$  symmetry with the carbon generator function depicted on the axes.

The p-orbitals for the carbon atom all have the same symmetry label ( $t_2$ ). One important consequence of this is that the orbitals are degenerate (equal in energy). While you would likely expect this for an isolated carbon atom, in compounds it is possible that the orbitals are no longer degenerate based on the shape of the molecule. The introduction of p-orbitals into our pictorial method adds one additional complication, p-orbitals are not symmetric and each lobe has a different sign for the wave function. In addition, p-orbitals also possess a nodal plane, a plane in which the probability of finding an electron is zero. In developing the LGO that matches with the  $p_z$ -orbital, these factors must be considered. For the  $p_z$ -orbital, the nodal plane is the xy plane. So, any hydrogen atoms that lie in the xy plane would be unable to interact with the carbon atom. That leads to an LGO that matches with the  $p_z$ -orbital as shown below (Fig. 5.4.1.3).

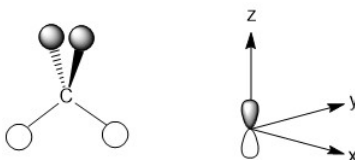


Figure 5.4.1.3 The LGO for the hydrogen atoms that has  $t_2$  symmetry with the carbon generator function depicted on the axes.

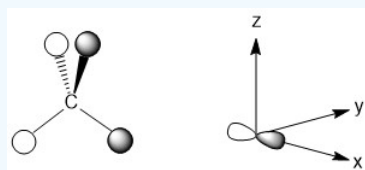
None of the hydrogen atoms are in the  $xy$  plane, so they are all capable of interacting. Notice that the change in sign of the carbon  $p_z$ -orbital impacts the way the orbitals on the hydrogen atoms are represented, but does not impact the ability of those hydrogen atoms to interact.

#### Exercise 5.4.1.5

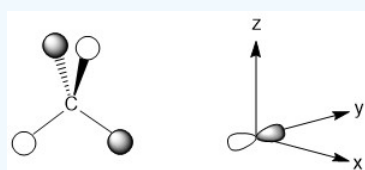
Using the remaining basis functions, sketch the rest of the LGOs for the hydrogen atoms in methane.

#### Answer

For the  $p_x$ -orbital, the nodal plane is the  $yz$  plane. Once again none of the hydrogen atoms are in this plane so they can all interact. The LGO is depicted below. Again, the  $p$ -orbital of carbon does not point directly at any of the hydrogen atoms, but they are still capable of interacting.



For the  $p_y$ -orbital, the nodal plane is the  $xz$  plane. Once again there are no hydrogen atoms that are unable to interact. This is a consequence of our decision to maximize the interactions possible in this highly symmetric molecule. The LGO is depicted below.



#### Step 4 - Constructing the MO diagram

The final step in the process is to construct the MO diagram for the molecule. Before we start constructing the MO diagram there is one final crucial question to be considered, are the atomic orbitals similar enough in energy to interact? We have actually done this to some extent already by ignoring the  $1s$  orbital on carbon as being too low in energy to interact. Compare the energy of the valence orbitals of the atoms that are interacting and if that difference is 15 eV or less, they are close enough in energy. Like many 'rules' you have learned in chemistry, the 15 eV difference is not absolute, but is a reasonable guideline. In the case of methane, all of the orbitals are close enough in energy to interact.

Atomic Number	Element	1s	2s	2p	3s	3p	4s	4p
1	H	-13.6						
2	He	-24.5						
3	Li		-5.5					
4	Be		-9.3					
5	B		-14.0	-8.3				
6	C		-19.5	-10.7				
7	N		-25.5	-13.1				
8	O		-32.4	-15.9				
9	F		-46.4	-18.7				
10	Ne		-48.5	-21.6				
11	Na				-5.2			

12	Mg				-7.7			
13	Al				-11.3	-6.0		
14	Si				-15.0	-7.8		
15	P				-18.7	-10.0		
16	S				-20.7	-12.0		
17	Cl				-25.3	-13.7		
18	Ar				-29.3	-15.9		
19	K						-4.3	
20	Ca						-6.1	
30	Zn						-9.4	
31	Ga						-12.6	-6.0
32	Ge						-15.6	-7.6
33	As						-17.6	-9.1
34	Se						-20.8	-11.0
35	Br						-24.1	-12.5
36	Kr						-27.5	-14.3

Table 5.4.1.3 Energy (eV) for valence orbitals of atoms from J.G. Verkade, *A Pictorial Approach to Molecular Bonding and Vibrations*, Springer-Verlag, New York, 1997, p. 69.

Building the MO diagram is similar to how it was done for diatomic molecules (Fig. 5.4.1.4). The central atom is placed on one side and the outer atoms, as a group, are placed on the other. The relative orbital energies are approximated based on the values in Table 5.4.1.3 in this case the hydrogen LGOs fall between the  $a_1$  and  $t_2$  orbitals for carbon. The hydrogen LGOs are depicted as being degenerate since they are all derived from hydrogen 1s orbitals. The molecular orbitals are drawn between the carbon and hydrogen atoms. The  $a_1$  atomic orbital on carbon has a matching  $a_1$  LGO from hydrogen and so these orbitals can combine to give a bonding MO and an antibonding MO. As the carbon  $a_1$  orbital is the lowest energy AO in this system it leads to the lowest energy MO. Recall that ABIMABTBIB, so it is not surprising that the lowest energy bonding orbital would give the highest energy antibonding orbital. Again, this is a rough guideline and not always the case. Dashed lines are often added to link orbitals with the same symmetry label. This is useful, but with more complex molecules can make the diagrams difficult to read. Finally, there are orbitals with  $t_2$  symmetry on both the carbon atom and from the hydrogen LGOs. Again, these can combine to give three degenerate bonding MOs and three degenerate antibonding MOs. The exact placement of these orbitals is not critical, however, the bonding orbitals should be lower in energy than the AO and LGOs and the antibonding should be higher. The eight valence electrons are added to the system using standard electron configuration principles (Aufbau, Pauli exclusion and Hund's rule).

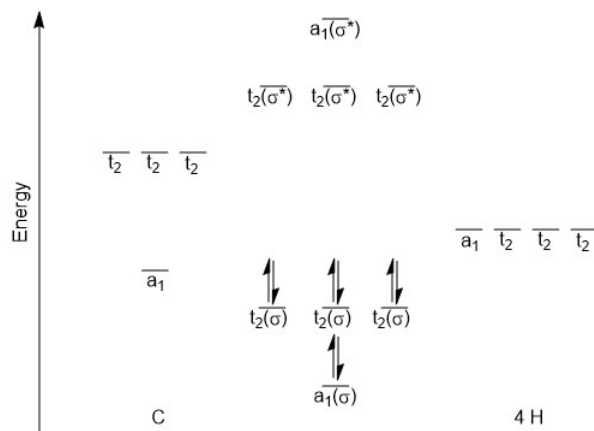


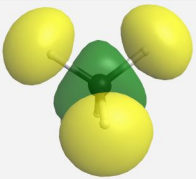
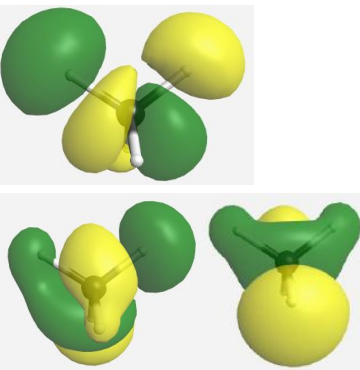
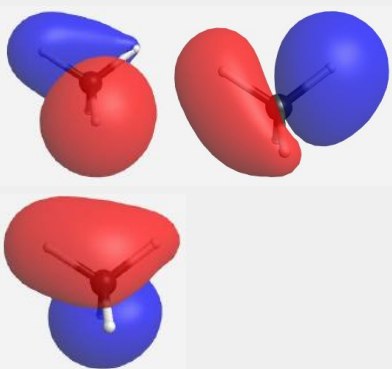
Figure 5.4.1.4 The MO diagram for  $\text{CH}_4$ .

For this system the bond order =  $\frac{8-0}{2} = 4$ . Notice that while this agrees with your original structure, the MO diagram shows something very different. The lowest energy bonding MO ( $a_1$  which is depicted in c) involves all five atoms sharing two electrons, not the carbon atom and one hydrogen atom sharing. The same would be true for the bonding  $t_2$  orbitals, more than 2 atoms are involved. In addition it would be worth noting that the HOMO would be a  $t_2$  orbital (remember they are degenerate so a specific one can not be distinguished) and the LUMO would be a  $t_2$  antibonding orbital.

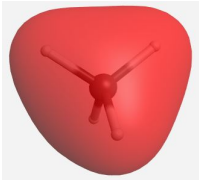
### How did we do?

Our pictorial method is qualitative but does a reasonable job of predicting the MO diagram. A more quantitative method would be to use computational methods to derive a more accurate MO diagram for this methane. The orbitals and their energies as calculated by [WebMO](#) are presented below (Table 5.4.1.4). Overall our MO diagram looks pretty good. We see that the bonding  $a_1$  orbital is approximately 5 eV lower in energy than the carbon  $a_1$  orbital. The  $a_1^*$  orbital is almost 40 eV higher in energy than the  $a_1$  LGO. This is an excellent representation of the ABIMABTBIB principle. A similar trend is noted for the  $t_2$  orbitals in which the bonding MOs are approximately 1.7 eV lower in energy than the LGOs and the  $t_2^*$  orbitals are approximately 14 eV higher in energy than the carbon 2p orbitals.

**(Table 5.4.1.4).** The MOs for  $\text{CH}_4$  as calculated and displayed by [WebMO](#). The data for  $\text{CF}_4$  was imported into [WebMO](#) from the [NIST Webbook](#) as a computed 3-D structure and calculations were performed using B3LYP-6-31G(d). The same perspective of the molecule is used throughout.

Symmetry Label	Orbital(s)	Energy (eV)
$a_1^*$		26.479
$t_2^*$		3.649
$t_2$		-15.334



$a_1$		-24.545
-------	---	---------

[5.4.1: Ligand Group Orbitals and Generator Functions](#) is shared under a [not declared](#) license and was authored, remixed, and/or curated by LibreTexts.

## SECTION OVERVIEW

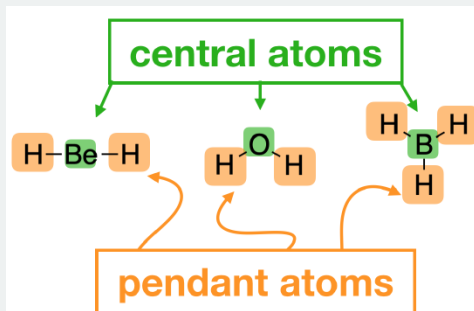
### 5.4.2: Polyatomic Molecules

We can extend the method we used for diatomic molecules to draw the molecular orbitals of more complicated, polyatomic molecules (molecules with more than two atoms). To combine several different atoms in a molecular orbital diagram, we will group orbitals from different atoms into sets that match the symmetry of a central atom. These **group orbitals** are also referred to as **symmetry adapted linear combinations (SALCs)**. We'll use a stepwise approach to do this as summarized below.

#### 📌 Symmetry adapted linear combinations (SALCs)

We need SALCs (aka group orbitals) to draw molecular orbital (MO) diagrams of *polyatomic* molecules. SALCs are groups of orbitals on **pendant atoms**. These groups of orbitals much match the symmetry of valence orbitals on the **central atom** in order to create a productive interaction. When we combine SALCs with the atomic orbitals on the central atom, we can generate an MO diagram that gives us information about the molecule's bonding and electronic states.

Below is a set of steps you can follow to find SALCs and draw an MO Diagram. Each step will be illustrated in detail through the examples in the subsections that follow this page.



- Find the **point group** of the molecule and assign Cartesian coordinates so that  $z$  is the principal axis.  
*Sometimes we can simplify things by looking only at the point group of the relevant orbitals.\* Only simplify when instructed to do so.*
- Identify and count the pendant atoms' valence orbitals.  
*Is there more than 1 type for each atom (ex. just  $s$ , or  $s$  and  $p$ ?) We expect 1 SALC for each ligand orbital.*
- Generate a **reducible representation ( $\Gamma$ )** for the group of pendant atom orbitals using the appropriate character table.  
*You have to do this for each set of orbital types. If you only have  $s$  orbitals for each ligand, you only need to generate 1 reducible representation. If you have  $p$  orbitals, you would generate additional  $\Gamma$ 's for  $p_x$ ,  $p_y$ , and  $p_z$ .*
- Break the  $\Gamma$  into its component **irreducible representations** from the character table. Note the symmetry of each irreducible representation, its associated orbitals, and their degeneracy.
- If you are asked to sketch the shapes of SALCs, determine what they "look like" using one of the following strategies.  
  - Shortcut:** if the reducible representations are listed with  $s$ ,  $p$ , or  $d$  orbitals in the character table, just draw them (... and skip steps b-c)
  - Systematic (Projection Operator) method:** Draw an expanded character table and draw your molecule with each ligand identified by letters or numbers ( $a, b, c...$  or  $i, j, k...$  or  $1, 2, 3...$ ) Determine where each pendant atom/orbital ends up under each of the operations of your expanded table. Project the values for each irreducible representation onto the chart you created and then add up the values. Positive and negative values are opposite signed orbitals.
- Draw the MO diagram by combining SALCs with AO's of like symmetry. When drawing SALC energy levels, remember that the more nodal planes in your SALC orbital drawing, the higher the energy for that SALC orbital.

\* When we are focused on orbitals, as in the case for finding group orbitals and drawing molecular orbital diagrams, the symmetry of the orbitals is what we are interested in. In the case of high-symmetry point groups, like  $D_{\infty h}$  and  $C_{\infty v}$ , even though the molecule may have a  $C_{\infty}$  axis, the orbitals do not necessarily retain this symmetry element. For example, the  $p_x$  orbital would not have a  $C_{\infty}$  axis, but rather a  $C_2$  axis. It is sufficient and useful to substitute  $D_{2h}$  for  $D_{\infty h}$  and  $C_{2v}$  for  $C_{\infty v}$  to simplify the problem.

#### 5.4.2.1: Bifluoride anion

5.4.2.2: Carbon Dioxide

5.4.2.3: H<sub>2</sub>O

5.4.2.4: NH<sub>3</sub>

---

5.4.2: Polyatomic Molecules is shared under a [CC BY-SA 4.0](#) license and was authored, remixed, and/or curated by LibreTexts.

## 5.4.2.1: Bifluoride anion

### Finding SALCs and drawing the MO diagram for $[\text{F-H-F}]^-$

The linear anion  $[\text{F-H-F}]^-$  is a good place to start as an example to illustrate the process of generating pendant atom SALCs and then constructing a molecular orbital diagram for a polyatomic molecule. We will proceed using the steps outlined on the [previous page](#) for generating SALCs and a molecular orbital diagram.

#### Step 1. Find the point group of the molecule and assign Cartesian coordinates so that $z$ is the principal axis.

We begin by assigning the appropriate point group for this molecule:  $D_{\infty h}$  (Figure 5.4.2.1.1). As mentioned in the [previous page](#), it is useful to substitute  $D_{2h}$  for  $D_{\infty h}$  when generating SALCs and molecular orbital diagrams. The  $z$  axis is assigned to be colinear with the principal axis, and in this case is the same as the  $C_{\infty}$  axis (Figure 5.4.2.1.1).

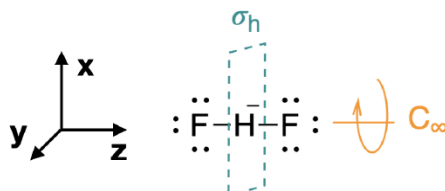


Figure 5.4.2.1.1: The  $[\text{FHF}]^-$  anion belongs to the  $D_{\infty h}$  point group. (CC-BY-NC-SA; Kathryn Haas)

#### Step 2. Identify and count the pendant atoms' valence orbitals.

The next step is to identify the valence orbitals on the pendant F atoms that will form SALCs. In most cases, you should consider all of the valence orbitals. In this case, each of the fluorine atoms has four valence orbitals ( $2s$ ,  $2p_x$ ,  $2p_y$ , and  $2p_z$ ). From these eight fluorine valence orbitals, we should expect eight group orbitals (SALCs).

#### 3. - 5. Generate SALCS (shortcut)

To draw these SALCs for this molecule is rather simple, and we don't need to follow all the steps of finding the  $\Gamma$ 's and reducing them. Rather, you can proceed as if you are creating bonding and antibonding molecular orbitals between the two F atoms, except that the F orbitals are separated by the H atom. Approximate sketches of the eight SALCs from F valence orbitals are shown in Figure 5.4.2.1.2

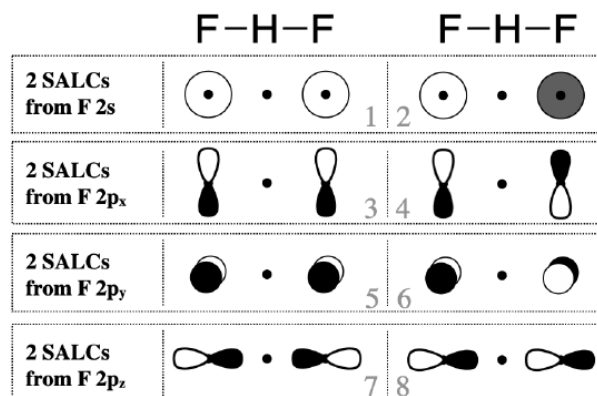


Figure 5.4.2.1.2: Eight SALCs from the valence orbitals of two fluorine atoms. (CC-BY-NC-SA; Kathryn Haas)

#### 6. Draw the MO diagram by combining SALCs with AO's of like symmetry.

SALCs can productively interact with the central atom only when symmetry is compatible. Just some of the groups of orbitals in Figure 5.4.2.1.2 possess appropriate symmetry to combine with the hydrogen atom valence orbital (the H  $1s$ ). In this simple case, you can decide whether orbitals have compatible symmetry by visually inspecting the shapes of the group orbitals. The F  $2p_y$  and  $2p_x$  orbitals do not have appropriate symmetry to bond to the H  $1s$  orbital because the nodes of these orbitals run through the center of the H  $1s$  orbital, thus we can eliminate all SALCs composed from F  $2p_x$  and  $2p_y$  (these are SALCs numbered 3-6 in Figure 5.4.2.1.2). On the other hand, the F  $2s$  and  $2p_z$  orbitals individually do have appropriate shape and direction in space for productive interaction with an H  $1s$  orbital. However only SALCs where the *entire group* has appropriate symmetry will combine

with H  $1s$  to produce bonding or antibonding molecular orbitals. Only the SALCs labeled with numbers 1 and 7 can combine with an  $s$  orbital in the center of the group. The ways in which these SALCs are able to combine with H  $1s$  are illustrated in Figure 5.4.2.1.3

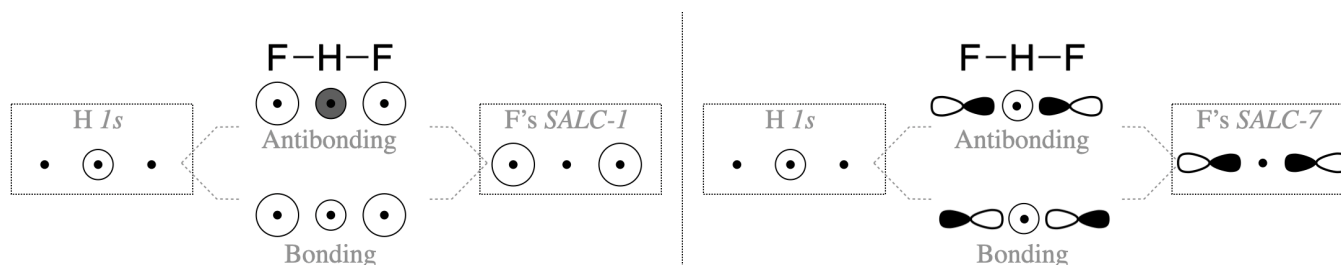


Figure 5.4.2.1.3: Combinations of a central H  $1s$  orbital with the group orbitals, SALC-1 and SALC-7 from Figure 5.4.2.1.2, to create bonding and antibonding interactions. (CC-BY-NC-SA; Kathryn Haas)

Before we assume that both SALC-1 and SALC-7 will combine with the H  $1s$  orbital, we must consider the energies of all atomic orbitals. The F  $2p_z$  orbital has a potential energy of  $-18.7$  eV (see Table 5.3.1). This is a good match for the H  $1s$  orbital ( $-13.6$  eV). However, the F  $2s$  orbital has a much lower energy of  $-46.37$  eV and would have weak interaction with the H  $1s$ .

The molecular orbital diagram for  $[\text{F-H-F}]^-$  is shown in Figure 5.4.2.1.4. Notice that all atomic orbitals, group orbitals (SALCs), and molecular orbitals in Figure 5.4.2.1.4 are assigned a symmetry label that corresponds to each element's symmetry under the  $D_{2h}$  point group. The molecular orbital labels correspond to **lower-case Mulliken Labels** of individual reducible representations from the  $D_{2h}$  character table. Upper-case symbols are used to indicate symmetry and irreducible representations, while lower-case symbols are used to indicate the identity of an orbital with that symmetry. The labeling methods described for simple diatomic linear molecules ( $\sigma, \pi$ ) are not sufficient to indicate the more complex symmetries of the molecular orbitals in polyatomic molecules. The use of lower-case Mulliken symbols is the most rigorous way to label the orbitals. Refer to your instructor for how you should label orbitals for any graded work.

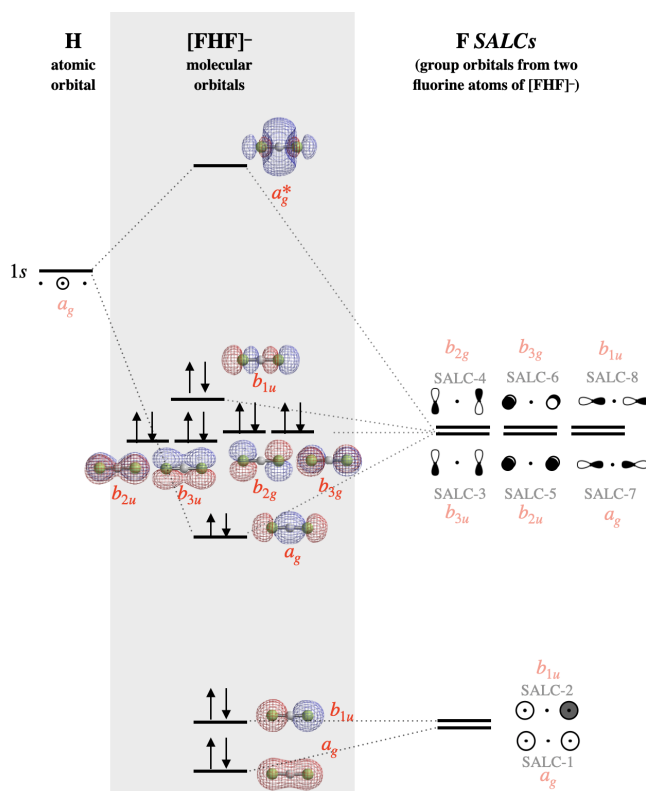
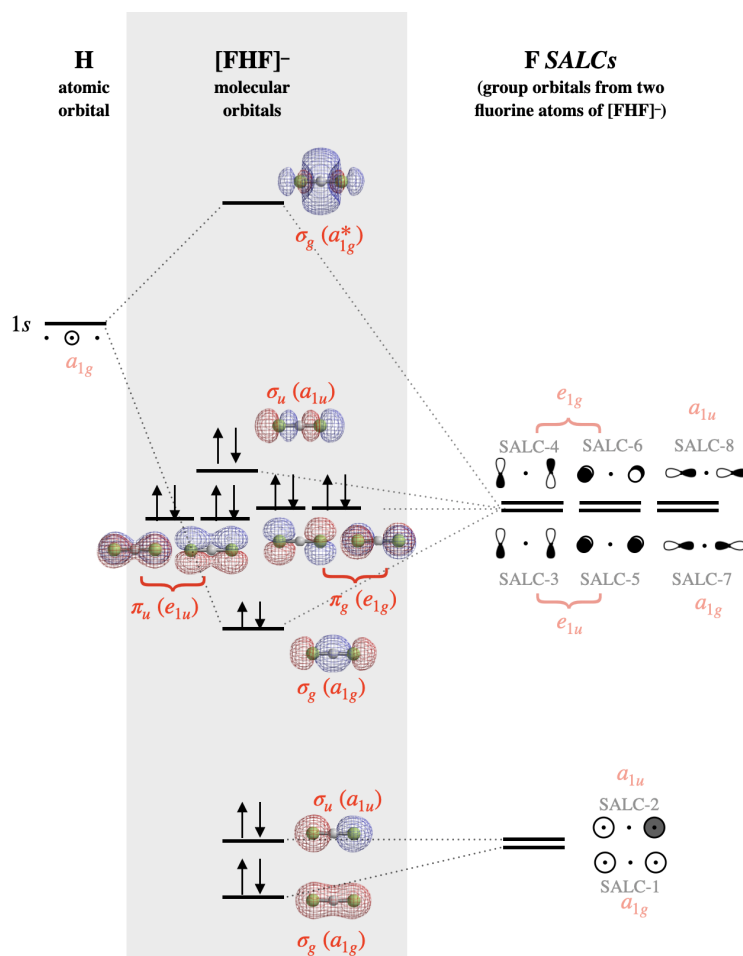


Figure 5.4.2.1.4: The molecular orbital diagram for  $[\text{F-H-F}]^-$ . The molecular orbital surfaces and relative energy levels were calculated using Spartan software. SALCs are labeled according to numbers assigned in Figure 5.4.2.1.2. The symmetry of each SALC and orbital under the  $D_{2h}$  point group is shown in red font. (CC-BY-NC-SA; Kathryn Haas)

**Click here for a version of Figure 5.4.2.1.4 using  $D_{\infty h}$  labeling:**

For high-symmetry groups, a shortcut is to use a lower-symmetry group that maintains the critical symmetry elements. In the case of the  $D_{\infty h}$  point group, it is often sufficient to use the approximation of the  $D_{2h}$  point group and character table. This is the same MO diagram as shown above, but using the symmetry labels appropriate for the  $D_{2h}$  approximation.



Alternate Figure 5.4.2.1.4: The molecular orbital diagram for  $[\text{F-H-F}]^-$ . The molecular orbital surfaces and relative energy levels were calculated using Spartan software. SALCs are labeled according to numbers assigned in Figure 5.4.2.1.2. The symmetry of each SALC and orbital under the  $D_{2h}$  point group is shown in red font. (CC-BY-NC-SA; Kathryn Haas)

### Constructing the MO diagram

After identifying the atomic orbitals and constructing SALCs, place the atomic orbitals of H on one side of the diagram and all SALCs from F on the other side. Molecular orbitals are in the center.

The lowest-energy fluorine SALCs will be those composed of the lowest-energy atomic orbitals of fluorine; these would be SALC-1 ( $a_{1g}$ ) and SALC-2 ( $a_{1u}$ ) that are constructed from fluorine  $s$  atomic orbitals. Of these two orbitals, the one with zero nodes would be slightly lower in energy than the one with one node. When these two orbitals form molecular orbitals, the completely symmetric SALC-1 will be mostly non-bonding with slight bonding character from minor combination with the hydrogen  $1s$  orbital. SALC-2, however, is symmetrically incompatible with hydrogen  $1s$  and will be a truly non-bonding orbital distributed over both F atoms.

The six SALCs constructed of fluorine  $p$  orbitals will have higher energy since the fluorine  $p$  atomic orbitals are higher in energy than the  $s$  orbitals (SALC-3 through SALC-8). Again, we expect SALCs with more nodes (SALC-4, -6, -8) to have slightly higher energy than those with fewer nodes (SALC-3, -5, -7). SALC-7 will form a bonding and antibonding interaction with the hydrogen  $1s$  orbital. All other SALCs are truly non-bonding, but are non-degenerate non-bonding orbitals.

In bifluoride, there is an important distinction between the Lewis structure and molecular orbital description of lone pairs. In Lewis theory, the lone pairs are localized to individual fluorine atoms, while in the molecular orbital description each lone pair is distributed over both fluorine atoms at once (see surface depiction of each molecular orbital in Figure 5.4.2.1.4).

5.4.2.1: Bifluoride anion is shared under a CC BY-SA 4.0 license and was authored, remixed, and/or curated by LibreTexts.

- 5.4.1: Bifluoride anion is licensed CC BY-SA 4.0.

## 5.4.2.2: Carbon Dioxide

### Construct SALCs and the molecular orbital diagram for CO<sub>2</sub>.

Carbon dioxide is another linear molecule. This example is slightly more complex than the previous example of the bifluoride anion. While bifluoride had only one valence orbital to consider in its central H atom (the 1s orbital), carbon dioxide has a larger central atom, and thus more valence orbitals that will interact with SALCs.

#### Preliminary Steps

**Step 1. Find the point group of the molecule and assign Cartesian coordinates so that z is the principal axis.**

The CO<sub>2</sub> molecule is linear and its point group is  $D_{\infty h}$ . The z axis is collinear with the  $C_{\infty}$  axis. We will use the  $D_{2h}$  point group as a substitute since the orbital symmetries are retained in the  $D_{2h}$  point group.

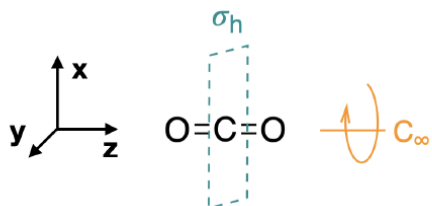


Figure 5.4.2.2.1: CO<sub>2</sub> belongs to the  $D_{\infty h}$  point group. (CC-BY-NC-SA; Kathryn Haas)

**Step 2. Identify and count the pendant atoms' valence orbitals.**

Each of the two pendant oxygen atoms has four valence orbitals;  $2s$ ,  $2p_x$ ,  $2p_y$ , and  $2p_z$ . Thus, we can expect a total of eight SALCs.

#### Generate SALCs

The SALCs for CO<sub>2</sub> are identical in shape and symmetry to those described in the previous example for the [bifluoride anion](#). But instead of cutting to the shortcut, we will systematically derive the SALCs here to demonstrate the process.

**Step 3. Generate the  $\Gamma$ 's**

Use the [D<sub>2h</sub> character table](#) to generate four reducible representations ( $\Gamma$ 's); one for each of the four types of pendant atom orbitals ( $s$ ,  $p_x$ ,  $p_y$ ,  $p_z$ ). For each  $s$  orbital, assign a value of 1 if it remains in place during the operation or zero if it moves out of its original place. For each  $p$  orbital, assign 1 if there is no change, -1 if it remains in place but is inverted, and 0 if it moves out of its original position. The four  $\Gamma$ 's are given below:

$D_{2h}$	$E$	$C_2(z)$	$C_2(y)$	$C_2(x)$	$i$	$\sigma(xy)$	$\sigma(xz)$	$\sigma(yz)$
$\Gamma_{2s}$	2	2	0	0	0	0	2	2
$\Gamma_{2p_x}$	2	-2	0	0	0	0	2	-2
$\Gamma_{2p_y}$	2	-2	0	0	0	0	-2	2
$\Gamma_{2p_z}$	2	2	0	0	0	0	2	2

**Step 4. Break  $\Gamma$ 's into irreducible representations for individual SALCs**

Reduce each  $\Gamma$  into its component irreducible representations. There are two strategies that can be used to do this. The quick and easy way is to do it "by inspection", but this only works well for simple cases. The other is by using the systematic approach for breaking a  $\Gamma$  into reducible representations [described previously in section 4.4.2](#) using the following formula:

$$\# \text{ of } i = \frac{1}{h} \sum (\# \text{ of operations in class}) \times (\chi_{\Gamma}) \times (\chi_i) \quad (5.4.2.2.1)$$

In other words, the number of irreducible representations of type  $i$  is equal to the sum of the number of operations in the class  $\times$  the character of the  $\Gamma_{modes}$   $\times$  the character of  $i$ , and that sum is divided by the order of the group ( $h$ ).

Using either approach results in the following eight irreducible representations ( $2A_g + 2B_{1u} + B_{2g} + B_{3u} + B_{3g} + B_{2u}$ ):



D <sub>2h</sub>	<i>E</i>	<i>C</i> <sub>2</sub> ( <i>z</i> )	<i>C</i> <sub>2</sub> ( <i>y</i> )	<i>C</i> <sub>2</sub> ( <i>x</i> )	<i>i</i>	σ( <i>xy</i> )	σ( <i>xz</i> )	σ( <i>yz</i> )	
Γ <sub>2s</sub> = A <sub>g</sub> + B <sub>1u</sub>	Γ <sub>2s</sub>	<b>2</b>	<b>2</b>	<b>0</b>	<b>0</b>	<b>0</b>	<b>0</b>	<b>2</b>	<b>2</b>
	<i>A<sub>g</sub></i>	1	1	1	1	1	1	1	1
	<i>B<sub>1u</sub></i>	1	1	−1	−1	−1	−1	1	1
Γ <sub>2p<sub>x</sub></sub> = B <sub>2g</sub> + B <sub>3u</sub>	Γ <sub>2p<sub>x</sub></sub>	<b>2</b>	<b>−2</b>	<b>0</b>	<b>0</b>	<b>0</b>	<b>0</b>	<b>2</b>	<b>−2</b>
	<i>B<sub>2g</sub></i>	1	−1	1	−1	1	−1	1	−1
	<i>B<sub>3u</sub></i>	1	−1	−1	1	−1	1	1	−1
Γ <sub>2p<sub>y</sub></sub> = B <sub>3g</sub> + B <sub>2u</sub>	Γ <sub>2p<sub>y</sub></sub>	<b>2</b>	<b>−2</b>	<b>0</b>	<b>0</b>	<b>0</b>	<b>0</b>	<b>−2</b>	<b>2</b>
	<i>B<sub>3g</sub></i>	1	−1	−1	1	1	−1	−1	1
	<i>B<sub>2u</sub></i>	1	−1	1	−1	−1	1	−1	1
Γ <sub>2p<sub>z</sub></sub> = A <sub>g</sub> + B <sub>1u</sub>	Γ <sub>2p<sub>z</sub></sub>	<b>2</b>	<b>2</b>	<b>0</b>	<b>0</b>	<b>0</b>	<b>0</b>	<b>2</b>	<b>2</b>
	<i>A<sub>g</sub></i>	1	1	1	1	1	1	1	1
	<i>B<sub>1u</sub></i>	1	1	−1	−1	−1	−1	1	1

### Step 5. Sketch the SALCs

From the systematic process above, you have found the symmetries (the irreducible representations) of all eight SALCs under the  $D_{2h}$  point group. To sketch the SALC that corresponds to each irreducible representation, again we use the [D<sub>2h</sub> character table](#), and specifically the functions listed on the right side columns of the table.

**Two  $A_g$  SALCs (one from  $s$  and one from  $p_z$ ):** The  $A_g$  SALCs are each singly degenerate and symmetric with respect to both the principal axis ( $z$ ) and the inversion center ( $i$ ) (based on its [Mulliken Label](#)). We can look at the functions in the  $D_{2h}$  character table that correspond to  $A_g$  and see that it is completely symmetric under the group (because the combination of  $x^2, y^2, z^2$  shows that it is totally symmetric). This would be the same symmetry as an  $s$  orbital on the central atom. From this information, we know that these SALCs must have symmetry compatible with an  $s$  orbital on the central atom, and we can draw the two  $A_g$  SALCs shown in Figure 5.4.2.2.2

**Two  $B_{1u}$  SALCs (one from  $s$  and one from  $p_z$ ):** The [Mulliken Label](#) tells us that the  $B_{1u}$  SALCs are each antisymmetric with respect to both the principal axis and the inversion center. The function,  $z$ , appearing with  $B_{1u}$  in the character table tells us that these SALCs have the same symmetry as the  $z$  axis, or a  $p_z$  orbital on the central atom. From this information, we know that these two SALCs should be compatible with a  $p_z$  orbital on the central atom, and we can draw the two  $B_{1u}$  SALCs shown in Figure 5.4.2.2.2

All other SALCs shown below are derived using a strategy similar to the one in the two cases described above.

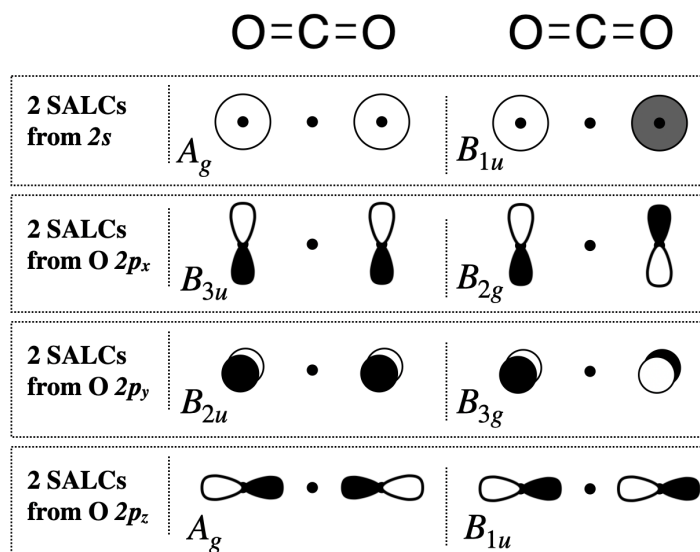


Figure 5.4.2.2.2: SALCs from the valence orbitals of oxygen atoms in CO<sub>2</sub>. (CC-BY-NC-SA; Kathryn Haas)

### Draw the MO diagram for CO<sub>2</sub>

#### Step 6. Combine SALCs with AO's of like symmetry.

First we identify the valence orbitals on carbon: there are four including  $2s$ ,  $2p_x$ ,  $2p_y$ , and  $2p_z$ . Now we identify the symmetry of each using the  $D_{2h}$  character table. The symmetry of a central  $s$  orbital corresponds to the combination of functions  $x^2$ ,  $y^2$ , and  $z^2$  in the character table; this is  $A_g$ . The  $p_z$  orbital corresponds to the symmetry of the linear function  $z$  in the character table; this is  $B_{1u}$ . And so on... The symmetries of the C valence orbitals are listed below.

$$\begin{aligned} 2s &= A_g \\ 2p_x &= B_{3u} \\ 2p_y &= B_{2u} \\ 2p_z &= B_{1u} \end{aligned}$$

Now that we have identified the symmetries of the eight oxygen SALCs and the four valence orbitals on carbon, we know which atomic orbitals and SALCs may combine based on compatible symmetries. We also need to know the relative [orbital energy](#) levels so that we can predict the relative strength of orbital interactions. The [orbital ionization energies](#) are listed in [Section 5.3](#).

With knowledge of both orbital symmetries and energies, we can construct the molecular orbital diagram. The carbon atom goes on one side of the diagram while the oxygen SALCs are drawn on the opposite side. Molecular orbitals are drawn in the center column of the diagram:

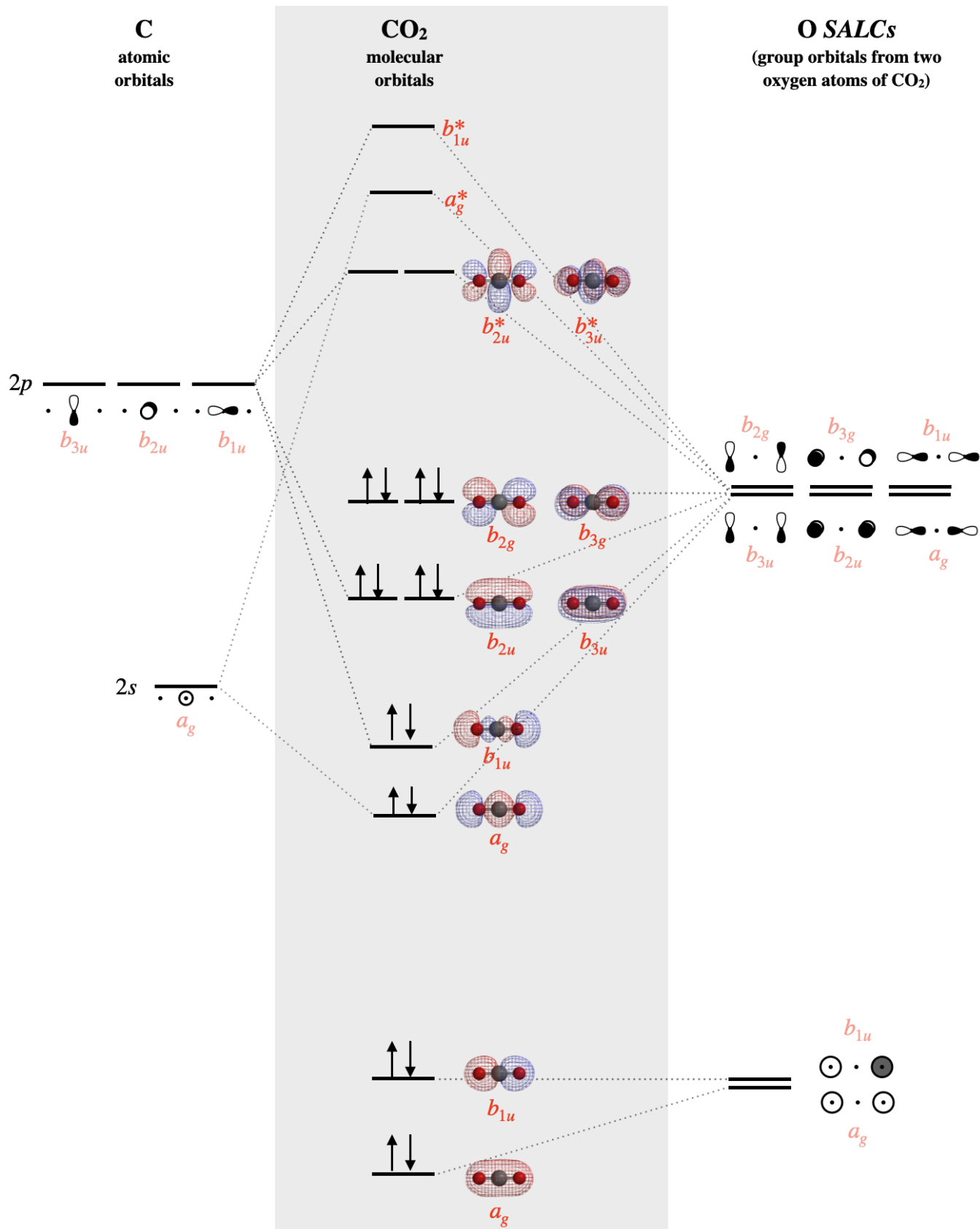


Figure 5.4.2.2.3: Molecular orbital diagram for carbon dioxide. (CC-BY-NC-SA; Kathryn Haas)

The SALCs on the right side of the diagram above are constructed from groups of either the  $2s$  atomic orbitals of oxygen, or the  $2p$  atomic orbitals of oxygen. Each SALC will combine with the atomic orbitals of carbon that have compatible symmetry; but the strength of the interaction depends on their relative energies. The individual valence atomic orbitals of oxygen have energies of  $-32.36\text{eV}$  ( $2s$ ) and  $-15.87\text{eV}$  ( $2p$ ), while the valence orbitals of carbon have energies of  $-19.47\text{eV}$  ( $2s$ ) and  $-10.66\text{eV}$  ( $2p$ ). The  $2s$  orbitals of the oxygen are far lower in energy ( $-32.36\text{eV}$ ) than all other valence orbitals, and so we should expect that molecular orbitals that are constructed from these oxygen  $2s$  will be mostly non-bonding. These mostly non-bonding orbitals are the  $a_{1g}$  and  $b_{1g}$  orbitals shown at the bottom of Figure 5.4.2.2.3 The  $a_g$  orbital is lower in energy than the  $b_{1u}$  due to slight mixing with other orbitals of  $a_g$  symmetry.

The bonding orbitals of  $\text{CO}_2$  include two *sigma* molecular orbitals of  $a_g$  and  $b_{1u}$  symmetry and two  $\pi$  molecular orbitals of  $b_{2u}$  and  $b_{3u}$  symmetry. Each of these bonding molecular orbitals possesses a higher-energy antibonding partner. The  $b_{2g}$  and  $b_{3g}$  SALCs that are formed from oxygen  $2p_x$  and  $2p_y$  orbitals have no compatible match with carbon valence orbitals; thus they form two  $b_{2g}$  and  $b_{3g}$  molecular orbitals, which are truly non-bonding and mostly oxygen in character. Still, notice that each orbital is spread across both oxygen atoms at once, and again we see that each non-bonding electron pair in the HOMO is very different in molecular orbital theory compared to Lewis theory. Each non-bonding pair is distributed over both oxygen atoms at once in molecular orbital theory, while in Lewis theory each lone pair is isolated to one atom or to localized bonds attached to that atom.

---

This page titled 5.4.2.2: Carbon Dioxide is shared under a CC BY-SA 4.0 license and was authored, remixed, and/or curated by Kathryn Haas.

- 5.4.2: Carbon Dioxide by Kathryn Haas is licensed CC BY-SA 4.0.

### 5.4.2.3: H<sub>2</sub>O

#### Construct SALCs and the molecular orbital diagram for H<sub>2</sub>O.

This is the first example so far that is not a linear molecule. Water is a bent molecule, and so it is important to remember that interactions of pendant ligands are dependent on their positions in space. You should consider the positions of the three atoms in water to be essentially fixed in relation to each other. The process for constructing the molecular orbital diagram *for a non-linear molecule*, like water, is similar to the process for linear molecules. We will walk through the steps below to construct the molecular orbital diagram of water.

#### Preliminary Steps

**Step 1. Find the point group of the molecule and assign Cartesian coordinates so that z is the principal axis.**

The H<sub>2</sub>O molecule is bent and its point group is  $C_{2v}$ . The z axis is collinear with the principal axis, the  $C_2$  axis. There is no need to simplify this problem, as we had done for previous examples. The  $C_{2v}$  point group is simple enough.

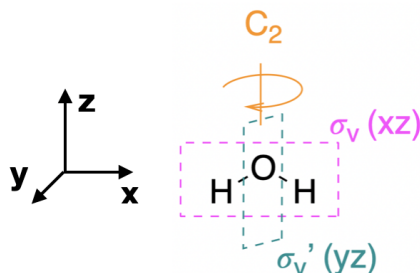


Figure 5.4.2.3.1: The water molecular is in the  $C_{2v}$  point group. (CC-BY-NC-SA; Kathryn Haas)

**Step 2. Identify and count the pendant atoms' valence orbitals.**

Each of the two pendant hydrogen atoms has one valence orbital, the  $1s$ . Thus, we can expect a total of two SALCs from these two atoms.

#### Generate SALCs

The SALCs for H<sub>2</sub>O are quite simple, yet we will systematically derive the SALCs here to demonstrate the process.

**Step 3. Generate the  $\Gamma$ 's**

Use the  $C_{2v}$  character table to generate one reducible representation ( $\Gamma$ ); in this case we need only one  $\Gamma$  because there is only one type of valence orbital (the  $1s$ ). For each  $s$  orbital, assign a value of 1 if it remains in place during the operation or zero if it moves out of its original place. The  $\Gamma$  is given below:

$C_{2v}$	$E$	$C_2$	$\sigma_v(xz)$	$\sigma_v'(yz)$
$\Gamma_{1s}$	2	0	2	0

**Step 4. Break  $\Gamma$ 's into irreducible representations for individual SALCs**

Reduce each  $\Gamma$  into its component irreducible representations. Using either of the processes described previously, we find that the  $\Gamma$  reduces to the two irreducible representations  $A_1$  and  $B_1$  under the  $C_{2v}$  point group.

$C_{2v}$	$E$	$C_2$	$\sigma_v(xz)$	$\sigma_v'(yz)$
$\Gamma_{1s}$	<b>2</b>	<b>0</b>	<b>2</b>	<b>0</b>
$A_1$	1	1	1	1
$B_1$	1	-1	1	-1

**Step 5. Sketch the SALCs**

From the systematic process above, you have found the symmetries (the irreducible representations) of both SALCs under the  $C_{2v}$  point group. To sketch the SALC that corresponds to each irreducible representation, again we use the  $C_{2v}$  character table, and specifically the functions listed on the right side columns of the table.

**One  $A_1$  SALC:** The  $A_1$  SALC is singly degenerate and symmetric with respect to both the principle axis ( $z$ ) and the inversion center ( $i$ ) (based on its [Mulliken Label](#)). We can look at the functions in the  $C_{2v}$  character table that correspond to  $A_1$  and see that it is completely symmetric under the group (because the combination of  $x^2, y^2, z^2$  shows that it is totally symmetric). This would be the same symmetry as an  $s$  orbital on the central oxygen atom. From this information, we know that this SALC must have symmetry compatible with an  $s$  orbital on the central atom. We can also see from the character table that the  $z$  axis, and thus a  $p_z$  orbital on oxygen, also possesses  $A_1$  symmetry. This tells us that in addition to being compatible with the oxygen  $s$  orbital, it should also be compatible with the oxygen  $p_z$  orbital. From this information we can draw the  $A_1$  SALC shown in Figure 5.4.2.3.2. *If it is not obvious how the  $A_1$  sketch in Fig. 5.4.2.3.2 is compatible with the  $s$  and  $p_z$  orbitals of oxygen, inspect the drawings corresponding to molecular orbitals  $2a_1$  and  $3a_1$  in Fig. 5.4.2.3.3*

**One  $B_1$  SALC:** The [Mulliken Label](#) tells us that the  $B_1$  SALC is singly degenerate and antisymmetric with respect to both the principal axis and the inversion center. The function,  $x$ , appearing with  $B_1$  in the character table tells us that this SALC has the same symmetry as the  $x$  axis, or a  $p_x$  orbital on the central oxygen atom. From this information, we know that this SALC should be compatible with a  $p_x$  orbital on the central atom, and we can draw the  $B_1$  SALCs shown in Figure 5.4.2.3.2. *If it is not obvious how the  $B_1$  sketch in Fig. 5.4.2.3.2 is compatible with the  $p_x$  orbital of oxygen, inspect the drawing corresponding to molecular orbital  $1b_1$  in Fig. 5.4.2.3.3*

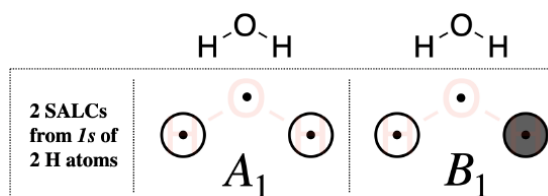


Figure 5.4.2.3.2: Sketch of the  $A_1$  and  $B_1$  hydrogen SALCs of water. (CC-BY-NC-SA; Kathryn Haas)

Not convinced about the sketches of these SALCs? You can convince yourself by putting them to the test. Try the exercise below.

#### ? Exercise 5.4.2.3.1

Perform all operations of the  $C_{2v}$  point group on the two sketches of H SALCs shown in Figure 5.4.2.3.2 and convince yourself that each sketch does possess the  $A_1$  and  $B_1$  symmetries assigned to them, respectively, under the  $C_{2v}$  point group.

#### Answer

Add texts here. Do not delete this text first.

### Draw the MO diagram for $H_2O$

#### Step 6. Combine SALCs with AO's of like symmetry.

First we must identify the valence orbitals on the central oxygen: there are four including  $2s$ ,  $2p_x$ ,  $2p_y$ , and  $2p_z$ . Now we identify the symmetry of each using the  $C_{2v}$  character table. The symmetry of a central  $2s$  orbital corresponds to the combination of functions  $x^2, y^2$ , and  $z^2$  in the character table; this is  $A_1$ . The  $p_z$  orbital also corresponds to  $A_1$ . And so on... The symmetries of oxygen valence orbitals are listed below.

$$\begin{aligned} 2s &= A_1 \\ 2p_x &= B_1 \\ 2p_y &= B_2 \\ 2p_z &= A_1 \end{aligned}$$

Now that we have identified the symmetries of the two hydrogen SALCs and the four valence orbitals on oxygen, we know which atomic orbitals and SALCs may combine based on compatible symmetries. We also need to know the relative [orbital energy](#) levels so that we can predict the relative strength of orbital interactions. The [orbital ionization energies are listed in Section 5.3.1](#).

With knowledge of both orbital symmetries and energies, we can construct the molecular orbital diagram. The valence orbitals of oxygen go on one side of the diagram while the hydrogen group orbitals are drawn on the opposite side. Molecular orbitals are drawn in the center column of the diagram, as shown in Figure 5.4.2.3.3

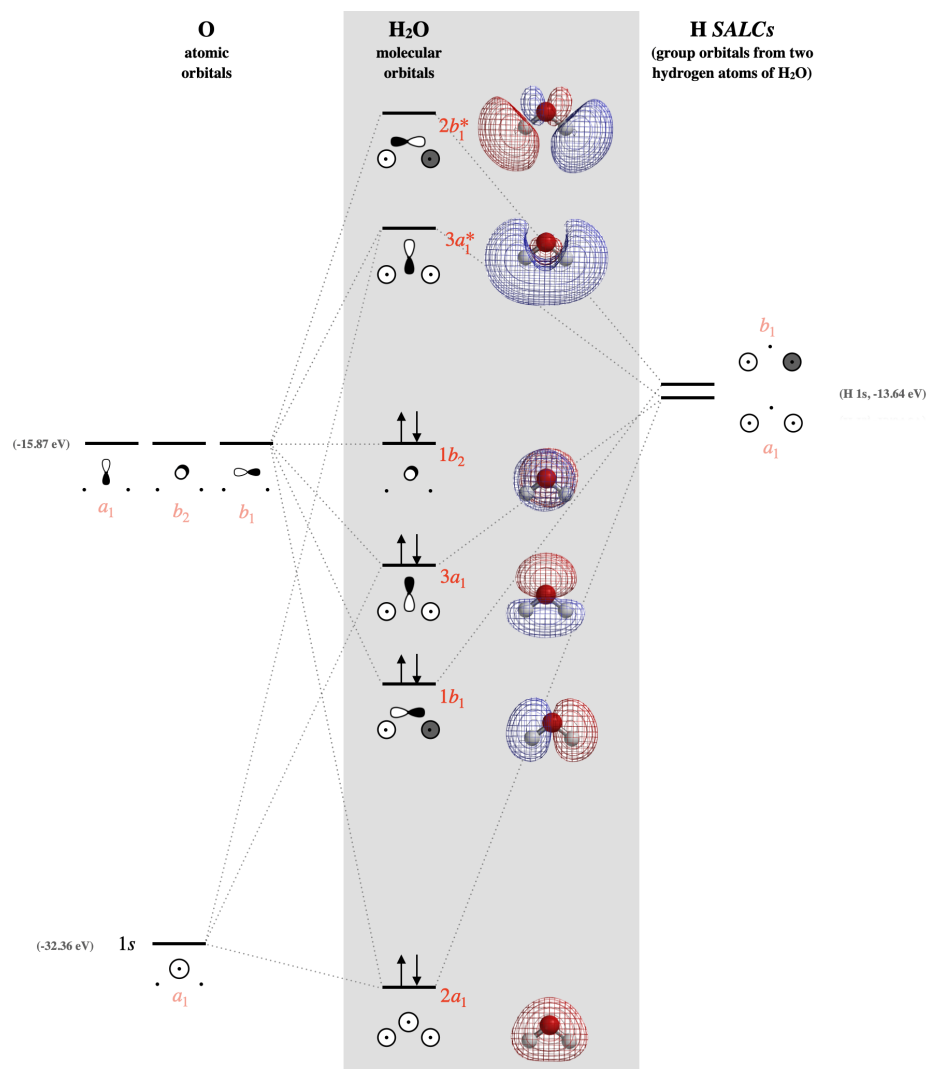


Figure 5.4.2.3.3: The molecular orbital diagram of water. Molecular orbital surfaces calculated using Spartan software. The surface of the 3a<sub>1</sub>\* orbital has been trimmed. (CC-BY-NC-SA; Kathryn Haas)

### ✓ Example 5.4.2.3.1

In the previous examples shown for the molecular orbital diagrams of the bifluoride anion and carbon dioxide, we discussed differences in the understanding of those molecules from molecular orbital theory compared to Lewis structures. Water contains two lone pairs in its Lewis structure. Compare the predictions about water's lone pairs of electrons and its reactivity based on (1) the combination of elementary models (Lewis, Valence Bond, and Hybridized Orbital theories) and (2) Molecular Orbital theory. Specifically address and explain how the elementary models differ from molecular orbital theory in the following respects:

- Where are the lone pairs in water?
- Are the two lone pairs equivalent or are they different?
- Where are sites on the molecule that will undergo reaction with electrophiles and nucleophiles?

#### Solution

**1) Elementary models:** The Lewis structure predicts that two lone pairs are (a) localized on the oxygen atom of water and that (b) both lone pairs are equivalent. The Lewis structure, combined with Valence Bond Theory, would predict that lone pairs occupy two equivalent hybridized  $sp^3$  atomic orbitals on oxygen. (c) Lewis theory would predict that the oxygen lone pairs are nucleophiles; thus an electrophile would react with the oxygen atom lone pairs. The polarized O-H bond leaves the H atoms as the most electrophilic locations on the water molecule; thus nucleophiles would react at the H atoms of water.

**2) Molecular orbital theory:** The molecular orbitals predict that (a) the two lone pairs of water are not equivalent, and that (b) each is distributed over the entire molecule. One lone pair is in the truly non-bonding  $1b_2$  orbital (Figure 5.4.2.3.3), which is also the HOMO. There is not another truly non-bonding orbital in the molecule, but the lowest-energy  $2a_1$  orbital could be considered mostly non-bonding due to the large energy difference between it and other valence orbitals. (c) Although the  $2a_1$  orbital can be considered mostly non-bonding, we cannot expect the electrons in  $2a_1$  to react readily, as they are in the lowest-energy molecular orbital. Molecular orbital theory predicts that reactions occur at the HOMO and LUMO orbitals. The HOMO reacts with electrophiles, and in this case, the HOMO is distributed over the top and bottom faces of the molecule, and is centered on the oxygen atom. The LUMO would react with nucleophiles. The LUMO is the orbital labeled  $3a_1^*$  in Figure 5.4.2.3.3 and has a major lobe that is distributed more heavily over the H atoms, and from this we should predict H atoms to be the preferred site of reaction for nucleophiles.

### Expressing molecular orbitals in terms of $\Psi$

The general expression for a molecular orbital, or the linear combination of atomic orbitals (LCAO), was given [previously](#) as  $\Psi = c_a\psi_a + c_b\psi_b$ . In this expression, the wavefunction of two atoms ( $\psi_a$  and  $\psi_b$ ) is combined to form the wavefunction of the molecular orbital. The coefficients  $c_a$  and  $c_b$  quantify the contribution of each atomic  $\psi$  to the molecular  $\Psi$ .

$$\Psi = c_a\psi_a + c_b\psi_b$$

In the case of polyatomic orbitals, each LCAO is constructed of atomic orbitals from a central atom and group orbitals (SALCs) from the pendent atoms. In the case of water, the expression above could be modified to give the expression below.

$$\Psi = c_{oxygen}(\psi_{oxygen}) + c_{SALCs}(N(\psi_{H_a} \pm \psi_{H_b}))$$

N represents the normalizing requirement that was mentioned [previously](#) in reference to the requirements for electron wavefunctions and probability functions. The normalizing requirement simply stated is the requirement that the probability of finding the electron in any orbital, including group orbitals, is 1. In general, the value of N for a group orbital is...

$$N = \frac{1}{\sum c_i^2}$$

...where  $c_i$  is the coefficient of each unique atomic orbital that contributes to the group. For the hydrogen SALCs of water, there are two atomic orbitals that contribute to equally to each SALC, and so the coefficient on each of the two orbitals is 1. This gives

$$N = \left( \frac{1}{\sqrt{1^2 + 1^2}} \right) = \frac{1}{\sqrt{2}} \text{ for the H SALCs of water.}$$

There are only two hydrogen SALCs: the one in which the hydrogen wavefunctions are added ( $N(\psi_{H_a} + \psi_{H_b})$ ) has  $A_1$  symmetry, and the one in which the hydrogen wavefunctions are subtracted ( $N(\psi_{H_a} - \psi_{H_b})$ ) has  $B_1$  symmetry.

The molecular orbitals from Figure 5.4.2.3.3 are expressed below in terms of their LCAO of individual wavefunctions. Yet, note that these expressions are simplifications that ignore orbital mixing. For example, as expressed below, they ignore contributions of oxygen  $2s$  to the higher energy molecular orbitals with  $A_1$  symmetry (the  $3a_1$  and  $3a_1^*$  in Figure 5.4.2.3.3).

MO	OxygenAO	HydrogenSALC	Description
$\Psi_{2a_1}$	$= c_{(ox1)}\psi(2s)$	$+ c_{(hy1)}[N(\psi_{H_a} + \psi_{H_b})]$	$c_{(hy1)}$ is positive; bonding, slightly nonbonding
$\Psi_{1b_1}$	$= c_{(ox2)}\psi(2p_x)$	$+ c_{(hy2)}[N(\psi_{H_a} - \psi_{H_b})]$	$c_{(hy2)}$ is positive; bonding
$\Psi_{3a_1}$	$= c_{(ox3)}\psi(2p_z)$	$+ c_{(hy3)}[N(\psi_{H_a} + \psi_{H_b})]$	$c_{(hy3)}$ is positive; bonding
$\Psi_{1b_2}$	$= \psi(2p_y)$		nonbonding
$\Psi_{3a_1}^*$	$= c_{(ox4)}\psi(2p_z)$	$+ c_{(hy4)}[N(\psi_{H_a} + \psi_{H_b})]$	$c_{(hy4)}$ is negative; antibonding
$\Psi_{1b_1}^*$	$= c_{(ox5)}\psi(2p_x)$	$+ c_{(hy5)}[N(\psi_{H_a} - \psi_{H_b})]$	$c_{(hy5)}$ is negative; antibonding

5.4.2.3: H<sub>2</sub>O is shared under a [CC BY-SA 4.0](#) license and was authored, remixed, and/or curated by LibreTexts.

- 5.4.3: H<sub>2</sub>O is licensed [CC BY-SA 4.0](#).



### 5.4.2.4: NH<sub>3</sub>

#### Construct SALCs and the molecular orbital diagram for NH<sub>3</sub>

This is the first example so far that has more than two pendant atoms and the first example in which the molecule has atoms that lie in three dimensions (i.e., it is not flat). Ammonia is a trigonal pyramidal molecule, with three pendant hydrogen atoms. The three-dimensional shape and the odd number of pendant atoms makes this example more complicated than the previous cases of [water](#), [carbon dioxide](#), and [bifluoride](#). In this case, sketching the shapes ([step 5](#)) of pendant atom SALCs is less straightforward; rather, an alternative method, the **projection operator method**, is preferred for generating pictorial representations of the SALCs.

As in previous examples, it is important to remember that interactions of pendant ligands are dependent on their positions in three-dimensional space. You should consider the positions of the four atoms in ammonia to be essentially fixed in relation to each other. We will walk through the steps used to construct the molecular orbital diagram of ammonia. The first few steps are the same as you've seen before:

#### Step 1. Find the point group of the molecule and assign Cartesian coordinates so that z is the principal axis.

The NH<sub>3</sub> molecule is trigonal pyramidal and its point group is  $C_{3v}$ . The z axis is collinear with the principal axis, the  $C_3$  axis.

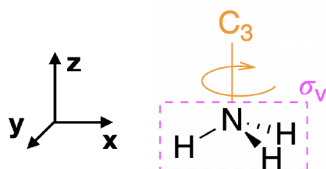


Figure 5.4.2.4.1: The ammonia molecule is in the  $C_{3v}$  point group. (CC-BY-NC-SA; Kathryn Haas)

#### Step 2. Identify and count the pendant atoms' valence orbitals.

Each of the three pendant hydrogen atoms has one valence orbital; the 1s. Thus, we can expect a total of three SALCs from these three atoms.

#### Step 3. Generate the $\Gamma$ 's

Use the  $C_{3v}$  [character table](#) to generate one reducible representation ( $\Gamma$ ); in this case we need only one  $\Gamma$  because there is only one type of valence orbital (the 1s). For each s orbital, assign a value of 1 if it remains in place during the operation or zero if it moves out of its original place. The  $\Gamma$  is given below:

$C_{3v}$	$E$	$2C_3$	$3\sigma_v$
$\Gamma_{1s}$	3	0	1

#### Step 4. Break $\Gamma$ 's into irreducible representations for individual SALCs

Reduce each  $\Gamma$  into its component irreducible representations. Using either of the processes described previously, we find that the  $\Gamma$  reduces to the two irreducible representations  $A_1$  and  $E$  under the  $C_{3v}$  point group.

$C_{3v}$	$E$	$2C_3$	$3\sigma_v$
$\Gamma_{1s}$	<b>3</b>	<b>0</b>	<b>2</b>
$A_1$	1	1	1
$E$	2	-1	0

Notice that we only found TWO irreducible representations. But, in fact we have THREE different SALCs. The  $E$  irreducible representation is doubly degenerate, which in this context means that it corresponds to two degenerate SALCs. Thus, we have already found the symmetries of the three SALCs for ammonia: Two of the SALCs are degenerate with  $E$  symmetry under the  $C_{3v}$  point group, while the third SALC has  $A_1$  symmetry.

#### Step 5. Sketch the SALCs using the PROJECTION OPERATOR METHOD

From the [first four steps](#) (described above), you have found the symmetries (the irreducible representations) of all three SALCs under the  $C_{3v}$  point group. To sketch the SALC that corresponds to each irreducible representation, again we use the  $C_{3v}$  [character table](#). But now we will introduce the **projection operator method** to derive the surface representation of each SALC.

### Step 5.1: Label the pendent atoms

In the projection operator method, first **label each of the pendant atoms so that we can distinguish identical atoms from one another**; for example, identify the three hydrogen atoms on ammonia as  $H_a$ ,  $H_b$ , and  $H_c$  (Figure 5.4.2.4.2).

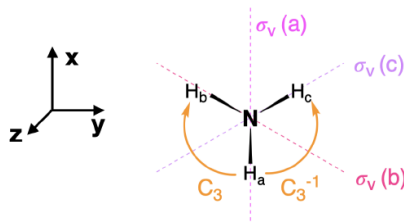


Figure 5.4.2.4.2: The three H's in  $\text{NH}_3$  are chemically identical, but we can distinguish them using labels for the purpose of applying the projection operator method. In this figure, we have placed the  $z$  axis along the principal  $C_3$  axis and placed the  $x$  axis colinear with one H. Each of the three H atoms has been labeled as  $H_a$ ,  $H_b$ , or  $H_c$ . The  $\sigma_v$  that is coplanar with each H is labeled similarly (a, b, c) to keep account of each individual plane of symmetry. (CC-BY-NC-SA; Kathryn Haas)

### Step 5.2: Create an expanded character table with one pendant atom's projected position after each operation

We will **perform each operation of the  $C_{3v}$  point group on this labeled molecule** and follow where one of the atoms is projected after the operation is complete. We will arbitrarily choose  $H_a$ . For example, upon performing the identity operation,  $E$ , the  $H_a$  atom is projected onto itself. On the other hand,  $H_a$  is projected onto  $H_b$  upon a clockwise  $C_3$  rotation (as drawn in Figure 5.4.2.4.2). We take into account the result of each operation using an expanded character table (refer to the table below, 5.4.2.4.1). In the expanded character table, each operation within each class is written separately (i.e.,  $2C_3$  is accounted for separately as  $C_3$  and  $C_3^{-1}$ ).

Table 5.4.2.4.1: The expanded character table, and the projection of  $H_a$  by each operation is shown below.

$C_{3v}$	$E$	$C_3$	$C_3^{-1}$	$\sigma_v(a)$	$\sigma_v(b)$	$\sigma_v(c)$
<b>Projection of <math>H_a</math></b>	$H_a$	$H_b$	$H_c$	$H_a$	$H_c$	$H_b$

(5.4.2.4.1)

### Step 5.3: Find the contribution of each pendant atom to each SALC

Next, **create a linear combination of the projections for each of the SALCs** (the irreducible representations found in step 4). For each of the irreducible representations, multiply the projection by the respective character of the operation.

$$\text{Contribution of each atom to the SALC} = \sum (\text{Projection of } H_a \times \chi)$$

The linear combination for all irreducible representations of  $C_{3v}$  is shown below.

Table 5.4.2.4.2: The symmetry adapted linear combination (SALC) for each irreducible representation of  $C_{3v}$  is shown.

$C_{3v}$	$E$	$C_3$	$C_3^{-1}$	$\sigma_v(a)$	$\sigma_v(b)$	$\sigma_v(c)$	Linear Combination
<b>Projection of <math>H_a</math></b>	$H_a$	$H_b$	$H_c$	$H_a$	$H_c$	$H_b$	
$A_1$	1	1	1	1	1	1	$= 2H_a + 2H_b + 2H_c$
$A_2$	1	1	1	-1	-1	-1	$= 0$
$E$	2	-1	-1	0	0	0	$= 2H_a - H_b - H_c$

(5.4.2.4.2)

Notice that there are only two irreducible representations that produce SALCs, and these are the same that were found in Step 4, above. This illustrates the fact that only the irreducible representations found through the reduction of the  $\Gamma$  will produce SALCs. We can ignore any irreducible representations that were not found in Step 4. Or, you can check your work in Step 4 by applying the projection operator to any irreducible representations not found in Step 4, and finding that they produce a sum of zero.

### Step 5.4: Sketch the SALCs

The meaning of the linear combinations found in Table 5.4.2.4.2 is as follows:

- Sketch the SALC with  $A_1$  symmetry:** The linear combination  $2H_a + 2H_b + 2H_c$  indicates all contributions to this SALC are of the same sign (of the wavefunction). Qualitatively, this means there is no node in this SALC. We can take this SALC almost literally to assume that all three H 1s wavefunctions contribute equally to the SALC. We can also use the fact that the  $A_1$  representation possesses the full symmetry of the  $C_{3v}$  point group, is compatible with an s orbital on N, and thus is a totally

symmetric SALC.

Quantitatively, we can apply the [normalizing factor, N](#), for this SALC. The linear combination for the  $A_1$  SALC in Table 5.4.2.4.2 shows us that the coefficient for each orbital is 1. Thus, the normalizing factor for the  $A_1$  SALC is

$N = \left( \frac{1}{\sqrt{1^2+1^2+1^2}} \right) = \frac{1}{\sqrt{3}}$ . This tells us that  $H_a$ ,  $H_b$ , and  $H_c$  each contribute  $\frac{1}{\sqrt{3}}$  to the normalized  $A_1$  group orbital:

$$A_1 \text{ group orbital} = \frac{1}{\sqrt{3}}[\psi_{H_a} + \psi_{H_b} + \psi_{H_c}]$$

This is shown visually in Figure 5.4.2.4.3

- **Sketch two SALCs with E symmetry:** The linear combination  $2H_a - H_b - H_c$  indicates that there are contributions with both positive and negative sign to the wavefunction for each of the  $E$  group orbitals. Qualitatively, this tells us that there is a node within each of these two SALCs, and that the total contribution of the positive portion of the wavefunction is equal to the contribution of the negative portion.

- **Finding the first E SALC:**

For one of the SALCs, we can take the linear combination from Table 5.4.2.4.2 almost literally: The contribution from  $H_a$  is equal and opposite to the sum of the contributions from  $H_b + H_c$ . This would result in a SALC as shown in Figure 5.4.2.4.3(E, left), that would have symmetry of the  $x$  axis and that would be compatible with the  $p_x$  orbital on N. The node exists in the  $yz$  plane and there is an equal contribution of positive and negative parts of the total wavefunction.

We can also apply the [normalizing factor, N](#), to find this SALC. The linear combination for the  $E$  SALC in Table 5.4.2.4.2 shows us that the coefficients for orbital contributions are 2, -1, and -1. Thus, the normalizing factor for the first  $E$  SALC is

$N = \left( \frac{1}{\sqrt{2^2+(-1)^2+(-1)^2}} \right) = \frac{1}{\sqrt{6}}$ . This normalized  $E$  group orbital is:

$$\text{First } E \text{ group orbital} = \frac{1}{\sqrt{6}}[2\psi_{H_a} - \psi_{H_b} - \psi_{H_c}]$$

This is shown visually in Figure 5.4.2.4.3(E, left).

- **Finding the second E SALC:**

The second SALC is less obvious at first glance. We must use clues from the character table to help us determine what it should "look like". Since the  $E$  representation transforms as the group,  $(x, y)$ , we know that one of the SALCs will have the symmetry of the  $x$  axis and  $p_x$  orbital on the central nitrogen atom, while the other should possess the symmetry of the  $y$  axis and be compatible with the  $p_y$  orbital on nitrogen. This alone could lead you to the sketch of the second SALC with  $E$  symmetry shown in Figure 5.4.2.4.3 (E, right). This second  $E$  SALC must have a node in the  $xz$  plane, and because  $H_a$  lies in this node,  $H_a$  cannot contribute to this group orbital. Retaining the fact that the positive and negative contributions of the linear combination must be equal, we can arrive at a SALC that has equal but opposite contributions of  $H_b$  and  $H_c$ , and no contribution by  $H_a$  (Figure 5.4.2.4.3 right).

We can also apply the [normalizing factor, N](#), to find this SALC. But we must apply the fact that  $H_a$  cannot contribute to the SALC with " $y$ " symmetry. We remove the contribution of  $H_a$ , leaving us with coefficients of 0 for  $H_a$  and 1 for  $H_b$  and  $H_c$ .

Thus, the normalizing factor for the second  $E$  SALC is  $N = \left( \frac{1}{\sqrt{0^2+1^2+1^2}} \right) = \frac{1}{\sqrt{2}}$ . To this, we must add positive and negative coefficients so that the entire wavefunction of this SALC is normalized. The result for this normalized  $E$  group orbital is:

$$\text{Second } E \text{ group orbital} = \frac{1}{\sqrt{2}}[\psi_{H_b} - \psi_{H_c}]$$

This is shown visually in Figure 5.4.2.4.3

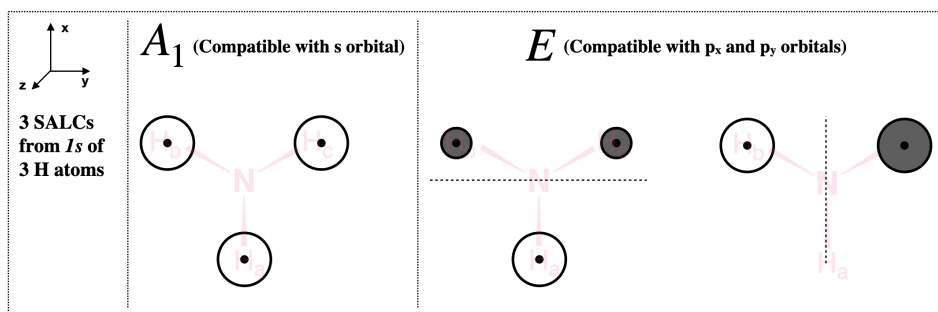


Figure 5.4.2.4.3: Sketches of H SALCs of ammonia from the perspective of the  $C_3$  axis ( $z$  axis). The  $A_1$  SALC is shown at the left, while two degenerate SALCs with  $E$  symmetry are shown on the right. Nodes for  $E$  group orbitals are shown as dashed lines. (CC-BY-NC-SA; Kathryn Haas)

#### Step 6. Combine SALCs with AO's of like symmetry to draw the MO diagram for $\text{NH}_3$

First we must identify the valence orbitals on the central nitrogen: there are four including  $2s$ ,  $2p_x$ ,  $2p_y$ , and  $2p_z$ . Now we identify the symmetry of each using the  $C_{3v}$  character table. The symmetry of a central  $2s$  orbital corresponds to the combination of functions  $x^2$ ,  $y^2$ , and  $z^2$  in the character table; this is  $A_1$ . The  $p_z$  orbital also corresponds to  $A_1$ . And so on... The symmetries of nitrogen valence orbitals are listed below.

$$\begin{aligned} 2s &= A_1 \\ (2p_x, 2p_y) &= E \\ 2p_z &= A_1 \end{aligned}$$

The next step is to get a sense of the relative energies of valence atomic orbitals for nitrogen and hydrogen, and then construct the molecular orbital diagram. The nitrogen  $2s$  orbital is about 12 eV lower in energy than a H  $1s$ . This difference is an acceptable energy-match for the H orbitals to interact, but would not usually result in a strong interaction. On the other hand, the nitrogen  $2p$  orbitals have an energy very close to the hydrogen  $1s$ , different by only 0.5 eV. Knowledge of the relative energies of the atomic orbitals tells us that, when constructing a diagram, we can place the H SALCs at an energy similar to that of the N  $2p$  orbitals, while the N  $2s$  is much lower (Figure 5.4.2.4.4).

The  $2s$  and  $2p_z$  orbitals have  $A_1$  symmetry and can combine with the  $A_1$  SALC. These orbitals will give three molecular orbitals. The  $2s$  orbital will not have strong interactions with the other orbitals of  $A_1$  symmetry due to the large energy difference. The  $2p_z$  orbital will not have good overlap with the wavefunctions for the three hydrogen orbitals due to their positions in space: The  $2p_z$  orbital has half of its angular distribution pointed away from the hydrogen orbitals, and half pointed toward the center of a triangle formed by the three hydrogen atoms. The nitrogen  $2s$  and  $2p_z$  will combine with the hydrogen SALC of  $A_1$  symmetry to give three molecular orbitals; one low-energy bonding orbital, one mid-energy non-bonding orbital, and one high-energy antibonding orbital. The mid-level non-bonding  $a_1$  molecular orbital is close in energy to, and resembles, the nitrogen  $2p_z$  orbital. The lowest energy  $a_1$  molecular orbital will be lower in energy, but be similar to the nitrogen  $2s$ .

The remaining two  $2p$  orbitals are degenerate and possess  $E$  symmetry under the  $C_{3v}$  point group. Although these orbitals are a good energy match, again, their orientation and positions in space do not allow for good orbital overlap, and their bonding and antibonding interactions are relatively weak compared to what we might otherwise expect from such a good energy match. The  $e$  atomic orbitals of nitrogen will combine with the  $e$  SALCs to give a set of two degenerate bonding molecular orbitals and a set of two degenerate antibonding orbitals (four total molecular orbitals of  $e$  symmetry). The MO diagram for  $\text{NH}_3$  is shown in Figure 5.4.2.4.4 with calculated electron density surfaces of each MO shown.

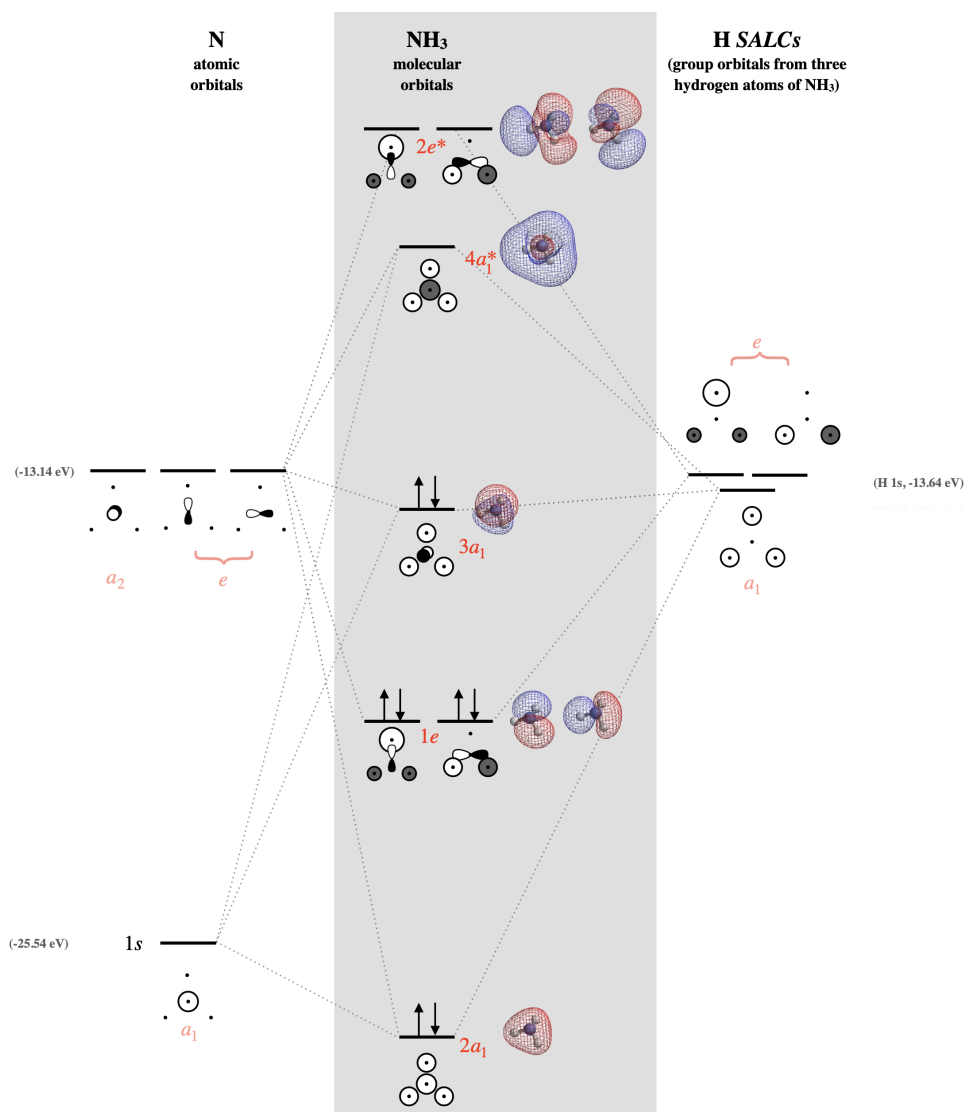


Figure 5.4.2.4.4: The molecular orbital diagram of ammonia. Molecular orbitals surfaces calculated using Spartan software. (CC-BY-NC-SA; Kathryn Haas)

This page titled 5.4.2.4: NH<sub>3</sub> is shared under a CC BY-SA 4.0 license and was authored, remixed, and/or curated by Kathryn Haas.

- 5.4.4: NH<sub>3</sub> by Kathryn Haas is licensed CC BY-SA 4.0.

### 5.4.3: Why is BeH<sub>2</sub> Linear and H<sub>2</sub>O Bent?

In this section, we will construct approximate molecular orbitals for a water molecule by considering a simple linear triatomic of the general form  $HXH$ , where  $X$  is a second row element. We will take a multi-centered molecular orbital approach instead of the two-centered valence bond/hybrid approach discussed previously. As with previous discussions of Molecular Orbitals, we approximate them as a linear combinations of atomic orbitals (LCAO). In molecular orbital theory linear combinations of **all** available (atomic) orbitals will form molecular orbitals. These are spread over the whole molecule, or delocalized, and in a quantum chemical interpretation they are called canonical orbitals. Since it is absolutely wrong to assume that there are only three types of  $sp^x$  hybrid orbitals, it is possible, that there are multiple different types of orbitals involved in bonding for a certain atom.

#### AH<sub>2</sub> Molecules

We want to construct a reasonable argument for the energetic ordering and structure of the molecular orbitals. We first note that each  $H$  will donate a  $1s$  orbital in the LCAO scheme, and  $A$  will likely donate at least  $2s$  and possible  $2p$  orbitals, depending on its chemical identity. In general, if we consider only the first row  $A$  elements, the molecule orbitals (via the LCAO) can be expressed as combination of  $1s$  orbitals on the two Hydrogens ( $H_1$  and  $H_2$ ) and the four  $n=2$  orbitals ( $2s$   $2p_x$   $2p_y$ ;  $2p_z$ ) on the  $A$  atom:

$$|\chi\rangle = a_1|1s\rangle_{H_1} + a_2|1s\rangle_{H_2} + a_3|2s\rangle_A + a_4|2p_x\rangle_A + a_5|2p_y\rangle_A + a_6|2p_z\rangle_A \quad (5.4.3.1)$$

These molecular orbitals were created with six atomic orbitals and hence six different  $|\chi\rangle$  molecular orbitals can be created. As with previous molecular orbitals problems, the coefficients of this expansion ( $\{a_i\}$ ) are determined by solving the secular determinant.

If we consider only linear  $AH_2$  molecules, then Equation 5.4.3.1 can be simplified by ignoring  $2p_x$  and  $2p_y$  atomic orbitals since they are perpendicular to the bonds and are hence non-bonding (only for linear  $AH_2$  molecules). Moreover, the molecule is symmetric about the center (the position of  $A$ ), hence the orbitals have to have the same symmetry.

Only the  $2p$  orbital of  $A$  that will overlap with  $1s$  of  $H$  is the  $2p_z$ . Hence, Equation 5.4.3.1 can be simplified to consider the combination

$$|\chi\rangle = a_1|1s\rangle_{H_1} + a_2|1s\rangle_{H_2} + a_3|2s\rangle_A + a_6|2p_z\rangle_A \quad (5.4.3.2)$$

Note that the two coefficients in front of the  $1s$  orbitals of hydrogen are the same by symmetry. This since no hydrogen is "special" and they must have the same contribution to the molecular orbital.

#### Mixing Amplitudes

How big should the  $2s$  orbital contributors of  $A$  be compared to the  $1s$  orbital of  $H$ ?

This depends on several things. First, is the nuclear charge on  $A$  and the second is the **electronegativity** difference between  $H$  and  $A$ . The first determines how quickly the  $2s$  orbitals, remembering that the exponential part is  $\exp(-Zr/a_0)$ , and the electronegativity difference determines the relative magnitude of  $H_1$  compared to  $H_2$ .

The six  $|\chi\rangle$  molecular orbitals from Equation 5.4.3.1 are shown in Figure 10.3.1 .

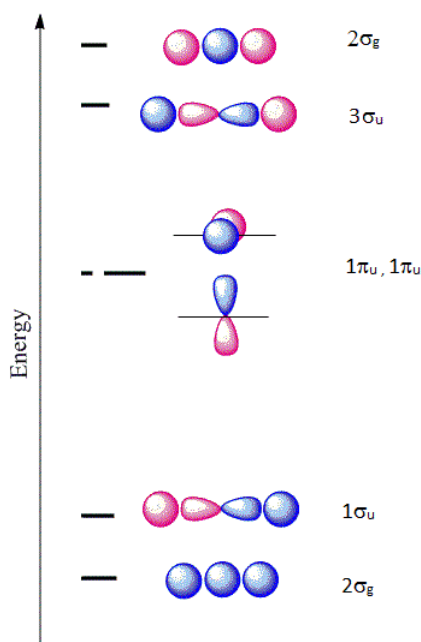


Figure 10.3.1 : The six molecular orbitals for the  $AH_2$  molecule constrained to a linear geometry. The symmetry labels for each molecular orbital are indicated.

The first molecular orbital  $|\chi_1\rangle$  constructed from Equation 5.4.3.1 is purely bonding because the  $2s$  orbital is positive near the  $A$  nucleus, but becomes negative as we go away from the nucleus. This orbital is also even (*gerade symmetry*), so we can denote it as a  $2\sigma_g$  orbital signifying that it is constructed from a  $2s$  orbital of  $A$  combined with the two  $1s$  orbitals of  $H$ . The only other MO that can be constructed that has the right symmetry is  $|\chi_6\rangle$  which is denoted as  $2\sigma_u$ . This is an antibonding molecular orbital and is also even (*gerade symmetry*). The corresponding wavefunctions are:

$$|\chi_1\rangle = a_1|1s\rangle_{H_1} + a_1|1s\rangle_{H_2} + a_3|2s\rangle_A$$

$$|\chi_6\rangle = a_1|1s\rangle_{H_1} + a_1|1s\rangle_{H_2} - a_3|2s\rangle_A$$

Next, if we combine a  $2p_z$  orbital of  $A$  with the  $1s$  of  $H$ , there are two possibilities that have the right symmetry. The first is

$$|\chi_2\rangle = a_1|1s\rangle_{H_1} + a_1|1s\rangle_{H_2} + a_6|2p_z\rangle_A$$

which is a bonding orbital and denoted as  $1\sigma_u$ . This is purely antibonding and has an odd symmetry (*ungerade*). The other combination is

$$|\chi_5\rangle = a_1|1s\rangle_{H_1} - a_1|1s\rangle_{H_2} + a_6|2p_z\rangle_A$$

Hence, we denote this as  $2\sigma_g$ . The orbitals  $2p_x$  and  $2p_y$  from  $X$  are nonbonding and become  $\pi_{2p_x}$  and  $\pi_{2p_y}$  nonbonding orbitals and designated as  $1\pi_u$  orbitals:

$$|\chi_3\rangle = |2p_x\rangle_A$$

$$|\chi_4\rangle = |2p_y\rangle_A$$

### Beryllium Hydride ( $BeH_2$ ) is Linear

Consider the  $BeF_2$  molecule: Be has a  $1s^2 2s^2$  electron configuration with is no unpaired electrons available for bonding. From a perspective of using only atomic orbitals to generate the bonding orbitals, we would conclude that the molecule could not exist since no free orbitals exist on  $Be$  to bond. Clearly, atomic orbitals are not adequate to describe orbitals in molecules, but this can be solved by allowing the  $2s$  and one  $2p$  orbital on Be to mix to form  $sp$  hybrid orbitals. The experimental H-Be-H bond angle is  $180^\circ$ . Presumably, one electron from Be is shared with each unpaired electrons from H. We could promote one electron from the  $2s$  orbital on Be to the  $2p$  orbital to get two unpaired electrons for bonding (predicting  $90^\circ$  bond angles, not  $180^\circ$ ). Thus the geometry is still not explained with atomic orbitals alone.

Be has 2s and 2p orbitals, and it is in the middle. H has 1s orbitals; there are 2 H atoms on the outside. We initially make combinations of the H atomic orbitals that we previously used to make diatomic hydrogen, except there is no overlap (i.e.,  $S = 0$ ). These combinations will mix with the 2s and 2p<sub>z</sub> on Be, as shown in Figure 10.3.2.

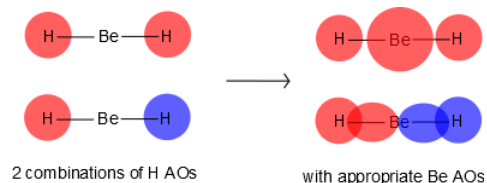


Figure 10.3.2 : Forming molecular orbitals for  $\text{BeH}_2$ .

Then we can put the Molecular Orbital diagram together, starting with the outside, drawing in bonding, non-bonding and anti-bonding MOs, and filling the electrons (Figure 10.3.3 ). The bond order is 2.

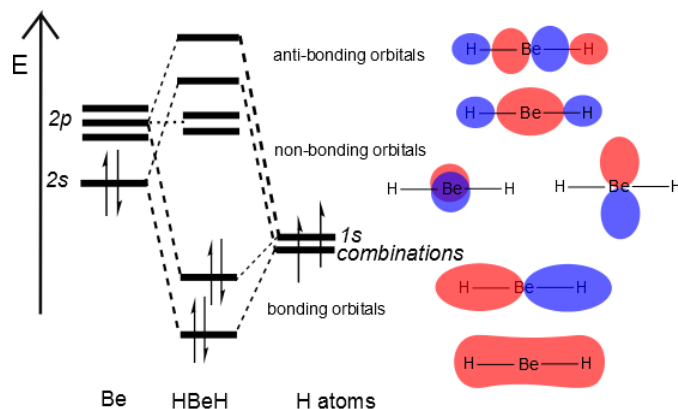


Figure 10.3.3 : Molecular orbitals diagram for  $\text{BeH}_2$ .

### Walsh Correlation Diagrams

Walsh diagrams, often called angular coordinate diagrams or correlation diagrams, are representations of calculated orbital energies of a molecule versus a distortion coordinate, used for making quick predictions about the geometries of small molecules. By plotting the change in molecular orbital levels of a molecule as a function of geometrical change, Walsh diagrams explain why molecules are more stable in certain spatial configurations (i.e. why water adopts a bent conformation).

A major application of Walsh diagrams is to explain the regularity in structure observed for related molecules having identical numbers of valence electrons (i.e. why  $\text{H}_2\text{O}$  and  $\text{H}_2\text{S}$  look similar), and to account for how molecules alter their geometries as their number of electrons or spin state changes. Additionally, Walsh diagrams can be used to predict distortions of molecular geometry from knowledge of how the LUMO (Lowest Unoccupied Molecular Orbital) affects the HOMO (Highest Occupied Molecular Orbital) when the molecule experiences geometrical perturbation. Walsh's rule for predicting shapes of molecules states that a molecule will adopt a structure that best provides the most stability for its HOMO. If a particular structural change does not perturb the HOMO, the closest occupied molecular orbital governs the preference for geometrical orientation.



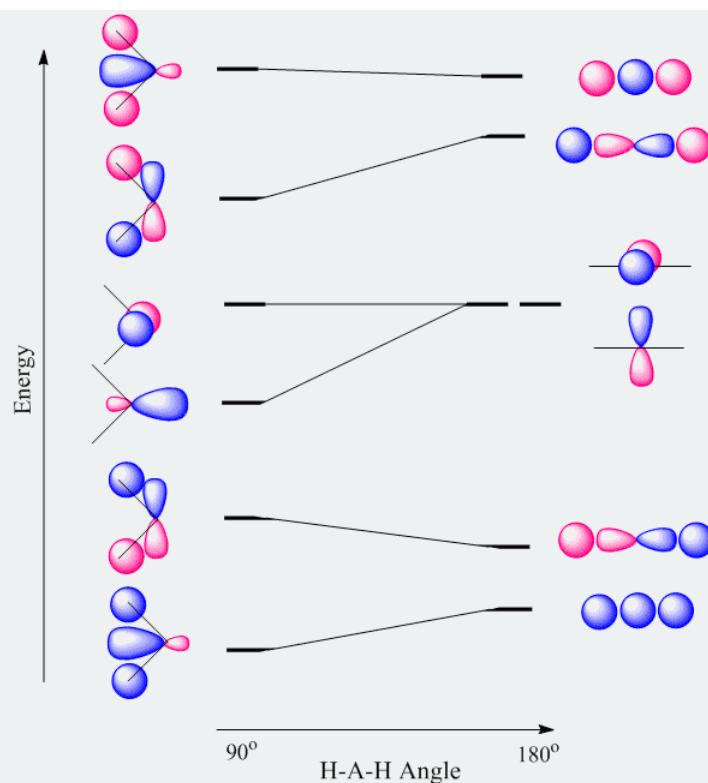


Figure 10.3.4 : A Walsh diagram for an  $AH_2$  molecule. (public domain).

For the  $AH_2$  molecular system, Walsh produced the first angular correlation diagram by plotting the orbital energy curves for the canonical molecular orbitals while changing the bond angle from  $90^\circ$  to  $180^\circ$  (Figure 10.3.4 ). As the bond angle is distorted, the energy for each of the orbitals can be followed along the lines, allowing a quick approximation of molecular energy as a function of conformation.

A typical prediction result for water is an bond angle of  $90^\circ$ , which is not even close to the experimental value of  $104^\circ$ . At best, the method is able to differentiate between a bent and linear molecule.

*Walsh's rule for predicting shapes of molecules states that a molecule will adopt a structure that best provides the most stability for its HOMO. If a particular structural change does not perturb the HOMO, the closest occupied molecular orbital governs the preference for geometrical orientation.*

Figure 10.3.4 illustrates the difference between the actual linear case we just analyzed and the truly bent molecule, e.g.  $H_2O$ . The geometry changes the ordering somewhat, but the qualitative picture we obtain from the linear case makes it a useful construction. The oxygen atomic orbitals are labeled according to their symmetry (Figure 10.3.5 ) as  $a_1$  for the 2s orbital and  $b_1$  ( $2p_x$ ),  $b_2$  ( $2p_y$ ) and  $a_1$  ( $2p_z$ ) for the three 2p orbitals. The two hydrogen 1s orbitals are premixed to form  $a_1$  and  $b_2$  molecular orbitals.

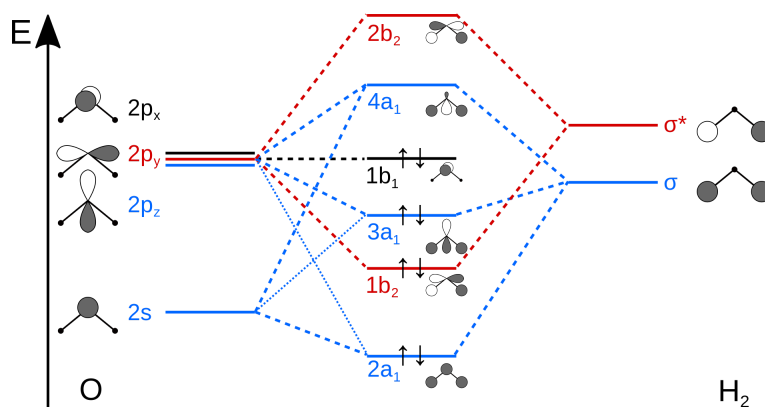


Figure 10.3.5 : MO diagram for water. (CC-SA-BY-3.0; Officer781).

Mixing takes place between same-symmetry orbitals of comparable energy resulting a new set of MO's for water:

- 2a<sub>1</sub> MO from mixing of the oxygen 2s atomic orbital and the hydrogen σ MO. Small oxygen 2p<sub>z</sub> atomic orbital admixture strengthens bonding and lowers the orbital energy.
- 1b<sub>2</sub> MO from mixing of the oxygen 2p<sub>y</sub> atomic orbital and the hydrogen σ\* MO.
- 3a<sub>1</sub> MO from mixing of the oxygen 2p<sub>z</sub> atomic orbital and the hydrogen σ MO. Small oxygen 2s atomic orbital admixture weakens bonding and raises the orbital energy.
- 1b<sub>1</sub> nonbonding MO from the oxygen 2p<sub>x</sub> atomic orbital (the p-orbital perpendicular to the molecular plane).

In the water molecule the highest occupied orbital, (1b<sub>1</sub>) is non-bonding and highly localized on the oxygen atom, similar to the non-bonding orbitals of hydrogen fluoride. The next lowest orbital (2a<sub>1</sub>) can be thought of as a non-bonding orbital, as it has a lobe pointing away from the two hydrogens. From the lower energy bonding orbitals, it is possible to see that oxygen also takes more than its "fair share" of the total electron density. The electronic configuration of water in the ground state (Figure 10.3.5 ) is therefore

$$(a_1)^2(b_2)^2(a_1)^2(b_1)^2$$

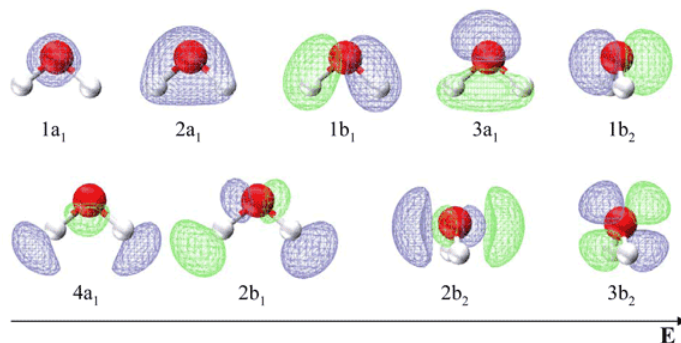


Figure 10.3.5 . Image from Anna Krylov (USC)

Table 10.3.1 list the respective LCAO coefficients for the six atomic orbitals. Table 10.3.1 combines the energy values with the description derived from the character table for molecules of point group C<sub>2v</sub>

Table 10.3.1 : LCAO Coefficients of first six molecular orbitals of water

Energy	Symbol	s(H)	s(O)	p <sub>x</sub> (O)	p <sub>y</sub> (O)	p <sub>z</sub> (O)	s(H)
6.728	2b <sub>2</sub>	0.525	0	0	-0.669	0	-0.525
5.440	3a <sub>1</sub>	-0.553	0.306	0	0	-0.544	0.553
-12.191	1b <sub>1</sub>	0	0	-1.000	0	0	0
-14.467	2a <sub>1</sub>	-0.309	0.354	0	0	0.827	-0.309
-19.113	1b <sub>2</sub>	-0.473	0	0	-0.743	0	0.473

Energy	Symbol	s(H)	s(O)	p <sub>x</sub> (O)	p <sub>y</sub> (O)	p <sub>z</sub> (O)	s(H)
-40.032	1a <sub>1</sub>	0.315	0.884	0	0	-0.143	0.315

Note in contrast to the valence bond theory discussed previous for water, the two lone electron pairs are **not in identical orbitals**. The 1b<sub>1</sub> MO is a lone pair, while the 3a<sub>1</sub>, 1b<sub>2</sub> and 2a<sub>1</sub> MO's can be localized to give two O–H bonds and an in-plane lone pair. This is in agreement with the experimentally measured photoelectron spectrum discussed in the next section.

## Summary

Walsh correlation diagram is a plot of molecular orbital energy as a function of some systematic change in molecular geometry. For example, the correlation between orbital energies and bond angle for an  $AH_2$  molecule. The geometry of a molecule is determined by which possible structure is lowest in energy. We can use the Walsh diagram to determine the energy trends based on which orbitals are occupied.

## Contributors and Attributions

- Mark Tuckerman (New York University)
- Emily V Eames (City College of San Francisco)

5.4.3: Why is BeH<sub>2</sub> Linear and H<sub>2</sub>O Bent? is shared under a CC BY-NC-SA 4.0 license and was authored, remixed, and/or curated by LibreTexts.

- 10.3: BeH<sub>2</sub> is Linear and H<sub>2</sub>O is Bent is licensed CC BY-NC-SA 4.0.

## 5.5: Pi Bonding and Hypervalency

---

Learning objectives for this unit are to:

- Use group theory and the central atom generator function method to determine the symmetries and draw pictures of ligand group orbitals (LGOs) that include pi bonding interactions
  - Derive molecular orbital energy diagrams for polyatomic molecules with pi bonding based on the interactions between the central atom AOs and the LGOs
  - Explain the concept of hypervalency and identify molecules that are hypervalent
  - Determine in what cases d-orbitals may or may not participate in the formation of hybrid atomic orbitals
  - Use ionic resonance hybrids to explain bonding in hypervalent compounds
  - Use 3c-4e bonds and MO theory to explain bonding in hypervalent compounds
- 

5.5: Pi Bonding and Hypervalency is shared under a [not declared](#) license and was authored, remixed, and/or curated by LibreTexts.

## 5.5.1: BF<sub>3</sub>

The case of boron trifluoride (BF<sub>3</sub>) is an example of a molecule with one more layer of complexity than the other examples we have seen in previous sections in this chapter. (BF<sub>3</sub>) is more complex than previous examples because it is the first case in which there are multiple types of valence orbitals on the pendant atoms. (BF<sub>3</sub>) possesses *s* and *p* orbitals on *both* the central atom and all of the pendant atoms. We can follow the same steps that we have previously to derive other molecular orbital diagrams; however, there is one important difference; we will treat each type of pendant orbital as an individual set of SALCs.

**Step 1. Find the point group of the molecule and assign Cartesian coordinates so that *z* is the principal axis.**

The BF<sub>3</sub> molecule is trigonal planar, and its point group is *D*<sub>3h</sub>. The *z* axis is colinear with the principle axis, the *C*<sub>3</sub> axis.

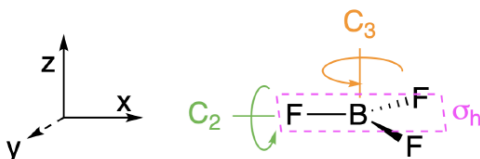


Figure 5.5.1.1: The molecule is in the *D*<sub>3h</sub> point group. (CC-BY-NC-SA; Kathryn Haas)

**Step 2. Identify and count the pendant atoms' valence orbitals.**

Each of the three pendant fluorine atoms has four valence orbitals: one *2s* and three *2p* orbitals. Thus, we can expect a total of twelve SALCs from the three atoms. However, we will treat each type of orbital from the F atoms as its own set; each will have its own set of coordinates, with the *y* axis along the M-L bond. Thus we expect the following:

- One set of *2s* SALCs: there is one *2s* orbital on each of three atoms. This set will have three SALCs.
- One set of *2p<sub>x</sub>* SALCs: there is one *2p<sub>x</sub>* orbital on each of three atoms. Each of these individual orbitals is perpendicular to the M-L bond and coplanar with the molecule. This set will have three SALCs.
- One set of *2p<sub>y</sub>* SALCs: there is one *2p<sub>y</sub>* orbital on each of three atoms. Each of these individual orbitals is colinear with the M-L bond. This set will have three SALCs.
- One set of *2p<sub>z</sub>* SALCs: there is one *2p<sub>z</sub>* orbital on each of three atoms. Each of these individual orbitals is perpendicular to the M-L bond and parallel with the principal axis of the molecule. This set will have three SALCs.

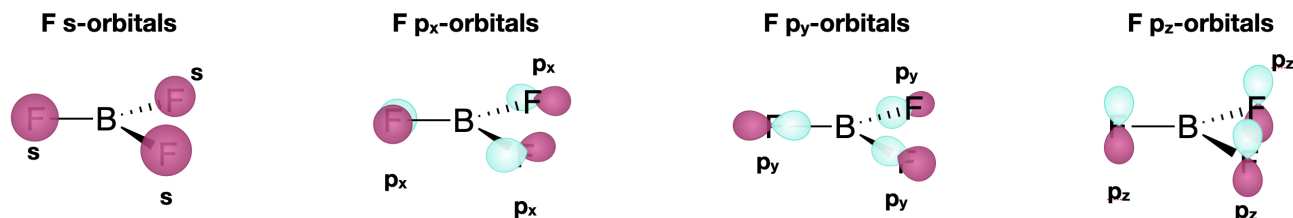


Figure 5.5.1.2: Individual sets of pendant fluorine atomic orbitals will create separate sets of SALCs. (CC-BY-SA; Kathryn Haas)

**Step 3. Generate the  $\Gamma$ 's for each set of SALCs**

Use the *D*<sub>3h</sub> character table to generate one reducible representation ( $\Gamma$ ) for each of the four sets of pendant atomic orbitals shown in Figure 5.5.1.2 in this case we need four  $\Gamma$  because there are four types of valence orbital (the *s*, *p<sub>x</sub>*, *p<sub>y</sub>*, *p<sub>z</sub>*).

- For the set of *s* orbitals: perform the operation for each class in the character table. Each *s* orbital is assigned a value depending on whether it moves or not: assign a value of 1 if it remains in place during the operation, or 0 (zero) if it moves out of its original place.
- for each set of *p* orbitals: Now there are phases (signs of the wavefunction), so a negative value is possible. Assign a value of 1 to each *p* orbital if it remains in place and in phase during the operation; assign a -1 if the atom's position remains, while the phase of the orbital is inverted (the positive lobe moves to the position of the negative lobe and vice versa); assign a 0 if it moves out of its original position.

The  $\Gamma$  for each type is given below:

$D_{3h}$	$E$	$2C_3$	$3C_2$	$\sigma_h$	$2S_3$	$3\sigma_v$
$\Gamma_{2s}$	3	0	1	3	0	1
$\Gamma_{2p_x}$	3	0	-1	3	0	-1
$\Gamma_{2p_y}$	3	0	1	3	0	1
$\Gamma_{2p_z}$	3	0	-1	-3	0	1

#### Step 4. Break $\Gamma$ 's into irreducible representations for individual SALCs

Reduce each  $\Gamma$  into its component irreducible representations. Using either of the processes described previously, we find that each of the  $\Gamma$  reduces to two irreducible representations under the  $D_{3h}$  point group; in each case one is singly degenerate ( $A$ ) and the other doubly degenerate ( $E$ ). This equates to three SALCs for each  $\Gamma$  (orbital type) and a total of twelve SALCs. This should give us confidence! We were in fact expecting 12 SALCs because we found that there were twelve pendant atomic orbitals to start with.

$D_{3h}$	$E$	$2C_3$	$3C_2$	$\sigma_h$	$2S_3$	$3\sigma_v$
$\Gamma_{2s}$	<b>3</b>	<b>0</b>	<b>1</b>	<b>3</b>	<b>0</b>	<b>1</b>
$A'_1$	1	1	1	1	1	1
$E'$	2	-1	0	2	-1	0

$D_{3h}$	$E$	$2C_3$	$3C_2$	$\sigma_h$	$2S_3$	$3\sigma_v$
$\Gamma_{2p_x}$	<b>3</b>	<b>0</b>	<b>-1</b>	<b>3</b>	<b>0</b>	<b>-1</b>
$A'_2$	1	1	-1	1	1	-1
$E'$	2	-1	0	2	-1	0

$D_{3h}$	$E$	$2C_3$	$3C_2$	$\sigma_h$	$2S_3$	$3\sigma_v$
$\Gamma_{2p_y}$	<b>3</b>	<b>0</b>	<b>1</b>	<b>3</b>	<b>0</b>	<b>1</b>
$A'_1$	1	1	1	1	1	1
$E'$	2	-1	0	2	-1	0

$D_{3h}$	$E$	$2C_3$	$3C_2$	$\sigma_h$	$2S_3$	$3\sigma_v$
$\Gamma_{2p_z}$	<b>3</b>	<b>0</b>	<b>-1</b>	<b>-3</b>	<b>0</b>	<b>1</b>
$A_2''$	1	1	-1	-1	-1	1
$E''$	2	-1	0	-2	1	0

#### Step 5: Sketch the SALCs

We'll skip this step for now to make this problem simpler.

#### Step 6: Draw the MO diagram by combining SALCs with AO's of like symmetry.

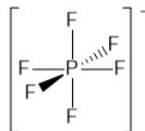
We now know the symmetries of different pendant orbital SALCs - and it is helpful if we also know their relative energies, and the energies of the valence orbitals on the central boron atom. We can make predictions based on periodic trends, or we can use a [table of ionization energies](#) as a guide. The symmetries of the boron  $2s$  and  $2p$  orbitals can be found from the  $D_{3h}$  character table.

5.5.1:  $BF_3$  is shared under a [CC BY-SA 4.0](#) license and was authored, remixed, and/or curated by LibreTexts.

- 5.4.4:  $NH_3$  by Kathryn Haas is licensed [CC BY-SA 4.0](#).

## 5.5.2: Expanded Octets and Molecular Orbitals

In organic chemistry the octet rule is closer to a law; do not make more than four bonds to carbon! However, once you start dealing with atoms in the third row of the periodic table, the octet rule becomes a bit more of a guideline. Consider the common anion, hexafluorophosphate,  $\text{PF}_6^-$  (Figure 5.5.2.1), in which we draw the phosphorous atom with six bonds giving it an apparently electron count of 12.



**Figure 5.5.2.1.** The structure of the hexafluorophosphate anion.

The bonding in these types of systems is a bit more involved and to fully appreciate it we must consider the molecular orbital diagram for such a molecule. This will be done using the same techniques as were used in the previous section, but some adjustments will need to be made as we progress from the Lewis structure to the molecular orbital diagram.

### Step 1 - Drawing the structure and determining the hybridization of the central atom

#### Exercise 5.5.2.1

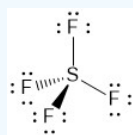
Using VSEPR, draw the three-dimensional structure of sulfur tetrafluoride ( $\text{SF}_4$ ).

#### Answer

Sulfur has 6 valence electrons and fluorine has 7 giving a total of 34 electrons in this molecule.

To start, you would draw bonds between sulfur and each of the fluorine atoms which would use 8 of the 34 electrons.

As fluorine is more electronegative, the next step would be to give each fluorine 3 lone pair in order to fill their octets. This will use 26 of the remaining electrons. At this point you might be tempted to stop as the sulfur atom and all of the fluorine atoms have an octet.



The problem is that this structure only accounts for 32 of our 34 electrons. As fluorine is an element in the 2<sup>nd</sup> row, we will not add the missing electrons to any of the fluorine atoms. That leaves sulfur as the only option. Checking the formal charge on each of the atoms supports this placement.

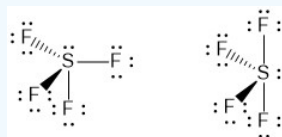
Formal Charge = number of valence electrons - (2 x number of lone pair + number of bonds)

$$\text{FC}_\text{F} = 7 - (2(3) + 1) = 0$$

$$\text{FC}_\text{S} = 6 - (2(1) + 4) = 0$$

This makes the sulfur  $\text{AX}_4\text{E}_1$  so the structure is going to be based on  $\text{AX}_5\text{E}_0$  which is trigonal bipyramidal.

There are two possible options for the structure, but the rules for VSEPR say that the lone pair should be as far away from other electrons as possible. In this structure that would be one of the equatorial positions and so the structure on the right (see-saw) is the correct one.



### Exercise 5.5.2.2

What orbitals need to be considered for hybridization on the central sulfur atom?

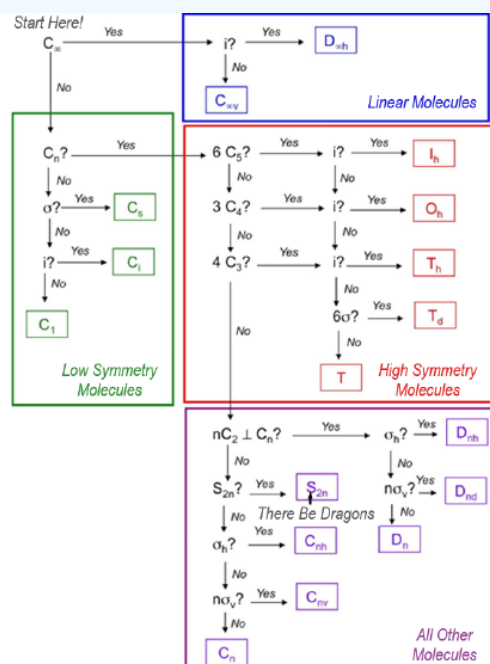
#### Answer

We need a total of 5 hybrid orbitals to account for the 4 fluorine atoms and the lone pair. That means we need to incorporate a d-orbital which will give  $sp^3d$  hybridization. The particular d-orbital that is used would be the  $d_{z^2}$  orbital.

### Step 2 - Determine the point group of the molecule and assign the generator functions

#### Exercise 5.5.2.3

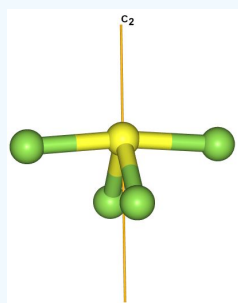
What is the point group of sulfur hexafluoride?



#### Answer

$SF_4$  does not have an infinite rotation axis.

There one rotation axis passing through the lone pair which is  $C_2$ .



There are not 6  $C_5$  axes.

There are not 3  $C_4$  axes.

There are not 4  $C_3$  axes.

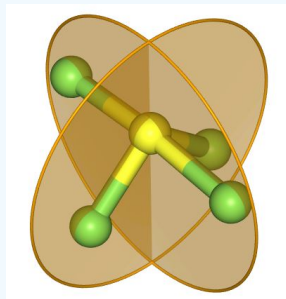
There are no perpendicular  $C_2$  axes.



There is not an  $S_4$  axis.

There is not a perpendicular mirror plane.

There are however two mirror planes.



The point group of  $SF_4$  is  $C_{2v}$ .

Once again we need the [character table](#) for the point group of  $SF_4$ . Shown below are two different representations for the character table for the  $C_{2v}$  point group. The first is the full character table. Although we ignored it in the methane example, this does include the d-orbital needed for hybridization. In the abbreviated character table the d-orbital has just been incorporated.

$C_{2v}$	E	$C_2$	$\sigma_v (xz)$	$\sigma_v (yz)$	Linear Functions	Quadratic Functions
$A_1$	+1	+1	+1	+1	z	$x^2, y^2, z^2$
$A_2$	+1	+1	-1	-1	$R_z$	xy
$B_1$	+1	-1	+1	-1	x, $R_y$	xz
$B_2$	+1	-1	-1	+1	z, $R_x$	yz

Table 5.5.2.1: Full character table for the  $C_{2v}$  point group.

$C_{2v}$	Orbitals
$A_1$	s, $p_z$ , $d_{z^2}$
$A_2$	
$B_1$	$p_x$
$B_2$	$p_y$

Table 5.5.2.2 Abbreviated character table for the  $C_{2v}$  point group.

#### Exercise 5.5.2.4

What are the symmetry labels for the orbitals on sulfur used to make  $SF_4$ .

**Answer**

s -  $a_1$

$p_x$  -  $b_1$

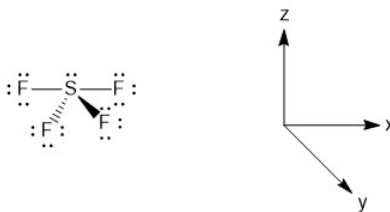
$p_y$  -  $b_2$

$p_z$  -  $a_1$

$d_{z^2}$  -  $a_1$

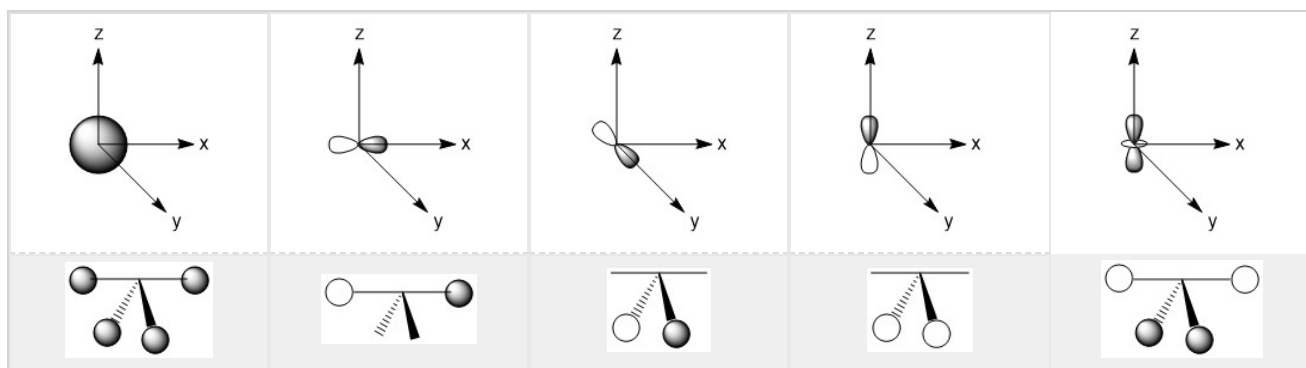
### Step 3 - Making the LGOs

Before making the LGOs, we need to assign axis labels to the molecule. While there are many ways to do this, the proper convention is to assign the principle axis to be the z-axis (Figure 5.5.2.2).



**Figure 5.5.2.2.** Assignment of the axes in  $\text{SF}_4$ .

As mentioned in the previous section, we can treat terminal halides using this method. To make the pictures less cluttered, the halides will be represented just as the hydrogen atoms were and we will ignore the lone pair on the fluorine atoms. Based on the assigned axes above, the LGOs can be drawn to match the orbitals on the sulfur atom (Figure 5.5.2.3).



**Figure 5.5.2.3.** LGOs in  $\text{SF}_4$ .

#### Step 3a - A few new twists

Before we go to step 4, we have a little bit of extra work to do. There are two features in this molecule that we have not dealt with before, the lone pair and the use of d-orbitals. Let's begin with the lone pair as this is something that could be encountered in molecules that do not break the octet rule. We know that this molecule has a lone pair on the sulfur atom. That lone pair has to be accounted for and must occupy one of the orbitals we considered as our basis functions. The question is, which orbital? The best option would be an orbital on the central atom that has no symmetry matched LGO. An example of this would be if all of the outer atoms in a molecule were sitting in the nodal plane of a p-orbital. We do not have that case in this example, so now we need to dig a little deeper. Our next best option is to consider all of the atomic orbitals of the central atom and ask which has the least amount of direct interaction with a LGO. The s-orbital on sulfur has interaction with all four fluorine atoms so it is not a good candidate. The p-orbitals all have interactions with two fluorine atoms, so they are slightly better options. In looking closer at the p-orbitals we see that the  $p_x$  orbital has very direct overlap with two fluorine atoms; the orbital is pointing directly at two atoms and both lobes interact. This is greater than the overlap of the  $p_y$  orbital in which the LGO does not lie directly on the y-axis. However, both lobes of the  $p_y$  orbital are interacting with the LGO. The  $p_z$  orbital is somewhat similar in that the LGO does not lie along the z-axis. However, for this orbital, only one lobe of the sulfur  $p_z$  is interacting with the LGO. So, given the options for the location of the lone pair,  $p_z > p_y > p_x > s$ , we must assign the  $p_z$  ( $a_1$ ) orbital to be the one with the lone pair. You may have noticed that the  $d_{z^2}$  was not considered in the previous discussion. That is because the  $d_{z^2}$  orbital is not accessible energetically. It is too high in energy to participate in any meaningful bonding in this molecule. While, we draw an LGO that would match this orbital, we do not consider any possible bonding or antibonding interaction between the LGO and the  $d_{z^2}$  orbital. This is going to become very critical in the next step.

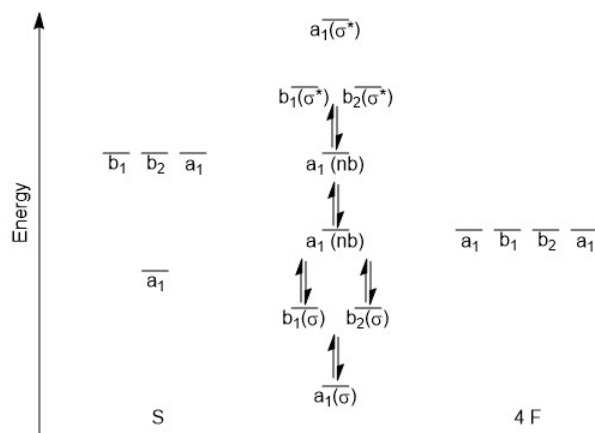
#### Step 4 - Constructing the MO diagram

In looking at the orbital energies from the previous section, we see that the 2s orbital of fluorine is MUCH lower in energy than the 2p of fluorine or the 3s and 3p of sulfur. It will not interact and does not need to be considered for this diagram. The 2p orbitals of

fluorine fall between the 3s and 3p orbitals of sulfur. We will be bringing together a total of eight orbitals. Why only eight? Let's consider each of the combinations above (Figure 5.5.2.3).

- Remember, we are ignoring the extra lone pairs on fluorine so that leaves a total of 12 orbitals that will not be shown in our diagram.
- The s-orbital ( $a_1$ ) from sulfur and the corresponding LGO will make a bonding and antibonding set.
- The  $p_x$  orbital ( $b_1$ ) orbital from sulfur and the corresponding LGO will make a bonding and antibonding set.
- The  $p_y$  orbital ( $b_2$ ) orbital from sulfur and the corresponding LGO will make a bonding and antibonding set.
- The  $p_z$  orbital ( $a_1$ ) has been assigned as the orbital holding the lone pair so we ignore the LGO it could interact with. Note that this does not mean that the fluorine orbitals do not contribute to this orbital, but for the purpose of constructing the MO diagram we will ignore any contribution.
- The  $d_{z^2}$  orbital ( $a_1$ ) of sulfur is not energetically accessible so we do not include it, but we do consider the LGO that would interact with it.

In sketching the MO diagram, the s-orbital of sulfur is the lowest energy orbital depicted and as such will give the lowest energy bonding MO and likely the highest energy antibonding MO. We will have two  $a_1$  orbitals that will be labeled as non-bonding (nb), one for the  $p_z$  orbital with the lone pair, and one for the LGO that would match the  $d_{z^2}$  orbital. As we are considering the orbitals to be localized on specific atoms, we will not change their energy from that of the atomic orbital from which they are derived. That leaves the  $b_1$  and  $b_2$  orbitals that will make a bonding and antibonding set. At first glance, you might expect these to be degenerate as they both are derived from p-orbitals on sulfur and the corresponding LGOs. However, upon examining the pictures above, (Figure 5.5.2.3), it might be expected that the  $b_1$  bonding orbital might be slightly lower in energy than the  $b_2$  since there is a more direct overlap between the sulfur orbital and the LGO. For now we will treat the orbitals as being degenerate. This would lead to a MO diagram as pictured below (Figure 5.5.2.4).



(Figure 5.5.2.4). MO diagram for  $\text{SF}_4$ .

Overall, this would give a bond order =  $\frac{6-0}{2} = 3$  which is quite different from the Lewis structure. The bonding in structures of p-block elements with 'expanded' octets is not as straightforward as the Lewis structure might suggest. There are filled bonding orbitals that involve more than two atoms. There are also significant ionic contributions to what is typically drawn as covalent bonds.

#### How did we do?

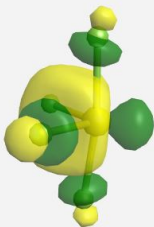
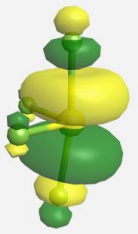
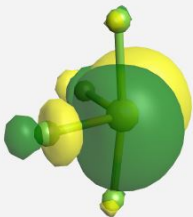
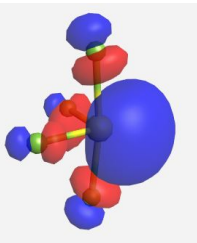
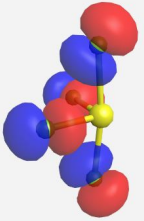
Our MO diagram was generated using a pictorial method. Using computational methods it is possible to derive a more accurate MO diagram for this molecule. Show below are the orbitals and their energies as calculated by WebMO (Table 5.5.2.3). Overall our MO diagram looks pretty good. We see a VERY slight difference in the energy of the  $b_1$  and  $b_2$  bonding orbitals. This difference is more pronounced in the antibonding orbitals. Based on the ABIMABTBIB principle, it is not surprising that we see a greater difference in the antibonding orbitals. So our approximation of the  $b_1$  and  $b_2$  orbitals as being degenerate is not unreasonable for the bonding MOs but not accurate for the antibonding.

You may also notice that all of the fluorine contributions are from p-orbitals. The 2s orbital of fluorine is much too low in energy to participate in these interactions. So the only orbital involved in bonding with the sulfur would be the p-orbital pointing directly at

the sulfur atom. This justifies our treatment of the fluorine as being hydrogen-like. Again, we are ignoring any possible  $\pi$ -bonding interactions in this molecule.

We also estimated that the  $a_1$  (nb) would not change in energy much from the atomic orbitals they were derived from. The energy for the  $a_1$  (nb) derived from the sulfur  $p_z$  is -12.049 eV which compares very favorably to the value of -12.0 eV for the 3p orbital of sulfur found in the previous page. For the  $a_1$  (nb) LGO, the energy was calculated to be -17.853 eV which is slightly higher than the -18.7 eV listed for the 2p orbitals of fluorine. Again, while not completely accurate, our pictorial method did a fairly reasonable job of generating the MO diagram.

**(Table 5.5.2.3).** The MOs for  $\text{SF}_4$  (ignoring the lone pairs) as calculated and displayed by [WebMO](#). The data for  $\text{SF}_4$  was imported into [WebMO](#) from the [NIST Webbook](#) as a computed 3-D structure and calculations were performed using B3LYP-6-31G(d).

Orbital	Label	Energy (eV)
	$a_1^*$	0.517
	$b_1^*$	-1.950
	$b_2^*$	-4.083
	$a_1$ (nb)	-12.049
	$a_1$ (nb)	-17.853

	$b_2$	-18.559
	$b_1$	-18.697
	$a_1$	-20.655

5.5.2: Expanded Octets and Molecular Orbitals is shared under a [not declared](#) license and was authored, remixed, and/or curated by LibreTexts.

## CHAPTER OVERVIEW

### Unit 6: Solid State Chemistry

#### 6.1: Solid State Structures

##### 6.1.1: Cubic Lattices and Close Packing

##### 6.1.2: Ionic Radii and Radius Ratios

#### 6.2: Crystalline Solids

##### 6.2.1: Types of Crystalline Solids

##### 6.2.2: Alloys and Intermetallics

##### 6.2.3: The Imperfect Solid State

#### 6.3: X-Ray Crystallography of Solids

##### 6.3.1: Miller Indices (hkl)

##### 6.3.2: X-rays and X-ray Diffraction

##### 6.3.3: Powder X-ray Diffraction

#### 6.4: Energetics of Ionic Solids

##### 6.4.1: Lattice Enthalpies of Ionic Solids

##### 6.4.2: Born Haber Cycles

##### 6.4.3: Lattice Energies and Solubility

##### 6.4.4: Theoretical Lattice Energy Calculations

##### 6.4.5: Kapustinskii Equation

#### 6.5: Band Theory and Conductivity

##### 6.5.1: Bonding in Metals and Semiconductors

##### 6.5.2: The Fermi Level

##### 6.5.3: Semiconductors- Band Gaps, Colors, Conductivity and Doping

##### 6.5.4: Periodic Trends- Metals, Semiconductors, and Insulators

##### 6.5.5: Semiconductor p-n Junctions

##### 6.5.6: Diodes, LEDs and Solar Cells

##### 6.5.7: Superconductors

---

Unit 6: Solid State Chemistry is shared under a [not declared](#) license and was authored, remixed, and/or curated by LibreTexts.

## 6.1: Solid State Structures

---

Learning objectives for this unit are to:

- Describe and identify a unit cell within a 2D or 3D lattice
  - Identify, describe, and compare the common Bravais Lattices, including primitive cubic, body-centered cubic, face-centered cubic (or cubic closest packed), and hexagonal closest-packed
  - Identify the locations and comparative sizes of tetrahedral, octahedral, and cubic holes within a closest-packed lattice
  - Use the “radius ratio rule” to predict lattice types for ionic solids and explain why certain types of holes are filled or empty
  - Calculate edge length, density, and packing efficiency for a given lattice
  - Determine the metallic or ionic radius given the lattice type and density
  - Determine the number of atoms per unit cell, the coordination number per atom, and the atom stoichiometry given a picture or description of a lattice structure
  - Describe the following common ionic structural motifs: sodium chloride, sphalerite, wurtzite, fluorite, and anti-fluorite.
- 

6.1: Solid State Structures is shared under a [not declared](#) license and was authored, remixed, and/or curated by LibreTexts.

## 6.1.1: Cubic Lattices and Close Packing

### Close-Packing of Identical Spheres

Crystals are of course three-dimensional objects, but we will begin by exploring the properties of arrays in two-dimensional space. This will make it easier to develop some of the basic ideas without the added complication of getting you to visualize in 3-D — something that often requires a bit of practice. Suppose you have a dozen or so marbles. How can you arrange them in a single compact layer on a table top? Obviously, they must be in contact with each other in order to minimize the area they cover. It turns out that there are two efficient ways of achieving this:



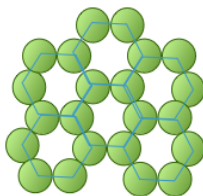
The essential difference here is that any marble within the interior of the square-packed array is in contact with four other marbles, while this number rises to six in the hexagonal-packed arrangement. It should also be apparent that the latter scheme covers a smaller area (contains less empty space) and is therefore a more efficient packing arrangement. If you are good at geometry, you can show that square packing covers 78 percent of the area, while hexagonal packing yields 91 percent coverage.

If we go from the world of marbles to that of atoms, which kind of packing would the atoms of a given element prefer?



If the atoms are identical and are bound together mainly by dispersion forces which are completely non-directional, they will favor a structure in which as many atoms can be in direct contact as possible. This will, of course, be the hexagonal arrangement.

Directed chemical bonds between atoms have a major effect on the packing. The version of hexagonal packing shown at the right occurs in the form of carbon known as *graphite* which forms 2-dimensional sheets. Each carbon atom within a sheet is bonded to three other carbon atoms. The result is just the basic hexagonal structure with some atoms missing.



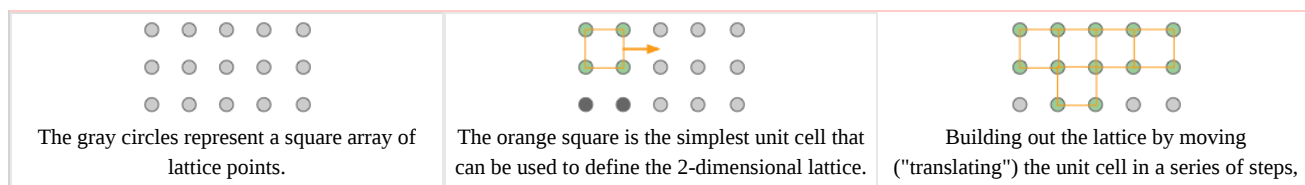
The coordination number of 3 reflects the  $sp^2$ -hybridization of carbon in graphite, resulting in plane-trigonal bonding and thus the sheet structure. Adjacent sheets are bound by weak dispersion forces, allowing the sheets to slip over one another and giving rise to the lubricating and flaking properties of graphite.

### Lattices

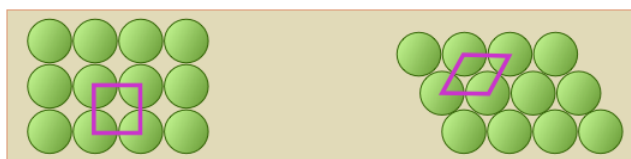
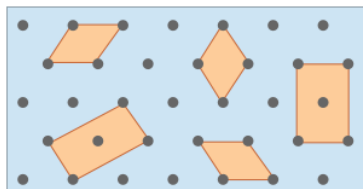
The underlying order of a crystalline solid can be represented by an array of regularly spaced points that indicate the locations of the crystal's basic structural units. This array is called a crystal lattice. Crystal lattices can be thought of as being built up from repeating units containing just a few atoms. These repeating units act much as a rubber stamp: press it on the paper, move ("translate") it by an amount equal to the lattice spacing, and stamp the paper again.



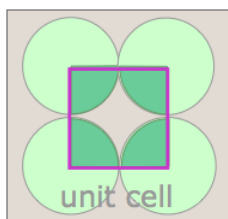




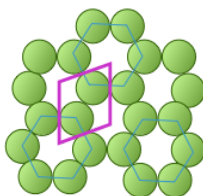
Although real crystals do not actually grow in this manner, this process is conceptually important because it allows us to classify a lattice type in terms of the simple repeating unit that is used to "build" it. We call this shape the *unit cell*. Any number of primitive shapes can be used to define the unit cell of a given crystal lattice. The one that is actually used is largely a matter of convenience, and it may contain a lattice point in its center, as you see in two of the unit cells shown here. In general, the best unit cell is the simplest one that is capable of building out the lattice.



Shown above are unit cells for the close-packed square and hexagonal lattices we discussed near the start of this lesson. Although we could use a hexagon for the second of these lattices, the rhombus is preferred because it is simpler.



Notice that in both of these lattices, the corners of the unit cells are centered on a lattice point. This means that an atom or molecule located on this point in a real crystal lattice is shared with its neighboring cells. As is shown more clearly here for a two-dimensional square-packed lattice, a single unit cell can claim "ownership" of only one-quarter of each molecule, and thus "contains"  $4 \times \frac{1}{4} = 1$  molecule.

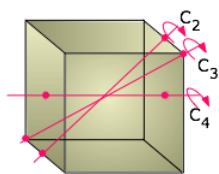


The unit cell of the graphite form of carbon is also a rhombus, in keeping with the hexagonal symmetry of this arrangement. Notice that to generate this structure from the unit cell, we need to shift the cell in both the  $x$ - and  $y$ - directions in order to leave empty spaces at the correct spots. We could alternatively use regular hexagons as the unit cells, but the  $x+y$  shifts would still be required, so the simpler rhombus is usually preferred. As you will see in the next section, the empty spaces within these unit cells play an important role when we move from two- to three-dimensional lattices.

## Cubic crystals

In order to keep this lesson within reasonable bounds, we are limiting it mostly to crystals belonging to the so-called *cubic* system. In doing so, we can develop the major concepts that are useful for understanding more complicated structures (as if there are not

enough complications in cubics alone!) But in addition, it happens that cubic crystals are very commonly encountered; most metallic elements have cubic structures, and so does ordinary salt, sodium chloride.

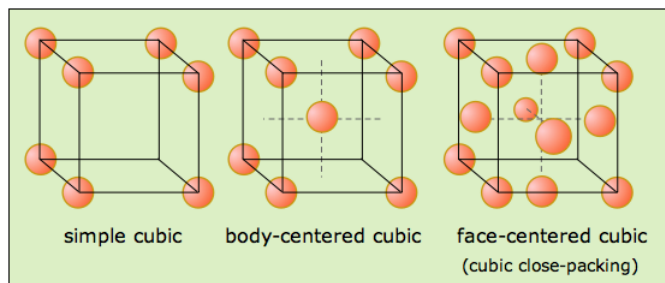


We usually think of a cubic shape in terms of the equality of its edge lengths and the  $90^\circ$  angles between its sides, but there is another way of classifying shapes that chemists find very useful. This is to look at what *geometric transformations* (such as rotations around an axis) we can perform that leave the appearance unchanged. For example, you can rotate a cube  $90^\circ$  around an axis perpendicular to any pair of its six faces without making any apparent change to it. We say that the cube possesses three mutually perpendicular *four-fold rotational axes*, abbreviated  $C_4$  axes. But if you think about it, a cube can also be rotated around the axes that extend between opposite corners; in this case, it takes three  $120^\circ$  rotations to go through a complete circle, so these axes (also four in number) are three-fold or  $C_3$  axes.

Cubic crystals belong to one of the seven crystal systems whose lattice points can be extended indefinitely to fill three-dimensional space and which can be constructed by successive translations (movements) of a primitive unit cell in three dimensions. As we will see below, the cubic system, as well as some of the others, can have variants in which additional lattice points can be placed at the center of the unit or at the center of each face.

### The three types of cubic lattices

The three Bravais lattices which form the cubic crystal system are shown here.

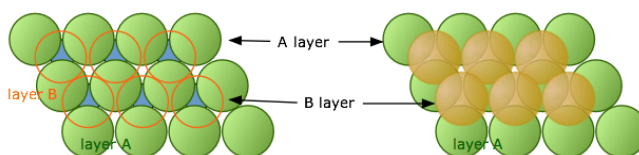


Structural examples of all three are known, with body- and face-centered (BCC and FCC) being much more common; most metallic elements crystallize in one of these latter forms. But although the simple cubic structure is uncommon by itself, it turns out that many BCC and FCC structures composed of ions can be regarded as interpenetrating combinations of two simple cubic lattices, one made up of positive ions and the other of negative ions. Notice that only the FCC structure, which we will describe below, is a close-packed lattice within the cubic system.

### Close-packed lattices in three dimensions

Close-packed lattices allow the maximum amount of interaction between atoms. If these interactions are mainly attractive, then close-packing usually leads to more energetically stable structures. These lattice geometries are widely seen in metallic, atomic, and simple ionic crystals.

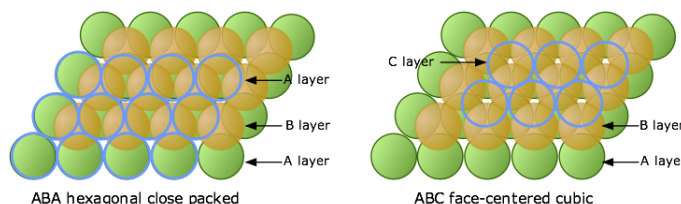
As we pointed out above, hexagonal packing of a single layer is more efficient than square-packing, so this is where we begin. Imagine that we start with the single layer of green atoms shown below. We will call this the A layer. If we place a second layer of atoms (orange) on top of the A-layer, we would expect the atoms of the new layer to nestle in the hollows in the first layer. But if all the atoms are identical, only some of these void spaces will be accessible.



In the diagram on the left, notice that there are two classes of void spaces between the A atoms; one set (colored blue) has a vertex pointing up, while the other set (not colored) has down-pointing vertices. Each void space constitutes a depression in which atoms of a second layer (the B-layer) can nest. The two sets of void spaces are completely equivalent, but only one of these sets can be occupied by a second layer of atoms whose size is similar to those in the bottom layer. In the illustration on the right above we have arbitrarily placed the B-layer atoms in the blue voids, but could just as well have selected the white ones.

### Two choices for the third layer lead to two different close-packed lattice types

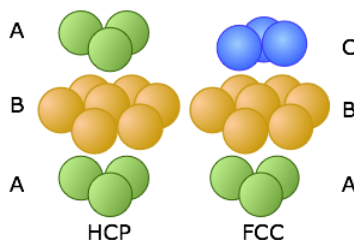
Now consider what happens when we lay down a third layer of atoms. These will fit into the void spaces within the B-layer. As before, there are two sets of these positions, but unlike the case described above, they are not equivalent.



The atoms in the third layer are represented by open blue circles in order to avoid obscuring the layers underneath. In the illustration on the left, this third layer is placed on the B-layer at locations that are directly above the atoms of the A-layer, so our third layer is just another A layer. If we add still more layers, the vertical sequence A-B-A-B-A-B-A... repeats indefinitely.

In the diagram on the right above, the blue atoms have been placed above the white (unoccupied) void spaces in layer A. Because this third layer is displaced horizontally (in our view) from layer A, we will call it layer C. As we add more layers of atoms, the sequence of layers is A-B-C-A-B-C-A-B-C..., so we call it ABC packing.

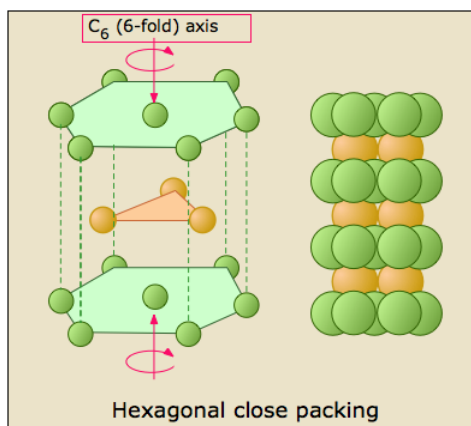
For the purposes of clarity, only three atoms of the A and C layers are shown in these diagrams. But in reality, each layer consists of an extended hexagonal array; the two layers are simply displaced from one another.



These two diagrams that show exploded views of the vertical stacking further illustrate the rather small fundamental difference between these two arrangements— but, as you will see below, they have widely divergent structural consequences. Note the opposite orientations of the A and C layers

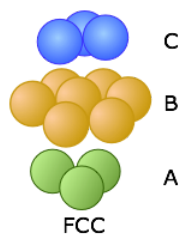
### The Hexagonal closed-packed structure

The HCP stacking shown on the left just above takes us out of the cubic crystal system into the hexagonal system, so we will not say much more about it here except to point out each atom has 12 nearest neighbors: six in its own layer, and three in each layer above and below it.

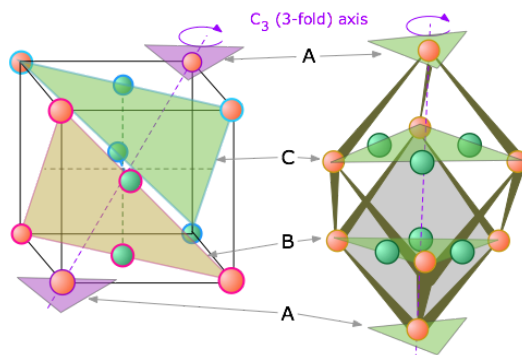


### The cubic close-packed structure

Below we reproduce the FCC structure that was shown above.



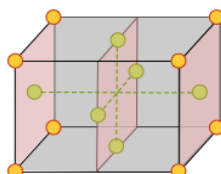
You will notice that the B-layer atoms form a hexagon, but this is a *cubic* structure. How can this be? The answer is that the FCC stack is inclined with respect to the faces of the cube, and is in fact coincident with one of the three-fold axes that passes through opposite corners. It requires a bit of study to see the relationship, and we have provided two views to help you. The one on the left shows the cube in the normal isometric projection; the one on the right looks down upon the top of the cube at a slightly inclined angle.



Both the CCP and HCP structures fill 74 percent of the available space when the atoms have the same size. You should see that the two shaded planes cutting along diagonals within the interior of the cube contain atoms of different colors, meaning that they belong to different layers of the CCP stack. Each plane contains three atoms from the B layer and three from the C layer, thus reducing the symmetry to  $C_3$ , which a cubic lattice must have.

### The FCC unit cell

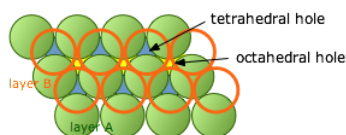
The figure below shows the the face-centered cubic unit cell of a cubic-close packed lattice.



How many atoms are contained in a unit cell? Each corner atom is shared with eight adjacent unit cells and so a single unit cell can claim only  $1/8$  of each of the eight corner atoms. Similarly, each of the six atoms centered on a face is only half-owned by the cell. The grand total is then  $(8 \times 1/8) + (6 \times 1/2) = 4$  atoms per unit cell.

## Interstitial Void Spaces

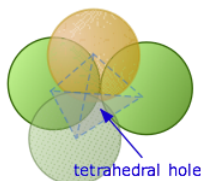
The atoms in each layer in these close-packing stacks sit in a depression in the layer below it. As we explained above, these void spaces are not completely filled. (It is geometrically impossible for more than two identical spheres to be in contact at a single point.) We will see later that these *interstitial void spaces* can sometimes accommodate additional (but generally smaller) atoms or ions.



If we look down on top of two layers of close-packed spheres, we can pick out two classes of void spaces which we call *tetrahedral* and *octahedral holes*.

### Tetrahedral holes

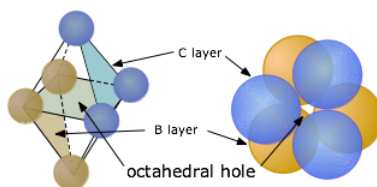
If we direct our attention to a region in the above diagram where a single atom is in contact with the three atoms in the layers directly below it, the void space is known as a *tetrahedral hole*. A similar space will be found between this single atom and the three atoms (not shown) that would lie on top of it in an extended lattice. Any interstitial atom that might occupy this site will interact with the four atoms surrounding it, so this is also called a *four-coordinate interstitial space*.



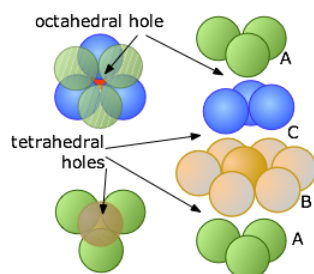
Don't be misled by this name; the boundaries of the void space are spherical sections, not tetrahedra. The tetrahedron is just an imaginary construction whose four corners point to the centers of the four atoms that are in contact.

### Octahedral holes

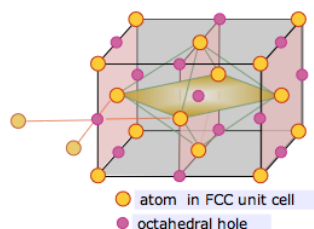
Similarly, when two sets of three trigonally-oriented spheres are in close-packed contact, they will be oriented  $60^\circ$  apart and the centers of the spheres will define the six corners of an imaginary octahedron centered in the void space between the two layers, so we call these *octahedral holes* or *six-coordinate interstitial sites*. Octahedral sites are larger than tetrahedral sites.



An octahedron has six corners and eight sides. We usually draw octahedra as a double square pyramid standing on one corner (left), but in order to visualize the octahedral shape in a close-packed lattice, it is better to think of the octahedron as lying on one of its faces (right).



Each sphere in a close-packed lattice is associated with one octahedral site, whereas there are only half as many tetrahedral sites. This can be seen in this diagram that shows the central atom in the B layer in alignment with the hollows in the C and A layers above and below.



The face-centered cubic unit cell contains a single octahedral hole within itself, but octahedral holes shared with adjacent cells exist at the centers of each edge. Each of these twelve edge-located sites is shared with four adjacent cells, and thus contributes  $(12 \times \frac{1}{4}) = 3$  atoms to the cell. Added to the single hole contained in the middle of the cell, this makes a total of 4 octahedral sites per unit cell. This is the same as the number we calculated above for the number of atoms in the cell.

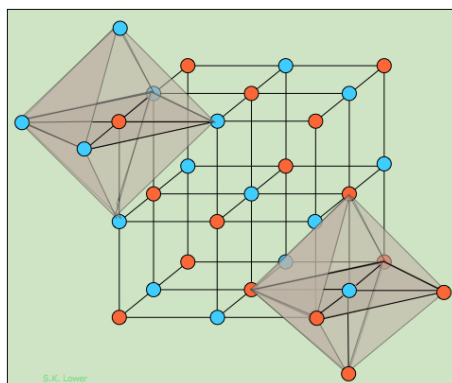
## Common cubic close-packed structures

It can be shown from elementary trigonometry that an atom will fit exactly into an octahedral site if its radius is 0.414 as great as that of the host atoms. The corresponding figure for the smaller tetrahedral holes is 0.225.

Many pure metals and compounds form face-centered cubic (cubic close-packed) structures. The existence of tetrahedral and octahedral holes in these lattices presents an opportunity for "foreign" atoms to occupy some or all of these interstitial sites. In order to retain close-packing, the interstitial atoms must be small enough to fit into these holes without disrupting the host CCP lattice. When these atoms are too large, which is commonly the case in ionic compounds, the atoms in the interstitial sites will push the host atoms apart so that the face-centered cubic lattice is somewhat opened up and loses its close-packing character.

### The rock-salt structure

Alkali halides that crystallize with the "rock-salt" structure exemplified by sodium chloride can be regarded either as a FCC structure of one kind of ion in which the octahedral holes are occupied by ions of opposite charge, or as two interpenetrating FCC lattices made up of the two kinds of ions. The two shaded octahedra illustrate the identical coordination of the two kinds of ions; each atom or ion of a given kind is surrounded by six of the opposite kind, resulting in a coordination expressed as (6:6).

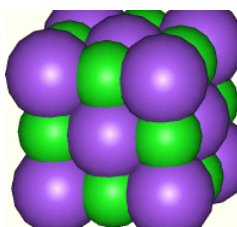


How many NaCl units are contained in the unit cell? If we ignore the atoms that were placed outside the cell in order to construct the octahedra, you should be able to count fourteen "orange" atoms and thirteen "blue" ones. But many of these are shared with adjacent unit cells.

An atom at the corner of the cube is shared by eight adjacent cubes, and thus makes a  $1/8$  contribution to any one cell. Similarly, the center of an edge is common to four other cells, and an atom centered in a face is shared with two cells. Taking all this into consideration, you should be able to confirm the following tally showing that there are four AB units in a unit cell of this kind.

Orange	Blue
8 at corners: $8 \times 1/8 = 1$	12 at edge centers: $12 \times 1/4 = 3$
6 at face centers: $6 \times 1/2 = 3$	1 at body center = 1
total: 4	total: 4

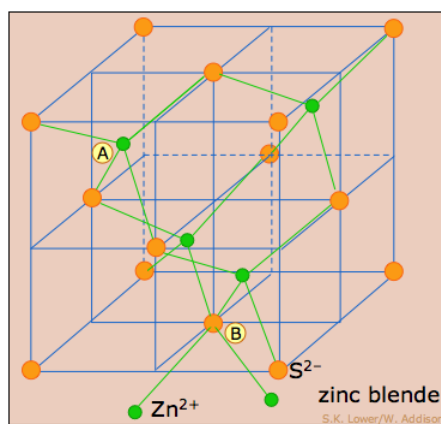
If we take into consideration the actual sizes of the ions ( $\text{Na}^+ = 116 \text{ pm}$ ,  $\text{Cl}^- = 167 \text{ pm}$ ), it is apparent that neither ion will fit into the octahedral holes with a CCP lattice composed of the other ion, so the actual structure of NaCl is somewhat expanded beyond the close-packed model.



The space-filling model on the right depicts a face-centered cubic unit cell of chloride ions (purple), with the sodium ions (green) occupying the octahedral sites.

#### The zinc-blende structure: using some tetrahedral holes

Since there are two tetrahedral sites for every atom in a close-packed lattice, we can have binary compounds of 1:1 or 1:2 stoichiometry depending on whether half or all of the tetrahedral holes are occupied. Zinc-blende is the mineralogical name for zinc sulfide,  $\text{ZnS}$ . An impure form known as *sphalerite* is the major ore from which zinc is obtained.

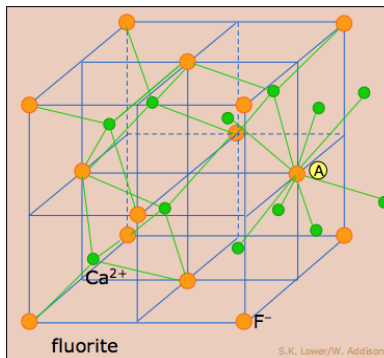


This structure consists essentially of a FCC (CCP) lattice of sulfur atoms (orange) (equivalent to the lattice of chloride ions in NaCl) in which zinc ions (green) occupy half of the tetrahedral sites. As with any FCC lattice, there are four atoms of sulfur per unit cell, and the the four zinc atoms are totally contained in the unit cell. Each atom in this structure has **four** nearest neighbors, and is thus tetrahedrally coordinated.

It is interesting to note that if all the atoms are replaced with carbon, this would correspond to the *diamond* structure.

### The fluorite structure: all tetrahedral sites occupied

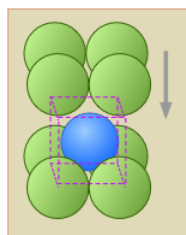
Fluorite,  $\text{CaF}_2$ , having twice as many ions of fluoride as of calcium, makes use of all eight tetrahedral holes in the CPP lattice of calcium ions (orange) depicted here. To help you understand this structure, we have shown some of the octahedral sites in the next cell on the right; you can see that the calcium ion at **A** is surrounded by eight fluoride ions, and this is of course the case for all of the calcium sites. Since each fluoride ion has four nearest-neighbor calcium ions, the coordination in this structure is described as (8:4).



Although the radii of the two ions ( $\text{F}^- = 117 \text{ pm}$ ,  $\text{Ca}^{2+} = 126 \text{ pm}$ ) does not allow true close packing, they are similar enough that one could just as well describe the structure as a FCC lattice of fluoride ions with calcium ions in the octahedral holes.

### Simple- and body-centered cubic structures

In Section 4 we saw that the only cubic lattice that can allow close packing is the face-centered cubic structure. The simplest of the three cubic lattice types, the *simple cubic lattice*, lacks the hexagonally-arranged layers that are required for close packing. But as shown in this exploded view, the void space between the two square-packed layers of this cell constitutes an octahedral hole that can accommodate another atom, yielding a packing arrangement that in favorable cases can approximate true close-packing. Each second-layer B atom (blue) resides within the unit cell defined the A layers above and below it.

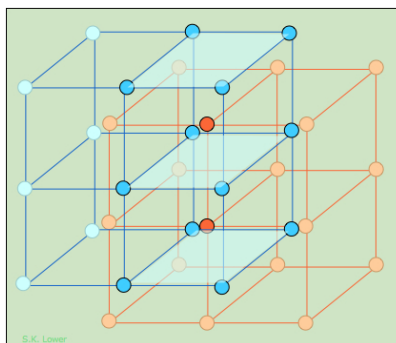


The A and B atoms can be of the same kind or they can be different. If they are the same, we have a *body-centered cubic lattice*. If they are different, and especially if they are oppositely-charged ions (as in the CsCl structure), there are size restrictions: if the B atom is too large to fit into the interstitial space, or if it is so small that the A layers (which all carry the same electric charge) come into contact without sufficient A-B coulombic attractions, this structural arrangement may not be stable.

### The cesium chloride structure

CsCl is the common model for the BCC structure. As with so many other structures involving two different atoms or ions, we can regard the same basic structure in different ways. Thus if we look beyond a single unit cell, we see that CsCl can be represented as two interpenetrating simple cubic lattices in which each atom occupies an octahedral hole within the cubes of the other lattice.





This page titled [6.1.1: Cubic Lattices and Close Packing](#) is shared under a [CC BY 3.0](#) license and was authored, remixed, and/or curated by [Stephen Lower](#) via [source content](#) that was edited to the style and standards of the LibreTexts platform.

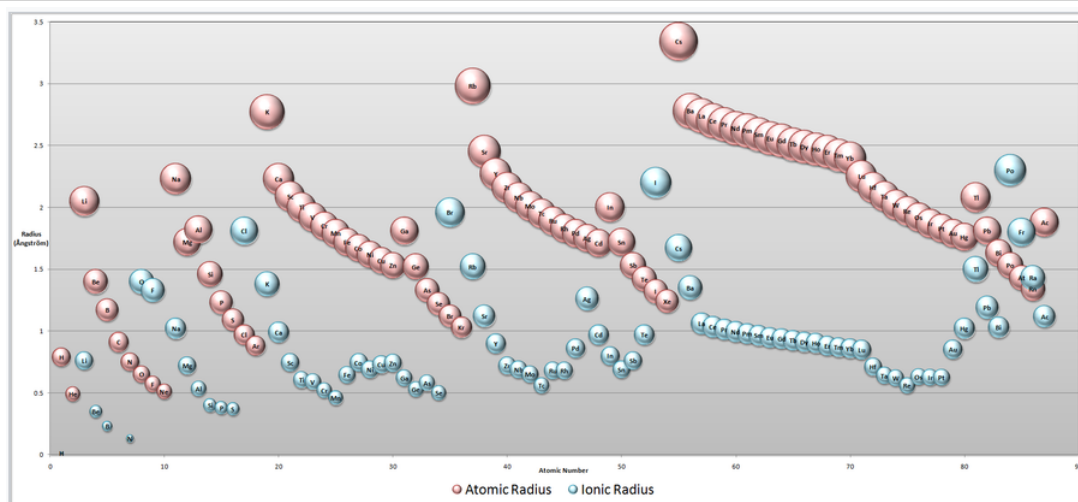
- **7.8: Cubic Lattices and Close Packing** by [Stephen Lower](#) is licensed [CC BY 3.0](#). Original source: <http://www.chem1.com/acad/webtext/virtualtextbook.html>.

## 6.1.2: Ionic Radii and Radius Ratios

Atoms in crystals are held together by electrostatic forces, van der Waals interactions, and covalent bonding. It follows that arrangements of atoms that can maximize the strength of these attractive interactions should be most favorable and lead to the most commonly observed crystal structures.

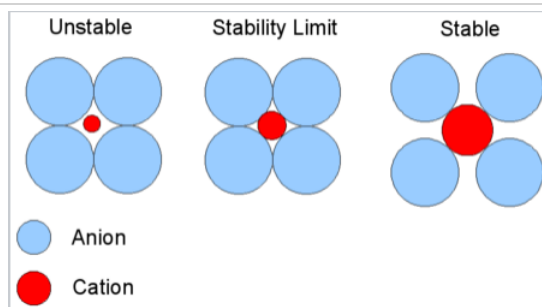
### Radius ratio rules

Early crystallographers had trouble solving the structures of inorganic solids using X-ray diffraction because some of the mathematical tools for analyzing the data had not yet been developed. Once a trial structure was proposed, it was relatively easy to calculate the diffraction pattern, but it was difficult to go the other way (from the diffraction pattern to the structure) if nothing was known *a priori* about the arrangement of atoms in the unit cell. It was (and still is!) important to develop some guidelines for guessing the coordination numbers and bonding geometries of atoms in crystals. The first such rules were proposed by Linus Pauling, who considered how one might pack together oppositely charged spheres of different radii. Pauling proposed from geometric considerations that the quality of the "fit" depended on the **radius ratio** of the anion and the cation.



**Atomic and Ionic Radii.** Note that cations are always smaller than the neutral atom (pink) of the same element, whereas anions are larger. Going from left to right across any row of the periodic table, neutral atoms and cations contract in size because of increasing nuclear charge. (click for larger image)

The basic idea of radius ratio rules is illustrated at the right. We consider that the anion is the packing atom in the crystal and the smaller cation fills interstitial sites ("holes"). Cations will find arrangements in which they can contact the largest number of anions. If the cation can touch all of its nearest neighbor anions, as shown at the right for a small cation in contact with larger anions, then the fit is good. If the cation is too small for a given site, that coordination number will be unstable and it will prefer a lower coordination number structure. The table below gives the ranges of cation/anion radius ratios that give the best fit for a given coordination geometry.



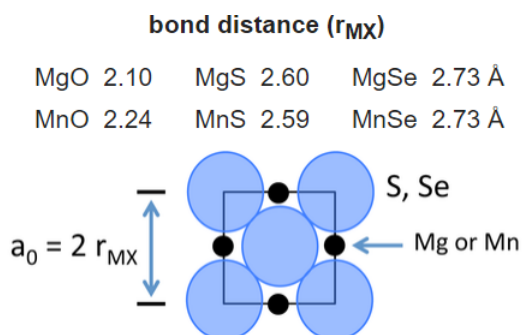
**Critical Radius Ratio.** This diagram is for coordination number six: 4 anions in the plane are shown, 1 is above the plane and 1 is below. The stability limit is at  $r_C/r_A = 0.414$

Coordination number	Geometry	$\rho = r_{\text{cation}}/r_{\text{anion}}$
2	linear	0 - 0.155
3	triangular	0.155 - 0.225
4	tetrahedral	0.225 - 0.414
4	square planar	0.414 - 0.732
6	octahedral	0.414 - 0.732
8	cubic	0.732 - 1.0
12	cuboctahedral	1.0

There are unfortunately several challenges with using this idea to predict crystal structures:

- We don't know the radii of individual ions
- Atoms in crystals are not really ions - there is a varying degree of covalency depending electronegativity differences
- Bond distances (and therefore ionic radii) depend on bond strength and coordination number (remember Pauling's rule  $D(n) = D(1) - 0.6 \log n$ )
- Ionic radii depend on oxidation state (higher charge => smaller cation size, larger anion size)

We can build up a table of ionic radii by assuming that the bond length is the sum of the radii ( $r_+ + r_-$ ) if the ions are in contact in the crystal. Consider for example the compounds  $\text{MgX}$  and  $\text{MnX}$ , where  $\text{X} = \text{O}, \text{S}, \text{Se}$ . All of these compounds crystallize in the NaCl structure:



For the two larger anions ( $\text{S}^{2-}$  and  $\text{Se}^{2-}$ ), the unit cell dimensions are the same for both cations. This suggests that the anions are in contact in these structures. From geometric considerations, the anion radius in this case is given by:

$$r_{-} = \frac{r_{\text{MX}}}{\sqrt{2}}$$

and thus the radii of the  $\text{S}^{2-}$  and  $\text{Se}^{2-}$  ions are 1.84 and 1.93 Å, respectively. Once the sizes of these anions are fixed, we can obtain a self-consistent set of cation and anion radii from the lattice constants of many MX compounds.

How well does this model work? Let's consider the structures of tetravalent metal oxides ( $\text{MO}_2$ ), using Pauling radii and the predictions of the radius ratio model:

Oxide $\text{MO}_2$	Radius ratio	Predicted coord. no.	Observed coord no. (structure)
$\text{CO}_2$	~0.1	2	2 (linear molecule)
$\text{SiO}_2$	0.32	4	4 (various tetrahedral structures)
$\text{GeO}_2$	0.43	4	4 (silica-like structures)
"	0.54	6	6 (rutile)
$\text{TiO}_2$	0.59	6	6 (rutile)
$\text{ZrO}_2$	0.68	6	7 (baddleyite)
"	0.77	8	8 (fluorite)

ThO <sub>2</sub>	0.95	8	8 (fluorite)
------------------	------	---	--------------

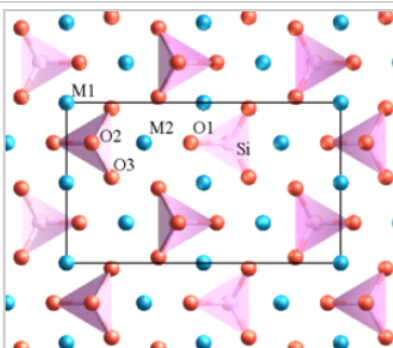
Note that cations have different radii depending on their coordination numbers, and thus different radius ratios are calculated for Ge<sup>4+</sup> with coordination numbers 4 and 6, and for Zr<sup>4+</sup> with coordination numbers 6 and 8.

For this series of oxides, the model appears to work quite well. The correct coordination number is predicted in all cases, and borderline cases such as GeO<sub>2</sub> and ZrO<sub>2</sub> are found in structures with different coordination numbers. The model also correctly predicts the structures of BeF<sub>2</sub> (SiO<sub>2</sub> type), MgF<sub>2</sub> (rutile), and CaF<sub>2</sub> (fluorite).

What about the alkali halides NaCl, KBr, LiI, CsF, etc.? All of them have the NaCl structure except for CsCl, CsBr, and CsI, which have the CsCl (8-8) structure. In this case the radius ratio model fails rather badly. The Li<sup>+</sup> salts LiBr and LiI are predicted to have tetrahedral structures, and KF is predicted to have an 8-8 structure like CsCl. We can try adjusting the radii (e.g., making the cations larger and anions smaller), but the best we can do with the alkali halides is predict about half of their structures correctly. Since the alkali halides are clearly ionic compounds, this failure suggests that there is something very wrong with the radius ratio model, and its success with MO<sub>2</sub> compounds was coincidental.

In addition to the radius ratio rule, Linus Pauling developed other useful rules that are helpful in rationalizing and also predicting the structures of inorganic compounds. Pauling's rules<sup>[1]</sup> state that:

- Stable structures are **locally electroneutral**. For example, in the structure of the double perovskite Sr<sub>2</sub>FeMoO<sub>6</sub>, MO<sub>6</sub> (M = Fe<sup>2+</sup>, Mo<sup>6+</sup>) octahedra share all their vertices, and Sr<sup>2+</sup> ions fill the cubooctahedral cavities that are flanked by eight MO<sub>6</sub> octahedra.<sup>[2]</sup> Each O<sup>2-</sup> ion is coordinated to one Fe<sup>2+</sup> and one Mo<sup>6+</sup> ion in order to achieve local electroneutrality, and thus the FeO<sub>6</sub> and MoO<sub>6</sub> octahedra alternate in the structure.
- **Cation-cation repulsion** should be minimized. Anion polyhedra can share vertices (as in the perovskite structure) without any energetic penalty. Shared polyhedral edges, and especially shared faces, cause cation-cation repulsion and should be avoided. For example, in rutile, the most stable polymorph of TiO<sub>2</sub>, the TiO<sub>6</sub> octahedra share vertices and two opposite edges, forming ribbons in the structure. In anatase TiO<sub>2</sub>, each octahedron shares four edges so the anatase polymorph is less thermodynamically stable.
- **Highly charged cations** in anion polyhedra tend not to share edges or even vertices, especially when the coordination number is low. For example, in orthosilicates such as olivine (M<sub>2</sub>SiO<sub>4</sub>), there are isolated SiO<sub>4</sub><sup>4-</sup> tetrahedra.



Structure of olivine. M (Mg or Fe) = blue spheres, Si = pink tetrahedra, O = red spheres.

As we will soon see, all of Pauling's rules are justified on the basis of lattice energy considerations. In ionic compounds, the arrangement of atoms that maximizes anion-cation interactions while minimizing cation-cation and anion-anion contacts is energetically the best.

6.1.2: Ionic Radii and Radius Ratios is shared under a CC BY-SA license and was authored, remixed, and/or curated by LibreTexts.

- **9.1: Ionic Radii and Radius Ratios** by Chemistry 310 is licensed CC BY-SA 4.0. Original source: [https://en.wikibooks.org/wiki/Introduction\\_to\\_Inorganic\\_Chemistry](https://en.wikibooks.org/wiki/Introduction_to_Inorganic_Chemistry).

## 6.2: Crystalline Solids

---

Learning objectives for this unit are to:

- Compare and contrast the structures and properties of the four types of crystalline solids
  - Explain the concept of polymorphism
  - Describe and/or identify substitutional, interstitial, and intermetallic alloys
  - Compare and contrast intrinsic and extrinsic defects, and point, line and plane defects
  - Describe and/or identify Schottky and Frenkel defects
- 

6.2: Crystalline Solids is shared under a [not declared](#) license and was authored, remixed, and/or curated by LibreTexts.

## 6.2.1: Types of Crystalline Solids

When most liquids are cooled, they eventually freeze and form crystalline solids, solids in which the atoms, ions, or molecules are arranged in a definite repeating pattern. It is also possible for a liquid to freeze before its molecules become arranged in an orderly pattern. The resulting materials are called amorphous solids or noncrystalline solids (or, sometimes, glasses). The particles of such solids lack an ordered internal structure and are randomly arranged (Figure 6.2.1.1).

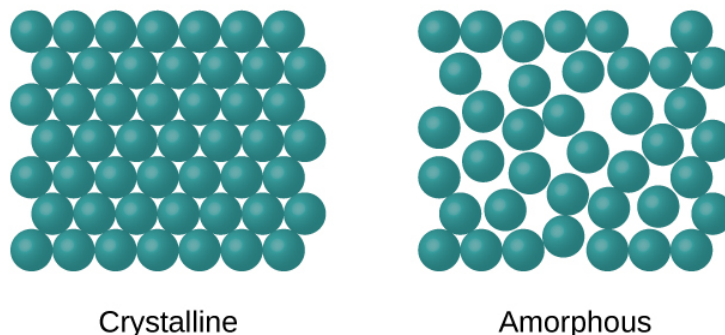


Figure 6.2.1.1: The entities of a solid phase may be arranged in a regular, repeating pattern (crystalline solids) or randomly (amorphous).

The crystalline arrangement shows many circles drawn in rows and stacked together tightly. The amorphous arrangement shows many circles spread slightly apart and in no organized pattern.

Metals and ionic compounds typically form ordered, crystalline solids. Substances that consist of large molecules, or a mixture of molecules whose movements are more restricted, often form amorphous solids. For examples, candle waxes are amorphous solids composed of large hydrocarbon molecules. Some substances, such as boron oxide (Figure 6.2.1.2), can form either crystalline or amorphous solids, depending on the conditions under which it is produced. Also, amorphous solids may undergo a transition to the crystalline state under appropriate conditions.

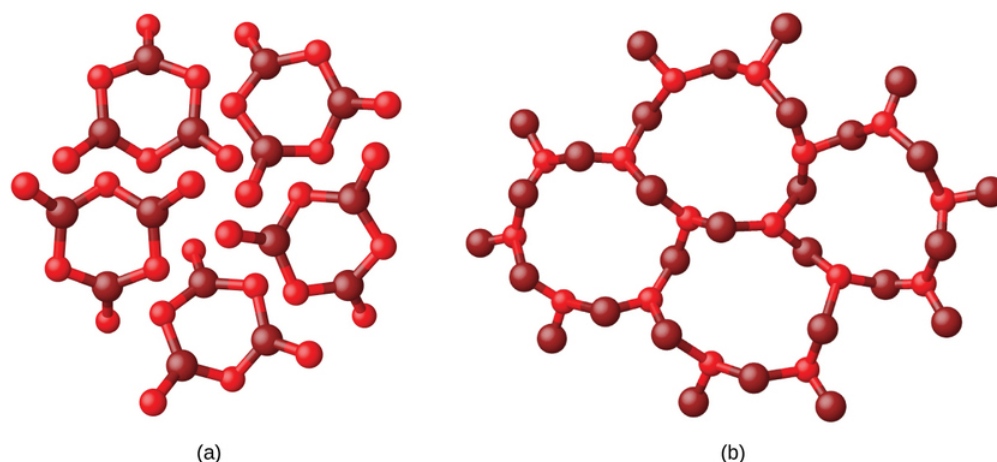


Figure 6.2.1.2: (a) Diboron trioxide,  $B_2O_3$ , is normally found as a white, amorphous solid (a glass), which has a high degree of disorder in its structure. (b) By careful, extended heating, it can be converted into a crystalline form of  $B_2O_3$ , which has a very ordered arrangement.

The first structure of diboron trioxide shows five identical and separated hexagonal rings. The second structure of diboron trioxide shows a more interconnected structure with four large rings forming a more stable structure.

Crystalline solids are generally classified according to the nature of the forces that hold its particles together. These forces are primarily responsible for the physical properties exhibited by the bulk solids. The following sections provide descriptions of the major types of crystalline solids: ionic, metallic, covalent network, and molecular.

### Ionic Solids

Ionic solids, such as sodium chloride and nickel oxide, are composed of positive and negative ions that are held together by electrostatic attractions, which can be quite strong (Figure 6.2.1.3). Many ionic crystals also have high melting points. This is due to the very strong attractions between the ions—in ionic compounds, the attractions between full charges are (much) larger than

those between the partial charges in polar molecular compounds. This will be looked at in more detail in a later discussion of lattice energies. Although they are hard, they also tend to be brittle, and they shatter rather than bend. Ionic solids do not conduct electricity; however, they do conduct when molten or dissolved because their ions are free to move. Many simple compounds formed by the reaction of a metallic element with a nonmetallic element are ionic.

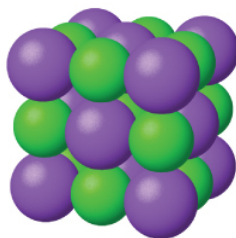


Figure 6.2.1.3: Sodium chloride is an ionic solid.

A cube composed of purple and green spheres is shown. The cube has dimensions of three by three spheres. The purple spheres are slightly larger than the green spheres.

## Metallic Solids

Metallic solids such as crystals of copper, aluminum, and iron are formed by metal atoms. Figure 6.2.1.4 The structure of metallic crystals is often described as a uniform distribution of atomic nuclei within a “sea” of delocalized electrons. The atoms within such a metallic solid are held together by a unique force known as *metallic bonding* that gives rise to many useful and varied bulk properties. All exhibit high thermal and electrical conductivity, metallic luster, and malleability. Many are very hard and quite strong. Because of their malleability (the ability to deform under pressure or hammering), they do not shatter and, therefore, make useful construction materials. The melting points of the metals vary widely. Mercury is a liquid at room temperature, and the alkali metals melt below 200 °C. Several post-transition metals also have low melting points, whereas the transition metals melt at temperatures above 1000 °C. These differences reflect differences in strengths of metallic bonding among the metals.

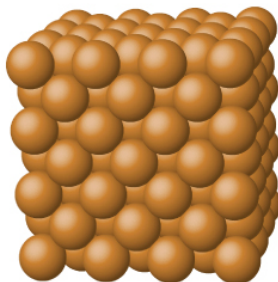


Figure 6.2.1.4: Copper is a metallic solid.

## Covalent Network Solids

Covalent network solids include crystals of diamond, silicon, some other nonmetals, and some covalent compounds such as silicon dioxide (sand) and silicon carbide (carborundum, the abrasive on sandpaper). Many minerals have networks of covalent bonds. The atoms in these solids are held together by a network of covalent bonds, as shown in Figure 6.2.1.5 To break or to melt a covalent network solid, covalent bonds must be broken. Because covalent bonds are relatively strong, covalent network solids are typically characterized by hardness, strength, and high melting points. For example, diamond is one of the hardest substances known and melts above 3500 °C.

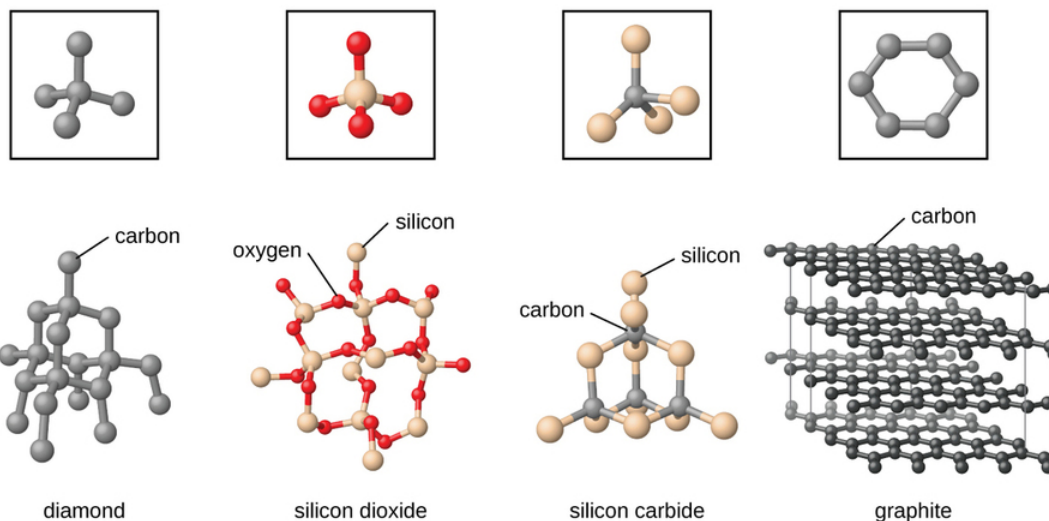


Figure 6.2.1.5. A covalent crystal contains a three-dimensional network of covalent bonds, as illustrated by the structures of diamond, silicon dioxide, silicon carbide, and graphite. Graphite is an exceptional example, composed of planar sheets of covalent crystals that are held together in layers by noncovalent forces. Unlike typical covalent solids, graphite is very soft and electrically conductive.

The complex three dimensional structure of diamond, silicon dioxide, silicon carbide and graphite is shown along with a smaller repeating unit of the structure shown above each structure.

## Molecular Solids

Molecular solids, such as ice, sucrose (table sugar), and iodine, as shown in Figure 6.2.1.6 are composed of neutral molecules. The strengths of the attractive forces between the units present in different crystals vary widely, as indicated by the melting points of the crystals. Small symmetrical molecules (nonpolar molecules), such as  $H_2$ ,  $N_2$ ,  $O_2$ , and  $F_2$ , have weak attractive forces and form molecular solids with very low melting points (below  $-200\text{ }^{\circ}\text{C}$ ). Substances consisting of larger, nonpolar molecules have larger attractive forces and melt at higher temperatures. Molecular solids composed of molecules with permanent dipole moments (polar molecules) melt at still higher temperatures. Examples include ice (melting point,  $0\text{ }^{\circ}\text{C}$ ) and table sugar (melting point,  $185\text{ }^{\circ}\text{C}$ ).

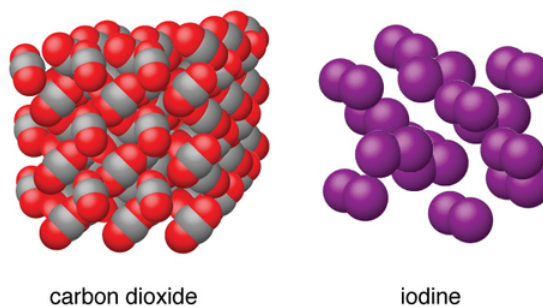


Figure 6.2.1.6: Carbon dioxide ( $CO_2$ ) consists of small, nonpolar molecules and forms a molecular solid with a melting point of  $-78\text{ }^{\circ}\text{C}$ . Iodine ( $I_2$ ) consists of larger, nonpolar molecules and forms a molecular solid that melts at  $114\text{ }^{\circ}\text{C}$ .

On the left, many red and grey molecules are densely stacked in a 3-D drawing to represent carbon dioxide. On the right, purple molecules are scattered randomly to represent iodine.

## Properties of Solids

A crystalline solid, like those listed in Table 6.2.1.1 has a precise melting temperature because each atom or molecule of the same type is held in place with the same forces or energy. Thus, the attractions between the units that make up the crystal all have the same strength and all require the same amount of energy to be broken. The gradual softening of an amorphous material differs dramatically from the distinct melting of a crystalline solid. This results from the structural nonequivalence of the molecules in the amorphous solid. Some forces are weaker than others, and when an amorphous material is heated, the weakest intermolecular attractions break first. As the temperature is increased further, the stronger attractions are broken. Thus amorphous materials soften over a range of temperatures.

Table 6.2.1.1: Types of Crystalline Solids and Their Properties



Type of Solid	Type of Particles	Type of Attractions	Properties	Examples
ionic	ions	ionic bonds	hard, brittle, conducts electricity as a liquid but not as a solid, high to very high melting points	NaCl, Al <sub>2</sub> O <sub>3</sub>
metallic	atoms of electropositive elements	metallic bonds	shiny, malleable, ductile, conducts heat and electricity well, variable hardness and melting temperature	Cu, Fe, Ti, Pb, U
covalent network	atoms of electronegative elements	covalent bonds	very hard, not conductive, very high melting points	C (diamond), SiO <sub>2</sub> , SiC
molecular	molecules (or atoms)	IMFs	variable hardness, variable brittleness, not conductive, low melting points	H <sub>2</sub> O, CO <sub>2</sub> , I <sub>2</sub> , C <sub>12</sub> H <sub>22</sub> O <sub>11</sub>

### Graphene: Material of the Future

Carbon is an essential element in our world. The unique properties of carbon atoms allow the existence of carbon-based life forms such as ourselves. Carbon forms a huge variety of substances that we use on a daily basis, including those shown in Figure 6.2.1.7. You may be familiar with diamond and graphite, the two most common *allotropes* of carbon. (Allotropes are different structural forms of the same element.) Diamond is one of the hardest-known substances, whereas graphite is soft enough to be used as pencil lead. These very different properties stem from the different arrangements of the carbon atoms in the different allotropes.

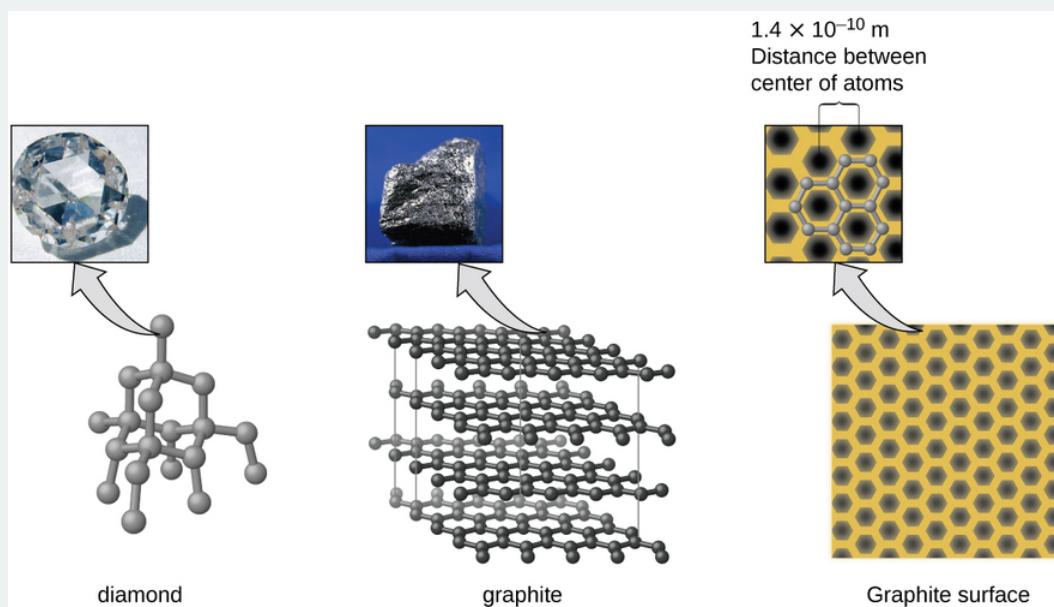


Figure 6.2.1.7: Diamond is extremely hard because of the strong bonding between carbon atoms in all directions. Graphite (in pencil lead) rubs off onto paper due to the weak attractions between the carbon layers. An image of a graphite surface shows the distance between the centers of adjacent carbon atoms. (credit left photo: modification of work by Steve Jurvetson; credit middle photo: modification of work by United States Geological Survey)

A close up of a piece of diamond shows a three dimensional structure of a complex network of well bonded carbon atoms. A close up of a graphite shows several layers of carbon sheets. Each sheet is composed of a repeated and connected hexagonal structure of carbon atoms. The third diagram shows that the distance between the center of atoms is 1.4 times 10 to the power of negative 10 meters.

You may be less familiar with a recently discovered form of carbon: graphene. Graphene was first isolated in 2004 by using tape to peel off thinner and thinner layers from graphite. It is essentially a single sheet (one atom thick) of graphite. Graphene, illustrated in Figure 6.2.1.8 is not only strong and lightweight, but it is also an excellent conductor of electricity and heat.

These properties may prove very useful in a wide range of applications, such as vastly improved computer chips and circuits, better batteries and solar cells, and stronger and lighter structural materials. The 2010 Nobel Prize in Physics was awarded to Andre Geim and Konstantin Novoselov for their pioneering work with graphene.

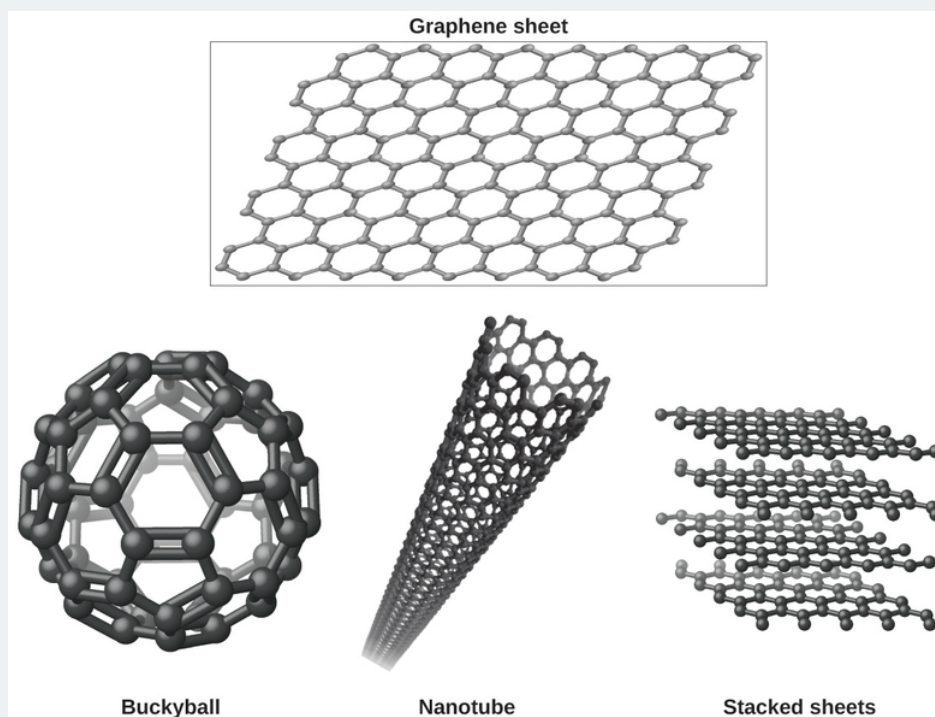


Figure 6.2.1.8: Graphene sheets can be formed into buckyballs, nanotubes, and stacked layers.

A sheet of interconnected hexagonal rings is shown at the top. Below it, a buckyball is shown which is a sphere composed of hexagonal rings. In the lower middle image, a nanotube is shown that is made by rolling a graphene sheet into a tube. In the lower right image, stacked sheets made up of four horizontal sheets composed of joined, hexagonal rings are shown.

## Crystal Defects

In a crystalline solid, the atoms, ions, or molecules are arranged in a definite repeating pattern, but occasional defects may occur in the pattern. Several types of defects are known, as illustrated in Figure 6.2.1.9. Vacancies are defects that occur when positions that should contain atoms or ions are vacant. Less commonly, some atoms or ions in a crystal may occupy positions, called interstitial sites, located between the regular positions for atoms. Other distortions are found in impure crystals, as, for example, when the cations, anions, or molecules of the impurity are too large to fit into the regular positions without distorting the structure. Trace amounts of impurities are sometimes added to a crystal (a process known as *doping*) in order to create defects in the structure that yield desirable changes in its properties. For example, silicon crystals are doped with varying amounts of different elements to yield suitable electrical properties for their use in the manufacture of semiconductors and computer chips.

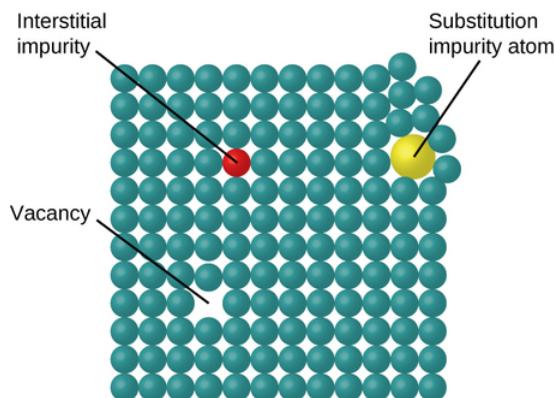


Figure 6.2.1.9: Types of crystal defects include vacancies, interstitial atoms, and substitution impurities.

## Summary

Some substances form crystalline solids consisting of particles in a very organized structure; others form amorphous (noncrystalline) solids with an internal structure that is not ordered. The main types of crystalline solids are ionic solids, metallic solids, covalent network solids, and molecular solids. The properties of the different kinds of crystalline solids are due to the types of particles of which they consist, the arrangements of the particles, and the strengths of the attractions between them. Because their particles experience identical attractions, crystalline solids have distinct melting temperatures; the particles in amorphous solids experience a range of interactions, so they soften gradually and melt over a range of temperatures. Some crystalline solids have defects in the definite repeating pattern of their particles. These defects (which include vacancies, atoms or ions not in the regular positions, and impurities) change physical properties such as electrical conductivity, which is exploited in the silicon crystals used to manufacture computer chips.

---

This page titled [6.2.1: Types of Crystalline Solids](#) is shared under a [CC BY 4.0](#) license and was authored, remixed, and/or curated by [OpenStax](#).

- [10.6: The Solid State of Matter](#) by [OpenStax](#) is licensed [CC BY 4.0](#). Original source: <https://openstax.org/details/books/chemistry-2e>.

## 6.2.2: Alloys and Intermetallics

When a molten metal is mixed with another substance, there are two mechanisms that can cause an alloy to form: (1) *atom exchange* or (2) *interstitial mechanism*. The relative size of each element in the mix plays a primary role in determining which mechanism will occur.

### Substitutional Alloys

When the atoms are relatively similar in size, the atom exchange method usually happens, where some of the atoms composing the metallic crystals are substituted with atoms of the other constituent. This is called a *substitutional alloy*. Examples of substitutional alloys include bronze and brass, in which some of the copper atoms are substituted with either tin or zinc atoms.

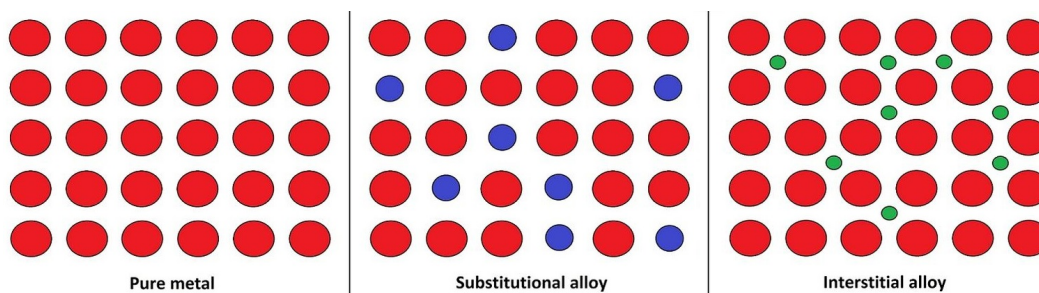


Figure 6.2.2.1: Different atomic mechanisms of alloy formation, showing pure metal, substitutional, and interstitial structures. (CCO; Hbf878 via Wikipedia)

### Why Substitutional Alloys Occur: Bonding

The bonding between two metals is best described as a combination of metallic electron "sharing" and covalent bonding, one can't occur without the other and the proportion of one to the other changes depending on the constituents involved. Metals share their electrons throughout their structure, this flow of electrons is the reason behind many of the characteristics associated with metals, including their ability to act as conductors. The different amount and strength of covalent bonds can change depending on the different specific metals involved and how they are mixed. The covalent bonding is what is responsible for the crystal structure as well as the melting point and various other physical properties.

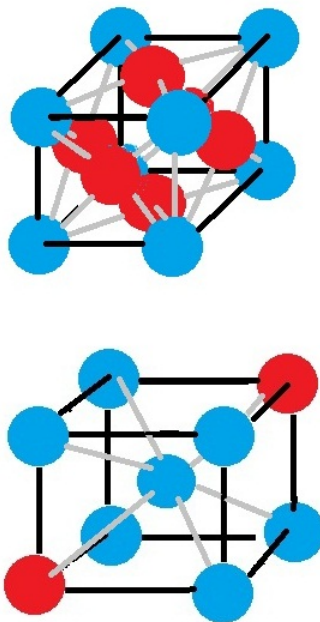


Figure 6.2.2.2: Examples of Substitutional Metal Alloys. Depending on the specific type of substitutional alloy they can have multiple crystal structures. Two of the possible structures include Face Center Cubic (left), and Cubic Center Cubic (right). The structure of the metal alloy is not limited to these two structures, but combined they represent a large portion of the common alloys.

As the similarities between the electron structure of the metals involved in the alloy increase, the metallic characteristics of the alloy decrease. Pure metals are useful but their applications are often limited to each individual metal's properties. Alloys allow metal mixtures that have increased resistance to oxidation, increased strength, conductivity, and melting point; Essentially any property can be manipulated by adjusting alloy concentrations. An example could be Brass Door fixtures, they are strong and resist corrosion better than pure zinc or copper, the two major metals that constitute a brass alloy. The combination also has a low melting point allowing it to be easily cast into many different shapes and sizes.<sup>(1)</sup> There are many other aspects of substitutional alloys that could be explored in depth, but the basic concept is the idea that each individual metal in an alloy give the final product its chemical and physical properties.

Substitutional alloys played an important role in the development of human society and culture as we know it today. The Bronze age itself is named after the Substitutional alloy consisting of tin in a metallic solution of copper. Ancient bronzes are very impure, or even mislabeled, containing large amounts of zinc and arsenic as well as lots of impurities. These many substitutional alloys allowed for stronger tools and weapons, they allowed for increased productivity in the workshop as well as on the battlefield. The need for raw materials like tin and copper for the production of bronze also spurred an increase in trade, since their ores are rarely found together. The current chemical understanding of substitutional alloys would not be so in depth if it weren't for the usefulness of the alloys to humans.

### Interstitial Alloys

With the interstitial mechanism, one atom is usually much smaller than the other, so cannot successfully replace an atom in the crystals of the base metal. The smaller atoms become trapped in the spaces between the atoms in the crystal matrix, called the *interstices*. This is referred to as an *interstitial alloy*. Steel is an example of an interstitial alloy, because the very small carbon atoms fit into interstices of the iron matrix. Stainless steel is an example of a combination of interstitial and substitutional alloys, because the carbon atoms fit into the interstices, but some of the iron atoms are replaced with nickel and chromium atoms.

### Intermetallics

Intermetallic compounds are solid phases containing two or more metallic elements, with optionally one or more non-metallic elements, whose crystal structure differs from that of the other constituents.

## Summary

An alloy is a mixture of metals that has bulk metallic properties different from those of its constituent elements. Alloys can be formed by substituting one metal atom for another of similar size in the lattice (substitutional alloys), by inserting smaller atoms into holes in the metal lattice (interstitial alloys), or by a combination of both. Although the elemental composition of most alloys can vary over wide ranges, certain metals combine in only fixed proportions to form intermetallic compounds.

## References

1. Smallman, R. E., Ngan, A. H. W., & Smallman, R. E. (2007). *Physical metallurgy and advanced materials*. Amsterdam: Butterworth Heinemann.
2. Wang, F. E.. (2005). *Bonding theory for metals and alloys*. Amsterdam: Elsevier.
3. Dickinson, O. T. P. K. (1994). *The Aegean Bronze age*. Cambridge world archeology. Cambridge: Cambridge University Press.

## Problems

1. Are substitutional metal alloys naturally occurring on earth's surface?
2. What are two characteristics of a metal required for a substitutional alloy to form?
3. Can Oxygen or Nitrogen be a part of the crystal structure of a substitutional alloy?

## Solutions

1. No, the oxidizing nature of the earth's atmosphere, as well as the need for specific and concentrated metals keeps these from being found naturally occurring.
2. Similar radii and similar electronegativity.
3. Only metallic elements can form the necessary metallic bonds that allow alloys to form.

---

6.2.2: Alloys and Intermetallics is shared under a [not declared](#) license and was authored, remixed, and/or curated by LibreTexts.

- [6.7A: Substitutional Alloys](#) is licensed [CC BY-NC-SA 4.0](#).

## 6.2.3: The Imperfect Solid State

### 6.2.3.1: INTRODUCTION

Real crystals are never perfect: they always contain a considerable density of defects and imperfections that affect their physical, chemical, mechanical and electronic properties. The existence of defects also plays an important role in various technological processes and phenomena such as annealing, precipitation, diffusion, sintering, oxidation and others. It should be noted that defects do not necessarily have adverse effects on the properties of materials. There are many situations in which a judicious control of the types and amounts of imperfections can bring about specific characteristics desired in a system. This can be achieved by proper processing techniques. In fact, “defect engineering” is emerging as an important activity.

All defects and imperfections can be conveniently considered under four main divisions: *point defects*, *line defects* or dislocations, *planar defects* or interfacial or grain boundary defects, and *volume defects*. We can also add here *macroscopic* or *bulk defects* such as pores, cracks and foreign inclusions that are introduced during production and processing of the solid state. Point defects are inherent to the equilibrium state and thus determined by temperature, pressure and composition of a given system. The presence and concentration of other defects, however, depend on the way the solid was originally formed and subsequently processed.

Briefly consider the effects of *imperfections* or crystal defects on a few important properties of solids. The electrical behavior of semiconductors, for example, is largely controlled by crystal imperfections. The conductivity of silicon can thus be altered in type (n or p) and by over eight orders of magnitude through the addition of minute amounts of electrically active dopant elements. In this case, each atom of dopant, substitutionally incorporated, represents a point defect in the silicon lattice. The fact that such small amounts of impurity atoms can significantly alter the electrical properties of semiconductors is responsible for the development of the transistor and has opened up the entire field of solid state device technology. Practically none of the semiconducting properties that led to these engineering accomplishments are found in a “perfect” crystal. They are properties peculiar to the defective solid state.

The existence of dislocations (line defects) in crystals provides a mechanism by which permanent change of shape or mechanical deformation can occur. A crystalline solid free of dislocations is brittle and practically useless as an engineering material. While the existence of dislocations in crystals insures ductility (ability to deform), the theoretical strength of crystalline solids is drastically reduced by their presence.

We should recognize that dislocations play a central role in the determination of such important properties as strength and ductility. In fact, virtually all mechanical properties of crystalline solids are to a significant extent controlled by the behavior of line imperfections.

The ability of a ferromagnetic material (such as iron, nickel or iron oxide) to be magnetized and demagnetized depends in large part on the presence of two-dimensional imperfections known as *Bloch walls*. These interfaces are boundaries between two regions of the crystal which have a different magnetic state. As magnetization occurs, these defects migrate and by their motion provide the material with a net magnetic moment. Without the existence of Bloch walls all ferromagnetic materials would be permanent magnets. In fact, electromagnets would not exist if it were not for this type of defect.

The presence of surface defects such as cracks causes brittle materials like glass to break at small applied stresses. This fact is familiar to anyone who has broken a glass tube by first filing a small notch (or crack) into the surface. Removal of cracks from the surface of glass either by etching in hydrofluoric acid or by flame polishing almost always raises the fracture strength. For example, glass in the absence of any surface cracks has a fracture strength of  $\sim 10^{10}$  Newton/m<sup>2</sup> (as opposed to real glass which has a fracture strength of  $\sim 0^7$  Newton /m<sup>2</sup> ).

### 6.2.3.2: POINT DEFECTS

#### 6.2.3.2.1: Formation of Point Defects

An incontrovertible law of nature states: “Nothing is perfect”. This law applies to humans as well as to the inorganic world of crystalline solids and can be formulated as the 2nd law of thermodynamics:

$$F = H - TS \quad (1)$$

where  $F$  is the free energy of a given system,  $H$  is the heat content or enthalpy and  $TS$  is the entropy, or disorder, term. If a reaction takes place at a temperature  $T$ , we find the change in  $F$  ( $\Delta F$ ) related to a change in  $H$  ( $\Delta H$ ), the heat content, and possibly also a



change in TS ( $T\Delta S$ ). Such is the case when defects are formed in a perfect solid: The energy distribution in a solid (Maxwell-Boltzmann) suggests that a number of individual atoms may acquire enough thermal energy to be displaced from the equilibrium lattice site into an interstitial position. This process of point defect formation requires energy and leads to lattice strain which constitutes, as discussed earlier, an increase in the heat content of the system ( $\Delta H$  is positive and increases linearly with the number of defects formed). The departure from perfection by the generation of defects leads to disorder ( $\Delta S$  is positive). The magnitude of disorder generated ( $\Delta S$ ) is very large during the initial step from perfection to slight disarray, but the increase in disorder (with a given number of defects generated) decreases as the overall disorder increases.

Correspondingly the term  $T\Delta S$  drops rapidly at the beginning and then flattens out. The net result (fig. 1), free energy, exhibits a minimum for a certain number of defects in the

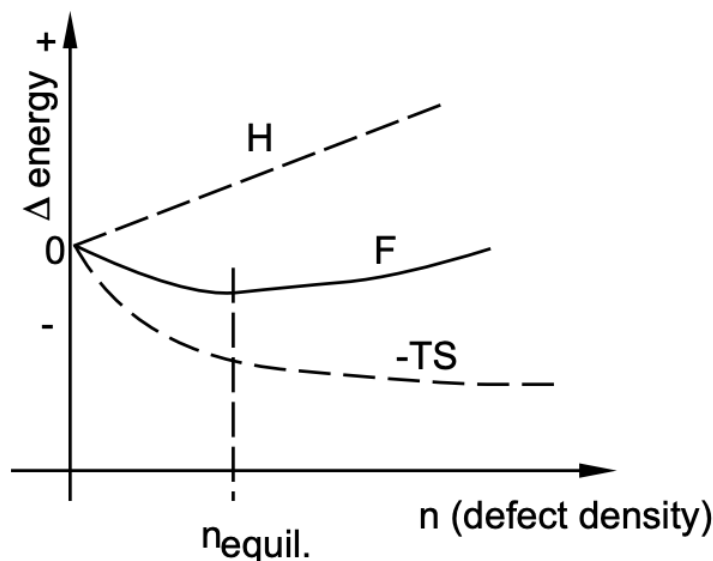


Figure 1 Thermodynamics of point defect formation

solid [equilibrium defect density =  $f$  (temperature)]; the  $F_{\text{minimum}}$  suggests also that the transition from perfection to equilibrium defect structure is spontaneous: it occurs naturally!

While the detailed mechanisms for the formation of atomic vacancies in solids are still the subject of extensive research, the associated equilibrium energetics are clear: calculations of the thermal energy of atoms in a lattice show that the average vibrational energy of lattice atoms is much less than 1eV (the approximate energy change associated with vacancy formation, i.e., the least amount of energy required to form a vacancy) at room temperature. Therefore a lattice atom will only acquire the energy  $\Delta H_d$ , the energy required to form the defect, upon the occurrence of a large energy fluctuation. Since the relative probability of an atom having an energy  $\Delta H_d$  or more in excess of the ground state energy is  $e^{-\Delta H_d/kT}$ , the probability that an atomic site is vacant varies in the same way. In a (molar) crystal containing  $N$  atomic sites, the number  $n_d$  of vacant sites is, therefore,

$$n_d = ANe^{-\Delta H_d/kT} \quad (2)$$

where

- $n_d$  is the number of defects (in equilibrium at  $T$ )
- $N$  is the total number of atomic sites per mole
- $\Delta H_d$  is the energy necessary to form the defect
- $T$  is the absolute temperature (K)
- $k$  is the Boltzmann constant
- $A$  is a proportionality constant

#### 6.2.3.2.2: Point Defects in "Pure" Metallic Systems

Point defects in "pure" crystalline metals are defects of atomic dimensions, such as impurity atoms, the absence of a matrix atom and/or the presence of a matrix atom in the wrong place. Some of these point defects are shown in fig. 2. An impurity atom



that occupies a normal lattice site is called a *substitutional impurity atom* and an impurity atom found in the interstice between matrix atoms is called an *interstitial impurity atom*. Whether a foreign atom will occupy a substitutional

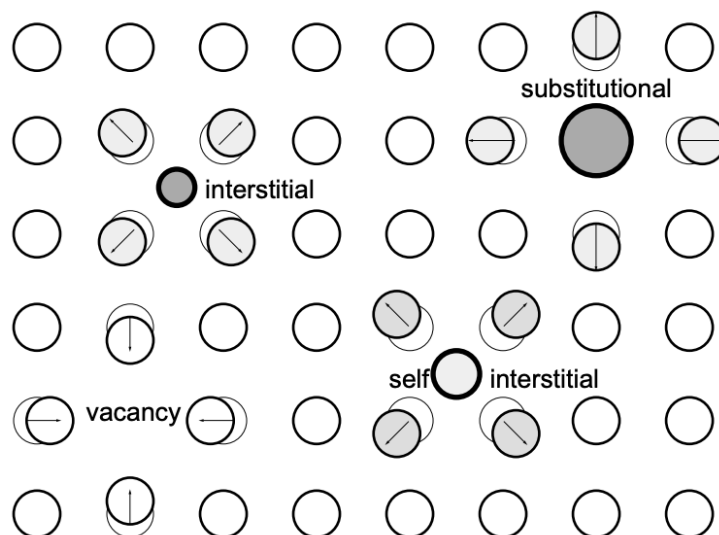


Figure 2 Point defects in crystalline solids

or interstitial site depends largely on the size of the atom relative to the size of the site. Small atoms are usually interstitial impurities, while larger atoms are usually substitutional impurities.

A *vacancy* is an atom site, normally occupied in the perfect crystal, from which an atom is missing. Often the term “vacancy” is used to denote a so-called *Schottky defect*, which is formed when an atom or an ion leaves a normal lattice site and repositions itself in a lattice site on the surface of the crystal. This may be the result of atomic rearrangement in an existing crystal at a high temperature when atomic mobility is high because of increased thermal vibrations. A vacancy may also originate in the process of crystallization as a result of local disturbances during the growth of new atomic planes on the crystal surface. Vacancies are point defects of a size nearly equal to the size of the original (occupied) site; the energy of the formation of a vacancy is relatively low - usually less than 1 eV.

The number of vacancies at equilibrium at each temperature in a crystal can be determined from eq. (2), in which  $\Delta H_d$  is the energy necessary to take an atom from a regular site of the crystal and place it on the surface for a Schottky-type defect. When a solid is heated a new higher equilibrium concentration of vacancies is established, usually first at crystal surfaces and then in the vicinity of dislocations and grain boundaries which provide sites for the atoms which have left their normal lattice site. Vacancies gradually spread throughout the crystal (from the surfaces into the bulk). On cooling the vacancy concentration is lowered by “diffusion of vacancies” to grain boundaries or dislocations, which act as sinks. In both cases, the new equilibrium vacancy concentration is established only after a finite amount of time. The rate at which vacancies move from point to point in the lattice decreases exponentially with decreasing temperature. Thus, on very rapid cooling (quenching) from a high temperature near the melting point most of the vacancies do not have time to diffuse to sinks and are said to be “frozen in”. This gives a considerably greater (“non-equilibrium”) concentration of vacancies in quenched specimens than that indicated by the thermal equilibrium value.

The concentration of vacant lattice sites in pure materials is very small at low temperatures - about one vacancy every  $10^8$  atom sites - and increases with increasing temperature to about one vacancy every  $10^3$  sites at the melting temperature. Vacancies are important because they control the rate of matrix (or substitutional) atom diffusion - i.e., atoms are able to move around in a crystalline solid primarily because of the presence of vacancies. (The mechanism by which they move is the same as that associated with moving a car in a filled parking lot to the exit). This is shown schematically in fig. 3. *Self-interstitials* are generally not encountered in close-packed

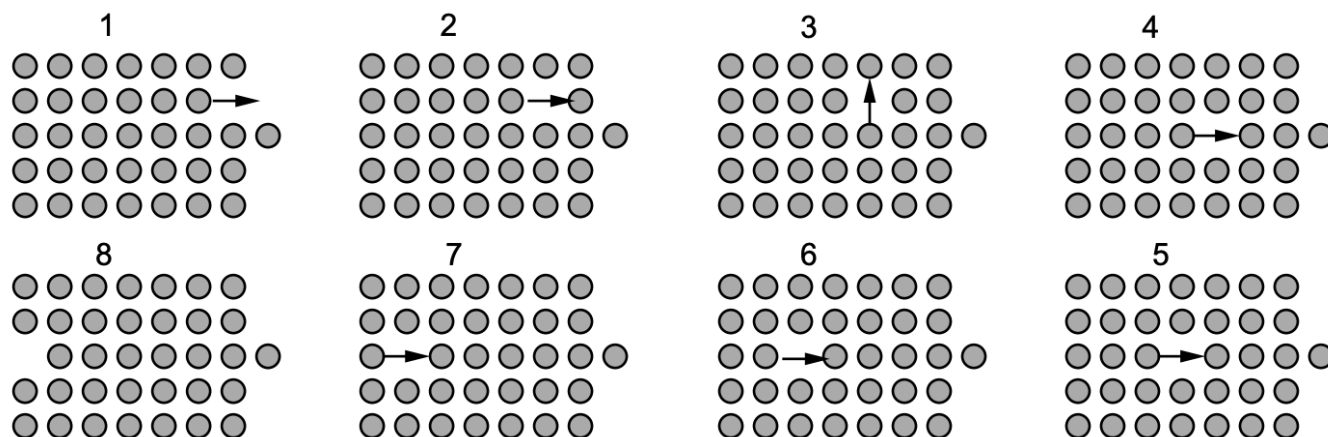


Figure 3 Dynamics of vacancy movements in a close packed solid

metallic systems, but may be introduced by irradiation. For example, high-energy neutrons from atomic fission can knock metal atoms from their regular sites into interstitial sites, creating vacancy-interstitial pairs.

#### 6.2.3.2.3: Point Defects in Ionic Solids

Point defects in ionic structures differ from those found in pure elements because of the charge neutrality requirement. For example, in a pure monovalent ionic material a cation vacancy must have associated with it either a cation interstitial or an anion vacancy to maintain charge neutrality. Similar requirements hold for anion vacancies. A vacancy pair defect (migration of a cation and an anion to the surface) is usually called a *Schottky imperfection*, and a vacancy-interstitial pair defect is referred to as a *Frenkel imperfection* (an anion or cation has left its lattice position, which becomes a vacancy, and has moved to an interstitial position). These two types of imperfections are shown in fig. 4. Self-interstitials are much more common in ionic structures than in pure elements because many ionic compounds have relatively large interstitial sites available. That is, there are often interstitial sites in the unit cell that have nearly the

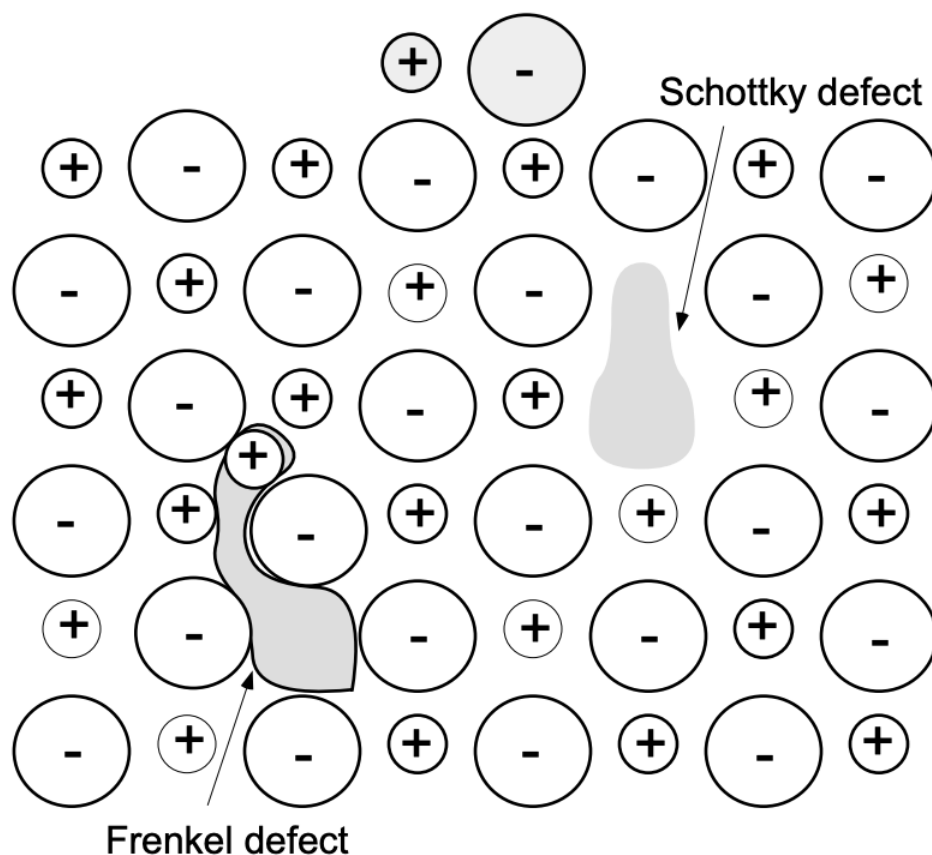


Figure 4 Point defects in ionic solids

same surroundings as normal atom sites. (For example, in BeO the Be atoms fill only one-half the available tetrahedral sites, leaving four possible cation interstitial sites per unit cell. Thus a Be atom could go from a regular lattice site to an almost equivalent interstitial site with little distortion of the lattice.)

*Foreign atoms* in ionic crystals produce defects that also must maintain charge neutrality. For example, in NaCl a monovalent cation, such as lithium, may simply replace one of the sodium ions as a substitutional impurity. But a divalent cation, such as calcium, replacing a sodium ion must be accompanied by either a cation vacancy or an anion interstitial if charge neutrality is to be maintained. Correspondingly, monovalent impurity cations in a divalent structure (e.g., Na in MgO) must be accompanied by an appropriate number of cation interstitials or anion vacancies.

#### 6.2.3.2.4: Point Defects in Covalently Bonded Solids

*Substitutional impurities* in covalently bonded materials can create a unique imperfection in the electronic structure if the impurity atom is from a group in the periodic table other than the matrix atoms. For example, you already considered Group V and Group III elements in a Group IV matrix, such as As or B in Si.

When foreign atoms are incorporated into a crystal structure, whether in substitutional or interstitial sites, we say that the resulting phase is a *solid solution* of the matrix material (solvent) and the foreign atoms (solute). The term “solid solution”, however, is not restricted to the low solute contents of doped semiconductor systems; there are many solid solutions, such as metallic alloys, that comprise a wide composition range.

#### 6.2.3.3: LINE DEFECTS

Line imperfections, or *dislocations*, in crystalline solids are defects that produce lattice distortions centered about a line. A dislocation is simply the edge of an extra inserted fractional plane of atoms (fig. 5). Normally the symbol  $\perp$  is used to represent a *positive*

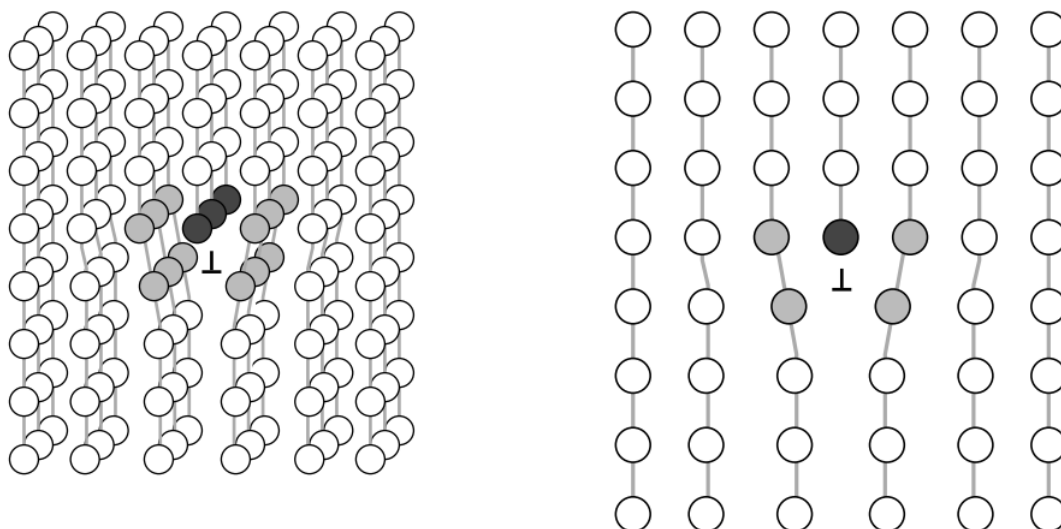


Figure 5 Schematic presentation of a dislocation; the last row of atoms (dark) in the inserted fractional plane *dislocation* (extra fractional plane) and  $\top$  is used to represent a *negative dislocation* (missing fractional plane).

The importance of dislocations is readily demonstrated in the deformation of crystalline materials. The plane in which a dislocation moves through the lattice is called a *slip plane*. With an applied shear stress the dislocation moves, atomic row by atomic row, and one part of the crystal is displaced relative to the other. When the dislocation has passed through the crystal, the portion of the crystal above the *slip plane* has shifted one atomic distance relative to the portion below the slip plane. In other words, the motion of the dislocation has caused the crystal to change its shape - to be permanently deformed (fig. 6).

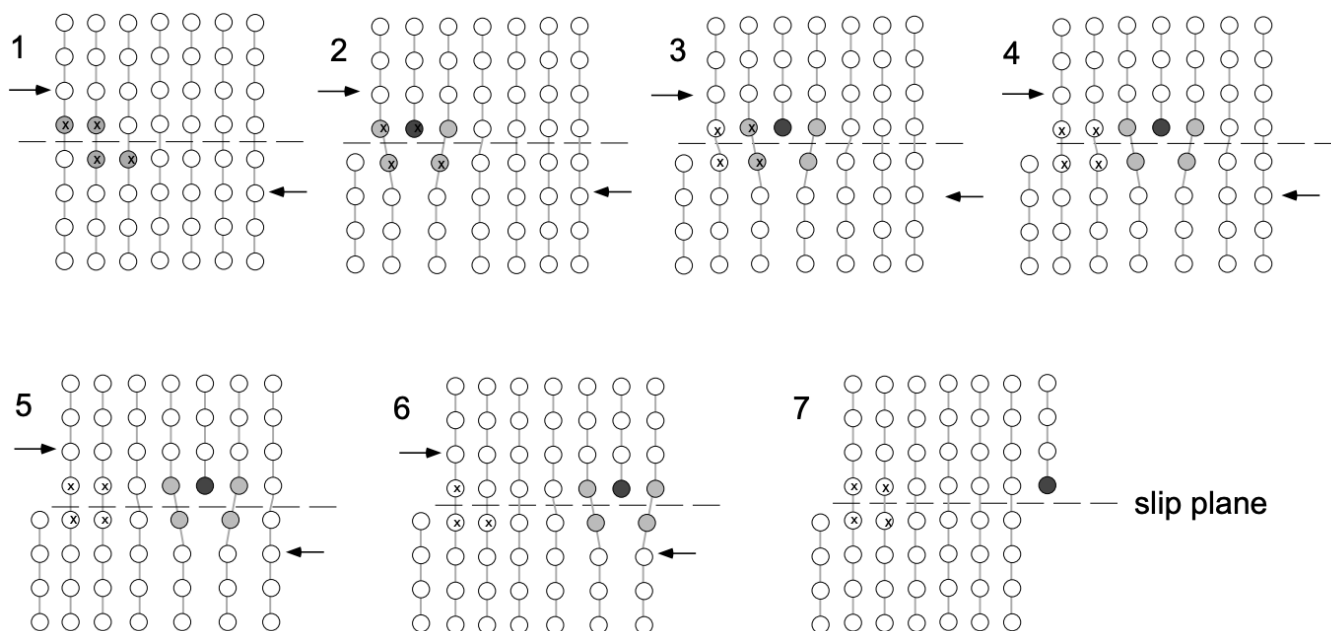


Figure 6 Plastic deformation of crystalline solid by slip associated with stress induced motion of dislocation

Please note: on either side of the dislocation the crystal lattice is essentially perfect, but in the immediate vicinity of the dislocation the lattice is severely distorted. For a positive edge dislocation, the presence of the extra half plane causes the atoms above the slip plane to be put in compression, while those below the slip plane are put in tension. Consequently, the edge dislocation will have a stress field around it that is compressive above the slip plane and tensile below the slip plane.

#### Plastic Deformation By Slip:

When single crystals of metal (or semiconductor) are pulled in tension, they will begin to deform (elongate) plastically at relatively low stress levels, and “blocks” of the crystals slide over one another because of dislocation motion. Simultaneously, so-called

*slip lines* appear on their surface. It is found that deformation by slip occurs most easily on planes with high atomic density and with large interplanar spacing, while the direction of slip is in all instances an atomically “close-packed direction”. For FCC structures we therefore observe as the primary slip system  $\{111\}$  planes in direction, while in BCC structures the primary slip occurs on  $\{110\}$  planes in directions. (It should be noted that an alternate deformation mechanism is “deformation twinning”, presently not to be considered.)

#### Dislocation Climb:

Climb is the name given to the motion of dislocations when the extra “half” plane is extended farther into a crystal or partially withdrawn from it. Clearly, the climb process is not a motion of the plane, but rather its growth or shrinking as a result of the addition of atoms or “vacancies” respectively from the environment of the dislocation (fig. 7).

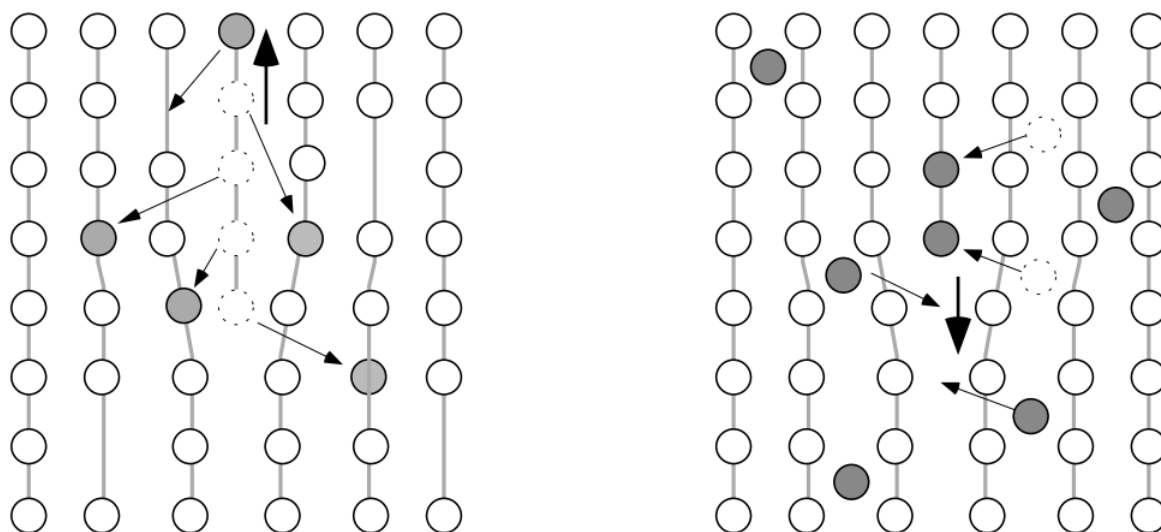


Figure 7 Dislocation climb by (a) loss of atoms to surrounding vacancies and (b) incorporation of interstitial atoms.

#### Multiplication of Dislocations:

Since during slip each dislocation leaves the matrix, macroscopic deformation could not take place given normal dislocation densities in the range of  $10^6 - 10^8/\text{cm}^3$ . Examination of the deformed crystals indicates that multiplication of dislocations takes place during deformation. While there are a multitude of multiplication mechanisms, the one most extensively studied is the Frank-Read Source (not to be discussed in detail).

#### Dislocation Interactions:

The relative ease with which dislocations move across a solid matrix can be attributed to the severe displacements of atoms in the core of dislocations. If these local stresses are reduced, the mobility of dislocations - and thus the ease of slip - is reduced. It is found that impurities in the vicinity of dislocation cores tend to reduce the local distortion energy of the dislocations and thus stabilize the system against slip. In many systems impurities are intentionally added (e.g., solid solution hardening) to increase the strength of materials. Similarly, micro-precipitates tend to impede dislocation motion (e.g., precipitation hardening).

### 6.2.3.4: INTERFACIAL IMPERFECTIONS

The several different types of interfacial, or planar imperfections, in solids can be grouped into the following categories:

1. Interfaces between solids and gases, which are called *free surfaces*;
2. Interfaces between regions where there is a change in the electronic structure, but no change in the periodicity of atom arrangement, known as *domain boundaries*;
3. Interfaces between two crystals or grains of the same phase where there is an orientation difference in the atom arrangement across the interface; these interfaces are called *grain boundaries*;
4. Interfaces between different phases, called *phase boundaries*, where there is generally a change of chemical composition and atom arrangement across the interface.

Grain boundaries are peculiar to crystalline solids, while free surfaces, domain boundaries and phase boundaries are found in both crystalline and amorphous solids.

#### 6.2.3.4.1: Free Surfaces

Because of their finite size, all solid materials have free surfaces. The arrangement of atoms at a free surface differs slightly from the interior structure because the surface atoms do not have neighboring atoms on one side. Usually the atoms near the surface have the same crystal structure but a slightly larger lattice parameter than the interior atoms.

Perhaps the most important aspect of free surfaces is the *surface energy* ( $\gamma$ ) associated with surfaces of any solid. The source of this surface energy may be seen by considering the surroundings of atoms on the surface and in the interior of a solid. To bring an atom from the interior to the surface, we must either break or distort some bonds - thereby increasing the energy. The surface energy is defined as the increase in energy per unit area of new surface formed. In crystalline solids, the surface energy depends on the crystallographic orientation of the surface - those surfaces that are planes of densest atomic packing are also the planes of lowest surface energy. This is because atoms on these surfaces have fewer of their bonds broken or, equivalently, have a larger number of nearest neighbors within the plane of the surface. Typical values of surface energies of solids range from about  $10^{-1}$  to  $1 \text{ J/m}^2$ . Generally, the stronger the bonding in the crystal, the higher the surface energy.

Surface energies can be reduced by the adsorption of foreign atoms or molecules from the surrounding atmosphere. For example, in mica the surface energy of freshly cleaved material in a vacuum is much higher than the surface energy of the same surface cleaved in air. In this instance, oxygen is adsorbed from the air to partially satisfy the broken bonds at the surface. Impurity atom adsorption makes it almost impossible to maintain atomically clean surfaces. As a result, surface properties such as electron emission, rates of evaporation and rates of chemical reactions are extremely dependent on the presence of any adsorbed impurities. These properties will be different if the measurements are made under conditions giving different surface adsorption.

#### 6.2.3.4.2: Grain Boundaries

Grain boundaries separate regions of different crystallographic orientation. The simplest form of a grain boundary is an interface composed of a parallel array of edge dislocations. This particular type of boundary is called a tilt boundary because the misorientation is in the form of a simple tilt about an axis, parallel to the dislocations. Tilt boundaries are referred to as low-angle boundaries because the angle of misorientation is generally less than  $10^\circ$ .

When a grain boundary has a misorientation greater than  $10^\circ$  or  $15^\circ$ , it is no longer practical to think of the boundary as being made up of dislocations because the spacing of the dislocations would be so small that they would lose their individual identity. The grain boundary represents a region a few atomic diameters wide where there is a transition in atomic periodicity between adjacent crystals or grains.

Grain boundaries have an interfacial energy because of the disruption in atomic periodicity in the vicinity of the boundary and the broken bonds that exist across the interface. The interfacial energy of grain boundaries is generally less than that of a free surface because the atoms in a grain boundary are surrounded on all sides by other atoms and have only a few broken or distorted bonds.

Solids with grain boundaries are referred to as *polycrystalline*, since the structure is composed of many crystals - each with a different crystallographic orientation. In the case of iron the grain boundary structure can be revealed by preferential chemical attack (*etching*) at the grain boundaries, while the grain structure in polyethylene is revealed by the use of polarized light. The grain structure is usually specified by giving average grain diameter or by using a scheme developed by the American Society for Testing and Materials (ASTM). In the ASTM procedure the grain size is specified by a "grain size number" ( $n$ ) where

$$N = 2^{n-1} \quad (6.2.3.1)$$

with  $N$  equal to the number of grains per square inch when the sample is viewed at 100X magnification. For example, at a magnification of  $X = 100$ , a material with grain size number 8 will show 128 grains per inch<sup>2</sup> - this material in effect has (at  $X = 1$ )  $1.28 \times 10^6$  grains per square inch. If the grains are approximately square in cross section, this corresponds to an average grain dimension of  $8.8 \times 10^{-4} \text{ in}^*$ .

In polycrystalline samples the individual grains usually have a random crystallographic orientation with respect to one another, and the grain structure is referred to as *randomly oriented*. In some instances, however, the grains all have the same orientation to within a few degrees. In this instance the material is said to have a *preferred orientation* or *texture*.

#### 6.2.3.4.3: Phase Boundaries

A *phase* is defined as a *homogeneous, physically distinct and mechanically separable portion of the material with a given chemical composition and structure*. Phases may be substitutional or interstitial solid solutions, ordered alloys or compounds, amorphous substances or even pure elements; a crystalline phase in the solid state may be either polycrystalline or exist as a single crystal.



Solids composed of more than one element may - and often do - consist of a number of phases. For example, a dentist's drill, something painfully familiar to all of us, consists of a mixture of small single crystals of tungsten carbide surrounded by a matrix of cobalt. Here the cobalt forms a continuous phase. Polyphase materials such as the dentist's drill are generally referred to as *composite materials*. Composite materials have great importance in the engineering world because they have many attractive properties that set them apart from single-phase materials. For example, the dentist's drill has good abrasive characteristics (due to the hard carbide particles) and good toughness and impact resistance (due to the continuous cobalt matrix). Neither the tungsten carbide nor the cobalt has both abrasion resistance and impact resistance, yet the proper combination of the two phases yields a composite structure with the desired properties.

\*

ASTM has as yet not issued specifications in SI units!

The nature of the interface separating various phases is very much like a grain boundary. Boundaries between two phases of different chemical composition and different crystal structure are similar to grain boundaries, while boundaries between different phases with similar crystal structures and crystallographic orientations may be analogous to low-angle grain boundaries in both energy and structure.

The concept of a solid consisting of a continuous phase and a discontinuous phase (or phases) leads to a simple classification of the various types of composite materials. Table 1 gives this classification, which is based on the structure (whether amorphous or crystalline) of the continuous and discontinuous phases.

**TABLE 1**  
**Classification of Composite or Multiphase Materials**

Continuous Phase	Discontinuous Phase (or Phases)	Examples
Crystalline	Crystalline	All metallic systems such as cast iron, steel, soft solder, etc.; most natural rocks such as granite and marble.
Crystalline	Amorphous	None of practical significance.
Amorphous	Crystalline	Most man-made ceramics such as building bricks and electrical insulator porcelain, concrete, partially crystalline polymers, some polymer-crystalline particle composites.
Amorphous	Amorphous	Fiberglass, asphalt, wood, hydrated cement, other gels.

This page titled [6.2.3: The Imperfect Solid State](#) is shared under a [CC BY-NC-SA 4.0](#) license and was authored, remixed, and/or curated by Donald Sadoway (MIT OpenCourseWare) .

## 6.3: X-Ray Crystallography of Solids

---

Learning objectives for this unit are to:

- Determine the Miller indices of a lattice plane from its intercepts with the edges of the unit cell
  - Visualize and draw a lattice plane when given its Miller indices
  - Describe the properties of X-rays
  - Explain the concept of diffraction as it applies to crystalline lattices
  - Know the equation for Bragg diffraction and use the equation to calculate lattice spacings, diffraction angles, and x-ray wavelengths
  - Compare and contrast single crystal and powder XRD techniques
  - Understand the information contained within a powder XRD pattern, including how the locations and intensities of peaks vary with changes in a crystalline lattice
- 

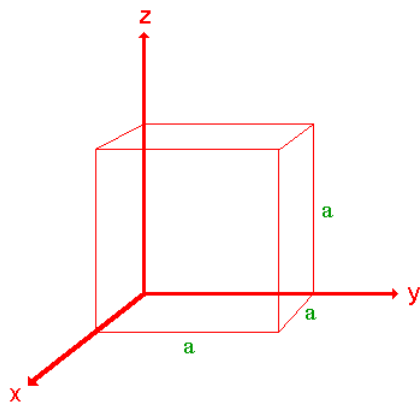
6.3: X-Ray Crystallography of Solids is shared under a [not declared](#) license and was authored, remixed, and/or curated by LibreTexts.



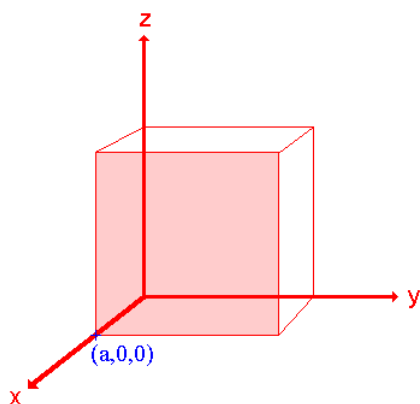
### 6.3.1: Miller Indices (hkl)

The orientation of a surface or a crystal plane may be defined by considering how the plane (or indeed any parallel plane) intersects the main crystallographic axes of the solid. The application of a set of rules leads to the assignment of the Miller Indices ( $hkl$ ), which are a set of numbers which quantify the intercepts and thus may be used to uniquely identify the plane or surface.

The following treatment of the procedure used to assign the Miller Indices is a simplified one and only a **cubic** crystal system (one having a cubic unit cell with dimensions  $a \times a \times a$ ) will be considered.



The procedure is most easily illustrated using an example so we will first consider the following surface/plane:



**Step 1:** Identify the intercepts on the  $x$ -,  $y$ - and  $z$ - axes.

In this case the intercept on the  $x$ -axis is at  $x = a$  ( at the point  $(a,0,0)$  ), but the surface is parallel to the  $y$ - and  $z$ -axes - strictly therefore there is no intercept on these two axes but we shall consider the intercept to be at infinity ( $\infty$ ) for the special case where the plane is parallel to an axis. The intercepts on the  $x$ -,  $y$ - and  $z$ -axes are thus  $a, \infty, \infty$ .

**Step 2:** Specify the intercepts in fractional co-ordinates

Co-ordinates are converted to fractional co-ordinates by dividing by the respective cell-dimension - for example, a point  $(x,y,z)$  in a unit cell of dimensions  $a \times b \times c$  has fractional co-ordinates of  $(x/a, y/b, z/c)$ . In the case of a cubic unit cell each co-ordinate will simply be divided by the cubic cell constant,  $a$ . This gives

Fractional Intercepts =  $a/a, \infty/a, \infty/a$  i.e.  $1, \infty, \infty$ .

**Step 3:** Take the reciprocals of the fractional intercepts

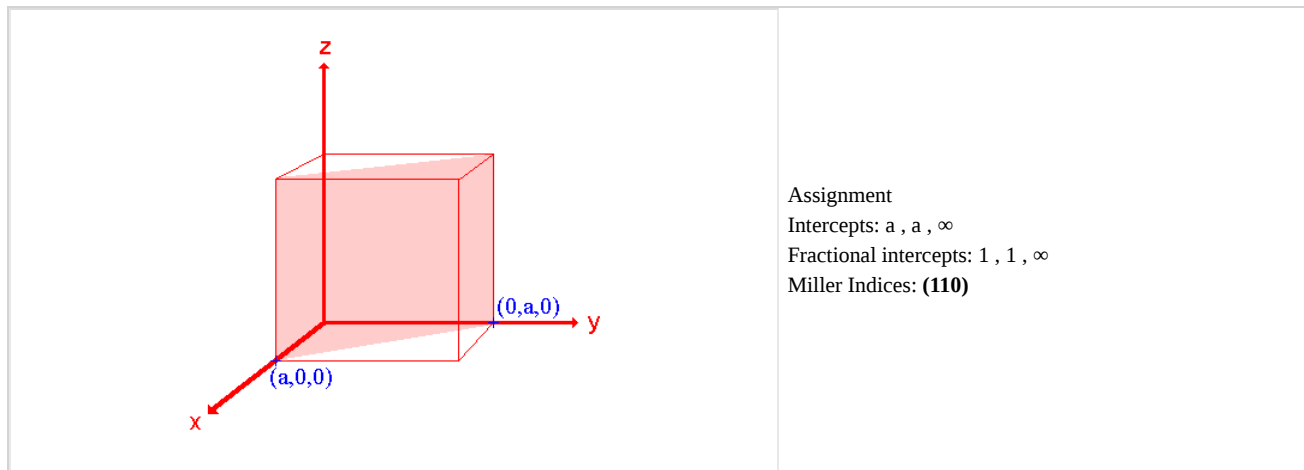
This final manipulation generates the Miller Indices which (by convention) should then be specified without being separated by any commas or other symbols. The Miller Indices are also enclosed within standard brackets (...) when one is specifying a unique surface such as that being considered here.

The reciprocals of 1 and  $\infty$  are 1 and 0 respectively, thus yielding Miller Indices **(100)**.

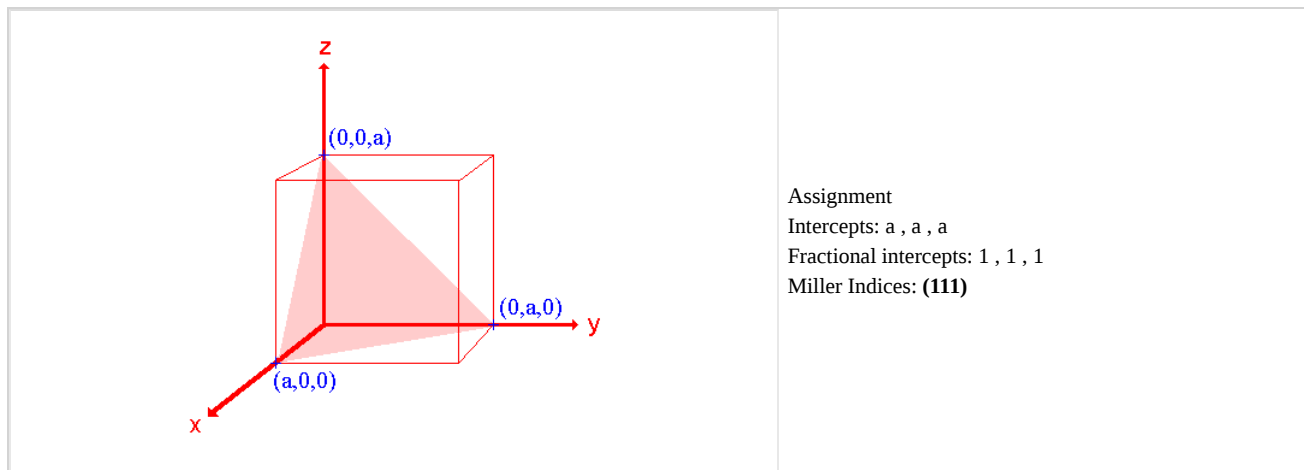
So the surface/plane illustrated is the (100) plane of the cubic crystal.

### Other Examples

#### 1. The (110) surface

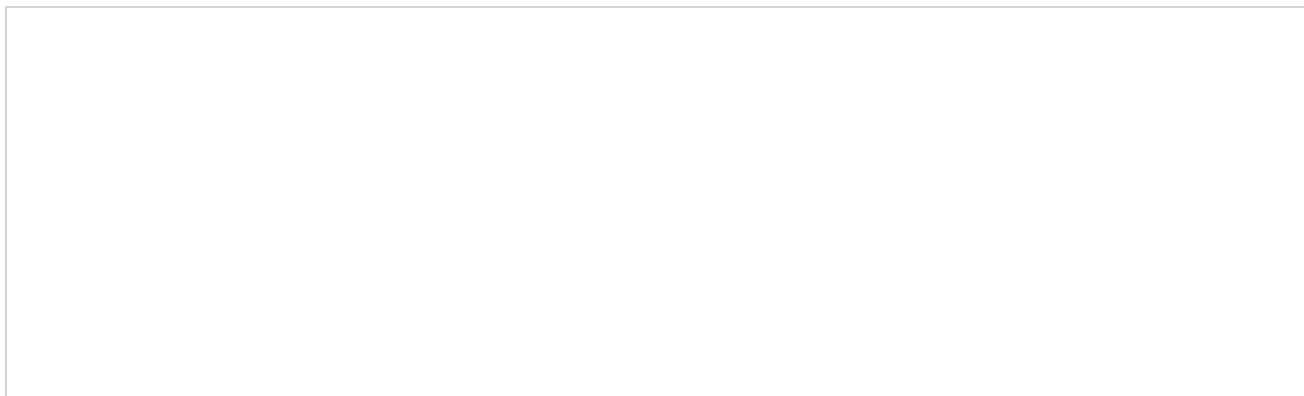


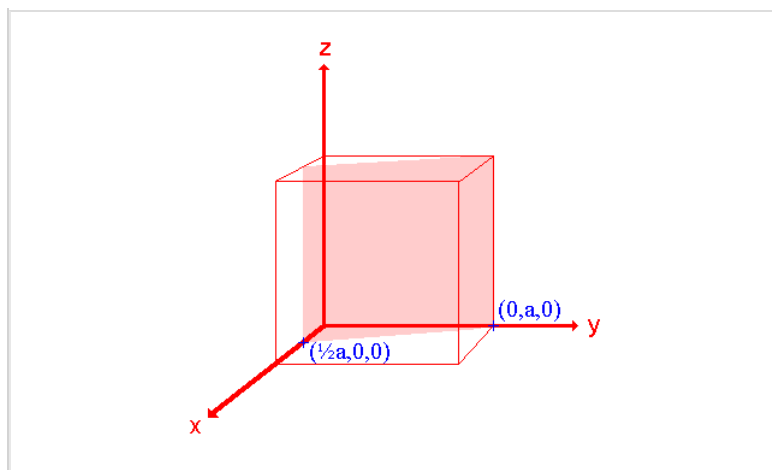
#### 2. The (111) surface



The (100), (110) and (111) surfaces considered above are the so-called **low index surfaces** of a cubic crystal system (the "low" refers to the Miller indices being small numbers - 0 or 1 in this case). These surfaces have a particular importance but there are an infinite number of other planes that may be defined using Miller index notation. We shall just look at one more ...

#### 3. The (210) surface





Assignment

Intercepts:  $\frac{1}{2}a$ ,  $a$ ,  $\infty$

Fractional intercepts:  $\frac{1}{2}$ ,  $1$ ,  $\infty$

Miller Indices: **(210)**

Further notes:

- i. in some instances the Miller indices are best multiplied or divided through by a common number in order to simplify them by, for example, removing a common factor. This operation of multiplication simply generates a parallel plane which is at a different distance from the origin of the particular unit cell being considered. e.g. (200) is transformed to (100) by dividing through by 2.
- ii. if any of the intercepts are at negative values on the axes then the negative sign will carry through into the Miller indices; in such cases the negative sign is actually denoted by overstriking the relevant number. e.g. (00-1) is instead denoted by  $(00\bar{1})$
- iii. in the *hcp* crystal system there are four principal axes; this leads to four Miller Indices e.g. you may see articles referring to an *hcp* (0001) surface. It is worth noting, however, that the intercepts on the first three axes are necessarily related and not completely independent; consequently the values of the first three Miller indices are also linked by a simple mathematical relationship.

## Contributors and Attributions

- [Roger Nix](#) (Queen Mary, University of London)

This page titled [6.3.1: Miller Indices \(hkl\)](#) is shared under a [not declared](#) license and was authored, remixed, and/or curated by [Roger Nix](#).

## 6.3.2: X-rays and X-ray Diffraction

### 6.3.2.1: HISTORICAL INTRODUCTION

X-rays were discovered during the summer of 1895 by Wilhelm Röntgen at the University of Würzburg (Germany). Röntgen was interested in the *cathode rays* (beams of electrons) developed in discharge tubes, but it is not clear exactly which aspects of cathode rays he intended to study. By chance he noticed that a fluorescent screen ( $\text{ZnS} + \text{Mn}^{++}$ ) lying on a table some distance from the discharge tube emitted a flash of light each time an electrical discharge was passed through the tube. Realizing that he had come upon something completely new, he devoted his energies to investigating the properties of the unknown ray "X" which produced this effect. The announcement of this discovery appeared in December 1895 as a concise ten page publication.

The announcement of the discovery of X-rays was received with great interest by the public. Röntgen himself prepared the first photographs of the bones in a living hand, and use of the radiation was quickly adopted in medicine. In the succeeding fifteen years, however, very few fundamental insights were gained into the nature of X-radiation. There was some indication that the rays were waves, but the evidence was not clear-cut and could be interpreted in several ways. Then, at the University of Munich in 1912, Max von Laue performed one of the most significant experiments of modern physics. At his suggestion, Paul Knipping (who had just completed a doctoral thesis with Röntgen) and Walter Friedrich (a newly appointed assistant to Sommerfeld) directed a beam of X-rays at a crystal of copper sulfate and attempted to record the scattered beams on a photographic plate. The first experiment was unsuccessful. The result of a second experiment was successful. They observed the presence of spots produced by diffracted X-ray beams grouped around a larger central spot where the incident X-ray beam struck the film. This experiment demonstrated conclusively that X-radiation consisted of waves and, further, that the crystals were composed of atoms arranged on a *space lattice*.

### 6.3.2.2: ORIGIN OF X-RAY SPECTRA

The interpretation of X-ray spectra according to the Bohr theory (LN-1) of electronic levels was first (and correctly) proposed by W. Kossel in 1920: the electrons in an atom are arranged in shells (K, L, M, N, corresponding to  $n = 1, 2, 3, 4, \dots$ , etc.). Theory predicts that the energy differences between successive shells increase with decreasing  $n$  and that the electron transition from  $n = 2$  to  $n = 1$  results in the emission of very energetic (short wavelength) radiation (fig. 1), while outer shell transitions (say, from  $n = 5$  to  $n = 4$ ) yield low energy radiation (long wavelength). For hydrogen, you recall, the wave number of the emitted radiation associated with a particular electron transition is given by the Rydberg equation:

$$\bar{\nu} = \left( \frac{1}{n_i^2} - \frac{1}{n_f^2} \right) R$$

For "hydrogen-like" atoms with the atomic number  $Z$  (containing one electron only) the corresponding Rydberg equation becomes:

$$\bar{\nu} = \left( \frac{1}{n_i^2} - \frac{1}{n_f^2} \right) RZ^2$$

From this relationship it is apparent that the energy difference associated with electron transitions increases strongly with the atomic number and that the wavelength of radiation emitted during such transitions moves with increasing  $Z$  from the  $10^{-7}$  m range to the  $10^{-10}$  m range (radiation now defined as X-rays).

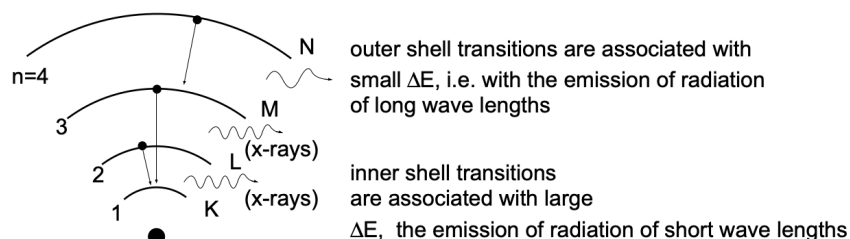


Figure 1 X-rays are generated by inner shell electron transitions

To bring about such inner shell transitions requires the generation of an *electron vacancy*: an electron must be removed, for example from the K shell ( $n = 1$ ), of an atom. Such a vacancy is conveniently produced in an X-ray tube by an electron beam (generated by a heated filament which is made a cathode) impinging, after being subjected to an accelerating potential of several

kV, into a target material made anode (fig. 2). The impinging electrons will transfer part of their energy to electrons of the target material and result in electronic excitation. If the energy of the arriving electrons is high enough, some may knock out a K shell electron in the target and thus generate a vacancy. [It should be clear that a  $K \rightarrow L$  excitation cannot take place since the L shell is filled: excitation must involve  $(n = 1) \rightarrow (n = \infty)$ .] When such a vacancy is generated, it can readily be filled by an electron from the L shell or the M shell of the same atom. These internal electron transitions give rise to the emission of "characteristic" X-radiation which, because of its short wavelength, has extremely high "penetrating" power.

Since an electron beam is used to generate X-rays, the X-ray tube has to be evacuated: to dissipate the energy flux arriving at the target, the anode support (onto which the target is mounted) is water-cooled.

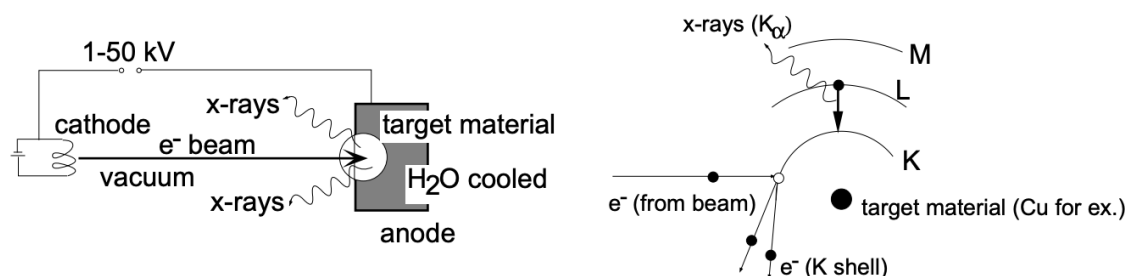


Figure 2 Generation of x-rays

Under standard operating conditions, the characteristic radiation emitted by the target comprises two sharp lines, referred to as  $K_\alpha$  and  $K_\beta$  lines (fig. 3). They are associated, respectively, with electron transitions from  $n = 2$  to  $n = 1$  and from  $n = 3$  to  $n = 1$ .

Emitted X-ray spectra were extensively studied by H.G.J. Moseley who established the relationship between the wavelength of characteristic radiation and the atomic number  $Z$  of the radiation emitting target material (fig. 4). Experimentally he found that the  $K_\alpha$  lines for various target materials (elements) exhibit the relationship:

$$\lambda K_\alpha \propto \frac{1}{Z^2} \quad (\bar{\nu} K_\alpha \propto Z^2)$$

Moseley's empirical relationship (which reflects a behavior in agreement with the Rydberg equation) can be quantified. While the energy levels associated with outer electron transitions are significantly affected by the "screening" effect of inner electrons (which is variable and cannot as yet be determined from first principles), the conditions associated with X-ray generation are simple. Very generally, the screening effect of the innermost electrons on the nuclear charge is accounted for in an effective nuclear charge  $(Z - \sigma)$  and the Rydberg equation assumes the form:

$$\bar{\nu} = \left( \frac{1}{n_i^2} - \frac{1}{n_f^2} \right) R(Z - \sigma)^2$$

where  $\sigma$  = screening effect

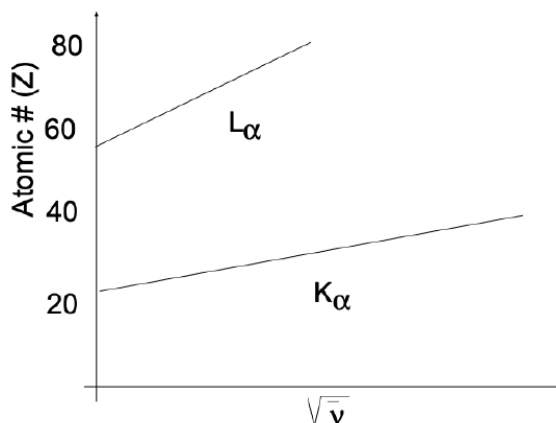


Figure 4 Moseley relationship for  $K_\alpha$  and  $L_\alpha$  radiation

Considering the transition  $n_2 \rightarrow n_1$ , screening of the full nuclear charge is only provided by the one electron remaining in the K shell. Thus it is possible to use the modified Rydberg equation, taking  $\sigma = 1$ . Accordingly, we have:

$$\bar{\nu} K_{\alpha} = \left( \frac{1}{2^2} - \frac{1}{1^2} \right) R(Z-1)^2 = -\frac{3}{4} R(Z-1)^2$$

where:  $R$  = Rydberg constant and  $Z$  = atomic number of the target material. [The minus sign (-) only reflects radiative energy given off by the system.]

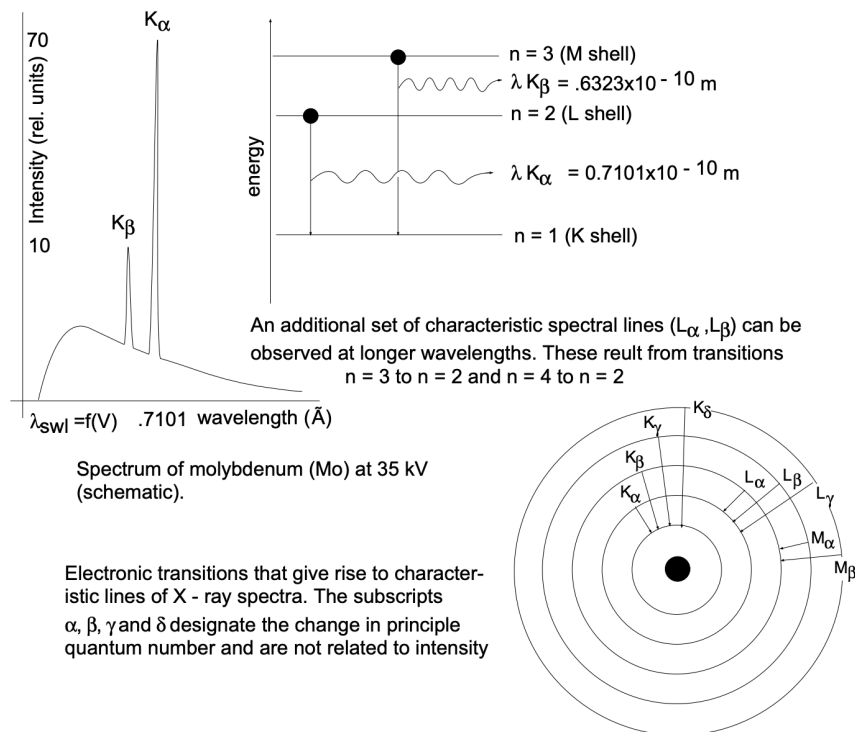


Figure 3 Electronic transitions giving rise to characteristic X-ray spectra.

Similarly, for the characteristic  $L_{\alpha}$  series of spectral lines ( $n = 3$  to  $n = 2$ ) we find, after removal of one L electron, that the screening of the electrons in the K shell and the remaining electrons in the L shell reduces the nuclear charge by 7.4 (empirical value).

$$\bar{\nu} L_{\alpha} = \left( \frac{1}{3^2} - \frac{1}{2^2} \right) R(Z-7.4)^2 = -\frac{5}{36} R(Z-7.4)^2$$

A second look at the X-ray spectrum of a Mo target, obtained with an electron accelerating potential of 35kV (fig. 5), shows that the characteristic radiation ( $K_{\alpha}, K_{\beta}$ ) appears superimposed on a continuous spectrum (continuously varying  $\lambda$ ) of lower and varying intensity. This continuous spectrum is referred to as **bremstrahlung** (*braking radiation*) and has the following origin. Electrons, impinging on the target material, may lose their energy by transferring it to orbiting electrons, as discussed above; in many instances, however, the electrons may come into the proximity of the force fields of *target nuclei* and, in doing so, will be "slowed down" or decelerated to a varying degree,

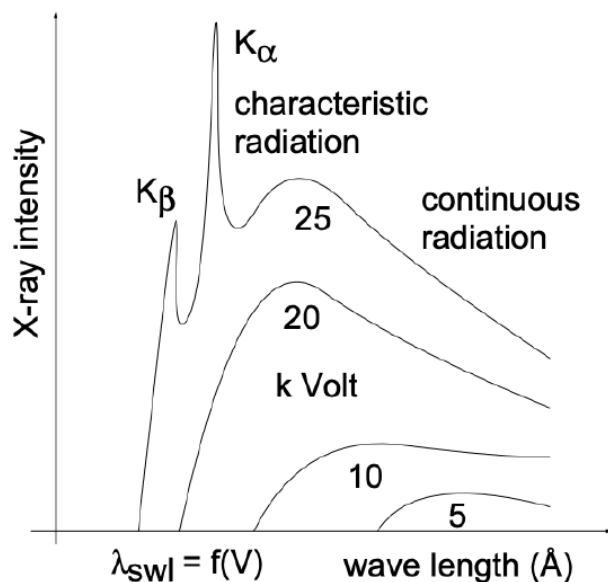
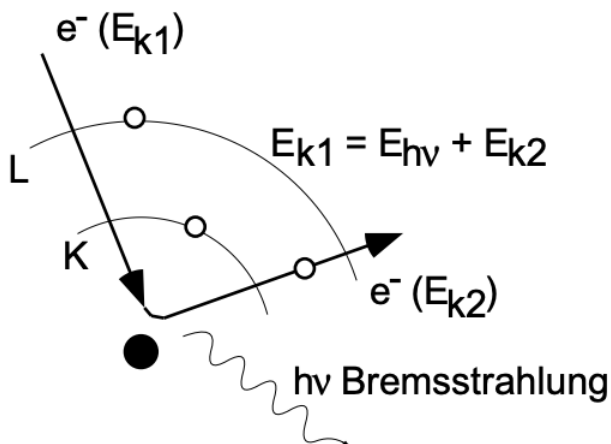


Figure 5 X-ray spectrum of Mo target as a function of applied Voltage.

ranging from imperceptible deceleration to total arrest. The energy lost in this slowing down process is emitted in the form of radiation (braking radiation, or bremsstrahlung). This energy conversion, as indicated, can range from partial to complete (fig. 6). The



$$\text{for } E_{k2} = 0, E_{(h\nu)\text{max}} = E_{k1} = \lambda_{\text{SWL}} = h\nu = eV ; \lambda_{\text{swl}} = hc/eV$$

Figure 6 Origin of Bremsstrahlung; the continuous part of the X-ray spectrum

incident electrons have an energy of  $e \cdot V$  (electronic charge times accelerating Voltage) in the form of kinetic energy ( $mv^2/2$ ), and their total energy conversion gives rise to a *Shortest Wavelength (SWL)* - the cut-off of the continuous spectrum for decreasing values of  $\lambda$  (fig. 5). Analytically, we have:

$$eV = h\nu_{\text{max}} = h \frac{c}{\lambda_{\text{SWL}}} ; \lambda_{\text{SWL}} = \frac{hc}{eV}$$

From this relationship it is evident that the cut-off of the continuous spectrum toward decreasing  $\lambda$ 's ( $\lambda_{\text{SWL}}$ ) is controlled by the accelerating potential (fig. 5).

### 6.3.2.3: "FINE STRUCTURE" OF CHARACTERISTIC X-RAYS

It is customary to consider the characteristic X-ray spectral lines as discrete lines ( $K_{\alpha}$ ,  $K_{\beta}$ ,  $L_{\alpha}$ ,  $L_{\beta}$ , etc.). In reality, they are not discrete since the electron shells involved in the associated electron transitions have energy *sublevels* (s, p, d orbitals). These

sublevels give rise to a "fine structure" insofar as the  $K_{\alpha}$  lines are doublets composed of  $K_{\alpha 1}$  and  $K_{\alpha 2}$  lines. Similarly,  $L_{\alpha}$ ,  $L_{\beta}$ , etc., exhibit a fine structure.

These considerations suggest that X-ray spectra contain information concerning the energetics of electronic states. Obviously, analysis of X-rays emitted from a target of unknown composition can be used for a quantitative chemical analysis. [This approach is taken routinely in advanced scanning electron microscopy (SEM) where X-rays, generated by the focused electron-beam, are analyzed in an appropriate spectrometer.]

In fundamental studies it is also of interest to analyze soft (long  $\lambda$ ) X-ray spectra. For example, take the generation of X-rays in sodium (Na). By generating an electron vacancy in the K shell, a series of  $K_{\alpha}$  and  $K_{\beta}$  lines will result. The cascading electron generates vacancies in the  $2p$  level, which in turn can be filled by electrons entering from the  $3s$  level (generation of "soft" X-rays). If the X-rays are generated in a Na vapor, the  $3s \rightarrow 2p$  transition will yield a sharp line; on the other hand, if X-rays are analyzed in sodium metal, the same transition results in the emission of a continuous broad band, about 30Å in width. This finding confirms the existence of an *energy band* (discussed earlier).

An analysis of the width and intensity distribution of the X-ray band provides experimental data concerning the energy band width and the energy state density distribution within the energy band (fig. 7).

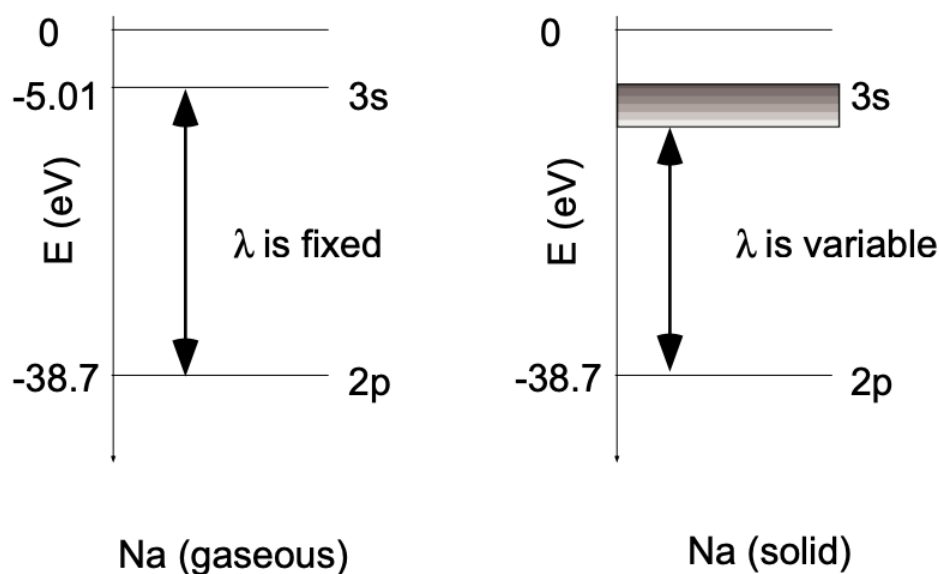


Figure 7 Soft X-rays from  $3s - 2p$  transitions in solid Na and Na vapor

#### 6.3.2.4: X-RAYS FOR STRUCTURAL ANALYSIS

The extensive use of X-rays for the analysis of atomic structural arrangements is based on the fact that waves undergo a phenomenon called *diffraction* when interacting with systems (diffracting centers) which are spaced at distances of the same order of magnitude as the wavelength of the particular radiation considered. X-ray diffraction in crystalline solids takes place because the atomic spacings are in the  $10^{-10}$  m range, as are the wavelengths of X-rays.

#### 6.3.2.5: DIFFRACTION AND BRAGG'S LAW

The atomic structure of crystalline solids is commonly determined using one of several different X-ray diffraction techniques. Complementary structure information can also be obtained through electron and neutron diffraction. In all instances, the radiation used must have wavelengths in the range of 0.1 to 10Å because the resolution (or smallest object separation distance) to which any radiation can yield useful information is about equal to the wavelength of the radiation, and the average distance between adjacent atoms in solids is about  $10^{-10}$  m (1Å). Since there is no convenient way to focus X-rays with lenses and to magnify images, we do not attempt to look directly at atoms. Rather, we consider the interference effects of X-rays when scattered by the atoms, comprising a crystal lattice. This is analogous to studying the structure of an optical diffraction grating by examining the interference pattern produced when we shine visible light on the grating. (The spacing of lines on a grating is about 0.5 to 1  $\mu\text{m}$  and the wavelength of visible radiation ranges from 0.4 to 0.8  $\mu\text{m}$ .) In the optical grating the ruled lines act as scattering centers, whereas in a crystal it is the atoms (more correctly, the electrons about the atom) which scatter the incident radiation.



The geometrical conditions which must be satisfied for diffraction to occur in a crystal were first established by Bragg. He considered a monochromatic (single wavelength) beam of X-rays with coherent radiation (X-rays of common wave front) to be incident on a crystal, as shown in fig. 8. Moreover, he established that the atoms which

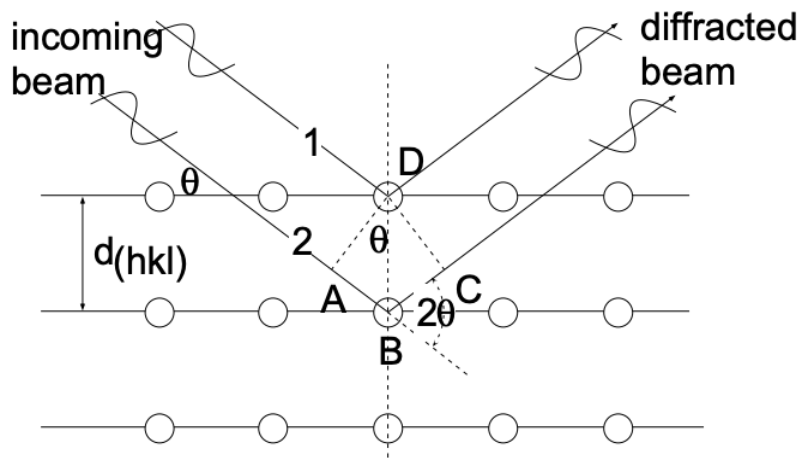


Figure 8 Bragg's law, assuming the planes of atoms behave as reflecting planes.

constitute the actual scattering centers can be represented by sets of parallel planes (in which the atoms are located) which act as mirrors and "reflect" the X-rays. In cubic systems the spacing of these planes,  $d_{(hkl)}$  (see LN – 4), is related to the lattice constant (a):

$$d_{(hkl)} = \frac{a}{\sqrt{h^2 + k^2 + l^2}} \quad (1)$$

For constructive interference of the scattered X-rays (the appearance of a diffraction peak) it is required that the beams, scattered on successive planes, be "in phase" (have again a common wave front) after they leave the surface of the crystal. In terms of the beams labeled 1 and 2 in fig. 8 this requires that the distance  $\overline{AB} + \overline{BC}$  be equal to an integral number of wavelengths ( $\lambda$ ) of the incident radiation. Accordingly:

$$\overline{AB} + \overline{BC} = n\lambda \quad (n = 1, 2, 3, \dots)$$

Since  $\overline{AB} = \overline{BC}$  and  $\sin \theta = \frac{\overline{AB}}{d_{(hkl)}} \left[ \overline{AB} = d_{(hkl)} \sin \theta \right]$ :

$$n\lambda = 2 d_{(hkl)} \sin \theta \quad (2)$$

This relation is referred to as *Bragg's Law* and describes the angular position of the diffracted beam in terms of  $\lambda$  and  $d_{(hkl)}$ . In most instances of interest we deal with first order diffraction ( $n = 1$ ) and, accordingly, Bragg's law is:

$$\lambda = 2d_{(hkl)} \sin \theta$$

[We are able to make  $n = 1$  because we can always interpret a diffraction peak for  $n = 2, 3, \dots$  as diffraction from  $(nh \ nkl)$  planes - i.e., from planes with one-nth the interplanar spacing of  $d_{(hkl)}$ .]

If we consider fig. 8 as representative for a "diffractometer" set-up (fig. 11), we have a collimated beam of X-rays impinging on a (100) set of planes and at  $2\theta$  to the incident beam a detector which registers the intensity of radiation. For a glancing incident beam (small  $\theta$ ) the detector will register only background radiation. As  $\theta$  increases to a value for which  $2d \sin \theta = \lambda$ , the detector will register high intensity radiation - we have a diffraction peak. From the above it is evident that the diffraction angle ( $\theta$ ) increases as the interplanar spacing,  $d_{(hkl)}$ , decreases.

The diffraction experiment as presently considered is intended to provide quantitative information on the volume (the lattice constant  $a$ ) and shape characteristics (SC, BCC, FCC) of the unit cell. The intensity of diffraction peaks depends on the phase relationships between the radiation scattered by all the atoms in the unit cell. As a result, it happens quite often that the intensity of a particular peak, whose presence is predicted by Bragg's law, is zero. (This is because Bragg's law deals not with atom positions, but only with the size and shape of the unit cell.) For example, consider the intensity of the (100) diffraction peak of a crystal which has a BCC unit cell. The phase relationships show that the X-rays scattered at the top and bottom faces of the unit cell, (100)

planes, interfere constructively, but are  $180^\circ$  out of phase with the X-rays scattered by the atom at the center of the unit cell. The resultant intensity is therefore zero. The rules which govern the presence of particular diffraction peaks in the different cubic Bravais lattices (SC, BCC and FCC) are given in Table I.

TABLE I. Selection Rules for Diffraction Peaks in Cubic Systems

Bravais Lattice	Reflections Present	Reflections Absent
Simple Cubic	All	None
Body-Centered Cubic	$(h + k + l) = \text{even}$	$(h + k + l) = \text{odd}$
Face-Centered Cubic	$h, k, l$ unmixed (either all odd or all even)	$h, k, l$ mixed

The rules given are strictly true only for unit cells where a single atom is associated with each lattice point. (Unit cells with more than one atom per lattice point may have their atoms arranged in positions such that reflections cancel. For example, diamond has an FCC Bravais lattice with two atoms per lattice point. All reflections present in diamond have unmixed indices, but reflections such as  $\{200\}$ ,  $\{222\}$  and  $\{420\}$  are missing. The fact that all reflections present have unmixed indices indicates that the Bravais lattice is FCC – the extra missing reflections give additional information as to the exact atom arrangement.)

A hypothetical diffraction experiment: A material is known to be of simple cubic structure; determine  $a$ , the lattice constant, by X-ray diffraction. In theory, the question may be answered by placing the crystal into a diffractometer, rotating it into all possible positions relative to the incident X-ray beam and recording all diffracting  $2\theta$  values. From the above we know that the smallest observed  $\theta$  value must correspond to diffraction on  $\{100\}$  planes and also that  $d_{(100)} = a$ . We may now use Bragg's equation to determine  $a$ , the lattice constant:

$$\lambda = 2d \sin \theta = 2a \sin \theta$$

$$a = \frac{\lambda}{2 \sin \theta}$$

There are two simplifying assumptions in this problem: (1) we know the system is SC and (2) we are able, through rotation, to bring all planes present into diffraction conditions.

### 6.3.2.6: EXPERIMENTAL APPROACHES TO X-RAY DIFFRACTION

In the context of this course we are interested in making use of X-ray diffraction for the purpose of (a) identifying (cubic) crystal systems, (b) determining the lattice constant,  $a$ , and (c) identifying particular planes or meaningful orientations. The possible approaches can, in principle, be identified through an examination of Bragg's law. The Bragg condition for particular  $d_{(hkl)}$  values can be satisfied by adjusting either one of two experimental variables: (a)  $\lambda$ , the wavelength of the X-ray beam used, or (b)  $\theta$ , the orientation of the crystal planes relative to the incident X-rays.

(a) Fixed  $\theta$ , Variable  $\lambda$ : One means of satisfying Bragg's law is to irradiate a stationary single crystal ( $\theta$  fixed for all planes within the crystal) with an X-ray beam of "white" radiation, which contains the characteristic and continuous spectrum produced by an X-ray tube. (For  $\lambda$  variable we have the simultaneous exposure of a crystal to a range of  $\lambda$  values). Each set of planes will reflect (diffract) the particular  $\lambda$  which satisfies the Bragg condition for the fixed  $\theta$ . The diffracted beams may conveniently be recorded with a Polaroid camera or, alternately, with an electronic imaging device. It is possible to analyze either the transmitted or the back-reflected X-rays. This experimental procedure is referred to as the **Laue technique** (fig. 9); it is mostly conducted in the back-reflection mode. Note that the approach taken makes it possible to determine the values of  $\theta$  for each reflection, but not the corresponding  $\lambda$ . Therefore, the technique cannot be used, for example, to determine lattice constants. However, it is very valuable if particular planes or crystal orientations are to be identified.

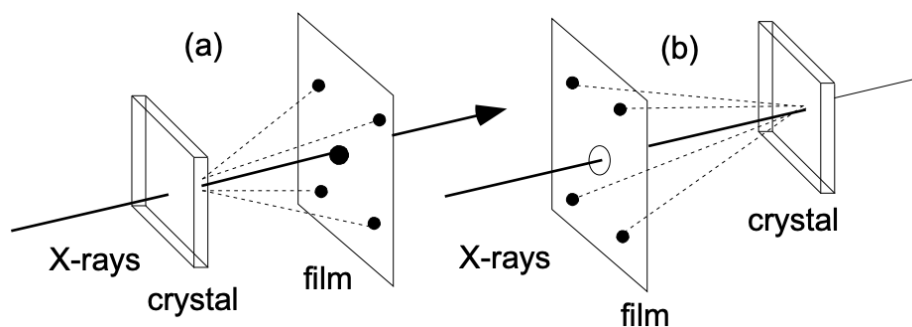


Figure 9: Laue diffraction in (a) transmission and (b) back-reflection mode. Long

This is a figure with information about the process described in this section.

The figure has several sections of important information:

- This is the description of the first section.
- The middle section of the figure contains this information.
- The third and final section of the figure has this information.

(b) Fixed  $\lambda$  (Monochromatic X-Rays), Variable  $\theta$ : The basic prerequisite for this approach is the availability of a monochromatic X-radiation of known wavelength ( $\lambda$ ). Such radiation can be conveniently obtained by using a crystal (i.e., its diffracting property) as a filter or monochromator (fig. 10). Filter action is achieved by positioning the crystal in such a way that the unfiltered radiation emitted by the X-ray tube becomes incident at an angle,  $\theta$ , on a set of low index planes which satisfy Bragg's law for the highest intensity radiation ( $K_\alpha$ ) emitted. The condition of a fixed  $\lambda$  and variable  $\theta$  is experimentally used in two techniques. Using a **diffractometer** (fig. 11), we place a sample (ground to a powder) into the center of a rotating stage and expose it to a monochromatic X-ray beam. The sample is rotated into diffraction condition and the diffraction angle determined.

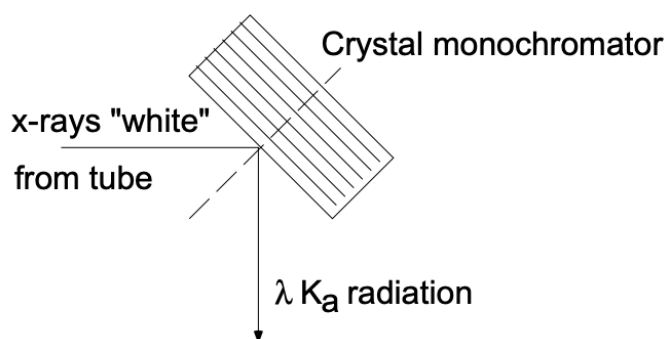


Figure 10 Isolation of monochromatic radiation from target radiation

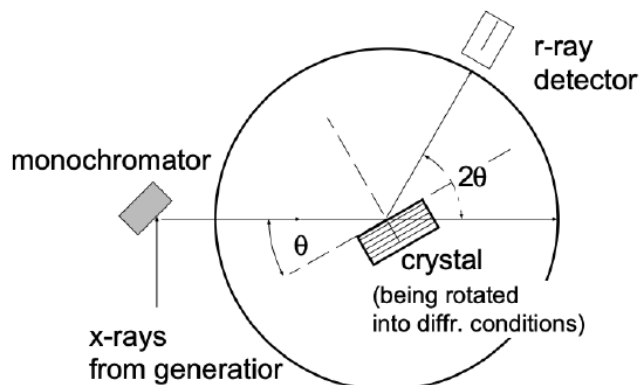


Figure 11 X-ray Diffractometer setup.

In the **Debye-Scherrer method** (fig.12) the sample is ground to a powder and placed (in an ampoule) into the center of a Debye-Scherrer camera. Exposed to monochromatic X-rays, in this way a large number of diffracted cone-shaped beams are generated

such that the semiangles of the cones measure  $2\theta$ , or twice the Bragg angle for the particular diffracting crystallographic planes. The reason diffracted beams are cone-shaped is that the planes in question (within the multitude of randomly oriented grains) give rise to diffraction for any orientation around the incident beam as long as the incident beam forms the appropriate Bragg angle with these planes – thus there is a rotational symmetry of the diffracted beams about the direction of the incident beam. Those planes with the largest interplanar spacing have the smallest Bragg angle,  $\theta$ .

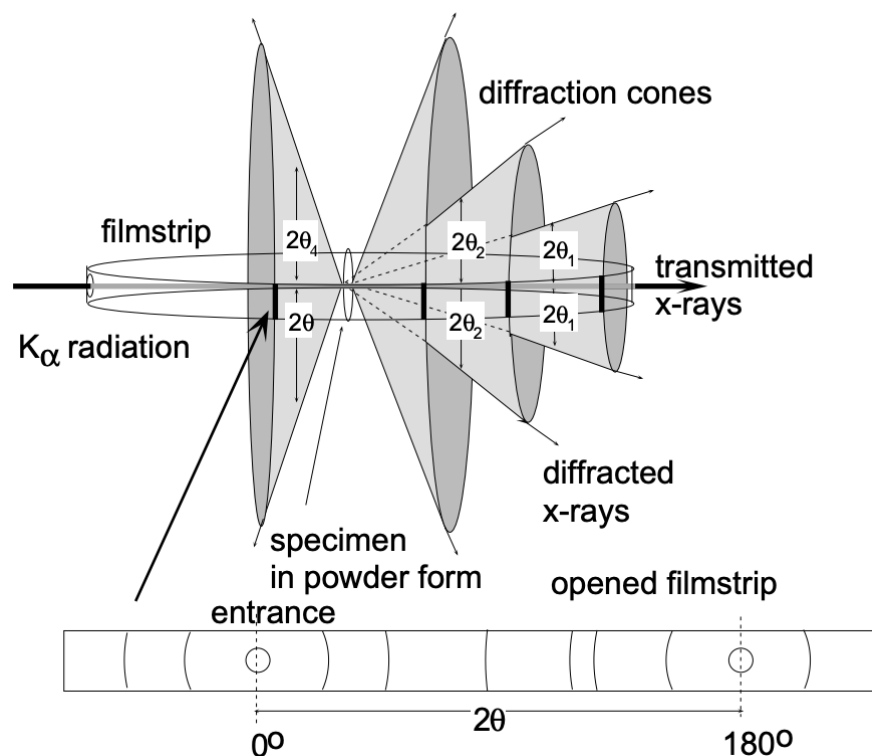


Figure 12 Debye-Scherrer powder diffraction setup and analysis

In a Debye-Scherrer arrangement, after exposing a powder of a crystalline material to monochromatic X-rays, the developed film strip will exhibit diffraction patterns such as indicated in fig. 12. Each diffraction peak (dark line) on the film strip corresponds to constructive interference at planes of a particular interplanar spacing  $[d_{(hkl)}]$ . The problem now consists of "indexing" the individual lines - i.e., determining the Miller indices (hkl) for the diffraction lines:

$$\begin{aligned} \text{Bragg: } \lambda &= 2 d_{(hkl)} \sin \theta & d_{(hkl)} &= \frac{a}{\sqrt{h^2 + k^2 + l^2}} \\ \lambda^2 &= 4 d_{(hkl)}^2 \sin^2 \theta & d_{(hkl)}^2 &= \frac{a^2}{(h^2 + k^2 + l^2)} \end{aligned}$$

Substitution and rearrangement of above yields:

$$\frac{\sin^2 \theta}{(h^2 + k^2 + l^2)} = \frac{\lambda^2}{4a^2} = \text{const.}$$

Accordingly, we find that for all lines ( $\theta$  values) of a given pattern, the relationship

$$\frac{\sin^2 \theta_1}{(h^2 + k^2 + l^2)_1} = \frac{\sin^2 \theta_2}{(h^2 + k^2 + l^2)_2} = \frac{\sin^2 \theta_3}{(h^2 + k^2 + l^2)_3} = \text{const.}$$

holds. Since the sum  $(h^2 + k^2 + l^2)$  is always integral and  $\lambda^2/4a^2$  is a constant, the problem of indexing the pattern of a cubic system is one of finding a set of integers  $(h^2 + k^2 + l^2)$  which will yield a constant quotient when divided one by one into the observed  $\sin^2 \theta$  values. (Certain integers such as 7, 15, 23, etc. are impossible because they cannot be formed by the sum of three squared integers.)

Indexing in step-by-step sequence is thus performed as follows:  $\theta$  values of the lines are obtained from the geometric relationship of the unrolled film strip. Between the exit hole of the X-ray beam ( $2\theta = 0^\circ$ ) and the entrance hole ( $2\theta = 180^\circ$ ) the angular relationship is linear (fig. 12). The increasing  $\theta$  values for successive lines are indexed  $\theta_1, \theta_2, \theta_3$ , etc., and  $\sin^2 \theta$  is determined for each. If the system is simple cubic we know that all planes present will lead to diffraction and the successive lines (increasing  $\theta$ ) result from diffraction on planes with decreasing interplanar spacing: (100), (110), (111), (200), (210), (211), (220), etc. From equation (3) above we recognize:

$$\frac{\sin^2 \theta_1}{1} = \frac{\sin^2 \theta_2}{2} = \frac{\sin^2 \theta_3}{3} = \frac{\sin^2 \theta_4}{4} = \frac{\sin^2 \theta_5}{5} = \text{const.}$$

If the system is BCC, however, we know from the selection rules that only planes for which  $(h + k + l) = \text{even}$  will reflect. Thus:

$$\frac{\sin^2 \theta_1}{2} = \frac{\sin^2 \theta_2}{4} = \frac{\sin^2 \theta_3}{6} = \frac{\sin^2 \theta_4}{8} \text{ etc.} = \text{const.}$$

[SC can be differentiated from BCC through the fact that no sum of three squared integers can yield 7, but 14 can be obtained from planes (321)].

For FCC systems, the selection rules indicate reflections on planes with unmixed h,k,l indices:

$$\frac{\sin^2 \theta_1}{3} = \frac{\sin^2 \theta_2}{4} = \frac{\sin^2 \theta_3}{8} = \text{const.}$$

After proper indexing, the constant is obtained:

$$\frac{\sin^2 \theta}{(h^2 + k^2 + L^2)} = \text{const.}$$

and the particular Bravais lattice is identified. The lattice constant of the unit cell is subsequently obtained, knowing the wavelength of the incident radiation:

$$\begin{aligned} \frac{\sin^2 \theta}{(h^2 + k^2 + l^2)} &= \text{const.} = \frac{\lambda^2}{4a^2} \\ a^2 &= \frac{\lambda^2}{4 \sin^2 \theta} (h^2 + k^2 + l^2) \\ a &= \frac{\lambda}{2 \sin \theta} \sqrt{(h^2 + k^2 + l^2)} \end{aligned}$$

This page titled [6.3.2: X-rays and X-ray Diffraction](#) is shared under a [CC BY-NC-SA 4.0](#) license and was authored, remixed, and/or curated by [Donald Sadoway \(MIT OpenCourseWare\)](#).

### 6.3.3: Powder X-ray Diffraction

When an X-ray is shined on a crystal, it diffracts in a pattern characteristic of the structure. In powder X-ray diffraction, the diffraction pattern is obtained from a powder of the material, rather than an individual crystal. Powder diffraction is often easier and more convenient than single crystal diffraction since it does not require individual crystals be made. Powder X-ray diffraction (XRD) also obtains a diffraction pattern for the bulk material of a crystalline solid, rather than of a single crystal, which doesn't necessarily represent the overall material. A diffraction pattern plots intensity against the angle of the detector,  $2\theta$ .

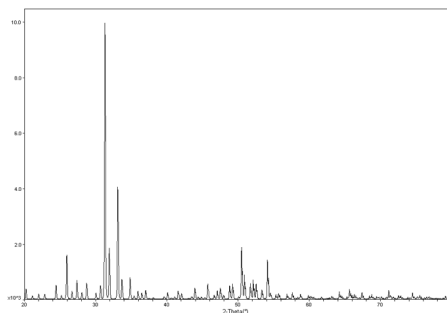
#### Introduction

Since most materials have unique diffraction patterns, compounds can be identified by using a database of diffraction patterns. The purity of a sample can also be determined from its diffraction pattern, as well as the composition of any impurities present. A diffraction pattern can also be used to determine and refine the lattice parameters of a crystal structure. A theoretical structure can also be refined using a method known as **Rietveld refinement**. The particle size of the powder can also be determined by using the Scherrer formula, which relates the particle size to the peak width. The Scherrer formula is

$$t = \frac{0.9\lambda}{\sqrt{B_M^2 - B_S^2} \cos \theta} \quad (6.3.3.1)$$

with

- $\lambda$  is the x-ray wavelength,
- $B_M$  is the observed peak width,
- $B_S$  is the peak width of a crystalline standard, and
- $\theta$  is the angle of diffraction.



To the left is an example XRD pattern for  $Ba_{24}Ge_{100}$ . The x axis is  $2\theta$  and the y axis is the intensity.

#### References

1. Dann, S.E. *Reactions and Characterization of SOLIDS*. Royal Society of Chemistry, USA (2002).
2. Skoog, D.A.; Holler, F.J.; Crouch, S.R. *Principles of Instrumental Analysis*. Sixth Edition, Thomson Brooks/Cole, USA (2007).

#### Contributors and Attributions

- Jason Grebenkemper

6.3.3: Powder X-ray Diffraction is shared under a [not declared](#) license and was authored, remixed, and/or curated by LibreTexts.

## 6.4: Energetics of Ionic Solids

---

Learning objectives for this unit are to:

- Use Coulomb's Law and periodic trends to explain and predict the properties of ionic compounds such as lattice energies and melting points
  - Given appropriate thermodynamic data, use a Born-Haber cycle to calculate experimental lattice energy of an ionic compound
  - Use the Born-Landé and Kapustinskii equations to calculate lattice energy of an ionic compound
  - Explain discrepancies between experimental and theoretical values for lattice energies
- 

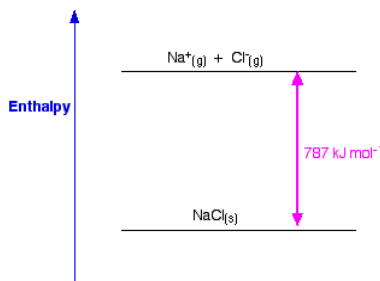
6.4: Energetics of Ionic Solids is shared under a [not declared](#) license and was authored, remixed, and/or curated by LibreTexts.

## 6.4.1: Lattice Enthalpies of Ionic Solids

**Lattice enthalpy** is a measure of the strength of the forces between the ions in an ionic solid. The greater the **lattice enthalpy**, the stronger the forces. This page introduces lattice enthalpies (lattice energies) and Born-Haber cycles.

### Defining Lattice Enthalpy

There are two different ways of defining lattice enthalpy which directly contradict each other, and you will find both in common use. In fact, there is a simple way of sorting this out, but many sources do not use it. Lattice enthalpy is a measure of the strength of the forces between the ions in an ionic solid. The greater the lattice enthalpy, the stronger the forces. Those forces are only completely broken when the ions are present as gaseous ions, scattered so far apart that there is negligible attraction between them. You can show this on a simple enthalpy diagram.



For sodium chloride, the solid is more stable than the gaseous ions by  $787 \text{ kJ mol}^{-1}$ , and that is a measure of the strength of the attractions between the ions in the solid. Remember that energy (in this case heat energy) is released when bonds are made, and is required to break bonds.

So lattice enthalpy could be described in either of two ways.

- It could be described as the enthalpy change when 1 mole of sodium chloride (or whatever) was formed from its scattered gaseous ions. In other words, you are looking at a downward arrow on the diagram.
- Or, it could be described as the enthalpy change when 1 mole of sodium chloride (or whatever) is broken up to form its scattered gaseous ions. In other words, you are looking at an upward arrow on the diagram.

Both refer to the same enthalpy diagram, but one looks at it from the point of view of making the lattice, and the other from the point of view of breaking it up. Unfortunately, both of these are often described as "lattice enthalpy".

#### Definitions

- The *lattice dissociation enthalpy* is the enthalpy change needed to convert 1 mole of solid crystal into its scattered gaseous ions. Lattice dissociation enthalpies are **always positive**.
- The *lattice formation enthalpy* is the enthalpy change when 1 mole of solid crystal is formed from its separated gaseous ions. Lattice formation enthalpies are **always negative**.

This is an absurdly confusing situation which is easily resolved by never using the term "lattice enthalpy" without qualifying it.

- You should talk about "lattice dissociation enthalpy" if you want to talk about the amount of energy needed to split up a lattice into its scattered gaseous ions. For NaCl, the lattice dissociation enthalpy is  $+787 \text{ kJ mol}^{-1}$ .
- You should talk about "lattice formation enthalpy" if you want to talk about the amount of energy released when a lattice is formed from its scattered gaseous ions. For NaCl, the lattice formation enthalpy is  $-787 \text{ kJ mol}^{-1}$ .

That immediately removes any possibility of confusion.

### Factors affecting Lattice Enthalpy

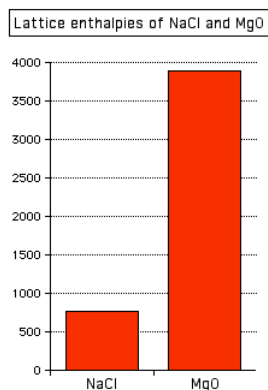
The two main factors affecting lattice enthalpy are

- The charges on the ions and
- The ionic radii (which affects the distance between the ions).



## The charges on the ions

Sodium chloride and magnesium oxide have exactly the same arrangements of ions in the crystal lattice, but the lattice enthalpies are very different.

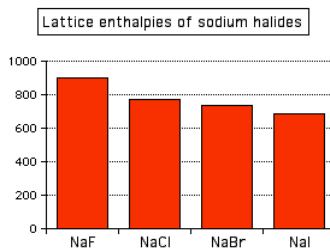


You can see that the lattice enthalpy of magnesium oxide is much greater than that of sodium chloride. That's because in magnesium oxide,  $2+$  ions are attracting  $2-$  ions; in sodium chloride, the attraction is only between  $1+$  and  $1-$  ions.

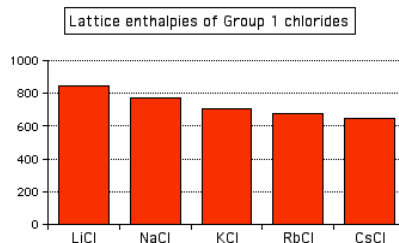
## The Radius of the Ions

The lattice enthalpy of magnesium oxide is also increased relative to sodium chloride because magnesium ions are smaller than sodium ions, and oxide ions are smaller than chloride ions. That means that the ions are closer together in the lattice, and that increases the strength of the attractions.

This effect of ion size on lattice enthalpy is clearly observed as you go down a Group in the Periodic Table. For example, as you go down Group 7 of the Periodic Table from fluorine to iodine, you would expect the lattice enthalpies of their sodium salts to fall as the negative ions get bigger - and that is the case:



Attractions are governed by the distances between the centers of the oppositely charged ions, and that distance is obviously greater as the negative ion gets bigger. And you can see exactly the same effect if as you go down Group 1. The next bar chart shows the lattice enthalpies of the Group 1 chlorides.



## Contributors and Attributions

- Jim Clark ([Chemguide.co.uk](http://Chemguide.co.uk))

This page titled [6.4.1: Lattice Enthalpies of Ionic Solids](#) is shared under a [CC BY-NC 4.0](#) license and was authored, remixed, and/or curated by [Jim Clark](#).

- [Lattice Enthalpies and Born Haber Cycles](#) by [Jim Clark](#) is licensed [CC BY-NC 4.0](#).

## 6.4.2: Born Haber Cycles

### Calculating Lattice Enthalpy

It is impossible to measure the enthalpy change starting from a solid crystal and converting it into its scattered gaseous ions. It is even more difficult to imagine how you could do the reverse - start with scattered gaseous ions and measure the enthalpy change when these convert to a solid crystal. Instead, lattice enthalpies always have to be calculated, and there are two entirely different ways in which this can be done.

1. You can use a [Hess's Law](#) cycle (in this case called a Born-Haber cycle) involving enthalpy changes which can be measured. Lattice enthalpies calculated in this way are described as experimental values.
2. Or you can do physics-style calculations working out how much energy would be released, for example, when ions considered as point charges come together to make a lattice. These are described as theoretical values. In fact, in this case, what you are actually calculating are properly described as lattice energies.

### Born-Haber Cycles

#### Standard Atomization Enthalpies

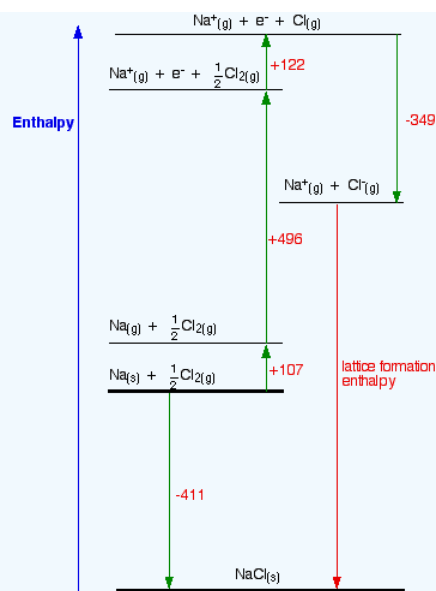
Before we start talking about Born-Haber cycles, we need to define the **atomization enthalpy**,  $\Delta H_a^\circ$ . The standard atomization enthalpy is the enthalpy change when 1 mole of gaseous atoms is formed from the element in its standard state. Enthalpy change of atomization is always positive. You are always going to have to supply energy to break an element into its separate gaseous atoms. All of the following equations represent changes involving atomization enthalpy:



Notice particularly that the "mol<sup>-1</sup>" is per mole of atoms **formed** - NOT per mole of element that you start with. You will quite commonly have to write fractions into the left-hand side of the equation. Getting this wrong is a common mistake.

#### ✓ Example 6.4.2.1: Born-Haber Cycle for NaCl

Consider a Born-Haber cycle for sodium chloride, and then talk it through carefully afterwards. You will see that I have arbitrarily decided to draw this for lattice formation enthalpy. If you wanted to draw it for lattice dissociation enthalpy, the red arrow would be reversed - pointing upwards.



Focus to start with on the higher of the two thicker horizontal lines. We are starting here with the elements sodium and chlorine in their standard states. Notice that we only need half a mole of chlorine gas in order to end up with 1 mole of NaCl. The arrow pointing down from this to the lower thick line represents the enthalpy change of formation of sodium chloride.

The Born-Haber cycle now imagines this formation of sodium chloride as happening in a whole set of small changes, most of which we know the enthalpy changes for - except, of course, for the lattice enthalpy that we want to calculate.

- The +107 is the atomization enthalpy of sodium. We have to produce gaseous atoms so that we can use the next stage in the cycle.
- The +496 is the first ionization energy of sodium. Remember that first ionization energies go from gaseous atoms to gaseous singly charged positive ions.
- The +122 is the atomization enthalpy of chlorine. Again, we have to produce gaseous atoms so that we can use the next stage in the cycle.
- The -349 is the first electron affinity of chlorine. Remember that first electron affinities go from gaseous atoms to gaseous singly charged negative ions.
- And finally, we have the positive and negative gaseous ions that we can convert into the solid sodium chloride using the lattice formation enthalpy.

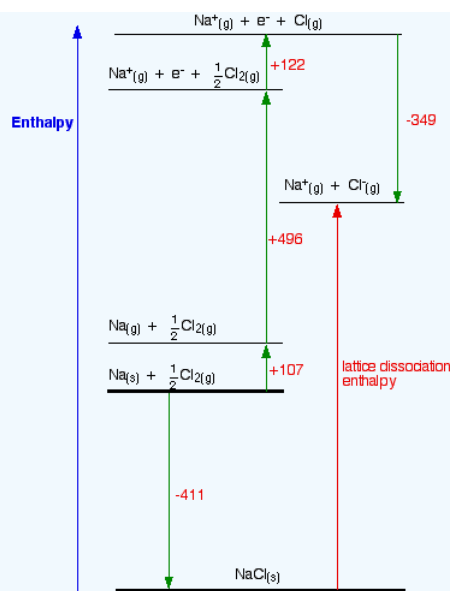
Now we can use Hess' Law and find two different routes around the diagram which we can equate. As drawn, the two routes are obvious. The diagram is set up to provide two different routes between the thick lines. So, from the cycle we get the calculations directly underneath it . . .

$$-411 = +107 + 496 + 122 - 349 + \text{LE}$$

$$\text{LE} = -411 - 107 - 496 - 122 + 349$$

$$\text{LE} = -787 \text{ kJ mol}^{-1}$$

How would this be different if you had drawn a lattice dissociation enthalpy in your diagram? Your diagram would now look like this:



The only difference in the diagram is the direction the lattice enthalpy arrow is pointing. It does, of course, mean that you have to find two new routes. You cannot use the original one, because that would go against the flow of the lattice enthalpy arrow. This time both routes would start from the elements in their standard states, and finish at the gaseous ions.

$$-411 + \text{LE} = +107 + 496 + 122 - 349$$

$$\text{LE} = +107 + 496 + 122 - 349 + 411$$

$$\text{LE} = +787 \text{ kJ mol}^{-1}$$

Once again, the cycle sorts out the sign of the lattice enthalpy.

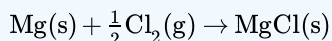
#### ✓ Example 6.4.2.2: Born-Haber Cycle for $\text{MgCl}_2$

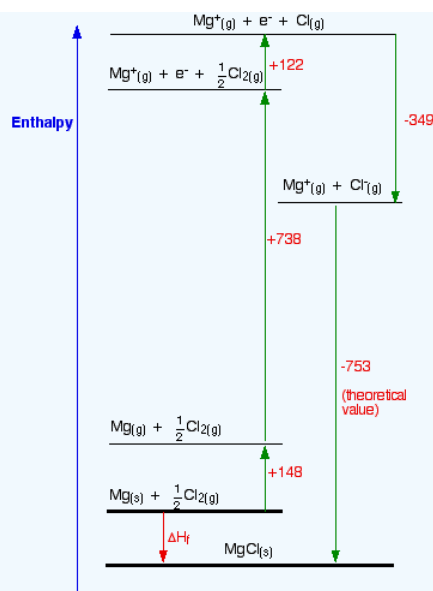
The question arises as to why, from an energetics point of view, magnesium chloride is  $\text{MgCl}_2$  rather than  $\text{MgCl}$  or  $\text{MgCl}_3$  (or any other formula you might like to choose). It turns out that  $\text{MgCl}_2$  is the formula of the compound which has the most negative enthalpy change of formation - in other words, it is the most stable one relative to the elements magnesium and chlorine.

Let's look at this in terms of Born-Haber cycles of and contrast the enthalpy change of formation for the imaginary compounds  $\text{MgCl}$  and  $\text{MgCl}_3$ . That means that we will have to use theoretical values of their lattice enthalpies. We cannot use experimental ones, because these compounds obviously do not exist! I'm taking theoretical values for lattice enthalpies for these compounds that I found on the web. I can't confirm these, but all the other values used by that source were accurate. The exact values do not matter too much anyway, because the results are so dramatically clear-cut.

##### 1. The Born-Haber cycle for $\text{MgCl}$

We will start with the compound  $\text{MgCl}$ , because that cycle is just like the  $\text{NaCl}$  one we have already looked at.





Find two routes around this without going against the flow of any arrows. That's easy:

$$\Delta H_f = +148 + 738 + 122 - 349 - 753$$

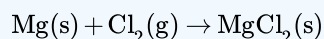
$$\Delta H_f = -94 \text{ kJ mol}^{-1}$$

So the compound MgCl is definitely energetically **more stable** than its elements. I have drawn this cycle very roughly to scale, but that is going to become more and more difficult as we look at the other two possible formulae. So I am going to rewrite it as a table. You can see from the diagram that the enthalpy change of formation can be found just by adding up all the other numbers in the cycle, and we can do this just as well in a table.

	kJ
atomization enthalpy of Mg	+148
1st IE of Mg	+738
atomization enthalpy of Cl	+122
electron affinity of Cl	-349
lattice enthalpy	-753
<b>calculated <math>\Delta H_f</math></b>	<b>-94</b>

## 2. The Born-Haber cycle for $\text{MgCl}_2$

The equation for the enthalpy change of formation this time is



So how does that change the numbers in the Born-Haber cycle?

- You need to add in the second ionization energy of magnesium, because you are making a 2+ ion.
- You need to multiply the atomization enthalpy of chlorine by 2, because you need 2 moles of gaseous chlorine atoms.
- You need to multiply the electron affinity of chlorine by 2, because you are making 2 moles of chloride ions.
- You obviously need a different value for lattice enthalpy.

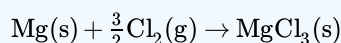
	kJ
atomization enthalpy of Mg	+148

	kJ
1st IE of Mg	+738
2nd IE of Mg	+1451
atomization enthalpy of Cl (x 2)	+244
electron affinity of Cl (x 2)	-698
lattice enthalpy	-2526
calculated $\Delta H_f$	-643

You can see that much more energy is released when you make  $\text{MgCl}_2$  than when you make  $\text{MgCl}$ . Why is that? You need to put in more energy to ionize the magnesium to give a 2+ ion, but a lot more energy is released as lattice enthalpy. That is because there are stronger ionic attractions between 1- ions and 2+ ions than between the 1- and 1+ ions in  $\text{MgCl}$ . So what about  $\text{MgCl}_3$ ? The lattice energy here would be even greater.

### 3. The Born-Haber cycle for $\text{MgCl}_3$

The equation for the enthalpy change of formation this time is



So how does that change the numbers in the Born-Haber cycle this time?

- You need to add in the third ionization energy of magnesium, because you are making a 3+ ion.
- You need to multiply the atomization enthalpy of chlorine by 3, because you need 3 moles of gaseous chlorine atoms.
- You need to multiply the electron affinity of chlorine by 3, because you are making 3 moles of chloride ions.
- You again need a different value for lattice enthalpy.

	kJ
atomization enthalpy of Mg	+148
1st IE of Mg	+738
2nd IE of Mg	+1451
3rd IE of Mg	+7733
atomization enthalpy of Cl (x 3)	+366
electron affinity of Cl (x 3)	-1047
lattice enthalpy	-5440
calculated $\Delta H_f$	+3949

This time, the compound is hugely energetically unstable, both with respect to its elements, and also to other compounds that could be formed. You would need to supply nearly 4000 kJ to get 1 mole of  $\text{MgCl}_3$  to form!

Look carefully at the reason for this. The lattice enthalpy is the **highest** for all these possible compounds, but it is not high enough to make up for the very large third ionization energy of magnesium.

Why is the third ionization energy so big? The first two electrons to be removed from magnesium come from the 3s level. The third one comes from the 2p. That is closer to the nucleus, and lacks a layer of screening as well - and so much more energy is needed to remove it. The 3s electrons are screened from the nucleus by the 1 level and 2 level electrons. The 2p electrons are only screened by the 1 level (plus a bit of help from the 2s electrons).

### Conclusion

Magnesium chloride is  $\text{MgCl}_2$  because this is the combination of magnesium and chlorine which produces the most energetically stable compound - the one with the most negative enthalpy change of formation.

### Contributors and Attributions

- Jim Clark ([Chemguide.co.uk](http://Chemguide.co.uk))

---

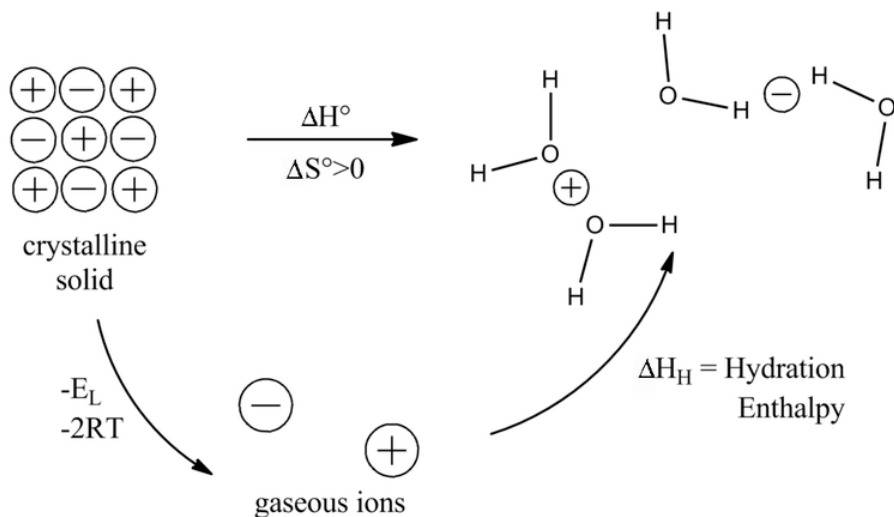
This page titled [6.4.2: Born Haber Cycles](#) is shared under a [CC BY-NC 4.0](#) license and was authored, remixed, and/or curated by [Jim Clark](#).

- [Lattice Enthalpies and Born Haber Cycles](#) by [Jim Clark](#) is licensed [CC BY-NC 4.0](#).



### 6.4.3: Lattice Energies and Solubility

Lattice energies can also help predict compound solubilities. Let's consider a Born-Haber cycle for dissolving a salt in water. We can imagine this as the sum of two processes: (1) the vaporization of the salt to produce gaseous ions, characterized by the lattice enthalpy, and (2) the hydration of those ions to produce the solution. The enthalpy change for the overall process is the sum of those two steps. We know that the entropy change for dissolution of a solid is positive, so the solubility depends on the enthalpy change for the overall process.



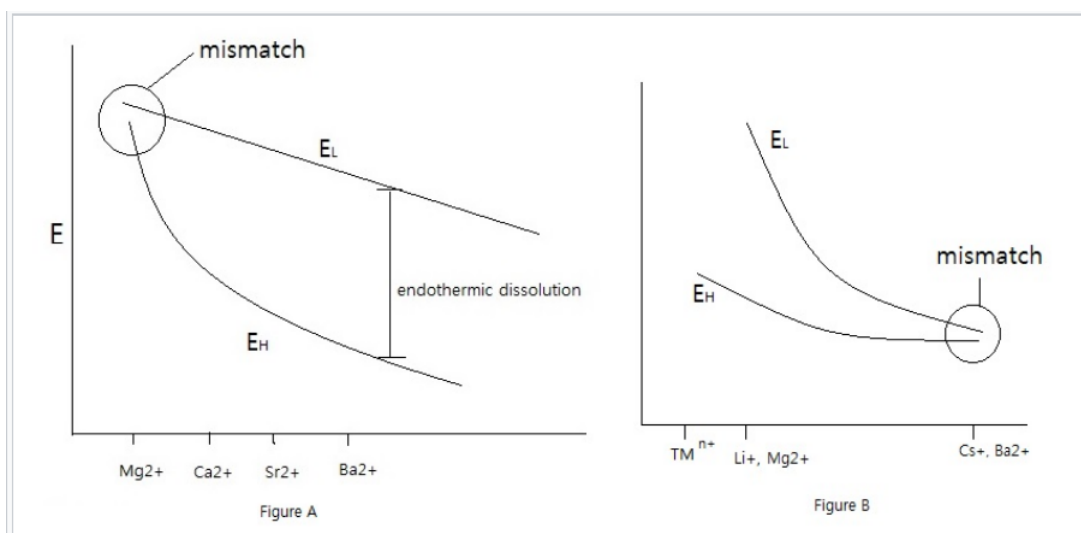
Here we need to consider the trends in both the lattice energy  $E_L$  and the hydration energy  $E_H$ . The lattice energy depends on the sum of the anion and cation radii ( $r_+ + r_-$ ), whereas the hydration energy has separate anion and cation terms. Generally the solvation of small ions (typically cations) dominates the hydration energy because of the  $1/r^2$  dependence.

$$E_L \propto \frac{1}{r_+ + r_-} \quad (6.4.3.1)$$

$$E_H \propto \frac{1}{r_+^2} + \frac{1}{r_-^2} \quad (6.4.3.2)$$

For salts that contain large anions,  $E_L$  doesn't change much as  $r_+$  changes. That is because the anion dominates the  $r_+ + r_-$  term in the denominator of the formula for  $E_L$ . On the other hand,  $E_H$  changes substantially with  $r_+$ , especially for small cations.

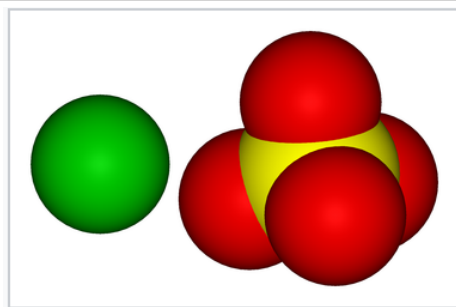
As a result, sulfate salts of small divalent cations, such as  $\text{MgSO}_4$  (epsom salts), are soluble, whereas the lower hydration energy of  $\text{Ba}^{2+}$  in  $\text{BaSO}_4$  makes that salt insoluble ( $K_{sp} = 10^{-10}$ ).



Left:  $E_L$  diagram for sulfate salts. The large  $\text{SO}_4^{2-}$  ion is size-mismatched to small cations such as  $\text{Mg}^{2+}$ , which have large hydration energies, resulting soluble salts. With larger cations such as  $\text{Ba}^{2+}$ , which have lower  $E_H$ , the lattice energy exceeds the solvation enthalpy and the salts are insoluble. Right: In the case of small anions such as  $\text{F}^-$  and  $\text{OH}^-$ , the lattice energy dominates with small cations such as transition metal ions ( $\text{TM}^{n+}$ ),  $\text{Mg}^{2+}$ , and  $\text{Li}^+$ . Anion-cation size mismatch occurs with larger cations, such as  $\text{Cs}^+$  and  $\text{Ba}^{2+}$ , which make soluble fluoride salts.

For small anions,  $E_L$  is more sensitive to  $r_+$ , whereas  $E_H$  does not depend on  $r_+$  as strongly. For fluorides and hydroxides,  $\text{LiF}$  is slightly soluble whereas  $\text{CsF}$  is very soluble, and  $\text{Mg}(\text{OH})_2$  is insoluble whereas  $\text{Ba}(\text{OH})_2$  is very soluble.

Putting both trends together, we see that **low solubility** is most often encountered when the **anion and cation match well in their sizes**, especially when one or both are **multiply charged**.



Space-filling models showing the van der Waals surfaces of  $\text{Ba}^{2+}$  and  $\text{SO}_4^{2-}$ . The similarity in size of the two ions contributes to the low solubility of  $\text{BaSO}_4$  in water.

Combining all our conclusions about solubility, we note the following trends:

- 1) Increasing **size mismatch** between the anion and cation leads to greater solubility, so  $\text{CsF}$  and  $\text{LiI}$  are the most soluble alkali halides.
- 2) Increasing **covalency** leads to lower solubility in the salts (due to larger  $E_L$ . For example,  $\text{AgF}$ ,  $\text{AgCl}$ ,  $\text{AgBr}$ , and  $\text{AgI}$  exhibit progressively lower solubility because of increasing covalency.  
 $\text{AgF} > \text{AgCl} > \text{AgBr} > \text{AgI}$
- 3) Increasing the **charge on the anion** lowers the solubility because the increase in  $E_L$  is large relative to the increase in  $E_H$ .
- 4) Small, polyvalent cations (having large  $E_H$ ) make **soluble salts with large, univalent anions** such as  $\text{I}^-$ ,  $\text{NO}_3^-$ ,  $\text{ClO}_4^-$ ,  $\text{PF}_6^-$ , and acetate.

**Examples:** Salts of transition metal and lanthanide ions

- $\text{Ln}^{3+}$ : Nitrate salts are soluble, but oxides and hydroxides are insoluble.

- $\text{Fe}^{3+}$ : Perchlorate is soluble, but sulfate is insoluble.

5) Multiple charged anions such as  $\text{O}^{2-}$ ,  $\text{S}^{2-}$ ,  $\text{PO}_4^{3-}$ , and  $\text{SO}_4^{2-}$  make insoluble salts with most  $\text{M}^{2+}$ ,  $\text{M}^{3+}$ , and  $\text{M}^{4+}$  metals.

---

6.4.3: Lattice Energies and Solubility is shared under a [CC BY-SA](#) license and was authored, remixed, and/or curated by LibreTexts.

- **9.12: Lattice Energies and Solubility** by Chemistry 310 is licensed [CC BY-SA 4.0](#). Original source: [https://en.wikibooks.org/wiki/Introduction\\_to\\_Inorganic\\_Chemistry](https://en.wikibooks.org/wiki/Introduction_to_Inorganic_Chemistry).

## 6.4.4: Theoretical Lattice Energy Calculations

### Lattice Energy

Many ionic compounds have simple structures. Because the forces holding the atoms together are primarily electrostatic, we can calculate the cohesive energy of the crystal lattice with good accuracy. Interesting questions to ask about these lattice energy calculations are:

- How accurate are lattice energy calculations?
- What do they teach us about the chemical bonds in ionic crystals?
- Can we use lattice energies to predict properties such as solubility, stability, and reactivity?
- Can we use lattice energies to predict the crystal structures of ionic compounds?

Let's start by looking at the forces that hold ionic lattices together. There are mainly two kinds of force that determine the energy of an ionic bond.

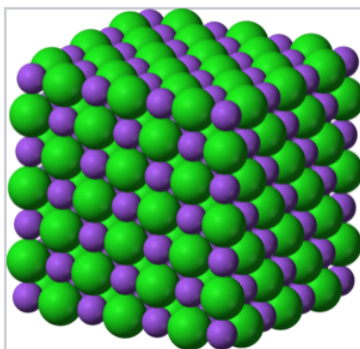


Figure 6.4.4.1: The NaCl crystal structure is the archetype for calculating lattice energies and computing enthalpies of formation from [Born-Haber cycles](#).

### Electrostatic force

Electrostatic force is the attraction and repulsion between ions described by Coulomb's Law. Two ions with charges  $z_+$  and  $z_-$ , separated by a distance  $r$ , experience a force  $F$ :

$$\mathbf{F} = -\frac{e^2}{4\pi\epsilon_0} \frac{z_+ z_-}{r^2} \quad (6.4.4.1)$$

where

$$e = 1.6022 \times 10^{-19} \text{ C}$$

$$4\pi\epsilon_0 = 1.112 \times 10^{-10} \text{ C}^2/(\text{J m})$$

This force is attractive for ions of opposite charge and repulsive for ions of the same charge.

### Closed-shell repulsion

When electrons in the core shells of one ion overlap with those of another ion, there is a repulsive force due to the Pauli exclusion principle. A third electron cannot enter an orbital that already contains two electrons. This force is short range, and is typically modeled as falling off exponentially or with a high power of the distance  $r$  between atoms. For example, in the Born approximation,  $B$  is a constant and  $\rho$  is a number with units of length, which is usually empirically determined from compressibility data. A typical value of  $\rho$  is  $0.345 \text{ \AA}$ .

$$\mathbf{E}_{repulsion} = B \exp\left(\frac{-r}{\rho}\right) \quad (6.4.4.2)$$

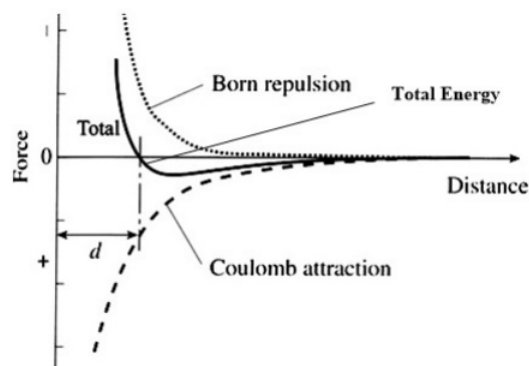


Figure 6.4.4.2: Total energy of an ionic bond (solid) determined by the combination of Coulombic attraction (dashed) and Born (closed-shell) repulsion (dotted).

The energy of the ionic bond between two atoms is then calculated as the combination of net electrostatic and the closed-shell repulsion energies, as shown in Figure 6.4.4.2. Note that for the moment we are ignoring the attractive van der Waals forces between ions. For a pair of ions, the equilibrium distance between ions is determined by the minimum in the total energy curve.

### Madelung Constant

We can use the above equations to calculate the lattice energy of a crystal by summing up the interactions between all pairs of ions. Because the closed-shell repulsion force is short range, this term is typically calculated only for interactions between neighboring ions. However, the Coulomb force is long range, and must be calculated over the entire crystal. This problem was first solved in 1918 by Erwin Madelung, a German physicist.

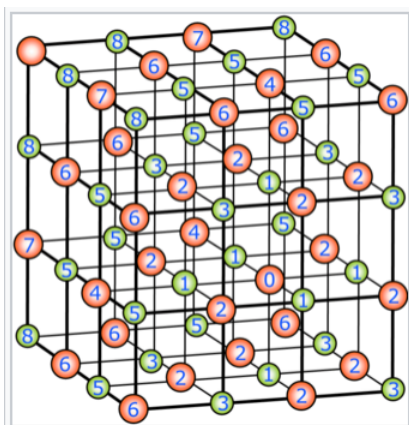


Figure 6.4.4.3: The Madelung constant is calculated by summing up electrostatic interactions with ion labeled 0 in the expanding spheres method. Each number designates the order in which it is summed. For example, ions labeled 1 represent the six nearest neighbors (attractive interaction), ions labeled 2 are the 12 next nearest neighbors (repulsive interaction) and so on.

Consider an ion in the NaCl structure labeled "0" in Figure 6.4.4.3. We can see that the nearest neighbor interactions (+ -) with ions labeled "1" are attractive, the next nearest neighbor interactions (- - and + +) are repulsive, and so on. In the NaCl structure, counting from the ion in the center of the unit cell, there are 6 nearest neighbors (on the faces of the cube), 12 next nearest neighbors (on the edges of the cube), 8 in the next shell (at the vertices of the cube), and so on. Their distances from ion "0" increase progressively:  $r_o$ ,  $\sqrt{2} r_o$ ,  $\sqrt{3} r_o$ , and so on, where  $r_o$  is the nearest neighbor distance.

We can now write the electrostatic energy at ion "0" as:

$$E_{elec} = -6 \frac{e^2}{4\pi\epsilon_0} \frac{z_+ z_-}{r_o} + 12 \frac{e^2}{4\pi\epsilon_0} \frac{z_+ z_-}{\sqrt{2} r_o} - 8 \frac{e^2}{4\pi\epsilon_0} \frac{z_+ z_-}{\sqrt{3} r_o} + \dots \quad (6.4.4.3)$$

Factoring out constants and the nearest-neighbor bond distance  $r_o$  we obtain:

$$E_{elec} = \frac{e^2}{4\pi\epsilon_0} \frac{z_+ z_-}{r_o} \left( 6 - \frac{12}{\sqrt{2}} + \frac{8}{\sqrt{3}} - \frac{6}{\sqrt{4}} + \dots \right) \quad (6.4.4.4)$$

Where the sum in parentheses, which is unitless, slowly converges to a value of  $A = 1.74756$ . Generalizing this formula for any three-dimensional ionic crystal we get a function:

$$E_{elec} = \frac{e^2}{4\pi\epsilon_0} \frac{z_+z_-}{r_o} N A \quad (6.4.4.5)$$

where  $N$  is Avogadro's number (because we are calculating energy per mole of ions) and  $A$  is called the *Madelung constant*. The **Madelung constant** depends only on the geometrical arrangement of the ions and so it varies between different types of crystal structures, but within a given structure type it does not change. Thus MgO and NaCl have the same Madelung constant because they both have the NaCl structure.

Table 6.4.4.1: Madelung Constants

Compound	Crystal Lattice	$M$	$A : C$	Type
NaCl	NaCl	1.74756	6 : 6	Rock salt
CsCl	CsCl	1.76267	6 : 6	CsCl type
CaF <sub>2</sub>	Cubic	2.51939	8 : 4	Fluorite
CdCl <sub>2</sub>	Hexagonal	2.244	6 : 3	
MgF <sub>2</sub>	Tetragonal	2.381		
ZnS (wurtzite)	Hexagonal	1.64132	4 : 4	Wurtzite
TiO <sub>2</sub> (rutile)	Tetragonal	2.408	6 : 3	Rutile
bSiO <sub>2</sub>	Hexagonal	2.2197		
Al <sub>2</sub> O <sub>3</sub>	Rhombohedral	4.1719	6 : 4	Corundum

$A$  is the number of anions coordinated to cation and  $C$  is the numbers of cations coordinated to anion.

## Born–Landé Equation

There are other factors to consider for the evaluation of lattice energy and the treatment by Max Born and Alfred Lande led to the formula for the evaluation of lattice energy for a mole of **crystalline solid**. The Born–Landé equation (Equation 6.4.4.6) is a means of calculating the lattice energy of a crystalline ionic compound and derived from the electrostatic potential of the ionic lattice and a repulsive potential energy term

$$U = \frac{N_A M Z^2 e^2}{4\pi\epsilon_0 r} \left( 1 - \frac{1}{n} \right) \quad (6.4.4.6)$$

where

- $N_A$  is Avogadro constant;
- $M$  is the Madelung constant for the lattice
- $z^+$  is the charge number of cation
- $z^-$  is the charge number of anion
- $e$  is elementary charge,  $1.6022 \times 10^{-19}$  C
- $\epsilon_0$  is the permittivity of free space
- $r_0$  is the distance to closest ion
- $n$  is the **Born exponent** that is typically between 5 and 12 and is determined experimentally.  $n$  is a number related to the electronic configurations of the ions involved (Table 6.4.4.3).

Table 6.4.4.2:  $n$  values for select solids

Atom/Molecule	$n$
He	5
Ne	7
Ar	9

Atom/Molecule	<i>n</i>
Kr	10
Xe	12
LiF	5.9
LiCl	8.0
LiBr	8.7
NaCl	9.1
NaBr	9.5

#### Example 6.4.4.1: NaCl

Estimate the lattice energy for NaCl.

##### Solution

Using the values giving in the discussion above, the estimation is given by

$$U_{NaCl} = \frac{(6.022 \times 10^{23}/mol)(1.74756)(1.6022 \times 10^{-19})^2(1.747558)}{4\pi (8.854 \times 10^{-12} C^2/m)(282 \times 10^{-12} m)} \left(1 - \frac{1}{9.1}\right)$$

$$= -756 \text{ kJ/mol}$$

Much more should be considered in order to evaluate the lattice energy accurately, but the above calculation leads you to a good start. When methods to evaluate the energy of crystallization or lattice energy lead to reliable values, these values can be used in the [Born-Hable cycle](#) to evaluate other chemical properties, for example the electron affinity, which is really difficult to determine directly by experiment.



Figure 6.4.4.4: Lithium fluoride (shown here as a large single crystal in a beaker of water) is the only alkali halide that is not freely soluble in water. The lattice energy of LiF is the most negative of the alkali fluorides because  $\text{Li}^+$  and  $\text{F}^-$  are both small ions and lattice energy is proportional to  $1/r_0$ .

6.4.4: Theoretical Lattice Energy Calculations is shared under a [CC BY-NC-SA 4.0](#) license and was authored, remixed, and/or curated by LibreTexts.

- [5.2: Energetics of Ionic Solids- Lattice Energy](#) is licensed [CC BY-NC-SA 4.0](#).
- [9.3: Energetics of Crystalline Solids- The Ionic Model](#) by Chemistry 310 is licensed [CC BY-SA 4.0](#). Original source: [https://en.wikibooks.org/wiki/Introduction\\_to\\_Inorganic\\_Chemistry](https://en.wikibooks.org/wiki/Introduction_to_Inorganic_Chemistry).
- [6.13E: Madelung Constants](#) is licensed [CC BY-NC-SA 4.0](#).

## 6.4.5: Kapustinskii Equation

From the discussion above, it is clear that the lattice energy,  $E_L$ , of an ionic crystal can be calculated with reasonable accuracy if the structure is known. But how can we calculate  $E_L$  for a new or hypothetical compound of unknown structure? Recall that the reduced Madelung constant is about the same for different crystal structures. Russian chemist A. F. Kapustinskii recognized this fact and devised a formula that allows one to calculate  $E_L$  for any compound if we know the univalent radii of the constituent ions. [5]

The Madelung constant,  $A$ , is proportional to the number of ions ( $n$ ) in formula unit, so dividing by the  $n$  gives similar values as shown in the table below:

**$A/n \sim \text{invariant}$**

Structure	$A/n$
NaCl	0.874
CsCl	0.882
Rutile	0.803
Fluorite	0.800

Kapustinskii noticed that the difference in ionic radii between  $M^+$  and  $M^{2+}$  (the monovalent vs. divalent radius) largely compensates for the differences in  $A/n$  between monovalent (NaCl, CsCl) and divalent (rutile,  $\text{CaF}_2$ ) structures. He thus arrived at a lattice energy formula using an average Madelung constant, corrected to monovalent radii. In the **Kapustinskii formula**, the lattice energy (kJ/mol) is given by:

$$E_L = \frac{1213.8 z_+ z_- n}{r_+ + r_-} \left( 1 - \frac{0.345}{r_+ + r_-} \right) \quad (6.4.5.1)$$

Here the sum of the monovalent radii is used in place of  $r_0$ , the bond distance in the Born-Mayer equation. The beauty of this formula is that it requires no knowledge of the structure of the compound. Therefore it can be used, in combination with Born-Haber cycles, to predict the stability of unknown compounds. As we show below, this is a broadly useful tool in guiding syntheses and predicting the reactivity of inorganic solids.

6.4.5: Kapustinskii Equation is shared under a [CC BY-SA](#) license and was authored, remixed, and/or curated by LibreTexts.

- **9.5: Kapustinskii Equation** by [Chemistry 310](#) is licensed [CC BY-SA 4.0](#). Original source: [https://en.wikibooks.org/wiki/Introduction\\_to\\_Inorganic\\_Chemistry](https://en.wikibooks.org/wiki/Introduction_to_Inorganic_Chemistry).



## 6.5: Band Theory and Conductivity

---

Learning objectives for this unit are to:

- Explain the origins of band theory and define valence and conduction bands
  - Classify materials as conductors, insulators, or semiconductors, and describe their conductivity
  - Use band theory to explain the manner in which conductors and semiconductors allow for the movement of electrons
  - Rationalize or predict trends in band gaps based on periodic properties
  - Explain how doping alters the electrical conductivity of a solid state material
  - Identify, compare, and design p- and n-type semiconductors
  - Calculate band gaps, carrier concentrations, and electrical conductivity of materials
- 

6.5: Band Theory and Conductivity is shared under a [not declared](#) license and was authored, remixed, and/or curated by LibreTexts.

## 6.5.1: Bonding in Metals and Semiconductors

### Band Theory

Band theory was developed with some help from the knowledge gained during the quantum revolution in science. In 1928, Felix Bloch had the idea to take the quantum theory and apply it to solids. In 1927, Walter Heitler and Fritz London discovered bands—very closely spaced orbitals with not much difference in energy. One way to conceptualize band theory is to view it as an extension of [molecular orbital theory](#) where the number of atomic orbitals mixed is increased to an infinite number and the energy difference between the molecular orbitals formed approaches 0 (Figure 6.5.1.1).

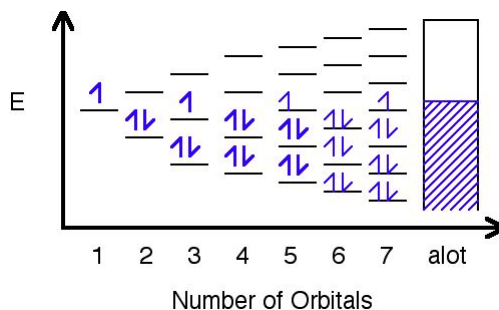


Figure 6.5.1.1: In this image, orbitals are represented by the black horizontal lines, and they are being filled with an increasing number of electrons as their amount increases. Eventually, as more orbitals are added, the space in between them decreases to hardly anything, and as a result, a band is formed where the orbitals have been filled.

example: Na

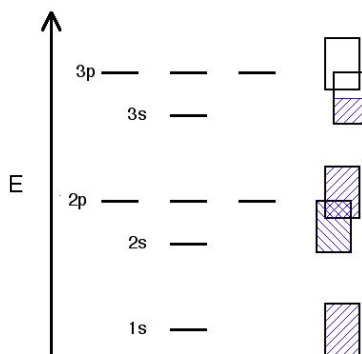


Figure 6.5.1.2: Bands diagram of sodium metal. Filled bands are blue and empty bands are white. Because the 3s orbital is half filled in Na, the band formed from the 3s orbitals is also half filled.

Different metals will produce different combinations of filled and half filled bands depending on their valence electron configuration. Sodium's bands are shown in Figure 6.5.1.2. As you can see, bands may overlap each other (the bands are shown askew to be able to tell the difference between different bands). The lowest unoccupied band is called the conduction band, and the highest occupied band is called the valence band.

Bands will follow a trend as you go across a period:

- In Na, the 3s band is 1/2 full.
- In Mg, the 3s band is full.
- In Al, the 3s band is full and the 3p band is 1/2 full... and so on.

In order for the material to conduct electricity, electrons should be in the conduction band where they are able to move freely through the material. The probability of finding an electron in the conduction band is shown by the equation:

$$P = \frac{1}{e^{\frac{\Delta E}{k_b T}} + 1} \quad (6.5.1.1)$$

The  $\Delta E$  in the equation stands for the energy gap between the valence and conduction bands.  $k_b$  is the Boltzmann constant and  $T$  is temperature in K. That equation and the table below show that the larger the band gap between the valence band and the

conduction band, the less likely electrons are to be found in the conduction band. This is because they don't have sufficient energy to make the jump up to the conduction band.

Table 6.5.1.1: Band Gaps and Conduction Band Electron Densities for Group 4 Elements

ELEMENT	$\Delta E(\text{kJ/mol})$ of energy gap	# of electrons/cm <sup>3</sup> in conduction band	material type
C (diamond)	524	$10^{-27}$	insulator
Si	117	$10^9$	semiconductor
Ge	66	$10^{13}$	semiconductor

## Conductors, Insulators and Semiconductors

The conductivity of materials is directly related to the band gap and the probability of having electrons in the conduction band. Materials can be divided into three classes based on their band gaps (Figure 6.5.1.3).

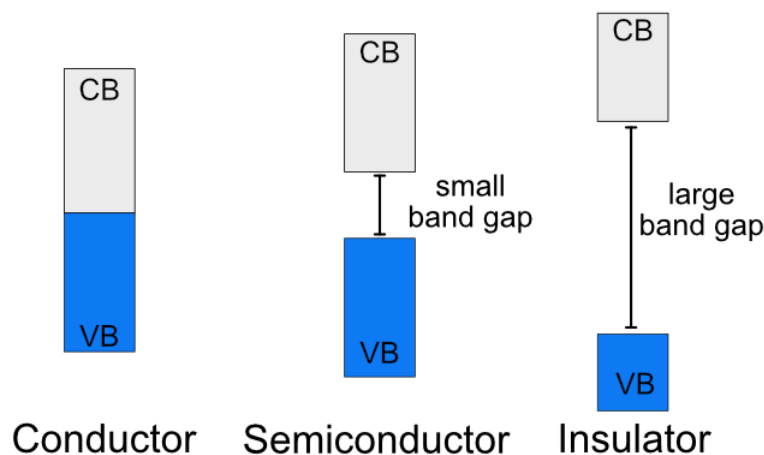


Figure 6.5.1.3: Illustration of the energy difference between the valence band (VB) and conduction band (CB) in conductors, semiconductors and insulators. (CC BY-NC-SA; Catherine McCusker)

### Conductors

Conductors have no band gap between their valence and conduction bands, since they overlap. There is no barrier for electrons to move from the valence to conduction band. Electrons can move freely through the material, which makes it able to conduct electricity. When the temperature of a conductor increases, the resistivity increases (and the conductivity decreases). Conductivity and resistivity are inversely proportional to each other. When conductivity is low, resistivity is high. When resistivity is low, conductivity is high. Since conductivity is the measure of how easily electricity flows, electrical resistivity measures how much a material resists the flow of electricity. As electrons move through a material, they come into contact with nuclei in the material. Collisions slow the electrons down. Each collision increases the resistivity of the material, and as temperature increases the electron are more likely to have collisions.

### Insulators

Insulators have a large band gap between the valence and conduction bands. In insulators electrons do not have sufficient energy to jump from the valence band to the conduction band and the probability of finding an electron in the conduction band approaches 0. An insulator material won't conduct any electricity at any temperature.

### Semiconductors

Semiconductors are an intermediate between conductors and insulators. They have a small energy gap between the valence band and the conduction band. Some electrons have sufficient energy that they can make the jump up to the conduction band. Semiconductors can conduct electricity, but not as easily as conductors. The probability of finding electrons in the conduction

band of a semiconductor, and therefore its ability to conduct electricity, will vary with the band gap and the temperature. Unlike conductors, semiconductors are more conductive at higher temperatures because more electrons have the energy to jump into the conduction band. There are two types of semiconductors: **intrinsic** and **extrinsic**.

### Intrinsic Semiconductors

An intrinsic semiconductor is a pure material with a small band gap. For every electron that jumps into the conduction band, the missing electron will generate a hole that can move freely in the valence band. Both conduction band electrons and valence band holes can contribute to conducting electricity. The number of holes will equal the number of electrons that have jumped.

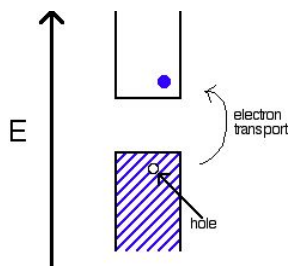


Figure 6.5.1.4: Illustration of an intrinsic semiconductor. The electron in the conduction band (blue dot) leaves behind a vacancy (hole) in the valence band (white dot).

### Extrinsic Semiconductors

Extrinsic semiconductors are not good conductors in their pure forms, they have larger band gaps than intrinsic semiconductors. In extrinsic semiconductors, the conductivity is controlled by purposefully adding small amounts of impurities to the material. This process is called doping. Doping, or adding impurities to the lattice can change the electrical conductivity of the lattice and therefore vary the efficiency of the semiconductor. In extrinsic semiconductors, the number of valence band holes will not equal the number of conduction band electrons. Silicon is one of the most common extrinsic semiconductors. If silicon is doped with an atom with fewer electrons, such as boron, electrons from the silicon valence band can hop to the boron atoms, leaving holes in the valence band to conduct electricity. If silicon is doped with an atom with more electrons, such as phosphorus, the extra electron from the phosphorus atoms can jump into the silicon conduction band.

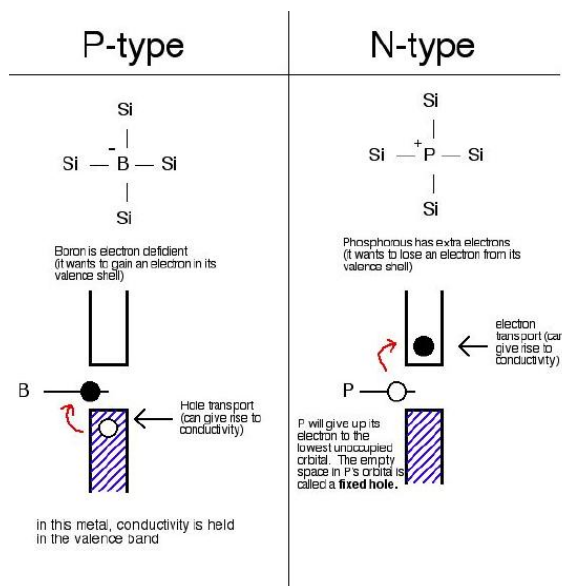


Figure 6.5.1.5: P-type (left) n-type (right) silicon semiconductors. In the p-type an electron from the valence band can jump to a vacancy on boron, leaving a hole in the valence band. In the n-type an electron from the phosphorus dopant can jump into the conduction band.

### Exercise 6.5.1.1

Describe the difference between a valence band and a conduction band

#### Answer

The valence band is the highest band with electrons in it, the equivalent of the HOMO in MO theory. The conduction band is the highest band with no electrons in it, the equivalent of the LUMO in MO theory.

### Exercise 6.5.1.2

A conductor material and a semiconductor material have the same conductivity at 100 K. Which will be more conductive when the temperature is increased to 200 K?

#### Answer

The conductivity of conductors will decrease as the temperature increases and the conductivity of semiconductors will increase as the temperature increases. Therefore at higher temperature the semiconductor material will have higher conductivity.

## References

1. Electrical Conductivity and Resistivity, Heaney, Michael, Electrical Measurement, Signal Processing, and Displays. Jul 2003
2. Levy, Peter M., and Shufeng Zhang. "Electrical Conductivity of Magnetic Multilayered Structures." *Physical Review Letters* 65.13 (1990): 1643-646. Print.
3. Petrucci, Harwood, Herring, Madura. GENERAL CHEMISTRY Principles and Modern Applications 9th Edition. Macmillan Publishing Co: New Jersey. 1989.
4. Moore, John T. Chemistry Made Simple. Random House Inc: New York. 2004.

## Contributors and Attributions

- Michael Ford (UCD) and Alexandra Christman (UCD)
- Sierra Blair (UCD)
- Jim Clark ([Chemguide.co.uk](http://Chemguide.co.uk))

6.5.1: Bonding in Metals and Semiconductors is shared under a [CC BY-NC-SA 4.0](https://creativecommons.org/licenses/by-nc-sa/4.0/) license and was authored, remixed, and/or curated by LibreTexts.

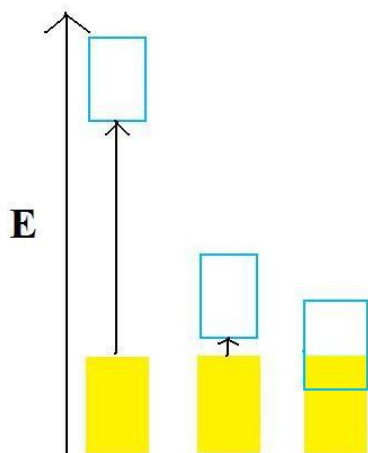
- [5.5: Bonding in Metals and Semiconductors](#) is licensed [CC BY-NC-SA 4.0](https://creativecommons.org/licenses/by-nc-sa/4.0/).
- [6.8A: Electrical Conductivity and Resistivity](#) is licensed [CC BY-NC-SA 4.0](https://creativecommons.org/licenses/by-nc-sa/4.0/).

## 6.5.2: The Fermi Level

The Fermi Level is the energy level which is occupied by the electron orbital at temperature equals 0 K. The level of occupancy determines the conductivity of different materials. For solid materials such as metals, the orbital occupancy can be calculated by making an approximation based on the crystalline structure. These orbitals, combined with the energy level, determine whether the material is an insulator, semi-conductor, or conductor. The orbitals are categorized according to its energy. The lower energy orbitals combine and form a band called the valence electron band, and the higher energy orbitals combine to form a band called the conduction band. There is a gap between the valence and conduction band called the energy gap; the larger the energy gap, the more energy it is required to transfer the electron from the valence band to the conduction band.

### Energy Band Diagram

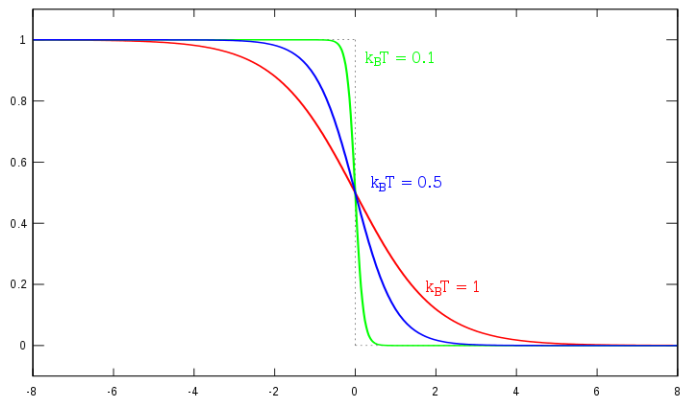
The diagram below is an example of an energy band diagram. The upper box represents the conduction band, the lower box represents the valence band, and the yellow is the occupancy level of electrons. The conductivity of a material can be determined by the energy diagram. In order to conduct electricity, an electron must make a transition into another state since electrons cannot occupy the same quantum states. When the electron cannot make that transition, it will be not be able to conduct electricity. When the band is completely filled, the closest state an electron to transfer to will be the states in the conduction band, and that would require the electron to jump over the band gap, thus making it more difficult to conduct electricity. With this rule, it is easy to tell the difference between insulator, semi-conductor, and conductors. The energy band on the left side is an insulator because if an electron wants to go into a higher energy state, it will need to jump through that huge energy gap. Since it requires a large amount of energy to move the electron, the material will have a difficult time conducting electricity. The energy band in the middle is a semi-conductor because although the electrons have to jump across the energy gap, the energy gap is small. If an electron wants to make a transition, it will require very little energy since they are all in the same energy band. Thus, for the material in the middle, although it will have difficulty conducting electricity, it is not impossible. The energy band in the right is a conductor. Although the valence band is filled just like the insulator and semi-conductor, the conduction band overlaps the valence band. If an electron wants to make a transition, it will require very little amount of energy. Which means the material on the right can conduct electricity very easily.



### Fermi Level

The electrons that occupies the orbits are described by Fermi-Dirac distribution as the figure below, the distribution takes on the form of:

$$f(E) = \frac{1}{1 + \exp[(E - \mu)/kT]}$$



[http://upload.wikimedia.org/wikipedi...irac\\_distr.svg](http://upload.wikimedia.org/wikipedi...irac_distr.svg)

Where  $E$  is the energy of the system,  $\mu$  is the Fermi level,  $k_B$  is the Boltzmann constant, and  $T$  is the temperature. The Fermi-Dirac distribution accounts for the population level at different energies. The Fermi level is at  $e/\mu = 1$  and  $k_B T = \mu$ . Whenever the system is at the Fermi level, the population  $n$  is equal to  $1/2$ . The tail part in the exponential is very important for the conductivity of semi-conductors. If you can bring the Fermi level high enough, then part of the tail will go over to the conduction band. Thus, the electron will have an easier time making a transition to the conduction band and the conductivity will increase. The conductivity can also be affected by factors such as temperature and purity. From the distribution, the temperature has a direct effect on how the energy states are populated. When temperature increases the tail of the exponential gets longer and wider, thus making the conduction band level population more accessible. For Semi-conductor materials, having an access to the conduction band level means it can conduct electricity with energy, which means the conductivity of the material is increased. The purity also affects the Fermi level. Purity defects with atoms that have excess electrons would bring the Fermi level up, and making it easier for electrons to jump into the conduction band.

## References

1. Kittel, Charles. Introduction to Solid State Physics. Eighth edition. New Jersey: John Wiley & Sons, Inc, 2005.
2. Griffiths, Davis. Introduction to Quantum Mechanics. Second edition. New Jersey: Pearson Education, Inc, 2005.
3. Band energies.jpg

## Problems

1. Besides the Fermi Level, what other factor determines the population in different energy levels?

answer: Temperature

2. What is the difference between a semi-conductor and an insulator?

answer: A semi-conductor has a smaller band gap and therefore, while more difficult than a conductor, is able to conduct electricity if you put in enough energy.

3. What does the Fermi level determine?

answer: The Fermi level determines several factors. It determines the population at different energy levels. It also determines how easily can the material conduct electricity. As your Fermi level approaches your conduction band energy, it will be easier for the electrons from the valence band to travel to the conduction band.

---

6.5.2: The Fermi Level is shared under a [not declared](#) license and was authored, remixed, and/or curated by LibreTexts.

### 6.5.3: Semiconductors- Band Gaps, Colors, Conductivity and Doping

Semiconductors, as we noted above, are somewhat arbitrarily defined as insulators with **band gap energy**  $\leq 3.0 \text{ eV}$  ( $\sim 290 \text{ kJ/mol}$ ). This cutoff is chosen because, as we will see, the conductivity of undoped semiconductors drops off exponentially with the band gap energy and at  $3.0 \text{ eV}$  it is very low. Also, materials with wider band gaps (e.g.  $\text{SrTiO}_3$ ,  $E_{\text{gap}} = 3.2 \text{ eV}$ ) do not absorb light in the visible part of the spectrum

There are a number of places where we find semiconductors in the periodic table:

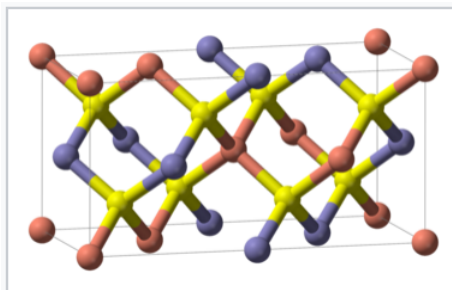
- Early transition metal oxides and nitrides, especially those with  $d^0$  electron counts such as  $\text{TiO}_2$ ,  $\text{TaON}$ , and  $\text{WO}_3$
- Oxides of later 3d elements such as  $\text{Fe}_2\text{O}_3$ ,  $\text{NiO}$ , and  $\text{Cu}_2\text{O}$
- Layered transition metal chalcogenides with  $d^0$ ,  $d^2$  and  $d^6$  electron counts including  $\text{TiS}_2$ ,  $\text{ZrS}_2$ ,  $\text{MoS}_2$ ,  $\text{WSe}_2$ , and  $\text{PtS}_2$
- $d^{10}$  copper and silver halides, e.g.,  $\text{CuI}$ ,  $\text{AgBr}$ , and  $\text{AgI}$
- Zincblende- and wurtzite-structure compounds of the p-block elements, especially those that are isoelectronic with Si or Ge, such as  $\text{GaAs}$  and  $\text{CdTe}$ . While these are most common, there are other p-block semiconductors that are not isoelectronic and have different structures, including  $\text{GaS}$ ,  $\text{PbS}$ , and  $\text{Se}$ .



A 2" wafer cut from a GaAs single crystal. GaAs, like many p-block semiconductors, has the zincblende structure.

The **p-block octet semiconductors** are by far the most studied and important for technological applications, and are the ones that we will discuss in detail.

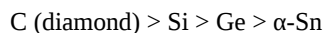
**Zincblende- and wurtzite-structure** semiconductors have 8 valence electrons per 2 atoms. These combinations include 4-4 (Si, Ge,  $\text{SiC}$ ,...), 3-5 ( $\text{GaAs}$ ,  $\text{AlSb}$ ,  $\text{InP}$ ,...), 2-6 ( $\text{CdSe}$ ,  $\text{HgTe}$ ,  $\text{ZnO}$ ,...), and 1-7 ( $\text{AgCl}$ ,  $\text{CuBr}$ ,...) semiconductors. Other variations that add up to an octet configuration are also possible, such as  $\text{Cu}^{\text{I}}\text{In}^{\text{III}}\text{Se}_2$ , which has the **chalcopyrite** structure, shown at the right.



The **chalcopyrite structure** is adopted by  $\text{ABX}_2$  octet semiconductors such as  $\text{Cu}^{\text{I}}\text{In}^{\text{III}}\text{Se}_2$  and  $\text{Cd}^{\text{II}}\text{Sn}^{\text{IV}}\text{P}_2$ . The unit cell is doubled relative to the parent **zincblende structure** because of the ordered arrangement of cations. Each anion (yellow) is coordinated by two cations of each type (blue and red).

How does the **band gap energy** vary with **composition**? There are two important trends

(1) Going **down a group** in the periodic table, the gap **decreases**:





$E_{\text{gap}}$  (eV): 5.4 1.1 0.7 0.0

This trend can be understood by recalling that  $E_{\text{gap}}$  is related to the **energy splitting between bonding and antibonding orbitals**. This difference decreases (and bonds become weaker) as the principal quantum number increases.

(2) For isoelectronic compounds, **increasing ionicity** results in a **larger band gap**.

Ge < GaAs < ZnSe

0.7 1.4 2.8 eV

Sn < InSb < CdTe < AgI

0.0 0.2 1.6 2.8 eV

This trend can also be understood from a simple MO picture, as we discussed in Ch. 2. As the electronegativity difference  $\Delta\chi$  increases, so does the energy difference between bonding and antibonding orbitals.

The band gap is a very important property of a semiconductor because it determines its color and conductivity. Many of the applications of semiconductors are related to band gaps:

- Narrow gap materials ( $\text{Hg}_x\text{Cd}_{1-x}\text{Te}$ ,  $\text{VO}_2$ , InSb,  $\text{Bi}_2\text{Te}_3$ ) are used as infrared photodetectors and thermoelectrics (which convert heat to electricity).
- Wider gap materials (Si, GaAs, GaP, GaN, CdTe,  $\text{CuIn}_x\text{Ga}_{1-x}\text{Se}_2$ ) are used in electronics, light-emitting diodes, and solar cells.



Color wheel showing the colors and wavelengths of emitted light.

Semiconductor solid solutions such as  $\text{GaAs}_{1-x}\text{P}_x$  have band gaps that are intermediate between the end member compounds, in this case GaAs and GaP (both zincblende structure). Often, there is a linear relation between composition and band gap, which is referred to as **Vegard's Law**. This "law" is often violated in real materials, but nevertheless offers useful guidance for designing materials with specific band gaps. For example, red and orange light-emitting diodes (LED's) are made from solid solutions with compositions of  $\text{GaP}_{0.40}\text{As}_{0.60}$  and  $\text{GaP}_{0.65}\text{As}_{0.35}$ , respectively. Increasing the mole fraction of the lighter element (P) results in a larger band gap, and thus a higher energy of emitted photons.

### Colors of semiconductors

The color of absorbed and emitted light both depend on the band gap of the semiconductor. Visible light covers the range of approximately 390-700 nm, or 1.8-3.1 eV. The **color of emitted light** from an LED or semiconductor laser corresponds to the band gap energy and can be read off the color wheel shown at the right.



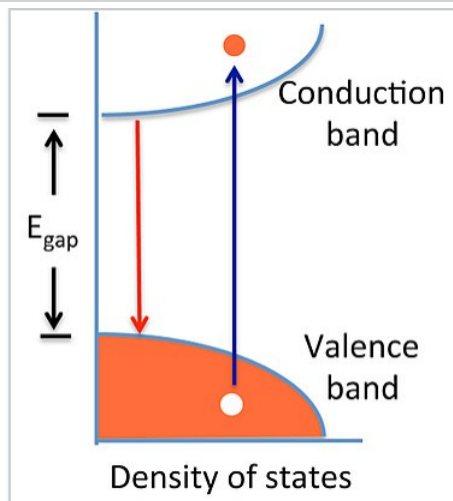
Fe<sub>2</sub>O<sub>3</sub> powder is reddish orange because of its 2.2 eV band gap

The color of **absorbed light** includes the band gap energy, but also all colors of higher energy (shorter wavelength), because electrons can be excited from the valence band to a range of energies in the conduction band. Thus semiconductors with band gaps in the infrared (e.g., Si, 1.1 eV and GaAs, 1.4 eV) appear black because they absorb all colors of visible light. Wide band gap semiconductors such as TiO<sub>2</sub> (3.0 eV) are white because they absorb only in the UV. Fe<sub>2</sub>O<sub>3</sub> has a band gap of 2.2 eV and thus absorbs light with  $\lambda < 560$  nm. It thus appears reddish-orange (the colors of light reflected from Fe<sub>2</sub>O<sub>3</sub>) because it absorbs green, blue, and violet light. Similarly, CdS ( $E_{\text{gap}} = 2.6$  eV) is yellow because it absorbs blue and violet light.

### Electrons and holes in semiconductors

Pure (undoped) semiconductors can conduct electricity when electrons are promoted, either by heat or light, from the valence band to the conduction band. The promotion of an **electron** (e<sup>-</sup>) leaves behind a **hole** (h<sup>+</sup>) in the valence band. The hole, which is the absence of an electron in a bonding orbital, is also a mobile charge carrier, but with a positive charge. The motion of holes in the lattice can be pictured as analogous to the movement of an empty seat in a crowded theater. An empty seat in the middle of a row can move to the end of the row (to accommodate a person arriving late to the movie) if everyone moves over by one seat. Because the movement of the hole is in the opposite direction of electron movement, it acts as a positive charge carrier in an electric field.

The opposite process of excitation, which creates an electron-hole pair, is their recombination. When a conduction band electron drops down to recombine with a valence band hole, both are annihilated and energy is released. This release of energy is responsible for the emission of light in LEDs.



An electron-hole pair is created by adding heat or light energy  $E \geq E_{\text{gap}}$  to a semiconductor (blue arrow). The electron-hole pair recombines to release energy equal to  $E_{\text{gap}}$  (red arrow).

At equilibrium, the creation and annihilation of electron-hole pairs proceed at equal rates. This dynamic equilibrium is analogous to the dissociation-association equilibrium of H<sup>+</sup> and OH<sup>-</sup> ions in water. We can write a mass action expression:

$$n \times p = K_{eq} = n_i^2$$

where  $n$  and  $p$  represent the number density of electrons and holes, respectively, in units of  $\text{cm}^{-3}$ . The intrinsic carrier concentration,  $n_i$ , is equal to the number density of electrons or holes in an undoped semiconductor, where  $n = p = n_i$ .

Note the similarity to the equation for water autodissociation:

$$[H^+][OH^-] = K_w$$

By analogy, we will see that when we increase  $n$  (e.g., by doping),  $p$  will decrease, and vice-versa, but their product will remain constant at a given temperature.

**Temperature dependence of the carrier concentration.** Using the equations  $K_{eq} = e^{(\frac{-\Delta G^o}{RT})}$  and  $\Delta G^o = \Delta H^o - T\Delta S^o$ , we can write:

$$n \times p = n_i^2 = e^{(\frac{\Delta S^o}{R})} e^{(\frac{-\Delta H^o}{RT})} \quad (6.5.3.1)$$

The entropy change for creating electron hole pairs is given by:

$$\Delta S^o = R \ln(N_V) + R \ln(N_V) = R \ln(N_C N_V) \quad (6.5.3.2)$$

where  $N_V$  and  $N_C$  are the effective density of states in the valence and conduction bands, respectively.

and thus we obtain

$$n_i^2 = N_C N_V e^{(-\Delta H^o / RT)} \quad (6.5.3.3)$$

Since the volume change is negligible,  $\Delta H^o \approx \Delta E^o$ , and therefore  $\frac{\Delta H^o}{R} \approx \frac{E_{gap}}{k}$ , from which we obtain

$$n_i^2 = N_C N_V e^{(\frac{-E_{gap}}{kT})} \quad (6.5.3.4)$$

and finally

$$n = p = n_i = (N_C N_V)^{\frac{1}{2}} e^{(\frac{-E_{gap}}{2kT})} \quad (6.5.3.5)$$

For pure Si ( $E_{gap} = 1.1 \text{ eV}$ ) with  $N \approx 10^{22}/\text{cm}^3$ , we can calculate from this equation a carrier density  $n_i$  of approximately  $10^{10}/\text{cm}^3$  at 300 K. This is about 12 orders of magnitude lower than the valence electron density of Al, the element just to the left of Si in the periodic table. Thus we expect the conductivity of pure semiconductors to be many orders of magnitude lower than those of metals.

## Conductivity of intrinsic semiconductors

The conductivity ( $\sigma$ ) is the product of the number density of carriers ( $n$  or  $p$ ), their charge ( $e$ ), and their mobility ( $\mu$ ). Recall from Chapter 6 that  $\mu$  is the ratio of the carrier drift velocity to the electric field and has units of  $\text{cm}^2/\text{Volt-second}$ . Typically electrons and holes have somewhat different mobilities ( $\mu_e$  and  $\mu_h$ , respectively) so the conductivity is given by:

$$\sigma = ne\mu_e + pe\mu_h \quad (6.5.3.6)$$

For either type of charge carrier, we recall from Ch. 6 that the mobility  $\mu$  is given by:

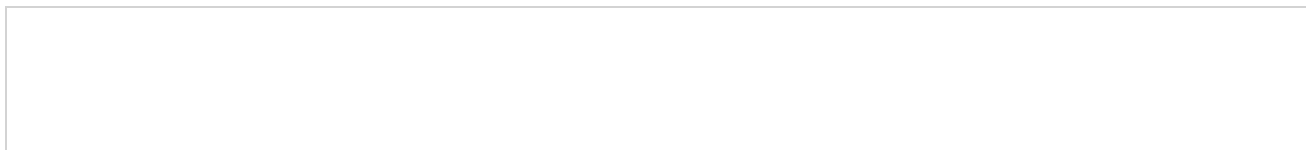
$$\mu = \frac{v_{drift}}{E} = \frac{e\tau}{m} \quad (6.5.3.7)$$

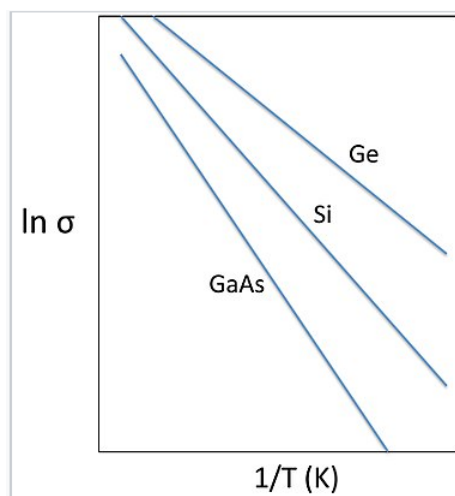
where  $e$  is the fundamental unit of charge,  $\tau$  is the scattering time, and  $m$  is the effective mass of the charge carrier.

Taking an average of the electron and hole mobilities, and using  $n = p$ , we obtain

$$\sigma = \sigma_o e^{(\frac{-E_{gap}}{2kT})}, \text{ where } \sigma_o = 2(N_C N_V)^{\frac{1}{2}} e\mu \quad (6.5.3.8)$$

By measuring the conductivity as a function of temperature, it is possible to obtain the activation energy for conduction, which is  $E_{gap}/2$ . This kind of plot, which resembles an Arrhenius plot, is shown at the right for three different undoped semiconductors. The slope of the line in each case is  $-E_{gap}/2k$ .



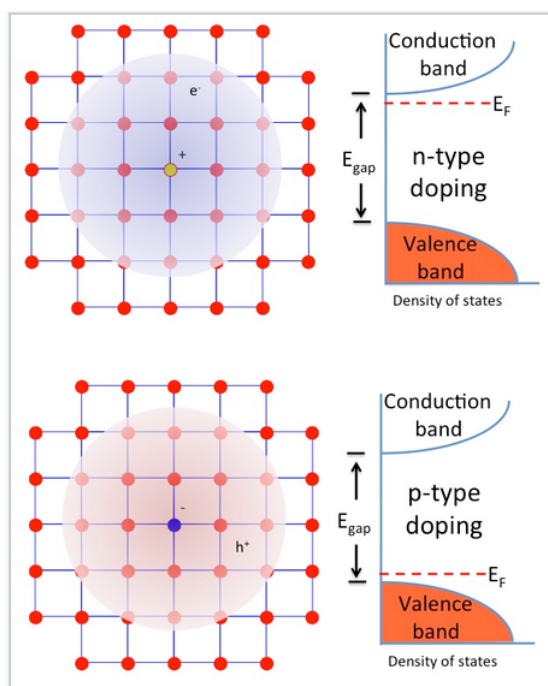


Plots of  $\ln(\sigma)$  vs. inverse temperature for intrinsic semiconductors Ge ( $E_{\text{gap}} = 0.7$  eV), Si (1.1 eV) and GaAs (1.4 eV). The slope of the line is  $-E_{\text{gap}}/2k$ .

**Doping of semiconductors.** Almost all applications of semiconductors involve controlled **doping**, which is the substitution of impurity atoms, into the lattice. Very small amounts of dopants (in the parts-per-million range) dramatically affect the conductivity of semiconductors. For this reason, very pure semiconductor materials that are carefully doped - both in terms of the concentration and spatial distribution of impurity atoms - are needed.

**n- and p-type doping.** In crystalline Si, each atom has four valence electrons and makes four bonds to its neighbors. This is exactly the right number of electrons to completely fill the valence band of the semiconductor. Introducing a phosphorus atom into the lattice (the positively charged atom in the figure at the right) adds an extra electron, because P has five valence electrons and only needs four to make bonds to its neighbors. The extra electron, at low temperature, is bound to the phosphorus atom in a hydrogen-like molecular orbital that is much larger than the 3s orbital of an isolated P atom because of the high dielectric constant of the semiconductor. In silicon, this "expanded" Bohr radius is about 42 Å, i.e., 80 times larger than in the hydrogen atom. The energy needed to ionize this electron - to allow it to move freely in the lattice - is only about 40–50 meV, which is not much larger than the thermal energy (26 meV) at room temperature. Therefore the Fermi level lies just below the conduction band edge, and a large fraction of these extra electrons are promoted to the conduction band at room temperature, leaving behind fixed positive charges on the P atom sites. The crystal is **n-doped**, meaning that the majority carrier (electron) is negatively charged.

Alternatively, boron can be substituted for silicon in the lattice, resulting in **p-type** doping, in which the majority carrier (hole) is positively charged. Boron has only three valence electrons, and "borrows" one from the Si lattice, creating a positively charged hole that exists in a large hydrogen-like orbital around the B atom. This hole can become delocalized by promoting an electron from the valence band to fill the localized hole state. Again, this process requires only 40–50 meV, and so at room temperature a large fraction of the holes introduced by boron doping exist in delocalized valence band states. The Fermi level (the electron energy level that has a 50% probability of occupancy at zero temperature) lies just above the valence band edge in a p-type semiconductor.



n- and p-type doping of semiconductors involves substitution of electron donor atoms (light orange) or acceptor atoms (blue) into the lattice. These substitutions introduce extra electrons or holes, respectively, which are easily ionized by thermal energy to become free carriers. The Fermi level of a doped semiconductor is a few tens of mV below the conduction band (n-type) or above the valence band (p-type).

As noted above, the doping of semiconductors dramatically changes their conductivity. For example, the intrinsic carrier concentration in Si at 300 K is about  $10^{10} \text{ cm}^{-3}$ . The mass action equilibrium for electrons and holes also applies to doped semiconductors, so we can write:

$$n \times p = n_i^2 = 10^{20} \text{ cm}^{-6} \text{ at } 300\text{K} \quad (6.5.3.9)$$

If we substitute P for Si at the level of one part-per-million, the concentration of electrons is about  $10^{16} \text{ cm}^{-3}$ , since there are approximately  $10^{22} \text{ Si atoms/cm}^3$  in the crystal. According to the mass action equation, if  $n = 10^{16}$ , then  $p = 10^4 \text{ cm}^{-3}$ . There are three consequences of this calculation:

- The density of carriers in the doped semiconductor ( $10^{16} \text{ cm}^{-3}$ ) is much higher than in the undoped material ( $\sim 10^{10} \text{ cm}^{-3}$ ), so the conductivity is also many orders of magnitude higher.
- The activation energy for conduction is only 40–50 meV, so the conductivity does not change much with temperature (unlike in the intrinsic semiconductor)
- The minority carriers (in this case holes) do not contribute to the conductivity, because their concentration is so much lower than that of the majority carrier (electrons).

Similarly, for p-type materials, the conductivity is dominated by holes, and is also much higher than that of the intrinsic semiconductor.

**Chemistry of semiconductor doping.** Sometimes it is not immediately obvious what kind of doping (n- or p-type) is induced by "messing up" a semiconductor crystal lattice. In addition to substitution of impurity atoms on normal lattice sites (the examples given above for Si), it is also possible to dope with vacancies - missing atoms - and with interstitials - extra atoms on sites that are not ordinarily occupied. Some simple rules are as follows:

- For substitutions, adding an **atom to the right** in the periodic table results in **n-type** doping, and an atom to the **left** in **p-type** doping.

For example, when  $\text{TiO}_2$  is doped with Nb on some of the Ti sites, or with F on O sites, the result is n-type doping. In both cases, the impurity atom has one more valence electron than the atom for which it was substituted. Similarly, substituting a small amount of Zn for Ga in GaAs, or a small amount of Li for Ni in NiO, results in p-type doping.

- **Anion vacancies** result in **n-type** doping, and **cation vacancies** in **p-type** doping.

Examples are anion vacancies in  $\text{CdS}_{1-x}$  and  $\text{WO}_{3-x}$ , both of which give n-type semiconductors, and copper vacancies in  $\text{Cu}_{1-x}\text{O}$ , which gives a p-type semiconductor.

- **Interstitial cations** (e.g. Li) donate electrons to the lattice resulting in **n-type** doping. Interstitial anions are rather rare but would result in p-type doping.

Sometimes, there can be both p- and n-type dopants in the same crystal, for example B and P impurities in a Si lattice, or cation and anion vacancies in a metal oxide lattice. In this case, the two kinds of doping **compensate** each other, and the doping type is determined by the one that is in higher concentration. A dopant can also be present on more than one site. For example, Si can occupy both the Ga and As sites in GaAs, and the two substitutions compensate each other. Si has a slight preference for the Ga site, however, resulting in n-type doping.

---

6.5.3: Semiconductors- Band Gaps, Colors, Conductivity and Doping is shared under a [CC BY-SA](#) license and was authored, remixed, and/or curated by LibreTexts.

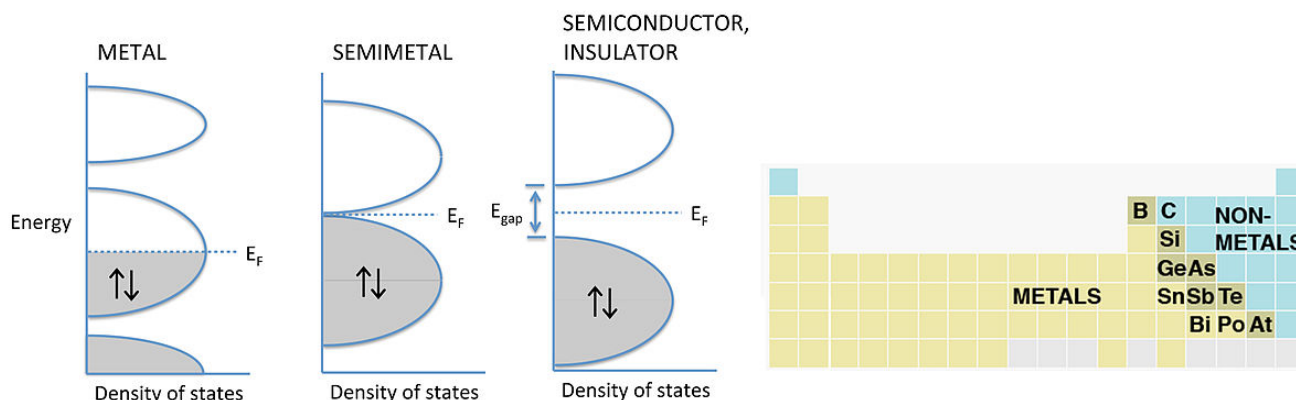
- **10.5: Semiconductors- Band Gaps, Colors, Conductivity and Doping** by Chemistry 310 is licensed [CC BY-SA 4.0](#). Original source: [https://en.wikibooks.org/wiki/Introduction\\_to\\_Inorganic\\_Chemistry](https://en.wikibooks.org/wiki/Introduction_to_Inorganic_Chemistry).

### 6.5.4: Periodic Trends- Metals, Semiconductors, and Insulators

As we consider periodic trends in the electronic properties of materials, it is important to review some of the key bonding trends we have learned in earlier chapters:

- Going down the periodic table, atoms in solids tend to adopt structures with higher coordination numbers.
- The second row of the periodic table is special, with strong s-p hybridization and  $\pi$ -bonding between atoms.
- Electrons in higher quantum shells are less strongly bound, so the energy difference between bonding and antibonding orbitals becomes smaller for heavier atoms.

We also know that most of the elements in the periodic table are metals, but the elements in the top right corner are insulating under ordinary conditions (1 atm. pressure) and tend to obey the octet rule in their compounds.



At the transition between metals and non-metals in the periodic table we encounter a crossover in electronic properties, as well as in other properties such as the acidity of the oxides (see Ch. 3). The group of elements at the border is loosely referred to as the metalloids. Several of these elements (such as C, Sn, and As) can exist as different allotropes that can be metals, insulators, or something in between.

A more rigorous delineation of the electronic properties of these elements (and of many compounds) can be made by considering their band structures and the **temperature dependence of the electronic conductivity**. As we have previously discussed, metals have partially filled energy bands, meaning that the Fermi level intersects a partially filled band. With increasing temperature, metals become poorer conductors because lattice vibrations (which are called phonons in the physics literature) scatter the mobile valence electrons. In contrast, semiconductors and insulators, which have filled and empty bands, become better conductors at higher temperature, since some electrons are thermally excited to the lowest empty band. The distinction between insulators and semiconductors is arbitrary, and from the point of view of metal-insulator transitions, all semiconductors are insulators. We typically call an insulator a semiconductor if its band gap ( $E_{\text{gap}}$ ) is less than about 3 eV. A semimetal is a material that has a band gap near zero, examples being single sheets of  $sp^2$ -bonded carbon (graphene) and elemental Bi. Like a narrow gap semiconductor, a semimetal has higher conductivity at higher temperature.

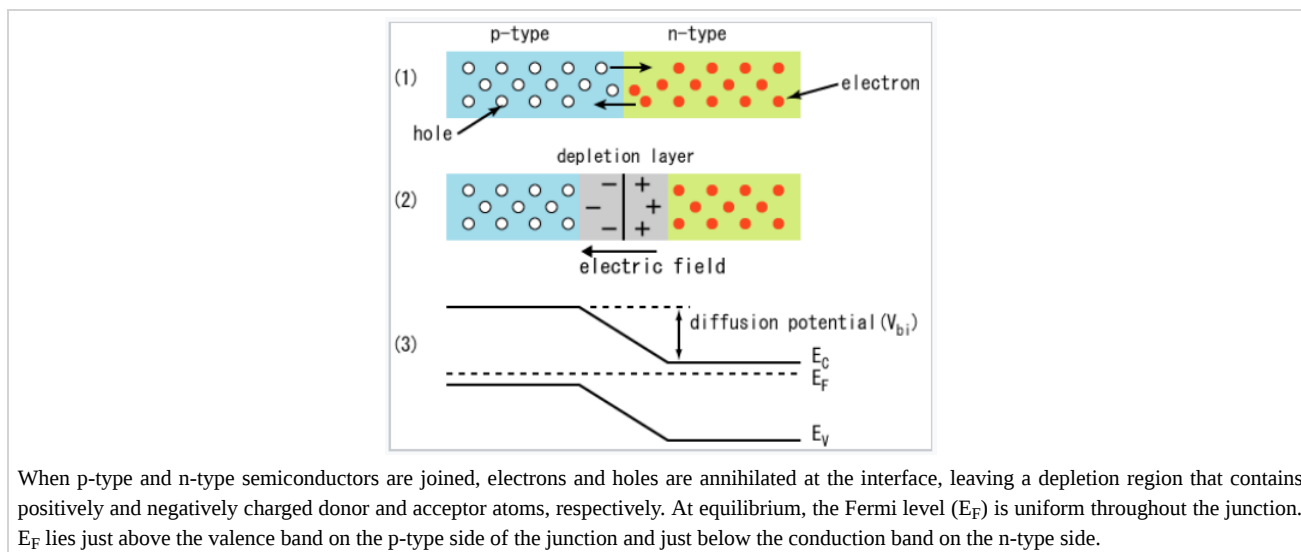
6.5.4: Periodic Trends- Metals, Semiconductors, and Insulators is shared under a [CC BY-SA](#) license and was authored, remixed, and/or curated by LibreTexts.

- **10.4: Periodic Trends- Metals, Semiconductors, and Insulators** by Chemistry 310 is licensed [CC BY-SA 4.0](#). Original source: [https://en.wikibooks.org/wiki/Introduction\\_to\\_Inorganic\\_Chemistry](https://en.wikibooks.org/wiki/Introduction_to_Inorganic_Chemistry).

## 6.5.5: Semiconductor p-n Junctions

**Semiconductor p-n junctions** are important in many kinds of electronic devices, including diodes, transistors, light-emitting diodes, and photovoltaic cells. To understand the operation of these devices, we first need to look at what happens to electrons and holes when we bring p-type and n-type semiconductors together. At the junction between the two materials, mobile electrons and holes annihilate each other, leaving behind the fixed + and - charges of the electron donor and electron acceptor dopants, respectively. For example, on the n-side of a silicon p-n junction, the positively charged dopants are  $P^+$  ions and on the p-side the negatively charged dopants are  $B^-$ . The presence of these uncompensated electrical charges creates an electric field, the **built-in field** of the p-n junction. The region that contains these charges (and a very low density of mobile electrons or holes) is called the **depletion region**.

The electric field, which is created in the depletion region by electron-hole recombination, repels both the electrons (on the n-side) and holes (on the p-side) away from the junction. The concentration gradient of electrons and holes, however, tends to move them in the opposite direction by diffusion. At equilibrium, the flux of mobile carriers is zero because the field-driven migration flux is equal and opposite to the concentration-driven diffusion flux.



The width of the depletion layer depends on the screening length in the semiconductor, which in turn depends on the dopant density. At high doping levels, the depletion layer is narrow (tens of nanometers across), whereas at low doping density it can be as thick as 1  $\mu\text{m}$ . The depletion region is the only place where the electric field is nonzero, and the only place where the bands bend. Elsewhere in the semiconductor the field is zero and the bands are flat.

In the middle of p-n junction, the Fermi level energy,  $E_F$ , is halfway between the valence band, VB, and the conduction band, CB, and the semiconductor is intrinsic ( $n = p = n_i$ )

6.5.5: Semiconductor p-n Junctions is shared under a [CC BY-SA](#) license and was authored, remixed, and/or curated by LibreTexts.

- **10.6: Semiconductor p-n Junctions** by Chemistry 310 is licensed [CC BY-SA 4.0](#). Original source: [https://en.wikibooks.org/wiki/Introduction\\_to\\_Inorganic\\_Chemistry](https://en.wikibooks.org/wiki/Introduction_to_Inorganic_Chemistry).



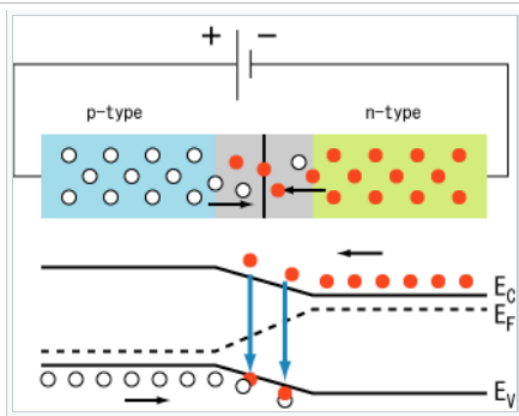
## 6.5.6: Diodes, LEDs and Solar Cells

**Diodes** are semiconductor devices that allow current to flow in only one direction. Diodes act as rectifiers in electronic circuits, and also as efficient light emitters (in LEDs) and solar cells (in photovoltaics). The basic structure of a diode is a junction between a p-type and an n-type semiconductor, called a p-n junction. Typically, diodes are made from a single semiconductor crystal into which p- and n- dopants are introduced.



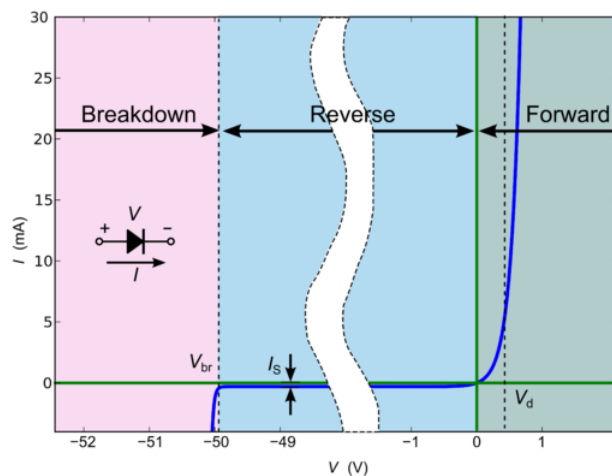
Closeup of a diode, showing the square-shaped semiconductor crystal (*black object on left*) (John Maushammer, [Wikipedia](#), CC-BY-SA)

If the n-side of a diode is biased at positive potential and the p-side is biased negative, electrons are drawn to the n-side and holes to the p-side. This reinforces the built in potential of the p-n junction, the width of the depletion layer increases, and very little current flows. This polarization direction is referred to as "back bias." If the diode is biased the other way, carriers are driven into the junction where they recombine. The electric field is diminished, the bands are flattened, and current flows easily since the applied bias lowers the built-in potential. This is called "forward bias."



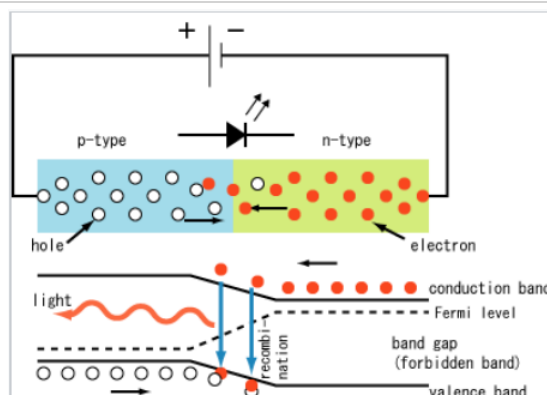
Electrons (red) and holes (white) in a forward-biased diode. (S-kei, [Wikipedia](#), CC-BY-SA)

The figure on the left illustrates a forward-biased diode, through which current flows easily. As electrons and holes are driven into the junction (black arrows in lower left figure), they recombine (downward blue arrows), producing light and/or heat. The Fermi level in the diode is indicated as the dotted line. There is a drop in the Fermi level (equal to the applied bias) across the depletion layer. The corresponding diode i-V curve is shown on the right. The current rises exponentially with applied voltage in the forward bias direction, and there is very little leakage current under reverse bias. At very high reverse bias (typically tens of volts) diodes undergo avalanche breakdown and a large reverse current flows.



Diode i-V curve

A **light-emitting diode** or **LED** is a kind of diode that converts some of the energy of electron-hole recombination into light. This radiative recombination process always occurs in competition with non-radiative recombination, in which the energy is simply converted to heat. When light is emitted from an LED, the photon energy is equal to the bandgap energy. Because of this, LED lights have pure colors and narrow emission spectra relative to other light sources, such as incandescent and fluorescent lights. LED lights are energy-efficient and thus are typically cool to the touch.



Light-emitting diode (LED). (S-kei. [Wikipedia](#), CC-BY-SA)

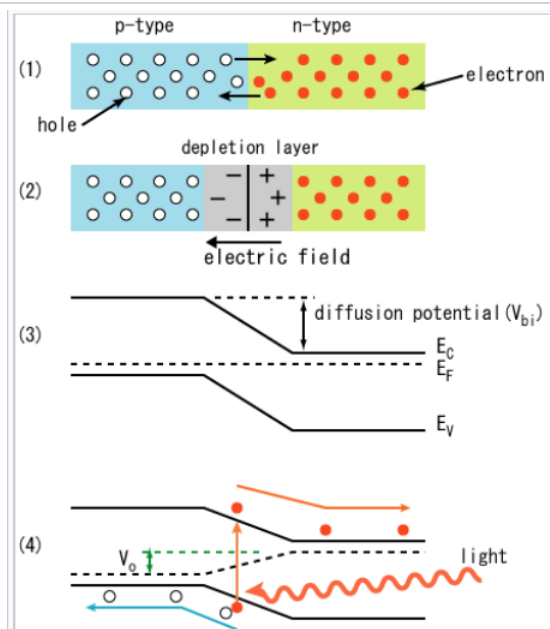
**Direct-gap** semiconductors such as GaAs and GaP have efficient luminescence and are also good light absorbers. In direct gap semiconductors, there is no momentum change involved in electron-hole creation or recombination. That is, the electrons and holes originate at the same value of the momentum wavevector  $\mathbf{k}$ , which we encountered in Ch. 6.  $\mathbf{k}$  is related to the momentum (also a vector quantity) by  $\mathbf{p} = \hbar\mathbf{k}/2\pi$ . In a direct-gap semiconductor, the top of the valence band and the bottom of the conduction band most typically both occur at  $\mathbf{k} = 0$ . Since the momentum of the photon is close to zero, photon absorption and emission are strongly allowed (and thus kinetically fast). Polar semiconductors such as GaAs, GaN, and CdSe are typically direct-gap materials. **Indirect-gap** semiconductors such as Si and Ge absorb and emit light very weakly because the valence band maximum and conduction band minimum do not occur at the same point in  $\mathbf{k}$ -space. This means that a lattice vibration (a phonon) must also be created or annihilated in order to conserve momentum. Since this "three body" (electron, hole, phonon) process has low probability, the radiative recombination of electrons and holes is slow relative to non-radiative decay - the thermalization of electron-hole energy as lattice vibrations - in indirect-gap semiconductors. The momentum selection rule thus prevents light absorption/emission and there are no pure Si LEDs or Si-based lasers.



Prof. Shuji Nakamura holding a blue LED.

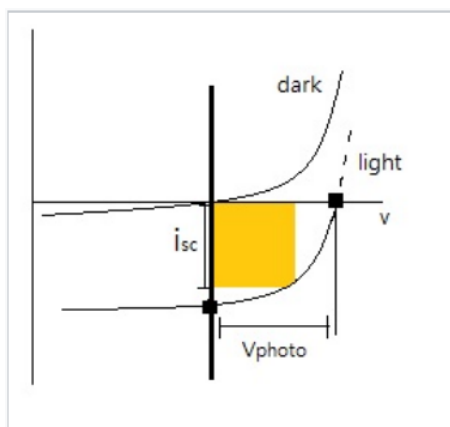
While red, orange, yellow, and green LEDs can be fabricated relatively easily from AlP-GaAs solid solutions, it was initially very difficult to fabricate blue LEDs because the best direct gap semiconductor with a bandgap in the right energy range is a nitride, GaN, which is difficult to make and to dope p-type. Working at Nichia Corporation in Japan, Shuji Nakamura succeeded in developing a manufacturable process for p-GaN, which is the basis of the blue LED. Because of the importance of this work in the development of information storage (Blu-Ray technology) and full-spectrum, energy-efficient LED lighting, Nakamura shared the 2014 Nobel Prize in Physics with Isamu Asaki and Hiroshi Amano, both of whom had made earlier contributions to the development of GaN diodes.

A **Solar cell**, or photovoltaic cell, converts light absorbed in a p-n junction directly to electricity by the photovoltaic effect. Photovoltaics is the field of technology and research related to the development of solar cells for conversion of solar energy to electricity. Sometimes the term solar cell is reserved for devices intended specifically to capture energy from sunlight, whereas the term photovoltaic cell is used when the light source is unspecified.



Photovoltaic effect in a semiconductor p-n junction. (S-kei. [Wikipedia](#), CC-BY-SA)

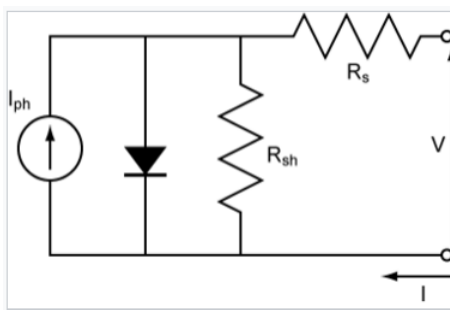
Photocurrent in p-n junction solar cells flows in the diode reverse bias direction. In the dark, the solar cell simply acts as a diode. In the light, the photocurrent can be thought of as a constant current source, which is added to the i-V characteristic of the diode. The relationship between the dark and light current in a photovoltaic cell is shown in the diagram at the left.



Current-voltage characteristic of a solar cell in the dark and under illumination with band gap light. The short-circuit photocurrent is indicated as  $i_{sc}$ , and the open-circuit photovoltage is  $V_{photo}$ . The maximum power generated by the solar cell is determined by the area of the orange box.

The built-in electric field of the p-n junction separates  $e^- h^+$  pairs that are formed by absorption of bandgap light in the depletion region. The electrons flow downhill, towards the n-type side of the junction, the holes flow uphill towards the p-side. If  $h\nu \geq E_{gap}$ , light can be absorbed by promoting an electron from the valence band to the conduction band. Any excess energy is rapidly thermalized. Light with  $h\nu > E_g$  thus can store only  $E_g$  worth of energy in an  $e^- h^+$  pair. If light is absorbed outside of depletion region, i.e., on the n- or p-side of the junction where there is no electric field, minority carriers must diffuse into the junction in order to be collected. This process occurs in competition with electron-hole recombination. Because impurity atoms and lattice defects make efficient recombination centers, semiconductors used in solar cells (especially indirect-gap materials such as Si, which must be relatively thick in order to absorb most of the solar spectrum) must be very pure. Most of the cost of silicon solar cells is associated with the process of purifying elemental silicon and growing large single crystals from the melt.

In the photodiode i-V curve above,  $V_{photo}$  is typically only about 70% of the bandgap energy  $E_{gap}$ . The photocurrent is limited by the photon flux, the recombination rate, and the re-emission of absorbed light.<sup>[6]</sup> The area of the orange rectangle indicates the power generated by the solar cell, which can be calculated as  $P = i \times V$ . In good single crystal or polycrystalline solar cells made of Si, GaAs, CdTe,  $CuIn_xGa_{1-x}Se_2$ , or  $(CH_3NH_3)PbI_3$  the quantum yield (the ratio of short circuit photocurrent to photon flux) is close to unity.

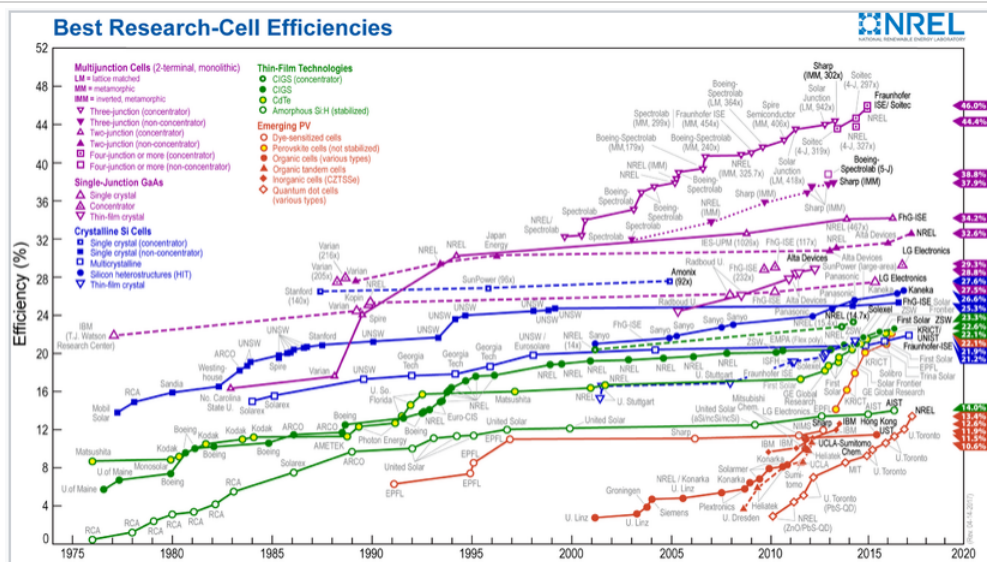


The equivalent circuit of a p-n junction solar cell, which results in the "light" i-V curve shown in the figure above. The solar cell is effectively a diode with a reverse-bias current source provided by light-generated electrons and holes. The shunt resistance ( $R_{sh}$ ) in the equivalent circuit represents parasitic electron-hole recombination. A high shunt resistance (low recombination rate) and low series resistance ( $R_s$ ) are needed for high solar cell efficiency.

Solar cells have many current applications. Individual cells are used for powering small devices such as electronic calculators. Photovoltaic arrays generate a form of renewable electricity, particularly useful in situations where electrical power from the grid is unavailable such as in remote area power systems, Earth-orbiting satellites and space probes, remote radio-telephones and water pumping applications. Photovoltaic electricity is also increasingly deployed in grid-tied electrical systems.

The cost of installed photovoltaics (calculated on a per-watt basis) has dropped over the past decade at a rate of about 13% per year, and has already reached grid parity in Germany and a number of other countries.<sup>[7]</sup> Photovoltaic grid parity is anticipated in U.S. power markets in the 2020 timeframe.<sup>[8]</sup> A major driver in the progressively lower cost of photovoltaic power is the steadily

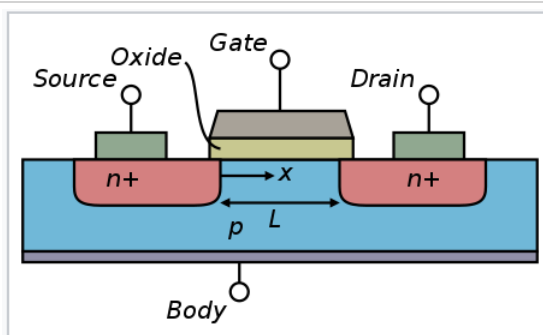
increasing efficiency of solar cells, which is shown in the graphic at the right. Higher efficiency solar cells require less area to deliver the same amount of power, and this lowers the "balance of system" costs such as wiring, roof mounting, etc., which scale as the area of the solar panels. Progress towards higher efficiency reflects improved processes for making photovoltaic materials such as silicon and gallium arsenide, as well as the discovery of new materials. Silicon solar cells are a mature technology, so they are now in the flat part of the learning curve and are approaching their maximum theoretical efficiencies. Newer technologies such as organic photovoltaics, quantum dot solar cells, and lead halide perovskite cells are still in the rising part of the learning curve.



Reported timeline of solar cell energy conversion efficiencies since 1976 (National Renewable Energy Laboratory)

A **field effect transistor (FET)** is a transistor that uses an electric field to control the width of a conducting channel and thus the current in a semiconductor material. It is classified as unipolar transistor, in contrast to bipolar transistors.

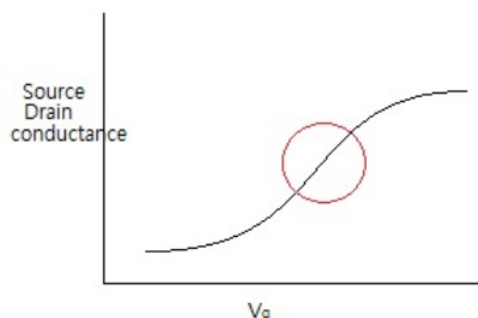
Field effect transistors function as current amplifiers. The typical structure of Si-based FETs is one in which two n-type regions (the source and the drain) are separated by a p-type region. An oxide insulator over the p-type region separates a metal gate lead from the semiconductor. This structure is called a metal-oxide-semiconductor FET (or MOSFET). When voltage is applied between source and drain, current cannot flow because either the n-p or the p-n junction is back-biased. When a positive potential is applied to the gate, however, electrons are driven towards the gate, and locally the semiconductor is "inverted" to n-type. Then the current flows easily between the n-type source and drain through the n-channel. The current flow between the source and drain is many times larger than the current through the gate, and thus the FET can act as an amplifier. Current flow can also represent a logical "1," so FETs are also used in digital logic.



Cross section of an n-type MOSFET

In electronic devices such as microprocessors, field-effect transistors are kept in the off-state most of the time in order to minimize background current and power consumption. The FET shown above, which has n-type source and drain regions, is called an NMOS transistor. In a PMOS transistor, the source and drain regions are p-type and the gate is n-type. In **CMOS** (complementary metal-oxide semiconductor) integrated circuits, both NMOS and PMOS transistors are used. CMOS circuits are constructed in such a way

that all PMOS transistors must have either an input from the voltage source or from another PMOS transistor. Similarly, all NMOS transistors must have either an input from ground or from another NMOS transistor. This arrangement results in low static power consumption.



Transistors are most useful in the range of gate voltage (indicated by the red circle in the figure at the left) where the source-drain current changes rapidly. In this region it is possible to effect a large change in current between source and drain when a small signal is applied to the gate. An important figure of merit for FETs is the **subthreshold slope**, which is the slope a plot of  $\log(\text{current})$  vs.  $V_{\text{gate}}$ . An ideal subthreshold slope is one decade of current per 60 mV of gate bias. Typically, a decade change in source-drain current can be achieved with a change in gate voltage of  $\sim 70$  mV. The performance of FETs as switches and amplifiers is limited by the subthreshold slope, which in turn is limited by the capacitance of the gate. It is desirable to have a very high gate capacitance, which requires a thin insulating oxide, but also to have a small leakage current, which requires a thick oxide. A current challenge in the semiconductor industry is to continue to scale FETs to even smaller nanoscale dimensions while maintaining acceptable values of these parameters. This is being done by developing new gate insulator materials that have higher dielectric constants than silicon oxide and do not undergo redox reactions with silicon or with metal gate leads. Only a few known materials (such as hafnium oxynitride and hafnium silicates) currently meet these stringent requirements.

---

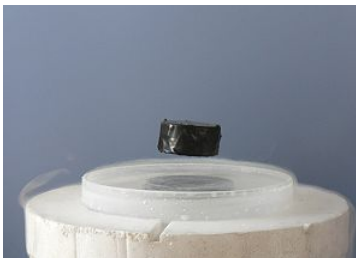
6.5.6: Diodes, LEDs and Solar Cells is shared under a [CC BY-SA](#) license and was authored, remixed, and/or curated by LibreTexts.

- **10.7: Diodes, LEDs and Solar Cells** by Chemistry 310 is licensed [CC BY-SA 4.0](#). Original source: [https://en.wikibooks.org/wiki/Introduction\\_to\\_Inorganic\\_Chemistry](https://en.wikibooks.org/wiki/Introduction_to_Inorganic_Chemistry).

## 6.5.7: Superconductors

Superconductivity refers to the flow of electrical current in a material with zero resistance. Such materials are very important for use in electromagnets, e.g., in magnetic resonance imaging (MRI) and nuclear magnetic resonance (NMR) machines, because once the current starts flowing in the coils of these magnets it doesn't stop. Magnetic levitation using superconductors - which, below a critical field strength, are perfect diamagnets that are not penetrated by magnetic flux lines - is also potentially relevant to future technologies such as magnetically levitated trains.

The phenomenon of superconductivity, first discovered in Hg metal in 1911 by Onnes, continues to be only partially understood. It is of great interest to physicists as a macroscopic quantum phenomenon, and to chemists and materials scientists who try to make better superconductors (especially those that superconduct at higher temperatures) and devices derived from them, such as superconducting quantum interference devices (SQUIDs), which are extremely sensitive magnetometers.

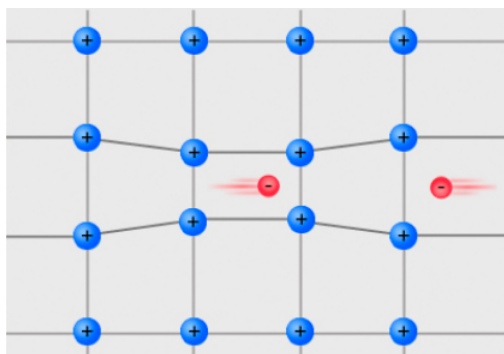


A magnet levitating above a high-temperature superconductor, cooled with liquid nitrogen. Persistent electric current flows on the surface of the superconductor, excluding the magnetic field of the magnet. This current effectively forms an electromagnet that repels the magnet.

### Spin pairing and zero resistance

The transition from the metallic to the superconducting state is related to the quantum phenomena of Bose-Einstein condensation and superfluidity. Individual electrons have spin =  $1/2$ , and as such are fermions (particles with half-integer spin). Because of the Pauli exclusion principle, no more than two fermions can occupy the same quantum state (such as an orbital in a molecule or a solid). The familiar consequence of this rule is the aufbau filling of orbitals with spin-paired electrons in each energy level. In contrast, particles with integer spins - which are called bosons - do not have this restriction, and any number of bosons can occupy the same quantized energy level.

Superconductivity occurs when electrons spin pair into so-called Cooper pairs, which can travel through the lattice together. The electrons in a Cooper pair, although spin-paired, have a long-distance relationship: the spatial extent of a Cooper pair is a few nanometers in cuprate superconductors, and up to one micron in low  $T_c$  superconductors such as aluminum. Because its overall spin angular momentum is zero, a Cooper pair is a boson. When the temperature is low enough, the Cooper pairs "condense" into the lowest energy level. The second lowest energy level - which is typically a few meV above the ground state - is not accessible to them as long as the energy gap is larger than the thermal energy,  $kT$ . The scattering of electrons by the lattice then becomes forbidden by energy conservation because scattering dissipates energy, and the Cooper pairs cannot change their energy state. Thus the resistance (which arises from scattering, as we learned in Ch. 6) drops abruptly to zero below  $T_c$ . However, the Cooper pairs can be broken apart when they move fast, and thus superconductors turn back into normal metals (even below  $T_c$ ) above some critical current density  $j_c$ . This phenomenon is also related to the critical magnetic field,  $H_c$ , that quenches superconductivity.

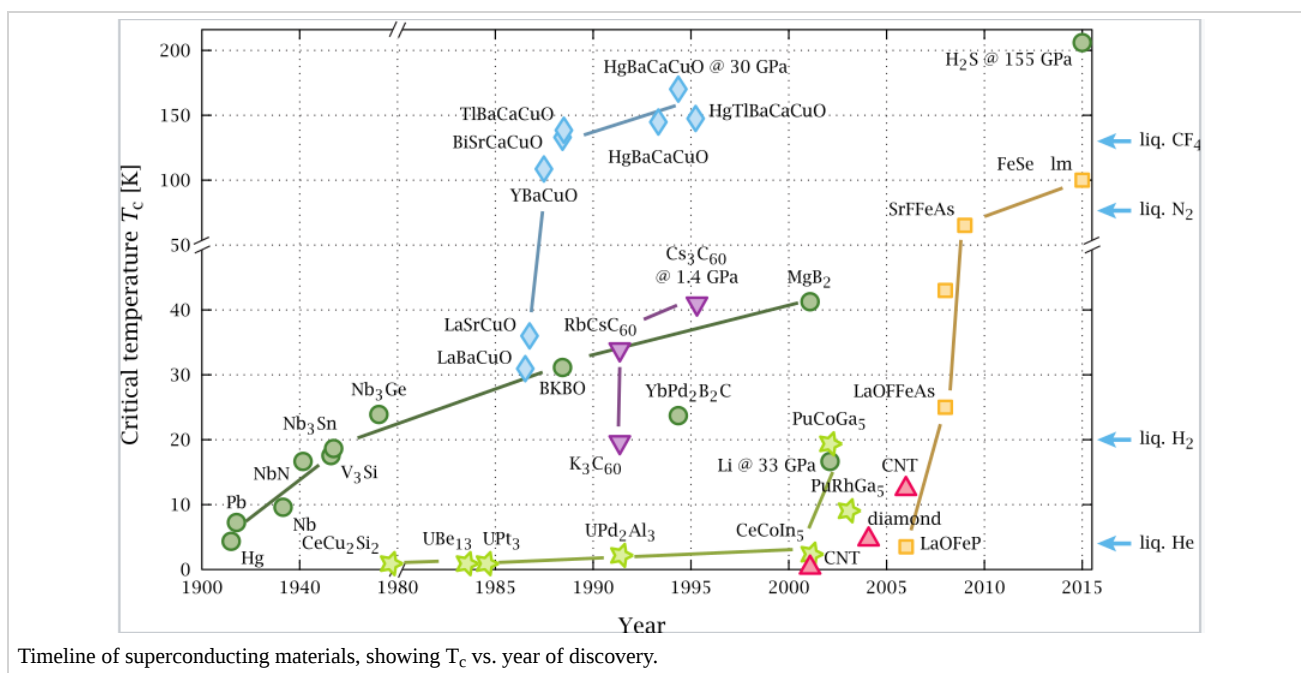




## A trampoline for electrons

What causes electrons, which repel each other because of their negative charge, to pair up and travel together in superconductors? The mechanism - which must involve some kind of attractive interaction between electrons - is well understood for "conventional" superconductors which have relatively low transition temperatures, but is not yet known with certainty for high temperature oxide superconductors. In conventional, or BCS superconductors, the spin pairing is mediated by the lattice as shown in the figure at the left. A strong electron-lattice interaction causes a distortion in the lattice as an electron moves through. This elastic deformation is felt as an attractive force by a second electron moving in the opposite direction. This can be thought of as analogous to the interaction of two people jumping on a trampoline. The weight of the first person on the trampoline creates a "well" that attracts the second one, and they tend to move together (even if they don't like each other). Strange as this interaction seems, it is supported experimentally by isotope effects on  $T_c$  and by quantitative predictions of  $T_c$  values in conventional superconductors.

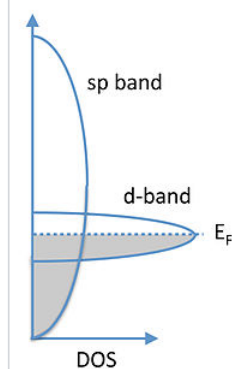
**Bad metals make good superconductors.** All superconductors are "normal" metals - with finite electrical resistance - above their critical transition temperature,  $T_c$ . If you ask where in the periodic table one might look for superconductors, the answer is surprising. The most conductive metals (Ag, Au, Cu, Cs, etc.) make the worst superconductors, i.e., they have the lowest superconducting transition temperatures, in many cases below 0.01 K. Conversely "bad" metals, such as niobium alloys, certain copper oxides,  $K_xBa_{1-x}BiO_3$ ,  $MgB_2$ , FeSe, and alkali salts of  $C_{60}^{n-}$  anions, can have relatively high transition temperatures.



We observe that most good superconductors appear in composition space very **near a metal-insulator transition**. In terms of our microscopic picture, orbital overlap in superconductors is poor, just barely enough to make them act as metals ( $\Delta \approx U$ ) above  $T_c$ . In the normal state, superconductors with high  $T_c$  - which can be as high as 150 K - are typically "bad" metals. An important characteristic of such metals is that the **mean free path** of electrons (in the normal state, above  $T_c$ ) is on the order of the lattice spacing, i.e., **only a few Å**. In contrast, we learned in Ch. 6 that good metals such as Au, Ag, and Cu have electron mean free paths that are two orders of magnitude longer (ca. 40 nm). In a bad metal, the electron "feels" the lattice rather strongly, whereas in a good metal, the electrons are insensitive to small changes in the distance between metal atoms.

What does the band picture look like for a bad metal? The key point is that because orbital overlap is poor, the metal has a **high density of states** at the Fermi level. This is a universal property of high temperature superconductors and provides a clue of where to look for new and improved superconducting materials. Recall that transition elements in the middle of the 3d series (Cr, Fe, Co, Ni) were magnetic because of poor orbital overlap and weak d-d bonding. The elements below these - especially Nb, Ta, and W - have just barely enough d-d orbital overlap to be on the metallic side of the metal-insulator transition and to be "bad" metals. Carbides and nitrides of these elements are typically superconducting, with the carbon and nitrogen atoms serving to adjust the valence electron density, as illustrated in the table below.





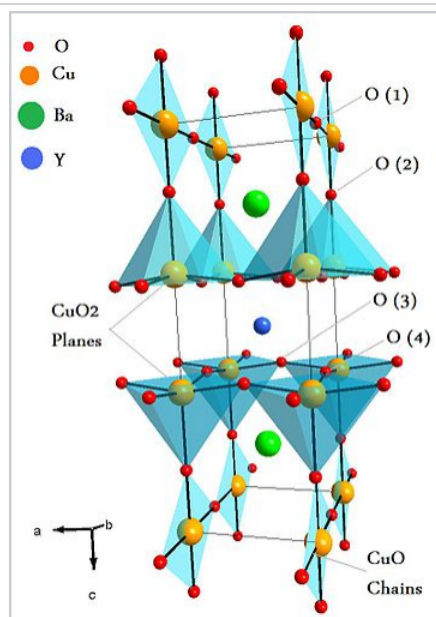
Generic E vs. DOS for a bad metal.

Compound	NbC	Mo <sub>2</sub> N	TaC	VN	NbN	TaN	Nb <sub>3</sub> Ge
T <sub>c</sub> (K)	11.1	5.0	9.7	7.5	15.2	17.8	22.3

## High T<sub>c</sub> superconductors

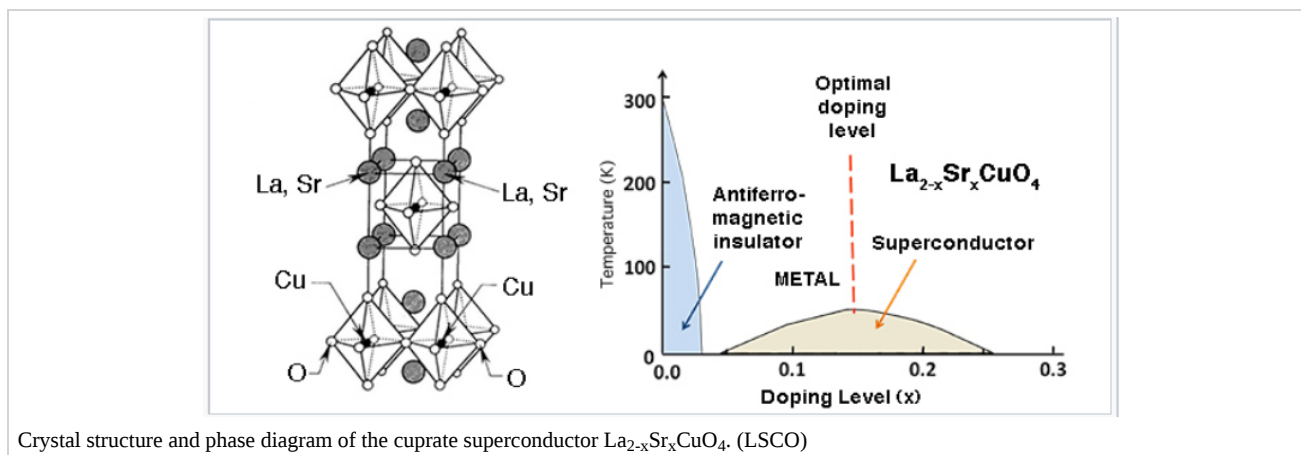
In addition to having weak orbital overlap in the metallic state - which results in a high DOS at E<sub>F</sub> - high temperature superconductors also typically contain elements in mixed oxidation states (for example, Cu<sup>2+/3+</sup> or Bi<sup>3+/5+</sup>) that are close in energy to the O<sup>2-/O<sup>-</sup></sup> couple in the lattice. At ambient pressure, cuprate superconductors have the highest known T<sub>c</sub> values, ranging between about 35 and 150 K. The crystal structures of these materials are almost all variants of the perovskite lattice, as shown at the right for the 1-2-3 superconductor YBa<sub>2</sub>Cu<sub>3</sub>O<sub>7-δ</sub>. An ideal perovskite lattice would have formula ABO<sub>3</sub> = A<sub>3</sub>B<sub>3</sub>O<sub>9</sub>. In YBa<sub>2</sub>Cu<sub>3</sub>O<sub>7-δ</sub>, Y and Ba occupy the A cation sites, Cu occupies the B sites, and two of the nine O atoms are missing.

The YBa<sub>2</sub>Cu<sub>3</sub>O<sub>7-δ</sub> lattice consists of mixed-valent copper(II/III) oxide sheets capped by oxygen atoms to form CuO<sub>5</sub> square pyramids. These sheets encapsulate the Y<sup>3+</sup> cations. Copper(II) oxide ribbons that share the apical oxygen atoms of the square pyramids run in one direction through the structure. In YBa<sub>2</sub>Cu<sub>3</sub>O<sub>7-δ</sub> and related materials, one component of the structure (here the Cu-O ribbons) acts as a **charge reservoir** to control the doping of the planar CuO<sub>2</sub> sheets, which are the elements of the structure that carry the supercurrent. Cuprate superconductors with Bi, Tl, or Hg-containing charge reservoir layers and multiple, eclipsed CuO<sub>2</sub> sheets in the unit cell tend to have the highest T<sub>c</sub> values.



Crystal structure of YBa<sub>2</sub>Cu<sub>3</sub>O<sub>7-δ</sub> (YBCO), the first superconductor with T<sub>c</sub> above the boiling point of liquid nitrogen.

The connection between the metal-insulator transition and superconductivity is nicely illustrated in the phase diagram of  $\text{La}_{2-x}\text{Sr}_x\text{CuO}_4$ , the first cuprate superconductor, which was discovered in 1986 by Georg Bednorz and K. Alex Müller. This compound has a rather simple structure in which rocksalt  $\text{La}(\text{Sr})\text{O}$  layers are intergrown with perovskite  $\text{La}(\text{Sr})\text{CuO}_3$  layers. Undoped  $\text{La}_2\text{CuO}_4$  contains only  $\text{Cu}^{2+}$  ions and is an antiferromagnetic insulator. As a small amount of  $\text{Sr}^{2+}$  is substituted for  $\text{La}^{3+}$ , some of the  $\text{Cu}^{2+}$  is oxidized to  $\text{Cu}^{3+}$ , and the lattice is doped with holes. As the doping level increases, the antiferromagnetic phase undergoes a first-order phase transition to a "bad" metal, and at slightly higher doping density the superconducting phase appears. The proximity of the superconducting phase to the metal-insulator transition is a hallmark of cuprate superconductors. A maximum  $T_c$  of 35K is observed at  $x = 0.15$ . Doping at higher levels moves the Fermi level beyond the point of highest DOS in the d-band of Cu and the superconducting phase then gradually disappears. It is interesting to compare this phase diagram with that of  $\text{V}_2\text{O}_3$  (above), which also undergoes an antiferromagnetic insulator to "bad" metal transition as it is doped.



This page titled [6.5.7: Superconductors](#) is shared under a [CC BY-SA 4.0](#) license and was authored, remixed, and/or curated by [Chemistry 310 \(Wikibook\)](#) via [source content](#) that was edited to the style and standards of the LibreTexts platform.

- **10.3: Superconductors** by [Chemistry 310](#) is licensed [CC BY-SA 4.0](#). Original source: [https://en.wikibooks.org/wiki/Introduction\\_to\\_Inorganic\\_Chemistry](https://en.wikibooks.org/wiki/Introduction_to_Inorganic_Chemistry).

## CHAPTER OVERVIEW

### Unit 7: Acid-Base and Donor-Acceptor Chemistry

#### 7.1: Acid Base Chemistry

##### 7.1.1: Arrhenius Model

##### 7.1.2: Brønsted-Lowry Model

##### 7.1.3: Metal Ions as Acids

##### 7.1.4: Autoionization and Solvent Leveling

##### 7.1.5: Lewis Model and Frontier Orbitals

#### 7.2: Hard Soft Acid Base Theory

##### 7.2.1: Hard and Soft Acids and Bases

##### 7.2.2: Applications of Hard Soft Acid Base Theory

##### 7.2.3: Theoretical Interpretation of HSAB Theory

#### 7.3: Unit 7 Practice Problems

---

Unit 7: Acid-Base and Donor-Acceptor Chemistry is shared under a [not declared](#) license and was authored, remixed, and/or curated by LibreTexts.

## 7.1: Acid Base Chemistry

---

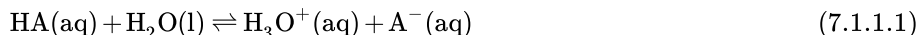
Learning objectives for this unit are to:

- Compare and contrast Arrhenius, Bronsted-Lowry, and Lewis concepts of acids and bases
  - Identify and classify atoms, ions, and molecules as acids or bases
  - Describe and rationalize acid/base chemistry in non-aqueous systems
  - Explain the concept of solvent leveling and identify the strongest possible acids and bases for a given solvent system
  - Differentiate between coordinate covalent/dative bonds and covalent/ionic bonds
  - Identify frontier orbitals in MO energy level diagrams
  - Describe how metal cations lower the pKa of bound water molecules
  - Identify and rationalize trends in acid strength of metal cations
  - Predict and rationalize trends in Lewis base strength based on inductive and steric effects
- 

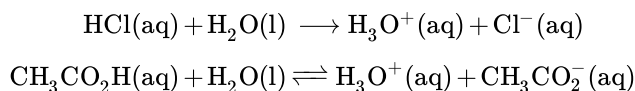
7.1: Acid Base Chemistry is shared under a [not declared](#) license and was authored, remixed, and/or curated by LibreTexts.

## 7.1.1: Arrhenius Model

The Arrhenius acid-base concept defines acids and bases in terms of how they affect the amount of hydronium ions,  $\text{H}_3\text{O}^+$ , (and by extension hydroxide ions,  $\text{OH}^-$ ) in aqueous solutions. Simply, in the Arrhenius definition an acid is a substance that increases the concentration of hydronium ions when it is dissolved in water. This typically occurs when the acid dissociates by loss of a proton to water according to the general equation:



where A is the deprotonated form of the acid. For example, what hydrochloric and acetic acid,  $\text{CH}_3\text{CO}_2\text{H}$ , have in common is that both increase the amount of hydronium ion when they are dissociated in solution.



In terms of the Arrhenius definition, the major difference between hydrochloric and acetic acid is that hydrochloric acid dissociates completely in solution to yield stoichiometric amounts of  $\text{H}_3\text{O}^+$ , while acetic acid only partially dissociates. Acids like HCl that completely dissociate in water are classified as strong in the Arrhenius definition, while those like acetic acid that do not are classified as weak.

Although all weak acids incompletely dissociate, the extent of dissociation can vary widely. The relative strengths of weak Arrhenius acids is conveniently expressed in terms of the equilibrium constant for their acid dissociation reaction,  $K_a$ .

$$K_a = \frac{[\text{H}^+][\text{A}^-]}{[\text{HA}]}$$

The  $\text{p}K_a$  values for selected weak acids are given in Table 7.1.1.1

Table 7.1.1.1: Values of  $K_a$ ,  $\text{p}K_a$ ,  $K_b$ , and  $\text{p}K_b$  for selected monoprotic acids.

Acid	HA	$K_a$	$\text{p}K_a$	$\text{A}^-$	$K_b$	$\text{p}K_b$
sulfuric acid (2nd ionization)	$\text{HSO}_4^-$	$1.0 \times 10^{-2}$	1.99	$\text{SO}_4^{2-}$	$9.8 \times 10^{-13}$	12.01
hydrofluoric acid	$\text{HF}$	$6.3 \times 10^{-4}$	3.20	$\text{F}^-$	$1.6 \times 10^{-11}$	10.80
nitrous acid	$\text{HNO}_2$	$5.6 \times 10^{-4}$	3.25	$\text{NO}_2^-$	$1.8 \times 10^{-11}$	10.75
formic acid	$\text{HCO}_2\text{H}$	$1.78 \times 10^{-4}$	3.750	$\text{HCO}_2^-$	$5.6 \times 10^{-11}$	10.25
benzoic acid	$\text{C}_6\text{H}_5\text{CO}_2\text{H}$	$6.3 \times 10^{-5}$	4.20	$\text{C}_6\text{H}_5\text{CO}_2^-$	$1.6 \times 10^{-10}$	9.80
acetic acid	$\text{CH}_3\text{CO}_2\text{H}$	$1.7 \times 10^{-5}$	4.76	$\text{CH}_3\text{CO}_2^-$	$5.8 \times 10^{-10}$	9.24
pyridinium ion	$\text{C}_5\text{H}_5\text{NH}^+$	$5.9 \times 10^{-6}$	5.23	$\text{C}_5\text{H}_5\text{N}$	$1.7 \times 10^{-9}$	8.77
hypochlorous acid	$\text{HOCl}$	$4.0 \times 10^{-8}$	7.40	$\text{OCl}^-$	$2.5 \times 10^{-7}$	6.60
hydrocyanic acid	$\text{HCN}$	$6.2 \times 10^{-10}$	9.21	$\text{CN}^-$	$1.6 \times 10^{-5}$	4.79
ammonium ion	$\text{NH}_4^+$	$5.6 \times 10^{-10}$	9.25	$\text{NH}_3$	$1.8 \times 10^{-5}$	4.75
water	$\text{H}_2\text{O}$	$1.0 \times 10^{-14}$	14.00	$\text{OH}^-$	1.00	0.00
acetylene	$\text{C}_2\text{H}_2$	$1 \times 10^{-26}$	26.0	$\text{HC}_2^-$	$1 \times 10^{12}$	-12.0
ammonia	$\text{NH}_3$	$1 \times 10^{-35}$	35.0	$\text{NH}_2^-$	$1 \times 10^{21}$	-21.0

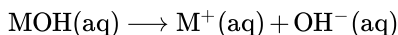
\*The number in parentheses indicates the ionization step referred to for a polyprotic acid.

As can be seen from the table the  $K_a$  values for weak acids are less than one (otherwise they would not be weak) and vary over many orders of magnitude. Consequently it is customary to tabulate acid ionization constants as  $\text{p}K_a$  values:

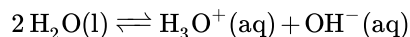
$$\text{p}K_a = -\log K_a$$

Because  $pK_a$  values essentially place the  $K_a$  values on a negative base ten logarithmic scale, the stronger the weak acid, the lower its  $pK_a$ . Weak acids with larger  $K_a$  values will have lower  $pK_a$  values than weaker acids with smaller  $K_a$ . Moreover, each unit increase or decrease in the  $pK_a$  corresponds to a tenfold increase or decrease in the corresponding  $K_a$ .

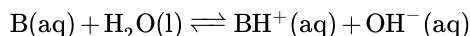
While Arrhenius acids increase the concentration of  $H_3O^+$  in aqueous solution, Arrhenius bases decrease  $H_3O^+$ . Strong bases do this stoichiometrically. Most are hydroxide salts of alkali metals or quaternary ammonium salts that dissociate completely when dissolved in water:



This added hydroxide decreases the concentration of  $H_3O^+$  by shifting the water autoionization equilibrium towards water.



In contrast, most weak bases react with water to produce an equilibrium concentration of hydroxide ion according to the base dissociation reaction



in which B is the weak base. The ionization constant for this reaction, called the **base ionization constant** or  $K_b$ , is typically used as a measure of a weak base's strength.

Because both hydroxide and hydronium ion are products of water autoionization, the concentrations of hydronium ion and hydroxide ion in aqueous solution will vary reciprocally with one another. This means that Arrhenius acids can be recognized as substances that decrease the hydroxide concentration and Arrhenius bases as substances that increase it.

Since the Arrhenius acid-base concept is concerned about the state of the water autoionization reaction, Arrhenius acids and bases may also be recognized by their effect on the solution pH. Arrhenius acids decrease the pH and Arrhenius bases will increase it.

#### NOTE

To qualify as an Arrhenius acid, upon the introduction to water, the chemical must cause, either directly or otherwise:

- an increase in the aqueous hydronium concentration,
- a decrease in the aqueous hydroxide concentration, or
- a decrease in the solution pH.

Conversely, to qualify as an Arrhenius base, upon the introduction to water, the chemical must cause, either directly or otherwise:

- a decrease in the aqueous hydronium concentration,
- an increase in the aqueous hydroxide concentration, or
- an increase in the solution pH.

Because the Arrhenius acid-base model defines acids and bases in terms of their impact on the state of an aqueous solution the Arrhenius concept is unable to describe reactions in nonaqueous solvents, gases, molten liquids, and the solid state. Consequently other models should be used to describe reactions involving the transfer of  $H^+$  and other fragments in nonaqueous media.

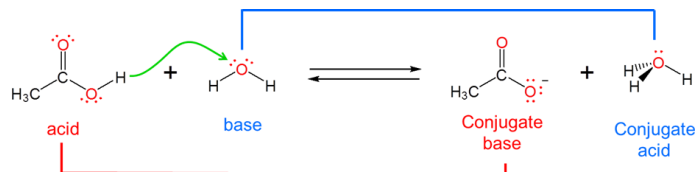
7.1.1: Arrhenius Model is shared under a [not declared](#) license and was authored, remixed, and/or curated by Stephen M. Contakes.

- [7.1A: Acid-Base Theories and Concepts](#) by Stephen M. Contakes is licensed [CC BY-NC 4.0](#).
- [6.2: Arrhenius Concept](#) by Stephen M. Contakes has no license indicated.

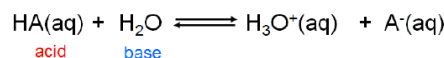
## 7.1.2: Brønsted-Lowry Model

### The Brønsted-Lowry Acid Base Concept

The Brønsted-Lowry acid base concept overcomes the Arrhenius system's inability to describe reactions that take place outside of aqueous solution by moving the focus away from the solution and onto the acid and base themselves. It does this by redefining acid-base reactivity as involving the transfer of a hydrogen ion,  $H^+$ , between an acid and a base. Specifically, a Brønsted acid is a substance that loses a  $H^+$  ion by donating it to a base. This means that a Brønsted base is defined as a substance which accepts  $H^+$  from an acid when it reacts.

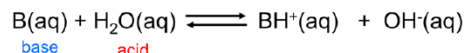


Because the Brønsted-Lowry concept is concerned with  $H^+$  ion transfer rather than the creation of a particular chemical species it is able to handle a diverse array of acid-base concepts. In fact, from the viewpoint of the Brønsted-Lowry concept, Arrhenius acids and bases are just a special case involving hydrogen ion donation and acceptance involving water. Arrhenius acids donate  $H^+$  ion to water, which acts as a Brønsted base to give  $H_3O^+$



(7.1.2.1)

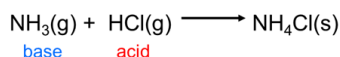
Similarly, Arrhenius bases act as Brønsted bases in accepting a hydrogen ion from the Brønsted acid water:



(7.1.2.2)

In this way it can be seen that Arrhenius acids and bases are defined in terms of their causing hydrogen ions to be donated to and abstracted from water, respectively, while Brønsted acids and bases are defined in terms of their ability to donate and accept hydrogen ions to and from anything.

Because the Brønsted-Lowry concept can handle any sort of hydrogen ion transfer it readily accommodates many reactions that Arrhenius theory cannot, including those that take place outside of water, such as the reaction between gaseous hydrochloric acid and ammonia:



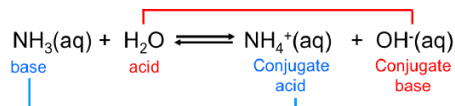
(7.1.2.3)

The classification of acids as strong or weak usually refers to their ability to donate or abstract hydrogen ions to or from water to give  $H_3O^+$  and  $OH^-$ , respectively, - *i.e.* their Arrhenius acidity and basicity. However, acids and bases may be classified as strong and weak under the Brønsted-Lowry definition based on whether they completely transfer or accept hydrogen ions; it is just that in this case it is important to specify the conditions under which a given acid or base acts strong or weak. For example, acetic acid acts as a weak base in water but is a strong base in triethylamine, since in the latter case it completely transfers a hydrogen ion to triethylamine to give triethylammonium acetate. Alternatively, the acidity or basicity of a compound may be specified using a thermodynamic scale like the [Hammett acidity](#).

### Conjugate Acids and Bases

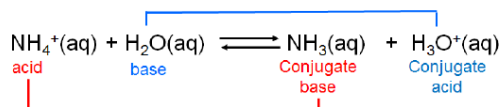
By redefining acids and bases in terms of hydrogen ion donation and acceptance the Brønsted-Lowry system makes it easy to recognize that when an acid loses its hydrogen ion it becomes a substance that is capable of receiving it back again, namely a base.

Consider, for example, the base dissociation of ammonia in water. When ammonia acts as a Brønsted base and receives a hydrogen ion from water ammonium ion and hydroxide are formed:



(7.1.2.4)

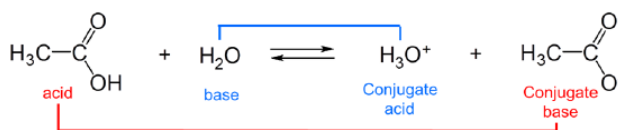
The ammonium ion is itself a weak acid that can undergo dissociation:



(7.1.2.5)

In this case ammonia and ammonium ion are acid-base conjugates. In general acids and bases that differ by a *single ionizable hydrogen ion* are said to be conjugates of one another.

The strengths of conjugates vary reciprocally with one another so that the stronger the acid the weaker the base and vice versa. For example, in water, acetic acid acts as a weak Brønsted acid:



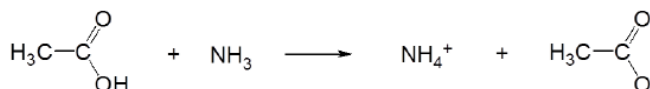
(7.1.2.6)

and acetic acid's conjugate base, acetate, acts as a weak Brønsted base.



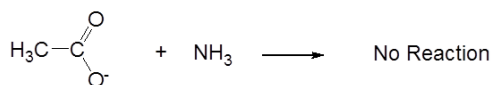
(7.1.2.7)

However, in liquid ammonia acetic acid acts as a strong Brønsted acid:



(7.1.2.8)

while its conjugate base, acetate, is neutral.



(7.1.2.9)

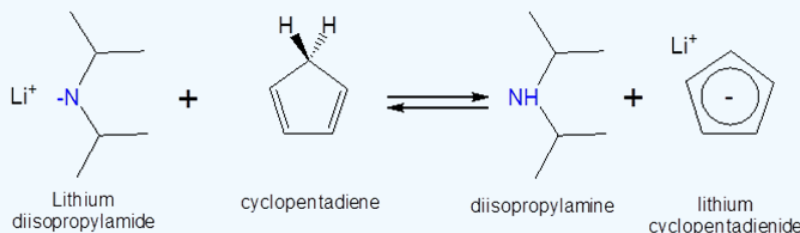
The reciprocal relationship between the strengths of acids and their conjugate bases has several consequences:

1. Under conditions when an acid or base acts as a weak acid or base its conjugate acts as weak as well. Conversely, when an acid or base acts as a strong acid or base its conjugate acts as a neutral species.
2. When a Brønsted acid and base react with one another the equilibrium favors formation of the weakest acid-base pair. That is why the acid-base reaction between acetic acid and ammonia in liquid ammonia proceeded to give the weak acid ammonium ion and neutral acetate. This consequence is particularly important for understanding the behavior of acids and bases in nonaqueous solvents, as illustrated by the following example.



### ✓ Example 7.1.2.1

Can a solution of lithium diisopropylamide in heptane be used to form lithium cyclopentadienide? The  $pK_a$  of cyclopentadiene and diisopropylamine are ~15 and 40, respectively, and the proposed reaction is as follows:



#### Solution:

Since cyclopentadiene is a stronger acid than diisopropylamine (the stronger the acid the lower the  $pK_a$ ) the equilibrium will favor protonation of the diisopropylamine by cyclopentadiene. Consequently addition of a heptane solution lithium diisopropylamide to monomeric cyclopentadiene should give lithium cyclopentadienide.

## Molecular Structure and Brønsted Acidity and Basicity

Because the acidity of a given substance depends on the interplay between the relatively large values of its proton affinity and the energy associated with solvation of an acid's conjugate base it can be sometimes difficult to estimate the strength of an acid in a given solvent in the absence of detailed computations. Nevertheless a variety of simple ideas may be used to roughly estimate the relative strengths of acids. These should never be substituted for a detailed consideration of solvation but can serve as useful aids when thinking about trends and designing new Brønsted acids and bases.

Some simple factors that it can be helpful to consider when thinking about the strength of a given acid or base are:

### Bond strength effects

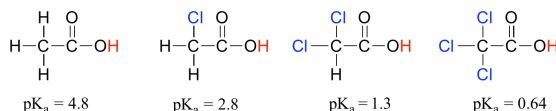
The weaker the bond to the ionizable hydrogen, the stronger the acid. Strongly bonded hydrogen ions are difficult to remove, weakly bonded ones much less so.

### Inductive effects

Inductive effects involve the donation or withdrawal of electrons from an atom by a group connected to it through bonds. Electron donating groups increase the electron density while electron withdrawing groups decrease it. Atoms or groups that withdraw electron density away from a center increase its acidity while those which donate electrons to the center decrease its acidity. The reasons for this follow from the heterolytic bond cleavage of acid ionization:



- When a bond to hydrogen is more polarized away from the H (more like  $^{\delta-}E-H^{\delta+}$ ) it is easier to cleave off the hydrogen ion from that E-H bond. This may be seen from how the  $pK_a$  values of acetic acid and its mono-, di-, and tri-chlorinated derivatives decreases with the extent of chlorination of the methyl group.



- Polarized E-H bonds also make for stronger Brønsted acids because the resulting  $E:^-$  conjugate base is more stable.

This leads to the third major factor that should be considered when thinking about acid strength.

### Electronegativity effects

The more stable the acid's conjugate base, the stronger the Brønsted acid. All reactions are in theory reversible and so when considering the propensity of an acid to donate hydrogen ions it can be helpful to look at the reverse of hydrogen ion donation,

namely protonation of the acid's conjugate base. If deprotonation of the acid gives a very stable conjugate base then deprotonation of the acid will be more favorable.

Two factors determine the stability of an acid's conjugate base.

- Conjugate bases in which a small amount of charge is on a large atom, spread over a large number of atoms, and on electronegative atoms tend to be more stable. Conjugate bases in which a small amount of charge is spread over a large number of electronegative atoms are especially stable. That is why magic acid, a mixture of HF and  $SbF_5$ , is so acidic; the single negative charge on its conjugate base is spread over six F atoms and on Sb in  $SbF_6^-$ .
- Groups which tend to inductively polarize E-H bonds also tend to stabilize the conjugate base formed when that bond ionizes. In general, the more electronegative an atom, the better able it is to bear a negative charge. All other things being equal weaker bases have negative charges on more electronegative atoms; stronger bases have negative charges on less electronegative atoms. This is apparent from how inductive effects lead to an increase in the acidity of E-H bonds as the electronegativity of the element to which the acidic hydrogen is bound increases from left to right across a row of the periodic table. This horizontal periodic trend in acidity and basicity is apparent from the homologous series below in Figure 7.1.2.1.

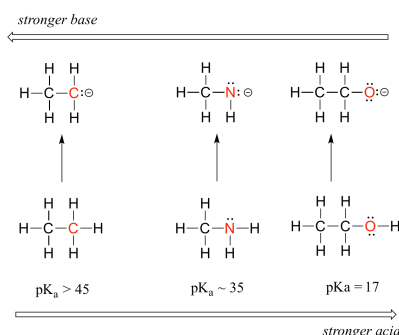


Figure 7.1.2.1: Horizontal periodic trend in acidity and basicity.

Notice how the inductive polarization of the E-H bond which results in greater acidity contributes to the greater stability of the conjugate base. For the case above look at where the negative charge ends up in each conjugate base. In the conjugate base of ethane, the negative charge is borne by a carbon atom, while on the conjugate base of methylamine and ethanol the negative charge is located on a nitrogen and an oxygen, respectively. Remember that **electronegativity** also increases as we move from left to right along a row of the periodic table, meaning that oxygen is the most electronegative of the three atoms, and carbon the least.

Thus, the methoxide anion is the most stable (lowest energy, least basic) of the three conjugate bases, and the ethyl carbanion anion is the least stable (highest energy, most basic). Conversely, ethanol is the strongest acid, and ethane the weakest acid.

### Size effects

There are two classes of size effects to be considered:

- The larger the atom to which a H is bound in an E-H bond, the weaker the bond and the stronger the acid.
- Increased charge delocalization with increasing size. Electrostatic charges, whether positive or negative, are more stable when they are 'spread out' over a larger area. The greater the volume over which charge is spread in the acid's conjugate base, the more stable that base and the stronger the acid.

The impact of size effects are readily seen in the increase in acidity of the hydrogen halides, as illustrated by the vertical periodic trend in acidity and basicity below in Figure 7.1.2.2

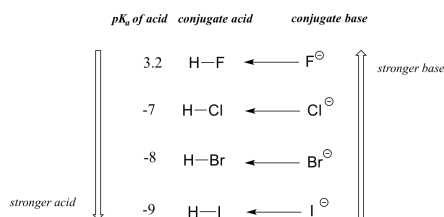
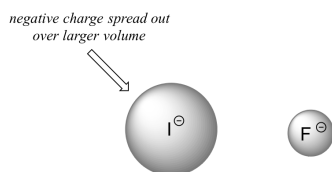


Figure 7.1.2.2: Vertical periodic trend in acidity and basicity.

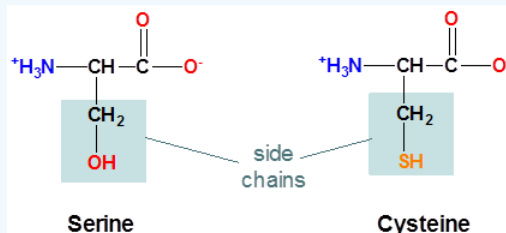
On going vertically down the halogen group from F to I the H-X bond strength decreases in the acid, making it easier to ionize, while the charge becomes more diffuse in the resultant  $X^-$  ion, making the conjugate base more stable.



The increase in the acidity of the hydrogen halides down a group suggests that size effects are more important than inductive effects. In the case of the hydrogen halides because fluorine is the most electronegative halogen element, we might expect fluoride to also be the least basic halogen ion. But in fact, it is the *least* stable, and the most basic! It turns out that when moving vertically in the periodic table, the *size* of the atom trumps its electronegativity with regard to basicity. The atomic radius of iodine is approximately twice that of fluorine, so in an iodide ion, the negative charge is spread out over a significantly larger volume.

### ? Exercise 7.1.2.1

The structure of the amino acids serine and cysteine are shown below. Which do expect will have the more acidic side chain?

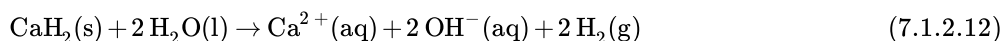
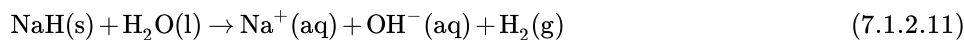


### Answer

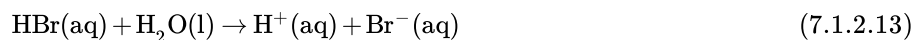
Cysteine, since the cysteine side chain possesses an ionizable S-H bond while serine's side chain possesses an ionizable O-H bond. Since S is larger than O cysteine's S-H bond will be weaker than serine's O-H bond and cysteine side chain's thiolate conjugate base more stable than the serine side chain's alkoxide conjugate base. In fact, the side chain  $pK_a$  of cysteine is 8.3 while serine is considered to be nonionizable under physiological conditions.

## Binary Hydrides

The compounds formed between the elements and hydrogen are called binary hydrides. All such compounds can in principle act as Brønsted acids in reactions with a suitably strong base. However, as the electronegativity decreases down a group and increases from left to right across the periodic table the acidity of binary hydrides increases. In fact, on the left side of the periodic table the hydrides of extremely electropositive alkali and alkaline earth metals are not acidic but basic. They are perhaps best considered to be ionic salts of the hydride ion ( $H^-$ ). Consequently substances such as NaH and  $CaH_2$  tend to act as Brønsted bases in their reactions.



On the right side of the periodic table the binary hydrides of the nonmetals exhibit appreciable acidity.



For this reason the binary nonmetal hydrides are termed acidic hydrides. Nevertheless not all are equally acidic. The dilute aqueous acid ionization constants for these hydrides are given in Figure 7.1.2.3 As can be seen from the constants in Figure 7.1.2.2 the ability of the hydrides to transfer a hydrogen to water increases across a period and down a group.

CH <sub>4</sub> 10 <sup>-46</sup>	NH <sub>3</sub> 10 <sup>-35</sup>	H <sub>2</sub> O 10 <sup>-16</sup>	HF 10 <sup>-3</sup>
	PH <sub>3</sub> 10 <sup>-27</sup>	H <sub>2</sub> S 10 <sup>-7</sup>	HCl 10 <sup>7</sup>
		H <sub>2</sub> Te 10 <sup>-3</sup>	HBr 10 <sup>9</sup>
			HI 10 <sup>10</sup>

Figure 7.1.2.3: The acid ionization constants of nonmetal hydrides increase across a period and down a group.

These trends are largely due to changes in the electronegativity and size of the nonmetal atom:

1. Going across a period the acid strength increases as there is an increase in electronegativity and the molecule gets more polar, with the hydrogen getting a larger partial positive charge. This makes it easier to heterolytically cleave the E-H bond to produce a stable anion.



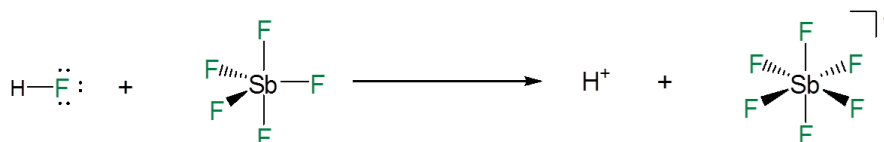
2. Going down a group the acid strength increases because the bond strength decreases as a function of increasing size of the nonmetal, and this has a larger effect than the electronegativity. In fact HF is a weak acid because it is so small that the hydrogen-fluorine bond is so strong that it is hard to break. Remember, the weaker the bond, the stronger the acid strength. This is further illustrated in Table 7.1.2.1 where the weakest bond has produced the strongest acid.

Table 7.1.2.1 Acid strength as function of bond energy

Relative Acid Strength	HF	<<	HCl	<	HBr	<	HI
H-X Bond Energy (kJ/mol)	570		432		366		298
K <sub>a</sub>	10 <sup>-3</sup>		10 <sup>7</sup>		10 <sup>9</sup>		10 <sup>10</sup>

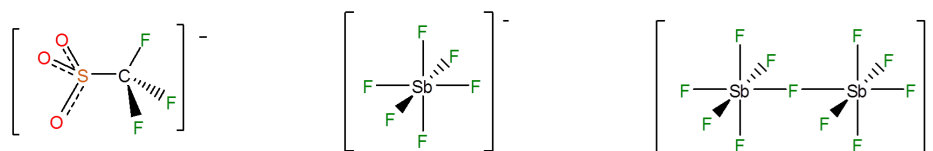
## Superacids

Superacids are acids that are more acidic than pure sulfuric acid. They are able to dissociate completely because when they do so they give an extremely stable anion in which the residual negative charge is distributed among multiple electronegative atoms. For example, in mixtures of HF and antimony pentafluoride the dissociation of a hydrogen ion from the HF is promoted by the formation of a Lewis acid-base adduct between the HF fluoride and SbF<sub>5</sub>.



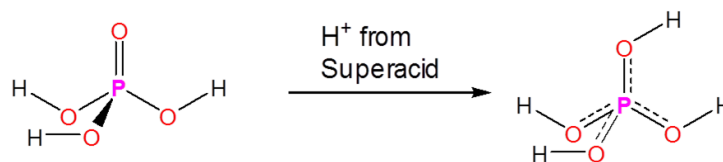
(7.1.2.15)

This gives extremely stable anions like SbF<sub>6</sub><sup>-</sup> and Sb<sub>2</sub>F<sub>11</sub><sup>-</sup>, in which a single negative charge is delocalized among many electronegative groups and atoms; of these CF<sub>3</sub> and F are particularly common.

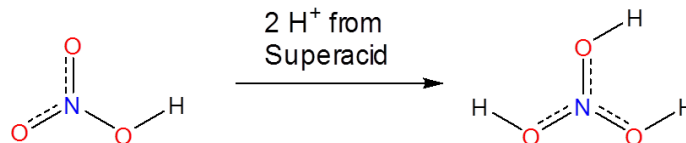


(7.1.2.16)

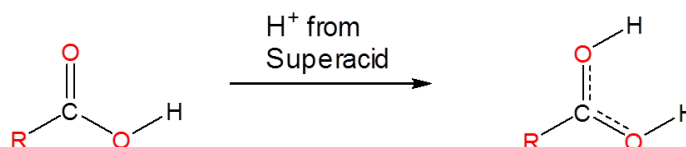
Superacids are able to protonate species that would otherwise act as neutral or even acidic species in water or aprotic media. Phosphoric, nitric, carboxylic, and other ordinary acids are all protonated when dissolved in superacids:



(7.1.2.17)

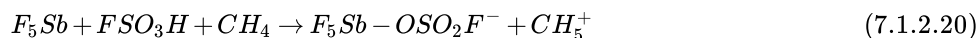


(7.1.2.18)



(7.1.2.19)

However, superacids also protonate many species that are not usually considered to have acid base properties. Even alkanes can be protonated and, in fact, superacids are used to generate carbocations in a variety of synthetic applications. They do this by protonating alkanes to give unstable species which then decompose to carbocations in further reactions. For example, Mixtures of  $SbF_5$  and  $FSO_3H$  called Magic Acid can even protonate methane, which subsequently decomposes to give a  $CH_5^+$  cation:

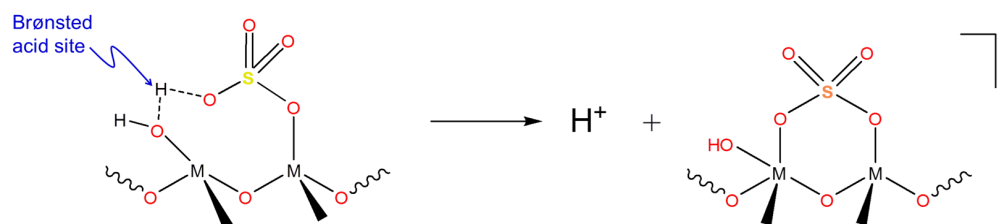


which subsequently decomposes to give an ordinary carbocation



### Solid superacids

Since liquid superacids are extremely corrosive and can be costly to separate from reaction mixtures solid superacids are used industrially instead. The main use these solid superacids to generate carbocations for use in hydrocarbon isomerization and alkylation chemistry. Many solid superacids consist of sulfuric acid/sulfates attached to a metal oxide surface to give structures similar to that shown below:



(7.1.2.22)

These structures exhibit Hammett acidity parameters in the superacid range. However, the mechanism by which these solid superacids generate carbocations isn't entirely clear since they contain both Brønsted acid sites (at OH) and Lewis acid sites (at M) that could be involved in the carbocation generation process.

### Oxyacids

Oxyacids (also known as oxoacids) are compounds of the general formula  $H_nEO_m$ , where E is a nonmetal or early transition metal and the acidic hydrogens are attached directly to oxygen (not E). This class of compounds includes such well-known acids as nitric acid,  $HNO_3$ , and phosphoric acid,  $H_3PO_4$ .



The acidity of oxyacids follows three trends:

### Electronegativity of the central atom

In a homologous series the acidity increases with the electronegativity of the central atom. Elements in the same group frequently form oxyacids of the same general formula. For example, chlorine, bromine, and iodine all form oxyacids of formula HOE: hypochlorous, hypobromous and hypoiodous acids. In the case of these homologous oxyacids the acidity is largely determined by the electronegativity of the central element. Central atoms which are better able to inductively pull electron density towards themselves make the oxygen-hydrogen bond that is to be ionized more polar and stabilize the conjugate base,  $\text{OE}^-$ . Thus the acid strength in such homologous series increases with the electronegativity of the central atom. This may be seen from the data for the hypohalous acids in Table 7.1.2.2 in which the acid strength increases with the electronegativity of the halogen so that the order of acidity is:



Table 7.1.2.2: Relationship of central atoms electronegativity to acid ionization constant in the hypohalous acids.

HOE	Electronegativity of E	$K_a$
HOCl	3.0	$4.0 \times 10^{-8}$
HOBr	2.8	$2.8 \times 10^{-9}$
HOI	2.5	$3.2 \times 10^{-11}$

Note this the influence of central atom electronegativity on the strength of oxyacids is exactly the opposite to that observed for the binary hydrides in Table *PageIndex*5, for which acidity increased down a group giving the order of acidity:



The reason for this is that in the hydrogen halides the bond to be broken (H-E bond) decreased in strength down the group while in oxyacids the bond to be broken is always an O-H bond and so varies much less in strength with the electronegativity of central atom.

### Central element's oxidation state

For oxoacids of a given central atom the acidity increases with the central element's oxidation state or, in other words, the number of oxygens bound to the central atom. Here we are looking at the trend for acids in which there are variable numbers of oxygen bound to a given central atom. An examples is the perchloric ( $\text{HClO}_4$ ), chloric ( $\text{HClO}_3$ ), chlorous ( $\text{HClO}_2$ ), and hypochlorous ( $\text{HClO}$ ) acid series. In such series the greater the number of oxygens the stronger the acid. This can be explained in several ways. From the viewpoint of the acid itself the key factor is again the inductive effect, in this case involving the ability of the oxygens attached to the central atom to pull on electron density across the OH bond. This is seen from the charge density diagram for the chlorine oxoacids shown in Figure 7.1.2.4 in which the partial positive charge on the acidic hydrogen increases with the number of oxygens present.

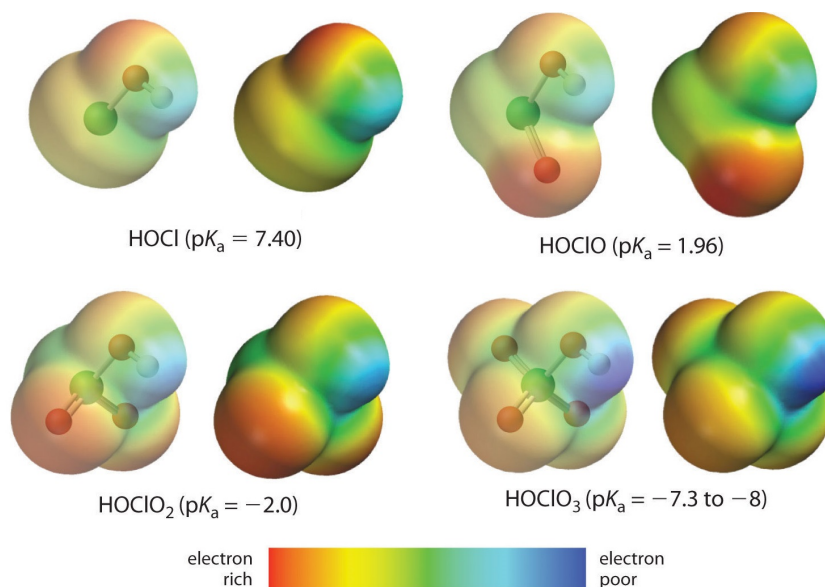


Figure 7.1.2.4: Increasing number of oxygens increases  $K_a$  as evidenced by the decreased electron density on the acidic hydrogen (which is most blue in HClO<sub>4</sub>). Note,  $K_a = 10^{-pK_a}$ , and so the larger  $pK_a$ , the smaller  $K_a$ . (CC BY-SA-NC; anonymous)

The increase in oxoacid acidity with the number of oxygens bound to the central atom may also be seen by considering the stability of the conjugate oxyanion. That the stability of the conjugate base increases with the number of oxygens may be seen from the charge distribution diagrams and Lewis bonding models for the chlorine oxyanions shown in figure 7.1.2.5. As the negative charge is spread over more oxygen atoms it becomes increasingly diffuse.

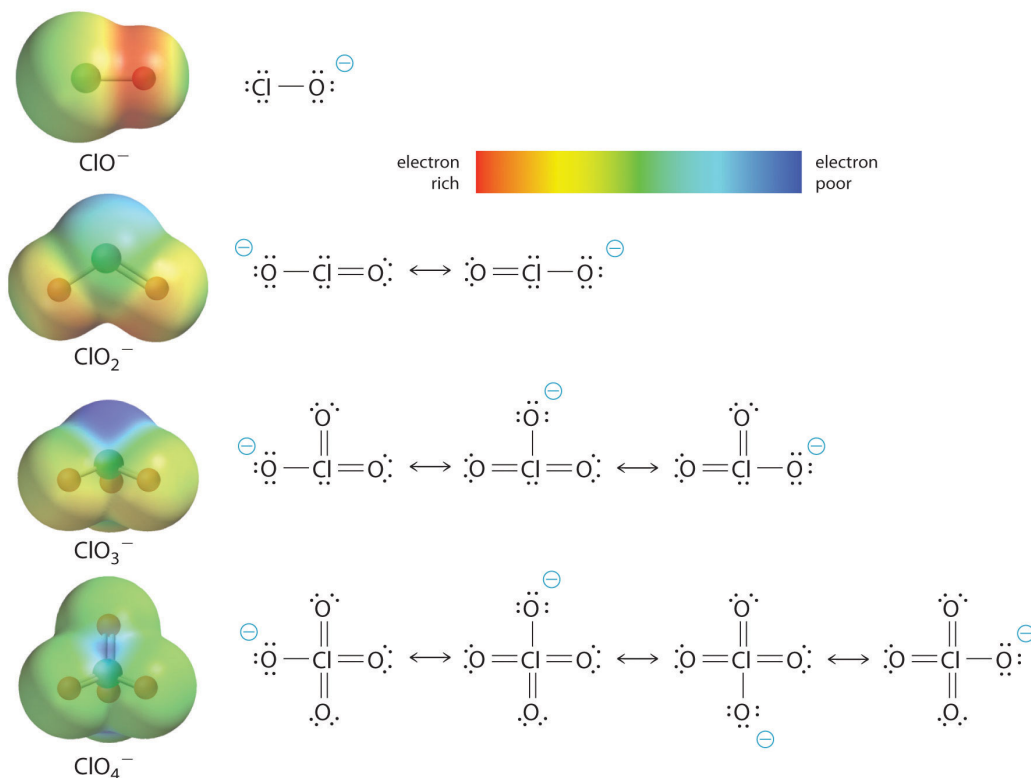


Figure 7.1.2.5: Increased diffusion of charge in chlorine oxyanions with increasing number of oxygens. The larger the ion the more dispersed the charge and thus the less the charge density, making the perchlorate the most stable anion in the series. Even the simplistic treatment of bonding depicted in the resonance structures correctly show an increased dispersion of the charge density. (CC BY-SA-NC 3.0; anonymous)

### ? Exercise 7.1.2.1

Sulfur and selenium both forms oxoacids of formula  $H_2EO_4$  where E is either S or Se. These are called sulfurous and selenous acid, respectively. Which oxoacid would you expect to be more acidic: selenous acid or sulfurous acid?

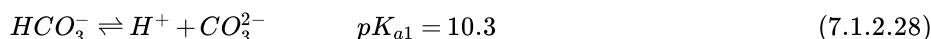
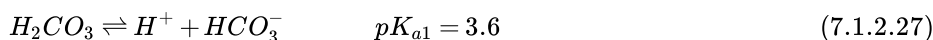
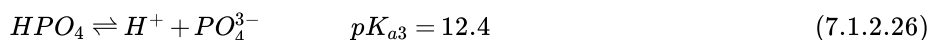
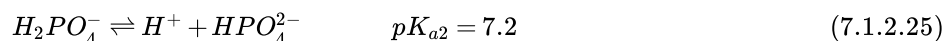
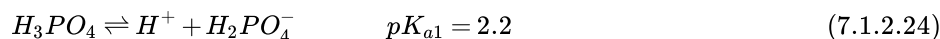
#### Answer

Sulfurous acid should be more acidic. Since sulfur is more electronegative than selenium sulfur will polarize OH bonds to a greater extent, making them more acidic. This prediction is borne out by a comparison of the  $pK_a$  values for the acids:

Acid	$pK_{a1}$	$pK_{a2}$
sulfurous acid, $H_2SO_3$	1.85	7.2
selenous acid, $H_2SeO_3$	2.62	8.32

### Successive proton removal

For polyprotic oxoacids the acidity decreases as each successive proton is removed. Oxoacids with multiple O-H bonds are called **polyprotic** since they can donate more than one hydrogen ion. In this case hydrogen ions are removed in successive ionization reactions. Examples include phosphoric and carbonic acid:



The dissociation constants for successive ionization constants decrease by about five orders of magnitude between successive hydrogen ions. This is reflected in Linus Pauling's rule for oxoacids and their oxyanions.

#### Pauling's Rules

1. The  $pK_a$  of an oxyacid of general formula  $E(OH)_q(O)_p$  is given by

$$pK_a = 8 - 5 \times p \quad (7.1.2.29)$$

2. As an oxoacid undergoes successive ionizations the  $pK_a$  increases by five each time.

The central theme of Pauling's Rules is that the more oxygen there are on the central atom, the more resonance structure that can be constructed of the conjugate base, which increases its stability and increases the acidity of the acid. However, as the acids successively ionize, they have fewer resonance structures. Pauling's Rules are phenomenological (i.e., not based on a theoretical basis). As with many empirical rules, they often work quite well, but they are approximations which may not work in all situations.

### ? Exercise 7.1.2.2: How well do Pauling's rules for oxoacids work?

Calculate the theoretical  $pK_a$  values for phosphoric and carbonic acid and their dissociation products and compare the results with the experimental  $pK_a$  values.

#### Answer

For phosphoric acid, Pauling's rules (Equation 7.1.2.29) predict the  $pK_a$  values quite well:

- $H_3PO_4$ :  $p = 3$  and  $q = 1$  and

$$pK_{a1, predicted} = 8 - 5 \times 1 = 3$$

This is slightly greater than the observed value of 2.2.

- $H_2PO_4^-$ :



$$pK_{a2,predicted} = pK_{a1,experimental} + 5 = 7.2$$

This Spot on with experiment.

- $HPO_4^{2-}$ :

$$pK_{a3,predicted} = pK_{a2,experimental} + 5 = 12.2$$

. This is slightly less than the experimental value of 12.4.

For carbonic acid Pauling's rules predict  $pK_{a1}$  reasonably well, but  $pK_{a2}$  less so:

- $H_2CO_3$ :  $p = 2$ ,  $q = 1$  and

$$pK_{a1,predicted} = 8 - 5 \times 1 = 3$$

This is slightly lower than the observed value of 3.6.

- $HCO_3^-$ :

$$pK_{a2,predicted} = pK_{a1,experimental} + 5 = 8.6$$

This is 1.7 units less than the experimental value of 10.3.

In some cases discrepancies between experimental  $pK_a$  values and those predicted by Pauling's rules suggest that structural rearrangements may be taking place upon ionization or else that the reported  $pK_a$  values do not really represent the ionization in question because they do not fully account for all the equilibria taking place in solution. In the case of carbonic acid, however, the reason for the discrepancy between the predicted and experimental  $pK_{a2}$  values is not entirely clear.

## References

1. Wulfsberg, G. *Principles of Descriptive Inorganic Chemistry* University Science Books, 1991, pp. 28-30.
2. (a) Gutmann, V. *Allg. Prakt. Chem.* 1970, 21, 116. (b) Gutmann, V. *Fortschr. Chem. Forsch.* 1972, 27, 59.
3. Burgess, J. *Metal Ions in Solution* Ellis Horwood, 1978, pg. 268.

## Contributors and Attributions

Stephen M. Contakes (Westmont College),

who expanded this section from a combination of

[https://chem.libretexts.org/Courses/University\\_of\\_Arkansas\\_Little\\_Rock/Chem\\_1403%3A\\_General\\_Chemistry\\_2/Text/16%3A\\_Acids\\_and\\_Bases/16.6%3A\\_Molecular\\_Structure%2C\\_Bonding%2C\\_and\\_Acid-Base\\_Behavior](https://chem.libretexts.org/Courses/University_of_Arkansas_Little_Rock/Chem_1403%3A_General_Chemistry_2/Text/16%3A_Acids_and_Bases/16.6%3A_Molecular_Structure%2C_Bonding%2C_and_Acid-Base_Behavior)

[https://chem.libretexts.org/Bookshelves/Organic\\_Chemistry/Book%3A\\_Organic\\_Chemistry\\_with\\_a\\_Biological\\_Emphasis\\_\(Soderberg\)/Chapter\\_07%3A\\_Organic\\_compounds\\_as\\_acids\\_and\\_bases/7.3%3A\\_Structural\\_effects\\_on\\_acidity\\_and\\_basicity](https://chem.libretexts.org/Bookshelves/Organic_Chemistry/Book%3A_Organic_Chemistry_with_a_Biological_Emphasis_(Soderberg)/Chapter_07%3A_Organic_compounds_as_acids_and_bases/7.3%3A_Structural_effects_on_acidity_and_basicity)

[https://chem.libretexts.org/Courses/University\\_of\\_Arkansas\\_Little\\_Rock/Chem\\_1403%3A\\_General\\_Chemistry\\_2/Text/16%3A\\_Acids\\_and\\_Bases/16.6%3A\\_Molecular\\_Structure%2C\\_Bonding%2C\\_and\\_Acid-Base\\_Behavior](https://chem.libretexts.org/Courses/University_of_Arkansas_Little_Rock/Chem_1403%3A_General_Chemistry_2/Text/16%3A_Acids_and_Bases/16.6%3A_Molecular_Structure%2C_Bonding%2C_and_Acid-Base_Behavior)

[https://chem.libretexts.org/Bookshelves/Organic\\_Chemistry/Book%3A\\_Organic\\_Chemistry\\_with\\_a\\_Biological\\_Emphasis\\_\(Soderberg\)/Chapter\\_07%3A\\_Organic\\_compounds\\_as\\_acids\\_and\\_bases/7.3%3A\\_Structural\\_effects\\_on\\_acidity\\_and\\_basicity](https://chem.libretexts.org/Bookshelves/Organic_Chemistry/Book%3A_Organic_Chemistry_with_a_Biological_Emphasis_(Soderberg)/Chapter_07%3A_Organic_compounds_as_acids_and_bases/7.3%3A_Structural_effects_on_acidity_and_basicity)

[https://chem.libretexts.org/Courses/University\\_of\\_Arkansas\\_Little\\_Rock/Chem\\_1403%3A\\_General\\_Chemistry\\_2/Text/16%3A\\_Acids\\_and\\_Bases/16.6%3A\\_Molecular\\_Structure%2C\\_Bonding%2C\\_and\\_Acid-Base\\_Behavior](https://chem.libretexts.org/Courses/University_of_Arkansas_Little_Rock/Chem_1403%3A_General_Chemistry_2/Text/16%3A_Acids_and_Bases/16.6%3A_Molecular_Structure%2C_Bonding%2C_and_Acid-Base_Behavior)

[https://chem.libretexts.org/Bookshelves/General\\_Chemistry/Map%3A\\_General\\_Chemistry\\_\(Petrucci\\_et\\_al.\)/16%3A\\_Acids\\_and\\_Bases/16.7%3A\\_Ions\\_as\\_Acids\\_and\\_Bases](https://chem.libretexts.org/Bookshelves/General_Chemistry/Map%3A_General_Chemistry_(Petrucci_et_al.)/16%3A_Acids_and_Bases/16.7%3A_Ions_as_Acids_and_Bases)

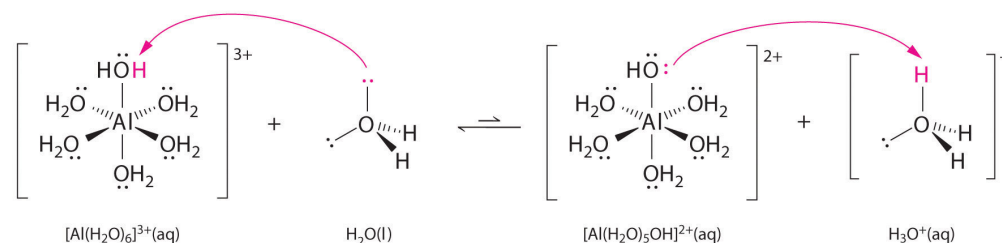
7.1.2: Brønsted-Lowry Model is shared under a CC BY-NC-SA 4.0 license and was authored, remixed, and/or curated by LibreTexts.

- **6.3.1: Brønsted-Lowry Concept** by Stephen M. Contakes is licensed CC BY 4.0.
- **6.2: Brønsted-Lowry Model** is licensed CC BY-NC-SA 4.0.
- **6.3.2: Rules of Thumb for thinking about the relationship between Molecular Structure and Brønsted Acidity and Basicity\*** has no license indicated.

- [6.3.3: The acid-base behavior of binary element hydrides is determined primarily by the element's electronegativity and secondarily by the element-hydrogen bond strength.\\*](#) has no license indicated.
- [6.3.4: Brønsted-Lowry Superacids and the Hammett Acidity Function](#) by Stephen M. Contakes has no license indicated.
- [6.3.7: The Acidity of an Oxoacid is Determined by the Electronegativity and Oxidation State of the Oxoacid's Central Atom\\*](#) by Stephen M. Contakes is licensed [CC BY-NC-SA 3.0](#).
- [6.3.11: Non-nucleophilic Brønsted-Lowry Superbases](#) by Stephen M. Contakes is licensed [CC BY-NC 4.0](#).
- [6.3.8: High Charge-to-Size Ratio Metal Ions Act as Brønsted Acids in Water](#) by Stephen M. Contakes is licensed [CC BY-NC-SA 4.0](#).

### 7.1.3: Metal Ions as Acids

Aqueous solutions of simple salts of metal ions can also be acidic, even though a metal ion cannot donate a proton directly to water to produce  $H_3O^+$ . Instead, a metal ion can act as a Lewis acid and interact with water, a Lewis base, by coordinating to a lone pair of electrons on the oxygen atom to form a hydrated metal ion.



A water molecule coordinated to a metal ion is more acidic than a free water molecule for two reasons. First, repulsive electrostatic interactions between the positively charged metal ion and the partially positively charged hydrogen atoms of the coordinated water molecule make it easier for the coordinated water to lose a proton.

Second, the positive charge on the  $Al^{3+}$  ion attracts electron density from the oxygen atoms of the water molecules, which decreases the electron density in the O–H bonds, as shown in Figure 7.1.3.6b. With less electron density between the O atoms and the H atoms, the O–H bonds are weaker than in a free  $H_2O$  molecule, making it easier to lose a  $H^+$  ion. This is shown schematically in Figure 7.1.3.1.

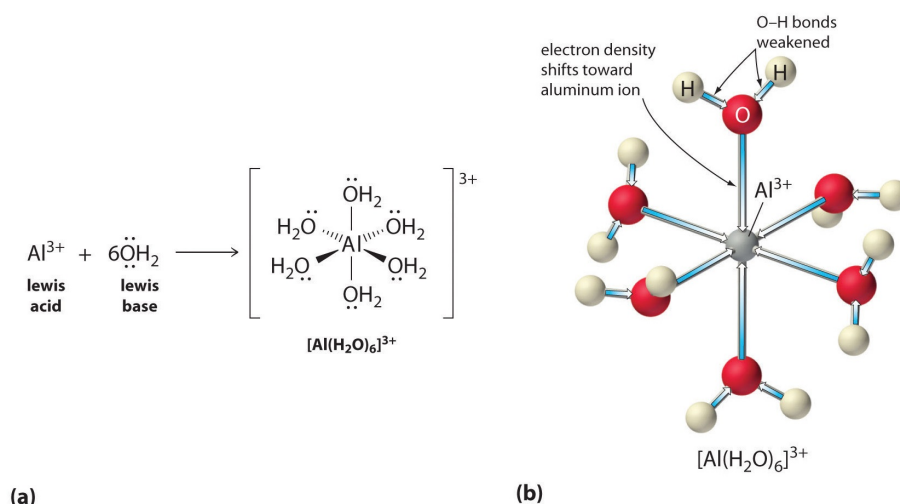


Figure 7.1.3.6: Effect of a Metal Ion on the Acidity of Water (a) Reaction of the metal ion  $Al^{3+}$  with water to form the hydrated metal ion is an example of a Lewis acid–base reaction. (b) The positive charge on the aluminum ion attracts electron density from the oxygen atoms, which shifts electron density away from the O–H bonds. The decrease in electron density weakens the O–H bonds in the water molecules and makes it easier for them to lose a proton. (CC BY-NC-SA 3.0; anonymous)

#### Trends in Acidity

The acidity of a given metal ion largely depends on its charge to size ratio and electronegativity, although in some cases hardness and ligand field effects also play a role. The magnitude of this effect depends on the following factors, of which the first two are generally considered the most important.

#### The charge on the metal ion

A divalent ion ( $M^{2+}$ ) has approximately twice as strong an effect on the electron density in a coordinated water molecule as a monovalent ion ( $M^+$ ) of the same radius.

#### The radius of the metal ion

For metal ions with the same charge, the smaller the ion, the shorter the internuclear distance to the oxygen atom of the water molecule and the greater the effect of the metal on the electron density distribution in the water molecule.

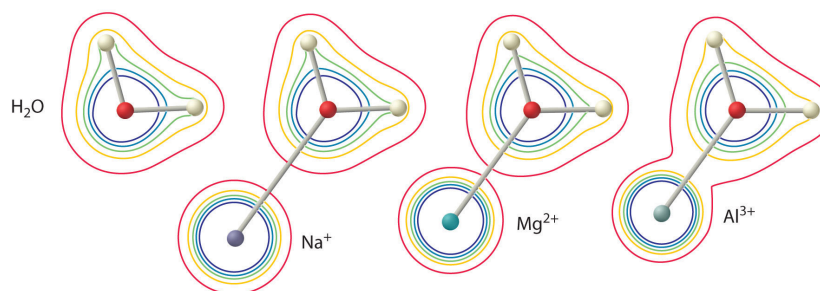
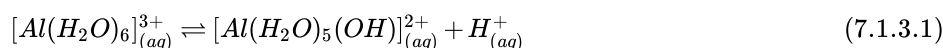


Figure 7.1.3.7: The Effect of the Charge and Radius of a Metal Ion on the Acidity of a Coordinated Water Molecule. The contours show the electron density on the O atoms and the H atoms in both a free water molecule (left) and water molecules coordinated to  $\text{Na}^+$ ,  $\text{Mg}^{2+}$ , and  $\text{Al}^{3+}$  ions. These contour maps demonstrate that the smallest, most highly charged metal ion ( $\text{Al}^{3+}$ ) causes the greatest decrease in electron density of the O–H bonds of the water molecule. Due to this effect, the acidity of hydrated metal ions increases as the charge on the metal ion increases and its radius decreases. (CC BY-NC-SA 3.0; anonymous)

The first two of these factors explain why most alkali metal cations exhibit little acidity while aqueous solutions of small, highly charged metal ions, such as  $\text{Al}^{3+}$  and  $\text{Fe}^{3+}$ , are acidic:



The  $[\text{Al}(\text{H}_2\text{O})_6]^{3+}$  ion has a  $pK_a$  of 5.0, making it almost as strong an acid as acetic acid. Because of the two factors described previously, the most important parameters for predicting the effect of a metal ion on the acidity of coordinated water molecules are the charge and ionic radius of the metal ion. Although the charge to size ratio is the simplest and most powerful predictor of metal ion acidity in water, three additional factors also can play a role:

### Electronegativity

All other things being equal more electronegative elements are better able to withdraw electron density from a bound water ligand and consequently better at enhancing the ability of that water molecule to lose a hydrogen ion.

### References

1. Wulfsberg, G. *Principles of Descriptive Inorganic Chemistry* University Science Books, 1991, pp. 28-30.
2. (a) Gutmann, V. *Allg. Prakt. Chem.* 1970, 21, 116. (b) Gutmann, V. *Fortschr. Chem. Forsch.* 1972, 27, 59.
3. Burgess, J. *Metal Ions in Solution* Ellis Horwood, 1978, pg. 268.

### Contributors and Attributions

Stephen M. Contakes (Westmont College),

who expanded this section from a combination of

[https://chem.libretexts.org/Courses/University\\_of\\_Arkansas\\_Little\\_Rock/Chem\\_1403%3A\\_General\\_Chemistry\\_2/Text/16%3A\\_Acids\\_and\\_Bases/16.6%3A\\_Molecular\\_Structure%2C\\_Bonding%2C\\_and\\_Acid-Base\\_Behavior](https://chem.libretexts.org/Courses/University_of_Arkansas_Little_Rock/Chem_1403%3A_General_Chemistry_2/Text/16%3A_Acids_and_Bases/16.6%3A_Molecular_Structure%2C_Bonding%2C_and_Acid-Base_Behavior)

[https://chem.libretexts.org/Bookshelves/Organic\\_Chemistry/Book%3A\\_Organic\\_Chemistry\\_with\\_a\\_Biological\\_Emphasis\\_\(Soderberg\)/Chapter\\_07%3A\\_Organic\\_compounds\\_as\\_acids\\_and\\_bases/7.3%3A\\_Structural\\_effects\\_on\\_acidity\\_and\\_basicity](https://chem.libretexts.org/Bookshelves/Organic_Chemistry/Book%3A_Organic_Chemistry_with_a_Biological_Emphasis_(Soderberg)/Chapter_07%3A_Organic_compounds_as_acids_and_bases/7.3%3A_Structural_effects_on_acidity_and_basicity)

[https://chem.libretexts.org/Courses/University\\_of\\_Arkansas\\_Little\\_Rock/Chem\\_1403%3A\\_General\\_Chemistry\\_2/Text/16%3A\\_Acids\\_and\\_Bases/16.6%3A\\_Molecular\\_Structure%2C\\_Bonding%2C\\_and\\_Acid-Base\\_Behavior](https://chem.libretexts.org/Courses/University_of_Arkansas_Little_Rock/Chem_1403%3A_General_Chemistry_2/Text/16%3A_Acids_and_Bases/16.6%3A_Molecular_Structure%2C_Bonding%2C_and_Acid-Base_Behavior)

[https://chem.libretexts.org/Bookshelves/Organic\\_Chemistry/Book%3A\\_Organic\\_Chemistry\\_with\\_a\\_Biological\\_Emphasis\\_\(Soderberg\)/Chapter\\_07%3A\\_Organic\\_compounds\\_as\\_acids\\_and\\_bases/7.3%3A\\_Structural\\_effects\\_on\\_acidity\\_and\\_basicity](https://chem.libretexts.org/Bookshelves/Organic_Chemistry/Book%3A_Organic_Chemistry_with_a_Biological_Emphasis_(Soderberg)/Chapter_07%3A_Organic_compounds_as_acids_and_bases/7.3%3A_Structural_effects_on_acidity_and_basicity)

[https://chem.libretexts.org/Courses/University\\_of\\_Arkansas\\_Little\\_Rock/Chem\\_1403%3A\\_General\\_Chemistry\\_2/Text/16%3A\\_Acids\\_and\\_Bases/16.6%3A\\_Molecular\\_Structure%2C\\_Bonding%2C\\_and\\_Acid-Base\\_Behavior](https://chem.libretexts.org/Courses/University_of_Arkansas_Little_Rock/Chem_1403%3A_General_Chemistry_2/Text/16%3A_Acids_and_Bases/16.6%3A_Molecular_Structure%2C_Bonding%2C_and_Acid-Base_Behavior)

[https://chem.libretexts.org/Bookshelves/General\\_Chemistry/Map%3A\\_General\\_Chemistry\\_\(Petrucci\\_et\\_al.\)/16%3A\\_Acids\\_and\\_Bases/16.7%3A\\_Ions\\_as\\_Acids\\_and\\_Bases](https://chem.libretexts.org/Bookshelves/General_Chemistry/Map%3A_General_Chemistry_(Petrucci_et_al.)/16%3A_Acids_and_Bases/16.7%3A_Ions_as_Acids_and_Bases)

7.1.3: Metal Ions as Acids is shared under a CC BY-NC-SA 4.0 license and was authored, remixed, and/or curated by LibreTexts.

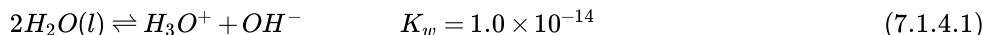
- 6.3.8: High Charge-to-Size Ratio Metal Ions Act as Brønsted Acids in Water by Stephen M. Contakes is licensed CC BY-NC-SA 4.0.

- [6.2: Brønsted-Lowry Model](#) is licensed [CC BY-NC-SA 4.0](#).
- [6.3.11: Non-nucleophilic Brønsted-Lowry Superbases](#) by Stephen M. Contakes is licensed [CC BY-NC 4.0](#).
- [6.3.2: Rules of Thumb for thinking about the relationship between Molecular Structure and Brønsted Acidity and Basicity\\*](#) has no license indicated.
- [6.3.3: The acid-base behavior of binary element hydrides is determined primarily by the element's electronegativity and secondarily by the element-hydrogen bond strength.\\*](#) has no license indicated.

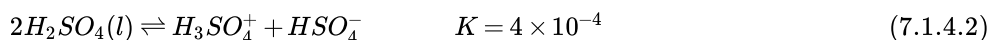
## 7.1.4: Autoionization and Solvent Leveling

### Solvent Autoionization

The Brønsted-Lowry concept allows for an understanding of hydrogen ion transfer chemistry in amphoteric protic solvents. Amphoteric protic solvents are those which can both accept and receive hydrogen ions. From the viewpoint of the Brønsted-Lowry concept the acid-base chemistry in these solvents is governed by autoionization equilibria analogous to water autoionization.

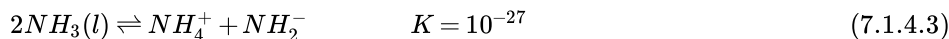


For example, sulfuric acid ionizes according to the equation:



The magnitude of the solvent autoionization constant in a given amphoteric solvent determines the amount of protonated and deprotonated\* solvent present. Since sulfuric acid's autoionization constant is much larger than that of water  $K_w = 10^{-14}$  the concentration of  $H_3SO_4^+$  and  $HSO_4^-$  present in pure sulfuric acid is  $\sim 0.02\text{ M}$ , much greater than the  $10^{-7}\text{ M}$   $H^+$  and  $OH^-$  present in pure water.

In contrast, ammonia's autoionization constant is much less than that of water and only  $\sim 10^{-27}\text{ M}$   $NH_4^+$  and  $NH_2^-$  are present in pure ammonia.



### Solvent Leveling Effect

The solvent leveling effect limits the strongest acid or base that can exist in acidic, basic, and amphoteric solvents. The conjugate acid and base of the solvent are the strongest Brønsted acid and bases that can exist in that solvent. To see why this is the case for acids consider the reaction between a Brønsted acid (HA) and solvent (S):



This equilibrium will favor dissociation of whichever is a stronger acid - HA or  $HS^+$ . If the acid is stronger it will mostly dissociate to give  $HS^+$ , while if the solvent's conjugate acid is stronger the acid will be mostly un-ionized and remain as HA.

Any acid significantly stronger than  $HS^+$  will act as a strong acid and effectively dissociate completely to give the solvent's conjugate acid  $HS^+$ . This also means that the relative acidity of acids stronger than  $HS^+$  cannot be distinguished in solvent S. This is called the leveling effect since the solvent "levels" the behavior of acids much stronger acids than it to that of complete dissociation. For example, there is no way to distinguish the acidity of strong acids like  $HClO_4$  and  $HCl$  in water since they both completely dissociate. However, it is possible to distinguish their relative acidities in solvents that are more weakly basic than the conjugate base of the strongest acid since then the acids will dissociate to different extents. Such solvents are called differentiating solvents. For example, acetonitrile (MeCN) acts as a differentiating solvent for  $HClO_4$  and  $HCl$ . Both  $HClO_4$  and  $HCl$  partially dissociate in MeCN, with the stronger acid  $HClO_4$  dissociating to a greater extent than  $HCl$ .

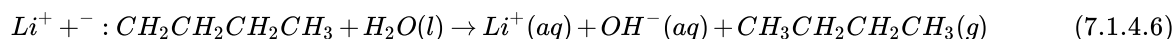
The leveling effect can also occur in basic solutions. The strongest Brønsted base, B, that can exist in a solvent is determined by the relative acidity of the solvent and the base's conjugate acid,  $BH^+$ , determines whether the base will remain unprotonated and able to act as a base in that solvent. If the solvent is represented this time as HS then the relevant equilibrium is:



The position of this equilibrium depends on whether B or  $S^-$  is the stronger base. If the solvent's conjugate base,  $S^-$ , is stronger then the base will remain unprotonated and available to act as a base. However, if B is a stronger base than  $S^-$  it will deprotonate the solvent to give  $BH^+$  and  $S^-$ . In this way the strongest base that can exist in a given solvent is the solvent's conjugate base. The relative strength of Brønsted bases can only be determined in solvents that are more weakly acidic than  $BH^+$ ; otherwise the bases will all be leveled to  $S^-$ .

It is important to consider the levelling effect of protic solvents when performing syntheses that require the use of basic reagents. For instance, hydride and carbanion reagents (Lithium aluminum hydride, Grignard reagents, alkylolithium reagents, etc.) cannot be used as nucleophiles in protic solvents like water, alcohols, or enolizable aldehydes and ketones. Since carbanions are stronger bases than these solvent's conjugate bases they will instead act as Brønsted bases and deprotonate the solvent. For example if one

adds n-butyllithium to water the result (along with much heat and possibly a fire) butane and a solution of lithium hydroxide will be obtained:



Since hydride and carbanion reagents cannot be used as nucleophiles in protic solvents like water or methanol they are commonly sold as solutions in solvents such as hexanes (for alkylolithium reagents) or tetrahydrofuran (for Grignard reagents and  $LiAlH_4$ ).

## References

1. Wulfsberg, G. *Principles of Descriptive Inorganic Chemistry* University Science Books, 1991, pp. 28-30.
2. (a) Gutmann, V. *Allg. Prakt. Chem.* 1970, 21, 116. (b) Gutmann, V. *Fortschr. Chem. Forsch.* 1972, 27, 59.
3. Burgess, J. *Metal Ions in Solution* Ellis Horwood, 1978, pg. 268.

## Contributors and Attributions

Stephen M. Contakes (Westmont College),

who expanded this section from a combination of

[https://chem.libretexts.org/Courses/University\\_of\\_Arkansas\\_Little\\_Rock/Chem\\_1403%3A\\_General\\_Chemistry\\_2/Text/16%3A\\_Acids\\_and\\_Bases/16.6%3A\\_Molecular\\_Structure%2C\\_Bonding%2C\\_and\\_Acid-Base\\_Behavior](https://chem.libretexts.org/Courses/University_of_Arkansas_Little_Rock/Chem_1403%3A_General_Chemistry_2/Text/16%3A_Acids_and_Bases/16.6%3A_Molecular_Structure%2C_Bonding%2C_and_Acid-Base_Behavior)

[https://chem.libretexts.org/Bookshelves/Organic\\_Chemistry/Book%3A\\_Organic\\_Chemistry\\_with\\_a\\_Biological\\_Emphasis\\_\(Soderberg\)/Chapter\\_07%3A\\_Organic\\_compounds\\_as\\_acids\\_and\\_bases/7.3%3A\\_Structural\\_effects\\_on\\_acidity\\_and\\_basicity](https://chem.libretexts.org/Bookshelves/Organic_Chemistry/Book%3A_Organic_Chemistry_with_a_Biological_Emphasis_(Soderberg)/Chapter_07%3A_Organic_compounds_as_acids_and_bases/7.3%3A_Structural_effects_on_acidity_and_basicity)

[https://chem.libretexts.org/Courses/University\\_of\\_Arkansas\\_Little\\_Rock/Chem\\_1403%3A\\_General\\_Chemistry\\_2/Text/16%3A\\_Acids\\_and\\_Bases/16.6%3A\\_Molecular\\_Structure%2C\\_Bonding%2C\\_and\\_Acid-Base\\_Behavior](https://chem.libretexts.org/Courses/University_of_Arkansas_Little_Rock/Chem_1403%3A_General_Chemistry_2/Text/16%3A_Acids_and_Bases/16.6%3A_Molecular_Structure%2C_Bonding%2C_and_Acid-Base_Behavior)

[https://chem.libretexts.org/Bookshelves/Organic\\_Chemistry/Book%3A\\_Organic\\_Chemistry\\_with\\_a\\_Biological\\_Emphasis\\_\(Soderberg\)/Chapter\\_07%3A\\_Organic\\_compounds\\_as\\_acids\\_and\\_bases/7.3%3A\\_Structural\\_effects\\_on\\_acidity\\_and\\_basicity](https://chem.libretexts.org/Bookshelves/Organic_Chemistry/Book%3A_Organic_Chemistry_with_a_Biological_Emphasis_(Soderberg)/Chapter_07%3A_Organic_compounds_as_acids_and_bases/7.3%3A_Structural_effects_on_acidity_and_basicity)

[https://chem.libretexts.org/Courses/University\\_of\\_Arkansas\\_Little\\_Rock/Chem\\_1403%3A\\_General\\_Chemistry\\_2/Text/16%3A\\_Acids\\_and\\_Bases/16.6%3A\\_Molecular\\_Structure%2C\\_Bonding%2C\\_and\\_Acid-Base\\_Behavior](https://chem.libretexts.org/Courses/University_of_Arkansas_Little_Rock/Chem_1403%3A_General_Chemistry_2/Text/16%3A_Acids_and_Bases/16.6%3A_Molecular_Structure%2C_Bonding%2C_and_Acid-Base_Behavior)

[https://chem.libretexts.org/Bookshelves/General\\_Chemistry/Map%3A\\_General\\_Chemistry\\_\(Petrucci\\_et\\_al.\)/16%3A\\_Acids\\_and\\_Bases/16.7%3A\\_Ions\\_as\\_Acids\\_and\\_Bases](https://chem.libretexts.org/Bookshelves/General_Chemistry/Map%3A_General_Chemistry_(Petrucci_et_al.)/16%3A_Acids_and_Bases/16.7%3A_Ions_as_Acids_and_Bases)

---

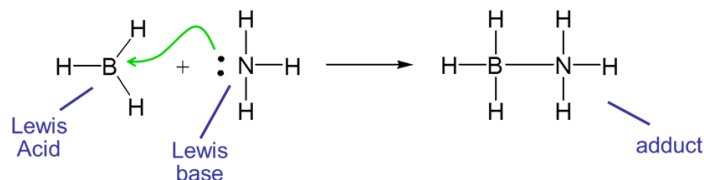
7.1.4: Autoionization and Solvent Leveling is shared under a [CC BY-NC-SA 4.0](https://creativecommons.org/licenses/by-nc-sa/4.0/) license and was authored, remixed, and/or curated by LibreTexts.

- **6.3.1: Brønsted-Lowry Concept** by Stephen M. Contakes is licensed [CC BY 4.0](https://creativecommons.org/licenses/by/4.0/).
- **6.2: Brønsted-Lowry Model** is licensed [CC BY-NC-SA 4.0](https://creativecommons.org/licenses/by-nc-sa/4.0/).
- **6.3.10: Acid-Base Chemistry in Amphoteric Solvents and the Solvent Leveling Effect** by Stephen M. Contakes is licensed [CC BY-NC 4.0](https://creativecommons.org/licenses/by-nc/4.0/).
- **6.3.11: Non-nucleophilic Brønsted-Lowry Superbases** by Stephen M. Contakes is licensed [CC BY-NC 4.0](https://creativecommons.org/licenses/by-nc/4.0/).
- **6.3.8: High Charge-to-Size Ratio Metal Ions Act as Brønsted Acids in Water** by Stephen M. Contakes is licensed [CC BY-NC-SA 4.0](https://creativecommons.org/licenses/by-nc-sa/4.0/).
- **6.3.2: Rules of Thumb for thinking about the relationship between Molecular Structure and Brønsted Acidity and Basicity\*** has no license indicated.
- **6.3.3: The acid-base behavior of binary element hydrides is determined primarily by the element's electronegativity and secondarily by the element-hydrogen bond strength.\*** has no license indicated.

## 7.1.5: Lewis Model and Frontier Orbitals

### Lewis Acids and Bases

The Lewis acid base concept generalizes the Brønsted and solvent system acid base concepts by describing acid-base reactions in terms of the donation and acceptance of an electron pair. Under the Lewis definition Lewis acids are electron pair acceptors and Lewis bases are electron pair donors. In Lewis acid-base reactions a Lewis base donates an electron pair to the Lewis acid, which accepts it. The reaction between borane,  $\text{BH}_3$ , and  $\text{NH}_3$  is the classic example:



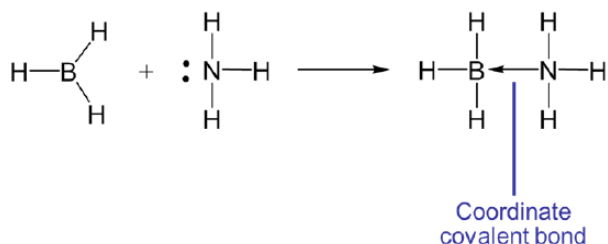
#### Definition: Lewis acid

A species that is an electron pair acceptor

#### Definition: Lewis base

A species that is an electron pair donor

In this case the Lewis acid-base reaction results in the formation of a bond between  $\text{BH}_3$  and  $\text{NH}_3$ . When the acid and base combine to form a larger unit that unit is said to be an adduct and the resulting bond is said to be a coordinate covalent or dative bond. Such coordinate covalent bonds are sometimes represented by an arrow that indicates the direction of electron donation from the base to the acid. For instance the reaction between  $\text{BH}_3$  and  $\text{NH}_3$  could also have been written as



The arrow notation for the coordinate covalent bond is really just a convenient formalism - a bookkeeping tool to help keep track of where the electrons came from and where they might return if the reverse reaction occurs.

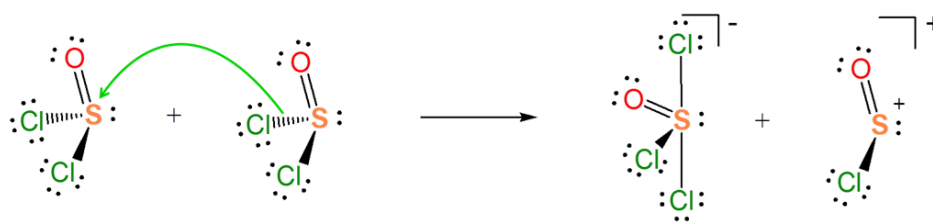
For example, in Brønsted acid base reactions the hydrogen ion is an acid because it accepts an electron pair from the Brønsted base. Consequently under the Lewis acid-base concept in Brønsted acid base reactions involve the formation of an adduct between  $\text{H}^+$  and a base.



(7.1.5.1)

The Lewis acid base concept nicely explains ionization reactions involving nonaqueous solvents. For instance, the autoionization of  $\text{SOCl}_2$  as an acid-base reaction between two  $\text{SOCl}_2$  molecules.





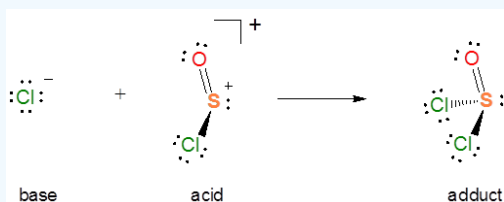
(7.1.5.2)

### Example 7.1.5.1

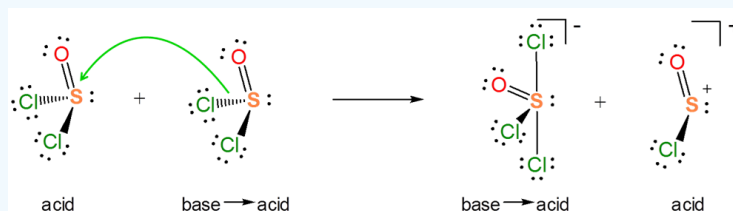
Explain how the autoionization of  $\text{SOCl}_2$  is a Lewis acid-base displacement reaction.

#### Solution

In the autoionization of  $\text{SOCl}_2$  the pair of electrons donated comes from the S-Cl bond and the S-Cl bond is broken to give a lone pair bearing  $\text{Cl}^-$  base and a  $\text{SOCl}^+$  Lewis acid fragment. If you are having trouble seeing how this works it can be instructive to consider the reverse of this process. It is a Lewis acid-base reaction to give a Lewis acid-base adduct:



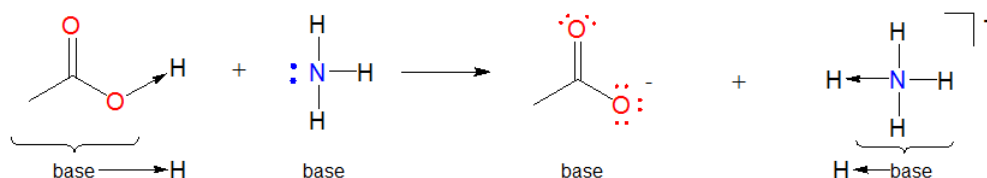
From the autoionization reaction it is also apparent that  $\text{SOCl}_2$  itself acts as a Lewis acid towards the liberated  $\text{Cl}^-$ . So the autoionization reaction involves a transfer of the base  $\text{Cl}^-$  between the two Lewis acids - a Lewis acid-base displacement reaction.



### Lewis acid-base model and chemical reactions

It can be helpful to keep several distinctions in mind when using the Lewis acid-base concept to describe chemical reactions.

- Many Lewis-Acid base reactions are displacement reactions. This is because the hydrogen ion is usually bound to something at the start of the reaction. In such cases the Lewis acid  $\text{H}^+$  unit is transferred from one Lewis base and another. Such acid-base reactions are sometimes called displacement reactions since the base group in the initial Lewis acid-base complex is displaced by the incoming Lewis base to generate another complex.



(7.1.5.3)

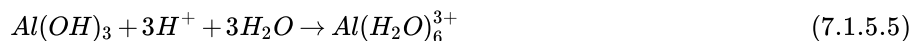
- Substances are sometimes considered amphoteric because they exhibit Lewis acidity and basicity at different types of atomic centers. The classic example is aluminum hydroxide,  $\text{Al}(\text{OH})_3$ . In water  $\text{Al}(\text{OH})_3$  can act as a Lewis acid towards  $\text{OH}^-$  ion. The reaction occurs by formation of an adduct at  $\text{Al}(\text{OH})_3$ 's  $\text{Al}^{3+}$  center:



Notice that in addition to acting as a Lewis acid, in this reaction  $\text{Al}(\text{OH})_3$

- does not act as a Brønsted acid or base since no  $\text{H}^+$  ion transfer occurs
- but does act as an Arrhenius acid since  $\text{OH}^-$  ion is consumed from solution, decreasing  $[\text{OH}^-]$  and increasing  $[\text{H}^+]$

In water  $\text{Al}(\text{OH})_3$  also acts as a Lewis base towards  $\text{H}^+$  through the lone pairs on its hydroxide ligands.



Notice that in addition to acting as a Lewis base, in this reaction  $\text{Al}(\text{OH})_3$  also acts as a

- Brønsted base since a  $\text{H}^+$  ion is transferred onto the  $\text{OH}^-$  ligand
- Arrhenius base since  $\text{H}^+$  ion is consumed from solution, decreasing  $[\text{H}^+]$
- Lewis acid at its  $\text{Al}^{3+}$  center since Al-O metal-ligand bonds are formed

## Frontier Orbitals

Another way the Lewis acid-base concept is widely employed for understanding chemical reactivity is through the frontier orbital approach to chemical reactions. The frontier orbital concept is a simplified version of [molecular orbital theory](#) where chemical bonding and reactivity are visualized in terms of the interactions between frontier molecular orbitals on the chemical species undergoing an interaction (*e.g.* molecules, atoms, ions, or groups as they interact to form a bond or undergo a reaction). Frontier orbitals are those at the frontier between occupied and unoccupied. They are often taken to be the highest energy occupied and lowest energy unoccupied molecular orbitals, called the HOMO and LUMO levels. However, it can sometimes be more convenient to think about them as atomic orbitals or Valence Bond approach-derived orbitals. When developing rough qualitative frontier orbital descriptions of the orbital interactions involved in a given system the choice of what types of orbitals to use is often a matter of what is the most informative and convenient.

In particular the frontier orbital concept envisions a Lewis acid-base interaction as involving an interaction between some of the frontier orbitals of the Lewis acid and base, specifically the donation of electrons from the bases' HOMO level into the acid's LUMO level. For example, in the frontier orbital approach adduct formation between  $\text{NH}_3$  and  $\text{BH}_3$  involves the donation of electrons from ammonia's HOMO into  $\text{BH}_3$ 's LUMO level.

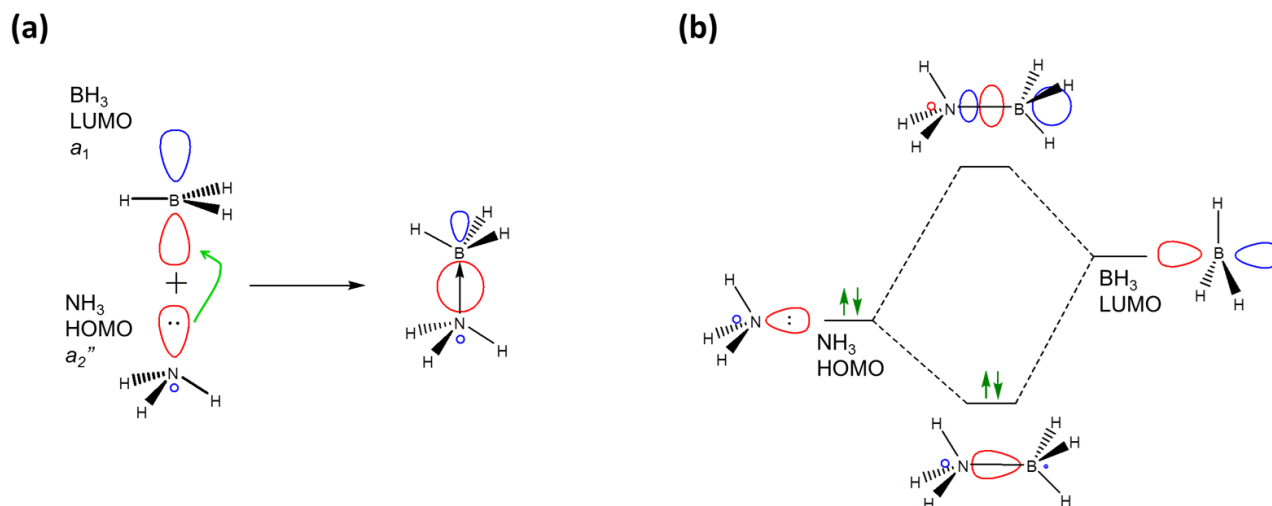


Figure 7.1.5.1: Frontier orbital picture of adduct formation between ammonia and borane. (a) As  $\text{NH}_3$  and  $\text{BH}_3$  approach one another interaction between the  $\text{NH}_3$  HOMO (lone pair on N) and  $\text{BH}_3$  LUMO (unoccupied, non-bonding 2p orbital) gives a bonding MO. (b) Partial molecular orbital diagram for  $\text{NH}_3 \rightarrow \text{BH}_3$  showing the stabilization of the base ( $\text{NH}_3$ ) lone pair in a sigma bonding MO on adduct formation.

As expected when two orbitals of the appropriate symmetry combine, the result of the interaction is the formation of a lower energy bonding orbital between the acid and base (Figure 7.1.5.1). Since it is occupied by an electron the net result of the interaction is the lowering of the base's lone pair as it interacts with the Lewis acid. In this case the interaction just follows the general pattern for Lewis-Acid base adduct formation, which is shown in Figure 7.1.5.2

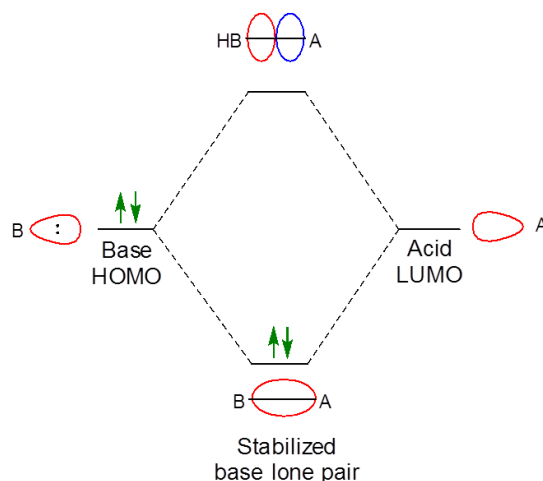
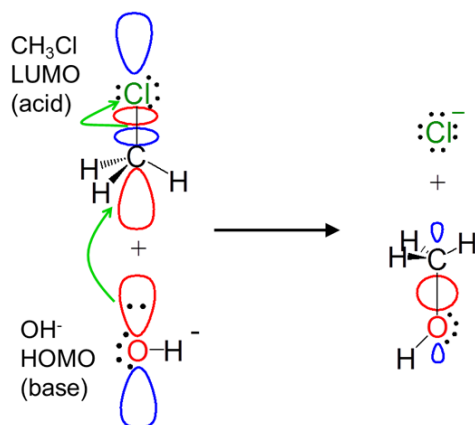


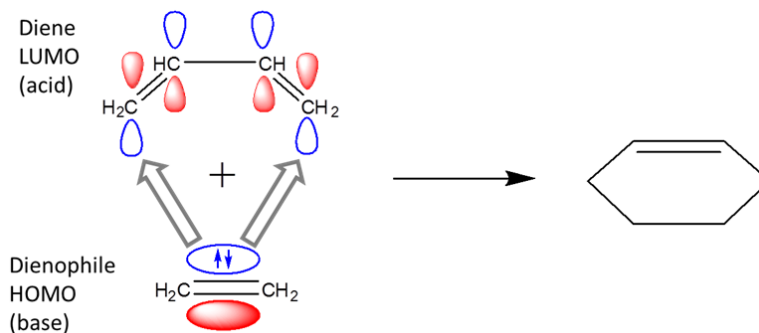
Figure 7.1.5.2: Generalized frontier orbital picture for adduct formation between a Lewis base (B) and a Lewis acid (A) involving stabilization of the lone pair of the base HOMO by formation of a bonding orbital with the acid LUMO. The relative energies of the acid LUMO and base HOMO affect the character of the bonding and antibonding MOs but are otherwise unimportant in determining the general features of the interaction. In some cases the base HOMO is higher in energy; in others the acid LUMO is higher in energy; in still others they are equal in energy. In any case the net result is the stabilization of the base lone pair.

The frontier orbital concept illuminates the orbital interactions involved in reactions. For instance, from a frontier orbital perspective the alkyl halide substitution reaction between hydroxide and  $\text{CH}_3\text{Cl}$  via the  $\text{S}_{\text{N}}2$  mechanism involves a Lewis acid-base interaction:

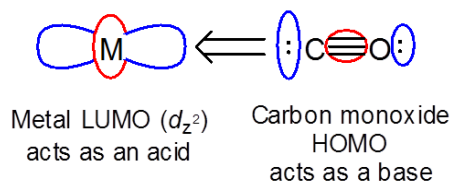


Notice how the frontier orbital approach even explains the displacement of the chloride leaving group. The donation of electrons from the hydroxide HOMO populates the antibonding  $\text{CH}_3\text{Cl}$  LUMO, breaking the  $\text{C-Cl}$  bond.

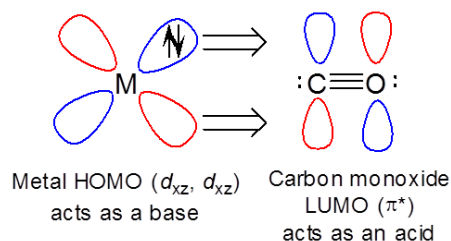
Using the frontier orbital approach it becomes apparent that pericyclic reactions are Lewis acid-base reactions. For example, in the Diels-Alder reaction the dienophile acts as a Lewis base and the diene as a Lewis acid.



The orbital interactions involved in a given reaction can include both reactants acting as both an acid and base. In these cases the HOMO of each reactant interacts with the LUMO of the other. A good example of this involves  $\Pi$ -type interactions between a metal ion with occupied  $d$  orbitals and a pi-acceptor ligand. The ligand acts as a base and the metal as an acid to give a M-CO single bond.

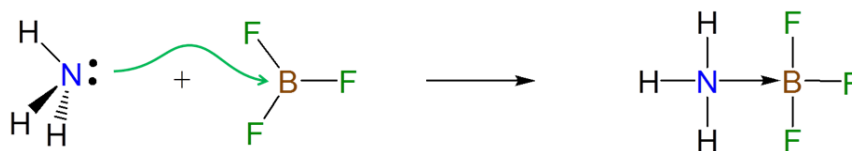


However, the metal can also act as a base towards the ligand LUMO ( $\pi^*$ ) orbitals. Bonding between metals and ligands will be discussed further in [chapter 9](#)



## Substituent Effects

The electrons donated from a Lewis base to a Lewis acid in a Lewis acid-base reaction are donated and accepted at particular atomic centers. For instance, the formation of an adduct between ammonia and  $\text{BF}_3$  involves the donation of the lone pair on the ammonia nitrogen atom to the Lewis acid site on  $\text{BF}_3$ .



Because Lewis acid-base reactions involve electron donation and acceptance at particular sites substituent groups which alter the electron density at a site through inductively donating or withdrawing electron density will affect the Lewis acid-base properties of that site. For instance, the  $\text{BF}_3$  affinities of 4-substituted pyridines increase slightly as the substituent on the aromatic ring is changed from electron donating Me to electron withdrawing  $\text{CF}_3$ .

	$\text{BF}_3$ Affinity (kJ/mol) <sup>a</sup>
	$115.7 \pm 0.4$
	$128.1 \pm 0.5$
	$134.1 \pm 0.6$

a) Data from Laurence, C.; Gal, J.-F. O., *Lewis basicity and Affinity Scales: Data and Measurement*. John Wiley: Chichester, West Sussex, U.K., 2010; pp. 91-101.

Substituent inductive effects are much as one might predict. Since Lewis bases donate electron pairs and Lewis acids accept them:

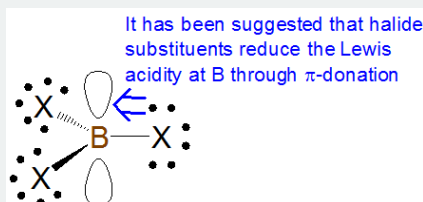
- electron withdrawing substituents tend to decrease the Lewis basicity of basic sites while electron donating substituents increase site Lewis basicity by making them more electron rich.
- electron withdrawing substituents increase the Lewis acidity of acidic sites by making those sites more electron deficient while electron donating substituents tend decrease Lewis acidity by making sites less electron deficient.

Nevertheless it can be difficult to predict substituent-based trends in Lewis acidity and basicity by inductive effects alone. This is because inductive effects are modest and often exists in competition with other substituent effects, such as

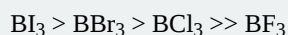
- Steric effects
- Hardness effects
- $\pi$ -donation and acceptance effects, which can increase or decrease electron density at a given site as well as create an energy barrier for any structural distortions that might occur on adduct formation.

### $\pi$ Donation and Acceptance and Lewis Acid-Base Affinity

As with  $\sigma$ -based induction effects  $\pi$ -donation tends to increase Lewis basicity and decrease Lewis acidity while  $\pi$ -withdrawal tends to decrease Lewis basicity and increase Lewis acidity. However, care needs to be taken in assessing the effect of  $\pi$ -donation effects on Lewis acidity and basicity. For example, some textbooks claim that the Lewis acidity of boron trihalides is dominated by the reduction of boron acidity through  $\pi$ -donation from the halide substituents:

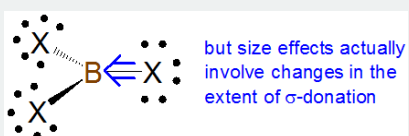


According to this explanation the extent of this  $\pi$ -donation decreases down the halogen group as the boron-halogen bond distance decreases. This is consistent with the observed trend in Lewis acidity of the boron trihalides towards most bases, which runs counter to that suggested by inductive effects alone:



However, computation work suggests that this explanation is incorrect since

- atomic size effects are important mainly for substituents in which the connected atom is row 3+ or higher
- atomic size effects mainly involve changes in the extent of  $\sigma$ -overlap. In other words the larger halogens are less able to reduce the electron deficiency at the boron center through  $\sigma$  interactions while  $\pi$ -interactions play little or no role.



### References:

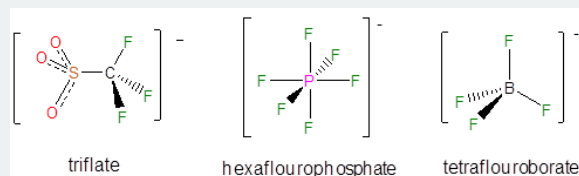
1. Plumley, J. A.; Evanseck, J. D., Periodic Trends and Index of Boron Lewis Acidity. *The Journal of Physical Chemistry A* 2009, 113 (20), 5985-5992.
2. Jupp, A. R.; Johnstone, T. C.; Stephan, D. W., Improving the Global Electrophilicity Index (GEI) as a Measure of Lewis Acidity. *Inorganic Chemistry* 2018, 57 (23), 14764-14771.

### Conjugate Bases of Brønsted Superacids

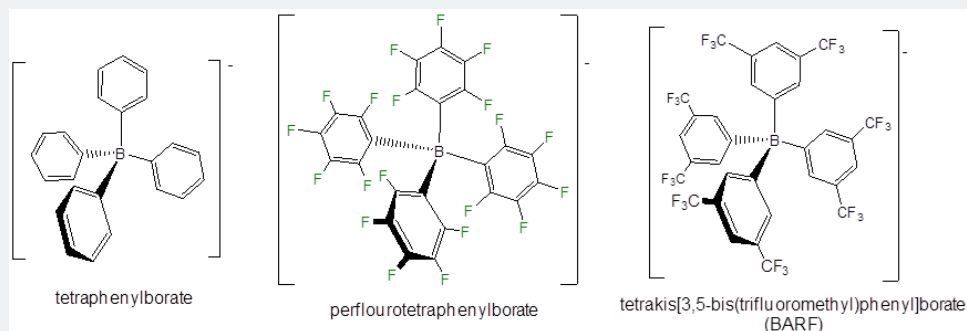
The nonreactivity of Brønsted superacids' conjugate bases towards hydrogen ions is often mirrored in nonreactivity towards other Lewis Acids/electrophiles, most notably metals. This makes these substances useful as inert or noncoordinating ions, although since all are reactive towards a suitably electrophilic centers they are perhaps better understood as weakly coordinating.

A number of noncoordinating anions are commonly used in synthetic and other applications. The conjugate base of perchloric acid, perchlorate, was a common noncoordinating inert anion in classical coordination chemistry and continues to be used

widely in electrochemistry. However metal perchlorate salts can be explosive, so synthesis of metal salts with perchlorate anions, especially on large scales is much less common in modern inorganic chemistry. In contrast, the conjugate bases of triflic acid, hexafluoroboric acid, and tetrafluoroboric acid are now more commonly used as counterions for when isolating reactive cations.



Even less reactive noncoordinating anions include derivatives of tetraphenylborate, particularly those with electron withdrawing substituents.



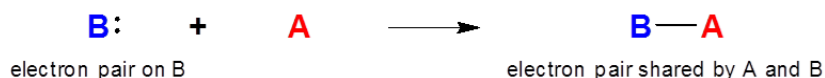
Other classes of noncoordinating ions include fluoroantimonate clusters, derivatives of the carborane anion ( $\text{CB}_{11}\text{H}_{11}^-$ ), and fluorinated aluminum tetraalkoxides.

#### References:

- Engesser, T. A.; Lichtenthaler, M. R.; Schleep, M.; Krossing, I., Reactive p-block cations stabilized by weakly coordinating anions. *Chemical Society Reviews* **2016**, 45 (4), 789-899.

### Lewis Acid-Base Adducts

When a Lewis acid-base adduct is formed electron density and negative charge is transferred from the Lewis base to the acid.



(7.1.5.6)

For example, the formation of an adduct between borane and ammonia involves the transfer of a small amount of electron density, as shown by the movement of negative charge from  $\text{NH}_3$  to  $\text{BH}_3$  depicted in Figure 7.1.5.3

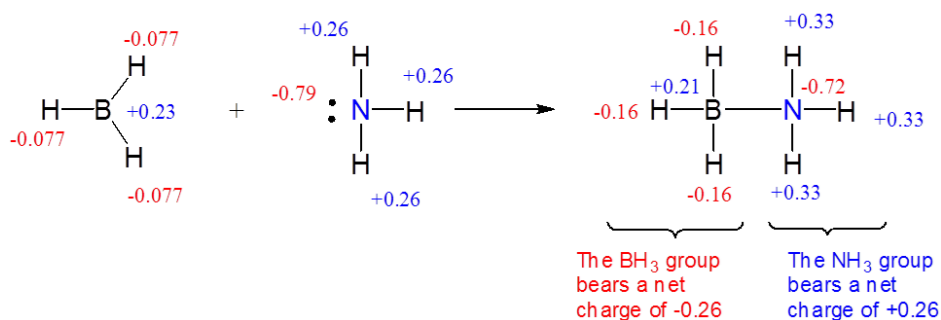


Figure 7.1.5.3: Calculated change in atomic charge distribution on formation of an adduct between  $\text{BH}_3$  and  $\text{NH}_3$  in the gas phase. All partial charges were calculated for geometry optimized molecules at the 6-31G\*\* level.

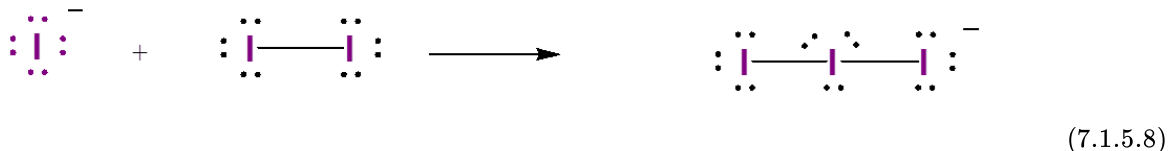
In many weakly bound Lewis acid-base complexes the transfer of electron density and consequently, charge, from the base group to the acid group is only partial:



Such Lewis acid-base adducts are commonly called **charge transfer complexes (CT complexes)** or **donor-acceptor complexes (DA complexes)**. In these

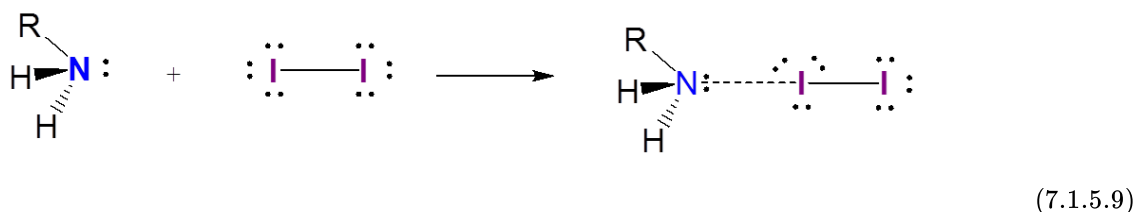
- the base is called the **donor (D)** since it is a net donor of electrons and, consequently, their negative charge
- the acid is called the **acceptor (A)** since it is a net acceptor of electrons and, consequently, their negative charge

A particularly well-known class of charge transfer complexes are the iodine charge transfer complexes. In iodine charge transfer complexes the  $I_2$  acts as a Lewis acid. This is possible since iodine is a Row 3+ element and so is capable of forming hypervalent complexes on reaction with a Lewis base. For example,  $I_2$  reacts with  $I^-$  to give the triiodide ion.

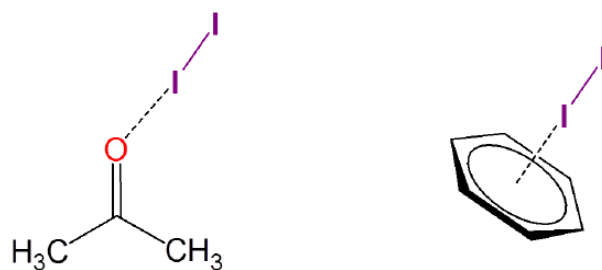


Triiodide is well-known from introductory chemistry from the bright blue color that appears when the triiodide is complexes with starch to give the dark blue starch-iodide complex.

In contrast to stable triiodide anion, iodine charge transfer complexes are only weakly associated. Complexes between iodine and amines are a well known example:



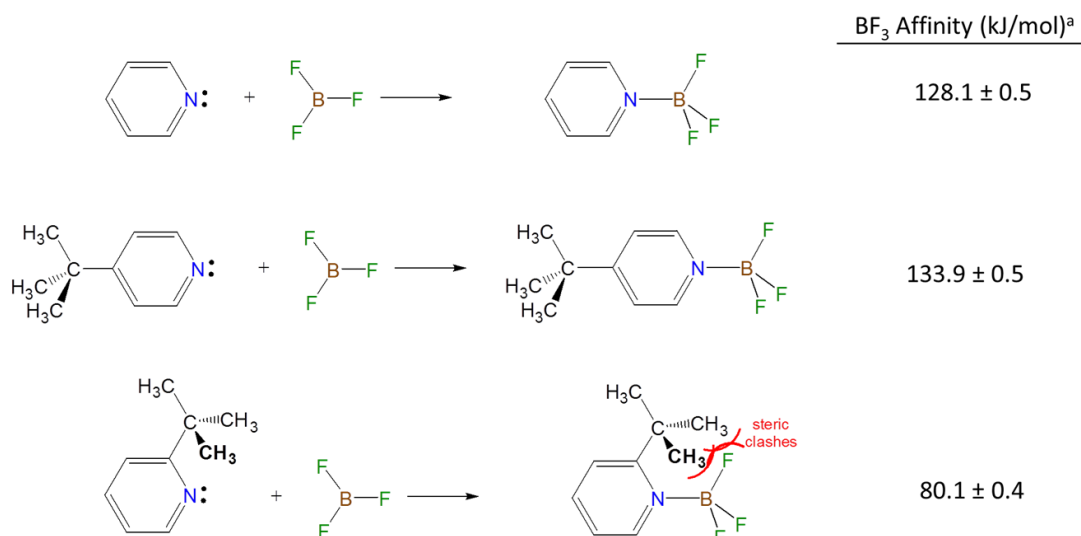
Iodine also forms weakly-associated charge transfer complexes with many solvents. For instance, iodine can weakly associate with both acetone and benzene:



## Steric Effects

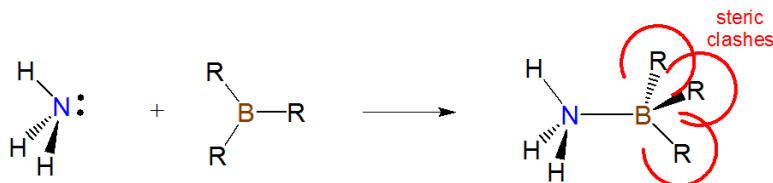
Steric effects can influence the ability of a Lewis acid or base to form adducts by introducing:

- front strain (F-strain)** whereby bulky groups make it difficult for the Lewis acid and Lewis base centers to approach and interact.



a) Data from Laurence, C.; Gal, J.-F. o., *Lewis basicity and Affinity Scales: Data and Measurement*. John Wiley: Chichester, West Sussex, U.K., 2010; pp. 91-101.

- **back strain (B-strain)** associated with steric interactions that do not directly impede the Lewis acid and base centers from interacting but instead occur as the acid and base rearrange on adduct formation. For instance, when trivalent boron compounds form adducts with amines the boron center changes from a more open trigonal pyramidal geometry to a more hindered tetrahedral one:



- **internal strain (I-strain)** is also associated with the geometry changes incident on adduct formation. However, while B-strain involves direct steric clashes that occur on adduct formation I-strain is the strain involved in deforming bond and torsional angles away from more stable local geometries. Thus it is more important for Lewis base centers embedded in rings or clusters.

## References

1. Alder, R. W., Strain effects on amine basicities. *Chemical Reviews* 1989, 89 (5), 1215-1223.

## Contributors and Attributions

Stephen M. Contakes, Westmont College

Consistent with the policy for original artwork made as part of this project, all unlabeled drawings of chemical structures are by Stephen Contakes and licensed under a [Creative Commons Attribution 4.0 International License](https://creativecommons.org/licenses/by-nc-sa/4.0/).

7.1.5: [Lewis Model and Frontier Orbitals](#) is shared under a [CC BY-NC-SA 4.0](https://creativecommons.org/licenses/by-nc-sa/4.0/) license and was authored, remixed, and/or curated by LibreTexts.

- [6.3: Lewis Concept and Frontier Orbitals](#) is licensed [CC BY-NC-SA 4.0](https://creativecommons.org/licenses/by-nc-sa/4.0/).
- [6.4: Lewis Concept and Frontier Orbitals](#) by Stephen M. Contakes is licensed [CC BY-NC 4.0](https://creativecommons.org/licenses/by-nc-sa/4.0/).
- [6.4.1: The frontier orbital approach considers Lewis acid-base reactions in terms of the donation of electrons from the base's highest occupied orbital into the acid's lowest unoccupied orbital.](#) by Stephen M. Contakes has no license indicated.
- [6.4.2: All other things being equal, electron withdrawing groups tend to make Lewis acids stronger and bases weaker while electron donating groups tend to make Lewis bases stronger and acids weaker](#) by Stephen M. Contakes has no license indicated.
- [6.4.3: The electronic spectra of charge transfer complexes illustrate the impact of frontier orbital interactions on the electronic structure of Lewis acid-base adducts](#) by Stephen M. Contakes is licensed [CC BY-NC 4.0](https://creativecommons.org/licenses/by-nc-sa/4.0/).
- [6.4.7: Bulky groups weaken the strength of Lewis acids and bases because they introduce steric strain into the resulting acid-base adduct.](#) by Stephen M. Contakes has no license indicated.



- [6.4.8: Frustrated Lewis pair chemistry uses Lewis acid and base sites within a molecule that are sterically restricted from forming an adduct with each other.](#) by Stephen M. Contakes is licensed [CC BY-NC 4.0](#).

## 7.2: Hard Soft Acid Base Theory

---

Learning objectives for this unit are to:

- Describe the basic tenets of Hard-Soft Acid-Base (HSAB) theory
  - Classify acids and bases as hard or soft based on HSAB theory
  - Predict whether reactants or products will be favored at equilibrium using HSAB
  - Determine the relative stability of complexes based upon HSAB theory
  - Rationalize solubility data based on HSAB theory
  - Apply HSAB theory to understand bioinorganic systems
- 

7.2: Hard Soft Acid Base Theory is shared under a [not declared](#) license and was authored, remixed, and/or curated by LibreTexts.

## 7.2.1: Hard and Soft Acids and Bases

### Origin of the Hard-Soft Acid-Base Principle

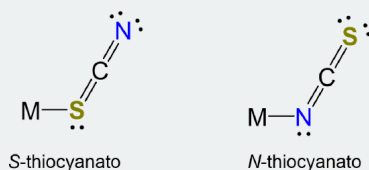
One of the strengths of the Lewis acid-base concept is the readiness with which it illuminates the role that covalent and electrostatic interactions in acid base behavior, specifically through its ability to explain chemical interactions in terms of frontier orbitals and the interactions between charged groups as electrons are donated from a base to an acid. However, simply acknowledging the presence of such interactions does little to illuminate the degree to which each mode of explanation best explains the bonding in a given system? To what extent is a given adduct better described as held together by covalent bonds as opposed to ionic ones - *e.g.* better described as a molecule rather than an ion pair? Moreover, does it even matter, given that the orbitals of quantum mechanics result from the combination of electrons' wavelike behavior with their electrostatic attraction to nuclei in either case? These questions and more are addressed by one of the most important conceptual tools in contemporary inorganic chemistry, the hard-soft acid-base principle.

The hard-soft acid-base (HSAB) principle stems from the recognition that some Lewis acids and bases seem to have a natural affinity for one another.\* Consider the following:

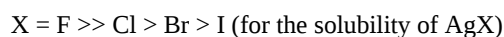
- Some metals are commonly found in nature as salts of chloride or as oxide ores while others are found in combination with sulfur. Geochemists even use the Goldschmidt classification scheme to classify the halide and oxide formers as lithophiles and the sulfide formers as chalcophiles.
- In living systems small highly charged metals ions like  $\text{Fe}^{3+}$  are usually found bound to N and O atoms while larger metals with lower charges such as  $\text{Zn}^{2+}$  are often found attached to at least one S atom. Similarly, metals prefer to bind to one coordination site over the other when forming complexes with ambidentate ligands. The most well-known instances involve complexes of cyanate and thiocyanate, which can coordinate metals through either the N or chalcogen atom. For instance,  $\text{Cu}^{2+}$  and  $\text{Zn}^{2+}$  form *N*-thiocyanato complexes in species like  $[\text{Cu}(\text{NCS})_2(\text{py})_2]$  and  $[\text{Zn}(\text{NCS})_4]^{2-}$  while their larger congeners  $\text{Au}^{3+}$  and  $\text{Hg}^{2+}$  preferentially forms *S*-thiocyanato complexes, giving species like  $[\text{Hg}(\text{SCN})_4]^{2-}$ .

#### Ambidentate ligands

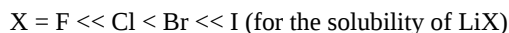
Ambidentate ligands possess multiple coordination sites through which a metal may bind. For instance, thiocyanate may coordinate metals (M) at either the S or N to give *S*-thiocyanato or *N*-thiocyanato complexes.



- The solubility trends for the alkali metal halides and silver halides are opposite, even though both involve salts of formula  $\text{M}^+\text{X}^-$  (salts can be thought of as involving Lewis acid-base adduct formation between the anions and cations). Specifically, although the silver halides are all relatively insoluble in water, the very modest solubility they possess follows the order:



In contrast, the much more ample solubility of the alkali metal halides\*\* follows the opposite order. For example, the order for the lithium halides is



#### Notes

\* Despite the fruitfulness of this observation, in general it is important to reduce the potential for observer bias by checking observations like these against compounds reported in the chemical literature and databases like the Inorganic Crystal Structure and Cambridge Crystallographic Databases.

\*\* These are very soluble in water, to the point where some solutions are perhaps better described as solutions of water in the halide.

## Qualitative HSAB Principle

The hard-soft acid-base principle is a conceptual tool for thinking about patterns of Lewis acid base reactivity. The explanation of the trends in metal distribution, halide salt solubility, and preferred metal coordination patterns is rooted in Arland, Chatt, and Davies' observation that *Lewis acids and bases could be classified into two groups based on their propensity to form stable compounds with one another* (e.g. acids in a class tend to form more stable adducts with bases in the same class than they did with bases in the other).<sup>1</sup> Arland, Chatt, and Davies somewhat boringly termed these groups class a and class b but today they are known by Ralph Pearson's name for them. Pearson called the class a acids and bases hard and class b acids and bases soft. These terms reflect how "soft" these substance's electron clouds are towards distortion or, in other words, their polarizability (Figure 7.2.1.1). Pearson terms acids and bases which are relatively polarizable **soft** and those which are difficult to polarize **hard**.

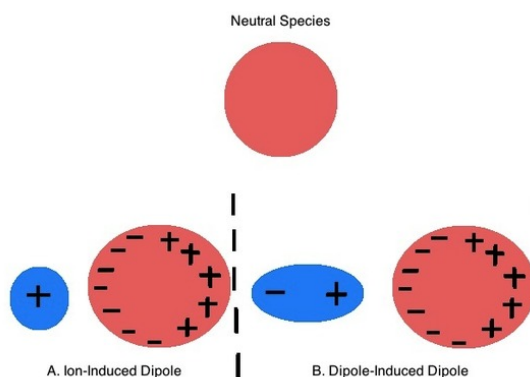


Figure 7.2.1.1: Polarizability refers to the ease with which a substance's electron cloud may be distorted under the action of an electric field. An fragment's polarizability determines the degree to which its electron cloud is distorted by A.) an Ion and B.) a polar molecule to induce a dipole moment. The figure is taken from (and the caption expanded from) Cox, Kelly and Dana Reusser "Polarizability" in

[https://chem.libretexts.org/Bookshelves/Physical\\_and\\_Theoretical\\_Chemistry\\_Textbook\\_Maps/Supplemental\\_Modules\\_\(Physical\\_and\\_Theoretical\\_Chemistry\)/Physical\\_Properties\\_of\\_Matter/Atomic\\_and\\_Molecular\\_Properties/Intermolecular\\_Forces/Specific\\_I](https://chem.libretexts.org/Bookshelves/Physical_and_Theoretical_Chemistry_Textbook_Maps/Supplemental_Modules_(Physical_and_Theoretical_Chemistry)/Physical_Properties_of_Matter/Atomic_and_Molecular_Properties/Intermolecular_Forces/Specific_Interactions/Polarizability)  
[nteractions/Polarizability](https://chem.libretexts.org/Bookshelves/Physical_and_Theoretical_Chemistry_Textbook_Maps/Supplemental_Modules_(Physical_and_Theoretical_Chemistry)/Physical_Properties_of_Matter/Atomic_and_Molecular_Properties/Intermolecular_Forces/Specific_I)

## Recognizing Hard and Soft Acids and Bases

**Hard acids and bases** come in two varieties:

1. hard acid and base sites which possess few valence electrons and for which polarization therefore involves distorting core electrons, which are difficult to distort because they are close to the nucleus and experience a high nuclear charge. The most common examples of such substances are Lewis acids hard acids towards the left of the periodic table.
2. hard acids and base sites with a high charge density (highly charged relative to size) and/or which are electron deficient. In these cases polarization involves distorting electrons that already experience strong unshielded electrostatic interactions.

**Soft acids and bases** also come in two varieties

1. soft acids and bases which possess many valence electrons and so are more readily polarized. In consequence, all other things being equal, soft acids and bases are more likely to be found towards the middle or right of the periodic table.
2. soft acids and bases with little charge density and/or which are relatively electron rich.

Note that the hard-soft classification should not be thought of as if all hard acids and bases are equally hard and all soft acids and bases equally soft. There is a graduation in hardness and softness and a number of intermediate acids and bases which do not fit neatly in either category. With this caveat in mind, representative **hard, soft, and borderline acids** are given below. Notice how they illustrate the trends just outlined.



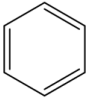
### Selected Hard Bases (Class a)

Nitrogen bases	Oxygen bases	small halides
$\text{NH}_2^-$	$\text{OH}^-$	$\text{CO}_3^{2-}$
$\text{NH}_3$	$\text{H}_2\text{O}$	$\text{RCO}_2^-$
$\text{RNH}_2$	$\text{ROH}$	$\text{NO}_3^-$
$\text{NH}_2\text{NH}_2$	$\text{ROR}$	$\text{PO}_4^{3-}$
		$\text{SO}_4^{2-}$

### Selected Borderline Bases

electron-poor Nitrogen bases	low oxidation state element oxyanions	intermediate halides
$\text{N}_3^-$		
$\text{NO}_2^-$	$\text{NO}_2^-$	
$\text{SCN}^-$	$\text{SO}_3^{2-}$	$\text{Br}^-$
$\text{N}_2$		

### Selected Soft Bases (Class b)

Carbon bases	P and As bases	Sulfur bases	large halides & pseudohalides
$\text{R}^-$	$\text{PR}_3$	$\text{RS}^-$	$\text{H}^-$
$\text{CO}$	$\text{P(OR)}_3$	$\text{RSH}$	$\text{I}^-$
$\text{CN}^-$	$\text{AsR}_3$	$\text{RSR}$	
$\text{RNC}$		$\text{SCN}^-$	
$\text{R}_2\text{C}=\text{CR}_2$ (alkenes)			
			

(electron-rich aromatics)

## Qualitative Estimation of the Relative Hardness and Softness of Lewis Acids and Bases

As can be seen from the examples above, **hard acids are relatively electron-poor and hard bases electron-rich** since they have comparatively

- small frontier orbitals, reflective of their relatively small atom/ion/fragment sizes
- high (for acids) or low (for bases) oxidation states on the base atom, reflected in a large positive formal charge (for acids) or negative formal charge (for bases)
- low polarizability, due to loss or gain of substantial numbers of electrons, or the localization of
  - positive charge on an electropositive element or an atom bearing electron-withdrawing substituents
  - negative charge on an electronegative element or an atom bearing electron-donating substituents

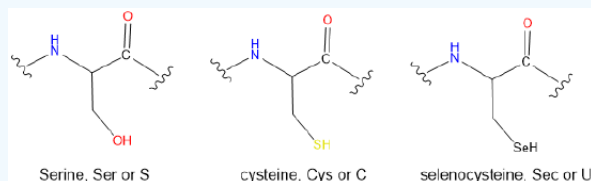
In contrast to hard acids and bases **soft acids are relatively electron-rich and soft bases larger and more electron poor** since they have comparatively

- large frontier orbitals, reflective of their relatively large atom/ion/fragment sizes
- low oxidation states, often resulting in small or nonexistent atomic charges
- high polarizability, as might be expected of species in which electron-electron repulsions are lower and electrons are spread over a large volume. Sometimes this is indicated by
  - positive charge on an electronegative element or an atom bearing electron-donating substituents
  - negative charge on an electropositive element or an atom bearing electron-withdrawing substituents

### ? Exercise 7.2.1.1

Rank the acid or bases in each set in increasing order of expected hardness?

- $\text{Cr}^{2+}$  and  $\text{Cr}^{3+}$
- $\text{H}^+$ ,  $\text{Cs}^+$ , and  $\text{Tl}^+$
- $\text{SCN}^-$  (acting as a base at N) and  $\text{SCN}^-$  (acting as a base at S)
- $\text{AlF}_3$ ,  $\text{AlH}_3$ ,  $\text{AlMe}_3$
- The side chains of the following proteinogenic amino acids



### Answer

- $\text{Cr}^{2+} < \text{Cr}^{3+}$  All other things being equal, hardness increases with oxidation state.
- $\text{Tl}^+ < \text{Cs}^+ < \text{H}^+$  The order reflects  $\text{Cs}^+$  and  $\text{Tl}^+$ 's larger size relative to  $\text{H}^+$  (which doesn't possess any electrons that can be polarized anyway) and that  $\text{Tl}^+$  still possesses two valence electrons while  $\text{Cs}^+$  possesses none.
- $\text{SCN}^-$  (acting as a base at S)  $<$   $\text{SCN}^-$  (acting as a base at N) The order reflects that N is more electronegative than S and possesses a more negative formal charge of -1.
 

Formal charge    0    0    -1
- $\text{AlH}_3 < \text{AlMe}_3$ ,  $\text{AlF}_3$  The hardness increases as the substituents on the Lewis acid Al center become less electron donating and more electron withdrawing (and, incidentally, harder bases) as their electronegativity increases in the order  $\text{H}^- < \text{CH}_3^- < \text{F}^-$ . Note that the order of electron donating ability for  $\text{H}^-$  and  $\text{CH}_3^-$  is the opposite observed for carbocations, for which hyperconjugation plays a larger role.
- $\text{Sec} < \text{Cys} < \text{Ser}$  The hardness increases as the electronegativity of the Lewis base chalcogen increases on going from a selenol to a thiol to an alcohol.

### References

- Ahrland, S.; Chatt, J.; Davies, N. R., The relative affinities of ligand atoms for acceptor molecules and ions. Quarterly Reviews, Chemical Society 1958, 12 (3), 265-276.
- Pearson, R. G., Hard and Soft Acids and Bases. Journal of the American Chemical Society 1963, 85 (22), 3533-3539.
- Fleming, I., Molecular orbitals and organic chemical reactions. Reference ed.; Wiley: Hoboken, N.J., 2010.

### Contributors and Attributions

Stephen M. Contakes (Westmont College)

7.2.1: Hard and Soft Acids and Bases is shared under a CC BY-NC-SA 4.0 license and was authored, remixed, and/or curated by LibreTexts.

- 6.6: Hard and Soft Acids and Bases by Stephen M. Contakes has no license indicated.
- 6.4: Hard and Soft Acids and Bases is licensed CC BY-NC-SA 4.0.
- 6.6.2: Hard-Hard and Soft-Soft preferences may be explained and quantified in terms of electrostatic and covalent and electronic stabilization on the stability of Lewis acid-base adducts by Stephen M. Contakes is licensed CC BY-NC 4.0.

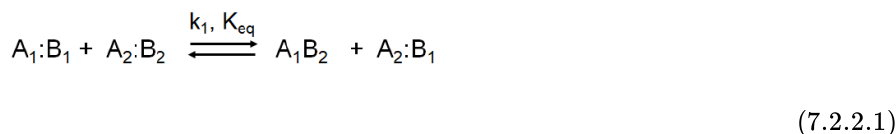
## 7.2.2: Applications of Hard Soft Acid Base Theory

The Hard-Soft acid-base principle (HSAB Principle) explains patterns in Lewis acid-base reactivity in terms of a *like reacts with like preference*. Both thermodynamically and kinetically hard acids prefer hard bases and soft acids soft bases. Specifically,

- Thermodynamically, hard acids form stronger acid-base complexes with hard bases while soft acids form stronger complexes with soft bases.
- Kinetically, hard acids/electrophiles react more quickly with hard bases/nucleophiles while soft acids/electrophiles react more quickly with soft bases/neucleophiles

Applications of the HSAB principle include

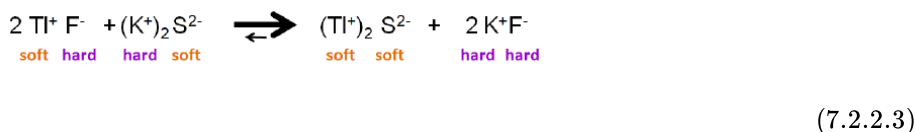
1. Predicting the equilibrium or speed of *Lewis acid-base metathesis and displacement reactions*. In a Lewis acid-base *metathesis reaction* the acids and bases swap partners



For example, the equilibrium position of the metathesis reaction between TlF and K<sub>2</sub>S favors the products:



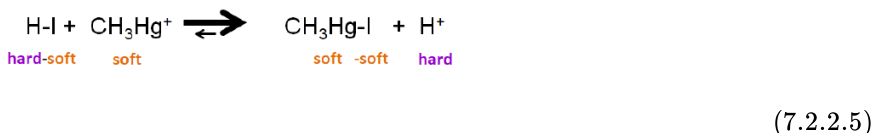
consistent with the HSAB's hard-hard and soft-soft preference.



The HSAB principle also allows for prediction of the position of displacement reactions, in which a Lewis acid or base forms an adduct using a base or acid from an existing Lewis acid-base complex. In these reactions, the displacement of acid or base from the reactant complex to may be thought of as a sort of metathesis reaction, one in which in the unbound acid or base switches places with one in the complex. For example, the reaction between HI and methylmercury cation

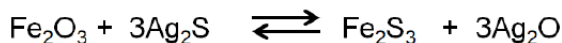


involves displacement of an iodide from HI to give CH<sub>3</sub>HgI. The position of the equilibrium favors CH<sub>3</sub>HgI since both CH<sub>3</sub>Hg<sup>+</sup> and I<sup>-</sup> are both soft, while H<sup>+</sup> is a hard acid.



### ? Exercise 7.2.2.2

Predict the position of equilibrium for the following reaction.



#### Answer

The equilibrium will favor the reactants ( $K < 1$ ) since the hard-hard and soft-soft interactions in the reactants are more stable than the hard-soft interactions in the products.





### ? Exercise 7.2.2.3

Predict whether K for the following equilibria will be  $\ll 1$ ,  $\sim 1$ , or  $\gg 1$ .

- $2\text{HF} + (\text{CH}_3\text{Hg})_2\text{S} \rightleftharpoons 2\text{CH}_3\text{HgF} + \text{H}_2\text{S}$
- $\text{Ag}(\text{NH}_3)_2^+ + 2\text{PH}_3 \rightleftharpoons \text{Ag}(\text{PH}_3)_2^+ + 2\text{NH}_3$
- $\text{Ag}(\text{PH}_3)_2^+ + 2\text{H}_3\text{B}-\text{SH}_2 \rightleftharpoons 2\text{H}_3\text{B}-\text{PH}_3 + \text{Ag}(\text{SH}_2)_2^+$
- $\text{H}_3\text{B}-\text{NH}_3 + \text{F}_3\text{B}-\text{SH}_2 \rightleftharpoons \text{H}_3\text{B}-\text{SH}_2 + \text{F}_3\text{B}-\text{NH}_3$

### Answer

- $K \ll 1$  since the reactant adducts are hard-hard and soft-soft while the products involve hard-soft interactions
- $K \gg 1$  since the reactant complex, diamine silver(I) is a complex of a hard base,  $\text{NH}_3$ , with the soft acid,  $\text{Ag}^+$ , while the product is a complex of the same soft acid with the soft base phosphine.
- $K \sim 1$  since all the adducts amongst the reactants and products involve soft acids and bases
- $K \gg 1$  since  $\text{BH}_3$  is a softer acid than  $\text{BF}_3$  so it will form a stronger complex with the softer base  $\text{H}_2\text{S}$  while the harder  $\text{BF}_3$  forms a stronger complex with the harder base  $\text{NH}_3$ .

2. Predicting the relative strengths of a given set of *Lewis acids or bases towards a particular substrate*. Consider, for example, the relative strengths of a  $\text{BH}_3$ ,  $\text{BMe}_3$ , and  $\text{BF}_3$  towards group 15 hydrides like  $\text{NH}_3$ ,  $\text{PH}_3$ , and  $\text{AsH}_3$ . Of the boranes listed, the hardest acid  $\text{BF}_3$  is the strongest acid towards the hard base  $\text{NH}_3$  while  $\text{BH}_3$  is the strongest towards  $\text{AsH}_3$ .<sup>†</sup>

### ? Exercise 7.2.2.4

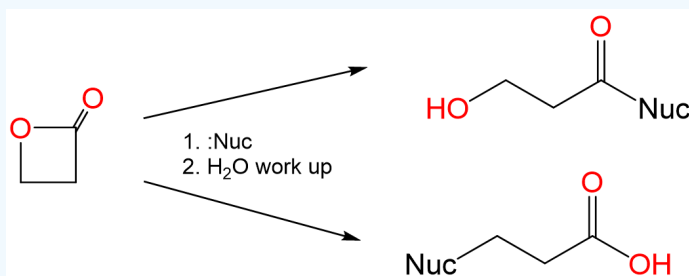
Which acid will form the most stable complex with CO -  $\text{BH}_3$ ,  $\text{BF}_3$ , or  $\text{BMe}_3$ ?

### Answer

$\text{BH}_3$ . Since CO forms complexes primarily through its carbon lone pair it is a soft base and so will form the strongest complex with the softest Lewis acid.

### ? Exercise 7.2.2.5

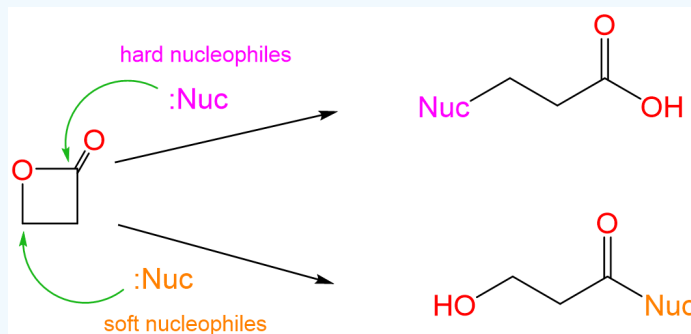
When lactones react with nucleophiles they can undergo ring opening reactions to give either an alcohol or carboxylic acid, as shown for propiolactone below:



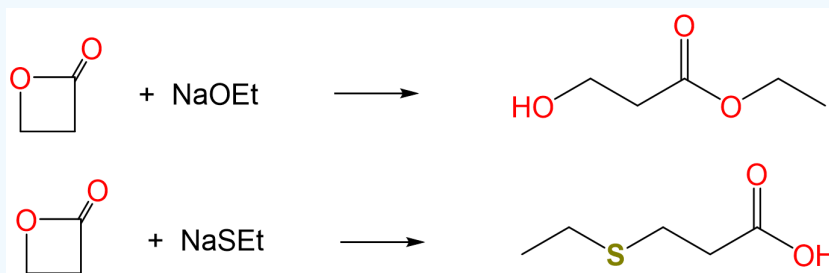
In the reaction above, sterically unhindered alkoxides give one product and sterically unhindered thioalkoxides the other. Explain why this is the case and predict the products of the reaction between propiolactone and the sodium salts of ethoxide and thioethoxide.

## Answer

The two reaction products correspond to nucleophilic attack at the lactones two electrophilic carbon centers. Specifically, the acid is produced by attack at the softer  $C^I$  center of the  $CH_2$  directly attached to the ester oxygen and the alcohol by nucleophilic attack at the harder  $C^{III}$  center of the ester carbonyl.



Consequently, it is reasonable to expect that the harder base ethoxide will nucleophilically attack the harder carbonyl carbon while the softer thioethoxide will attack the softer methylene carbon.



## Notes

\* Despite the fruitfulness of this observation, in general it is important to reduce the potential for observer bias by checking observations like these against compounds reported in the chemical literature and databases like the Inorganic Crystal Structure and Cambridge Crystallographic Databases.

\*\* These are very soluble in water, to the point where some solutions are perhaps better described as solutions of water in the halide.

† This can be predicted based on the relative hardness of  $BF_3$ ,  $BR_3$ , and  $BH_3$  in the list of hard and soft acids. However, for those of you who may be confused as to why H is considered a better electron donor for the purposes of softening a Lewis acid center while alkyl groups are better electron donors for the purposes of stabilizing carbocations in organic chemistry, the dominant effect is the lower electronegativity of H relative to carbon (in  $CH_3$ ). The effect of electron donation due to hyperconjugation isn't as great for thermodynamically stable bases like  $BX_3/BR_3$ .

## References

1. Ahrland, S.; Chatt, J.; Davies, N. R., The relative affinities of ligand atoms for acceptor molecules and ions. Quarterly Reviews, Chemical Society 1958, 12 (3), 265-276.
2. Pearson, R. G., Hard and Soft Acids and Bases. Journal of the American Chemical Society 1963, 85 (22), 3533-3539.
3. Fleming, I., Molecular orbitals and organic chemical reactions. Reference ed.; Wiley: Hoboken, N.J., 2010.

## Contributors and Attributions

Stephen M. Contakes (Westmont College)

7.2.2: Applications of Hard Soft Acid Base Theory is shared under a CC BY-NC-SA 4.0 license and was authored, remixed, and/or curated by LibreTexts.

- [6.6.2: Hard-Hard and Soft-Soft preferences may be explained and quantified in terms of electrostatic and covalent and electronic stabilization on the stability of Lewis acid-base adducts](#) by Stephen M. Contakes is licensed [CC BY-NC 4.0](#).
- [6.4: Hard and Soft Acids and Bases](#) is licensed [CC BY-NC-SA 4.0](#).
- [6.6: Hard and Soft Acids and Bases](#) by Stephen M. Contakes has no license indicated.

### 7.2.3: Theoretical Interpretation of HSAB Theory

The Theoretical Interpretation of the Hard Soft Acid-Base Principle is that hard-hard preferences reflect superior electrostatic stabilization while soft-soft preferences reflect superior covalent stabilization. The hard-hard and soft-soft preferences in Lewis acid-base interactions reflect that

- The lone pair of a hard base is strongly stabilized electrostatically by a hard acid
- The lone pair of a soft base is strongly stabilized by forming a covalent bond with a soft acid
- The lone pair of a hard or soft base is comparatively weakly stabilized by an acid opposite to it in hardness or softness since the overall electrostatic and covalent stabilization of the adduct is comparatively weak.

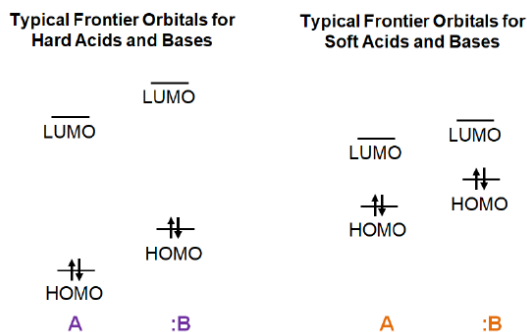
To see why this is the case it is helpful to divide the contributions to the interaction energy between an acid and a base as follows:

$$\text{Interaction Energy} = \underbrace{\text{Electrostatic attractions and repulsions of partial atomic charges}}_{\text{Ionic term}} + \underbrace{\text{Interactions between filled orbitals on one fragment and unfilled orbitals on the other}}_{\text{Covalent term}} + \underbrace{\text{Electrostatic repulsions between filled orbitals on the two fragments}}_{\text{Steric term}}$$

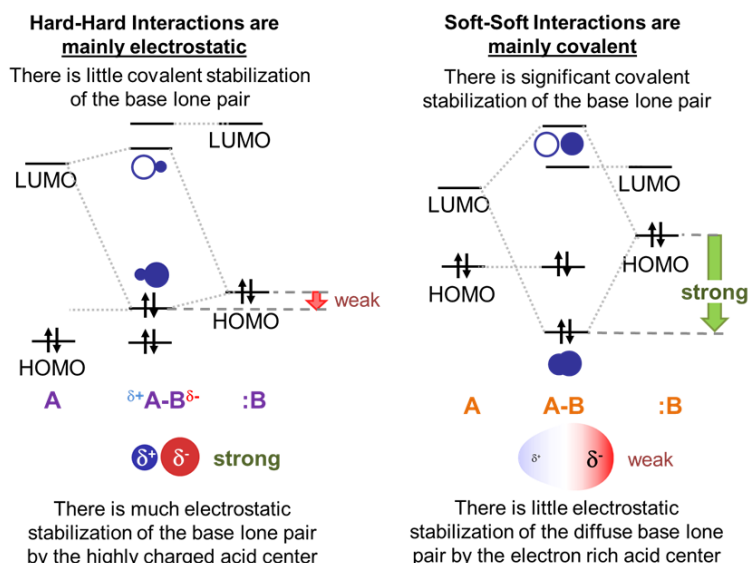
(7.2.3.1)

Of the three contributions to the interaction energy, only the ionic and covalent terms directly relate to the hardness of the interacting acid and base. One approach to thinking about how hardness influences the ionic and covalent contributions is to consider the frontier orbitals involved in the acid-base interaction. This is sometimes done through the use of the Salem-Klopman equation,<sup>1,\*</sup> although in the treatment which follows a more qualitative approach will be employed.

Both hard acids and bases will have comparatively low energy HOMO levels and high energy LUMO levels, with a correspondingly high HOMO-LUMO gap. In contrast, soft acids and bases will have comparatively high-energy HOMO levels and low-energy LUMO levels, giving a comparatively smaller HOMO-LUMO gap.



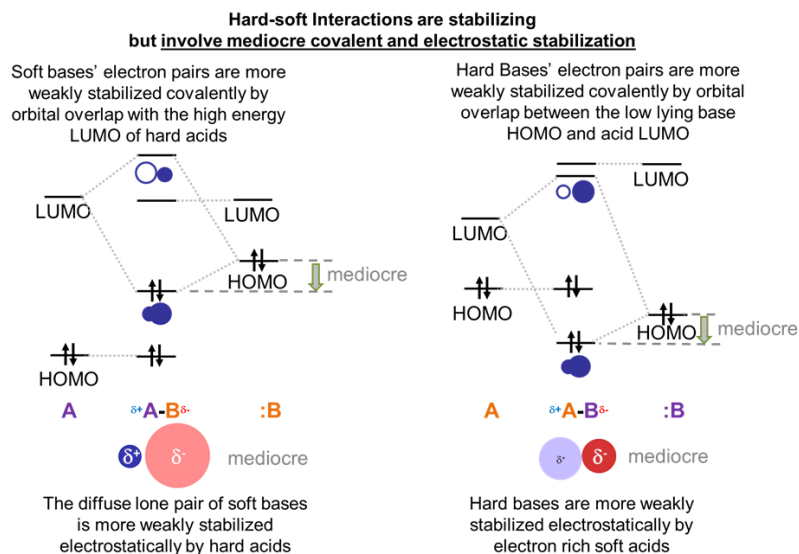
Given this, consider the frontier orbital interactions involved in the formation of an acid-base complex for the possible cases, as illustrated schematically below.



The large gap in energy between hard bases' highly stabilized HOMO lone pairs and the high energy LUMO of hard acids ensures that in **hard acid-hard base adducts the dominant stabilizing interaction will involve electrostatic attraction between the base lone pair and the electropositive Lewis acid center**. Fortunately, since the electron clouds in hard bases are relatively dense and electron rich while hard Lewis acids are highly charged and small these electrostatic interactions are strong.

In contrast, in **soft acid-soft base adducts the dominant stabilizing interaction will be covalent**. This is because the small gap in energy between a soft base HOMO and soft acid LUMO enables the formation of a well-stabilized bonding orbital with significant electron density between the acid and base.

The orbital interactions between hard acids and soft bases and soft acids and hard bases are intermediate between the hard acid-hard base and soft acid-soft base cases.



This means that the adducts are stable relative to free acid and base – just not as well stabilized as in the hard acid and hard base case. In the case of hard acids and soft bases the hard acids are less able to stabilize the soft bases' relatively diffuse electron pair electrostatically and there isn't as much covalent stabilization as in adducts of soft acids and bases due to hard acid's high energy.

## Notes

†† For more on the Salem-Klopman equation see Fleming, I., Molecular orbitals and organic chemical reactions. Reference ed.; Wiley: Hoboken, N.J., 2010; pp. 138-143.

## References

1. Ahrland, S.; Chatt, J.; Davies, N. R., The relative affinities of ligand atoms for acceptor molecules and ions. Quarterly Reviews, Chemical Society 1958, 12 (3), 265-276.
2. Pearson, R. G., Hard and Soft Acids and Bases. Journal of the American Chemical Society 1963, 85 (22), 3533-3539.
3. Fleming, I., Molecular orbitals and organic chemical reactions. Reference ed.; Wiley: Hoboken, N.J., 2010.

## Contributors and Attributions

Stephen M. Contakes (Westmont College)

---

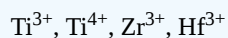
7.2.3: Theoretical Interpretation of HSAB Theory is shared under a [CC BY-NC-SA 4.0](#) license and was authored, remixed, and/or curated by LibreTexts.

- [6.4: Hard and Soft Acids and Bases](#) is licensed [CC BY-NC-SA 4.0](#).
- [6.6.2: Hard-Hard and Soft-Soft preferences may be explained and quantified in terms of electrostatic and covalent and electronic stabilization on the stability of Lewis acid-base adducts](#) by Stephen M. Contakes is licensed [CC BY-NC 4.0](#).
- [6.6: Hard and Soft Acids and Bases](#) by Stephen M. Contakes has no license indicated.

## 7.3: Unit 7 Practice Problems

### Exercise 1

Decide if the following species are acids or bases according to Lewis theory. Order them with respect to their hardness and polarizability.



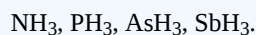
#### Answer

Hardness:  $\text{Ti}^{4+} > \text{Ti}^{3+} > \text{Zr}^{3+} > \text{Hf}^{3+}$

Polarizability:  $\text{Hf}^{3+} > \text{Zr}^{3+} > \text{Ti}^{3+} > \text{Ti}^{4+}$

### Exercise 2

Decide if the following species are acids or bases according to Lewis theory. Order them with respect to their hardness and polarizability.



#### Answer

Bases.

Hardness:  $\text{NH}_3 > \text{PH}_3 > \text{AsH}_3 > \text{SbH}_3$

Polarizability:  $\text{SbH}_3 > \text{AsH}_3 > \text{PH}_3 > \text{NH}_3$

### Exercise 3

CsI is much less soluble in water than CsF. Why?

#### Answer

Cs-F hard-hard interactions are stronger than Cs-I hard-soft interactions. Nonetheless, CsI is less soluble because of the small solvation enthalpy for  $\text{I}^-$  (weak hard-soft interaction between water and  $\text{I}^-$ ).

### Exercise 4

Order the following species with regard to their expected solubility in water: ZnS, CdS, HgS.

#### Answer



### Exercise 5

$\text{AlF}_3$  is insoluble in liquid HF but dissolves when NaF is present. When  $\text{BF}_3$  is added to the solution,  $\text{AlF}_3$  precipitates. Explain.

#### Answer

Hard-Hard interactions between H and F in H-F stronger than Hard-Hard interactions between  $\text{Al}^{3+}$  and  $\text{F}^-$ . Consequence: no reaction occurs (no formation of  $\text{AlF}_4^-$ ).

Hard-Hard interactions between  $\text{Al}^{3+}$  and  $\text{F}^-$  are stronger than hard-hard interactions between  $\text{Na}^+$  and  $\text{F}^-$ . Consequence:  $\text{AlF}_3$  dissolves to form  $\text{AlF}_4^-$ .

$\text{AlF}_3$  precipitates upon addition of  $\text{BF}_3$  because Al-F hard-hard interactions are weaker than B-F hard-hard interactions ( $\text{B}^{3+}$  is harder than  $\text{Al}^{3+}$ ).  $\text{AlF}_4^-(\text{aq}) + \text{BF}_3(\text{aq}) \rightarrow \text{BF}_4^-(\text{aq}) + \text{AlF}_3(\text{s})$ .

**Exercise 6**

Why were most of the metals used in early prehistory soft metals (in HSAB terminology)?

**Answer**

Because oxygen is the most abundant element in the earth crust. Thus most hard metals have formed oxides with oxygen. Soft metals do not easily combine with oxygen to form oxides. Therefore, they can be found more often in elemental form in nature. Because of that they have been used more often.

**Exercise 7**

Which of the following ions is the softest according to HSAB theory:

- a) oxide ( $O^{2-}$ )
- b) peroxide ( $O_2^{2-}$ )
- c) ozonide ( $O_3^-$ )

**Answer**

- c) ozonide ( $O_3^-$ )

**Exercise 8**

The oxidation of barium with oxygen gas yields barium peroxide while the oxidation of strontium with oxygen gas yields strontium oxide. Explain this from the standpoint of the HSAB theory.

**Answer**

Barium is softer, so it has a greater tendency to combine with the peroxide ion which is relatively soft compared to the oxide ion.

**Exercise 9**

A molecule with an electron pair in an antibonding HOMO will most likely undergo a reaction in which

- a) this molecule will get oxidized
- b) this molecule will be reduced
- c) this molecule will act as a donor in a Lewis acid base reaction.
- d) this molecule will act as an acceptor in a Lewis acid base reaction.

**Answer**

- a) this molecule will get oxidized

**Exercise 10**

When a dative bond is polarized toward the acceptor this indicates that

- a) the HOMO energy of the donor is higher than the LUMO energy of the acceptor.
- b) the HOMO energy of the donor is lower than the LUMO energy of the acceptor.
- c) the HOMO energy of the donor is equal to the LUMO energy of the acceptor.

**Answer**

- a) the HOMO energy of the donor is higher than the LUMO energy of the acceptor.



---

Dr. Kai Landskron ([Lehigh University](#)). If you like this textbook, please consider to make a donation to support the author's research at Lehigh University: [Click Here to Donate](#).

---

This page titled [7.3: Unit 7 Practice Problems](#) is shared under a [CC BY 4.0](#) license and was authored, remixed, and/or curated by [Kai Landskron](#).

- [Homework Problems Chapter 4](#) by [Kai Landskron](#) is licensed [CC BY 4.0](#).

## CHAPTER OVERVIEW

### Unit 8: Electronic Structure of Coordination Complexes

Coordination compounds are important to all areas of chemistry, engineering, the life and environmental sciences, and beyond. In the synthetic laboratory catalytic amounts of coordination compounds enable organic chemists to synthesize new compounds selectively and in high yield under mild conditions. Applied industrially, coordination compound catalysts serve as vital catalysts that facilitate the conversion of raw petrochemical or bio-derived feedstocks into useful industrial and consumer products. Without them life as we know it would be impossible, as many biochemical systems are coordination complexes. Examples include the hemoglobin that transports oxygen around our bodies and the myoglobin that stores it, the photosystems that harvest light and use light energy in photosynthesis, the constituents of the respiratory chain, and many of the enzymes involved in the expression and transmission of genetic information. In studying coordination chemistry you are about to take your first steps into a vast and exciting world.

#### 8.1: Introduction to Coordination Complexes

##### 8.1.1: What are Coordination Complexes?

##### 8.1.2: History of Coordination Complexes

##### 8.1.3: Nomenclature and Ligands

##### 8.1.4: Coordination Numbers and Structures

##### 8.1.5: Isomerism

#### 8.2: Crystal Field Theory

##### 8.2.1: Crystal Field Theory

##### 8.2.2: Crystal Field Stabilization Energy

##### 8.2.3: Non-octahedral Complexes

#### 8.3: Crystal Field Theory and Magnetism

##### 8.3.1: Jahn-Teller Distortions

##### 8.3.2: Magnetism

##### 8.3.3: Magnetic Moments of Transition Metals

##### 8.3.4: Ferro-, Ferri- and Antiferromagnetism

#### 8.4: Ligand Field Theory

##### 8.4.1: Ligand Field Theory

##### 8.4.2: The Spectrochemical Series

##### 8.4.3: Factors That Affect Ligand Field Splitting

##### 8.4.4: Octahedral vs. Tetrahedral Geometries

#### 8.5: Absorption Spectroscopy of Coordination Complexes

##### 8.5.1: Absorption of Light

##### 8.5.2: Colors of Coordination Complexes

##### 8.5.3: Charge-Transfer Spectra

#### 8.6: Tanabe Sugano Diagrams

##### 8.6.1: Tanabe-Sugano Diagrams

##### 8.6.2: Selection Rules

##### 8.6.3: Applications of Tanabe-Sugano Diagrams

##### 8.6.4: Tetrahedral Complexes

---

Unit 8: Electronic Structure of Coordination Complexes is shared under a [CC BY 4.0](#) license and was authored, remixed, and/or curated by Stephen M. Contakes.

## 8.1: Introduction to Coordination Complexes

---

Learning objectives for this unit are to:

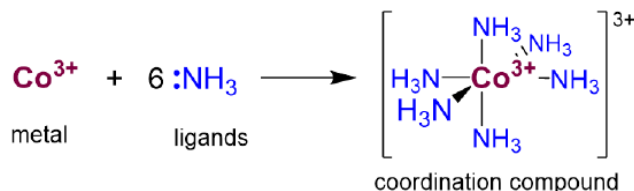
- Identify, name, and draw common coordination compound ligands, including chelates
  - Determine the charge on a metal or ligand in a chemical structure
  - Use a chemical name to draw a chemical structure and vice versa
  - Recognize, name, and draw structural, stereo, and optical isomers of coordination complexes
- 

8.1: Introduction to Coordination Complexes is shared under a [not declared](#) license and was authored, remixed, and/or curated by LibreTexts.

## 8.1.1: What are Coordination Complexes?

### What is a coordination compound?

**Coordination compounds** consist of one or more **metals** bound to one or more Lewis base **ligands**. For example, hexamineruthenium (3+) ion is a coordination complex in which six ammonia ligands coordinate a  $\text{Co}^{3+}$  ion, as shown in Scheme 8.1.1.1.



Scheme 8.1.1.1: Formation of hexamineruthenium(3+) ion from  $\text{Co}^{3+}$  and  $\text{NH}_3$ . (CC BY 4.0; Stephen Contakes)

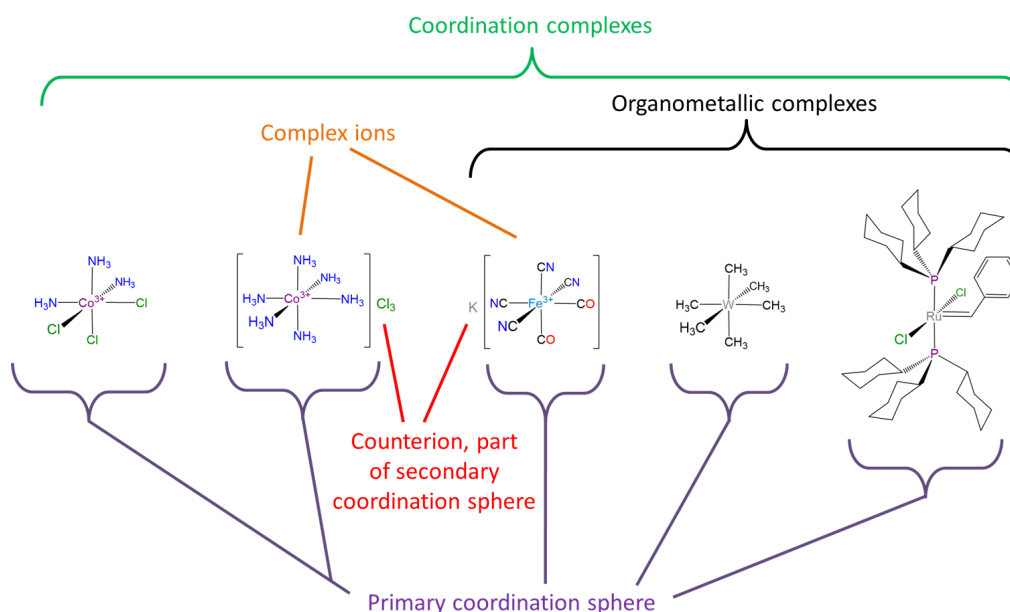
Such complexes are called coordination complexes because the ligand-metal bond may be thought of as a **coordinate covalent bond** in which both of the bonding electrons come from the ligand, which is then said to **coordinate** the metal. This coordinate covalent model is a very useful formalism for understanding the basic features of coordination chemistry, although it does not always accurately reflect the actual details of the bonding in every coordination complex. Nevertheless, even in those cases where the simple coordinate covalent bond model breaks down, the coordinate covalent bond concept supplies the language sophisticated models employ to describe the more complex bonding involved.

### Additional important terms

Some of the common widely used terms that follow from the coordinate covalent model of bonding in coordination complexes include:

- Coordination compounds are also called **coordination complexes**, **metal complexes**, or just **complexes**. The term **complex** refers to coordination compounds' composite nature, in that they may be thought of as comprising multiple ligand and metal ion parts that can be restored by breaking the coordinate covalent bonds holding the complex together. This is in contrast to inorganic or organic molecules which are more commonly thought about as whole molecules held together by the sharing of electrons contributed by all the atoms.
- Coordination complexes that are ions are called **complex ions**.
- Ligands bound to the coordination complex are said to reside in the **primary** or **inner coordination sphere**. These bound ligands are not readily exchangeable, in contrast to nearby counterions and solvent molecules, which are said to reside in the **secondary** or **outer coordination sphere**.
- The portion of the complex contributing the electron pairs is said to be the **donor** and the portion which receives them the **acceptor**. In conventional coordination compounds the ligand is the donor and the metal the acceptor. In these cases it would be equally convenient to refer to the ligand donor as the Lewis base and the metal acceptor as the Lewis acid. However, in more complex bonding scenarios there may be multiple electron pair donation and acceptance interactions taking place between each pair of atoms and donor-acceptor language will be more convenient.
- The number of ligand sites donating lone pairs to the central atom is referred to as the **coordination number**. For most complexes this will just be equal to the number of ligand atoms bound to the metal. In simple complexes it is just equal to the number of ligands. For instance, the cobalt in Scheme 8.1.1.1 has a coordination number of six.
- Although technically compounds with metal-carbon bonds are coordination complexes, the term coordination complex is sometimes used to refer to complexes which do not possess metal-carbon bonds in their primary coordination sphere. Complexes which possess metal-carbon bonds are called **organometallic compounds** instead. The use of the terms organometallic and coordination to distinguish organometallic compounds from other types of coordination compounds is often convenient since many organometallic ligands engage in more than simple  $\sigma$  donor-acceptor coordinate covalent bond formation with the metal center. However, this is true of some wholly inorganic ligands too, so it should always be kept in mind that organometallic compounds are just a type of coordination compound and that inorganic ligands can in principle be tuned to interact with a metal center in much the same way an organic ligand does.

A summary of some of the concepts and terms used to describe coordination compounds is given in Scheme 8.1.1.2



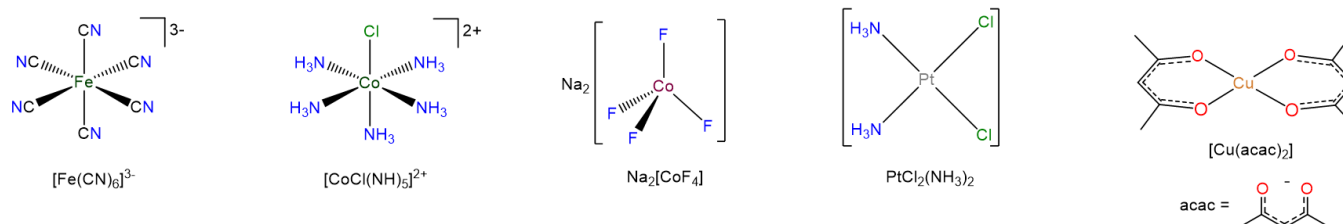
Scheme 8.1.1.2: Some terms used to describe coordination compounds. (CC BY 4.0; Stephen Contakes)

## The formulae of coordination complexes

The way the formulae of coordination complexes are written reflects the fact that it is often convenient to think of coordination compounds as a composite of metals and ligands. When writing the formula of a complex

- the atoms of a ligand are not added to those of the rest of the compound. Instead, the ligand atoms are kept together, if necessary by enclosing the ligand formula in parentheses or giving an abbreviation for the ligand.
- For complex ions the metal and ligands are enclosed in square brackets. Sometimes this is also done for neutral coordination compounds as well. In either case the brackets enclose those parts of the compound which comprise the primary coordination sphere; anything else is in the secondary coordination sphere outside.

A careful perusal of the examples in Scheme 8.1.1.3 should make the important features of this system clear.



Scheme 8.1.1.3: Formulae of coordination compounds and complex ions. (CC BY 4.0; Stephen Contakes)

8.1.1: What are Coordination Complexes? is shared under a CC BY 4.0 license and was authored, remixed, and/or curated by Stephen M. Contakes.

- 9.1: Prelude to Coordination Chemistry I - Structure and Isomers by Stephen M. Contakes is licensed CC BY 4.0.

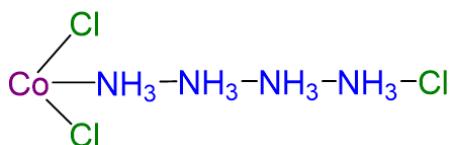
## 8.1.2: History of Coordination Complexes

### History of the Coordination Compounds

Coordination compounds have been known and used since antiquity; one of the oldest synthetic pigments is the blue pigment Egyptian blue, a copper complex of formula  $\text{CaCuSi}_4\text{O}_{10}$  used by the Egyptians since the third Millennium B.C. (in ancient China the Ba analogue, Han blue, was discovered independently). The blue color of Egyptian blue is due to interlocked  $\text{Cu}(\text{Si}_2\text{O}_7)_4$  units in which each copper is coordinated by four O atoms in a square planar arrangement. Later, in 1706, the Berlin painter Diesbach would discover another deep blue pigment, Prussian blue:  $\text{KFe}_2(\text{CN})_6$ .

Despite their long use, the chemical nature of coordination compounds was unclear for a number of reasons. For example, many compounds called “double salts” were known, such as  $\text{AlF}_3 \cdot 3 \text{KF}$ ,  $\text{Fe}(\text{CN})_2 \cdot 4 \text{KCN}$ , and  $\text{ZnCl}_2 \cdot 2 \text{CsCl}$ , which were combinations of simple salts in fixed and apparently arbitrary ratios. Why should  $\text{AlF}_3 \cdot 3 \text{KF}$  exist but not  $\text{AlF}_3 \cdot 4 \text{KF}$  or  $\text{AlF}_3 \cdot 2 \text{KF}$ ? And why should a 3:1  $\text{KF}:\text{AlF}_3$  mixture have different chemical and physical properties than either of its components? Similarly, adducts of metal salts with neutral molecules such as ammonia were also known—for example,  $\text{CoCl}_3 \cdot 6 \text{NH}_3$ , which was first prepared sometime before 1798. Like the double salts, the compositions of these adducts exhibited fixed and apparently arbitrary ratios of the components. For example,  $\text{CoCl}_3 \cdot 6 \text{NH}_3$ ,  $\text{CoCl}_3 \cdot 5 \text{NH}_3$ ,  $\text{CoCl}_3 \cdot 4 \text{NH}_3$ , and  $\text{CoCl}_3 \cdot 3 \text{NH}_3$  were all known and had very different properties, but despite all attempts, chemists could not prepare  $\text{CoCl}_3 \cdot 2 \text{NH}_3$  or  $\text{CoCl}_3 \cdot \text{NH}_3$ .

Although the chemical composition of such compounds was readily established by existing analytical methods, their chemical nature was puzzling and highly controversial. The major problem was that what we now call valence (i.e., the oxidation state) and coordination number were thought to be identical. As a result, highly implausible (to modern eyes at least) structures were proposed for such compounds. Of these the most influential was the Blomstrand-Jørgensen chain theory of bonding in coordination compounds, which predicted the “Chattanooga choo-choo” model for  $\text{CoCl}_3 \cdot 4 \text{NH}_3$  shown in Scheme 8.1.2.1



Scheme 8.1.2.1. Blomstrand-Jørgensen chain theory model of bonding in  $\text{CoCl}_3 \cdot 4 \text{NH}_3$ .

Nevertheless, this theory was not wholly illogical and, in fact, explained much of the analytical data on coordination compounds available to chemists of the time. This data included the electrical conductivity of aqueous solutions of these compounds, which was roughly proportional to the number of ions formed per mole, and the number of free chloride ions present, which could be determined by precipitating them gravimetrically as  $\text{AgCl}$ . In the case of  $\text{CoCl}_3 \cdot 4 \text{NH}_3$ , two ions and one chloride were produced when the compound was dissolved in water, which Jørgensen was able to explain using the chain structure shown above by postulating that chlorides attached to  $\text{NH}_3$  could dissociate while those attached to  $\text{Co}$  could not. The modern theory of coordination chemistry, which overthrew the chain theory, is based largely on the work of Alfred Werner (1866–1919; Nobel Prize in Chemistry in 1913). In a series of careful experiments carried out in the late 1880s and early 1890s, he examined the properties of several series of metal halide complexes with ammonia. For example, five different “adducts” of ammonia with  $\text{PtCl}_4$  were known at the time:  $\text{PtCl}_4 \cdot n \text{NH}_3$  ( $n = 2-6$ ). Some of Werner’s original data on these compounds are shown in Table 8.1.2.1. Werner’s data on  $\text{PtCl}_4 \cdot 6 \text{NH}_3$  in Table 8.1.2.1 showed that all the chloride ions were present as free chloride. In contrast,  $\text{PtCl}_4 \cdot 2 \text{NH}_3$ , was a neutral molecule that did not give free chloride ions when dissolved in water.

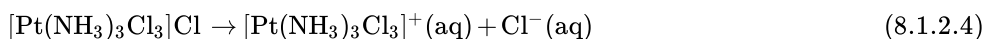
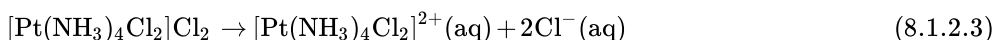
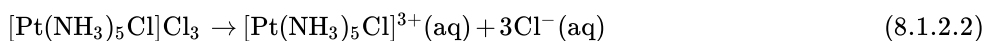
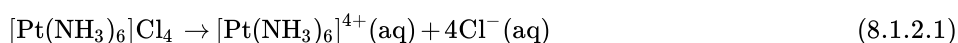
#### Alfred Werner (1866–1919)

Werner, the son of a factory worker, was born in Alsace. He developed an interest in chemistry at an early age, and he did his first independent research experiments at age 18. While doing his military service in southern Germany, he attended a series of chemistry lectures, and he subsequently received his PhD at the University of Zurich in Switzerland, where he was appointed professor of chemistry at age 29. He won the Nobel Prize in Chemistry in 1913 for his work on coordination compounds, which he performed as a graduate student and first presented at age 26. Apparently, Werner was so obsessed with solving the riddle of the structure of coordination compounds that his brain continued to work on the problem even while he was asleep. In 1891, when he was only 25, he woke up in the middle of the night and, in only a few hours, had laid the foundation for modern coordination chemistry.

Table 8.1.2.1: Werner's Data on Complexes of Ammonia with  $PtCl_4$

Complex	Conductivity ( $\text{ohm}^{-1}$ )	Number of Ions per Formula Unit	Number of $\text{Cl}^-$ Ions Precipitated by $\text{Ag}^+$
$\text{PtCl}_4 \cdot 6\text{NH}_3$	523	5	4
$\text{PtCl}_4 \cdot 5\text{NH}_3$	404	4	3
$\text{PtCl}_4 \cdot 4\text{NH}_3$	299	3	2
$\text{PtCl}_4 \cdot 3\text{NH}_3$	97	2	1
$\text{PtCl}_4 \cdot 2\text{NH}_3$	0	0	0

These data led Werner to postulate that metal ions have two different kinds of valence: (1) a primary valence (oxidation state) that corresponds to the positive charge on the metal ion and (2) a secondary valence (coordination number) that is the total number of ligands bound to the metal ion. If Pt had a primary valence of 4 and a secondary valence of 6, Werner could explain the properties of the  $\text{PtCl}_4 \cdot \text{NH}_3$  adducts by the following reactions, where the metal complex is enclosed in square brackets:

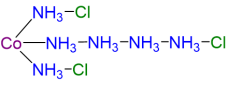
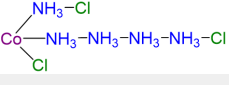
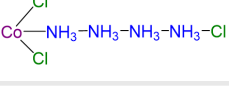
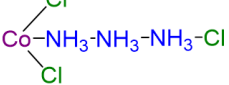


Further work showed that the two missing members of the series— $[\text{Pt}(\text{NH}_3)\text{Cl}_5]^-$  and  $[\text{PtCl}_6]^{2-}$ —could be prepared as their mono- and dipotassium salts, respectively. Similar studies established coordination numbers of 6 for  $\text{Co}^{3+}$  and  $\text{Cr}^{3+}$  and 4 for  $\text{Pt}^{2+}$  and  $\text{Pd}^{2+}$ .

### ? Exercise 8.1.2.1. The $\text{CoCl}_3 \cdot x\text{NH}_3$ series.

The series  $\text{CoCl}_3 \cdot x\text{NH}_3$  was particularly important in establishing the correctness of Werner's coordination theory over the rival chain theory. By ~1900 conductivity measurements suggested that the members of the series gave the number of ions shown in Table 8.1.2.1.

Table 8.1.2.1. The  $\text{CoCl}_3 \cdot x\text{NH}_3$  series according to coordination theory, chain theory, and experiment.

Compound	Color	Werner formulation	Blomstrand-Jørgensen chain theory formulation	Number of ions in solution
$\text{CoCl}_3 \cdot 6\text{NH}_3$	yellow	$[\text{Co}(\text{NH}_3)_6]\text{Cl}_3$		4
$\text{CoCl}_3 \cdot 5\text{NH}_3$	violet	$[\text{Co}(\text{NH}_3)_5\text{Cl}]\text{Cl}_2$		3
$\text{CoCl}_3 \cdot 4\text{NH}_3$	green	$[\text{Co}(\text{NH}_3)_4\text{Cl}_2]\text{Cl}$		2
$\text{CoCl}_3 \cdot 3\text{NH}_3$	orange	$[\text{Co}(\text{NH}_3)_4\text{Cl}_3]$		0

What does this data suggest about the relative explanatory power of Werner's coordination theory and chain theory? Explain.

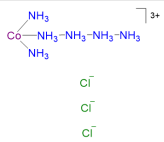
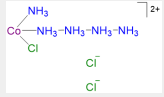
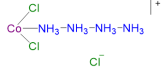
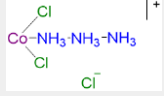
**Answer**

Remember that

- chain theory predicts that the number of ions is the number formed when the Cl atoms bound in a chain with  $\text{NH}_3$  dissociate.
- coordination theory predicts the number of ions based on the number of complex ions and their counterions.

Based on this the predictions of coordination theory and chain theory can be compared with the experimental data, as is done in Table 8.1.2.2

Table 8.1.2.2: Comparison of ions predicted for the  $\text{CoCl}_3 \cdot x\text{NH}_3$  series by coordination theory and chain theory with the number observed experimentally.

Compound	Color	Ions predicted by Werner's coordination theory	Number of ions predicted by coordination theory	Ions predicted by Blomstrand-Jørgensen chain theory	Number of ions predicted by chain theory	Observed Number of ions in solution
$\text{CoCl}_3 \cdot 6\text{NH}_3$	yellow	$[\text{Co}(\text{NH}_3)_6]^{3+}$ $\text{Cl}^-$ $\text{Cl}^-$ $\text{Cl}^-$	4		4	4
$\text{CoCl}_3 \cdot 5\text{NH}_3$	violet	$[\text{Co}(\text{NH}_3)_5\text{Cl}]^{2+}$ $\text{Cl}^-$ $\text{Cl}^-$	3		3	3
$\text{CoCl}_3 \cdot 4\text{NH}_3$	green	$[\text{Co}(\text{NH}_3)_4\text{Cl}_2]^+$ $\text{Cl}^-$	2		2	2
$\text{CoCl}_3 \cdot 3\text{NH}_3$	orange	None	0		2	0

As can be seen by comparing the number of ions predicted by coordination and chain theory in Table 8.1.2.2 coordination theory successfully explains all the observed ion counts, while chain theory fails to explain the lack of ions observed for  $\text{CoCl}_3 \cdot 3\text{NH}_3$ .

Nevertheless, as is often the case when developing theoretical models using data from real experimental investigations, these observations did not convince Jørgensen, who could point to the experimental difficulty of determining the number of ions present from solution conductivity data.

What ultimately convinced Jørgensen of the correctness of Werner's coordination model over his own chain theory was how Werner's explanation of the structure of cobalt coordination complexes using an octahedral coordination geometry explained the existence of isomers in Co complexes containing Cl and  $\text{NH}_3$  ligands. In the case of  $[\text{Co}(\text{NH}_3)_4\text{Cl}_2]\text{Cl}$  two isomers were known: one red and the other green. Because both compounds had the same chemical composition and the same number of groups of the same kind attached to the same metal, there had to be something different about the arrangement of the ligands around the metal ion. Werner's key insight was that the six ligands in  $[\text{Co}(\text{NH}_3)_4\text{Cl}_2]\text{Cl}$  had to be arranged at the vertices of an octahedron because that was the only structure consistent with the existence of two, and only two, stereoisomers (Figure 8.1.2.1). His conclusion was also corroborated by the existence of two and only two stereoisomers of the next compound in the series:  $\text{Co}(\text{NH}_3)_3\text{Cl}_3$ .



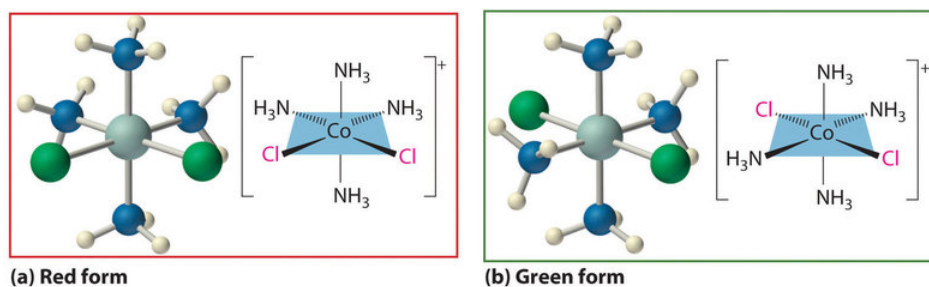


Figure 8.1.2.1. The  $[\text{Co}(\text{NH}_3)_4\text{Cl}_2]^+$  ion can have two different arrangements of the ligands, which results in different colors: if the two  $\text{Cl}^-$  ligands are next to each other (*cis*), the complex is red (a), but if they are opposite each other (*trans*), the complex is green (b).

### ✓ Example 8.1.2.1: Why did Werner propose an octahedral geometry for 6-coordinate complexes?

In Werner's time, many complexes of the general formula  $\text{MA}_4\text{B}_2$  were known, but no more than two different compounds with the same composition had been prepared for any metal. To confirm Werner's reasoning that this suggests these complexes possess an octahedral geometry, calculate the maximum number of different structures possible for six-coordinate  $\text{MA}_4\text{B}_2$  complexes with each of the three most symmetrical possible structures the ligands will form about the central metal - a hexagon, a trigonal prism, and an octahedron.

Assuming that the absence of evidence for additional compounds in this case serves as reasonable circumstantial evidence for their absence, what does the fact that no more than two forms of any  $\text{MA}_4\text{B}_2$  complex were known suggest about the three-dimensional structures of these complexes?

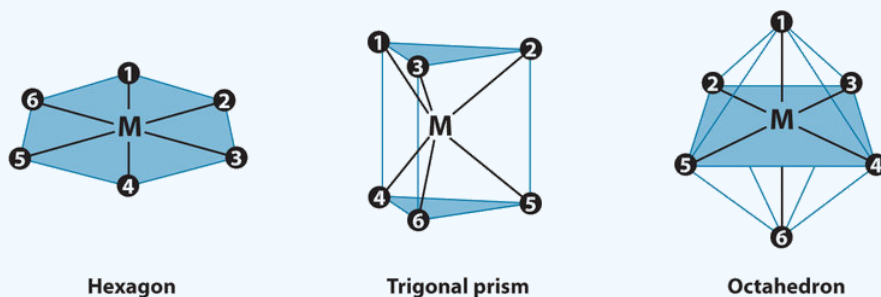
#### Solution

In this problem you are given

- the stoichiometry of the complexes,  $\text{MA}_4\text{B}_2$
- three possible coordination geometries - hexagonal, trigonal prismatic, and octahedral.

In order to calculate the number of isomers that could be present for each geometry it is best to follow a systematic approach. Since there are fewer B type ligands than A type ligands, the easiest way to do this for each geometry is to start by placing a B ligand at one vertex and then to determine how many different positions are available for the second B ligand.

The three regular six-coordinate structures are shown here, with each coordination position numbered so that we can keep track of the different arrangements of ligands. For each structure, all vertices are equivalent. We begin with a symmetrical  $\text{MA}_6$  complex and simply replace two of the A ligands in each structure to give an  $\text{MA}_4\text{B}_2$  complex:



For the hexagon, we place the first B ligand at position 1. There are now **three** possible places for the second B ligand:

- position 2 (or 6)
- position 3 (or 5)
- position 4

The (1, 2) and (1, 6) arrangements are chemically identical because the two B ligands are adjacent to each other. The (1, 3) and (1, 5) arrangements are also identical because in both cases the two B ligands are separated by an A ligand. Those of you who remember your organic chemistry might recognize that this situation is formally analogous to the *ortho*-, *meta*-, and *para*-isomerism in disubstituted benzenes.

Turning to the trigonal prism, we place the first B ligand at position 1. Again, there are three possible choices for the second B ligand:

- at position 2 or 3 on the same triangular face
- position 4 (on the other triangular face but adjacent to 1)
- position 5 or 6 (on the other triangular face but not adjacent to 1).

The (1, 2) and (1, 3) arrangements are chemically identical, as are the (1, 5) and (1, 6) arrangements.

In the octahedron, however, if we place the first B ligand at position 1, then we have only two choices for the second B ligand:

- position 2 (or 3 or 4 or 5)
- position 6.

In the latter, the two B ligands are at opposite vertices of the octahedron, with the metal lying directly between them. Although there are four possible arrangements for the former, they are chemically identical because in all cases the two B ligands are adjacent to each other.

The number of possible  $MA_4B_2$  arrangements for the three geometries is thus: hexagon, 3; trigonal prism, 3; and octahedron, 2. The fact that only two different forms were known for all  $MA_4B_2$  complexes that had been prepared suggested that the correct structure was the octahedron but did not prove it. For some reason one of the three arrangements possible for the other two structures could have been less stable or harder to prepare and had simply not yet been synthesized. When combined with analogous results for other types of complexes (e.g.,  $MA_3B_3$ ), however, the data were best explained by an octahedral structure for six-coordinate metal complexes.

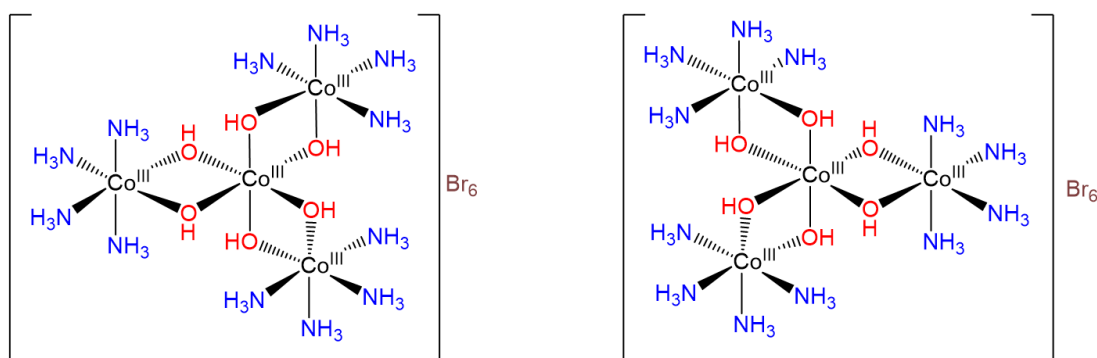
### ? Exercise 8.1.2.1

Determine the maximum number of structures that are possible for a four-coordinate  $MA_2B_2$  complex with either a square planar or a tetrahedral symmetrical structure.

#### Answer

square planar, 2; tetrahedral, 1

Even Werner's explanation of isomerism in coordination complexes in terms of octahedral and other recognized coordination geometries did not convince all chemists until he was able to resolve a racemic mixture of *d*- and *l*- $[Co\{Co(NH_3)_4(OH)_2\}_3]$  into its enantiomers, which are shown in Scheme 8.1.2.II. By doing so Werner demonstrated to chemists of his time (virtually none of whom knew group theory) that tetrahedral carbon atoms were not required for chirality;  $D_3$  octahedral complexes were also chiral.



Scheme 8.1.2.II: *d*- and *l*-enantiomers of  $[Co\{Co(NH_3)_4(OH)_2\}_3]$ , colloquially referred to as hexol. This work by Stephen Contakes is licensed under a [Creative Commons Attribution 4.0 International License](#).

8.1.2: History of Coordination Complexes is shared under a [CC BY-NC-SA 4.0](#) license and was authored, remixed, and/or curated by Stephen M. Contakes.

- 24.1: Werner's Theory of Coordination Compounds by Anonymous is licensed [CC BY-NC-SA 4.0](#).

## 8.1.3: Nomenclature and Ligands

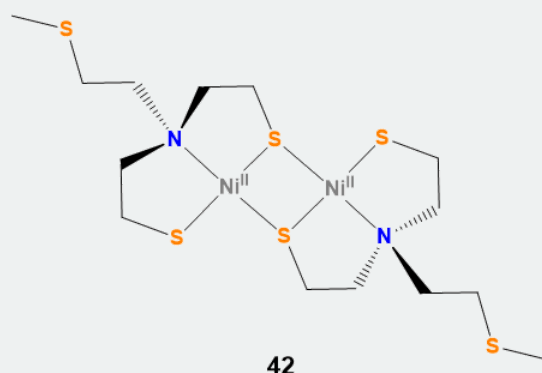
Systems of nomenclature and formulae are intended as tools, to be employed insofar as they are useful

There are well-established rules for both naming and writing the formulae of coordination compounds. The purpose of these rules is to facilitate clear and precise communication among chemists. As with all such rules, some are more burdensome than others to employ, and some serve more crucial roles in the communication process while others are more peripheral - and all are poorly used in the service of pedantic tyranny, especially when used against those who are otherwise doing good work. For this reason, you are urged to approach the rules in a spirit of generosity towards others in

- naming and writing formulas as reasonably accurately as you can so that ligands and metals are where readers expect them and thus can understand what you mean more easily.
- being gracious towards the many professional inorganic chemists who adhere loosely to some of the rules you are about to learn.
- recognizing that in cases when a structure is particularly complex and a picture may make be particularly useful, you should supply one (See the note below).

**Note 8.1.3.1:** Sometimes the most helpful name to give a compound is 42.

Even though the IUPAC nomenclature rules permit specification of even the most complex structures, it is often much easier and more effective to supply a numbered structure that can be referred to instead of the IUPAC name. Consider bis{[( $\mu$ -2-mercaptoethyl)(2-mercaptoethyl)-methylthioethylaminato (2-)]Nickel(II)}. Which is easier, to expect readers and hearers to work out the structure from that name or to just refer them to compound **42** in Scheme 8.1.3.1?



Scheme 8.1.3.1. Structure of bis{[( $\mu$ -2-mercaptoethyl)(2-mercaptoethyl)-methylthioethylaminato (2-)]Nickel(II)}. The authors of the synthesis of this compound in *Inorganic syntheses*<sup>1</sup> may have had to figure out an IUPAC name for this compound but if you have this scheme in your paper and your instructor is OK with it you can just call it **42**

### Coordination Complexes are named as the ligand derivatives of a metal

A variety of systems have been used for naming coordination compounds since the development of the discipline in the time of Alfred Werner. In this section the most common approaches as they are currently used by practicing chemists will be described. Those who need a more thorough and accurate acquaintance with the full IUPAC nomenclature rules are encouraged to consult the [IUPAC brief guide to inorganic nomenclature](#) followed by [complete guidelines, commonly known as the IUPAC red book](#). If those are still not enough a careful read of note 8.1.3.1 is suggested.

The systems for naming coordination compounds used at present are additive, meaning that they consider coordination compounds as comprising a central metal to which are added ligands. To specify the structure and bonding in this metal-ligand complex then involves:

1. when there are several different ways of attaching the metal and ligands, specifying the structural or stereoisomer
2. systematically listing the ligands in a way that, as necessary, conveys information about how they are linked to the metal and their stereochemistry

- providing the identity of the metal and its oxidation state, or if the oxidation state is unclear, at least the overall charge on the complex
- specifying any counterions present

Since the stereochemistry of coordination compounds forms the subject of the next section, in this section it will be addressed by simply giving the prefixes that designate stereochemistry as if they were self-evident. Do not worry about these for now. They will make sense after you have learned more about stereochemistry in the next section. At that time, you can go back over the examples in that section to solidify your understanding of how to name coordination compounds.

However, in order to name coordination compounds accurately you will need to learn how to think about and name ligands first.

## Ligands

Ligands are classified based on whether they bind to the metal center through a single site on the ligand or whether they bind at multiple sites. Ligands that bind through only a single site are called **monodentate** from the Latin word for tooth; in contrast, those which bind through multiple sites are called **chelating** after the Greek  $\chi\alpha\lambda\epsilon$  for “claw”. These relationships are summarized in Figure 8.1.3.1

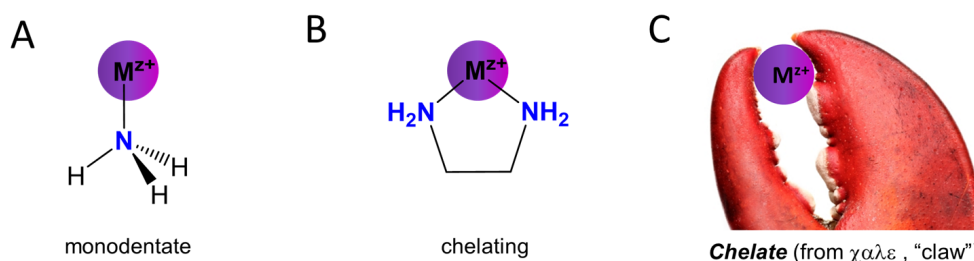
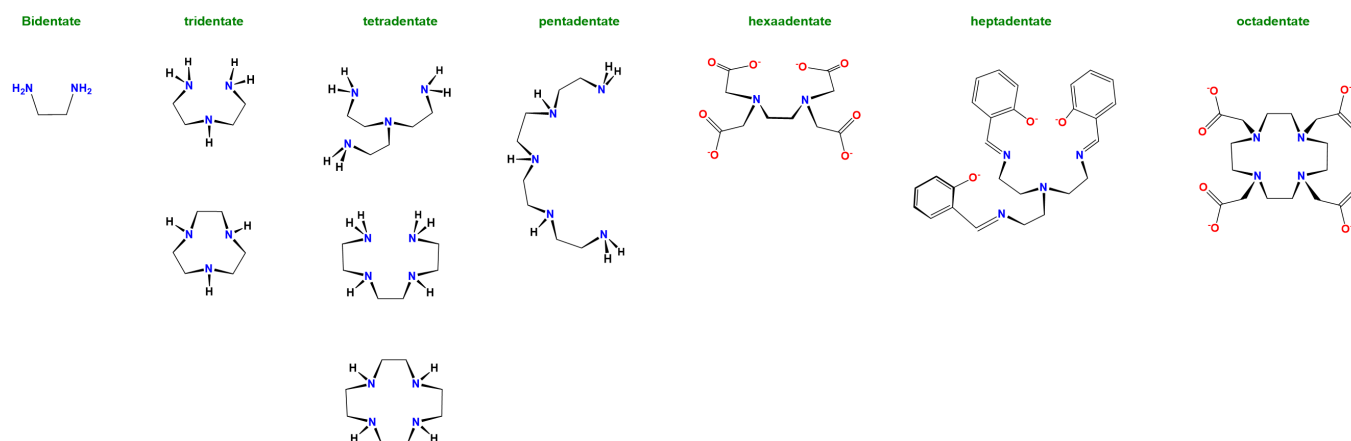


Figure 8.1.3.1. (A) Ammonia is a monodentate ligand while (B) ethylene diamine is a chelating ligand owing to its capacity to bind metals via its two amine functional groups. (C) Chelating ligands act like a lobster claw in attaching to the metal via multiple sites. The lobster claw image is adapted from <https://www.clipart.email/download/1127636.html>. Otherwise this work by Stephen Contakes is licensed under a [Creative Commons Attribution 4.0 International License](#).

Following naturally from the classification of non-chelating ligands as monodentate, chelating ligands are further classified according to the number of sites which they can use to bind a metal center. This number of binding sites is called the denticity and ligands are referred to as monodentate (non-chelating), bidentate, tridentate, etc., based on the number of sites available. Ligands with two binding sites have a denticity of two and are said to be bidentate; those with three are tridentate, four tetradentate, and so on. To illustrate this classification system examples of chelating ligands classified according to denticity are given in Scheme 8.1.3.1

**Scheme 8.1.3.1.** A selection of chelating ligands classified according to denticity.

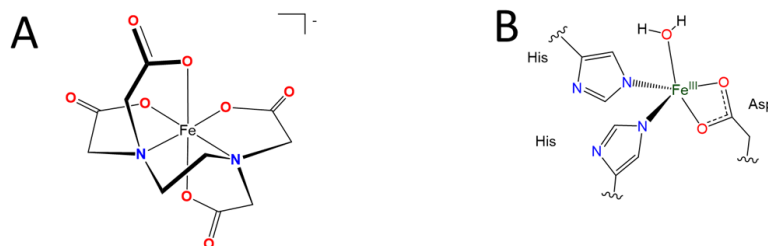


Scheme 8.1.3.IIA. Because only one oxygen per carboxylate typically binds, only one is counted when assigning a ligand's denticity. This work by Stephen Contakes is licensed under a [Creative Commons Attribution 4.0 International License](#).

Although only one carboxylate oxygen usually binds to a metal, it is still possible to bind a metal using both oxygens. As shown in Scheme 8.1.3.IIB complexes in which both carboxylates bind to a metal are known, and in fact are common in the active sites of

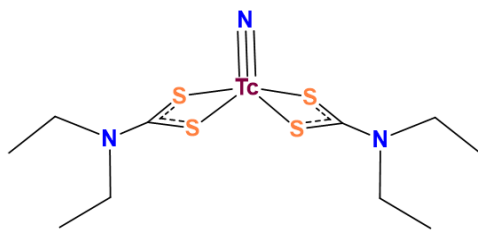
some enzymes. It is just that the binding of both oxygens gives a strained four-membered ring that is usually unstable.

**Scheme 8.1.3.II.** (A) Only one oxygen per carboxylate counts towards the denticity of EDTA since on binding the other oxygen generally points away from the metal center, as in the structure of  $\text{Fe}(\text{EDTA})^-$ . This does not mean that both oxygens of a carboxylate can *never* both bind to metal centers in a complex. (B) Structures in which both oxygens of a carboxylate side chain bind to a metal are sometimes found in the active sites of some of the nonheme iron enzymes your body uses to break down amino acids.



Scheme 8.1.3.III) Two atoms from one ligand bind and are classified as bidentate. This work by Stephen Contakes is licensed under a [Creative Commons Attribution 4.0 International License](https://creativecommons.org/licenses/by/4.0/).

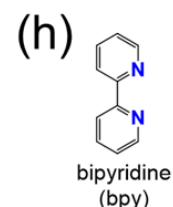
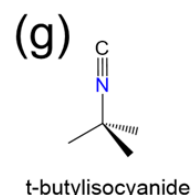
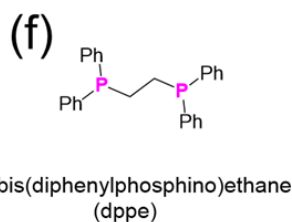
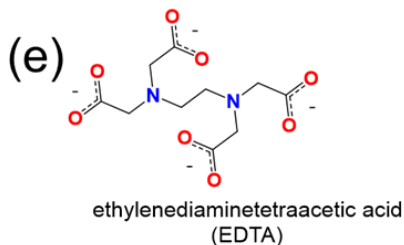
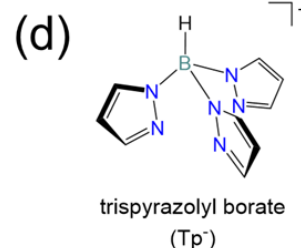
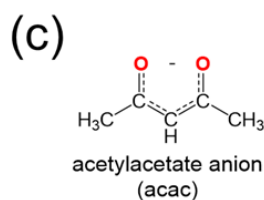
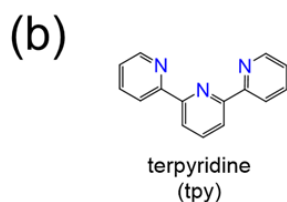
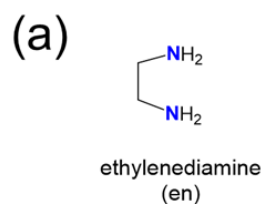
**Scheme 8.1.3.III.** As in this complex, dithiocarbamates commonly bind metals through both sulfur atoms. Consequently, dithiocarbamates are classified as bidentate. This work by Stephen Contakes is licensed under a [Creative Commons Attribution 4.0 International License](https://creativecommons.org/licenses/by/4.0/).



Because of these factors it is technically more correct to say that carboxylates *usually act as* monodentate ligands and dithiocarbamates bidentate ones than it is to say that carboxylates *are* monodentate ligands and dithiocarbamates bidentate ones. So in other words the ligand classifications presented here just represent common binding modes.

### ? Exercise 8.1.3.1

Determine the denticity of each ligand in the list below and classify them as monodentate, tridentate, etc.



Answer

- (a) bidentate
- (b) tridentate
- (c) bidentate
- (d) tridentate (only the lower N on each ring has a lone pair that can be used to bind the metal)
- (e) hexadentate (remember that each carboxylate only counts as one point of attachment)
- (f) bidentate
- (g) monodentate (through the lone pair on the isocyanide C)
- (h) bidentate

This experimentally-based classification of dithiocarbamates as bidentate and carboxylates as monodentate can be confusing to a beginner. Fortunately, such experimentally based classifications are embedded in the lists of common monodentate ligands as given in Table 8.1.3.1 and common chelating ligands in Table 8.1.3.2

A perusal of the ligands in Table 8.1.3.1 reveals that several can bind to a metal in multiple ways. For example, thiocyanate,  $\text{SCN}^-$  can bind metals through its S or N atoms. Such ligands are called **ambidentate ligands**. In naming an ambidentate ligand, the atom through which it attaches to the metal is commonly specified after the ligand name using the italicized element symbol or, more formally, a  $\kappa$  followed by the italicized element symbol. An example is given in Scheme 8.1.3.1<sup>2</sup>

**Scheme 8.1.3.1.** Two possible binding modes of nitrite acting as a ligand.<sup>3</sup>

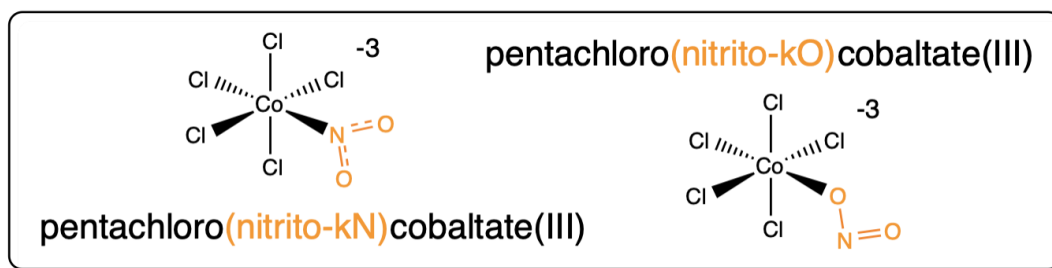
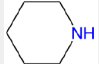
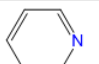
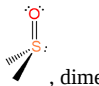
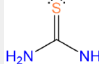


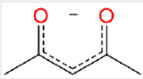
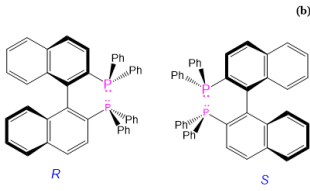
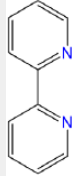


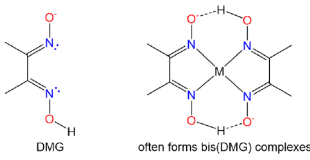
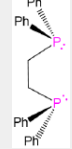
Table 8.1.3.1. Common monodentate ligands. Most chemists still prefer common names over the IUPAC ones.

Ligand	Common name	IUPAC name
$\text{H}^-$ (H ligands are always considered anions for naming purposes)	hydrido	hydrido
$\text{F}^-$	fluoro	fluorido
$\text{Cl}^-$	chloro	chlorido
$\text{Br}^-$	bromo	bromido
$\text{I}^-$	iodo	iodido
$\text{CN}^-$ , as M-CN	cyano	cyanido or cyanido- $\kappa\text{C}$ or cyanido-C
$\text{CN}^-$ , as M-NC	isocyano	isocyanido or cyanido- $\kappa\text{N}$ or cyanido-N
$\text{CH}_3\text{NC}$	methylisocyanide	methylisocyanide
$\text{N}_3^-$	azido	azido
$\text{SCN}^-$ , e.g. thiocyanate as M-SCN	thiocyanato	thiocyanato- $\kappa\text{S}$ or thiocyanato-S
$\text{NCS}^-$ , e.g. thiocyanate as M-NCS	isothiocyanato	thiocyanato- $\kappa\text{N}$ or thiocyanato-N
$\text{CH}_3\text{CO}_2^-$	acetato	ethanoato
$\text{N}^{3-}$	nitrido	nitrido
$\text{NH}^{2-}$	imido	azanediido

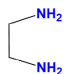

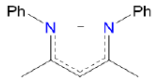
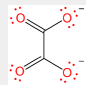
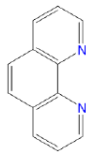
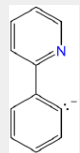
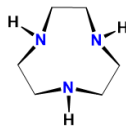
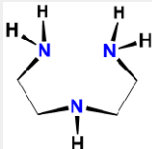
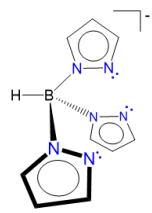
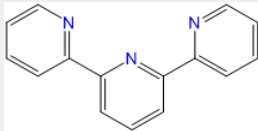
Ligand	Common name	IUPAC name
$\text{NH}_2^-$	amido	azanido
$\text{NH}_3$	ammine	ammine
$\text{RNH}_2, \text{R}_2\text{NH}, \text{R}_3\text{N}$	alkylamine, dialkylamine, trialkylamine ( <i>e.g.</i> methylamine for $\text{CH}_3\text{NH}_2$ )	alkylamine, dialkylamine, trialkylamine ( <i>e.g.</i> methylamine for $\text{CH}_3\text{NH}_2$ )
 , piperidine, abbreviated pip	piperidine	piperidine
 , pyridine, abbreviated py	pyridine	pyridine
$\text{CH}_3\text{CN}$ , acetonitrile, abbreviated MeCN	acetonitrile	acetonitrile
$\text{P}^{3-}$	phosphido	phosphido
$\text{PH}_3$	phosphine	phosphane
$\text{PR}_3$	trialkylphosphine ( <i>e.g.</i> trimethylphosphine for $\text{Me}_3\text{P}$ )	trialkylphosphane ( <i>e.g.</i> trimethylphosphane for $\text{Me}_3\text{P}$ )
$\text{PAR}_3$	triarylphosphine ( <i>e.g.</i> triphenylphosphine for $\text{Ph}_3\text{P}$ )	triarylphosphine ( <i>e.g.</i> triphenylphosphane for $\text{Ph}_3\text{P}$ )
 , dimethylsulfoxide or DMSO or dmso	dimethylsulfoxide (sometimes called dimethylsulfoxo but this usage is rare and violates the nomenclature rules for neutral ligands)	(methanesulfinyl)methane or dimethyl(oxido)sulfur
 , thiourea or tu	thiourea	thiourea
$\text{O}^{2-}$	oxo	oxido
$\text{OH}^-$	hydroxo	hydroxido
$\text{H}_2\text{O}$	aqua	aqua
$\text{S}^{2-}$	sulfo	sulfo
$\text{HS}^-$	hydrosulfido	hydrosulfido
$\text{RS}^-$	alkanethiolate ( <i>e.g.</i> ethanthiolate for $\text{EtS}^-$ )	thioalkanoate
$\text{H}_2\text{S}$	hydrogen sulfide	hydrogen sulfide
$\text{R}_2\text{S}$	alkylsulfanylalkane ( <i>e.g.</i> ethylsulfanylane for $\text{Et}_2\text{S}$ )	dialkyl sulfide
$\text{O}_2$	dioxygen	dioxygen
$\text{O}_2^-$ , superoxide	superoxido	dioxido(1-) or superoxido
$\text{O}_2^{2-}$ , peroxide	peroxido	dioxido(2-) or peroxido
$\text{N}_2$	dinitrogen	dinitrogen
$\text{NO}$ (are always considered neutral for naming purposes)	nitrosyl	nitrosyl
$\text{CO}$	carbonyl	carbonyl
$\text{CS}$	thiocarbonyl	thiocarbonyl
$\text{SO}$ , as $\text{M-SO}$	sulfinio	sulfur monoxide- $\kappa\text{S}$ or sulfur monoxide-S
$\text{NO}_2$ , as $\text{M-NO}_2$	nitryl	nitrogen dioxide- $\kappa\text{N}$ or nitrogen dioxide-N

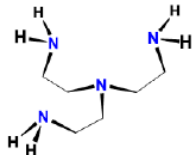
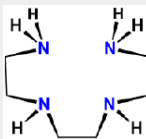
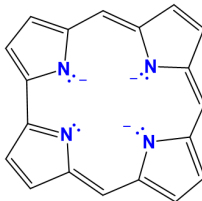
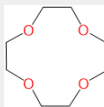
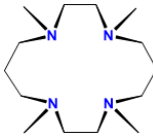
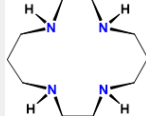
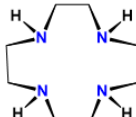
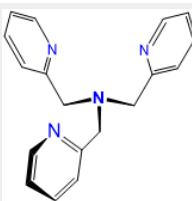
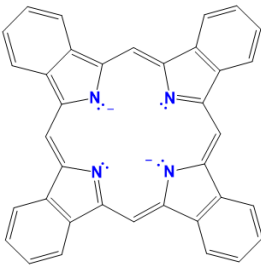
Ligand	Common name	IUPAC name
$\text{CO}_3^{2-}$	carbonato	carbonato
$\text{NO}_2^-$ , as M- $\text{NO}_2$	nitro or nitrito- <i>N</i>	nitrito- $\kappa N$ or nitrito- <i>N</i>
$\text{NO}_2^-$ , as M-ONO	nitrito or nitrito- <i>O</i>	nitrito- $\kappa O$ or nitrito- <i>O</i>
$\text{NO}_3^-$	nitrato	nitrato
$\text{SO}_3^{2-}$	sulfito	sulfito
$\text{SO}_4^{2-}$	sulfato	sulfato
$\text{S}_2\text{O}_3^{2-}$ , as M-S- $\text{SO}_2\text{-O}^-$	thiosulfato- <i>S</i>	thiosulfato- $\kappa S$ or thiosulfato- <i>S</i>
$\text{S}_2\text{O}_3^{2-}$ , as M-O- $\text{SO}_2\text{-S}^-$	thiosulfato- <i>O</i>	thiosulfato- $\kappa O$ or thiosulfato- <i>O</i>

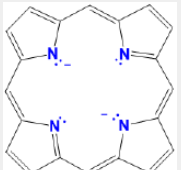
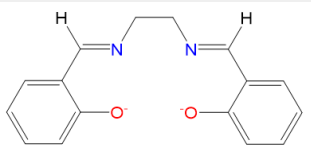
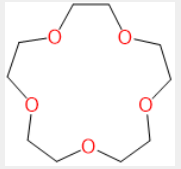
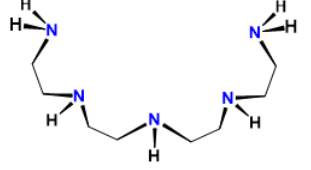
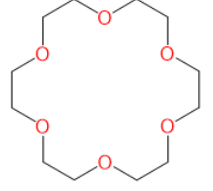
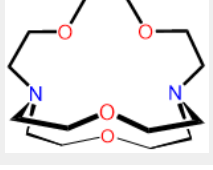
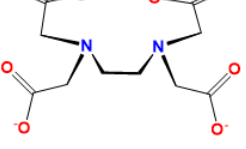
Table 8.1.3.2. Common chelating ligands organized by denticity. Most chemists use the common names and abbreviations to describe these ligands.

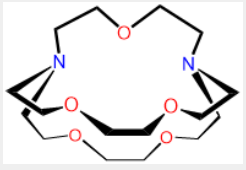
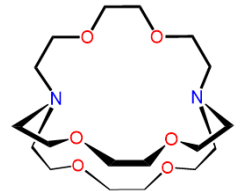
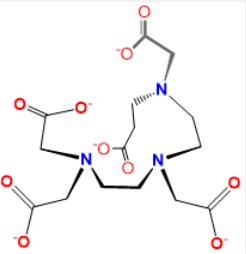
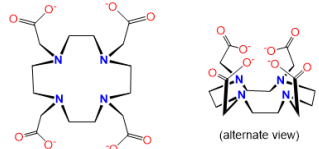
Common Ligand name	IUPAC ligand name	abbreviation (if applicable)	structure or representative/parent structure (shown in the ionization state in which they bind to a metal)
<i>bidentate ligands</i>			
acetylacetonato	2,4-pentanediono	acac	
R-BINAP and S-BINAP	<i>R</i> - or <i>S</i> -2,2'-bis(diphenylphosphino)-1,1'-binaphthyl	BINAP	
2,2'-bipyridine	2,2'-bipyridine	bpy or bipy	
cyclooctadiene	1,5-cyclooctadiene	COD	 (binding to the metal occurs through the alkene $\pi$ cloud)
dialkyldithiocarbamato	dialkylcarbamdithiolato	$\text{R}_2\text{NCS}_2^-$ or dtc	
dimethylglyoximato	butanedienedioxime	Hdmg or DMG	
diphenylphosphinoethane or 1,2-(diphenylphosphino)ethane	Ethane-1,2-diylbis(diphenylphosphane)	dppe	



Common Ligand name	IUPAC ligand name	abbreviation (if applicable)	structure or representative/parent structure (shown in the ionization state in which they bind to a metal)
ethylenediamine	Ethane-1,2-diamine	en	
ethylenedithiolato	Ethane-1,2-dithiolato	C <sub>2</sub> H <sub>2</sub> S <sub>2</sub> <sup>2-</sup>	
nacnac	<i>N,N'</i> -diphenyl-2,4-pentanediiiminato	nacnac	
oxalato	oxalato	ox	
1,10-phenanthroline or o-phenanthroline	1,10-phenanthroline	phen or o-phen	
phenylpyridinato	2-phenylpyridinato-C <sup>2</sup> , <i>N</i> or 2-phenylpyridinato-κC <sup>2</sup> , <i>N</i>	PPY	
<i>tridentate ligands</i>			
triazacyclononane	1,4,7-triazacyclononane	tacn	
diethylenetriamine	1,4,7-triazaheptane	dien	
pyrazoylborato (scorpionate)	hydrotris(pyrazo-1-yl)borato	Tp	
terpyridine or 2,2';6',2''-terpyridine	1 <sup>2</sup> ,2 <sup>2</sup> :2 <sup>6</sup> ,3 <sup>2</sup> -terpyridine or 2,6-bis(2-pyridyl)pyridine, tripyridyl, 2,2':6',2''-terpyridine	tpy or terpy	
<i>tetradentate ligands</i>			

Common Ligand name	IUPAC ligand name	abbreviation (if applicable)	structure or representative/parent structure (shown in the ionization state in which they bind to a metal)
$\beta$ , $\beta'$ , $\beta''$ -triaminotriethylamine	$\beta$ , $\beta'$ , $\beta''$ -tris(2-aminoethyl)amine	tren	
triethylenetetramine	1,4,7,10-tetraazadecane	trien	
corroles	variable and generally not used	cor or Cor	
12-crown-4	1,4,7,10-tetraoxacyclododecane	12-crown-4	
tetramethylcyclam	1,4,8,11-tetramethyl-1,4,8,11-tetraazacyclotetradecane	TMC or cyclam	
cyclam	1,4,8,11-tetraazacyclotetradecane	cyclam	
cyclen	1,4,7,10-tetraazacyclododecane	cyclen	
tris(2-pyridylmethyl)amine	1-pyridin-2-yl-N,N-bis(pyridin-2-ylmethyl)methanamine	tpa or TPA	
phthalocyanines	variable and generally not used	variable, usually a modified Pc	

Common Ligand name	IUPAC ligand name	abbreviation (if applicable)	structure or representative/parent structure (shown in the ionization state in which they bind to a metal)
porphyrins	variable and generally not used	variable, usually a modified por, Por, or P (e.g. TPP = tetraphenylporphyrin)	
salen	2,2'-ethylenebis(nitrilomethylidene)diphenoxido	salen	
<i>pentadentate ligands</i>			
15-crown-5	1,4,7,10,13-Pentaoxacyclopentadecane	15-crown-5	
tetraethylenepentamine	1,4,7,10,13-pentaazatridecane	tepa or TEPA	
<i>hexadentate ligands</i>			
18-crown-6	1,4,7,10,13,16-hexaoxacyclooctadecane	18-crown-6	
2,1,1-cryptand	4,7,13,18-Tetraoxa-1,10-diazabicyclo[8.5.5]icosane	2,1,1-crypt or [2.1.1]-cryptand kryptofix 211 and variations thereof	
ethylenediaminetetraaceto	2,2',2'',2'''-(Ethane-1,2-diyl)dinitrilo)tetraaceto	EDTA, edta, Y <sup>4-</sup>	
<i>heptadentate ligands</i>			

Common Ligand name	IUPAC ligand name	abbreviation (if applicable)	structure or representative/parent structure (shown in the ionization state in which they bind to a metal)
2,2,1-cryptand	4,7,13,16,21-pentaoxa-1,10-diazabicyclo[8.8.5]icosane	2,2,1-crypt or [2.2.1]-cryptand kryptofix 221 and variations thereof	
<i>octadentate ligands</i>			
2,2,2-cryptand	4,7,13,16,21,24-Hexaoxa-1,10-diazabicyclo[8.8.8]hexacosan	2,2,2-crypt or [2.2.2]-cryptand kryptofix 222 and variations thereof	
pentetate acid or diethylenetriaminepentaacetato or DTPA	2-[bis[2-[bis(carboxylatomethyl)amino]ethyl]amino]acetato	DTPA	
DOTA or tetraxetan	1,4,7,10-Tetraazacyclododecane-1,4,7,10-tetraacetic acid	Dota, DOTA	

## Rules for Naming Coordination Compounds

As explained above, the name of a coordination compound communicates

- as appropriate, information about isomerism
- systematically listing the ligands in a way that as necessary conveys information about their oxidation state and how they are linked to the metal
- the identity of the metal and its oxidation state
- any counterions present

Before going into these rules it is worth pointing out a few things.

1. It is easiest to learn these rules by starting with one or two of the rules, learning how to apply them, and then adding additional rules one at a time. To that end, instructors who wish to use a more programmed approach may find it convenient to first direct their students to [this page which focuses on getting the names of the ligands and metal right, without worrying about isomerism or stereochemistry](#).

2. The rules also assume some familiarity with common coordination geometries and patterns of isomerism in metal complexes. Thus it might be easiest to learn about [common coordination geometries](#) first, followed by [common patterns of isomerism in metal complexes](#) before beginning this section. If you decide to dive right in to this section you might find it helpful to know that when applying nomenclature and formula rules most textbooks *assume*

- complexes in which the metal has a coordination number of six are octahedral
- complexes in which the metal has a coordination number of five are trigonal bipyramidal

- complexes in which  $\text{Pt}^{\text{II}}$ ,  $\text{Pd}^{\text{II}}$ , or  $\text{Rh}^{\text{I}}$ , or  $\text{Ir}^{\text{I}}$  have a coordination number of four are square planar
- other complexes in which the metal has a coordination number of four are tetrahedral

Like all assumptions these don't always work in real life but they should be good enough to get you through your first inorganic chemistry course.

For the pedants among you, note that the complexes given as examples and in exercises on this page have been selected for pedagogical utility. Although many are well-known compounds, others are hypothetical.

Now on to the rules.

**Rule 1:** If ions are present, name the cation first, followed by the anion.

Examples:

$\text{K}_2[\text{Pt}^{\text{II}}\text{Cl}_4]$  potassium tetrachloroplatinate(2-)

$[\text{Co}^{\text{III}}(\text{NH}_3)_6](\text{NO}_3)_3$  hexaamminecobalt(3+) nitrate

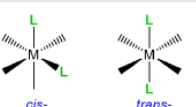
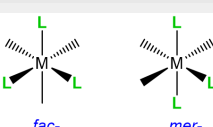
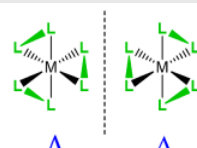
$[\text{Co}^{\text{III}}(\text{NH}_3)_6][\text{Cr}^{\text{III}}(\text{C}_2\text{O}_4)_3]$  hexaamminecobalt(3+) tris(oxalato)chromium(3-)

**Rule 2:** When multiple isomers are possible, designate the particular isomer in *italics* at the front of the name of each complex

If you have not yet learned about isomerism in coordination compounds skip this rule for now and return to it after you have.

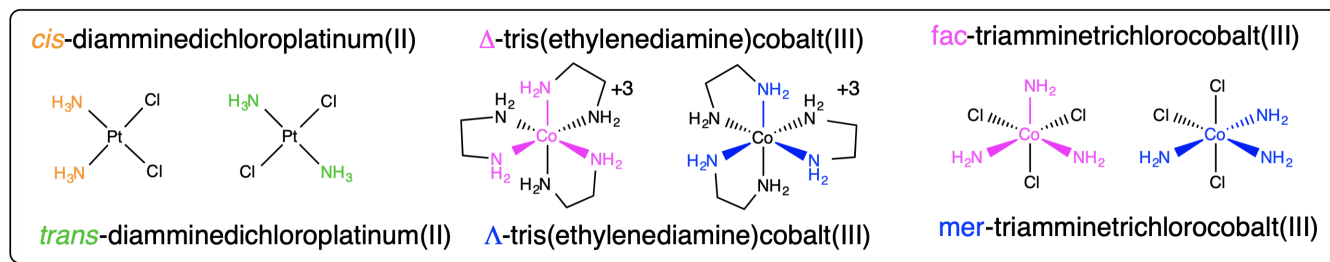
When a complex might exist as one of two stereoisomers, prefixes are commonly used to designate which isomer is present. The most common cases are listed in Table 8.1.3.3

Table 8.1.3.3. Prefixes used to specify isomerism about a metal center when naming and writing coordination compounds' formulae.

Type of isomerism	Graphical reminder	Prefixes
Geometric, <i>cis-</i> , <i>trans-</i>		<i>cis-</i> or <i>trans-</i>
Geometric, <i>fac-</i> / <i>mer-</i>		<i>fac-</i> or <i>mer-</i>
Enantiomers, $\Lambda$ -, $\Delta$ -		$\Lambda$ - or $\Delta$ -

Examples of how isomerism about a metal center is designated are given in Scheme 8.1.3.II

**Scheme 8.1.3.II.** Application of nomenclature rules for stereoisomerism about a metal.<sup>3</sup>



There are a number of other cases where it might be advisable to specify the stereochemistry of a complex. These cases involve specifying

- the coordination geometry about a metal center (octahedral, trigonal prismatic, tetrahedral, square planar, etc. )
- the geometry cannot be unambiguously described by a single *cis/trans* or *fac/mer* relationship of ligands

These cases may also be handled by using a designator to specify the coordination geometry and, as necessary, giving the position of ligated atoms in terms of designated numbered positions for that geometry. See the IUPAC red book for details as such cases fall outside the scope of what is normally advisable for an undergraduate course.

**Rule 3: Specify the identity, number, and as appropriate, isomerism of the ligands present in alphabetical order by ligand name.**

Before specifying the metal, the ligands are written as prefixes of the metal.

In specifying the ligands several rules are followed.

- The ligands are written in alphabetical order by the ligand name only; symbols are not considered and prefixes do not count in determining alphabetical order.

*Example:* In the name of the complex ion  $[\text{Co}(\text{NH}_3)_5\text{Cl}]^{2+}$ , pentamminechlorocobalt(II), the ammine ligand is named before the chloro ligand because the order is alphabetical by the ligand name by virtue of which ammine comes before chloro.

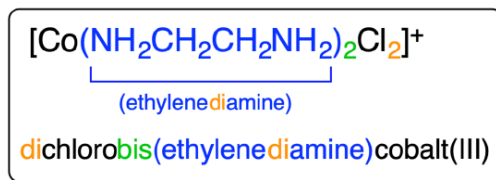
- Prefixes are used to indicate the number of each ligand present. Specifically, *di-*, *tri-*, *tetra-*, *penta-*, *hexa-*, etc. prefixes are used to indicate multiple ligands of the same type EXCEPT when the ligand is polydentate or its name already has a *di-*, *tri-*, *tetra-* etc. In that case *bis-*, *tris-*, *tetrakis-*, etc. are used instead. These prefix rules are summarized in Table 8.1.3.3

Table 8.1.3.3. Prefixes used to specify the number of a given ligand present.

Number of identical ligands	prefix used when the ligand name is simple	prefix used when the ligand is polydentate or its name already has a <i>di-</i> , <i>tri-</i> , <i>tetra-</i> etc.
2	di-	bis-
3	tri-	tris-
4	tetra-	tetrakis-
5	penta-	pentakis-
6	hexa-	hexakis-
7	hepta-	heptakis-
8	octa-	octakis-
9	nona-	nonakis-
10	deca-	decakis-

An example of the application of the prefix rule is given in Scheme 8.1.3.III

**Scheme 8.1.3.III** . Example of the use of prefixes to specify the number of ligands of each type in a complex.<sup>3</sup>



- Ligand names are based on their charge.

- Neutral and cationic ligand names are the same as the names of their neutral compounds with two caveats:
  - names that involve spaces should either be put in parentheses or the spaces should be eliminated (preferred)
 

*Example:* *cis*-dichlorobis(dimethyl sulfoxide)platinum(II) or *cis*-dichlorobis(dimethylsulfoxide)platinum(II)
  - A few ligands are given common names.
    - $\text{H}_2\text{O}$  = aqua

- $\text{NH}_3$  = ammine (notice that there are two n's)
- $\text{CO}$  = carbonyl
- $\text{CS}$  = thiocarbonyl
- $\text{NO}$  = nitrosyl
- For anionic ligands, the vowel at the end of their anion names is changed to an "-o"

Examples:  $\text{Cl}^-$  = chloro,  $\text{NH}_2^-$  = amido,  $\text{N}_3^-$  = azido

Caveat: some anionic ligands have common names that may also be used

Examples:

$\text{I}^-$  = iodo or iodino

$\text{CN}^-$  = cyano or cyanido

$\text{O}^{2-}$  = oxo or oxido

The IUPAC and common names of many ligands are given in Tables 8.1.3.1 and 8.1.3.2

- When an ambidentate ligand is present, the atom through which it is bound to the metal is indicated by giving either its element symbol or a  $\kappa$  and its element symbol in italics after the ligand name.

Example:

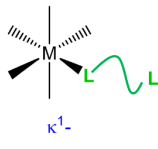
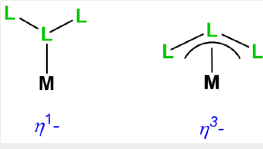
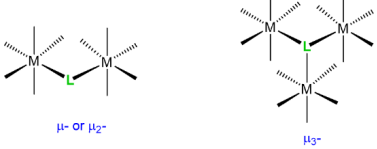
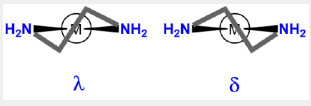
$\text{M-SCN}$  is thiocyanato-S or thiocyanato- $\kappa\text{S}$

$\text{M-NCS}$  = thiocyanato-N or thiocyanato- $\kappa\text{N}$

The use of  $\kappa$  and an element symbol to indicate how a ligand and metal are linked is called a **k-term**. More complex k-terms might also involve specifying the atoms by number, though their use is outside the scope of this text.

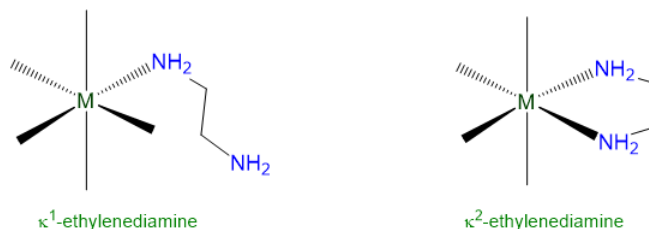
- As appropriate, additional information about the way a ligand is bound to the metal center and/or its stereochemistry is specified using a prefix. The prefixes to provide linkage and stereochemistry for ligands are given in Table 8.1.3.4

Table 8.1.3.4. Prefixes used to specify ligands' isomerism when naming and writing coordination compounds' formulae. Some of these types of isomerism will be discussed in later pages.

Type of isomerism	Graphical reminder	Prefixes
when a multidentate ligand binds through less than the full number of atoms	 $\kappa^1-$	$\kappa^n$ where n is the number of attached atoms; used when the attached atoms are not directly connected by a chemical bond. The metal-ligand bonding usually involves $\sigma$ -type coordination.
hapticity	 $\eta^1-$ $\eta^3-$	$\eta^n$ where n is the number of attached atoms; used when the coordinated atoms are all connected by bonds. Usually the metal-ligand bonding involves $\pi$ -type coordination. In speech, $\eta^1$ =monohapto; $\eta^2$ =dihapto; $\eta^3$ =trihapto, etc.
bridging ligands	 $\mu-$ or $\mu_2-$ $\mu_3-$	$\mu_n$ where n is the number of atoms bridged. The number n is usually omitted when n = 2.
chelating ligand ring twist	 $\lambda$ $\delta$	$\lambda$ - or $\delta$ -

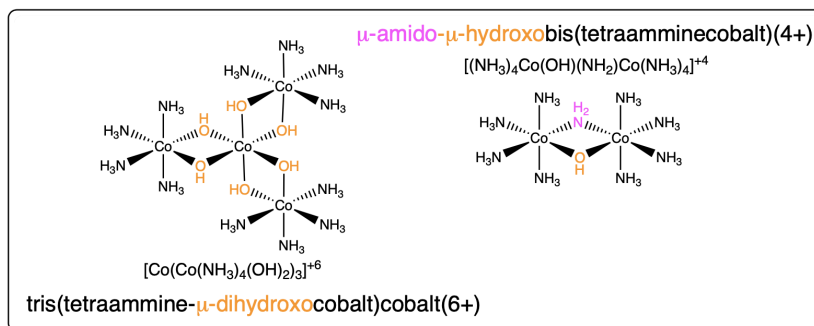
An example showing how the nomenclature rule is applied to a ligand that can have two coordination modes is given in Scheme 8.1.3.IV.

**Scheme 8.1.3.IV**. Use of the  $\kappa$  notation to specify the number of attached groups in a multidentate ligand.



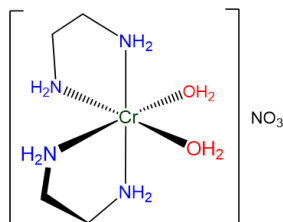
Scheme 8.1.3.V. The names of the complexes follow the rules described in 9.2.6: [multinuclear coordination complexes](#).

**Scheme 8.1.3.V**. Use of the  $\mu$  notation to specify bridging ligands in metal complexes.<sup>3</sup>



6. If desired, parentheses *may* be used to delineate a ligand name to make it easier to identify in the name of the complex. This can be particularly helpful when the entire name contains a lot of information to keep track of. An example is given in Scheme 8.1.3.VI

**Scheme 8.1.3.VI**. When naming the complex shown, *cis*-diaquabis(ethylenediamine)chromium(III) nitrate is easier to read than *cis*-diaquabisethylenediaminechromium(III) nitrate.



#### Rule 4: Specify the identity of the metal

- In neutral and cationic complexes the metal's name is used directly  
 - *e.g.* as in hexammineruthenium(III) for  $[\text{Ru}(\text{NH}_3)_6]^{3+}$
- In anionic complexes, -ate replaces -ium, -en, or -ese or adds to the metal name,  
 e.g., as in hexachloromanganate(IV) for  $\text{MnCl}_6^{2-}$
- In anionic complexes of some metals a Latin-derived name is used instead of the element's English name. These names are given in Table 8.1.3.5

Table 8.1.3.5. Latin terms for select metal Ions. Redrawn from this page describing the [nomenclature of coordination complexes](#).

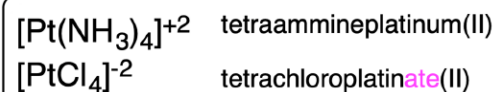
Transition Metal	Latin
Copper	Cuprate
Gold	Aurate
Iron	Ferrate
Lead	Plumbate
Silver	Argentate



Transition Metal	Latin
Tin	Stannate

An example of the application of the metal naming rules is given in Scheme \sf{\PageIndex{VII}}).

**Scheme 8.1.3.VII.** Example of the application of the metal specification rules to a cationic and an anionic platinum complex.<sup>3</sup>

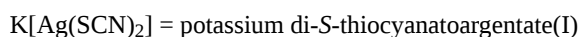
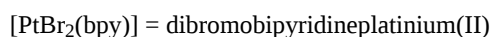
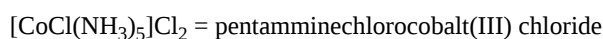


### Rule 5: Specify the oxidation state of the metal.

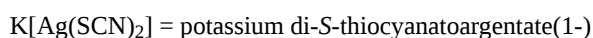
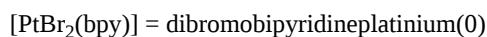
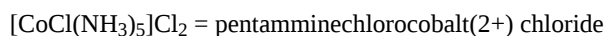
Two different systems are used to specify the oxidation state of the metal.

1. In the **Stock system** the metal's oxidation state is indicated in Roman numerals after the metal name.

*Examples:*



2. In the **Ewing-Bassett system** the charge on the complex is specified in Arabic numerals after the complex name. This provides a way of specifying a complex even when the oxidation state of the metal isn't known and, in cases where it is known, the value of the metal's oxidation state may be inferred from the complex ion's charge.

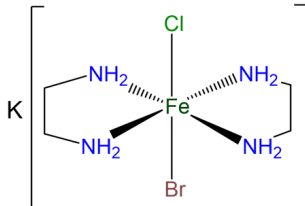
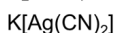
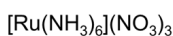


### Summary of rules for naming coordination complexes.

A graphical summary of the **rules for naming complexes** along with a few examples that you can use to review the nomenclature rules is given in Figure 8.1.3.1 This work by Stephen Contakes is licensed under a [Creative Commons Attribution 4.0 International License](https://creativecommons.org/licenses/by/4.0/).

stereochemical prefix-	Specify Ligands	Indicate Metal	Charge on the complex or metal oxidation state
As appropriate use <i>cis</i> -, <i>trans</i> -, <i>fac</i> -, <i>mer</i> -, $\Lambda$ -, $\Delta$ -, to indicate stereochemistry.	<p>What ligands and how many?</p> <ul style="list-style-type: none"> <li>List alphabetically by ligand name <ul style="list-style-type: none"> <li>Neutral – ligand name</li> <li>Carionic – ligand name</li> <li>Anionic – change last vowel to "o"</li> </ul> </li> <li>Indicate # by di-, tri-, tetra-, etc. (or bis-, tris-, tetrakis-, etc. if there is a di-, tri-, tetra-, etc. in the ligand name)</li> </ul> <p>As appropriate, how are the ligands arranged?</p> <ul style="list-style-type: none"> <li>Ambidentate – indicate linkage point by <math>\kappa</math> &amp; italicized element symbol</li> <li>other structure – use <math>\kappa^n</math>, <math>\eta^n</math>, <math>\mu_n</math>, <math>\lambda</math>-, <math>\delta</math>-</li> </ul> <p>For clarity, parentheses may be used to delineate ligands</p>	<p>Neutral, cationic: English name</p> <p>Anionic – change ending to "ate"</p> <ul style="list-style-type: none"> <li>Latin names for Ag, Au, Cu, Fe, Pb, Sn; English for others</li> </ul>	<p>Stock system: Metal Oxidation state in capital Roman numerals</p> <p>Ewing-Bassett system: Complex's charge in Arabic numerals</p>

**Examples:**



hexamine ruthenium(3+) nitrate

or

hexamine ruthenium(III) nitrate

potassium tetrachloroplatinate(2-)

or

potassium tetrachloroplatinate(II)

potassium dicyanoargentate(1-)

or

potassium dicyanoargentate(I)

potassium *trans*-bromochlorobis(ethylenediamine)iron(1+) (Ewing-Bassett)

-or-

potassium *trans*-bromochlorobis(ethylenediamine)iron(III) (Stock)

Figure 8.1.3.1. Summary of nomenclature rules for coordination complexes along with a few examples of their application.

When learning chemical nomenclature, practice makes perfect. The following examples and exercises are provided to give you this practice. Additional examples and exercises on the <https://chem.libretexts.org/> site include [a set of simple examples with explained solutions](#), [a set of simple exercises with solutions](#), and [a set of more challenging exercises without solutions](#).

### ? Exercise 8.1.3.2. Assigning metal oxidation states in a complex

In order to name a complex in the Stock system it is necessary to assign a formal oxidation state to the metal. For this reason it is important to be able to assign the oxidation state of a metal in a complex. Fortunately, this is easy to do if you remember

1. The sum of all atoms' oxidation states will equal the overall charge on the complex
2. When determining the metal's oxidation state the ligands can be treated as having an oxidation state equal to their charge - *i.e.*, the charge they possess in the form in which they coordinate the metal, so if they need to lose a proton to bind, don't forget to account for that.

Given the above, assign the oxidation state of the metal in the following real and hypothetical complexes.

- a.  $\text{K}_3[\text{Fe}(\text{CN})_6]$
- b.  $[\text{CoCl}(\text{NH}_3)_5](\text{NO}_3)_2$
- c.  $\text{K}_2[\text{PtCl}_4]$
- d.  $[\text{MnCl}(\text{por})]$
- e.  $[\text{Ru}(\text{bpy})_3]\text{Cl}_2$
- f.  $[\text{PdCl}_2(\text{dppe})]$
- g.  $[\text{Mn}(\text{en})_2(\text{SCN})_2]$

**Answer for  $\text{K}_3[\text{Fe}(\text{CN})_6]^{3-}$ .**

This contains  $[\text{Fe}(\text{CN})_6]^{3-}$ ; so  $\text{O.S.}_{\text{Fe}} + 6 \times (-1)$  (for  $\text{CN}^-$ ) = -3 (the complex's charge) so  $\text{O.S.}_{\text{Fe}} = +3$  or  $\text{Fe}^{3+}$ .

**Answer for  $[\text{CoCl}(\text{NH}_3)_5](\text{NO}_3)_2$ .**

This contains  $[\text{CoCl}(\text{NH}_3)_5]^{2+}$ ; so  $\text{O.S.}_{\text{Co}} + 1 \times (-1)$  (for  $\text{Cl}^-$ ) +  $0 \times 5$  (for  $\text{NH}_3$ ) = +2 (the complex's charge) so  $\text{O.S.}_{\text{Co}} = +3$  or  $\text{Co}^{3+}$ .

**Answer for  $\text{K}_2[\text{PtCl}_4]$ .**

This contains  $2\text{K}^+$  and  $[\text{PtCl}_4]^{2-}$ ; so  $\text{O.S.}_{\text{Pt}} + 4 \times (-1)$  (for  $\text{Cl}^-$ ) = -2 (the complex's charge) so  $\text{O.S.}_{\text{Pt}} = +2$  or  $\text{Pt}^{2+}$ .

**Answer for  $[\text{MnCl}(\text{por})]$ .**

$\text{O.S.}_{\text{Pt}} + 1 \times (-2)$  (for por; see [table 9.2.2](#)) +  $1 \times (-1)$  (for  $\text{Cl}^-$ ) = +0 (the complex's charge) so  $\text{O.S.}_{\text{Mn}} = +3$  or  $\text{Mn}^{3+}$ .

**Answer  $[\text{Ru}(\text{bpy})_3]\text{Cl}_2$ .**

The complex is  $[\text{Ru}(\text{bpy})_3]^{2+}$  so  $\text{O.S.}_{\text{Ru}} + 0 \times 3$  (for bpy) = +2 (the complex's charge) so  $\text{O.S.}_{\text{Ru}} = +2$  or  $\text{Ru}^{2+}$ .

**Answer  $[\text{PdCl}_2(\text{dppe})]$ .**

$\text{O.S.}_{\text{Pd}} + 2 \times (-1)$  (for  $\text{Cl}^-$ ) +  $0 \times 3$  (for dppe) = +0 (the complex's charge) so  $\text{O.S.}_{\text{Pd}} = +2$  or  $\text{Pd}^{2+}$ .

**Answer  $[\text{Mn}(\text{en})_2(\text{SCN})_2]$ .**

$\text{O.S.}_{\text{Mn}} + (2 \times 0)$  (for en) +  $2 \times (-1)$  (for  $\text{SCN}^-$ ) = +0 (the complex's charge) so  $\text{O.S.}_{\text{Mn}} = +2$  or  $\text{Mn}^{2+}$ .

### ? Exercise 8.1.3.3: Simple Nomenclature Problems.

Name the following compounds in both the Stock and Ewing-Bassett systems:

- $[\text{Ru}(\text{NH}_3)_6](\text{NO}_3)_3$
- $\text{K}_2[\text{PtCl}_4]$
- $\text{K}[\text{Ag}(\text{CN})_2]$
- $\text{Cs}[\text{CuBrCl}_2\text{F}]$
- $[\text{Cu}(\text{acac})_2]$

**Answer**

	Complex	Stock system name	Ewing-Bassett System name
a	$[\text{Ru}(\text{NH}_3)_6](\text{NO}_3)_3$	hexammineruthenium(III) nitrate	hexammineruthenium(3+) nitrate
b	$\text{K}_2[\text{PtCl}_4]$	potassium tetrachloroplatinate(II)	potassium tetrachloroplatinate(2-)
c	$\text{K}[\text{Ag}(\text{CN})_2]$	potassium dicyanoargentate(I)	potassium dicyanoargentate(1-)
d	$\text{Cs}_2[\text{CuBrCl}_2\text{F}]$	cesium bromodichlorofluorocuprate(II)	cesium bromodichlorofluorocuprate(2-)
e	$[\text{Cu}(\text{acac})_2]$	bis(acetylacetonato)copper(II)	bis(acetylacetonato)copper(0)

### ? Exercise 8.1.3.4: More simple nomenclature problems.

Name the following compounds and ions in both the Stock and Ewing-Bassett systems.

- $\text{Cu}(\text{OH})_4^-$
- $[\text{AuXe}_4]^{2+}$
- $\text{AuCl}_4^-$
- $\text{Fe}(\text{CN})_6^{3-}$
- $\text{K}_4[\text{Fe}(\text{CN})_6]$
- trans*- $[\text{Cu}(\text{en})_2(\text{NO}_2)_2]$  (the N is bound to Cu)
- cis*- $\text{IrCl}_2(\text{CO})(\text{PPh}_3)$  (ignore stereochemistry)
- $\text{IrCl}(\text{PPh}_3)_3$

**Answer**

	Compound	Stock System Name	Ewing-Bassett System Name
a	$\text{Cu}(\text{OH})_4^-$	tetrahydroxidocuprate(III) or tetrahydroxidocuprate(III)	tetrahydroxidocuprate(1-) or tetrahydroxidocuprate(1-)
b	$[\text{AuXe}_4]^{2+}$	tetraxenongold(II)	tetraxenongold(2+)
c	$\text{AuCl}_4^-$	tetrachloraurate(III)	tetrachloraurate(1-)
d	$\text{Fe}(\text{CN})_6^{3-}$	hexacyanoferrate(III) or hexacyanidoferrate(III)	hexacyanoferrate(3-) or hexacyanidoferrate(3-)
e	$\text{K}_4[\text{Fe}(\text{CN})_6]$	potassium hexacyanoferrate(II) or potassium hexacyanidoferrate(II)	potassium hexacyanoferrate(4-) or potassium hexacyanidoferrate(4-)
f	<i>trans</i> - $[\text{Cu}(\text{en})_2(\text{NO}_2)_2]$ (the N is bound to Cu)	bis(ethylenediamine)bisnitro copper(II) or bis(ethylenediamine)bis(nitrito- $\kappa N$ )copper(II)	bis(ethylenediamine)bisnitro copper(0) or bis(ethylenediamine)bis(nitrito- $\kappa N$ )copper(0)
g	<i>cis</i> - $\text{IrCl}_2(\text{CO})(\text{PPh}_3)$	<i>cis</i> -dichlorocarbonyltriphenylphosphineiridium(I) or <i>cis</i> -dichloro(carbonyl)(triphenylphosphine)iridium(I)	<i>cis</i> -dichlorocarbonyltriphenylphosphineiridium(0) or <i>cis</i> -dichloro(carbonyl)(triphenylphosphine)iridium(0)
h	$\text{IrCl}(\text{PPh}_3)_3$	chlorotris(triphenylphosphine)iridium(I)	chlorotris(triphenylphosphine)iridium(0)

### ? Exercise 8.1.3.5: Even more simple nomenclature problems.

Name the following compounds and ions in both the Stock and Ewing-Bassett systems. Ignore prefixes for designating isomers if you haven't learned about those.

- $\text{Fe}(\text{acac})_3$
- $\text{K}_2[\text{CuBr}_4]$
- $\text{ReH}_9$
- $[\text{Ag}(\text{NH}_3)_2]\text{BF}_4$
- $[\text{Ag}(\text{NH}_3)_2][\text{Ag}(\text{CN})_2]$
- $[\text{Ni}(\text{CN})_4]^{2-}$
- $[\text{Co}(\text{N}_3)(\text{NH}_3)_5]\text{SO}_4$
- $[\text{CoBrCl}(\text{H}_2\text{O})(\text{NH}_3)]\text{I}$  (ignore stereochemistry)

### Sample Answers

	Complex	Stock system name	Ewing-Bassett System name
a	$\text{Fe}(\text{acac})_3$	tris(acetoacetato)iron(III)	tris(acetoacetato)iron(0)
b	$\text{Na}_2[\text{CuBr}_4]$	sodium tetrabromocuprate(II)	sodium tetrabromocuprate(2-)
c	$[\text{Co}(\text{NH}_3)_6][\text{Co}(\text{ox})_3]$	hexamminecobalt(III) tris(oxalato)cobalt(III)	hexamminecobalt(3+) tris(oxalato)cobalt(3-)
d	$[\text{Ag}(\text{NH}_3)_2]\text{BF}_4$	diamminesilver(I) tetrafluoroborate	diamminesilver(1+) tetrafluoroborate
e	$[\text{Ag}(\text{NH}_3)_2][\text{Ag}(\text{CN})_2]$	diamminesilver(I) dicyanoargentate(I) or diamminesilver(I) dicyanidoargentate(I)	diamminesilver(1+) dicyanoargentate(1-) or diamminesilver(1+) dicyanidoargentate(1-)

	Complex	Stock system name	Ewing-Bassett System name
f	$[\text{Ni}(\text{CN})_4]^{2-}$	tetracyanonickelate(II) or tetracyanonickelate(II) ion	tetracyanonickelate(2-) or tetracyanonickelate(2-) ion
g	$[\text{Co}(\text{N}_3)(\text{NH}_3)_5]\text{SO}_4$	pentammineazidocobalt(III) sulfate	pentammineazidocobalt(2+) sulfate
h	$[\text{CoBrCl}(\text{H}_2\text{O})(\text{NH}_3)]\text{I}$ (ignore stereochemistry)	ammineaquabromochlorocobalt(III) iodide	ammineaquabromochlorocobalt(1+) iodide

### ? Exercise 8.1.3.6: Nomenclature problems, some of which involve consideration of isomerism.

Name the following compounds and ions in both the Stock and Ewing-Bassett systems. Ignore prefixes for designating isomers if you haven't learned about those.

- $\text{trans-}[\text{Cu}(\text{dppe})_2(\text{NO}_2)_2]$  (the N is bound to Cu)
- $[\text{Pd}(\text{en})_2(\text{SCN})_2]$ , with the thiocyanates bound Pd-SCN
- $[\text{Mn}(\text{CO})_6]\text{BPh}_4$  ( $\text{BPh}_4$  = tetraphenylborate)
- $\text{Rb}[\text{AgF}_4]$
- $\text{K}_2\text{ReH}_9$
- $\text{K}_3\text{CrCl}_6$
- $[\text{Ru}(\text{H}_2\text{O})_6]\text{Cl}_2$
- $[\text{cis-Fe}(\text{CO})_4\text{I}_2]$
- $\text{K}_2[\text{trans-Fe}(\text{CN})_4(\text{CO})_2]$
- $[\text{cis-MnCl}(\text{H}_2\text{O})_4(\text{NH}_3)](\text{NO}_3)$
- $\text{K}_3[\text{fac-RuCl}_3(\text{PMe}_3)_3]$

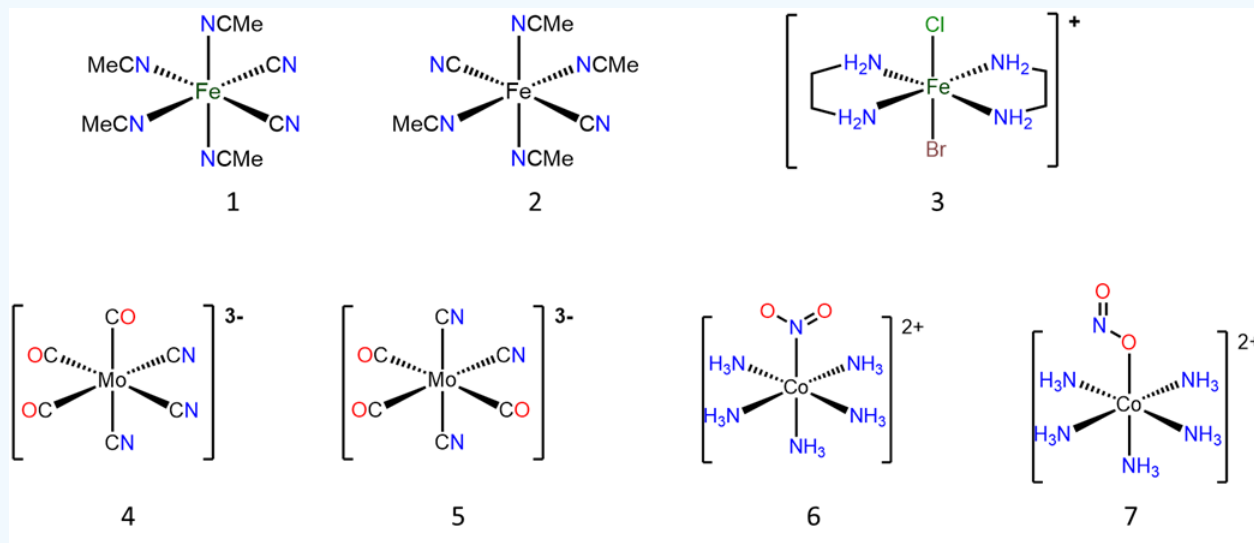
### Answer

	Complex	Stock system name	Ewing-Bassett System name
a	$\text{trans-}[\text{Cu}(\text{dppe})_2(\text{NO}_2)_2]$	<i>trans</i> -bis(diphenylphosphinoethane)bisnitrocopper(II) or <i>trans</i> -bis(diphenylphosphinoethane)bis(nitrito- $\kappa$ N)copper(II)	<i>trans</i> -bis(diphenylphosphinoethane)bisnitrocopper(0) or <i>trans</i> -bis(diphenylphosphino)ethanebis(nitrito- $\kappa$ N)copper(0)
b	$[\text{Pd}(\text{en})_2(\text{SCN})_2]$ , with the thiocyanates bound Pd-SCN	bis(ethylenediamine)bisthiocyanatopalladium(II) or bis(ethylenediamine)bis(thiocyanato-S)palladium(II) or bis(ethylenediamine)bis(thiocyanato- $\kappa$ S)palladium(II)	bis(ethylenediamine)bisthiocyanatopalladium(0) or bis(ethylenediamine)bis(thiocyanato-S)palladium(0) or bis(ethylenediamine)bis(thiocyanato- $\kappa$ S)palladium(0)
c	$[\text{Mn}(\text{CO})_6]\text{BPh}_4$	hexacarbonylmanganese(I) tetraphenylborate	hexacarbonylmanganese(1+) tetraphenylborate
d	$\text{Rb}[\text{AgF}_4]$	rubidium tetrafluoroargentate(III)	rubidium tetrafluoroargentate(1-)
e	$\text{K}_2\text{ReH}_9$	potassium nonahydridorhenium(VII)	potassium nonahydridorhenium(2-)
f	$\text{K}_3\text{CrCl}_6$ or $\text{K}_3[\text{CrCl}_6]$	potassium hexachlorochromium(III) or potassium hexachloridochromium(III)	potassium hexachlorochromium(3-) or potassium hexachloridochromium(3-)
g	$[\text{Ru}(\text{H}_2\text{O})_6]\text{Cl}_2$	hexaaquaruthenium(II) chloride	hexaaquaruthenium(2+) chloride

	Complex	Stock system name	Ewing-Bassett System name
h	$[cis-Fe(CO)_4I_2]$	<i>cis</i> -tetracarbonyldiiodoiron(II)	<i>cis</i> -tetracarbonyldiiodoiron(0)
i	$K_2[trans-Fe(CN)_4(CO)_2]$	potassium <i>trans</i> -dicarbonyltetracyanoferrate(II)	potassium <i>trans</i> -dicarbonyltetracyanoferrate(2-)
j	$[cis-MnCl(H_2O)_4(NH_3)](NO_3)$	<i>cis</i> -amminetetraaquachloromanganese(0) nitrate	<i>cis</i> -amminetetraaquachloromanganese(1+) nitrate
k	$K[fac-RuCl_3(PMe_3)_3]$	potassium <i>fac</i> -trichlorotris(triphenylphosphine)ruthenium(II)	potassium <i>fac</i> -trichlorotris(triphenylphosphine)ruthenium(1-)

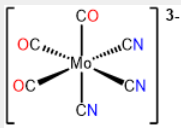
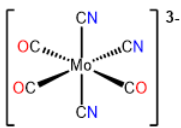

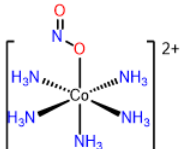
### ? Exercise 8.1.3.7

Name the compounds and ions below using both the Stock and Ewing-Bassett systems. Ignore prefixes for designating isomers if you haven't learned about those.



### Answer

#	Structure	Stock system name	Ewing-Bassett system name
1		<i>cis</i> -tetraacetonitriledicyanoiron(II) or <i>cis</i> -tetraacetonitriledicyanidoiron(II)	<i>cis</i> -tetraacetonitriledicyanoiron(0) or <i>cis</i> -tetraacetonitriledicyanidoiron(0)
2		<i>trans</i> -tetraacetonitriledicyanoiron(II) or <i>trans</i> -tetraacetonitriledicyanidoiron(II)	<i>trans</i> -tetraacetonitriledicyanoiron(0) or <i>trans</i> -tetraacetonitriledicyanidoiron(0)
3		<i>trans</i> -bromochlorobis(ethylenediamine)iron(III) or <i>trans</i> -bromidochloridobis(ethylenediamine)iron(III)	<i>trans</i> -bromochlorobis(ethylenediamine)iron(1+) or <i>trans</i> -bromidochloridobis(ethylenediamine)iron(1+)

#	Structure	Stock system name	Ewing-Bassett system name
4		<i>fac</i> -tricarbonyltricyanomolybdate(0) or <i>fac</i> -tricarbonyltricyanidomolybdate(0)	<i>fac</i> -tricarbonyltricyanomolybdate(3-) or <i>fac</i> -tricarbonyltricyanidomolybdate(3-)
5		<i>mer</i> -tricarbonyltricyanomolybdate(0) or <i>mer</i> -tricarbonyltricyanidomolybdate(0)	<i>mer</i> -tricarbonyltricyanomolybdate(3-) or <i>mer</i> -tricarbonyltricyanidomolybdate(3-)
6		pentamminenitrito- <i>N</i> -cobalt(III), pentamminenitrito- $\kappa$ <i>N</i> -cobalt(III), or pentamminenitrocobalt(III)	pentamminenitrito- <i>N</i> -cobalt(2+), pentamminenitrito- $\kappa$ <i>N</i> -cobalt(2+), or pentamminenitrocobalt(2+)
7		pentamminenitrito- <i>O</i> -cobalt(2+), pentamminenitrito- $\kappa$ <i>O</i> -cobalt(2+), or pentamminenitritocobalt(2+)	pentamminenitrito- <i>O</i> -cobalt(2+), pentamminenitrito- $\kappa$ <i>O</i> -cobalt(2+), or pentamminenitritocobalt(2+)

### ? Exercise 8.1.3.8

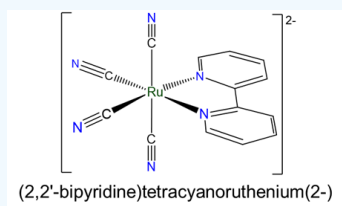
Draw structural formulae for the following compounds and ions. You may assume that

- complexes in which the metal has a coordination number of six are octahedral
- complexes in which the metal has a coordination number of five are trigonal bipyramidal
- complexes in which  $\text{Pt}^{\text{II}}$ ,  $\text{Pd}^{\text{II}}$ , or  $\text{Rh}^{\text{I}}$ , or  $\text{Ir}^{\text{I}}$  have a coordination number of four are square planar
- other complexes in which the metal has a coordination number of four will be tetrahedral

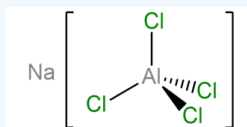
- (2,2'-bipyridine)tetracyanoruthenium(2-)
- sodium tetrachloroaluminate (note that since Al is a main group metal with a generally fixed oxidation state no oxidation state is given)
- pentaamminechlorocobalt(2+) sulfate
- carbonylhydridotris(triphenylphosphine)rhodium(I) (the ligands in this complex occupy sterically preferred positions)
- bromotrichlorocobaltate(III)
- hexaaquacopper(2+) sulfate
- sodium tris(oxalato)cobalt(III)
- fac*-(1,10-phenanthroline)tricarbonylchlororhenium(I)
- mer*-triaquatrichlorochromium(III)
- trans*-dichlorobis(ethylenediamine)platinum(IV)

### Answers

a

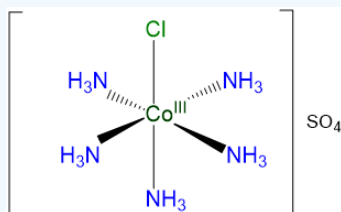


b



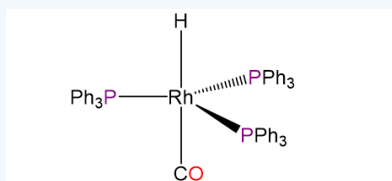
Sodium tetrachloroaluminate

c



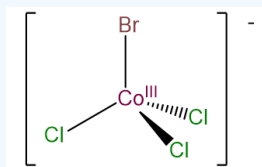
pentaamminechlorocobalt(2+) sulfate

d



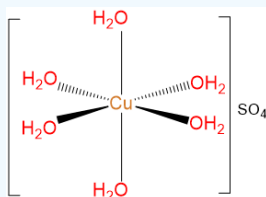
carbonylhydridotris(triphenylphosphine)rhodium(I)

e



bromotrichlorocobaltate(III)

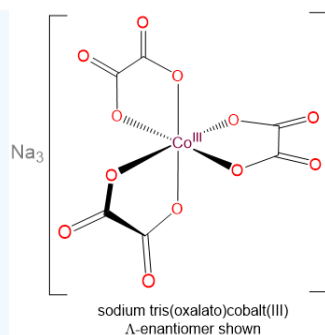
f



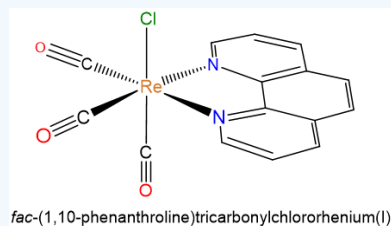
hexaaquacopper(2+) sulfate

g

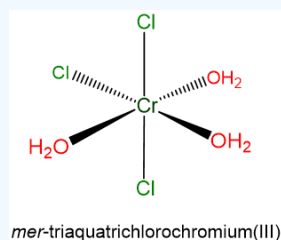




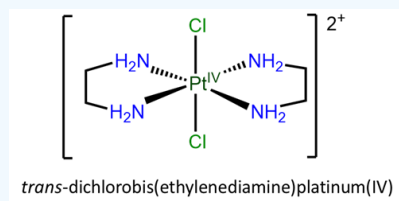
h



i

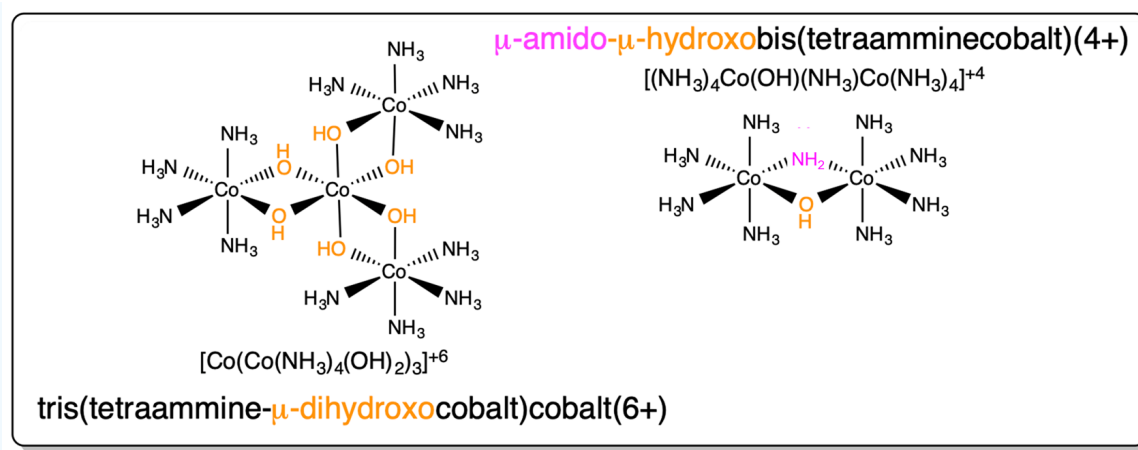


j



### ? Exercise 8.1.3.9.

The name of the structure named tris(tetraammine- $\mu$ -dihydroxocobalt)cobalt(6+) in Scheme 8.1.3.III (reproduced below) is incomplete. Give the complete name of the structure in both the Stock and Ewing-Basset systems.



### Answer

$\Delta$ -tris(tetraammine- $\mu$ -dihydroxocobalt)cobalt(6+) or  $\Delta$ -tris(tetraammine- $\mu$ -dihydroxocobalt(III)cobalt(III)

### Note: Rules for Writing the Formulae of Coordination Compounds

#### Rules for writing the formulae of coordination compounds

The rules for writing the formulae of coordination compounds follow the same convention used to specify their names. However, according to a myth that has been widely propagated on educational websites, the charge need not be listed. As organized predictable formulae can be easier to read and understand than haphazardly written ones, the rules for writing the formulae of coordination compounds have value. To support those who wish to employ them they are given in this section. The rules as given here are adapted from a [summary by Robert Lancashire](#).

1. If there are multiple ions present list the cations before anions.
2. Enclose all the constituents of each complex ion in square brackets.
3. For each complex ion,
  - o Give the **central metal** atom first.
  - o Then **ligands** next, listed in alphabetical order, ignoring prefixes according to the first letters in the ligand's symbol as written. This is true regardless of whether the symbol is an element symbol (like C, N, O, etc.) or a symbol for the ligand name (bpy, en, MeCN, etc.). Contrary to widely-circulated myths, the ligand's charge does not matter.<sup>4</sup>
  - o The formulae or abbreviations (*e.g.* en) for all polyatomic ligands should be enclosed in ordinary parentheses.
  - o As appropriate, use italicized atom symbols to indicate linkage isomerism and prefixes such as *cis*-, *trans*-, *fac*-, *mer*-,  $\Lambda$ -,  $\Delta$ -,  $\kappa^n$ ,  $\eta^n$ ,  $\mu_n$ ,  $\lambda$ -, or  $\delta$ - to indicate stereochemistry.
  - o When a ligand is bound to a metal through a particular atom, preferably place that atom closest to the metal - *e.g.*,  $[\text{Fe}(\text{CN})_6]^{3-}$  not  $[\text{Fe}(\text{NC})_6]^{3-}$  (Note: this rule is used primarily for ambidentate ligands; although IUPAC recommends that aqua ligands be written as  $\text{OH}_2$  when the O would be closest to its coordinated metal, they are still usually written as  $\text{H}_2\text{O}$ ).

These rules are graphically summarized in Figure 8.1.3.2

**prefix-** [ **Metal**(oxidation state)(**ligands**) ] **charge±**

**prefix-** [ **Metal**      oxidation state      (**ligands**) ] **charge±**

**prefix-** [ **Metal**      (**ligands**) ] **charge±**

As appropriate use *cis-*, *trans-*, *fac-*, *mer-*,  $\Lambda$ -,  $\Delta$ -, etc.

Usually goes before the brackets but may be placed inside to avoid ambiguity

Chemical symbol

Optional but use the stock system

Alphabetical by chemical symbol or abbreviation irrespective of ligand charge

Preferably place attached atoms nearest the metal

As appropriate, use  $\kappa$ °,  $\eta$ °,  $\mu$ °,  $\lambda$ -,  $\delta$ -, to indicate structure

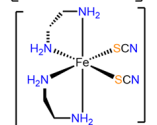
#### Multimetallic complexes:

1. Place bridging ligands after others of the same type in order of bridging multiplicity ( $\mu_4$  then  $\mu_3$  then  $\mu_2$  etc.)
2. May write ligands and metals in a way that indicates structure (e.g.  $[(\text{NH}_3)_5\text{Co}^{\text{II}}-\mu-(\text{OH})-\text{Cr}^{\text{III}}\text{Cl}_2]$  instead of  $[\text{CoCrCl}_2(\text{NH}_3)_5-\mu-\text{OH}]$ )

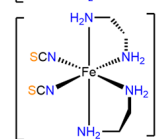
#### Examples:



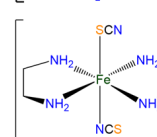
$[\text{Co}(\text{II})(\text{H}_2\text{O})(\text{NH}_3)_5]^{2+}$ ,  $[\text{Co}^{\text{II}}(\text{H}_2\text{O})(\text{NH}_3)_5]^{2+}$ ,  $[\text{Co}(\text{H}_2\text{O})(\text{NH}_3)_5]^{2+}$ ,  $[\text{Co}(\text{II})(\text{NH}_3)_5(\text{OH}_2)]^{2+}$ ,  $[\text{Co}^{\text{II}}(\text{NH}_3)_5(\text{OH}_2)]^{2+}$ , or  $[\text{Co}(\text{NH}_3)_5(\text{OH}_2)]^{2+}$



$\Delta$ -*cis*- $[\text{Fe}(\text{II})(\text{en})_2(\text{SCN})_2]$ ,  
 $\Delta$ -*cis*- $[\text{Fe}^{\text{II}}(\text{en})_2(\text{SCN})_2]$ , or  
 $\Delta$ -*cis*- $[\text{Fe}(\text{en})_2(\text{SCN})_2]$



$\Delta$ -*cis*- $[\text{Fe}(\text{II})(\text{en})_2(\text{NCS})_2]$ ,  
 $\Delta$ -*cis*- $[\text{Fe}^{\text{II}}(\text{en})_2(\text{NCS})_2]$ , or  
 $\Delta$ -*cis*- $[\text{Fe}(\text{en})_2(\text{NCS})_2]$

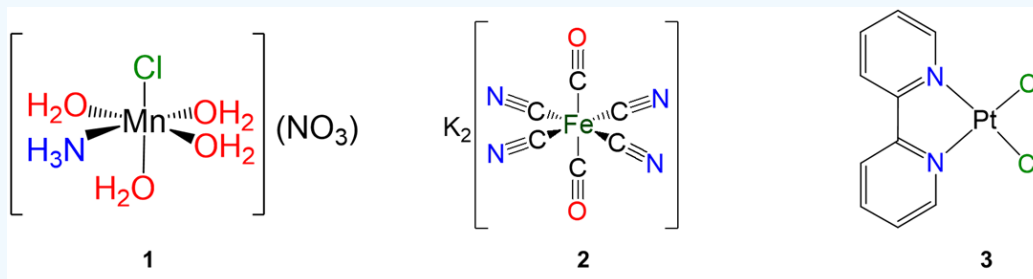


*trans*- $[\text{Fe}(\text{II})(\text{en})_2(\text{NCS})(\text{SCN})]$ ,  
*trans*- $[\text{Fe}^{\text{II}}(\text{en})_2(\text{NCS})(\text{SCN})]$ , or  
*trans*- $[\text{Fe}(\text{en})_2(\text{NCS})(\text{SCN})]$

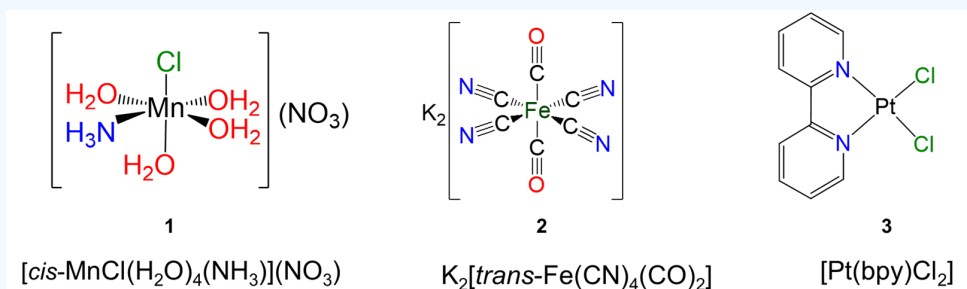
Figure 8.1.3.2. Summary of the rules for writing the formula of a coordination complexes along with a few examples of their application. This work by Stephen Contakes is licensed under a [Creative Commons Attribution 4.0 International License](https://creativecommons.org/licenses/by/4.0/).

#### ? Exercise 8.1.3.10

Give the formulae of the following complexes.



#### Answer

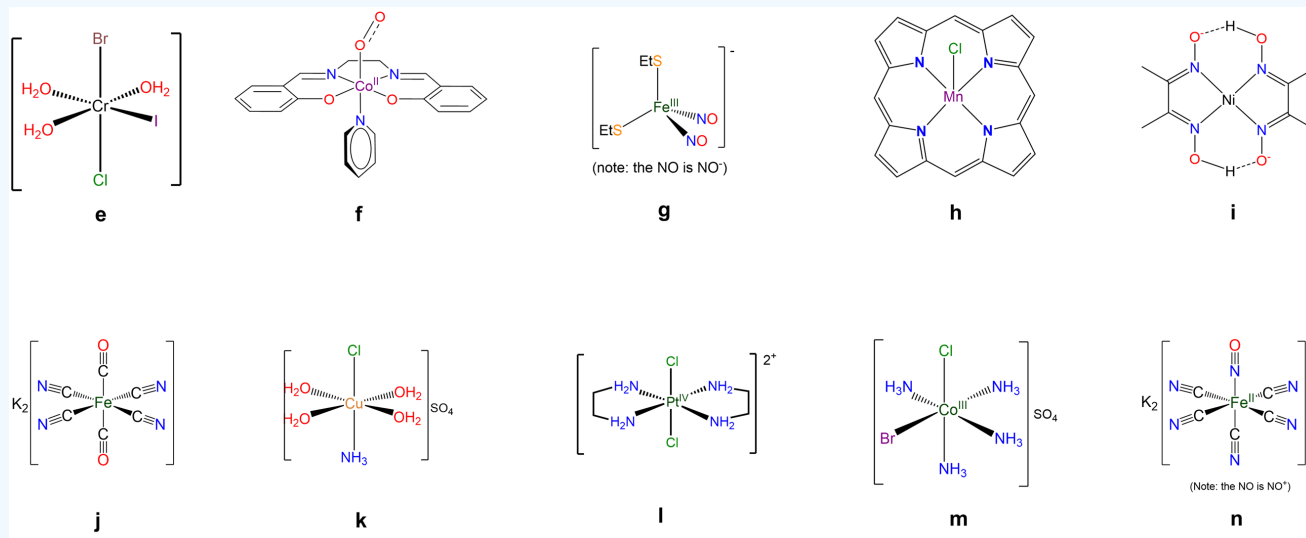


#### ? Exercise 8.1.3.11

Write formulae for each of the following compounds and ions. When multidentate ligands are present use suitable abbreviations.

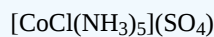
- a. pentaamminechlorocobalt(2+) sulfate
- b.  $\Delta$ -diamminebis(oxalato)manganate(III)
- c. *trans*-tetraacetoneitriledicyanoiron(II)

d. tricarbonyldichlorobis(triphenylphosphine)molybdenum

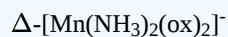


Answers

a.



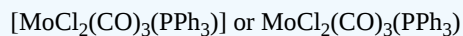
b.



c.



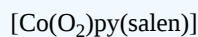
d.



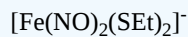
e.



f.



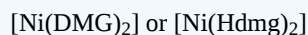
g.



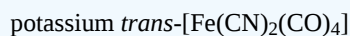
h.



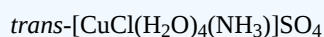
i.



j.



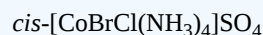
k.



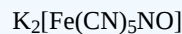
l.



m.



n.

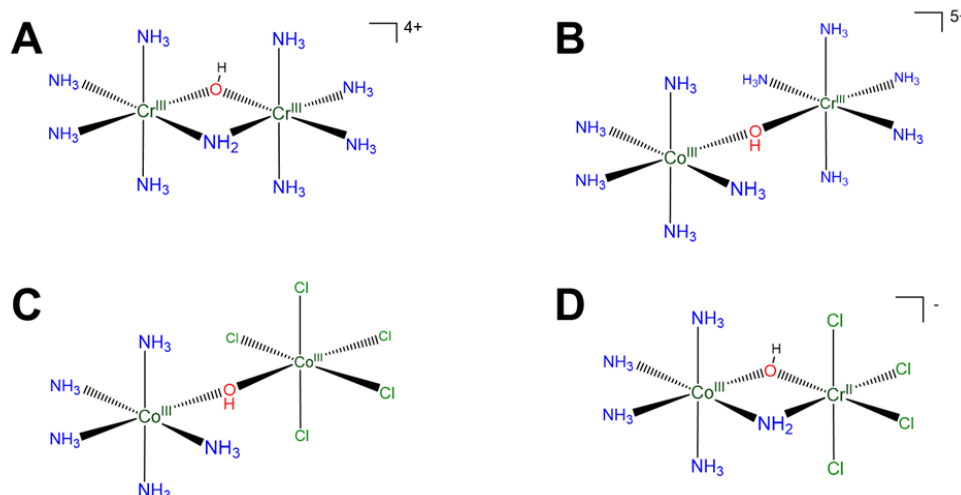


## Multinuclear coordination complexes

Multinuclear coordination complexes contain multiple metals connected by one or more bridging ligands. The structures of bridging complexes can usually be inferred from their  $\mu$ -tagged ligands in their names and formulae. For the benefit of instructors who wish to have their students name multinuclear complexes, the rules are presented below.

Multinuclear complexes are named differently depending on whether the groups on either side of the bridging ligands are identical or different, as shown in Scheme 8.1.3.VIII

**Scheme 8.1.3.VIII.** Multinuclear coordination complexes may be named differently depending on whether the groups on either side of the bridging ligands are the same or different. The groups are the same if the metal, ligands, and ligand arrangement are identical. This is true in A but in B the metals differ, in C the ligands differ, and in D both the metal and ligands differ.



## Naming multinuclear complexes

Let's look at the rules for naming symmetric and asymmetric multinuclear complexes.

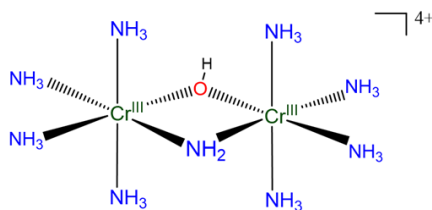
### Application of the IUPAC system and variants thereof to symmetric complexes

The IUPAC naming system helpfully avoids the sort of ambiguities and *ad hoc* choices involved in most textbook-level nomenclature systems for multimetallic complexes. Unfortunately, it is correspondingly difficult for beginners to employ. Thus it will only be applied in depth to the case of symmetric complexes. Symmetric complexes are particularly easy to name in the IUPAC system and several of its variants that find common use. In these

1. The ligands are given in alphabetical order. When there are bridging and non-bridging ligands of the same type the bridging ligands are given first. When there are multiple bridging ligands of the same type but which use different bridging modes (*e.g.*,  $\mu_4$ -,  $\mu_3$ -,  $\mu_2$ -), the bridging ligands are specified in decreasing order of bridging multiplicity, *e.g.*,  $\mu_3$ -sulfido-di- $\mu$ -sulfido.
2. The groups bridged are given afterwards using names that follow the ordinary rules. Generally this involves either
  - a. naming all the ligands followed by all the metals, in both cases using prefixes to indicate the number of each, or
  - b. naming each group of atoms individually as in the less formal naming system, using prefixes to indicate the number of ligands (this is an unofficial variant of the IUPAC system that some textbook authors seem to prefer).

These two rules are sufficient to describe simple symmetric bridging complexes.

Example: The compound in Scheme 8.1.3.VIIIA



may be named

[ $\mu$ -amido- $\mu$ -hydroxo-octaamminedichromium(4+)] ion

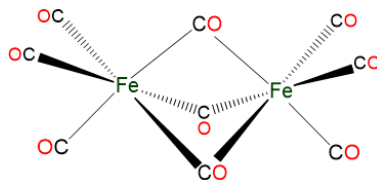
or

[ $\mu$ -amido- $\mu$ -hydroxo-bis(tetraamminechromium(III))] ion

or

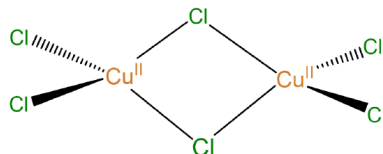
[ $\mu$ -amido- $\mu$ -hydroxo-bis(tetraamminechromium)(4+)] ion

Example: The complex<sup>5</sup>



may be named [tri- $\mu$ -carbonyl-bis(tricarbonyliron)(0)], [tri- $\mu$ -carbonyl-bis(tricarbonyliron(0))], or [tri- $\mu$ -carbonyl-hexacarbonyldiiron(0)]

Example: The complex



may be named di- $\mu$ -chlorido-tetrachloridodicopper(II), di- $\mu$ -chlorido-bis(dichlorocopper(II)), or di- $\mu$ -chlorido-bis(dichlorocopper)(0)

#### A note on the application of the IUPAC system and variants thereof to asymmetric complexes

For a symmetrical complex like the  $[\text{Cu}_2\text{Cl}_4(\mu\text{-Cl})_2]$  considered above it is enough to specify the existence of the two bridging and four terminal chloro ligands; there is no need to number the chloro ligands or to specify exactly which ones are involved in bridging or to clarify that the bridging involves  $\kappa^2$  coordination of the chloro ligands. In cases where the two metal centers or the chloro ligands differ it is necessary to specify the exact ligands and metals involved and how they are connected.

For example, a more extensive IUPAC name for  $[\text{Cu}_2\text{Cl}_4(\mu\text{-Cl})_2]$  in which the chloro ligands are individually and more completely specified would read di- $\mu_2$ -chlorido-tetrachlorido-1 $\kappa^2$ Cl,2 $\kappa^2$ Cl-dicopper(II).

Even more extensive systems would involve numbering the metals and specifying how they are connected together too. The details of how this is done are typically beyond the level of most undergraduate and graduate courses in inorganic chemistry. Those who want to know the details should consult [the red book](#). In many cases it is sufficient to reserve the use of formal IUPAC names for use in publications and to employ a convenient shorthand naming system for everyday use. An example of one type of system that is sometimes employed is given next.

#### Unofficial but commonly used methods applicable to complexes in which the groups bridged are identical or different.

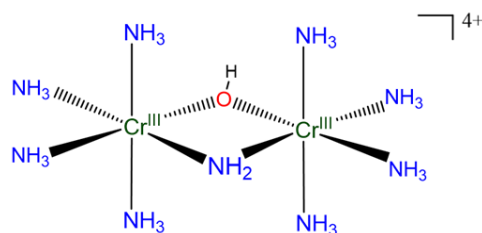
It can be quite complicated to use the IUPAC system to name asymmetric multinuclear coordination complexes. Fortunately it is rarely necessary and there are a variety of simpler somewhat *ad hoc* methods that work well for such cases. Since these methods

are commonly used by textbooks and inorganic instructors it is likely worth your while to learn about their general features. In these methods

1. A multinuclear complex is named as a derivative of one of the metal centers and the other metal centers and their ligands are treated as ligands to the prioritized metal center.
2. Unfortunately, most of the time the choice of which metals are part of the ligands and which one is central is made haphazardly. In other words, there is no agreed upon system for assigning which metal center is the central metal and which should be regarded as part of the ligands around it. One way to be more systematic about the selection of the central and ligand-embedded metals is to assign the central metal as the metal of highest priority in the IUPAC priority rules. In the IUPAC priority rules, the central metal is the highest priority metal alphabetically by name; then if there is a tie the ligands on each tied metal center are ranked alphabetically and the tied metal center with the highest priority (or most highest priority) ligands wins.
3. The metal centers not chosen as the primary metal center and all ligands around them, including those bridging to the winning metal center, are then treated as a single ligand that coordinates the winning metal center.
4. When naming the ligands and the overall complex, again there is much that is haphazard. However, in the best systems each coordination sphere is named using the same rules as for mononuclear complexes - *i.e.*, the ligands are given in alphabetical order, etc.
  - This is true of any metal center-containing ligands.
  - When there is a bridging and non-bridging ligand of the same type, the bridging ligands are given first. When there are multiple bridging ligands of the same type but which use different bridging modes (*e.g.*  $\mu_4^-$ ,  $\mu_3^-$ ,  $\mu_2^-$ ), the ligands are specified in decreasing order of bridging multiplicity, *e.g.*  $\mu_3$ -sulfido-di- $\mu$ -sulfido.

Let's apply these rules to the examples in Scheme 8.1.3.VIII

Compound A:



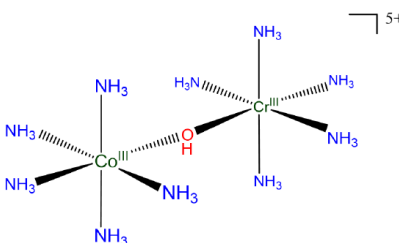
Using hydroxo for the  $\text{OH}^-$ , it may be named

$[(\mu\text{-amido-tetraammine-}\mu\text{-hydroxochromium(III)})\text{tetraamminechromium(III)}]$  ion

or

$[(\mu\text{-amido-tetraammine-}\mu\text{-hydroxochromium})\text{chromium(4+)}]$  ion

Compound B:



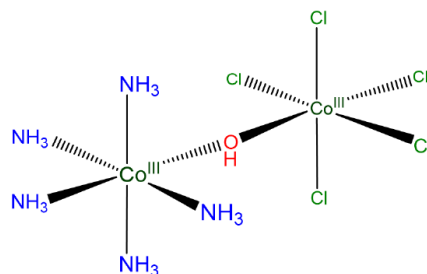
Using hydroxo for the  $\text{OH}^-$ , it may be named

$[(\text{pentaammine-}\mu\text{-hydroxocobalt(III)})\text{tetraamminechromium(III)}]$  ion

or

$[(\text{pentaammine-}\mu\text{-hydroxocobalt})\text{tetraamminechromium(5+)}]$  ion

Compound C:



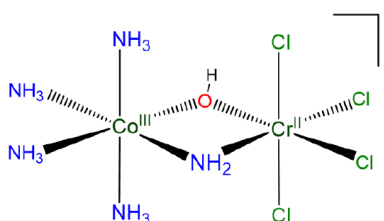
Using hydroxo for  $\text{OH}^-$ , it may be named

[pentaammine(pentachloro- $\mu$ -hydroxocobalt(III))cobalt(III)]

or

[pentaammine(pentachloro- $\mu$ -hydroxocobalt)cobalt](0)

Compound D:



Using hydroxo for  $\text{OH}^-$  and chloro for  $\text{Cl}^-$ , it may be named

[pentaammine(pentachloro- $\mu$ -hydroxocobalt(III))chromate(III)] ion

or

[(tetrammine- $\mu$ -ammine- $\mu$ -hydroxocobalt)tetrachlorochromate](1-) ion

As can be seen from the examples above this system gives serviceable names for multimetallic complexes but those names are not the IUPAC names and so should not be used to describe complexes outside of pedagogical and informal settings.

### Writing and interpreting formulae for multinuclear complexes

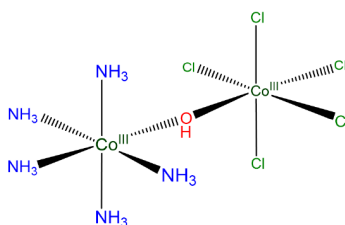
The rules for writing formulae for multinuclear complexes are the same as for mononuclear ones with two added details:

1. Write bridging ligands after nonbridging ligands of the same type. For example,  $\text{Cu}_2\text{Cl}_6$  should be written as  $[\text{Cu}_2\text{Cl}_4(\mu\text{-Cl})_2]$
2. However, you may ignore that and other rules if you find it helpful to keep groups of metals and ligands together in a way that better conveys how the atoms are connected. Just as the structure of ethane may be more clearly conveyed as  $\text{H}_3\text{CCH}_3$  instead of  $\text{CH}_3\text{CH}_3$ , the complex  $[\text{Cu}_2\text{Cl}_4(\mu\text{-Cl})_2]$  may be written as  $[(\text{Cl}_2\text{Cu})(\mu\text{-Cl})_2(\text{CuCl}_2)]$ .

*Other Examples:*

For dichromate write,  $[\text{Cr}_2\text{O}_6(\mu\text{-O})]^{2-}$  or  $[\text{O}_5\text{Cr}-\mu\text{-O}-\text{CrO}_5]^{2-}$

For compound C of Scheme 8.1.3.VIII

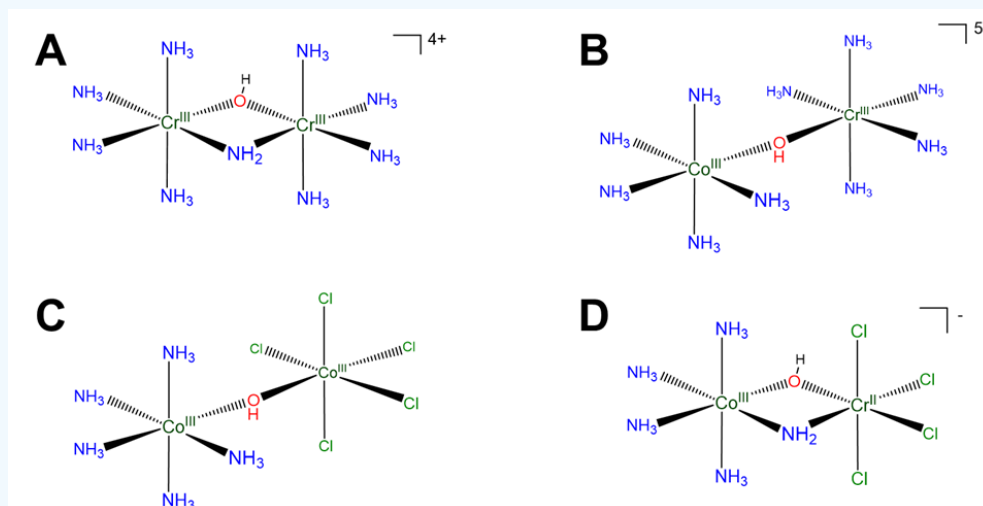


write  $[\text{Co}_2\text{Cl}_5(\text{NH}_3)_5(\mu\text{-OH})]$  or, even better,  $[(\text{H}_3\text{N})_5\text{Co}(\mu\text{-OH})\text{CoCl}_5]$ .



### ? Exercise 8.1.3.10

Write reasonable formulae for complexes A, B, and D in Scheme 8.1.3.VIII which for convenience is reproduced below.



#### Sample answers for A

$[\text{Cr}_2(\text{NH}_3)_8-\mu(\text{NH}_2)-\mu(\text{OH})]^{4+}$  or  $[(\text{H}_3\text{N})_4\text{Cr}^{\text{III}}-\mu(\text{NH}_2)-\mu(\text{OH})-\text{Cr}^{\text{II}}(\text{NH}_3)_4]$  and variants thereof involving writing the  $\text{H}_3\text{N}$  as  $\text{NH}_3$ ,  $\mu$  as  $\mu_2$ , etc.

#### Sample answers for B

$[\text{CoCr}(\text{NH}_3)_{10}-\mu(\text{OH})]^{5+}$  or, better,  $[(\text{H}_3\text{N})_5\text{Co}^{\text{III}}-\mu(\text{OH})-\text{Cr}^{\text{III}}(\text{NH}_3)_5]^{5+}$

#### Sample answers for C

This was already done as an example above,  $[\text{Co}_2\text{Cl}_5(\text{NH}_3)_5-\mu(\text{OH})]$  or, better,  $[(\text{NH}_3)_5\text{Co}^{\text{III}}-\mu(\text{OH})-\text{Co}^{\text{III}}\text{Cl}_5]$  and variants thereof

#### Sample answers for D

$[\text{CoCrCl}_4(\text{NH}_3)_4-\mu(\text{NH}_2)-\mu(\text{OH})]$  or, better,  $[(\text{H}_3\text{N})_4\text{Co}^{\text{III}}-\mu(\text{NH}_2)-\mu(\text{OH})-\text{Cr}^{\text{II}}\text{Cl}_4]$

## References

1. International Union of Pure and Applied Chemistry *Nomenclature of Inorganic Chemistry* Cambridge, UK, 2005.
2. The structure and name is taken from Choudhury, S. B.; Allan, C. B.; Maroney, M.; Woodward, A. D.; Lucas, C. R. *Inorg. Synth.* **1998**, 32, 98-107.
3. Haas, K. Naming Transition Metal Complexes. [https://chem.libretexts.org/Courses/Saint\\_Mary's\\_College%2C\\_Notre\\_Dame%2C\\_IN/CHEM\\_342%3A\\_Bioinorganic\\_Chemistry/Readings/Week\\_2%3A\\_Introduction\\_to\\_Metal-Ligand\\_Interactions\\_and\\_Biomolecules/2.1\\_Transition\\_metal\\_complexes/2.1.6%3A\\_Naming\\_Transition\\_Metal\\_Complexes](https://chem.libretexts.org/Courses/Saint_Mary's_College%2C_Notre_Dame%2C_IN/CHEM_342%3A_Bioinorganic_Chemistry/Readings/Week_2%3A_Introduction_to_Metal-Ligand_Interactions_and_Biomolecules/2.1_Transition_metal_complexes/2.1.6%3A_Naming_Transition_Metal_Complexes)
4. There is a widely-circulated myth that anionic ligands should be named before neutral ones. This myth is false. According to the IUPAC red book (bolding mine):

IR-2.15.3.4: Ordering ligands in formulae and names in formulae of coordination compounds,

The formulae or abbreviations representing the ligands **are cited in alphabetical order as the general rule**. Bridging ligands are cited immediately after terminal ligands of the same kind, if any, and in increasing order of bridging multiplicity. (See also Sections IR-9.2.3 and IR-9.2.5.)

IR-9.2.3.1 Sequence of symbols within the coordination formula

(i) The central atom symbol(s) is (are) listed first.

(ii) The **ligand symbols (line formulae, abbreviations or acronyms)** are then listed in alphabetical order (see Section IR-4.4.2.2).<sup>5</sup> Thus, CH<sub>3</sub>CN, MeCN and NCMe would be ordered under C, M and N respectively, and CO precedes Cl because single letter symbols precede two letter symbols. **The placement of the ligand in the list does not depend on the charge of the ligand.**

(iii) More information is conveyed by formulae that show ligands with the donor atom nearest the central atom; this procedure is recommended wherever possible, even for coordinated water.

5. Technically organometallic complexes are named according to slightly different rules but the coordination compound naming system works here. Note that this complex was once thought to possess an Fe-Fe bond, in accordance with the predictions of the 18-electron rule. Consequently, older sources often give an [Fe-Fe] after the name to reflect the presence of that bond. However, as the complex is no longer thought to possess an Fe-Fe bond it is omitted here.

## Contributors and Attributions

Stephen Contakes, Westmont College, to whom comments, corrections, and criticisms should be addressed.

with some examples taken from [Naming Transition Metal Complexes](#) by Kathryn Haas.

Consistent with the policy for original artwork made as part of this project, all unlabeled drawings of chemical structures are by Stephen Contakes and licensed under a [Creative Commons Attribution 4.0 International License](#).

---

8.1.3: Nomenclature and Ligands is shared under a [not declared](#) license and was authored, remixed, and/or curated by Stephen M. Contakes.

- [9.3: Nomenclature and Ligands](#) by Stephen M. Contakes has no license indicated.

## 8.1.4: Coordination Numbers and Structures

### 8.1.4.1 Why do coordination complexes form the structures they do?

As with all chemical structure, coordination complexes form the structures they do so as to best stabilize the metal center and ligands through the formation of metal-ligand bonds while avoiding destabilizing interactions like steric repulsions. The issue then is how many metal-ligand bonds should be formed and how those bonds should be arranged spatially to give the largest net stabilization possible. This question will eventually be [considered in detail in connection with the nature of bonding in coordination compounds](#). For now, it will be helpful to think about it in terms of seven factors:

#### 8.1.4.1.1 The stabilizing effect of metal-ligand bond formation.

The driving force for complex formation is the stabilization of electrons in covalent chemical bonds. In the vast majority of cases, this largely involves stabilization of the ligand lone pair as it experiences the effective nuclear charge of the metal, although a few instances involve stabilization of metal electrons by ligand nuclei (inverse ligand fields). Regardless, metal-ligand bond formation is stabilizing and classified by the way it preferences the addition of ligands to the complex.

#### 8.1.4.1.2 Steric effects, specifically steric repulsions between ligands.

One reason coordination numbers do not increase indefinitely is that only so many ligands can fit around a metal. Exactly how many depends on

- *the size of the metal center.* This is one of the more important factors. Many metals tend to exhibit preferred coordination numbers, which depend on their oxidation state and size as shown in Figure 8.1.4.1. Larger inner transition metals like the Lanthanides and Actinides can accommodate 9-12 sterically undemanding ligands, while the smaller transition metals tend to accommodate up to six, although larger coordination numbers are more common for low valent metals and as size increases on moving from right to left across the transition metal block of the periodic table. Thus, the early transition metal molybdenum forms seven- and eight-coordinate  $[\text{Mo}^{\text{III}}(\text{CN})_7]^{4-}$  and  $[\text{Mo}^{\text{IV}}(\text{CN})_8]^{4-}$  with the sterically undemanding cyano ligand.
- *the size of the ligands.* As long as ligands are not excessively rigid and bulky, their size is less important than the size of the metal in determining the number of ligands that coordinate. Ligands' ability to donate electrons to the metal center also tends to influence coordination number more than ligand size. However, all other things being equal for a given metal and ligand donor ability, small ligands allow higher coordination numbers while fewer bulky ligands will fit around the metal center.
- *how the ligand bonds to the metal.* Again, all other things being equal, ligands that are more sterically demanding in the vicinity of the metal center tend to limit the ability of other ligands to bind more than those which bind through a small extended group. For example, a bulky isocyanide like  $t\text{-BuCN}$  will sterically crowd the metal less than a bulky phosphine like  $t\text{-BuH}_2\text{P}$  would. For this reason the effective size of a ligand is sometimes rated in terms of either a cone angle of space they are estimated to occupy around the metal (called the Tolman cone angle, it is commonly used to evaluate phosphines' steric bulk) or in terms of the percentage of the metal's coordination sphere the ligand occupies (called the percent buried volume, it is used to estimate the steric impact of  $N$ -heterocyclic carbenes).

3	4	5	6	7	8	9	10	11	12
Sc Sc <sup>3+</sup>	Ti Ti <sup>2-4+</sup>	V V <sup>2-4+</sup>	Cr Cr <sup>2-3+</sup>	Mn Mn <sup>1-3+</sup>	Fe Fe <sup>2-3+</sup>	Co Co <sup>+</sup> Co <sup>2-3+</sup>	Ni Ni <sup>2+</sup> Ni <sup>3+</sup>	Cu Cu <sup>+</sup> Cu <sup>2+</sup>	Zn Zn <sup>2+</sup>
Y Y <sup>3+</sup>	Zr Zr <sup>4+</sup>	Nb Nb <sup>5+</sup>	Mo Mo <sup>2+</sup> Mo <sup>3-5+</sup> Mo <sup>6+</sup>	Tc Tc <sup>3+</sup>	Ru Ru <sup>2-3+</sup>	Rh Rh <sup>+</sup> Rh <sup>3+</sup>	Pd Pd <sup>2+</sup> Pd <sup>4+</sup>	Ag Ag <sup>+</sup>	Cd Cd <sup>2+</sup>
La-Lu	Hf Hf <sup>4+</sup>	Ta Ta <sup>5+</sup>	W W <sup>2+</sup> W <sup>4-6+</sup>	Re Re <sup>1,3-5+</sup> Re <sup>7+</sup>	Os Os <sup>2-4,6+</sup>	Ir Ir <sup>+</sup> Ir <sup>3+</sup>	Pt Pt <sup>2+</sup> Pt <sup>4+</sup>	Au Au <sup>+</sup> Au <sup>3+</sup>	Hg Hg <sup>2+</sup>
Ac-Lr	Rf	Db	Sg	Bh	Hs	Mt	Ds	Rg	Cn

**Key**

= linear   
 = square planar   
 = square pyramidal   
 = trigonal bipyramidal   
 = octahedral   
 = capped trigonal prismatic   
 = trigonal prismatic   
 = square planar/ elongated octahedral

Figure 8.1.4.1. Preferred coordination geometries of the transition elements. Assignments are as reported in reference 1 except for Cu<sup>2+</sup>, which is assigned above as square planar/elongated octahedral instead of the square planar assignment given in that work. This work by Stephen Contakes is licensed under a [Creative Commons Attribution 4.0 International License](https://creativecommons.org/licenses/by/4.0/).

#### 8.1.4.1.3 Repulsion between M-L bonding electrons on different ligands.

For many complexes, steric effects are neither the only effects nor the most important. Among the additional factors that should be considered are the repulsions that occur between the electrons that different ligands donate to the metal-ligand bonding. These electron-electron repulsions affect the

- Coordination number.** When a ligand donates its electrons to a metal center to form a new metal-ligand bond, the electron density around the metal increases, raising the overall energy of the other M-L bonding electrons. This increased repulsion often limits the number of coordinated ligands. As more ligands are added, the electron-electron repulsions keep increasing until the lowering of energy of the ligand electrons in the new bond is insufficient to compensate for the raising of energy of the existing M-L bonding electrons. Based on this effect alone,
  - larger metals tend to achieve higher coordination numbers than smaller ones because the electron-electron repulsions are spread across a larger coordination sphere.
  - With a given metal, ligands that are more electron donating have a greater tendency to form complexes with lower coordination numbers with a given metal than similar neutral ones do. This is why anionic ligands (which tend to be better electron donors) tend to give lower coordination numbers than comparable neutral ligands (which tend to be weaker donors). Thus Co<sup>2+</sup> forms CoCl<sub>4</sub><sup>2-</sup> with chloro ligands but [Co(H<sub>2</sub>O)<sub>6</sub>]<sup>2+</sup> with aqua ligands.
- Coordination geometry.** In the **Kepert model** for the shapes of coordination complexes, this intraligand repulsion determines the most stable coordination geometry by causing the ligands to move as far apart from one another on the metal's coordination sphere as possible.

Formally, according to the **Kepert model**

- any of the metal's valence electrons not involved in metal-ligand bonds occupy (n-1)d orbitals and function as core electrons. As core electrons they do not influence the molecular shape.
- electrons involved in bonding to a given ligand constitute an electron group that repels all other electron groups around the metal.
- all other things being equal, the complex will form the geometry that maximizes the intra-electron group repulsions.

Notice the similarities of these postulates to those of VSEPR theory. In predicting coordination geometries in terms of electron-electron repulsions, the Kepert model is just an extension of VSEPR theory to coordination compounds. The difference between

VSEPR theory and the Kepert model is that in the Kepert model, only electrons involved in metal-ligand bonds count.

Coordination geometries predicted by the Kepert model for coordination numbers two through nine are given in Figure 8.1.4.2 As may be seen from the geometries listed in Figure 8.1.4.2 these are just equivalent to VSEPR geometries for cases in which the number of electron groups is equal to the coordination number.

The difference between optimal and suboptimal coordination geometries is greater with few ligands, and becomes smaller as ligands become increasingly dispersed across the metal's coordination sphere. In complexes containing five, seven, eight, or higher coordinate metals, there are a number of geometries that are similar in energy to the preferred geometry. These geometries, which should be regarded as accessible, are also listed in Figure 8.1.4.2

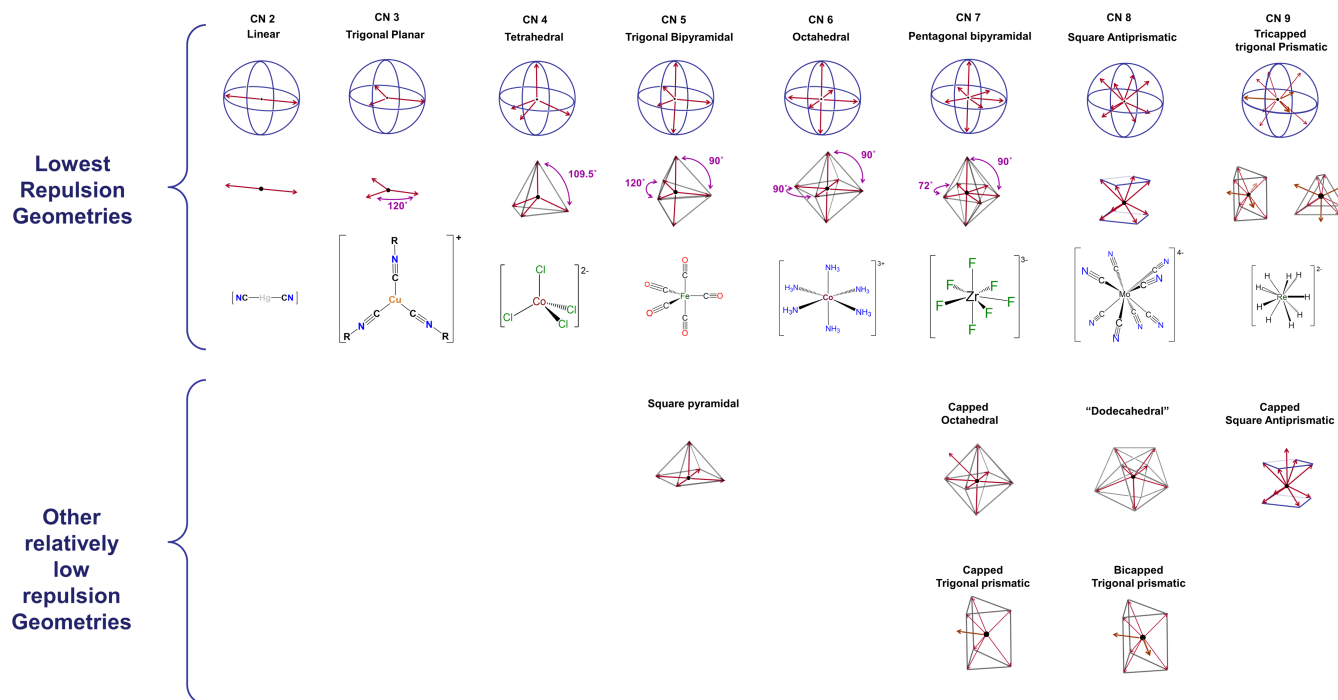


Figure 8.1.4.2. Coordination geometries predicted by the Kepert model for coordination numbers two through nine along with other coordination geometries similar in energy to the lowest repulsion geometry. This work by Stephen Contakes is licensed under a [Creative Commons Attribution 4.0 International License](https://creativecommons.org/licenses/by/4.0/).

#### 8.1.4.1.4 d-electron effects

A few coordination geometries are noticeably absent from the Kepert-preferred and Kepert-accessible geometries in Figure 8.1.4.1. These include the trigonal prismatic geometries formed by compounds like  $\text{W}(\text{CH}_3)_6$  and the very common square planar geometry illustrated by complexes like  $[\text{PtCl}_4]^{2-}$  and  $[\text{IrCl}(\text{PPh}_3)_2]$ . One of the reasons the Kepert model fails to predict the existence of such structures is its neglect of directional interactions involving  $d$  electrons on the metal center. Metal  $d$  electrons exert a profound influence on almost all properties of transition metal complexes, including their structures. The way in which this occurs will be explored at length in [the next chapter](#). For now, it is enough to note that both the ligand-donated electrons surrounding a metal center and the electrons occupying particular  $d$  orbitals on that metal are oriented in specific directions relative to one another. Because of this, the strength of the interactions between the ligand and metal  $d$  electrons depends on the number of  $d$  electrons present, how strongly metal-ligand binding affects their energy, and how the ligands are arranged about the metal center. The impact of these effects, here termed ligand field effects, differs from case to case and can include

- distortions of the complex's geometry. For instance, an ideal octahedral coordination geometry might be tetragonally distorted by flattening or elongating it.
- imparting a strong preference for non-Kepert coordination geometries. This is why, for example, 2nd and 3rd row complexes in which the metal has a  $d^8$  electron configuration are almost always square planar.
- stabilizing non-Kepert geometries enough to permit complexes to adopt them in the presence of a rigid or semirigid ligand that prefers to coordinate the metal in that geometry.<sup>3</sup>

Because of these effects, square planar and trigonal prismatic geometries are also observed, and the list of coordination geometries given in Figure 8.1.4.2 may be extended to that shown in Figure 8.1.4.3

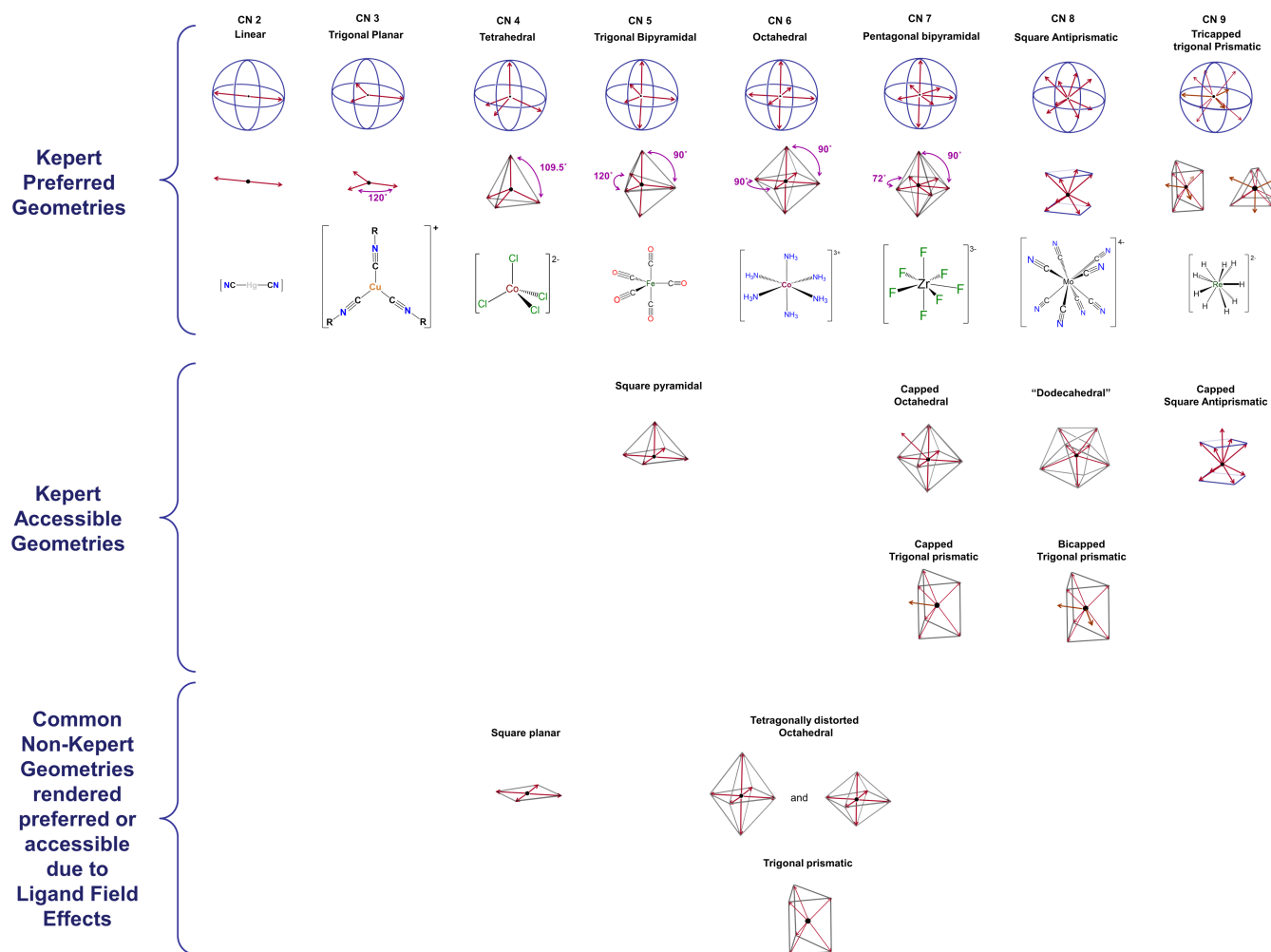


Figure 8.1.4.3. Coordination geometries accessible for 2-9 coordinate complexes even without constraint by rigid or semirigid ligands. This work by Stephen Contakes is licensed under a [Creative Commons Attribution 4.0 International License](https://creativecommons.org/licenses/by/4.0/).

#### 8.1.4.1.5 Ligand constraints imposed by rigid or semirigid ligands

Rigid or semirigid ligands influence the coordination geometry of metal complexes in two main ways:

- Bulky rigid ligands that crowd the metal center prevent other ligands from binding. Thus such ligands are useful for preparing low-coordinate complexes.
- Rigid and semirigid ligands can impose their preferred coordination geometry on a metal center. This is because these ligands energetically prefer to adopt a particular conformation when they bind a metal center. In doing so they shift the coordination geometry energy landscape toward that preferred geometry. If the shift is large enough relative to the native preference due to ligand repulsion and ligand field effects, the complex will either adopt the ligand-preferred geometry or be distorted in the direction of the ligand-preferred geometry. Examples are given in Figure 8.1.4.4

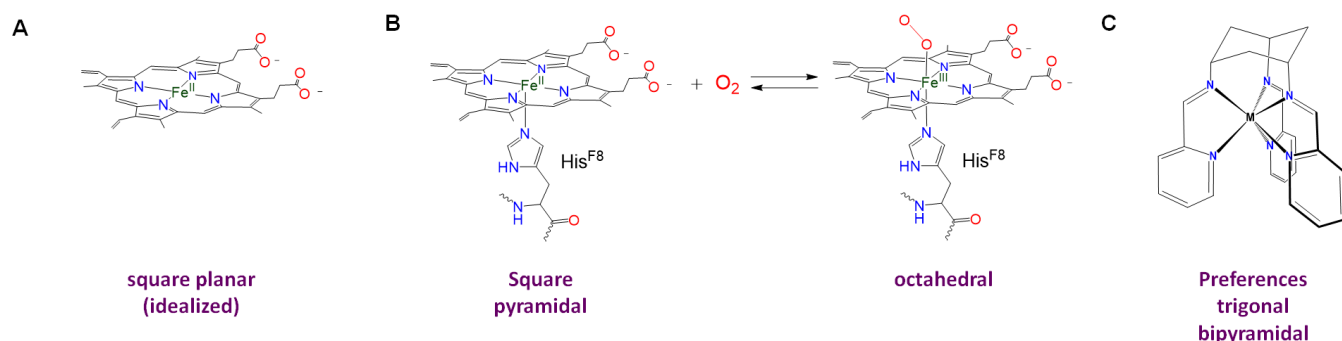


Figure 8.1.4.4. Examples of rigid/semirigid ligands that can impose their preferred coordination geometry on a metal center. Porphyrins, phthalocyanines and related macrocycles tend to impose a slightly bent square planar coordination geometry, although (B) many such complexes, including the iron of myoglobin's heme cofactor, coordinate additional ligands to give square planar or octahedral complexes. (C) Synthetic multidentate ligands have been developed to preference trigonal prismatic coordination geometries, including the one shown here. It forms roughly trigonal prismatic complexes with  $\text{Co}^{\text{II}}$  and  $\text{Zn}^{\text{II}}$ , albeit imperfect ones.<sup>3</sup> This work by Stephen Contakes is licensed under a [Creative Commons Attribution 4.0 International License](https://creativecommons.org/licenses/by/4.0/).

The influence of ligands on coordination geometry is important in living systems, in which proteins and nucleic acids can act as rigid or semirigid ligands. The ability of these ligands to distort the coordination geometries of metal atoms in ways that enable them to perform specific functions is so common that the resulting distorted geometries are termed entactic states. A particularly spectacular case of an entactic state involves the blue copper proteins azurin and plastocyanin, the structure of which is given in Figure 8.1.4.5

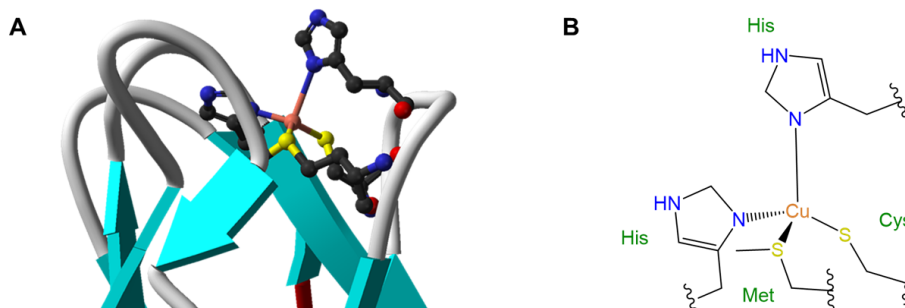


Figure 8.1.4.5. (A) Structure and (B) schematic of the plastocyanin active site showing the distorted tetrahedral coordination environment that the protein imposes on the copper center (tan), which is most evident from the long vertically oriented Cu-Histidine bond. The image in part A is cropped from an original image by Ben Mills - Own work, Public Domain, <https://commons.wikimedia.org/w/index.php?curid=6202620>. The image in part B is by Stephen Contakes and licensed under a [Creative Commons Attribution 4.0 International License](https://creativecommons.org/licenses/by/4.0/).

As may be seen from the structure in Figure 8.1.4.5 the copper in plastocyanin exhibits a distorted tetrahedral coordination geometry. The protein is said to act like a medieval torture device called a rack in stretching the metal into its distorted geometry. This distortion makes it easier for the copper center to undergo facile redox reactions, enabling it to better function as an electron carrier.

#### 8.1.4.1.6 Crystal packing effects, in which the energy-lowering packing of molecules and ions in a crystal drives the distortion of a complex's structure away from what it would adopt in the gas phase or solution

This effect is similar to that of ligand constraints except that in this case it arises not from the structure internal to a ligand but out of the forces involved in maximizing the stabilization energy of a crystal. With lower coordination number complexes, packing effects can shift the conformations of flexible ligands but only give rise to very small distortions of the overall coordination geometry. Packing effects can drive a shift in the overall coordination geometry of higher coordination number complexes, for which packing effects are significant relative to the small difference in energy between geometries. Thus while  $[\text{Mo}(\text{CN})_8]^{4-}$  has a square antiprismatic coordination geometry, in solution it exhibits a dodecahedral coordination geometry in the crystals of many of its salts.

#### 8.1.4.1.7 Relativistic effects on orbital energies

The proximity of fast moving electrons to massive nuclei in the heavier transition elements results in relativistic expansion and contraction of orbitals. The net results are that

- heavier elements tend to be smaller than expected. This effect preferences lower coordination numbers.
- the relative energies of orbitals shift. Orbitals which become contracted are lowered in energy while those which are expanded increase in energy, as shown for the case of gold in Figure 8.1.4.6A

The combination of smaller sizes and altered orbital energies affects coordination preferences. Relativistic effects contribute to the greater tendency of  $\text{Au}^{\text{I}}$  relative to other group 11 metals to form linear two-coordinate complexes. As shown in Figure 8.1.4.6B, the relative closeness in energy of the 6s and 5d orbitals of gold makes mixing of these orbitals more favorable, facilitating the ability of gold to form two-coordinate complexes with strong sigma bonds oriented  $180^\circ$  from one another.

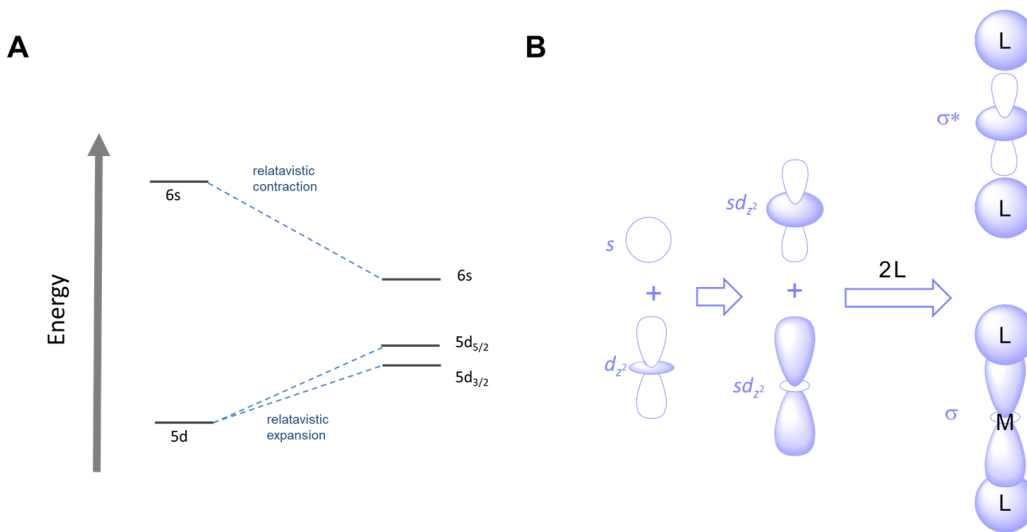


Figure 8.1.4.6. (A) Gold experiences relativistic expansion and contraction of its 5d and 6s orbitals, resulting in shifts to their relative energies. (B) This makes mixing of these orbitals more favorable, facilitating the ability of gold to form two-coordinate complexes with strong sigma bonds that involve considerable  $sd_{z^2}$  character. This work by Stephen Contakes is licensed under a [Creative Commons Attribution 4.0 International License](#).

#### 8.1.4.2 What structures do coordination complexes form?

Metal complexes with coordination numbers ranging from one to 16 are known, although values greater than seven are rare for the transition metals. In this section, examples of common coordination geometries will be presented in order of coordination number.

##### 8.1.4.2.1 Coordination Number 1.

Condensed phase monocoordinate complexes are unknown for the transition metals, although the post-transition metals Tl and In form monocoordinate complexes with the bulky ligands triazapentadienyl and 2,6-tris(2,4,6-triisopropylphenyl)benzene as shown in Figure 8.1.4.7.

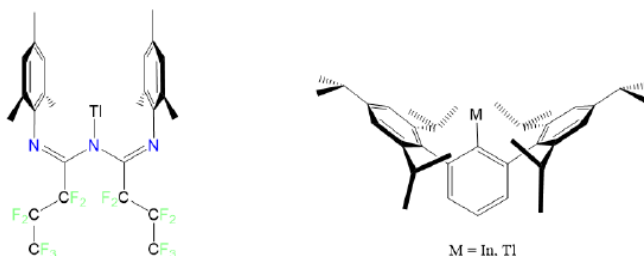
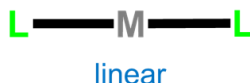


Figure 8.1.4.7. No monocoordinate transition metal complexes are known, but  $\text{Tl}^+$  and  $\text{In}^+$  form monocoordinate complexes with extremely bulky ligands. This work by Stephen Contakes is licensed under a [Creative Commons Attribution 4.0 International License](#).



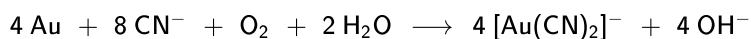
#### 8.1.4.2.2 Coordination Number 2.

A coordination number of 2 is rare outside of  $d^{10}$  complexes of the group 11 metals and mercury, specifically,  $\text{Cu}^+$ ,  $\text{Ag}^+$ ,  $\text{Au}^+$ , and  $\text{Hg}_2^{2+}$ . In accordance with the predictions of the Kepert model these give **linear complexes**.



Among these,

- $\text{Cu}^+$  more commonly gives tetrahedral complexes but can be coaxed to give linear ones. The most prominent example is  $[\text{CuCl}_2]^-$ , which forms when  $\text{CuCl}$  is treated with concentrated  $\text{HCl}$  under anoxic conditions.
- $\text{Ag}^+$  also commonly forms tetrahedral or trigonal planar complexes but can give linear ones. The most prominent example is  $[\text{Ag}(\text{NH}_3)_2]^+$ , which can be formed by treating silver salts with concentrated aqueous or liquid ammonia.
- $\text{Au}^+$  almost always forms linear complexes, but many of these formally two-coordinate complexes associate as depicted in Figure 8.1.4.8 The ability of  $\text{Au}^+$  to form linear complexes with cyanide is even used to selectively extract metallic gold from low grade ores. The stability of  $[\text{Au}(\text{CN})_2]^-$  means that the dissolution of metallic gold in aqueous cyanide is thermodynamically favorable under aerobic conditions.



- $\text{Hg}_2^{2+}$ , like  $\text{Au}^+$ , benefits from relativistic effects and more commonly forms two-coordinate complexes with a linear geometry. Among these is  $[\text{Hg}(\text{CN})_2]$ . However, its preference for linearity is not as rigid as for  $\text{Au}^+$ , and so complexes with a variety of coordination geometries are known.

And by means of honorary mention, the mercury(I) ion,  $\text{Hg}_2^{2+}$ , forms linear complexes of the type  $\text{L-Hg-Hg-L}$ , although since  $\text{Hg}_2^{2+}$  is often considered as a single unit, these aren't always considered to be two-coordinate complexes.

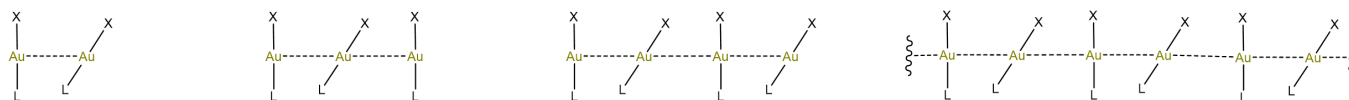


Figure 8.1.4.8. Many "linear" gold complexes associate side-on to form dimers, trimers, tetramers, and chains. Although in this chapter  $\text{L}$  is usually taken to represent a generic ligand, in this scheme  $\text{L}$  represents a neutral ligand that donates two electrons to the metal ( $\text{py}$ ,  $\text{PR}_3$ ,  $\text{CO}$ , etc.) and  $\text{X}$  an anionic one (e.g.,  $\text{Cl}^-$ ,  $\text{CN}^-$ , etc.). Exactly which structure forms depends on the identity of  $\text{L}$  and  $\text{X}$ . Redrawn from reference 5. This work by Stephen Contakes is licensed under a [Creative Commons Attribution 4.0 International License](#).

Two-coordinate complexes may also be formed through the use of bulky ligands that only allow for the binding of two to the metal center. The classic examples are given in Figure 8.1.4.9

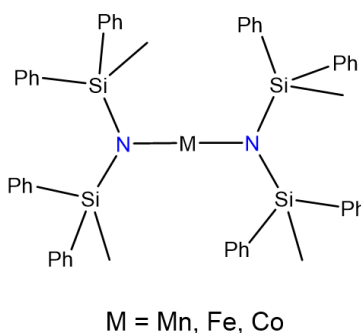


Figure 8.1.4.9. Two-coordinate complexes form between  $\text{Mn}^{2+}$ ,  $\text{Fe}^{2+}$ , and  $\text{Co}^{2+}$  with  $\text{N}(\text{SiMePh}_2)_2$ .<sup>6</sup> This work by Stephen Contakes is licensed under a [Creative Commons Attribution 4.0 International License](#).

#### 8.1.4.2.3 Coordination Number 3

Three-coordinate complexes are similar to two-coordinate ones in that they are rare and, aside from the constraining influence of ligands, usually limited to  $d^{10}$  metal ions such as  $\text{Cu}^+$ ,  $\text{Ag}^+$ ,  $\text{Au}^+$ ,  $\text{Hg}_2^{2+}$ , and  $\text{Pt}(0)$ . As expected from the Kepert model, in the absence of constraining ligands, three-coordinate complexes are trigonal planar.

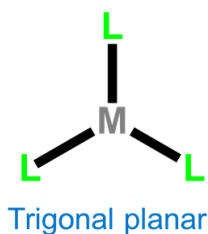


Figure 8.1.4.10.

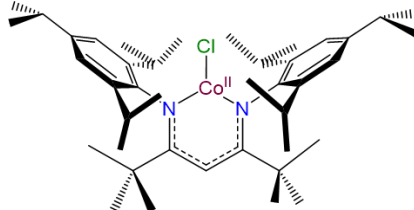
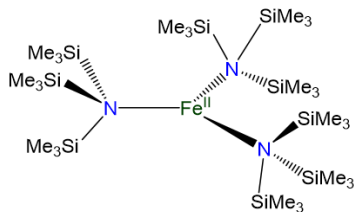
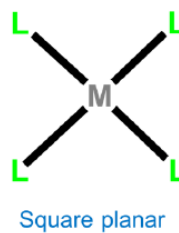
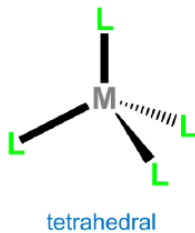


Figure 8.1.4.10. Three-coordinate complexes prepared using bulky and semirigid ligands. This work by Stephen Contakes is licensed under a [Creative Commons Attribution 4.0 International License](https://creativecommons.org/licenses/by/4.0/).

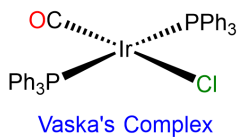
#### 8.1.4.2.4 Coordination Number 4

The two common four-coordinate geometries are tetrahedral and square planar.



**Tetrahedral complexes** are commonly formed by metals possessing either a  $d^0$  or  $d^{10}$  electron configuration. Monometallic examples of  $d^0$  configurations include  $\text{TiCl}_4$ ,  $\text{VO}_4^{3-}$ ,  $\text{WS}_4^{2-}$ ,  $\text{MnO}_4^-$ ,  $\text{CrO}_4^{2-}$ , and  $\text{OsO}_4$ , while  $d^{10}$  examples are  $[\text{Ni}(\text{CO})_4]$ ,  $[\text{HgBr}_4]^{2-}$ ,  $[\text{ZnCl}_4]^{2-}$ , and  $[\text{CdI}_4]^{2-}$ . For other electron configurations, tetrahedral complexes are known but much less common. Examples usually involve good donor ligands and include  $[\text{FeCl}_4]^-$  ( $d^5$ ),  $[\text{CoCl}_4]^{2-}$  ( $d^6$ ), and  $[\text{NiCl}_4]^{2-}$  ( $d^7$ ).

Second and third row transition metal centers with  $d^8$  electron configurations like  $\text{Rh}^+$ ,  $\text{Ir}^+$ ,  $\text{Pd}^{2+}$ ,  $\text{Pt}^{2+}$ , and  $\text{Au}^{3+}$  almost exclusively exhibit **square planar geometries**. Beyond this, square planar geometries are often formed by  $\text{Ni}^{2+}$  ( $d^8$ ),  $\text{Ni}^{3+}$  ( $d^7$ ), and  $\text{Cu}^{2+}$  ( $d^9$ ). Examples of square planar complexes include  $[\text{Cu}(\text{acac})_2]$ ;  $[\text{PtCl}_4]^{2-}$ ; Wilkinson's catalyst,  $[\text{RhCl}(\text{PPh}_3)_3]$ ; and Vaska's complex,  $\text{trans-}[\text{Ir}(\text{CO})\text{Cl}(\text{PPh}_3)_2]$ .



#### 8.1.4.2.5 Coordination Number 5

The two common coordination geometries for five-coordinate complexes are trigonal bipyramidal and square pyramidal.

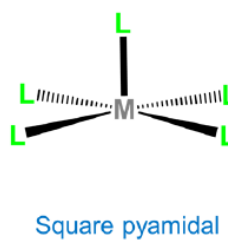
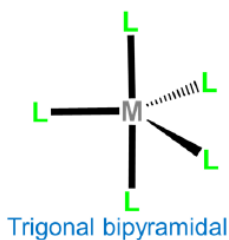


Figure 8.1.4.11.

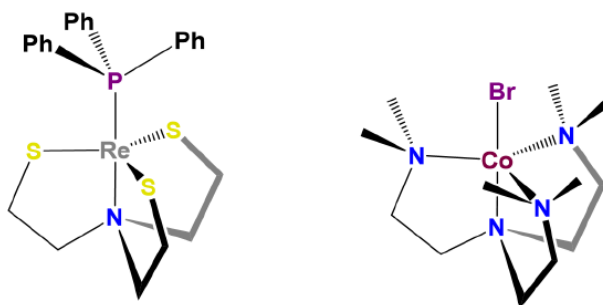


Figure 8.1.4.11. Some tripodal ligands preference the formation of trigonal bipyramidal complexes. This work by Stephen Contakes is licensed under a [Creative Commons Attribution 4.0 International License](#).

Homoleptic  $[\text{Ni}(\text{CN})_5]^{3-}$  possesses a square pyramidal structure, although the geometry is more common for macrocyclic complexes like the iron protoporphyrin of deoxymyoglobin shown in figure 8.1.4.4 and for complexes containing oxo and nitrido ligands, examples of which are shown in Figure 8.1.4.12

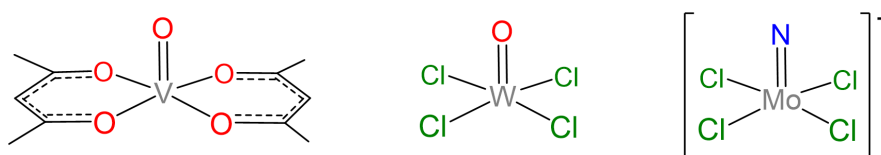


Figure 8.1.4.12. Some square pyramidal oxo and nitrido complexes. This work by Stephen Contakes is licensed under a [Creative Commons Attribution 4.0 International License](#).

In the absence of rigid constraining ligands, the relatively low energy difference between the trigonal bipyramidal and square pyramidal coordination geometries provides a mechanism for interconversion of the axial and equatorial ligands in a trigonal planar complex. For example, pentacarbonyliron(0) exhibits fluxionality involving a square pyramidal intermediate via a Berry pseudorotation mechanism, as shown in Figure 8.1.4.13

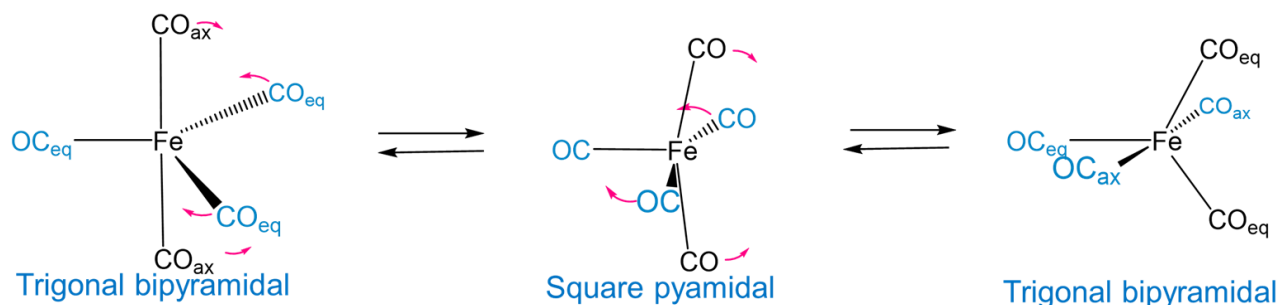


Figure 8.1.4.13. Fluxionality in pentacarbonyliron(0) involves exchange of axial and equatorial carbonyl ligands via Berry pseudorotation. Interconversion of the axial and equatorial carbonyl groups occurs faster than the NMR timescale at room temperature. As a result the  $^{13}\text{C}$  NMR spectrum of  $\text{Fe}(\text{CO})_5$  exhibits a single signal rather than two separate signals for the axial and equatorial carbonyl carbons. This work by Stephen Contakes is licensed under a [Creative Commons Attribution 4.0 International License](#).

#### 8.1.4.2.6 Coordination Number 6

The two common coordination geometries for coordination number 8 are octahedral and trigonal prismatic.

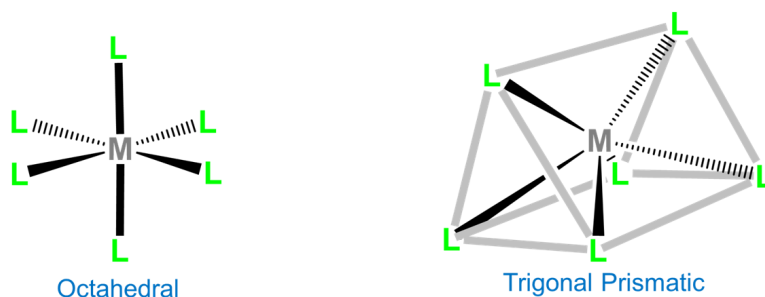


Figure 8.1.4.14.

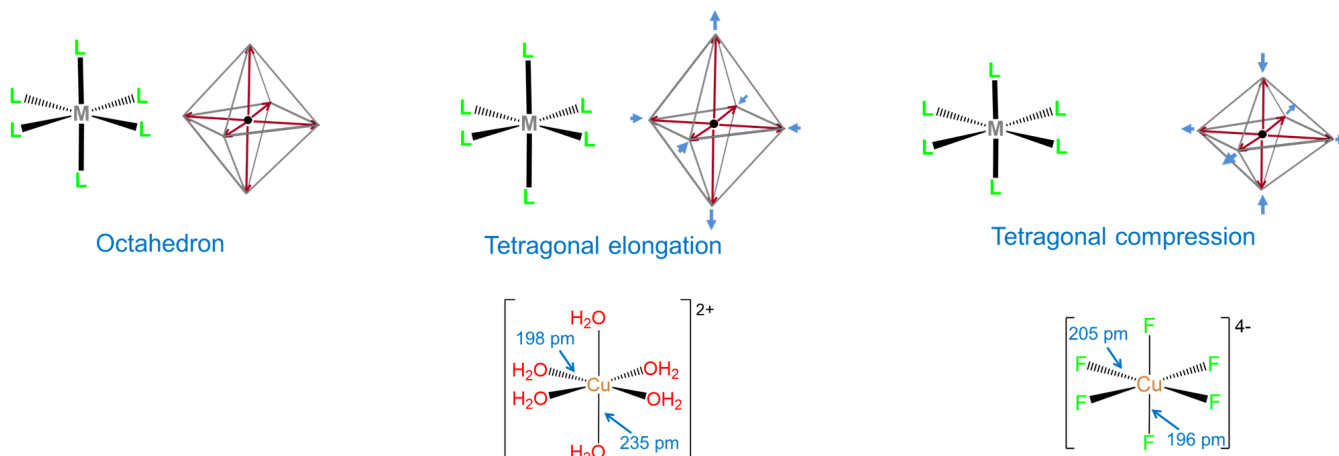


Figure 8.1.4.14. Tetragonal distortions commonly occur for  $d^4$ ,  $d^7$ , and  $d^9$  octahedral complexes. The most common type involves axial elongation in which the octahedron is stretched along a single *trans*-L-M-L axis, but axial compressions in which the octahedron is compressed along such an axis instead are sometimes observed. An example of an axial elongated complex is  $[\text{Cu}(\text{H}_2\text{O})_6]^{2+}$  in solution, while  $[\text{CuF}_6]^{4-}$  is axially compressed when doped into a  $\text{Ba}_2\text{ZrF}_6$  lattice (it is elongated when doped into a -----). Bond distances are taken from references 7 and 8. This work by Stephen Contakes is licensed under a [Creative Commons Attribution 4.0 International License](https://creativecommons.org/licenses/by/4.0/).

**Trigonal prismatic coordination** is related to octahedral coordination as shown in Figure 8.1.4.15. As may be seen in Figure 8.1.4.15, an octahedral coordination sphere is just a trigonal antiprism in which all edge lengths are identical. Rotation of one triangular face relative to its opposite until the two are eclipsed gives a trigonal prismatic geometry. In fact, since continuation of this rotation gives another octahedral complex, the trigonal prismatic geometry is an intermediate in isomerization reactions involving octahedral complexes.

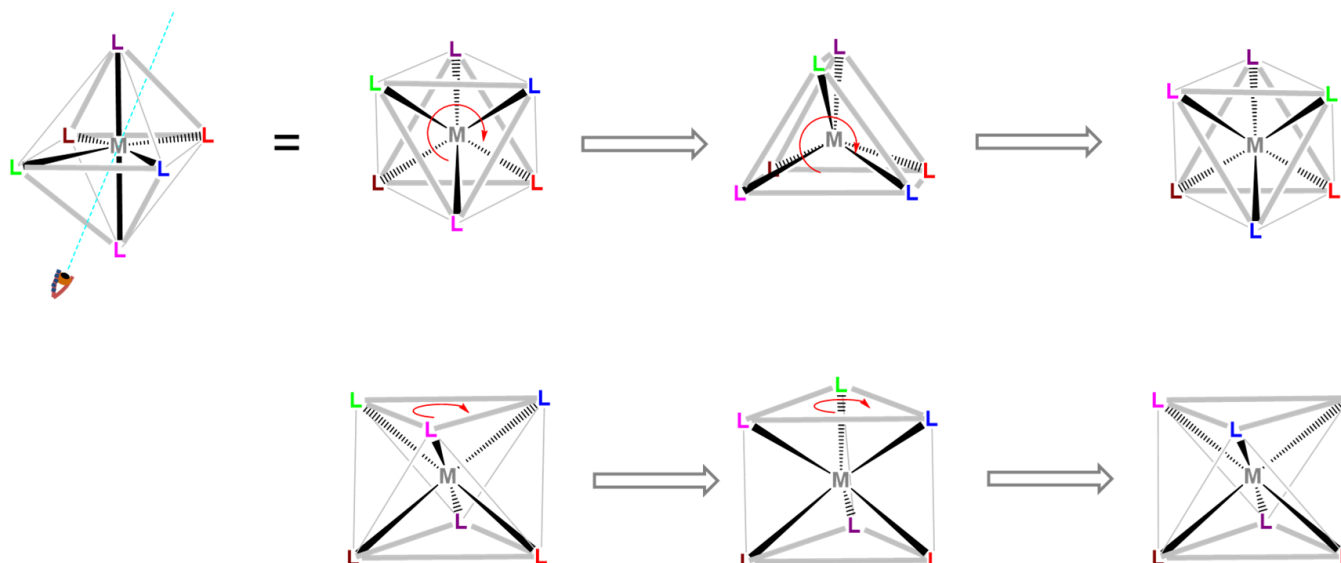


Figure 8.1.4.15. Since an octahedron is a trigonal antiprism, a trigonal prism may be produced by rotating or "twisting" one face of the octahedron relative to its opposite. Since continuation of the rotation gives an isomer of the original octahedron, when the energy landscape for twists like these is thermally or photochemically accessible, such twists provide one pathway for isomerization reactions involving octahedral complexes. In tris- and bis-chelates, such isomerizations are said to occur by Bailar and Ray-Dutt twists, which differ only in the relationship between the chelate rings and the faces twisted. Top: View looking down an axis bisecting a pair of opposing faces. Bottom: View perpendicular to that shown at top. This work by Stephen Contakes is licensed under a [Creative Commons Attribution 4.0 International License](https://creativecommons.org/licenses/by/4.0/).

In contrast to octahedral coordination geometries, trigonal prismatic coordination (and distorted versions thereof) are rare and occur mostly for  $d^0$ ,  $d^1$ , and  $d^2$  configurations. Examples of trigonal prismatic metal centers include the  $d^2$   $\text{Mo}^{4+}$  centers in  $\text{MoS}_2$ ,  $d^1$   $[\text{Re}(\text{S}_2\text{C}_2\text{Ph}_2)_3]^-$ , and  $d^0$   $[\text{Ta}(\text{CH}_3)_6]^-$ , of which the latter two structures are given in Figure 8.1.4.16. Semirigid ligands like that shown in Figure 8.1.4.4C may be used to encourage the adoption of a trigonal prismatic geometry, although once the number of  $d$  electrons present exceeds two, the preference for octahedral coordination is too great for a trigonal prismatic geometry to occur.

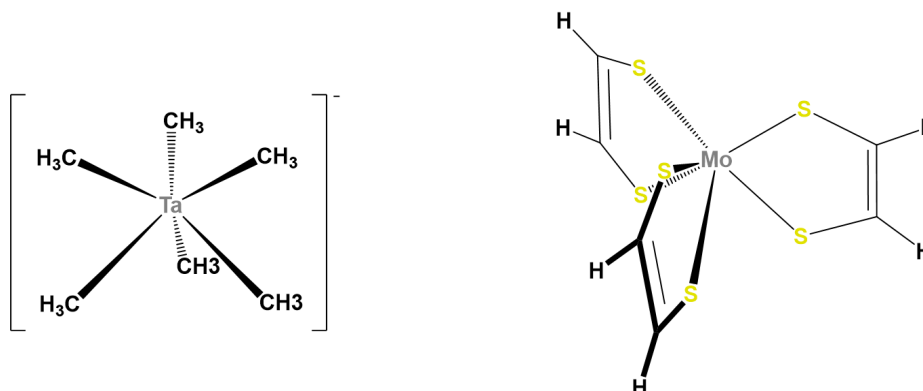
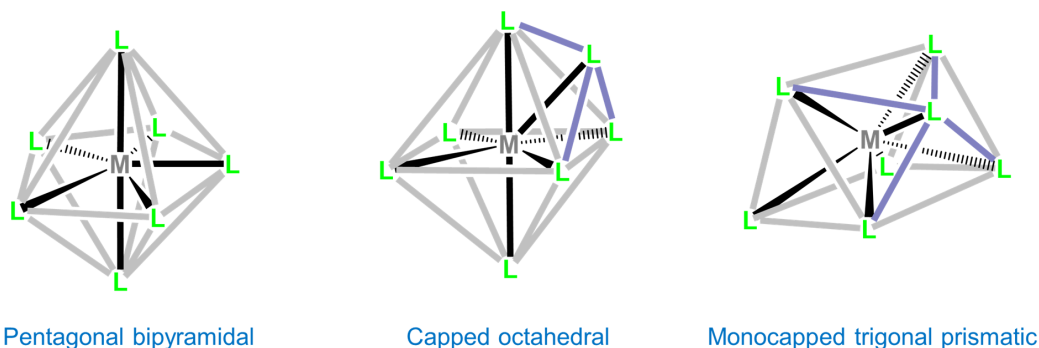


Figure 8.1.4.16. The complexes  $[\text{Ta}(\text{CH}_3)_6]^-$  and  $[\text{Mo}(\text{S}_2\text{C}_2\text{H}_2)_3]$  adopt a trigonal prismatic geometry. Trigonal prismatic coordination is common for  $d^0$  and  $d^1$  complexes with alkyl and dithiolene ligands. It is also typical for the dithiolene ligands to coordinate along the rectangular edges of the trigonal prism instead of the triangular ones. This work by Stephen Contakes is licensed under a [Creative Commons Attribution 4.0 International License](https://creativecommons.org/licenses/by/4.0/).

#### 8.1.4.2.7 Coordination Number 7

Seven-coordinate complexes are rare outside of the relatively large early transition metals, lanthanides, and actinides. The three common seven-coordinate geometries are pentagonal bipyramidal, monocapped octahedral, and monocapped trigonal prismatic. The latter two are often called capped octahedral and capped trigonal prismatic, with the mono- prefix being understood.



Although intraligand repulsions are smaller in the pentagonal bipyramidal coordination geometry than the capped octahedral and capped trigonal prismatic geometries, the difference is small, and the three structures are often close in energy. As a result the structure observed is often dependent on ligand-based constraints, crystal packing, and solvent effects that preference one geometry over the others.

Heptacyano complexes are often pentagonal bipyramidal. Examples include  $[\text{Mo}(\text{CN})_7]^{3-}$ ,  $[\text{W}(\text{CN})_7]^{3-}$ , and  $[\text{Os}(\text{CN})_7]^{3-}$ . Seven-coordinate complexes containing oxo ligands commonly are pentagonal bipyramidal with the oxo ligand(s) in the less sterically hindered axial position. Examples include  $[\text{NbOF}_6]^{3-}$  and, for the inner transition metals,  $[\text{UO}_2\text{F}_5]^{3-}$ . Ligands that have been used to promote formation of seven-coordinate species include 15-crown-5 and 2,2':6',2'':6'',2'''-quaterpyridine. Representative complexes are given in Figure 8.1.4.17.

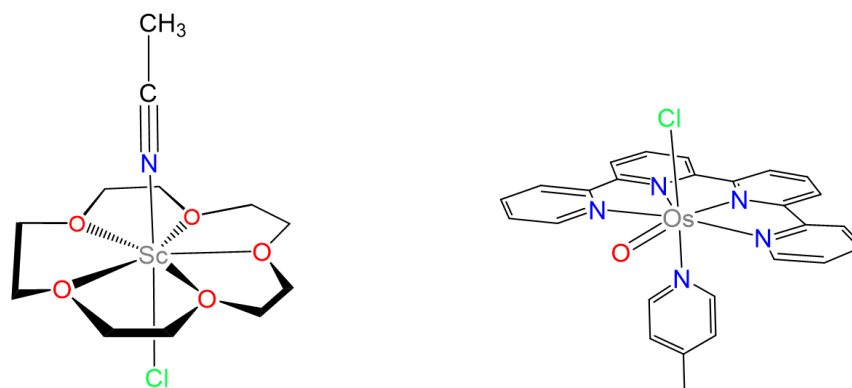


Figure 8.1.4.17. Seven-coordinate complexes containing ligands that encourage the formation of seven-coordinate geometries. Note that while in  $[\text{NbOF}_6]^{3-}$  and  $[\text{UO}_2\text{F}_5]^{3-}$  the oxo ligands occupy axial positions, the Osmium complex shown possesses an oxo ligand in an equatorial position. This is likely because the parent octahedral complex, in which the oxo ligand is not present, possesses an expanded outer N-Os-N angle of  $121.655^\circ$  that opens to  $154.161^\circ$  to accommodate the oxo group. Drawn based on the structures reported in references 9 and 10. This work by Stephen Contakes is licensed under a [Creative Commons Attribution 4.0 International License](https://creativecommons.org/licenses/by/4.0/).

Capped trigonal prismatic geometries are common for complexes of the early transition metals. Examples include  $[\text{NbF}_7]^{2-}$ ,  $[\text{TaF}_7]^{2-}$ , and  $[\text{ZrF}_7]^{3-}$  in  $(\text{NH}_4)_3[\text{ZrF}_7]$ .

Capped octahedral geometries are found in  $[\text{MoMe}_7]^-$ ,  $[\text{WMe}_7]^-$ , and  $[\text{WBr}_3(\text{CO})_4]$ , which contains three pairs of *trans*-Br and CO with the final CO capping the octahedron's  $(\text{CO})_3$  face, as shown in Figure 8.1.4.18

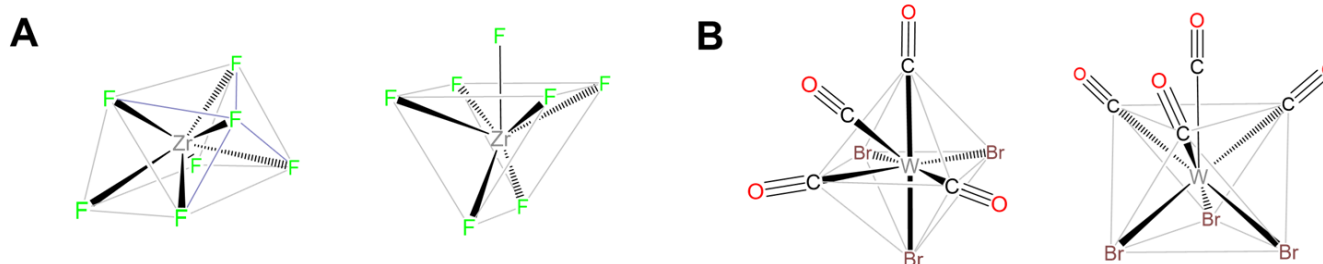


Figure 8.1.4.18. Examples of complexes that adopt monocapped trigonal prismatic and monocapped octahedral geometries. (A) Two views of the structure of (A) capped trigonalprismatic  $[\text{ZrF}_7]^{3-}$  and (B) capped octahedral  $[\text{WBr}_3(\text{CO})_4]$ . This work by Stephen Contakes is licensed under a [Creative Commons Attribution 4.0 International License](https://creativecommons.org/licenses/by/4.0/).

In seven- and higher-coordinate complexes, ligand and crystal packing effects frequently give distorted coordination geometries. These geometries are intermediate between two or more of the idealized seven coordinate geometries, making it difficult to tell exactly which structure they are a distortion of (Figure 8.1.4.19).

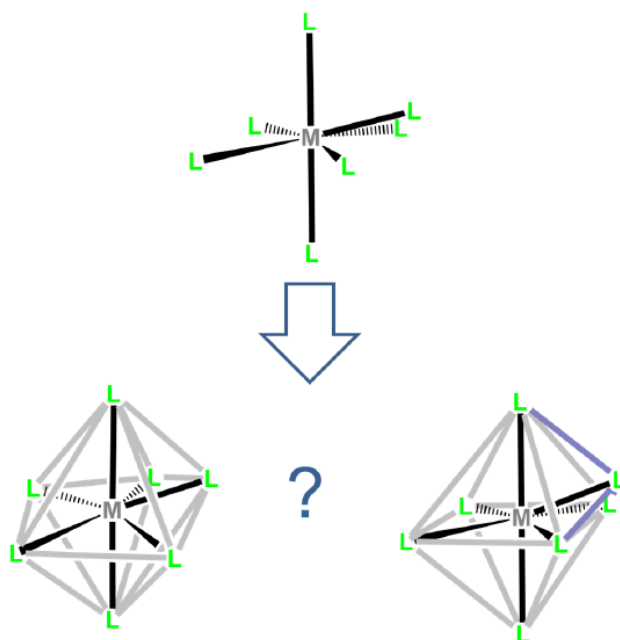


Figure 8.1.4.19. Many seven-coordinate structures are distorted and can be difficult to classify. For example, how should the geometry of this complex be described - as distorted trigonal bipyramidal or distorted monocapped octahedral? This work by Stephen Contakes is licensed under a [Creative Commons Attribution 4.0 International License](#).

#### 8.1.4.2.8 Coordination Number 8

Eight-coordinate complexes are rare and occurs in discrete molecules and ions only for the relatively large early transition metals, lanthanides, and actinides. The three common eight-coordinate geometries are square antiprismatic, dodecahedral, and bicapped trigonal prismatic. In contrast, the cubic coordination geometry is only found in ionic lattices like that of CsCl and in complexes of the inner transition metals such as  $\text{Na}_3[\text{UF}_8]$ .

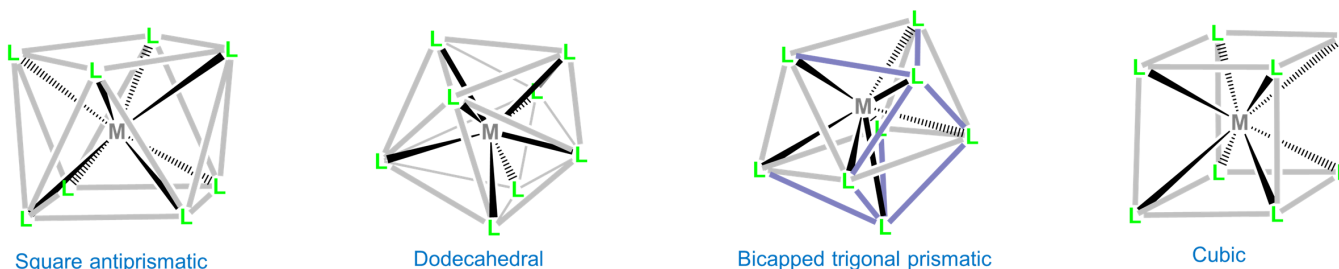


Figure 8.1.4.20. The square antiprism may be made by twisting one face of a cube relative to another, and the dodecahedron by folding opposing faces towards one another.

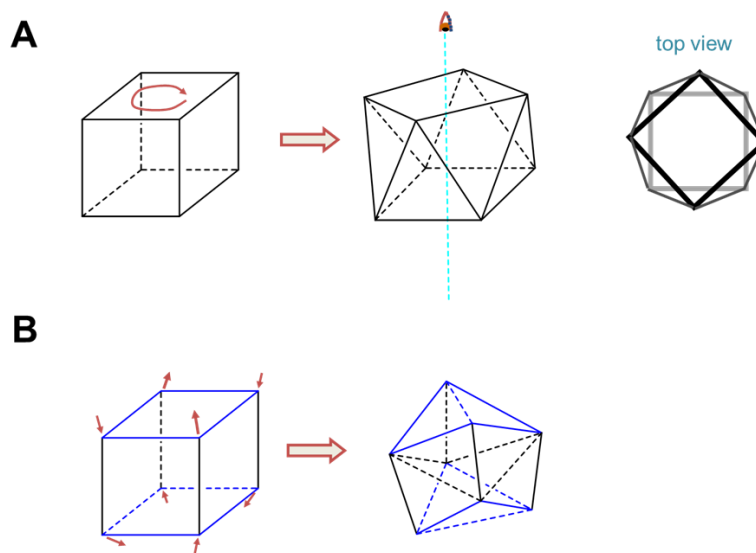


Figure 8.1.4.20. The (A) square antiprismatic and (B) dodecahedral coordination geometries are distorted cubic geometries. (A) The square antiprismatic coordination geometry is just a cubic coordination geometry in which one face has been rotated  $45^\circ$  relative to its opposite (and for which the distance between those faces need not be equal to the distance between adjacent atoms within a face) (B) The dodecahedral geometry may be thought of as a cube in which opposing faces are folded up and down relative to one another as shown. This work by Stephen Contakes is licensed under a [Creative Commons Attribution 4.0 International License](https://creativecommons.org/licenses/by/4.0/).

As with other high-coordinate structures, the energy difference between these eightfold coordination geometries is small enough that packing effects can significantly influence the observed structure. For example, octacyanomolybdates commonly adopt a square antiprismatic coordination geometry but depending on the counterions present can give dodecahedral or bicapped trigonal prismatic complexes. Examples are given in Figure 8.1.4.21

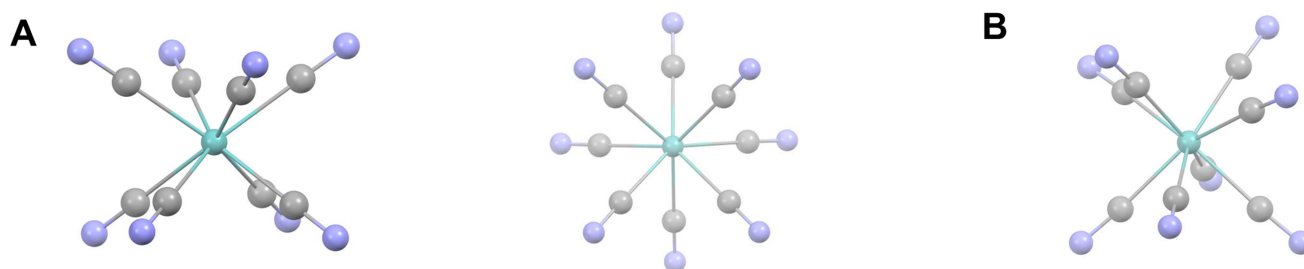
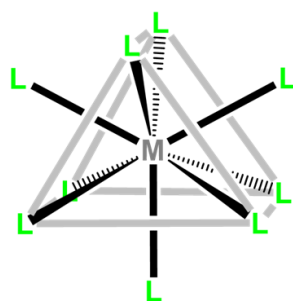


Figure 8.1.4.21: Structures reported for (A) square antiprismatic  $[\text{Mo}(\text{CN})_8]^{3-}$  as a solid 4,4'-Diazenediylidipyridinium salt and (B) dodecahedral  $[\text{Mo}(\text{CN})_8]^{4-}$  as a solid tetra-n-butylammonium salt.

#### 8.1.4.2.9 Coordination Number 9

Again, nine-coordinate complexes typically require larger transition metals, lanthanides, and actinides. Coordination geometries are typically either tricapped trigonal prismatic or idiosyncratically determined by the ligands. Simple examples include the aqua complexes  $[\text{Sc}(\text{H}_2\text{O})_9]^{3+}$ ,  $[\text{Y}(\text{H}_2\text{O})_9]^{3+}$ , and  $[\text{La}(\text{H}_2\text{O})_9]^{3+}$ , as well as  $[\text{TcH}_9]^{2-}$  and  $[\text{ReH}_9]^{2-}$ .





Tricapped trigonal Antiprism

Figure 8.1.4.22.

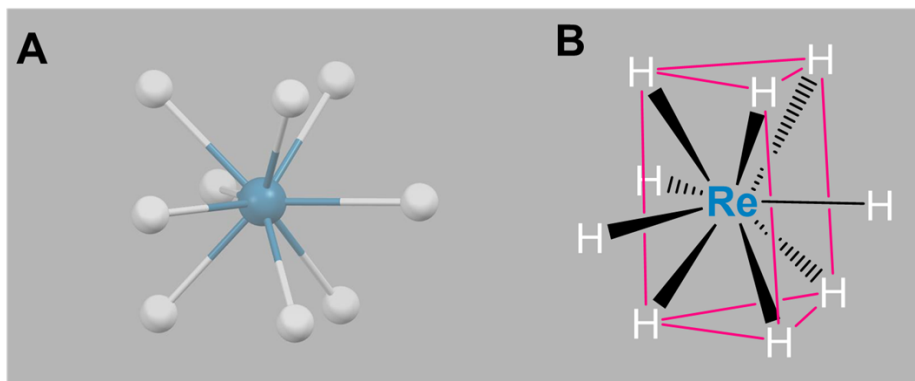


Figure 8.1.4.22. (A) Structure of  $[\text{ReH}_9]^{2-}$  in  $\text{K}_2[\text{ReH}_9]$  and (B) schematic showing how the structure maps onto a tricapped trigonal pyramidal coordination geometry. This work by Stephen Contakes is licensed under a [Creative Commons Attribution 4.0 International License](https://creativecommons.org/licenses/by/4.0/).

#### 8.1.4.2.10 Coordination Numbers 10-16

Coordination numbers higher than nine are extremely rare for compounds that bind in  $\kappa$  fashion (form conventional metal-ligand bonds)<sup>14</sup> and usually involve some combination of large metals, sterically undemanding ligands, and special ligand structures that promote higher coordination. Noteworthy examples include

1. Twelve-coordinate  $[\text{Hf}(\text{BH}_4)_4]$ , which illustrates how small multidentate ligands promote higher coordination numbers. As shown in Figure 8.1.4.23  $[\text{Hf}(\text{BH}_4)_4]$  has a cubooctahedral structure in which  $\text{BH}_4^-$  acts as a tridentate ligand, with  $\text{BH}_3$  units occupying triangular faces of the cubooctahedron to give a tetrahedron of  $\text{BH}_4^-$  ligands around the Hf.

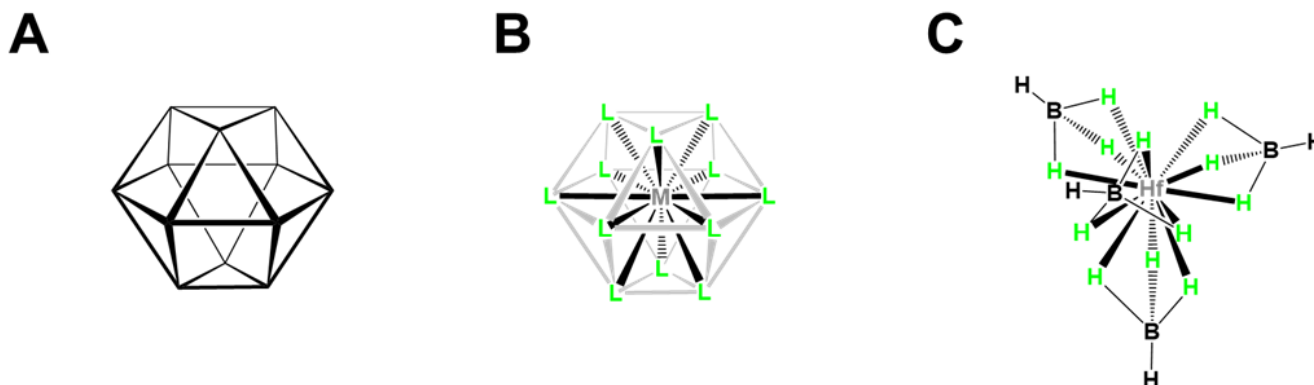
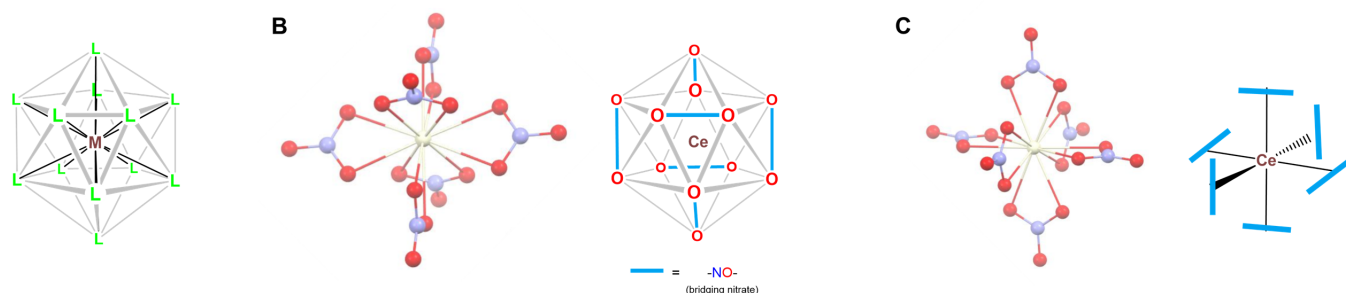


Figure 8.1.4.23. The anticubooctahedral coordination geometry is observed for  $[\text{Hf}(\text{BH}_4)_4]$ . (A) An anticubooctahedron consists of a hexagonal ring capped with antiparallel triangles above and below the ring. (B) Idealized anticubooctahedral complex. (C) Structure of  $[\text{Hf}(\text{BH}_4)_4]$ . This work by Stephen Contakes is licensed under a [Creative Commons Attribution 4.0 International License](https://creativecommons.org/licenses/by/4.0/).

2. Twelve-coordinate  $[\text{Ce}(\text{NO}_3)_6]^{2-}$ , in which the nitrate oxygens define an icosahedral coordination geometry as shown in Figure 8.1.4.24 The nitrates in the structure bind the Ce center in bidentate fashion in an octahedral array.



3. Fifteen-coordinate  $[\text{Th}(\text{H}_3\text{BNMe}_2\text{BH}_3)_4]$ , which also uses bridging H-B-H units that occupy little of the coordination sphere. In  $[\text{Th}(\text{H}_3\text{BNMe}_2\text{BH}_3)_4]$ , three of the four  $\text{H}_3\text{BNMe}_2\text{BH}_3$  ligands bind in  $\kappa^4$  fashion and one binds  $\kappa^3$ , giving the fifteen fold coordination.<sup>16</sup>
4. Sixteen-coordinate  $[\text{CoB}_{16}]^-$ , which possesses the highest coordination number yet observed. Its structure is given in Figure 8.1.4.25 The coordination geometry is an octahedral antiprism, and the complex should be considered to involve a Co center in the midst of a  $\text{B}_{16}^-$  "molecular drum" held together by cluster bonds.

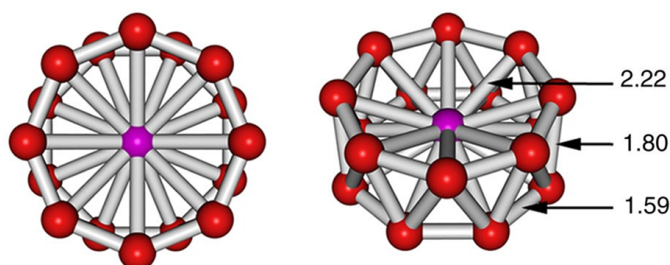


Figure 2A from Popov, I., Jian, T., Lopez, G. *et al.* Cobalt-centered boron molecular drums with the highest coordination number in the  $\text{CoB}_{16}^-$  cluster. *Nat Commun* **6**, 8654 (2015). <https://doi.org/10.1038/ncomms9654>, which is licensed in that publication under a Creative Commons Attribution 4.0 International License.

### 8.1.4.3 References

- Dudev, M.; Wang, J.; Dudev, T.; Lim, C., Factors Governing the Metal Coordination Number in Metal Complexes from Cambridge Structural Database Analyses. *The Journal of Physical Chemistry B* **2006**, *110*(4), 1889-1895.
- Kuppuraj, G.; Dudev, M.; Lim, C., Factors Governing Metal–Ligand Distances and Coordination Geometries of Metal Complexes. *The Journal of Physical Chemistry B* 2009, *113* (9), 2952-2960.
- Cremades, E.; Echeverría, J.; Alvarez, S., The Trigonal Prism in Coordination Chemistry. *Chemistry – A European Journal* 2010, *16* (34), 10380-10396.
- Xiong, X.-G.; Wang, Y.-L.; Xu, C.-Q.; Qiu, Y.-H.; Wang, L.-S.; Li, J., On the gold–ligand covalency in linear  $[\text{AuX}_2]^-$  complexes. *Dalton Transactions* 2015, *44* (12), 5535-5546.
- Concepción Gimeno, M. The Chemistry of Gold in Laguna, Antonio (ed.) *Modern Supramolecular Gold Chemistry: Gold-Metal Interactions and Applications*. Wiley, 2008.
- Andersen, R. A.; Faegri, K.; Green, J. C.; Haaland, A.; Lappert, M. F.; Leung, W. P.; Rypdal, K., Synthesis of bis[bis(trimethylsilyl)amido]iron(II). Structure and bonding in  $\text{M}[\text{N}(\text{SiMe}_3)_2]_2$  (M = manganese, iron, cobalt): two-coordinate transition-metal amides. *Inorganic Chemistry* 1988, *27* (10), 1782-1786.
- Persson, I., Hydrated metal ions in aqueous solution: How regular are their structures? *Pure and Applied Chemistry* 2010, *82*(10), 1901.
- Aramburu, J. A.; García-Fernández, P.; García-Lastra, J. M.; Moreno, M., Jahn–Teller and Non-Jahn–Teller Systems Involving  $\text{CuF}_6^{4-}$  Units: Role of the Internal Electric Field in  $\text{Ba}_2\text{ZnF}_6:\text{Cu}^{2+}$  and Other Insulating Systems. *The Journal of Physical Chemistry C* 2017, *121*(9), 5215-5224.

9. Brown, M. D.; Levason, W.; Murray, D. C.; Popham, M. C.; Reid, G.; Webster, M., Primary and secondary coordination of crown ethers to scandium(III). Synthesis, properties and structures of the reaction products of  $\text{ScCl}_3(\text{thf})_3$ ,  $\text{ScCl}_3 \cdot 6\text{H}_2\text{O}$  and  $\text{Sc}(\text{NO}_3)_3 \cdot 5\text{H}_2\text{O}$  with crown ethers. *Dalton Transactions* 2003, (5), 857-865.
10. Liu, Y.; Ng, S.-M.; Lam, W. W. Y.; Yiu, S.-M.; Lau, T.-C., A Highly Reactive Seven-Coordinate Osmium(V) Oxo Complex:  $[\text{OsV}(\text{O})(\text{qpy})(\text{pic})\text{Cl}]^{2+}$ . *Angewandte Chemie International Edition* 2016, 55 (1), 288-291.
11. Popov, I., Jian, T., Lopez, G. *et al.* Cobalt-centred boron molecular drums with the highest coordination number in the  $\text{CoB}_{16}^-$  cluster. *Nat Commun* **6**, 8654 (2015). <https://doi.org/10.1038/ncomms9654>
12. The structures are rendered from cif data reported in the following publications: (A) square antiprismatic  $[\text{Mo}(\text{CN})_8]^{3-}$ : Wen-Yan Liu, Hu Zhou, Ai-Hua Yuan, *Acta Crystallographica Section E: Structure Reports Online*, 2008, 64, m1151, (B) dodecahedral  $[\text{Mo}(\text{CN})_8]^{4-}$ : B.J.Corden, J.A.Cunningham, R.Eisenberg, *Inorganic Chemistry*, 1970, 9, 356.
13. The structure of  $\text{ReH}_9^{2-}$  is rendered from the structure reported in Abrahams, S.C.; Ginsberg, A.P.; Knox, K. Transition metal-hydrogen compounds. II. The crystal and molecular structure of potassium rhenium hydride,  $\text{K}_2\text{ReH}_9$  *Inorganic Chemistry*, **1964**, 3, 558-567.
14. There are other complexes in which a metal may be said to interact with more than sixteen "ligand atoms", but these are not usually considered to possess a higher coordination number. For example, in some  $\pi$  complexes like  $\eta^5\text{-Cp}_4\text{U}$ , technically there are 20 C atoms fastened to the U, but these complexes are better considered as 12-coordinate than twenty (since each cyclopentadienyl ring is isolobal with a *fac*-coordinated set of 3 L ligands), while the metal centers in endohedral fullerene species like  $\text{La@C}_{60}$  do not interact with all sixty carbon atoms at once, and so are better thought of as a metal trapped in a spacious sixty-carbon cage.
15. Zalkin, A.; Forrester, J.D.; Templeton, D.H. Crystal structure of cerium magnesium nitrate hydrate *Journal of Chemical Physics*, **1963**, 39, 2881-2891.
16. Daly, S. R.; Piccoli, P. M. B.; Schultz, A. J.; Todorova, T. K.; Gagliardi, L.; Girolami, G. S., Synthesis and Properties of a Fifteen-Coordinate Complex: The Thorium Aminodiborane  $[\text{Th}(\text{H}_3\text{BNMe}_2\text{BH}_3)_4]$ . *Angewandte Chemie International Edition* 2010, 49 (19), 3379-3381.
17. Popov, I., Jian, T., Lopez, G., Boldyrev, A. I.; Wang, L.-S. Cobalt-centred boron molecular drums with the highest coordination number in the  $\text{CoB}_{16}^-$  cluster. *Nat Commun* **6**, 8654 (2015).

8.1.4: Coordination Numbers and Structures is shared under a [CC BY 4.0](#) license and was authored, remixed, and/or curated by Stephen M. Contakes.

- [9.5: Coordination Numbers and Structures](#) by Stephen M. Contakes is licensed [CC BY 4.0](#).

## 8.1.5: Isomerism

Metal complexes present a rich, interesting, and diverse structural chemistry. Major points of variation in the structural chemistry of metal complexes include

1. **coordination number** and **coordination geometry**, which involve differences in how many ligands surround a central metal and their overall geometric arrangement. Examples of the latter include the tetrahedral and square planar geometries commonly observed for four-coordinate metal centers. Tetrahedral, square planar, and octahedral coordination serve as a backdrop to the discussion of isomerism on this page. Readers who are unfamiliar with these structures might consider reading the [section on coordination geometries](#) before this one.
2. **structural isomerism** involves differences in how potential ligand atoms are bound to metals in a complex. Possibilities for structural isomerism include
  - linkage or ambidentate isomerism
  - hydrate/solvate isomerism
  - ionization isomerism
  - coordination isomerism.

Of these, linkage isomerism should always be considered when working with ambidentate ligands. As classifications, the last three forms of structural isomerism are mainly of academic interest since they represent permutations of ordinary structure patterns for solvates, salts, and coordination complexes, respectively.

3. **stereochemistry**, which includes
  - which coordination geometry is adopted for a metal with a given set of ligands in a particular oxidation state. For instance,  $[\text{Ni}^{\text{II}}\text{Cl}_4]^{2-}$  is tetrahedral while  $[\text{Pt}^{\text{II}}\text{Cl}_4]^{2-}$  is square planar. Since this geometry is usually fixed by the metal and ligands it is typically not a source of stereoisomeric variety.
  - metal-centric stereoisomerism involving possible variations in where ligands are located relative to one another around the metal. The possibilities depend on the coordination number, geometry, and number of different types of ligands. For instance, square planar complexes can exhibit *cis*-/ *trans*- isomerism while tetrahedral ones cannot. Tetrahedral complexes with four different ligands exhibit *R* and *S* chirality but complexes of that type are relatively rare. The more common cases include *cis* and *trans* isomerism in square planar complexes and *cis* & *trans*-, *mer* & *fac*-, and  $\Lambda$  &  $\Delta$  isomerism in octahedral ones, although some multidentate ligands present additional possibilities for stereochemical variation
  - Stereoisomerism centered on the ligands bound to a metal center. Possibilities include
    - stereoisomerism inherent to a ligand. This would include cases where the ligand itself is chiral or, as in the case of amines, exists as a rapidly interconverting mixture of isomers. Thus this sort of stereoisomerism is an extension of the isomerism encountered in ordinary organic and other main group compounds. The main new issues introduced by binding of such ligands to a metal center involve the creation of new possibilities for diastereoisomerism based on the stereochemistry of the metal center and the freezing out of stereocenter inversion on binding to a metal. The latter is particularly important for amines, which as free amines racemize rapidly by nitrogen inversion.
    - or conformational isomerism involving five-membered **chelate rings** created when a multidentate ligand binds to a metal. This isomerism is often called chelate ring twist since individual rings can exhibit one of two conformations depending on how they twist on binding.

A summary of these forms of isomerism is given in Figure 8.1.5.1

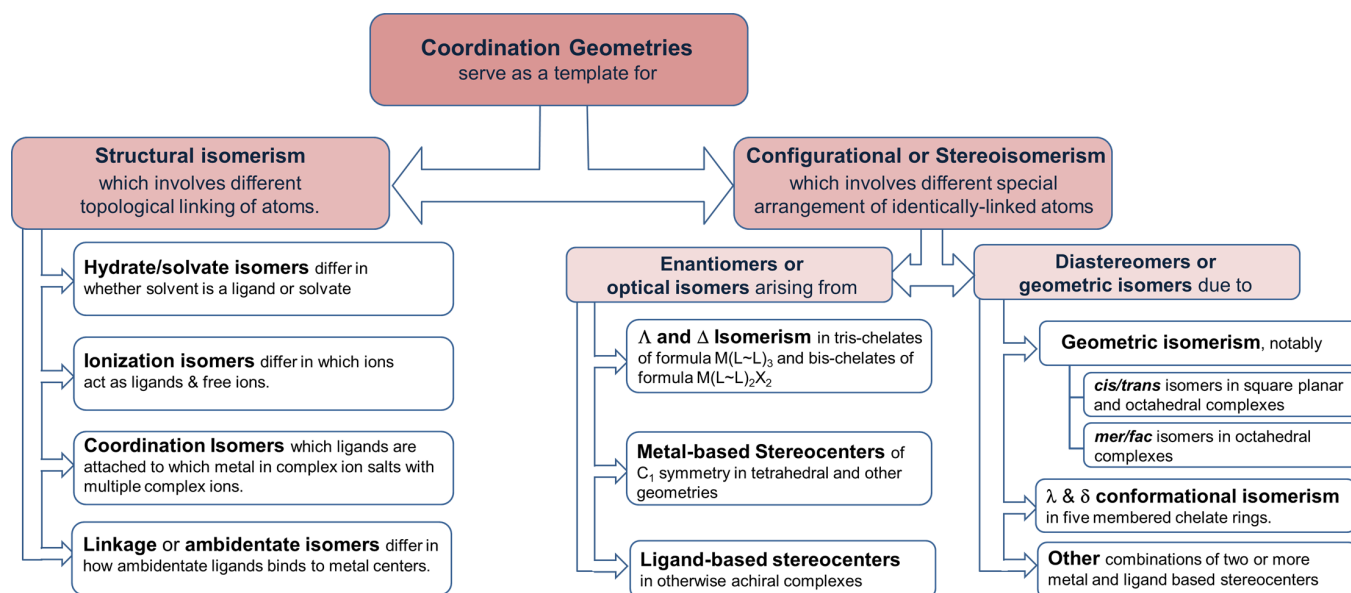


Figure 8.1.5.1. Relationship among the common types of isomerism in metal complexes. This work by Stephen Contakes is licensed under a [Creative Commons Attribution 4.0 International License](#).

## Structural isomers

Structural isomerism involves different topological linkages of atoms. Differences in atomic linkages distinctive to coordination chemistry involve the linkages between metals and ligands. The main variations are:

### 1. Hydrate/solvate isomerism

Solvate isomers differ in terms of whether a molecule acts as a ligand or whether it acts as a solvate by occupying a lattice site in the crystal. Among solvate isomers, the case in which water is the ligand or solvate is the best known. The resulting isomers are called **hydrate isomers** after the term for water acting as a solvate, hydrate. A well-known example that illustrates how solvate isomerism works is the series  $[\text{CrCl}_x(\text{H}_2\text{O})_{6-x}]\text{Cl}_{3-x} \cdot x\text{H}_2\text{O}$ , for which  $x = 0-2$ . The structures of the complex ions involved in this series are shown in Figure 8.1.5.2<sup>1</sup>

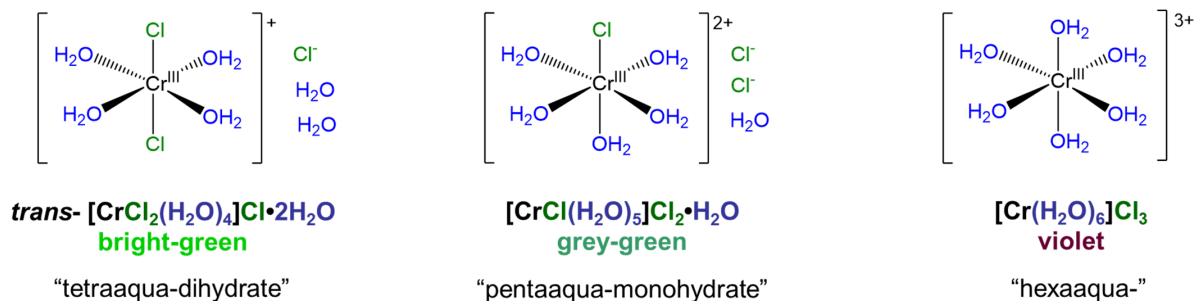


Figure 8.1.5.2. Complexes of the hydrate isomer series  $[\text{CrCl}_x(\text{H}_2\text{O})_{6-x}]\text{Cl}_{3-x} \cdot x\text{H}_2\text{O}$  ( $x = 0-2$ ). This work by Stephen Contakes is licensed under a [Creative Commons Attribution 4.0 International License](#).

As can be seen from the compounds in Figure 8.1.5.2 hydrate isomers differ both in terms of whether water acts as a ligand or hydrate *and* in terms of whether a potential counterion acts as a counterion or ligand. Thus, in  $\text{trans-}[\text{CrCl}_2(\text{H}_2\text{O})_4]\text{Cl} \cdot 2\text{H}_2\text{O}$  two chlorides act as chloro ligands and four waters as aqua ligands while in  $[\text{CrCl}(\text{H}_2\text{O})_5]\text{Cl}_2 \cdot \text{H}_2\text{O}$  five water molecules act as aqua ligands while only one chloride acts as a chloro ligand. In this way, solvate isomers simply represent cases in which two or more of the possible permutations for metal ligand binding among a set of solvent and counterion molecules are stable.

### 2. Ionization isomerism

In **ionization isomerism** there are two or more potential ions that can act as ligands. The ionization isomers differ in terms of which of these ions act as counterions and which act as ligands. Consider, for instance, the complexes shown in Figure 8.1.5.3 These complexes differ in terms of whether the chloride or sulfate acts as a ligand, with the other acting as a counterion.

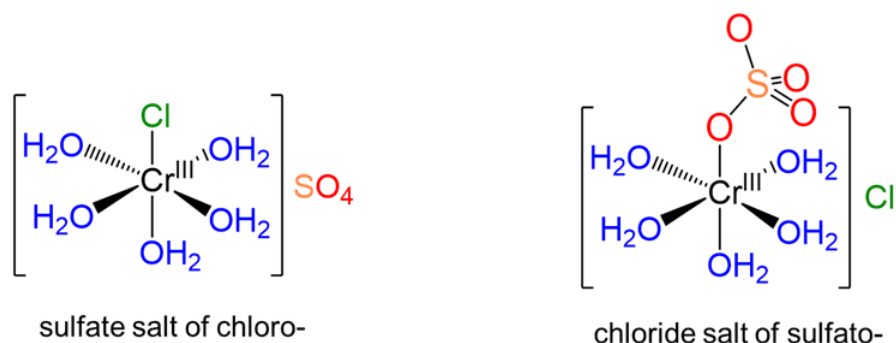


Figure 8.1.5.3. Ionization isomers comprising a pentaquachromium(III) fragment and the anions chloride and sulfate. As with all ionization isomers, the isomers differ in terms of which anion acts as a ligand and which a counterion. This work by Stephen Contakes is licensed under a [Creative Commons Attribution 4.0 International License](#).

### 3. Coordination isomerism

Coordination isomers exist in compounds containing two or more complexes, each of which possesses a different set of ligands that can in principle be swapped with a ligand of the other complex. An example involves  $[\text{Co}^{\text{III}}(\text{NH}_3)_6][\text{Cr}^{\text{III}}(\text{ox})_3]$ , depicted in Figure 8.1.5.4A<sup>1</sup> Coordination isomers of this complex involve swapping the ammine ligands around the  $\text{Co}^{3+}$  center for oxalato ligands surrounding the  $\text{Cr}^{3+}$  center. For instance, swapping all the ammine and oxalato ligands between the metal centers gives the coordination isomer  $[\text{Cr}^{\text{III}}(\text{NH}_3)_6][\text{Co}^{\text{III}}(\text{ox})_3]$  shown in Figure 8.1.5.4B

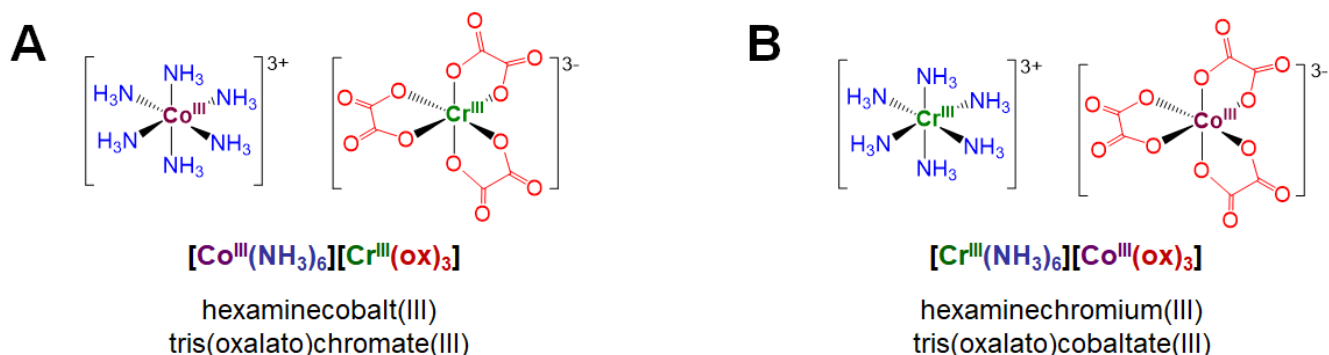
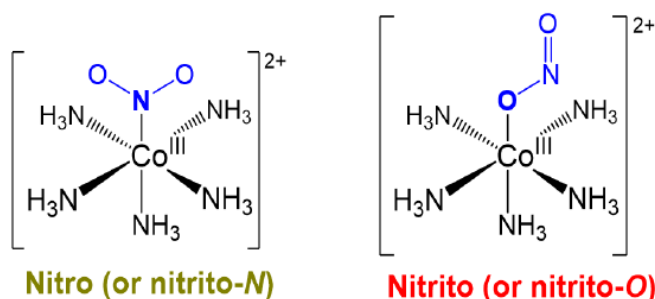


Figure 8.1.5.4. Two coordination isomers comprising a  $\text{Co}^{3+}$ ,  $\text{Cr}^{3+}$ , six  $\text{NH}_3$ , and three oxalato ligands. The isomers differ in terms of which ligand type is bound to which metal. This work by Stephen Contakes is licensed under a [Creative Commons Attribution 4.0 International License](#).

As classifications, hydrate/solvate, ionization, and coordination isomerism represent permutations of ordinary structure patterns for solvates, salts, and coordination complexes, respectively. As a result these forms of isomerism are rarely used as independent conceptual frameworks when thinking and talking about the structure of coordination compounds. Not so the final type of structural isomerism, linkage isomerism. That is because linkage isomerism has to do with the special *capacity* of ambidentate ligands to bind metals in multiple ways.

### 4. Linkage or ambidentate isomerism

Linkage or ambidentate isomers differ in how one or more ambidentate ligands bind to metal centers in a complex. The classic example dating from the work of Jørgensen and Werner is given in Scheme 8.1.5.1



Scheme 8.1.5.I. Linkage isomers of pentaamminenitritocobalt(III) ion. This work by Stephen Contakes is licensed under a [Creative Commons Attribution 4.0 International License](#).

Just as alkenes exist as *E* and *Z* isomers, compounds possessing ambidentate ligands exist as one among the possible linkage isomers. As such, when working with ambidentate ligands the particular linkage isomer formed should be determined experimentally and considered when interpreting the complex's chemical and physical behavior.

The main ambidentate ligands which give rise to linkage isomerism are

- cyanide,  $\text{CN}^-$
- thiocyanate,  $\text{SCN}^-$ , and the O and Se analogues,  $\text{OCN}^-$  and  $\text{SeCN}^-$
- nitrite,  $\text{NO}_2^-$
- sulfite,  $\text{SO}_3^-$
- nitrosyl,  $\text{NO}$

Although ambidentate ligands can bind metals in multiple ways, most exhibit a preferred binding mode (*i.e.*, prefer to bind metal centers in one of the possible ways). For instance, cyanide almost always binds through its carbon atom and thiocyanate almost always binds through its nitrogen ( $\mu\text{-N}$ ). However, the other binding mode can sometimes be formed kinetically or by using conditions that particularly favor its formation. Thus thiocyanate forms  $\text{M-SCN}^-$  linkages in the presence of exceptionally soft metal centers or in hard polar solvents (in which Lewis acid groups can stabilize the terminal nitrogen of a bound thiocyanate ligand).

Ambidentate ligands are of significant research interest because many don't just bind to metal centers in two ways; the linkage isomers sometimes have significantly different physical properties. In addition, the possibility of two binding modes introduces the possibility of exploiting linkage isomerism to take advantage of some of these ligands:

- different structural chemistry in different coordination modes. In mononuclear complexes the coordination mode influences which side of the ligand faces away from the complex and might be susceptible to stabilization by interaction with solvent. Additionally, the orientation of the ligand relative to the metal center might differ between one coordination mode and another. For instance, as predicted from the minor contributor to its resonance structure, thiocyanate binds nonlinearly via its S atom and linearly via its N (Figure 8.1.5.5). Because of this the apparent steric bulk of the ligand around the metal center might differ between forms.

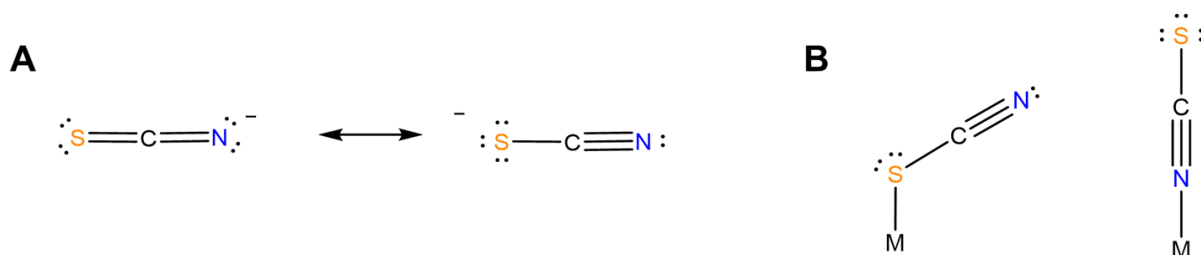


Figure 8.1.5.5. Thiocyanate generally prefers to bind metals nonlinearly but in some cases forms linear  $\text{M-SCN}$  bonds. This work by Stephen Contakes is licensed under a [Creative Commons Attribution 4.0 International License](#).

- bind two different metal centers at the same time, linking them together. Perhaps the best-known examples involve thiocyanate and cyanide. The latter forms linkages of the type  $\text{M-C}\equiv\text{N-M'}$ . In the dye Prussian blue these take the form  $\text{Fe}^{\text{II}}\text{-C}\equiv\text{N-Fe}^{\text{III}}$ . An example from the author's graduate research involved tetrahedral clusters containing four metal atoms linked by six cyano ligands, as shown in Figure 8.1.5.6



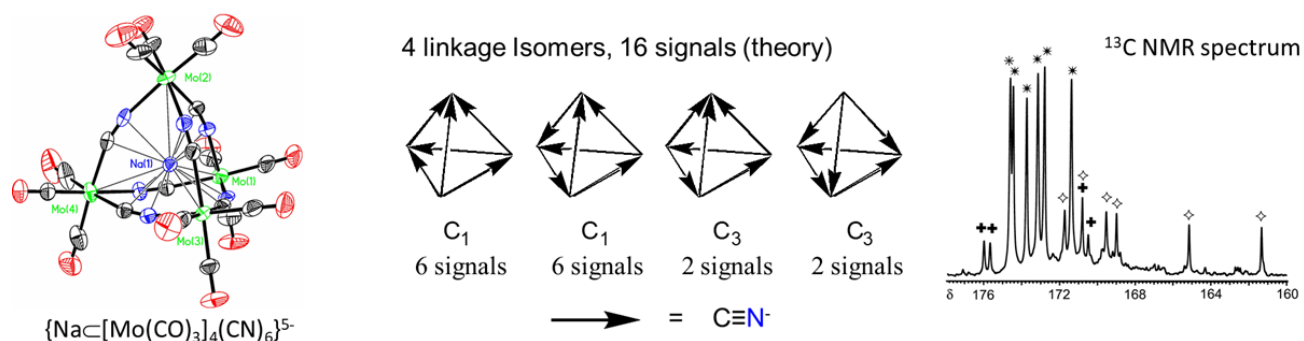


Figure 8.1.5.6. (A) Structure of  $\{Na@[Mo(CO)_3]_4(CN)_6\}^{5-}$  showing the linking of four Mo centers by six CN ligands. Thermal ellipsoids for the C atoms are shown in black; those of the N atoms in blue. (B) The complex exists as a mixture of four linkage isomers in which the bridging  $CN^-$  ligands are oriented in different ways, as may be seen from the presence of the expected sixteen signals in its  $^{13}C$  NMR spectrum. Based on work reported in reference 2.

c. can be induced to change from one binding mode to another in response to a stimulus. The classic example involves the light-driven transformation of the thermodynamically more stable yellow nitro complex of pentamminecobalt(III),  $[Co(NH_3)_5NO_2]^{2+}$  to the less stable red O-nitrito complex,  $[Co(NH_3)_5ONO]^{2+}$ . Less stable cyanometallate coordination networks like those in the red  $K\{Fe^{II}[Cr^{III}(CN)_6]\}$  transform into the more stable green  $K\{Fe^{II}[Cr^{III}(NC)_6]\}$  form on heating, as shown in Figure 8.1.5.7<sup>3</sup>

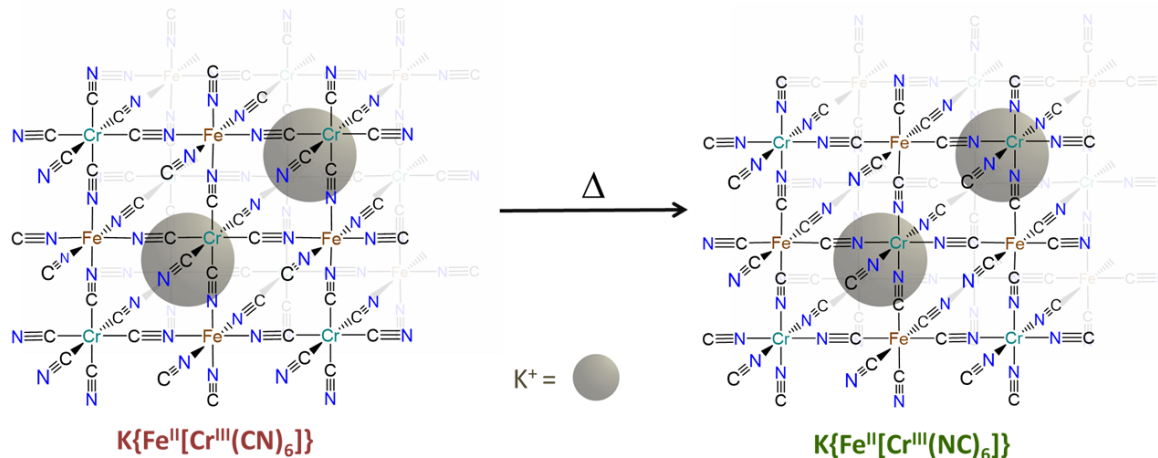


Figure 8.1.5.7. Thermally-induced transformation of one  $K\{Fe^{II}[Cr^{III}(CN)_6]\}$  into its more stable green linkage isomer  $K\{Fe^{II}[Cr^{III}(NC)_6]\}$  involves "flipping" the cyano ligands. This work by Stephen Contakes is licensed under a [Creative Commons Attribution 4.0 International License](https://creativecommons.org/licenses/by/4.0/).

### ? Exercise 8.1.5.1: Bridging ambidentate ligands and the Hard-Soft Acid-Base Principle.

The hard-soft acid-base principle helps explain the preference of bridging ambidentate ligands for particular binding modes. How might the greater stability of the green  $K\{Fe^{II}[Cr^{III}(NC)_6]\}$  over red  $K\{Fe^{II}[Cr^{III}(CN)_6]\}$  be explained in terms of the hard and soft acid-base concept?

#### Answer

The greater stability of  $K\{Fe^{II}[Cr^{III}(NC)_6]\}$  over  $K\{Fe^{II}[Cr^{III}(CN)_6]\}$  reflects the greater stability of the  $Fe^{II}-CN-Cr^{III}$  linkages in the former over the  $Fe^{II}-NC-Cr^{III}$  linkages in the latter. This is consistent with the preference for hard-hard and soft-soft Lewis acid-base interactions of the Hard-Soft Acid-Base Principle.

The  $Fe^{II}-CN-Cr^{III}$  linkages are more stable because they possess bonds between

- the softer Lewis acid ( $Fe^{II}$ ) and Lewis base (the C end of  $CN^-$ )
- the harder Lewis acid ( $Cr^{III}$ ) and Lewis base (the N end of  $CN^-$ )

In contrast, the  $Fe^{II}-NC-Cr^{III}$  linkages in the less stable linkage isomer involve bonds between

- the softer base (the C end of  $CN^-$ ) and harder acid ( $Cr^{III}$ )



- the harder base (the N end of  $\text{CN}^-$ ) and softer acid ( $\text{Fe}^{\text{II}}$ )

## Stereoisomerism

### Optical Isomerism/Chirality

Molecules of  $D_n$ ,  $C_n$ , or  $C_1$  symmetry with only proper rotation axes (including  $E = C_1$ ) are chiral and exhibit optical isomerism. As described in Figure 8.1.5.1, the main sources of such optical isomerism in coordination chemistry are:

#### 1. Chirality inherent to an organic or main group ligand.

This type of isomerism is just an extension of the sort described in undergraduate organic texts and consequently does not merit separate discussion here, other than to note that some forms of optical isomerism which are of little importance in organic chemistry lead to optical activity in coordination compounds. In particular, the **nitrogen inversion** process which serves to rapidly racemize chiral amines is frozen out on formation of a metal-ligand bond. Because of this chiral amine, ligands bound to a metal form non-interconvertible *R* and *S* enantiomers, as shown in Figure 8.1.5.8

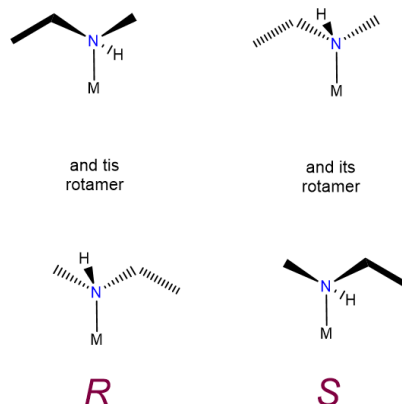


Figure 8.1.5.8. Two views of *R* and *S* enantiomers formed when the chiral amine ethylmethylamine binds a metal that are commonly used to represent chiral amines in complexes. This work by Stephen Contakes is licensed under a [Creative Commons Attribution 4.0 International License](#).

#### 2. Chirality arising from the symmetry of ligands about a metal center.

The two common situations through which such chirality arises involve:

##### i. Chirality at a tetrahedral metal center surrounded by four different ligand attachment points.

Such cases are often referred to as MABCD or Mabcd where M stands for the metal and a, b, c, and d the four different ligand attachment points. An example of such a complex is given in Figure 8.1.5.9A. The chirality of such complexes is analogous to the chirality arising from a tetrahedral carbon stereocenter. There are two caveats, though. First, it is not enough to have a four-coordinate complex; the metal must possess tetrahedral symmetry since, as shown in Figure 8.1.5.9B, square planar M complexes with four different ligands are identical to their mirror images. Second, such chirality is most easily realized using macrocyclic ligands like proteins. Metal ligand bonds involving sterically unhindered monodentate complexes like that in the example of Figure 8.1.5.9A are in general weaker and more flexible than analogous carbon-carbon bonds. Consequently, in such cases it is likely that the enantiomers would interconvert through a fluxional process, making their resolution difficult if not impossible.

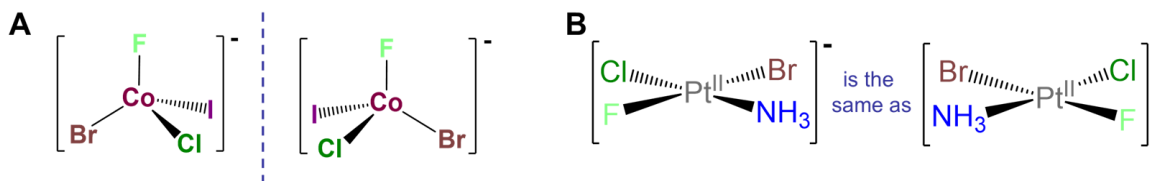


Figure 8.1.5.9. (A) In principle tetrahedral metal centers surrounded by four different ligands (Mabcd) exhibit chirality analogous to the chirality of tetrahedral carbon stereocenters; (B) in contrast, square planar Macbd complexes like  $[\text{PtBrClF}(\text{NH}_3)]^-$  are not chiral since they are the same as their mirror images. (It is easiest to see this by either working out its point group ( $C_s$ ) or by rotating the left  $[\text{PtBrClF}(\text{NH}_3)]^-$  structure clockwise 180 degrees to give its mirror image. This work by Stephen Contakes is licensed under a [Creative Commons Attribution 4.0 International License](#).

ii.  $\Lambda$  and  $\Delta$  isomerism at octahedral metal centers surrounded by two or three chelating ligands.  
Specifically,

- Octahedral tris-chelates of formula  $M(L\sim L)_3$  exhibit  $D_3$  symmetry.
- cis-octahedral bis-chelates of formula  $M(L\sim L)_2XY$  exhibit  $C_2$  or  $C_1$  symmetry:  $C_2$  if  $X = Y$  and  $C_1$  if  $X \neq Y$ .

As shown in Figure 8.1.5.10A octahedral tris-chelates like  $[V(ox)_3]^{3-}$  are chiral and can exist as nonsuperimposable  $\Lambda$  and  $\Delta$  enantiomers. The chirality of these tris-chelates is analogous to that of pinwheels. As shown in Figure 8.1.5.10B when looking directly at the head of any individual pinwheel from above, the blades will be angled from back to front going around the pinwheel in either the clockwise or counterclockwise direction. As shown in Figure 8.1.5.10C the case for which the blades are angled in the clockwise direction is analogous to the  $\Lambda$  enantiomer and the case when they are angled in the counterclockwise direction the  $\Delta$ .

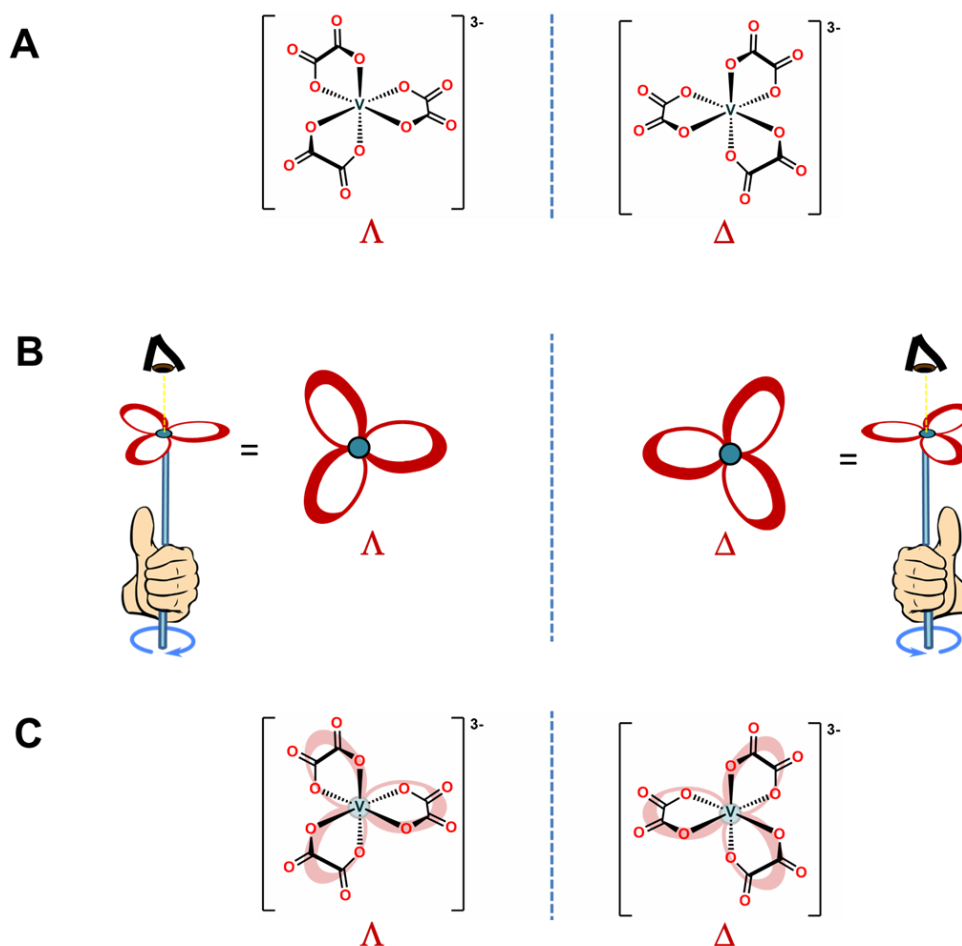


Figure 8.1.5.10. (A) Octahedral tris-chelates like  $[V(ox)_3]^{3-}$  are chiral and can exist as  $\Lambda$  and  $\Delta$  enantiomers. (B) The chirality in these systems is analogous to that of a pinwheel, with the  $\Lambda$  enantiomer exhibiting the symmetry of a left-handed pinwheel and the  $\Delta$  enantiomer that of a right handed one. (C) The pinwheel-like nature of  $\Lambda$  and  $\Delta$  enantiomers is easiest to see by overlaying the structures of  $[V(ox)_3]^{3-}$  from A with the pinwheel structures of B. One way to recognize  $\Lambda$  and  $\Delta$  enantiomers is to draw them in these projections. If a left hand is curled around the  $\Lambda$  enantiomer with the thumb facing up the curl of the fingers will flow from the back of each ligand towards the front. The same will be true if the right hand is curled around the  $\Delta$  enantiomer. Credits: Although the image is largely an original drawing, the hand images used in part B are adapted from an image by SVGguru / CC BY-SA (<https://creativecommons.org/licenses/by-sa/4.0>). Otherwise this work by Stephen Contakes is licensed under a [Creative Commons Attribution 4.0 International License](https://creativecommons.org/licenses/by-sa/4.0).

The  $\Lambda$  and  $\Delta$  chirality in octahedral bis-chelates is analogous to that in the tris-chelates except this time the third chelating ligand is replaced by an arbitrary pair of ligands. This lowers the symmetry of the complex to either  $C_2$  or  $C_1$ , as shown for the  $C_2$  complex  $[CoCl_2(en)_2]^+$  in Figure 8.1.5.11A In either case the result is that such complexes exist as  $\Lambda$  and  $\Delta$  enantiomers analogous to those in the metal tris-chelates, as shown in Figure 8.1.5.11B

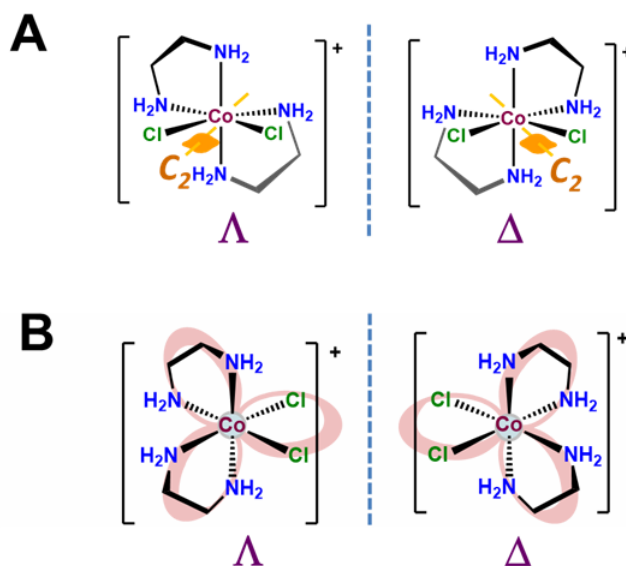


Figure 8.1.5.9C. This work by Stephen Contakes is licensed under a [Creative Commons Attribution 4.0 International License](#).

Octahedral complexes containing ligands with denticities of four or more also exhibit  $\Lambda$  and  $\Delta$  chirality; it is just that in such cases the bound ligand defines multiple rings within the complex that can be defined as existing in either  $\Lambda$  or  $\Delta$  orientations relative to each other. The procedure for making these assignments is beyond the scope of most introductory inorganic courses but the result is that such complexes are designated as  $\Lambda\Lambda$ ,  $\Delta\Delta$ ,  $\Delta\Lambda$ ,  $\Delta\Delta\Delta$ , etc., depending on the number of relationships involving the rings defined by the bound ligand. Interested readers should consult reference 4 for more details.

#### Circular dichroism may be used to characterize optically active metal complexes.

At the present the most definitive way to determine the absolute configuration of an optically active coordination compound is to determine its 3D molecular structure using single crystal X-ray crystallography.<sup>5</sup> However, as that is not always possible or convenient, the optical activity of coordination complexes is also commonly studied using circular dichroism (CD) spectroscopy. CD spectroscopy is used because, unlike most chiral organics, optically active coordination complexes possess low-energy electronic transitions that occur in the far UV and visible range. This means that it is often convenient to use the ability of a complex to refract and absorb different circular polarizations of light to derive information about both the configuration of an optically active complex and its electronic structure. The focus of this section will be to explain how the determination of absolute configuration by circular dichroism and optical rotatory dispersion work, as well as the relationship of these techniques to the more ordinary sort of polarimetry used to measure optical rotation in organic systems. Only brief notes will be made about the instrumental and electronic structure applications of these techniques since the electronic spectra of metal complexes will be discussed in [Chapter 11: Coordination Chemistry III - Electronic Spectra](#) and the [instrumental aspects of CD are well-treated elsewhere](#).

Both polarimetry and circular dichroism spectroscopy are grounded in the recognition that plane polarized light is equivalent to a superposition of left and right circularly polarized light, as shown in Figure 8.1.5.12

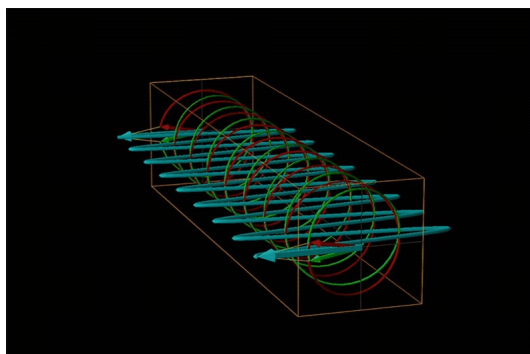


Figure 8.1.5.12. Angled and front view of plane polarized light (light blue) as the vector sum of left circularly polarized light (red) and right circularly polarized light (green). Created using EMANIM Version 1.2 (2011 July) by Andras Szilagyi ([www.enzim.hu/~szia/emanim](http://www.enzim.hu/~szia/emanim)). This work by Stephen Contakes is licensed under a [Creative Commons Attribution 4.0 International License](https://creativecommons.org/licenses/by/4.0/).

When plane polarized light passes through a chiral medium, its left and right circularly polarized components move at different rates (*i.e.*, have different indices of refraction). This causes the plane of polarization to rotate in the direction of the faster component according to the relationship

$$\alpha = \frac{n_l - n_r}{\lambda}$$

where  $\alpha$  is the angle of rotation,  $\lambda$  the light's wavelength, and  $n_l$  and  $n_r$  the refractive indices experienced by left and right circularly polarized light.

An example of such a rotation is shown in Figure 8.1.5.13

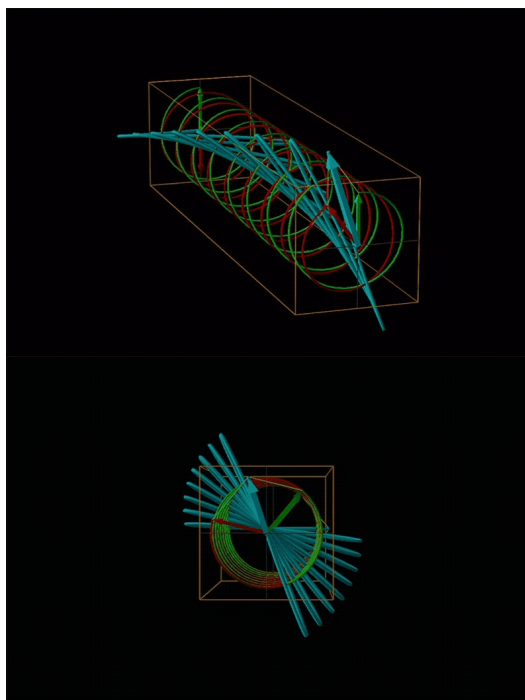


Figure 8.1.5.13. Angled and front view of plane polarized light (light blue) as it passes through a medium (represented by the orange box) in which left circularly polarized light (red) experiences a higher refractive index (and so moves slower) than right circularly polarized light (green). Created using EMANIM Version 1.2 (2011 July) by Andras Szilagyi ([www.enzim.hu/~szia/emanim](http://www.enzim.hu/~szia/emanim)) with a refractive index of 1.05 for left circularly polarized light and 1.00 for right circularly polarized light. This work by Stephen Contakes is licensed under a [Creative Commons Attribution 4.0 International License](https://creativecommons.org/licenses/by/4.0/).

Chemists typically call this rotation of light by a chiral medium optical rotation. In organic chemistry it is common to measure the optical rotation at the sodium D wavelength of 589.29 nm, a much longer wavelength than most organics are able to absorb. Because of this the optical rotations commonly measured by organic chemists are largely independent of absorption and mainly serve as a characteristic physical property similar to melting points or are used to establish the purity of a mixture of enantiomers. The sort of spectroscopic data used to characterize chiral coordination compounds more commonly makes use of the relationship between absorption and optical rotation.

In coordination chemistry the wavelength-dependence of optical rotation is used to discern information about compounds' electronic spectra. This measurement of the wavelength dependence of optical rotation is called **optical rotatory dispersion (ORD)** and the resulting plots are called optical rotatory dispersion or ORD spectra or curves. Such ORD curves are useful for characterizing the chiral environment in a coordination complex because the ORD curves exhibit a characteristic shape. This characteristic shape is because according to the **Cotton Effect**, the optical rotation changes sign at the absorption maximum of a chromophore in the compound. For one configuration the rotation will go from negative to positive with increasing wavelength and is called a **positive cotton effect**; for the other configuration the rotation will go from positive to negative or exhibit a **negative cotton effect**. This behavior is summarized in the top two curves of Figure 8.1.5.14

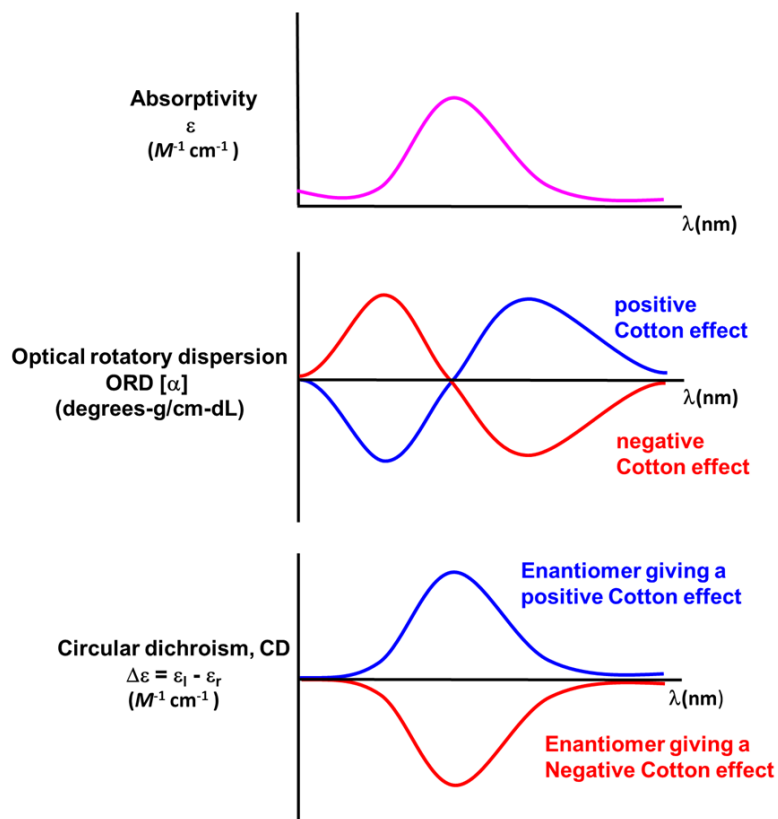


Figure 8.1.5.14. Idealized relationship between absorbance, ORD, and CD spectra for enantiomers exhibiting a positive and negative Cotton effect. This work by Stephen Contakes is licensed under a [Creative Commons Attribution 4.0 International License](https://creativecommons.org/licenses/by/4.0/).

A technique used even more often than ORD is **circular dichroism (CD)**, represented by the lowest spectrum in Figure 8.1.5.14. Circular dichroism arises from the differential absorption of left and right circularly polarized light by a chiral compound. This gives elliptically polarized light as shown in Figure 8.1.5.15

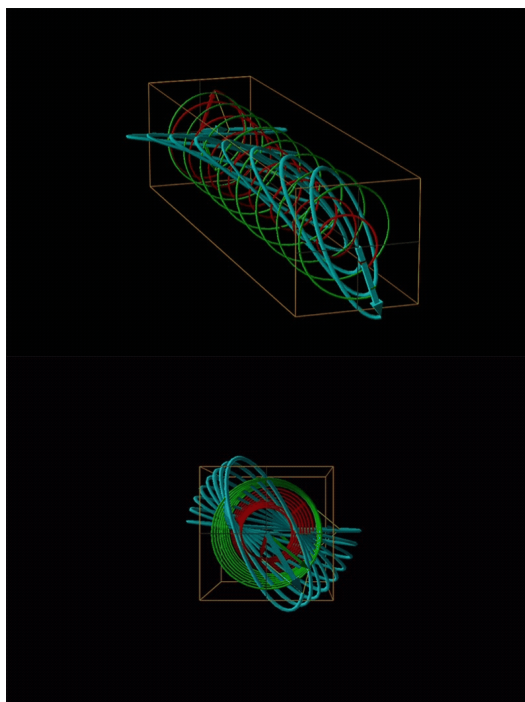


Figure 8.1.5.15. Angled and front view of plane polarized light (light blue) as it passes through a medium (represented by the orange box) in which left circularly polarized light (red) both experiences a higher refractive index and greater absorption than right circularly polarized light (green). Created using EMANIM Version 1.2 (2011 July) by Andras Szilagyi ([www.enzim.hu/~szia/emanim](http://www.enzim.hu/~szia/emanim)) with a refractive index of 1.05 and an extinction coefficient of 0.05 for left circularly polarized light and a refractive index of 1.00 and extinction coefficient of 0 for right circularly polarized light. This work by Stephen Contakes is licensed under a [Creative Commons Attribution 4.0 International License](https://creativecommons.org/licenses/by/4.0/).

In circular dichroism (CD) spectroscopy a sample is irradiated with polarized light resulting in the transmission of elliptically polarized light due to differential refraction and absorption of the polarized light's left and right circularly polarized components. For achiral molecules the handedness doesn't affect absorbance, but for chiral molecules, which chiral ground and excited states the handedness of an EM wave affects can determine how readily that wave can distort the chiral ground state into the chiral excited one. For this reason chiral molecules absorb left and right circularly polarized light differently.

In CD spectroscopy the magnitudes of the left and right circularly polarized components of light that is transmitted by the sample are measured and used to determine how much light of each was absorbed (just as in regular absorbance spectroscopy). The difference in absorption between left and right circularly polarized light constitutes the primary signal in CD spectroscopy. More specifically, circular dichroism spectra (CD spectra) show the difference in extinction coefficients for left and right circularly polarized light,  $\Delta\epsilon$ , as a function of wavelength, where

$$\Delta\epsilon = \epsilon_l - \epsilon_r$$

where  $\epsilon_l$  and  $\epsilon_r$  are the extinction coefficients observed with left and right circularly polarized light, respectively.

As with ORD spectra, the signs of the features in CD spectra like that of  $\Delta[\text{Co(en)}_3]\text{Cl}_3$  given in Figure 8.1.5.16 are enantiomer-dependent. As illustrated in the lower spectrum in Figure 8.1.5.14, the CD spectra of enantiomers mirror one another. Because of this difference in behavior it is possible in principle to determine the absolute configuration of a complex from its CD spectrum.

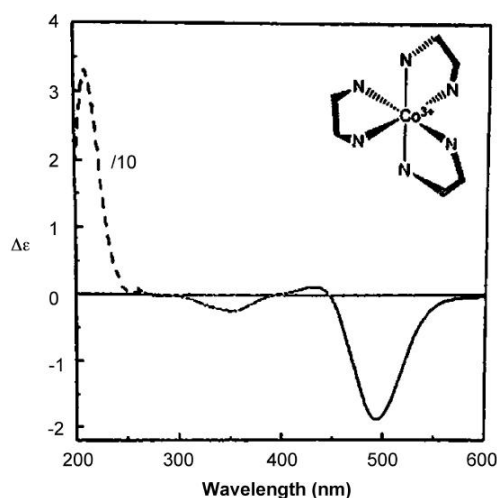


Figure 8.1.5.16. CD spectrum of  $\Delta$ -[Co(en)<sub>3</sub>]Cl<sub>3</sub>. Taken from reference 6.

There are several ways that ORD and CD spectra can be useful for determining the absolute configuration of a chiral complex.

1. First, the sign of the Cotton effect and peaks in CD spectra exhibited by a given absolute configuration is often consistent across a series of compounds. Thus if a new member of the series is isolated, its configuration can be determined based on which enantiomer has the same Cotton effect. For instance, if both the  $\Lambda$  isomer of a metal diimine complex like [Ru(bpy)<sub>3</sub>]<sup>2+</sup> exhibit a positive Cotton effect and a newly resolved metal diimine exhibits a negative Cotton effect it might reasonably be inferred that the newly-resolved complex is in the opposite or  $\Delta$  configuration.
2. Second, for some systems the expected sign of the Cotton effect and CD peaks for each enantiomer may be predicted semi-empirically based on the spatial locations of substituents relative to the chromophore (the part of the molecule that changes electronic structure during the transition), although the details are beyond the scope of the present discussion.
3. Consideration of interactions between multiple chromophores in a compound can be used to infer absolute configuration. Again, the details are beyond the scope of the present discussion. Interested readers are referred to reference 7 for details.

## Common patterns of Diastereomerism

### Geometric isomerism

Geometric isomerism involves differences in the geometric placement of atoms in a compound. In coordination chemistry, geometric isomerism involves differences in the relative placement of a set of ligands about a metal center. There are two main types:

#### *cis* and *trans* isomerism

This type of isomerism has to do with how two ligands are oriented relative to one another in a square planar or octahedral complex. As shown in Figure 8.1.5.17, ligands that are next to one another with a L-M-L bond angle of 90° are said to be *cis*; those on opposite sides of the metal with a L-M-L bond angle of 180° are in the *trans* arrangement.



Figure 8.1.5.17. *cis* and *trans* arrangement of ligands around (A) square planar and (B) octahedral metal centers. Since both types of complexes feature 90° L-M-L bond angles, the arrangements are fundamentally the same in both cases. This work by Stephen Contakes is licensed under a [Creative Commons Attribution 4.0 International License](https://creativecommons.org/licenses/by/4.0/).

Simple *cis* and *trans* geometric isomers can be identified when there are two identical ligands (A) or chelating ligands with distinguishable attachment points (A~B) oriented about either a square planar or octahedral center. Examples are given in Figure 8.1.5.18 Notice from the example given in Figure 8.1.5.18C that multidentate ligands have the potential to constrain complexes to adopt a particular geometry.



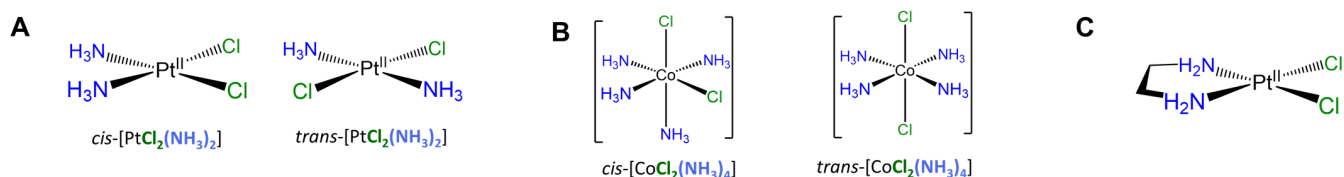


Figure 8.1.5.18. Examples of square planar and octahedral *cis* and *trans* isomers. (A) *cis* and *trans* isomers of  $[PtCl_2(NH_3)_2]$ ; the former is medically important. Sold under the name cisplatin, the *cis* isomer is used as a chemotherapy against various forms of cancer. (B) *cis* and *trans* isomers of  $[CoCl_2(NH_3)_4]$ , a compound of more academic interest. (C)  $PtCl_2(en)$  only exists as the *cis* isomer because the chelating en ligand can only bind in a *cis* arrangement. This work by Stephen Contakes is licensed under a [Creative Commons Attribution 4.0 International License](#).

Slightly more involved examples involve perturbations of the simple cases above in which there are multiple distinguishable *cis* and/or *trans* relationships. Two square planar examples are given in Figure 8.1.5.19

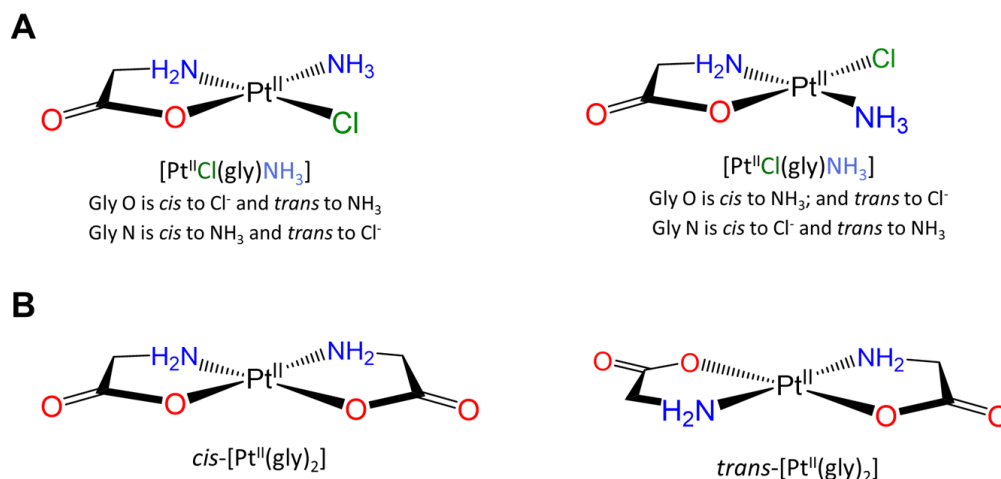


Figure 8.1.5.19. Examples of more complex square planar systems. (A) Geometric isomers of  $[PtCl(gly)NH_3]$ , a  $MA_2BC$  system for which A = gly<sup>-</sup>, B =  $Cl^-$ , and C =  $NH_3$ . Swapping of the ammine and chloro ligands changes both the *cis* and *trans* relationships involving the Gly ligand. (B) Geometric isomers of  $[Pt(gly)_2]$ , an  $M(A\sim B)_2$  system for which A = the  $\kappa O$  glycine carboxy group and B its  $\kappa N$  amine. The only possible geometric isomerism involves swapping the orientation of one glycine relative to the other. For this reason the two complexes shown can be designated as *cis* and *trans* isomers based on whether the  $\kappa O$  and  $\kappa N$  ends of the glycine are *cis* or *trans* to one another. This work by Stephen Contakes is licensed under a [Creative Commons Attribution 4.0 International License](#).

More complex examples of *cis* and *trans* relationships between ligands in octahedral complexes are given in the exercises that conclude this page, which also demonstrates how a systematic approach may be used to identify isomers.

### mer and fac isomerism

This type of isomerism has to do with how three ligands are oriented relative to one another in an octahedral complex. The arrangements are represented in Figure 8.1.5.20

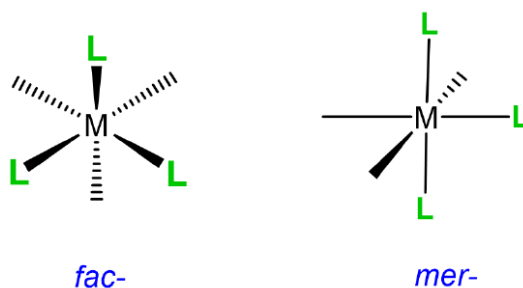


Figure 8.1.5.20. Simple representation of the *fac* and *mer* arrangements of ligands around an octahedral metal center. This work by Stephen Contakes is licensed under a [Creative Commons Attribution 4.0 International License](#).

Since it can help to visualize the *mer* and *fac* geometry from multiple points of view, several representations are given in Figure 8.1.5.21 As shown in Figure 8.1.5.21, in **fac** or **facial arrangements**, the ligands occupy the same "face" of the octahedral

coordination sphere, while in the **mer** or **meridional geometry** the ligands form a T shape in the same plane or its "meridian."<sup>8</sup>

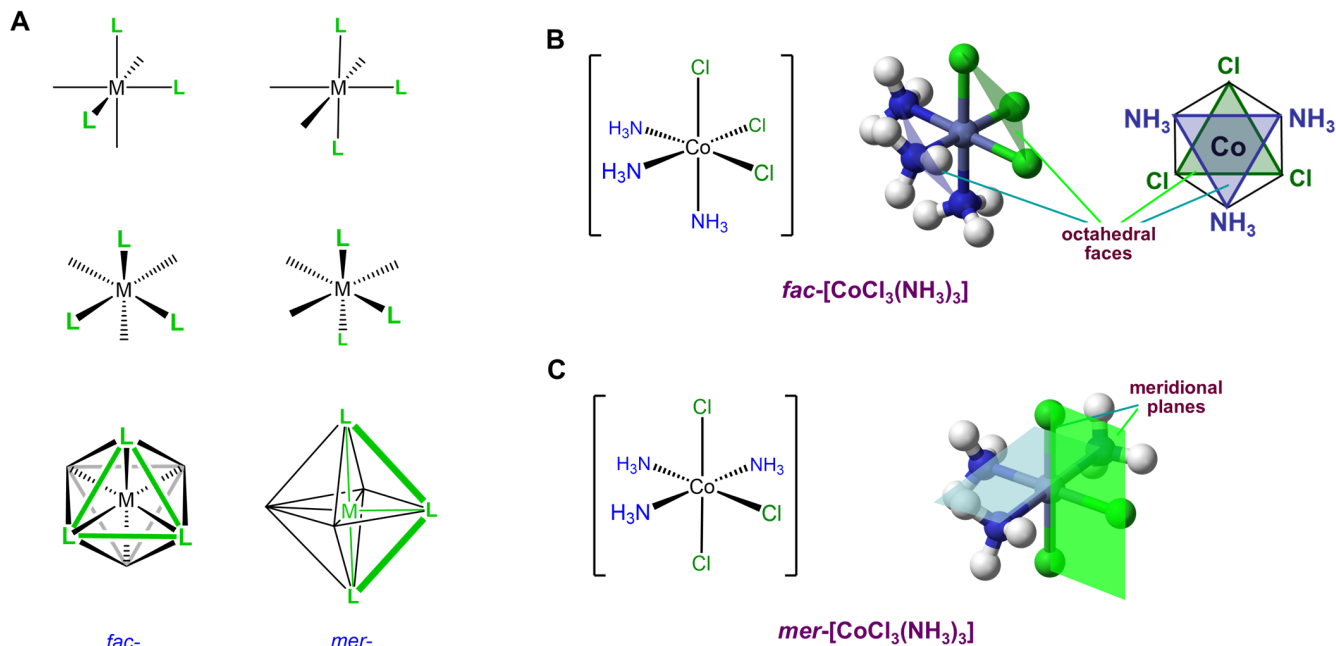


Figure 8.1.5.21. (A) Three projections of *fac* and *mer* arrangements of ligands around an octahedral metal center emphasizing that in the *fac* arrangement the ligands are oriented along a face of the octahedron while in the *mer* arrangement they are oriented in a plane. (B) Structure of *fac*-[CoCl<sub>3</sub>(NH<sub>3</sub>)<sub>3</sub>] showing the octahedral faces occupied by the chloro and amine ligands. (C) Structure of *mer*-[CoCl<sub>3</sub>(NH<sub>3</sub>)<sub>3</sub>] showing the planar arrangement of the chloro and ammine ligands. The ball and stick models are modified from images by Benjah-bmm27 - Own work, Public Domain, <https://commons.wikimedia.org/w/index.php?curid=1874872> and [curid=1874873](https://commons.wikimedia.org/w/index.php?curid=1874873). Otherwise this work by Stephen Contakes is licensed under a [Creative Commons Attribution 4.0 International License](#).

Octahedral complexes with three identical ligands oriented about an octahedral center can only exist in *mer* and *fac* arrangements. Consequently, such complexes can be designated as *mer* and *fac* isomers. Examples are given in Figure 8.1.5.22

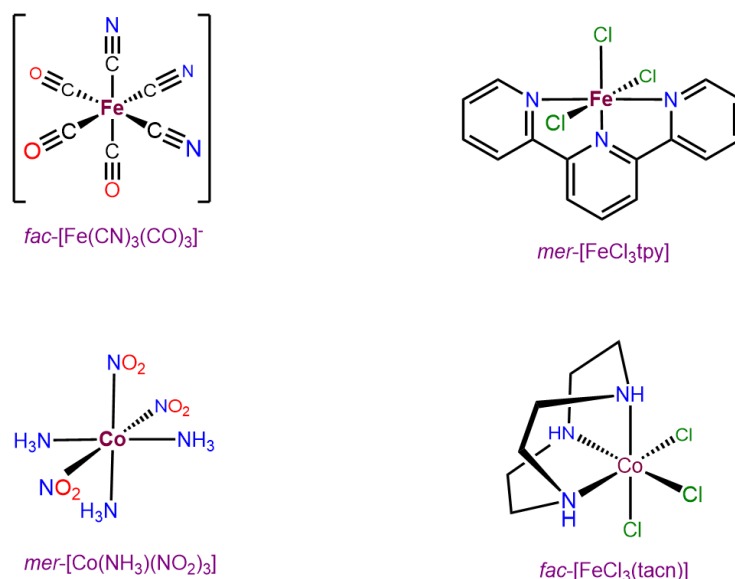


Figure 8.1.5.22. Examples of *fac* and *mer* octahedral complexes. Note how some chelating ligands preferentially bind to the metal in a *fac* or *mer* arrangement and, in so doing, force the other ligands to also form a *mer* or *fac* arrangement. This work by Stephen Contakes is licensed under a [Creative Commons Attribution 4.0 International License](#).

### Diastereomerism arising from multiple ligand-associated chiral centers

Diastereomerism can also arise when two or more chiral ligands bind to a metal center. Such cases typically give rise to a complex mixture of isomers, as shown by the example in Figure 8.1.5.23 As may be seen from Figure 8.1.5.23 the differences between

these isomers can arise from both changes in the stereochemical configuration of the ligand and the relationship of particular ligand centers relative to one another. For instance, the leftmost two structures in Figure 8.1.5.23 possess one *R* and *S* nitrogen center each but differ in whether the centers are oriented so that the *R* and *S* centers on the two ligands are *trans* or *cis* to one another.

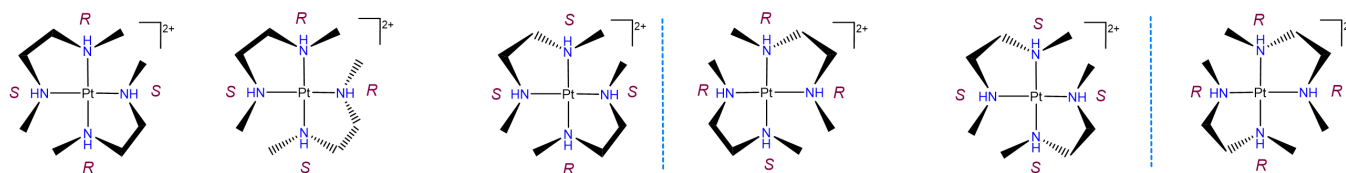


Figure 8.1.5.23. Diastereomers that can in principle be formed when two *N,N'*-dimethylethylenediamine ligands coordinate a  $\text{Pt}^{2+}$  center. This work by Stephen Contakes is licensed under a [Creative Commons Attribution 4.0 International License](#).

### Diastereomerism arising from $\lambda$ and $\delta$ ring conformation isomerism.

Chelate rings are formed when a chelating ligand binds a metal

As may also be seen from the structures in Figure 8.1.5.23 when a multidentate ligand coordinates a metal, the ligand and metal center comprise one or more **chelate rings**. Examples of such chelate rings are shown in Figure 8.1.5.24

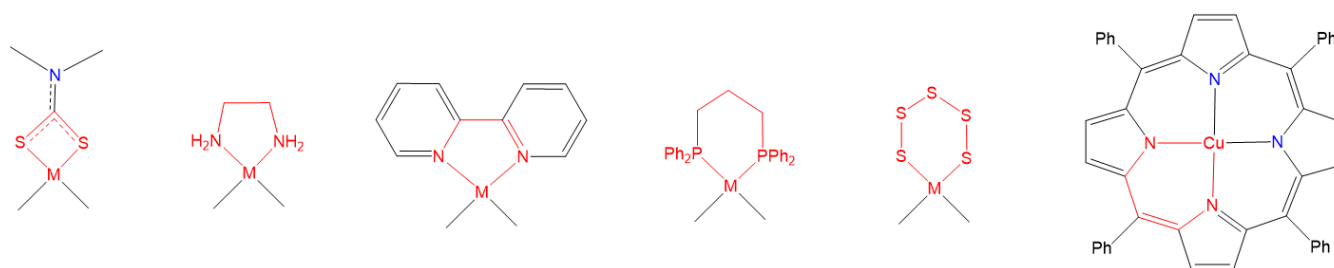


Figure 8.1.5.24. Four, five, and six-membered chelate rings (shown in red) formed by coordination of selected bidentate ligands to a metal center. This work by Stephen Contakes is licensed under a [Creative Commons Attribution 4.0 International License](#).

As may be inferred from the examples in Figure 8.1.5.24 chelate rings may be of different sizes, although four, six, and especially five-membered rings are particularly common. Exactly which ring sizes will be more stable for a given system depends on the coordination geometry and, due to differences in M-L bond lengths, to a lesser degree on the metal. As a result, for octahedral and square planar complexes with  $90^\circ$  L-M-L bond angles between *cis* ligands, *five-membered rings tend to be especially stable* (Figure 8.1.5.25).

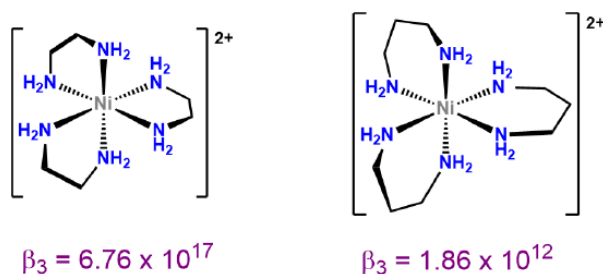


Figure 8.1.5.25. The greater stability of five-membered chelate rings involving  $\text{Ni}^{2+}$  and organic ligands is reflected in the higher overall formation constant ( $\beta_3$ ) for the five-membered chelate rings contained in  $[\text{Ni}(\text{en})_3]^{2+}$  compared to that of  $[\text{Ni}(\text{et})_3]^{2+}$ , which has six-membered rings. The data in this figure is taken from [Stability of Metal Complexes and Chelation](#) by Robert Lancashire. This work by Stephen Contakes is licensed under a [Creative Commons Attribution 4.0 International License](#).

Not all metal chelates prefer to form five-membered rings. The steric requirements of chelate rings depend on both the preferred coordination geometry of the metal center and the stereochemistry of the ligand. Both of these effects are typically considered in terms of preferred L-M-L bond angles. From the perspective of the metal center, the preferred bond angle is determined by the coordination geometry. Octahedral and square planar metals prefer  $90^\circ$  L-M-L bond angles, trigonal bipyramidal systems  $90$  and  $120^\circ$  L-M-L bond angles, and tetrahedral complexes  $109.5^\circ$  L-M-L angles. The larger preferred bond angles in tetrahedral and trigonal bipyramidal systems often require the formation of larger six or seven-membered chelate rings for maximum stability. The size of the chelate ring actually formed between a metal and ligand is determined by the ligand's structure. As the contributor of all the atoms in the chelate ring but one, the ligand directly determines the chelate ring size. More subtly, ligands naturally prefer to coordinate metals at a particular L-M-L angle, called the **bite angle**, as shown in Figure 8.1.5.26A Ligands with bite angles corresponding to the ideal L-M-L angle for a metal's preferred geometry tend to form more stable complexes, although in turn

ligand bite angles can cause metals with a weak coordination geometry preference to adopt the ligand's preferred geometry instead.<sup>10</sup> As may be seen from the values in Figure 8.1.5.26B bite angles roughly increase with the size of the chelate ring formed but are also influenced by the types of structures used to connect the ligand's Lewis base sites. This facilitates the use of diphosphine ligands to tailor the structure and reactivity of phosphine-containing organometallic catalysts.

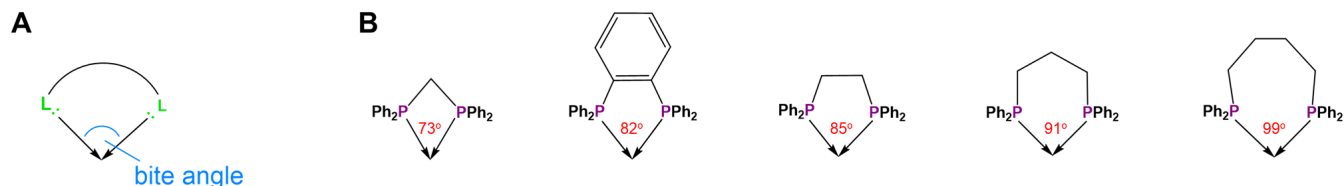


Figure 8.1.5.26. (A) Definition of the bite angle as the angle at which the ligand's preferred L-M-L angle when coordinating a metal center. (B) Bite angles of selected diphosphines.<sup>9</sup> The bite angles of many such diphosphines have been determined to facilitate the design of phosphine-containing organometallic catalysts. This work by Stephen Contakes is licensed under a [Creative Commons Attribution 4.0 International License](#).

$\lambda$  and  $\delta$  isomerism involves differences in the conformation of nonplanar five-membered chelate rings

As shown in Figure 8.1.5.27, some chelate ring systems are planar while others are not.

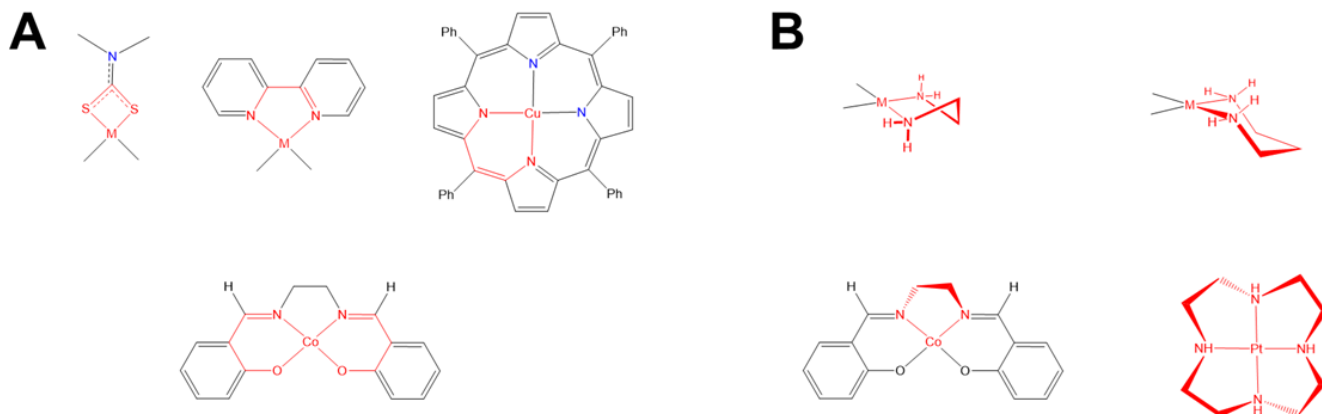


Figure 8.1.5.27. (A) Planar and (B) Nonplanar chelate rings shown highlighted in red. Notice how [Co(salen)] possesses a nonplanar chelate ring and two planar ones. This work by Stephen Contakes is licensed under a [Creative Commons Attribution 4.0 International License](#).

Among the nonplanar chelate ring systems are ligands like en and dppe, which contain tetrahedral C, N, O, P, and S atoms. Because these atoms create kinks in the chelate ring they introduce additional opportunities for diastereomerism due to differences in the chelate ring conformation, called **ring twist**. Ring twist in nonplanar systems has been most extensively explored for five-membered chelates like those formed by dppe and by en and other chelating amines. Unlike the more rigid four-membered chelate rings, five-membered chelates tend to be conformationally flexible, but not so conformationally flexible that their conformers are rapidly interconverting at room temperature (at least not when the rings are substituted to introduce additional steric strain). This balance between flexibility and rigidity enables some five-membered chelate rings to exist as mixtures of distinguishable conformational isomers at room temperature.

To understand the two most stable conformers that five-membered chelates rings tend to form, it is helpful to think of five-membered chelate rings as involving two components (Figure 8.1.5.28):

- a planar L-M-L group, where L are the atoms directly attached to the metal, M, and
- the remaining two ring atoms, E, which form a rigid E-E bar across the back of the chelate ring.

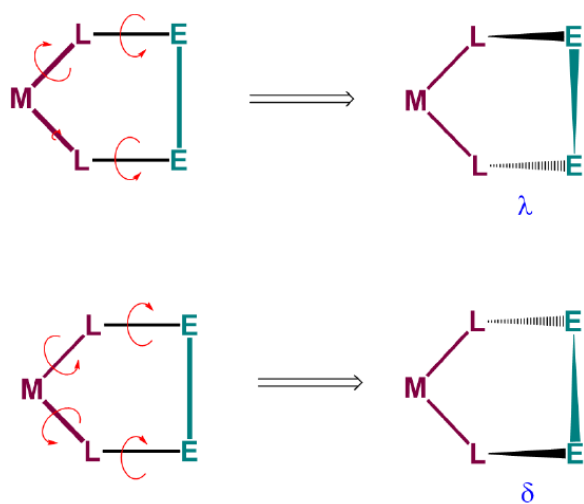
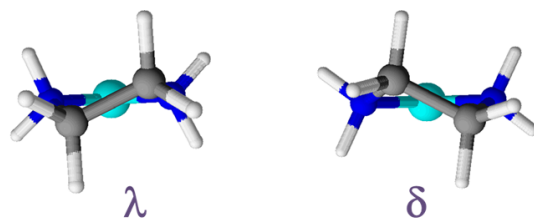


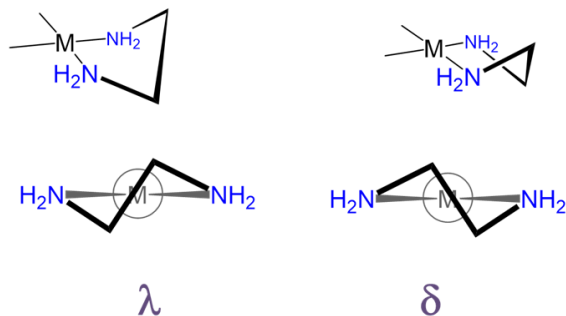
Figure 8.1.5.28. Five-membered chelate rings consist of a planar L-M-L group connected to a rigid E-E bar. Conformers arise as rotation about the M-L and L-E bonds causes twisting of the E-E bar relative to the L-M-L plane. This work by Stephen Contakes is licensed under a [Creative Commons Attribution 4.0 International License](https://creativecommons.org/licenses/by/4.0/).

As can be seen from Figure 8.1.5.28, rotation about the M-L and L-E bonds causes twisting of the E-E bar relative to the L-M-L plane. The two most stable conformers produced by these motions are the  $\lambda$  or  $\delta$  conformations as shown in Figures 8.1.5.29 and 8.1.5.29

A



B



C

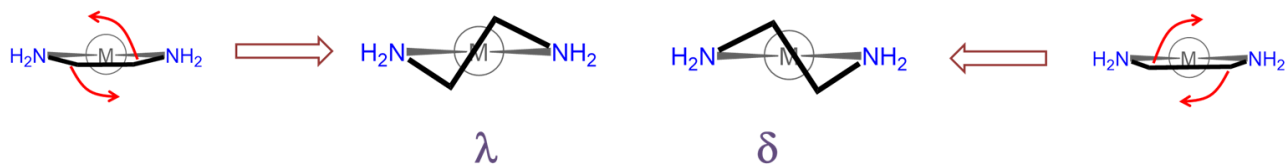


Figure 8.1.5.29. (A)  $\lambda$  and  $\delta$  ring twist in a square planar metal ethylenediamine complex (B) along with several ways to represent it in line drawing form. (C) Of these, the projection looking down an axis bisecting the chelate ring makes it easiest to see that, starting with a planar chelate ring the  $\lambda$  conformer corresponds to a counterclockwise twist of the  $\text{CH}_2\text{CH}_2$  bond relative to the N-M-N plane and the  $\delta$  conformer a clockwise twist relative to the N-M-N plane. This work by Stephen Contakes is licensed under a [Creative Commons Attribution 4.0 International License](https://creativecommons.org/licenses/by/4.0/).

The relative stability of the  $\lambda$  and  $\delta$  conformers will depend on the configuration of any stereocenters present and steric factors. As with organic ring systems, steric effects tend to favor conformers in which bulky groups are placed in the less sterically strained equatorial positions while the configuration of the stereocenters present can serve to restrict the allowable ring twist conformations, as illustrated in Figure 8.1.5.30 A detailed treatment of such systems is beyond the scope of this page. Interested readers are referred to reference 12 for more details.

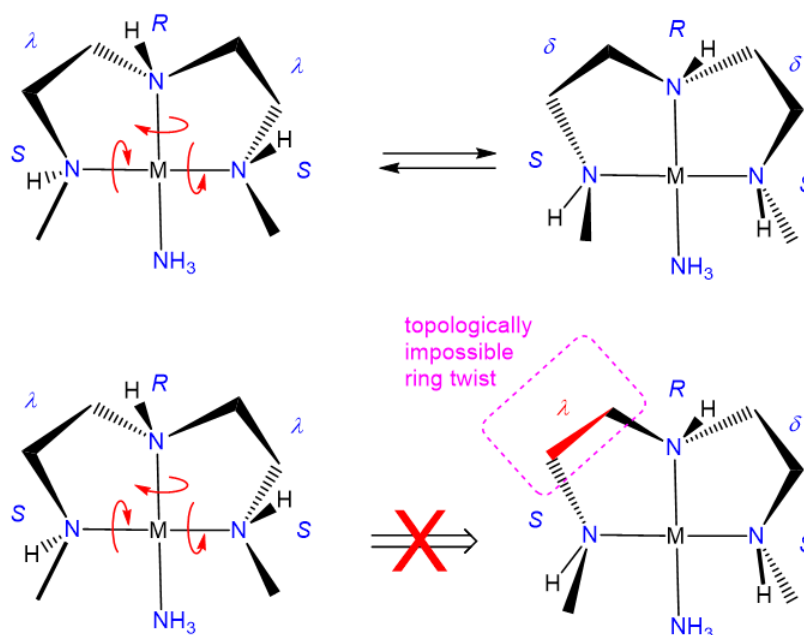


Figure 8.1.5.30. The configurations at nitrogen in the complex shown restrict the chelate ring conformations to either a  $\lambda\lambda$  or  $\delta\delta$  conformation because the rotations needed to enable a  $\lambda\delta$  configuration are topologically impossible. This work by Stephen Contakes is licensed under a [Creative Commons Attribution 4.0 International License](#).

In closing, it should be noted that it might seem to be making much of small effects in pointing out that one source of diastereomerism in metal complexes involves the freezing out of chelate ring conformations. However, that would be to mistake the impacts that ring conformations can have on the steric accessibility of a coordination site and shaping the course of processes that might occur there. As illustrated in Figure 8.1.5.31, a simple shift in the conformation of one ring in a square planar, pyramidal, or octahedral complex containing coplanar ethylene diamine ligands can exert a significant effect on the steric profile of the complex perpendicular to the  $MN_4$  square plane. Because of effects like these, ring conformation isomerism plays a role in the design of stereoselective transition metal catalysts.

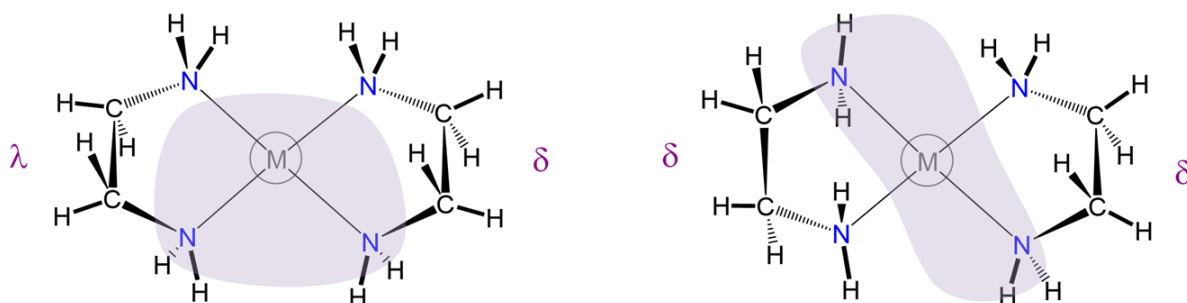


Figure 8.1.5.31. Schematic illustrating how the conformation of ethylenediamine ligands bound to a metal center affects the steric accessibility of the metal (shown shaded in violet) to potential ligands attempting to bind from above the  $MN_4$  plane. This work by Stephen Contakes is licensed under a [Creative Commons Attribution 4.0 International License](#).

## Exercises

### ? Exercise 8.1.5.1. Identify the type of isomerism

What type of isomers are

- $[\text{CoCl}(\text{NH}_3)_5](\text{NO}_3)$  and  $[\text{Co}(\text{NH}_3)_5(N\text{-NO}_2)]\text{Cl}$ ?
- $[\text{Co}(\text{NH}_3)_5\text{-CN-Ru}(\text{NH}_3)_5]^{4+}$  and  $[\text{Co}(\text{NH}_3)_5\text{-NC-Ru}(\text{NH}_3)_5]^{4+}$
- $[\text{Cr}(\text{CN})_5\text{-CN-Co}(\text{NH}_3)_5]$  and  $[\text{Co}(\text{CN})_5\text{-CN-Cr}(\text{NH}_3)_5]$
- cis*- $[\text{Mn}(\text{en})_2(\text{CN})_2]$  and *trans*- $[\text{Mn}(\text{en})_2(\text{CN})_2]$

**Answer a.**

Ionization isomers.

**Answer b.**

Linkage isomers.

**Answer c.**

Coordination isomers.

**Answer d.**

Geometric isomers, specifically *cis/trans* isomers.

### ? Exercise 8.1.5.2. Assigning metal oxidation states in a complex

Many properties of transition metal complexes depend on the metal's oxidation state. For instance,

- octahedral complexes of  $\text{Co}^{\text{II}}$  lose and gain ligands rapidly
- octahedral complexes of  $\text{Co}^{\text{III}}$  lose and gain ligands very slowly
- four-coordinate complexes are generally tetrahedral
- EXCEPT four-coordinate complexes of metals like  $\text{Pt}^{\text{II}}$ ,  $\text{Pd}^{\text{II}}$ ,  $\text{Rh}^{\text{I}}$ , and  $\text{Ir}^{\text{I}}$ , among others, are square planar

For this reason it is important to be able to estimate the formal oxidation state of a metal in a complex. Fortunately, this is easy to do if you remember

1. The sum of all atoms' oxidation states will equal the overall charge on the complex
2. When determining the metal's oxidation state, the ligands can be treated as having an oxidation state equal to their charge - *i.e.*, the charge they possess in the form in which they coordinate the metal - so if they need to lose a proton to bind, don't forget to account for that.

Given the above, estimate the oxidation state of the metal in the following real and hypothetical complexes.

- a.  $\text{Na}_4[\text{Fe}(\text{CN})_6]$
- b.  $[\text{Cu}(\text{phen})_2]\text{BF}_4$
- c.  $[\text{PtF}_4(\text{NH}_3)_2]$
- d.  $[\text{Ni}(\text{en})_2]\text{SO}_4$
- e.  $\text{Co}(\text{acac})_3$
- f.  $[\text{MnCl}(\text{O})(\text{salen})]$

**Answer for  $\text{Na}_4[\text{Fe}(\text{CN})_6]$ .**

This contains  $[\text{Fe}(\text{CN})_6]^{4-}$ ; so  $\text{O.S.}_{\text{Fe}} + 6 \times (-1)$  (for  $\text{CN}^-$ ) = -4 (the complex's charge) so  $\text{O.S.}_{\text{Fe}} = +2$  or  $\text{Fe}^{2+}$ .

**Answer for  $[\text{Cu}(\text{phen})_2]\text{BF}_4$ .**

Since tetrafluoroborate is a monoanion, the complex is  $[\text{Cu}(\text{phen})_2]^+$  so  $\text{O.S.}_{\text{Cu}} + 0 \times 2$  (for phen) = +1 (the complex's charge) so  $\text{O.S.}_{\text{Cu}} = +1$  or  $\text{Cu}^+$ .

**Answer for  $[\text{PtF}_4(\text{NH}_3)_2]$ .**

$\text{O.S.}_{\text{Pt}} + 4 \times (-1)$  (for  $\text{F}^-$ ) +  $0 \times 2$  (for  $\text{NH}_3$ ) = +0 (the complex's charge) so  $\text{O.S.}_{\text{Pt}} = +4$  or  $\text{Pt}^{4+}$ .

**Answer  $[\text{Ni}(\text{en})_2]\text{SO}_4$ .**

The complex is  $[\text{Ni}(\text{en})_2]^+$  so  $\text{O.S.}_{\text{Ni}} + 0 \times 2$  (for en) = +2 (the complex's charge) so  $\text{O.S.}_{\text{Ni}} = +2$  or  $\text{Ni}^{2+}$ .

**Answer  $\text{Co}(\text{acac})_3$ .**

$\text{O.S.}_{\text{Co}} + 3 \times (-1)$  (for acac; see [table 9.2.2](#)) = +0 (the complex's charge) so  $\text{O.S.}_{\text{Co}} = +3$  or  $\text{Co}^{3+}$ .

**Answer  $[\text{MnCl}(\text{O})(\text{salen})]$ .**

$\text{O.S.}_{\text{Mn}} + 1 \times (-1)$  (for  $\text{Cl}^-$ ) +  $1 \times (-2)$  (for oxo) +  $1 \times (-2)$  (for salen; see [table 9.2.2](#)) = +0 (the complex's charge) so  $\text{O.S.}_{\text{Mn}} = +5$  or  $\text{Mn}^{5+}$ .



### ? Exercise 8.1.5.3. Drawing isomers from descriptions

Draw structures that match the descriptions given, assuming that

- complexes in which the metal has a coordination number of six are octahedral
- complexes in which the metal has a coordination number of five are trigonal bipyramidal
- complexes in which  $\text{Pt}^{\text{II}}$ ,  $\text{Pd}^{\text{II}}$ , or  $\text{Rh}^{\text{I}}$ , or  $\text{Ir}^{\text{I}}$  have a coordination number of four are square planar
- other complexes in which the metal has a coordination number of four will be tetrahedral

a. *mer*-triammineaqua-*trans*-dichlorocobalt(III) ion

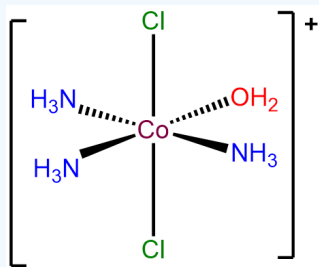
b.  $\Delta$ -diamminebis(oxalato)manganate(III)

c.  $[\text{CoCl}_4]^{2-}$

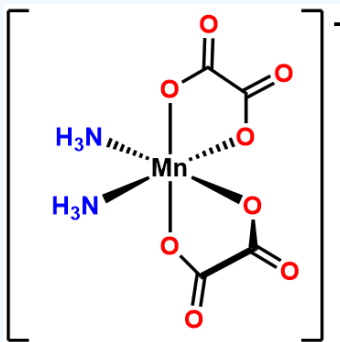
d. *trans*-diamminebis(ethylenediamine)Nickel(2+) tetracyanopalladate(2-)

e.  $\Lambda$ -bis(ethylenediamine)cobalt(III)-  $\mu$ -amido  $\mu$ -hydroxo- $\Delta$ -bis(ethylenediamine)cobalt(III)

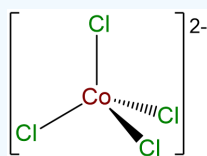
Answer a. *mer*-triammineaqua-*trans*-dichlorocobalt(III) ion.



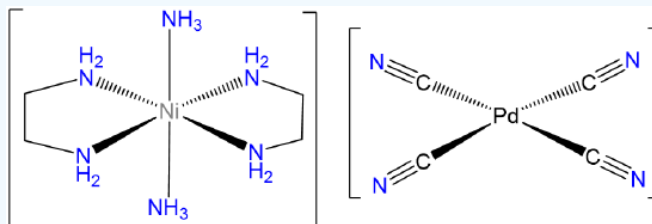
Answer b.  $\Delta$ -diamminebis(oxalato)manganate(III).



Answer c.  $[\text{CoCl}_4]^{2-}$ .

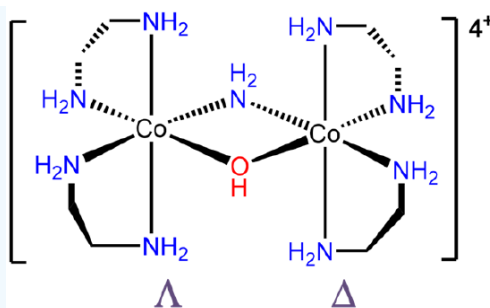


Answer d. *trans*-diamminebis(ethylenediamine)Nickel(2+) tetracyanopalladate(2-).



Note that since the Pd in  $[\text{Pd}(\text{CN})_4]^{2-}$  is  $\text{Pd}^{2+}$  it will be square planar.

Answer e.  $\Lambda$ -bis(ethylenediamine)cobalt(III)-  $\mu$ -amido  $\mu$ -hydroxo- $\Delta$ -bis(ethylenediamine)cobalt(III).



#### ? Exercise 8.1.5.4. Stereoisomers of complexes containing only monodentate ligands.

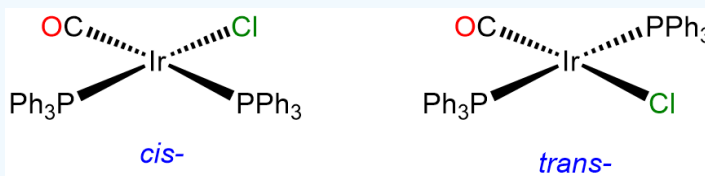
Draw all the stereoisomers of the following real and hypothetical complexes. You may assume that

- complexes in which the metal has a coordination number of six are octahedral
- complexes in which the metal has a coordination number of five are trigonal bipyramidal
- complexes in which  $\text{Pt}^{\text{II}}$ ,  $\text{Pd}^{\text{II}}$ , or  $\text{Rh}^{\text{I}}$ , or  $\text{Ir}^{\text{I}}$  have a coordination number of four are square planar
- other complexes in which the metal has a coordination number of four will be tetrahedral

- $[\text{IrCl}(\text{CO})(\text{PPh}_3)_2]$
- $[\text{CoCl}_3(\text{NH}_3)_3]$
- $[\text{CoCl}_2(\text{H}_2\text{O})_2(\text{NH}_3)_2]^+$
- $[\text{CoBrCl}(\text{H}_2\text{O})_2(\text{NH}_3)_2]^+$
- $[\text{CoBrCl}(\text{NH}_3)_3]$

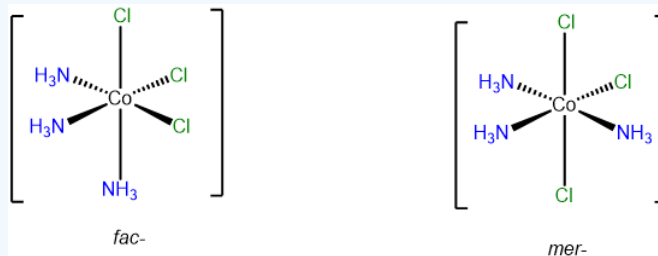
##### Answer a. $[\text{IrCl}(\text{CO})(\text{PPh}_3)_2]$

This is a 4-coordinate  $\text{Ir}^{\text{I}}$  complex and, as such will be square planar. Since two of the ligands are identical, it will have *cis* and *trans* isomers. The *trans* isomer is famous for its ability to form adducts and is called Vaska's complex.



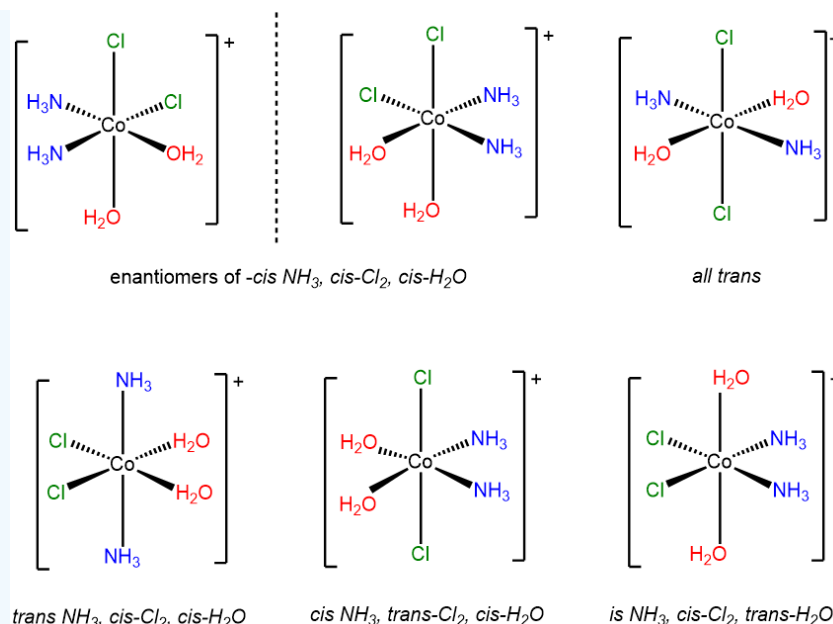
##### Answer b. $[\text{CoCl}_3(\text{NH}_3)_3]$

This complex contains three ammine and three chloro ligands and so will have *fac* and *mer* isomers.



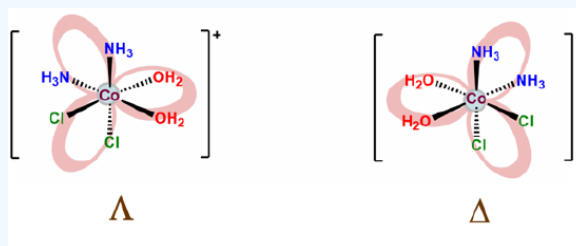
##### Answer c. $[\text{CoCl}_2(\text{H}_2\text{O})_2(\text{NH}_3)_2]^+$

This is a case of an  $\text{MA}_2\text{B}_2\text{C}_2$  system ( $\text{A} = \text{Cl}^-$ ,  $\text{B} = \text{H}_2\text{O}$ ,  $\text{C} = \text{NH}_3$ ) involving multiple *cis* and *trans* relationships. The six stereoisomers are shown below.



Since it may not be obvious how to arrive at a set of isomers like the ones above, it is worth considering how one might work through the possibilities for a system of ligands like this one. Several systems may be used to systematically identify isomers. One approach is the Macbdef system described in Note 8.1.5.1 at the end of these exercises. The solutions presented here and in subsequent problems employ a variant of that approach.

- Start by fixing one set of ligands. In this case the chloro ligands were first fixed as *cis* to one another. Then the remaining ligands might be *cis* or *trans* to one another, although since the *chloro* ligands are already *cis*, the ammine and aqua ligands cannot both be *trans* at the same time. Thus for *cis* chloro ligands the possibilities for the others are:
  - cis*- $\text{H}_2\text{O}$ , *cis*- $\text{NH}_3$ ,
  - cis*- $\text{H}_2\text{O}$ , *trans*- $\text{NH}_3$
  - trans*- $\text{H}_2\text{O}$ , *cis*- $\text{NH}_3$
- Swap the configuration of the ligand set you started with. In this case it means placing the chloro ligands *trans* to one another. From that configuration, the possibilities for the ammine and aqua ligands are
  - cis*- $\text{H}_2\text{O}$ , *cis*- $\text{NH}_3$ ,
  - trans*- $\text{H}_2\text{O}$ , *trans*- $\text{NH}_3$
- Check for enantiomers and create mirror images of any chiral complexes you drew. The easiest way to do this is to assign point groups. However, it turns out that the octahedral all-*cis* case is  $D_3$  and formally equivalent to the symmetry of a tris chelate, as shown below.

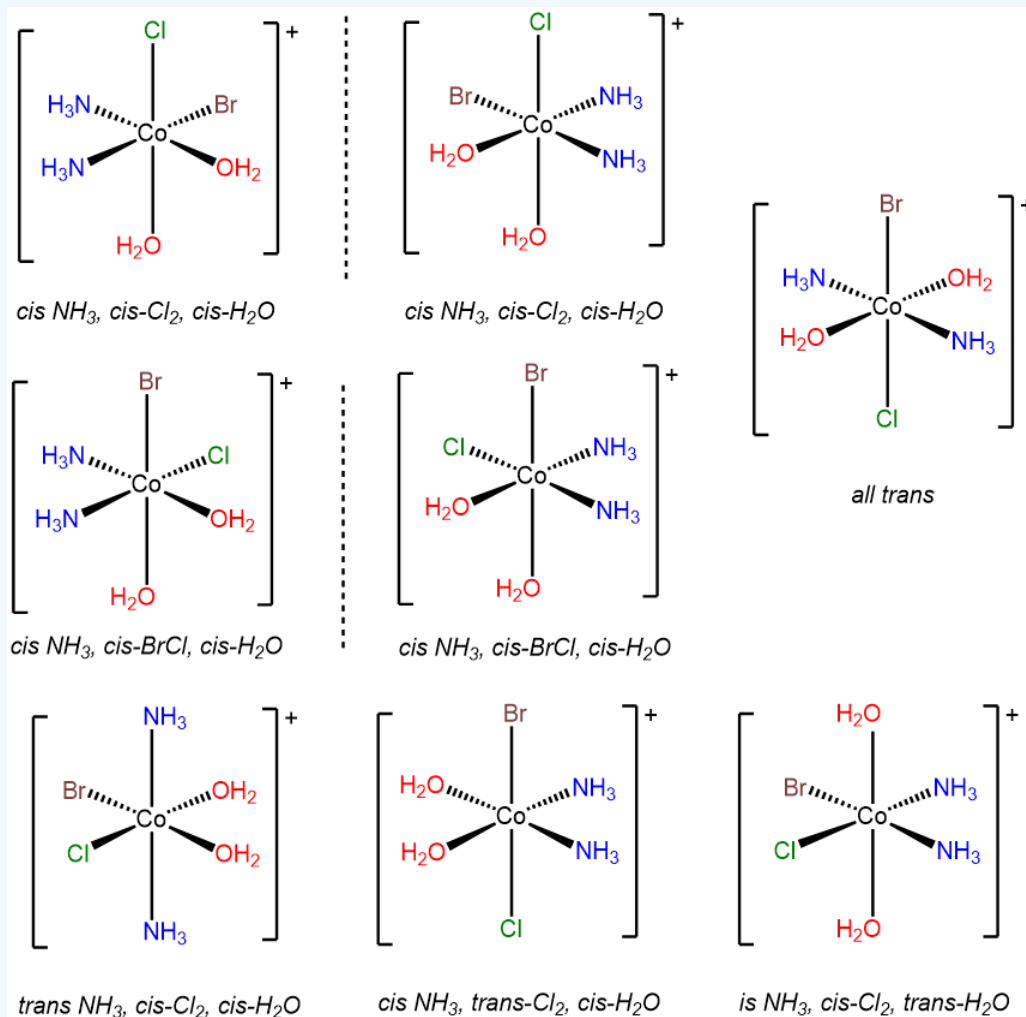


- finally, check to make sure you didn't include the same complex twice. Humans do make mistakes after all.

#### Answer d. $[\text{CoBrCl}(\text{H}_2\text{O})_2(\text{NH}_3)_2]^+$

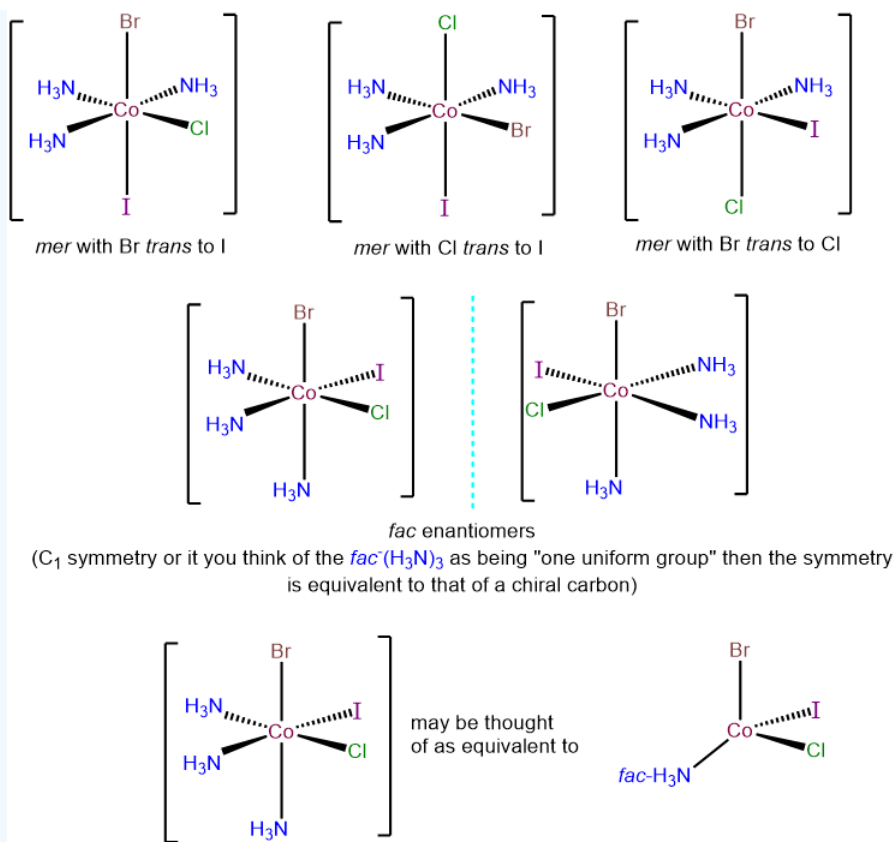
This problem is analogous to the one above except that this complex contains a bromo and chloro ligand in place of the two chloro ligands in  $[\text{CoCl}_2(\text{H}_2\text{O})_2(\text{NH}_3)_2]^+$ . Consequently, when the bromo and chloro ligands are *cis* to one

another, additional possibilities for isomers arise based on whether ammine or aqua ligands are *trans* to the chloro and bromo. The result is eight isomers.



#### Answer e. $[\text{CoBrClI}(\text{NH}_3)_3]$

There are two possibilities for this complex - a *fac*-( $\text{NH}_3$ )<sub>3</sub> and a *mer*-( $\text{NH}_3$ )<sub>3</sub> arrangement. These may be taken as starting points for examining the possible permutations for the  $\text{Cl}^-$ ,  $\text{Br}^-$ , and  $\text{I}^-$  ligands. The top row presents the three possibilities within the *mer*-( $\text{NH}_3$ )<sub>3</sub> arrangement; each corresponds to a different ligand *trans* to an ammine ligand. The bottom row presents the two possible isomers with a *fac*-( $\text{NH}_3$ )<sub>3</sub> arrangement. In each, the  $\text{Cl}^-$ ,  $\text{Br}^-$ , and  $\text{I}^-$  ligands are *trans* to ammine ligands. However, the complexes possess  $C_1$  symmetry and so are chiral and exist as enantiomers.



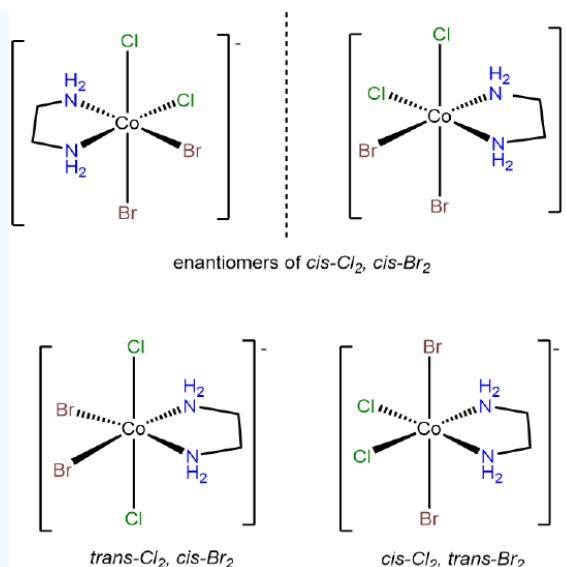
### ? Exercise 8.1.5.5. Stereoisomers of complexes with bidentate ligands (ignoring ring twist).

Ignoring ring twist, draw all the stereoisomers of the following real and hypothetical octahedral complexes.

- $[CoBr_2Cl_2(en)]^-$
- $[CoBrCl(en)_2]^+$
- $[CoBrCl(gly)_2]^-$
- $[Co(en)_3]^{3+}$
- $[Co(gly)_3]$

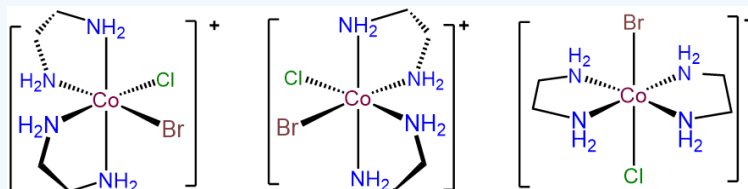
#### Answer a. $[CoBr_2Cl_2(en)]^-$

This complex is analogous to  $[CoCl_2(H_2O)_2(NH_3)_2]^+$  in possessing pairs of identical ligating groups. The main difference is that in  $[CoBr_2Cl_2(en)]^-$  the two amine ligating group of the en ligand are restricted to a *cis* arrangement. Under the MABCDEF system explained in Note 8.1.5.1  $[CoCl_2(H_2O)_2(NH_3)_2]^+$  may be  $MA_2B_2C_2$ , but this complex,  $[CoBr_2Cl_2(en)]^-$ , is  $M(AA)B_2C_2$ . The isomers are:



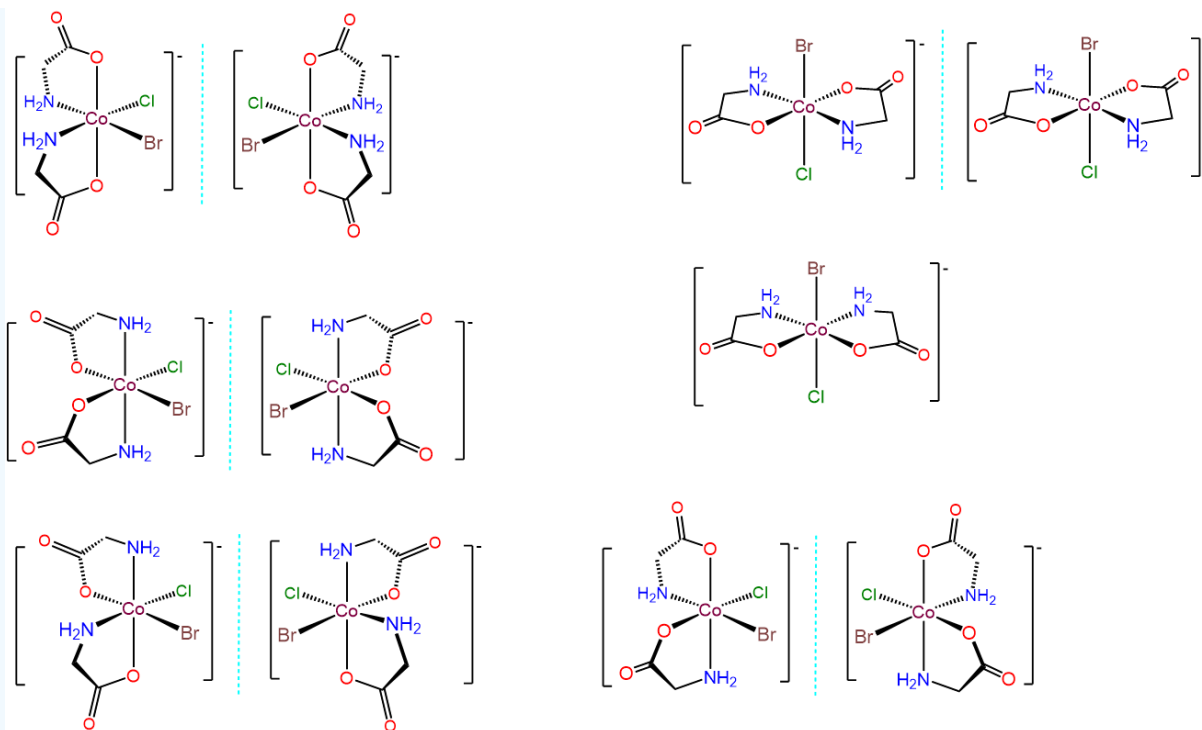
**Answer b. [CoBrCl(en)<sub>2</sub>]<sup>+</sup>**

The key to problems like this is to focus on the unique ligands, in this case Br<sup>-</sup> and Cl<sup>-</sup>. These can exist in either a *cis* or *trans* arrangement. The *trans* form is achiral, but in the case where Br<sup>-</sup> and Cl<sup>-</sup> are *cis*,  $\Lambda$  and  $\Delta$  enantiomers are possible. The result is three isomers.



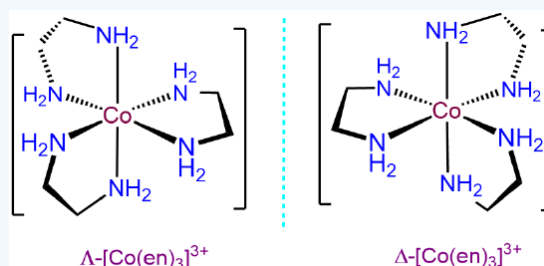
**Answer c. [CoBrCl(gly)<sub>2</sub>]<sup>-</sup>**

This case is analogous to the one above, but this time the bidentate ligand, gly, possesses distinguishable binding sites. Thus there are additional permutations involving how the gly ligands are bound relative to one another and/or whether the O or N end of the gly is bound *trans* to Br or Cl. The result is 11 different isomers, which are given below.



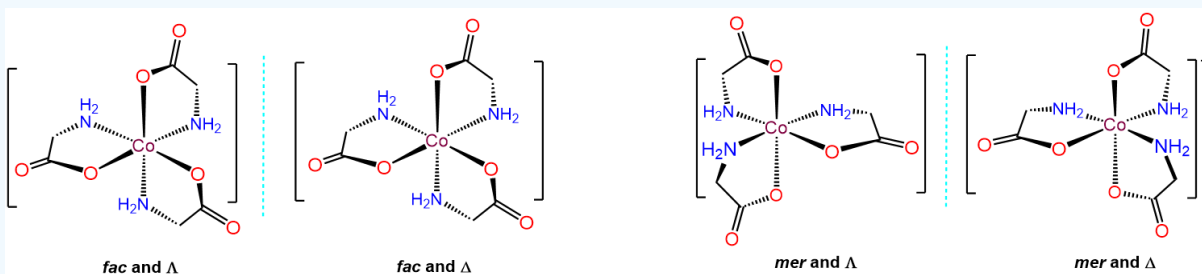
**Answer d.  $[\text{Co}(\text{en})_3]^{3+}$**

As a tris-chelate of symmetric bidentate ligands, ignoring ring twist,  $[\text{Co}(\text{en})_3]^{3+}$  will only exhibit  $\Lambda$  and  $\Delta$  isomerism.



**Answer e.  $[\text{Co}(\text{gly})_3]$**

Since there are three gly ligands, each of which have carboxy and amine ends, the allowable arrangements involve whether the resulting three carboxy and three amine ends are oriented in a *mer* or *fac* arrangement. This gives two possibilities, each of which can exist as either the  $\Lambda$  or  $\Delta$  enantiomer, for a total of four isomers, which are given below.



### ? Exercise 8.1.5.6. More stereoisomers: Now featuring linkage isomerism

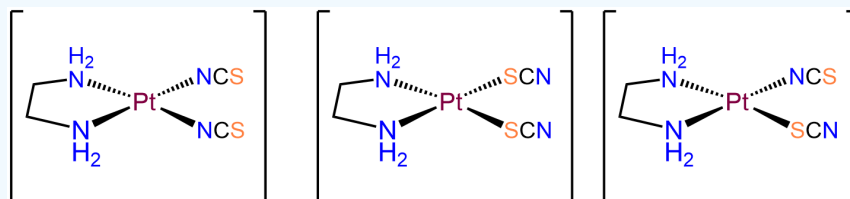
Ignoring ring twist, draw all chemically reasonable stereoisomers for the following real and hypothetical complexes. You may assume that

- complexes in which the metal has a coordination number of six are octahedral
- complexes in which the metal has a coordination number of five are trigonal bipyramidal
- complexes in which  $\text{Pt}^{\text{II}}$ ,  $\text{Pd}^{\text{II}}$ , or  $\text{Rh}^{\text{I}}$ , or  $\text{Ir}^{\text{I}}$  have a coordination number of four are square planar
- other complexes in which the metal has a coordination number of four will be tetrahedral

- $[\text{Pt}(\text{en})(\text{SCN})_2]$
- $[\text{Pt}(\text{NH}_3)_2(\text{SCN})_2]$
- $[\text{Co}(\text{en})_2(\text{SCN})_2]^+$

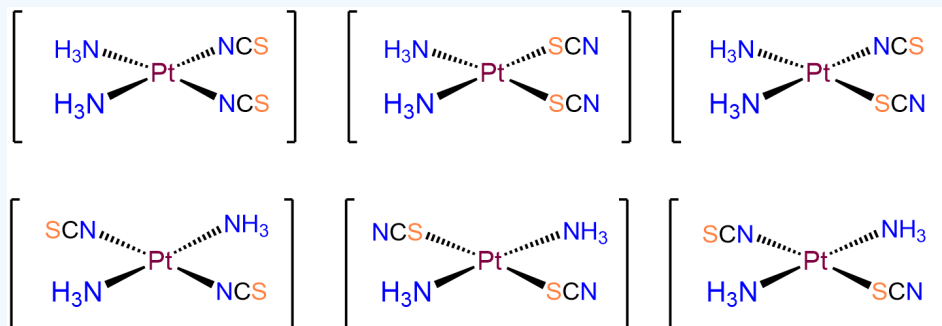
#### Answer a. $[\text{Pt}(\text{en})(\text{SCN})_2]$

The Pt in this neutral complex must be  $\text{Pt}^{2+}$  to balance the negative charges of the two  $\text{SCN}^-$  ligands. Complexes of  $\text{Pt}^{2+}$  are square planar and four coordinate, consistent with the bidentate en and two thiocyanato ligands. Of the ligands, the en ligand must bind in a *cis* arrangement. Consequently, the two  $\text{SCN}^-$  ligands will be in a *cis* arrangement as well. The isomers will therefore only differ in whether the two  $\text{SCN}^-$  bind  $\kappa\text{N}$  or  $\kappa\text{S}$ . The possibilities are:



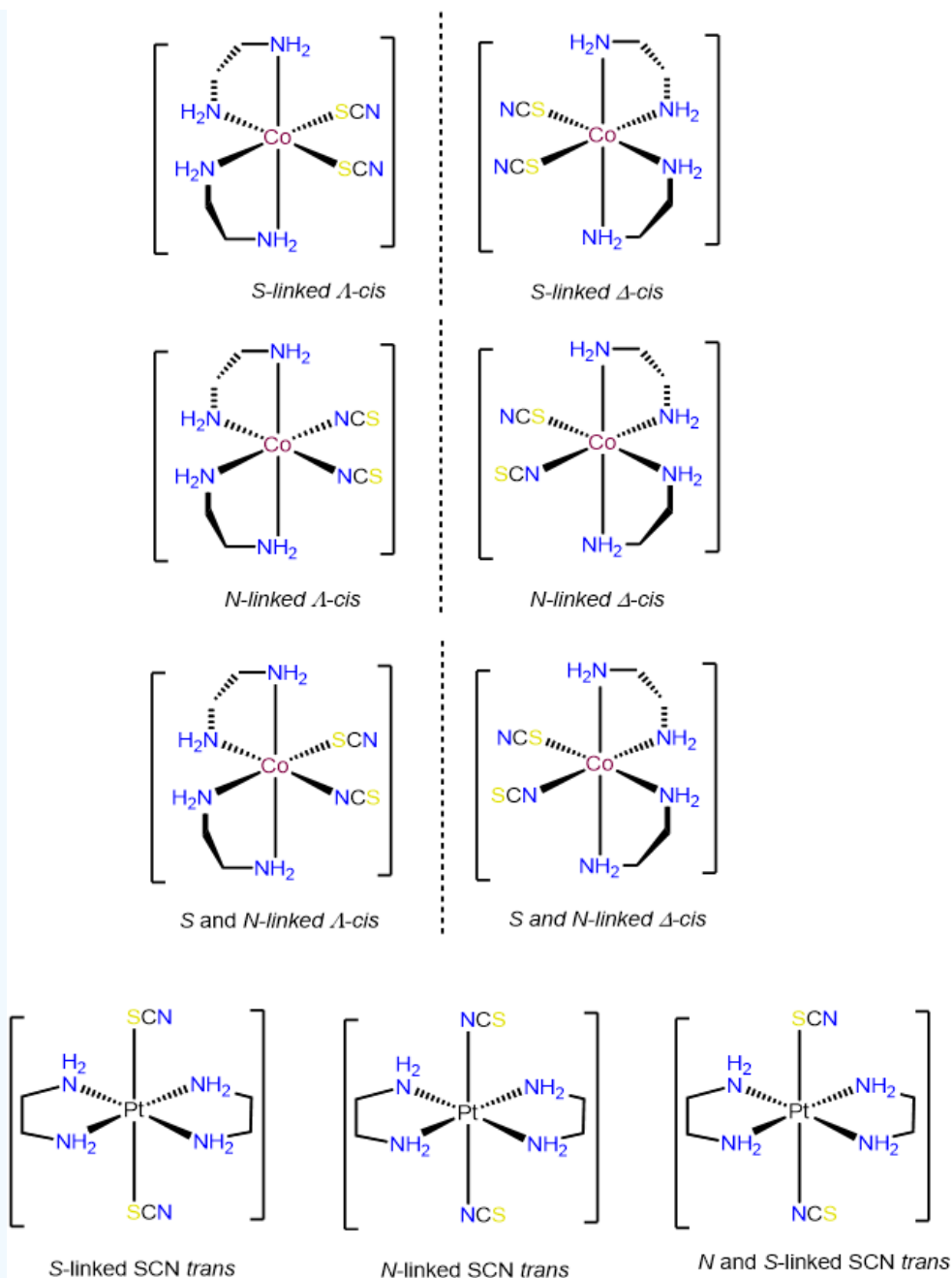
#### Answer b. $[\text{Pt}(\text{NH}_3)_2(\text{SCN})_2]$

As with the preceding example, this will be a square planar  $\text{Pt}^{2+}$  complex. The main difference is that this time the coordinated nitrogens are not constrained to adopt a *cis* arrangement so there will be both *cis* and *trans* isomers.



#### Answer c. $[\text{Co}(\text{en})_2(\text{SCN})_2]^+$





### ? Exercise 8.1.5.7. Stereoisomer free for all.

Ignoring ring twist, draw all chemically reasonable stereoisomers for the following real and hypothetical complexes. You may assume that

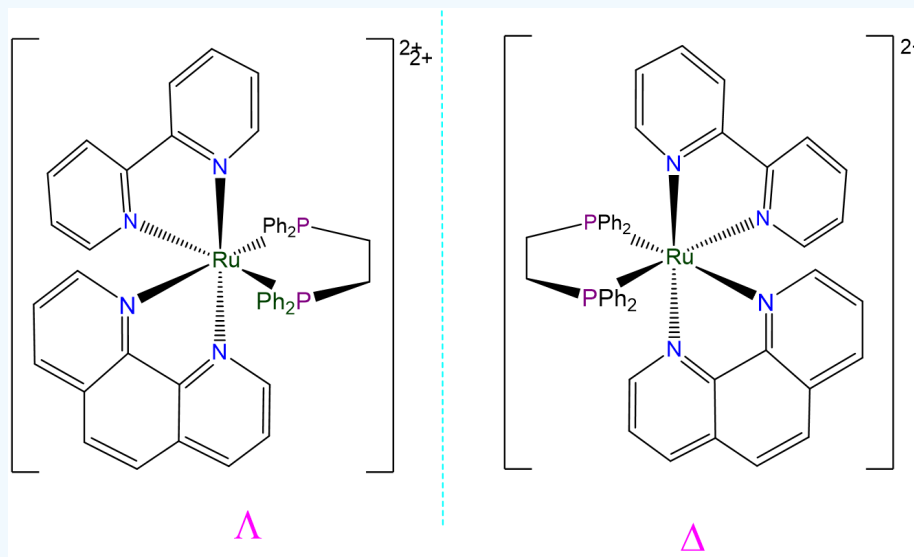
- complexes in which the metal has a coordination number of six are octahedral
- complexes in which the metal has a coordination number of five are trigonal bipyramidal
- complexes in which  $\text{Pt}^{\text{II}}$ ,  $\text{Pd}^{\text{II}}$ , or  $\text{Rh}^{\text{I}}$ , or  $\text{Ir}^{\text{I}}$  have a coordination number of four are square planar
- other complexes in which the metal has a coordination number of four will be tetrahedral

- $[\text{Ru}(\text{bpy})(\text{phen})(\text{dppe})]^{2+}$
- $[\text{CoClF}(\text{PPh}_3)(\text{py})]^-$
- $[\text{Ni}(\text{en})_2(\text{NO}_2)_2]$

- d.  $[\text{Fe}(\text{H}_2\text{O})_3(\text{SCN})_3]$
- e.  $[\text{PtClF}(\text{PPh}_3)(\text{py})]$
- f.  $[\text{CoBr}_2\text{Cl}(\text{NH}_3)_3]$

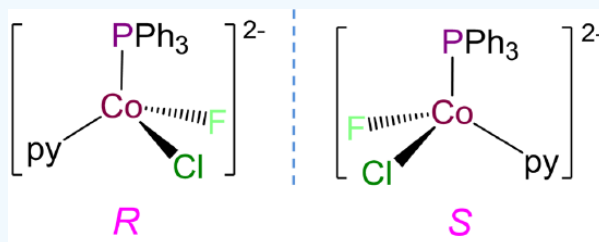
**Answer a.  $[\text{Ru}(\text{bpy})(\text{phen})(\text{dppe})]^{2+}$**

This complex is an octahedral tris-chelate containing symmetric ligands. As such it will exhibit  $\Lambda$  and  $\Delta$  isomers:



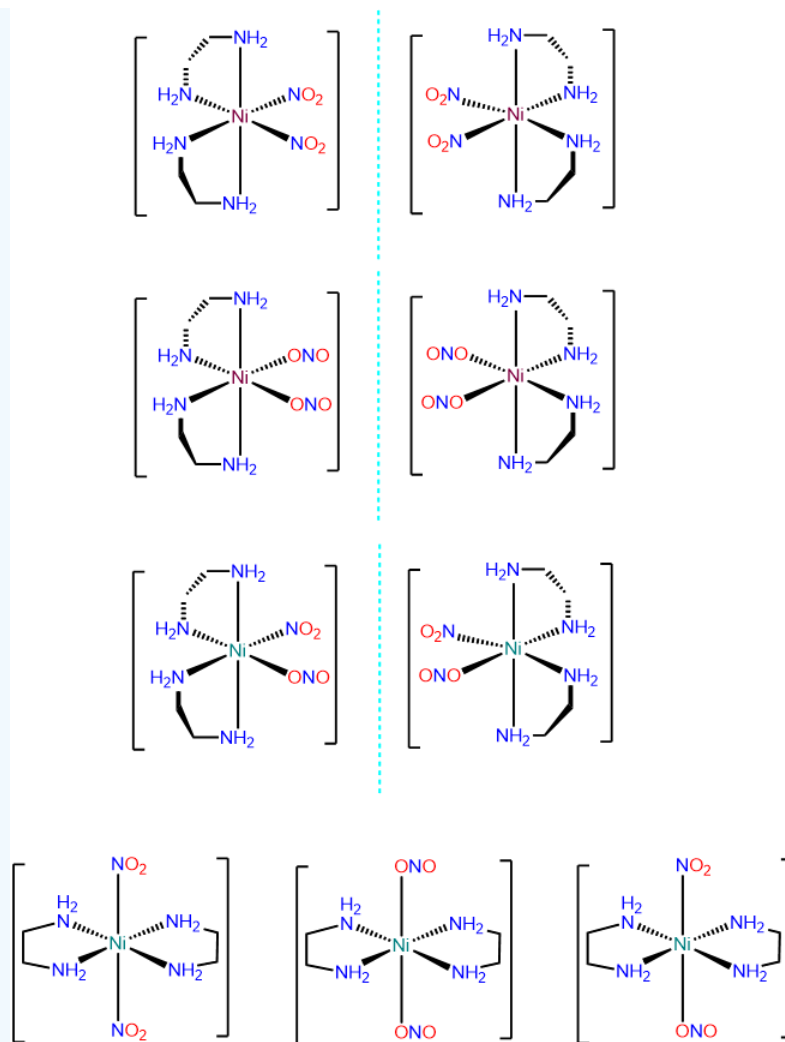
**Answer b.  $[\text{CoClF}(\text{PPh}_3)(\text{py})]^-$**

This complex has a coordination number of 4 and contains a  $\text{Co}^{2+}$  ion with a  $d^7$  electron configuration, so a tetrahedral geometry is expected. Tetrahedral complexes like this one with four different ligands are chiral and can form *R* and *S* enantiomers.



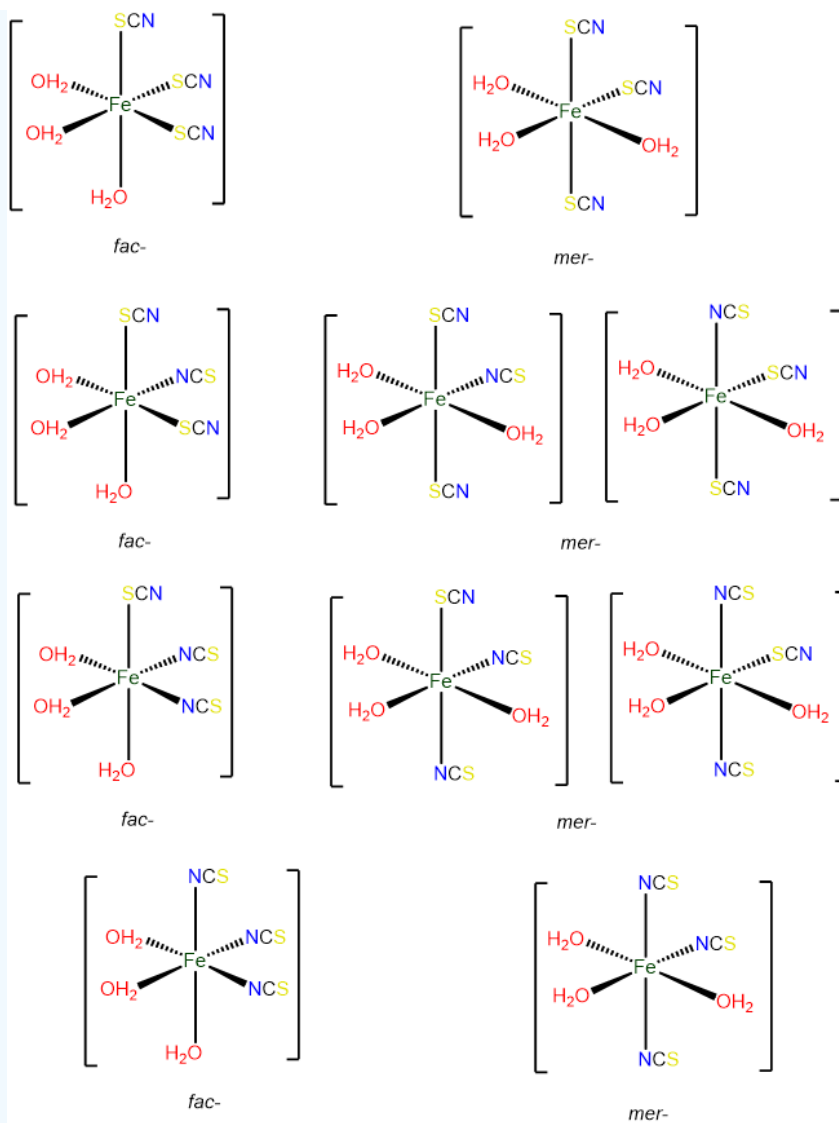
**Answer c.  $[\text{Ni}(\text{en})_2(\text{NO}_2)_2]$**

This is an octahedral bis-chelate and will exist in  $\Lambda$  and  $\Delta$  configurations. Within each configuration the  $\text{NO}_2^-$  ligands can exist as  $\kappa\text{N}$  and  $\kappa\text{O}$ , leading to the following possibilities:



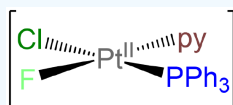
**Answer d.  $[\text{Fe}(\text{H}_2\text{O})_3(\text{SCN})_3]$**

As an octahedral complex with three identical ligands it can exist in *mer* and *fac* configurations, with the ambidentate SCN ligand providing additional possibilities for isomerism.



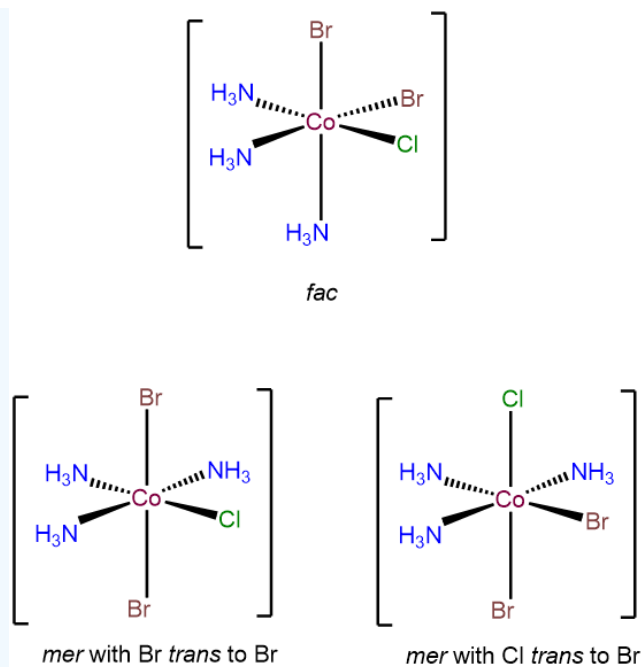
**Answer e. [PtClF(PPh<sub>3</sub>)(py)]**

As a square planar complex with four nonidentical ligands, this complex exists as a single isomer.



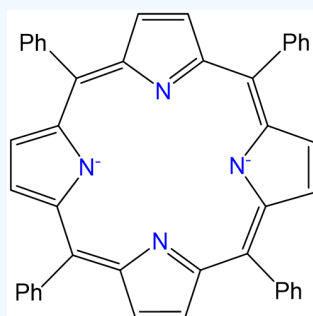
**Answer f. [CoBr<sub>2</sub>Cl(NH<sub>3</sub>)<sub>3</sub>]**

As an octahedral complex with three identical ligands it will exhibit *mer* and *fac* isomerism. In addition, it will have two *mer* configurations that differ in terms of the cis and trans relationships between the bromo and chloro ligands.



### ? Exercise 8.1.5.8

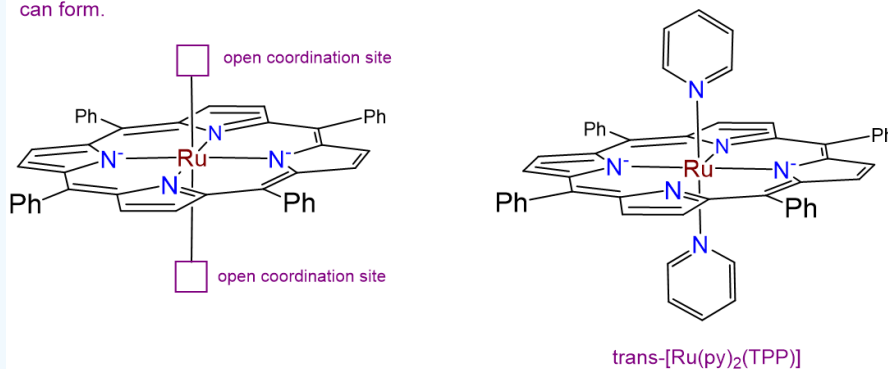
Complexes of formula  $\text{Ru}(\text{TPP})\text{py}_2$  have been prepared, in which TPP is tetraphenylporphyrin, which binds metals in the form given below. Draw all isomers of  $\text{Ru}(\text{TPP})\text{py}_2$ .



### Answer

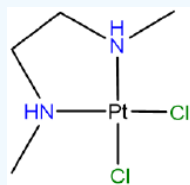
There is only one isomer. While normally complexes containing two identical ligands (in this case  $\text{py}$ ) can exhibit *cis* and *trans* isomerism, in this case the planar tetraphenylporphyrin ring ligates the  $\text{Ru}^{2+}$  ion in a square planar arrangement, as shown at left in the image below. This leaves only a pair of *trans* coordination sites for the chloro ligands to occupy, giving the isomer shown at right below.

When TPP ligates  $\text{Ru}^{2+}$  it leaves only *trans* open coordination sites so only the *trans* isomer can form.



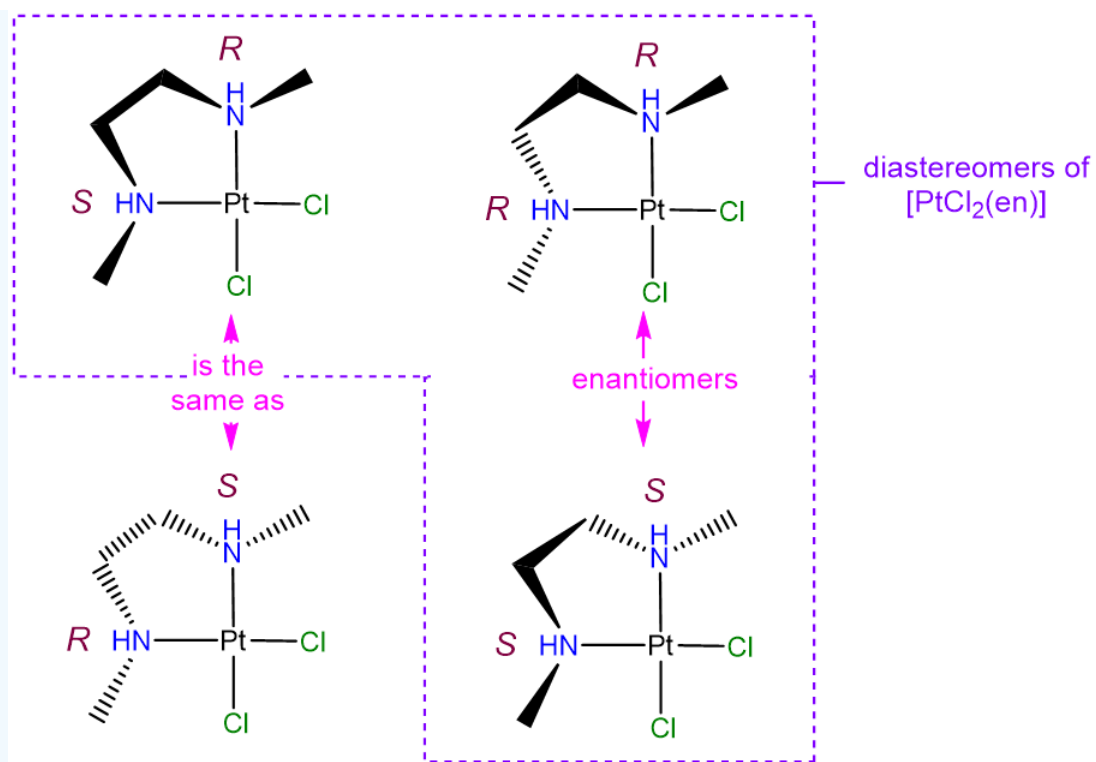
### ? Exercise 8.1.5.9

Draw the diastereomers formed due to the chirality of the amine nitrogen atoms in  $[\text{PtCl}_2(\text{N,N'}\text{-dimethylethane-1,2-diamine})]$  which has the atomic connectivity represented below



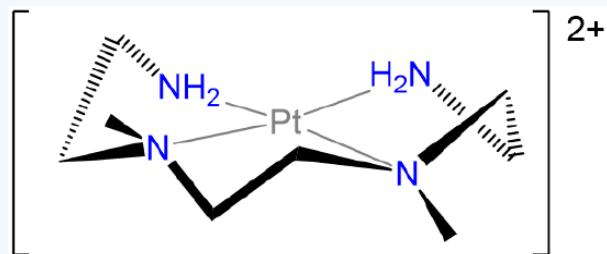
### Answer

The diastereomers will differ in whether the N atoms adopt an *R* or *S* configuration at the nitrogen atoms. The possible permutations are (*R,R*), (*S,S*), (*R,S*), and (*S,R*). However, as may be seen from the image below, the (*R,S*) and (*S,R*) configurations are identical (the two projections shown can be interconverted through a  $C_2$  rotation along an axis bisecting the  $\text{Cl-Pt-Cl}$  unit). As a result there are only three unique isomers. Of these, the (*R,R*) and (*S,S*) configurations are enantiomers (they are mirror images by reflection in the  $\text{PtCl}_2\text{N}_2$  plane). Note that in solving problems like this one it can be helpful to keep track of possible isomers by assigning the stereochemistry at each chiral center as *R* or *S* using the [Cahn-Ingold-Prelog-convention](#), though it is not strictly necessary to do so.

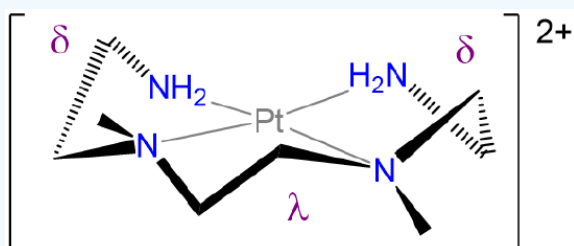


### ? Exercise 8.1.5.10

Label the conformations of all chelate rings in the structure below.



Answer



## Appendix: The MABCDEF bookkeeping system for identifying isomers

The Mabcdef or MABCDEF system is one method for identifying the number of isomers in an octahedral complex, although since it is really just a bookkeeping and organizational system it can easily be extended to other geometries as well. The M in Mabcdef stands for metal and the other letters are used to stand in for ligands. The basic approach involves

- classifying the ligands as A, B, C, D, E, or F in order of multiplicity. Thus for

$[\text{Cr}(\text{NH}_3)_6]^{3+}$  A =  $\text{NH}_3$ ; there are no B, C, D, E, or F ligands; and the complex is classified as  $\text{MA}_6$

$[\text{CoCl}(\text{NH}_3)_5]^{2+}$  A =  $\text{NH}_3$ , B =  $\text{Cl}^-$ , and the complex is  $\text{MA}_5\text{B}$

$[\text{CrCl}_2(\text{H}_2\text{O})_2(\text{NH}_3)_2]^+$  A =  $\text{Cl}^-$ , B =  $\text{H}_2\text{O}$ , C =  $\text{NH}_3$ , and the complex is  $\text{MA}_2\text{B}_2\text{C}_2$

- in the classification above, multidentate ligands are typically classified before monodentate ones and are designated AA, AB, ABC, ABA, etc. based on the symmetry of the attachment points. Thus

en has identical attachment amine points and is AA

gly has a carboxy and amine attachment points and is AB

trien is ABA

$\text{CoCl}_2(\text{en})_2^+$  is  $\text{M}(\text{AA})_2\text{B}_2$

$\text{CoCl}_2(\text{gly})_2^-$  is  $\text{M}(\text{AB})_2\text{C}_2$

$\text{CoCl}_2(\text{en})(\text{gly})$  is  $\text{M}(\text{AA})(\text{AB})\text{C}_2$

- Systematically list out the possible *trans* arrangements of ligands by
  - assigning one pair of ligands to be *trans* to one another.
  - Then systematically list out the other possible *trans* pairs by permuting the remaining *trans* arrangements. It can help to organize the permutations in a table, such as that shown below for an MABCDEF complex where A and B are assigned *trans*. In looking at the table notice how the second set of *trans* permutations is systematically varied. This helps ensure that no possibility is skipped.
  - Go through the list of isomers and remove any duplicates you generated so far. For instance, notice in the table below that the last three stereoisomers are identical with the first three (*e.g.*, stereoisomer 4 is identical to stereoisomer 3, 5 with 2, and 6 with 1).

Stereoisomer 1	Stereoisomer 2	Stereoisomer 3	Stereoisomer 4 (same as isomer 3)	Stereoisomer 5 (same as isomer 2)	Stereoisomer 6 (same as isomer 1)
<i>trans</i> AB (fixed)	<i>trans</i> AB (fixed)	<i>trans</i> AB (fixed)	<i>trans</i> AB (fixed)	<i>trans</i> AB (fixed)	<i>trans</i> AB (fixed)
<i>trans</i> CD	<i>trans</i> CE	<i>trans</i> CF	<i>trans</i> DE	<i>trans</i> DF	<i>trans</i> EF
<i>trans</i> EF	<i>trans</i> DF	<i>trans</i> DE	<i>trans</i> CF	<i>trans</i> CE	<i>trans</i> CD

- If the complex possesses multidentate ligands that demand that certain groups exist and *cis* pairs, then also remove any configurations which do not agree with the known binding capability of the ligand (*e.g.*, the two amine groups of ethylenediamine cannot be *trans* to one another, so if you have an en ligand, remove configurations like that from the list).
- Next, swap or permute the original *trans* pair and repeat the process you just followed. In the case of Mabcdef this gives the following results:

Isomer	"fixed" <i>trans</i> pair	Additional <i>trans</i> pairs	
1	AB	CD	EF
2	AB	CE	DF
3	AB	CF	DE
4	AC	BD	EF
5	AC	BE	BF



6	AC	BF	DE
7	AD	BC	EF
8	AD	BE	CF
9	AD	BF	CE
10	AE	BC	DF
11	AE	BD	CF
12	AE	BF	CD
13	AF	BC	DE
14	AF	BD	CE
15	AF	BE	CD

- Since the procedure explained above only identifies isomers based on unique *trans* pairings, **it does not identify when a configuration is chiral and corresponds to a pair of enantiomers**. Any enantiomers can be identified by drawing out the complexes and either classifying their point groups or by drawing their mirror images and checking if they are superimposable. In the MABCDEF case - *i.e.*, where all the ligands are different - all of the isomers identified have  $C_1$  symmetry so are chiral. This means there will be a pair of enantiomers for each, giving  $15 \times 2 = 30$  different stereoisomers.

## References

1. These examples are taken from <http://wwwchem.uwimona.edu.jm/courses/inorgnom.html>
2. Contakes S. M.; Rauchfuss, T.B. *Chem. Commun.* 2001, 553-554.
3. Shriver, D. F.; Shriver, S. A.; Anderson, S. E., *Inorg. Chem.* 1965, 4(5), 725-730.
4. Zelewsky, A. v., *Stereochemistry of Coordination Compounds* Wiley, 1996.
5. In the past it was difficult to determine absolute configurations from X-ray data alone, but recent advances have made it easier to do so.
6. Pavan M. V. Raja & Andrew R. Barron "Circular Dichroism Spectroscopy and its Application for Determination of Secondary Structure of Optically Active Species" in *Physical Methods in Chemistry and Nano Science* [https://chem.libretexts.org/Bookshelves/Analytical\\_Chemistry/Book%3A\\_Physical\\_Methods\\_in\\_Chemistry\\_and\\_Nano\\_Science\\_\(Barron\)/07%3A\\_Molecular\\_and\\_Solid\\_State\\_Structure/7.07%3A\\_Circular\\_Dichroism\\_Spectroscopy\\_and\\_its\\_Application\\_for\\_Determination\\_of\\_Secondary\\_Structure\\_of\\_Optically\\_Active\\_Species](https://chem.libretexts.org/Bookshelves/Analytical_Chemistry/Book%3A_Physical_Methods_in_Chemistry_and_Nano_Science_(Barron)/07%3A_Molecular_and_Solid_State_Structure/7.07%3A_Circular_Dichroism_Spectroscopy_and_its_Application_for_Determination_of_Secondary_Structure_of_Optically_Active_Species)
7. Berova, N.; Bari, L. D.; Pescitelli, G., *Chemical Society Reviews* 2007, 36 (6), 914-931.
8. Of course, if one set of ligands occupies a meridional plane, then the other three ligands will be oriented in an equatorial one. The reason they may both be considered meridional is because if the complex were rotated, the equatorial plane would be meridional and vice versa. From that point of view both might be considered meridional planes - albeit not at the same time.
9. Bite angles are taken from Mansell, S. M., Catalytic applications of small bite-angle diphosphorus ligands with single-atom linkers. *Dalton Transactions* 2017, 46 (44), 15157-15174.
10. Hancock, R. D., The pyridyl group in ligand design for selective metal ion complexation and sensing. *Chemical Society Reviews* 2013, 42 (4), 1500-1524.
11. Sasi, D.; Ramkumar, V.; Murthy, N. N., Bite-Angle-Regulated Coordination Geometries: Tetrahedral and Trigonal Bipyramidal in Ni(II) with Biphenyl-Appended (2-Pyridyl)alkylamine N,N'-Bidentate Ligands. *ACS Omega* 2017, 2 (6), 2474-2481.
12. Ehnbohm, A.; Ghosh, S. K.; Lewis, K. G.; Gladysz, J. A., Octahedral Werner complexes with substituted ethylenediamine ligands: a stereochemical primer for a historic series of compounds now emerging as a modern family of catalysts. *Chemical Society Reviews* 2016, 45 (24), 6799-6811.

8.1.5: Isomerism is shared under a [CC BY 4.0](https://creativecommons.org/licenses/by/4.0/) license and was authored, remixed, and/or curated by Stephen M. Contakes.

- [9.4: Isomerism](#) by Stephen M. Contakes is licensed [CC BY 4.0](#).

## 8.2: Crystal Field Theory

---

Learning objectives for this unit are to:

- Recall and draw shapes of common coordination complex geometries
  - Describe Berry pseudorotation and explain the experimental evidence that supports interconversion of trigonal bipyramidal and square planar geometries
  - Derive d-orbital splitting diagrams based on a given ligand field (coordination number and geometry)
  - Calculate crystal field/ligand field stabilization energies (CFSE/LFSE) for a metal ion in octahedral and tetrahedral transition metal complexes
  - Understand the difference between low and high spin complexes, determine the number of unpaired electrons for low-spin and high-spin configurations, and predict the spin state of a complex based on oxidation state and identity of the metal, identity of the ligands, and geometry of the complex.
  - Predict whether a four-coordinate complex will be tetrahedral or square planar based on the metal d-electron count and the electronics and sterics of the ligands
- 

8.2: Crystal Field Theory is shared under a [not declared](#) license and was authored, remixed, and/or curated by LibreTexts.

## 8.2.1: Crystal Field Theory

Crystal field theory (CFT) describes the breaking of orbital degeneracy in [transition metal complexes](#) due to the presence of [ligands](#). CFT qualitatively describes the strength of the metal-ligand bonds. Based on the strength of the metal-ligand bonds, the energy of the system is altered. This may lead to a change in [magnetic properties](#) as well as [color](#). This theory was developed by Hans Bethe and John Hasbrouck van Vleck.

### Basic Concept

In Crystal Field Theory, it is assumed that the ions are **simple point charges** (a simplification). When applied to alkali metal ions containing a symmetric sphere of charge, calculations of bond energies are generally quite successful. The approach taken uses classical potential energy equations that take into account the attractive and repulsive interactions between charged particles (that is, Coulomb's Law interactions).

$$E \propto \frac{q_1 q_2}{r}$$

with

- $E$  the bond energy between the charges and
- $q_1$  and  $q_2$  are the charges of the interacting ions and
- $r$  is the distance separating them.

This approach leads to the correct prediction that large cations of low charge, such as  $K^+$  and  $Na^+$ , should form few coordination compounds. For transition metal cations that contain varying numbers of d electrons in orbitals that are NOT spherically symmetric, however, the situation is quite different. The shapes and occupations of these d-orbitals then become important in building an accurate description of the bond energy and properties of the transition metal compound.

When examining a single transition metal ion, the five [d-orbitals](#) have the same energy (Figure 8.2.1.1). When ligands approach the metal ion, some experience more opposition from the d-orbital electrons than others based on the geometric structure of the molecule. Since ligands approach from different directions, not all d-orbitals interact directly. These interactions, however, create a splitting due to the electrostatic environment.

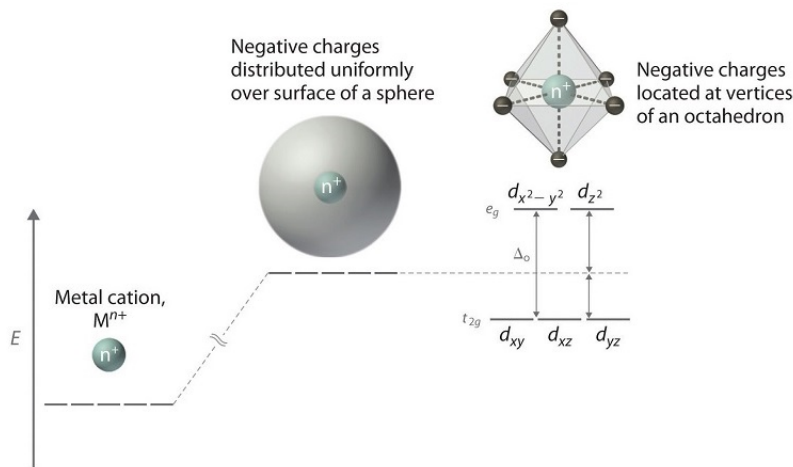


Figure 8.2.1.1: Distributing a charge of  $-6$  uniformly over a spherical surface surrounding a metal ion causes the energy of all five d orbitals to increase due to electrostatic repulsions, but the five d orbitals remain degenerate. Placing a charge of  $-1$  at each vertex of an octahedron causes the d orbitals to split into two groups with different energies: the  $d_{x^2-y^2}$  and  $d_{z^2}$  orbitals increase in energy, while the  $d_{xy}$ ,  $d_{xz}$ , and  $d_{yz}$  orbitals decrease in energy. The average energy of the five d orbitals is the same as for a spherical distribution of a  $-6$  charge, however. Attractive electrostatic interactions between the negatively charged ligands and the positively charged metal ion (far right) cause all five d orbitals to decrease in energy but does not affect the splittings of the orbitals. The two  $e_g$  orbitals point directly at the six negatively charged ligands, which increases their energy compared with a spherical distribution of negative charge. In contrast, the three  $t_{2g}$  orbitals point between the negatively charged ligands, which decreases their energy compared with a spherical distribution of charge.

For example, consider a molecule with octahedral geometry. Ligands approach the metal ion along the  $x$ ,  $y$ , and  $z$  axes. Therefore, the electrons in the  $d_{z^2}$  and  $d_{x^2-y^2}$  orbitals (which lie along these axes) experience greater repulsion. It requires more energy to have an electron in these orbitals than it would to put an electron in one of the other orbitals. This causes a splitting in the energy levels of the d-orbitals. This is known as **crystal field splitting**. For octahedral complexes, crystal field splitting is denoted by  $\Delta_o$  (or  $\Delta_{oct}$ ). The energies of the  $d_{z^2}$  and  $d_{x^2-y^2}$  orbitals increase due to greater interactions with the ligands. The  $d_{xy}$ ,  $d_{xz}$ , and  $d_{yz}$  orbitals decrease with respect to this normal energy level and become more stable.

### Electrons in Orbitals

According to the [Aufbau principle](#), electrons are filled from lower to higher energy orbitals (Figure 8.2.1.1). For the octahedral case above, this corresponds to the  $d_{xy}$ ,  $d_{xz}$ , and  $d_{yz}$  orbitals. Following [Hund's rule](#), electrons are filled in order to have the highest number of unpaired electrons. For example, if one had a  $d^3$  complex, there would be three unpaired electrons. If one were to add an electron, however, it has the ability to fill a higher energy orbital ( $d_{z^2}$  or  $d_{x^2-y^2}$ ) or pair with an electron residing in the  $d_{xy}$ ,  $d_{xz}$ , or  $d_{yz}$  orbitals. This pairing of the electrons requires energy ([spin pairing](#)).

energy). If the pairing energy is less than the crystal field splitting energy,  $\Delta_o$ , then the next electron will go into the  $d_{xy}$ ,  $d_{xz}$ , or  $d_{yz}$  orbitals due to stability. This situation allows for the least amount of unpaired electrons, and is known as **low spin**. If the pairing energy is greater than  $\Delta_o$ , then the next electron will go into the  $d_{z^2}$  or  $d_{x^2-y^2}$  orbitals as an unpaired electron. This situation allows for the most number of unpaired electrons, and is known as **high spin**. Ligands that cause a transition metal to have a small crystal field splitting, which leads to high spin, are called **weak-field ligands**. Ligands that produce a large crystal field splitting, which leads to low spin, are called **strong field ligands**.

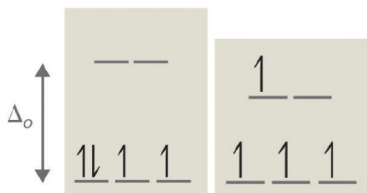
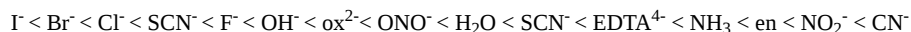


Figure 8.2.1.2: Low Spin, Strong Field ( $\Delta_o \gg P$ ) High Spin, Weak Field ( $\Delta_o \ll P$ ) Splitting for a  $d^4$  complex under a strong field (left) and a weak field (right). The strong field is a low spin complex, while the weak field is a high spin complex.

As mentioned above, CFT is based primarily on symmetry of ligands around a central metal/ion and how this anisotropic (properties depending on direction) ligand field affects the metal's atomic orbitals; the energies of which may increase, decrease or not be affected at all. Once the ligands' electrons interact with the electrons of the  $d$ -orbitals, the electrostatic interactions cause the energy levels of the  $d$ -orbital to fluctuate depending on the orientation and the nature of the ligands. For example, the **oxidation state** and the strength of the ligands determine splitting; the higher the oxidation state or the stronger the ligand, the larger the splitting. Ligands are classified as strong or weak based on the spectrochemical series:



Note that  $\text{SCN}^-$  and  $\text{NO}_2^-$  ligands are represented twice in the above spectrochemical series since there are two different Lewis base sites (e.g., free electron pairs to share) on each ligand (e.g., for the  $\text{SCN}^-$  ligand, the electron pair on the sulfur or the nitrogen can form the **coordinate covalent bond** to a metal). The specific atom that binds in such ligands is underlined.

In addition to octahedral complexes, two common geometries observed are that of tetrahedral and square planar. These complexes differ from the octahedral complexes in that the orbital levels are raised in energy due to the interference with electrons from ligands. For the tetrahedral complex, the  $d_{xy}$ ,  $d_{xz}$ , and  $d_{yz}$  orbitals are raised in energy while the  $d_{z^2}$ ,  $d_{x^2-y^2}$  orbitals are lowered. For the square planar complexes, there is greatest interaction with the  $d_{x^2-y^2}$  orbital and therefore it has higher energy. The next orbital with the greatest interaction is  $d_{xy}$ , followed below by  $d_{z^2}$ . The orbitals with the lowest energy are the  $d_{xz}$  and  $d_{yz}$  orbitals. There is a large energy separation between the  $d_{z^2}$  orbital and the  $d_{xz}$  and  $d_{yz}$  orbitals, meaning that the crystal field splitting energy is large. We find that the square planar complexes have the greatest crystal field splitting energy compared to all the other complexes. This means that most square planar complexes are low spin, strong field ligands.

## Description of $d$ -Orbitals

To understand CFT, one must understand the description of the lobes:

- $d_{xy}$ : lobes lie in-between the  $x$  and the  $y$  axes.
- $d_{xz}$ : lobes lie in-between the  $x$  and the  $z$  axes.
- $d_{yz}$ : lobes lie in-between the  $y$  and the  $z$  axes.
- $d_{x^2-y^2}$ : lobes lie on the  $x$  and  $y$  axes.
- $d_{z^2}$ : there are two lobes on the  $z$  axes and there is a donut shape ring that lies on the  $xy$  plane around the other two lobes.

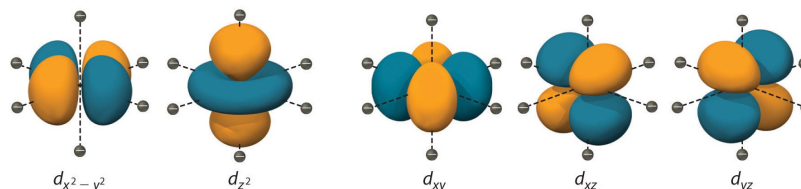


Figure 8.2.1.3: Spatial arrangement of ligands in the an octahedral ligand field with respect to the five  $d$ -orbitals.

## Octahedral Complexes

In an **octahedral complex**, there are six ligands attached to the central transition metal. The  $d$ -orbital splits into two different levels (Figure 8.2.1.4). The bottom three energy levels are named  $d_{xy}$ ,  $d_{xz}$ , and  $d_{yz}$  (collectively referred to as  $t_{2g}$ ). The two upper energy levels are named  $d_{x^2-y^2}$ , and  $d_{z^2}$  (collectively referred to as  $e_g$ ).

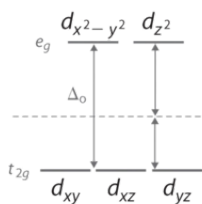


Figure 8.2.1.4.

The reason they split is because of the electrostatic interactions between the electrons of the ligand and the lobes of the d-orbital. In an octahedral, the electrons are attracted to the axes. Any orbital that has a lobe on the axes moves to a higher energy level. This means that in an octahedral, the energy levels of  $e_g$  are higher ( $0.6\Delta_o$ ) while  $t_{2g}$  is lower ( $0.4\Delta_o$ ). The distance that the electrons have to move from  $t_{2g}$  to  $e_g$  and it dictates the energy that the complex will absorb from white light, which will determine the **color**. Whether the complex is **paramagnetic or diamagnetic** will be determined by the spin state. If there are unpaired electrons, the complex is paramagnetic; if all electrons are paired, the complex is diamagnetic.

### Tetrahedral Complexes

In a tetrahedral complex, there are four ligands attached to the central metal. The d orbitals also split into two different energy levels. The top three consist of the  $d_{xy}$ ,  $d_{xz}$ , and  $d_{yz}$  orbitals. The bottom two consist of the  $d_{x^2-y^2}$  and  $d_{z^2}$  orbitals. The reason for this is due to poor orbital overlap between the metal and the ligand orbitals. The orbitals are directed on the axes, while the ligands are not.

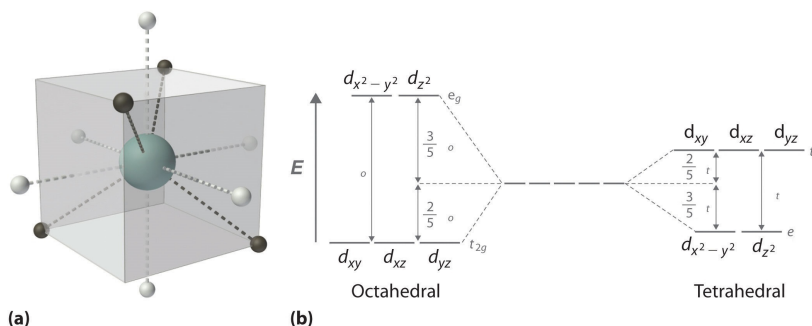


Figure 8.2.1.5: (a) Tetrahedral ligand field surrounding a central transition metal (blue sphere). (b) Splitting of the degenerate d-orbitals (without a ligand field) due to an octahedral ligand field (left diagram) and the tetrahedral field (right diagram).

The difference in the splitting energy is tetrahedral splitting constant ( $\Delta_t$ ), which is less than ( $\Delta_o$ ) for the same ligands:

$$\Delta_t = 0.44 \Delta_o \quad (8.2.1.1)$$

Consequently,  $\Delta_t$  is typically smaller than the **spin pairing energy**, so tetrahedral complexes are usually **high spin**.

### Square Planar Complexes

In a square planar, there are four ligands as well. However, the difference is that the electrons of the ligands are only attracted to the  $xy$  plane. Any orbital in the  $xy$  plane has a higher energy level (Figure 8.2.1.6). There are four different energy levels for the square planar (from the highest energy level to the lowest energy level):  $d_{x^2-y^2}$ ,  $d_{xy}$ ,  $d_{z^2}$ , and both  $d_{xz}$  and  $d_{yz}$ .

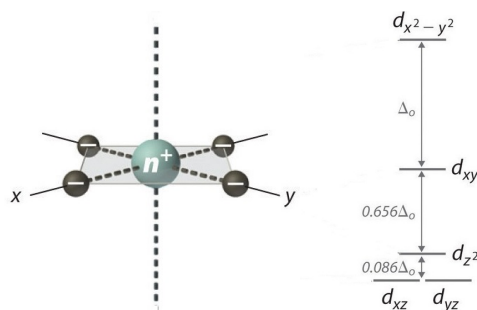


Figure 8.2.1.6: Splitting of the degenerate d-orbitals (without a ligand field) due to a square planar ligand field.

The splitting energy (from highest orbital to lowest orbital) is  $\Delta_{sp}$  and tends to be larger than  $\Delta_o$

$$\Delta_{sp} = 1.74 \Delta_o \quad (8.2.1.2)$$

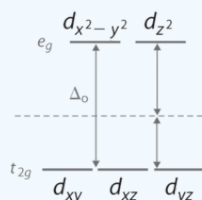
Moreover,  $\Delta_{sp}$  is also larger than the pairing energy, so the square planar complexes are usually **low spin** complexes.

### ✓ Example 8.2.1.1

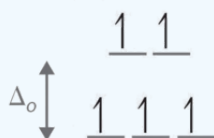
For the complex ion  $[\text{Fe}(\text{Cl})_6]^{3-}$  determine the number of d electrons for Fe, sketch the d-orbital energy levels and the distribution of d electrons among them, list the number of lone electrons, and label whether the complex is paramagnetic or diamagnetic.

#### Solution

- Step 1: Determine the oxidation state of Fe. Here it is  $\text{Fe}^{3+}$ . Based on its electron configuration,  $\text{Fe}^{3+}$  has **5 d-electrons**.
- Step 2: Determine the geometry of the ion. Here it is an octahedral which means the energy splitting should look like:



- Step 3: Determine whether the ligand induces is a strong or weak field spin by looking at the [spectrochemical series](#).  $\text{Cl}^-$  is a weak field ligand (i.e., it induces high spin complexes). Therefore, electrons fill all orbitals before being paired.



- Step four: Count the number of lone electrons. Here, there are **5 electrons**.
- Step five: The five unpaired electrons means this complex ion is **paramagnetic** (and strongly so).

### ✓ Example 8.2.1.2

A *tetrahedral* complex absorbs at 545 nm. What is the respective octahedral crystal field splitting ( $\Delta_o$ )? What is the color of the complex?

#### Solution

$$\begin{aligned}\Delta_t &= \frac{hc}{\lambda} \\ &= \frac{(6.626 \times 10^{-34} \text{ J} \cdot \text{s})(3 \times 10^8 \text{ m/s})}{545 \times 10^{-9} \text{ m}} \\ &= 3.65 \times 10^{-19} \text{ J}\end{aligned}$$

However, the *tetrahedral* splitting ( $\Delta_t$ ) is  $\sim 4/9$  that of the *octahedral* splitting ( $\Delta_o$ ).

$$\begin{aligned}\Delta_t &= 0.44\Delta_o \\ \Delta_o &= \frac{\Delta_t}{0.44} \\ &= \frac{3.65 \times 10^{-19} \text{ J}}{0.44} \\ &= 8.30 \times 10^{-18} \text{ J}\end{aligned}$$

This is the energy needed to promote *one* electron in *one* complex. Often the crystal field splitting is given per mole, which requires this number to be multiplied by Avogadro's Number ( $6.022 \times 10^{23}$ ).

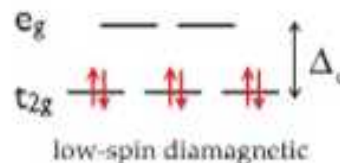
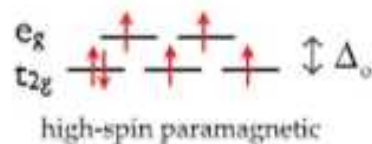
This complex appears red, since it absorbs in the complementary green color (determined via the color wheel).



Most ordinary materials have all electrons paired. Zero spin = diamagnetic (slight repulsion)

- Unpaired electrons have magnetic fields, so are attracted by an external field (paramagnetic)
- Permanently oriented spins are ferromagnetic

$d^6$  octahedral field



Video:

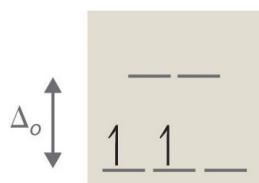
### Problems

For each of the following, sketch the d-orbital energy levels and the distribution of d electrons among them, state the geometry, list the number of d-electrons, list the number of lone electrons, and label whether they are paramagnetic or diamagnetic:

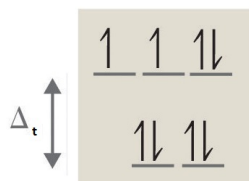
1.  $[\text{Ti}(\text{H}_2\text{O})_6]^{2+}$
2.  $[\text{NiCl}_4]^{2-}$
3.  $[\text{CoF}_6]^{3-}$  (also state whether this is low or high spin)
4.  $[\text{Co}(\text{NH}_3)_6]^{3+}$  (also state whether this is low or high spin)
5. True or False: Square Planar complex compounds are usually low spin.

### Answers

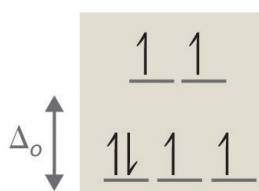
1. octahedral, 2, 2, paramagnetic



2. tetrahedral, 8, 2, paramagnetic (see [Octahedral vs. Tetrahedral Geometries](#))

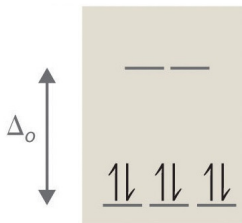


3. octahedral, 6, 4, paramagnetic, high spin





4. octahedral, 6, 0, diamagnetic, low spin



5. True

### Contributors and Attributions

- Asadullah Awan (UCD), Hong Truong (UCD)
- [Prof. Robert J. Lancashire](#) (The Department of Chemistry, University of the West Indies)

---

8.2.1: Crystal Field Theory is shared under a [CC BY-NC-SA 4.0](#) license and was authored, remixed, and/or curated by LibreTexts.

- [Crystal Field Theory](#) is licensed [CC BY-NC-SA 4.0](#).

## 8.2.2: Crystal Field Stabilization Energy

A consequence of [Crystal Field Theory](#) is that the distribution of electrons in the d orbitals may lead to net stabilization (decrease in energy) of some complexes depending on the specific ligand field geometry and metal d-electron configurations. It is a simple matter to calculate this stabilization since all that is needed is the electron configuration and knowledge of the splitting patterns.

### Definition: Crystal Field Stabilization Energy

The Crystal Field Stabilization Energy is defined as the energy of the electron configuration in the ligand field minus the energy of the electronic configuration in the isotropic field.

$$CFSE = \Delta E = E_{\text{ligand field}} - E_{\text{isotropic field}} \quad (8.2.2.1)$$

The CSFE will depend on multiple factors including:

- Geometry (which changes the d-orbital splitting patterns)
- Number of d-electrons
- [Spin Pairing Energy](#)
- Ligand character (via [Spectrochemical Series](#))

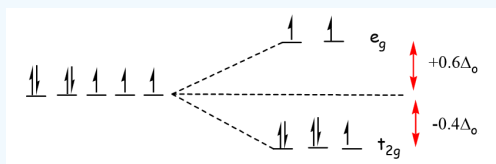
For an octahedral complex, an electron in the more stable  $t_{2g}$  subset is treated as contributing  $-2/5\Delta_o$  whereas an electron in the higher energy  $e_g$  subset contributes to a destabilization of  $+3/5\Delta_o$ . The final answer is then expressed as a multiple of the crystal field splitting parameter  $\Delta_o$ . If any electrons are paired within a single orbital, then the term  $P$  is used to represent the spin pairing energy.

### ✓ Example 8.2.2.1: CFSE for a high Spin $d^7$ complex

What is the Crystal Field Stabilization Energy for a high spin  $d^7$  octahedral complex?

#### Solution

The splitting pattern and electron configuration for both isotropic and octahedral ligand fields are compared below.



The energy of the isotropic field ( $E_{\text{isotropic field}}$ ) is

$$E_{\text{isotropic field}} = 7 \times 0 + 2P = 2P$$

The energy of the octahedral ligand field  $E_{\text{ligand field}}$  is

$$E_{\text{ligand field}} = (5 \times -2/5\Delta_o) + (2 \times 3/5\Delta_o) + 2P = -4/5\Delta_o + 2P$$

So via Equation 8.2.2.1, the CFSE is

$$\begin{aligned} CFSE &= E_{\text{ligand field}} - E_{\text{isotropic field}} \\ &= (-4/5\Delta_o + 2P) - 2P \\ &= -4/5\Delta_o \end{aligned}$$

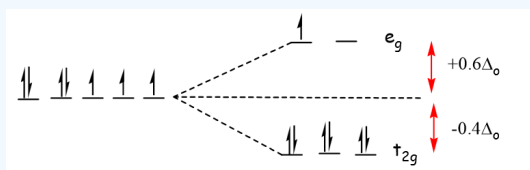
Notice that the Spin pairing Energy falls out in this case (and will when calculating the CFSE of high spin complexes) since the number of paired electrons in the ligand field is the same as that in isotropic field of the free metal ion.

### ✓ Example 8.2.2.2: CFSE for a Low Spin $d^7$ complex

What is the Crystal Field Stabilization Energy for a low spin  $d^7$  octahedral complex?

#### Solution

The splitting pattern and electron configuration for both isotropic and octahedral ligand fields are compared below.



The energy of the isotropic field is the same as calculated for the high spin configuration in Example 1:

$$E_{\text{isotropic field}} = 7 \times 0 + 2P = 2P$$

The energy of the octahedral ligand field  $E_{\text{ligand field}}$  is

$$\begin{aligned} E_{\text{ligand field}} &= (6 \times -2/5 \Delta_o) + (1 \times 3/5 \Delta_o) + 3P \\ &= -9/5 \Delta_o + 3P \end{aligned}$$

So via Equation 8.2.2.1, the CFSE is

$$\begin{aligned} CFSE &= E_{\text{ligand field}} - E_{\text{isotropic field}} \\ &= (-9/5 \Delta_o + 3P) - 2P \\ &= -9/5 \Delta_o + P \end{aligned}$$

Adding in the pairing energy since it will require extra energy to pair up one extra group of electrons. This appears more a more stable configuration than the high spin  $d^7$  configuration in Example 8.2.2.1, but we have then to take into consideration the Pairing energy  $P$  to know definitely, which varies between  $200 - 400 \text{ kJ mol}^{-1}$  depending on the metal.

Table 8.2.2.1: Crystal Field Stabilization Energies (CFSE) for high and low spin octahedral complexes

Total d-electrons	Isotropic Field	Octahedral Complex				Crystal Field Stabilization Energy	
		High Spin		Low Spin		High Spin	Low Spin
	$E_{\text{isotropic field}}$	Configuration	$E_{\text{ligand field}}$	Configuration	$E_{\text{ligand field}}$		
$d^0$	0	$t_{2g}^0 e_g^0$	0	$t_{2g}^0 e_g^0$	0	0	0
$d^1$	0	$t_{2g}^1 e_g^0$	$-2/5 \Delta_o$	$t_{2g}^1 e_g^0$	$-2/5 \Delta_o$	$-2/5 \Delta_o$	$-2/5 \Delta_o$
$d^2$	0	$t_{2g}^2 e_g^0$	$-4/5 \Delta_o$	$t_{2g}^2 e_g^0$	$-4/5 \Delta_o$	$-4/5 \Delta_o$	$-4/5 \Delta_o$
$d^3$	0	$t_{2g}^3 e_g^0$	$-6/5 \Delta_o$	$t_{2g}^3 e_g^0$	$-6/5 \Delta_o$	$-6/5 \Delta_o$	$-6/5 \Delta_o$
$d^4$	0	$t_{2g}^3 e_g^1$	$-3/5 \Delta_o$	$t_{2g}^4 e_g^0$	$-8/5 \Delta_o + P$	$-3/5 \Delta_o$	$-8/5 \Delta_o + P$
$d^5$	0	$t_{2g}^3 e_g^2$	$0 \Delta_o$	$t_{2g}^5 e_g^0$	$-10/5 \Delta_o + 2P$	$0 \Delta_o$	$-10/5 \Delta_o + 2P$
$d^6$	$P$	$t_{2g}^4 e_g^2$	$-2/5 \Delta_o + P$	$t_{2g}^6 e_g^0$	$-12/5 \Delta_o + 3P$	$-2/5 \Delta_o$	$-12/5 \Delta_o + P$
$d^7$	$2P$	$t_{2g}^5 e_g^2$	$-4/5 \Delta_o + 2P$	$t_{2g}^6 e_g^1$	$-9/5 \Delta_o + 3P$	$-4/5 \Delta_o$	$-9/5 \Delta_o + P$
$d^8$	$3P$	$t_{2g}^6 e_g^2$	$-6/5 \Delta_o + 3P$	$t_{2g}^6 e_g^2$	$-6/5 \Delta_o + 3P$	$-6/5 \Delta_o$	$-6/5 \Delta_o$
$d^9$	$4P$	$t_{2g}^6 e_g^3$	$-3/5 \Delta_o + 4P$	$t_{2g}^6 e_g^3$	$-3/5 \Delta_o + 4P$	$-3/5 \Delta_o$	$-3/5 \Delta_o$
$d^{10}$	$5P$	$t_{2g}^6 e_g^4$	$0 \Delta_o + 5P$	$t_{2g}^6 e_g^4$	$0 \Delta_o + 5P$	0	0

$P$  is the [spin pairing energy](#) and represents the energy required to pair up electrons within the same orbital. For a given metal ion  $P$  (pairing energy) is constant, but it does not vary with ligand and [oxidation state](#) of the metal ion).

## Octahedral Preference

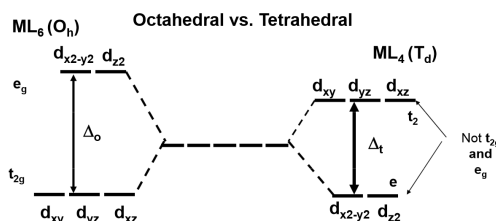
Similar CFSE values can be constructed for non-octahedral ligand field geometries once the knowledge of the d-orbital splitting is known and the electron configuration within those orbitals known, e.g., the tetrahedral complexes in Table 8.2.2.2 These energies geometries can then be contrasted to the octahedral CFSE to calculate a thermodynamic preference (Enthalpy-wise) for a metal-ligand combination to favor the octahedral geometry. This is quantified via a Octahedral Site Preference Energy defined below.

### Definition: Octahedral Site Preference Energies

The Octahedral Site Preference Energy (OSPE) is defined as the difference of CFSE energies for a non-octahedral complex and the octahedral complex. For comparing the preference of forming an octahedral ligand field vs. a tetrahedral ligand field, the OSPE is thus:

$$OSPE = CFSE_{(oct)} - CFSE_{(tet)} \quad (8.2.2.2)$$

The OSPE quantifies the preference of a complex to exhibit an octahedral geometry vs. a tetrahedral geometry.



Note: the conversion between  $\Delta_o$  and  $\Delta_t$  used for these calculations is:

$$\Delta_t \approx \frac{4}{9} \Delta_o \quad (8.2.2.3)$$

which is applicable for comparing octahedral and tetrahedral complexes that involve same ligands only.

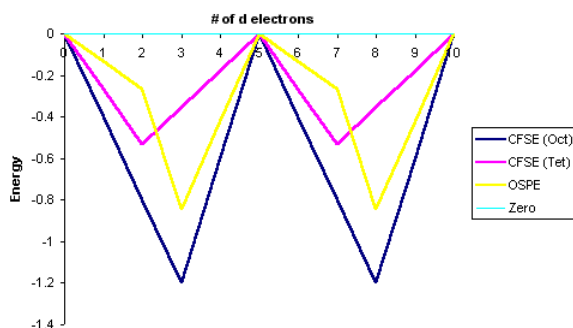
Table 8.2.2.2: Octahedral Site Preference Energies (OSPE)

Total d-electrons	CFSE(Octahedral)		CFSE(Tetrahedral)		OSPE (for high spin complexes)**
	High Spin	Low Spin	Configuration	Always High Spin*	
d <sup>0</sup>	0 $\Delta_o$	0 $\Delta_o$	e <sup>0</sup>	0 $\Delta_t$	0 $\Delta_o$
d <sup>1</sup>	-2/5 $\Delta_o$	-2/5 $\Delta_o$	e <sup>1</sup>	-3/5 $\Delta_t$	-6/45 $\Delta_o$
d <sup>2</sup>	-4/5 $\Delta_o$	-4/5 $\Delta_o$	e <sup>2</sup>	-6/5 $\Delta_t$	-12/45 $\Delta_o$
d <sup>3</sup>	-6/5 $\Delta_o$	-6/5 $\Delta_o$	e <sup>2</sup> t <sub>2</sub> <sup>1</sup>	-4/5 $\Delta_t$	-38/45 $\Delta_o$
d <sup>4</sup>	-3/5 $\Delta_o$	-8/5 $\Delta_o$ + P	e <sup>2</sup> t <sub>2</sub> <sup>2</sup>	-2/5 $\Delta_t$	-19/45 $\Delta_o$
d <sup>5</sup>	0 $\Delta_o$	-10/5 $\Delta_o$ + 2P	e <sup>2</sup> t <sub>2</sub> <sup>3</sup>	0 $\Delta_t$	0 $\Delta_o$
d <sup>6</sup>	-2/5 $\Delta_o$	-12/5 $\Delta_o$ + P	e <sup>3</sup> t <sub>2</sub> <sup>3</sup>	-3/5 $\Delta_t$	-6/45 $\Delta_o$
d <sup>7</sup>	-4/5 $\Delta_o$	-9/5 $\Delta_o$ + P	e <sup>4</sup> t <sub>2</sub> <sup>3</sup>	-6/5 $\Delta_t$	-12/45 $\Delta_o$
d <sup>8</sup>	-6/5 $\Delta_o$	-6/5 $\Delta_o$	e <sup>4</sup> t <sub>2</sub> <sup>4</sup>	-4/5 $\Delta_t$	-38/45 $\Delta_o$
d <sup>9</sup>	-3/5 $\Delta_o$	-3/5 $\Delta_o$	e <sup>4</sup> t <sub>2</sub> <sup>5</sup>	-2/5 $\Delta_t$	-19/45 $\Delta_o$
d <sup>10</sup>	0	0	e <sup>4</sup> t <sub>2</sub> <sup>6</sup>	0 $\Delta_t$	0 $\Delta_o$

$P$  is the [spin pairing energy](#) and represents the energy required to pair up electrons within the same orbital.

Tetrahedral complexes are always high spin since the splitting is appreciably smaller than  $P$  (Equation [8.2.2.3](#)).

After conversion with Equation 8.2.2.3 The data in Tables 8.2.2.1 and 8.2.2.2 are represented graphically by the curves in Figure 8.2.2.1 below for the high spin complexes only. The low spin complexes require knowledge of  $P$  to graph.



**Figure 8.2.2.1:** Crystal Field Stabilization Energies for both octahedral fields ( $CFSE_{oct}$ ) and tetrahedral fields ( $CFSE_{tet}$ ). Octahedral Site Preference Energies (OSPE) are in yellow. This is for high spin complexes.

From a simple inspection of Figure 8.2.2.1 the following observations can be made:

- The OSPE is *small* in  $d^1$ ,  $d^2$ ,  $d^5$ ,  $d^6$ ,  $d^7$  complexes and other factors influence the stability of the complexes including steric factors
- The OSPE is *large* in  $d^3$  and  $d^8$  complexes which strongly favor octahedral geometries

## Applications

The "double-humped" curve in Figure 8.2.2.1 is found for various properties of the first-row transition metals, including Hydration and [Lattice energies](#) of the M(II) ions, ionic radii as well as the stability of M(II) complexes. This suggests that these properties are somehow related to Crystal Field effects.

In the case of Hydration Energies describing the [complexation](#) of water ligands to a bare metal ion:

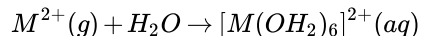
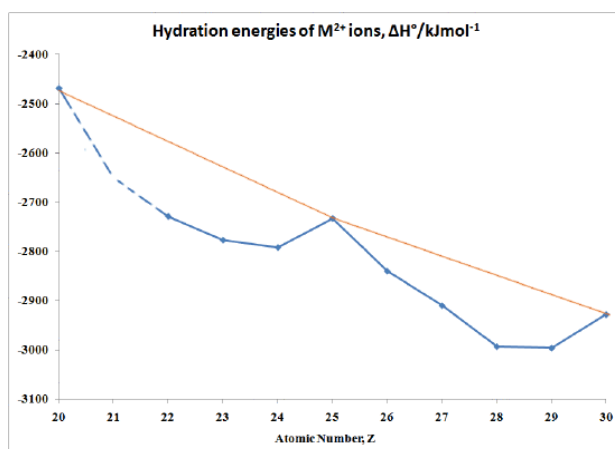


Table 8.2.2.3 and Figure 8.2.2.1 shows this type of curve. Note that in any series of this type not all the data are available since a number of ions are not very stable in the M(II) state.

Table 8.2.2.3: Hydration energies of  $M^{2+}$  ions

M	$\Delta H^\circ/\text{kJmol}^{-1}$	M	$\Delta H^\circ/\text{kJmol}^{-1}$
Ca	-2469	Fe	-2840
Sc	no stable 2+ ion	Co	-2910
Ti	-2729	Ni	-2993
>V	-2777	Cu	-2996
Cr	-2792	Zn	-2928
Mn	-2733		

Graphically the data in Table 2 can be represented by:



**Figure 8.2.2.2:** hydration energies of  $M^{2+}$  ions

### Contributors and Attributions

- [Prof. Robert J. Lancashire](#) (The Department of Chemistry, University of the West Indies)

8.2.2: Crystal Field Stabilization Energy is shared under a [CC BY-NC-SA 4.0](#) license and was authored, remixed, and/or curated by LibreTexts.

- [Crystal Field Stabilization Energy](#) is licensed [CC BY-NC-SA 4.0](#).

## 8.2.3: Non-octahedral Complexes

### Learning Objectives

- Understand the d-orbital degeneracies of square planar and tetrahedral metal complexes.

### Tetragonal and Square Planar Complexes

If two *trans*- ligands in an octahedral complex are either chemically different from the other four (as in *trans*-[Co(NH<sub>3</sub>)<sub>4</sub>Cl<sub>2</sub>]<sup>+</sup>), or at a different distance from the metal than the other four, the result is a tetragonally distorted octahedral complex. The electronic structures of such complexes are best viewed as the result of distorting an octahedral complex. Consider, for example, an octahedral complex such as [Co(NH<sub>3</sub>)<sub>6</sub>]<sup>3+</sup>: two *trans*- NH<sub>3</sub> molecules are slowly removed from the metal along the  $\pm z$  axes, as shown in the top half of Figure 8.2.3.1. As the two axial Co–N distances increase simultaneously, the d-orbitals that interact most strongly with the two axial ligands decrease in energy due to a decrease in electrostatic repulsions between the electrons in these orbitals and the negative ends of the ligand dipoles. The affected d orbitals are those with a component along the  $\pm z$  axes— $d_{z^2}$ ,  $d_{xz}$ , and  $d_{yz}$ . These orbitals are not affected equally, however: because the  $d_{z^2}$  orbital points directly at the two ligands being removed, its energy will decrease much more rapidly than the degenerate energies of the  $d_{xz}$  and  $d_{yz}$ , as shown in the bottom half of Figure 8.2.3.1. In addition, the effective positive charge on the metal increases somewhat as the axial ligands are removed, increasing the attraction between the four remaining ligands and the metal. This increases the extent of their interactions with the other two d orbitals and increases their energies. Again, the two d orbitals are not affected equally: because the  $d_{x^2-y^2}$  orbital points directly at the four in-plane ligands, its energy increases to a greater extent than the energy of the  $d_{xy}$  orbital, which points between the in-plane ligands. If the two axial ligands are moved infinitely far away from the metal, a square planar complex is formed. The energy of the  $d_{xy}$  orbital actually surpasses that of the  $d_{z^2}$  orbital in the process. The largest orbital splitting in a square planar complex, between the  $d_{x^2-y^2}$  and  $d_{xy}$  energy levels, is identical in magnitude to  $\Delta_o$ .

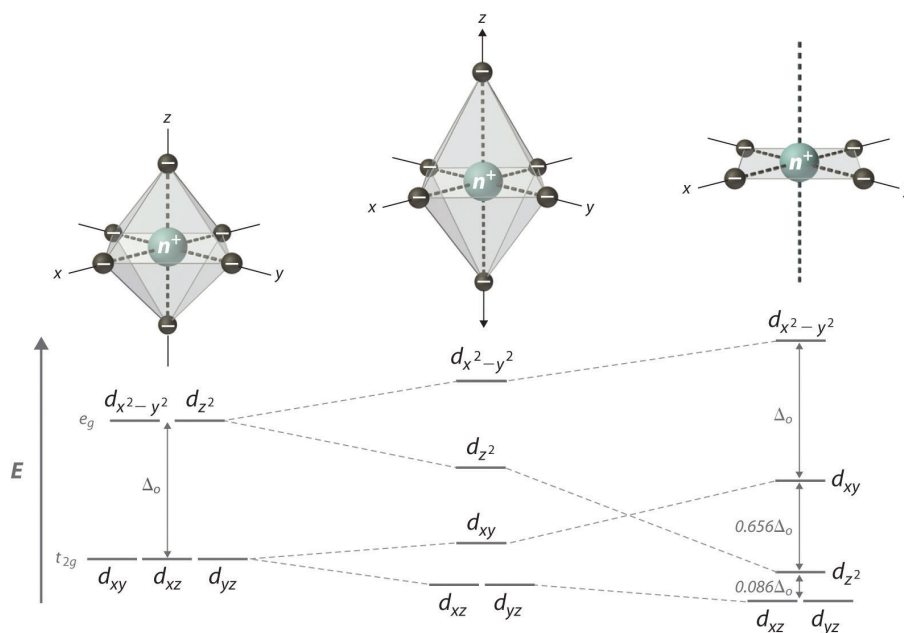


Figure 8.2.3.1 d-Orbital Splittings for Tetragonal and Square Planar Complexes. (CC BY-SA-NC; anonymous by request)

Moving the two axial ligands away from the metal ion along the  $z$  axis initially generates an elongated octahedral complex (the center compound of Figure 8.2.3.1) and eventually produces a square planar complex (right). As shown below the structures, an axial elongation causes the  $d_{z^2}$ ,  $d_{xz}$  and  $d_{yz}$  orbitals to decrease in energy and the  $d_{x^2-y^2}$  and  $d_{xy}$  orbitals to increase in energy. The change in energy is not the same for all five d orbitals. The  $d_{z^2}$  orbital has a smaller  $xy$  component than does the  $d_{xy}$  orbital, so it reaches a lower energy level; thus, the order of these orbitals is reversed.

## Tetrahedral Complexes

In a tetrahedral arrangement of four ligands around a metal ion, none of the ligands lies on any of the three coordinate axes (illustrated in part (a) in Figure 8.2.3.2); consequently, none of the five d orbitals points directly at the ligands. Nonetheless, the  $d_{xy}$ ,  $d_{xz}$ , and  $d_{yz}$  orbitals interact more strongly with the ligands than do  $d_{x^2-y^2}$  and  $d_{z^2}$ ; this again results in a splitting of the five d orbitals into two groups. The splitting of the energies of the orbitals in a tetrahedral complex ( $\Delta_t$ ) is much smaller than that for an octahedral complex ( $\Delta_o$ ), however, for two reasons: first, the d orbitals interact less strongly with the ligands in a tetrahedral arrangement; second, there are only four negatively-charged regions rather than six, which decreases the electrostatic interactions by one-third if all other factors are equal. It can be shown that for complexes of the same metal ion with the same charge, the same ligands, and the same M–L distance,  $\Delta_t = \frac{4}{9} \Delta_o$ . The relationship between the splitting of the five d orbitals in octahedral and tetrahedral crystal fields imposed by the same ligands is shown schematically in part (b) in Figure 8.2.3.2.

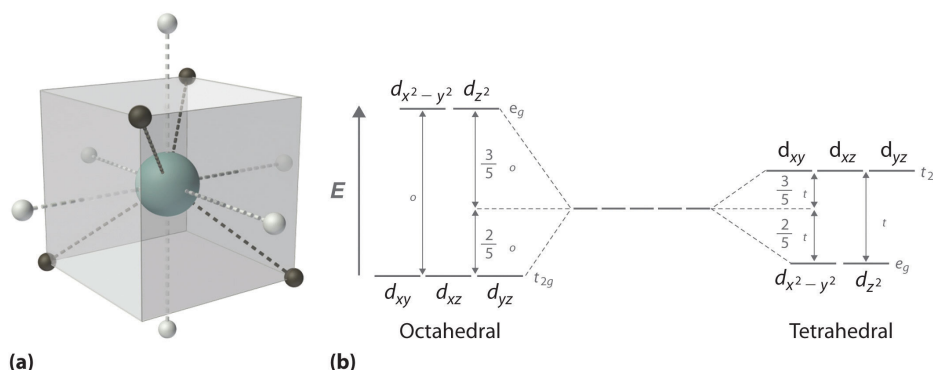


Figure 8.2.3.2: d-Orbital Splittings for a Tetrahedral Complex. (a) In a tetrahedral complex, none of the five d orbitals points directly at or between the ligands. (b) Because the  $d_{xy}$ ,  $d_{xz}$ , and  $d_{yz}$  orbitals (the  $t_{2g}$  orbitals) interact more strongly with the ligands than do the  $d_{x^2-y^2}$  and  $d_{z^2}$  orbitals (the  $e_g$  orbitals), the order of orbital energies in a tetrahedral complex is the opposite of the order in an octahedral complex. (CC BY-SA-NC; anonymous by request)

$\Delta_t < \Delta_o$  because of weaker d-orbital–ligand interactions and decreased electrostatic interactions.

### ✓ Example 8.2.3.1: Predicting Structure

For each complex, predict its structure, whether it is high spin or low spin, and the number of unpaired electrons present.

1.  $[Cu(NH_3)_4]^{2+}$
2.  $[Ni(CN)_4]^{2-}$

#### Solution

Because  $\Delta_o$  is so large for the second- and third-row transition metals, all four-coordinate complexes of these metals are square planar due to the much higher crystal field stabilization energy (CFSE) for square planar versus tetrahedral structures. The only exception is for  $d^{10}$  metal ions such as  $Cd^{2+}$ , which have zero CFSE and are therefore tetrahedral as predicted by the VSEPR model. Four-coordinate complexes of the first-row transition metals can be either square planar or tetrahedral; the former is favored by strong-field ligands, whereas the latter is favored by weak-field ligands. For example, the  $[Ni(CN)_4]^{2-}$  ion is square planar, while the  $[NiCl_4]^{2-}$  ion is tetrahedral.

1.

The copper in this complex is a  $d^9$  ion and it has a coordination number of 4. So it is probably either square planar or tetrahedral. To estimate which, we need to fill in the CFT splitting diagrams for each with 9 electrons and ask which has a lower energy. Comparing the square planar (Figure 8.2.3.1) splitting diagram with tetrahedral (Figure 8.2.3.2), suggests that 9 electrons will have a net lower total energy for square planar (since the  $d_{x^2-y^2}$  orbital is high in energy, the others are lower).

For the square planar structure, neither high nor low spin states are possible (only one state) with a single unpaired electron.

2.

The nickel in this complex is a  $d^8$  ion and it has a coordination number of 4. So it is probably either square planar or tetrahedral. To estimate which, we need to fill in the CFT splitting diagrams for each with 8 electrons and ask which has a



lower energy. Comparing the square planer (Figure 8.2.3.1) splitting diagram with tetrahedral (Figure 8.2.3.2), suggests that 8 electrons will have a net lower total energy for square planar (since the  $d_{x^2-y^2}$  orbital is high in energy, the others are lower).

For the square planar structure, it is a low spin complex since a high spin requires a lot of energy to promote to the  $d_{x^2-y^2}$  orbital. Hence, there are no unpaired electrons

### ? Exercise 8.2.3.1

What are the geometries of the following two complexes?

1.  $[\text{AlCl}_4]^-$
2.  $[\text{Ag}(\text{NH}_3)_2]^+$

#### Answer 1

tetrahedral

#### Answer 2

linear

## Summary

Distorting an octahedral complex by moving opposite ligands away from the metal produces a tetragonal or square planar arrangement, in which interactions with equatorial ligands become stronger. Because none of the d orbitals points directly at the ligands in a tetrahedral complex, these complexes have smaller values of the crystal field splitting energy  $\Delta_t$ . In tetrahedral molecular geometry, a central atom is located at the center of four substituents, which form the corners of a tetrahedron. Tetrahedral geometry is common for complexes where the metal has  $d^0$  or  $d^{10}$  electron configuration. The CFT diagram for tetrahedral complexes has  $d_{x^2-y^2}$  and  $d_{z^2}$  orbitals equally low in energy because they are between the ligand axis and experience little repulsion. In square planar molecular geometry, a central atom is surrounded by constituent atoms, which form the corners of a square on the same plane. The square planar geometry is prevalent for transition metal complexes with  $d^8$  configuration. The CFT diagram for square planar complexes can be derived from octahedral complexes yet the  $d_{x^2-y^2}$  level is the most destabilized and is left unfilled.

This page titled [8.2.3: Non-octahedral Complexes](#) is shared under a [CC BY-NC-SA 4.0](#) license and was authored, remixed, and/or curated by [Anonymous](#).

- [Non-octahedral Complexes](#) by Anonymous is licensed [CC BY-NC-SA 4.0](#).

## 8.3: Crystal Field Theory and Magnetism

---

Learning objectives for this unit are to:

- Predict if or explain why Jahn-Teller distortions will occur in a metal complex
  - Predict the magnetic properties of a complex based on its d-electron configuration and predict d-electron configurations based on magnetic properties
  - Calculate the spin-only magnetic moment ( $\mu_s$ ) for a complex given the number of unpaired electrons
  - Determine the number of unpaired electrons in a complex from the calculated  $\mu_{\text{eff}}$  and  $\mu_s$  values and determine the spin state of the complex from this information
  - Compare and contrast diamagnetism, paramagnetism, ferromagnetism, antiferromagnetism, and ferrimagnetism
- 

8.3: Crystal Field Theory and Magnetism is shared under a [not declared](#) license and was authored, remixed, and/or curated by LibreTexts.

## 8.3.1: Jahn-Teller Distortions

### Introduction to Jahn-Teller Distortion

The Jahn–Teller effect occurs because the unequal occupation of orbitals with identical energies is unfavorable. To avoid these unfavorable electronic configurations, molecules distort (lowering their symmetry) to render these orbitals no longer degenerate.<sup>[1]</sup> The Jahn–Teller distortion, describes the geometrical distortion of molecules and ions that result from certain electron configurations.<sup>[2]</sup> This distortion is normally observed among octahedral complexes where the two axial bonds can be compressed or elongated to result in a different bond length from those of the equatorial bonds as shown in Figure 8.3.1.1<sup>[3]</sup>

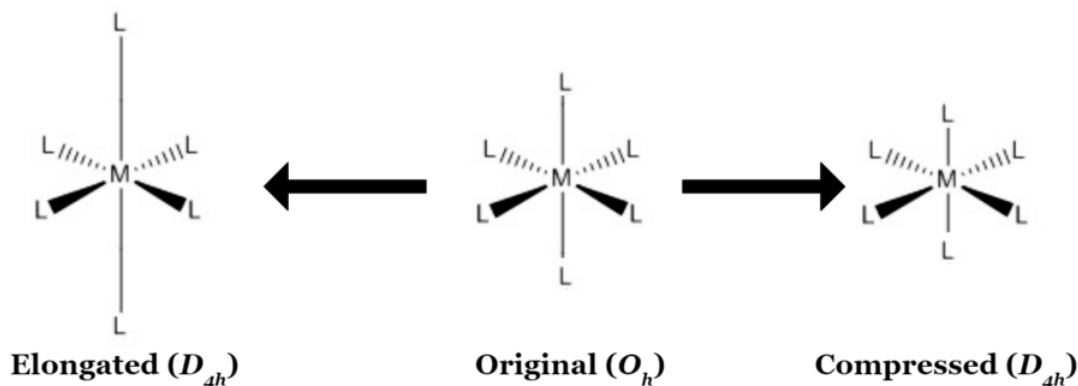


Figure 8.3.1.1: The geometric distortion of an octahedral complex

#### A Brief History of Jahn-Teller Distortion

In 1937, Hermann Jahn and Edward Teller postulated a theorem stating that "stability and degeneracy are not possible simultaneously unless the molecule is a linear one," in regards to its electronic state. This leads to a break in degeneracy which stabilizes the molecule and by consequence, reduces its symmetry.<sup>[4]</sup>

### Orbital Analysis of Jahn-Teller Distortion

#### Elongation Distortion

Elongation as shown in Figure 8.3.1.2 is the most common mechanism of distortion. In ideally octahedral complexes that experience Jahn–Teller distortion, the  $e_g^*$  orbitals change more in energy relative to the  $t_{2g}$  orbitals.<sup>[5]</sup>

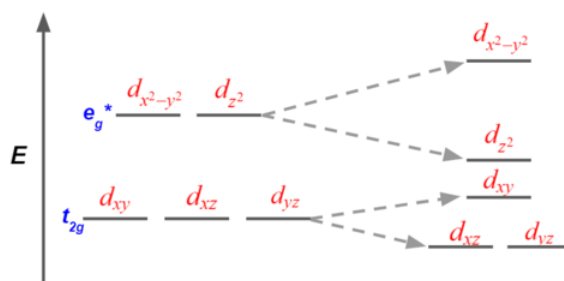


Figure 8.3.1.2: The d-orbitals undergo an elongation

When the octahedral complex undergoes an elongation, any of the metal d orbitals that carry a z-directional feature become lower in energy, ligands are easier to bond along z-direction. Geometrically, as the z-direction gets elongated, the repulsion energy and sterical hindrance along z-direction are lower to allow ligands easier to bond.

#### Compression Distortion

Compression as shown in Figure 8.3.1.3 happens less frequently than the elongation.

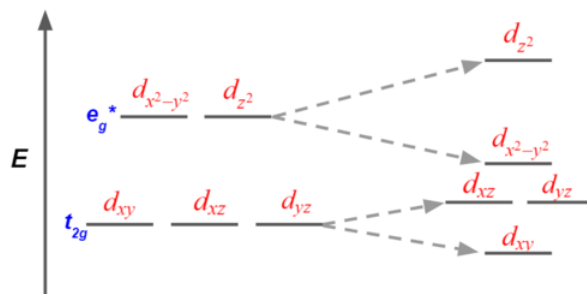


Figure 8.3.1.3: The d-orbitals undergo a compression

When the octahedral complex undergoes a compression, any of the metal d orbitals that carry a z-directional feature become higher in energy, ligands are harder to bond along z-direction. Geometrically, as the z-direction gets compressed, the repulsion energy and sterical hindrance along z-direction are higher, which makes ligands more difficult to bond.

[d-orbitals and their associated Jahn-Teller Distortion](#)

<b>d<sup>1</sup></b> (Compression)	<b>d<sup>2</sup></b> (Elongation)	<b>d<sup>3</sup></b> (No Jahn-Teller Distortion)

<b>d<sup>4</sup> Low-spin</b> (Compression)	<b>d<sup>4</sup> High-spin</b> (Must distort but cannot specify whether it is elongated or compressed.)	<b>d<sup>5</sup> Low-spin</b> (Elongation)	<b>d<sup>5</sup> High-spin</b> (No Jahn-Teller Distortion)

<b>d<sup>6</sup> Low-spin</b> (No Jahn-Teller Distortion)	<b>d<sup>6</sup> High-spin</b> (Compression)	<b>d<sup>7</sup> Low-spin</b> (Must distort but cannot specify whether it is elongated or compressed.)	<b>d<sup>7</sup> High-spin</b> (Elongation)

<b>d<sup>8</sup></b> (No Jahn-Teller Distortion)	<b>d<sup>9</sup></b> (Must distort but cannot specify whether it is elongated or compressed.)	<b>d<sup>10</sup></b> (No Jahn-Teller Distortion)

## The Strength of Jahn-Teller Distortion

## General Strength Trend of Jahn-Teller Distortion

For octahedral complexes:

- weak Jahn-Teller effect if  $t_{2g}$  is unevenly occupied
- strong Jahn-Teller effect if  $e_g$  is unevenly occupied

Table of Jahn-Teller Distortion Strength<sup>[6]</sup>

Number of d-electrons	1	2	3	4	5	6	7	8	9	10
High-spin	w	w	-	s	-	w	w	-	s	-
Low-spin	w	w	-	w	w	-	s	-	s	-

Figure 8.3.1.4: The table of d-orbitals Jahn-Teller distortion strength w = weak Jahn-Teller effect expected; s = strong Jahn-Teller effect expected; - = no Jahn-Teller distortion

## Jahn-Teller Distortion and Spectra

### Spectra of the First-order Jahn-Teller Distortion

In the first-order Jahn-Teller distortion, two electron transitions can be observed. This phenomenon can lead to a “double-hump” result on the absorption spectra as shown in Figure 8.3.1.5 and 8.3.1.6

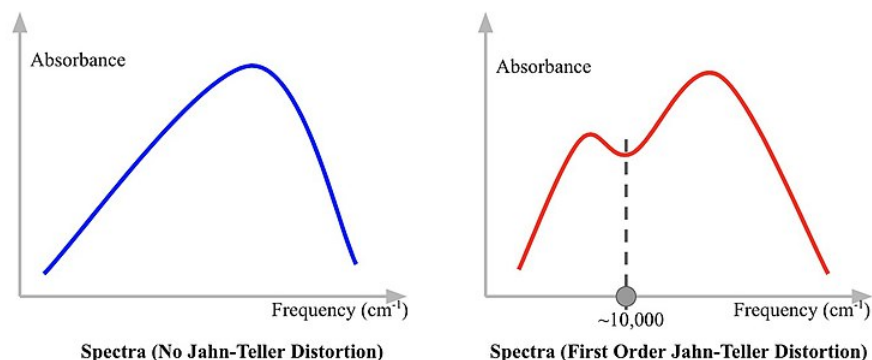


Figure 8.3.1.5: The absorption spectra of a first-order Jahn-Teller distortion

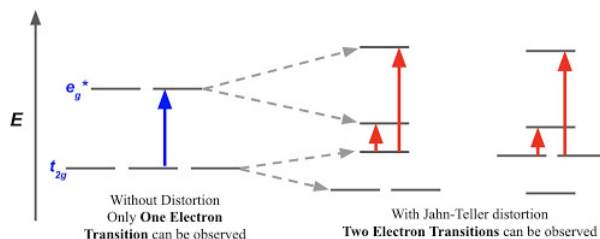


Figure 8.3.1.6: The electron transition in non-distorted (left) and distorted (right) orbitals

## The Second-order Jahn-Teller Distortion

### A brief introduction to the Second-order Jahn-Teller Distortion

The second order Jahn-Teller distortion occurs when the excited state of the transition metal has unequal occupation of d-orbitals with identical energies.<sup>[7]</sup> The ground state of the transition metal may not have unequal occupation of degenerate orbitals, therefore, the second order Jahn-Teller distortion is also called Pseudo Jahn-Teller distortion as shown in Figure 8.3.1.7.<sup>[8]</sup>

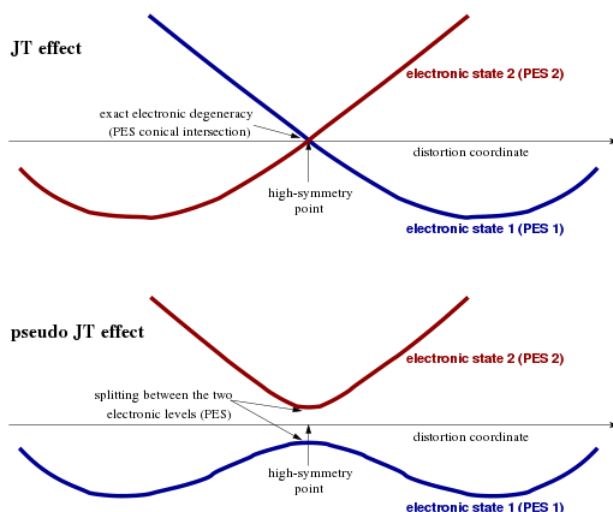


Figure 8.3.1.7: Energy profiles in a Pseudo Jahn-Teller distortion versus the Jahn-Teller distortion

### Spectra of the Second-order Jahn-Teller Distortion

Since the second order Jahn-Teller distortion occurs in excited state, the trough on the spectra likely located at higher frequency, thus higher in energy, as shown in Figure 8.3.1.8

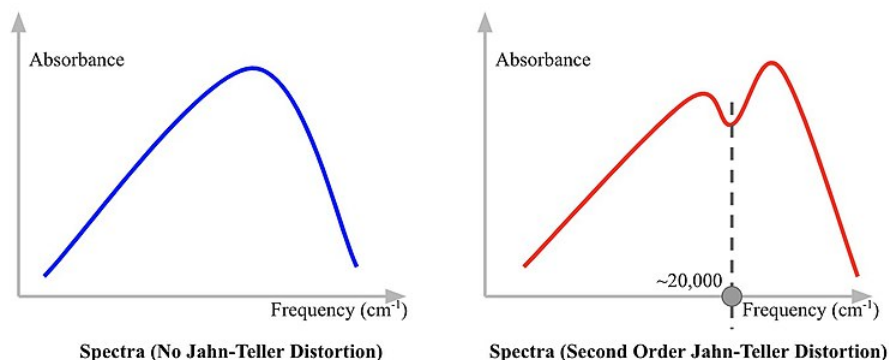


Figure 8.3.1.8: The absorption spectra of a second-order Jahn-Teller distortion

**Figure 8.3.1.8.**

### References

1. Libretexts. "Jahn-Teller Distortions." Chemistry LibreTexts, Libretexts, 23 Apr. 2019,
2. Libretexts. "5.7: Jahn-Teller Effect." *Chemistry LibreTexts*, Libretexts, 23 Apr. 2019
3. Libretexts. "Jahn-Teller Distortions." *Chemistry LibreTexts*, Libretexts, 23 Apr. 2019
4. "Jahn-Teller Effect." Wikipedia, Wikimedia Foundation, 7 Mar. 2019
5. Libretexts. "Jahn-Teller Distortions." Chemistry LibreTexts, Libretexts, 23 Apr. 2019
6. Miessler, Gary L., et al. *Inorganic Chemistry*. Pearson, 2014.
7. Bersuker, Isaac B. (9 January 2013). "Pseudo-Jahn-Teller Effect—A Two-State Paradigm in Formation, Deformation, and Transformation of Molecular Systems and Solids". *Chemical Reviews*. American Chemical Society (ACS). 113 (3): 1351–1390. doi:10.1021/cr300279n. ISSN 0009-2665.
8. "File:Jahn-Teller and Pseudo Jahn-Teller Effects.svg." File:Jahn-Teller and Pseudo Jahn-Teller Effects.svg - Wikimedia Commons

This page titled [8.3.1: Jahn-Teller Distortions](#) is shared under a [CC BY-SA 4.0](#) license and was authored, remixed, and/or curated by [Wikipedia](#) via [source content](#) that was edited to the style and standards of the LibreTexts platform.

- **1.17: Jahn-Teller Distortions** by Wikipedia is licensed [CC BY-SA 4.0](#). Original source: [https://en.wikibooks.org/wiki/Advanced\\_Inorganic\\_Chemistry](https://en.wikibooks.org/wiki/Advanced_Inorganic_Chemistry).

## 8.3.2: Magnetism

Movement of an electrical charge (which is the basis of electric currents) generates a magnetic field in a material. Magnetism is therefore a characteristic property of all materials that contain electrically charged particles and for most purposes can be considered to be entirely of electronic origin.

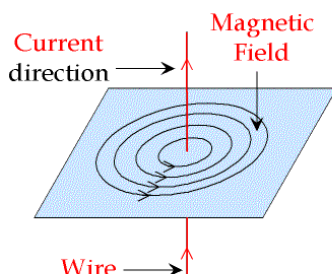


Figure 8.3.2.1: The Right Hand Rule for an induced magnetic field

In an atom, the magnetic field is due to the coupled spin and orbital magnetic moments associated with the motion of electrons. The spin magnetic moment is due to the precession of the electrons about their own axes whereas the orbital magnetic moment is due to the motion of electrons around the nucleus. The resultant combination of the spin and orbital magnetic moments of the constituent atoms of a material gives rise to the observed magnetic properties.

Historically, magnetism has been recognized for thousands of years. An account, that is probably apochryphal, tells of a shepherd called Magnes in Crete who around 900 B.C discovered the naturally occurring magnet lodestone (a form of the the spinel magnetite,  $\text{Fe}_3\text{O}_4$ ) in a region later named Magnesia. Supposedly while he was walking over a deposit, the lodestone pulled the nails out of his sandals and the metal tip from his staff.

### The Classical Theory of Magnetism

The classical theory of magnetism was well developed before quantum mechanics. [Lenz's Law](#) states that when a substance is placed within a magnetic field,  $H$ , the field within the substance,  $B$ , differs from  $H$  by the induced field,  $4\pi I$ , which is proportional to the intensity of magnetization,  $I$ . That is;

$$B = H + 4\pi I \quad (8.3.2.1)$$

where  $B$  is the magnetic field within the substance and  $H$  is the applied magnetic field and  $I$  is the intensity of magnetization

#### Lenz's Law (1834)

Lenz's Law can also be written as

$$\frac{B}{H} = 1 + \frac{4\pi I}{H} \quad (8.3.2.2)$$

or

$$\frac{B}{H} = 1 + 4\pi\kappa \quad (8.3.2.3)$$

where

- $B/H$  is called the magnetic permeability of the material and
- $\kappa$  is the magnetic susceptibility per unit volume, ( $I/H$ )

By definition,  $\kappa$  in a vacuum is zero, so under those conditions the equation would reduce to  $B = H$ . It is usually more convenient to measure mass than volume and the mass susceptibility,  $\chi_g$ , is related to the volume susceptibility,  $\kappa$ , through the density.

$$\chi_g = \frac{\kappa}{\rho} \quad (8.3.2.4)$$



where  $\rho$  is the density.

Finally to get our measured quantity on a basis that can be related to atomic properties, we convert to molar susceptibility

$$\chi_m = \chi_g \times RMM \quad (8.3.2.5)$$

Since this value includes the underlying diamagnetism of paired electrons, it is necessary to correct for the diamagnetic portion of  $\chi_m$  to get a corrected paramagnetic susceptibility.

$$\chi'_m = \chi_m + \chi_{dia} \quad (8.3.2.6)$$

Examples of these corrections are tabulated below.

Table 8.3.2.1: Table of Diamagnetic Corrections (Pascal's constants,  $10^{-6}$  c.g.s. units)

Ion	DC	Ion	DC
Na <sup>+</sup>	6.8	Co <sup>2+</sup>	12.8
K <sup>+</sup>	14.9	Co <sup>3+</sup>	12.8
NH <sub>4</sub> <sup>+</sup>	13.3	Ni <sup>2+</sup>	12.8
Hg <sup>2+</sup>	40	VO <sup>2+</sup>	12.5
Fe <sup>2+</sup>	12.8	Mn <sup>3+</sup>	12.5
Fe <sup>3+</sup>	12.8	Cr <sup>3+</sup>	12.5
Cu <sup>2+</sup>	12.8	Cl <sup>-</sup>	23.4
Br <sup>-</sup>	34.6	SO <sub>4</sub> <sup>2-</sup>	40.1
I <sup>-</sup>	50.6	OH <sup>-</sup>	12
NO <sub>3</sub> <sup>-</sup>	18.9	C <sub>2</sub> O <sub>4</sub> <sup>2-</sup>	34
ClO <sub>4</sub> <sup>-</sup>	32	OAc <sup>-</sup>	31.5
IO <sub>4</sub> <sup>-</sup>	51.9	pyr	49.2
CN <sup>-</sup>	13	Me-pyr	60
NCS <sup>-</sup>	26.2	Acac <sup>-</sup>	62.5
H <sub>2</sub> O	13	en	46.3
EDTA <sup>4-</sup>	~150	urea	33.4

these can be converted to S.I units of  $\text{m}^3 \text{mol}^{-1}$  by multiplying by  $4 \pi \times 10^{-7}$

There are numerous methods for measuring magnetic susceptibilities, including, the **Gouy, Evans and Faraday methods**. These all depend on measuring the force exerted upon a sample when it is placed in a magnetic field. The more paramagnetic the sample, the more strongly it will be drawn toward the more intense part of the field.

### Determination of Magnetic Susceptibility

- **The Gouy Method:** The underlying theory of the Gouy method is described here and a form for calculating the magnetic moment from the collected data is available as well.
- **The Evans method:** The Evans balance measures the change in current required to keep a pair of suspended magnets in place or balanced after the interaction of the magnetic field with the sample. The Evans balance differs from that of the Gouy in that, in the former the permanent magnets are suspended and the position of the sample is kept constant while in the latter the position of the magnet is constant and the sample is suspended between the magnets.

### Orbital contribution to magnetic moments

From a quantum mechanics viewpoint, the magnetic moment is dependent on both spin and orbital angular momentum contributions. The spin-only formula used last year was given as:

$$\mu_{s.o.} = \sqrt{4S(S+1)} \quad (8.3.2.7)$$

and this can be modified to include the orbital angular momentum

$$\mu_{S+L} = \sqrt{4S(S+1) + L(L+1)} \quad (8.3.2.8)$$

An orbital angular momentum contribution is expected when the ground term is triply degenerate (i.e. a triplet state). These show temperature dependence as well.

In order for an electron to contribute to the orbital angular momentum the orbital in which it resides must be able to transform into an exactly identical and degenerate orbital by a simple rotation (it is the rotation of the electrons that induces the orbital contribution). For example, in an octahedral complex the degenerate  $t_{2g}$  set of orbitals ( $d_{xz}, d_{yx}, d_{yz}$ ) can be interconverted by a  $90^\circ$  rotation. However the orbitals in the  $e_g$  subset ( $d_{z^2}, d_{x^2-y^2}$ ) cannot be interconverted by rotation about any axis as the orbital shapes are different; therefore an electron in the  $e_g$  set does not contribute to the orbital angular momentum and is said to be quenched. In the free ion case the electrons can be transformed between any of the orbitals as they are all degenerate, but there will still be partial orbital quenching as the orbitals are not identical.

Electrons in the  $t_{2g}$  set do not always contribute to the orbital angular momentum. For example in the  $d^3, t_{2g}^3$  case, an electron in the  $d_{xz}$  orbital cannot by rotation be placed in the  $d_{yz}$  orbital as the orbital already has an electron of the same spin. This process is also called quenching.

Tetrahedral complexes can be treated in a similar way with the exception that we fill the  $e$  orbitals first, and the electrons in these do not contribute to the orbital angular momentum. The tables in the links below give a list of all  $d^1$  to  $d^9$  configurations including high and low spin complexes and a statement of whether or not a direct orbital contribution is expected.

- Octahedral complexes
- Tetrahedral complexes

### Contributors and Attributions

- [Prof. Robert J. Lancashire](#) (The Department of Chemistry, University of the West Indies)

---

8.3.2: Magnetism is shared under a [not declared](#) license and was authored, remixed, and/or curated by LibreTexts.

### 8.3.3: Magnetic Moments of Transition Metals

Magnetic moments are often used in conjunction with electronic spectra to gain information about the oxidation number and stereochemistry of the central metal ion in coordination complexes. A common laboratory procedure for the determination of the magnetic moment for a complex is the Gouy method which involves weighing a sample of the complex in the presence and absence of a magnetic field and observing the difference in weight. A template is provided for the calculations involved.

For first row transition metal ions in the free ion state, i.e. isolated ions in a vacuum, all 5 of the 3d orbitals are degenerate.

A simple crystal field theory approach to the bonding in these ions assumes that when they form octahedral complexes, the energy of the d orbitals are no longer degenerate but are split such that two orbitals, the  $d_{x^2-y^2}$  and the  $d_{z^2}$  ( $e_g$  subset) are at higher energy than the  $d_{xy}$ ,  $d_{xz}$ ,  $d_{yz}$  orbitals (the  $t_{2g}$  subset).

For octahedral ions with between 4 and 7 d electrons, this gives rise to 2 possible arrangements called either high spin/weak field or low spin/strong field respectively. The energy gap is dependent on the position of the coordinated ligands in the SPECTROCHEMICAL SERIES.

#### Note

A good starting point is to assume that all Co(III),  $d^6$  complexes are octahedral and LOW spin, i.e.  $t_{2g}^6$ .

In tetrahedral complexes, the energy levels of the orbitals are again split, such that the energy of two orbitals, the  $d_{x^2-y^2}$  and the  $d_{z^2}$  ( $e$  subset) are now at lower energy (more favored) than the remaining three  $d_{xy}$ ,  $d_{xz}$ ,  $d_{yz}$  (the  $t_2$  subset) which are destabilized.

*Tetrahedral complexes are ALL high spin since the difference between the 2 subsets of energies of the orbitals is much smaller than is found in octahedral complexes.*

The usual relationship quoted between them is:

$$\Delta_{tet} \approx \frac{4}{9} \Delta_{oct}$$

Square planar complexes are less common than tetrahedral and  $d^8$  e.g. Ni(II), Pd(II), Pt(II), etc, have a strong propensity to form square planar complexes. As with octahedral complexes, the energy gap between the  $d_{xy}$  and  $d_{x^2-y^2}$  is  $\Delta_{oct}$  and these are considered strong field / low spin hence they are all diamagnetic,  $\mu=0$  Bohr Magnetons (B.M.)

The formula used to calculate the spin-only magnetic moment can be written in two forms; the first based on the number of unpaired electrons,  $n$ , and the second based on the electron spin quantum number,  $S$ . Since for each unpaired electron,  $n = 1$  and  $S = 1/2$  then the two formulae are clearly related and the answer obtained must be identical.

$$\mu_{so} = \sqrt{n(n+2)}$$

$$\mu_{so} = \sqrt{4S(S+1)}$$

Comparison of calculated spin-only magnetic moments with experimental data for some octahedral complexes

Ion	Config	$\mu_{so}$ / B.M.	$\mu_{obs}$ / B.M.
Ti(III)	$d^1 (t_{2g}^1)$	$\sqrt{3} = 1.73$	1.6-1.7
V(III)	$d^2 (t_{2g}^2)$	$\sqrt{8} = 2.83$	2.7-2.9
Cr(III)	$d^3 (t_{2g}^3)$	$\sqrt{15} = 3.88$	3.7-3.9
Cr(II)	$d^4$ high spin ( $t_{2g}^3 e_g^1$ )	$\sqrt{24} = 4.90$	4.7-4.9
Cr(II)	$d^4$ low spin ( $t_{2g}^4$ )	$\sqrt{8} = 2.83$	3.2-3.3
Mn(II)/ Fe(III)	$d^5$ high spin ( $t_{2g}^3 e_g^2$ )	$\sqrt{35} = 5.92$	5.6-6.1
Mn(II)/ Fe(III)	$d^5$ low spin ( $t_{2g}^5$ )	$\sqrt{3} = 1.73$	1.8-2.1
Fe(II)	$d^6$ high spin ( $t_{2g}^4 e_g^2$ )	$\sqrt{24} = 4.90$	5.1-5.7

Ion	Config	$\mu_{so}$ / B.M.	$\mu_{obs}$ / B.M.
Co(III)	$d^6$ low spin ( $t_{2g}^6$ )	0	0
Co(II)	$d^7$ high spin ( $t_{2g}^5 e_g^2$ )	$\sqrt{15} = 3.88$	4.3-5.2
Co(II)	$d^7$ low spin ( $t_{2g}^6 e_g^1$ )	$\sqrt{3} = 1.73$	1.8
Ni(II)	$d^8$ ( $t_{2g}^6 e_g^2$ )	$\sqrt{8} = 2.83$	2.9-3.3
Cu(II)	$d^9$ ( $t_{2g}^6 e_g^3$ )	$\sqrt{3} = 1.73$	1.7-2.2

Comparison of calculated spin-only magnetic moments with experimental data for some tetrahedral complexes

Ion	Config	$\mu_{so}$ / B.M.	$\mu_{obs}$ / B.M.
Cr(V)	$d^1$ ( $e^1$ )	$\sqrt{3} = 1.73$	1.7-1.8
Cr(IV) / Mn(V)	$d_2$ ( $e^2$ )	$\sqrt{8} = 2.83$	2.6 - 2.8
Fe(V)	$d^3$ ( $e^2 t_2^1$ )	$\sqrt{15} = 3.88$	3.6-3.7
-	$d^4$ ( $e^2 t_2^2$ )	$\sqrt{24} = 4.90$	-
Mn(II)	$d^5$ ( $e^2 t_2^3$ )	$\sqrt{35} = 5.92$	5.9-6.2
Fe(II)	$d^6$ ( $e^3 t_2^3$ )	$\sqrt{24} = 4.90$	5.3-5.5
Co(II)	$d^7$ ( $e^4 t_2^3$ )	$\sqrt{15} = 3.88$	4.2-4.8
Ni(II)	$d^8$ ( $e^4 t_2^4$ )	$\sqrt{8} = 2.83$	3.7-4.0
Cu(II)	$d^9$ ( $e^4 t_2^5$ )	$\sqrt{3} = 1.73$	-

## Contributors and Attributions





- [Prof. Robert J. Lancashire](#) (The Department of Chemistry, University of the West Indies)

8.3.3: Magnetic Moments of Transition Metals is shared under a [CC BY-NC-SA 4.0](#) license and was authored, remixed, and/or curated by LibreTexts.

- [Magnetic Moments of Transition Metals](#) is licensed [CC BY-NC-SA 4.0](#).

### 8.3.4: Ferro-, Ferri- and Antiferromagnetism

The magnetism of metals and other materials are determined by the orbital and spin motions of the unpaired electrons and the way in which unpaired electrons align with each other. All magnetic substances are **paramagnetic** at sufficiently high temperature, where the thermal energy ( $kT$ ) exceeds the interaction energy between spins on neighboring atoms. Below a certain critical temperature, spins can adopt different kinds of ordered arrangements.

<b>Ferromagnetic</b> 	Below $T_C$ , spins are aligned parallel in magnetic domains
<b>Antiferromagnetic</b> 	Below $T_N$ , spins are aligned antiparallel in magnetic domains
<b>Ferrimagnetic</b> 	Below $T_C$ , spins are aligned antiparallel but do not cancel
<b>Paramagnetic</b> 	Spins are randomly oriented (any of the others above $T_C$ or $T_N$ )

A pictorial description of the ordering of spins in ferromagnetism, antiferromagnetism, ferrimagnetism, and paramagnetism

Let's begin by considering an individual atom in the bcc structure of iron metal. Fe is in group VIIIb of the periodic table, so it has eight valence electrons. The atom is promoted to the  $4s^13d^7$  state in order to make bonds. A localized picture of the d-electrons for an individual iron atom might look like this:



Since each unpaired electron has a spin moment of  $1/2$ , the total spin angular momentum,  $S$ , for this atom is:

$$S = 3 \frac{1}{2} = \frac{3}{2} \text{ (in units of } h/2\pi \text{)}$$

We can think of each Fe atom in the solid as a little bar magnet with a spin-only moment  $S$  of  $3/2$ . The spin moments of neighboring atoms can align in parallel ( $\uparrow \uparrow$ ), antiparallel ( $\uparrow \downarrow$ ), or random fashion. In bcc Fe, the tendency is to align parallel because of the positive sign of the exchange interaction. This results in **ferromagnetic** ordering, in which all the spins within a magnetic domain (typically hundreds of unit cells in width) have the same orientation, as shown in the figure at the right. Conversely, a negative exchange interaction between neighboring atoms in bcc Cr results in **antiferromagnetic** ordering. A third arrangement, **ferrimagnetic** ordering, results from an antiparallel alignment of spins on neighboring atoms when the magnetic moments of the neighbors are unequal. In this case, the spin moments do not cancel and there is a net magnetization. The ordering mechanism is like that of an antiferromagnetic solid, but the magnetic properties resemble those of a ferromagnet. Ferrimagnetic ordering is most common in metal oxides, as we will learn in Chapter 7.

#### Magnetization and susceptibility

The **magnetic susceptibility**,  $\chi$ , of a solid depends on the ordering of spins. Paramagnetic, ferromagnetic, antiferromagnetic, and ferrimagnetic solids all have  $\chi > 0$ , but the magnitude of their susceptibility varies with the kind of ordering and with temperature. We will see these kinds of magnetic ordering primarily among the **3d** and **4f** elements and their alloys and compounds. For example, Fe, Co, Ni,  $\text{Nd}_2\text{Fe}_{14}\text{B}$ ,  $\text{SmCo}_5$ , and  $\text{YCo}_5$  are all ferromagnets, Cr and MnO are antiferromagnets, and  $\text{Fe}_3\text{O}_4$  and  $\text{CoFe}_2\text{O}_4$  are ferrimagnets. Diamagnetic compounds have a weak *negative* susceptibility ( $\chi < 0$ ).

## Definitions

- $H$  = applied magnetic field (units: Henry (H))
- $B$  = induced magnetic field in a material (units: Tesla (T))
- $M$  = magnetization, which represents the magnetic moments within a material in the presence of an external field  $H$ .

Magnetic susceptibility  $\chi = M/H$

Usually,  $\chi$  is given in *molar* units in the *cgs* system:

$\chi_M$  = molar susceptibility (units:  $\text{cm}^3/\text{mol}$ )

Typical values of  $\chi_M$ :

Compound	Type of Magnetism	$\chi$ at 300K ( $\text{cm}^3/\text{mol}$ )
$\text{SiO}_2$	Diamagnetic	$-3 \times 10^{-4}$
Pt metal	Pauli paramagnetic	$+2 \times 10^{-4}$
$\text{Gd}_2(\text{SO}_4)_3 \cdot 8\text{H}_2\text{O}$	Paramagnetic	$+5 \times 10^{-2}$
Ni-Fe alloy	Ferromagnetic	$+10^4 - 10^6$

To correlate  $\chi$  with the number of unpaired electrons in a compound, we first correct for the small diamagnetic contribution of the core electrons:

$$\chi^{corr} = \chi^{obs} - \chi^{diamagnetic\ cores} \quad (8.3.4.1)$$

## Susceptibility of paramagnets

For a paramagnetic substance,

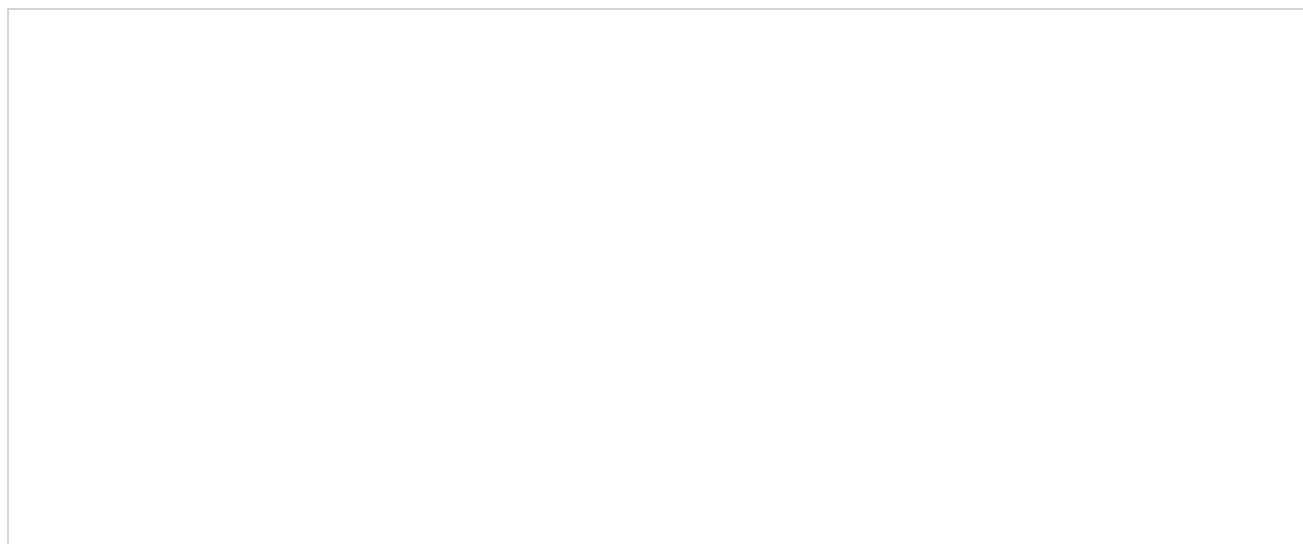
$$\chi_M^{corr} = \frac{C}{T} \quad (8.3.4.2)$$

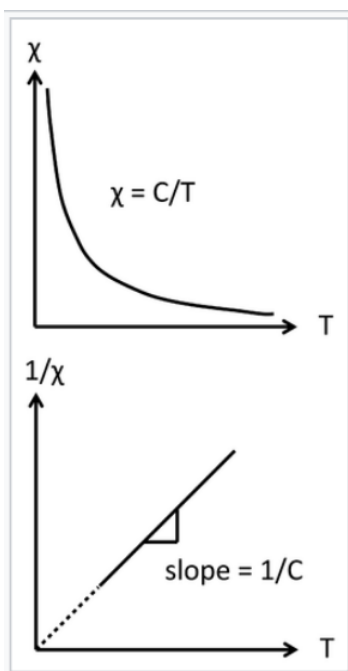
The inverse relationship between the magnetic susceptibility and  $T$ , the absolute temperature, is called **Curie's Law**, and the proportionality constant  $C$  is the **Curie constant**:

$$C = \frac{N_A}{3k_B} \mu_{eff}^2 \quad (8.3.4.3)$$

Note that  $C$  is not a "constant" in the usual sense, because it depends on  $\mu_{eff}$ , the **effective magnetic moment** of the molecule or ion, which in turn depends on its number of unpaired electrons:

$$\mu_{eff} = \sqrt{n(n+2)} \mu_B \quad (8.3.4.4)$$





Curie law behavior of a paramagnet. A plot of  $1/\chi$  vs. absolute temperature is a straight line, with a slope of  $1/C$  and an intercept of zero.

Here  $\mu_B$  is the Bohr magneton, a physical constant defined as  $\mu_B = eh/4\pi m_e = 9.274 \times 10^{-21}$  erg/gauss (in cgs units).

In cgs units, we can combine physical constants,

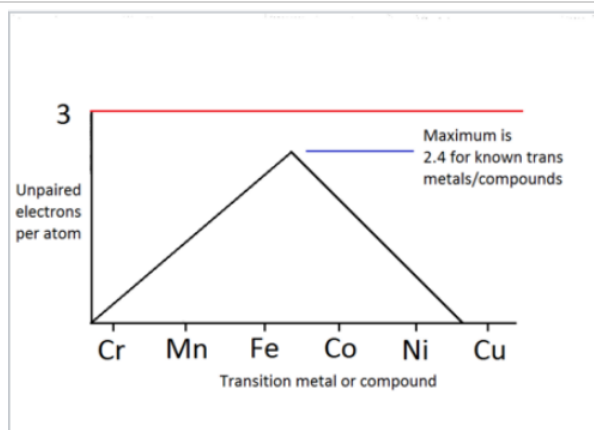
$$\frac{N_A}{3k_B} \mu_B^2 = .125 \quad (8.3.4.5)$$

Combining these equations, we obtain

$$\chi_M^{corr} = \frac{.125}{T} \left( \frac{\mu_{eff}}{\mu_B} \right)^2 \quad (8.3.4.6)$$

These equations relate the molar susceptibility, a bulk quantity that can be measured with a magnetometer, to  $\mu_{eff}$ , a quantity that can be calculated from the number of unpaired electrons,  $n$ . Two important points to note about this formula are:

- The magnetic susceptibility is inversely proportional to the absolute temperature, with a proportionality constant  $C$  (Curie's Law)
- So far we are talking only about paramagnetic substances, where there is no interaction between neighboring atoms.



Number of unpaired electrons per atom, determined from Curie constants of transition metals and their 1:1 alloys.

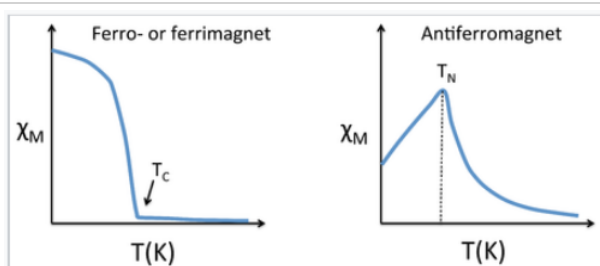
Returning to the isolated Fe atom with its three unpaired electrons, we can measure the Curie constant for iron metal (above the temperature of its transition to a paramagnetic solid) and compare it to the calculation of  $\mu_{eff}$ . Since  $n = 3$ , we calculate:

$$\mu_{eff} = \sqrt{(3)(5)}\mu_B = 3.87\mu_B \quad (8.3.4.7)$$

The plot at the right shows the number of unpaired electrons per atom, calculated from measured Curie constants, for the magnetic elements and 1:1 alloys in the 3d series. The plot peaks at a value of 2.4 spins per atom, slightly lower than we calculated for an isolated iron atom. This reflects the fact that there is some pairing of d-electrons, i.e., that they do contribute somewhat to bonding in this part of the periodic table.

### Susceptibility of ferro-, ferri-, and antiferromagnets

Below a certain critical temperature, the spins of a solid paramagnetic substance order and the susceptibility deviates from simple Curie-law behavior. Because the ordering depends on the short-range exchange interaction, this critical temperature varies widely. Metals and alloys in the 3d series tend to have high critical temperatures because the atoms are directly bonded to each other and the interaction is strong. For example, Fe and Co have critical temperatures (also called the Curie temperature,  $T_C$ , for ferromagnetic substances) of 1043 and 1400 K, respectively. The Curie temperature is determined by the strength of the magnetic exchange interaction and by the number of unpaired electrons per atom. The number of unpaired electrons peaks between Fe and Co as the d-band is filled, and the exchange interaction is stronger for Co than for Fe. In contrast to ferromagnetic metals and alloys, paramagnetic salts of transition metal ions typically have critical temperatures below 1K because the magnetic ions are not directly bonded to each other and thus their spins are very weakly coupled in the solid state. For example, in gadolinium sulfate, the paramagnetic  $Gd^{3+}$  ions are isolated from each other by  $SO_4^{2-}$  ions.



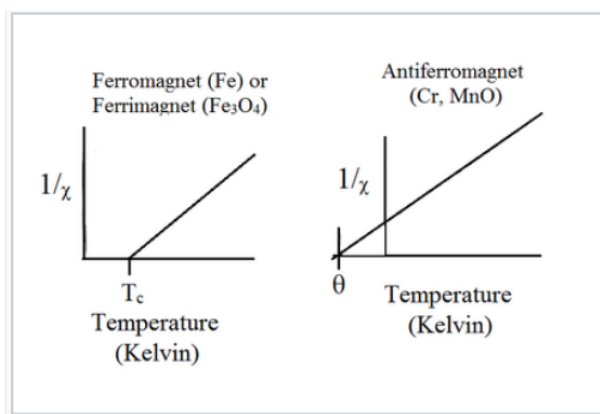
Magnetic susceptibility vs temperature (Kelvin) for ferrimagnetic, ferromagnetic, and antiferromagnetic materials

Above the critical temperature  $T_C$ , **ferromagnetic** compounds become paramagnetic and obey the **Curie-Weiss law**:

$$\chi = \frac{C}{T - T_c} \quad (8.3.4.8)$$

This is similar to the Curie law, except that the plot of  $1/\chi$  vs.  $T$  is shifted to a positive intercept  $T_C$  on the temperature axis. This reflects the fact that ferromagnetic materials (in their paramagnetic state) have a greater tendency for their spins to align in a magnetic field than an ordinary paramagnet in which the spins do not interact with each other. Ferrimagnets follow the same kind of ordering behavior. Typical plots of  $\chi$  vs.  $T$  and  $1/\chi$  vs.  $T$  for ferro-/ferrimagnets are shown above and below.





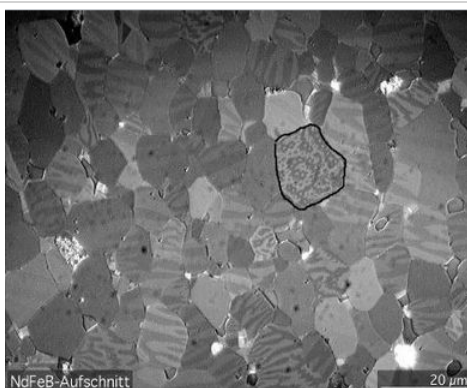
Plots of  $1/\chi$  vs.  $T$  for ferromagnets, ferrimagnets, and antiferromagnets.

**Antiferromagnetic** solids are also paramagnetic above a critical temperature, which is called the Néel temperature,  $T_N$ . For antiferromagnets,  $\chi$  reaches a maximum at  $T_N$  and is smaller at higher temperature (where the paramagnetic spins are further disordered by thermal energy) and at lower temperature (where the spins pair up). Typically, antiferromagnets retain some positive susceptibility even at very low temperature because of canting of their paired spins. However the maximum value of  $\chi$  is much lower for an antiferromagnet than it is for a ferro- or ferrimagnet. The Curie-Weiss law is also modified for an antiferromagnet, reflecting the tendency of spins (in the paramagnetic state above  $T_N$ ) to resist parallel ordering. A plot of  $1/\chi$  vs.  $T$  intercepts the temperature axis at a negative temperature,  $-\theta$ , and the Curie-Weiss law becomes:

$$\chi = \frac{C}{T + \theta} \quad (8.3.4.9)$$

### Ordering of spins below $T_C$

Below  $T_C$ , the spins align spontaneously in ferro- and ferrimagnets. Complex magnetization behavior is observed that depends on the history of the sample. For example, if a ferromagnetic material is cooled in the absence of an applied magnetic field, it forms a mosaic structure of magnetic domains that each have internally aligned spins. However, neighboring domains tend to align the opposite way in order to minimize the total energy of the system. This is illustrated in the figure at the left for a Nd-Fe-B magnet. The sample consists of 5-10  $\mu\text{m}$  wide crystal grains that can be easily distinguished by the sharp boundaries in the image. Within each grain are a series of lighter and darker stripes (imaged by using the optical Kerr effect) that are ferromagnetic domains with opposite orientations. Averaged over the whole sample, these domains have random orientation so the net magnetization is zero.



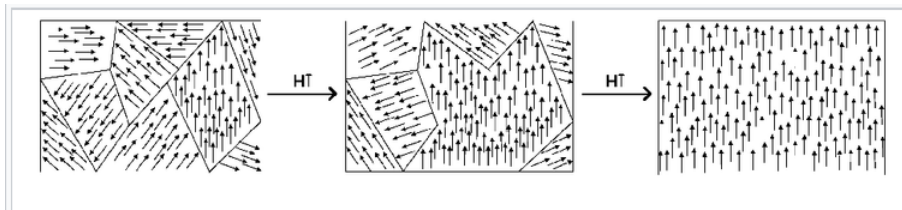
Microcrystalline grains within a piece of  $\text{Nd}_2\text{Fe}_{14}\text{B}$  (the alloy used in neodymium magnets) with magnetic domains made visible with a Kerr microscope. The domains are the light and dark stripes visible within each grain.

When a sample like this one is magnetized (i.e., exposed to a strong magnetic field), the domain walls move and the favorably aligned domains grow at the expense of those with the opposite orientation. This transformation can be seen in real time in the Kerr microscope. The domain walls are typically hundreds of atoms wide, so movement of a domain wall involves a cooperative tilting of spin orientation (analogous to "the wave" in a sports stadium) and is a relatively low energy process.



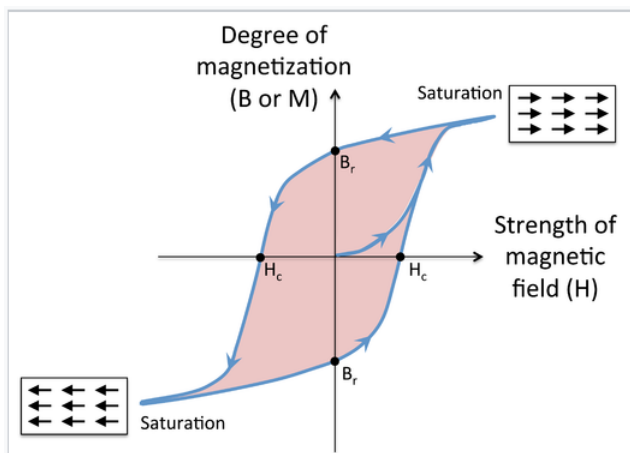
The movement of domain walls in a grain of silicon steel is driven in this movie by increasing the external magnetic field in the "downward" direction, and is imaged using a Kerr microscope. White areas are domains with their magnetization directed up, dark areas - which eventually comprise the entire grain - are domains with their magnetization directed down.

The process of magnetization moves the solid away from its lowest energy state (random domain orientation), so magnetization involves input of energy. When the external magnetic field is removed, the domain walls relax somewhat, but the solid (especially in the case of a "hard" magnet) can retain much of its magnetization. If you have ever magnetized a nail or a paper clip by using a permanent magnet, what you were doing was moving the walls of the magnetic domains inside the ferromagnet. The object thereafter retains the "memory" of its magnetization. However, annealing a permanent magnet destroys the magnetization by returning the system to its lowest energy state in which all the magnetic domains cancel each other.



Rotation of orientation and increase in size of magnetic domains in response to an externally applied magnetic field.

**Magnetic hysteresis.** Cycling a ferro- or ferrimagnetic material in a magnetic field results in hysteresis in the magnetization of the material, as shown in the figure at the left. At the beginning, the magnetization is zero, but it begins to rise rapidly as the magnetic field is applied. At high field, the magnetic domains are aligned and the magnetization is said to be saturated. When the field is removed, a certain **remanent magnetization** (indicated as the point  $B_r$  on the graph) is retained, i.e., the material is magnetized. Applying a field in the opposite direction begins to orient the magnetic domains in the other direction, and at a field  $H_c$  (the **coercive field**), the magnetization of the sample is reduced to zero. Eventually the material reaches saturation in the opposite direction, and when the field is removed again, it has remanent magnetization  $B_r$ , but in the opposite direction. As the field continues to reverse, the magnet follows the hysteresis loop as indicated by the arrows. The area of colored region inside the loop is proportional to the magnetic work done in each cycle. When the field cycles rapidly (for example, in the core of a transformer, or in read-write cycles of a magnetic disk) this work is turned into heat.



Magnetization of a ferro- or ferrimagnet vs. applied magnetic field  $H$ . Starting at the origin, the upward curve is the initial magnetization curve. The downward curve after saturation, along with the lower return curve, form the main loop. The intercepts  $H_c$  and  $B_r$  are the coercivity and remanent magnetization.

This page titled [8.3.4: Ferro-, Ferri- and Antiferromagnetism](#) is shared under a [CC BY-SA 4.0](#) license and was authored, remixed, and/or curated by [Chemistry 310 \(Wikibook\)](#) via [source content](#) that was edited to the style and standards of the LibreTexts platform.

- [6.8: Ferro-, Ferri- and Antiferromagnetism](#) by [Chemistry 310](#) is licensed [CC BY-SA 4.0](#). Original source: [https://en.wikibooks.org/wiki/Introduction\\_to\\_Inorganic\\_Chemistry](https://en.wikibooks.org/wiki/Introduction_to_Inorganic_Chemistry).

## 8.4: Ligand Field Theory

---

Learning objectives for this unit are to:

- Identify and classify ligands as s-donor, s-donor/p-donor, and s-donor/p-acceptor based on the type of bonding interaction they can have with a metal atom
  - Derive MO diagrams for  $ML_6$  complexes with s-donor, s-donor/p-donor, and s-donor/p-acceptor ligands
  - Explain why and how sigma-donor, s-donor, s-donor/p-donor, and s-donor/p-acceptor ligands affect the magnitude of  $D_o$
  - Rationalize the spectrochemical series based on ligand field theory
  - Describe the orbital interactions involved in p-backbonding
  - Predict or explain changes in bond length, bond strength, and CO stretching frequencies due to p-backbonding interactions
- 

8.4: Ligand Field Theory is shared under a [not declared](#) license and was authored, remixed, and/or curated by LibreTexts.

## 8.4.1: Ligand Field Theory

### Extension of Crystal Field Theory

Experimentally it is known that the [nature of the ligand](#) plays an important role in the magnitude of the crystal field splitting in metal complexes and can determine whether a complex is high or low spin. Empirically ligands can be ordered in the spectrochemical series, but using crystal field theory we cannot rationalize where ligands fall in the series. For example, why is the neutral CO one of the strongest field ligands in the series while the anionic halogens are weak field ligands? To understand why ligands behave differently we have to consider how ligand orbitals interact with the metal d orbitals. Ligand field theory is essentially a combination between [crystal field theory](#) and [molecular orbital theory](#) where we focus only on the orbital overlap between the metal d orbitals and select ligand orbitals (rather than considering all of the valence orbitals on both the metal and ligand)

### Metal-Ligand $\sigma$ Bonding

The bond between a metal and a ligand is primarily a Lewis acid-base interaction where the ligand is a Lewis base and donates a pair of electron to the metal, the Lewis acid. This interaction forms a [coordinate covalent bond](#). As with molecular orbital theory we have to decide how (or if) the ligand lone pairs will overlap with each of the d orbitals, and what type of bonding will be formed. In an octahedral complex the ligands and their lone pairs lie along the x, y, and z axes. As shown in Figure 8.4.1.1, the two on axis d orbitals ( $d_{x^2-y^2}$  and  $d_{z^2}$ ) have to correct orientation to form sigma bonds with the ligands. With the three off axis d orbitals ( $d_{xy}$ ,  $d_{xz}$ , and  $d_{yz}$ ) the ligand lone pair overlaps with a node in these orbitals (Figure 8.4.1.1c). This means there is no net overlap and no bonding (or antibonding) molecular orbital can be formed.

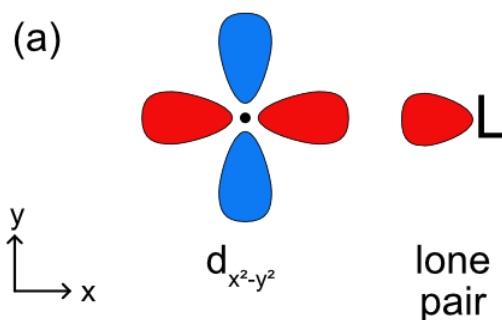


Figure 8.4.1.1a: Overlap between a ligand lone pair orbital and the metal  $d_{x^2-y^2}$  orbital to form a sigma bond (CC BY-NC-SA, Catherine McCusker)

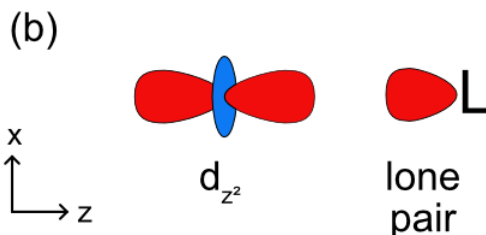


Figure 8.4.1.1b: Overlap between a ligand lone pair orbital and the metal  $d_{z^2}$  orbital to form a sigma bond (CC BY-NC-SA, Catherine McCusker)

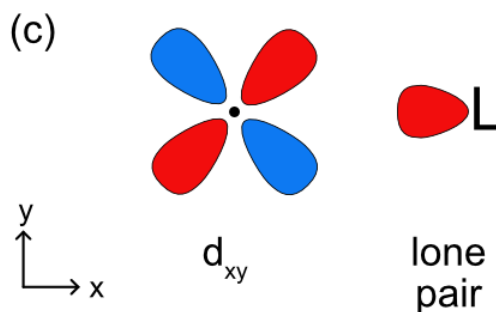


Figure 8.4.1.1c: There is no net overlap between the ligand lone pair orbital and the  $d_{xy}$  metal orbital, so this is a non bonding interaction (CC BY-NC-SA, Catherine McCusker)

Knowing this, we can construct a ligand field splitting diagram (a simplified molecular orbital diagram) (Figure 8.4.1.2). In the free metal ion all 5 of the d orbitals are degenerate and before they interact with the metal all 6 of the ligand lone pair orbitals are at the same energy as well. Generally, based on electronegativity the ligand lone pair orbitals will be lower in energy than the metal d orbitals. When the ligand lone pairs interact with metal d orbitals the on axis set of d orbitals ( $d_{x^2-y^2}$  and  $d_{z^2}$ ) will form sigma bonding ( $e_g$ ) and sigma antibonding ( $e_g^*$ ) molecular orbitals. The off axis set of d orbitals are nonbonding and are not stabilized or destabilized by the ligand lone pairs. Unlike a complete molecular orbital diagrams, a ligand field diagram won't necessarily have the same number of molecular orbitals as atomic orbitals because not every possible bonding interaction is included (for example, any overlap between the ligand orbitals and the metal s and p orbitals are not included). As in crystal field theory we can define an octahedral ligand field splitting energy ( $\Delta_o$ ), which will be the difference between the two molecular orbitals with the most metal d orbital character. In Figure 8.4.1.2 the  $t_{2g}$  set of d orbitals are nonbonding and therefore 100% metal character. The  $e_g$  bonding orbital is closer in energy to the ligand lone pairs and will have a higher % contribution from the ligands, and the  $e_g^*$  antibonding orbital is closer in energy to the metal d orbitals and will have a higher % contribution from the metal. The relevant energy difference is between the  $t_{2g}$  and  $e_g^*$  orbitals, as highlighted in green in Figure 8.4.1.2. The splitting energy will increase as there is a stronger interaction between the metal and ligand orbitals (based on the criteria discussed previously) and the  $e_g^*$  is more destabilized.

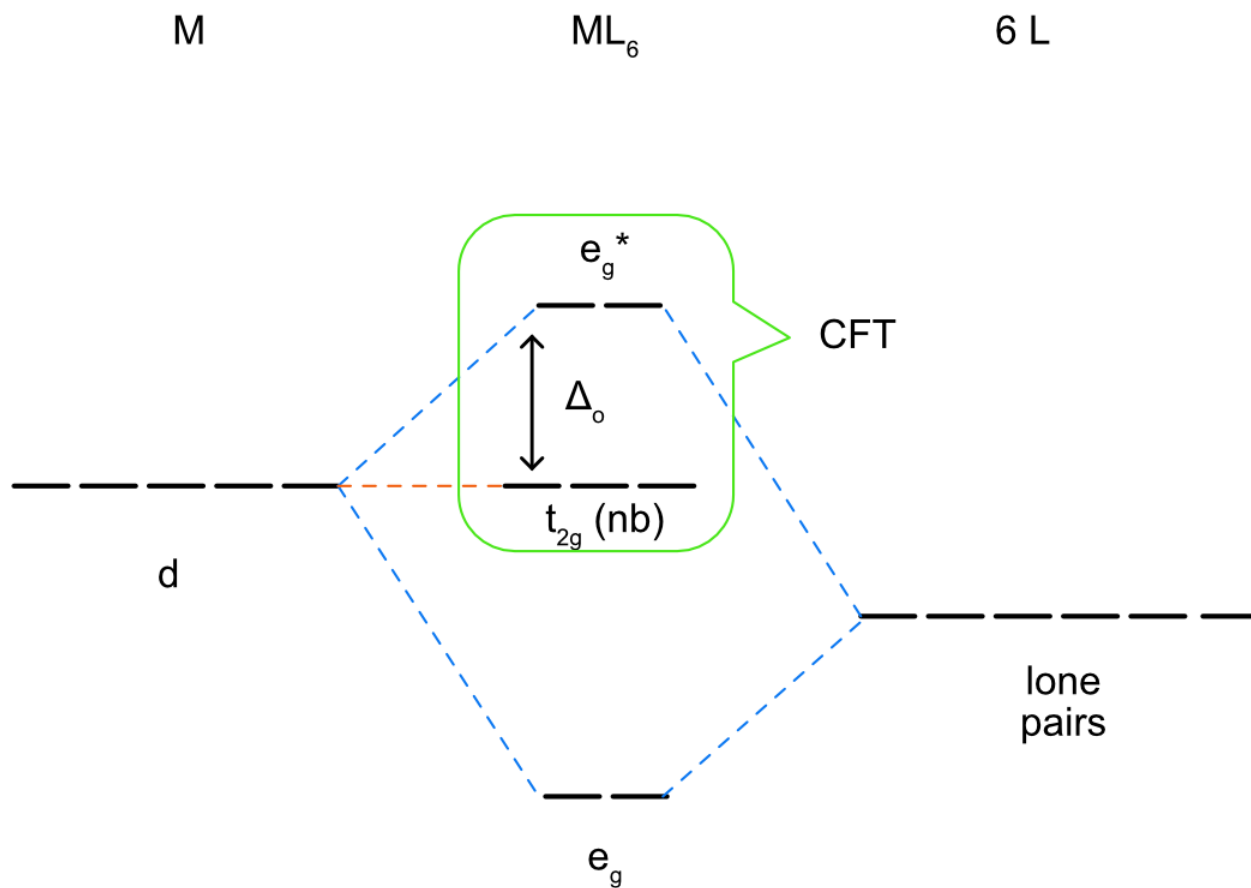


Figure 8.4.1.2: Octahedral ligand field splitting diagram for only sigma bonding. The  $d_{x^2-y^2}$  and  $d_{z^2}$  metal orbitals form sigma bonding ( $e_g$ ) and antibonding molecular orbitals ( $e_g^*$ ). The  $d_{xy}$ ,  $d_{xz}$ , and  $d_{yz}$  orbitals are nonbonding ( $t_{2g}$  (nb)). The green outline highlights the portion of the diagram that is equivalent to the crystal field splitting diagram. (CC BY-NC-SA; Catherine McCusker)

### Metal-Ligand $\pi$ Bonding

In addition to sigma bonding, some ligands have orbitals available which can form  $\pi$  bonds with metals as well. These could include p orbitals on a single donor atom such as a halogen ion or  $\pi$  bonding or antibonding molecular orbitals on a molecular ligand. To determine how  $\pi$  bonding will change the ligand field splitting picture in Figure 8.4.1.2 we will visualize how a ligand p orbital will interact with the metal d orbitals. The  $d_{x^2-y^2}$  and  $d_{z^2}$  orbitals do not have the correct symmetry to form any type of bond with a ligand p orbital as shown in Figures 8.4.1.3a – b. The  $d_{xy}$ ,  $d_{xz}$ , and  $d_{yz}$  orbitals all have the correct symmetry to form  $\pi$  bonds with a ligand p orbital (Figure 8.4.1.3c).

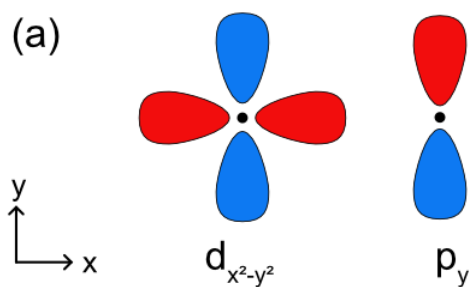


Figure 8.4.1.3a: There is no net overlap between the ligand p orbital and the  $d_{x^2-y^2}$  metal orbital, so this is a non bonding interaction (CC BY-NC-SA, Catherine McCusker)

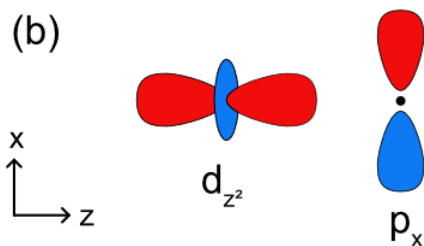


Figure 8.4.1.3b: There is no net overlap between the ligand p orbital and the  $d_{z^2}$  metal orbital, so this is a non bonding interaction (CC BY-NC-SA, Catherine McCusker)

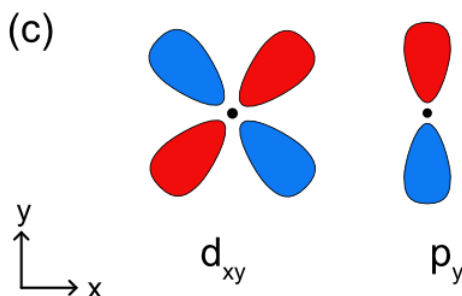


Figure 8.4.1.3c: Overlap between a ligand p orbital and the metal  $d_{xy}$  orbital to form a  $\pi$  bond (CC BY-NC-SA, Catherine McCusker)

Unlike metal-ligand  $\sigma$  bonding, where electrons are always donated from the ligand to the metal, electrons in metal-ligand  $\pi$  bonding can be donated from either the metal or the ligand depending on the nature of the orbitals involved. In cases where ligands have empty p or  $\pi$  symmetry orbitals that are close in energy to the metal d orbitals, they can accept electrons from a filled metal orbital. This is also known as  $\pi$  backbonding because the direction of electron donation is opposite of that found in sigma metal ligand bonding. These ligands are called  $\pi$  acceptor ligands. In cases where ligands have filled p or  $\pi$  symmetry orbitals that are close in energy to the metal d orbitals, they can donate electrons to an empty metal orbital. These ligands are called  $\pi$  donor ligands.

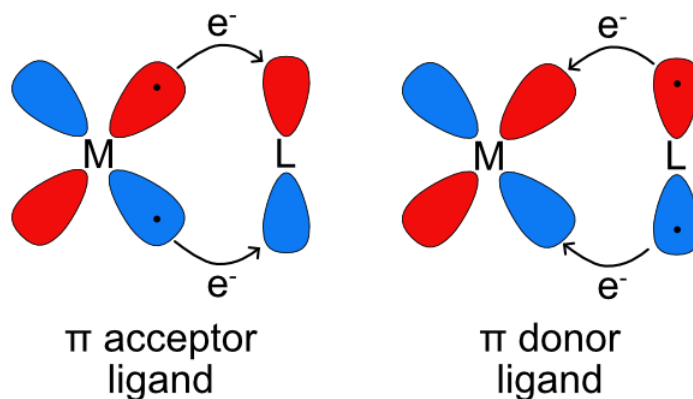


Figure 8.4.1.4: Illustration of metal-ligand  $\pi$  bonding with  $\pi$  acceptor and donor ligands. Filled orbitals are represented with black dots. (CC BY-NC-SA, Catherine McCusker)

### $\pi$ Acceptors

Ligands that are  $\pi$  acceptors have empty, low energy  $\pi$  symmetry orbitals available to accept electrons from the metal center. Most often this is a  $\pi^*$  antibonding molecular orbital but it could also be an empty p orbital. Due to the aufbau principle, these empty orbitals will be higher in energy than any filled lone pairs on the ligands and will also generally be higher energy than the metal d orbitals. Similar to [multiple bonding in main group compounds](#)  $\pi$  bonding always occurs in combination with sigma bonding so in the ligand field splitting diagram of metal-ligand bonding with a  $\pi$  acceptor ligand the lone pairs for sigma bonding must be included as well as the empty orbitals for  $\pi$  bonding. As seen in Figure 8.4.1.3 the  $d_{x^2-y^2}$  and  $d_{z^2}$  orbitals do not overlap with the ligand p orbitals. The on axis d orbitals will form sigma bonding ( $e_g$ ) and sigma antibonding ( $e_g^*$ ) molecular orbitals. Unlike the sigma bonding only diagram, the off axis d orbitals ( $d_{xy}$ ,  $d_{xz}$ , and  $d_{yz}$ ) overlap with the ligand p orbitals to form  $\pi$  bonding ( $t_{2g}$ ) and  $\pi$  antibonding ( $t_{2g}^*$ ) molecular orbitals as seen in Figure 8.4.1.5 Rather than being nonbonding, like in the sigma bonding only picture, the metal based  $t_{2g}$  molecular orbital is bonding. This increases the energy difference between the  $t_{2g}$  and  $e_g^*$  and therefore increases  $\Delta_o$ .



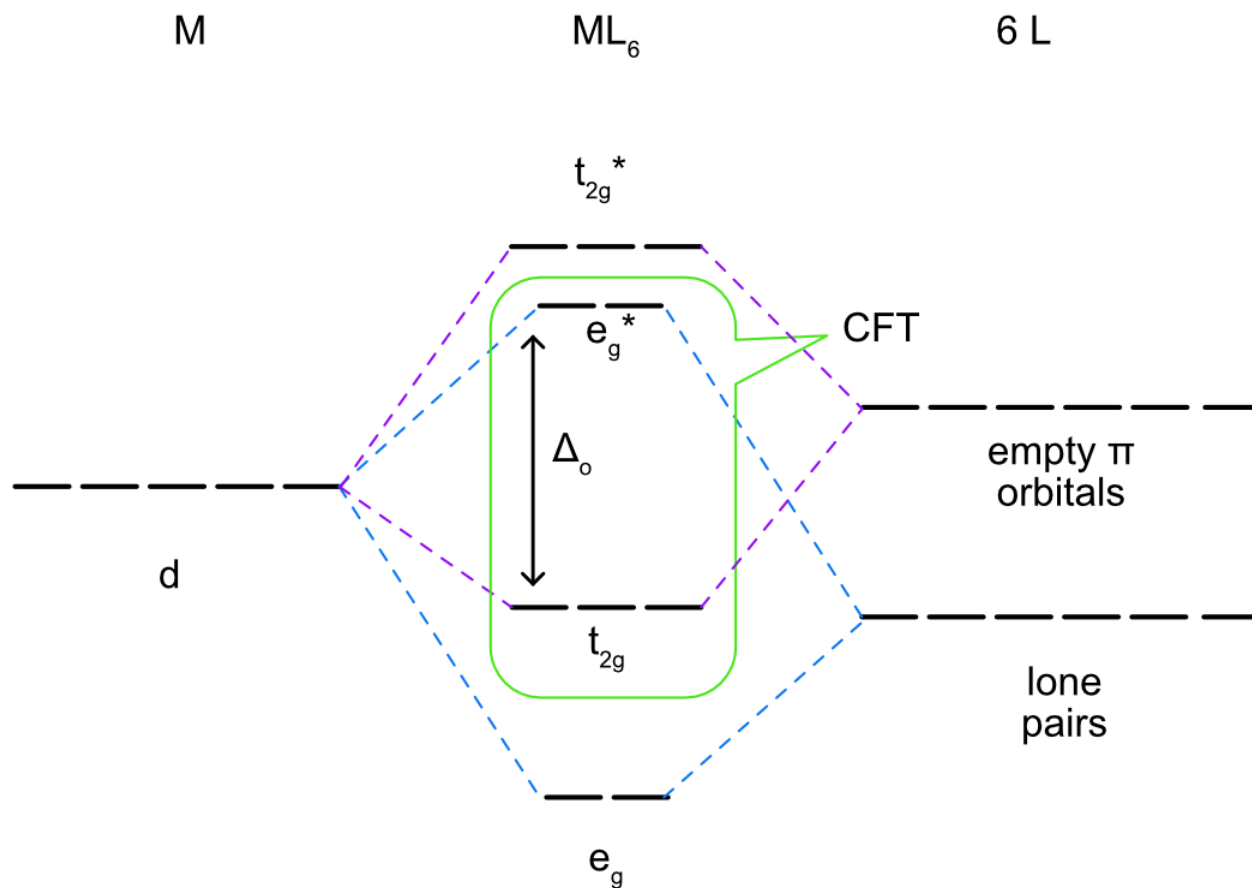


Figure 8.4.1.5: Octahedral ligand field splitting diagram with a  $\pi$  acceptor ligand. The  $d_{x^2-y^2}$  and  $d_{z^2}$  metal orbitals form sigma bonding ( $e_g$ ) and antibonding molecular orbitals ( $e_g^*$ ) with the ligand lone pairs. The  $d_{xy}$ ,  $d_{xz}$ , and  $d_{yz}$  orbitals form pi bonding ( $t_{2g}$ ) and pi antibonding molecular orbitals ( $t_{2g}^*$ ) with the empty  $\pi$  symmetry orbitals. The green outline highlights the portion of the diagram that is equivalent to the crystal field splitting diagram. (CC BY-NC-SA; Catherine McCusker)

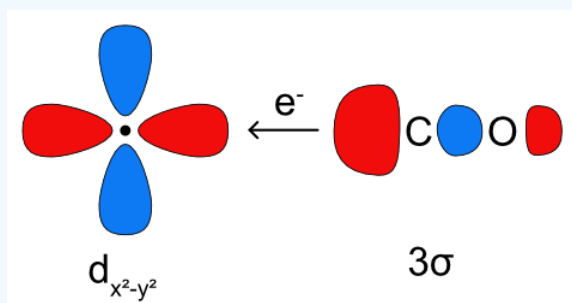
#### Exercise 8.4.1.1

Carbon monoxide is one of the most common, and strongest  $\pi$  acceptor ligands in inorganic chemistry. Refer to the [molecular orbital diagram of CO](#) and sketch likely metal-ligand orbital interactions for both sigma and pi bonding in a metal-CO complex. Indicate the direction of electron donation in both cases.

#### Answer

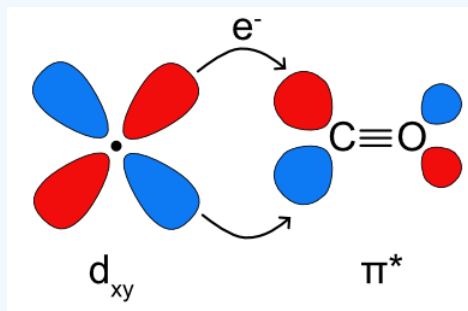
##### Sigma bonding:

Sigma bonding between a metal ion and a CO ligand involves overlap between the HOMO of CO ( $3\sigma$ ) and the metal  $d_{x^2-y^2}$  or  $d_{z^2}$  orbitals. Electrons are donated from the ligand to the metal.



##### Pi bonding:

Pi bonding between a metal ion and CO ligand involves overlap between the LUMO of CO ( $\pi^*$ ) and the metal  $d_{xy}$ ,  $d_{xz}$ , or  $d_{yz}$  orbitals. Electrons are donated from the metal to the ligand.



### $\pi$ Donor Ligands

Ligands that are  $\pi$  donors have filled  $\pi$  symmetry orbitals that are high enough in energy to donate electrons to the metal center. Most often this is a filled p orbital, but it could also be a  $\pi$  bonding molecular orbital. As lone pairs are generally the highest occupied orbitals in a molecule, the filled  $\pi$  orbitals will be lower in energy as seen in Figure 8.4.1.6 The sigma interaction between the ligand lone pairs and the metal  $d_{x^2-y^2}$  and  $d_{z^2}$  remain the same as previously described, forming the  $e_g$  bonding and  $e_g^*$  antibonding molecular orbitals. The  $d_{xy}$ ,  $d_{xz}$ , and  $d_{yz}$  overlap with the filled  $\pi$  orbitals to form  $\pi$  bonding ( $t_{2g}$ ) and  $\pi$  antibonding ( $t_{2g}^*$ ) molecular orbitals. The difference between the *pi* acceptor and donor ligands is the energy and character of the  $t_{2g}$  and  $t_{2g}^*$  molecular orbitals. In the  $\pi$  acceptor case above, the  $t_{2g}$  orbital is above the  $e_g$  and has a higher contribution from the metal and the  $t_{2g}^*$  is above the  $e_g^*$  and has a higher contribution from the ligand. In the  $\pi$  donor case the opposite is true. The  $t_{2g}$  orbital is below the  $e_g$  and has a higher contribution from the ligand and the  $t_{2g}^*$  is below the  $e_g^*$  and has a higher contribution from the metal. In this case  $\Delta_o$  is smaller than in the sigma only picture because the  $t_{2g}$  symmetry molecular orbital has gone from nonbonding to antibonding and the energy difference between  $t_{2g}^*$  and  $e_g^*$  is smaller.

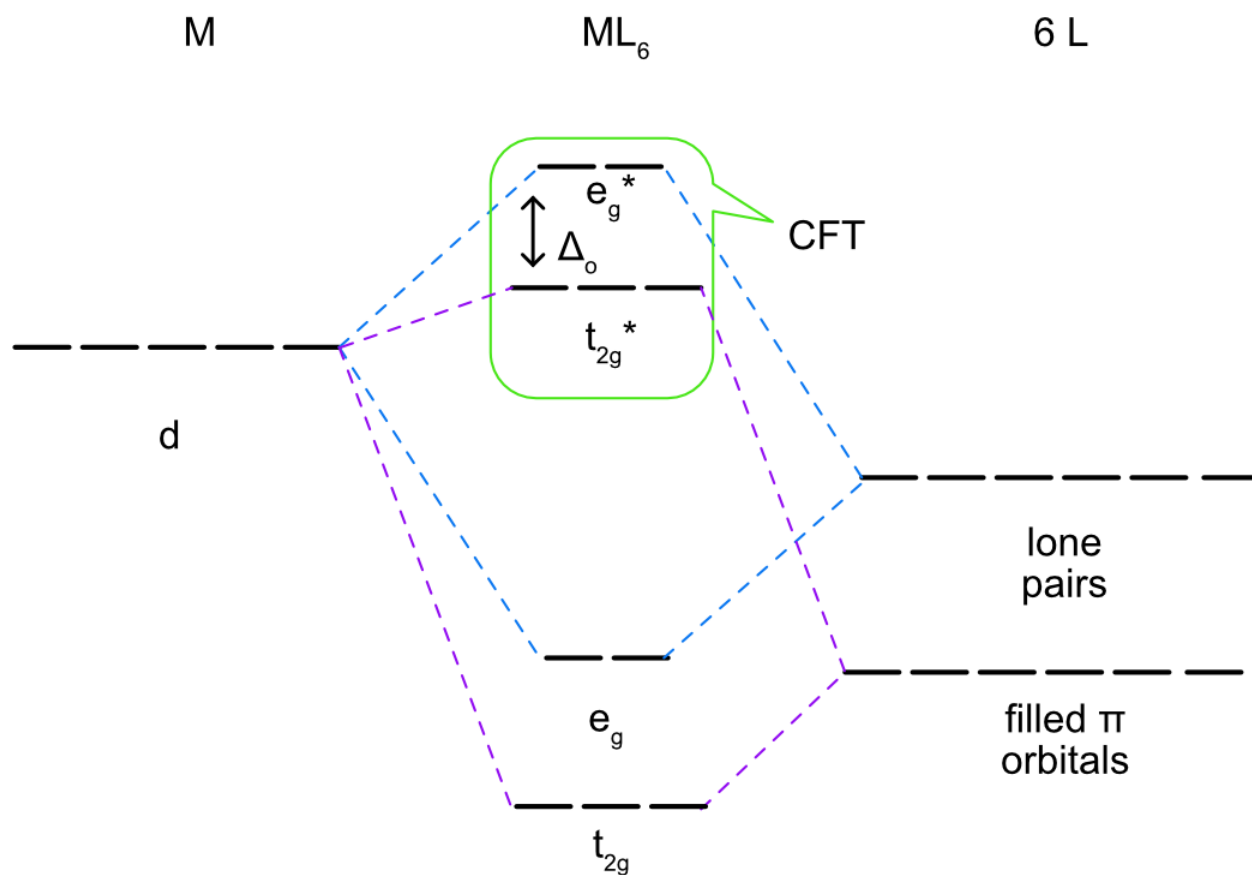


Figure 8.4.1.6: Octahedral ligand field splitting diagram with a  $\pi$  donor ligand. The  $d_{x^2-y^2}$  and  $d_{z^2}$  metal orbitals form sigma bonding ( $e_g$ ) and antibonding molecular orbitals ( $e_g^*$ ) with the ligand lone pairs. The  $d_{xy}$ ,  $d_{xz}$ , and  $d_{yz}$  orbital form pi bonding ( $t_{2g}$ ) and pi antibonding molecular orbitals ( $t_{2g}^*$ ) with the filled  $\pi$  symmetry orbitals. The green outline highlights the portion of the diagram that is equivalent to the crystal field splitting diagram. (CC BY-NC-SA; Catherine McCusker)

## The Spectrochemical Series

As discussed above, crystal field theory alone can't distinguish the behaviors of different ligands or explain why some ligands inherently produce larger splittings than others. Armed with ligand field theory we can now revisit the spectrochemical series and explain why ligands fall where they do within the series.

### Strong field ligands

Strong field ligands are ones that produce large splittings between the d orbitals and form low spin complexes. Examples of strong field ligands include CO,  $\text{CN}^-$ , and  $\text{NO}_2$ . From a ligand field theory perspective all three of these ligands have strong  $\pi$  bonds (either double or triple bonds) and have empty  $\pi^*$  molecular orbitals available for backbonding. Strong field ligands are both sigma donors (all ligands are sigma donors) and  $\pi$  acceptors.  $\pi$  backbonding between a metal and a ligand stabilizes the metal based  $t_{2g}$  molecular orbital and increases  $\Delta_o$ .

### Weak field ligands

Weak field ligands are ones that produce small splittings between the d orbitals and form high spin complexes. Examples of weak field ligands include the halogens,  $\text{OH}^-$  and  $\text{H}_2\text{O}$ . From a ligand field perspective these ions or molecules all have filled orbitals which can  $\pi$  bond with the metal d orbitals. In the case of the halogens these are filled p orbitals and in the case of  $\text{OH}^-$  and  $\text{H}_2\text{O}$  these are lone pairs which are perpendicular to the metal-ligand bond. Weak field ligands are both sigma donors and  $\pi$  donors. The  $\pi$  donation from the ligand to the metal destabilizes the metal based  $t_{2g}$  molecular orbital and decreases  $\Delta_o$ .

### Intermediate field ligands

Intermediate field ligands produce intermediate splittings between the d orbitals and could form high or low spin complexes. Examples of intermediate field ligands include  $\text{NH}_3$  or ethylenediamine (en). From a ligand field perspective these ligands only have a single lone pair available for sigma bonding. All of the other orbitals on nitrogen are used for sigma bonding to the H or C atoms within the molecule. Intermediate ligands are those which are only sigma donors, and are not  $\pi$  donors or  $\pi$  acceptors. In this case the  $t_{2g}$  symmetry d orbitals are nonbonding and the  $\Delta_o$  is determined by the strength of the metal ligand sigma interaction (and amount of destabilization of the  $e_g^*$  molecular orbital)

---

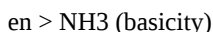
This page titled [8.4.1: Ligand Field Theory](#) is shared under a [CC BY-NC-SA 4.0](#) license and was authored, remixed, and/or curated by [Catherine McCusker](#).

- [9.5: Ligand Field Theory](#) by [Catherine McCusker](#) is licensed [CC BY-NC-SA 4.0](#).

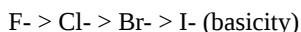
## 8.4.2: The Spectrochemical Series

The spectrochemical series was determined through an examination of the absorption spectra of a series of octahedral Co(III) complexes by Tsuchida in the 1930's. The position of the d-d absorption band is influenced by the field strength of the ligand, which leads to greater or lesser values of  $\Delta_o$ . That interaction depends on both the relative energies of the metal and ligand orbitals and the degree of overlap between these orbitals. The closer in energy the two orbitals are to each other, the greater the interaction. Also, the greater the overlap between the two orbitals, the greater the interaction.

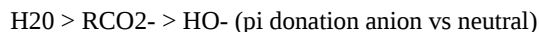
Recall that sigma donors simply donate a lone pair to the metal but do not have additional metal-ligand interactions. The classic example is ammonia. The nitrogen in ammonia has only one lone pair to donate and is a simple sigma donor. Ethylenediamine,  $\text{NH}_2\text{CH}_2\text{CH}_2\text{NH}_2$  (en), is also a sigma donor because it has a single lone pair on each nitrogen atom. The en ligand is a slightly stronger sigma donor than ammonia. The difference is explained by the slightly stronger basicity of en compared to ammonia; the nitrogen lone pairs in en are better donors to both protons and metal ions.



The common pi donors include the halides and some oxygen donors. In these cases, the donor atom has an additional lone pair (or more) which may engage in formation of a pi bond by donation to a metal d orbital. Among the halides, fluoride produces the largest field splitting and iodide the smallest. This trend is also explained in terms of the relative basicity of these halides; fluoride is more basic than bromide. In addition, there is also understood to be better overlap between fluorine's p orbital and the d acceptor of a positively charged metal ion, compared to larger halides such as iodine.



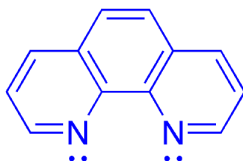
Oxygen donors do not follow this basicity trend. Hydroxide is thought to act as a better pi donor than water, partly because of its negative charge. A carboxylate ligand is not quite as strong a pi donor as hydroxide, probably because its lone pair is delocalized into the carbonyl group.



The pi acceptors include familiar examples such as carbon monoxide (carbonyl ligand) as well as the aromatic phenanthroline.



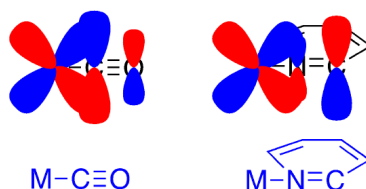
The phenanthroline may be an unfamiliar ligand. It is an aromatic amine, like pyridine. Other aromatic ligands, if they donate through a lone pair such as a phenyl,  $\text{C}_6\text{H}_5^-$ , can also be considered pi acceptors. These compounds feature a pi bond that includes the donor atom, so there is a  $\pi^*$  orbital at that position capable of undergoing back-donation from the metal.



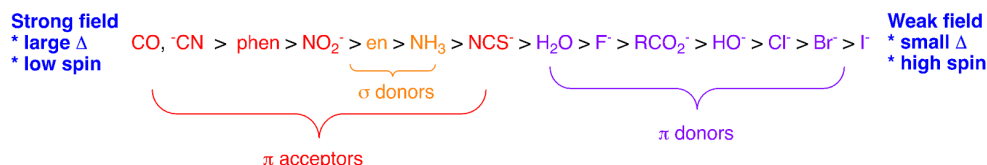
phenanthroline (phen)

Again, there are subtle variations among the field strengths exhibited by these pi acceptors, and there may be several factors contributing to those differences. For example, the cyanide is only slightly weaker field than the isoelectronic carbon monoxide. That small difference may be due to the negative charge on the cyanide rendering it a weaker electron acceptor. On the other hand, phenanthroline is neutral, but it is still a weaker donor than carbon monoxide. That weaker field may be due to the smaller lobe on the nitrogen atom in the  $\pi^*$  orbital in phenanthroline. Because nitrogen is more electronegative than carbon, it makes a greater contribution to the  $\text{C}=\text{N}$  pi bonding orbital than carbon; the opposite is true in the antibonding orbital. Carbon monoxide, in contrast, features a larger lobe on carbon in its  $\pi^*$  orbital. The result is better metal-ligand pi overlap with carbon monoxide than with phenanthroline.

Phosphines are also commonly considered to be pi acceptors, for subtle reasons that have been subject to some debate.<sup>1</sup>

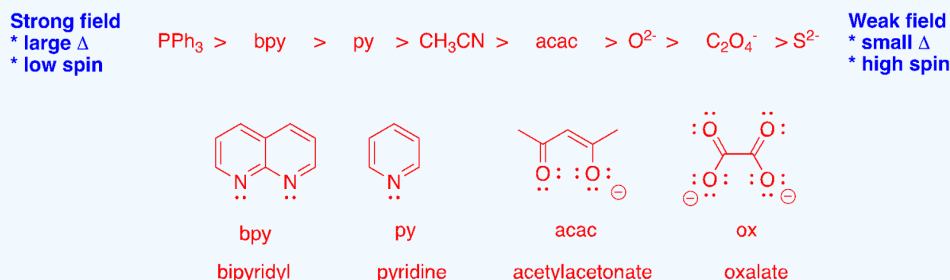


All three of these series can be collated to arrive at a combined list, which is a more complete spectrochemical series. Note that there may be some overlap between the different types of donors. Nevertheless, the overall trend holds: pi acceptors lead to the greatest field splitting on average, whereas di donors lead to the smallest.



#### ✓ Example 8.4.2.1

Some additional common ligands are displayed according to field strength, below. Classify these ligands as pi donors, sigma donors, or pi acceptors.



#### Solution

$PPh_3$ , based on its structure, appears to be a sigma donor only because it has just one lone pair on the donor atom. However, phosphines tend to behave as pi acceptors; that is, they appear to withdraw some electron density from the metal as indicated by the response of reporter ligands such as CO.

Bpy, py and  $CH_3CN$  (acetonitrile) all appear to be pi acceptors. Like phen, they behave as weak pi acceptors.

Acac, oxide, oxalate and sulfide are all pi donors. The donor atom in each case has a lone pair in addition to the sigma donor pair.

#### References

1. Wolczanski, P. T. "Flipping the Oxidation State Formalism: Charge Distribution in Organometallic Complexes as Reported by Carbon Monoxide". *Organometallics* **2017**, 36, 622-631.

This page titled [8.4.2: The Spectrochemical Series](#) is shared under a [CC BY-NC 4.0](#) license and was authored, remixed, and/or curated by [Chris Schaller](#).

## 8.4.3: Factors That Affect Ligand Field Splitting

### Magnitude of Ligand Field Splitting

The magnitude of the ligand field splitting ( $\Delta$ ) dictates whether a complex with four, five, six, or seven d electrons (in an octahedral complex) is high spin or low spin, which affects its magnetic properties, structure, and reactivity. Large values of  $\Delta$  (i.e.,  $\Delta > P$ ) yield a low-spin complex, whereas small values of  $\Delta$  (i.e.,  $\Delta < P$ ) produce a high-spin complex. The magnitude of  $\Delta$  depends on four factors: the valence of the metal, the principal quantum number of the metal (and thus its location in the periodic table), the geometry, and the nature of the ligand(s). Values of  $\Delta$  for some representative transition metal complexes are given in Table 8.4.3.1.

Table 8.4.3.1: Ligand Field Splitting Energies for Some Octahedral ( $\Delta_o$ )\* and Tetrahedral ( $\Delta_t$ ) Transition-Metal Complexes

Octahedral Complexes	$\Delta_o$ ( $\text{cm}^{-1}$ )	Octahedral Complexes	$\Delta_o$ ( $\text{cm}^{-1}$ )	Tetrahedral Complexes	$\Delta_t$ ( $\text{cm}^{-1}$ )
$[\text{Ti}(\text{H}_2\text{O})_6]^{3+}$	20,300	$[\text{Fe}(\text{CN})_6]^{4-}$	32,800	$\text{VCl}_4$	9010
$[\text{V}(\text{H}_2\text{O})_6]^{2+}$	12,600	$[\text{Fe}(\text{CN})_6]^{3-}$	35,000	$[\text{CoCl}_4]^{2-}$	3300
$[\text{V}(\text{H}_2\text{O})_6]^{3+}$	18,900	$[\text{CoF}_6]^{3-}$	13,000	$[\text{CoBr}_4]^{2-}$	2900
$[\text{CrCl}_6]^{3-}$	13,000	$[\text{Co}(\text{H}_2\text{O})_6]^{2+}$	9300	$[\text{CoI}_4]^{2-}$	2700
$[\text{Cr}(\text{H}_2\text{O})_6]^{2+}$	13,900	$[\text{Co}(\text{H}_2\text{O})_6]^{3+}$	27,000		
$[\text{Cr}(\text{H}_2\text{O})_6]^{3+}$	17,400	$[\text{Co}(\text{NH}_3)_6]^{3+}$	22,900		
$[\text{Cr}(\text{NH}_3)_6]^{3+}$	21,500	$[\text{Co}(\text{CN})_6]^{3-}$	34,800		
$[\text{Cr}(\text{CN})_6]^{3-}$	26,600	$[\text{Ni}(\text{H}_2\text{O})_6]^{2+}$	8500		
$\text{Cr}(\text{CO})_6$	34,150	$[\text{Ni}(\text{NH}_3)_6]^{2+}$	10,800		
$[\text{MnCl}_6]^{4-}$	7500	$[\text{RhCl}_6]^{3-}$	20,400		
$[\text{Mn}(\text{H}_2\text{O})_6]^{2+}$	8500	$[\text{Rh}(\text{H}_2\text{O})_6]^{3+}$	27,000		
$[\text{MnCl}_6]^{3-}$	20,000	$[\text{Rh}(\text{NH}_3)_6]^{3+}$	34,000		
$[\text{Mn}(\text{H}_2\text{O})_6]^{3+}$	21,000	$[\text{Rh}(\text{CN})_6]^{3-}$	45,500		
$[\text{Fe}(\text{H}_2\text{O})_6]^{2+}$	10,400	$[\text{IrCl}_6]^{3-}$	25,000		
$[\text{Fe}(\text{H}_2\text{O})_6]^{3+}$	14,300	$[\text{Ir}(\text{NH}_3)_6]^{3+}$	41,000		

\*Energies obtained by spectroscopic measurements are often given in units of wave numbers ( $\text{cm}^{-1}$ ); the wave number is the reciprocal of the wavelength of the corresponding electromagnetic radiation expressed in centimeters:  $1 \text{ cm}^{-1} = 11.96 \text{ J/mol}$ .

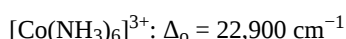
Source of data: Duward F. Shriver, Peter W. Atkins, and Cooper H. Langford, Inorganic Chemistry, 2nd ed. (New York: W. H. Freeman and Company, 1994).

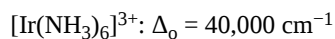
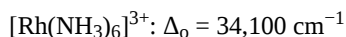
### Valence of the metal

Increasing the valence of a metal ion has two effects: the radius of the metal decreases and ligands are more strongly attracted to it due to Coulombic attraction. Both factors decrease the metal–ligand distance, which in turn causes the ligands to interact more strongly with the d-orbitals. Consequently, the magnitude of  $\Delta_o$  increases as the valence of the metal increases. Typically,  $\Delta_o$  for a M(III) is about 50% greater than for the M(II) of the same metal; for example, for  $[\text{V}(\text{H}_2\text{O})_6]^{2+}$ ,  $\Delta_o = 11,800 \text{ cm}^{-1}$ ; for  $[\text{V}(\text{H}_2\text{O})_6]^{3+}$ ,  $\Delta_o = 17,850 \text{ cm}^{-1}$ .

### Principal quantum number of the metal

For a series of complexes of metals from the same group in the periodic table with the same charge and the same ligands, the magnitude of  $\Delta_o$  increases with increasing principal quantum number:  $\Delta(3d) < \Delta(4d) < \Delta(5d)$ . The data for hexaammine complexes of the trivalent Group 9 metals illustrate this point:





The increase in  $\Delta$  with increasing principal quantum number is due to the larger [radial extension of the d orbitals as n increases](#). In addition, repulsive ligand–ligand interactions are most important for smaller metal ions. Relatively speaking, this results in shorter M–L distances and stronger d orbital–ligand interactions. The increase in  $\Delta$  going from 3d to 4d and 5d is so large that all 4d and 5d metals will form low spin complexes.

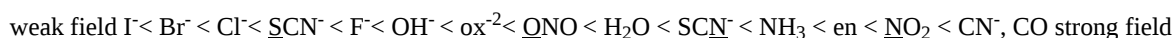
### Geometry of the complex

The number of ligands in a complex as well as how well the ligand geometry overlaps with the d orbitals is also a factor in the magnitude of the ligand field splitting. For example, comparing octahedral and tetrahedral geometries the octahedral geometry has 6 ligands, and those 6 ligands overlap directly with the two d orbitals that lie along the axes,  $d_{x^2-y^2}$  and  $d_{z^2}$ . The tetrahedral geometry has fewer ligands than octahedral, and those ligands overlap less ideally with the ligands that lie between the axes,  $d_{xy}$ ,  $d_{xz}$ , and  $d_{yz}$ . Because of this the ligand field splitting of a tetrahedral complex is generally less than half ( $\frac{4}{9}$  than an octahedral complex with the same metal and ligands. For example  $[\text{FeCl}_4]^-$  has a  $\Delta_t = 5,200 \text{ cm}^{-1}$  and  $[\text{FeCl}_6]^{3-}$  has a  $\Delta_o = 11,600 \text{ cm}^{-1}$ .

### Nature of the ligands

In crystal field theory ligands are all modeled as negative point charges, which means that all ligands should behave identically. Experimentally, it is found that the  $\Delta_o$  observed for a series of complexes of the same metal ion depends strongly on the nature of the ligands. For a series of chemically similar ligands, the magnitude of  $\Delta_o$  decreases as the size of the donor atom increases. For example,  $\Delta_o$  values for halide complexes generally decrease in the order  $\text{F} > \text{Cl} > \text{Br} > \text{I}$  because smaller, more localized charges, such as we see for F, interact more strongly with the d-orbitals of the metal. In addition, a small neutral ligand with a highly localized lone pair, such as  $\text{NH}_3$ , results in significantly larger  $\Delta_o$  values than might be expected. Because the lone pair points directly at the metal ion, the electron density along the M–L axis is greater than for a spherical anion such as F. The experimentally observed order of the crystal field splitting energies produced by different ligands is called the spectrochemical series.

Ligands are classified as strong field or weak field based on the spectrochemical series:



Note that  $\text{SCN}$  and  $\text{NO}_2$  ligands are represented twice in the above spectrochemical series since there are two different Lewis base sites (e.g., free electron pairs to share) on each ligand (e.g., for the  $\text{SCN}$  ligand, the electron pair on the sulfur or the nitrogen can form the bond to a metal). The specific atom that binds in such ligands is underlined. Ligands on the weak field end of the series (halogens,  $\text{OH}$ ,  $\text{H}_2\text{O}$ ) will tend to form high spin complexes and ligands on the strong field end of the series ( $\text{CN}$ ,  $\text{CO}$ ,  $\text{NO}_2$ ) will tend to form low spin complexes. Intermediate ligands in the middle of the series could form high or low spin complexes depending on other factors.

#### How to determine if a complex is high or low spin

- How many d electrons does the complex have?
  - Only complexes with 4-7 d electrons have high spin and low spin configurations
- What period is the metal?
  - 3d metals could either be high or low spin
  - 4d and 5d metals will ALWAYS be low spin
- What is the geometry of the complex?
  - Tetrahedral complexes with 3d metals will almost always be high spin because  [\$\Delta\_t\$  is generally less than spin pairing energy](#)
  - Square planar complexes will almost always be low spin because they are favored over tetrahedral [when crystal field splitting is large](#)
  - Octahedral complexes could be either high or low spin
- What are the ligands?
  - Strong field ligands will form low spin complexes
  - Weak field ligands will form high spin complexes



- Intermediate field ligands could form high or low spin complexes. Additional information (like number of unpaired electrons) is needed

- Adapted by Catherine McCusker (East Tennessee State University)

---

8.4.3: Factors That Affect Ligand Field Splitting is shared under a [CC BY-NC-SA 4.0](#) license and was authored, remixed, and/or curated by LibreTexts.

- **9.4: Factors That Affect Crystal Field Splitting** is licensed [CC BY-NC-SA 4.0](#).

## 8.4.4: Octahedral vs. Tetrahedral Geometries

How do we tell whether a particular complex is octahedral, tetrahedral, or square planar? Obviously if we know the formula, we can make an educated guess: something of the type  $ML_6$  will almost always be octahedral (there is an alternative geometry for 6-coordinate complexes, called trigonal prismatic, but it's pretty rare), whereas something of formula  $ML_4$  will usually be *tetrahedral* unless the metal atom has the  $d^8$  electron configuration, in which case it will probably be *square planar*. But what if we take a particular metal ion and a particular ligand? Can we predict whether it will form an octahedral or a tetrahedral complex, for example? To an extent, the answer is yes... we can certainly say what factors will encourage the formation of tetrahedral complexes instead of the more usual octahedral.

The Crystal Field Stabilization Energy (CFSE) is the additional stabilization gained by the splitting of the orbitals according to the [crystal field theory](#), against the energy of the original five degenerate d orbitals. So, for example, in a  $d^1$  situation such as  $[Ti(OH_2)_6]^{3+}$ , putting the electron into one of the orbitals of the  $t_{2g}$  level gains  $-0.4 \Delta_o$  of CFSE. Generally speaking, octahedral complexes will be favored over tetrahedral ones because:

- It is more (energetically) favorable to form six bonds rather than four
- The CFSE is usually greater for octahedral than tetrahedral complexes. Remember that  $\Delta_o$  is bigger than  $\Delta_{tet}$  (in fact,  $\Delta_{tet}$  is approximately  $4/9 \Delta_o$ ).

If we make the assumption that  $\Delta_{tet} = 4/9 \Delta_o$ , we can calculate the difference in stabilization energy between octahedral and tetrahedral geometries by referencing everything in terms of  $\Delta_o$ .

### ✓ Example 8.4.4.1: $d^3$ Stabilized Structures

Which is the preferred configuration for a  $d^3$  metal: tetrahedral or octahedral?

#### Solution

To answer this, the *Crystal Field Stabilization Energy* has to be calculated for a ( $d^3$  metal in both configurations. The geometry with the greater stabilization will be the preferred geometry.

- For a  $d^3$  *octahedral* configuration, the *Crystal Field Stabilization Energy* is

$$3 \times -0.4\Delta_o = -1.2\Delta_o$$

- For a  $d^3$  *tetrahedral* configuration (assuming high spin), the *Crystal Field Stabilization Energy* is

$$-0.8\Delta_{tet}$$

Remember that because  $\Delta_{tet}$  is less than half the size of  $\Delta_o$ , tetrahedral complexes are often high spin. We can now put this in terms of  $\Delta_o$  (we can make this comparison because we're considering the same metal ion and the same ligand: all that's changing is the geometry)

So for tetrahedral  $d^3$ , the Crystal Field Stabilization Energy is:

$$CFSE = -0.8 \times 4/9 \Delta_o = -0.355 \Delta_o.$$

And the difference in Crystal Field Stabilization Energy between the two geometries will be:

$$1.2 - 0.355 = 0.845 \Delta_o.$$

If we do a similar calculation for the other configurations, we can construct a Table of  $\Delta_o$ ,  $\Delta_{tet}$  and the difference between them (we'll ignore their signs since we're looking for the difference between them).

Table 8.4.4.1: Crystal Field Stabilization Energies (not splitting parameters). This table compares the values of the CFSE for octahedral and tetrahedral geometries, assuming high spin configurations. The units are  $\Delta_o$ , and we're assuming that  $\Delta_{tet} = 4/9 \Delta_o$ .

	Octahedral	Tetrahedral	Difference
$d^0, d^5, d^{10}$	0	0	0
$d^1, d^6$	0.4	0.27	0.13
$d^2, d^7$	0.8	0.53	0.27

	Octahedral	Tetrahedral	Difference
$d^3, d^8$	1.2	0.36	0.84
$d^4, d^9$	0.6	0.18	0.42

These values can be plotted:.

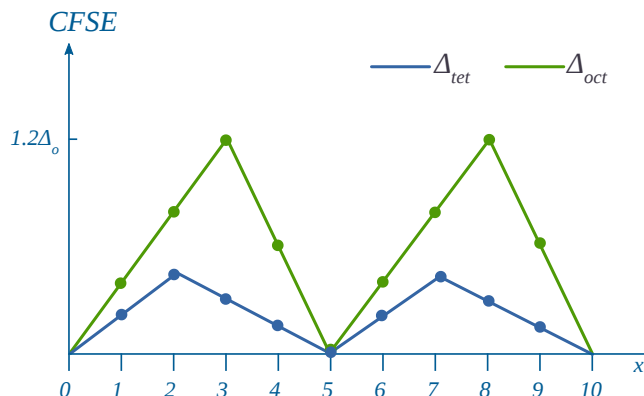


Figure 8.4.4.1: Crystal Field Stabilization Energy as a function of d-electrons for a hypothetical molecule in the octahedral (green curve) and tetrahedral (blue curve) geometries. (CC BY-NC; Ümit Kaya)

Notice that the Crystal Field Stabilization Energy almost always favors octahedral over tetrahedral in most cases, but the degree of favorability varies with the *electronic configuration*. In other words, for  $d^1$  there's only a small gap between the oct and tet lines, whereas at  $d^3$  and  $d^8$  there's a big gap. However, for  $d^0$ ,  $d^5$  high spin and  $d^{10}$ , there is **no** CFSE difference between octahedral and tetrahedral. The ordering of favorability of octahedral over tetrahedral is:

$$d^3, d^8 > d^4, d^9 > d^2, d^7 > d^1, d^6 > d^0, d^5, d^{10}$$

The units of the graph are  $\Delta_o$ . So if we have strong field ligands present,  $\Delta_o$  will be bigger anyway (according to the spectrochemical series), and any energy difference between the oct and tet lines will be all the greater for it. A bigger  $\Delta_o$  might also push the complexes over to low spin. Similarly, as we saw previously, high oxidation states and metals from the 2nd and 3rd rows of the transition series will also push up  $\Delta_o$ .

On the other hand, if large or highly charged ligands are present, they may suffer large interligand repulsions and thus prefer a lower coordination number (4 instead of 6). Consequently if you set out to make something that would have a tetrahedral geometry, you would use large, negatively charged, weak field ligands, and use a metal atom with a  $d^0$ ,  $d^5$  or  $d^{10}$  configuration from the first row of the transition series (though of course having weak field ligands doesn't matter in these three configurations because the difference between oct and tet is 0  $\Delta_o$ ). As Table 2 shows, you can find tetrahedral complexes for most configurations, but there are very few for  $d^3$  and  $d^8$ .

Table 8.4.4.2: Tetrahedral complexes of different d electron counts

$d^0$	$\text{MnO}_4^-$	$d^5$	$\text{MnCl}_4^{2-}$
$d^1$	$\text{TiCl}_4^-$	$d^6$	$\text{FeCl}_4^{2-}$
$d^2$	$\text{Cr(OR)}_4$	$d^7$	$\text{CoCl}_4^{2-}$

## Contributors and Attributions

- Dr Mike Morris, March 2001

8.4.4: Octahedral vs. Tetrahedral Geometries is shared under a CC BY-NC-SA 4.0 license and was authored, remixed, and/or curated by LibreTexts.

- Octahedral vs. Tetrahedral Geometries is licensed CC BY-NC-SA 4.0.

## 8.5: Absorption Spectroscopy of Coordination Complexes

---

Learning objectives for this unit are to:

- Know the definitions and properties of  $d \rightarrow d$ , MLCT, LMCT, and  $p \rightarrow p^*$  electronic transitions, including relative energies and intensities
- Explain or predict how the magnitude of the d-orbital splitting will influence the absorption properties of a coordination complex and vice versa

---

8.5: Absorption Spectroscopy of Coordination Complexes is shared under a [not declared](#) license and was authored, remixed, and/or curated by LibreTexts.

## 8.5.1: Absorption of Light

### Introduction

The d-orbital splitting in coordination complexes results in a gap ( $\Delta$ ) that happens to be just the right magnitude to absorb visible light. Because metal complexes can absorb visible light, they display an array of colors. Not only is the color attractive to the eye, it is an indication of the chemical and physical properties of the metal complex. The color (like the magnitude of  $\Delta$ ) depends on the identity of the metal ion, the coordination geometry, and the ligand identity. Chemists don't just "look" at color, though - we measure it using electronic absorption spectroscopy. This is usually done in a lab using a UV-visible spectrophotometer.

An example of such a measurement is shown below in Figure 8.5.1.1 for a Cu(II) complex. The sample appears a pink color to the eye, and when it is measured using a UV-visible spectrophotometer, it is shown to absorb visible light at approximately 530 nm. The absorption spectrum can indicate the oxidation state of Cu, the ligands bound to the Cu(II) ion, and the coordination geometry. The color of the solution in Figure 8.5.1.1 is a shade of pink.

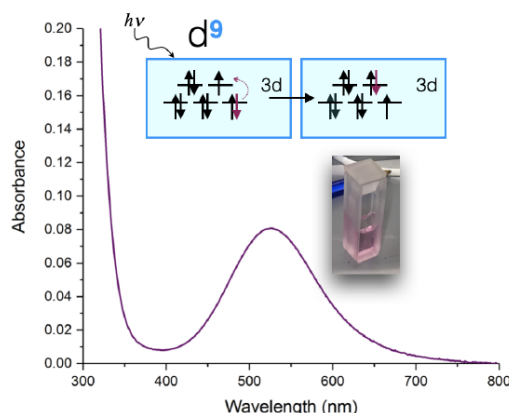


Figure 8.5.1.1: A UV-visible spectrum of a Cu(II)-peptide complex. A photo of the sample shows its pink color. The splitting diagram for its approximation as an octahedral complex is shown, where an electronic transition from  $t_{2g}$  to  $e_g$  is shown. (CC-BY-NC-SA; Kathryn Haas)

### We observe the complementary color of light absorbed

The absorption spectrum shown above in Figure 8.5.1.1 is a simple case in which only one absorption band is observed in the visible region of the spectrum. In a simple case like this, the color of a complex can be predicted as the complementary color of the light absorbed by the solution. When a solution or object absorbs a certain wavelength, we see the complementary color; or the color opposite to the absorbed wavelength on the color wheel in Figure 8.5.1.2. In the case of the Cu(II) complex spectrum shown in Figure 8.5.1.1, the color of the light absorbed at 530 nm is green, and the predicted color observed is pink.

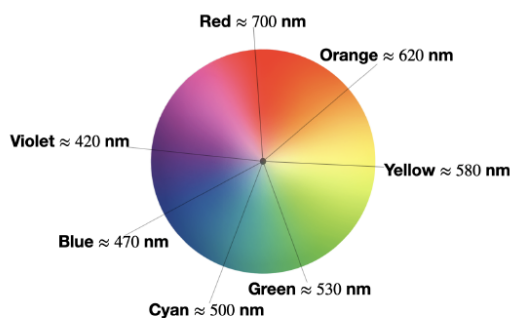


Figure 8.5.1.2: Color wheel with approximate wavelengths of colors. (CC-BY-NC-SA; Kathryn Haas)

The table below lists the approximate colors of absorption corresponding to wavelengths of light absorbed, and gives similar information to that deduced from Figure 8.5.1.2

Table 8.5.1.1: Approximate wavelengths of absorption and their complementary colors observed. \* This prediction is limited to simple cases where there is only one absorption band in the visible spectrum.

--	--

$\lambda$ absorbed	$E$ ( $\text{cm}^{-1}$ )	$E$ (eV)	Approximate color absorbed	Predicted color observed (by eye)
$> 700 \text{ nm}$	$< 14,000 \frac{1}{\text{cm}}$	$< 1.77 \text{ eV}$	Infrared	not observable
$\approx 700 - 635 \text{ nm}$	$\approx 14,300 - 16,000 \frac{1}{\text{cm}}$	$\approx 1.77 - 1.95 \text{ eV}$	Red	Green
$\approx 635 - 590 \text{ nm}$	$\approx 15,700 - 16,900 \frac{1}{\text{cm}}$	$\approx 1.95 - 2.10 \text{ eV}$	Orange	Blue
$\approx 590 - 560 \text{ nm}$	$\approx 16,900 - 17,900 \frac{1}{\text{cm}}$	$\approx 2.10 - 2.21 \text{ eV}$	Yellow	Violet
$\approx 560 - 520 \text{ nm}$	$\approx 17,900 - 19,200 \frac{1}{\text{cm}}$	$\approx 2.21 - 2.38 \text{ eV}$	Green	Red
$\approx 520 - 490 \text{ nm}$	$\approx 19,200 - 20,400 \frac{1}{\text{cm}}$	$\approx 2.38 - 2.53 \text{ eV}$	Cyan	Red-Orange
$\approx 490 - 450 \text{ nm}$	$\approx 20,400 - 22,200 \frac{1}{\text{cm}}$	$\approx 2.53 - 2.76 \text{ eV}$	Blue	Orange
$400 - 450 \text{ nm}$	$\approx 22,200 - 25,000 \frac{1}{\text{cm}}$	$\approx 2.76 - 3.10 \text{ eV}$	Violet	Yellow
$< 400 \text{ nm}$	$> 25,000 \frac{1}{\text{cm}}$	$> 3.10 \text{ eV}$	Ultraviolet (UV)	not observable

### Energy of electronic absorption

The absorption spectrum of a metal complex can be used to calculate the splitting energy,  $\Delta$ , when the absorption corresponds to a  $d \rightarrow d$  transition. Let's use the  $d^9$  Cu(II) complex (discussed above) as an example. A  $d^9$  metal ion has only one visible-light  $d \rightarrow d$  transition. Let's assume that the coordination geometry is *approximately* octahedral (although it is actually a [Jahn-Teller distorted octahedron](#), and more like a square plane). If we assume it's octahedral, then the  $d$ -orbital splitting diagram (see Figure 8.5.1.1) leads us to expect one electronic transition: an electron is excited from the  $t_{2g}$  to  $e_g$ . The energy absorbed is equal to the energy of the  $\Delta$ .

Many cases are not as simple as a  $d^9$  octahedral case because there are multiple possible electronic transitions, and also multiple absorption bands in the UV-vis spectrum. In these more complex cases, the actual energy of the transition are affected by differences in electron-electron repulsion energies in the ground state and the excited states. We will learn how to account for multiple possible excited states and electron-electron repulsions using Tanabe-Sugano diagrams later in this chapter.

---

This page titled [8.5.1: Absorption of Light](#) is shared under a [not declared](#) license and was authored, remixed, and/or curated by [Kathryn Haas](#).

- [11.1: Absorption of Light](#) by [Kathryn Haas](#) has no license indicated.

## 8.5.2: Colors of Coordination Complexes

The color for a [coordination complex](#) can be predicted using the [Crystal Field Theory \(CFT\)](#). Knowing the color can have a number of useful applications, such as the creation of pigments for dyes in the textile industry. The tendency for coordination complexes to display such a wide array of colors is merely coincidental; their absorption energies happen to fall within range of the visible light spectrum. Chemists and physicists often study the color of a substance not to understand its sheer appearance, but because color is an indicator of a chemical's physical properties on the atomic level.

### The Electromagnetic Spectrum

The [electromagnetic spectrum](#) (EM) spectrum is made up of photons of different wavelengths. Photons, unique in displaying the properties of both waves and particles, create visible light and colors in a small portion of the EM spectrum. This visible light portion has wavelengths in approximately the 400-700 nanometer range (a nanometer, "nm," is  $10^{-9}$  meters). Each specific wavelength corresponds to a different color (Figure 8.5.2.1), and when all the wavelengths are present, it appears as white light.

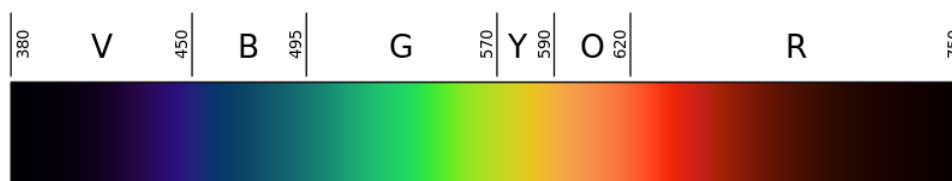


Figure 8.5.2.1: A linear representation of the visible light spectrum. (Public Domain; [Gringer](#) via Wikipedia)

The wavelength and frequency of a wave are inversely proportional: as one increases, the other decreases; this is a consequence of all light traveling at the same speed.

$$\lambda \propto \nu^{-1}$$

Because of this relationship, blue light has a much higher frequency and more energy than red light.

### Perceiving Color

Color is perceived in two ways, through additive mixing, where different colors are made by combining different colors of light, and through subtractive mixing, where different wavelengths of light are taken out so that the light is no longer pure white. For colors of coordination complexes, subtractive mixing is considered. As shown in Figure 8.5.2.2 the idea behind subtractive mixing is that white light (which is made from all the colors mixed together) interacts with an object. The object absorbs some of the light, and then reflects or transmits (or both, depending on the object) the rest of the light, which contacts the eye. The object is perceived as whichever color is not absorbed. In Figure 8.5.2.2 white light (simplified as green, red, and blue bands) is shone through a solution. The solution absorbs the red and green wavelengths; however, the blue light is reflected and passes through, so the solution appears blue. This procedure takes place whenever an object displays visible color. If none of the light is absorbed, and all is reflected back off, the object appears white; if all of the light is absorbed, and there is none left to reflect or transmit through, the object appears black.

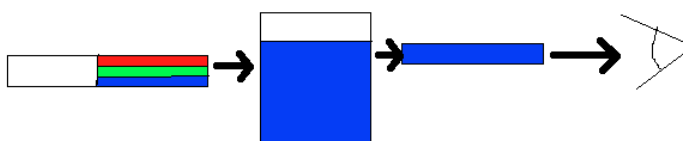


Figure 8.5.2.2: Subtractive mixing

### Colors of Coordination Complexes: Crystal Field Splitting

When ligands attach to a transition metal to form a coordination complex, electrons in the d orbital split into high energy and low energy orbitals. The difference in energy of the two levels is denoted as  $\Delta$ , and it is a characteristic property both of the metal and the ligands. This is illustrated in Figure 8.5.2.3 the "o" subscript on the  $\Delta$  indicates that the complex has octahedral geometry.

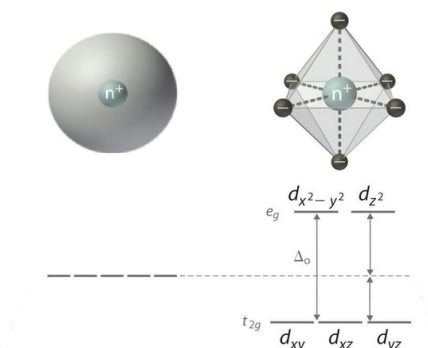


Figure 8.5.2.3: d-Orbitals Splitting in an octahedral ligand field. (CC BY-SA-NC; anonymous by request)

If  $\Delta_o$  is large, and much energy is required to promote electrons into the high energy orbitals, the electrons will instead pair in the lower energy orbitals, resulting in a "low spin" complex (Figure 8.5.2.4A); however, if  $\Delta_o$  is small, and it takes little energy to occupy the higher orbitals, the electrons will do so, and remain unpaired (until there are more than five electrons), resulting in a "high spin" complex (Figure 8.5.2.4B). Different ligands are associated with either **high or low spin** —a "strong field" ligand results in a large  $\Delta_o$  and a low spin configuration, while a "weak field" ligand results in a small  $\Delta_o$  and a high spin configuration. For more details, see the [Crystal Field Theory \(CFT\)](#) page.

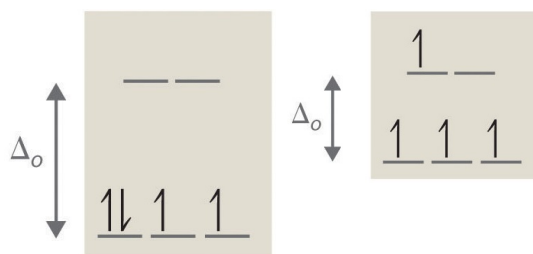


Figure 8.5.2.4: (a) Low Spin, Strong Field ( $\Delta_o > P$ ). (b): High Spin, Weak Field ( $\Delta_o < P$ ). (CC BY-SA-NC; anonymous)

A photon equal to the energy difference  $\Delta_o$  can be absorbed, promoting an electron to the higher energy level. As certain wavelengths are absorbed in this process, subtractive color mixing occurs and the coordination complex solution becomes colored. If the ions have a noble gas configuration, and have no unpaired electrons, the solutions appear colorless; in reality, they still have a measured energy and absorb certain wavelengths of light, but these wavelengths are not in the visible portion of the EM spectrum and no color is perceived by the eye.

In general, a larger  $\Delta_o$  indicates that higher energy photons are absorbed, and the solution appears further to the left on the EM spectrum shown in Figure 8.5.2.1 This relationship is described in the equation

$$\Delta_o = hc/\lambda$$

where  $h$  and  $c$  are constants, and  $\lambda$  is the wavelength of light absorbed.

Using a color wheel can be useful for determining what color a solution will appear based on what wavelengths it absorbs (Figure 8.5.2.6). If a complex absorbs a particular color, it will have the appearance of whatever color is directly opposite it on the wheel. For example, if a complex is known to absorb photons in the orange range, it can be concluded that the solution will look blue. This concept can be used in reverse to determine  $\Delta$  for a complex from the color of its solution.



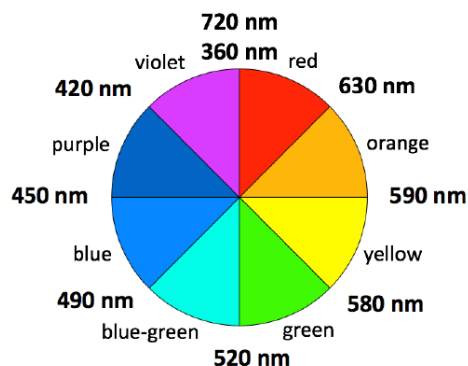


Figure 8.5.2.5: Color wheel with wavelengths marked (CC BY-SA 4.0 International; Tem5psu via [source](#))

### Relating the Colors of Coordination Complexes to the Spectrochemical Series

According to the Crystal Field Theory, ligands that have smaller  $\Delta_o$  values are considered "weak field" and will absorb lower-energy light with longer  $\lambda$  values (ie a "red shift"). Ligands that have larger  $\Delta_o$  values are considered "strong field" and will absorb higher-energy light with shorter  $\lambda$  values (ie a "blue shift"). This relates to the colors seen in a coordination complex. Weaker-field ligands induce the absorption of longer wavelength (lower frequency=lower energy) light than stronger-field ligands since their respective  $\Delta_o$  values are **smaller** than the electron pairing energy.

The energy difference,  $\Delta_o$ , determines the color of the coordination complex. According to the **spectrochemical series**, the high spin ligands are considered "weak field," and absorb longer wavelengths of light (weak  $\Delta_o$ ), while complexes with low spin ligands absorb light of greater frequency (high  $\Delta_o$ ). The color seen is the complementary color of the color associated with the absorbed wavelength. To predict which possible colors and their corresponding wavelengths are absorbed, the [spectrochemical series](#) can be used:

(Strong field/large  $\Delta_o$ /low spin) (weak field/ small  $\Delta_o$ /high spin)



#### ✓ Example 8.5.2.1

If a solution with a dissolved octahedral complex appears yellow to the eye, what wavelength of light does it absorb? Is this complex expected to be low spin or high spin?

#### Solution

A solution that looks yellow absorbs light that is violet, which is roughly 410 nm from the color wheel. Since it absorbs high energy, the electrons must be raised to a higher level, and  $\Delta_o$  is high, so the complex is likely to be low spin.

#### ✓ Example 8.5.2.2

An octahedral metal complex absorbs light with wavelength 535 nm. What is the crystal field splitting  $\Delta_o$  for the complex? What color is it to the eye?

#### Solution

To solve this question, we need to use the equation

$$\Delta_o = \frac{hc}{\lambda}$$

with

- $h$  is Planck's constant and is  $6.625 \times 10^{-34} \text{ J} \cdot \text{s}$  and
- $c$  is the speed of light and is  $2.998 \times 10^8 \text{ m/s}$ .

It is also important to remember that 1 nm is equal to  $1 \times 10^{-9}$  meters. With all this information, the final equation looks like this:

$$\Delta_o = \frac{(6.625 \times 10^{-34} \text{ J} \cdot \text{s})(2.998 \times 10^8 \text{ m/s})}{(535 \text{ nm}) \left( \frac{1 \text{ m}}{1 \times 10^9 \text{ nm}} \right)} = 3.712 \text{ J/molecule}$$

It is not necessary to use any equations to solve the second part of the problem. Light that is 535 nm is green, and because green light is absorbed, the complex appears red (refer to Figures 8.5.2.1 and 8.5.2.6 for this information).

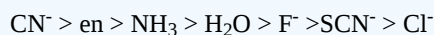
Note: the fact that the complex is octahedral makes no impact when solving this problem. Although the splitting is different for complexes of different structures, the mechanics of solving the problem are identical.

### ✓ Example 8.5.2.3

There are two solutions, one orange and one blue. Both solutions are known to be made up of a cobalt complex; however, one has chloride ions as ligands, while the other has ammonia ligands. Which solution is expected to be orange?

#### Solution

In order to solve this problem, it is necessary to know the relative strengths of the ligands involved. A sample ligand strength list is given here, but see Crystal Field Splitting for a more complete list:



From this information, it is clear that  $\text{NH}_3$  is a stronger ligand than  $\text{Cl}^-$ , which means that the complex involving  $\text{NH}_3$  has a greater  $\Delta$ , and the complex will be low spin. Because of the larger  $\Delta$ , the electrons absorb higher energy photons, and the solution will have the appearance of a lower energy color. Since orange light is less energetic than blue light, the  $\text{NH}_3$  containing solution is predicted to be orange

## References

1. Cox, P. A. Instant Notes Inorganic Chemistry. Second ed. Grand Rapids: Garland, Incorporated, 2004.
2. Nassau, Kurt. The Physics and Chemistry of Color : The Fifteen Causes of Color. Second ed. New York: Wiley-Interscience, 2001.
3. Petrucci, Ralph H., William S. Harwood, and Geoff E. Herring. General Chemistry : Principles and Modern Applications. Ninth ed. Upper Saddle River: Prentice Hall PTR, 2006.
4. Petrucci, Ralph H., Carey Bissonnette, F. Geoffrey Herring, Jeffrey D. Madura. General Chemistry: Principles and Modern Applications. Tenth Ed. Upper Saddle River: Pearson Education, Inc. 2011.

## Problems

1. What color will a complex be that absorbs light that is 600 nm be?
2. What color will a complex an octahedral complex appear if it has a  $\Delta_o$  of  $3.75 \times 10^{-19} \text{ J}$ ?
3. Would you expect a violet solution to be high spin or low spin? What about a red solution?
4. There are two solutions, one which is yellow and another which is violet. The solutions are  $[\text{Co}(\text{H}_2\text{O})_6]^{3+}$  and  $[\text{Co}(\text{CN})_6]^{3-}$ . What are the colors of each solution?

## Answers

1. Blue. The color absorbed is orange.
2. It is red. Using  $\Delta = hc/\lambda$ ,  $h = 6.626 \times 10^{-34} \text{ J} \cdot \text{s}$ ,  $c = 2.998 \times 10^8 \text{ m/s}$ , wavelength would equal 530 nm. So green is absorbed, and the complementary color of green is red, so red is the color of the complex.
3. It would be high spin. The complementary color of violet is yellow, which has a wavelength of 570 nm. For a red solution, the complementary color absorbed is green, with a wavelength of 530 nm, so it would be considered low spin.
4.  $[\text{Co}(\text{H}_2\text{O})_6]^{3+}$  is violet and  $[\text{Co}(\text{CN})_6]^{3-}$  is yellow. Looking at the spectrochemical series,  $\text{H}_2\text{O}$  is a weak field ligand, so it absorbs colors of long wavelengths—in this case, the longer wavelength is yellow, so the color reflected is violet.  $\text{CN}^-$  is a strong field ligand, so it absorbs colors of shorter wavelengths—in this case, the shorter wavelength is violet, so the color reflected is yellow.

## Contributors and Attributions

- Deyu Wang (UCD)

---

8.5.2: Colors of Coordination Complexes is shared under a [CC BY](#) license and was authored, remixed, and/or curated by LibreTexts.

- [Colors of Coordination Complexes](#) is licensed [CC BY 4.0](#).

## 8.5.3: Charge-Transfer Spectra

### Charge Transfer Transitions

$\text{Zn}^{2+}$		$d^{10}$ ion	white
$[\text{Cu}(\text{MeCN})_4]^+$	Cu(I)	$d^{10}$ ion	colourless
$[\text{Cu}(\text{phen})_2]^+$	Cu(I)	$d^{10}$ ion	dark orange
$\text{TiF}_4$		$d^0$ ion	white
$\text{TiCl}_4$		$d^0$ ion	white
$\text{TiBr}_4$		$d^0$ ion	orange
$\text{TiI}_4$		$d^0$ ion	dark brown
$[\text{MnO}_4]^-$	Mn(VII)	$d^0$ ion	extremely purple
$[\text{Cr}_2\text{O}_7]^-$	Cr(VI)	$d^0$ ion	bright orange

Figure 8.5.3.1: Some examples of complexes with  $d^0$  and  $d^{10}$  electron configurations, and their colors. Attribution: E.R. Schofield.

We are still not done with our electronic spectra. Thus far, we have only considered transitions of d-electrons between d-orbitals, and their terms. These are called d-d transitions. However, there are also so-called charge transfer transitions possible, which are not d-d transitions. We can easily see that there must be transitions other than d-d transitions when we look at the colors of  $d^{10}$  and  $d^0$  ions. For those, there are no d-d transitions possible. Therefore, they all should be colorless. However, that is not always true. Some of these ions are indeed colorless, but some are not (Figure 8.5.3.2). For example,  $\text{Zn}^{2+}$ , a  $d^{10}$  ion, is colorless in complexes, but not Cu(I), which is also  $d^{10}$ . While tetrakis(acetonitrile)copper(+) is colorless, bis(phenanthrene) copper(+) is dark orange.  $d^0$  ions have similar properties: While  $\text{TiF}_4$  and  $\text{TiCl}_4$  are colorless,  $\text{TiBr}_4$  is orange, and  $\text{TiI}_4$  is brown. Some  $d^0$  species are even extremely colorful, for example, permanganate with  $\text{Mn}^{7+}$ , which is extremely purple, and dichromate with Cr(VI), which is bright orange.

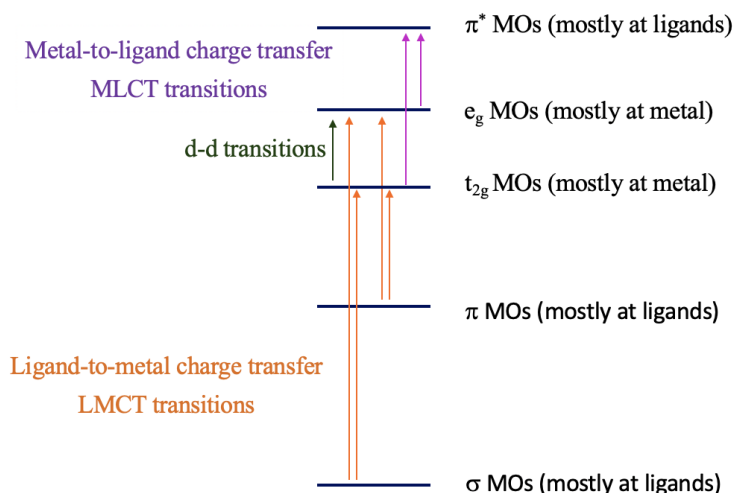


Figure 8.5.3.2: Charge-transfer transitions. Attribution: E.R. Schofield.



The explanation for these phenomena is charge-transfer transitions (8.5.3.2). There are two types of charge-transfer transitions: ligand-to-metal (LMCT) and metal-to-ligand (MLCT) charge transfer transitions. For the ligand-to-metal transitions, electrons from bonding  $\sigma$  and  $\pi$ -orbitals get excited into metal d-orbitals in the ligand field, for example the  $t_{2g}$  and the  $e_g$  orbitals in an octahedral complex. If the energy difference between the  $\sigma/\pi$ -orbitals and the d-orbitals is small enough, then this electron transition is associated with the absorption of visible light. The transition is called a ligand-to-metal transition because the ligand  $\sigma/\pi$ -orbitals are mostly located at the ligands, while the metal-d-orbitals in a ligand field are mostly located at the metal. Vice versa, the metal-to-ligand transition involves the transition of an electron from metal d-orbitals in a ligand field to ligand  $\pi^*$ -orbitals. This

essentially moves electron density from the metal to the ligand, hence the name ligand-to-metal-charge transfer transition. If the energy-difference between the ligand  $\pi^*$  and the metal orbitals is small enough, then the absorption occurs in the visible range. Charge-transfer transitions are usually both spin- and Laporte allowed; hence, if they occur, the color is often very intense. How can we distinguish between d-d and charge transfer transitions? Charge transfer transitions often change in energy as the solvent polarity is varied (solvatochromic), as there is a change in polarity of the complex associated with the charge transfer transition. This can be used to distinguish between d-d transitions and charge-transfer bands.

## LMCT Transitions

Can we predict when the energy windows between the bonding molecular orbitals and the metal d-orbitals are small enough for LMCT transitions in the visible to take place? Generally, it would be desirable if the energy of the metal orbitals were as low as possible and the energy of the bonding ligand orbitals were as high as possible. The energy of metal d-orbitals decreases with increasing positive charge at the metal because the effective nuclear charge on the metal increases. This means that very high metal oxidation states favor LMCT transitions. The d-orbitals should have few or no electrons, so that electrons can be promoted into the orbitals, and orbital energy decreases because electron-electron repulsion is minimized. Examples are Mn(VII), Cr(VI), and Ti(IV). The energy of MOs from bonding ligand orbitals increases when the ligand orbitals have high energy; this is typically the case for  $\pi$ -donor ligands with a negative charge (Fig. 8.2.21).

Ligand properties	Metal ion properties
Ligand MOs: high energy	Valence orbitals: low energy
$\pi$ -donor electrons	high positive charge
Negatively charged ligands	Few or no d electrons
$O^{2-}$ , $Cl^-$ , $Br^-$ , $I^-$	Eg. Mn(VII), Cr(VI), Ti(IV)

8.5.3.1: The properties of the metal ions and ligands suitable for LMCT transitions.  $MnO_4^-$  is deep purple due to LMCT transitions (Attribution: Benjah-bmm27 / Public domain <https://commons.wikimedia.org/wiki/File:Permanganate-sample.jpg>) and (Attribution: Pradana Aumars / CC0 <https://commons.wikimedia.org/wiki/File:Entrations.jpg>), respectively.

Examples of ligands are oxo- and halo ligands. This explains, for example, the LMCT transitions in permanganate. The Mn is in the very high oxidation state +7, and the ligands are oxo-ligands, which are  $\pi$ -donors with a 2- negative charge. The transitions are both Laporte and spin-allowed, leading to a very high intensity of light absorption, and thus color (Fig. 8.2.21).

## MLCT Transitions

What are favorable metal ion and ligand properties for a metal-to-ligand transition, then? In this case we would like to keep the energy of the metal orbitals as high as possible so that the energy difference between a metal d-orbital and a  $\pi^*$ -orbital is minimized. This is accomplished when the positive charge at the metal ion is small, and there are many d-electrons that can repel each other, thereby increasing orbital energies, for example Cu(I), Fig. 8.2.22.

#### Metal ion properties

low metal ion charge

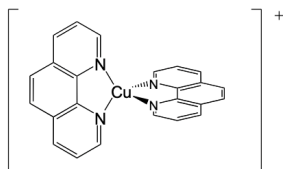
many electrons

Cu(I),  $d^{10}$  ion

#### Ligand properties

$\pi$ -acceptor ligand with low-lying  $\pi^*$  orbitals

1,10-phenanthroline,  $CN^-$ , CO,  $SCN^-$



$[Cu(phen)_2]^+$ , dark orange

#### 8.5.3.3: bis(phenanthroline) copper(+). Attribution: E.R. Schofield.

The ligand should be a  $\pi$ -acceptor with low-lying  $\pi^*$ -orbitals - for example, phenanthroline,  $CN^-$ ,  $SCN^-$ , and CO. The bis(phenanthroline) copper(+) ion, for instance, is dark orange and has an MLCT absorption band at 458 nm. This MLCT transfer is both spin and Laporte-allowed.

It should be mentioned that some complexes allow for both metal-to-ligand and ligand-to-metal transitions. For example, in the  $Cr(CO)_6$  complex, the  $\sigma$ -orbitals are high enough and the  $\pi^*$ -orbitals are low enough in energy to allow for light absorption in the visible range. Finally, intraligand bands are also possible when the ligand is a chromophore.

Dr. Kai Landskron ([Lehigh University](#)). If you like this textbook, please consider to make a donation to support the author's research at Lehigh University: [Click Here to Donate](#).

This page titled [8.5.3: Charge-Transfer Spectra](#) is shared under a [not declared](#) license and was authored, remixed, and/or curated by [Kathryn Haas](#).

- [8.2: Term splitting in ligand fields, selection rules, Tanabe-Sugano diagrams. Metal to ligand, and ligand to metal transitions](#) by Kai Landskron is licensed CC BY 4.0.

## 8.6: Tanabe Sugano Diagrams

---

Learning objectives for this unit are to:

- Know the information provided by a Tanabe Sugano diagram
  - Determine the ground state term symbol for an electron configuration, including total angular momentum and multiplicity
  - Know the conditions under which an electronic transition will be spin-allowed or spin-forbidden and how this affects the intensity of the observed transitions
  - Use Tanabe Sugano diagrams to assign peaks in absorption spectra to specific electronic transitions and calculate  $D_0$  and  $B$  based on absorption spectra
  - Rationalize or predict values for Racah  $B$  based on the size and charge of a metal ion
  - Explain why Racah  $B$  is smaller for complexes compared to free ions
  - Calculate the nephelauxetic factor  $b$  and relate the results to metal-ligand bond covalency
- 

8.6: Tanabe Sugano Diagrams is shared under a [not declared](#) license and was authored, remixed, and/or curated by LibreTexts.

## 8.6.1: Tanabe-Sugano Diagrams

### Introduction

Tanabe-Sugano Diagrams are a form of correlation diagrams. These diagrams show relative energies of terms (eg. electronic microstates) by plotting the splitting energy and the field strength in terms of the Racah Parameter,  $B$  (plotted as  $\frac{E}{B}$  vs  $\frac{\Delta}{B}$ ). The Racah parameter accounts for  $d$ -electron-electron repulsions that affect the energies of the terms (and thus the transition energy). These diagrams are useful for interpreting electronic spectra. Specifically, the diagrams can be used to qualitatively predict the number of spin-allowed and spin-forbidden transitions, the relative intensities of these transitions, and their relative energies. The diagrams can also be used to estimate the  $d$ -orbital splitting energy ( $\Delta$  or  $10D_q$ ) and the strength of field necessary to cause transition between high- and low-spin.

**The Tanabe-Sugano diagrams shown below can be used to interpret the spectra of octahedral complexes of a given electron configuration.** The diagrams for octahedral complexes for  $d^2$ ,  $d^3$ ,  $d^4$ ,  $d^5$ ,  $d^6$ ,  $d^7$  and  $d^8$  are given below. The Tanabe-Sugano diagrams for  $d^0$ ,  $d^1$ ,  $d^9$  and  $d^{10}$  are unnecessary. In the case of  $d^0$  and  $d^{10}$ , there are no possible  $d-d$  transitions because the  $d$ -orbitals are either completely empty or completely full. In the case of  $d^1$ , there is only one free ion term ( $^2D$ ) that is split into a ground state  $^2T_{2g}$  and excited state  $^2E_g$ . There are no electron-electron repulsions to consider, and there is only one possible transition, so the Tanabe-Sugano diagram is unnecessary for  $d^1$ . The case of  $d^9$  is similar and related to  $d^1$  by the "positive hole" concept. In the case of  $d^9$ , the lone  $^2D$  free ion term is split into a ground state  $^2E_g$  term and an excited state  $^2T_{2g}$  term. There is just one transition possible and so the Tanabe-Sugano diagram for  $d^9$  is also unnecessary. In some cases, there are two versions given; a complete version and a simplified version. All diagrams are shown in full-page size.

These diagrams can also be used to interpret the electronic spectra of **tetrahedral complexes**. For a tetrahedral complex with  $d^m$ , use the diagram given below for  $d^{10-m}$ . All "g" subscripts on the terms are irrelevant for tetrahedrons.



Octahedron with 2 d-electrons

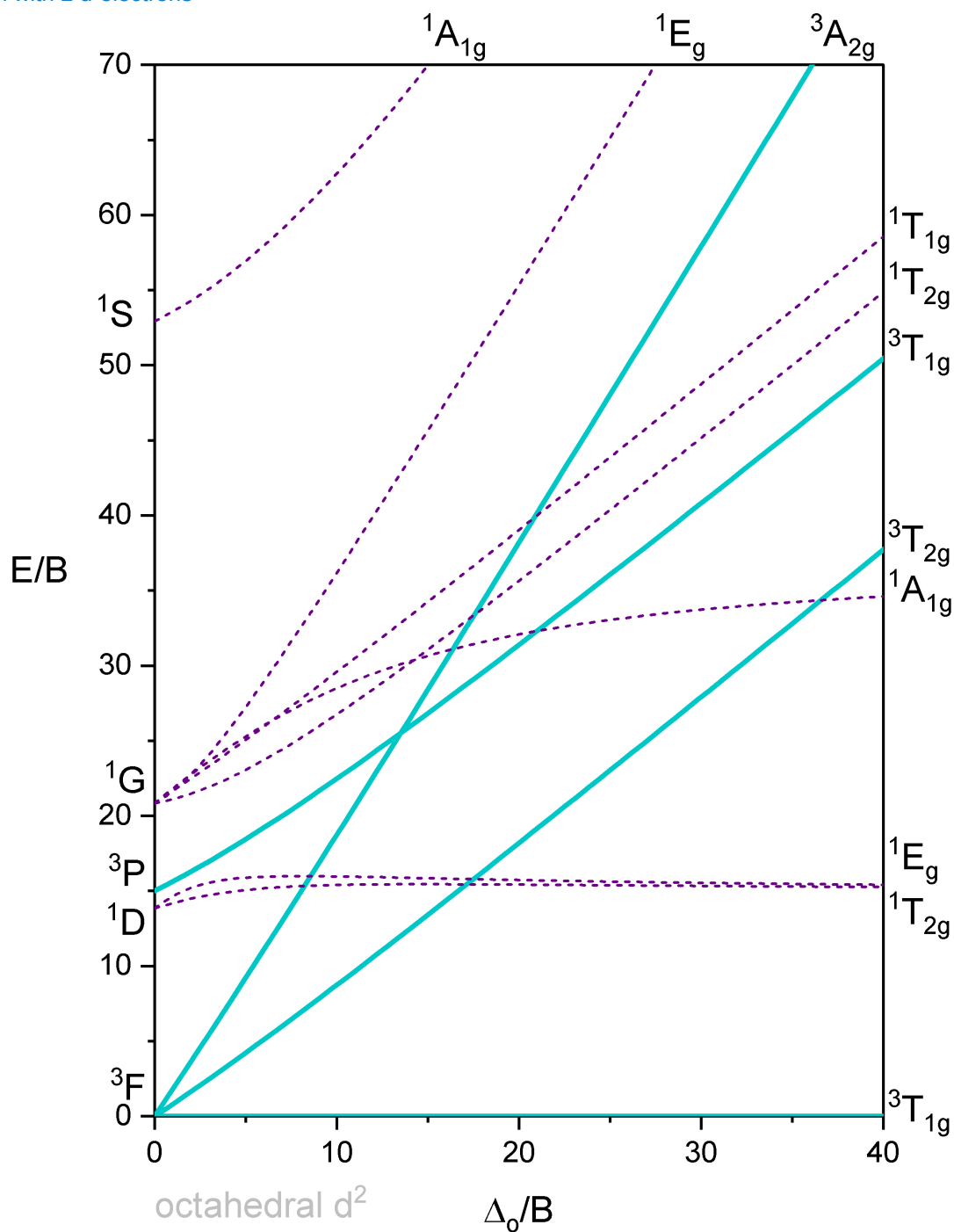


Figure 8.6.1.2:  $d^2$ : Tanabe-Sugano Diagram for octahedral metal complex with two  $d$  electrons. For convenience, terms that can accommodate spin-allowed transitions from the ground state are indicated by solid lines. Terms that have different multiplicity than the ground state are shown in dashed lines. (CC-BY-SA; Kathryn Haas)

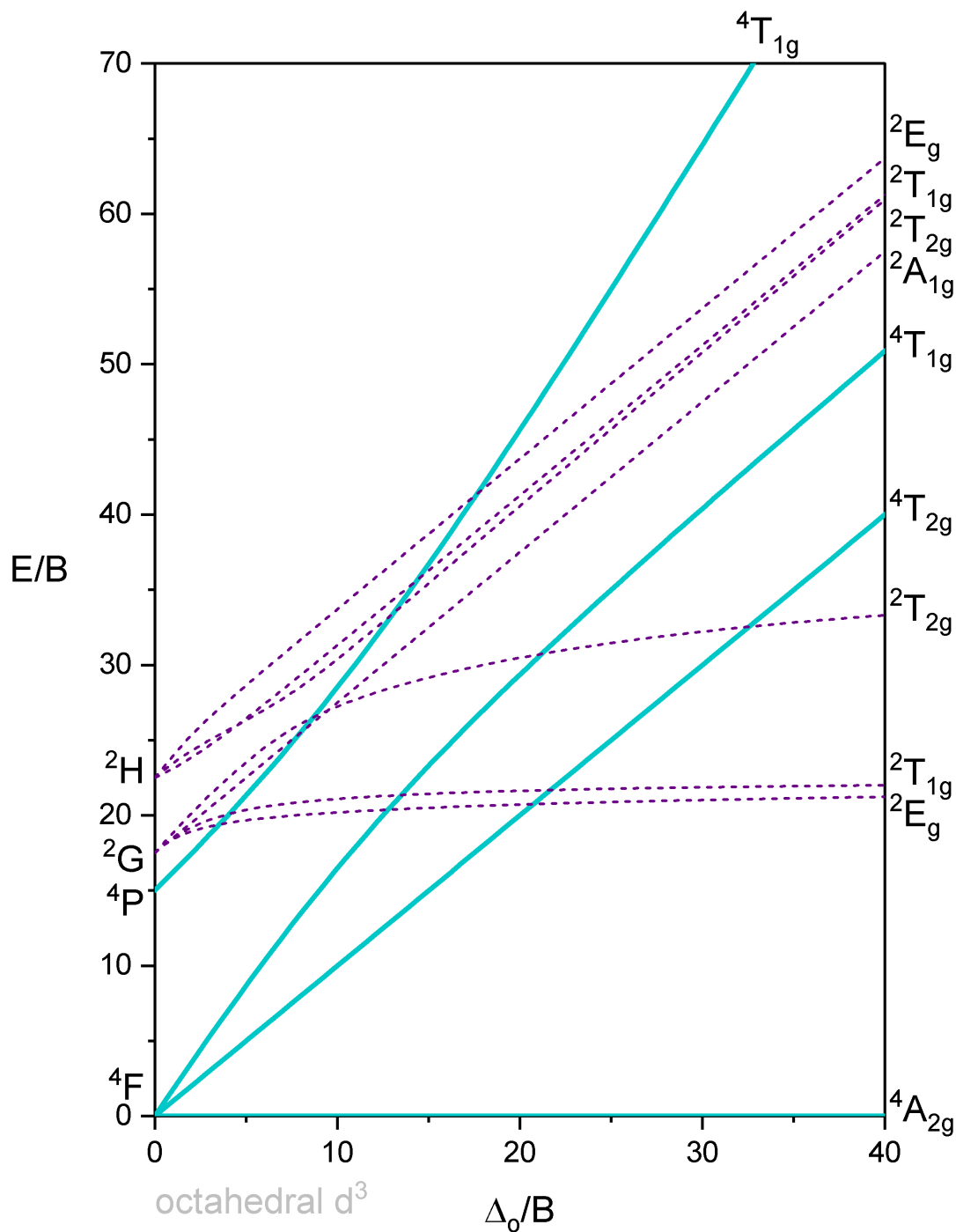


Figure 8.6.1.2:  $d^3$ : Tanabe-Sugano Diagram for octahedral metal complex with three  $d$  electrons. For convenience, terms that can accommodate spin-allowed transitions from the ground state are indicated by solid lines. Terms that have different multiplicity than the ground state are shown in dashed lines. (CC-BY-SA; Kathryn Haas)

### Octahedron with 4 d-electrons

Figure 3 shows a Tanabe-Sugano diagram that includes all terms. A simplified version of the  $d^4$  Tanabe-Sugano Diagram is shown below in Figure 4.

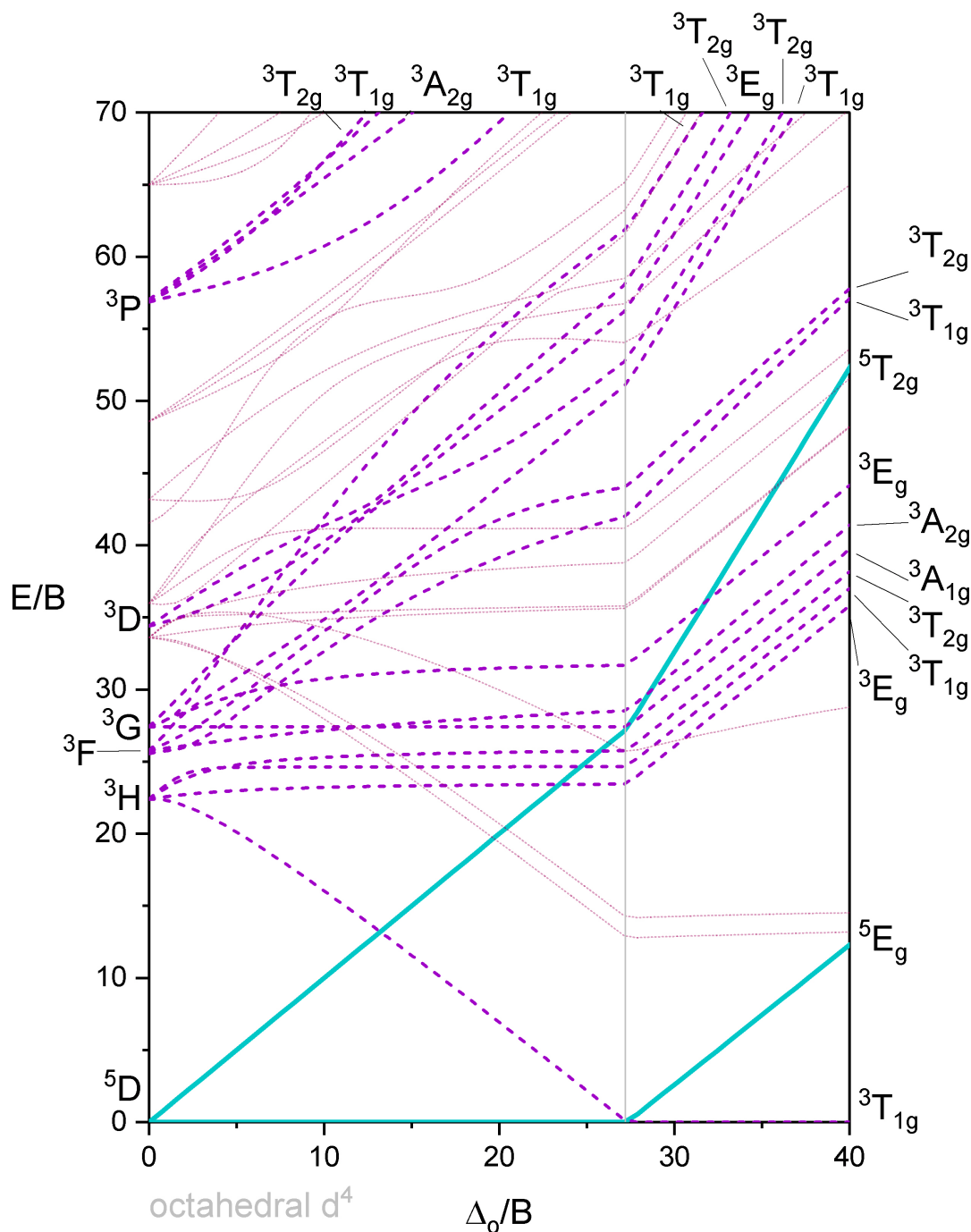


Figure 8.6.1.3:  $d^4$ , full: Tanabe-Sugano Diagram for octahedral metal complex with four  $d$  electrons. A grey vertical line at  $27.2 \frac{\Delta_o}{B}$  divides high spin from low spin cases. For convenience, terms that can accommodate spin-allowed transitions from the pentet ground state in high spin (left of grey line) are indicated by heavy solid lines. Terms that can accommodate spin-allowed transitions from the low spin triplet ground state are shown in heavy dashed lines. Terms that have different multiplicity than either pentet or triplet ground states are shown in lighter dotted lines. For a simplified version of the  $d^4$  diagram, see Figure 8.6.1.4. (CC-BY-SA; Kathryn Haas)

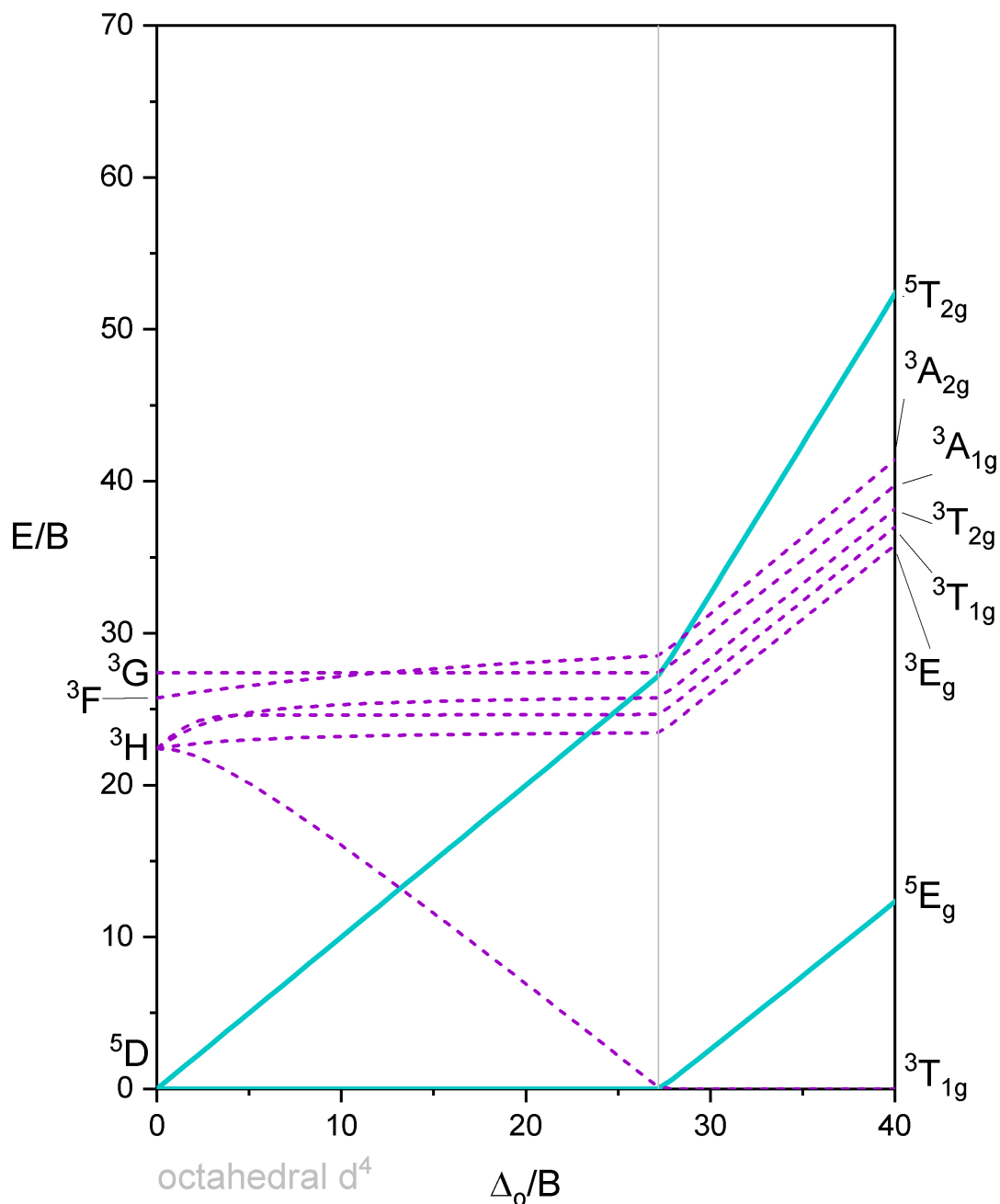


Figure 8.6.1.4:  $d^4$ , simplified: Tanabe-Sugano Diagram for octahedral metal complex with four  $d$  electrons. A grey vertical line at  $27.2 \frac{\Delta_o}{B}$  divides high spin from low spin cases. For convenience, terms that can accommodate spin-allowed transitions from the pentet ground state in high spin (left of grey line) are indicated by heavy solid lines. Terms that can accommodate spin-allowed transitions from the low spin triplet ground state are shown in heavy dashed lines. This version of the  $d^4$  Tanabe Sugano Diagram is abbreviated in that it shows only the spin-allowed terms that are most relevant for interpreting UV-visible spectra. For the full version of a  $d^4$  diagram, see Figure 8.6.1.3. (CC-BY-SA; Kathryn Haas)

### Octahedron with 5 d-electrons

Figure 5 shows a Tanabe-Sugano diagram that includes all terms. A simplified version of the  $d^5$  Tanabe-Sugano Diagram is shown below in Figure 6.

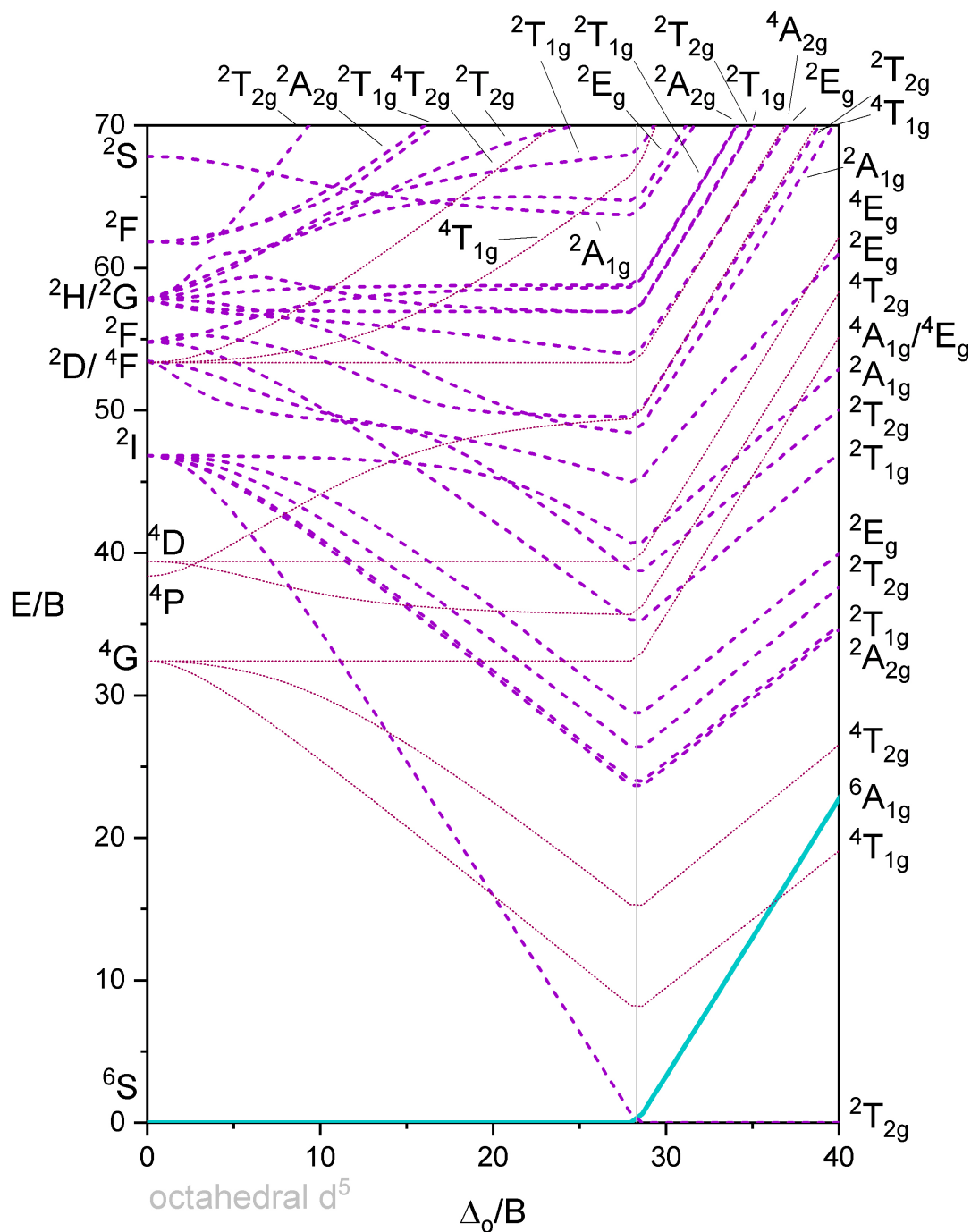


Figure 8.6.1.5:  $d^5$ , full: Tanabe-Sugano Diagram for octahedral metal complex with five  $d$  electrons. A grey vertical line at  $27.3 \frac{\Delta_o}{B}$  divides high spin from low spin cases. For convenience, terms that can accommodate spin-allowed transitions from the sextet ground state in high spin (left of grey line) are indicated by heavy solid lines. Terms that can accommodate spin-allowed transitions from the low spin doublet ground state are shown in heavy dashed lines. Terms that have different multiplicity than ground states are shown in lighter dotted lines. For a simplified version of the  $d^5$  diagram, see Figure 8.6.1.6. (CC-BY-SA; Kathryn Haas)

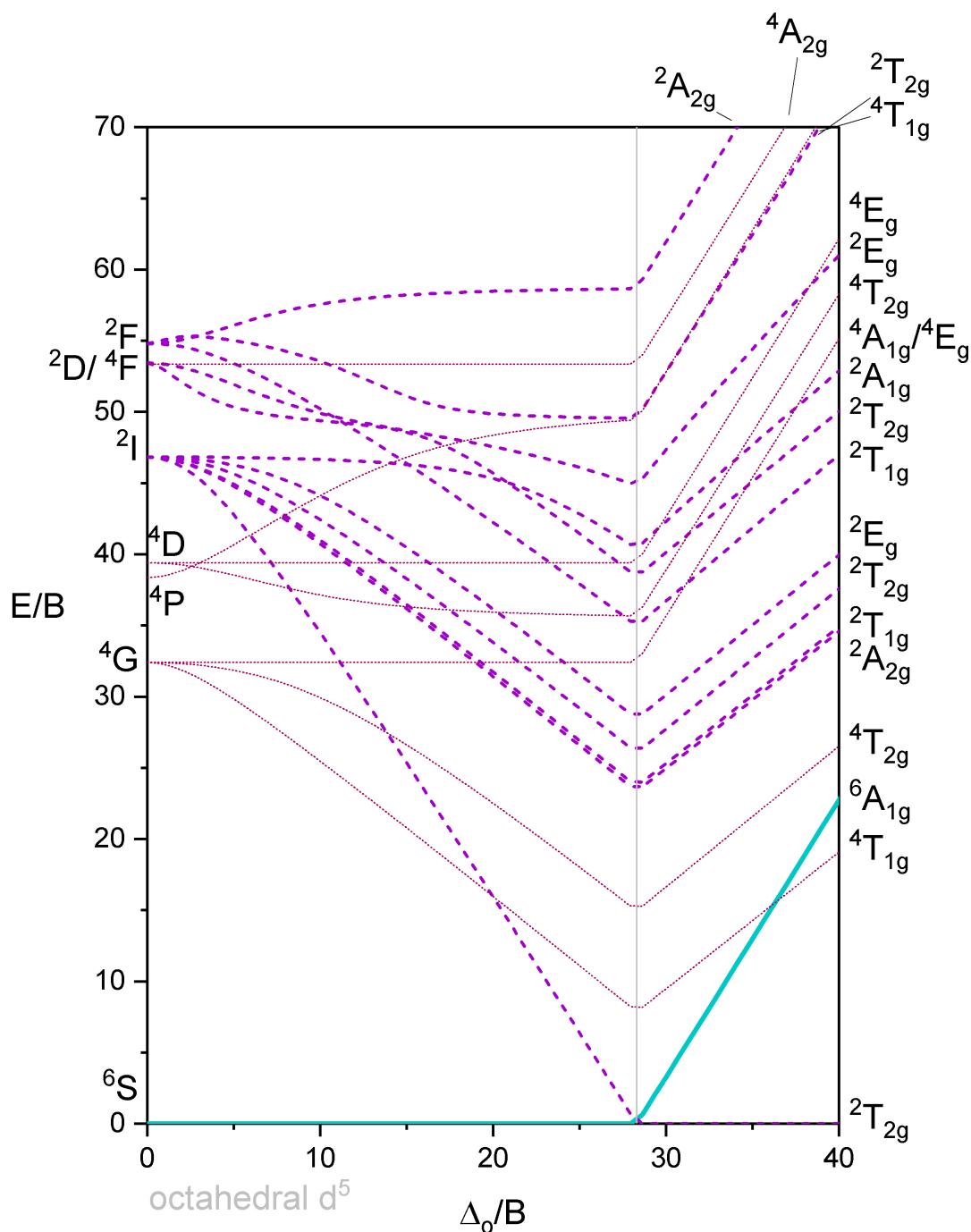


Figure 8.6.1.6:  $d^5$ , simple: Tanabe-Sugano Diagram for octahedral metal complex with five  $d$  electrons. A grey vertical line at  $27.3 \frac{\Delta_o}{B}$  divides high spin from low spin cases. For convenience, terms that can accommodate spin-allowed transitions from the sextet ground state in high spin (left of grey line) are indicated by heavy solid lines. Terms that can accommodate spin-allowed transitions from the low spin doublet ground state are shown in heavy dashed lines. Terms that have different multiplicity than ground states are shown in lighter dotted lines. This version of the  $d^5$  Tanabe Sugano Diagram is abbreviated for simplicity and for the purpose of interpreting UV-visible spectra. For the full version of a  $d^5$  diagram, see Figure 8.6.1.5 (CC-BY-SA; Kathryn Haas)

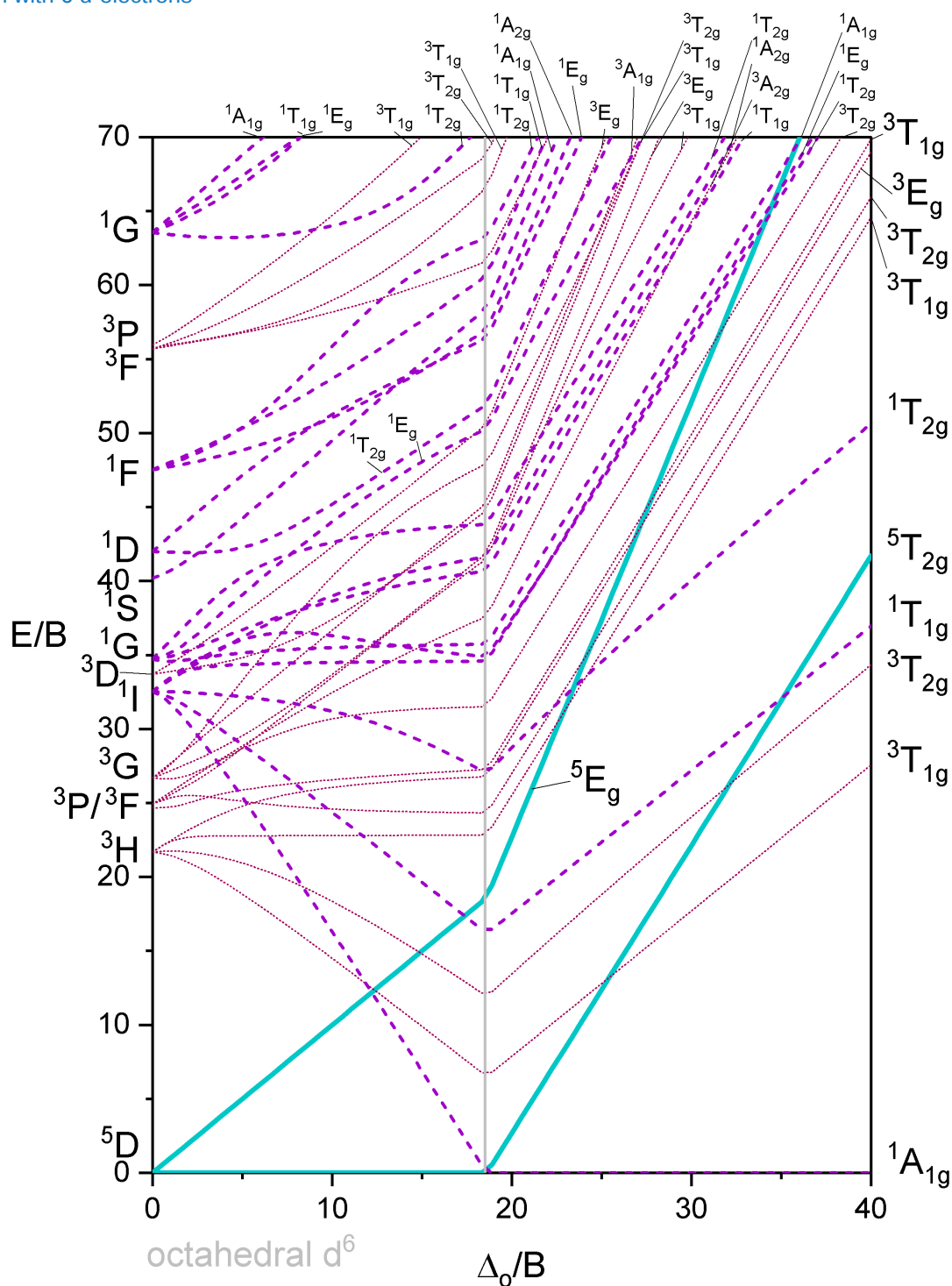


Figure 8.6.1.7:  $d^6$ : Tanabe-Sugano Diagram for octahedral metal complex with six  $d$  electrons. A grey vertical line at  $18.5 \frac{\Delta_o}{B}$  divides high spin from low spin cases. For convenience, terms that can accommodate spin-allowed transitions from the pentet ground state in high spin (left of grey line) are indicated by heavy solid lines. Terms that can accommodate spin-allowed transitions from the low spin singlet ground state are shown in heavy dashed lines. Terms that have different multiplicity than ground states are shown in lighter dotted lines. (CC-BY-SA; Kathryn Haas)

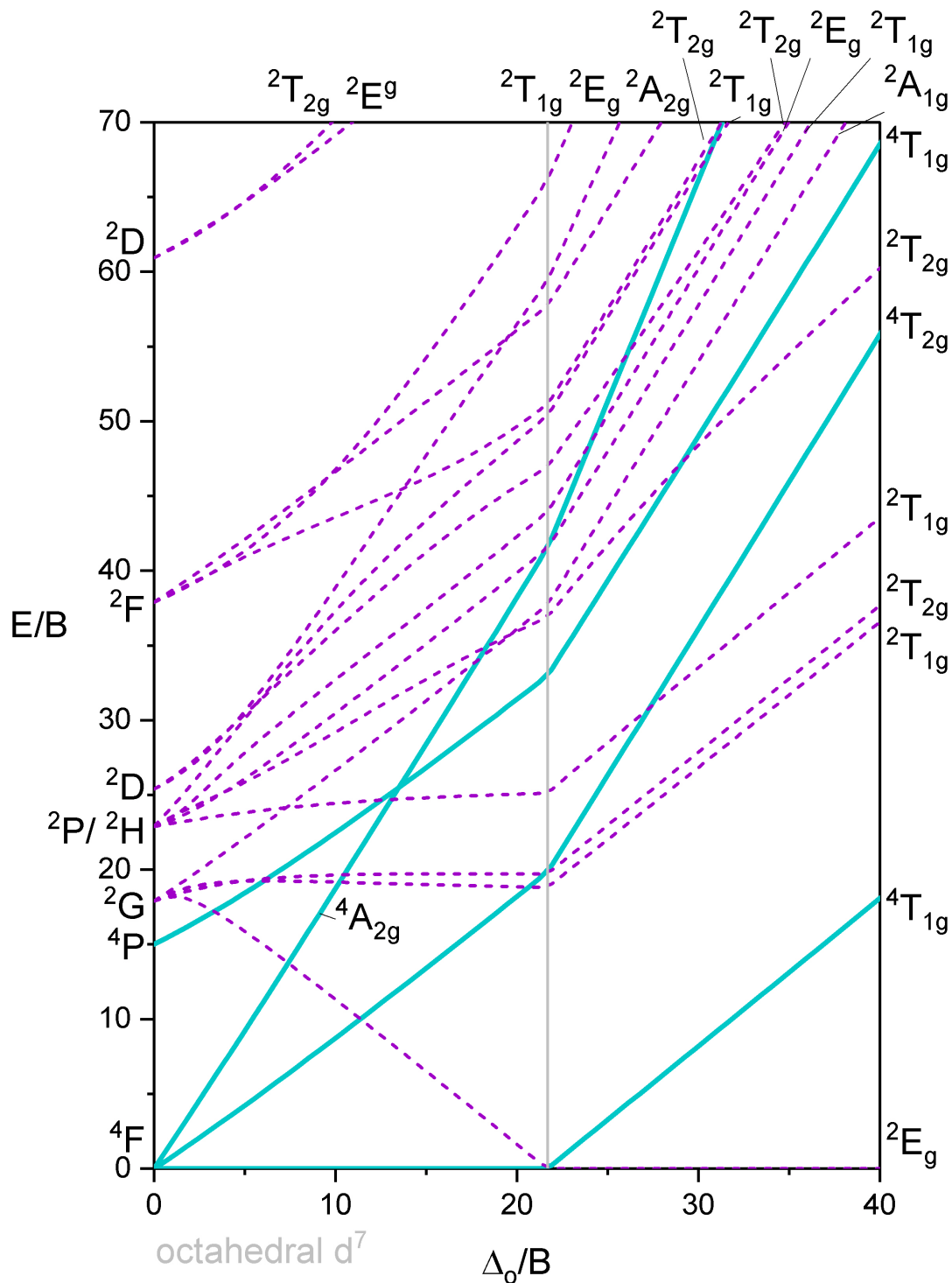


Figure 8.6.1.8:  $d^7$ : Tanabe-Sugano Diagram for octahedral metal complex with seven  $d$  electrons. A grey vertical line at  $21.7 \frac{\Delta_o}{B}$  divides high spin from low spin cases. For convenience, terms that can accommodate spin-allowed transitions from the quartet ground state in high spin (left of grey line) are indicated by heavy solid lines. Terms that can accommodate spin-allowed transitions from the low spin doublet ground state are shown in heavy dashed lines. (CC-BY-SA; Kathryn Haas)



Octahedron with 8 d-electrons

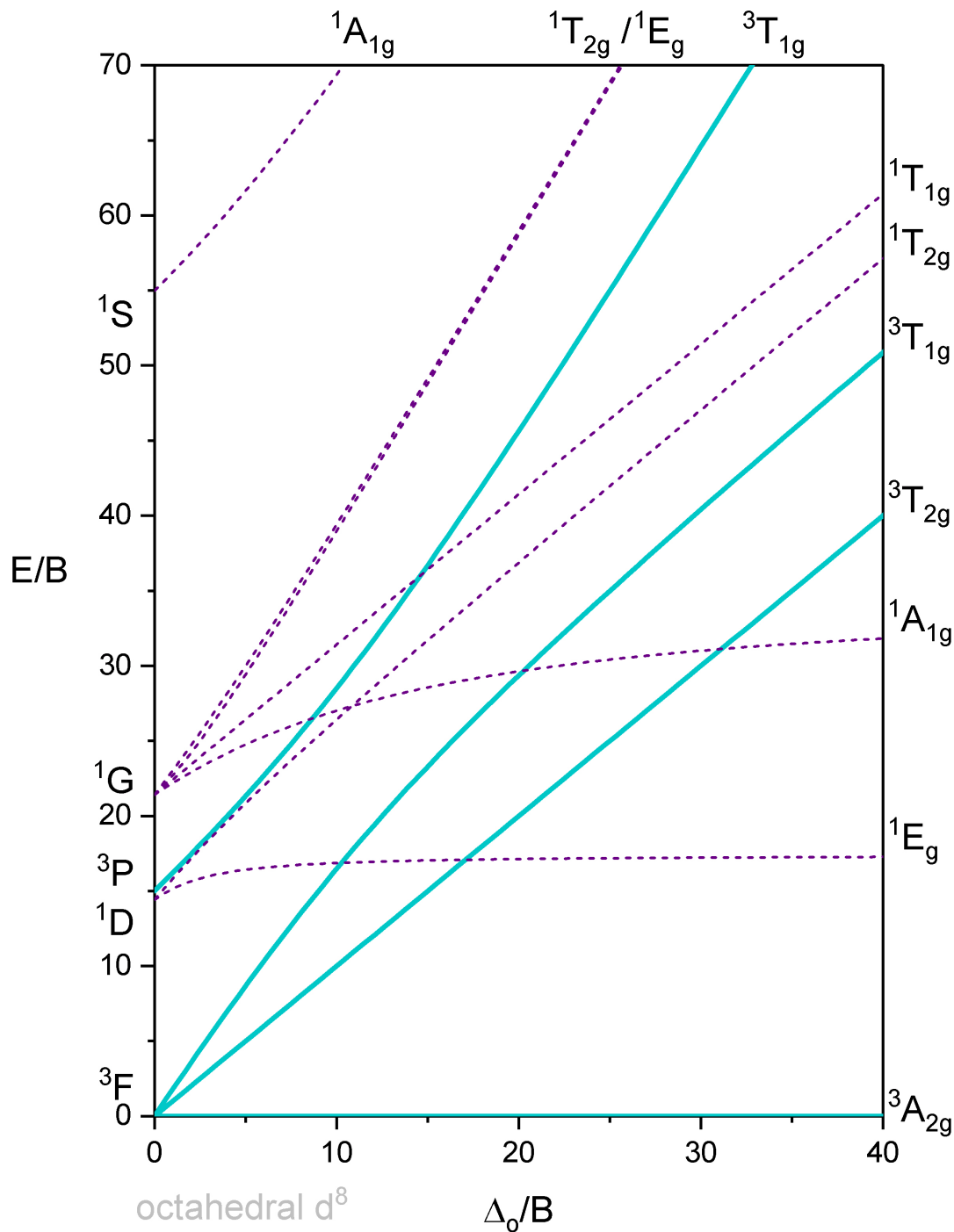


Figure 8.6.1.9:  $d^8$ : Tanabe-Sugano Diagram for octahedral metal complex with eight  $d$  electrons. For convenience, terms that can accommodate spin-allowed transitions from the ground state are indicated by solid lines. Terms that have different multiplicity than the ground state are shown in dashed lines. (CC-BY-SA; Kathryn Haas)

## 8.6.2: Selection Rules

Electronic transitions between states of different energies give rise to electronic spectra. However, some transitions are more probable, and thus more intense, than others. In UV-vis spectroscopy, for example, the transitions that are "allowed" can give rise to absorption bands that are much more intense than transitions that are "forbidden". To be clear, "forbidden" transitions are still possible, and are sometimes observable, but are less intense because they happen less frequently than "allowed" transition when the molecules are exposed to electromagnetic radiation.

### Selection Rules that govern Electronic Transitions

The Selection Rules governing transitions between electronic energy levels (including microstates and terms) are:

1. **The Spin Selection Rule**,  $\Delta S = 0$ .
2. **The Laporte (or orbital) Selection Rule**, for centrosymmetric molecules  $g \rightarrow u$  or  $u \rightarrow g$ , or  $\Delta l = \pm 1$ .

### Selection rules that govern electronic transitions

#### Spin selection rule

The Spin Selection Rule forbids transitions between states with different total spin, and thus different spin multiplicity. This rule allows transitions only between states with the same total intrinsic spin ( $\Delta S = 0$ ), and thus the same spin multiplicity value in the term symbol. In other words, the direction of the promoted electron's spin should not change. Just in case it is not obvious yet, the spin multiplicity is the left superscript in the term symbol, so this rule allows transitions between terms with the same superscript. For example, this rule would allow a transition from a  $^3T$  term to a  $^3A$  term, but not from  $^3T$  to  $^2D$ .

#### Laporte (orbital) Selection Rule

The Laporte Selection Rule applies to molecules that have a center of symmetry (aka center of inversion, centrosymmetric). This rule forbids transitions between states with the same parity (symmetry) with respect to an inversion center ( $i$ ). Parity is indicated on molecular orbitals and on term symbols with subscripts  $g$  (gerade, or even) and  $u$  (ungerade, or uneven). Transitions between  $u$  and  $g$  terms are allowed (eg  $T_{2g} \rightarrow T_{1u}$  is allowed), but those between two  $g$  or two  $u$  terms are forbidden (eg  $T_{2g} \rightarrow T_{1g}$  is forbidden). Because different types of orbitals have different symmetries with respect to  $i$ , this rule is sometimes referred to as the "orbital selection rule". It forbids transitions within one type of orbital subshell. For example,  $p$  orbitals are antisymmetric with respect to  $i$ , while both  $s$  and  $d$  orbitals are symmetric with respect to  $i$ . This rule forbids  $s \rightarrow s$ ,  $p \rightarrow p$ ,  $d \rightarrow d$ , and  $d \rightarrow s$  transitions, but allows transition between  $d \rightarrow p$  and  $d \rightarrow s$  orbitals. This rule is important in transition metal complexes because it forbids  $d-d$  transitions in centrosymmetric geometries, including octahedral and linear coordination geometries.

Despite these selection rules,  $d \rightarrow d$  transitions are a hallmark feature of octahedral transition metal complexes, and are often responsible for their brilliant colors. These  $d \rightarrow d$  transitions, and other forbidden transitions may still occur, primarily through relaxation of these rules in specific cases.

### Breaking the rules!

Relaxation of the Laporte and Spin Selection Rules can occur through:

- **Vibronic coupling:** the bonds of metal complexes vibrate and may cause temporary distortions in molecular symmetry. These distortions can cause temporary loss in symmetry (as well as some orbital mixing), and thus allow  $d \rightarrow d$  transitions in those moments of distortion. Despite being forbidden by the Laporte Selection rule, the  $d \rightarrow d$  transitions in octahedral complexes appear, but are weak (of low intensity) with molar absorptivities  $\leq 100 \text{ M}^{-1} \text{ cm}^{-1}$ .
- **Orbital Mixing:** In the case of octahedral complexes,  $\pi$ -acceptor and  $\pi$ -donor ligands can mix with the  $d$ -orbitals so that transitions are no longer purely  $d \rightarrow d$  (but these are usually considered "charge transfer" transitions, not  $d \rightarrow d$ ). In the case of tetrahedral complexes, the molecule has no center of symmetry (thus no  $u$  or  $g$  subscripts on the terms). In the valence orbital model, a tetrahedral molecule is said to have  $sp^3$  and  $sd^3$  hybridized orbitals, while MO theory predicts MO's with mixtures of some  $s$ ,  $p$ , and  $d$  character - this mixing of orbital types can allow transitions between "mixed" orbitals that would otherwise be forbidden in "pure" orbitals. A similar phenomenon would occur in octahedrons with significant distortion, or in other coordination geometries that provide potential for orbital mixing.

- **Spin-Orbit coupling:** This gives rise to spin-forbidden bands of low intensity, usually with very weak molar absorptivities approximately  $\leq 1 M^{-1} cm^{-1}$ . This phenomenon is usually more important for transition metals of the second row  $4d$  and beyond.

#### ? Exercise 8.6.2.1

Consider the  $d^2$  case presented in a [previous section](#). The free ion terms for  $d^2$  were found to be  $^3F$ ,  $^1G$ ,  $^3P$ ,  $^1D$ ,  $^1S$ . First, identify the ground state term. Then identify the Spin-Allowed excitations starting from the ground state.

#### Answer

The ground state is  $^3F$ . There is only one spin-allowed transition:  $^3F \rightarrow ^3P$ .

The spin-forbidden transitions from  $^3F$  include  $^3F \rightarrow ^1D$ ,  $^3F \rightarrow ^1G$ , and  $^3F \rightarrow ^1S$ .

This page titled [8.6.2: Selection Rules](#) is shared under a [not declared](#) license and was authored, remixed, and/or curated by [Kathryn Haas](#).

- [Selection Rules for Electronic Spectra of Transition Metal Complexes](#) by [Robert J. Lancashire](#) is licensed [CC BY 4.0](#).

### 8.6.3: Applications of Tanabe-Sugano Diagrams

The Tanabe-Sugano diagrams can be used to interpret absorption spectra and gain insight into the properties of a coordination complex. For example, you could use the appropriate diagram to predict the number of transitions, assign the identity of a specific transition, or calculate the value of  $\Delta$  for a specific metal complex.

#### How to use the Tanabe-Sugano Diagrams

1. Determine the  $d$ -electron count of the metal ion of interest.
2. Choose the appropriate Tanabe-Sugano diagram: this is the one matching the  $d$ -electron count of the metal ion. There is a full list of [Tanabe-Sugano diagrams in the Resources Section](#).
3. Acquire an electronic spectrum of the metal complex and identify  $\lambda_{max}$  for spin-allowed (strong intensity) and spin forbidden (weak intensity) transitions.
4. Convert wavelength ( $\lambda_{max}$ ) to energy (E) in wavenumbers ( $cm^{-1}$ ) and generate energy ratios relative to the lowest-energy allowed transition. (i.e.  $\frac{E_2}{E_1}$  and  $\frac{E_3}{E_1}$ ).
5. Using a ruler, slide it across the printed Tanabe-Sugano diagram until the E/B ratios between lines is equivalent to the ratios found in step 4.
6. Solve for B using the E/B values (y-axis, step 4) and  $\Delta_{oct}/B$  (x-axis, step 5) to yield the ligand field splitting energy, *Delta* (Sometimes this is labeled as  $10D_q$ , and it is useful to know that  $\Delta = 10D_q$ ).

#### ✓ Example 8.6.3.1: Chromium Splitting

A  $Cr^{3+}$  metal complex has strong transitions and  $\lambda_{max}$  at

- 431.03 nm,
- 781.25 nm, and
- 1,250 nm.

Determine the  $\Delta_{oct}$  for this complex.

#### Solution

1. Cr has 6 electrons.  $Cr^{3+}$  has three electrons, so it has a d-configuration of  $d^3$
2. Locate the  $d^3$  Tanabe-Sugano diagram
3. Convert to wavenumbers:

$$\frac{10^7 (nm/cm)}{1250 nm} = 8,000 cm^{-1} \quad (8.6.3.1)$$

$$\frac{10^7 (nm/cm)}{781.25 nm} = 13,600 cm^{-1} \quad (8.6.3.2)$$

$$\frac{10^7 (nm/cm)}{431.03 nm} = 23,200 cm^{-1} \quad (8.6.3.3)$$

4. Allowed transitions are  ${}^4T_{1g} \leftarrow {}^4A_{2g}$ ,  ${}^4T_{1g} \leftarrow {}^4A_{2g}$  and  ${}^4T_{2g} \leftarrow {}^4A_{2g}$ .

Transition	Energy $cm^{-1}$	Ratios to lowest
${}^4T_{1g} \leftarrow {}^4A_{2g}$	23,200	2.9
${}^4T_{1g} \leftarrow {}^4A_{2g}$	13,600	1.7
${}^4T_{2g} \leftarrow {}^4A_{2g}$	8,000	1

5. Sliding the ruler perpendicular to the x-axis of the  $d^3$  diagram yields the following values:

$\Delta_{oct}/B$	10	20	30	40
Height $E(v_3)/B$	29	45	64	84

$\Delta_{\text{oct}}/B$	10	20	30	40
Height $E(v_2)/B$	17	30	40	51
Height $E(v_1)/B$	10	20	30	40
Ratio $E(v_3)/E(v_1)$	2.9	2.25	2.13	2.1
Ratio $E(v_2)/E(v_1)$	1.7	1.5	1.33	1.275

6. Based on the two tables above it should be assessed that the  $\Delta_{\text{oct}}/B$  value is 10. B is found by dividing E by the height.

Energy $\text{cm}^{-1}$	Height	B
23,200	29	800
13,600	17	800
8,000	10	800

7. Next multiply  $\Delta_{\text{oct}}/B$  by B to yield the  $\Delta_{\text{oct}}$  energy.

$$10 \times 800 = 8000 \text{ cm}^{-1} = \Delta_{\text{oct}} \quad (8.6.3.4)$$

Each problem is of varying complexity as several steps may be needed to find the correct  $\Delta_{\text{oct}}/B$  values that yield the proper energy ratios.

This page titled [8.6.3: Applications of Tanabe-Sugano Diagrams](#) is shared under a [not declared](#) license and was authored, remixed, and/or curated by [Kathryn Haas](#).

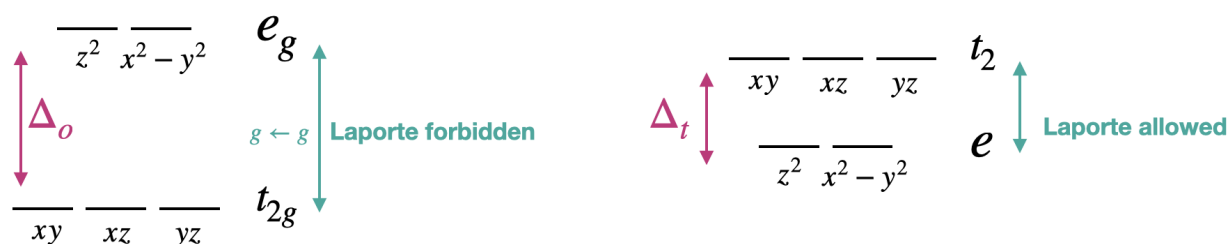
## 8.6.4: Tetrahedral Complexes

### Transitions in tetrahedral complexes are Laporte-allowed

Tetrahedral metal complexes often have more intense electronic transitions than their octahedral counterparts. This is due to the fact that the  $d-d$  transitions in a tetrahedron are allowed by the Laporte selection rule, while  $d-d$  transitions in an octahedral complex are Laporte-forbidden. Recall that the Laporte selection rule applies to centrosymmetric complexes only. The Laporte rule applies to octahedral complexes but not to tetrahedral complexes because a tetrahedron does not have a center of inversion. Notice that the terms (and orbital labels) in a tetrahedron do not include the  $g$  subscripts that are present under octahedral symmetry (Figure 8.6.4.1). The splitting pattern of a tetrahedral complex is exactly opposite to the octahedral case. In the case of a tetrahedron, however, the " $g$ " subscripts are inappropriate because of the tetrahedron's lack of a center of inversion, and transitions between the terms in a tetrahedron do not violate the Laporte Rule.

Another way to explain this in terms of electron transitions between orbitals is through the orbital mixing required to form a tetrahedral complex. Orbital types (i.e.,  $s, p, d$ ) must mix to form the molecular orbitals of a tetrahedral transition metal complex. The mixing of  $s$  and  $p$  orbitals with the  $d$  orbitals allows transitions that are forbidden in the case of pure  $d$ -orbitals.

It is also worth noting that  $\Delta_t = \frac{4}{9}\Delta_o$ . The smaller  $\Delta$  for transition metals means that the tetrahedral complexes can absorb at a lower energy and longer wavelength relative to an analogous octahedron.



### Octahedral field

### Tetrahedral field

Figure 8.6.4.1:  $d-d$  transitions in octahedral complexes are Laporte-forbidden, while those in tetrahedral complexes are Laporte-allowed. (CC\_BY\_SA; Kathryn Haas)

### Tanabe-Sugano diagrams for tetrahedral complexes

Due to the opposite splitting pattern, the transitions for a  $d^n$  tetrahedral complex are sufficiently represented by the  $d^{10-n}$  Tanabe-Sugano diagram (just drop the  $g$  subscripts from the diagrams). For example, the electronic spectrum of a  $d^8$  tetrahedral complex (e.g.,  $[\text{Ni}(\text{H}_2\text{O})_6]^{2+}$ ) can be interpreted using the  $d^2$  Tanabe-Sugano diagram.

This page titled 8.6.4: Tetrahedral Complexes is shared under a [not declared](#) license and was authored, remixed, and/or curated by Kathryn Haas.

## CHAPTER OVERVIEW

### Unit 9: Reactions of Coordination Complexes

#### 9.1: Substitution Reactions

##### 9.1.1: Review of Reaction Thermodynamics and Kinetics

##### 9.1.2: Introduction to Substitution Reactions

##### 9.1.3: Ligand Substitution Mechanisms

##### 9.1.4: Some Reasons for Differing Mechanisms

###### 9.1.4.1: Dissociation

###### 9.1.4.2: Associative Mechanisms

##### 9.1.5: Thermodynamic Stability and Chelate Effect

##### 9.1.6: Kinetic Lability

##### 9.1.7: The Trans Effect

#### 9.2: RedOx Reactions

##### 9.2.1: Redox Mechanisms

##### 9.2.2: Inner Sphere Electron Transfer

##### 9.2.3: Outer Sphere Electron Transfer

#### 9.3: Unit 9 Practice Problems

---

This page titled [Unit 9: Reactions of Coordination Complexes](#) is shared under a [not declared](#) license and was authored, remixed, and/or curated by [Kathryn Haas](#).

## 9.1: Substitution Reactions

---

Lecture objectives for this unit are to:

- Compare and contrast the properties of labile, inert, stable, and unstable as used to describe coordination compounds
  - Compare and contrast the three mechanistic pathways (dissociative, associative, and interchange) for ligand substitution reactions
  - Describe the conditions that favor associative or dissociative mechanisms
  - Use reaction order and kinetic data to differentiate between possible mechanistic pathways
  - Describe the chelate effect and explain its entropic origin
  - Use the Irving-Williams series to explain the stability of coordination complexes based on LFSE
  - Predict or explain the lability of coordination complexes based on charge, size, LFSE, bond strength, and ligand nucleophilicity
  - Use the trans effect to predict or explain the product of a square planar substitution reaction
- 

9.1: Substitution Reactions is shared under a [not declared](#) license and was authored, remixed, and/or curated by LibreTexts.



## 9.1.1: Review of Reaction Thermodynamics and Kinetics

### Review of reaction coordinate diagrams and terms

Before we begin our discussion of reactions, let's review some of the vocabulary and models that chemists use to understand reactions.

A chemical reaction can be represented with a reaction coordinate diagram in which the total potential energy of a state is plotted in the vertical  $y$  axis, and the "**reaction coordinate**" (sometimes also referred to as "reaction progress", or "extent of reaction") is plotted on the horizontal  $x$  axis. The reaction coordinate is often drawn as the progress of a reaction from reactants (R) on the left to products (P) on the right.\* Examples of reaction coordinate diagrams for a one-step and a two-step reaction are shown in Figure 9.1.1.1. Notice the difference in the reaction profile that depends on the number of reaction steps. A one-step reaction has one "hill" shape, while a two step reaction takes on a "saddle" shape.

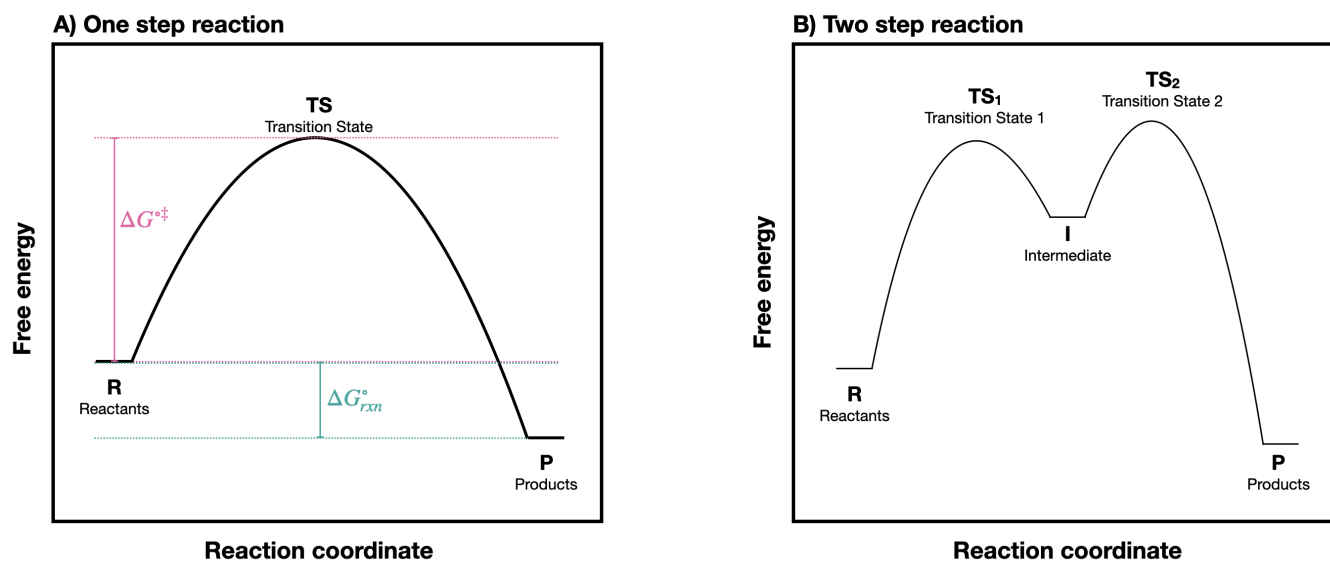


Figure 9.1.1.1: Examples of a reaction coordinate diagram for a one-step reaction (left), and a two-step reaction (right). (CC-BY-SA; Kathryn Haas)

\*Many students find it helpful to envision the horizontal axis in an reaction coordinate diagram as being analogous to the progress bar at the bottom of a youtube video.

### Thermodynamics

The difference in energy between reactants (R) and products (P) indicates whether reactants or products will dominate at thermodynamic equilibrium. At standard conditions, this difference is the standard Gibbs Free Energy of the reaction ( $\Delta G^{\circ}_{rxn}$  or  $\Delta G^{\circ}$ ). The Gibbs free-energy change is a combination of enthalpy change ( $\Delta H^{\circ}$ ) and entropy change ( $\Delta S^{\circ}$ ):

$$\Delta G^{\circ} = \Delta H^{\circ} - T\Delta S^{\circ}$$

where

- $T$  is the temperature in Kelvin (recall that the Kelvin temperature is simply the Celsius temperature plus 273.15).
- Enthalpy change ( $\Delta H^{\circ}$ ) is the heat released or absorbed by the reaction.
- Entropy change ( $\Delta S^{\circ}$ ) is the change in disorder from reactants to products. In a reaction in which one molecule cleaves into two smaller molecules, for example, disorder increases, so  $\Delta S^{\circ}$  is positive.

The standard Gibbs free energy change for a reaction can be related to the reaction's equilibrium constant  $K_{eq}$  by the equation:

$$\Delta G^{\circ} = -RT \ln K_{eq}$$

where  $R$  is the gas constant (8.314 J/mol×K) and  $T$  is the temperature in Kelvin (K).

A negative value for  $\Delta G^{\circ}_{rxn}$  (an exergonic reaction) corresponds to  $K_{eq}$  being greater than 1, an equilibrium constant which favors product formation. Conversely, an endergonic reaction has a positive value of  $\Delta G^{\circ}$ , and a  $K_{eq}$  between 0 and 1.

## Kinetics

The highest point between two energy minima is a transition state (TS). The difference in energies of the reactant and the highest-energy TS is the standard free energy of activation ( $\Delta G^\ddagger$ ). The activation energy, in combination with the temperature at which the reaction is being run, determines the rate of a reaction: the higher the activation energy, the slower the reaction. The rate constant ( $k$ ) is the proportionality constant relating the rate of the reaction to the concentrations of reactants. The relationship between activation energy and the rate constant,  $k$ , is given by the Arrhenius equation:

$$k = Ae^{-\frac{E_a}{RT}} \quad \text{or} \quad \ln k = \ln A - \frac{E_a}{RT}$$

A rate law is an expression showing the relationship of the reaction rate to the concentrations of each reactant. The rate is defined as the change in reactants or products over time. For example, in a reaction of two reactants ( $R_1$  and  $R_2$ ) to form product (P), a rate law could be written as follows:

$$\frac{d[P]}{dt} = k[R_1][R_2]$$

The rate law above is second order overall, and first order with respect to both  $R_1$  and  $R_2$ . The order indicates the power of reactant concentrations for individual reactants or overall for the reaction.

In a one-step reaction, the product is formed in one step. There is an energy barrier to overcome so that this process can happen. At the height of that energy barrier is the TS. In a one-step reaction, there is one transition state. In contrast, in a two-step reaction, there are two transition states and an intermediate (denoted by the letter I). The first step from R to I, passes over transition state  $TS_1$ , is endergonic. The second step passing through transition state  $TS_2$  is exergonic. The intermediate (I) is thus depicted as an energy 'valley' (a local energy minimum) situated between the two energy maxima;  $TS_1$  and  $TS_2$ .

In Figure 9.1.1.B, notice that the energy barrier for the first step is larger than the energy barrier for the second step. This means that the first step is slower than the second. In a multi-step reaction, the slowest step - the step with the largest energy barrier - is referred to as the rate-limiting or rate-determining step. The rate-determining step can be thought of as the 'bottleneck' of the reaction: a factor which affects the rate-determining step will affect the overall rate of the reaction. Conversely, a factor which affects only a much faster step will not significantly affect the rate of the overall reaction.

## Summary and Key Terms

Reaction coordinate diagrams convey some very important ideas about how the reaction can proceed, and about the thermodynamics and kinetics of the reaction. In the sections that follow, the following key terms will be used:



### Description of Key Terms

**Reactants (R):** The molecular species that are the starting materials for a chemical reaction. These are often written at the left side of a reaction coordinate diagram.

**Products (P):** The molecular species that result from a chemical reaction. These are often written at the right side of a reaction coordinate diagram.

**Transition State (TS):** a transition state is the transient species that exists at an energy maximum. In other words, TS's are highest-energy structures along a reaction pathway. Hammond's postulate suggests that the structure of a transition state should resemble the lower-energy species (R, P, or I) adjacent to it along the reaction coordinate, and most closely resembles the structure of the species closest in energy.

**Intermediate (I):** an intermediate is a high-energy structure at a local minimum. Intermediates are sometimes thought of as long-lived transition states. Unlike transition states, intermediates sometimes exist long enough and in high enough concentration to be detectable experimentally.

**Microscopic reversibility:** if a reaction can proceed in the forward direction from R to P, then in principle, it can also proceed in the reverse direction from P to R. There may be many possibilities for how a reaction *could* happen, but the lowest-energy pathway in the forward direction is also the lowest energy pathway in the reverse direction. In other words, the reactions passes through the same lowest-energy I and TS in the forward and reverse directions.

**Steady-State Approximation:** the concentration of an intermediate is assumed to react as quickly as it forms. This approximation allows us to assume that concentration of an intermediate remains "steady" throughout the reaction progress. This approximation is useful for analysis of reaction kinetics.

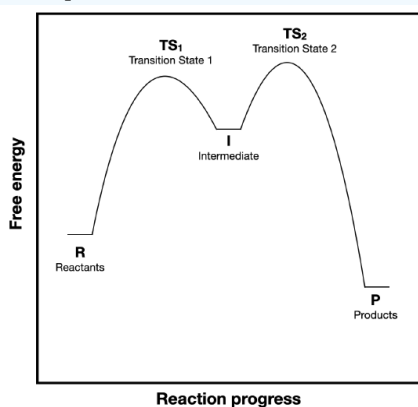
**Order:** The order of a reaction indicates the power of total reactant concentration in a kinetic rate law. The order of a reactant indicates that reactant's power in the rate law. For example, is a rate law that is  $\text{Rate} = k[A]^2[B]$ , the reaction is second order in A, first order in B and third order overall. If there were also a reactant, C, that was not part of the rate law, the reaction would be zero order with respect to C.

### ? Exercise 9.1.1.1

Figure 9.1.1.1 is replicated below for convenience. This figure shows a reaction coordinate diagram for a two-step reaction.

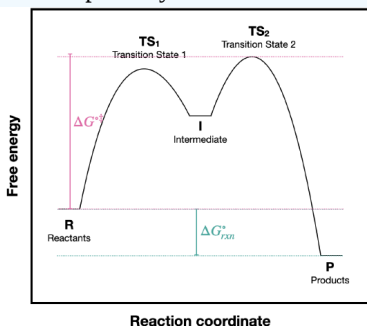
a. ( $\Delta G^\circ$ ) and  $\Delta G^{\ddagger}$  are labeled on Figure 9.1.1.1A but not on Figure 9.1.1.1B Add the appropriate labels to diagram B. (copied below for convenience).

b. Consider the energy barriers for the first and second steps and explain why the steady-state approximation is a valid assumption.

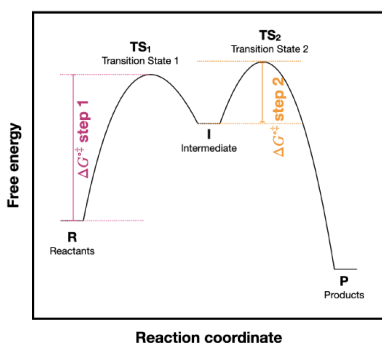


### Answer

a) The activation energy for this reaction is the difference between R and  $TS_2$  because  $TS_2$  is the highest energy along the reaction pathway.



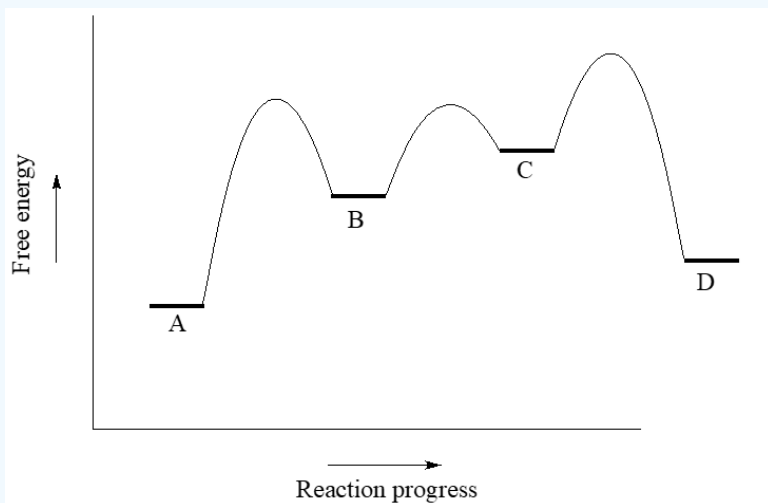
b) The activation energy for step 2 is much smaller than for step 1. This tells us that step 2 occurs faster than step 1. So, the concentration of intermediate should not increase over the course of the reaction, and it should react at least as fast as it is formed. The fact that the activation barrier for step 2 is less than for step one allows us to assume that [I] does not change over the course of the reaction. This should generally be true for all intermediates.



### ? Exercise 9.1.1.1

Use the reaction coordinate diagram below to answer the questions.

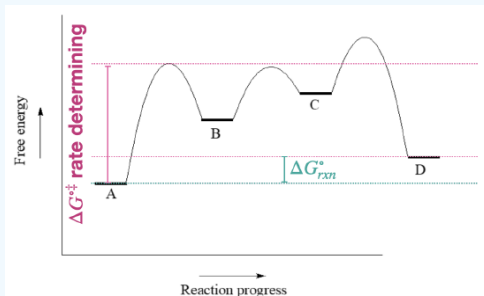
- Is the overall reaction endergonic or exergonic in the forward (A to D) direction?
- How many steps does the reaction mechanism have?
- How many intermediates does the reaction mechanism have?
- Redraw the diagram if necessary. Add a label showing the energy barrier for the rate-determining step of the forward reaction.
- Add a label showing  $\Delta G_{\text{rxn}}^{\circ}$  for the reverse reaction (D to A).
- What is the fastest reaction step, considering both the forward and reverse directions?



### Answer

- Is the overall reaction endergonic or exergonic in the forward (A to D) direction?
- How many steps does the reaction mechanism have?
- How many intermediates does the reaction mechanism have?
- The first step is rate determining since it has the largest activation barrier.

e.  $\Delta G_{\text{rxn}}^{\circ}$  for the reverse reaction (D to A) is the same as for the forward direction, with a reverse of its sign.



f. The fastest step has the lowest barriers: this would be the step to/from B and C.

Organic Chemistry With a Biological Emphasis by Tim Soderberg (University of Minnesota, Morris)

Curated or created by Kathryn Haas

This page titled 9.1.1: Review of Reaction Thermodynamics and Kinetics is shared under a CC BY-NC 3.0 license and was authored, remixed, and/or curated by Kathryn Haas.

- 6.3: A Quick Review of Thermodynamics and Kinetics by Tim Soderberg is licensed CC BY-NC-SA 4.0. Original source: [https://digitalcommons.morris.umn.edu/chem\\_facpubs/1/](https://digitalcommons.morris.umn.edu/chem_facpubs/1/).

## 9.1.2: Introduction to Substitution Reactions

Ligand substitution refers to the replacement of one ligand in a coordination complex with another ligand.

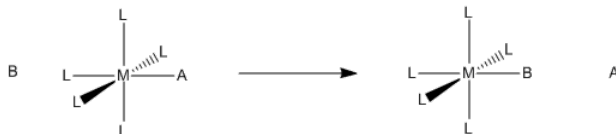


Figure 9.1.2.1: Substitution of one ligand for another in a coordination complex.

Remember, a ligand in coordination chemistry is just a Lewis base that binds to a metal atom or ion. It does so by donating a lone pair (or other pair of electrons). Generally, this donation is reversible. The donor can always take its electrons back. Typically, there may be some balance between the metal's need for more electrons and the donor's attraction for its own electrons; donor atoms are frequently more electronegative than the metal.

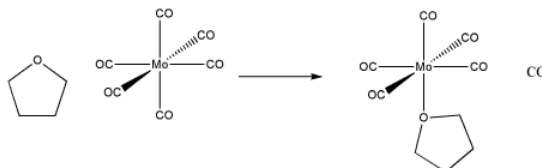


Figure 9.1.2.2: An example of ligand substitution. THF replaces a carbon monoxide in this molybdenum complex.

Even though the reaction is pretty simple, it can occur in different ways.

That is, the elementary steps involved in the reaction can occur in different orders. The elementary reactions are the individual bond-making or bond-breaking events that lead to an overall change. Sometimes the order of steps is referred to as the mechanism or the mechanistic pathway.

- The mechanism is the order of elementary reaction steps.
- Elementary reaction steps are individual bond-making and breaking steps.

You may have seen reaction mechanisms before. For example, carbonyl addition chemistry can involve lengthy mechanisms, in which a number of proton transfers and other bond-making and bond-breaking steps must occur to get from one state to another. Because ligand substitution is simpler than that, it is a good place to study mechanism in a little more depth, without getting overwhelmed by the details.

The sequence of steps in the mechanism influences how different factors will impact the reaction. For example, changing concentrations of different components in a reaction mixture can affect the time it takes for a reaction to finish.

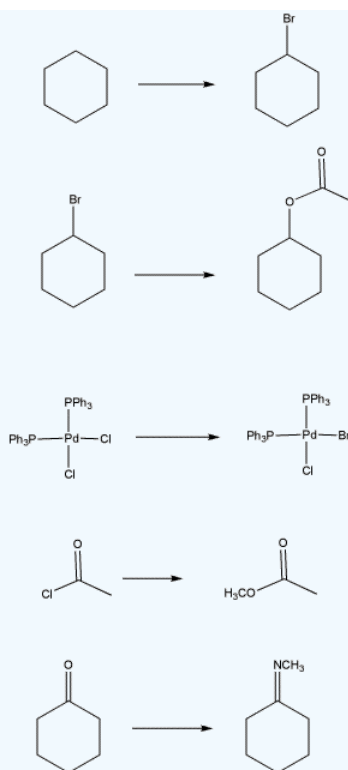
- The mechanism can have a dramatic impact on the outcome of the reaction under different circumstances.

These kinds of considerations have a dramatic impact on industrial processes such as pharmaceutical production. In that setting, chemical engineers need to make decisions about how much of each reactant must be admitted to a reaction mixture and how long they should be allowed to react together. If they allow the reaction to proceed for too long, there may be “side-reactions” that start to occur, interfering with the quality of the product, and they will waste valuable time in the production pipeline. If they don’t allow it to react long enough, the reaction may not finish, and the product will be contaminated with leftover starting materials.

In this chapter, we will look at how this simple reaction can occur in different ways. We will see some different methods that are used to tell which way the reaction occurs (i.e. evidence of what is really happening). We will also look at some different factors that may influence whether the reaction is likely to occur one way or the other (i.e. reasons it is happening that way, or reasons we expect it will happen that way).

### ? Exercise 9.1.2.1

Some kind of substitution occurs in each of the following reactions: an atom or group replaces another. In each case, identify what is being replaced, and what replaces it.



**Answer a**

a bromine atom replaces a hydrogen atom

**Answer b**

an acetate group (ethanoyl ester) replaces a bromine atom

**Answer c**

a bromine atom replaces a chlorine atom (or ions)

**Answer d**

a methoxy group replaces a chlorine atom

**Answer e**

a methylamino group replaces an oxygen atom

This page titled [9.1.2: Introduction to Substitution Reactions](#) is shared under a [not declared](#) license and was authored, remixed, and/or curated by Kathryn Haas.

- **3.1: Introduction to Substitution** by Chris Schaller is licensed [CC BY-NC 3.0](#). Original source: <https://employees.csbsju.edu/cschaller/ROBI2.htm>.

## 9.1.3: Ligand Substitution Mechanisms

### Ligand Substitution Reactions

Ligand substitution is one of the simplest reactions a metal complex may undergo. In general, ligand substitution involves the exchange of one ligand for another, with no change in oxidation state at the metal center. The incoming and outgoing ligands may be neutral or ionic but the charge of the complex changes if the ligand charge changes. Keep charge conservation in mind when writing out ligand substitutions.

How do we know when a ligand substitution reaction is favorable? The thermodynamics of the reaction depend on the relative strength of the two metal-ligand bonds, and the stability of the departing and incoming ligands (or salts of the ligand, if they're ionic). It's often useful to think of X-for-X substitutions like acid-base reactions, with the metal and spectator ligands serving as a "glorified proton." Like acid-base equilibria in organic chemistry, we look to the relative stability of the two charged species (the free ligands) to draw conclusions. Of course, we don't necessarily need to rely just on thermodynamics to drive ligand substitution reactions. Photochemistry, neighboring-group participation, relative concentrations, and other tools can facilitate otherwise difficult substitutions.

Ligand substitution is characterized by a continuum of mechanisms bound by associative (A) and dissociative (D) extremes. At the associative extreme, the incoming ligand first forms a bond to the metal, then the departing ligand takes its lone pair and leaves. At the dissociative extreme, the order of events is opposite—the departing ligand leaves, then the incoming ligand comes in. Associative substitution is common for square planar (like d8 complexes of Ni, Pd, and Pt), while dissociative substitution is more common for octahedral complexes. Then again, reality is often more complicated than these extremes. In some cases, evidence is available for simultaneous dissociation and association, and this mechanism has been given the name interchange (IA or ID).

### Associative Substitution

The associative substitution reaction is the inorganic analog of an S<sub>N</sub>2 reaction. In associative ligand substitution, the incoming ligand (Y) forms a new bond with the metal (M) before the bond to the leaving ligand (X) breaks. The first step, formation of the new M-Y bond is generally rate-determining. A typical mechanism for associative ligand substitution in both octahedral and square planar complexes is shown in Figure 9.1.3.1.



In an octahedral complex the intermediate is 7 coordinate, so associative ligand exchange in octahedral complexes is rare and only favored with larger metal ions and ligands that are not sterically demanding. In contrast, ligand substitution in square planar complexes almost always occurs via an associative mechanism, involving approach of the incoming ligand to the open coordination sites above or below the plane. Let's begin with the kinetics of the reaction. How can we spot an associative mechanism in experimental data, and what are some of the consequences of this mechanism?



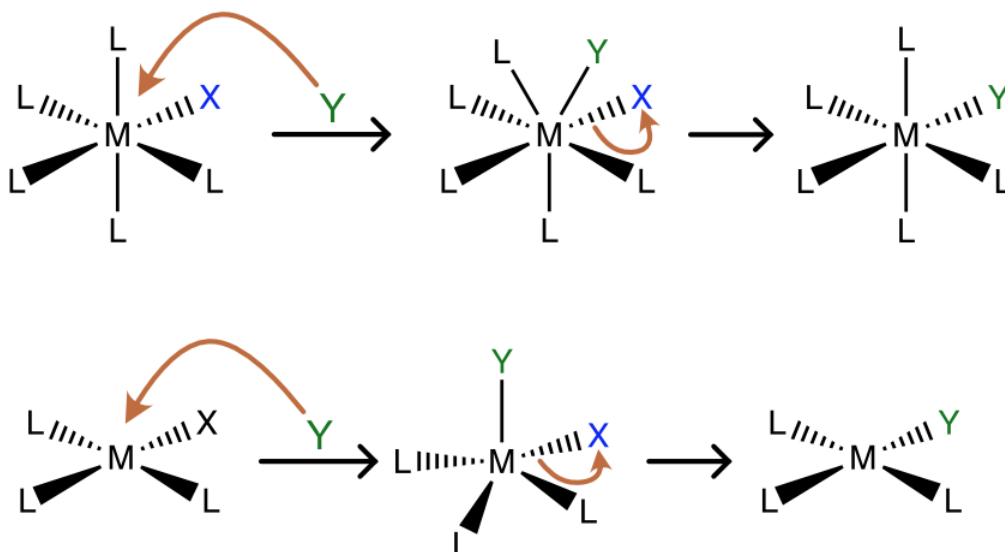


Figure 9.1.3.1: Scheme of associative ligand substitution in an octahedral (top) and square planar (bottom) metal complex. (CC BY-NC-SA; Catherine McCusker)

### Reaction Kinetics



$$\frac{d[L_nM-Y]}{dt} = \text{rate} = k_1 [L_nM-X][Y] \quad (9.1.3.3)$$

Reaction kinetics are commonly used to elucidate reaction mechanisms, and ligand substitution is no exception. Different mechanisms of substitution may follow different rate laws, so plotting the dependence of reaction rate on concentration often allows us to distinguish mechanisms. In the associative mechanism, the rate law is second order overall, first order in both  $L_nMX$  and  $Y$ . (Figure 9.1.3.2). If a large excess of  $Y$  is used in the reaction it will become **pseudo first order**, where the reaction appears first order because the  $[Y]$  doesn't change significantly over the course of the reaction.

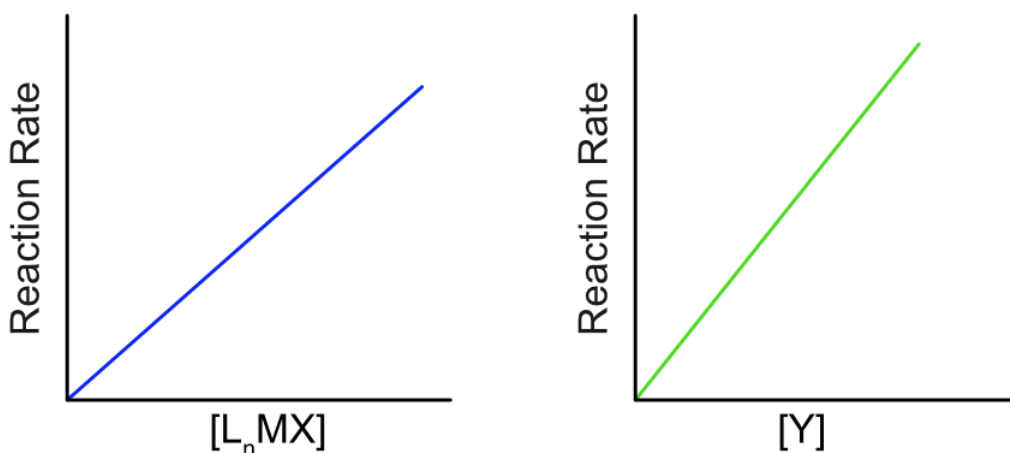


Figure 9.1.3.2: Dependence of associative reaction rate on concentration of the starting metal complex  $[ML_nX]$  and the incoming ligand  $[Y]$ . (CC BY-NC-SA; Catherine McCusker)

### Dissociative Substitution

The associative substitution mechanism is unlikely for 6 coordinate complexes. For octahedral complexes dissociative substitution mechanisms involving 5 coordinate intermediates are more likely. In

a slow step, the departing ligand leaves, generating a coordinatively unsaturated 5 coordinate intermediate. The incoming ligand then enters the coordination sphere of the metal to generate the product. We'll focus on the kinetics of the reaction and the nature of the unsaturated intermediate (which influences the stereochemistry of the reaction). The reverse of the first step, re-coordination of the departing ligand (rate constant  $k_{-1}$ ), is often competitive with dissociation.

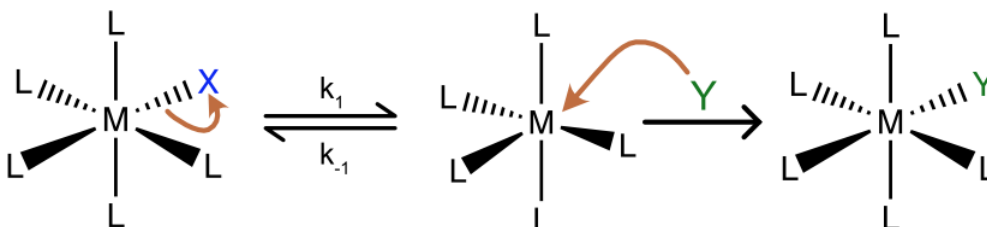
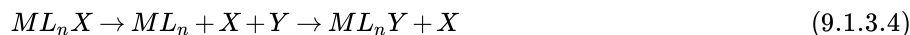


Figure 9.1.3.3: A general scheme for dissociative ligand substitution in an octahedral complex. (CC BY-NC-SA; Catherine McCusker)

### Reaction Kinetics

Let's begin with the general situation in which  $k_1$  and  $k_{-1}$  are similar in magnitude. Since  $k_1$  is rate limiting,  $k_2$ , the rate of the second step is assumed to be much larger than  $k_1$  and  $k_{-1}$ . Most importantly, we need to assume that variation in the concentration of the unsaturated intermediate is essentially zero. This is called the [steady state approximation](#), and it allows us to set up an equation that relates reaction rate to observable concentrations.

$$\text{rate} = k_2[L_nM][Y] \quad (9.1.3.5)$$

Of course, the unsaturated complex is present in very small concentration and is unmeasurable, so this equation doesn't help us much. We need to remove the concentration of the unmeasurable intermediate from (1), and the steady state approximation helps us do this. We can express variation in the concentration of the unsaturated intermediate as (processes that make it) minus (processes that destroy it), multiplying by an arbitrary time length to make the units work out. All of that equals zero, according to the steady state approximation.

$$\Delta[L_nM] = 0 = (k_1[L_nM-X] - k_{-1}[L_nM][X] - k_2[L_nM][Y])\Delta t \quad (9.1.3.6)$$

$$0 = k_1[L_nM-X] - k_{-1}[L_nM][X] - k_2[L_nM][Y] \quad (9.1.3.7)$$

Rearranging to solve for  $[L_nM]$ , we arrive at the following.

$$[L_nM] = k_1 \frac{[L_nM-X]}{(k_{-1}[X] + k_2[Y])} \quad (9.1.3.8)$$

Finally, substituting into Equation 9.1.3.5 we reach a verifiable rate equation.

$$\text{rate} = k_2 k_1 \frac{[L_nM-X][Y]}{(k_{-1}[X] + k_2[Y])} \quad (9.1.3.9)$$

When  $k_{-1}$  is negligibly small, Equation 9.1.3.9 reduces to the familiar Equation 9.1.3.10 typical of dissociative reactions like  $S_N1$ .

$$\text{rate} = k_1[L_nM-X] \quad (9.1.3.10)$$

This rate does not depend on the concentration of incoming ligand. For reactions that are better described by Equation 9.1.3.9 we can use a large excess of Y to make  $k_2[Y]$  far greater than  $k_{-1}[X]$ , essentially forcing the reaction to fit Equation 9.1.3.10

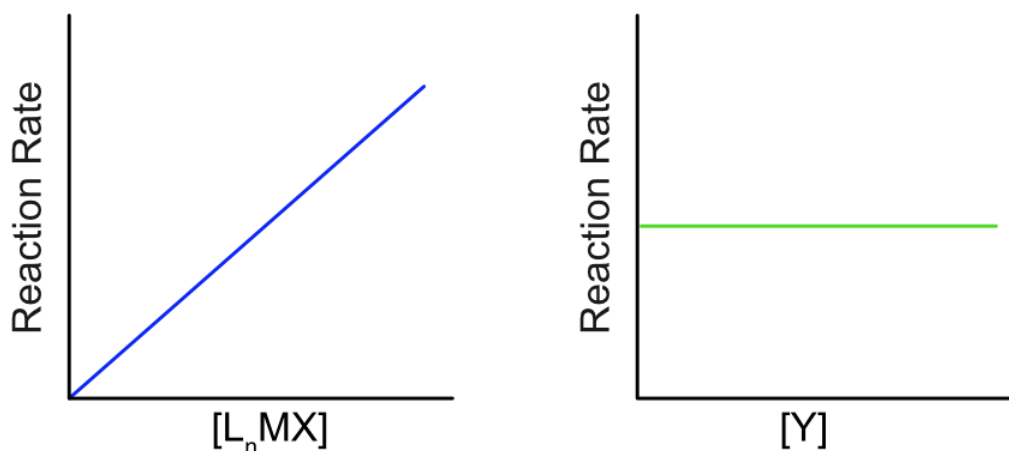


Figure 9.1.3.4: Dependence of dissociative reaction rate on concentration of the starting metal complex  $[ML_nX]$  and the incoming ligand  $[Y]$ . (CC BY-NC-SA; Catherine McCusker)

### Stereochemistry

Dissociation of a ligand from an octahedral complex generates an unsaturated  $ML_5$  intermediate. The five coordinate intermediate could adopt either a trigonal bipyramidal (TBP) geometry or a square pyramidal geometry (SP). Both steric and electronic factors combine to determine which geometry is most favorable. For example, with 6 d electrons an issue arises with the TBP geometry. With 6 d electrons, the TBP geometry has two unpaired electrons in degenerate orbitals. Unpaired electrons in degenerate orbitals lead to [Jahn-Teller distortion](#). For a TBP geometry, distortion to a SP or a distorted TBP geometry removes the degeneracy, and so five-coordinate d6 complexes typically have square pyramidal or distorted TBP geometries.

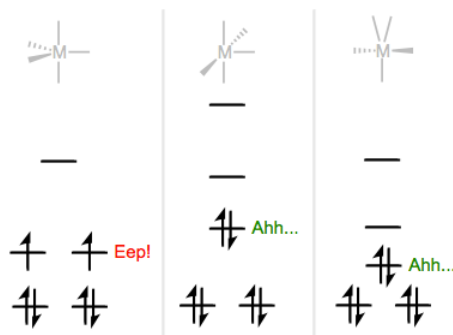


Figure 9.1.3.5: TBP geometry (left) is electronically disfavored for d6 metals. Distorted TBP (right) and SP (center) geometries are favored.

When the intermediate adopts square pyramidal geometry, the incoming ligand can simply approach where the departing ligand left, resulting in retention of stereochemistry. Inversion is more likely when the intermediate is a distorted trigonal bipyramid.

### Factors That Favor Dissociative Substitution

In general, introducing structural features that either stabilize the unsaturated intermediate or destabilize the starting complex can encourage dissociative substitution. Both of these strategies lower the activation barrier for the reaction.

Let's begin with features that stabilize the unsaturated intermediate. Electronically, the intermediate loves it when its d electron count is nicely matched to its crystal field orbitals. As you study inorganic chemistry, you'll learn that there are certain "natural" d electron counts for particular geometries that fit well with the metal-centered orbitals predicted by [crystal field theory](#). Octahedral geometry is great for six d electrons, for example, and square planar geometry loves eight d electrons. Complexes with "natural" d electron counts—but bearing one extra ligand—are ripe for dissociative substitution. The classic examples are d<sup>8</sup> TBP complexes, which become d<sup>8</sup> square planar complexes (think Pt(II) and Pd(II)) upon dissociation. Similar factors actually can also stabilize the starting complexes, making them less reactive in dissociative substitution reactions. For example, low spin d<sup>6</sup> octahedral complexes are particularly happy, and react most slowly in dissociative substitutions.

Destabilization of the starting complex is commonly accomplished by adding steric bulk to its ligands. Naturally, dissociation relieves steric congestion in the starting complex. Chelation has the opposite effect, and tends to steel the starting complex against dissociation.

$$ML_n \xrightleftharpoons{K_d} ML_{n-1} + L$$

L	Cone Angle	$K_d$
$P(OEt)_3$	109	$< 10^{-10}$
$P(O-C_6H_4-OEt)_3$	128	$6 \cdot 10^{-10}$
$P(Oi-Pr)_3$	130	$2.7 \cdot 10^{-5}$
$P(O-C_6H_4-Me)_3$	141	$4 \cdot 10^{-2}$
$PPh_3$	145	huge

*As steric bulk on the ligand increases, dissociation becomes more favorable.*

## Interchange Substitution

Real life chemical reactions don't always fall neatly into one of the categories above. In some cases the M-X bond can break and the M-Y bond can form simultaneously. An interchange reaction is a concerted reaction without an intermediate. The transition state is a species where the bond to Y is partially formed and the bond to X is partially broken as seen in Figure 9.1.3.6 If the new M-Y bond forms faster than the M-X bond breaks that is an associative interchange (IA) reaction and if the M-X bond breaks faster than the new M-Y bond forms that is a dissociative interchange reaction (ID)

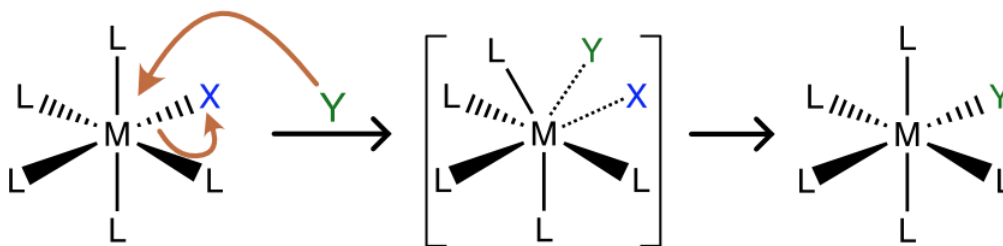


Figure 9.1.3.6: A general scheme for an interchange ligand substitution reaction. Species in brackets is the transition state, not an intermediate. (CC BY-NC-SA; Catherine McCusker)

## Contributors and Attributions

- [Dr. Michael Evans](#) (Georgia Tech)
- Modified by Catherine McCusker (East Tennessee State University)

This page titled [9.1.3: Ligand Substitution Mechanisms](#) is shared under a [CC BY-NC-SA 4.0](#) license and was authored, remixed, and/or curated by [Michael Evans](#).

- [10.3: Ligand Substitution Mechanisms](#) by [Michael Evans](#) is licensed [CC BY-NC-SA 4.0](#).
- [4.2: Associative Ligand Substitution](#) by [Michael Evans](#) is licensed [CC BY-NC-SA 4.0](#).
- [4.3: Dissociative Ligand Substitution Reactions](#) by [Michael Evans](#) is licensed [CC BY-NC-SA 4.0](#).
- [4.4: Ligand substitution](#) by [Michael Evans](#) is licensed [CC BY-NC-SA 4.0](#).

### 9.1.4: Some Reasons for Differing Mechanisms

We usually look for physical reasons why a given compound might undergo a reaction via one mechanism and not another. That ability adds to our understanding of chemistry. If we can take information and give it predictive value, then we may be able to make educated decisions about what is probably happening with new reactions.

Why might a reaction undergo a dissociative reaction rather than an associative one? What factors might prevent an associative pathway?

One reason may be that there is not enough room. In an associative step, an additional ligand comes in and binds to the metal. If it is already crowded, that may be difficult.

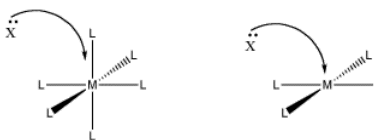


Figure 9.1.4.1: The role of steric crowding in ligand substitution. In one of these cases, the associative mechanism is less favored because of crowding that will occur in the transition state.

- Steric crowding may lead to a dissociative, rather than associative, mechanism.

Another reason has to do with electronics. Maybe the compound cannot easily accept an additional bonding pair. That may be the case if the compound already has eighteen electrons.

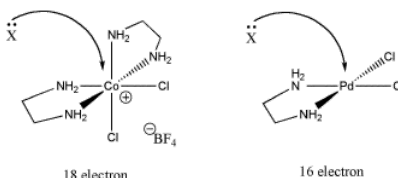


Figure 9.1.4.2: The role of electron count in ligand substitution. In one of these cases, the associative mechanism is less favored because the metal is already electronically saturated.

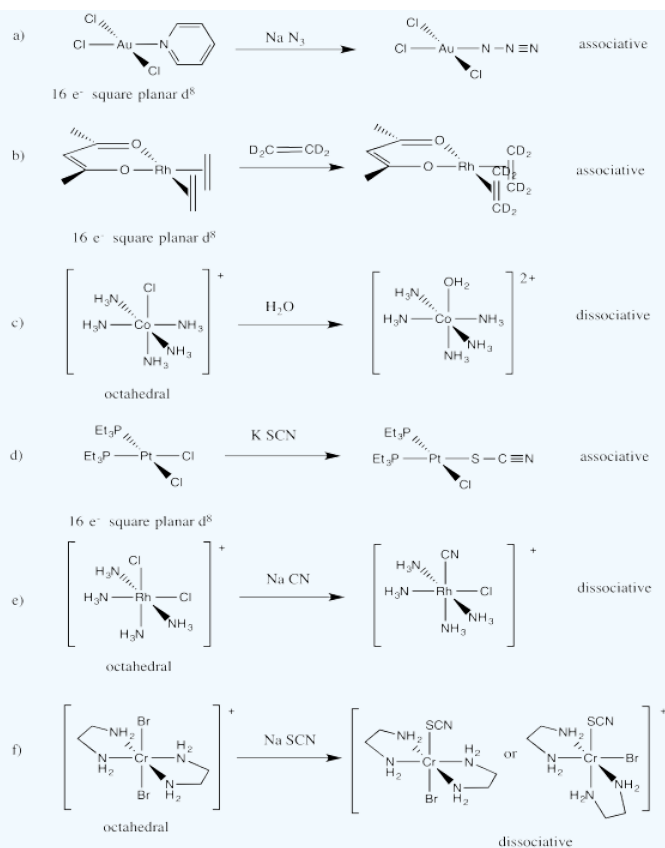
- Electronic saturation may lead to a dissociative, rather than associative, mechanism.

However, if there is less crowding, and more electrons can be accommodated, an associative pathway may result.

#### ? Exercise 9.1.4.1

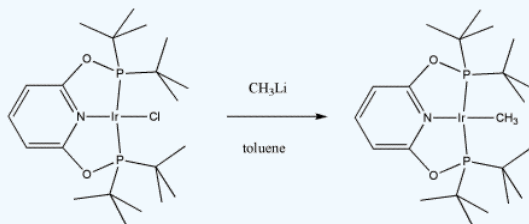
- Draw structures for the following reactions. Pay attention to geometry.
- Predict whether each of the substitutions would occur through associative or dissociative mechanisms.
  - $\text{AuCl}_3\text{py} + \text{Na N}_3 \rightarrow \text{Na}^+ [\text{AuCl}_3\text{N}_3]^- + \text{py}$
  - $\text{Rh}(\text{C}_2\text{H}_4)_2(\text{acac}) + \text{C}_2\text{D}_4 \rightarrow \text{Rh}(\text{C}_2\text{D}_4)_2(\text{acac}) + \text{C}_2\text{H}_4$
  - $[\text{Co}(\text{NH}_3)_5\text{Cl}]^{2+} + \text{H}_2\text{O} \rightarrow [\text{Co}(\text{NH}_3)_5(\text{OH}_2)]^{2+} + \text{Cl}^-$
  - $\text{trans}-(\text{Et}_3\text{P})_2\text{PtCl}_2 + ^-\text{SCN} \rightarrow \text{trans}-(\text{Et}_3\text{P})_2\text{PtCl}(\text{SCN}) + \text{Cl}^-$
  - $\text{Rh}(\text{NH}_3)_4\text{Cl}_2^+ + ^-\text{CN} \rightarrow \text{Rh}(\text{NH}_3)_4\text{Cl}(\text{CN})^+ + \text{Cl}^-$
  - $\text{trans}[\text{Cr}(\text{en})_2\text{Br}_2]^+ + ^-\text{SCN} \rightarrow \text{cis- and trans-}[\text{Cr}(\text{en})_2\text{Br}(\text{SCN})]^+ + \text{Br}^-$

**Answer**



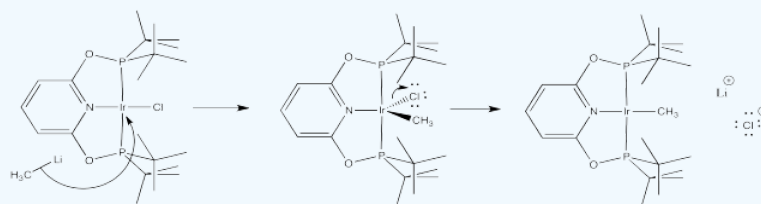
### ? Exercise 9.1.4.2

Maurice Brookhart of UNC, Chapel Hill, makes organometallic compounds in order to study fundamental questions about reactivity. In this case, he has reported making a new compound capable of "C-H activation", a reaction in which unreactive C-H bonds can be forced to break. This process holds the future promise of converting coal and natural gas into important commodities currently obtained from petroleum.



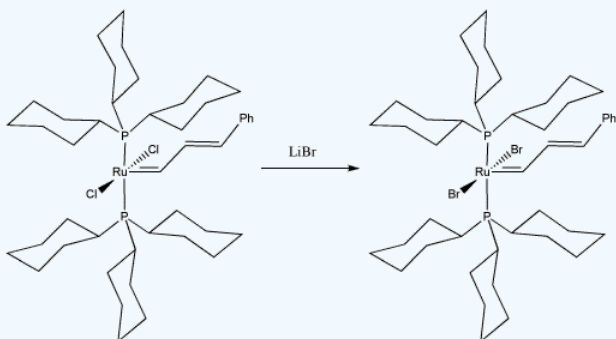
- Draw, with curved arrows, a mechanism for the ligand substitution in the synthesis of this C-H activating complex.
- Explain your reasons for your choice of reaction mechanism.

**Answer**



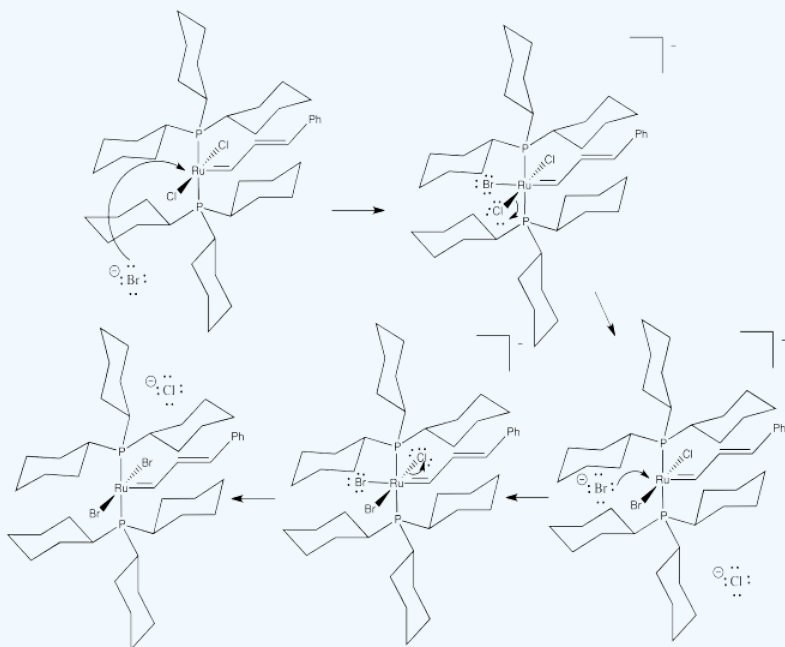
### ? Exercise 9.1.4.3

Bob Grubbs of Cal Tech was awarded the Nobel Prize in chemistry for his development of catalysts for olefin metathesis. Olefin metathesis is important both in the reforming of petroleum and in the synthesis of important commodities such as pharmaceuticals. In the following study, he replaced chlorides on a "Grubbs Generation I catalyst" to study the effect on the olefin metathesis reaction.



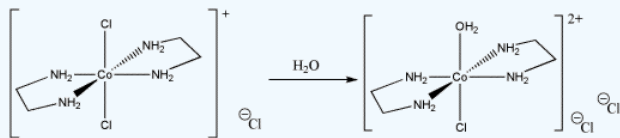
- Draw, with curved arrows, a mechanism for the ligand substitution in this complex.
- Explain your reasons for your choice of reaction mechanism.
- What factor(s) do you think Grubbs hoped to study by making this substitution in the catalyst?

**Answer**



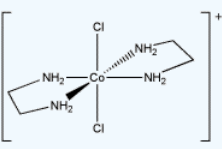
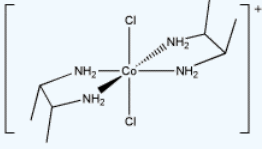
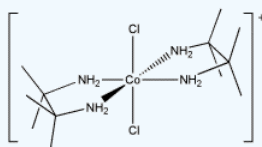
### ? Exercise 9.1.4.4

Sometimes, kinetic studies can give insight into a reaction if controlled changes in the reaction produce measurable results.



- Draw, with curved arrows, a mechanism for the ligand substitution in this reaction.

- b) Explain your reasons for your choice of reaction mechanism.  
c) Explain the following kinetic data.

complex	substitution rate constant
	$3.2 \times 10^{-5} \text{ s}^{-1}$
	$4.1 \times 10^{-3} \text{ s}^{-1}$
	too fast to measure easily

### ? Exercise 9.1.4.5

Several different structures were proposed for  $\text{Ni}(\text{cysteine})_2^{2-}$ . Kinetic studies of substitution in this complex showed the rate was dependent in the concentration of both the metal complex and the incoming ligand. Which structure do you think is correct? Why?

This page titled [9.1.4: Some Reasons for Differing Mechanisms](#) is shared under a [CC BY-NC 3.0](#) license and was authored, remixed, and/or curated by [Kathryn Haas](#).

- [3.6: Some Reasons for Differing Mechanisms](#) by [Chris Schaller](#) is licensed [CC BY-NC 3.0](#). Original source: <https://employees.csbsju.edu/cschaller/ROBI2.htm>.



### 9.1.4.1: Dissociation

Consider what must happen for the simplest case of a purely dissociative (D) reaction mechanism for an octahedral metal complex. The first step, and the rate-limiting step must be dissociation of one ligand to form an intermediate with a lower coordination number. Such a situation, where an octahedral complex loses a ligand, X, to become a square pyramidal intermediate is shown below in Figure 9.1.4.1.1

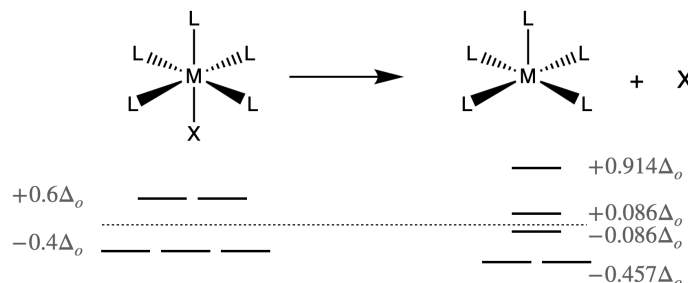


Figure 9.1.4.1.1: Dissociation of a ligand to form a square pyramidal intermediate. This would be the first step of a dissociative (D) reaction mechanism. The Ligand Field Activation Energy (LFAE) can be calculated from the splitting energies of the octahedron compared to the square planar intermediate. (CC-BY-SA; Kathryn Haas)

If the dissociation of a ligand is rate-determining, factors that lower the energy of the transition state or intermediate structures will speed the reaction rate. Here we could consider the differences in ligand-field stabilization energy (LFSE). The difference between the LFSE of the octahedral reactant and that of the intermediate is defined as the ligand field activation energy (LFAE). The LFAE can be calculated for a given *d*-electron count for an octahedral reactant and a square pyramidal intermediate using the information provided in Figure 9.1.4.1.1. Metal ions with particularly low (more negative) LFAE values tend to be more labile, while those with particularly high (less negative) values tend to be more inert. However, most octahedral complexes are expected to react through dissociative mechanisms due to the unfavorable steric crowding that must occur during an associative pathway.

The ease by which the M-X bond is broken will also influence rate of a dissociative reaction, and this can be probed experimentally. The following experiments can give evidence that support the argument that a reaction occurs by a dissociative pathway, or that it is dissociatively activated.

#### Experimental evidence that supports dissociative mechanism

##### 1. Identity of the entering ligand has little effect on reaction rate.

If dissociation is the rate-determining step, the identity of the entering ligand, Y, should have little effect on the reaction rate. Therefore, an experiment that varies Y while holding X constant can indicate whether or not Y is involved in the rate-determining step. If the identity of Y has little effect on rate, then it must not be involved in the rate-determining step. Such experimental evidence can be taken as evidence of a dissociative mechanism. For example, the rate constants for reaction of  $[\text{Cr}(\text{NH}_3)_5\text{H}_2\text{O}]^{3+}$  with different incoming ligands, shown below, has rate constants of similar magnitude (they are approximately within one order of magnitude), indicating a dissociatively activated mechanism. In this case, other lines of evidence suggest this is a reaction with a  $I_d$  mechanism.

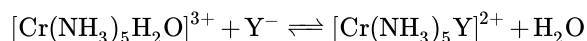


Table 9.1.4.1.1: Rate Constants for Exchange of Aquo Ligand of pentaammineaquo chromium(III) ion by incoming ligand, Y (chemical equation shown above). There is little effect of the identity of the incoming ligand on the rate constant. This data was sourced from Miessler, Fischer and Tarr's *Inorganic Chemistry*, 5th edition, pg 449.

Entering Ligand, Y <sup>-</sup>	Rate Constant, $k_1$ ( $10^{-4} \text{ M}^{-1} \text{ s}^{-1}$ )
NCS <sup>-</sup>	4.2
Cl <sup>-</sup>	0.7
Br <sup>-</sup>	3.7
CF <sub>3</sub> CO <sub>2</sub> <sup>-</sup>	1.4

## 2. Steric Crowding of the Metal Complex

Steric crowding of the metal complex would inhibit a dissociative pathway through steric crowding of the entering ligand. However, steric crowding can increase the stability of the intermediate after dissociation of the ligand from the crowded octahedral complex. If the reaction rate increases with steric crowding of the reactant complex, this is taken as evidence to support a dissociative mechanism.

## 3. Volume of Activation

One molecule generally takes up less space than two separate molecules. This usually holds true in solution. Measurement of a rate constant's dependence on pressure can be used to determine the volume of activation ( $\Delta V_{act}$ ) and give insight into the mechanism of that reaction. In a dissociation mechanism, the dissociation causes one metal complex to become two separate molecules. Thus, the intermediate should, in principle, take up more space than the reactant complex. In a situation like this, we expect that the rate of reaction should decrease with increasing pressure, giving a positive value for  $\Delta V_{act}$ . However, solvation of ions can influence volume, and this should be considered in interpretation of pressure-dependence data.

## 4. Increased coulombic attraction with the leaving group decreases reaction rate.

Coulombic (electrostatic) attraction between the dissociating ligand, X, and the metal complex should slow ligand dissociation. Coulombic attraction increases with increased magnitude of charges and with decreased distance. If the reaction rate slows with increased charge of the metal ion or the ligand itself, this is taken as evidence of a dissociative mechanism. Likewise, if rate decreases as the radius of the central metal ion is decreased, this is evidence to support a dissociative mechanism.

## 5. Increased strength of the M-X bond decreases reaction rate.

Free energy relationships between the formation constant of M-X and the kinetic rate constant of the reaction can provide evidence to support a dissociative mechanism (Discussed in the next section).

---

This page titled [9.1.4.1: Dissociation](#) is shared under a [not declared](#) license and was authored, remixed, and/or curated by [Kathryn Haas](#).

### 9.1.4.2: Associative Mechanisms

Associative mechanisms tend to be less common for octahedral complexes as a result of steric hindrance of the metal ion by six ligands. However, reactions of octahedral complexes with associative character are more likely if the ligands have low steric bulk and/or the central metal ion is larger with longer bonds (as in the case of  $4d$  and  $5d$  metal ions). Reactions of octahedrons have also been observed in cases of low  $d$ -electron count or low electron density around the central ion, presumably making nucleophilic reaction more favorable. If an octahedral complex is determined to have associative character, in most cases it is associatively-active interchange ( $I_a$ ).

The evidence that supports arguments for associative mechanisms is somewhat the opposite as that which would support dissociative character. One typical piece of evidence that supports an associative pathway is **a large effect of the incoming ligand on the reaction rate constant**. For example, in the reaction of hexaaquo chromium (III) ion ( $[\text{Cr}(\text{H}_2\text{O})_6]^{3+}$ ) with various incoming ligands (shown below), rate constants vary by several orders of magnitude. This data is evidence of an associative mechanism ( $I_a$ ). In contrast, the reaction of pentaammineaquo chromium (III) ion ( $[\text{Cr}(\text{NH}_3)_5\text{H}_2\text{O}]^{3+}$ ) occurs by an associative mechanism (data shown in [Section 12.4.1](#)). The difference in reaction mechanisms for different chromium (III) complexes can be justified by the different electron densities around their metal ion center. The ammine ligand is a stronger sigma donor and thus the metal center is more electron rich in the case of  $[\text{Cr}(\text{NH}_3)_5\text{H}_2\text{O}]^{3+}$ . Nucleophilic reaction by an incoming ligand is thus more likely in the case of  $[\text{Cr}(\text{H}_2\text{O})_6]^{3+}$ , which has a more electrophilic center.

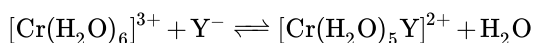


Table 9.1.4.2.1 : Rate Constants for Exchange of Aquo Ligand of hexaaquo chromium(III) ion by incoming ligand, Y (chemical equation shown above). There is little effect of the identity of the incoming ligand on the rate constant. This data was sourced from Miessler, Fischer and Tarr's *Inorganic Chemistry*, 5th edition, pg 449.

Entering Ligand, $\text{Y}^-$	Rate Constant, $k_1$ ( $10^{-4} \text{ M}^{-1} \text{ s}^{-1}$ )
$\text{NCS}^-$	180
$\text{NO}_3^-$	73
$\text{Cl}^-$	2.9
$\text{Br}^-$	0.9
$\text{I}^-$	0.08

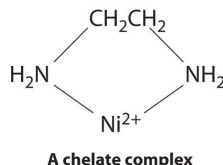
Another piece of evidence that can support associative mechanisms is the temperature-dependence of the rate law, which in turn can yield the entropy of activation (represented as  $\Delta S^\ddagger$  or  $\Delta S_{act}$ ). When an incoming ligand associates with a metal complex and two molecules become one, there would be a negative change in the entropy (entropy decreases). A negative value for the entropy of activation indicates an associative pathway. An example of this is in the substitution of the aquo ligand in  $[\text{Ru}(\text{EDTA})(\text{H}_2\text{O})]^-$ , which has a negative value of  $\Delta S^\ddagger$ , indicating an  $I_a$  mechanism.

This page titled [9.1.4.2: Associative Mechanisms](#) is shared under a [not declared](#) license and was authored, remixed, and/or curated by [Kathryn Haas](#).

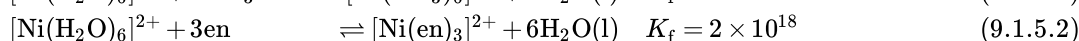
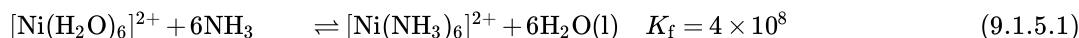
## 9.1.5: Thermodynamic Stability and Chelate Effect

### Chelate Complexes

As seen in [Chapter 8](#), ligands like chloride, water, and ammonia are monodentate. More complex ligands can, however, be bidentate, tridentate, or, in general, polydentate. Ethylenediamine ( $\text{H}_2\text{NCH}_2\text{CH}_2\text{NH}_2$ , often abbreviated as en) and diethylenetriamine ( $\text{H}_2\text{NCH}_2\text{CH}_2\text{NHCH}_2\text{CH}_2\text{NH}_2$ , often abbreviated as dien) are examples of a bidentate and a tridentate ligand, respectively, because each nitrogen atom has a lone pair that can be shared with a metal ion. When a bidentate ligand such as ethylenediamine binds to a metal such as  $\text{Ni}^{2+}$ , a five-membered ring is formed. A metal-containing ring like that shown is called a chelate ring. Correspondingly, a polydentate ligand is a chelating agent, and complexes that contain polydentate ligands are called chelate complexes.



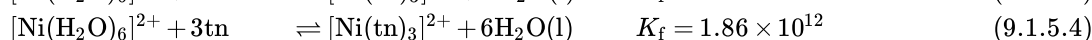
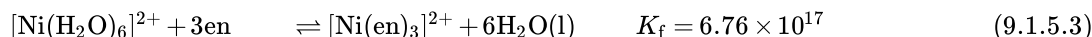
Experimentally, it is observed that metal complexes of polydentate ligands are significantly more stable than the corresponding complexes of chemically similar monodentate ligands; this increase in stability is called the chelate effect. For example, the complex of  $\text{Ni}^{2+}$  with three ethylenediamine ligands,  $[\text{Ni}(\text{en})_3]^{2+}$ , should be chemically similar to the  $\text{Ni}^{2+}$  complex with six ammonia ligands,  $[\text{Ni}(\text{NH}_3)_6]^{2+}$ . In fact, the equilibrium constant for the formation of  $[\text{Ni}(\text{en})_3]^{2+}$  is almost 10 orders of magnitude larger than the equilibrium constant for the formation of  $[\text{Ni}(\text{NH}_3)_6]^{2+}$  ([Table E4](#)):



The formation constants are formulated as [ligand exchange](#) reactions with aqua ligands being displaced by new ligands ( $\text{NH}_3$  or en) in the examples above.

*Chelate complexes are more stable than the analogous complexes with monodentate ligands.*

The stability of a chelate complex depends on the size of the chelate rings. For ligands with a flexible organic backbone like ethylenediamine, complexes that contain five-membered chelate rings, which have almost no strain, are significantly more stable than complexes with six-membered chelate rings, which are in turn much more stable than complexes with four- or seven-membered rings. For example, the complex of nickel (II) with three ethylenediamine ligands is about 363,000 times more stable than the corresponding nickel (II) complex with trimethylenediamine ( $\text{H}_2\text{NCH}_2\text{CH}_2\text{CH}_2\text{NH}_2$ , abbreviated as tn):



\*The above measurements were done in a solution of ionic strength 0.15 at 25° C.

#### Example 9.1.5.1

Arrange  $[\text{Cr}(\text{en})_3]^{3+}$ ,  $[\text{CrCl}_6]^{3-}$ ,  $[\text{CrF}_6]^{3-}$ , and  $[\text{Cr}(\text{NH}_3)_6]^{3+}$  in order of increasing stability.

**Given:** four Cr(III) complexes

**Asked for:** relative stabilities

**Strategy:**

A Determine the relative basicity of the ligands to identify the most stable complexes.

B Decide whether any complexes are further stabilized by a chelate effect and arrange the complexes in order of increasing stability.

**Solution**

A The metal ion is the same in each case:  $\text{Cr}^{3+}$ . Consequently, we must focus on the properties of the ligands to determine the stabilities of the complexes. Because the stability of a metal complex increases as the basicity of the ligands increases, we need to determine the relative basicity of the four ligands. Our earlier discussion of acid–base properties suggests that ammonia and ethylenediamine, with nitrogen donor atoms, are the most basic ligands. The fluoride ion is a stronger base (it has a higher charge-to-radius ratio) than chloride, so the order of stability expected due to ligand basicity is



B Because of the chelate effect, we expect ethylenediamine to form a stronger complex with  $\text{Cr}^{3+}$  than ammonia. Consequently, the likely order of increasing stability is



### Exercise 9.1.5.1

Arrange  $[\text{Co}(\text{NH}_3)_6]^{3+}$ ,  $[\text{CoF}_6]^{3-}$ , and  $[\text{Co}(\text{en})_3]^{3+}$  in order of decreasing stability.

**Answer:**  $[\text{Co}(\text{en})_3]^{3+} > [\text{Co}(\text{NH}_3)_6]^{3+} > [\text{CoF}_6]^{3-}$

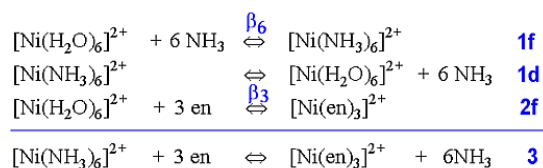
## The Chelate Effect

The chelate effect can be seen by comparing the reaction of a chelating ligand and a metal ion with the corresponding reaction involving comparable monodentate ligands. For example, comparison of the binding of 2,2'-bipyridine with pyridine or 1,2-diaminoethane (ethylenediamine=en) with ammonia. It has been known for many years that a comparison of this type always shows that the complex resulting from coordination with the chelating ligand is **much more thermodynamically stable**. This can be seen by looking at the values for adding two monodentates compared with adding one bidentate, or adding four monodentates compared to two bidentates, or adding six monodentates compared to three bidentates.

*The Chelate Effect is that complexes resulting from coordination with the chelating ligand is much more thermodynamically stable than complexes with non-chelating ligands.*

A number of points should be highlighted from the formation constants in Table E4. In Table 9.1.5.1, it can be seen that the  $\Delta H^\circ$  values for the formation steps are almost identical, that is, heat is evolved to about the same extent whether forming a complex involving monodentate ligands or bidentate ligands. What is seen to vary significantly is the  $\Delta S^\circ$  term which changes from negative (unfavorable) to positive (favorable). Note as well that there is a dramatic increase in the size of the  $\Delta S^\circ$  term for adding two compared to adding four monodentate ligands. ( $-5$  to  $-35 \text{ JK}^{-1}\text{mol}^{-1}$ ). What does this imply, if we consider  $\Delta S^\circ$  to give a measure of disorder?

In the case of complex formation of  $\text{Ni}^{2+}$  with ammonia or 1,2-diaminoethane, by rewriting the equilibria, the following equations are produced.



Using the equilibrium constant for the reaction (3 above) where the *three* bidentate ligands replace the *six* monodentate ligands, we find that at a temperature of  $25^\circ \text{C}$ :

$$\Delta G^\circ = -2.303 RT \log_{10} K \quad (9.1.5.5)$$

$$= -2.303 RT (18.28 - 8.61) \quad (9.1.5.6)$$

$$= -54 \text{ kJ mol}^{-1} \quad (9.1.5.7)$$

Based on measurements made over a range of temperatures, it is possible to break down the  $\Delta G^\circ$  term into the enthalpy and entropy components.

$$\Delta G^\circ = \Delta H^\circ - T\Delta S^\circ \quad (9.1.5.8)$$

The result is that:  $\Delta H^\circ = -29 \text{ kJ mol}^{-1}$

$$\begin{aligned} -T\Delta S^\circ &= -25 \text{ kJ mol}^{-1} \\ &\text{and at 25C (298K)} \\ \Delta S^\circ &= +88 \text{ J K}^{-1} \text{ mol}^{-1} \end{aligned}$$

### Caution

For many years, these numbers have been **incorrectly recorded** in textbooks. For example, the third edition of "Basic Inorganic Chemistry" by F.A. Cotton, G. Wilkinson and P.L. Gaus, John Wiley & Sons, Inc, 1995, on page 186 gives the values as:

$$\begin{aligned} \Delta G^\circ &= -67 \text{ kJ mol}^{-1} \\ \Delta H^\circ &= -12 \text{ kJ mol}^{-1} \\ -T\Delta S^\circ &= -55 \text{ kJ mol}^{-1} \end{aligned}$$

The conclusion they drew from these incorrect numbers was that the chelate effect was essentially an entropy effect, since the  $T\Delta S^\circ$  contribution was nearly 5 times bigger than  $\Delta H^\circ$ .

In fact, the breakdown of the  $\Delta G^\circ$  into  $\Delta H^\circ$  and  $T\Delta S^\circ$  shows that the two terms are nearly equal (-29 and -25 kJ mol<sup>-1</sup>, respectively) with the  $\Delta H^\circ$  term a little bigger! The entropy term found is still much larger than for reactions involving a non-chelating ligand substitution at a metal ion. How can we explain this enhanced contribution from entropy? One explanation is to count the number of species on the left and right hand side of the equation above.

It will be seen that on the left-hand-side there are 4 species, whereas on the right-hand-side there are 7 species, that is a net gain of 3 species occurs as the reaction proceeds. This can account for the increase in entropy since it represents an increase in the disorder of the system. An alternative view comes from trying to understand how the reactions might proceed. To form a complex with 6 monodentates requires 6 separate favorable collisions between the metal ion and the ligand molecules. To form the tris-bidentate metal complex requires an initial collision for the first ligand to attach by one arm but remember that the other arm is always going to be nearby and only requires a rotation of the other end to enable the ligand to form the chelate ring.

If you consider dissociation steps, then when a monodentate group is displaced, it is lost into the bulk of the solution. On the other hand, if one end of a bidentate group is displaced the other arm is still attached and it is only a matter of the arm rotating around and it can be reattached again. **Both** conditions favor the formation of the complex with bidentate groups rather than monodentate groups.

This page titled [9.1.5: Thermodynamic Stability and Chelate Effect](#) is shared under a [CC BY-NC-SA 4.0](#) license and was authored, remixed, and/or curated by [Robert J. Lancashire](#).

- [10.1: Thermodynamic Stability of Metal Complexes](#) by [Robert J. Lancashire](#) is licensed [CC BY-NC-SA 4.0](#).

## 9.1.6: Kinetic Lability

### Kinetics of Substitution Reactions

Kinetics is a branch of chemistry that is concerned with the rates of chemical reactions. In this section, we will discuss the rates of metal-ligand (M-L) substitution reactions.

Let's start with some examples. In the table below are three examples of ligand substitution reactions of hexaquo metal complexes to form hexaammine complexes. These reactions are nearly identical with the exception of the metal ion. The products are thermodynamically favored in all cases.

Reaction	Rate constant ( $k$ )	Labile or Inert
$[\text{Ni}(\text{OH}_2)]^{2+} + 6 \text{NH}_3 \rightleftharpoons [\text{Ni}(\text{NH}_3)_6]^{2+}$	$k = 10^4 \text{ s}^{-1}$ (1 ns)	Labile (happens in < 1 min)
$[\text{Cr}(\text{OH}_2)]^{3+} + 6 \text{NH}_3 \rightleftharpoons [\text{Cr}(\text{NH}_3)_6]^{3+}$	$k = 10^{-3} \text{ s}^{-1}$ (6 days)	Inert (slow, takes hours)
$[\text{Cu}(\text{OH}_2)]^{2+} + 6 \text{NH}_3 \rightleftharpoons [\text{Cu}(\text{NH}_3)_6]^{2+}$	$k = 10^8 \text{ s}^{-1}$	Very Labile (happens in seconds)

#### Definitions

- **Kinetically Labile** - Metal complexes that undergo "kinetically fast" substitution reactions are **kinetically labile**. Taube suggested that these are reactions in which half of the reactant is consumed in one minute or less ( $t_{1/2} < 1 \text{ min}$ ).
- **Kinetically Inert** - Metal complexes that undergo "kinetically slow" substitution reactions are **kinetically inert** or **non-labile**. Taube suggested that these are reactions in which  $t_{1/2} > 1 \text{ min}$ .

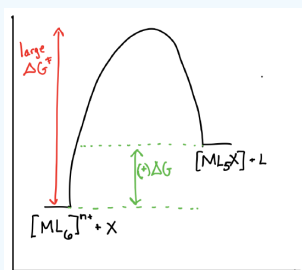
A common pitfall is to confuse the meaning of kinetic terms, like *labile* and *inert*, with thermodynamic terms, like *stable* and *unstable*. It is important to distinguish between kinetics and thermodynamics. For example, the complex  $[\text{Fe}(\text{H}_2\text{O})\text{Cl}]^{2+}$  has a large formation constant and is thermodynamically stable; yet it is also labile. On the other hand, the complex  $[\text{Co}(\text{NH}_3)_6]^{3+}$  is unstable in acidic aqueous solution and decomposes spontaneously to  $[\text{Co}(\text{H}_2\text{O})_6]^{3+}$ ; yet it decomposes slowly because it is inert. It is good practice to use clear terms such as "kinetically labile" or "kinetically inert" and "thermodynamically stable" and "thermodynamically unstable".

#### ? Exercise 9.1.6.1

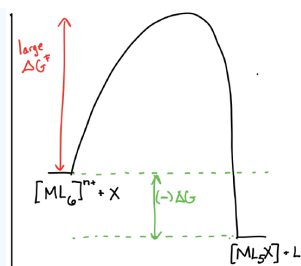
Draw the reaction coordinate diagrams for a reaction of the form  $[\text{ML}_6]^{n+} + \text{X} \rightleftharpoons [\text{ML}_5\text{X}]^{n+} + \text{L}$  in the following scenarios:

- $[\text{ML}_6]^{n+}$  is thermodynamically stable and kinetically inert.
- $[\text{ML}_6]^{n+}$  is thermodynamically unstable and kinetically inert.
- $[\text{ML}_6]^{n+}$  is thermodynamically stable and kinetically labile.
- $[\text{ML}_6]^{n+}$  is thermodynamically unstable and kinetically labile.

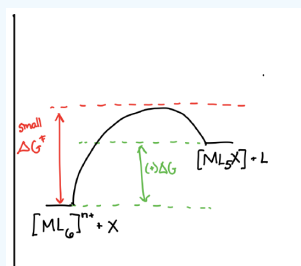
Answer a)



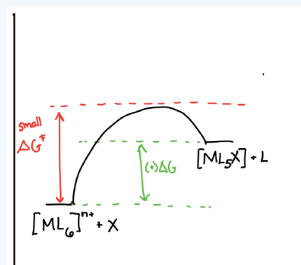
Answer b)



Answer c)



Answer d)



### Factors that affect rates of substitution reactions:

Some of the factors that affect the kinetic rates of ligand substitution are the same factors that affect thermodynamic stability (see [Chapter 10](#)). The same factors that make a complex stable can also make it more inert. Why are kinetic factors related to thermodynamic stability? It is because the structure and stability of the reactant complex is related to the structure and stability of the transition state. The reactant complex must change its geometry to form an intermediate or transition state. When the reactant is particularly stable, it can result in a higher activation energy associated with moving away from the stable configuration. However, it is incorrect to assume that stability is *always* correlated with reaction rates. Kinetic and thermodynamic factors are related, yet separate.

There are three important factors that influence kinetic rate of substitution:

1. **Ligand Field Stabilization Energy (LFSE):** Electron configurations that place electrons in higher-energy orbitals (particularly antibonding orbitals) result in more labile complexes. As long as there are not electrons in higher-energy orbitals, the lability correlates roughly with LFSE. The more negative the LFSE, the more inert.
2. **Coulombic attraction between the metal and ligand:** In general, higher charge density on the metal ion or on the ligand(s) leads to stronger electrostatic attraction between metal and ligand. Stronger Coulombic attraction generally leads to slower dissociation steps and faster association steps. The effect that these have on the reaction rate depends on elementary steps that take part in the rate-determine step(s).
3. **Denticity:** Multi-dentate ligands create particularly inert complexes as a result of the kinetic chelate effect.

All three considerations are described in more detail below.



### ? Exercise 9.1.6.2

In which compound from each pair would you expect the strongest ionic bonds? Why?

- a) LiF vs KBr
- b)  $\text{CaCl}_2$  vs. KCl

#### Answer a

The ions in LiF are both smaller than in KBr, so the force of attraction between the ions in LiF is greater because of the smaller separation between the charges.

#### Answer b

Calcium has a 2+ charge in  $\text{CaCl}_2$ , whereas potassium has only a + charge, so the chloride ions are more strongly attracted to the calcium than to the potassium.

### Taube's observations of metal complex substitution rates

Henry Taube (Nobel Prize, 1983) tried to understand kinetic lability by comparing the factors that govern bond strengths to observations about the rates of reaction of coordination complexes. He saw some things that were unsurprising. He also drew some new conclusions based on ligand field theory.

Taube observed that **many  $M^{+1}$  ions ( $M = \text{metal}$ ) are more labile than many  $M^{+3}$  ions**, in general. That isn't too surprising, since metal ions function as electrophiles (Lewis acids) and ligands function as nucleophiles (Lewis bases) in forming coordination complexes. In other words, *metals with higher charges ought to be stronger Lewis acids, and so they should bind ligands more tightly*. However, there were exceptions to that general rule. For example, Taube also observed that  $\text{Mo}_5^+$  compounds are more labile than  $\text{Mo}_3^+$  compounds. So, there must be more going on here than *just* the effects of electrostatic attraction.

Another factor that governs ionic bond strengths is the *size of the ion*. Typically, **ions with smaller atomic radii form stronger bonds** than ions with larger radii. Taube observed that  $\text{Al}^{3+}$ ,  $\text{V}^{3+}$ ,  $\text{Fe}^{3+}$  and  $\text{Ga}^{3+}$  ions are all about the same size. All these ions exchange ligands at about the same rate. That isn't surprising, because they have the same charge and the same radius. However,  $\text{Cr}^{3+}$  is also about the same size as those ions and it also has the same charge, but it is much less labile. Once again, there are exceptions to our regular expectations based on simple electrostatic considerations. Furthermore, 4d and 5d transition metals ( $\text{Y} \rightarrow \text{Cd}$ , and  $\text{Ac} \rightarrow \text{Hg}$ ) are much more inert than 3d transition metals ( $\text{Sc} \rightarrow \text{Zn}$ ). This is unexpected when we consider size; the 4d and 5d metals are much larger than the 3d metals. This unexpected behavior tells us that electrostatics alone cannot predict lability.

Taube came up with a hypothesis that could explain the seeming contradictory observations described above: *kinetic lability must be affected by d-electron configuration*. This idea forms the basis of Taube's rules about lability.

For example, metals like  $\text{Ni}^{2+}$  and  $\text{Cu}^{2+}$  are very labile. The d orbital splitting diagrams for those compounds would have d electrons in the  $e_g$  set. Remember, the  $e_g$  set arises from interaction with the ligand donor orbitals; this set corresponds to a  $\sigma$  antibonding level.

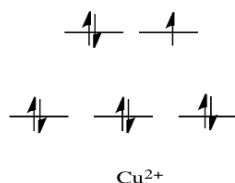


Figure 9.1.6.1:  $d^9$ -electron configuration assuming octahedral geometry.

By comparison,  $\text{V}^{2+}$  is rather inert. The d orbital splitting diagram in this case has electrons in the  $t_{2g}$  set, but none in the  $e_g$  set.

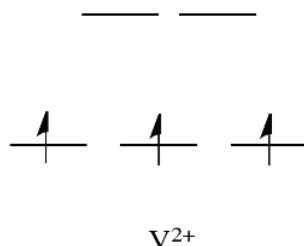


Figure 9.1.6.2:  $d^3$ -electron configuration assuming octahedral geometry.

So, having electrons in the higher energy, antibonding  $e_g$  level weakens the bond to the ligand, so the ligand can be replaced more easily. In the absence of those higher energy electrons, the bond to the ligand is stronger, and the ligand isn't replaced as easily.

On the other hand, metals like  $\text{Ca}^{2+}$ ,  $\text{Sc}^{3+}$  and  $\text{Ti}^{4+}$  are pretty labile. The d orbital splitting diagrams in those cases are pretty simple: there are no d-electrons at all in these ions.

That means having no electrons in these mostly non-bonding levels leaves the complex susceptible to ligand replacement. But it's hard to see why population of an orbital that is mostly non-bonding would have an effect on ligand bond strength.

Instead, this factor probably has something to do with the part of ligand substitution that we have ignored so far. Not only does one ligand need to leave, but a second one needs to bond in its place. So, having an empty orbital for the ligand to donate electrons into (or, put another way, not having electrons in the way that may complicate donation from the ligand) makes that part of the reaction easier.

### ? Exercise 9.1.6.3

Consider all possible electron configurations for octahedral complexes ( $d^0$  to  $d^{10}$ , high spin and low spin cases): predict whether each case would be inert, intermediate, or labile.

#### Answer

	Kinetically Inert (Slow)	Kinetically Labile (Fast)
$d^n$ electron count and ligand field strength	Octahedral configurations with empty $e_g$ orbitals: <ul style="list-style-type: none"> <li><math>d^3</math></li> <li>low-spin <math>d^4, d^5, d^6</math></li> </ul> Strong-field $d^8$ (square planar)	Octahedral configurations with occupied $e_g$ orbitals: <ul style="list-style-type: none"> <li><math>d^1, d^2, d^7, d^9, d^{10}</math></li> <li>high-spin <math>d^4, d^5, d^6</math></li> </ul> Weak-field $d^8$ (usually tetrahedral)

### ? Exercise 9.1.6.4

Put the metal ions in order of decreasing reaction rate (from labile to inert):

- a)  $\text{Al}^{3+}$ ,  $\text{Na}^+$ ,  $\text{Mg}^{2+}$   
 b)  $\text{Ca}^{2+}$ ,  $\text{Mg}^{2+}$ ,  $\text{Sr}^{2+}$

#### Answer (a)

Most Labile to most inert:  $\text{Na}^+ > \text{Mg}^{2+} > \text{Al}^{3+}$

These are metal ions with similar size and varying charge. They are in order of increasing charge and increasing density from left to right.

#### Answer (b)

Most labile to most inert:  $\text{Sr}^{2+} > \text{Ca}^{2+} > \text{Mg}^{2+}$

These metal ions have the same charge, and vary in size. They are in order of decreasing charge and increasing charge density from left to right.

### ? Exercise 9.1.6.5

Some metals, like  $\text{Mn}^{2+}$ , can be either labile or inert, depending on whether they are high spin or low spin. Explain why using d orbital splitting diagrams.

#### Answer

Add texts here. Do not delete this text first.

### ? Exercise 9.1.6.6

Predict whether the following metals, in octahedral complexes, are labile or not.

- a)  $\text{Co}^{3+}$  (high spin)
- b)  $\text{Co}^{3+}$  (low spin)
- c)  $\text{Fe}^{2+}$  (low spin)
- d)  $\text{Fe}^{2+}$  (high spin)
- e)  $\text{Zn}^{2+}$

#### Answer

##### Answer a

labile (electrons in higher energy d orbital set)

##### Answer b

not labile (all electrons in lower energy d orbitals)

##### Answer c

not labile (all electrons in lower energy d orbitals)

##### Answer d

labile (electrons in higher energy d orbital set)

##### Answer e

labile (electrons in higher energy d orbital set)

### Generalizations for how metal ion affects kinetics:

These are some generalizations about how the kinetics of substitution is affected by the metal ion identity and the  $d^n$  electron configuration.

1. s-block metals are very labile, except for those with very high charge density (eg.  $\text{Mg}^{2+}$  is inert)
2.  $d^{10}$  metals are labile (eg:  $\text{Zn}^{2+}$ ,  $\text{Cu}^+$ ,  $\text{Hg}^{2+}$ )
3. Other ions with a full shell are labile (eg:  $\text{Ln}^{3+}$  of f-block)
4. 3d  $M^{2+}$ , when high spin, are generally labile (eg.  $\text{Cu}^{2+}$  is very labile)
5. 4d and 5d are usually inert due to higher LFSE (low spin, high LFSE)
6.  $M^{2+}$  is more labile than the same metal as  $M^{3+}$
7.  $d^3$  and low spin  $d^6$  are inert (eg.  $\text{Cr}^{3+}$ ,  $\text{Co}^{3+}$ , low spin  $\text{Fe}^{2+}$ )

### Chelate Complexes

In addition to considering factors related to the metal ion and charge or covalent character of metal-ligand bonds, an important consideration is the effect a chelate ligand on reaction kinetics. This effect is also discussed in more detail later in this chapter (Section 12.4.5).

### Recall the Thermodynamic Chelate Effect

Chelating complexes tend to be more stable than complexes with monodentate ligands. This is called the “thermodynamic chelate effect”. The effect deserves an explanation. The explanation is the increase of entropy that occurs when two or more monodentate ligands are replaced by a chelating ligand. The entropy increases because the overall number of particles increases as the substitution takes place.

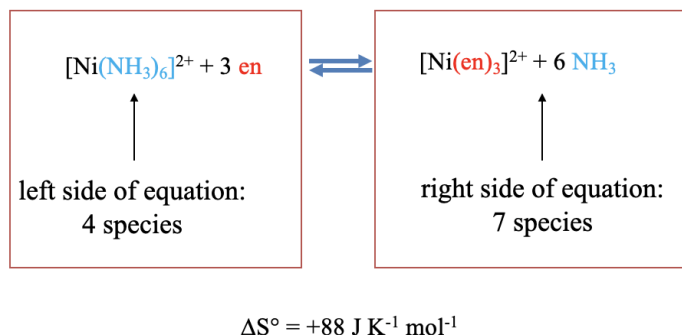


Figure 9.1.6.3: Example of the thermodynamic chelate effect

For example, the substitution of six ammine ligands in the hexaammine nickel (2+) complex by three ethylenediamine chelating ligands increases the number of molecules from four to seven, and hence the entropy increases, in this case by 88 J K<sup>-1</sup> and mol<sup>-1</sup> (Figure 9.1.6.3)

### The Kinetic Chelate Effect

In addition to the thermodynamic chelate effect, there is the kinetic chelate effect. Chelate complexes are frequently more inert than complexes with monodentate ligands. Chelate complexes are more inert for two reasons (Figure 9.1.6.4).

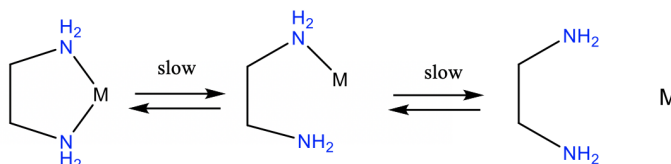


Figure 9.1.6.4: Illustration of the kinetic chelate effect

Firstly, the whole ligands needs to rotate and bend in order to cleave the first metal-ligand bond. This requires time and slows the kinetics of the bond cleavage. The second reason is that the detached donor atom cannot leave the proximity of the complex because the ligand is still attached via the other donor atom. This increases the probability of the re-formation of the metal-ligand bond which decreases the probability of both bonds being cleaved.

Chris P Schaller, Ph.D., (College of Saint Benedict / Saint John's University)

Curated or created by Kathryn Haas

Dr. Kai Landskron (Lehigh University). If you like this textbook, please consider to make a donation to support the author's research at Lehigh University: [Click Here to Donate](#).

This page titled 9.1.6: Kinetic Lability is shared under a [not declared](#) license and was authored, remixed, and/or curated by Kathryn Haas.

- 9.1: Substitution Reactions and their Mechanisms by Kai Landskron is licensed CC BY 4.0.

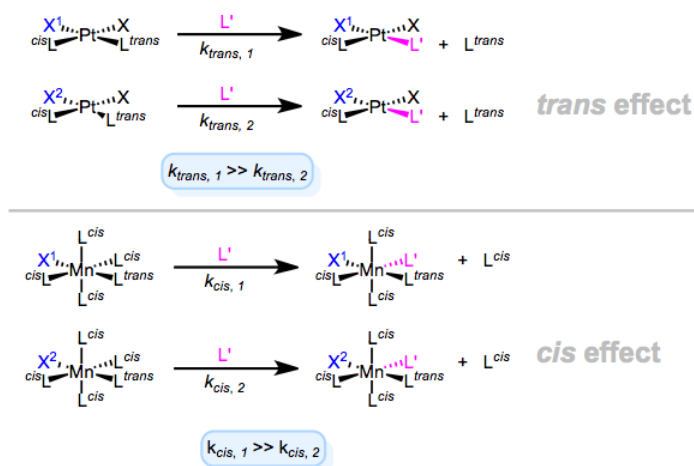
## 9.1.7: The Trans Effect

The trans effect is an ancient but venerable observation. First noted by Chernyaev in 1926, the trans effect and its conceptual siblings (the trans influence, cis influence, and cis effect) are easy enough to comprehend. That is, it's simple enough to know what they are. To understand why they are, on the other hand, is much more difficult.

### Definitions & Examples

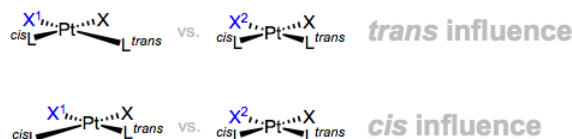
Let's begin with definitions: what is the trans effect? There's some confusion on this point, so we need to be careful. The trans effect proper, which is often called the kinetic trans effect, refers to the observation that certain ligands increase the rate of ligand substitution when positioned trans to the departing ligand. The key word in that last sentence is "rate"—the trans effect proper is a kinetic effect. The trans influence refers to the impact of a ligand on the length of the bond trans to it in the ground state of a complex. The key phrase there is "ground state"—this is a thermodynamic effect, so it's sometimes called the thermodynamic trans effect. Adding to the insanity, cis effects and cis influences have also been observed. Evidently, ligands may also influence the kinetics or thermodynamics of their cis neighbors. All of these phenomena are independent of the metal center, but do depend profoundly on the geometry of the metal (more on that shortly).

Kinetic trans and cis effects are shown in the figure below. In both cases, we see that  $X^1$  exhibits a stronger effect than  $X^2$ . The geometries shown are those for which each effect is most commonly observed. The metals and oxidation states shown are prototypical.



**Figure 1:** The kinetic trans and cis effects in action.  $X^1$  is the stronger (trans/cis)-effect ligand in these examples.

On to the influences, which are simpler to illustrate since they're concerned with ground states, not reactions. The lengthened bonds below are exaggerated.



**Figure 2:** The trans and cis influences in action. Note the elongated bond lengths.

And there we have it folks, the thermodynamic and kinetic cis/trans effects. It's worth keeping in mind that the kinetic trans effect is most common for d8 square planar complexes, and the kinetic cis effect is most common for d6 octahedral complexes (particularly when the departing L is CO). But a lingering question remains: what makes for a strong trans effect ligand?

### Origins of Effects & Influences

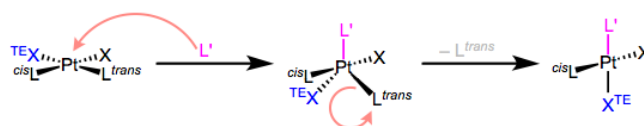
The trans effect and its cousins are all electronic, not steric effects. So, the electronic properties of the ligand dictate the strength of its trans effect. Let's finally dig into the trans effect series:

(weak)  $F^-$ ,  $HO^-$ ,  $H_2O$   $< NH_3 < py < Cl^- < Br^- < I^-$ ,  $SCN^-$ ,  $NO_2^-$ ,  $SC(NH_2)_2$ ,  $Ph^- < SO_3^{2-} < PR_3 < AsR_3$ ,  $SR_2$ ,  $H_3C^- < H^-$ ,  $NO$ ,  $CO$ ,  $NC^-$ ,  $C_2H_4$  (strong)

What's the electronic progression here? It's clear that electronegativity decreases across the series:  $F^- < Cl^- < Br^- < I^- < H_3C^-$ . From a bonding perspective, we can say that ligands with strong trans effects are strong  $\sigma$ -donors (or  $\sigma$ -bases). Yet  $\sigma$ -donation doesn't tell the whole story. What about ethylene and carbon monoxide, which both appear at the top of the heap? Neither of these ligands are strong  $\sigma$ -donors, but their  $\pi$  systems do interact with the metal center through backbonding. Consider the following sub-series:  $S=C=N^- < PR_3 < CO$ . Backbonding increases across this series, along with the strength of the trans effect. Strong backbonders—better known as  $\pi$ -acceptors or  $\pi$ -acids—exhibit strong trans effects.

Strong trans effect = strong  $\sigma$ -donor + strong  $\pi$ -acceptor

Wonderful! Using these ideas we can identify ligands with strong trans effects. But we can dive deeper down the rabbit hole: why does this particular combination of electronic factors lead to a strong trans effect? To understand this, we need to know the mechanism of the ligand substitution reaction that's sped up by strong trans effect ligands. For 16-electron Pt(II) complexes, associative substitution is par for the course. The incoming ligand binds to the metal first, forming an 18-electron complex (yay!), which jettisons a ligand to yield a new 16-electron product. The mechanism in all its glory is shown in the figure below.



**Figure 3:** The mechanism of associative ligand substitution of Pt(II) complexes.

Some very important points about this mechanism:

- The incoming ligand always sits at an equatorial site in the trigonal bipyramidal intermediate. More on this another day, but I think of this result as governed by the principle of least motion. Consider the molecular gymnastics that would have to happen to place the incoming ligand in an axial position.
- Two ligands in the square plane are “pushed down” and become the other two equatorial ligands.
- Owing to microscopic reversibility, the leaving group must be one of the equatorial ligands.

The third point reveals that once  $L'$  has “pushed down” XTE and Ltrans, Ltrans has no choice but to leave (assuming XTE stays put). Thus, the trans effect has nothing to do with the second step of the mechanism, which is not rate determining anyway. The key is the first step—in particular, the “pushing down” event. Apparently, ligands with strong trans effects like to be pushed down. They like to occupy the equatorial plane of the TBP geometry. Now here's the kicker: the equatorial sites of the TBP geometry are more  $\pi$  basic than the axial sites. The equatorial plane is just the xy-plane of the metal center, and the d orbitals in that plane (when occupied) are great electron sources for  $\pi$ -acidic ligands. Thus,  $\pi$ -acidic ligands want to occupy those equatorial sites, to receive the benefits of strong backbonding! Boom; strong  $\pi$ -acids encourage loss of the ligand trans to themselves.



**Figure 4:** The equatorial sites of TBP metals are rich in electrons that can  $\pi$  bond.

What about those pesky  $\sigma$  donors? Well, we can imagine that in a square planar complex, a ligand and its trans partner are competing for donation into the same d orbital. Strong  $\sigma$  donation from a ligand should thus weaken the bond trans to it. Although this is the thermodynamic trans effect (trans influence) in action, the resulting destabilization of the ground state relative to the transition state is a kinetic effect. On the whole, the barrier to substitution of the trans ligand goes down as  $\sigma$ -donating strength goes up.

This idea of “competition for the metal center” is a nice heuristic to use when thinking about the trans and cis influences. The type of metallic orbital involved in M–L bonding determines the strength of L's trans and cis influences on neighboring ligands that also need that metallic orbital for bonding. For example: both influences are large if the metal's s orbital is a significant contributor to M–L bonding, since it's non-directional; the trans influence is much greater than the cis influence when metallic p orbitals are primarily involved in M–L. For a deeper explanation of these ideas, see [this paper](#).

## Summing up

Perhaps the most valuable lesson from a study of the trans effect is that many concepts from organometallic chemistry involve more than meets the eye. Geometric effects and influences are real icebergs, in the sense that the observations and trends are easy to grasp, but difficult to explain. We had to dig all the way into the mechanism of associative ligand substitution before a satisfactory explanation emerged!

## Contributors

Dr. Michael Evans ([Georgia Tech](#))

---

9.1.7: The Trans Effect is shared under a [CC BY-NC-SA 4.0](#) license and was authored, remixed, and/or curated by LibreTexts.

## 9.2: RedOx Reactions

---

Lecture objectives for this unit are to:

- Identify coordination complexes being oxidized and reduced in a redox reaction
  - Compare and contrast inner and outer sphere electron transfer mechanisms
  - Recall the factors required for an inner sphere electron transfer to occur
  - Predict or explain observed rates of outer sphere electron transfer reactions based upon structures of the complexes
- 

9.2: RedOx Reactions is shared under a [not declared](#) license and was authored, remixed, and/or curated by LibreTexts.



### 9.2.1: Redox Mechanisms

---

The oxidation state of a metal ion can be changed by **reduction/oxidation** (redox) reactions in which electrons are transferred between a metal center and another species. The other species could be another metal ion or some other redox partner. In the case of metal complexes, the electron transfer often occurs at the metal center, changing the oxidation state of the metal ion(s) involved. This section will focus on the redox reactions involving change in metal ion oxidation state.

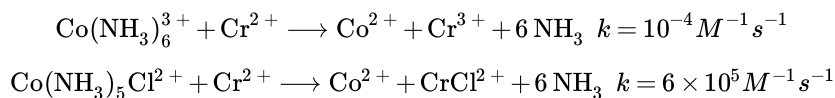
There are two general mechanisms by which electrons can be transferred to or from a metal center. The definition of these two mechanisms depends on whether the redox partner is bound within the metal ion's inner sphere (bound directly to the metal ion), or whether it is just nearby the metal complex (in the metal ion's outer sphere). If the redox partner is bound to the metal ion itself, it is called an **inner-sphere electron transfer**. Electrons can also be transferred between two species that are close in proximity, but not bound to one another. When electrons are transferred to or from a metal through close proximity, but not through direct bonds to the metal center, it is an **outer-sphere electron transfer**.

---

This page titled [9.2.1: Redox Mechanisms](#) is shared under a [not declared](#) license and was authored, remixed, and/or curated by [Kathryn Haas](#).

## 9.2.2: Inner Sphere Electron Transfer

In some cases, electron transfers occur much more quickly in the presence of certain ligands. For example, compare the rate constants for the following two electron transfer reactions, involving almost exactly the same complexes:



(Note: aqua ligands are omitted for simplicity. Ions, unless noted otherwise, are aqua complexes.)

Notice two things: first, when there is a chloride ligand involved, the reaction is much faster. Second, after the reaction, the chloride ligand has been transferred to the chromium ion. Possibly, those two events are part of the same phenomenon.

Similar rate enhancements have been reported for reactions in which other halide ligands are involved in the coordination sphere of one of the metals.

In the 1960's, Henry Taube of Stanford University proposed that halides (and other ligands) may promote electron transfer via bridging effects. What he meant was that the chloride ion could use one of its additional lone pairs to bind to the chromium ion. It would then be bound to both metals at the same time, forming a bridge between them. Perhaps the chloride could act as a conduit for electron transfer. The chloride might then remain attached to the chromium, to which it had already formed a bond, leaving the cobalt behind.

Electron transfers that occur via ligands shared by the two metals undergoing oxidation and reduction are termed "inner sphere" electron transfers. Taube was awarded the Nobel Prize in chemistry in 1983; the award was based on his work on the mechanism of electron transfer reactions.

### ? Exercise 9.2.2.1

Take another look at the two electron transfer reactions involving the cobalt and chromium ion, above.

- What geometry is adopted by these complexes?
- Are these species high spin or low spin?
- Draw d orbital splitting diagrams for each complex.
- Explain why electron transfer is accompanied by loss of the ammonia ligands from the cobalt complex.
- The chloride is lost from the cobalt complex after electron transfer. Why does it remain on the chromium?

#### Answer a

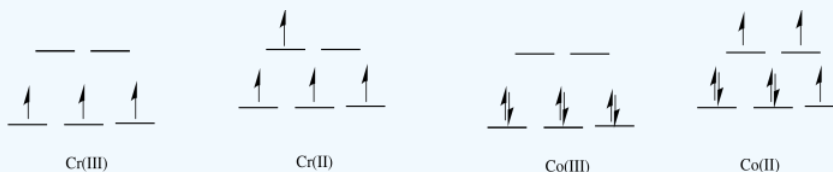
- octahedral

#### Answer b

- In the first row,  $2^+$  complexes are almost always high spin. However,  $3^+$  complexes are sometimes low spin.

#### Answer c

- 



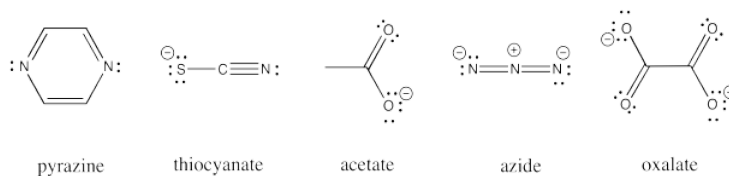
#### Answer d

- The Co(II) complex is high spin and labile. The ligands are easily replaced by water.

#### Answer e

- The Cr(III) complex is only  $d^3$ ; it is inert.

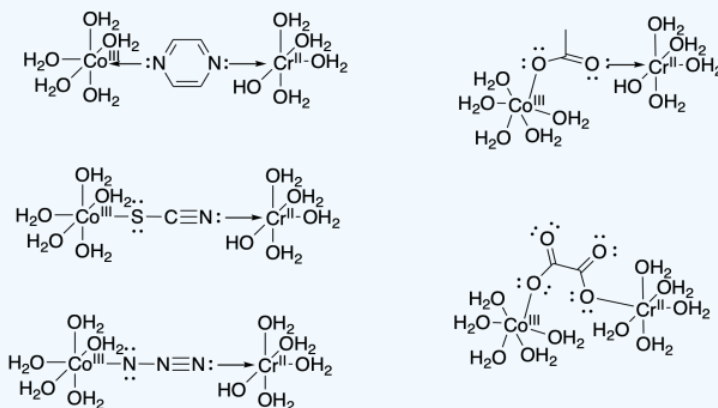
Other ligands can be involved in inner sphere electron transfers. These ligands include carboxylates, oxalate, azide, thiocyanate, and pyrazine ligands. All of these ligands have additional lone pairs with which to bind a second metal ion.



### ? Exercise 9.2.2.2

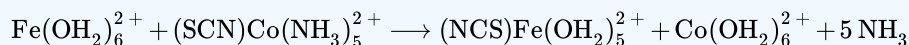
Draw an example of each of the ligands listed above bridging between a cobalt(III) and chromium(II) aqua complex.

**Answer**

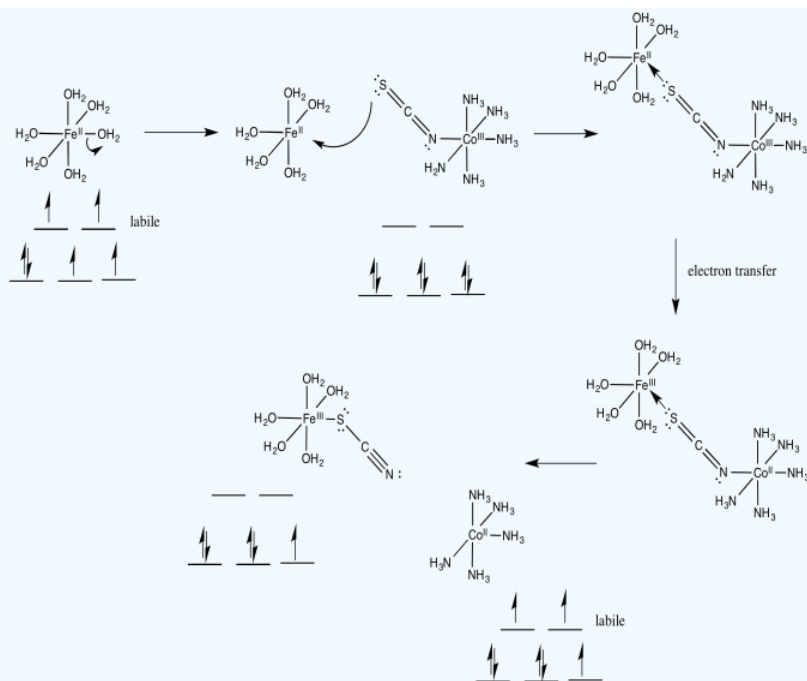


### ? Exercise 9.2.2.3

Explain, with structures and d orbital splitting diagrams, how the products are formed in the following reaction, in aqueous solution.



**Answer**



How does the electron travel over the bridge?

Once the bridge is in place, the electron transfer may take place via either of two mechanisms. Suppose the bridging ligand is a chloride. The first step might actually involve an electron transfer from chlorine to the metal; that is, the chloride could donate one electron from one of its idle lone pairs. This electron could subsequently be replaced by an electron transfer from metal to chlorine.



Sometimes, we talk about the place where an electron *used to be*, describing it as a "hole". In this mechanism, the electron donated from the bridging chloride ligand leaves behind a hole. The hole is then filled with an electron donated from the other metal.

Alternatively, an electron might first be transferred from metal to chlorine, which subsequently passes an electron along to the other metal. In the case of chlorine, this idea may be unsatisfactory, because chlorine already has a full octet. Nevertheless, some of the other bridging ligands may have low-lying unoccupied molecular orbitals that could be populated by this extra electron, temporarily.

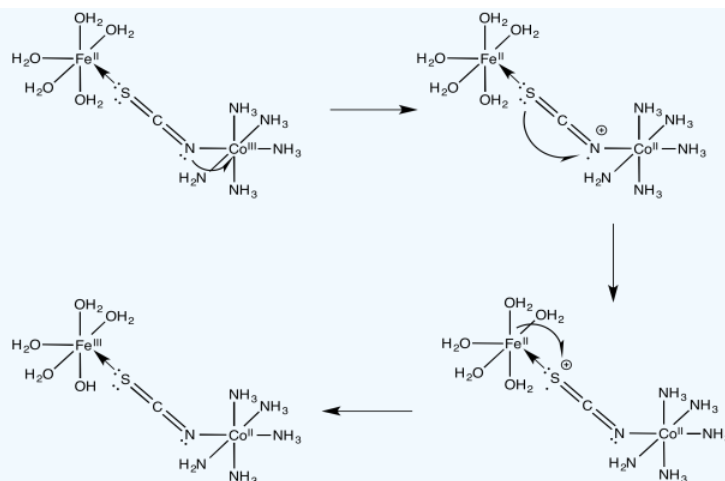


### ? Exercise 9.2.2.4

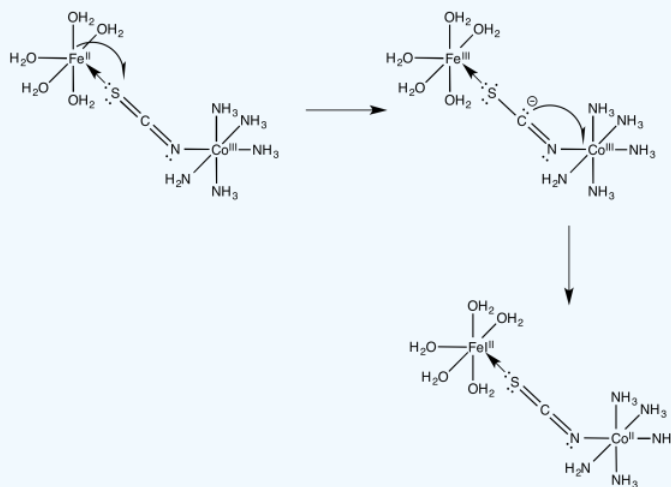
For the iron / cobalt electron transfer in problem Exercise 9.2.2.3(RO9.3.), show

- an electron transfer mechanism via a hole migration along the bridge
- an electron transfer mechanism via an electron migration along the bridge

**Answer a**



Answer b



### ? Exercise 9.2.2.5

One of the many contributions to the barrier for electron transfer between metal ions is internal electronic reorganization.

a) Draw d orbital splitting diagrams for each of the following metal ions in an octahedral environment.

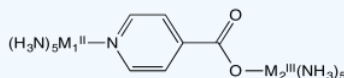
Ru(II) or Os(II)

Ru(III) or Os(III)

Co(II)

Co(III)

Flash photolysis is a method in which an electron can be moved instantly “uphill” from one metal to another (e.g. from  $\text{M}_2^{\text{II}}$  to  $\text{M}_1^{\text{III}}$ , below); the electron transfer rate can then be measured as the electron “drops” back from  $\text{M}_1^{\text{II}}$  to  $\text{M}_2^{\text{III}}$ .



b) Explain the relative rates of electron transfer reaction in this system, as measured by flash photolysis in the table below.

$\text{M}_1^{\text{II}}$	$\text{M}_2^{\text{III}}$	$k_{\text{obs}} \text{ s}^{-1}$
Os	Ru	$> 5 \times 10^9$

Os

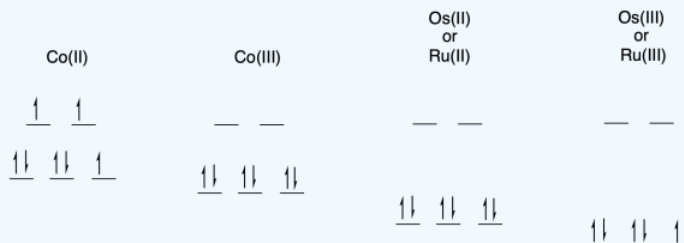
Co

$1.9 \times 10^5$

c) Does the reaction above probably occur via an inner sphere or by an outer sphere pathway? Why?

**Answer a**

a)



**Answer b**

b) The electron transfer between Os(II) and Ru(III) will not involve any electron reorganization because both are low spin to begin with. However, the electron transfer between Os(II) and Co(III) will result in cobalt changing from low spin to high spin. The need to move electrons between different d orbitals on the cobalt will add to the barrier, slowing down the reaction.

**Answer c**

c) The pathway is probably inner sphere because of the bridging ligand. Furthermore, the conjugation in the bridging ligand would help in conducting an electron from one end of the ligand to the other, either through an electron mechanism or a hole mechanism.

### ? Exercise 9.2.2.6

Outer sphere electron transfer rates depend on the free energy change of the reaction ( $\Delta G^\circ$ ) and the distance between oxidant and reductant (d) according to the relation

$$\text{Rate constant} = k = Ae^{(-\Delta G)}e^{-d}$$

a) What happens to the rate of the reaction as distance increases between reactants?

One potential problem in measuring rates of intramolecular electron transfer (i.e. *within* a molecule) is competition from intermolecular electron transfer (*between* molecules).

b) What would you do in the flash photolysis experiment above to discourage intermolecular electron transfer?

c) How could you confirm whether you were successful in discouraging intermolecular reaction?

**Answer a**

a) The rate decreases exponentially as distance increases.

**Answer b**

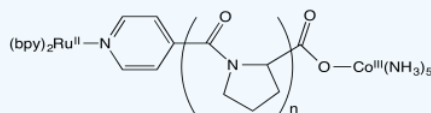
b) You might keep the concentration low in order to increase the distance between molecules, reducing the likelihood of an outer-sphere electron transfer.

**Answer c**

c) If you ran the experiment at a series of dilutions, intramolecular electron transfer would be unaffected but outer sphere electron transfer would not. If the rates were the same across a number of different concentrations, the reaction would probably be intramolecular.

### ? Exercise 9.2.2.7

Stephan Isied and coworkers at Rutgers measured the following electron transfer rates between metal centers separated by a peptide. (*Chem Rev* **1992**, 92, 381-394)



- The proline repeating unit is crucial in ensuring a steady increase in distance between metal centers with increased repeat units,  $n$ . Why?
- An inner sphere pathway in this case is expected to be somewhat slow because of the lack of conjugation in the polyproline bridge. Explain why.
- Plot the data below, with  $\log k$  on the y axis (range from 4-9) and  $d$  on the x axis (12-24 Angstroms).

$n$	$d$ (Å)	$k_{\text{obs}}$ ( $\text{s}^{-1}$ )
1	12.2	$5 \times 10^8$
2	14.8	$1.6 \times 10^7$
3	18.1	$2.3 \times 10^5$
4	21.3	$5.1 \times 10^4$
5	24.1	$1.8 \times 10^4$

- A linear relationship is in agreement with Marcus theory;  $\log k = -c \times d$ . Is your plot linear?

Isied offers a number of possible explanations for the data, all of which involve two competing reaction pathways.

- Suggest one explanation for the data.

#### Answer a

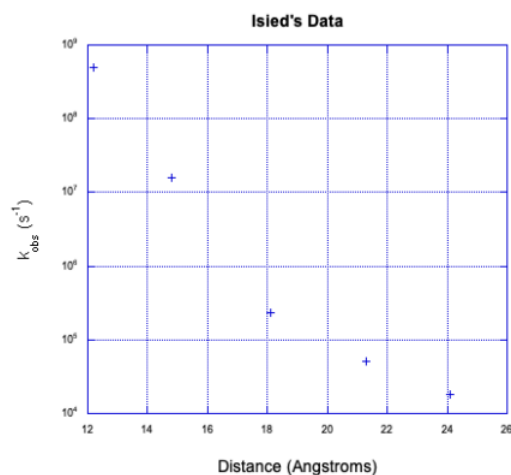
- Rings are frequently used to introduce conformational rigidity (or decrease conformational flexibility), limiting the range of potential shapes a molecule could adopt. If the molecule can't wiggle around as much, then the distance between the ends of the molecule should be more constant.

#### Answer b

- Although the ligand is bridging, it would be difficult to picture either an electron or hole mechanism of inner sphere electron transfer. There are few pi bonds or lone pairs to use as places to put electrons or temporarily remove electrons from, shuttling the electrons from place to place along the ligand. A conjugated system would be much more likely to carry out inner sphere electron transfer.

#### Answer c

-



**Answer d**

d) The data is not linear.

**Answer e**

e) The data appear to show two lines that cross. That's a classic symptom of two competing mechanisms. The faster mechanism, to the left, is probably an intramolecular electron transfer. The slower mechanism, to the right, may be an intermolecular electron transfer.

---

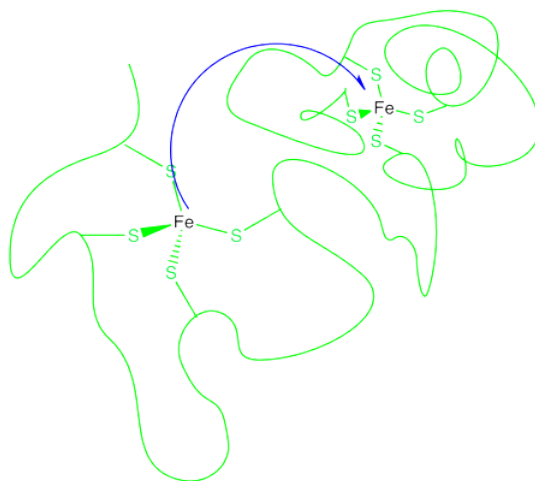
This page titled [9.2.2: Inner Sphere Electron Transfer](#) is shared under a [CC BY-NC](#) license and was authored, remixed, and/or curated by [Kathryn Haas](#).

- **1.10: Inner Sphere Electron Transfer** by [Chris Schaller](#) is licensed [CC BY-NC 3.0](#). Original source: <https://employees.csbsju.edu/cschaller/ROBI3.htm>.



### 9.2.3: Outer Sphere Electron Transfer

How does an electron get from one metal to another? This might be a more difficult task than it seems. In biochemistry, an electron may need to be transferred a considerable distance. Often, when the transfer occurs between two metals, the metal ions may be constrained in particular binding sites within a protein, or even in two different proteins.



That means the electron must travel through space to reach its destination. Its ability to do so is generally limited to just a few Angstroms (remember, an Angstrom is roughly the distance of a bond). Still, it can react with something a few bond lengths away. Most things need to actually bump into a partner before they can react with it.

This long distance hop is called an outer sphere electron transfer. The two metals react without ever contacting each other, without getting into each others' coordination spheres. Of course, there are limitations to the distance involved, and the further away the metals, the less likely the reaction. But an outer sphere electron transfer seems a little magical.

#### Barrier to Reaction: A Qualitative Picture of Marcus Theory

So, what holds the electron back? What is the barrier to the reaction? Rudy Marcus at Caltech has developed a mathematical approach to understanding the kinetics of electron transfer, in work he did beginning in the late 1950's. We will take a very qualitative look at some of the ideas in what is referred to as "Marcus Theory". An electron is small and very fast. All those big, heavy atoms involved in the picture are lumbering and slow. The barrier to the reaction has little to do with the electron's ability to whiz around, although even that is limited by distance. Instead, it has everything to do with all of those things that are barely moving compared to the electron.

Imagine an iron(II) ion is passing an electron to an iron(III) ion. After the electron transfer, they have switched identities; the first has become an iron(III) and the second has become an iron(II) ion.

Nothing could be simpler. The trouble is, there are big differences between an iron(II) ion and an iron(III) ion. For example, in a coordination complex, they have very different bond distances. Why is that a problem? Because when the electron hops, the two iron atoms find themselves in sub-optimal coordination environments.

#### ? Exercise 9.2.3.1

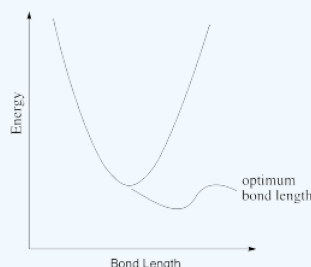
Suppose an electron is transferred from an Fe(II) to a Cu(II) ion. Describe how the bond lengths might change in each case, and why. Don't worry about what the specific ligands are.

#### Answer

The bonds to iron would contract because the increased charge on the iron would attract the ligand donor electrons more strongly. The bonds to copper would lengthen because of the lower charge on the copper.

### ? Exercise 9.2.3.2

In reality, a bond length is not static. If there is a little energy around, the bond can lengthen and shorten a little bit, or vibrate. A typical graph of molecular energy vs. bond length is shown below.



- Why do you think energy increases when the bond gets shorter than optimal?
- Why do you think energy increases when the bond gets longer than optimal?
- In the following drawings, energy is being added as we go from left to right. Describe what is happening to the bond length as available energy increases.

#### Answer a

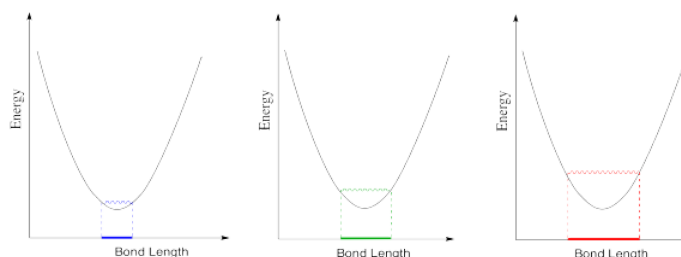
- Most likely there are repulsive forces between ligands if the bonds get too short.

#### Answer b

- Insufficient overlap between metal and ligand orbitals would weaken the bond and raise the energy.

#### Answer c

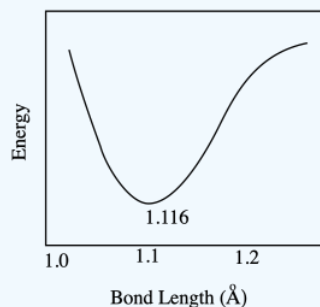
- The range of possible bond lengths gets broader as energy is increased. The bond has more latitude, with both longer and shorter bonds allowed at higher energy.



### ? Exercise 9.2.3.3

The optimum C-O bond length in a carbon dioxide molecule is 1.116 Å. Draw a graph of what happens to internal energy when this bond length varies between 1.10 Å and 1.20 Å. Don't worry about quantitative labels on the energy axis.

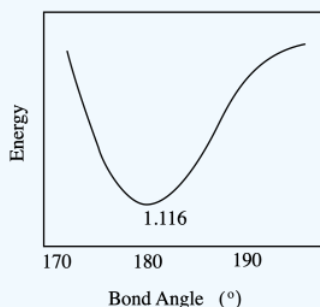
#### Answer



### ? Exercise 9.2.3.4

The optimum O-C-O bond angle in a carbon dioxide molecule is  $180^\circ$ . Draw a graph of what happens to internal energy when this bond angle varies between  $170^\circ$  and  $190^\circ$ . Don't worry about quantitative labels on the energy axis.

**Answer**



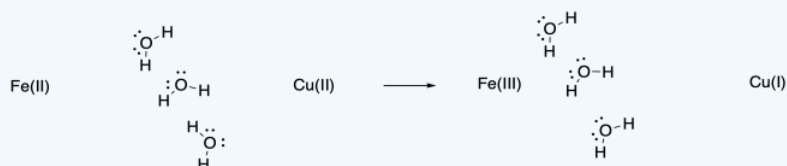
The barrier to electron transfer has to do with reorganizations of all those big atoms before the electron makes the jump. In terms of the coordination sphere, those reorganizations involve bond vibrations, and bond vibrations cost energy. Outside the coordination sphere, solvent molecules have to reorganize, too. Remember, ion stability is highly influenced by the surrounding medium.

### ? Exercise 9.2.3.5

Draw a Fe(II) ion and a Cu(II) ion with three water molecules located somewhere in between them. Don't worry about the ligands on the iron or copper. Show how the water molecules might change position or orientation if an electron is transferred from iron to copper.

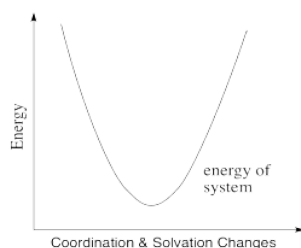
**Answer**

The water molecules may pivot toward the more highly charged Fe(III), or they may shift closer to it because of the attraction between the ion and the dipole of the water molecule.



Keep in mind that such adjustments would happen in non-polar solvents, too, although they would involve weaker IMFs such as ion - induced dipole interactions.

Thus, the energetic changes needed before electron transfer can occur involve a variety of changes, including bond lengths of several ligands, bond angles, solvent molecules, and so on. The whole system, involving both metals, has some optimum set of positions of minimum energy. Any deviations from those positions requires added energy. In the following energy diagram, the x axis no longer defines one particular parameter. Now it lumps all changes in the system onto one axis. This picture is a little more abstract than when we are just looking at one bond length or one bond angle, but the concept is similar: there is an optimum set of positions for the atoms in this system, and it would require an input of energy in order to move any of them away from their optimum position.

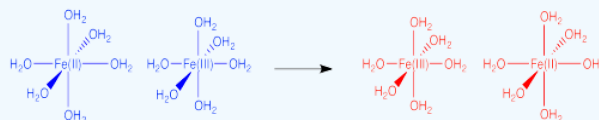


It is thought that these kinds of reorganizations -- involving solvent molecules, bond lengths, coordination geometry and so on -- actually occur prior to electron transfer. They happen via random motions of the molecules involved. However, once they have happened, there is nothing to hold the electron back. Its motion is so rapid that it can immediately find itself on the other atom before anything has a chance to move again.

Consequently, the barrier to electron transfer is just the amount of energy needed for all of those heavy atoms to get to some set of coordinates that would be accessible in the first state, before the electron is transferred, but that would also be accessible in the second state, after the electron is transferred.

### ? Exercise 9.2.3.6

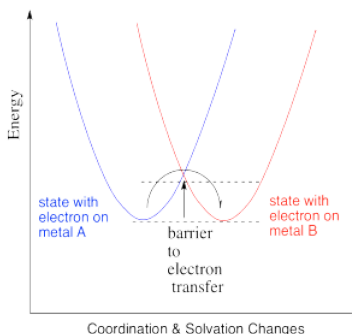
Describe some of the changes that contribute to the barrier to electron transfer in the following case.



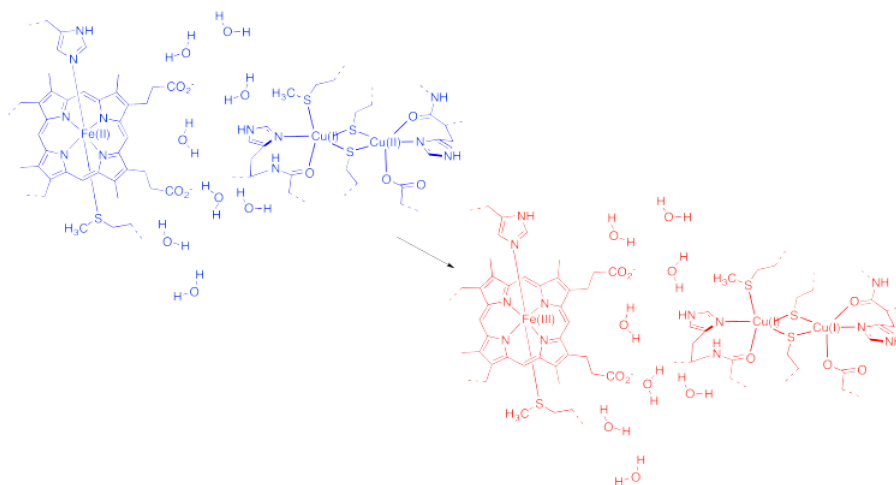
### Answer

The reactants and products are very similar in this case. However, the Fe(III) complex has shorter bonds than the Fe(II) complex because of greater electrostatic interaction between the metal ion and the ligands. These changes in bond length needed in order to get ready to change from Fe(III) to Fe(II) (or the reverse) pose a major barrier to the reaction.

In the drawing below, an electron is transferred from one metal to another metal of the same kind, so the two are just switching oxidation states. For example, it could be an iron(II) and an iron(III), as pictured in the problem above. In the blue state, one iron has the extra electron, and in the red state it is the other iron that has the extra electron. The energy of the two states are the same, and the reduction potential involved in this transfer is zero. However, there would be some atomic reorganizations needed to get the coordination and solvation environments adjusted to the electron transfer. The ligand atoms and solvent molecules have shifted in the change from one state to another, and so our energy surfaces have shifted along the x axis to reflect that reorganization.



That example isn't very interesting, because we don't form anything new on the product side. Instead, let's picture an electron transfer from one metal to a very different one. For example, maybe the electron is transferred from cytochrome c to the "copper A" center in cytochrome c oxidase, an important protein involved in respiratory electron transfer.



### ? Exercise 9.2.3.7

In the drawing above, some water molecules are included between the two metal centres.

- Explain what happens to the water molecules in order to allow electron transfer to occur, and why.
- Suppose there were a different solvent, other than water, between the complexes. How might that affect the barrier to the reaction?

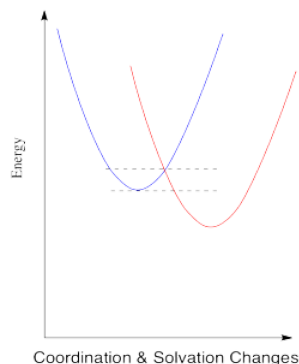
#### Answer a

a) The drawing is an oversimplification, but in general the water molecules are shown reorienting after the electron transfer because of ion-dipole interactions. In this case, the waters are shown orienting to present their negative ends to the more positive iron atom after the electron transfer. In reality, in a protein there are lots of other charges (including charges on the ligand) that may take part in additional ion-dipole interactions.

#### Answer b

b) Because electron transfer is so fast, atomic and molecular reorganisations are actually thought to happen before the electron transfer. The water molecules would happen to shift into a position that would provide the greatest possible stabilisation for the ions and then the electron would be transferred. A less polar solvent than water would be less able to stabilize ions and the electron would be slower to transfer as a result. In addition, a less polar solvent than water would be a poor medium to transmit an electron, which is charged and therefore stabilized by interactions with polar solvents.

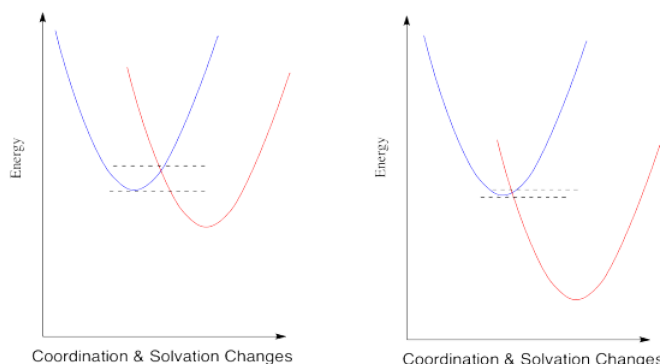
The energy diagram for the case involving two different metals is very similar, except that now there is a difference in energy between the two states. The reduction potential is no longer zero. We'll assume the reduction potential is positive, and so the free energy change is negative. Energy goes down upon electron transfer.



Compare this picture to the one for the degenerate case, when the electron is just transferred to a new metal of the same type. A positive reduction potential (or a negative free energy change) has the effect of sliding the energy surface for the red state

downwards. As a result, the intersection point between the two surfaces also slides downwards. Since that is the point at which the electron can slide from one state to the other, the barrier to the reaction decreases.

What would happen if the reduction potential were even more positive? Let's see in the picture below.



The trend continues. According to this interpretation of the kinetics of electron transfer, the more exothermic the reaction, the lower its barrier will be. It isn't always the case that kinetics tracks along with thermodynamics, but this might be one of them.

But is all of this really true? We should take a look at some experimental data and see whether it truly works this way.

Oxidant	$E^\circ$	$k$ ( $M^{-1}s^{-1}$ ) (margin of error shown in parentheses)
$Co(diene)(NH_3)_2^{3+}$	0.12	3.0(4)
$Co(diene)H_2O)NCS^{2+}$	0.38	11(1)
$Co(diene)(H_2O)_2^{3+}$	0.53	800(100)
$Co(EDTA)$	0.60	6000(1000)

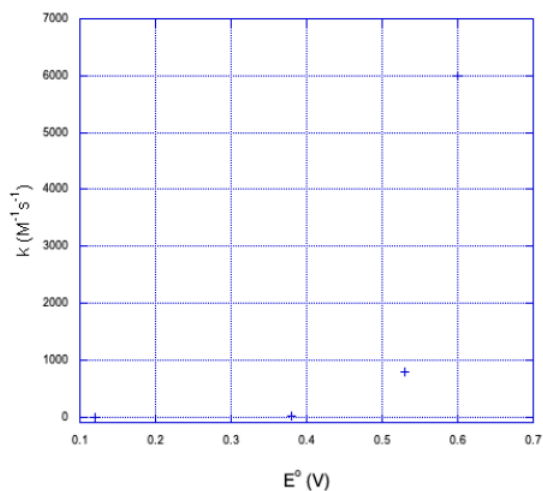
As the reduction potential becomes more positive, free energy gets more negative, and the rate of the reaction dramatically increases. So far, Marcus theory seems to get things right.

### ? Exercise 9.2.3.8

- Plot the data in the above table.
- How would you describe the relationship? Is it linear? Is it exponential? Is it direct? Is it inverse?
- Plot rate constant versus free energy change. How does this graph compare to the first one?

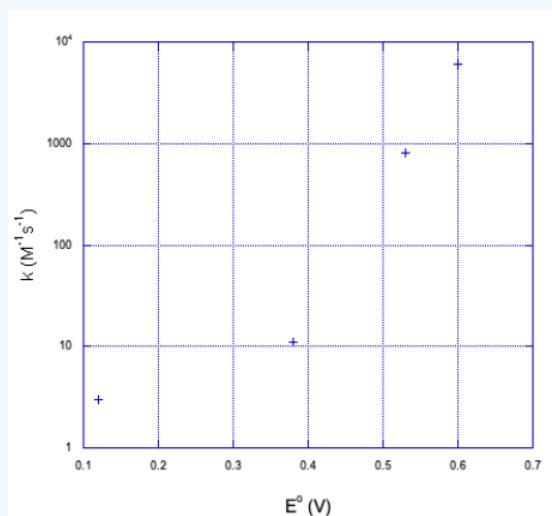
#### Answer a

- Here is a plot of the data.



**Answer b**

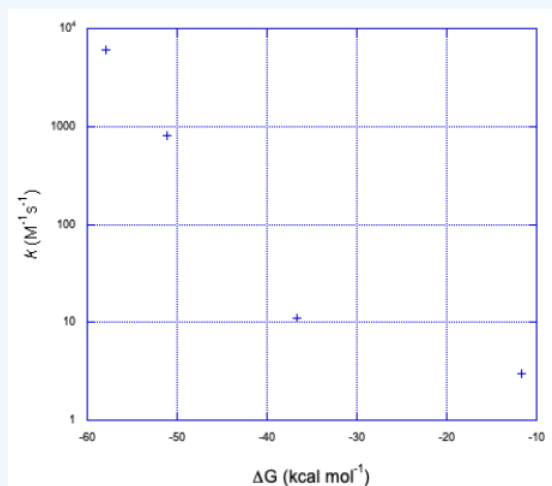
b) It doesn't look linear. If we plot the y axis on a log scale, things become a little more linear.



It looks closer to a logarithmic relationship than a linear one.

**Answer c**

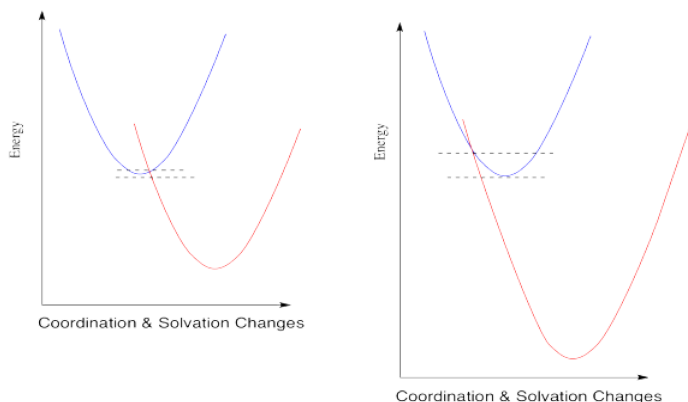
c) Assuming one electron transfer:



The graph takes the same form but in the opposite direction along the x axis.

## Marcus Inverted Region

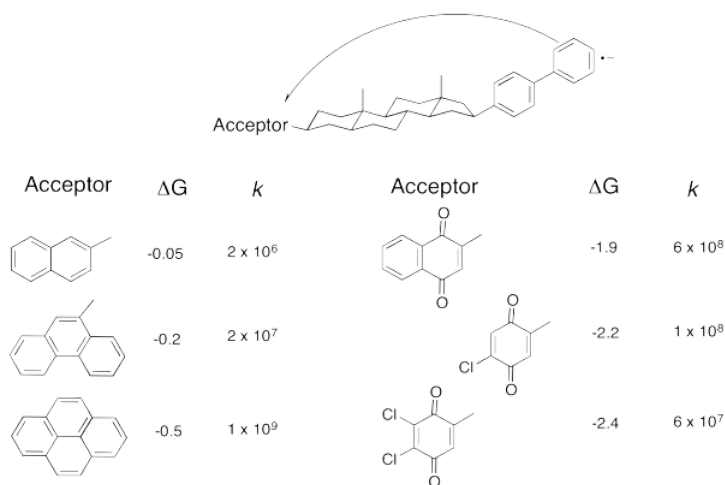
When you look a little closer at Marcus theory, though, things get a little strange. Suppose we make one more change and see what happens when the reduction potential becomes *even more* positive.



So, if Marcus is correct, at some point as the reduction potential continues to get more positive, reactions start to slow down again. They don't just reach a maximum rate and hold steady at that plateau; the barrier gets higher and higher and the reactions get slower and slower. If you feel a little skeptical about that, you're in good company.

Marcus always maintained that this phenomenon was a valid aspect of the theory, and not just some aberration that should be ignored. The fact that nobody had ever actually observed such a trend didn't bother him. The reason we didn't see this kind of thing, he said, was that we just hadn't developed technology that was good enough to measure these kind of rates accurately.

But technology did catch up. Just take a look at the following data (from Miller, *J. Am.Chem. Soc.* **1984**, 3047).



Don't worry that there are no metals involved anymore. An electron transfer is an electron transfer. Here, an electron is sent from the aromatic substructure on the right to the substructure on the left. By varying the part on the left, we can adjust the reduction potential (or the free energy change, as reported here).

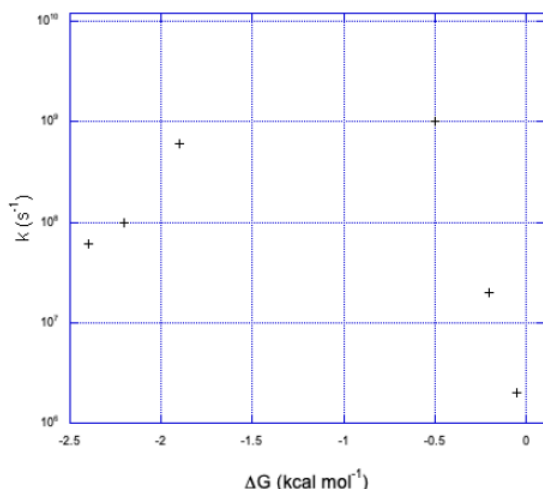
### ? Exercise 9.2.3.9

- Plot the data in the above table.
- How would you describe the relationship?

Answer a

a)





#### Answer b

b) We can see two sides of an inverted curve. The reaction gets much faster as the free energy becomes more negative, but at some point the rate begins to decrease again.

As the reaction becomes more exergonic, the rate increases, but then it hits a maximum and decreases again. Data like this means that the "Marcus Inverted Region" is a real phenomenon. Are you convinced? So were other people. In 1992, Marcus was awarded the Nobel Prize in Chemistry for this work.

#### ? Exercise 9.2.3.10

Take a look at the donor/acceptor molecule used in Williams' study, above. a) Why do you suppose the free energy change is pretty small for the first three compounds in the table? b) Why does the free energy change continue to get bigger over the last three compounds in the table?

#### Answer

The acceptor compound becomes an anion when it accepts an electron. The first three compounds do not appear to be strongly electrophilic; they can accept electrons simply because of resonance stability of the resulting anion. The last three have electron withdrawing groups (chlorines and oxygens) that would stabilize the anion even further.

#### ? Exercise 9.2.3.11

The rates of electron transfer between cobalt complexes of the bidentate bipyridyl ligand,  $\text{Co}(\text{bipy})_3^{n+}$ , are strongly dependent upon oxidation state in the redox pair. Electron transfer between  $\text{Co(I)}/\text{Co(II)}$  occurs with a rate constant of about  $10^9 \text{ M}^{-1}\text{s}^{-1}$ , whereas the reaction between  $\text{Co(II)}/\text{Co(III)}$  species proceeds with  $k = 18 \text{ M}^{-1}\text{s}^{-1}$ .

- What geometry is adopted by these complexes?
- Are these species high spin or low spin?
- Draw d orbital splitting diagrams for each complex.
- Explain why electron transfer is so much more facile for the  $\text{Co(I)}/\text{Co(II)}$  pair than for the  $\text{Co(II)}/\text{Co(III)}$  pair.

#### Answer a

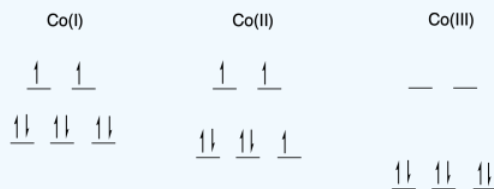
a) octahedral; bpy is a bidentate ligand.

#### Answer b

b) Co is first row;  $\text{Co(I)}$  and  $\text{Co(II)}$  have relatively low charge. Usually we would expect them to be high spin.  $\text{Co(III)}$  is at a cut-off point in the first row; it is just electronegative enough that it is usually low spin.

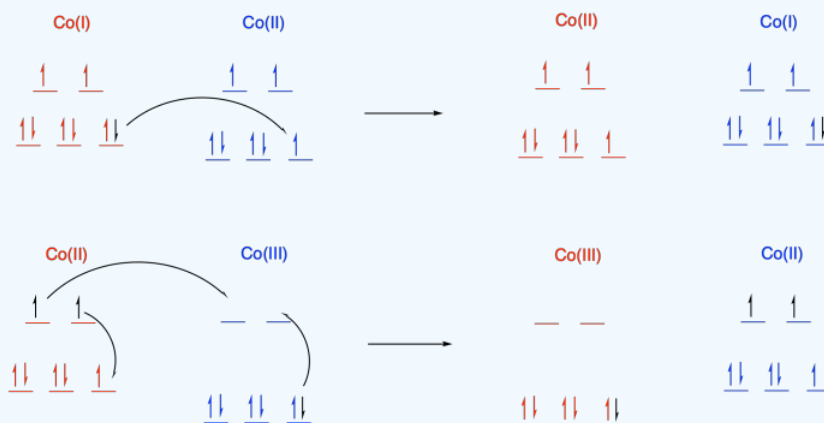
#### Answer c

c)



#### Answer d

d) In a transfer from Co(II) to Co(III), there is additional reorganization needed because the metal changes between high and low spin. Not only does one electron have to move from one metal to another metal, but additional electrons have to shuffle from one orbital to another on the same metal to accommodate the change. These reorganizations have a barrier, slowing the reaction.



This page titled 9.2.3: Outer Sphere Electron Transfer is shared under a CC BY-NC license and was authored, remixed, and/or curated by Kathryn Haas.

- 1.9: Outer Sphere Electron Transfer by Chris Schaller is licensed CC BY-NC 3.0. Original source: <https://employees.csbsju.edu/cschaller/ROBI3.htm>.

## 9.3: Unit 9 Practice Problems

### Exercise 1

An associative mechanism is favored when

- a) the oxidation state of the metal is high
- b) the coordination number of the metal is low
- c) the complex has bulky ligands
- d) the metal –ligand bonds are labile.

**Answer**

- b) the coordination number of the metal is low

### Exercise 2

Which of the following metal-ligand bonds would you expect to have the highest thermodynamic stability?

- a) Hg-S
- b) Hg-O
- c) Hg-N
- d) Hg-F

**Answer**

- a) Hg-S

### Exercise 3

Chelate complexes are thermodynamically particularly stable because

- a) The substitution of a simple ligand by a chelating ligand is enthalpically particularly favorable.
- b) The substitution of a simple ligand by a chelating ligand is entropically particularly favorable.
- c) Chelating ligands are more inert than simple ligands.

**Answer**

- b) The substitution of a simple ligand by a chelating ligand is entropically particularly favorable.

### Exercise 4

What is true about complexes that undergo metal to ligand charge transfer?

- a) The metal ion has no or few d electrons
- b) The ligands are good pi-acceptors
- c) The metal ions have a high charge.

**Answer**

- b) The ligands are good pi-acceptors

This page titled [9.3: Unit 9 Practice Problems](#) is shared under a [CC BY 4.0](#) license and was authored, remixed, and/or curated by [Kai Landskron](#).

- [Homework Problems Chapter 9](#) by Kai Landskron is licensed [CC BY 4.0](#).

## CHAPTER OVERVIEW

### Unit 10: Organometallic Chemistry

#### 10.1: Organometallic Complexes

##### 10.1.1: Introduction to Organometallic Chemistry

##### 10.1.2: Ligand Nomenclature and Classification

##### 10.1.3: Survey of Common Organometallic Ligands

##### 10.1.4: Electron Counting and the 18 Electron Rule

#### 10.2: Organometallic Reactions

##### 10.2.1: Ligand Dissociation and Substitution

##### 10.2.2: Oxidative Addition

##### 10.2.3: Reductive Elimination

##### 10.2.4: Migratory Insertion- 1,2-Insertions

##### 10.2.5: $\beta$ -Elimination Reactions

##### 10.2.6: Organometallic Catalysts

---

This page titled [Unit 10: Organometallic Chemistry](#) is shared under a [not declared](#) license and was authored, remixed, and/or curated by [Kathryn Haas](#).

## 10.1: Organometallic Complexes

---

Learning objectives for this unit are to:

- Recognize common organometallic ligands and modes of binding
  - Classify ligands as X-type or L-type based on the covalent bond classification method
  - Determine the d electron count, oxidation state, and overall electron count for organometallic complexes
- 

10.1: Organometallic Complexes is shared under a [not declared](#) license and was authored, remixed, and/or curated by LibreTexts.

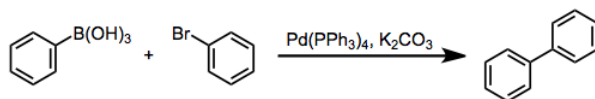
## 10.1.1: Introduction to Organometallic Chemistry

### What is Organometallic Chemistry?

This chapter will introduce a subfield of inorganic coordination chemistry; organometallic chemistry. Let's begin with a few simple questions: what is organometallic chemistry? What, after studying organometallic chemistry, will we know about the world that we didn't know before? Why is the subject worth studying? And what kinds of problems is the subject meant to address? The purpose of this introduction is twofold: (1) to help motivate us as we move forward (that is, to remind us that there is a point to all this!); and (2) to illustrate the kinds of problems we'll be able to address using concepts from the field. You might be surprised by the spine-chilling power you feel after learning about the behavior of organometallic compounds and reactions!

Put most bluntly, **organometallic chemistry is the study of compounds containing, and reactions involving, metal-carbon bonds**. The metal-carbon bond may be transient or temporary, but if one exists during a reaction or in a compound of interest, we're squarely in the domain of organometallic chemistry. Despite the denotational importance of the M-C bond, bonds between metals and the other common elements of organic chemistry also appear in organometallic chemistry: metal-nitrogen, metal-oxygen, metal-halogen, and even metal-hydrogen bonds all play a role. Metals cover a vast swath of the periodic table and include the alkali metals (group 1), alkali earth metals (group 2), transition metals (groups 3-12), the main group metals (groups 13-15, "under the stairs"), and the lanthanides and actinides. We will focus most prominently on the behavior of the transition metals, so called because they cover the transition between the electropositive group 2 elements and the more electron-rich main group elements.

Why is organometallic chemistry worth studying? Well, for me, it mostly comes down to synthetic flexibility. There's a reason the "organo" comes first in "organometallic chemistry"—our goal is usually the creation of new bonds in *organic* compounds. The metals tend to just be along for the ride (although their influence, obviously, is essential). And the fact is that you can do things with organometallic chemistry that you cannot do using straight-up organic chemistry. Case in point:



*The venerable Suzuki reaction...unthinkable without palladium!*

The establishment of the bond between the phenyl rings through a means other than dumb luck seems unthinkable to the organic chemist, but it's natural for the palladium-equipped metal-organicker. Bromobenzene looks like a potential electrophile at the bromine-bearing carbon, and if you're familiar with hydroboration you might see phenylboronic acid as a potential nucleophile at the boron-bearing carbon. Catalytic palladium makes it all happen! Organometallic chemistry is full of these mind-bending transformations, and can expand the synthetic toolbox of the organic chemist considerably.

To throw another motive into the mix for the non-specialist (or the synthesis-spurning chemist), organometallic chemistry is full of intriguing stories of scientific inquiry and discovery. Exploring how researchers take a new organometallic reaction from "ooh pretty" to strong predictive power is instructive for anyone interested in "how science works," in a practical sense. We'll examine a number of classical experiments in organometallic chemistry, both for their value to the field and their contributions to the general nature of scientific inquiry.

What kinds of problems should we be able to address as we move forward? Here's a bulleted list of the most commonly encountered types of problems in an organometallic chemistry course:

- Describe the structure of an organometallic complex...
- Predict the product of the given reaction conditions...
- Draw a reasonable mechanism based on evidence...
- Devise a synthetic route to synthesize a target organometallic compound...
- Explain the observation(s)...
- Predict the results of a series of experiments...

The first four are pretty standard organic-esque problems, but it's the last two, more general classes that really make organometallic chemistry compelling. Just imagine putting yourself in the shoes of the pioneers and making the same predictions they did!

There you have it, a short introduction to organometallic chemistry and why it's worth studying. The rest of this chapter will describe what organometallic chemistry really is...it will be helpful to keep these motives in mind as you study. Keep a thirst for predictive power, and it's hard to go wrong with organometallic chemistry!

### Resources for learning organometallic chemistry

For the penny-pinching student or layman, there are several good resources for organometallic chemistry on the Web. Nothing as exhaustive as Reusch's Virtual Textbook of Organic Chemistry exists for organometallic chemistry, but the base of resources available on the Web is growing. Rob Toreki's [Organometallic HyperTextBook](#) could use a CSS refresh, but contains some nice introductions to different organometallic concepts and reactions. Try the electron-counting quiz!

[VIPER](#) is a collection of electronic resources for teaching and learning inorganic chemistry, and includes a nice section on organometallic chemistry featuring laboratory assignments, lecture notes, and classroom activities. Awesome public lecture notes are available from Budzelaar at the University of Manitoba and Shaughnessy at Alabama (Roll Tide?). For practice problems, check out Fu's OpenCourseWare material from MIT and Shaughnessy's problem sets.

## Historical Background and Introduction to Metallocenes

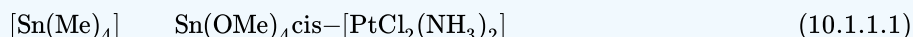
### Definition: Organometallic Complex

**Organometallic Complex:** A complex with bonding interactions between a metal atom and one or more carbon atoms of an organic group or molecule.

An **organometallic complex** is defined as a complex with bonding interactions between one or more carbon atoms of an organic group or molecule and at least one metal atom. It is important to understand that *just the presence of an organic ligand is not sufficient to define an organometallic compound*. If there are organic ligands present, but no metal-carbon bonds, the complex is said to be "**metal-organic**". There must be interactions between a carbon and a metal for the complex to be considered organometallic.

### ✓ Example 10.1.1.1

Which of the molecules below is an organometallic complex?



#### Solution

The tetramethyl tin ( $\text{Sn}(\text{Me})_4$ ) has metal-carbon bonds, and thus it is an organometallic complex.

Tetramethoxy tin ( $\text{Sn}(\text{OMe})_4$ ) has metal-oxygen bonds. It lacks metal-carbon bonds, but it does contain organic ligands; thus it is a "metal-organic" complex rather than organometallic.

Cisplatin ( $\text{cis-}[\text{PtCl}_2(\text{NH}_3)_2]$ ) contains no carbon and thus it is neither organometallic or metal-organic; it is just a coordination compound.

## Industrial Importance of Organometallic Compounds

Organometallic compounds are a very important class of compounds in industry. For example, tens of thousand of tons of aluminum and tin alkyl compounds are produced each year for industrial purposes. The use of organometallic compounds as catalysts to produce other compounds is even more important. Organometallic catalysts are used for a range of industrial syntheses from manufacture of commodity polymers like polypropylene and polyethylene to production of simple organic molecules like acetaldehyde and acetic acid. These compounds are produced at a scale in the order of millions of tons per year.

## History of Organometallic Chemistry

Let us take a historical approach to organometallic chemistry and see how the field has evolved. Arguably, the first organometallic compound was kakodyl oxide, an organo-arsenic compound (Figure 10.1.1.2). It was accidentally produced by the French chemist Louis Cadet in 1760 when he was working on inks. He heated arsenic oxide and potassium acetate and obtained a red-brown oily liquid, known as Cadet's fuming liquid. It consists mostly of cacodyl and cacodyl oxide (Figure 10.1.1.2). In cacodyl, there is an As-As bond and two methyl groups attached to each As atom. In the other product, cacodyl oxide, there is an O atom bridging the

two As atoms, and each As is bound to two methyl groups. The names of these two compounds come from the greek word "kakodes", meaning "bad smell". Indeed, they have a very intense, garlic-like smell. The reaction can be used to identify arsenic in samples. For instance, if you suspected your food was poisoned with arsenic, you could heat a sample together with potassium acetate. If a bad, garlic-like smell evolved, this would indicate that there is arsenic in your sample.

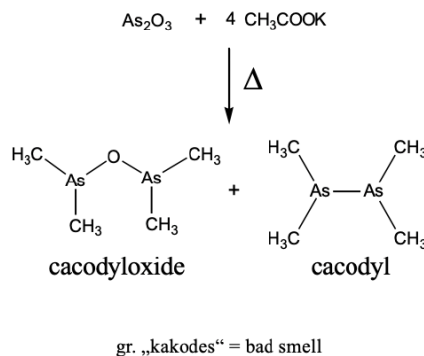


Figure 10.1.1.2: Cacodyl and cacodyl oxide

Another important milestone in coordination chemistry was the discovery of Zeise's salt by the Danish chemist William Zeise in 1827 (Figure 10.1.1.3). Zeise's salt was the first olefin complex in which an olefin was bound side-on to a metal using its  $\pi$ -electrons for  $\sigma$ -bonding. Zeise observed that when sodium hexachloroplatinate (2-) was heated in ethanol, a compound with the composition  $\text{Na}[\text{PtCl}_3(\text{C}_2\text{H}_4)]$  could be isolated. The chemical composition of the compound suggested that there was a  $\text{C}_2\text{H}_4$  organic fragment bonded to the platinum, but it was not clear how.

This question was only answered more than 100 years later in 1969 with the crystal structure analysis of Zeise's salt. The crystal structure revealed that an ethylene molecule was bound side-on to the platinum (Figure 10.1.1.3). The two carbon atoms had about the same distance to the Pt arguing that they were equally strongly involved in the bonding with Pt. The first C had a distance of 216 pm while the second carbon had a distance of 215 pm. The ethylene molecule was oriented perpendicular to the plane made of the three chloro ligands and the platinum atom. The Cl-Pt-Cl bond angles were near  $90^\circ$ . Overall, the structure could be described as a structure derived from a square planar structure with the ethylene as the fourth ligand that would stand perpendicular to the plane in order to minimize steric repulsion with the chloro ligands.

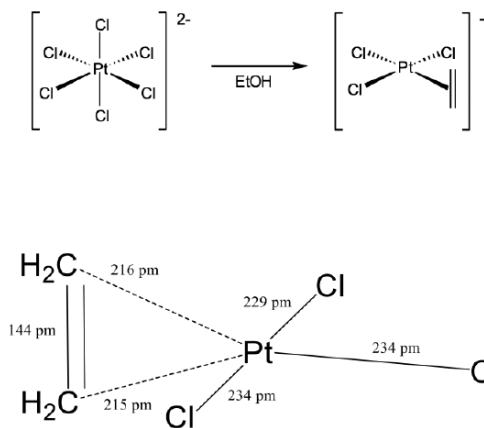


Figure 10.1.1.3: Zeise's salt: Synthesis and crystal structure.

An important question was how to describe the bonding in the compound. It was noteworthy that the C-C bond length in Zeise's salt was significantly longer (144 pm) than that in a free ethylene molecule (134 pm). Based on the bond-strength bond-length concept this argued that the bond was weaker than a regular  $\text{C}=\text{C}$  double bond, and that the bond order was smaller than 2. What could explain this lower bond order and the side-on coordination of the ethylene in Zeise's salt?

The answer is that the ethylene molecule uses its  $\pi$ -electrons for  $\sigma$ -bonding with a metal d-orbital (Figure 10.1.1.4). You can see above that the lobe of a  $d_{x^2-y^2}$  orbital has the correct orientation to overlap with the bonding  $\pi$ -orbitals of the ethylene ligand in a  $\sigma$ -fashion. Through this interaction electron density gets donated from the bonding ligand  $\pi$ -orbital into the metal-d-orbital. This results in a lower electron density for  $\pi$ -bonding within the ligand, and thus the bond order is decreased. In addition, there is



another effect that lowers the bond order. A metal d-orbital can interact with the  $\pi^*$ -orbitals in  $\pi$ -fashion. In this process, electron density can be donated from the metal d-orbital into the empty  $\pi$ -orbitals of the ligand. The increased electron density in the  $\pi$ -orbitals further decreases the bond order.

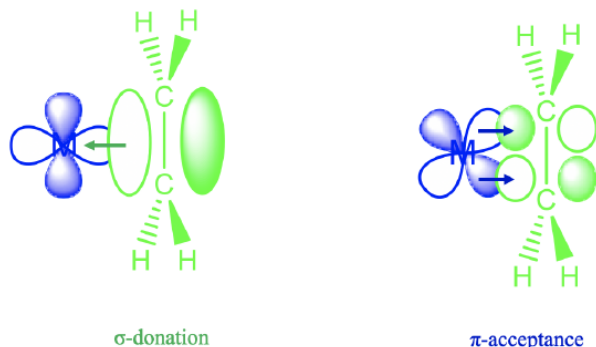


Figure 10.1.1.4: An orbital view of bonding in Zeise's salt

In 1890, a further milestone in organometallic chemistry was reached with the synthesis of the first carbonyl complex, the nickel tetracarbonyl. Nickel tetracarbonyl is a colorless liquid that boils at 43°C. The compound was prepared by the German chemist Ludwig Mond. Nickel tetracarbonyl forms spontaneously from nickel metal and carbon monoxide at room temperature. The reaction is the basis of the Mond-process that is used up to date in order to purify nickel (Figure 10.1.1.5). Carbon monoxide gas can be streamed over impure Ni metal at temperatures of 50-60°C to form  $\text{Ni}(\text{CO})_4$  in gaseous form. Impurities are left behind in solid form. Then, the nickel tetracarbonyl is thermally decomposed at ca. 220° to form nickel and carbon monoxide. The process can be varied to produce nickel in powder form, as spheres (Figure 10.1.1.5), and as coatings. The Mond process is still used despite the very high toxicity of nickel tetracarbonyl.

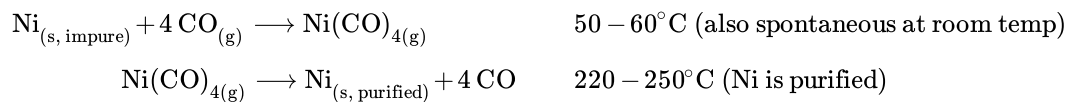
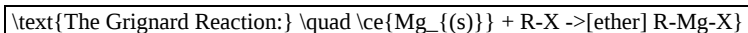


Figure 10.1.1.5: Purified Ni spheres prepared through the Mond process (René Rausch, [Nickel kugeln](#), CC BY-SA 3.0 DE)

In 1900 the first Grignard reagents were discovered. Victor Grignard (Figure 10.1.1.9) was an enthusiastic young French chemist who discovered how to make organomagnesium halides ( $\text{RMgX}$ ) while working for his Ph.D.. His supervisor, Sabatier, had been trying this chemistry for some time, but Victor was the genius who solved the problem. Organomagnesium halides form from magnesium and organic halides in ethers. This discovery in 1900 changed the course of organic chemistry and won Grignard and Sabatier the Nobel Prize in 1912.



In 1917, the first lithium alkyls were prepared by Wilhelm Schlenk. Like Grignard reagents, lithium alkyls are very valuable reactants in synthetic organic chemistry. Lithium alkyls are very air-sensitive compounds, and some even self-ignite in air (for example tert-butyl lithium is explosive when exposed to air). Therefore, they need to be handled carefully under inert gas. So that the reactions could be carried out under air-free conditions, Wilhelm Schlenk made an important invention: The Schlenk-lines (Figure 10.1.1.6). The Schlenk lines allow a chemist to remove all gas (air) from a reaction flask and back-fill the flask with an inert gas. A Schlenk line has a dual manifold with several ports. One manifold is connected to a source of purified inert gas, while the other is connected to a vacuum pump. The inert-gas line is vented through an oil bubbler, while solvent vapors and gaseous reaction products are prevented from contaminating the vacuum pump by a liquid nitrogen or dry ice/acetone cold trap. Special stopcocks or Teflon taps allow vacuum or inert gas to be selected without the need for placing the sample on a separate line.



Figure 10.1.1.6: A Schlenk-line ([Polimerek](#), [Double vac line front view](#), [CC BY-SA 3.0](#)).

### Discovery of Metallocenes

The discoveries discussed above were important milestones in the development of organometallic chemistry. But the field expanded more rapidly with the discovery of the first metallocene: ferrocene. Like often in science, ferrocene was discovered through an accident. In 1951 Peter Pauson and Thomas Kealy attempted to synthesize the organic compound fulvalene through oxidative coupling of cyclopentadienyl magnesium chloride with iron (III) chloride. However, instead of obtaining fulvalene they observed the formation hydrofulvalene together with an orange powder with “remarkable stability”. Analysis of the powder showed that the chemical compound contained two cyclopentadienyl rings and one iron atom. According to the knowledge on bonding in organometallic compounds that was known at the time Kealy and Pauson suggested a structure for the molecule in which two cyclopentadienyl group were bound to a single Fe atom via two Fe-C bonds (Figure 10.1.1.7).

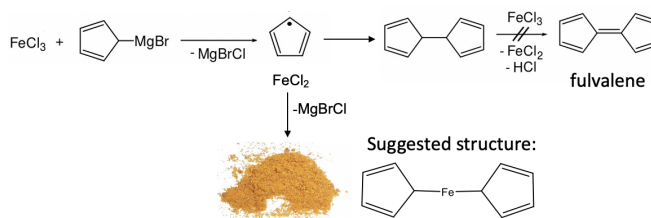
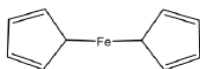


Figure 10.1.1.7: Synthesis of ferrocene (Attribution: T.J. Kealy, P.L. Pauson, Nature 1951, 168, 1039.)

However, the remarkable stability of the compound was in contradiction to the proposed structure. The structure would be a 10 electron complex which would be highly coordinatively unsaturated. This would be inconsistent with the observed stability. We can briefly practice our electron counting skills again in order to prove that there are only 10 electrons (Figure 10.1.1.8). (Electron counting will be discussed in more depth later in this chapter)



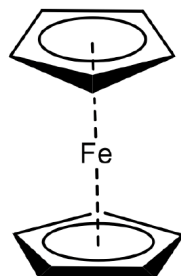
Structure is coordinatively unsaturated and has 10 valence electrons.

Fe:	8e
Ox-State (+2):	-2e
Ligands:	2x2e = 4e
Sum:	10e

Figure 10.1.1.8: Electron counting in the wrong structure for  $\text{Fe}(\text{Cp})_2$

The compound was stable in air, and could be sublimed without decomposition. Further, the double-bonds in the cyclopentadienyl rings resisted hydrogenation. In addition, the structure was inconsistent with spectroscopic observations. Only one C-H stretch vibration was observed in the IR and only one signal was observed in the  $^1\text{H}$  NMR. Kealy and Pauson's structure would have been consistent with three C-H stretch vibrations and three NMR resonances. For these reasons, Kealy's and Pauson's structure was soon questioned. Ernst Otto Fischer at University of Munich and Sir Geoffrey Wilkinson at Harvard University (Figure 10.1.1.9) suggested an alternative structure that was very different from all known organometallic structures. The bonding in this structure was completely different from all bonding concepts considered thus far for organometallics. What structure did they propose? They proposed a sandwich structure in which the two aromatic cyclopentadienyl anions would sandwich an  $\text{Fe}^{2+}$  ion. What would be the

bonding in this structure? The cyclopentadienyl anion would donate its six  $\pi$ -electrons into the valence orbitals of the metal. Thus, all five carbon atoms would be equally involved in the bonding, the ligand would act as a  $\eta^5$ -ligand. Because of the donation of  $\pi$ -electrons in the cyclopentadiene unit, the structure was called “ferrocene”. The ferrocene structure would explain the stability and low reactivity of the compound.



**Ferrocene**

Figure 10.1.1.9: The sandwich structure of ferrocene

Electron-counting gives an 18 electron complex (Figure 10.1.1.10). Let us verify this using the oxidation state method. Fe would contribute eight electrons in the neutral state. The ligands would be considered as cyclopentadienyl anions with a 1- charge. This would give an oxidation state of +2 for Fe reducing the number of electrons from eight to six. The two ligands would contribute six electrons each giving twelve electrons.  $12+6=18$ . Hence, the structure fulfills the 18 electron rule. The structure is also consistent with the spectroscopic observation of one NMR resonance and one C-H stretch vibration. All these were excellent arguments to support the ferrocene sandwich structure, however they were not an absolute proof. The proof finally came with the X-ray crystal structure determination which unambiguously confirmed the sandwich structure.

Fe:	8e
Ox-State (+2):	-2e
Ligands:	$2 \times 6e = 12e$
Sum:	18e

Figure 10.1.1.10: Electron counting in ferrocene using the oxidation state method

Dr. Kai Landskron ([Lehigh University](#)). If you like this textbook, please consider to make a donation to support the author's research at Lehigh University: [Click Here to Donate](#).

This page titled [10.1.1: Introduction to Organometallic Chemistry](#) is shared under a [not declared](#) license and was authored, remixed, and/or curated by [Kathryn Haas](#).

- [1.2: What is Organometallic Chemistry?](#) by Michael Evans is licensed [CC BY-NC-SA 4.0](#).
- [1.1: Resources for Organometallic Chemistry](#) by Michael Evans is licensed [CC BY-NC-SA 4.0](#).
- [10.1: Historical Background and Introduction into Metallocenes](#) by Kai Landskron is licensed [CC BY 4.0](#).

## 10.1.2: Ligand Nomenclature and Classification

The nomenclature of coordination compounds was described in an earlier section ([Section 9.2](#)). Organometallic compounds are named using this same system, so it may be helpful to review before proceeding. Here, we will point out some of the symbols and terminology that are used heavily in naming organometallic complexes.

### Hapticity

The eta ( $\eta$ ) symbol is used to indicate the variable **hapticity** of ligands with conjugated  $\pi$  systems. For example, the cyclopentadiene anion ( $\text{Cp}$ ,  $\text{C}_5\text{H}_5^-$ ) ligand has the capability to coordinate a metal ion in several ways due to its cyclic conjugated  $\pi$  system. The hapticity (the number of atoms involved in the metal bonding interaction) must be indicated in the formula with the  $\eta^n$  notation, and in the name with the appropriate prefix. Figure 10.1.2.1 illustrates three different hapticities, and the relevant formula symbols and names.

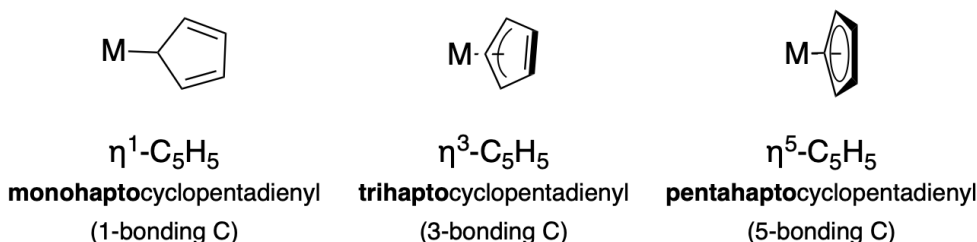


Figure 10.1.2.1: The cyclopentadiene anion is shown coordinating to a metal ion (M) using three different coordination modes: On the left, Cp as a monohapto ligand. In the center, Cp is shown bonding to a metal in a trihapto fashion where the metal interacts with three carbons. On the right, Cp is shown bonding in a pentahapto fashion, where the five ligand carbons interact equally through the  $\pi$  system. (CC-BY-SA 4.0; Kathryn Haas)

Another common ligand is the  $\pi$ -allyl anion ( $\text{C}_3\text{H}_3^-$ ), which can coordinate in either an  $\eta^1$  or  $\eta^3$  fashion, as illustrated below (Figure 10.1.2.2).

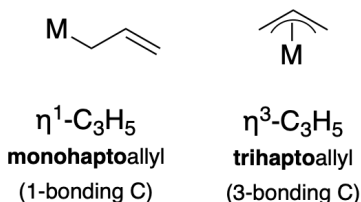


Figure 10.1.2.2: The allyl anion is shown coordinating in a  $\eta^1$  and  $\eta^3$  modes. (CC-BY-SA 4.0; Kathryn Haas)

### Bridging ligands

Ligands that bridge two or more metal ions are indicated using the symbol, mu ( $\mu$ ). For a ligand that bridges  $n$  metal ions, the symbol is written as  $\mu_n$ . However the subscript is often omitted when  $n = 2$ . Some examples of the carbonyl ligand are given below. More specific rules for naming are found in [Section 9.2](#).

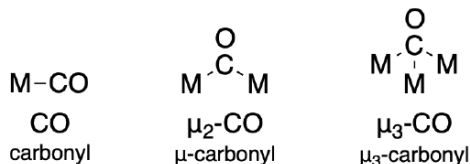
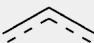




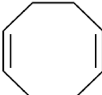


Figure 10.1.2.3: The carbonyl ligand is shown as a terminal ligand (with no  $\mu$  necessary), bridging two metals ( $\mu_2$ ), and bridging three metals ( $\mu_3$ ). (CC-BY-SA 4.0; Kathryn Haas)

### Common Ligands and Classifications

Some common organic ligands found in organometallic compounds are listed below with their names and structures.

Name	Structure	CBC description
Alkyl	$\text{—CR}_3$	X
Carbonyl	$\text{:C}\equiv\text{O:}$	L
Carbene (alkylidene)	$\text{=C}$	$\text{X}_2$
Carbyne (alkylidyne)	$\text{}\equiv\text{C—}$	$\text{X}_3$
Ethylene	$\text{H}_2\text{C=CH}_2$	L
Acetylene	$\text{HC}\equiv\text{CH}$	L
Acyl	$\text{—C(=O)R}$	X
$\pi$ -allyl ( $\text{C}_3\text{H}_5^-$ )		X for $\eta^1$ LX for $\eta^3$
Cyclopropenyl (cyclo- $\text{C}_3\text{H}_3$ )		X for $\eta^1$ LX for $\eta^3$
Cyclobutadiene (cyclo- $\text{C}_4\text{H}_4$ )		$\text{L}_2$ for $\eta^4$
Cyclopentadienyl (cyclo- $\text{C}_5\text{H}_5$ , Cp)		X for $\eta^1$ LX for $\eta^3$ $\text{L}_2\text{X}$ for $\eta^5$
Benzene		$\text{L}_3$ for $\eta^6$
1,5-cyclooctadiene (1,5-COD)		$\text{L}_2$ for $\eta^4$

## Covalent Bond Classification Method (CBC)

Later in this chapter, you will learn to count electrons. The way in which you count depends on what counting scheme you choose to use. But in any case, the way in which we "count" the electrons from ligands depends on the ligand type. The covalent bond classification method (CBC) has been in use since the late 1990's to classify ligands in organometallic complexes. This method classifies ligands into three main types as follows. (see Application of the Covalent Bond Classification Method for the Teaching of Inorganic Chemistry. Malcolm L. H. Green and Gerard Parkin, Journal of Chemical Education 2014 91 (6), 807-816, DOI: 10.1021/ed400504f.)

CBC Ligand Class/Type	Examples	Use in neutral Ligand Method of Electron Counting	Use in Donor Pair Method of Electron Counting
X-type	$\text{H—, Cl—, H}_3\text{C}^-$	Considered neutral Donates 1 electron to the metal	Considered anionic Donates 2 electrons to the metal
L-type	$\text{CO, NH}_3, \text{H}_2\text{O}$	Considered neutral Donates 2 electrons to the metal	Considered neutral Donates 2 electrons to the metal

CBC Ligand Class/Type	Examples	Use in neutral Ligand Method of Electron Counting	Use in Donor Pair Method of Electron Counting
Z-type (rarely used)	$\text{BR}_3$ , Lewis acids	Considered neutral Accepts 2 electrons	Considered cationic Donates 0 electrons

This page titled [10.1.2: Ligand Nomenclature and Classification](#) is shared under a [not declared](#) license and was authored, remixed, and/or curated by [Kathryn Haas](#).

### 10.1.3: Survey of Common Organometallic Ligands

There are some classes of ligands and modes of bonding that are important and in some cases unique to organometallic complexes and reactions. Before discussing reactions of organometallic complexes we will start with an overview of ligands common to organometallic complexes. In organometallic reactions, ligands can be either spectators, not chemically involved or changed during the reaction, or actors, chemically changed during the reaction. Similar to enzymes, a substrate will often bond to an organometallic catalyst as a ligand undergo a chemical transformation, and leave as a product.

#### Carbon Monoxide

Carbon monoxide is a neutral strong field ligand that we have [discussed previously](#). We've seen that there are two bonding interactions at play in the metal carbonyl bond: a ligand-to-metal  $n \rightarrow d_\sigma$  interaction ( $\sigma$  donation) and a metal-to-ligand  $d_\pi \rightarrow \pi^*$  interaction ( $\pi$  accepting). The latter interaction is called backbonding because the metal donates electron density back to the ligand.

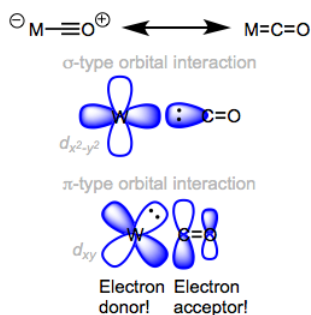


Figure 10.1.3.1: Orbital interactions in  $\text{M}=\text{C}=\text{O}$ . (Copyright; Michael Evans)

CO is a fair  $\sigma$ -donor (or  $\sigma$ -base) and a good  $\pi$ -acceptor (or  $\pi$ -acid). The properties of ligated CO depend profoundly upon the identity of the metal center. More specifically, the electronic properties of the metal center dictate the importance of backbonding in metal carbonyl complexes. Most bluntly, *more electron-rich metal centers are better at backbonding to CO*. Why is it important to ascertain the strength of backbonding?

#### Backbonding and CO vibrational frequency

Infrared spectroscopy has famously been used to empirically support the idea of backbonding. The table below arranges some metal carbonyl complexes in “periodic” order and provides the frequency corresponding to the  $\text{C}=\text{O}$  stretching mode. Notice that without exception, every complexed CO has a stretching frequency lower than that of free CO. Backbonding is to blame! When a metal donates electrons into a  $\pi^*$  antibonding MO on CO, the  $\text{C}-\text{O}$  bond order is lowered and the bond strength is weakened. According to [Hooke's law](#), assuming all other things are equal, when the force constant (bond strength) decreases the vibrational frequency also decreases. Complexes with the strongest metal-CO backbonding will have the lowest frequency CO bond vibration(s).

Free CO 2143 $\text{cm}^{-1}$					
$\text{V}(\text{CO})_6$ 1976 $\text{cm}^{-1}$	$\text{Cr}(\text{CO})_6$ 2000 $\text{cm}^{-1}$	$\text{Mn}_2(\text{CO})_{10}$ 2013 $\text{cm}^{-1}$	$\text{Fe}(\text{CO})_5$ 2023 $\text{cm}^{-1}$	$\text{Co}_2(\text{CO})_8$ 2044 $\text{cm}^{-1}$	$\text{Ni}(\text{CO})_4$ 2057 $\text{cm}^{-1}$
$[\text{Ti}(\text{CO})_6]^{2-}$ 1747 $\text{cm}^{-1}$					

Figure 10.1.3.2: CO stretching frequencies in metal-carbonyl complexes. (Copyright; Michael Evans)

The figure above depicts a clear increase in frequency (an increase in  $\text{C}-\text{O}$  bond order) as we move left to right across the periodic table. This finding may seem odd if we consider that the number of  $d$  electrons in the neutral metal increases as we move left to right. Shouldn't metal centers with more  $d$  electrons be better at backbonding (and more “electron rich”)? What's going on here? Recall the periodic trend in *orbital energy*. As we move left to right, the  $d$  orbital energies decrease and the energies of the  $d_\pi$  and  $\pi^*$  orbitals separate. As a result, the backbonding orbital interaction becomes worse ([remember that strong orbital interactions require well-matched orbital energies](#)) as we move toward the more electronegative late transition metals. We can draw an analogy to enamines and enols from organic chemistry. The more electronegative oxygen atom in the enol is a worse electron donor than the enamine's nitrogen atom.

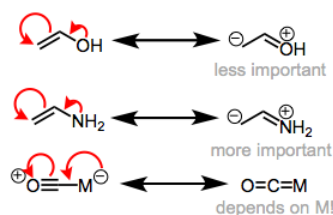


Figure 10.1.3.3: The importance of backbonding depends on the electronegativity of the metal and its electron density. (Copyright; Michael Evans)

Of course, the contribution of other ligands on the metal center to backbonding cannot be forgotten, either. Logically, electron-donating ligands will tend to make the backbond stronger (they make the metal a better electron donor), while electron-withdrawing ligands will worsen backbonding. Adding electron-rich phosphine ligands to a metal center, for instance, *decreases* the CO stretching frequency due to *improved* backbonding.

### CO as a bridging ligand

Carbonyl ligands are famously able to bridge multiple metal centers. Bonding in bridged carbonyl complexes may be either “traditional” or delocalized, depending on the structure of the complex and the bridging mode. The variety of bridging modes stems from the different electron donors and acceptors present on the the CO ligand (and the possibility of delocalized bonding). Known bridging modes are shown in the figure below.

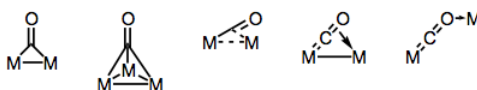
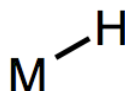


Figure 10.1.3.4: Building bridges with carbonyl ligands. (Copyright; Michael Evans)

### Metal Hydrides

Metal hydrides occupy an important place in transition metal organometallic chemistry as the M–H bonds can undergo insertion reactions with a variety of unsaturated organic substrates yielding numerous organometallic compounds with M–C bonds. Not only the metal hydrides are needed as synthetic reagents for preparing the transition metal organometallic compounds but they also are required for important hydride insertion steps in many catalytic processes. The first transition metal hydride compound was reported by W. Heiber in 1931 when he synthesized  $\text{Fe}(\text{CO})_4\text{H}_2$ . Though he claimed that the  $\text{Fe}(\text{CO})_4\text{H}_2$  contained Fe–H bond, it was not accepted until 1950s, when the concept of normal covalent M–H bond was widely recognized.



### Spectroscopic identification

The metal hydride moieties are easily detectable in  $^1\text{H}$  NMR as they appear upfield of TMS in the region between 0 to -60 ppm, where no other H resonances appear. The hydride moieties usually couple with metal centers possessing nuclear spins. Similarly, the hydride moieties also couple with the adjacent metal bound phosphine ligands, if present in the complex, exhibiting characteristic *cis* ( $J = 15 - 30$  Hz) and *trans* ( $J = 90 - 150$  Hz) coupling constants. In the IR spectroscopy, the M–H frequencies appear between  $(1500 - 2200) \text{ cm}^{-1}$  but their intensities are mostly weak. Crystallographic detection of metal hydride moiety is difficult as hydrogen atoms in general are poor scatterer of X-rays. Located adjacent to a metal atom in a M–H bond, the detection of hydrogen atom thus becomes challenging and as a consequence the X-ray crystallographic method systematically underestimates the M–H internuclear distance by  $\sim 0.1 \text{ \AA}$ . However, better data could be obtained by performing the X-ray diffraction studies at a low temperature in which the thermal motion of the atoms are significantly reduced. In light of these facts, the neutron diffraction becomes a powerful method for detection of the metal hydride moieties as hydrogen scatters neutrons more effectively and hence the M–H bond distances can be measured more accurately. A limitation of neutron diffraction method is that large sized crystals are required for the study.



## Bridging hydrides

Bridging hydrides are an intriguing class of ligands. A question to ponder: how can a ligand associated with only two electrons possibly bridge two metal centers? How can two electrons hold three atoms together? Enter the magic of three-center, two-electron bonding. We can envision the M–H sigma bond as an electron donor itself! With this in mind, we can imagine that hydrides are able to bind end-on to one metal and side-on to another. Consistent with the idea that bridging is the result of “end-on + side-on” bonding, bond angles of bridging hydrides are never 180°.

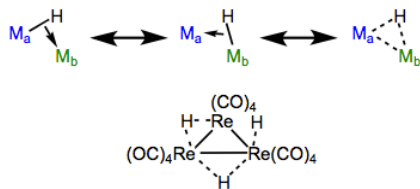


Figure 10.1.3.5: Resonance forms of bridging hydrides, with an example. Sigma complexes like these show up in other contexts

## Phosphines

Phosphines are most notable for their remarkable electronic and steric tunability and their “innocence”—they tend to avoid participating directly in reactions, but have the ability to profoundly modulate the electronic properties of the metal center to which they’re bound. Furthermore, because the energy barrier to inversion is quite high, “chiral-at-phosphorus” ligands can be isolated in enantioenriched form and introduced to metal centers, bringing asymmetry just about as close to the metal as it can get in chiral complexes. The one stable isotope of P ( $^{31}P$ ) is NMR active so  $^{31}P$  NMR is often used to characterize complexes and reactions involving phosphine ligands. Soft phosphines match up very well with the soft low-valent transition metals. Electron-poor phosphines are even good  $\pi$ -acids.



## Bonding

Like CO, phosphines are neutral  $\sigma$  donors and  $\pi$  acceptors that formally contribute two electrons to the metal center. Unlike CO, most phosphines are not small enough for more than four to bond to a single metal center (and for large R, the number is even smaller). Steric hindrance becomes a problem when five or more  $PR_3$  ligands try to make their way into the space around the metal. Bridging by phosphines is extremely rare, but ligands containing multiple phosphine donors such as [diphenylphosphinoethane](#) metal center are common. For entropic reasons, chelating ligands like these bind to a single metal center at multiple points if possible, instead of attaching to two different metal centers (the aptly named chelate effect). An important characteristic of chelating phosphines is bite angle, defined as the predominant P–M–P angle in known complexes of the ligand. When the preferred bite angle of the ligand doesn't match the ideal bond angles of the geometry (i.e. 90° for octahedral) that introduces strain, and potentially reactivity into the complex.

The predominant orbital interaction contributing to phosphine binding is the one we expect, a lone pair on phosphorus donating to an empty metal d orbital. The electronic nature of the R groups influences the electron-donating ability of the phosphorus atom. For instance, alkylphosphines, which possess P–Csp<sup>3</sup> bonds, tend to be better electron donors than arylphosphines, which possess P–Csp<sup>2</sup> bonds. The rationale here is the greater electronegativity of the sp<sup>2</sup> hybrid orbital versus the sp<sup>3</sup> hybrid, which causes the phosphorus atom to hold more tightly to its lone pair when bound to an sp<sup>2</sup> carbon. The same idea applies when electron-withdrawing and -donating groups are incorporated into R: the electron density on P is low when R contains electron-withdrawing groups and high when R contains electron-donating groups.

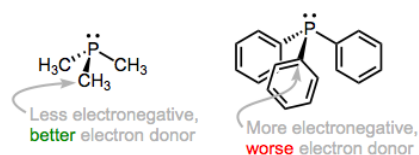


Figure 10.1.3.6: As we add electronegative R groups, the phosphorus atom (and the metal to which it's bound) become more electron poor.

Like CO, phosphines participate in backbonding to a certain degree; however, the phenomenon here is of a fundamentally different nature than CO backbonding. For one thing, phosphines lack a  $\pi^*$  orbital. In the days of yore, chemists attributed backbonding in phosphine complexes to an interaction between a metallic  $d\pi$  orbital and an empty 3d orbital on phosphorus. However, this idea has elegantly been proven bogus, and a much more organic-friendly explanation has taken its place (no d orbitals on P required). In an illuminating series of experiments, M–P and P–R bond lengths were measured via crystallography for several redox pairs of complexes.

M–P	2.218 Å	2.230 Å	M–P	2.146 Å	2.261 Å
P–R	1.846 Å	1.829 Å	P–R	1.598 Å	1.578 Å

Figure 10.1.3.7: Upon oxidation, M–P bond lengths increase and P–R bond lengths decrease.

Oxidation decreases the ability of the metal to backbond, because it removes electron density from the metal. This explains the increases in M–P bond length—just imagine a decrease the M–P bond order due to decreased backbonding. And the decrease in P–R bond length? It's important to see that invoking only the phosphorus 3d orbitals would not explain changes in the P–R bond lengths, as the 3d atomic orbitals are most definitely localized on phosphorus. Instead, we must invoke the participation of  $\sigma^*P-R$  orbitals in phosphine backbonding to account for the P–R length decreases. The figure below depicts one of the interactions involved in M–P backbonding, a  $d\pi \rightarrow \sigma^*$  interaction (an orthogonal  $d\pi \rightarrow \sigma^*$  interaction also plays a role). As with CO, a resonance structure depicting an  $M=P$  double bond is a useful heuristic! Naturally, R groups that are better able to stabilize negative charge—that is, electron-withdrawing groups—facilitate backbonding in phosphines. Electron-rich metals help too.

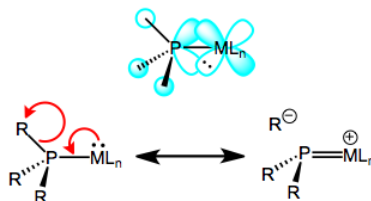


Figure 10.1.3.8: Backbonding in phosphines, a sigma-bond-breaking affair.

### Cone Angle

The steric and electronic properties of phosphines vary enormously. Tolman devised some intriguing parameters that characterize the steric and electronic properties of this class of ligands. To address sterics, he developed the idea of cone angle—the apex angle of a cone formed by a point 2.28 Å from the phosphorus atom (an idealized M–P bond length), and the outermost edges of atoms in the R groups, when the R groups are folded back as much as possible. Wider cone angles, Tolman reasoned, indicate greater steric congestion around the phosphorus atom. To address electronics, Tolman used the CO stretching frequency ( $\nu_{CO}$ ) of mixed phosphine-carbonyl complexes. Specifically, he used  $Ni(CO)_3L$  complexes, where L is a tertiary phosphine, as his standard.

: Illustration of the cone angle in phosphines. (CC BY-NC-SA; Catherine McCusker)

[illegible]

Notice the trifluorophosphine stuck in the “very small, very withdrawing” corner, and its utter opposite, the gargantuan tri(tert-butyl)phosphine in the “extremely bulky, very donating” corner.

## General Properties

The diagram illustrates the formation of molecular orbitals (MOs) from atomic orbitals (AOs). On the left, a  $d_{x^2-y^2}$  orbital is shown with four lobes (two red, two blue) and a central node labeled 'M'. A coordinate system with x and y axes is provided. In the middle, a ligand orbital (L) is shown as a red oval with a vertical line and 'L' at each end. On the right, the resulting  $\sigma$  MO and  $\sigma^*$  MO are shown. The  $\sigma$  MO is formed by the constructive overlap of the  $d_{x^2-y^2}$  and L orbitals, resulting in a single red lobe. The  $\sigma^*$  MO is formed by the destructive overlap, resulting in two lobes (one red, one blue) with a central node. A coordinate system with x and y axes is also provided for the  $\sigma^*$  MO.

The first thing to realize about  $\sigma$  complexes is that they are highly sensitive to steric bulk. Any old  $\sigma$  bond won't do; hydrogen at one end of the binding bond or the other (or both) is necessary. The best studied  $\sigma$  complexes involve dihydrogen ( $H_2$ ), so let's start

there.

### Dihydrogen complexes

Mildly backbonding metals may bind dihydrogen “side on.” Like side-on binding in  $\pi$  complexes, there are two important orbital interactions at play here:  $\sigma\text{H-H} \rightarrow d\sigma$  and  $d\pi \rightarrow \sigma^*\text{H-H}$ . Dihydrogen complexes can “tautomerize” to  $(\text{H})_2$  isomers through oxidative addition of the H-H bond to the metal. We should expect more electron-rich metal centers to favor the  $\text{X}_2$  isomer, since these should donate more strongly into the  $\sigma^*\text{H-H}$  orbital. This idea was masterfully demonstrated in a study by Morris, in which he showed that  $\text{H}_2$  complexes of  $\pi$ -basic metal centers show all the signs of dihydride complexes, rather than hydrogen complexes. More generally, metal centers in  $\sigma$  complexes need a good balance of  $\pi$  basicity and  $\sigma$  acidity (I like to call this the “Goldilocks effect”). Because of the need for balance,  $\sigma$  complexes are most common for centrally located metals (groups 6-9).

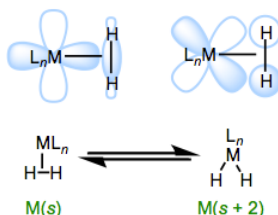


Figure 10.1.3.11: Orbital interactions and  $\text{L-X}_2$  equilibrium in  $\sigma$  complexes.

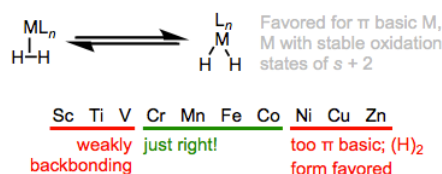
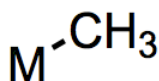


Figure 10.1.3.12: Oxidative addition of  $\text{H}_2$  is important for electron-rich,  $\pi$ -basic metal centers. Groups 6-9 hit the “Goldilocks” spot.

### Metal Alkyls

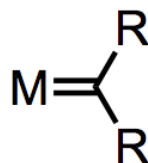


Alkyl or aryl transition metal compounds have M-C single bonds. In spite of many attempts over most of the course of chemical history, their isolation was unsuccessful and it was long considered that all M-C bonds were essentially unstable. Stable alkyl complexes began to be prepared gradually only from the 1950s.  $\text{Cp}_2\text{ZrCl}(\text{Pr})\text{WMe}_6$ ,  $\text{CpFeMe}(\text{CO})_2$ ,  $\text{CoMe}(\text{py})(\text{dmg})_2$ , ( $\text{dmg}$  = dimethylglyoximate),  $\text{IrCl}(\text{X})(\text{Et})(\text{CO})(\text{PPh}_3)_2$ ,  $\text{NiEt}_2(\text{bipy})$ ,  $\text{PtCl}(\text{Et})(\text{PET}_3)_2$  are some representative compounds. Among various synthetic processes so far developed, the reactions of compounds containing M-halogen bonds with main-group metal-alkyl compounds, such as a Grignard reagent or an organolithium compound, are common synthetic routes. Especially vitamin  $\text{B}_{12}$ , of which Dorothy Hodgkin (1964 Nobel Prize) determined the structure, is known to have a very stable Co-C bond. Metal alkyl compounds which have only alkyl ligand, such as  $\text{WMe}_6$ , are called homoleptic alkyls.

It is gradually accepted that a major cause of the instability of alkyl complexes is the low activation energy of their decomposition rather than a low M-C bond energy. The most general decomposition path is  $\beta$  elimination. Namely, the bonding interaction of a hydrocarbon ligand with the central transition metal tends to result in the formation of a metal hydride and an olefin. Such an interaction is called an **agostic interaction**. Although an alkyl and an aryl ligand are 1-electron ligands, they are regarded as anions when the oxidation number of the metal is counted. The hydride ligand, H, resembles the alkyl ligand in this aspect.

### Carbenes

In this section we’ll investigate two classes of carbenes, which are characterized by a metal-carbon double bond. Fischer carbenes and Shrock carbenes are usually  $\sigma$  ligands, but they may be either nucleophilic or electrophilic, depending on the nature of the R groups and metal. In addition, these ligands present some interesting synthetic problems: because free carbenes are quite unstable, ligand substitution reactions can’t be used for metal carbene synthesis.



### Fisher vs Schrock carbenes

Metal carbenes all possess a metal-carbon double bond. What's interesting for us about this double bond is that there are multiple ways to deconstruct it to determine the metal's oxidation state and number of d electrons. We could give one pair of electrons to the metal center and one to the ligand. This procedure nicely illustrates why compounds containing  $M=C$  bonds are called "metal carbenoids"—the deconstructed ligand is a neutral carbenoid. Alternatively, we could give both pairs of electrons to the ligand and think of it as a dianionic ligand. The appropriate procedure depends on the ligand's substituents and the electronic nature of the metal. The figure below summarizes the two deconstruction procedures.

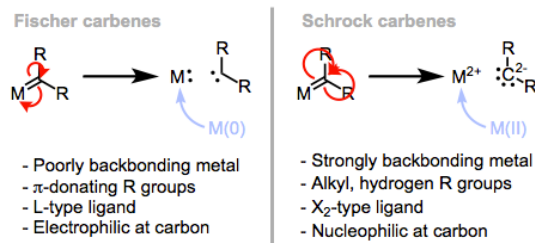
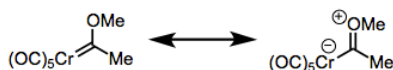


Figure 10.1.3.13: The proper method of deconstruction depends on the electronic nature of the ligand and metal.

When the metal possesses  $\pi$ -acidic ligands and the R groups are  $\pi$ -basic, the complex is best described as an L-type Fischer carbene and the oxidation state of the metal is unaffected by the carbene ligand. When the ligands are "neutral" ( $R = H$ , alkyl) and the metal is a good backbonder—that is, in the absence of  $\pi$ -acidic ligands and electronegative late metals—the complex is best described as an anionic  $X_2$ -type Schrock carbene. Notice that the oxidation state of the metal depends on our deconstruction method. In organometallic complexes it isn't uncommon for the oxidation state of the metal and ligand to be ambiguous.

Deconstruction reveals the typical behavior of the methylene carbon in each class of complex. The methylene carbon of Schrock carbenes, on which electron density is piled through backbonding, is nucleophilic. On the other hand, the methylene carbon of Fischer carbons is electrophilic, because backbonding is weak and does not compensate for  $\sigma$ -donation from the ligand to the metal. To spot a Fischer carbene, be on the lookout for reasonable zwitterionic resonance structures like the one at right below.

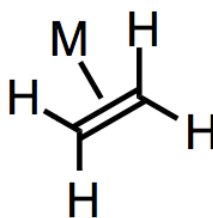


*Thanks to the  $\pi$ -accepting CO ligands, the metal handles the negative charge well. This is a Fischer carbene.*

The clever reader may notice that we haven't mentioned  $\pi$ -acidic R groups, such as carbonyls. Complexes of this type are best described as Fischer carbenes as well, as the ligand is still electrophilic. However, complexes of this type are difficult to handle and crazy reactive (see below) without a  $\pi$ -basic substituent to hold them in check. Take care when diagnosing the behavior of metal carbenes. In these complexes, there is often a subtle interplay between the R groups on the carbene and other ligands on the metal. In practice, many carbenes are intermediate between the Fischer and Schrock ideals.

### $\pi$ Systems

In contrast to neutral spectator ligands,  $\pi$  systems most often play an important role in the reactivity of the organometallic complexes of which they are a part (since they act in reactions, they're called "actors").  $\pi$  systems do useful chemistry, not just with the metal center, but also with other ligands and external reagents. Thus, in addition to thinking about how  $\pi$  systems affect the steric and electronic properties of the metal center, we need to start considering the metal's effect on the ligand and how we might expect the ligand to behave as an active participant in reactions. To the extent that structure determines reactivity—a commonly repeated, and extremely powerful maxim in organic chemistry—we can think about possibilities for chemical change without knowing the elementary steps of organometallic chemistry in detail yet.



## General Properties

Similar to  $\sigma$  complexes, the  $\pi$  bonding orbitals of alkenes, alkynes, carbonyls, and other unsaturated compounds may overlap with  $d\sigma$  orbitals on metal centers. This is the classic ligand HOMO  $\rightarrow$  metal LUMO interaction that we've seen many times. Because of this electron donation from the  $\pi$  system to the metal center, coordinated  $\pi$  systems often act electrophilic, even if the starting alkene was nucleophilic. The  $\pi \rightarrow d\sigma$  orbital interaction is central to the structure and reactivity of  $\pi$ -system complexes.  $\pi$  systems are also often subject to important backbonding interactions. We'll focus on alkenes here, but these same ideas apply to carbonyls, alkynes, and other unsaturated ligands bound through their  $\pi$  clouds. For alkene ligands, the relative importance of "normal" bonding and backbonding is nicely captured by the relative importance of the two resonance structures in Figure 10.1.3.14



Figure 10.1.3.14: Resonance forms of alkene ligands. In 1 backbonding is weak and in 2 the backbonding is strong.

Complexes of weakly backbonding metals, such as the electronegative late metals, are best represented by the traditional dative resonance structure 1. But complexes of strong backbonders, such as electropositive Ti(II), are often best drawn in the metallacyclopropane form 2. Bond lengths and angles in the alkene change substantially upon coordination to a strongly backbonding metal. We see an elongation of the C=C bond (consistent with decreased bond order) and some pyramidalization of the alkene carbons (consistent with a change in hybridization from  $sp^2$  to  $sp^3$ ). A complete orbital picture of sigma bonding and pi backbonding in alkenes is shown in Figure 10.1.3.15

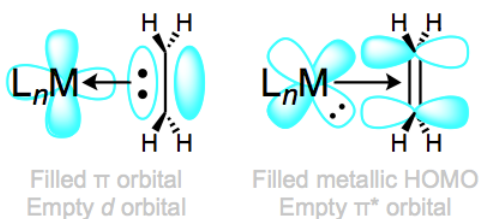
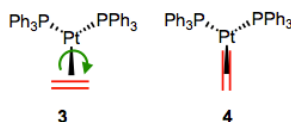


Figure 10.1.3.15: Normal sigma bonding and pi backbonding in alkene complexes.

Here's an interesting question with stereochemical implications: what is the orientation of the alkene relative to the other ligands? From what we've discussed so far, we can surmise that one face of the alkene must point toward the metal center. Put differently, the bonding axis must be normal to the plane of the alkene. However, this restriction says nothing about rotation about the bonding axis, which spins the alkene ligand like a pinwheel. Is a particular orientation preferred, or can we think about the alkene as a circular smudge over time? The figure below depicts two possible orientations of the alkene ligand in a trigonal planar complex. Other orientations make less sense because they would involve inefficient orbital overlap with the metal's orthogonal d orbitals. Which one is favored?



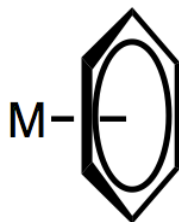
Two limiting cases for alkene orientation in a trigonal planar complex.

First of all, we need to notice that these two complexes are diastereomeric. They have different energies as a result, so one must be favored over the other. Steric considerations suggest that complex 4 ought to be more stable (in most complexes, steric factors dictate alkene orientation). To dig a little deeper, let's consider any electronic factors that may influence the preferred geometry. We've already seen that [electronic factors can overcome steric considerations when it comes to complex geometry](#). To begin, we

need to consider the crystal field orbitals of the complex as a whole. Verify on your own that in this  $d^{10}$ , Pt(0) complex, the crystal-field HOMOs are the  $d_{xy}$  and  $d_{x^2-y^2}$  orbitals. Where are these orbitals located in space? In the xy-plane! Only the alkene in **3** can engage in efficient backbonding with the metal center. In cases when the metal is electron rich and/or the alkene is electron poor, complexes like **3** can sometimes be favored in spite of sterics.

## Arenes

Arenes or aromatic ligands are neutral ligands that may serve either as actors or spectators. Arenes commonly bind to metals through more than two atoms, although  $\eta^2$ -arene ligands are known. Structurally, most  $\eta^6$ -arenes tend to remain planar after binding to metals. Both sigma bonding and pi backbonding are possible for arene ligands; however, arenes are stronger sigma donors than CO and backbonding is less important for these ligands. The reactivity of arenes changes dramatically upon metal binding, along lines that we would expect for strongly electron-donating ligands. After coordinating to a transition metal, the arene usually becomes a better electrophile (particularly when the metal is electron poor). Thus, metal coordination can enable otherwise difficult nucleophilic aromatic substitution reactions.



## General Properties

The coordination of an aromatic compound to a metal center through its aromatic  $\pi$  MOs removes electron density from the ring.  $\pi \rightarrow d\sigma$  (sigma bonding) and  $d\pi \rightarrow \pi^*$  (backbonding) orbital interactions are possible for arene ligands, with the former being much more important, typically. To simplify drawings, you often see chemists draw arenes involving a circle and single central line to represent the  $\pi \rightarrow d\sigma$  orbital interaction. Despite the single line these are not simple 2 electron donors. For instance,  $\eta^6$ -arenes are best describes as six-electron donors.

Multiple coordination modes are possible for arene ligands. When all six atoms of a benzene ring are bound to the metal ( $\eta^6$ -mode), the ring is flat and C–C bond lengths are slightly longer than those in free benzene. The ring is bent and non-aromatic in  $\eta^4$ -mode, so that the four atoms bound to the metal are coplanar while the other  $\pi$  bond is out of the plane. Even  $\eta^2$ -arene ligands bound through one double bond are known. Coordination of one  $\pi$  bond results in dearomatization and makes  $\eta^2$ -benzene behave more like butadiene, and furan act more like a vinyl ether. With naphthalene as ligand, there are multiple  $\eta^2$  isomers that could form; the isomer observed is the one that retains aromaticity in the free portion of the ligand. In fact, this result is general for polycyclic aromatic hydrocarbons: binding maximizes aromaticity in the free portion of the ligand. Arene ligands are usually hydrocarbons, not heterocycles. Why? Aromatic heterocycles, such as pyridine, more commonly bind using their basic lone pairs. That said, a few heterocycles form important  $\pi$  complexes. Thiophene is perhaps the most heavily studied, as the [desulfurization](#) of thiophene from fossil fuels is an industrially useful process.

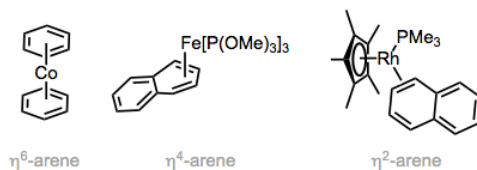


Figure 10.1.3.16: Arene ligands exhibit multiple coordination modes.

## Odd Numbered $\pi$ Systems

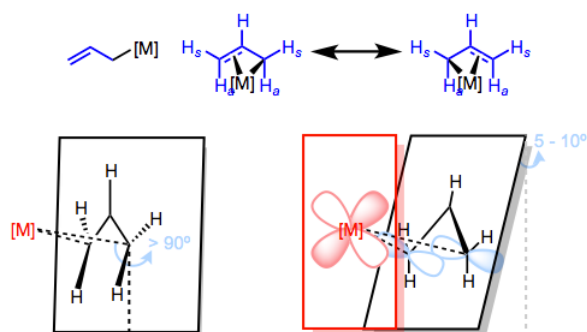
Odd-numbered  $\pi$  systems—most notably, the allyl and cyclopentadienyl ligands—are formally monoanionic ligands which donate  $n+1$  electrons (i.e.  $\eta^5$  cyclopentadienyl ligand is a 6 electron donor). To illustrate the plurality of equally important resonance structures for this class of ligands, we often just draw a curved line from one end of the  $\pi$  system to the other. Yet, even this form is not perfect, as it obscures the possibility that the datively bound atoms may dissociate from the metal center, forming  $\sigma$ -allyl or ring-slipped ligands. What do the odd-numbered  $\pi$  systems really look like, and how do they really behave?





## Metal Allyls

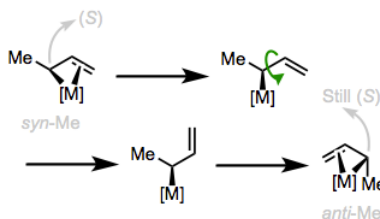
Allyls are often actor ligands, most famously in allylic substitution reactions. The allyl ligand is an interesting beast because it may bind to metals in two ways. When its double bond does not become involved in binding to the metal, allyl is a simple anionic ligand bound covalently through one carbon—basically, a monodentate alkyl! Alternatively, allyl can act as a bidentate LX-type ligand, bound to the metal through all three conjugated atoms. The LX or “trihapto” form can be represented using one of two resonance forms, or (more common) the “aromatic” form seen in the illustration above.



*Can we use FMO theory to explain the wonky geometry of the allyl ligand?*

The lower half of the figure above illustrates the slightly weird character of the geometry of allyl ligands. In a previous post on even-numbered  $\pi$  systems, we investigated the orientation of the ligand with respect to the metal and came to some logical conclusions by invoking FMO theory and backbonding. A similar treatment of the allyl ligand leads us to similar conclusions: the plane of the allyl ligand should be parallel to the xy-plane of the metal center and normal to the z-axis. In reality, the allyl plane is slightly canted to optimize orbital overlap—but we can see at the right of the figure above that  $\pi^2$ -dxy orbital overlap is key. Also note the rotation of the anti hydrogens (anti to the central C–H, that is) toward the metal center to improve orbital overlap.

Exchange of the syn and anti substituents can occur through  $\sigma,\pi$ -isomerization followed by bond rotation and formation of the isomerized trihapto form. Notice that the configuration of the stereocenter bearing the methyl group is unaffected by the isomerization! It should be noted that 1,3-disubstituted allyl complexes almost exclusively adopt a syn,syn configuration without danger of isomerization.



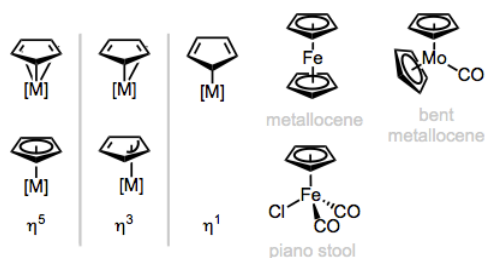
*The methylene and central C–H simply change places!*

## Metal Cyclopentadienyls

Upon deconstruction, the cyclopentadienyl (Cp) ligand yields the aromatic cyclopentadienyl anion, an L2X-type ligand. Cp is normally an  $\eta^5$ -ligand, but  $\eta^3$  (LX) and  $\eta^1$  (X) forms are known in cases where the other ligands on the metal center are tightly bound.  $\eta^1$ -Cyclopentadienyl ligands can sometimes be fluxional—the metal has the ability to “jump” from atom to atom. Variations on the Cp ligand include Cp\* ( $C_5Me_5$ ) and the monomethyl version ( $C_5H_4Me$ ). A single Cp may bond alongside other ligands (in “half-sandwich” or “piano-stool” complexes), or paired up with a second Cp ligand in metallocenes. The piano-stool and bent



metallocene complexes are most interesting for us, since these have potential for open coordination sites—metallocenes tend to be relatively stable and boring.



*Binding modes of Cp and general classes of Cp complexes.*

## Contributors and Attributions

- [Dr. Michael Evans](#) (Georgia Tech)
- Modified by Catherine McCusker (East Tennessee State University)

This page titled [10.1.3: Survey of Common Organometallic Ligands](#) is shared under a [CC BY-NC-SA 4.0](#) license and was authored, remixed, and/or curated by [Michael Evans](#).

- [2: Organometallic Ligands](#) by [Michael Evans](#) is licensed [CC BY-NC-SA 4.0](#).
- [11.1: Organometallic Ligands](#) by [Michael Evans](#) is licensed [CC BY-NC-SA 4.0](#).
- [2.2: Carbon Monoxide](#) by [Michael Evans](#) has no license indicated.
- [2.6: Metal Hydrides](#) by [Michael Evans](#) is licensed [CC BY-NC-SA 4.0](#).
- [2.9: Phosphines](#) by [Michael Evans](#) is licensed [CC BY-NC-SA 4.0](#).
- [2.3: σ Complexes](#) by [Michael Evans](#) is licensed [CC BY-NC-SA 4.0](#).
- [2.5: Metal Alkyls](#) by [Michael Evans](#) is licensed [CC BY-NC-SA 4.0](#).
- [2.1: Carbenes](#) by [Michael Evans](#) is licensed [CC BY-NC-SA 4.0](#).
- [2.10: π Systems](#) by [Michael Evans](#) is licensed [CC BY-NC-SA 4.0](#).
- [2.8: Odd-numbered π Systems](#) by [Michael Evans](#) is licensed [CC BY-NC-SA 4.0](#).

## 10.1.4: Electron Counting and the 18 Electron Rule

The 18 Electron Rule is a useful tool to predict the structure and reactivity of organometallic complexes. It describes the tendency of the central metal to achieve the noble gas configuration in its valence shell, and is somewhat analogous to the octet rule in a simplified rationale. Exceptions to this rule exist, depending on the energy and character of atomic and molecular orbitals.<sup>[1]</sup>

### The 18 Electron Rule

#### The General Rule

Atoms tend to have all its valence orbitals occupied by paired electrons. For transition metals, the valence orbitals consist of  $ns$ ,  $3np$  and  $5(n-1)d$  orbitals, leading to its tendency of being surrounded by 18 electrons. This is somewhat analogous to the octet and Lewis structure rules of main group elements in a simplified rationale.

Structures that satisfy this preferred electron structure are described as electron-precise. Transition metal complexes with 18 electrons are also referred to as saturated, and there will be no other empty low-lying orbitals available for extra ligand coordination. Complexes with less than 18 electron counts are unsaturated and can electronically bind to additional ligands.

#### Exceptions to The Rule

The 18 electron rule is usually followed in metal complexes with strong field ligands that are good  $\sigma$  donors and  $\pi$  acceptors (for example, CO ligands). The energy difference ( $\Delta_0$ ) between  $t_{2g}$  and  $e_g^*$  orbitals is very large, and in this case the three  $t_{2g}$  orbitals become bonding and are always filled, while the two  $e_g^*$  orbitals are strongly antibonding and are always empty.

However, when  $\Delta_0$  between  $t_{2g}$  and  $e_g^*$  orbitals are small, for example, in the case of first row transition metals with weaker field ligands, the antibonding character of  $e_g^*$  orbitals weakens, and the complex can have up to 22 electrons.

On the other hand, less than 18 electrons may be observed in complexes of 4th and 5th row transition metals with high oxidation states. In this case,  $\Delta_0$  is relatively large due to increased repulsion between  $d$  orbitals of metals and the ligands. The  $e_g^*$  orbitals are strongly antibonding and remains empty, while  $t_{2g}$  orbitals are non-bonding, and may be occupied by 0-6 electrons.<sup>[2]</sup>

Still, generally, the types of ligands in a complex determine if the complex would follow the 18 electron rule or not.

A few common examples of exceptions to 18 electron rules include:<sup>[3]</sup>

- 16-electron complexes: The metal center is usually low-spin and is in  $d^8$  configuration. These complexes adopt square planar structure, such as Rh(I), Ni(II), Pd(II), and Pt(II) complexes. In a lot of catalytic reactions, the organometallic catalysts convert back and forth between 18 and 16 electron configurations, and thus completes a catalytic cycle.
- Bulky ligands may hinder the completion of 18 electron rule. Examples include complexes with agostic interaction.<sup>[4]</sup> <sup>[5]</sup>
- Complexes with ligands of strong  $\pi$ -donating characters often violate 18 electron rule. Examples of this kind of ligands include  $F^-$ ,  $O^{2-}$ ,  $RO^-$  and  $RN^{2-}$ .

### Electron Counting Methods

There are two widely used methods for electron counting of complexes - covalent method and ionic ligand method. Both of the two methods are applicable to all organometallic complexes, and should give the same electron count.

#### Covalent Method

In this method, all metal-ligand bonds are considered covalent. Ligands are considered neutral in charge, and may donate either 2, 1 or zero electrons to the bond. For example, ligands such as CO and  $NH_3$  are considered to have filled valence and contribute 2 electrons. Halide and hydroxo groups, however, do not have octet structure in neutral state, and contribute 1 electron to the bonding. Ligands such as  $BF_3$  do not have any free electron available, and the two electrons for bonding would come from the metal center.

Steps for covalent counting method:

1. Identify the group number of the metal center.
2. Identify the number of electrons contributed by the ligands.
3. Identify the overall charge of the metal-ligand complex.
4. At the presence of metal-metal bond, one electron is counted towards each metal center in a bond.

5. Add up the group number of the metal center and the  $e^-$  count of the ligands, then take into consider the overall charge of the complex to obtain the final electron count.

### Ionic Method

The ionic method always assigns filled valences to the ligands. For example, H group is now considered  $H^-$ , as well as other groups such as halide, hydroxyl and methyl groups. These groups now contribute one more electron than they do in covalent method, and oxidize the metal center when a bond is formed. Groups with neutral charge in octet structure, such as CO and  $NH_3$ , behaves the same as in valence methods.

Steps for ionic counting method:

1. Determine the overall charge of the metal complex.
2. Identify the charges of the ligands, and the numbers of  $e^-$ s they donate.
3. Determine the number of valence electrons of the metal center, so that the oxidation state of the metal and charges of the ligands balance the overall charge of the complex. ( $E^-$  count of metal center = Metal atom group number +  $\sum$ (charges of ionic ligands) – overall charge of the complex)
4. If metal-metal bond is present, one bond counts for one electron for each metal atom.
5. Add up the electron count of the metal center and the ligands.

### Electron Counts of Some Common Ligands <sup>[6]</sup>

Ligand	Covalent	Ionic	Charge
H	1	2 ( $H^-$ )	-1
Cl, Br, I	1	2 ( $X^-$ )	-1
OH, OR	1	2 ( $OH^-$ , $OR^-$ )	-1
CN	1	2 ( $CN^-$ )	-1
$CH_3$ , $CR_3$	1	2 ( $CH_3^-$ , $CR_3^-$ )	-1
NO (bent M-N-O)	1	2 ( $NO^-$ )	-1
NO (linear M-N-O)	3	2 ( $NO^+$ )	+1
CO, $PR_3$	2	2	0
$NH_3$ , $H_2O$	2	2	0
$=CRR'$ (carbene)	2	2	0
$H_2C=CH_2$ (ethylene)	2	2	0
CNR	2	2	0
$=O$ , $=S$	2	4 ( $O^{2-}$ , $S^{2-}$ )	-2
$\eta^3-C_3H_5$ ( $\pi$ -allyl)	3	2 ( $C_3H_5^+$ )	+1
$\equiv CR$ (carbyne)	3	3	0
$\equiv N$	3	6 ( $N^{3-}$ )	-3
en (Ethylenediamine)	4	4	0
bipy (Bipyridine)	4	4	0
butadiene	4	4	0
$\eta^5-C_5H_5$ (cyclopentadienyl)	5	6 ( $C_5H_5^-$ )	-1
$\eta^6-C_6H_6$ (benzene)	6	6	0
$\eta^7-C_7H_7$ (cycloheptatrienyl)	7	6 ( $C_7H_7^+$ )	+1

## Examples

Examples of Electron Counting of Some Organometallic Complexes<sup>[7]</sup>

Complexes	Covalent Method	Ionic Method	Total Number of Electrons
$(\eta^5\text{-C}_5\text{H}_5)_2\text{Fe}$	<ul style="list-style-type: none"> <li>Fe gives <math>8e^-</math></li> <li>2 <math>\eta^5\text{-C}_5\text{H}_5</math> give <math>2 \times 5e^-</math></li> <li>Complex Charge is 0</li> </ul>	<ul style="list-style-type: none"> <li>Fe(II) gives <math>6e^-</math></li> <li>2 <math>\eta^5\text{-C}_5\text{H}_5^-</math> give <math>2 \times 6e^-</math></li> </ul>	18
$[\text{V}(\text{CO})_7]^+$	<ul style="list-style-type: none"> <li>V gives <math>5e^-</math></li> <li>7 CO give <math>7 \times 2e^-</math></li> <li>Complex Charge is +1 (<math>-1e^-</math>)</li> </ul>	<ul style="list-style-type: none"> <li>V(I) gives <math>4e^-</math></li> <li>7 CO give <math>7 \times 2e^-</math></li> </ul>	18
$[\text{Re}(\text{CO})_5(\text{PF}_3)]^+$	<ul style="list-style-type: none"> <li>Re gives <math>7e^-</math></li> <li>5 CO give <math>5 \times 2e^-</math></li> <li><math>\text{PF}_3</math> gives <math>2e^-</math></li> <li>Complex Charge is +1 (<math>-1e^-</math>)</li> </ul>	<ul style="list-style-type: none"> <li>Re(I) gives <math>6e^-</math></li> <li>2 CO give <math>5 \times 2e^-</math></li> <li><math>\text{PF}_3</math> gives <math>2e^-</math></li> </ul>	18

## References

- "18 electron rule" - Wikipedia, 18 May 2019.
- Libretexts 24.3-The 18 electron rule  
[https://chem.libretexts.org/Bookshelves/Inorganic\\_Chemistry/Map%3A\\_Inorganic\\_Chemistry\\_\(Housecroft\)/24%3A\\_Organometallic\\_chemistry%3A\\_d-block\\_elements/24.03%3A\\_The\\_18-electron\\_Rule](https://chem.libretexts.org/Bookshelves/Inorganic_Chemistry/Map%3A_Inorganic_Chemistry_(Housecroft)/24%3A_Organometallic_chemistry%3A_d-block_elements/24.03%3A_The_18-electron_Rule)
- "18 electron rule" - Wikipedia, 18 May 2019.
- "Agostic Interaction" - Wikipedia, 9 November 2018.
- International Union of Pure and Applied Chemistry. "agostic interaction". *Compendium of Chemical Terminology* Internet edition.
- Miessler, G.; Tarr, D. (1998). Inorganic Chemistry. New Jersey: Prentice-Hall. pp. 430.
- Miessler, G.; Tarr, D. (1998). Inorganic Chemistry. New Jersey: Prentice-Hall. pp. 430.

This page titled [10.1.4: Electron Counting and the 18 Electron Rule](#) is shared under a [CC BY-SA 4.0](#) license and was authored, remixed, and/or curated by [Wikipedia](#) via [source content](#) that was edited to the style and standards of the LibreTexts platform.

- 1.19: Electron Counting and the 18 Electron Rule** by Wikipedia is licensed [CC BY-SA 4.0](#). Original source: [https://en.wikibooks.org/wiki/Advanced\\_Inorganic\\_Chemistry](https://en.wikibooks.org/wiki/Advanced_Inorganic_Chemistry).

## 10.2: Organometallic Reactions

---

Learning objectives for this unit are to:

- Know the key characteristics of the five reaction classes (ligand association/dissociation, oxidative addition/reductive elimination, cycloaddition/retrocycloaddition, b-elimination/b-insertion; a-elimination/a-insertion)
  - Classify reactions based on the changes in coordination number, oxidation state, and total electron count
  - Predict the product(s) of a reaction given a reactant and reaction class
- 

10.2: Organometallic Reactions is shared under a [not declared](#) license and was authored, remixed, and/or curated by LibreTexts.

## 10.2.1: Ligand Dissociation and Substitution

As discussed previously, ligand substitution is characterized by a continuum of mechanisms bound by associative (A) and dissociative (D) extremes. At the associative extreme, the first step is an Associative reaction; the incoming ligand forms a bond to the metal and creates an intermediate of higher coordination number. Then the departing ligand takes its lone pair and leaves. At the dissociative extreme, the first step is a Dissociative reaction and the order of events is opposite; a ligand departs and a new complex with lower coordination number forms. Then, a new ligand associates with the complex in the second step. Sometimes, instead of reacting, the "intermediate" is simply a stable complex with a different coordination number than the reactant.

The most common reactions that are used to create new complexes are Dissociations and Substitutions (involving both Dissociation and Association steps). Associative substitution is common for 16-electron complexes (like  $d^8$  complexes of Ni, Pd, and Pt), while both Dissociation and Dissociative Substitution are the norm for 18-electron complexes. Then again, reality is often more complicated than these extremes. In some cases, evidence is available for interchange ( $I_a$  or  $I_d$ ).

In this subsection, we'll explore ligand substitution reactions and mechanisms in the context of organometallic chemistry. We'd like to be able to (a) predict whether a mechanism is likely to be associative or dissociative; (b) propose a reasonable mechanism from given experimental data; and (c) describe the results we'd expect given a particular mechanism. Keep these goals in mind as you learn the theoretical and experimental nuts and bolts of substitution reactions.

### Dissociation

Carbonyl compounds are known to undergo dissociation reactions upon heating or irradiation with light. For example, upon heating, the cyclopentadienylmolybdenum tricarbonyl dimer ( $\text{Cp}_2\text{Mo}_2(\text{CO})_6$ ), where Cp is the cyclopentadienyl ligand) loses a CO ligand from each Mo ion, and a triple bond between the Mo ions is formed (Top, Figure 10.2.1.1). An example of a photoactivated dissociation of CO is the case of neutral iron pentacarbonyl,  $\text{Fe}(\text{CO})_5$ . Irradiation of  $\text{Fe}(\text{CO})_5$  with UV produces  $\text{Fe}(\text{CO})_4$  (Bottom, Figure 10.2.1.1).

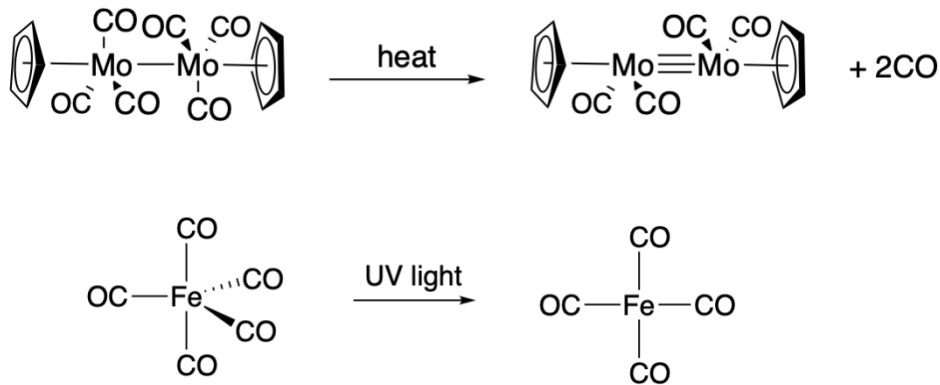


Figure 10.2.1.1: Dissociation reactions: Top, the thermally-activated dissociation of CO from cyclopentadienylmolybdenum tricarbonyl dimer. Bottom, the photochemically-activated dissociation of CO from ironpentacarbonyl. (CC-BY-SA; Kathryn Haas)

However, in each of the cases shown above, the product complex is reactive toward ligand association, usually resulting in an overall substitution. The cyclopentadienylmolybdenum dicarbonyl dimer shown on the top of Figure 10.2.1.1 binds a variety of substrates across the metal-metal triple bond. And the iron tetracarbonyl complex shown on the bottom in Figure 10.2.1.1 readily captures a variety of ligands to result in an [overall substitution \(example given below\)](#); when a ligand does not associate with it,  $\text{Fe}_2(\text{CO})_9$  is produced.

Sources: [Iron Pentacarbonyl](#) and [Cyclopentadienylmolybdenum tricarbonyl dimer](#) articles from Wikipedia.

### Dissociative Substitution

Associative substitution is unlikely for saturated, 18-electron complexes—coordination of another ligand would produce a 20-electron intermediate. For 18-electron complexes, dissociative substitution mechanisms involving 16-electron intermediates are more likely. In a slow step with positive entropy of activation, the departing ligand leaves, generating a coordinatively unsaturated

intermediate. The incoming ligand then enters the coordination sphere of the metal to generate the product. For the remainder of this post, we'll focus on the kinetics of the reaction and the nature of the unsaturated intermediate (which influences the stereochemistry of the reaction). The reverse of the first step, re-coordination of the departing ligand (rate constant  $k_{-1}$ ), is often competitive with dissociation.

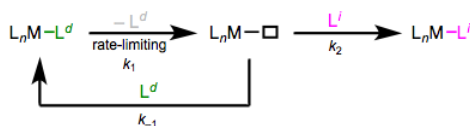


Figure 10.2.1.7: A general scheme for dissociative ligand substitution. There's more to the intermediate than meets the eye! (Michael Evans)

## Reaction Kinetics

Let's begin with the general situation in which  $k_1$  and  $k_{-1}$  are similar in magnitude. Since  $k_1$  is rate limiting,  $k_2$  is assumed to be much larger than  $k_1$  and  $k_{-1}$ . Most importantly, we need to assume that variation in the concentration of the unsaturated intermediate is essentially zero. This is called the steady state approximation, and it allows us to set up an equation that relates reaction rate to observable concentrations. Hold onto that for a second; first, we can use step 2 to establish a preliminary rate expression.

$$\text{rate} = k_2 [L_nM-\diamond] [Li] \quad (1)$$

Of course, the unsaturated complex is present in very small concentration and is unmeasurable, so this equation doesn't help us much. We need to remove the concentration of the unmeasurable intermediate from (1), and the steady state approximation helps us do this. We can express variation in the concentration of the unsaturated intermediate as (processes that make it) minus (processes that destroy it), multiplying by an arbitrary time length to make the units work out. All of that equals zero, according to the SS approximation. The painful math is almost over! Since  $\Delta t$  must not be zero, the other factor, the collection of terms, must equal zero.

$$\Delta [L_nM-\diamond] = 0 = (k_1 [L_nM-L^d] - k_{-1} [L_nM-\diamond] [L^d] - k_2 [L_nM-\diamond] [Li]) \Delta t \quad (2)$$

$$0 = k_1 [L_nM-L^d] - k_{-1} [L_nM-\diamond] [L^d] - k_2 [L_nM-\diamond] [Li] \quad (3)$$

Rearranging to solve for  $[L_nM-\diamond]$ , we arrive at the following.

$$[L_nM-\diamond] = k_1 \frac{[L_nM-L^d]}{(k_{-1} [L^d] + k_2 [Li])} \quad (4)$$

Finally, substituting into equation (1) we reach a verifiable rate equation.

$$\text{rate} = k_2 k_1 \frac{[L_nM-L^d] [Li]}{(k_{-1} [L^d] + k_2 [Li])} \quad (5)$$

When  $k_{-1}$  is negligibly small, (5) reduces to the familiar equation (6), typical of dissociative reactions like  $S_N1$ .

$$\text{rate} = k_1 [L_nM-L^d] \quad (6)$$

Unlike the associative rate law, this rate does not depend on the concentration of incoming ligand. For reactions that are better described by (5), we can drown the reaction in incoming ligand to make  $k_2 [Li]$  far greater than  $k_{-1} [L^d]$ , essentially forcing the reaction to fit equation (6).

## The Unsaturated Intermediate & Stereochemistry

Dissociation of a ligand from an octahedral complex generates an unsaturated  $ML_5$  intermediate. When all five of the remaining ligands are L-type, as in  $Cr(CO)_5$ , the metal has 6 d electrons for a total electron count of 16. The trigonal bipyramidal geometry presents electronic problems (unpaired electrons) for 6 d electrons, as the figure below shows. The orbital energy levels come from [crystal field theory](#). Distortion to a square pyramid or a distorted TBP geometry removes the electronic issue, and so five-coordinate d6 complexes typically have square pyramidal or distorted TBP geometries. This is just the [geometry prediction](#) process in action!

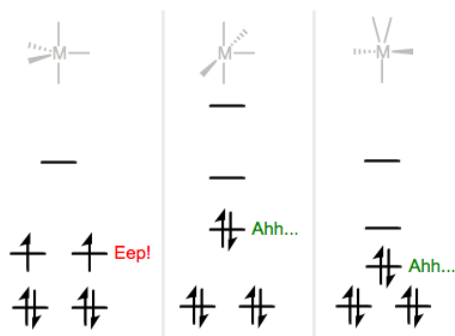


Figure 10.2.1.8: TBP geometry is electronically disfavored for d6 metals. Distorted TBP and SP geometries are favored. (Michael Evans)

When the intermediate adopts square pyramidal geometry (favored for good  $\pi$ -acceptors and  $\sigma$ -donors...why?), the incoming ligand can simply approach where the departing ligand left, resulting in retention of stereochemistry. Inversion is more likely when the intermediate is a distorted trigonal bipyramid (favored for good  $\pi$ -donors). As we've already seen for associative substitution, fluxionality in the five-coordinate intermediate can complicate the stereochemistry of the reaction.

### Encouraging Dissociative Substitution

In general, introducing structural features that either stabilize the unsaturated intermediate or destabilize the starting complex can encourage dissociative substitution. Both of these strategies lower the activation barrier for the reaction. Other, quirky ways to encourage dissociation include photochemical methods, oxidation/reduction, and ligand abstraction.

Let's begin with features that stabilize the unsaturated intermediate. Electronically, the intermediate loves it when its d electron count is nicely matched to its crystal field orbitals. As you study organometallic chemistry, you'll learn that there are certain "natural" d electron counts for particular geometries that fit well with the metal-centered orbitals predicted by [crystal field theory](#). Octahedral geometry is great for six d electrons, for example, and square planar geometry loves eight d electrons. Complexes with "natural" d electron counts—but bearing one extra ligand—are ripe for dissociative substitution. The classic examples are d8 TBP complexes, which become d8 square planar complexes (think Pt(II) and Pd(II)) upon dissociation. Similar factors actually stabilize starting 18-electron complexes, making them less reactive in dissociative substitution reactions. d6 octahedral complexes are particularly happy, and react most slowly in dissociative substitutions. The three most common types of 18-electron complexes, from fastest to slowest at dissociative substitution, are:



Destabilization of the starting complex is commonly accomplished by adding steric bulk to its ligands. Naturally, dissociation relieves steric congestion in the starting complex. Chelation has the opposite effect, and tends to steel the starting complex against dissociation.

L	Cone Angle	$K_d$
P(OEt) <sub>3</sub>	109	$< 10^{-10}$
P(O-C <sub>6</sub> H <sub>4</sub> -OEt) <sub>3</sub>	128	$6 \times 10^{-10}$
P(O <i>i</i> -Pr) <sub>3</sub>	130	$2.7 \times 10^{-5}$
P(O-C <sub>6</sub> H <sub>4</sub> -Me) <sub>3</sub>	141	$4 \times 10^{-2}$
PPh <sub>3</sub>	145	huge

Figure 10.2.1.9: As steric bulk on the ligand increases, dissociation becomes more favorable. (Michael Evans)

I plan to cover the "quirky" methods in a post of their own, but these include strategies like N-oxides for CO removal, photochemical cleavage of the metal-departing ligand bond, and the use of silver cation to abstract halide ligands. Oxidation and



reduction can also be used to encourage substitution: 17- and 19-electron complexes are much more reactive toward substitution than their 18-electron analogues.

## Associative Substitutions

Despite the sanctity of the 18-electron rule in organometallic chemistry, a wide variety of stable complexes possess fewer than 18 total electrons at the metal center. Perhaps the most famous examples of these complexes are 14- and 16-electron complexes of group 10 metals (Ni, Pt, Pd). Ligand substitution in complexes of this class typically occurs via an associative mechanism, involving approach of the incoming ligand to the complex before departure of the leaving group. If we keep this principle in mind, it seems easy enough to predict when ligand substitution is likely to be associative. But how can we spot an associative mechanism in experimental data, and what are some of the consequences of this mechanism?

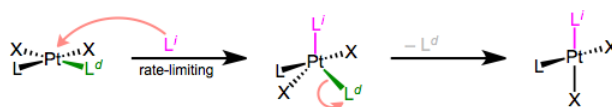


Figure 10.2.1.2: Associative substitution. (Michael Evans)

The prototypical mechanism of associative ligand substitution. The first step is rate-determining. A typical mechanism for associative ligand substitution is shown above. It should be noted that square pyramidal geometry is also possible for the intermediate, but is less common. Let's begin with the kinetics of the reaction.

### Reaction Kinetics for Associative Reactions

Reaction kinetics are commonly used to elucidate organometallic reaction mechanisms, and ligand substitution is no exception. Different mechanisms of substitution may follow different rate laws, so plotting the dependence of reaction rate on concentration often allows us to distinguish mechanisms. Associative substitution's rate law is analogous to that of the  $S_N2$  reaction—rate depends on the concentrations of both starting materials.



$$\frac{d[L_nM-L^i]}{dt} = \text{rate} = k_1[L_nM-L^d][L^i] \quad (10.2.1.2)$$

The easiest way to determine this rate law is to use pseudo-first-order conditions. Although the rate law is second order overall, if we could somehow render the concentration of the incoming ligand unchanging, the reaction would appear first order. The observed rate constant under these conditions reflects the constancy of the incoming ligand's concentration ( $k_{obs} = k_1[L^i]$ , where both  $k_1$  and  $[L^i]$  are constants). How can we make the concentration of the incoming ligand invariant, you ask? We can drown the reaction in ligand to achieve this. The teensy weensy bit actually used up in the reaction has a negligible effect on the concentration of the "sea" of starting ligand we began with. The observed rate is equal to  $k_{obs}[L_nM-L^d]$ , as shown by the purple trace below. By determining  $k_{obs}$  at a variety of  $[L^i]$  values, we can finally isolate  $k_1$ , the rate constant for the slow step. The red trace below at right shows the idea.

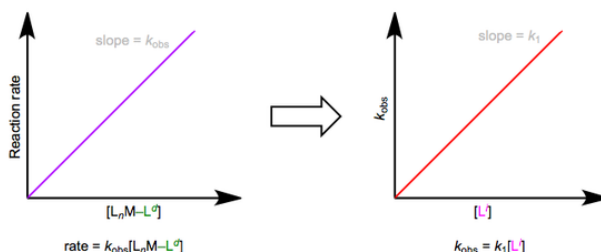


Figure 10.2.1.3: Associative substitution under pseudo-first-order conditions. The reaction is "swamped out" with incoming ligand. (Michael Evans)

In many cases, the red trace ends up with a non-zero y-intercept...curious, if we limit ourselves to the simple mechanism shown in the first figure of this post. A non-zero intercept suggests a more complex mechanism. We need to add a new term (called  $k_s$  for reasons to become clear shortly) to our first set of equations:

$$\text{rate} = (k_1[L^i] + k_s)[L_nM-L^d] \quad (10.2.1.3)$$

$$k_{obs} = k_1[L_i] + k_s \quad (10.2.1.4)$$

The full rate law suggests that some other step (with rate  $k_s[\text{LnM-Ld}]$ ) independent of incoming ligand is involved in the mechanism. To explain this observation, we can invoke the solvent as a reactant. Solvent can associate with the complex first in a slow step, then incoming ligand can displace the solvent in a fast step. Solvent concentration doesn't enter the rate law because, well, it's drowning the reactants and its concentration undergoes negligible change! An example of this mechanism in the context of [Pt\(II\) chemistry](#) is shown below.

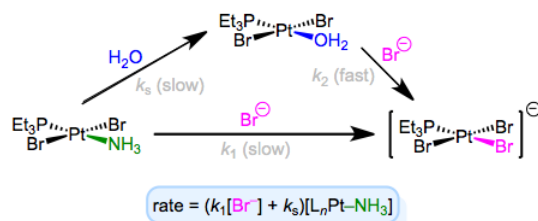


Figure 10.2.1.4: Associative substitution with solvent participation—a head-scratching mechanism for many an organometallic grad student! (Michael Evans)

As an aside, it's worth mentioning that the entropy of activation of associative substitution is typically negative. Entropy decreases as the incoming ligand and complex come together in the rate-determining step. Dissociative substitution shows the opposite behavior: loss of the departing ligand in the RDS increases entropy, resulting in positive entropy of activation.

### Stereochemistry of Associative Substitution

As we saw in discussions of the trans effect, the entering and departing ligands both occupy equatorial positions in the trigonal bipyramidal intermediate. Microscopic reversibility is to blame: the mechanism of the forward substitution (displacement of the leaving by the incoming ligand) must be the same as the mechanism of the reverse reaction (displacement of the incoming by the leaving ligand). This can be a confusing point, so let's examine an alternative mechanism that violates microscopic reversibility.

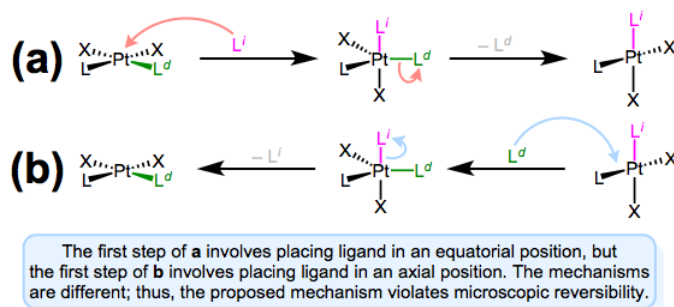


Figure 10.2.1.5: A mechanism involving approach to an axial position and departure from an equatorial position violates microscopic reversibility. Forward and reverse reactions a and b differ! (Michael Evans)

The figure above shows why a mechanism involving axial approach and equatorial departure (or vice versa) is not possible. The forward and reverse reactions differ, in fact, in both steps. In forward mechanism a, the incoming ligand enters an axial site. But in the reverse reaction, the incoming ligand (viz., the departing ligand in mechanism a) sits on an equatorial site. The second steps of each mechanism differ too—a involves loss of an equatorial ligand, while b involves loss of an axial ligand. Long story short, this mechanism violates microscopic reversibility. And what about a mechanism involving axial approach and axial departure? Such a mechanism is unlikely on [electronic grounds](#). The equatorial sites are more electron rich than the axial sites, and  $\sigma$  bonding to the axial  $d_{z^2}$  orbital is expected to be strong. Intuitively, then, loss of ligand from an axial site is less favorable than loss from an equatorial site.

I know what you're thinking: what the heck does all of this have to do with stereochemistry? Notice that, in the equatorial-equatorial mechanism (first figure of this post), the axial ligands don't move at all. The configuration of the starting complex is thus retained in the product. Although retention is "normal," complications often arise because five-coordinate TBP complexes—like other odd-coordinate organometallic complexes—are often fluxional. Axial and equatorial ligands can rapidly exchange through a process called [Berry pseudorotation](#), which resembles the axial ligands "cutting through" a pair of equatorial ligands like scissors (animation!). Fluxionality means that all stereochemical bets are off, since any ligand can feasibly occupy an equatorial site. In the example below, the departing ligand starts out cis to L, but the incoming ligand ends up trans to L.

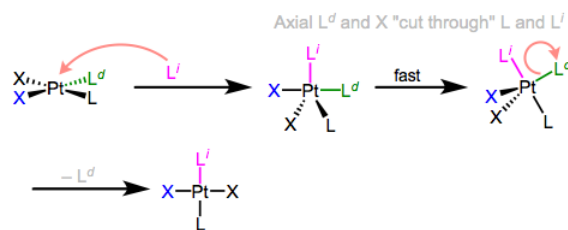


Figure 10.2.1.6: Berry pseudorotation in the midst of associative ligand substitution. (Michael Evans)

### Associative Substitution in 18-electron Complexes?

Associative substitution can occur in 18-electron complexes if it's preceded by the dissociation of a ligand. For example, changes in the hapticity of cyclopentadienyl or indenyl ligands may open up a coordination site, which can be occupied by a new ligand to kick off associative substitution. An allyl ligand may convert from its  $\pi$  to  $\sigma$  form, leaving an open coordination site where the  $\pi$  bond left. A particularly interesting case is the **nitrosyl ligand**—conversion from its linear to bent form opens up a site for coordination of an external ligand.

### Summary of Associative Substitution

Associative ligand substitution is common for complexes with 16 total electrons or fewer. The reaction is characterized by a second-order rate law, the possibility of solvent participation, and a trigonal bipyramidal intermediate that is often fluxional. An open coordination site is essential for associative substitution, but such sites are often hidden in the dynamism of 18-electron complexes with labile ligands.

Dr. Michael Evans (Georgia Tech)

### Quirky Substitutions

Over the years, a variety of “quirky” substitution methods have been developed. All of these have the common goal of facilitating substitution in complexes that would otherwise be inert. It's an age-old challenge: how can we turn a stable complex into something unstable enough to react? Photochemical excitation, oxidation/reduction, and radical chains all do the job, and have all been well studied. We'll look at a few examples in this post—remember these methods when simple associative or dissociative substitution won't get the job done.

### Photochemical Substitution

Substitution reactions of dative ligands—most famously, CO—may be facilitated by photochemical excitation. We just discussed the photochemically-activated dissociation of CO from ironpentacarbonyl above; that reaction is often used to accomplish substitution of a CO ligand. Other CO complexes also undergo photochemically-activated CO substitution reactions. [Two examples](#) are shown below. The first reaction yields only monosubstituted product without ultraviolet light, even in the presence of a strongly donating phosphine.

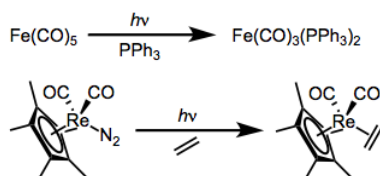


Figure 10.2.1.10: Dissociative photochemical substitutions of CO and dinitrogen. (Michael Evans)

All signs point to dissociative mechanisms for these reactions (the starting complexes have 18 total electrons each). Excitation, then, must increase the M–L antibonding character of the complex's electrons; exactly how this increase in antibonding character happens has been a matter of some debate. Originally, the prevailing explanation was that the LUMO bears M–L antibonding character, and excitation kicks an electron up from the HOMO to the LUMO, encouraging cleavage of the M–L bond. A more recent, more subtle explanation backed by calculations supports the involvement of a [metal-to-ligand charge-transfer](#) state along with the “classical” ligand-field excited state.

## Oxidation/Reduction

Imagine a screaming baby without her pacifier—that's a nice analogy for an odd-electron organometallic complex. Complexes bearing 17 and 19 total electrons are much more reactive toward substitution than their even-electron counterparts. Single-electron oxidation and reduction ("popping out the pacifier," if you will) can thus be used to efficiently turn on substitution. As you might expect, oxidation and reduction work best on electron-rich and electron-poor complexes, respectively. The Mn complex in the oxidative example below, for instance, includes a strongly donating MeCp group (not shown).

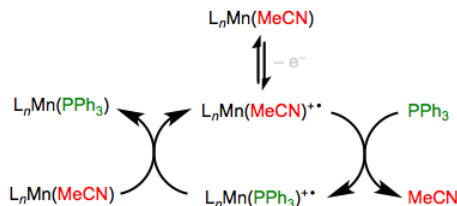


Figure 10.2.1.11: Oxidation accelerates substitution in electron-rich complexes through a chain process. (Michael Evans)

Reduction works well for electron-poor metal carbonyl complexes, which are happy to accept an additional electron.

There is a two-electron oxidation method that's also worth knowing: the oxidation of CO with amine oxides. This nifty little method releases carbon dioxide, amine, and an unsaturated complex that may be quenched by a ligand hanging around. The trick is addition to the CO ligand followed by elimination of the unsaturated complex. As the oxidized CO<sub>2</sub> and reduced amine float away, the metal complex finds another ligand.

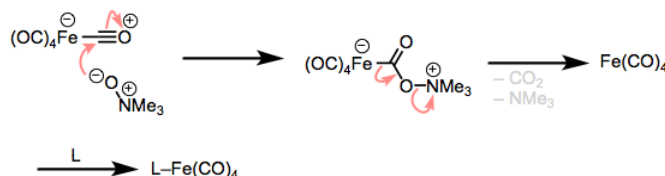


Figure 10.2.1.12: Oxidation of CO with amine oxides. A fun method for dissociative substitution of metal carbonyls! (Michael Evans)

## Radical Chain Processes

Atom abstraction from 18-electron complexes produces neutral 17-electron intermediates, which are susceptible to ligand substitution via radical chain mechanisms. The fact that the intermediates are neutral distinguishes these methods from oxidation-based methods. First-row metal hydrides are great for these reactions, owing to their relatively weak M-H bonds. One example is shown below.

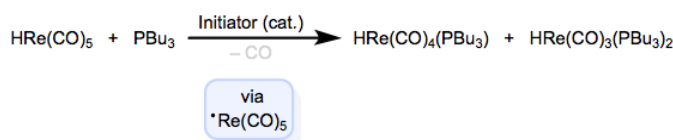


Figure 10.2.1.13: Radical-chain substitution involving atom abstraction. (Michael Evans)

After abstraction of the hydrogen atom by initiator, substitution is rapid and may occur multiple times. Propagation begins anew when the substituted radical abstracts hydrogen from the starting material to regenerate the propagating radical and form the product. These quirky methods are nice to have in your back pocket when you're backed into a synthetic corner—sometimes, conventional associative and dissociative substitution just won't do the job. In the next post, we'll press on to oxidative addition.

Template:Evans

This page titled [10.2.1: Ligand Dissociation and Substitution](#) is shared under a [not declared](#) license and was authored, remixed, and/or curated by [Kathryn Haas](#).

- [4.4: Ligand substitution](#) by [Michael Evans](#) is licensed [CC BY-NC-SA 4.0](#).
- [4.3: Dissociative Ligand Substitution Reactions](#) by [Michael Evans](#) is licensed [CC BY-NC-SA 4.0](#).
- [4.2: Associative Ligand Substitution](#) by [Michael Evans](#) is licensed [CC BY-NC-SA 4.0](#).
- [4.10: Quirky Ligand Substitutions](#) by [Michael Evans](#) is licensed [CC BY-NC-SA 4.0](#).

## 10.2.2: Oxidative Addition

### Overview

In the next few sections we will introduce reactions that are unique to organometallic complexes and play important roles in organometallic catalysis. The first reaction type is oxidative addition. As the name implies, the oxidative addition reaction involves increasing the coordination number of the metal complex by two and oxidizing the metal center by two electrons as shown in Figure 10.2.2.1 The metal donates two electrons to break the A-B bond and form two new bonds, M-A and M-B.

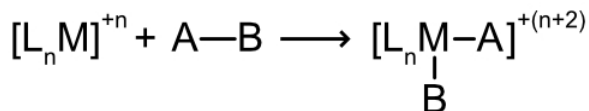


Figure 10.2.2.1: General scheme for oxidative addition. (CC BY-NC-SA; Catherine McCusker)

How important are oxidative additions? Very. The addition of dihydrogen ( $H_2$ ) is an important step in catalytic hydrogenation reactions. Organometallic C-H activations depend on oxidative additions of C-H bonds. In a fundamental sense, oxidative additions of organic compounds are commonly used to establish critical metal-carbon bonds. Non-polar oxidative additions get the ball rolling in all kinds of catalytic organometallic reactions. Here the mechanisms and important trends associated with oxidative additions are discussed.

### Oxidative Additions of $H_2$

Electron-rich metal centers with open coordination sites (or the ability to form them) undergo oxidative additions with dihydrogen gas. The actual addition step is concerted, but before the addition step, some interesting gymnastics are going on. The status of the  $\sigma$  complex that forms prior to H-H insertion is an open question—for some reactions it is a [transition state](#), others a discrete [intermediate](#). In either case, the two new hydride ligands end up cis to one another. Subsequent isomerization may occur to give a trans dihydride.

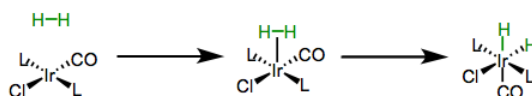


Figure 10.2.2.2: Oxidative addition of dihydrogen to Vaska's complex. Note the cis arrangement of the hydride ligands.

### Oxidative Additions of Silanes (H-Si)

Silanes bearing Si-H bonds may react with organometallic complexes in oxidative addition reactions. [Spectroscopic experiments](#) support the intermediacy of a silyl  $\sigma$  complex before insertion. Since the mechanism is concerted, oxidative addition occurs with retention of configuration at Si. The usual pair of forward bonding ( $\sigma Si-H \rightarrow d\sigma$ ) and backbonding ( $d\pi \rightarrow \sigma^* Si-H$ ) orbital interactions are at play here. File this reaction away as a great method for the synthesis of silyl complexes.

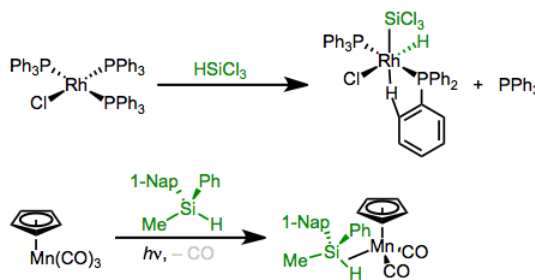


Figure 10.2.2.3: Si-H bonds undergo oxidative addition to electron-rich metal complexes. Electron-poor complexes may stop at the  $\sigma$  complex stage

### Oxidative Additions of C-H Bonds

Needless to say, oxidative addition reactions of C-H bonds are highly prized among organometallic chemists. As simple as it is to make silyl complexes through oxidative addition, analogous reactions of C-H bonds that yield alkyl hydride complexes are harder

to come by. The thermodynamics of C–H oxidative addition tell us whether it's favorable, and depend heavily on the nature of the organometallic complex. The sum of the bond energies of the new M–C and M–H bonds must exceed the sum of the energies of the C–H bond and any M–L bonds broken during the reaction. For many complexes, the balance is not in favor of oxidative addition. For example, the square planar [Vaska's complex](#) ( $\text{L}_2(\text{CO})\text{IrCl}$ ;  $\text{L} = \text{PPh}_3$ ) seems like a great candidate for oxidative addition of methane—at least to the extent that the product will be six-coordinate and octahedral. However, thermodynamics is a problem:

$$104 (\text{C-H}) - [60 (\text{Ir-H}) + 35 (\text{Ir-Me})] + 9 \text{ kcal/mol (entropy)} = 18 \text{ kcal/mol}$$

18 kcal/mol is prohibitively high in energy, and playing with the temperature to adjust the entropy factor can't "save" the reaction. More electron-rich complexes exhibit favorable thermodynamics for insertions of C–H bonds. The example below is so favorable ( $104 - [75 + 55] + 9 = -17 \text{ kcal/mol}$ ) that the product is a rock.

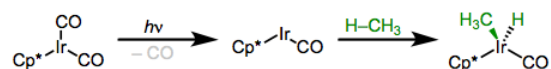


Figure 10.2.2.4: This thermodynamically favorable C–H oxidative addition is helped by the electron-donating  $\text{Cp}^*$  ligand.

Arenes undergo C–H oxidative addition faster (and more favorably) than alkanes for several reasons. It [seems likely](#) that an intermediate arene  $\pi$  complex and/or C–H  $\sigma$  complex precede insertion, and these complexes ought to be more stable than alkyl  $\sigma$  complexes. In addition, metal-aryl bonds tend to be stronger than metal-alkyl bonds.

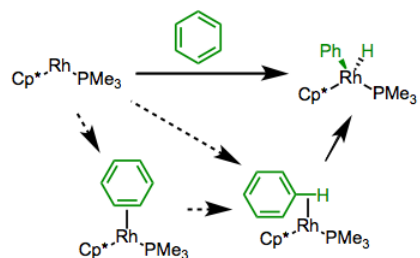


Figure 10.2.2.5: Mechanistic possibilities for the oxidative addition of arene C–H bonds.

## Contributors and Attributions

- [Dr. Michael Evans](#) ([Georgia Tech](#))
- Modified by Catherine McCusker ([East Tennessee University](#))

10.2.2: Oxidative Addition is shared under a [CC BY-NC-SA 4.0](#) license and was authored, remixed, and/or curated by LibreTexts.

- [11.3: Oxidative Addition](#) is licensed [CC BY-NC-SA 4.0](#).

### 10.2.3: Reductive Elimination

Reductive elimination is the microscopic reverse of oxidative addition. It is literally oxidative addition run in reverse. Chemically, reductive elimination and oxidative addition share the same reaction coordinate. The only difference between their reaction coordinate diagrams relates to what we call “reactants” and “products.” Thus, their mechanisms depend on one another, and trends in the speed and extent of oxidative additions correspond to opposite trends in reductive eliminations. In this section, we’ll address reductive elimination in a general sense, as we did for [oxidative addition](#).



Figure 10.2.3.1:A general reductive elimination scheme. The oxidation state of the metal decreases by two units, and open coordination sites become available.

During reductive elimination, the electrons in the M–X bond head toward ligand Y, and the electrons in M–Y head to the metal. The eliminating ligands are always anionic. On the whole, the oxidation state of the metal decreases by two units, two new open coordination sites become available, and an X–Y bond forms. What does the change in oxidation state suggest about changes in electron density at the metal? As suggested by the name “reductive,” the metal gains electrons. The ligands lose electrons as the new X–Y bond cannot possibly be polarized to both X and Y, as the original M–X and M–Y bonds were.

It’s been observed in a [number of cases](#) that a ligand dissociates from octahedral complexes before concerted reductive elimination occurs. Presumably, dissociation to form a distorted trigonal bipyramidal geometry brings the eliminating groups closer to one another to facilitate elimination. Square planar complexes may either take on an additional fifth ligand or lose a ligand to form an odd-coordinate complex before reductive elimination. Direct reductive elimination without dissociation or association is possible, too.

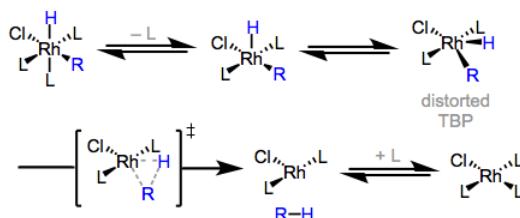


Figure 10.2.3.2:Reductive elimination is faster from five-coordinate than six-coordinate complexes.

Reactivity trends in reductive elimination are opposite those of oxidative addition. More [electron-rich ligands](#) bearing electron-donating groups react more rapidly, since the ligands lose electron density as the reaction proceeds. More electron-poor metal centers—bearing  $\pi$ -acidic ligands and/or ligands with electron-withdrawing groups—react more rapidly, since the metal center gains electrons. Sterically bulky ancillary ligands promote reductive elimination since the release of X and Y can “ease” steric strain in the starting complex. Steric hindrance helps explain, for example, why coordination of a fifth ligand to a square planar complex promotes reductive elimination [even though](#) coordination increases electron density at the metal center. A second example: trends in rates of reductive eliminations of alkanes parallel the steric demands of the eliminating ligands: C–C > C–H > H–H.

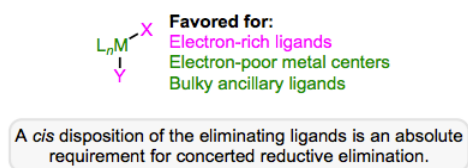


Figure 10.2.3.3: Reactivity trends for reductive eliminations.

Mechanistic trends for reductive elimination actually parallel trends in mechanisms of oxidative addition, since these two reactions are the microscopic reverse of one another. Non-polar and moderately polar ligands react by concerted or radical mechanisms; highly polarized ligands and/or very electrophilic metal complexes react by ionic ( $S_N2$ ) mechanisms. The thermodynamics of

reductive elimination must be favorable in order for it to occur! Most carbon–halogen reductive eliminations, for example, are thermodynamically unfavorable (this has turned out to be a good thing, especially for cross-coupling reactions).

Reductive elimination is an important step in many catalytic cycles—it usually comes near the “end” of catalytic mechanisms, just before product formation. For some catalytic cycles it’s the turnover-limiting step, making it very important to consider. [Hydrocyanation](#) is a classic example; in the mechanism of this reaction, reductive elimination of C–CN is the slow step. Electron-poor alkyl ligands, derived from electron-poor olefins like unsaturated ketones, are bad enough at reductive elimination to prevent turnover altogether.

## Contributors and Attributions

Dr. Michael Evans ([Georgia Tech](#))

---

10.2.3: [Reductive Elimination](#) is shared under a [CC BY-NC-SA 4.0](#) license and was authored, remixed, and/or curated by LibreTexts.

- [11.4: Reductive Elimination](#) is licensed [CC BY-NC-SA 4.0](#).



## 10.2.4: Migratory Insertion- 1,2-Insertions

### Overview

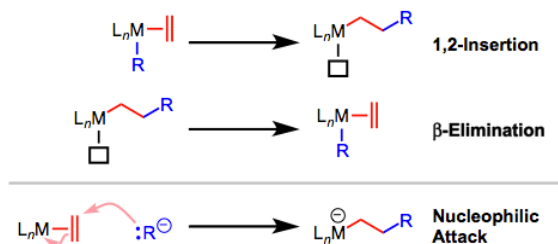


Figure 10.2.4.1: 1,2-Insertion is distinct from nucleophilic/electrophilic attack on coordinated ligands.

Insertions of  $\pi$  systems into M-X bonds are appealing in the sense that they establish two new  $\sigma$  bonds in one step, in a stereocontrolled manner. 1,2-insertions generate a vacant site on the metal, which is usually filled by external ligand. For unsymmetrical alkenes, it's important to think about site selectivity: which atom of the alkene will end up bound to metal, and which to the other ligand? To make predictions about site selectivity we can appeal to the classic picture of the M-X bond as  $M^+X^-$ . Asymmetric, polarized  $\pi$  ligands contain one atom with excess partial charge; this atom hooks up with the complementary atom in the M-R bond during insertion. Resonance is our best friend here!

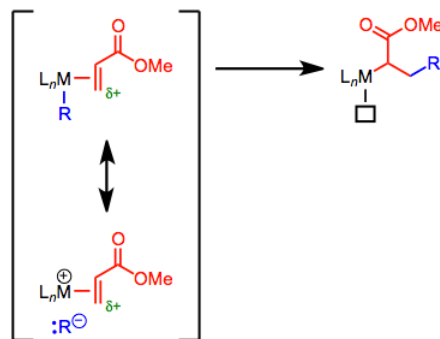


Figure 10.2.4.2: The site selectivity of 1,2-insertion can be predicted using resonance forms and partial charges.

A nice study by [Yu and Spencer](#) illustrates these effects in homogeneous palladium- and rhodium-catalyzed hydrogenation reactions. Unactivated alkenes generally exhibit lower site selectivity than activated ones, although steric differences between the two ends of the double bond can promote selectivity.

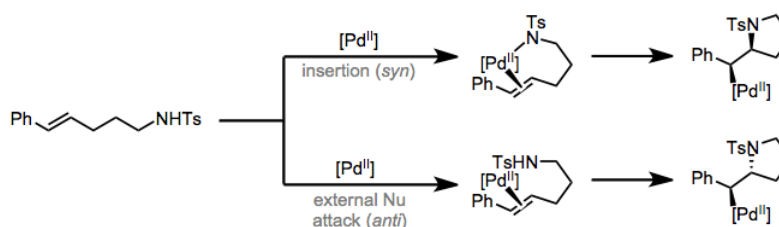
### Reactivity Trends in 1,2-Insertions

The thermodynamics of 1,2-insertions of alkenes depend strongly on the alkene, but we can gain great insight by examining the structure of the product alkyl. Coordinated alkenes that give strong metal-alkyl bonds after migratory insertion tend to undergo the process. Hence, electron-withdrawing groups, such as carbonyls and fluorine atoms, tend to encourage migratory insertion—remember that alkyl complexes bearing these groups tend to have stable M-C bonds.

Insertions of alkenes into both M-H and M-R (R = alkyl) are favored thermodynamically, but the kinetics of M-R insertion are much slower. This observation reflects a pervasive trend in organometallic chemistry: M-H bonds react more rapidly than M-R bonds. The same is true of the reverse,  $\beta$ -elimination. Even in cases when both hydride and alkyl elimination are thermodynamically favored,  $\beta$ -hydride elimination is much faster. Although insertion into M-R is relatively slow, this elementary step is critical for olefin polymerizations that form polyalkenes ([Ziegler-Natta polymerization](#)). This reaction deserves a post all its own!

As the strength of the M-X bond increases, the likelihood that an L-type  $\pi$  ligand will insert into the bond goes down. Hence, while insertions into M-H and M-C are relatively common, insertions into M-N and M-O bonds are more rare. [Lanthanides](#) and palladium are known to promote insertion into M-N in some cases, but products with identical connectivity can come from external attack of nitrogen on a coordinated  $\pi$  ligand. The diastereoselectivity of these reactions provides [mechanistic insight](#)—

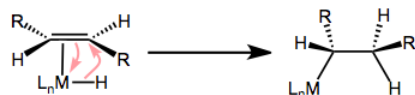
since migratory insertion is syn (see below), a syn relationship between Pd and N is to be expected in the products of migratory insertion. An anti relationship indicates external attack by nitrogen or oxygen.



*The diastereoselectivity of formal insertions provides insight about their mechanisms.*

## Stereochemistry of 1,2-Insertions

1,2-Insertion may establish two stereocenters at once, so the stereochemistry of the process is critical! Furthermore, 1,2-insertions and  $\beta$ -eliminations are bound by important stereoelectronic requirements. An analogy can be made to the E2 elimination of organic chemistry, which also has strict stereoelectronic demands. For migratory insertion to proceed, the alkene and X-type ligand must be synclinal during insertion; as a consequence of this alignment, X and ML<sub>n</sub> end up on the same face of the alkene after insertion. In other words, insertions into alkenes take place in a syn fashion. Complexes that have difficulty achieving a coplanar arrangement of C=C and M–X undergo insertion very slowly, if at all.

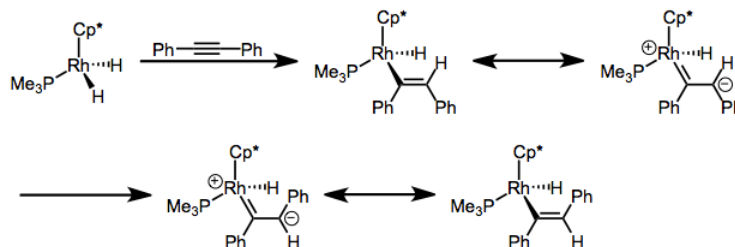


*1,2-Insertions take place in a syn fashion. The metal and X end up bound to the same face of the alkene.*

This observation has important implications for  $\beta$ -elimination, too—the eliminating X and the metal must have the ability to align syn.

## Insertions of Other $\pi$ Systems

To close this section, let's examine insertions into  $\pi$  ligands other than alkenes briefly. Insertions of alkynes into metal-hydride bonds are known, and are sometimes involved in reactions that I refer to collectively as “hydrostuffylation”: hydrosilylation, hydroesterification, hydrogenation, and other net H–X additions across the  $\pi$  bond. Strangely, some insertions of alkynes yield trans products, even though cis products are to be expected from syn addition of M–X. The mechanisms of these processes involve initial syn addition followed by isomerization to the trans complex via an interesting resonance form. The cis complex is the kinetic product, but it isomerizes over time to the more thermodynamically stable trans complex.



*Migratory insertions of alkynes into M–H produce alkenyl complexes, which have been known to isomerize.*

The strongly donating Cp\* ligand supports the legitimacy of the zwitterionic resonance form—and suggests that the C=C bond may be weaker than it first appears!

Polyenes can participate in migratory insertion, and insertions of polyenes are usually quite favored because stabilized  $\pi$ -allyl complexes result. In one [mind-bending case](#), a coordinated arene inserts into an M–Me bond in a syn fashion!

Have you ever stopped to consider that the addition of methyllithium to an aldehyde is a formal insertion of the carbonyl group into the Li–Me bond? It's true! We can think of these as (very) early-metal “insertion” reactions. Despite this precedent, migratory insertion reactions of carbonyls and imines into late-metal hydride and alkyl bonds are surprisingly hard to come by. [Rhodium](#) is

the most famous metal that can make this happen—rhodium has been used in complexes for [arylation](#) and vinylation, for example. Insertion of  $X=C$  into the  $M-R$  bond is usually followed by  $\beta$ -hydride elimination, which has the nifty effect of replacing H in aldehydes and aldimines with an aryl or vinyl group.

## Contributors and Attributions

[Dr. Michael Evans](#) ([Georgia Tech](#))

---

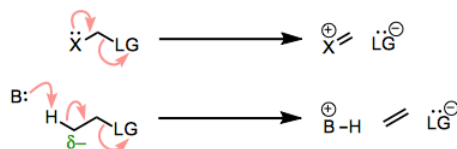
[10.2.4: Migratory Insertion- 1,2-Insertions](#) is shared under a [CC BY-NC-SA 4.0](#) license and was authored, remixed, and/or curated by LibreTexts.

- [11.5: Migratory Insertion- 1,2-Insertions](#) is licensed [CC BY-NC-SA 4.0](#).

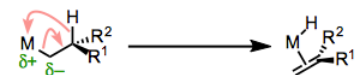
## 10.2.5: $\beta$ -Elimination Reactions

In organic chemistry class, one learns that elimination reactions involve the cleavage of a  $\sigma$  bond and formation of a  $\pi$  bond. A nucleophilic pair of electrons (either from another bond or a lone pair) heads into a new  $\pi$  bond as a leaving group departs. This process is called  $\beta$ -elimination because the bond  $\beta$  to the nucleophilic pair of electrons breaks. Transition metal complexes can participate in their own version of  $\beta$ -elimination, and [metal alkyl complexes](#) famously do so. Almost by definition, metal alkyls contain a nucleophilic bond—the M–C bond! This bond can be so polarized toward carbon, in fact, that it can promote the elimination of some of the world's worst leaving groups, like  $\text{--H}$  and  $\text{--CH}_3$ . Unlike the organic case, however, the leaving group is not lost completely in organometallic  $\beta$ -eliminations. As the metal donates electrons, it receives electrons from the departing leaving group. When the reaction is complete, the metal has picked up a new  $\pi$ -bound ligand and exchanged one X-type ligand for another.

### organic $\beta$ -eliminations



### organometallic $\beta$ -eliminations



- There is no change in oxidation state at M.
- Total electron count increases by 2.
- A new  $\pi$ -bound ligand appears on M.

Comparing organic and organometallic  $\beta$ -eliminations. A nucleophilic bond or lone pair promotes loss or migration of a leaving group.

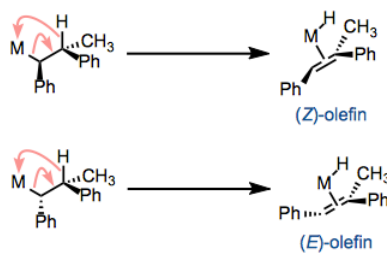
In this post, we'll flesh out the mechanism of  $\beta$ -elimination reactions by looking at the conditions required for their occurrence and their reactivity trends. Many of the trends associated with  $\beta$ -eliminations are the opposite of analogous trends in [1,2-insertion reactions](#). A future post will address other types of elimination reactions.

### $\beta$ -Hydride Elimination

The most famous and ubiquitous type of  $\beta$ -elimination is  **$\beta$ -hydride elimination**, which involves the formation of a  $\pi$  bond and an M–H bond. Metal alkyls that contain  $\beta$ -hydrogens experience rapid elimination of these hydrogens, provided a few other conditions are met.

The complex must have an open coordination site and an accessible, empty orbital on the metal center. The leaving group ( $\text{--H}$ ) needs a place to land. Notice that after  $\beta$ -elimination, the metal has picked up one more ligand—it needs an empty spot for that ligand for elimination to occur. We can envision hydride “attacking” the empty orbital on the metal center as an important orbital interaction in this process.

The  $\text{M--C}_\alpha$  and  $\text{C}_\beta\text{--H}$  bonds must have the ability to align in a syn coplanar arrangement. By “syn coplanar” we mean that all four atoms are in a plane and that the  $\text{M--C}_\alpha$  and  $\text{C}_\beta\text{--H}$  bonds are on the same side of the  $\text{C}_\alpha\text{--C}_\beta$  bond (a dihedral angle of  $0^\circ$ ). You can see that conformation in the figure above. In the syn coplanar arrangement, the  $\text{C--H}$  bond departing from the ligand is optimally lined up with the empty orbital on the metal center. Hindered or cyclic complexes that cannot achieve this conformation do not undergo  $\beta$ -hydride elimination. The need for a syn coplanar conformation has important implications for eliminations that may establish diastereomeric olefins:  $\beta$ -elimination is stereospecific. One diastereomer leads to the (E)-olefin, and the other leads to the (Z)-olefin.



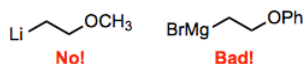
$\beta$ -elimination is stereospecific. One diastereomer of reactant leads to the (Z)-olefin and the other to the (E)-olefin.

The complex must possess 16 or fewer total electrons. Examine the first figure one more time—notice that the total electron count of the complex increases by 2 during  $\beta$ -hydride elimination. Complexes with 18 total electrons don't undergo  $\beta$ -elimination because the product would end up with 20 total electrons. Of course, dissociation of a loose ligand can produce a 16-electron complex pretty easily, so watch out for ligand dissociation when considering the possibility of  $\beta$ -elimination in a complex. Ligand dissociation may be reversible, but  $\beta$ -Hydride elimination is almost always irreversible.

The metal must bear at least 2 d electrons. Now this seems a bit strange, as the metal has served as nothing but an empty bin for electrons in our discussion so far. Why would the metal center need electrons for  $\beta$ -hydride elimination to occur? The answer lies in an old friend: backbonding. The  $\sigma_{\text{C-H}} \rightarrow \text{M}$  orbital interaction mentioned above is not enough to promote elimination on its own; an  $\text{M} \rightarrow \sigma^*_{\text{C-H}}$  interaction is also required! I've said it before, and I'll say it again: backbonding is everywhere in organometallic chemistry. If you can understand and articulate it, you'll blow your instructor's mind.

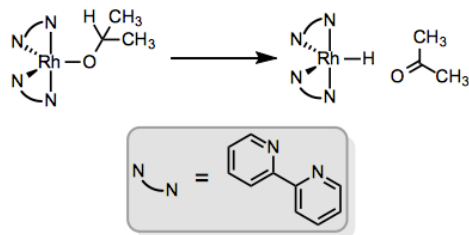
### Other $\beta$ -Elimination Reactions

The leaving group does not need to be hydrogen, of course, and a number of more electronegative groups come to mind as better candidates for leaving groups.  $\beta$ -Alkoxy and  $\beta$ -amino eliminations are usually thermodynamically favored thanks to the formation of strong M–O and M–N bonds, respectively. These reactions are so favored in  $\beta$ -alkoxyalkyl “complexes” of alkali and alkaline earth metals (R–Li, R–MgBr, etc.) that using these as  $\sigma$ -nucleophiles at carbon is untenable. Such compounds eliminate immediately upon their formation. I had an organic synthesis professor in undergrad who was obsessed with this—using a  $\beta$ -alkoxyalkyl lithium or  $\beta$ -alkoxyalkyl Grignard reagent in a synthesis was a recipe for red ink.  $\beta$ -Haloalkyls were naturally off limits too.



Watch out...these are not stable compounds!

The atom bound to the metal doesn't have to be carbon.  $\beta$ -Elimination of alkoxy ligands affords ketones or aldehydes bound to oxygen or through the C=O  $\pi$  bond (this step is important in many [transfer hydrogenations](#), and an analogous process occurs in the [Oppenauer](#) oxidation). Amido ligands can undergo  $\beta$ -elimination to afford complexes of imines; however, this process tends to be slower than  $\beta$ -alkoxy elimination.



$\beta$ -Elimination helps transfer the elements of dihydrogen from one organic compound to another.

Incidentally, I haven't seen any examples in which the  $\beta$  atom is not carbon, but would be interested if anyone knows of an example!

## Applications of $\beta$ -Eliminations

As with many concepts in organometallic chemistry, there are two ways to think about applications of  $\beta$ -elimination. One can take either the “inorganic” perspective, which focuses on the metal center, or the “organic” perspective, which focuses on the ligands.

With the metal center in focus, we can recognize that  $\beta$ -hydride elimination has the wonderful side effect of establishing an M–H bond—a feat generally difficult to achieve in a selective manner via oxidative addition of X–H. If the ligand from which the hydrogen came displaced something more electronegative, the whole process represents reduction at the metal center. For example, imagine rhodium(III) chloride is mixed with sodium isopropoxide,  $\text{NaOCH}(\text{CH}_3)_2$ . The isopropoxide easily displaces chloride, and subsequent  $\beta$ -hydride elimination affords a rhodium hydride, formally reduced with respect to the chloride starting material. See p. 236 of [this review](#) for more.

With the ligand in focus, we see that the organic ligand is oxidized in the course of  $\beta$ -hydride elimination. Notice that the metal is reduced and the ligand oxidized! A  $\pi$  bond replaces a  $\sigma$  bond in the ligand, and if the conditions are right, this represents a bona fide oxidation (as opposed to a mere elimination). For example, oxidative addition into a C–H bond followed by  $\beta$ -hydride elimination at a C–H bond next door sets up an alkene where two adjacent C–H bonds existed before, an oxidation process. These [dehydrogenation reactions](#) are incredibly appealing in a theoretical sense, but still at an early stage when it comes to scope and practicality.

## Summary

We already encountered  $\beta$ -hydride elimination in an earlier series of posts on [metal alkyl complexes](#), where we noted that it's a very common decomposition pathway for metal alkyls.  $\beta$ -Hydride elimination isn't all bad, however, as it can be an important step in catalytic reactions that result in the oxidation of organic substrates (dehydrogenations and transfer hydrogenations) and in reactions that reduce metal halides to metal hydrides. The general idea of  $\beta$ -elimination involves the transfer of a leaving group from a ligand to the metal center with simultaneous formation of a  $\pi$  bond in the ligand.  $\beta$ -Elimination requires an open coordination site and at least two d electrons on the metal center, and eliminations of chiral complexes are stereospecific. The leaving group is commonly hydrogen, but need not be—the more electronegative the leaving group, the more favorable the elimination. Stronger  $\pi$  bonds in the product also encourage  $\beta$ -elimination, so eliminations that form carbonyl compounds or imines are common.

In the next post, we'll explore other types of organometallic elimination reactions, which establish  $\pi$  bonds at different positions in metal alkyl or other complexes.  $\alpha$ -Eliminations, for example, establish metal-carbon, -oxygen, or -nitrogen multiple bonds, which are generally difficult to forge through other means

[Dr. Michael Evans](#) ([Georgia Tech](#))

---

10.2.5:  $\beta$ -Elimination Reactions is shared under a [CC BY-NC-SA 4.0](#) license and was authored, remixed, and/or curated by LibreTexts.

## 10.2.6: Organometallic Catalysts

### Overview

The different types of organometallic reactions discussed in the previous sections can be combined together into catalytic cycles to produce valuable chemicals or perform otherwise difficult chemical reactions. While the organometallic catalyst will undergo a number of transformations over the course of the cycle, it will return to its original active state at the end of the reaction. By definition catalysts are reactive, because of this the metal complex added to a reaction is at times a more stable precatalyst which must undergo a reaction such as ligand dissociation to form the active catalyst.

### Hydrogenation Catalysis

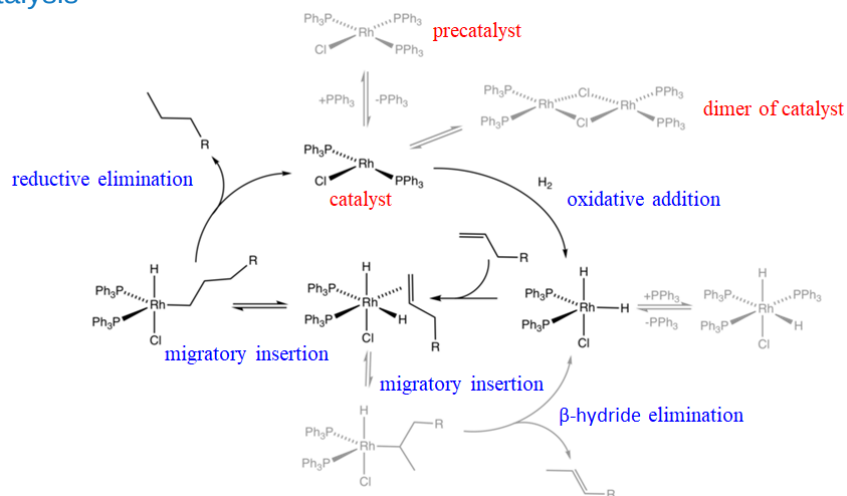


Figure 10.2.6.1: Mechanism of the Wilkinson hydrogenation catalyst (CC BY-SA; Smokefoot via Wikimedia Commons)

Migratory insertions play an important role in catalysis. For example a Rh-catalyst called Wilkinson's catalyst is an effective hydrogenation catalyst for olefins. The mechanism of the hydrogenation involves a combination of oxidative additions, olefin migratory (1,2) insertions, and reductive eliminations as shown in Figure 10.2.6.1. Wilkinson's catalyst is the square planar chlorotris(triphenylphosphine)rhodium(I) complex. This molecule is actually a precatalyst that becomes the active catalyst when it loses a triphenylphosphine ligand producing chlorobis(triphenylphosphine)rhodium(I). The loss of this ligand is a reversible reaction, and thus the catalyst is in chemical equilibrium with the precatalyst. The active catalyst is also in chemical equilibrium with its dimer. The chlorobis(triphenylphosphine)rhodium(I) catalyst can undergo an oxidative addition in the presence of hydrogen to form a trigonal bipyramidal chlorodihydridobis(triphenylphosphine)rhodium(III) complex. This species is in chemical equilibrium with an octahedral chlorodihydridotris(triphenylphosphine)rhodium(III) species that can form due to the presence of free triphenylphosphine ligands in the system. The trigonal bipyramidal species can then add an olefin ligand that binds side-on to the Rh. Because the olefin is in cis-position to the hydride ligand it can undergo a 1,2 insertion. The Rh-C bond can either form with the first or the second carbon in the carbon chain of the olefin, giving a linear and a branched alkyl complex, respectively. The branched complex can undergo a  $\beta$ -hydride elimination thereby reforming the trigonal bipyramidal Rh-complex, and an olefin. This reaction is a side-reaction because the branched alkyl complex is sterically more crowded than the linear complex. The linear alkyl Rh complex can undergo a reductive elimination to form the linear alkane and the  $\text{RhCl}(\text{PPh}_3)_2$  catalyst. This completes the catalytic cycle, and a new cycle can start.

### Ziegler-Natta Polymerization

Another example of an organometallic catalytic reaction is the Ziegler-Natta olefin polymerization. This reaction is of high industrial importance for the production of polymers like polyethylene. There are both heterogeneous and homogeneous Ziegler-Natta catalysts. The mechanism for the homogeneous catalysts is generally well understood. Homogeneous catalysts are typically metallocene catalysts.

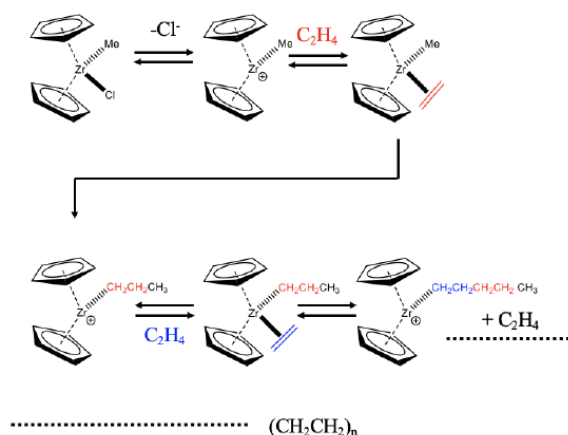
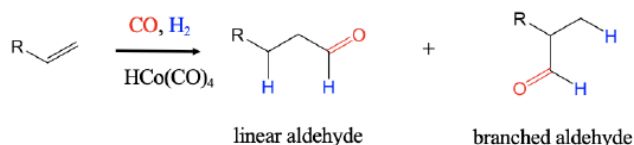


Figure 10.2.6.2: Mechanism for Zirconium-based Ziegler-Natta catalysis (Attribution: A. Vedernikov, U Maryland (modified).)

An example of a zirconium-based catalyst is shown in Figure 10.2.6.2. The catalyst is a coordinatively unsaturated complex cation with two cyclopentadienyl rings and a methyl group. The catalyst is formed from its precatalyst, a neutral molecule with an additional chloride ligand. The catalyst oxidatively adds an olefin like an ethylene molecule to the coordinatively unsaturated site. This step is followed by a 1,2b insertion step that produces a propyl group. The migratory insertion leads to the formation of a vacant site, that can be reoccupied by another ethylene molecule. This molecule can insert into the propyl chain thereby prolonging the propyl chain to a pentyl chain. The olefin insertion step generates another vacant site that can be reoccupied by a new ethylene molecule. Repeating the catalytic cycle many times eventually leads to polyethylene.

### Catalytic Olefin Hydroformylation



100°C, up to 100 atm of CO and H<sub>2</sub>

Figure 10.2.6.3: Scheme for catalytic olefin hydroformylation

A further important industrial reaction is the catalytic hydroformylation reaction, also known as oxo-process. It was discovered in 1938 by Otto Roelen at BASF. In the hydroformylation reaction an H atom and a formyl group are added to an alkene to form aldehydes. The reaction can produce both branched and linear aldehydes from terminal alkenes, CO, and H<sub>2</sub> using a carbonyl hydrides such as HCo(CO)<sub>4</sub> as a catalyst. The reaction is performed at about 100°C at a pressure of up to 100 atm.

### Mechanism

How does the hydroformylation work mechanistically?



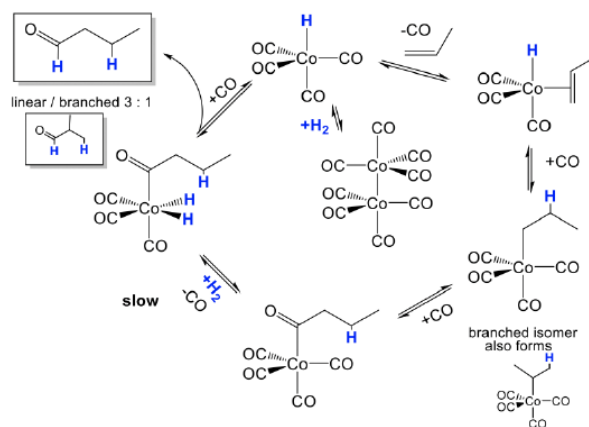


Figure 10.2.6.4: Mechanism of the catalytic olefin hydroformylation by  $\text{HCo(CO)}_4$  (Attribution: A. Vedernikov, U Maryland (modified).)

The mechanism is illustrated for the hydroformylation of propene in Figure 10.2.6.4. The actual catalyst  $\text{HCo(CO)}_4$  is first formed from its precatalyst  $\text{Co}_2(\text{CO})_8$  in the presence of  $\text{H}_2$  in a dinuclear oxidative addition reaction. The catalyst can undergo a substitution reaction in which a CO ligand is replaced by the olefin that binds side-on to the cobalt. This species can then undergo a migratory 1,2 olefin insertion reaction. This leads to a mixture of linear and branched alkyl groups attached to the Co. A new CO ligand can add to the vacant site. The alkyl group can then insert into a carbonyl group in another migratory insertion step, and the vacant site can be reoccupied by a new CO molecule. Then,  $\text{H}_2$  is added in an oxidative addition. This is the slowest and rate-limiting step in the catalytic cycle. From the addition product the aldehyde can then be eliminated in a reductive elimination reaction. Addition of CO regenerates the catalyst, and the catalytic cycle can begin again.

## Hydrocarbonylations

After the hydroformylation, a number of other hydrocarbonylations were developed, and industrially deployed.

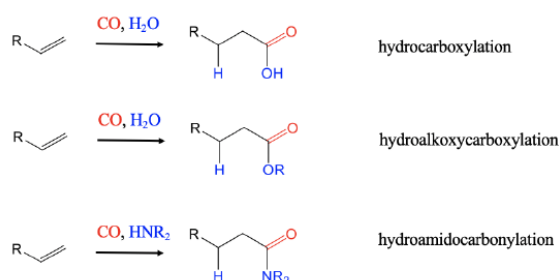


Figure 10.2.6.5: Hydrocarbonylation reactions

When hydrogen is replaced by  $\text{H}_2\text{O}$  hydrocarboxylations of alkenes lead to carboxylic acids (Figure 10.2.6.5). With an alcohol instead of  $\text{H}_2$ , hydroalkoxycarboxylations lead to esters. The employment of amines instead of  $\text{H}_2$  leads to amides in hydroamidocarboxylation reactions.

## Monsanto Acetic Acid Process

Another carbonylation reaction involving an organometallic catalyst is the Monsanto acetic acid process. It has been introduced by Monsanto in the 1970s for the industrial production of acetic acid from methanol. The reaction involves dual catalysis with HI and  $[\text{RhI}_2(\text{CO})_2]^-$  as co-catalysts. How does this reaction work?

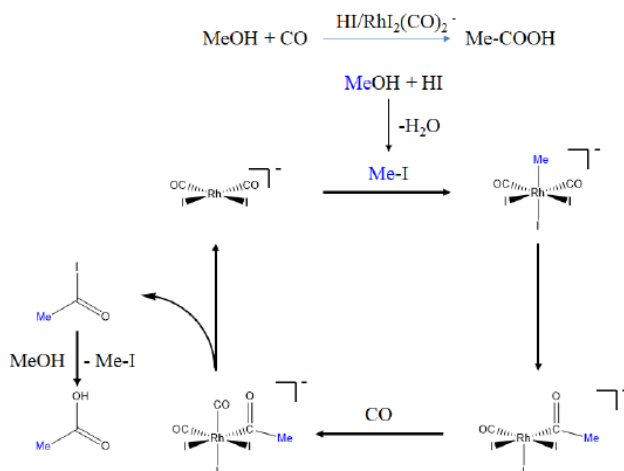


Figure 10.2.6.6: The catalytic cycle in the Monsanto acetic acid process

In the first step methanol reacts with HI to form methyl iodide. The methyl iodide then reacts with the Rh-catalyst in an oxidative addition reaction in which a methyl and an iodo group are added in trans-fashion to the square-planar Rh-complex to give an octahedral complex. The octahedral complex then undergoes a migratory insertion reaction with CO producing an acyl group and a vacant site. A CO molecule can then add to the vacant site. The acetyl iodide can then be eliminated in a reductive elimination to reform the Rh-catalyst thereby closing the catalytic cycle. The acetyl iodide can then react with methanol to form new methyl iodide and acetic acid. The methyl iodide can start a new catalytic cycle with the Rh-catalyst.

## Olefin Metathesis

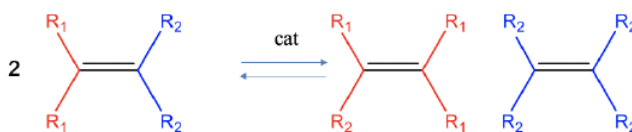


Figure 10.2.6.7: Scheme for olefin metathesis

Olefin metathesis is a reaction which allows to cut and rearrange C=C double bonds in olefins to make new olefins Figure 10.2.6.7. Formally, the carbon-carbon bond of the reactant is cleaved homoleptically and the two carbene fragments are combined in a different way. This reaction is typically an equilibrium reaction, and neither the reactants nor the products are clearly favored. This reaction is catalyzed by molybdenum arylamido carbene complexes or ruthenium carbene complexes.

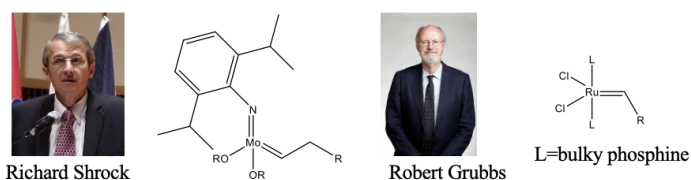


Figure 10.2.6.8: Shrock catalyst (left) (CC BY-SA; Materials scientist via Wikimedia Commons) and Grubbs catalyst (right) (CC BY-SA; The Royal Society via Wikimedia Commons)

The former are called Shrock catalysts, and the latter Grubbs catalysts named after their discoverers Richard Shrock and Robert Grubbs who received the Nobel prize for Chemistry in 2005 (Figure 10.2.6.8). The Shrock catalysts are more active, but also very sensitive to air and water. The Grubbs catalysts, while less active, are less sensitive to air and water.

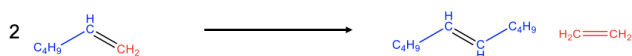


Figure 10.2.6.9: Scheme for regular metathesis

Olefin metathesis often allows for simpler preparation of olefins compared to other methods. Olefin metathesis is particularly powerful when one olefin product is gaseous because then it can be quite easily removed from the chemical equilibrium by purging. This drives the chemical equilibrium to the right side. An example is the preparation of 5-decene from 1-hexene. Cleavage of the C=C double bond in the hexene leads to C<sub>5</sub> and C<sub>1</sub> carbene fragments (Figure 10.2.6.9). The two C<sub>1</sub> fragments can combine

to form ethylene and the two C<sub>5</sub> fragments combine to 5-decene. The ethylene is volatile and can be purged from the reaction system thereby driving the chemical reaction to the right side.

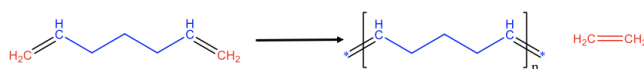


Figure 10.2.6.10: Acyclic diene metathesis (ADMET)

The same principles can also be applied to produce polymers from dienes with two terminal C=C double bonds at the chain ends. This is called acyclic diene metathesis (ADMET), Figure 10.2.6.10 For instance the cleavage of the two terminal double bonds in a diene with seven C atoms leads to C<sub>1</sub> and C<sub>5</sub> fragments. The C<sub>1</sub> fragments can combine to form ethylene, and the C<sub>5</sub> fragments can combine to make an unsaturated polymer of the type [CH(CH<sub>2</sub>)<sub>3</sub>CH]<sub>n</sub>. Again, the reaction can be driven to the right side by removing the gaseous ethylene from the reaction mixture through purging.

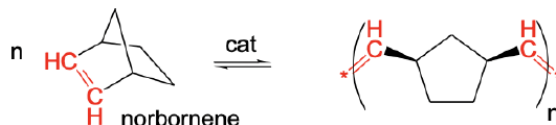


Figure 10.2.6.11: Ring-opening metathesis polymerization (ROMP)

Another variation of olefin metathesis is ring-opening metathesis polymerization (ROMP). It allows to make polymers from strained cycloolefins, for example norbornene. The reaction driving force is the relief of the strain. Because the strain is removed in the polymer, the chemical equilibrium lies far on the right side. The reaction product in norbornene is a polymer with 5-membered rings that are interconnected by ethylene -CH=CH- units (Figure 10.2.6.11).

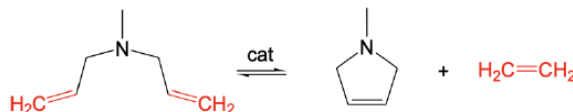


Figure 10.2.6.12: Ring-closing metathesis (RCM)

The opposite of ROMP is ring-closure metathesis (RCM). RCM allows for the preparation of unstrained rings with C=C double bonds from dienes with C=C double bonds that are five or six carbon atoms apart. This distance is suitable to produce unstrained rings. In the shown example a five-membered ring with a C=C double bond is formed from a diene with terminal C=C double bonds that are five atoms apart.

## Mechanism

What is the mechanism of olefin metathesis?

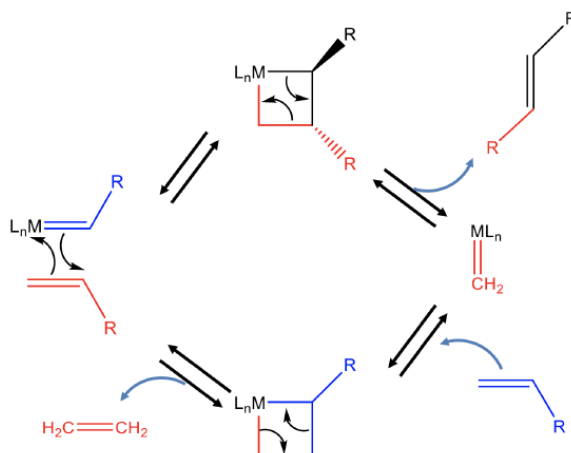


Figure 10.2.6.13: The mechanism of olefin metathesis

In the first step, the alkene adds to the the carbene fragment of the catalyst in a 2+2 cycloaddition reaction to produce an unstable intermediate with a highly strained four-membered ring (Figure 10.2.6.13). This four membered ring can open to produce the first

new alkene product  $R-CH=CH-R$  and a metal carbene species. This metal carbene can react with another reactant olefin to form another highly strained 4-ring intermediate via a 2+2 cycloaddition reaction. This ring can then reopen again to produce the second alkene metathesis product, in this case ethylene, and the original catalyst. The regenerated catalyst can then start a new catalytic cycle.

## Carbon-Carbon Cross Coupling Reactions

The palladium catalyzed cross-coupling reactions are a class of highly successful reactions with applications in the organic synthesis to have emerged recently. The reactions carry out a coupling of the aryl, vinyl or alkyl halide substrates with different organometallic nucleophiles and as such encompasses a family of C-C cross-coupling reactions that are dependent on the nature of nucleophiles like that of the B based ones in the Suzuki-Miyaura coupling, the Sn based ones in the Stille coupling, the Si based ones in the Hiyama coupling, the Zn based ones in the Negishi coupling and the Mg based ones in the Kumada coupling reactions (Figure 10.2.6.14).

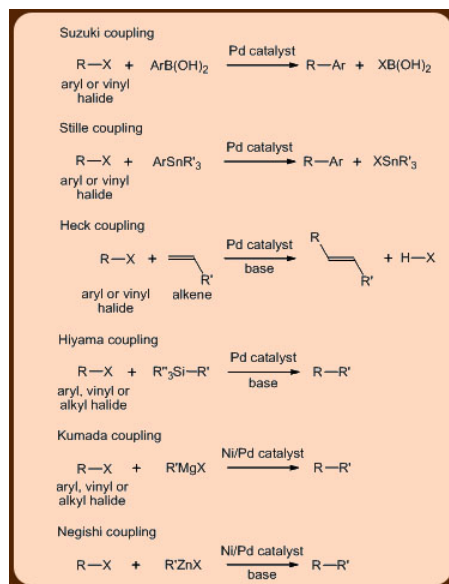


Figure 10.2.6.14: Various types of the palladium mediated C-C cross-coupling reactions.

An unique feature of these reactions is the exclusive formation of the cross-coupled product without the accompaniment of any homo-coupled product. Another interesting feature of these coupling reactions is that they proceed *via* a common mechanism involving three steps that include the oxidative addition, the transmetalation and the reductive elimination reactions (Figure 10.2.6.15 and 10.2.6.16).

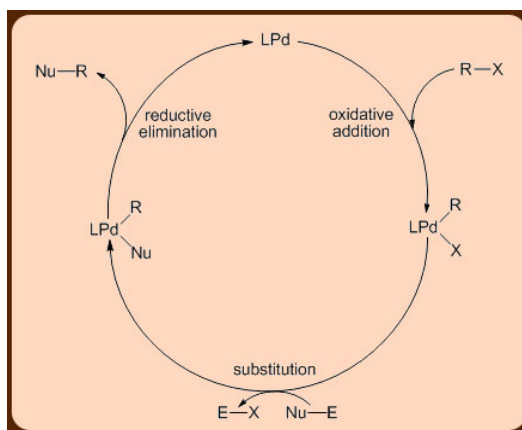


Figure 10.2.6.15: A general catalytic cycle for the palladium mediated C-C cross-coupling reactions.

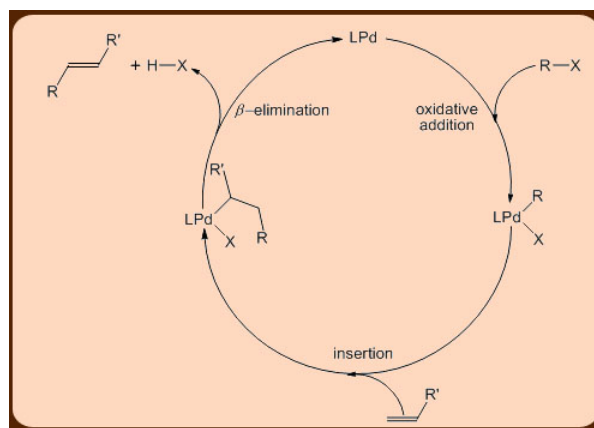


Figure 10.2.6.16: A catalytic cycle for the palladium mediated Heck coupling reaction.

## Summary

Organometallic complexes play a pivotal role in several successful homogeneous catalysis reactions like that of the hydroformylation and the C–C cross-coupling reactions. These reactions are important because of the fact that both of the hydroformylation and the C–C cross-coupling reactions give more value added products compared to the starting reactants. The palladium catalyzed C–C cross-coupling reactions are a class of highly successful reactions that have permanently impacted the area of organic synthesis in a profound way to an extent that the 2010 Nobel prize has been conferred on one of these reactions thereby recognizing the importance of the C–C cross-coupling reactions.

## Contributors and Attributions

- <http://nptel.ac.in/courses/104101006/31>
- Dr. Kai Landskron ([Lehigh University](#)). If you like this textbook, please consider to make a donation to support the author's research at Lehigh University: [Click Here to Donate](#).

10.2.6: Organometallic Catalysts is shared under a [CC BY-NC-SA 4.0](#) license and was authored, remixed, and/or curated by LibreTexts.

- **12.2: Organometallic Catalysts** by Kai Landskron is licensed [CC BY 4.0](#).
- **11.7: Organometallic Catalysts** is licensed [CC BY-NC-SA 4.0](#).
- **25.5F: C–C cross-coupling reactions** is licensed [CC BY-NC-SA 4.0](#).

# Index

## A

### A values

[9.1.3: Ligand Substitution Mechanisms](#)

### ammonia ligands

[9.1.5: Thermodynamic Stability and Chelate Effect](#)

### amorphous solid

[6.2.1: Types of Crystalline Solids](#)

### analogous complexes

[9.1.5: Thermodynamic Stability and Chelate Effect](#)

### arenes

[10.1.3: Survey of Common Organometallic Ligands](#)

### Associative Substitution

[9.1.3: Ligand Substitution Mechanisms](#)

### atomic radius

[1.4.5: Lanthanide Contraction](#)

### atomization enthalpy

[6.4.1: Lattice Enthalpies of Ionic Solids](#)

[6.4.2: Born Haber Cycles](#)

### aufbau principle

[1.3.3: Aufbau Principle](#)

### autoionization

[7.1.2: Brønsted-Lowry Model](#)

[7.1.3: Metal Ions as Acids](#)

[7.1.4: Autoionization and Solvent Leveling](#)

## B

### band gap

[6.5.1: Bonding in Metals and Semiconductors](#)

### band theory

[6.5.1: Bonding in Metals and Semiconductors](#)

### bent

[2.2.6: Valence Shell Electron-Pair Repulsion](#)

### Beryllium

[2.2.5: Limitation of Lewis Theory](#)

### block diagonal

[4.2.2: Representations of Point Groups](#)

### body centered cubic

[6.1.1: Cubic Lattices and Close Packing](#)

### bond angle

[2.2.6: Valence Shell Electron-Pair Repulsion](#)

### Boron

[2.2.5: Limitation of Lewis Theory](#)

## C

### carbene

[10.1.3: Survey of Common Organometallic Ligands](#)

### Carbon monoxide

[10.1.3: Survey of Common Organometallic Ligands](#)

### character (matrix)

[4.2.2: Representations of Point Groups](#)

### character table

[4.2.3: Character Tables](#)

### Chelate complexes

[9.1.5: Thermodynamic Stability and Chelate Effect](#)

### chelate effect

[9.1.5: Thermodynamic Stability and Chelate Effect](#)

### chelate ring

[8.1.5: Isomerism](#)

### Chelation

[9.1.5: Thermodynamic Stability and Chelate Effect](#)

### chirality

[3.2.3: Chirality](#)

### closed packing

[6.1.1: Cubic Lattices and Close Packing](#)

### conductors

[6.5.1: Bonding in Metals and Semiconductors](#)

### coordinate covalent bond

[8.1.1: What are Coordination Complexes?](#)

### coordination complex

[8.5.2: Colors of Coordination Complexes](#)

### Coordination Complexes

[8.5.2: Colors of Coordination Complexes](#)

### coordination compounds

[8.1.1: What are Coordination Complexes?](#)

### covalent network solid

[6.2.1: Types of Crystalline Solids](#)

### crystal field splitting

[8.2.2: Crystal Field Stabilization Energy](#)

[8.4.3: Factors That Affect Ligand Field Splitting](#)

### crystal field stabilization energy

[8.2.2: Crystal Field Stabilization Energy](#)

[8.4.4: Octahedral vs. Tetrahedral Geometries](#)

### crystal field theory

[8.2.1: Crystal Field Theory](#)

[8.2.2: Crystal Field Stabilization Energy](#)

[8.5.2: Colors of Coordination Complexes](#)

### crystalline solid

[6.2.1: Types of Crystalline Solids](#)

### Cubic Lattices

[6.1.1: Cubic Lattices and Close Packing](#)

### cyclopentadienyl ligands

[10.1.3: Survey of Common Organometallic Ligands](#)

## D

### D Block Contraction

[1.4.5: Lanthanide Contraction](#)

### Diode

[6.5.6: Diodes, LEDs and Solar Cells](#)

### dipole moment

[2.2.6: Valence Shell Electron-Pair Repulsion](#)

[2.2.10: Molecular Polarity](#)

## E

### effective nuclear charge

[1.3.2: Shielding](#)

[1.4.1: Effective Nuclear Charge](#)

### electromagnetic spectrum

[8.5.2: Colors of Coordination Complexes](#)

### electron affinity

[1.4.3: Electron Affinity](#)

### electron shielding

[1.3.4: Slater's Rules](#)

### electronegativity

[2.2.9: Electronegativity and Atomic Size Effects](#)

### enantiomers

[3.2.3: Chirality](#)

### ethylenediamine ligands

[9.1.5: Thermodynamic Stability and Chelate Effect](#)

### expanded valence

[2.2.4: Expanded Octets](#)

## F

### Fajans' Rules

[2.1.3: Polarizability and Percent Ionic Character](#)

### formal charge

[2.2.2: Formal Charge](#)

### frontier MOs

[7.1.5: Lewis Model and Frontier Orbitals](#)

### Frontier Orbitals

[7.1.5: Lewis Model and Frontier Orbitals](#)

## G

### group theory

[3.2.1: Molecular Point Groups](#)

## H

### hard acids

[7.2.1: Hard and Soft Acids and Bases](#)

[7.2.2: Applications of Hard Soft Acid Base Theory](#)

[7.2.3: Theoretical Interpretation of HSAB Theory](#)

### hard base

[7.2.1: Hard and Soft Acids and Bases](#)

[7.2.2: Applications of Hard Soft Acid Base Theory](#)

[7.2.3: Theoretical Interpretation of HSAB Theory](#)

### Hexagonal Closest Packed

[6.1.1: Cubic Lattices and Close Packing](#)

### high spin

[8.2.2: Crystal Field Stabilization Energy](#)

[8.4.3: Factors That Affect Ligand Field Splitting](#)

### hydration

[8.2.2: Crystal Field Stabilization Energy](#)

### hydride

[10.1.3: Survey of Common Organometallic Ligands](#)

### Hydrohalic Acids

[7.1.2: Brønsted-Lowry Model](#)

[7.1.3: Metal Ions as Acids](#)

[7.1.4: Autoionization and Solvent Leveling](#)

### hypervalency

[2.2.1: Lewis Electron-Dot Diagrams](#)

[2.2.4: Expanded Octets](#)

### hypovalency

[2.2.1: Lewis Electron-Dot Diagrams](#)

[2.2.5: Limitation of Lewis Theory](#)

## I

### identity operation

[3.1.1: Definitions and Examples](#)

### improper rotation

[3.1.1: Definitions and Examples](#)

### inductive effect

[7.1.5: Lewis Model and Frontier Orbitals](#)

### insulator

[6.5.1: Bonding in Metals and Semiconductors](#)

### Interchange

[9.1.3: Ligand Substitution Mechanisms](#)

### interstitial sites

[6.1.1: Cubic Lattices and Close Packing](#)

[6.2.1: Types of Crystalline Solids](#)

### ionic solid

[6.2.1: Types of Crystalline Solids](#)

### ionization energy

[1.4.2: Ionization energy](#)

[1.4.5: Lanthanide Contraction](#)

### ionization potential

[1.4.2: Ionization energy](#)

### isomerism

[8.1.5: Isomerism](#)

## K

### Kapustinskii equation

[6.4.5: Kapustinskii Equation](#)

### Kepert Model

[8.1.4: Coordination Numbers and Structures](#)

## L

### Lanthanide Contraction

[1.4.5: Lanthanide Contraction](#)

### lattice enthalpy

[6.4.1: Lattice Enthalpies of Ionic Solids](#)

[6.4.2: Born Haber Cycles](#)

### Lenz's Law

[8.3.2: Magnetism](#)

### Lewis Acid

[7.1.5: Lewis Model and Frontier Orbitals](#)

### Ligand Field Theory

[8.4.1: Ligand Field Theory](#)

### ligand substitution

[9.1.3: Ligand Substitution Mechanisms](#)

[10.2.1: Ligand Dissociation and Substitution](#)

### Linear

[2.2.6: Valence Shell Electron-Pair Repulsion](#)

### Linear Combination of Atomic Orbitals (LCAO)

[5.2.1: Formation of Molecular Orbitals from Atomic Orbitals](#)

### low spin

[8.2.2: Crystal Field Stabilization Energy](#)

[8.4.3: Factors That Affect Ligand Field Splitting](#)

## M

### magnetic moments

[8.3.3: Magnetic Moments of Transition Metals](#)

### magnetic permeability

[8.3.2: Magnetism](#)

### magnetism

[8.3.2: Magnetism](#)

### Marcus Theory

[9.2.3: Outer Sphere Electron Transfer](#)

### metal alkyl complexes

[10.1.3: Survey of Common Organometallic Ligands](#)

### Metal Complexes

[9.1.5: Thermodynamic Stability and Chelate Effect](#)

### metallic solid

[6.2.1: Types of Crystalline Solids](#)

### millier indicies

[6.3.1: Miller Indices \(hkl\)](#)

### molecular solid

[6.2.1: Types of Crystalline Solids](#)

### monodentate

[9.1.5: Thermodynamic Stability and Chelate Effect](#)

### monodentate ligands

[9.1.5: Thermodynamic Stability and Chelate Effect](#)

## O

### Octahedral

[2.2.6: Valence Shell Electron-Pair Repulsion](#)

### octahedral hole

[6.1.1: Cubic Lattices and Close Packing](#)

### Octahedral Preference

[8.2.2: Crystal Field Stabilization Energy](#)

### Octahedral Site Preference Energy

[8.2.2: Crystal Field Stabilization Energy](#)

### orbital mixing

[5.3.1.2: Orbital Mixing](#)

### Organometallic Ligands

[10.1.3: Survey of Common Organometallic Ligands](#)

### Outer Sphere Electron Transfer

[9.2.3: Outer Sphere Electron Transfer](#)

### overall symmetry

[3.1.1: Definitions and Examples](#)

### Oxidative addition

[10.2.2: Oxidative Addition](#)

### oxyacids

[7.1.2: Brønsted-Lowry Model](#)

[7.1.3: Metal Ions as Acids](#)

[7.1.4: Autoionization and Solvent Leveling](#)

## P

### penetration

[1.3.2: Shielding](#)

[1.4.1: Effective Nuclear Charge](#)

### phosphines

[10.1.3: Survey of Common Organometallic Ligands](#)

### Photoelectron Spectroscopy

[5.3.1.4: Photoelectron Spectroscopy](#)

### pi acceptor

[8.4.1: Ligand Field Theory](#)

### pi donor

[8.4.1: Ligand Field Theory](#)

### point groups

[3.2.1: Molecular Point Groups](#)

[3.2.2: Assigning Point Groups](#)

### polarizability

[7.2.1: Hard and Soft Acids and Bases](#)

[7.2.2: Applications of Hard Soft Acid Base Theory](#)

[7.2.3: Theoretical Interpretation of HSAB Theory](#)

### proper rotation

[3.1.1: Definitions and Examples](#)

## R

### resonance

[2.2.3: Resonance](#)

### Resonance Structures

[2.2.3: Resonance](#)

### rotation axis

[4.2.2: Representations of Point Groups](#)

## S

### Sabatier Principle

[3.1.1: Definitions and Examples](#)

### SALC

[5.4.2.2: Carbon Dioxide](#)

### Scandide Contraction

[1.4.5: Lanthanide Contraction](#)

### Schoenflies symbol

[3.1.1: Definitions and Examples](#)

### seesaw

[2.2.6: Valence Shell Electron-Pair Repulsion](#)

### semiconductor

[6.5.1: Bonding in Metals and Semiconductors](#)

### shielding

[1.3.2: Shielding](#)

[1.3.4: Slater's Rules](#)

[1.4.1: Effective Nuclear Charge](#)

### shielding effect

[1.4.5: Lanthanide Contraction](#)

### sigma donor

[8.4.1: Ligand Field Theory](#)

### simple cubic structure

[6.1.1: Cubic Lattices and Close Packing](#)

### Slater's Rules

[1.3.4: Slater's Rules](#)

### soft acid

[7.2.1: Hard and Soft Acids and Bases](#)

[7.2.2: Applications of Hard Soft Acid Base Theory](#)

[7.2.3: Theoretical Interpretation of HSAB Theory](#)

### soft bases

[7.2.1: Hard and Soft Acids and Bases](#)

[7.2.2: Applications of Hard Soft Acid Base Theory](#)

[7.2.3: Theoretical Interpretation of HSAB Theory](#)

### spectrochemical series

[8.4.2: The Spectrochemical Series](#)

[8.4.3: Factors That Affect Ligand Field Splitting](#)

[8.5.2: Colors of Coordination Complexes](#)

### spin pairing energy

[8.2.2: Crystal Field Stabilization Energy](#)

### square pyramidal

[2.2.6: Valence Shell Electron-Pair Repulsion](#)

### steric effect

[7.1.5: Lewis Model and Frontier Orbitals](#)

### strong field

[8.4.1: Ligand Field Theory](#)

### substitutional alloy

[6.2.2: Alloys and Intermetallics](#)

### substitutions

[9.1.3: Ligand Substitution Mechanisms](#)

[10.2.1: Ligand Dissociation and Substitution](#)

### Superacid

[7.1.2: Brønsted-Lowry Model](#)

[7.1.3: Metal Ions as Acids](#)

[7.1.4: Autoionization and Solvent Leveling](#)

### superconductor

[6.5.7: Superconductors](#)

### Symmetry

[3.2.1: Molecular Point Groups](#)

### Symmetry Adapted Linear Combinations

[5.4.2: Polyatomic Molecules](#)

### symmetry elements

[3.1.1: Definitions and Examples](#)

### symmetry operation

[4.2.2: Representations of Point Groups](#)

### symmetry operations

[3.1.1: Definitions and Examples](#)

## T

### Tetrahedral

[2.2.6: Valence Shell Electron-Pair Repulsion](#)

### tetrahedral hole

[6.1.1: Cubic Lattices and Close Packing](#)

### thermodynamically

[9.1.5: Thermodynamic Stability and Chelate Effect](#)

### thermodynamically stable

[9.1.5: Thermodynamic Stability and Chelate Effect](#)

### trigonal bipyramidal

[2.2.6: Valence Shell Electron-Pair Repulsion](#)

### Trigonal Planar

[2.2.6: Valence Shell Electron-Pair Repulsion](#)

### trigonal prismatic coordination

[8.1.4: Coordination Numbers and Structures](#)

### trigonal pyramidal

[2.2.6: Valence Shell Electron-Pair Repulsion](#)

### trimethylenediamine

[9.1.5: Thermodynamic Stability and Chelate Effect](#)

## V

### vacancy

[6.2.1: Types of Crystalline Solids](#)

### valence shell electron pair repulsion theory

[2.2.6: Valence Shell Electron-Pair Repulsion](#)

### VSEPR

[2.2.6: Valence Shell Electron-Pair Repulsion](#)

## W

### Walsh diagrams

[5.4.3: Why is BeH<sub>2</sub> Linear and H<sub>2</sub>O Bent?](#)

## weak field

[8.4.1: Ligand Field Theory](#)

## Z

### zeroth ionization energy

[1.4.3: Electron Affinity](#)





## Detailed Licensing

### Overview

**Title:** [CHEM322: Inorganic Chemistry](#)

**Webpages:** 197

**Applicable Restrictions:** Noncommercial

#### All licenses found:

- [Undeclared](#): 41.1% (81 pages)
- [CC BY-SA 4.0](#): 26.9% (53 pages)
- [CC BY-NC-SA 4.0](#): 18.8% (37 pages)
- [CC BY 4.0](#): 6.6% (13 pages)
- [CC BY-NC 4.0](#): 3.6% (7 pages)
- [CC BY-NC 3.0](#): 2% (4 pages)
- [CC BY-SA 3.0](#): 0.5% (1 page)
- [CC BY 3.0](#): 0.5% (1 page)

### By Page

- [CHEM322: Inorganic Chemistry - Undeclared](#)
  - [Front Matter - Undeclared](#)
    - [TitlePage - Undeclared](#)
    - [InfoPage - Undeclared](#)
    - [Table of Contents - Undeclared](#)
    - [Licensing - Undeclared](#)
    - [What is Inorganic Chemistry? - Undeclared](#)
    - [Licensing - Undeclared](#)
  - [Unit 1: Atomic Structure - Undeclared](#)
    - [1.1: Historical Development of Atomic Theory - CC BY-SA 4.0](#)
      - [1.1.1: Early Experiments of Atomic Theory - CC BY-SA 4.0](#)
      - [1.1.2: Discovery of Subatomic Particles - CC BY-SA 4.0](#)
      - [1.1.3: Quantization of Energy and Bohr Model of the Atom - CC BY-SA 4.0](#)
      - [1.1.4: Wave-Particle Duality - CC BY-SA 4.0](#)
    - [1.2: Electronic Structure of the Atom - CC BY-SA 4.0](#)
      - [1.2.1: Wave Quantization and Particle in a Box - CC BY-SA 4.0](#)
      - [1.2.2: The Schrodinger Equation - CC BY-SA 4.0](#)
      - [1.2.3: Quantum Numbers and Atomic Wave Functions - CC BY-SA 4.0](#)
    - [1.3: Multi-Electron Atoms - CC BY-SA 4.0](#)
      - [1.3.1: Orbital Energies - CC BY-SA 4.0](#)
      - [1.3.2: Shielding - CC BY-SA 4.0](#)
      - [1.3.3: Aufbau Principle - CC BY-SA 4.0](#)
      - [1.3.4: Slater's Rules - CC BY-SA 4.0](#)
  - [1.4: Periodic Properties of the Elements - CC BY-SA 4.0](#)
    - [1.4.1: Effective Nuclear Charge - CC BY-SA 4.0](#)
    - [1.4.2: Ionization energy - CC BY-SA 3.0](#)
    - [1.4.3: Electron Affinity - CC BY-SA 4.0](#)
    - [1.4.4: Covalent and Ionic Radii - CC BY-SA 4.0](#)
    - [1.4.5: Lanthanide Contraction - CC BY-SA 4.0](#)
    - [1.4.6: The Uniqueness Principle - CC BY-SA 4.0](#)
  - [1.5: Unit 1 Practice Problems - CC BY-SA 4.0](#)
- [Unit 2: Molecular Structure - Undeclared](#)
  - [2.1: Chemical Bonding - Undeclared](#)
    - [2.1.1: Types of Chemical Bonds - Undeclared](#)
    - [2.1.2: Electronegativity and the Bonding Continuum - CC BY 4.0](#)
    - [2.1.3: Polarizability and Percent Ionic Character - CC BY-NC-SA 4.0](#)
  - [2.2: Lewis Structures and Molecular Shape - Undeclared](#)
    - [2.2.1: Lewis Electron-Dot Diagrams - CC BY-NC-SA 4.0](#)
    - [2.2.2: Formal Charge - CC BY-NC-SA 4.0](#)
    - [2.2.3: Resonance - CC BY-NC-SA 4.0](#)
    - [2.2.4: Expanded Octets - CC BY-NC-SA 4.0](#)
    - [2.2.5: Limitation of Lewis Theory - CC BY-NC-SA 4.0](#)
    - [2.2.6: Valence Shell Electron-Pair Repulsion - CC BY-NC-SA 4.0](#)
    - [2.2.7: Lone Pair Repulsion - Undeclared](#)
    - [2.2.8: Multiple Bonds - Undeclared](#)
    - [2.2.9: Electronegativity and Atomic Size Effects - Undeclared](#)

- 2.2.10: Molecular Polarity - *Undeclared*
- Unit 3: Molecular Symmetry - *CC BY 4.0*
  - 3.1: Symmetry Elements and Operations LOs - *Undeclared*
    - 3.1.1: Definitions and Examples - *CC BY 4.0*
  - 3.2: Point Groups - *Undeclared*
    - 3.2.1: Molecular Point Groups - *CC BY-NC-SA 4.0*
    - 3.2.2: Assigning Point Groups - *Undeclared*
    - 3.2.3: Chirality - *CC BY-NC 4.0*
  - 3.3: Unit 3 Practice Problems - *CC BY 4.0*
- Unit 4: Group Theory - *Undeclared*
  - 4.1: Groups - *Undeclared*
    - 4.1.1: Properties of Groups - *Undeclared*
  - 4.2: Representations and Character Tables - *Undeclared*
    - 4.2.1: Matrices - *Undeclared*
    - 4.2.2: Representations of Point Groups - *Undeclared*
    - 4.2.3: Character Tables - *Undeclared*
  - 4.3: Application to Vibrational Spectroscopy - *Undeclared*
    - 4.3.1: Molecular Vibrations - *CC BY-NC 4.0*
  - 4.4: Unit 4 Practice Problems - *CC BY 4.0*
- Unit 5: Molecular Orbitals - *CC BY-SA 4.0*
  - 5.1: Valence Bond Theory - *Undeclared*
    - 5.1.1: The Shapes of Molecules (VSEPR Theory) and Orbital Hybridization - *CC BY-SA 4.0*
  - 5.2: Linear Combination of Atomic Orbitals - *Undeclared*
    - 5.2.1: Formation of Molecular Orbitals from Atomic Orbitals - *CC BY-SA 4.0*
    - 5.2.2: Molecular Orbitals from s Orbitals - *CC BY-NC 3.0*
    - 5.2.3: Molecular Orbitals from p Orbitals - *CC BY-NC 3.0*
    - 5.2.4: Molecular orbitals from d orbitals - *CC BY-SA 4.0*
    - 5.2.5: Nonbonding Orbitals and Other Factors - *CC BY-SA 4.0*
  - 5.3: Diatomic MO Diagrams - *Undeclared*
    - 5.3.1: Homonuclear Diatomic Molecules - *CC BY-SA 4.0*
      - 5.3.1.1: Molecular Orbitals - *CC BY-SA 4.0*
      - 5.3.1.2: Orbital Mixing - *CC BY-SA 4.0*
      - 5.3.1.3: Diatomic Molecules of the First and Second Periods - *CC BY-SA 4.0*
    - 5.3.1.4: Photoelectron Spectroscopy - *CC BY-SA 4.0*
  - 5.3.2: Heteronuclear Diatomic Molecules - *CC BY-SA 4.0*
    - 5.3.2.1: Orbital ionization energies - *CC BY-SA 4.0*
    - 5.3.2.2: Polar bonds - *CC BY-SA 4.0*
    - 5.3.2.3: Ionic Compounds and Molecular Orbitals - *CC BY-SA 4.0*
  - 5.4: Polyatomic MO Diagrams - *Undeclared*
    - 5.4.1: Ligand Group Orbitals and Generator Functions - *Undeclared*
    - 5.4.2: Polyatomic Molecules - *CC BY-SA 4.0*
      - 5.4.2.1: Bifluoride anion - *CC BY-SA 4.0*
      - 5.4.2.2: Carbon Dioxide - *CC BY-SA 4.0*
      - 5.4.2.3: H<sub>2</sub>O - *CC BY-SA 4.0*
      - 5.4.2.4: NH<sub>3</sub> - *CC BY-SA 4.0*
    - 5.4.3: Why is BeH<sub>2</sub> Linear and H<sub>2</sub>O Bent? - *CC BY-NC-SA 4.0*
  - 5.5: Pi Bonding and Hypervalency - *Undeclared*
    - 5.5.1: BF<sub>3</sub> - *CC BY-SA 4.0*
    - 5.5.2: Expanded Octets and Molecular Orbitals - *Undeclared*
- Unit 6: Solid State Chemistry - *Undeclared*
  - 6.1: Solid State Structures - *Undeclared*
    - 6.1.1: Cubic Lattices and Close Packing - *CC BY 3.0*
    - 6.1.2: Ionic Radii and Radius Ratios - *CC BY-SA 4.0*
  - 6.2: Crystalline Solids - *Undeclared*
    - 6.2.1: Types of Crystalline Solids - *CC BY 4.0*
    - 6.2.2: Alloys and Intermetallics - *Undeclared*
    - 6.2.3: The Imperfect Solid State - *CC BY-NC-SA 4.0*
  - 6.3: X-Ray Crystallography of Solids - *Undeclared*
    - 6.3.1: Miller Indices (hkl) - *Undeclared*
    - 6.3.2: X-rays and X-ray Diffraction - *CC BY-NC-SA 4.0*
    - 6.3.3: Powder X-ray Diffraction - *Undeclared*
  - 6.4: Energetics of Ionic Solids - *Undeclared*
    - 6.4.1: Lattice Enthalpies of Ionic Solids - *CC BY-NC 4.0*
    - 6.4.2: Born Haber Cycles - *CC BY-NC 4.0*
    - 6.4.3: Lattice Energies and Solubility - *CC BY-SA 4.0*
    - 6.4.4: Theoretical Lattice Energy Calculations - *CC BY-NC-SA 4.0*
    - 6.4.5: Kapustinskii Equation - *CC BY-SA 4.0*
  - 6.5: Band Theory and Conductivity - *Undeclared*

- 6.5.1: Bonding in Metals and Semiconductors - *CC BY-NC-SA 4.0*
  - 6.5.2: The Fermi Level - *Undeclared*
  - 6.5.3: Semiconductors- Band Gaps, Colors, Conductivity and Doping - *CC BY-SA 4.0*
  - 6.5.4: Periodic Trends- Metals, Semiconductors, and Insulators - *CC BY-SA 4.0*
  - 6.5.5: Semiconductor p-n Junctions - *CC BY-SA 4.0*
  - 6.5.6: Diodes, LEDs and Solar Cells - *CC BY-SA 4.0*
  - 6.5.7: Superconductors - *CC BY-SA 4.0*
- Unit 7: Acid-Base and Donor-Acceptor Chemistry - *Undeclared*
  - 7.1: Acid Base Chemistry - *Undeclared*
    - 7.1.1: Arrhenius Model - *Undeclared*
    - 7.1.2: Brønsted-Lowry Model - *CC BY-NC-SA 4.0*
    - 7.1.3: Metal Ions as Acids - *CC BY-NC-SA 4.0*
    - 7.1.4: Autoionization and Solvent Leveling - *CC BY-NC-SA 4.0*
    - 7.1.5: Lewis Model and Frontier Orbitals - *CC BY-NC-SA 4.0*
  - 7.2: Hard Soft Acid Base Theory - *Undeclared*
    - 7.2.1: Hard and Soft Acids and Bases - *CC BY-NC-SA 4.0*
    - 7.2.2: Applications of Hard Soft Acid Base Theory - *CC BY-NC-SA 4.0*
    - 7.2.3: Theoretical Interpretation of HSAB Theory - *CC BY-NC-SA 4.0*
  - 7.3: Unit 7 Practice Problems - *CC BY 4.0*
- Unit 8: Electronic Structure of Coordination Complexes - *CC BY 4.0*
  - 8.1: Introduction to Coordination Complexes - *Undeclared*
    - 8.1.1: What are Coordination Complexes? - *CC BY 4.0*
    - 8.1.2: History of Coordination Complexes - *CC BY-NC-SA 4.0*
    - 8.1.3: Nomenclature and Ligands - *Undeclared*
    - 8.1.4: Coordination Numbers and Structures - *CC BY 4.0*
    - 8.1.5: Isomerism - *CC BY 4.0*
  - 8.2: Crystal Field Theory - *Undeclared*
    - 8.2.1: Crystal Field Theory - *CC BY-NC-SA 4.0*
    - 8.2.2: Crystal Field Stabilization Energy - *CC BY-NC-SA 4.0*
    - 8.2.3: Non-octahedral Complexes - *CC BY-NC-SA 4.0*
  - 8.3: Crystal Field Theory and Magnetism - *Undeclared*
    - 8.3.1: Jahn-Teller Distortions - *CC BY-SA 4.0*
    - 8.3.2: Magnetism - *Undeclared*
    - 8.3.3: Magnetic Moments of Transition Metals - *CC BY-NC-SA 4.0*
    - 8.3.4: Ferro-, Ferri- and Antiferromagnetism - *CC BY-SA 4.0*
  - 8.4: Ligand Field Theory - *Undeclared*
    - 8.4.1: Ligand Field Theory - *CC BY-NC-SA 4.0*
    - 8.4.2: The Spectrochemical Series - *CC BY-NC 4.0*
    - 8.4.3: Factors That Affect Ligand Field Splitting - *CC BY-NC-SA 4.0*
    - 8.4.4: Octahedral vs. Tetrahedral Geometries - *CC BY-NC-SA 4.0*
  - 8.5: Absorption Spectroscopy of Coordination Complexes - *Undeclared*
    - 8.5.1: Absorption of Light - *Undeclared*
    - 8.5.2: Colors of Coordination Complexes - *CC BY 4.0*
    - 8.5.3: Charge-Transfer Spectra - *Undeclared*
  - 8.6: Tanabe Sugano Diagrams - *Undeclared*
    - 8.6.1: Tanabe-Sugano Diagrams - *CC BY-SA 4.0*
    - 8.6.2: Selection Rules - *Undeclared*
    - 8.6.3: Applications of Tanabe-Sugano Diagrams - *Undeclared*
    - 8.6.4: Tetrahedral Complexes - *Undeclared*
- Unit 9: Reactions of Coordination Complexes - *Undeclared*
  - 9.1: Substitution Reactions - *Undeclared*
    - 9.1.1: Review of Reaction Thermodynamics and Kinetics - *CC BY-NC 3.0*
    - 9.1.2: Introduction to Substitution Reactions - *Undeclared*
    - 9.1.3: Ligand Substitution Mechanisms - *CC BY-NC-SA 4.0*
    - 9.1.4: Some Reasons for Differing Mechanisms - *CC BY-NC 3.0*
      - 9.1.4.1: Dissociation - *Undeclared*
      - 9.1.4.2: Associative Mechanisms - *Undeclared*
    - 9.1.5: Thermodynamic Stability and Chelate Effect - *CC BY-NC-SA 4.0*
    - 9.1.6: Kinetic Lability - *Undeclared*
    - 9.1.7: The Trans Effect - *CC BY-NC-SA 4.0*
  - 9.2: RedOx Reactions - *Undeclared*
    - 9.2.1: Redox Mechanisms - *Undeclared*
    - 9.2.2: Inner Sphere Electron Transfer - *CC BY-NC 4.0*
    - 9.2.3: Outer Sphere Electron Transfer - *CC BY-NC 4.0*
  - 9.3: Unit 9 Practice Problems - *CC BY 4.0*

- Unit 10: Organometallic Chemistry - *Undeclared*
  - 10.1: Organometallic Complexes - *Undeclared*
    - 10.1.1: Introduction to Organometallic Chemistry - *Undeclared*
    - 10.1.2: Ligand Nomenclature and Classification - *Undeclared*
    - 10.1.3: Survey of Common Organometallic Ligands - *CC BY-NC-SA 4.0*
    - 10.1.4: Electron Counting and the 18 Electron Rule - *CC BY-SA 4.0*
  - 10.2: Organometallic Reactions - *Undeclared*
    - 10.2.1: Ligand Dissociation and Substitution - *Undeclared*
    - 10.2.2: Oxidative Addition - *CC BY-NC-SA 4.0*
    - 10.2.3: Reductive Elimination - *CC BY-NC-SA 4.0*
    - 10.2.4: Migratory Insertion- 1,2-Insertions - *CC BY-NC-SA 4.0*
    - 10.2.5:  $\beta$ -Elimination Reactions - *CC BY-NC-SA 4.0*
    - 10.2.6: Organometallic Catalysts - *CC BY-NC-SA 4.0*
- Back Matter - *Undeclared*
  - Index - *Undeclared*
  - Glossary - *Undeclared*
  - Detailed Licensing - *Undeclared*
  - Detailed Licensing - *Undeclared*

## Detailed Licensing

### Overview

**Title:** [CHEM322: Inorganic Chemistry](#)

**Webpages:** 197

**Applicable Restrictions:** Noncommercial

#### All licenses found:

- [Undeclared](#): 41.1% (81 pages)
- [CC BY-SA 4.0](#): 26.9% (53 pages)
- [CC BY-NC-SA 4.0](#): 18.8% (37 pages)
- [CC BY 4.0](#): 6.6% (13 pages)
- [CC BY-NC 4.0](#): 3.6% (7 pages)
- [CC BY-NC 3.0](#): 2% (4 pages)
- [CC BY-SA 3.0](#): 0.5% (1 page)
- [CC BY 3.0](#): 0.5% (1 page)

### By Page

- [CHEM322: Inorganic Chemistry - Undeclared](#)
  - [Front Matter - Undeclared](#)
    - [TitlePage - Undeclared](#)
    - [InfoPage - Undeclared](#)
    - [Table of Contents - Undeclared](#)
    - [Licensing - Undeclared](#)
    - [What is Inorganic Chemistry? - Undeclared](#)
    - [Licensing - Undeclared](#)
  - [Unit 1: Atomic Structure - Undeclared](#)
    - [1.1: Historical Development of Atomic Theory - CC BY-SA 4.0](#)
      - [1.1.1: Early Experiments of Atomic Theory - CC BY-SA 4.0](#)
      - [1.1.2: Discovery of Subatomic Particles - CC BY-SA 4.0](#)
      - [1.1.3: Quantization of Energy and Bohr Model of the Atom - CC BY-SA 4.0](#)
      - [1.1.4: Wave-Particle Duality - CC BY-SA 4.0](#)
    - [1.2: Electronic Structure of the Atom - CC BY-SA 4.0](#)
      - [1.2.1: Wave Quantization and Particle in a Box - CC BY-SA 4.0](#)
      - [1.2.2: The Schrodinger Equation - CC BY-SA 4.0](#)
      - [1.2.3: Quantum Numbers and Atomic Wave Functions - CC BY-SA 4.0](#)
    - [1.3: Multi-Electron Atoms - CC BY-SA 4.0](#)
      - [1.3.1: Orbital Energies - CC BY-SA 4.0](#)
      - [1.3.2: Shielding - CC BY-SA 4.0](#)
      - [1.3.3: Aufbau Principle - CC BY-SA 4.0](#)
      - [1.3.4: Slater's Rules - CC BY-SA 4.0](#)
  - [1.4: Periodic Properties of the Elements - CC BY-SA 4.0](#)
    - [1.4.1: Effective Nuclear Charge - CC BY-SA 4.0](#)
    - [1.4.2: Ionization energy - CC BY-SA 3.0](#)
    - [1.4.3: Electron Affinity - CC BY-SA 4.0](#)
    - [1.4.4: Covalent and Ionic Radii - CC BY-SA 4.0](#)
    - [1.4.5: Lanthanide Contraction - CC BY-SA 4.0](#)
    - [1.4.6: The Uniqueness Principle - CC BY-SA 4.0](#)
  - [1.5: Unit 1 Practice Problems - CC BY-SA 4.0](#)
- [Unit 2: Molecular Structure - Undeclared](#)
  - [2.1: Chemical Bonding - Undeclared](#)
    - [2.1.1: Types of Chemical Bonds - Undeclared](#)
    - [2.1.2: Electronegativity and the Bonding Continuum - CC BY 4.0](#)
    - [2.1.3: Polarizability and Percent Ionic Character - CC BY-NC-SA 4.0](#)
  - [2.2: Lewis Structures and Molecular Shape - Undeclared](#)
    - [2.2.1: Lewis Electron-Dot Diagrams - CC BY-NC-SA 4.0](#)
    - [2.2.2: Formal Charge - CC BY-NC-SA 4.0](#)
    - [2.2.3: Resonance - CC BY-NC-SA 4.0](#)
    - [2.2.4: Expanded Octets - CC BY-NC-SA 4.0](#)
    - [2.2.5: Limitation of Lewis Theory - CC BY-NC-SA 4.0](#)
    - [2.2.6: Valence Shell Electron-Pair Repulsion - CC BY-NC-SA 4.0](#)
    - [2.2.7: Lone Pair Repulsion - Undeclared](#)
    - [2.2.8: Multiple Bonds - Undeclared](#)
    - [2.2.9: Electronegativity and Atomic Size Effects - Undeclared](#)

- 2.2.10: Molecular Polarity - *Undeclared*
- Unit 3: Molecular Symmetry - *CC BY 4.0*
  - 3.1: Symmetry Elements and Operations LOs - *Undeclared*
    - 3.1.1: Definitions and Examples - *CC BY 4.0*
  - 3.2: Point Groups - *Undeclared*
    - 3.2.1: Molecular Point Groups - *CC BY-NC-SA 4.0*
    - 3.2.2: Assigning Point Groups - *Undeclared*
    - 3.2.3: Chirality - *CC BY-NC 4.0*
  - 3.3: Unit 3 Practice Problems - *CC BY 4.0*
- Unit 4: Group Theory - *Undeclared*
  - 4.1: Groups - *Undeclared*
    - 4.1.1: Properties of Groups - *Undeclared*
  - 4.2: Representations and Character Tables - *Undeclared*
    - 4.2.1: Matrices - *Undeclared*
    - 4.2.2: Representations of Point Groups - *Undeclared*
    - 4.2.3: Character Tables - *Undeclared*
  - 4.3: Application to Vibrational Spectroscopy - *Undeclared*
    - 4.3.1: Molecular Vibrations - *CC BY-NC 4.0*
  - 4.4: Unit 4 Practice Problems - *CC BY 4.0*
- Unit 5: Molecular Orbitals - *CC BY-SA 4.0*
  - 5.1: Valence Bond Theory - *Undeclared*
    - 5.1.1: The Shapes of Molecules (VSEPR Theory) and Orbital Hybridization - *CC BY-SA 4.0*
  - 5.2: Linear Combination of Atomic Orbitals - *Undeclared*
    - 5.2.1: Formation of Molecular Orbitals from Atomic Orbitals - *CC BY-SA 4.0*
    - 5.2.2: Molecular Orbitals from s Orbitals - *CC BY-NC 3.0*
    - 5.2.3: Molecular Orbitals from p Orbitals - *CC BY-NC 3.0*
    - 5.2.4: Molecular orbitals from d orbitals - *CC BY-SA 4.0*
    - 5.2.5: Nonbonding Orbitals and Other Factors - *CC BY-SA 4.0*
  - 5.3: Diatomic MO Diagrams - *Undeclared*
    - 5.3.1: Homonuclear Diatomic Molecules - *CC BY-SA 4.0*
      - 5.3.1.1: Molecular Orbitals - *CC BY-SA 4.0*
      - 5.3.1.2: Orbital Mixing - *CC BY-SA 4.0*
      - 5.3.1.3: Diatomic Molecules of the First and Second Periods - *CC BY-SA 4.0*
    - 5.3.1.4: Photoelectron Spectroscopy - *CC BY-SA 4.0*
  - 5.3.2: Heteronuclear Diatomic Molecules - *CC BY-SA 4.0*
    - 5.3.2.1: Orbital ionization energies - *CC BY-SA 4.0*
    - 5.3.2.2: Polar bonds - *CC BY-SA 4.0*
    - 5.3.2.3: Ionic Compounds and Molecular Orbitals - *CC BY-SA 4.0*
  - 5.4: Polyatomic MO Diagrams - *Undeclared*
    - 5.4.1: Ligand Group Orbitals and Generator Functions - *Undeclared*
    - 5.4.2: Polyatomic Molecules - *CC BY-SA 4.0*
      - 5.4.2.1: Bifluoride anion - *CC BY-SA 4.0*
      - 5.4.2.2: Carbon Dioxide - *CC BY-SA 4.0*
      - 5.4.2.3: H<sub>2</sub>O - *CC BY-SA 4.0*
      - 5.4.2.4: NH<sub>3</sub> - *CC BY-SA 4.0*
    - 5.4.3: Why is BeH<sub>2</sub> Linear and H<sub>2</sub>O Bent? - *CC BY-NC-SA 4.0*
  - 5.5: Pi Bonding and Hypervalency - *Undeclared*
    - 5.5.1: BF<sub>3</sub> - *CC BY-SA 4.0*
    - 5.5.2: Expanded Octets and Molecular Orbitals - *Undeclared*
- Unit 6: Solid State Chemistry - *Undeclared*
  - 6.1: Solid State Structures - *Undeclared*
    - 6.1.1: Cubic Lattices and Close Packing - *CC BY 3.0*
    - 6.1.2: Ionic Radii and Radius Ratios - *CC BY-SA 4.0*
  - 6.2: Crystalline Solids - *Undeclared*
    - 6.2.1: Types of Crystalline Solids - *CC BY 4.0*
    - 6.2.2: Alloys and Intermetallics - *Undeclared*
    - 6.2.3: The Imperfect Solid State - *CC BY-NC-SA 4.0*
  - 6.3: X-Ray Crystallography of Solids - *Undeclared*
    - 6.3.1: Miller Indices (hkl) - *Undeclared*
    - 6.3.2: X-rays and X-ray Diffraction - *CC BY-NC-SA 4.0*
    - 6.3.3: Powder X-ray Diffraction - *Undeclared*
  - 6.4: Energetics of Ionic Solids - *Undeclared*
    - 6.4.1: Lattice Enthalpies of Ionic Solids - *CC BY-NC 4.0*
    - 6.4.2: Born Haber Cycles - *CC BY-NC 4.0*
    - 6.4.3: Lattice Energies and Solubility - *CC BY-SA 4.0*
    - 6.4.4: Theoretical Lattice Energy Calculations - *CC BY-NC-SA 4.0*
    - 6.4.5: Kapustinskii Equation - *CC BY-SA 4.0*
  - 6.5: Band Theory and Conductivity - *Undeclared*

- 6.5.1: Bonding in Metals and Semiconductors - *CC BY-NC-SA 4.0*
  - 6.5.2: The Fermi Level - *Undeclared*
  - 6.5.3: Semiconductors- Band Gaps, Colors, Conductivity and Doping - *CC BY-SA 4.0*
  - 6.5.4: Periodic Trends- Metals, Semiconductors, and Insulators - *CC BY-SA 4.0*
  - 6.5.5: Semiconductor p-n Junctions - *CC BY-SA 4.0*
  - 6.5.6: Diodes, LEDs and Solar Cells - *CC BY-SA 4.0*
  - 6.5.7: Superconductors - *CC BY-SA 4.0*
- Unit 7: Acid-Base and Donor-Acceptor Chemistry - *Undeclared*
  - 7.1: Acid Base Chemistry - *Undeclared*
    - 7.1.1: Arrhenius Model - *Undeclared*
    - 7.1.2: Brønsted-Lowry Model - *CC BY-NC-SA 4.0*
    - 7.1.3: Metal Ions as Acids - *CC BY-NC-SA 4.0*
    - 7.1.4: Autoionization and Solvent Leveling - *CC BY-NC-SA 4.0*
    - 7.1.5: Lewis Model and Frontier Orbitals - *CC BY-NC-SA 4.0*
  - 7.2: Hard Soft Acid Base Theory - *Undeclared*
    - 7.2.1: Hard and Soft Acids and Bases - *CC BY-NC-SA 4.0*
    - 7.2.2: Applications of Hard Soft Acid Base Theory - *CC BY-NC-SA 4.0*
    - 7.2.3: Theoretical Interpretation of HSAB Theory - *CC BY-NC-SA 4.0*
  - 7.3: Unit 7 Practice Problems - *CC BY 4.0*
- Unit 8: Electronic Structure of Coordination Complexes - *CC BY 4.0*
  - 8.1: Introduction to Coordination Complexes - *Undeclared*
    - 8.1.1: What are Coordination Complexes? - *CC BY 4.0*
    - 8.1.2: History of Coordination Complexes - *CC BY-NC-SA 4.0*
    - 8.1.3: Nomenclature and Ligands - *Undeclared*
    - 8.1.4: Coordination Numbers and Structures - *CC BY 4.0*
    - 8.1.5: Isomerism - *CC BY 4.0*
  - 8.2: Crystal Field Theory - *Undeclared*
    - 8.2.1: Crystal Field Theory - *CC BY-NC-SA 4.0*
    - 8.2.2: Crystal Field Stabilization Energy - *CC BY-NC-SA 4.0*
    - 8.2.3: Non-octahedral Complexes - *CC BY-NC-SA 4.0*
  - 8.3: Crystal Field Theory and Magnetism - *Undeclared*
    - 8.3.1: Jahn-Teller Distortions - *CC BY-SA 4.0*
    - 8.3.2: Magnetism - *Undeclared*
    - 8.3.3: Magnetic Moments of Transition Metals - *CC BY-NC-SA 4.0*
    - 8.3.4: Ferro-, Ferri- and Antiferromagnetism - *CC BY-SA 4.0*
  - 8.4: Ligand Field Theory - *Undeclared*
    - 8.4.1: Ligand Field Theory - *CC BY-NC-SA 4.0*
    - 8.4.2: The Spectrochemical Series - *CC BY-NC 4.0*
    - 8.4.3: Factors That Affect Ligand Field Splitting - *CC BY-NC-SA 4.0*
    - 8.4.4: Octahedral vs. Tetrahedral Geometries - *CC BY-NC-SA 4.0*
  - 8.5: Absorption Spectroscopy of Coordination Complexes - *Undeclared*
    - 8.5.1: Absorption of Light - *Undeclared*
    - 8.5.2: Colors of Coordination Complexes - *CC BY 4.0*
    - 8.5.3: Charge-Transfer Spectra - *Undeclared*
  - 8.6: Tanabe Sugano Diagrams - *Undeclared*
    - 8.6.1: Tanabe-Sugano Diagrams - *CC BY-SA 4.0*
    - 8.6.2: Selection Rules - *Undeclared*
    - 8.6.3: Applications of Tanabe-Sugano Diagrams - *Undeclared*
    - 8.6.4: Tetrahedral Complexes - *Undeclared*
- Unit 9: Reactions of Coordination Complexes - *Undeclared*
  - 9.1: Substitution Reactions - *Undeclared*
    - 9.1.1: Review of Reaction Thermodynamics and Kinetics - *CC BY-NC 3.0*
    - 9.1.2: Introduction to Substitution Reactions - *Undeclared*
    - 9.1.3: Ligand Substitution Mechanisms - *CC BY-NC-SA 4.0*
    - 9.1.4: Some Reasons for Differing Mechanisms - *CC BY-NC 3.0*
      - 9.1.4.1: Dissociation - *Undeclared*
      - 9.1.4.2: Associative Mechanisms - *Undeclared*
    - 9.1.5: Thermodynamic Stability and Chelate Effect - *CC BY-NC-SA 4.0*
    - 9.1.6: Kinetic Lability - *Undeclared*
    - 9.1.7: The Trans Effect - *CC BY-NC-SA 4.0*
  - 9.2: RedOx Reactions - *Undeclared*
    - 9.2.1: Redox Mechanisms - *Undeclared*
    - 9.2.2: Inner Sphere Electron Transfer - *CC BY-NC 4.0*
    - 9.2.3: Outer Sphere Electron Transfer - *CC BY-NC 4.0*
  - 9.3: Unit 9 Practice Problems - *CC BY 4.0*



- Unit 10: Organometallic Chemistry - *Undeclared*
  - 10.1: Organometallic Complexes - *Undeclared*
    - 10.1.1: Introduction to Organometallic Chemistry - *Undeclared*
    - 10.1.2: Ligand Nomenclature and Classification - *Undeclared*
    - 10.1.3: Survey of Common Organometallic Ligands - *CC BY-NC-SA 4.0*
    - 10.1.4: Electron Counting and the 18 Electron Rule - *CC BY-SA 4.0*
  - 10.2: Organometallic Reactions - *Undeclared*
    - 10.2.1: Ligand Dissociation and Substitution - *Undeclared*
    - 10.2.2: Oxidative Addition - *CC BY-NC-SA 4.0*
    - 10.2.3: Reductive Elimination - *CC BY-NC-SA 4.0*
    - 10.2.4: Migratory Insertion- 1,2-Insertions - *CC BY-NC-SA 4.0*
    - 10.2.5:  $\beta$ -Elimination Reactions - *CC BY-NC-SA 4.0*
    - 10.2.6: Organometallic Catalysts - *CC BY-NC-SA 4.0*
- Back Matter - *Undeclared*
  - Index - *Undeclared*
  - Glossary - *Undeclared*
  - Detailed Licensing - *Undeclared*
  - Detailed Licensing - *Undeclared*